VOLUME 26 / NUMBER 24
DECEMBER 23, 1988
ACC. NOS. N88-29715 TO N88-30583

STAR
AN ABSTRACT JOURNAL

Scientific and Technical Aerospace Reports

PRODUCED BY THE
SCIENTIFIC AND TECHNICAL
INFORMATION
DIVISION

NASA

NATIONAL AERONAUTICS AND SPACE ADMINISTRATION

WHAT YOU CAN DO FOR *STAR*

All users of this abstract service are urged to forward reports to be considered for announcement in *STAR*. This will aid NASA in its efforts to provide the fullest possible coverage of all scientific and technical publications that might support aeronautics and space research and development. If you have prepared relevant reports (other than those that you will transmit to NASA, DoD, or DOE through the usual contract- or grant-reporting channels), please send them for consideration to the NASA Scientific and Technical Information Facility, P.O. Box 8757, B.W.I. Airport, Maryland 21240.

Reprints of journal articles, book chapters, and conference papers are also welcome. These will be considered for announcement in *STAR's* companion journal, *International Aerospace Abstracts.*

You may specify a particular source to be included in a report announcement if you wish; otherwise the report will be placed on public sale at the National Technical Information Service. Copyrighted publications will be announced but not distributed or sold.

PURCHASE OF *STAR*

The semimonthly issues are available for sale by the Superintendent of Documents, U.S. Government Printing Office, Washington, D.C. 20402.

PUBLISHED BY:

UNITED STATES GOVERNMENT
NATIONAL AERONAUTICS AND SPACE ADMINISTRATION
SCIENTIFIC AND TECHNICAL INFORMATION DIVISION
Scientific and Technical Aerospace Reports, Volume 26, is prepared by the NASA Scientific and Technical Information Facility operated for the National Aeronautics and Space Administration by RMS Associates.

The Administrator of the National Aeronautics and Space Administration has determined that the publication of this periodical is necessary in the transaction of the public business required by law of this Agency. Use of funds for printing this periodical has been approved by the Director of the Office of Management and Budget through March 22, 1989.

US ISSN 0036-8741

INTRODUCTION

Scientific and Technical Aerospace Reports (STAR) is a major component of a comprehensive National Aeronautics and Space Administration information system covering aeronautics, space, and supporting disciplines. *STAR* is issued on the 8th and 23rd of each month and announces current publications of the following types:

- NASA, NASA contractor, and NASA grantee reports
- Reports issued by other U.S. Government Agencies, domestic and foreign institutions, universities, and private firms
- Translations in report form
- NASA-owned patents and patent applications
- Dissertations and theses

Journal, book, and conference literature, cover-to-cover journal translations, and certain foreign dissertations are announced in a companion journal, *International Aerospace Abstracts (IAA)*, available on subscription from the American Institute of Aeronautics and Astronautics, Technical Information Service, 555 West 57th Street, 12th Floor, New York, New York 10019.

SUBJECT SCOPE

Subject scope of *STAR*, and *IAA* includes all aspects of aeronautics and space research and development, supporting basic and applied research, and applications. Aerospace aspects of earth resources, energy development, conservation, oceanography, environmental protection, urban transportation, and other topics of high national priority are also covered.

OTHER NASA PUBLICATIONS

Other NASA publications and information services are described in the publication, *The NASA Scientific and Technical Information System ... and How to Use It*, available without charge from the NASA Scientific and Technical Information Facility, P.O. Box 8757, B.W.I. Airport, Maryland 21240.

HOW TO USE *STAR* SUBJECT CATEGORIES

STAR is categorized by 10 major subject divisions divided into 76 specific subject categories and one general category/division. The major subject divisions are listed in the Table of Contents, together with a note for each that defines its scope and provides any cross-references. For example:

AERONAUTICS

Includes aeronautics (general); aerodynamics; air transportation and safety; aircraft communications and navigation; aircraft design, testing and performance; aircraft instrumentation; aircraft propulsion and power; aircraft stability and control; and research and support facilities (air).

For related information see also *Astronautics*.

Each major division is further divided into as many as nine specific categories, which are identified by category numbers.

Abstracts in *STAR* are grouped by specific category, the categories appearing in sequential order. Category breaks in the abstract section are identified by the category number and title, and a scope note. Cross-references to other categories are provided as appropriate. For example:

02 AERODYNAMICS

Includes aerodynamics of bodies, combinations, wings, rotors, and control surfaces; and internal flow in ducts and turbomachinery.

For related information see also *34 Fluid Mechanics and Heat Transfer.*

CROSS-REFERENCES

Individual *STAR* abstracts are not ordinarily cross-referenced, except for certain conference reports or book translations that have had separate abstracts written for their component papers or chapters. Citations and abstracts of the components follow immediately after those of the parent document. When the subject content of a component differs sufficiently from the general content of the parent, a cross-reference citation also is printed at the end of the category to which it normally would have been assigned if it were independent.

DOCUMENTS ON MICROFICHE

Documents on microfiche[1] are designated by a pound sign (#) following the accession number. The pound sign is used without regard to the source or quality of the microfiche.

AVAILABILITIES

One or more sources from which a document announced in *STAR* is available to the public is given in each citation. The most commonly indicated sources and their acronyms or abbreviations are listed below. If the publication is available from a source other than those listed, the publisher and his address will be displayed on the availability line or in combination with the corporate source line.

Avail: NTIS. Sold by the National Technical Information Service. Prices for hard copy (HC) and microfiche (MF) are indicated by a price code following the letters HC or MF in the *STAR* citation. Current values for the price codes are given in the tables on page vii.

Initially distributed microfiche under the NTIS SRIM (Selected Research in Microfiche) is available at greatly reduced unit prices. For this service and for information concerning subscription to NASA printed reports, consult the NTIS Subscription Section, Springfield, Va. 22161.

NOTE ON ORDERING DOCUMENTS: When ordering NASA publications (those followed by the * symbol), use the N accession number. NASA patent applications (only the specifications are offered) should be ordered by the US-Patent-Appl-SN number. Non-NASA publications (no asterisk) should be ordered by the AD, PB, or other *report number* shown on the last line of the citation, not by the N accession number. It is also advisable to cite the title and other bibliographic identification.

Avail: SOD (or GPO). Sold by the Superintendent of Documents, U.S. Government Printing Office, in hard copy. The current price and order number are given following the availability line. (NTIS will fill microfiche requests, as indicated above, for those documents identified by a # symbol.)

(1) A microfiche is a transparent sheet of film, 105 by 148 mm in size, containing as many as 60 to 98 pages of information reduced to micro images (not to exceed 26:1 reduction).

Avail: BLL (formerly NLL): British Library Lending Division, Boston Spa, Wetherby, Yorkshire, England. Photocopies available from this organization at the price shown. (If none is given, inquiry should be addressed to the BLL.)

Avail: DOE Depository Libraries. Organizations in U.S. cities and abroad that maintain collections of Department of Energy reports, usually in microfiche form, are listed in *Energy Research Abstracts.* Services available from the DOE and its depositories are described in a booklet, *DOE Technical Information Center - Its Functions and Services* (TID-4660), which may be obtained without charge from the DOE Technical Information Center.

Avail: ESDU. Pricing information on specific data, computer programs, and details on ESDU topic categories can be obtained from ESDU International Ltd. Requesters in North America should use the Virginia address while all other requesters should use the London address, both of which are on page vi.

Avail: Fachinformationszentrum, Karlsruhe. Sold by the Fachinformationszentrum Energie, Physik, Mathematik GMBH, Eggenstein Leopoldshafen, Federal Republic of Germany, at the price shown in deutschmarks (DM).

Avail: HMSO. Publications of Her Majesty's Stationery Office are sold in the U.S. by Pendragon House, Inc. (PHI), Redwood City, California. The U.S. price (including a service and mailing charge) is given, or a conversion table may be obtained from PHI.

Avail: NASA Public Document Rooms. Documents so indicated may be examined at or purchased from the National Aeronautics and Space Administration, Public Documents Room (Room 126), 600 Independence Ave., S.W., Washington, D.C. 20546, or public document rooms located at each of the NASA research centers, the NASA Space Technology Laboratories, and the NASA Pasadena Office at the Jet Propulsion Laboratory.

Avail: Univ. Microfilms. Documents so indicated are dissertations selected from *Dissertation Abstracts* and are sold by University Microfilms as xerographic copy (HC) and microfilm. All requests should cite the author and the Order Number as they appear in the citation.

Avail: US Patent and Trademark Office. Sold by Commissioner of Patents and Trademarks, U.S. Patent and Trademark Office, at the standard price of $1.50 each, postage free. (See discussion of NASA patents and patent applications below.)

Avail: (US Sales Only). These foreign documents are available to users within the United States from the National Technical Information Service (NTIS). They are available to users outside the United States through the International Nuclear Information Service (INIS) representative in their country, or by applying directly to the issuing organization.

Avail: USGS. Originals of many reports from the U.S. Geological Survey, which may contain color illustrations, or otherwise may not have the quality of illustrations preserved in the microfiche or facsimile reproduction, may be examined by the public at the libraries of the USGS field offices whose addresses are listed in this Introduction. The libraries may be queried concerning the availability of specific documents and the possible utilization of local copying services, such as color reproduction.

Avail: Issuing Activity, or Corporate Author, or no indication of availability. Inquiries as to the availability of these documents should be addressed to the organization shown in the citation as the corporate author of the document.

NASA PATENTS AND PATENT APPLICATIONS

Patents and patent applications owned by NASA are announced in *STAR* under appropriate subject categories and are referenced in the *STAR* indexes. In the Report/Accession Number Index, patents are indexed by the NASA Case Number (which appears in lieu of the report number in other indexes), the U.S. Patent Number, the U.S. Patent Application Serial Number, and the U.S. Patent Class. Patent applications for which patents have not yet been issued are indexed by the NASA Case Number and the U.S. Patent Application Serial Number.

NASA *patent application specifications* are sold in paper copy by the National Technical Information Service at price code A02. Microfiche are sold at price code A01. The US-Patent-Appl-SN- number should be used in ordering either paper copy or microfiche from NTIS. Printed copies of *patents* (which are not microfiched) are available for purchase at $1.50 per copy from:

Commissioner of Patents and Trademarks
U.S. Patent and Trademark Office
Washington, D.C. 20231

When ordering patents, the U.S. Patent Number should be used, and payment must be remitted in advance, preferably by money order or check payable to the Commissioner of Patents and Trademarks. Prepaid purchase coupons for ordering are also available from the Patent and Trademark Office. The patents and patent applications announced in *STAR* are owned by NASA and are available for royalty-free licensing. Requests for licensing terms and further information should be addressed to:

Associate General Counsel for Intellectual Property/Code GP
National Aeronautics and Space Administration
Washington, D.C. 20546

ELIGIBILITY AND REGISTRATION FOR NASA INFORMATION PRODUCTS AND SERVICES

A variety of services is available to organizations of the following types that have registered with NASA to receive specific services or products:

1. NASA offices, research centers, contractors, subcontractors, grantees, and consultants;
2. Other U.S. Government agencies and their contractors;
3. Libraries in the United States that have arrangements with NASA to maintain collections of NASA documents for public reference;
4. Other organizations in the United States having a need for NASA documents in work related to aeronautics and space research;
5. Organizations abroad that have established reciprocal document exchange arrangements with NASA.

Only the central service points or central points of document acquisition and control within qualified organizations are eligible to register for NASA products and services. Domestic organizations that may be eligible to receive various classes of NASA publications and services should address their requests for registration or for further information to:

NASA Scientific and Technical Information Facility
ATTN: Registration Activity
P.O. Box 8757
B.W.I. Airport, Maryland 21240

Organizations abroad should direct requests to the same address, but to the attention of: International Exchange Program.

AVAILABILITY OF *STAR* ABSTRACTS ON MICROFICHE

Microfiche of the abstract sections of this issue and other issues of *STAR* are available on annual subscription from NTIS as PB88-911300, Attn: Subscriptions, 5285 Port Royal Road, Springfield, Virginia 22161. Annual subscription rates are $70.00 North America; $140.00 foreign. Abstract sections for previous years retroactive to 1964 are available at the current rates. Microfiche for individual *STAR* issue abstract sections are not available.

PUBLIC COLLECTIONS OF NASA DOCUMENTS

DOMESTIC: NASA and NASA-sponsored documents and a large number of aerospace publications are available to the public for reference purposes at the library maintained by the American Institute of Aeronautics and Astronautics, Technical Information Service, 555 West 57th Street, 12th Floor, New York, New York 10019

EUROPEAN: An extensive collection of NASA and NASA-sponsored publications is maintained by the British Library Lending Division, Boston Spa, Wetherby, Yorkshire, England for public access. The British Library Lending Division also has available many of the non-NASA publications cited in *STAR*. European requesters may purchase facsimile copy or microfiche of NASA and NASA-sponsored documents, those identified by both the symbols # and * from ESA - Information Retrieval Service European Space Agency, 8-10 rue Mario-Nikis, 75738 Paris CEDEX 15, France.

FEDERAL DEPOSITORY LIBRARY PROGRAM

In order to provide the general public with greater access to U.S. Government publications, Congress established the Federal Depository Library Program under the Government Printing Office (GPO), with 50 regional depositories responsible for permanent retention of material, inter-library loan, and reference services. At least one copy of nearly every NASA and NASA-sponsored publication, either in printed or microfiche format, is received and retained by the 50 regional depositories. A list of the regional GPO libraries, arranged alphabetically by state, appears on the inside back cover. These libraries are *not* sales outlets. A local library can contact a Regional Depository to help locate specific reports, or direct contact may be made by an individual.

ADDRESSES OF ORGANIZATIONS

American Institute of Aeronautics and Astronautics
Technical Information Service
555 West 57th Street, 12th Floor
New York, New York 10019

British Library Lending Division,
Boston Spa, Wetherby, Yorkshire,
England

Commissioner of Patents and Trademarks
U.S. Patent and Trademark Office
Washington, D.C. 20231

Department of Energy
Technical Information Center
P.O. Box 62
Oak Ridge, Tennessee 37830

ESA-Information Retrieval Service
ESRIN
Via Galileo Galilei
00044 Frascati (Rome) Italy

ESDU International, Ltd.
1495 Chain Bridge Road
McLean, Virginia 22101

ESDU International, Ltd.
251-259 Regent Street
London, W1R 7AD, England

Fachinformationszentrum Energie, Physik, Mathematik GMBH
7514 Eggenstein Leopoldshafen
Federal Republic of Germany

Her Majesty's Stationery Office
P.O. Box 569, S.E. 1
London, England

NASA Scientific and Technical Information Facility
P.O. Box 8757
B.W.I. Airport, Maryland 21240

National Aeronautics and Space Administration
Scientific and Technical Information Division (NTT-1)
Washington, D.C. 20546

National Technical Information Service
5285 Port Royal Road
Springfield, Virginia 22161

Pendragon House, Inc.
899 Broadway Avenue
Redwood City, California 94063

Superintendent of Documents
U.S. Government Printing Office
Washington, D.C. 20402

University Microfilms
A Xerox Company
300 North Zeeb Road
Ann Arbor, Michigan 48106

University Microfilms, Ltd.
Tylers Green
London, England

U.S. Geological Survey Library
National Center - MS 950
12201 Sunrise Valley Drive
Reston, Virginia 22092

U.S. Geological Survey Library
2255 North Gemini Drive
Flagstaff, Arizona 86001

U.S. Geological Survey
345 Middlefield Road
Menlo Park, California 94025

U.S. Geological Survey Library
Box 25046
Denver Federal Center, MS914
Denver, Colorado 80225

NTIS PRICE SCHEDULES

(Effective January 1, 1988)

Schedule A
STANDARD PRICE DOCUMENTS AND MICROFICHE

PRICE CODE	NORTH AMERICAN PRICE	FOREIGN PRICE
A01	$ 6.95	$13.90
A02	9.95	19.90
A03	12.95	25.90
A04-A05	14.95	29.90
A06-A09	19.95	39.90
A10-A13	25.95	51.90
A14-A17	32.95	65.90
A18-A21	38.95	77.90
A22-A25	44.95	89.90
A99	*	*
NO1	49.50	89.90
NO2	48.00	80.00

Schedule E
EXCEPTION PRICE DOCUMENTS AND MICROFICHE

PRICE CODE	NORTH AMERICAN PRICE	FOREIGN PRICE
E01	$ 8.50	17.00
E02	11.00	22.00
E03	12.00	24.00
E04	14.50	29.00
E05	16.50	33.00
E06	19.00	38.00
E07	21.50	43.00
E08	24.00	48.00
E09	26.50	53.00
E10	29.00	58.00
E11	31.50	63.00
E12	34.00	68.00
E13	36.50	73.00
E14	39.50	79.00
E15	43.00	86.00
E16	47.00	94.00
E17	51.00	102.00
E18	55.00	110.00
E19	61.00	122.00
E20	71.00	142.00
E99	*	*

* Contact NTIS for price quote.

IMPORTANT NOTICE

NTIS Shipping and Handling Charges

U.S., Canada, Mexico — ADD $3.00 per TOTAL ORDER

All Other Countries — ADD $4.00 per TOTAL ORDER

Exceptions — Does NOT apply to:

ORDERS REQUESTING NTIS RUSH HANDLING

ORDERS FOR SUBSCRIPTION OR STANDING ORDER PRODUCTS *ONLY*

NOTE: Each additional delivery address on an order requires a separate shipping and handling charge.

VOLUME 26 NUMBER 24 / DECEMBER 23, 1988

TABLE OF CONTENTS

AERONAUTICS

Includes aeronautics (general); aerodynamics; air transportation and safety; aircraft communications and navigation; aircraft design, testing and performance; aircraft instrumentation; aircraft propulsion and power; aircraft stability and control; and research and support facilities (air).

For related information see also *Astronautics.*

01 AERONAUTICS (GENERAL) 3311

02 AERODYNAMICS 3315

Includes aerodynamics of bodies, combinations, wings, rotors, and control surfaces; and internal flow in ducts and turbomachinery.

For related information see also *34 Fluid Mechanics and Heat Transfer*

03 AIR TRANSPORTATION AND SAFETY 3322

Includes passenger and cargo air transport operations; and aircraft accidents.

For related information see also *16 Space Transportation* and *85 Urban Technology and Transportation.*

04 AIRCRAFT COMMUNICATIONS AND NAVIGATION 3322

Includes digital and voice communication with aircraft; air navigation systems (satellite and ground based); and air traffic control.

For related information see also *17 Space Communications, Spacecraft Communications, Command and Tracking* and *32 Communications and Radar.*

05 AIRCRAFT DESIGN, TESTING AND PERFORMANCE 3323

Includes aircraft simulation technology.

For related information see also *18 Spacecraft Design, Testing and Performance* and *39 Structural Mechanics.* For land transportation vehicles see *85 Urban Technology and Transportation.*

06 AIRCRAFT INSTRUMENTATION 3324

Includes cockpit and cabin display devices; and flight instruments.

For related information see also *19 Spacecraft Instrumentation* and *35 Instrumentation and Photography.*

07 AIRCRAFT PROPULSION AND POWER 3325

Includes prime propulsion systems and systems components, e.g., gas turbine engines and compressors; and onboard auxiliary power plants for aircraft.

For related information see also *20 Spacecraft Propulsion and Power, 28 Propellants and Fuels,* and *44 Energy Production and Conversion.*

08 AIRCRAFT STABILITY AND CONTROL 3328

Includes aircraft handling qualities; piloting; flight controls; and autopilots.

For related information see also *05 Aircraft Design, Testing and Performance.*

09 RESEARCH AND SUPPORT FACILITIES (AIR) 3329

Includes airports, hangars and runways; aircraft repair and overhaul facilities; wind tunnels; shock tubes; and aircraft engine test stands.

For related information see also *14 Ground Support Systems and Facilities (Space).*

ASTRONAUTICS

Includes astronautics (general); astrodynamics; ground support systems and facilities (space); launch vehicles and space vehicles; space transportation; space communications, spacecraft communications, command and tracking; spacecraft design, testing and performance; spacecraft instrumentation; and spacecraft propulsion and power.

For related information see also *Aeronautics*

12 ASTRONAUTICS (GENERAL) 3330

For extraterrestrial exploration see *91 Lunar and Planetary Exploration.*

13 ASTRODYNAMICS 3331

Includes powered and free-flight trajectories; and orbital and launching dynamics.

14 GROUND SUPPORT SYSTEMS AND FACILITIES (SPACE) 3332

Includes launch complexes, research and production facilities; ground support equipment, e.g., mobile transporters; and simulators.

For related information see also *09 Research and Support Facilities (Air).*

15 LAUNCH VEHICLES AND SPACE VEHICLES 3332

Includes boosters; operating problems of launch/space vehicle systems; and reusable vehicles.

For related information see also *20 Spacecraft Propulsion and Power.*

16 SPACE TRANSPORTATION 3332

Includes passenger and cargo space transportation, e.g., shuttle operations; and space rescue techniques.

For related information see also *03 Air Transportation and Safety* and *18 Spacecraft Design, Testing and Performance.* For space suits see *54 Man/System Technology and Life Support.*

17 SPACE COMMUNICATIONS, SPACECRAFT COMMUNICATIONS, COMMAND AND TRACKING N.A.

Includes telemetry; space communications networks; astronavigation and guidance; and radio blackout.

For related information see also *04 Aircraft Communications and Navigation* and *32 Communications and Radar.*

18 SPACECRAFT DESIGN, TESTING AND PERFORMANCE 3333

Includes satellites; space platforms; space stations; spacecraft systems and components such as thermal and environmental controls; and attitude controls.

For life support systems see *54 Man/System Technology and Life Support.* For related information see also *05 Aircraft Design, Testing and Performance, 39 Structural Mechanics,* and *16 Space Transportation.*

19 SPACECRAFT INSTRUMENTATION 3336

For related information see also *06 Aircraft Instrumentation* and *35 Instrumentation and Photography.*

20 SPACECRAFT PROPULSION AND POWER 3336

Includes main propulsion systems and components, e.g. rocket engines; and spacecraft auxiliary power sources.

For related information see also *07 Aircraft Propulsion and Power, 28 Propellants and Fuels, 44 Energy Production and Conversion,* and *15 Launch Vehicles and Space Vehicles.*

CHEMISTRY AND MATERIALS

Includes chemistry and materials (general); composite materials; inorganic and physical chemistry; metallic materials; nonmetallic materials; propellants and fuels; and materials processing.

23 CHEMISTRY AND MATERIALS (GENERAL) N.A.

24 COMPOSITE MATERIALS 3339

Includes physical, chemical, and mechanical properties of laminates and other composite materials.

For ceramic materials see *27 Nonmetallic Materials.*

25 INORGANIC AND PHYSICAL CHEMISTRY 3342

Includes chemical analysis, e.g., chromatography; combustion theory; electrochemistry; and photochemistry.

For related information see also *77 Thermodynamics and Statistical Physics.*

26 METALLIC MATERIALS 3353

Includes physical, chemical, and mechanical properties of metals, e.g., corrosion; and metallurgy.

27 NONMETALLIC MATERIALS 3354

Includes physical, chemical, and mechanical properties of plastics, elastomers, lubricants, polymers, textiles, adhesives, and ceramic materials.

For composite materials see *24 Composite Materials.*

28 PROPELLANTS AND FUELS 3356

Includes rocket propellants, igniters and oxidizers; their storage and handling procedures; and aircraft fuels.

For related information see also *07 Aircraft Propulsion and Power, 20 Spacecraft Propulsion and Power,* and *44 Energy Production and Conversion.*

29 MATERIALS PROCESSING 3358

Includes space-based development of products and processes for commercial application.

For biological materials see *55 Space Biology.*

ENGINEERING

Includes engineering (general); communications and radar; electronics and electrical engineering; fluid mechanics and heat transfer; instrumentation and photography; lasers and masers; mechanical engineering; quality assurance and reliability; and structural mechanics.

For related information see also *Physics.*

31 ENGINEERING (GENERAL) 3358

Includes vacuum technology; control engineering; display engineering; cryogenics; and fire prevention.

32 COMMUNICATIONS AND RADAR 3359

Includes radar; land and global communications; communications theory; and optical communications.

For related information see also *04 Aircraft Communications and Navigation* and *17 Space Communications, Spacecraft Communications, Command and Tracking.* For search and rescue see *03 Air Transportation and Safety,* and *16 Space Transportation.*

33 ELECTRONICS AND ELECTRICAL ENGINEERING 3365

Includes test equipment and maintainability; components, e.g., tunnel diodes and transistors; microminiaturization; and integrated circuitry.

For related information see also *60 Computer Operations and Hardware* and *76 Solid-State Physics.*

34 FLUID MECHANICS AND HEAT TRANSFER 3368

Includes boundary layers; hydrodynamics; fluidics; mass transfer and ablation cooling.

For related information see also *02 Aerodynamics* and *77 Thermodynamics and Statistical Physics.*

35 INSTRUMENTATION AND PHOTOGRAPHY 3374

Includes remote sensors; measuring instruments and gages; detectors; cameras and photographic supplies; and holography.

For aerial photography see *43 Earth Resources and Remote Sensing.* For related information see also *06 Aircraft Instrumentation* and *19 Spacecraft Instrumentation.*

36 LASERS AND MASERS 3377

Includes parametric amplifiers.

For related information see also *76 Solid-State Physics.*

37 MECHANICAL ENGINEERING 3379

Includes auxiliary systems (nonpower); machine elements and processes; and mechanical equipment.

38 QUALITY ASSURANCE AND RELIABILITY 3381

Includes product sampling procedures and techniques; and quality control.

39 STRUCTURAL MECHANICS 3382

Includes structural element design and weight analysis; fatigue; and thermal stress.

For applications see *05 Aircraft Design, Testing and Performance* and *18 Spacecraft Design, Testing and Performance.*

GEOSCIENCES

Includes geosciences (general); earth resources and remote sensing; energy production and conversion; environment pollution; geophysics; meteorology and climatology; and oceanography.

For related information see also *Space Sciences.*

42 GEOSCIENCES (GENERAL) **N.A.**

43 EARTH RESOURCES AND REMOTE SENSING **3385**

Includes remote sensing of earth resources by aircraft and spacecraft; photogrammetry; and aerial photography.

For instrumentation see *35 Instrumentation and Photography.*

44 ENERGY PRODUCTION AND CONVERSION **3389**

Includes specific energy conversion systems, e.g., fuel cells; global sources of energy; geophysical conversion; and windpower.

For related information see also *07 Aircraft Propulsion and Power, 20 Spacecraft Propulsion and Power,* and *28 Propellants and Fuels.*

45 ENVIRONMENT POLLUTION **3389**

Includes atmospheric, noise, thermal, and water pollution.

46 GEOPHYSICS **3390**

Includes aeronomy; upper and lower atmosphere studies; ionospheric and magnetospheric physics; and geomagnetism.

For space radiation see *93 Space Radiation.*

47 METEOROLOGY AND CLIMATOLOGY **3403**

Includes weather forecasting and modification.

48 OCEANOGRAPHY **3405**

Includes biological, dynamic, and physical oceanography; and marine resources.

For related information see also *43 Earth Resources and Remote Sensing.*

LIFE SCIENCES

Includes life sciences (general); aerospace medicine; behavioral sciences; man/system technology and life support; and space biology.

51 LIFE SCIENCES (GENERAL) **3406**

52 AEROSPACE MEDICINE **3406**

Includes physiological factors; biological effects of radiation; and effects of weightlessness on man and animals.

53 BEHAVIORAL SCIENCES **3408**

Includes psychological factors; individual and group behavior; crew training and evaluation; and psychiatric research.

54 MAN/SYSTEM TECHNOLOGY AND LIFE SUPPORT **3409**

Includes human engineering; biotechnology; and space suits and protective clothing.

For related information see also *16 Space Transportation.*

55 SPACE BIOLOGY **N.A.**

Includes exobiology; planetary biology; and extraterrestrial life.

MATHEMATICAL AND COMPUTER SCIENCES

Includes mathematical and computer sciences (general); computer operations and hardware; computer programming and software; computer systems; cybernetics; numerical analysis; statistics and probability; systems analysis; and theoretical mathematics.

59 MATHEMATICAL AND COMPUTER SCIENCES (GENERAL) **N.A.**

60 COMPUTER OPERATIONS AND HARDWARE **3411**

Includes hardware for computer graphics, firmware, and data processing.

For components see *33 Electronics and Electrical Engineering.*

61 COMPUTER PROGRAMMING AND SOFTWARE **3411**

Includes computer programs, routines, algorithms, and specific applications, e.g., CAD/CAM.

62 COMPUTER SYSTEMS **3414**

Includes computer networks and special application computer systems.

63 CYBERNETICS **3414**

Includes feedback and control theory, artificial intelligence, robotics and expert systems.

For related information see also *54 Man/System Technology and Life Support.*

64 NUMERICAL ANALYSIS **3424**

Includes iteration, difference equations, and numerical approximation.

65 STATISTICS AND PROBABILITY **3426**

Includes data sampling and smoothing; Monte Carlo method; and stochastic processes.

66 SYSTEMS ANALYSIS **3426**

Includes mathematical modeling; network analysis; and operations research.

67 THEORETICAL MATHEMATICS **N.A.**

Includes topology and number theory.

PHYSICS

Includes physics (general); acoustics; atomic and molecular physics; nuclear and high-energy physics; optics; plasma physics; solid-state physics; and thermodynamics and statistical physics.

For related information see also *Engineering.*

70 PHYSICS (GENERAL) **3427**

For precision time and time interval (PTTI) see *35 Instrumentation and Photography;* for geophysics, astrophysics or solar physics see *46 Geophysics, 90 Astrophysics,* or *92 Solar Physics.*

71 ACOUSTICS 3427
Includes sound generation, transmission, and attenuation.
For noise pollution see *45 Environment Pollution.*

72 ATOMIC AND MOLECULAR PHYSICS 3428
Includes atomic structure, electron properties, and molecular spectra.

73 NUCLEAR AND HIGH-ENERGY PHYSICS 3428
Includes elementary and nuclear particles; and reactor theory.
For space radiation see *93 Space Radiation.*

74 OPTICS 3428
Includes light phenomena and optical devices.
For lasers see *36 Lasers and Masers.*

75 PLASMA PHYSICS 3431
Includes magnetohydrodynamics and plasma fusion.
For ionospheric plasmas see *46 Geophysics.* For space plasmas see *90 Astrophysics.*

76 SOLID-STATE PHYSICS 3432
Includes superconductivity.
For related information see also *33 Electronics and Electrical Engineering* and *36 Lasers and Masers.*

77 THERMODYNAMICS AND STATISTICAL PHYSICS 3435
Includes quantum mechanics; theoretical physics; and Bose and Fermi statistics.
For related information see also *25 Inorganic and Physical Chemistry* and *34 Fluid Mechanics and Heat Transfer.*

SOCIAL SCIENCES

Includes social sciences (general); administration and management; documentation and information science; economics and cost analysis; law, political science, and space policy; and urban technology and transportation.

80 SOCIAL SCIENCES (GENERAL) N.A.
Includes educational matters.

81 ADMINISTRATION AND MANAGEMENT 3435
Includes management planning and research.

82 DOCUMENTATION AND INFORMATION SCIENCE 3435
Includes information management; information storage and retrieval technology; technical writing; graphic arts; and micrography.
For computer documentation see *61 Computer Programming and Software.*

83 ECONOMICS AND COST ANALYSIS 3439
Includes cost effectiveness studies.

84 LAW, POLITICAL SCIENCE AND SPACE POLICY N.A.
Includes NASA appropriation hearings; aviation law; space law and policy; international law; international cooperation; and patent policy.

85 URBAN TECHNOLOGY AND TRANSPORTATION 3440
Includes applications of space technology to urban problems; technology transfer; technology assessment; and surface and mass transportation.
For related information see *03 Air Transportation and Safety, 16 Space Transportation,* and *44 Energy Production and Conversion.*

SPACE SCIENCES

Includes space sciences (general); astronomy; astrophysics; lunar and planetary exploration; solar physics; and space radiation.
For related information see also *Geosciences.*

88 SPACE SCIENCES (GENERAL) 3440

89 ASTRONOMY 3452
Includes radio, gamma-ray, and infrared astronomy; and astrometry.

90 ASTROPHYSICS 3454
Includes cosmology; celestial mechanics; space plasmas; and interstellar and interplanetary gases and dust.
For related information see also *75 Plasma Physics.*

91 LUNAR AND PLANETARY EXPLORATION 3456
Includes planetology; and manned and unmanned flights.
For spacecraft design or space stations see *18 Spacecraft Design, Testing and Performance.*

92 SOLAR PHYSICS 3458
Includes solar activity, solar flares, solar radiation and sunspots.
For related information see *93 Space Radiation.*

93 SPACE RADIATION 3459
Includes cosmic radiation; and inner and outer earth's radiation belts.
For biological effects of radiation see *52 Aerospace Medicine.* For theory see *73 Nuclear and High-Energy Physics.*

GENERAL

Includes aeronautical, astronautical, and space science related histories, biographies, and pertinent reports too broad for categorization; histories or broad overviews of NASA programs.

99 GENERAL 3459

Note: N.A. means that no abstracts were assigned to this category for this issue.

SUBJECT INDEX I-1
PERSONAL AUTHOR INDEX I-55
CORPORATE SOURCE INDEX I-63
CONTRACT NUMBER INDEX I-75
REPORT/ACCESSION NUMBER INDEX I-77

TYPICAL CITATION AND ABSTRACT

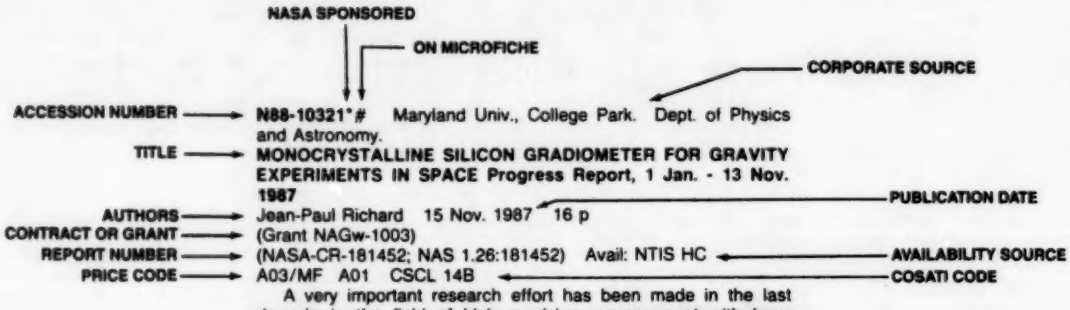

A very important research effort has been made in the last decade in the field of high precision measurement with laser instrumentation. The development of a space borne gradiometer operating at a high sensitivity level using laser measurement of the distance between proof mass over a short base line of order one meter is discussed. Two aspects of laser technology make it a promising tool for gradiometry measurements: quantum limited accuracy and absolute distance measurements. The quantum limit associated with laser instrumentation was formulated. The relevant quantum and classical sources of errors in laser measurements were reviewed and corresponding laser performance requirements for gradient measurements were evaluated. Some mechanical quality factor measurements were made on simple resonant monocrystalline silicon suspensions. It was discovered that the use of zero derivative restoring forces to position the gradiometer test masses will dramatically reduce the gradiometer temperature control requirements. A laser beam side injection scheme was discovered which permits rejection of common mode accelerations. These concepts are briefly discussed. Author

VOLUME 26 NUMBER 24 / DECEMBER 23, 1988

Scientific and Technical Aerospace Reports

A Semimonthly Publication of the National Aeronautics and Space Administration

01 AERONAUTICS (GENERAL)

N88-29715*# National Aeronautics and Space Administration. Langley Research Center, Hampton, Va.
NONLINEAR TOLLMIEN-SCHLICHTING/VORTEX INTERACTION IN BOUNDARY LAYERS Final Report
P. Hall and F. T. Smith (University Coll., London, England) Aug. 1988 37 p Submitted for publication
(Contract NAS1-18107)
(NASA-CR-181698; ICASE-88-46; NAS 1.26:181698) Avail: NTIS HC A03/MF A01 CSCL 01B

The nonlinear reaction between two oblique 3-D Tollmein-Schlichting (TS) waves and their induced streamwise-vortex flow is considered theoretically for an imcompressible boundary layer. The same theory applies to the destabilization of an incident vortex motion by subharmonic TS waves, followed by interaction. The scales and flow structure involved are addressed for high Reynolds numbers. The nonlionear interaction is powerful, starting at quite low amplitudes with a triple-deck structure for the TS waves but a large-scale structure for the induced vortex, after which strong nonlinear amplification occurs. This includes nonparallel-flow effects. The nonlinear interaction is governed by a partial differential system for the vortex flow coupled with an ordinary-differential one for the TS pressure. The solution properties found sometimes produce a breakup within a finite distance and sometimes further downstream, depending on the input amplitudes upstream and on the wave angles, and that then leads to the second stages of interaction associated with higher amplitudes, the main second stages giving either long-scale phenomena significantly affected by nonparallelism or shorter quasi-parallel ones governed by the full nonlinear triple-deck response. Author

N88-29716*# National Aeronautics and Space Administration. Langley Research Center, Hampton, Va.
THE STRONG NONLINEAR INTERACTION OF TOLLMIEN-SCHLICHTING WAVES AND TAYLOR-GOERTLER VORTICES IN CURVED CHANNEL FLOW Final Report
J. Bennett, P. Hall, and F. T. Smith (University Coll., London, England) Aug. 1988 35 p Submitted for publication
(Contracts NAS1-18107; NAS1-18605)
(NASA-CR-181697; ICASE-88-45; NAS 1.26:181697) Avail: NTIS HC A03/MF A01 CSCL 01B

Viscous fluid flows with curved streamlines can support both centrifugal and viscous traveling wave instabilities. Here the interaction of these instabilities in the context of the fully developed flow in a curved channel is discussed. The viscous (Tollmein-Schlichting) instability is described asymptotically at high Reynolds numbers and it is found that it can induce a Taylor-Goertler flow even at extremely small amplitudes. In this interaction, the Tollmein-Schlichting wave can drive a vortex state with wavelength either comparable with the channel width or the wavelength of lower branch viscous modes. The nonlinear equations which describe these interactions are solved for nonlinear equilibrium states. Author

N88-29717# Advisory Group for Aerospace Research and Development, Neuilly-Sur-Seine (France). Structures and Materials Panel.
THE FLIGHT OF FLEXIBLE AIRCRAFT IN TURBULENCE: STATE-OF-THE-ART IN THE DESCRIPTION AND MODELLING OF ATMOSPHERIC TURBULENCE
Jun. 1988 111 p Meeting held in Cesme, Turkey, 4-9 Oct. 1987
(AGARD-R-734-Add; ISBN-92-835-0458-5) Copyright Avail: NTIS HC A06/MF A01

The large scale use of flight recorders by commercial airlines, coupled with the enhanced quality of results offered by modern computer based reduction processes makes it possible to broaden knowledge of the phenomenon of atmospheric turbulence. At the same time, new methods for predicting the response of flexible aircraft to turbulence are being proposed, and novel gust alleviation systems are being designed and tested. The presentations made at a workshop held for the discussion of these ideas are given. For individual titles, see N88-29718 through N88-29724.

N88-29718# Federal Aviation Administration, Seattle, Wash.
CURRENT AND PROPOSED GUST CRITERIA AND ANALYSIS METHODS: AN FAA OVERVIEW **c08**
Terence J. Barnes *In* AGARD, The Flight of Flexible Aircraft in Turbulence: State-of-the-Art in the Description and Modelling of Atmospheric Turbulence Jun. 1988 12 p (For primary document see N88-29717 24-01)
Copyright Avail: NTIS HC A06/MF A01

An FAA overview is presented of the gust criteria and analysis methods used in the various types of flight vehicle certified under the FAR's. The current criteria for small airplanes, transports, and rotorcraft are presented, and the status of proposed criteria for the tilt rotor and aerospace plane are discussed. The amount of discussion on each class of vehicle depends on the significance of gust loads as design loads, and the importance of vehicle flexibility. Transport airplane gust criteria development, usage and problems are discussed in some detail. Analysis methods used by U.S. industry are covered in a separate paper. Author

N88-29719# Technische Univ., Brunswick (West Germany). Inst. for Guidance and Control.
FLIGHT TEST EQUIPMENT FOR THE ON-BOARD MEASUREMENT OF WIND TURBULENCE **c06**
G. Schaenzer, M. Swolinsky, and P. Voersmann (Aerodata Flugmesstechnik G.m.b.H., Brunswick, West Germany) *In* AGARD, The Flight of Flexible Aircraft in Turbulence: State-of-the-Art in the Description and Modelling of Atmospheric Turbulence Jun. 1988 11 p (For primary document see N88-29717 24-01)
Copyright Avail: NTIS HC A06/MF A01

The knowledge of the actual wind and turbulence situation along the flight path of an aircraft is an important factor in the area of meteorological and aeronautical research. Different flight test programs for the onboard implementation of offline and online wind and turbulence measuring systems are presented. The theoretical principle of the determination of all three components of the wind vector is stated. A summary of the installed sensors, the data acquisition systems and computer equipment is presented and the essential effects of sensor errors on the accuracy of wind determination are discussed. Author

N88-29720# National Aerospace Lab., Emmeloord (Netherlands).
MATCHING P.S.D.: DESIGN LOADS **c05**
R. Noback *In* AGARD, The Flight of Flexible Aircraft in Turbulence: State-of-the-Art in the Description and Modelling of Atmospheric Turbulence Jun. 1988 12 p Sponsored by the Netherlands Agency for Aerospace Programs (For primary document see N88-29717 24-01)
Copyright Avail: NTIS HC A06/MF A01

A method to match loads obtained with the Design Envelope criterion of the power spectral density method is presented. Consistent sets of design load conditions can be generated using the correlation coefficients between the loads. Two of these sets are proposed for practical use. Author

N88-29721# Lockheed Aeronautical Systems Co., Burbank, Calif. Dynamic Loads Div.
A SUMMARY OF METHODS FOR ESTABLISHING AIRFRAME DESIGN LOADS FROM CONTINUOUS GUST DESIGN CRITERIA **c05**
Richard N. Moon *In* AGARD, The Flight of Flexible Aircraft in Turbulence: State-of-the-Art in the Description and Modelling of Atmospheric Turbulence Jun. 1988 40 p (For primary document see N88-29717 24-01)
Copyright Avail: NTIS HC A06/MF A01

Continuous gust design criteria for airframe design are specified in FAR 25, JAR 25 and various U.S. military specs. Two forms of criterion, the design envelope approach and the mission analysis, are usually referenced as an acceptable means of compliance. However, these criteria do not provide methods of applying the statistical results of the airframe manufacturer, subject to approval of the certifying agency. Some of the methods that are currently used by U.S. airframe manufacturers are summarized. Continuous gust design requirements from various certifying agencies are reviewed. A brief discussion is also provided on the methods employed to include the effect of the L-1011 Tristar active controls wing load alleviation system on the loads due to corrective roll control in turbulence. Author

N88-29722# Messerschmitt-Boelkow-Blohm G.m.b.H., Hamburg (West Germany). Civil and Transport Aircraft Div.
COMPARISON OF THE INFLUENCE OF DIFFERENT GUST MODELS ON STRUCTURAL DESIGN **c05**
Manfred Molzow *In* AGARD, The Flight of Flexible Aircraft in Turbulence: State-of-the-Art in the Description and Modelling of Atmospheric Turbulence Jun. 1988 17 p (For primary document see N88-29717 24-01)
Copyright Avail: NTIS HC A06/MF A01

Depending on the country of certification, different gust models and means of compliance of the airworthiness requirements have to be covered in structural design of civil transport aircraft. The influence on aircraft design from gust models, aircraft modeling, and control systems and laws is demonstrated on example of a short to medium range transport aircraft. Recommendations for future harmonized approaches in gust methods and modeling are given. Author

N88-29723# Office National d'Etudes et de Recherches Aeronautiques, Paris (France).
MEASURED AND PREDICTED RESPONSES OF THE NORD 260 AIRCRAFT TO THE LOW ALTITUDE ATMOSPHERIC TURBULENCE **c08**
J. L. Meurzec and F. Poirion *In* AGARD, The Flight of Flexible Aircraft in Turbulence: State-of-the-Art in the Description and Modelling of Atmospheric Turbulence Jun. 1988 9 p (For primary document see N88-29717 24-01)
Copyright Avail: NTIS HC A06/MF A01

A program of in situ measures using the Nord 260 plane equipped with accelerometers has allowed the comparison of the predicted and the measured responses of the flexible aircraft to turbulence. It shows a good agreement between the two sets of results and it emphasizes the better modeling of the turbulence using the isotropic model rather than the cylindrical one. Author

N88-29724# Civil Aviation Authority, Redhill (England). Airworthiness Div.
A REVIEW OF MEASURED GUST RESPONSES IN THE LIGHT OF MODERN ANALYSIS METHODS **c08**
V. Card *In* AGARD, The Flight of Flexible Aircraft in Turbulence: State-of-the-Art in the Description and Modelling of Atmospheric Turbulence Jun. 1988 14 p (For primary document see N88-29717 24-01)
Copyright Avail: NTIS HC A06/MF A01

In the past simplified models of aircraft used to assess operational gust statistics have led to conservative estimates of derived gust exceedances. Modern refinements in aircraft modeling techniques have gradually introduced conservatism in the process of calculating gust loads. Gust statistics reviewed in the light of these modern analytical methods support the CAA view that gust velocities developed for use with simple rigid aircraft models are too severe for use with a modern dynamic analysis. Even in the light of improved safety targets, a 10 per cent reduction in design gust velocity can be readily justified. Further reductions may be justified on the basis of mission analysis considerations, or by investigation of more recent acceleration statistics collected by the current generation of transport aircraft. In the latter case, it will be essential to account for all relevant features of the subject aircraft in the derivation of gust velocities so as to obtain a true picture of the gust statistics. Author

N88-29725# Advisory Group for Aerospace Research and Development, Neuilly-Sur-Seine (France). Structures and Materials Panel.
THE FLIGHT OF FLEXIBLE AIRCRAFT IN TURBULENCE: STATE-OF-THE-ART IN THE DESCRIPTION AND MODELLING OF ATMOSPHERIC TURBULENCE
Dec. 1987 187 p Meeting held in Athens, Greece, 28 Sep. - 3 Oct. 1986
(AGARD-R-734; ISBN-92-835-0426-7) Copyright Avail: NTIS HC A09/MF A01

The flight of flexible aircraft in turbulence was studied. Presentations given at the first of two workshops on the subject are provided. Topics covered here are: (1) Measurements of turbulence by specially equipped aircraft, and (2) Data collection and reduction of incremental accelerations observed in commercial flights. For individual titles, see N88-29726 through N88-29734.

N88-29726*# National Aeronautics and Space Administration. Langley Research Center, Hampton, Va.
STATUS REVIEW OF ATMOSPHERE TURBULENCE AND AIRCRAFT RESPONSE **c08**
J. C. Houbolt *In* AGARD, The Flight of Flexible Aircraft in Turbulence: State-of-the-Art in the Description and Modelling at Atmospheric Turbulence Dec. 1987 11 p (For primary document see N88-29725 24-01)
Copyright Avail: NTIS HC A09/MF A01 CSCL 01C

A brief review is made of the understanding of aircraft encounter of atmospheric turbulence, both from the point of view of describing or modeling the turbulence and with respect to the ability to calculate resulting airplane loads. Some of the more recent studies of gust measurements and of reducing airline gust response data are discussed. Special attention is given to gust analysis requirements as involved in airplane certification and whether there is a need for additional or different requirements. A review is made of a recent study in which amazingly simple and universal gust response equations were discovered; the possible impact of these new findings on future work is indicated. Author

N88-29727*# National Aeronautics and Space Administration. Langley Research Center, Hampton, Va.
A SUMMARY OF ATMOSPHERIC TURBULENCE MEASUREMENTS WITH SPECIALLY-EQUIPPED AIRCRAFT IN THE US **c47**
H. N. Murrow *In* AGARD, The Flight of Flexible Aircraft in Turbulence: State-of the Art in the Description and Modelling of Atmospheric Turbulence Dec. 1987 11 p (For primary

document see N88-29725 24-01)
Copyright Avail: NTIS HC A09/MF A01 CSCL 04B

The technique of measurement of atmospheric turbulence in the form of true gust velocity is summarized. Specific aspects pointed out are related to NASA programs conducted over the last 15 years. Liberal use is made of references for details. Some recommendations resulting from a Spring 1986 workshop on atmospheric turbulence are also presented. Author

N88-29728# Royal Aircraft Establishment, Bedford (England).
MEASUREMENT AND ANALYSIS OF LOW ALTITUDE ATMOSPHERIC TURBULENCE OBTAINED USING A SPECIALLY INSTRUMENTED GNAT AIRCRAFT **c47**
G. W. Foster and J. G. Jones *In* AGARD, The Flight of Flexible Aircraft in Turbulence: State-of-the Art in the Description and Modelling of Atmospheric Turbulence Dec. 1987 45 p (For primary document see N88-29725 24-01)
Copyright Avail: NTIS HC A09/MF A01

Detailed measurements of atmospheric turbulence made by a specially instrumented Gnat aircraft at altitudes below one thousand feet over a variety of terrains are described. A program of flying yielded about 400 runs for which time histories of the three components of turbulence are available. These runs are analyzed to give parameters which summarize the statistical characteristics of the turbulence encountered. A very strong relationship between two parameters from the Statistical Discrete Gust Analysis technique and one from the Power Spectral Density technique is identified. Author

N88-29729# Taylor (J.), Camberley (England).
AN INTERIM COMPARISON OF OPERATIONAL CG RECORDS IN TURBULENCE ON SMALL AND LARGE CIVIL AIRCRAFT **c08**
J. Taylor *In* AGARD, The Flight of Flexible Aircraft in Turbulence: State-of-the-Art in the Description and Modelling of Atmospheric Turbulence Dec. 1987 31 p (For primary document see N88-29725 24-01)
Copyright Avail: NTIS HC A09/MF A01

Operational records have been made on British Airways aircraft for the period May 1980 to April 1985 and analyzed for about 650,000 flying hours on a number of different aircraft. Records were obtained for about 2 to 5 minutes of Normal Acceleration, Pitch Angle, Roll Angle, Height and Speed for nearly all those events which had an increment of 1 g or more, i.e., 29 events; similar records were also obtained for nearly all those events with an increment of 0.5 g or more with flaps down from May 1983 to April 1985, i.e., 33 events. An interim examination of the 29 events with 1 excess g or more, with special emphasis on 15 of them is made and includes an estimate of the interaction of maneuvers and turbulence, an estimate of the frequency of occurrence of high level intensity gusts and of the equiprobability relationships of gust levels and gust gradients. It was found that gusts that are important for a particular response are strongly dependent on the rate per sub 5 km at which zero crossings occur in that response. Using the Kaynes formula for gust intensity and zero crossings, it was found that the equiprobability relationships of gust levels and gust gradients can be represented on a single diagram for all sizes of aircraft at all heights. Author

N88-29730# National Aeronautical Establishment, Ottawa (Ontario). Flight Research Lab.
THE NAE ATMOSPHERIC RESEARCH AIRCRAFT **c06**
J. I. MacPherson and S. W. Baillie *In* AGARD, The Flight of Flexible Aircraft in Turbulence: State-of-the-Art in the Description and Modelling of Atmospheric Turbulence Dec. 1987 19 p (For primary document see N88-29725 24-01)
Copyright Avail: NTIS HC A09/MF A01

The Flight Research Laboratory of the NAE of Canada operates a T-33 and a Twin Otter aircraft instrumented for atmospheric research studies. The instrumentation in the aircraft is described with emphasis on the strapped down inertial Doppler system used to derive the mean and turbulent components of the atmospheric motion. Example data from several research projects are presented to demonstrate the measurement and analysis capabilities of the aircraft and their data playback facilities. Author

N88-29731# National Aeronautical Establishment, Ottawa (Ontario). Unsteady Aerodynamics Lab.
AIRCRAFT DYNAMICS: AERODYNAMIC ASPECTS AND WIND TUNNEL TECHNIQUES **c02**
K. J. Orlik-Rueckemann *In* AGARD, The Flight of Flexible Aircraft in Turbulence: State-of-the-Art in the Description and Modelling of Atmospheric Turbulence Dec. 1987 14 p Previously announced as N88-13320 (For primary document see N88-29725 24-01)
Copyright Avail: NTIS HC A09/MF A01

The dynamic behavior of modern fighter aircraft depends more and more on unsteady aerodynamics. Until recently, the designer concentrated on classical problems such as aeroelasticity and flutter. Dynamic stability parameters were most often determined by low angle of attack calculation methods, without much recourse to experiment. The results obtained from the few dynamic experiments performed were used to confirm the absence of problems rather than as design parameters. New requirements for fighter aircraft performance include the ability to fly at high angles of attack in the presence of extensive regions of separated or vortical flows, relaxed static stability, greatly increased agility, and an interest in unorthodox geometries such as closely coupled canard or tail first configurations. The time lags and unsteady phenomena associated with flow fields resulting from rapid maneuvers and large amplitude motions significantly affect the dynamic behavior of modern fighter aircraft and become as important for aircraft design as the classical static performance criteria. A review is made of the various aerodynamic aspects affecting aircraft dynamic behavior and some experimental techniques. Author

N88-29732# British Aerospace Aircraft Group, Weybridge (England). Military Aircraft Div.
RE-ASSESSMENT OF GUST STATISTICS USING CAADRP DATA **c08**
B. W. Payne, A. E. Dudman, and K. C. Griffiths *In* AGARD, The Flight of Flexible Aircraft in Turbulence: State-of-the-Art in the Description and Modelling of Atmospheric Turbulence Dec. 1987 22 p (For primary document see N88-29725 24-01)
Copyright Avail: NTIS HC A09/MF A01

The measured incremental c.g. accelerations of the BAC 1-11 operating on scheduled flights are compared with the equivalent theoretical predictions in a gust environment. Some of the results of the study are: (1) An analysis of the measured Civil Airworthiness Authority Data Recording Program data, based upon a significant 58,733 flying hours, gave an incremental vertical c.g. acceleration of 1.25 g at the datum probability value of 2 x .00005 exceedances per hour; (2) The theoretical predictions from all the flight segments in the Mission Analysis gave an incremental c.g. acceleration of .238 g at the datum exceedance value; and (3) Therefore in the comparison between the measured and predicted analyses for a similar mission considerable differences were found with measured frequencies of exceedance of about one half those predicted using current airworthiness requirements. Author

N88-29733# National Aerospace Lab., Amsterdam (Netherlands).
ACQUISITION OF GUST STATISTICS FROM AIDS-RECORDED DATA **c47**
J. B. deJonge, A. J. P. vanderWekken, and R. Noback *In* AGARD, The Flight of Flexible Aircraft in Turbulence: State-of-the-Art in the Description and Modelling of Atmospheric Turbulence Dec. 1987 14 p Previously announced as N88-14586 (For primary document see N88-29725 24-01)
Copyright Avail: NTIS HC A09/MF A01

The procedures applied to reduce B-747 acceleration data from greater than 100,000 flight hours to derived gust velocities are described. The results are presented and compared with other data sources. The validity of the assumptions made in the derivation are discussed. Author

N88-29734# Office National d'Etudes et de Recherches Aerospatiales, Paris (France).
EXTREME GUSTS DISTRIBUTION **c47**
Gabriel Coupry *In* AGARD, The Flight of Flexible Aircraft in Turbulence: State-of-the-Art in the Description and Modelling of Atmospheric Turbulence Dec. 1987 9 p In FRENCH; ENGLISH summary Original language document was announced in IAA as A87-44328 (For primary document see N88-29725 24-01)
Copyright Avail: NTIS HC A09/MF A01

A model of extreme atmospheric turbulence is proposed based on 5 years of commercial flight data for events with load factors in encess of 0.5. The Pratt formula is found to lead to incoherent atmospheric descriptions, while the Hall formula, with appropriate choice of scale, is found to lead to a coherent turbulence description which is relatively independent of the type of aircraft considered. For strong turbulences, the average number of overshoots by a nautical mile are found to decrease exponentially with gust amplitude. The incidences of gusts exceeding a threshold value are found to obey a Poisson distribution whose mean decreases exponentially with amplitude, indicating that the probability of the occurrence of big gusts can be represented by Gumbel's extreme value theory. Author

N88-29735# Advisory Group for Aerospace Research and Development, Neuilly-Sur-Seine (France). Flight Mechanics Panel.
ADVANCES IN FLYING QUALITIES
May 1988 194 p Lecture held in Delft, Netherlands, 26-27 May 1988, in Rome, Italy, 30-31 May 1988, and in Torrance, Calif., 15-16 Jun. 1988
(AGARD-LS-157; ISBN-92-835-0461-5) Copyright Avail: NTIS HC A09/MF A01

Judging the suitability of an aircraft to safely and effectively perform its mission without undue pilot skill and discomfort is what flying qualities is all about. Central to such judgement, and to the design of suitable aircraft plus flight control systems, is an understanding of what the pilot can do with ease and comfort or conversely what bothers him. The lectures are designed to impart such understanding to both novice and seasoned practioners in flying qualities and flight control and thereby to provide the bridge required to extend flying qualities requirements from simple classic response aircraft, to the responses attending the use of full time active control. Mathematical models of pilot control behavior are explained. The application of various model to flying qualities are discussed; and the influences, regarding the generic likes and dislikes of pilots drawn from such studies are listed. For individual titles, see N88-29736 through N88-29742.

N88-29736# Systems Technology, Inc., Hawthorne, Calif.
PILOT MODELING **c54**
Duane T. McRuer *In* AGARD, Advances in Flying Qualities May 1988 30 p (For primary document see N88-29735 24-01)
Copyright Avail: NTIS HC A09/MF A01

A description is presented of pilot control behavior in general. The essential features of pilot dynamics are emphasized for closed loop control of an aircraft. The crossover model is presented as the simplest and most useful model for the majority of flying qualities analyses. Two models are developed in some detail: a structural isomorphic form which accounts for some human subsystems as well as the total input output behavior; and an algorithmic optimal control model which attempts to mimic the pilot's total response only. Both full and divided attention conditions are treated.
Author

N88-29737# Systems Technology, Inc., Hawthorne, Calif.
PILOT MODELING APPLICATIONS **c54**
Irving L. Ashkenas *In* AGARD, Advances in Flying Qualities May 1988 38 p (For primary document see N88-29735 24-01)
Copyright Avail: NTIS HC A09/MF A01

The role of pilot opinion and rating in defining flying qualities, and the pilot adapted control behavior that impinges on such ratings are delineated and discussed. This is preparatory to the exemplary application of frequency domain pilot models to the examination and elucidation of a variety of flying qualities situations. This examination starts with single loop situations which progress in complexity; and then shifts to multiple loop cases, which also progress in complexity. This succession is designed to increasingly reveal the basic pilot centered requirements for good flying qualities. Such requirements, which stem from easily achieved pilot adaption and good resulting closed loop responses, are more generally applicable to new unknown situations than are classical requirements on the open loop controlled element dynamic parameters. However, the latter do in fact influence the ease of piloted closure and the resulting closed loop responses so, when properly expressed in terms of characteristics in the projected crossover frequency region, may also achieve a degree of generality. The pilot centered requirements illustrated by the examples are collected and briefly discussed. Author

N88-29738# National Aerospace Lab., Amsterdam (Netherlands).
LOW-SPEED LONGITUDINAL FLYING QUALITIES OF MODERN TRANSPORT AIRCRAFT **c05**
H. A. Mooij *In* AGARD, Advances in Flying Qualities May 1988 16 p (For primary document see N88-29735 24-01)
Copyright Avail: NTIS HC A09/MF A01

The suitability of an aircraft with respect to human control is determined by its handling qualities. In modern transport aircraft the handling qualities are determined to a high degree by the flight control system. An introduction to the following aspects of closed loop flight control systems for modern transport aircraft is given: stabilization and maneuvering functions, candidate implementation forms, manipulators for flight control, and mathematical representations of the airframe/flight control system combination required for prediction and evaluation purposes. Regarding criteria for good handling qualities of transport aircraft, the terminal flight phase (takeoff, initial climb, final approach and landing) are of prime interest. A treatise on a number of promising quantitative criteria for transport aircraft equipped with advanced flight control systems is given. Two groups of criteria are distinguished: criteria based on the dynamic characteristics of the aircraft alone and criteria based on the dynamic characteristics of the pilot/aircraft closed loop system. In the latter case, a quasi-linear describing function for the human controller behavior is used. Author

N88-29739# Systems Technology, Inc., Hawthorne, Calif.
ADVANCES IN FLYING QUALITIES: CONCEPTS AND CRITERIA FOR A MISSION ORIENTED FLYING QUALITIES SPECIFICATION **c05**
Roger H. Hoh *In* AGARD, Advances in Flying Qualities May 1988 28 p (For primary document see N88-29735 24-01)
Copyright Avail: NTIS HC A09/MF A01

There has been considerable activity over the past 8 years to upgrade the military flying qualities specifications for conventional aircraft, as well as for V/STOLs and helicopters. The primary objectives of these upgrades has been to account for the use of high gain, high authority augmentation, and to more directly reflect the requirements of the intended missions into the specifications. The methodologies developed to accomplish the latter objective are summarized. A brief overview of the Lower Order Equivalent Systems and Bandwidth criteria follows. Problems with the specification of control sensitivity, and potential solutions are then discussed, followed by a brief presentation of the use of time vs frequency domain criteria. An empirical method to combine the Cooper-Harper Handling Qualities Ratings (HQRs) from each axis of control into an overall rating is then presented. Finally, a proposed specification for precision flare and landing is given, followed by an example application of the method. Author

N88-29740# Air Force Wright Aeronautical Labs., Wright-Patterson AFB, Ohio.
A SECOND LOOK AT MIL PRIME FLYING QUALITIES REQUIREMENTS **c05**
Robert J. Woodcock *In* AGARD, Advances in Flying Qualities

May 1988 15 p (For primary document see N88-29735 24-01)
Copyright Avail: NTIS HC A09/MF A01

Current and projected applications of flying qualities criteria are addressed. The current state of the art, its deficiencies, and needs for further work are addressed. The rationale for the new U.S. Military Standard and Handbook on flying qualities is briefly discussed. With advanced vehicles, the scope of flying qualities is expanding, opening new areas to investigate and creating new problems. With relaxed static stability now commonly used, control margin is a prime safety consideration: control must be available for stabilization, maneuvering and recovery from any possible attitude, as well as for trim. Flying qualities aspects of agility include the need for nonlinear flying qualities metrics, and control systems that provide both rapid maneuvering and good damping for tight tracking. For all aspect engagement, the pilot needs to be thoroughly integrated with displays, automatic flight control modes and other systems. For dynamic longitudinal flying qualities, MIL-STD 1797 presents the Control Anticipation Parameter of an equivalent classical system as a primary criterion, but gives several alternatives in recognition of other problems. Author

N88-29741# Pisa Univ. (Italy). Dipartimento di Ingegneria Aerospaziale.
THE OPTIMAL CONTROL PILOT MODEL AND APPLICATIONS c54
Mario Innocenti *In* AGARD, Advances in Flying Qualities May 1988 17 p (For primary document see N88-29735 24-01)
Copyright Avail: NTIS HC A09/MF A01

The modeling of the human pilot behavior plays an important role in the preliminary analysis of aircraft handling qualities. This is especially true when the designer is confronted with nonconventional aircraft dynamics, tasks and/or lack of sufficient handling qualities data base. One modeling technique is reviewed which was developed in the early 1970's and has been widely used since then: the optimal control model of the human pilot. The model has been validated in a number of tasks and used in the analysis as well as the synthesis of manual control loops. The capabilities of the model are evaluated in the pilot rating prediction, in the analysis and in the synthesis of pilot/vehicle control loops from the handling qualities standpoint. Author

N88-29742# British Aerospace Public Ltd. Co., Preston (England).
THE ROLE OF SIMULATION IN FLYING QUALITIES AND FLIGHT CONTROL SYSTEM RELATED DEVELOPMENT c09
A. G. Barnes *In* AGARD, Advances in Flying Qualities May 1988 21 p (For primary document see N88-29735 24-01)
Copyright Avail: NTIS HC A09/MF A01

Flight simulation makes a vital contribution to the understanding of flying quality requirements and to the clearance of modern aircraft flight controls. The background to the use of simulators, both airborne and ground based is presented, and the experimental techniques, including validation and hardware requirements are discussed. The limitations which equipments can impose are presented, and examples are given of the use of flight simulation in flying qualities research. Finally, the techniques required for the clearance of current designs are highlighted, and a direction for future research is indicated. Author

N88-29743*# National Aeronautics and Space Administration. Langley Research Center, Hampton, Va.
ON THE GENERATION OF MEAN FLOWS BY THE INTERACTION OF GOERTLER VORTICES AND TOLLMIEN-SCHLICHTING WAVES IN CURVED CHANNEL FLOWS Final Report
Andrew P. Bassom and Philip Hall (Exeter Univ., England) Jul. 1988 40 p Submitted for publication
(Contracts NAS1-18107; NAS1-18605)
(NASA-CR-181690; ICASE-88-43; NAS 1.26:181690) Avail: NTIS HC A03/MF A01 CSCL 01B

There are many fluid flows where the onset of transition can be caused by different instability mechanisms which compete in the nonlinear regime. The interaction of a centrifugal instability mechanism with the viscous mechanism which causes Tollmein-Schlichting waves is discussed. The interaction between these modes can be strong enough to drive the mean state; the interaction is investigated in the context of curved channel flows so as to avoid difficulties associated with boundary layer growth. Essentially it was found that the mean state adjusts itself so that any modes present are neutrally stable even at finite amplitude. In the first instance, the mean state driven by a vortex of short wavelength in the absence of Tollmein-Schlichting waves is considered. It is shown that for a given channel curvature and vortex wavelength, there is an upper limit to the mass flow rate which the channel can support as the pressure gradient is increased. When the Tollmein-Schlichting waves are present, then the nonlinear differential equation to determine the mean state is modified. Author

02 AERODYNAMICS

Includes aerodynamics of bodies, combinations, wings, rotors, and control surfaces; and internal flow in ducts and turbomachinery.

For related information see also *34 Fluid Mechanics and Heat Transfer.*

N88-29744*# Chrysler Corp., New Orleans, La. Military Public Electronic Systems.
SPACE SHUTTLE PHASE B WIND TUNNEL MODEL AND TEST INFORMATION. VOLUME 3: LAUNCH CONFIGURATION
J. L. Glynn and D. E. Poucher Jul. 1988 549 p
(Contract NAS1-18276)
(NASA-CR-178416-Vol-3-Pt-2; NAS 1.26:178416-Vol-3-Pt-2; DMS-DB-02-Vol-3-Pt-2) Avail: NTIS HC A23/MF A01 CSCL 01A

Archived wind tunnel data are available for flyback booster or other alternative recoverable configurations as well as reusable orbiters studied during initial development (Phase B) of the Space Shuttle. Considerable wind tunnel data was acquired by the competing contractors and the NASA Centers for an extensive variety of configurations with an array of wing and body planforms. All contractor and NASA wind tunnel data acquired in the Phase B development have been compiled into a data base and are available for application to current winged flyback or recoverable booster aerodynamic studies. The Space Shuttle Phase B Wind Tunnel Database is structured by vehicle component and configuration type. Basic components include booster, orbiter and launch vehicle. Booster configuration types include straight and delta wings, canard, cylindrical, retroglide and twin body. Orbital configuration types include straight and delta wings, lifting body, drop tanks and double delta wings. This is Volume 3 (Part 2) of the report -- Launch Configuration -- which includes booster and orbiter components in various stacked and tandem combinations. Author

N88-29745*# Chrysler Corp., New Orleans, La. Military Public Electronic Systems.
SPACE SHUTTLE PHASE B WIND TUNNEL MODEL AND TEST INFORMATION. VOLUME 1: BOOSTER CONFIGURATION
J. L. Glynn and D. E. Poucher Jul. 1988 388 p
(Contract NAS1-18276)
(NASA-CR-178414-Vol-1-Pt-1; NAS 1.26:178414-Vol-1-Pt-1; DMS-DB-02-Vol-1-Pt-1) Avail: NTIS HC A17/MF A01 CSCL 01A

Archived wind tunnel test data are available for flyback booster or other alternative recoverable configurations as well as reusable orbiters studied during initial development (Phase B) of the Space Shuttle. Considerable wind tunnel data was acquired by the competing contractors and the NASA Centers for an extensive variety of configurations with an array of wing and body planforms. All contractor and NASA wind tunnel test data acquired in the Phase B development have been compiled into a database and are available for application to current winged flyback or recoverable booster aerodynamic studies. The Space Shuttle Phase

B Wind Tunnel Database is structured by vehicle component and configuration type. Basic components include the booster, the orbiter and the launch vehicle. Booster configuration types include straight and delta wings, canard, cylindrical, retroglide and twin body. Orbiter configuration types include straight and delta wings, lifting body, drop tanks, and double delta wings. Launch configurations include booster and orbiter components in various stacked and tandem combinations. This is Volume 1 (Part 1) of the report -- Booster Configuration. Author

N88-29746*# National Aeronautics and Space Administration. Lewis Research Center, Cleveland, Ohio.
ANALYSIS AND OPTIMIZATION OF TRUNCATED SCARF NOZZLES SUBJECT TO EXTERNAL FLOW CONDITIONS M.S. Thesis - Toledo Univ.
Rickey J. Shyne Aug. 1988 88 p
(NASA-TM-100955; E-4146; NAS 1.15:100955) Avail: NTIS HC A05/MF A01 CSCL 01A

Results of a calculation of an optimized truncated scarfed nozzle were compared. The truncated scarfed nozzle was designed for an exit Mach number of 6.0, i.e., the Mach number at the last nozzle characteristic is 6.0, with an external flow Mach number of 5.0. The nozzle was designed by the Rao method for optimum thrust nozzles modified for 2-D flow and truncated scarfed nozzle applications. This design was analyzed using a shock-fitting method for 2-D supersonic flows. Excellent agreement was achieved between the design and analysis. Truncation of the lower nozzle wall (cowl) revealed that there is an optimum length for truncating the cowl without degrading the nozzle performance. Truncation of the nozzle cowl past this optimal length should be analyzed in trade-off studies for thrust loss versus gross vehicle weight. Plots of the oblique shock wave equations were also identified which will allow computation of slip line angle, dynamic pressure coefficient, or ambient Mach number for various specific heat ratios. Author

N88-29747# Southwest Research Inst., San Antonio, Tex.
A STUDY OF THE EFFECT OF RANDOM INPUT MOTION ON LOW REYNOLDS NUMBER FLOWS Final Report, Sep. 1985 - Nov. 1987
James F. Unruh, Joel T. Park, and James E. Johnson May 1988 64 p
(Contract N00014-85-C-0840)
(AD-A195559; SwRI-8814) Avail: NTIS HC A04/MF A01 CSCL 20D

The SwRI (Southwest Research Institute) large water tunnel was modified by the addition of a large test section (.71 m x .81 m x 1.8 m long) to provide low Reynolds number flows with low blockage for models in a highly separated flow condition. Flow characteristics are documented and other physical features are described. The feasibility of conducting water tunnel experiments involving unsteady aero-hydrodynamics was demonstrated by performing a series of flow visualization studies on a oscillating airfoil (NACA 0012). This experiment was carried out at a reduced frequency of 0.26 and at a Reynolds number of 50,000. For this condition, the flow was not fully separated until 17 degress angle of attack, and the downstream wash of the separated flow occurred at 22 degrees. GRA

N88-29748# Air Force Inst. of Tech., Wright-Patterson AFB, Ohio.
NUMERICAL SOLUTIONS OF UNSTEADY INVISCID TRANSONIC TURBINE CASCADE FLOWS Ph.D. Thesis
Richard M. Moore May 1988 281 p
(AD-A196111; AFIT/CI/NR-88-8) Avail: NTIS HC A13/MF A01 CSCL 20D

A numerical analysis has been developed to solve 2-D inviscid transonic turbine-type cascade flowfields. This analysis combines accuracy comparable to that of the numerical method of characteristics with the efficiency of finite difference methods. The MacCormack explicit finite difference method is used to solve the unsteady Euler equations. Steady solutions are calculated as asymptotic solutions in time. A conservation variable formulation of the Kentzer method has been developed in this investigation and is used to derive appropriate equations for the flowfield boundaries. The Kentzer method is based on characteristic theory, but uses a finite difference method, consistent with the method used at interior points, to integrate the appropriate boundary equations. A grid generator has been developed to crease C-type grids around cascade blades using techniques similar to the Poisson equation grid generation techniques developed by Steger and Sorensen. Two different planar turbine-type cascades have been studied. The AACE II cascade blades are typical of the nozzle blades found in the first stator in a turbine. The GMA 400 cascade blades are typical of later turbine stator blades. GRA

N88-29749*# National Aeronautics and Space Administration. Langley Research Center, Hampton, Va.
ADAPTIVE MESH GENERATION FOR VISCOUS FLOWS USING DELAUNAY TRIANGULATION
Dimitri J. Mavriplis Aug. 1988 16 p
(Contract NAS1-18107)
(NASA-CR-181699; ICASE-88-47; NAS 1.26:181699) Avail: NTIS HC A03/MF A01 CSCL 01A

A method for generating an unstructured triangular mesh in two dimensions, suitable for computing high Reynolds number flows over arbitrary configurations is presented. The method is based on a Delaunay triangulation, which is performed in a locally stretched space, in order to obtain very high aspect ratio triangles in the boundary layer and the wake regions. It is shown how the method can be coupled with an unstructured Navier-Stokes solver to produce a solution adaptive mesh generation procedure for viscous flows. Author

N88-29750*# National Aeronautics and Space Administration. Ames Research Center, Moffett Field, Calif.
THREE-DIMENSIONAL NAVIER-STOKES SIMULATIONS OF TURBINE ROTOR-STATOR INTERACTION
Man Mohan Rai Mar. 1988 6 p
(NASA-TM-100081; A-88106; NAS 1.15:100081) Avail: NTIS HC A02/MF A01 CSCL 01A

Fluid flows within turbomachinery tend to be extremely complex in nature. Understanding such flows is crucial to improving current designs of turbomachinery. The computational approach can be used to great advantage in understanding flows in turbomachinery. A finite difference, unsteady, thin layer, Navier-Stokes approach to calculating the flow within an axial turbine stage is presented. The relative motion between the stator and rotor airfoils is made possible with the use of patched grids that move relative to each other. The calculation includes endwall and tip leakage effects. An introduction to the rotor-stator problem and sample results in the form of time averaged surface pressures are presented. The numerical data are compared with experimental data and the agreement between the two is found to be good. Author

N88-29751*# National Aeronautics and Space Administration. Ames Research Center, Moffett Field, Calif.
A STREAMWISE UPWIND ALGORITHM FOR THE EULER AND NAVIER-STOKES EQUATIONS APPLIED TO TRANSONIC FLOWS
Peter M. Goorjian Sep. 1988 9 p
(NASA-TM-101019; A-88259; NAS 1.15:101019) Avail: NTIS HC A02/MF A01 CSCL 01A

A new algorithm was developed for the Euler and Navier-Stokes equations that uses upwind differencing based on the streamwise direction. This algorithm is time accurate and can be used in codes for calculating unsteady transonic flows over wings. Such codes can be used for the flutter analysis of wings. In this algorithm, the coordinate system is locally rotated to align with the streamwise direction. For differencing the convective terms in the streamwise direction, a new form of flux splitting is employed, in which the biasing depends on the local Mach number. In the plane perpendicular to the stream direction, the new flux splitting uses the condition of no flow in that local plane. By using a locally rotated coordinate system, the convective flux vector biasing depends on the total Mach number. Hence, the switching of the

flux vector biasing occurs across shock waves and the proper domain of dependence is used in supersonic regions. For comparison, many other upwind methods switch differencing based on Mach number of shock waves in multidimensional flows. The formulas for the convective flux vector differencing do not contain any user specified parameters. So, the amount of numerical dissipation is automatically determined. Author

N88-29752*# National Aeronautics and Space Administration. Langley Research Center, Hampton, Va.
AERODYNAMICS IN GROUND EFFECT AND PREDICTED LANDING GROUND ROLL OF A FIGHTER CONFIGURATION WITH A SECONDARY-NOZZLE THRUST REVERSER
Daniel W. Banks Oct. 1988 131 p
(NASA-TP-2834; L-16435; NAS 1.60:2834) Avail: NTIS HC A07/MF A01 CSCL 01A

An experimental investigation of the in-ground effect aerodynamic characteristics and predicted landing-ground-roll performance of wing-canard fighter configuration with a secondary nozzle thrust reverser was completed. These tests were conducted in the Langley 14 by 22 foot Subsonic Wind Tunnel using a model equipped with a pneumatic jet for thrust simulation of nozzle pressure ratios up to 4.0. The model was tested in the landing rollout configuration at approx. wheel touchdown height for a range of decreasing dynamic pressure from 50 psf down to 10 psf. Landing-ground-roll predictions of the configuration were calculated using the wind tunnel results. Author

N88-29753*# National Aeronautics and Space Administration, Washington, D.C.
A PRELIMINARY INVESTIGATION OF DRAG REDUCTION AND MECHANISM FOR A BLUNT BODY OF REVOLUTION WITH SLANTED BASE
Xuejian Xia and Xiaoshen Yu Aug. 1988 17 p Transl. into ENGLISH from Acta Aerodynamica Sinica (People's Republic of China), v. 4, Mar. 1986 p 99-107 Transl. by Scientific Translation Service, Santa Barbara, Calif.
(Contract NASw-4307)
(NASA-TT-20349; NAS 1.77:20349) Avail: NTIS HC A03/MF A01 CSCL 01A

This is a preliminary study of the drag reduction effect and its mechanism of a blunt body of revolution with a 21-deg slant angle by using a series of base plates. Drag coefficients were measured to investigate the effect of base installation position and plate height. An effective drag reduction device was found. Through the measurement of base pressure and total pressure distribution and flow pattern display, flow characteristics and drag reduction mechanism in the vortex near the wake were investigated. Author

N88-29754*# National Aeronautics and Space Administration. Langley Research Center, Hampton, Va.
APPLICATION OF UNSTEADY AERODYNAMIC METHODS FOR TRANSONIC AEROELASTIC ANALYSIS
Woodrow Whitlow, Jr. Sep. 1988 10 p Presented at the 16th Congress of the International Council of the Aeronautical Sciences, Jerusalem, Israel, 28 Aug. - 2 Sep. 1988
(NASA-TM-100665; NAS 1.15:100665) Avail: NTIS HC A02/MF A01 CSCL 01A

Aerodynamic methods for aeroelastic analysis are applied to various flow problems. These methods include those that solve the three dimensional transonic small disturbance (TSD) potential equation, the two dimensional (2-D) full potential (FP) equation, and the 2-D thin layer Navier-Stokes equations. Flutter analysis performed using TSD aerodynamics show that such methods can be used to analyze some aeroelastic phenomena. For thicker bodies and larger amplitude motions, a nonisentropic FP method is presented. The unsteady FP equation is modified to model the entropy jumps across shock waves. The conservative form of the modified equation is solved in generalized coordinates using an implicit, approximate factorization method. Pressures calculated on the NLR 7301 and NACA 64A010A airfoils using the nonisentropic FP method are presented. It is shown that modeling shock generated entropy extends the range of validity of the FP method. A Navier-Stokes code is correlated with pressures measured on a supercritical airfoil at transonic speeds. When corrections are made for wind tunnel wall effects, the calculations correlate well with the measured data. Author

N88-29755# Advisory Group for Aerospace Research and Development, Neuilly-Sur-Seine (France). Fluid Dynamics Panel.
SPECIAL COURSE ON MISSILE AERODYNAMICS
Apr. 1988 429 p Course held in Rhode-Saint-Genese, Belgium, 30 Mar. - 3 Apr. 1987, in Athens, Greece, 18-19 May 1987, and in Ankara, Turkey, 21-22 May 1987
(AGARD-R-754; ISBN-92-835-0452-6) Copyright Avail: NTIS HC A19/MF A01

Topics addressed include: a survey of aerodynamic problems encountered on existing and future missiles and of the most important predictive methods; the criteria that define the required prediction accuracy; nonlinear aerodynamic effects; engineering computation methods used for calculating stability and control for conventional and unconventional missiles; the roles of intake in the propulsion system of turbojet and ramjet powered missiles; internal and external aerodynamic aspects of the induction system; computer aided design; prediction of aerodynamic heating; base flows with and without propulsion; and next generation supersonic and hypersonic missiles. For individual titles, see N88-29756 through N88-29766.

N88-29756# McDonnell-Douglas Astronautics Co., St. Louis, Mo.
ACCURACY CRITERIA FOR EVALUATING SUPERSONIC AERODYNAMIC COEFFICIENT PREDICTIONS
J. E. Williams and R. J. Krieger *In* AGARD, Special Course on Missile Aerodynamics Apr. 1988 18 p Sponsored in part by Department of the Air Force, Washington, D.C. (For primary document see N88-29755 24-02)
Copyright Avail: NTIS HC A19/MF A01

Aerodynamic prediction methods are traditionally compared with wind tunnel test data. However, the assessment of accuracy is left to an arbitrary interpretation. An accuracy criteria was developed that defines the required prediction accuracy in terms of allowable errors in missile performance and design parameters. Equations were selected that relate these parameters to the aerodynamic drag, stability, and control coefficients. These equations are differentiated with respect to the aerodynamic coefficients and simplified when possible. Allowable errors in the performance or design parameters are estimated, based on preliminary design requirements, and the required aerodynamic coefficient accuracy calculated. The results allow a quantitative evaluation of prediction accuracy. Author

N88-29757# Nielsen Engineering and Research, Inc., Mountain View, Calif. Missile and Store Separation Aerodynamics.
SURVEY ON NONLINEAR EFFECTS
Marnix F. E. Dillenius and Stanley C. Perkins, Jr. *In* AGARD, Special Course on Missile Aerodynamics Apr. 1988 101 p (For primary document see N88-29755 24-02)
Copyright Avail: NTIS HC A19/MF A01

A survey of experimental observations and intermediate level prediction methods aimed at nonlinear aerodynamic characteristics of tactical missiles is described. A description is given of the major differences between missile and aircraft flight and configuration characteristics. The importance of vortical interference and nonlinear compressibility due to shocks is stressed. Nonlinearities associated with deformable fin design, supersonic fin on body interference, wraparound finds, and unsteady flight are discussed. Summarized accounts are provided for the effects of asymmetric body vortex shedding and vortex bursting on overall missile aerodynamic characteristics. Physical examples are given that show vortex structures and shock formations in vapor screen and schlieren pictures. In many instances, the nonlinear aerodynamic effects are illustrated by theoretical results obtained with and without the relevant nonlinearity. Short descriptions are given of intermediate level panel-based missile aerodynamic prediction

methods with special attention to the models incorporated to account for vortical and nonlinear compressibility effects. The descriptions include applications to additive force analysis for supersonic inlets and to deformable fins. Additional comparisons with experimental data are provided and the nonlinear effects pointed out. Presently available methods and future needs are summarized in the concluding remarks. Author

N88-29758# PRC Kentron, Inc., Hampton, Va.
SEMI-EMPIRICAL METHODS FOR CONVENTIONAL AND UNCONVENTIONAL MISSILES
Michael J. Hemsch *In* AGARD, Special Course on Missile Aerodynamics Apr. 1988 21 p (For primary document see N88-29755 24-02)
Copyright Avail: NTIS HC A19/MF A01

In the development and use of semi-empirical methods for prediction of the aerodynamic characteristics of modern missiles, one fact is exploited more than any other: the slenderness of the airframes and of the flows surrounding them. The first mathematical attempts to use this face were made over thirty years ago and resulted in classical slender-body theory and the universally-known Pitts, Nielsen, and Kaatari method for conventional missiles. It is shown that invoking slenderness for a missile in supersonic high angle-of-attack flow yields similarity forms which correlate data for affine bodies and wings in a particularly useful way. The equivalent angle-of-attack concept which is rooted in classical slender body theory is also presented together with extensions required for flows with high crossflow Mach number, one of the similarity variables. Finally, it is shown that the classical two-term fits to normal-force and center-of-pressure-location data for isolated wings and bodies are inferior to one-term power-law fits to the data in similarity form. Author

N88-29759# Naval Surface Weapons Center, Silver Spring, Md.
SPACE MARCHING EULER SOLVERS
Andrew B. Wardlaw, Jr. *In* AGARD, Special Course on Missile Aerodynamics Apr. 1988 32 p (For primary document see N88-29755 24-02)
Copyright Avail: NTIS HC A19/MF A01

Space marching Euler solvers for tactical missiles are examined. These solvers are applicable to missiles in supersonic flight provided that the flow field remains supersonic everywhere. The introductory section outlines progress to date and is followed by a discussion of numerical methods which were used to compute the flow about tactical missiles. Four different codes are described which are available for treating missile body shapes. Results from these computational methods are presented for body-alone, body-wing, and body-wing-tail cases. Force coefficients, surface pressures, and flow field predictions are compared to experiment. Reasonable agreement is obtained, illustrating the feasibility of using these methods in the design process. The limitation of the Euler equations are also discussed. Author

N88-29760# MATRA Service Aerodynamique, Velizy-Villacoublay (France).
NUMERICAL METHODS: EULER TIME DEPENDENT SOLVER
J. J. Chattot *In* AGARD, Special Course on Missile Aerodynamics Apr. 1988 28 p (For primary document see N88-29755 24-02)
Copyright Avail: NTIS HC A19/MF A01

The EULER time dependent solver of MATRA is described and the fundamental problem of separated flow simulation with an inviscid model is addressed, in particular separation on a smooth surface. Applications pertinent to missile aerodynamics, ranging from simple configurations to complete missile flow simulations, are examined. Author

N88-29761# Dornier-Werke G.m.b.H., Friedrichshafen (West Germany).
PREDICTION OF DYNAMIC DERIVATIVES
Heinz Fuchs and Rolf Kapp *In* AGARD, Special Course on Missile Aerodynamics Apr. 1988 41 p (For primary document see N88-29755 24-02)
Copyright Avail: NTIS HC A19/MF A01

The dynamic derivatives are introduced by their mathematical definition derived from the general expansion of aerodynamic functions with respect to the relevant independent fluid motion variables. The common classification of the dynamic derivatives is evaluated in accordance with the definitions used at flight mechanical applications. This is shown with the examples of nonstationary motion types creating dynamic derivativa effects. Some basic aspects of a semiempirical method for the calculation of dynamic derivatives of missile configurations or military aircraft are shown. Results of the computer program DYNAM are presented in comparison with experimental results of different test rigs. For higher angles of attack the linear theory for the calculation of the derivatives with respect to q is extended by a cross-flow assumption using the cross-flow drag coefficient. In addition to the semiempirical prediction method of total missile or aircraft configurations there are nonstationary panel methods which are useful for the determination of dynamic derivativa of harmonic oscillating wings or wing-rudder systems. An overview of the different dynamic test rigs is given which are in use at the different aerodynamic test laboratories of FR Germany. Test results of a Dornier standard missile configuration are discussed. An outlook on future activities on the evaluation methods of the dynamic test rigs at the high angle-of-attack region is given. Author

N88-29762# British Aerospace Public Ltd. Co., Bristol (England). Naval and Electronic Systems Div.
AIR INTAKE AERODYNAMICS
C. S. Jell *In* AGARD, Special Course on Missile Aerodynamics Apr. 1988 62 p (For primary document see N88-29755 24-02)
Copyright Avail: NTIS HC A19/MF A01

The effective operation of airbreathing missiles is strongly dependent on the efficiency of the air intake system and its ability to supply the engine with air of adequate quality at all required flight conditions while minimizing any undesirable effects that the intakes may have on the overall aerodynamic characteristics of the missile. The role of the intake in the propulsion system of turbojet and ramjet powered missiles is described and both the internal and external aerodynamic aspect of the induction system are addressed. The features of various types of air intake commonly used for subsonic and supersonic operation are discussed. The causes and effects of flow instability and flow non-uniformity at engine entry are considered and the operational relationship between the engine and the intake is shown. Finally three major aspects of intake installation are discussed: namely the influence of the missile body flowfields on internal performance; the forces and moments generated by the internal flow; and the effect of the intakes and their associated fairings on the overall aerodynamic characteristics of the missile. Author

N88-29763# McDonnell-Douglas Astronautics Co., St. Louis, Mo.
SEMIEMPIRICAL METHODS FOR AIRBREATHING MISSILES
J. E. Williams and R. J. Krieger *In* AGARD, Special Course on Missile Aerodynamics Apr. 1988 12 p (For primary document see N88-29755 24-02)
Copyright Avail: NTIS HC A19/MF A01

A computer-aided design procedure is described for use in conceptual design for sizing and shaping supersonic noncircular missiles with turbojet or ramjet propulsion systems. The theoretical basis for the method which uses a sensitivity derivative approach is developed. Avionics, structures, payload, inlet, engine, fuel, aerodynamic and performance models are described. Inlet/engine sizing, external moldline shaping and interactive graphics design processes are presented. The synthesis procedure overcomes many of the major drawbacks of airbreathing missile synthesis. It has features such as: simple initial geometry setup for body, tails, and inlets; modeling of completely arbitrary missile shapes; noncircular subsystem packaging; noncircular and multiple inlet modeling; aerodynamic and performance shaping; low cost, short duration computer sessions; rapic convergence; and accurate aerodynamic predictions. Two example configuration shapings are provided to depict the sizing process. Author

N88-29764# Dornier-Werke G.m.b.H., Friedrichshafen (West Germany).
AERODYNAMIC HEATING OF MISSILES
Rolf Kapp, H. Mathauer, and H. Rieger *In* AGARD, Special Course on Missile Aerodynamics Apr. 1988 19 p (For primary document see N88-29755 24-02)
Copyright Avail: NTIS HC A19/MF A01

The results of investigations of the aerodynamic heatings of missiles are presented. First the applied basic semiempirical methods to determine the flow field about the isolated components of missiles are described and some possibilities to calculate the heat flux in the boundary layer are specified for different pointed or blunted body noses, such as conical, ogival, and hemispherical noses. The methods are valid for laminar and turbulent flow properties and in the transition region between laminar and turbulent. The calculated heat transfer factors or Stanton numbers are compared with experimental results. The agreement between theoretical and measured values is good. A theoretical method for the calculation of the flow field around missile configurations is presented. This method is based on the parabolization of the compressible, stationary Navier-Stokes equations (PNS-eq) and limited to supersonic Mach numbers. The quality of the results is demonstrated by comparison to corresponding tests results of other authors. Finally, a computational method is described to calculate the local time-dependent temperatures at the surface or inside the body. The configuration is divided into a number of volume elements, thus permitting numerical solution of the time varying equation of heat transfer. The resulting temperatures for some special configurations are plotted and when possible compared with experimental results. Author

N88-29765# Office National d'Etudes et de Recherches Aerospatiales, Paris (France).
PREDICTION OF BASE-FLOWS
J. Delery and R. G. Lacau (Societe Nationale Industrielle Aerospatiale, Paris, France) *In* AGARD, Special Course on Missile Aerodynamics Apr. 1988 72 p (For primary document see N88-29755 24-02)
Copyright Avail: NTIS HC A19/MF A01

The base region of a missile or a launcher is the seat of complex phenomena which can have important repercussions on vehicle performance. The fields they concern are many: afterbody drag, heat transfer, and interaction between external steam and the base. Thus prediction of these phenomena is of great practical interest for missile design. The basic principles underlying most of the methods currently used to compute base-flows are examined. These methods belong essentially to the following categories. In the Inviscid/Viscous Interactive approach, the outer inviscid flow and the viscous regions are computed together and made compatible along a common boundary. In the Multi-Component approach, the flowfield is decomposed into a limited number of regions which are treated by approximate methods and then patched together. This approach has led to the development of a large variety of practical methods which are still routinely used in industry. The last approach consists in solving the time averaged Navier-Stokes equations. Base-flows in the jet-off and jet-on situations are now computed by solving the full Navier-Stokes equations or the thin layer approximation of these equations. Although still costly in computer time and not always in good agreement with experiments because of the difficulty of modeling turbulence in such complex flows, the Navier-Stokes approach is particularly promising. It appears also as the most straightforward way to extend prediction capability to three-dimensional flows.
Author

N88-29766# McDonnell-Douglas Astronautics Co., St. Louis, Mo.
NEXT GENERATION MISSILE DESIGN
J. E. Williams and R. J. Krieger *In* AGARD, Special Course on Missile Aerodynamics Apr. 1988 12 p (For primary document see N88-29755 24-02)
Copyright Avail: NTIS HC A19/MF A01

Traditional long range cruise class missiles fly at low altitudes and subsonic speed. To meet operational requirements, the next generation missiles will fly at relative high altitudes and supersonic or hypersonic speeds. Because of economic constraints, low cost design and development approaches must be used. To illustrate these approaches, the results of the U.S. Air Force sponsored Aerodynamic Configured Missile (ACM) Program and the subsequent Low Cost Aerodynamic Configured Missile Demonstrator Program are summarized with emphasis on the impact of these studies on future missile concepts. The ACM program objective was to exploit the aerodynamic potential of supersonic cruise and maneuvering missiles to achieve significant improvements in performance. During three phases of effort over a 30 month period, configuration development, wind tunnel testing, and performance analyses were performed. The major uses of the program results to date are described. A low cost approach is described which uses existing equipment, standard airframe structural design, the existing ACM data base, trajectory shaping, and aggressive program planning. Two flight test options are then identified. Program plans, costs, and subset experimental programs are identified including growth versions with higher Mach number capability. Author

N88-29767# European Space Agency, Paris (France).
HISTORY OF AEROELASTICITY IN GERMANY FROM THE BEGINNING TO 1945
Peter Bublitz (Deutsche Forschungs- und Versuchsanstalt fuer Luft- und Raumfahrt, Goettingen, West Germany) Jul. 1988 466 p Transl. into ENGLISH of Geschicte der Entwicklung der Aeroelastik in Deutschland von den Anfaengen bis 1945 (Goettingen, Fed. Republic of Germany, DFVLR), Dec. 1986 319 p Original language document was announced as N88-10003
(ESA-TT-1082; DFVLR-Mitt-86-25; ETN-88-93050) Avail: NTIS HC A20/MF A01; original German version available from DFVLR, VB-PL-DO, 90 60 58, 5000 Cologne, Fed. Republic of Germany 98 deutsche marks

The history of research into the aeroelasticity problems of airframes in Germany is outlined. It is shown that almost 20 yr elapsed after the beginning of powered flight before the physics of such aeroelasticity problems as static divergence and flutter were properly understood. Even then, it was not possible to avoid the aeroelastic problems which arose from the rapid progress of aviation at the time. This led to the continual introduction of new research topics. ESA

N88-29768# Army Aviation Systems Command, St. Louis, Mo.
TEST OF AN 0.8-SCALE MODEL OF THE AH-64 APACHE IN THE NASA LANGLEY FULL-SCALE WIND TUNNEL
Frederick A. Raitch May 1988 49 p
(AD-A196129; USAAVSCOM-TM-87-D-5) Avail: NTIS HC A03/MF A01 CSCL 01A

This document summarizes the tests of an 0.8-scale model of the upper half of the AH-64 air vehicle in the NASA Langley full-scale tunnel, primarily to determine the large-scale blockage effects discovered during earlier tests of the same model in the NASA Langley 4- by 7-meter tunnel. As background information, and to provide continuity, the earlier program is outlined. The models were large and heavy, and therefore the balances had large capabilities. Yet, because of operational limitations with both wind tunnels involved, the only data that overlapped in flight conditions were at very low velocities. Thus, the results of these tests were inconclusive due to the time-honored difficulty of small differences in large numbers. This effect carried over into other, auxiliary tests performed during the same test series, each concerned with an attempt to detect small differences. GRA

N88-29769# Air Force Inst. of Tech., Wright-Patterson AFB, Ohio. School of Engineering.
ANGLE OF ATTACK AND SIDESLIP ESTIMATION USING AN INERTIAL REFERENCE PLATFORM M.S. Thesis
Joseph E. Zeis, Jr Jun. 1988 169 p
(AD-A194876; AFIT/GAE/AA/88J-2) Avail: NTIS HC A08/MF A01 CSCL 01B

Flight test concepts are developed for the estimation of angle

of attack (alpha) and sideslip (beta) using an inertial reference platform. This development was further broken down into real-time, inflight estimation of alpha and post-flight estimation of alpha and beta. Following theoretical development, the concepts were tested with NASA F-15A flight data and examined real-time during a NASA Highly Integrated Digital Engine Control (HIDEC) flight test using the F-15A aircraft. Angle of attack is a critical parameter in the maneuverable, high performance aircraft of today. Yet many errors are present in the current methods of obtaining this angle. An accurate method of alpha and beta estimation could eliminate the need for such probes, and allow these quantities to be used for a broad range of applications. An inflight estimator was developed for computational speed and accuracy using inertial navigation system linear accelerations and angular rates. A second system based on linear recursive modeling was developed for post-flight estimation of alpha and beta. The data and programs specified in this research are applicable only to those aircraft mentioned, but the methods of estimation are universal. GRA

N88-29770*# Chrysler Corp., New Orleans, La. Military Public Electronic Systems.

SPACE SHUTTLE PHASE B WIND TUNNEL MODEL AND TEST INFORMATION. VOLUME 1: BOOSTER CONFIGURATION

J. L. Glynn and D. E. Poucher Jul. 1988 355 p
(Contract NAS1-18276)
(NASA-CR-178414-Vol-1-Pt-2; NAS 1.26:178414-Vol-1-Pt-2; DMS-DB-02-Vol-1-Pt-2) Avail: NTIS HC A16/MF A01 CSCL 01A

Archived wind tunnel test data are available for flyback booster or other alternative recoverable configurations as well as reusable orbiters studied during initial development (Phase B) of the Space Shuttle. Considerable wind tunnel data was acquired by the competing contractors and the NASA Centers for an extensive variety of configurations with an array of wing and body planforms. All contractor and NASA wind tunnel test data acquired in the Phase B development have been compiled into a database and are available for application to current winged flyback or recoverable booster aerodynamic studies. The Space Shuttle Phase B Wind Tunnel Database is structured by vehicle component and configuration type. Basic components include the booster, the orbiter, and the launch vehicle. Booster configuration types include straight and delta wings, canard, cylindrical, retroglide and twin body. Orbiter configuration types include straight and delta wings, lifting body, drop tanks and double delta wings. Launch configurations include booster and orbiter components in various stacked and tandem combinations. This is Volume 1 (Part 2) of the report -- Booster Configuration. Author

N88-29771*# National Aeronautics and Space Administration. Lewis Research Center, Cleveland, Ohio.

EULER ANALYSIS OF A SWIRL RECOVERY VANE DESIGN FOR USE WITH AN ADVANCED SINGLE-ROTATION PROPFAN

Christopher J. Miller 1988 15 p Presented at the 24th Joint Propulsion Conference, Boston, Mass., 11-13 Jul. 1988; sponsored by AIAA, ASME, SAE and ASEE
(NASA-TM-101357; E-4387; NAS 1.15:101357; AIAA-88-3152) Avail: NTIS HC A03/MF A01 CSCL 01A

Recent work has demonstrated the propulsive efficiency improvement available from single- and counter-rotation propfans as compared with current technology high bypass ratio turbofans. The concept known as swirl recovery vanes (SRV) is examined through the use of a 3-D Euler code. At high speed cruise conditions, the SRV can improve the efficiency level of a single-rotation propfan, but a concern is to have adequate hub choke margin. The SRV was designed with 2-D methods and was predicted to have hub choking at Mach 0.8 cruise. The 3-D Euler analysis properly accounts for sweep effects and 3-D relief, and predicts that at cruise the SRV will recover roughly 5 percent of the 10 percent efficiency loss due to swirl and have a good hub choke margin. Author

N88-29772# Ballistic Research Labs., Aberdeen Proving Ground, Md.

COMPUTATIONAL AERODYNAMIC ANALYSIS FOR A RANGE-LIMITED 25mm TRAINING ROUND

Bernard J. Guidos and Walter B. Sturek Aug. 1987 56 p
(DA Proj. 1L1-62618-AH-80)
(AD-A185270; BRL-TR-2833) Avail: NTIS HC A04/MF A01 CSCL 01A

A computational aerodynamics study is presented for an initial design configuration intended for use as a training round for a 25 mm gun. The shell is designed with a nonaxisymmetric boattail which induced a large de-spin moment. The purpose for such a design is to limit the range of the round through aerodynamic destabilization. A computational aerodynamics study is reported using a thin layer Parabolized Navier-Stokes computational technique. Static aerodynamic coefficients and roll damping are computed for a range of supersonic Mach numbers and boattail lengths. Comparisons are made with computational predictions for axisymmetric configurations and firing range data. A six degree of freedom trajectory simulation code is used to estimate the early flight characteristics for the configurations of interest. Author

N88-29773*# National Aeronautics and Space Administration. Ames Research Center, Moffett Field, Calif.

THE PRESENT STATUS AND THE FUTURE OF MISSILE AERODYNAMICS

Jack N. Nielsen Jan. 1988 37 p
(NASA-TM-100063; A-87289; NAS 1.15:100063) Avail: NTIS HC A03/MF A01 CSCL 01A

Some recent developments in the state of the art in missile aerodynamics are reviewed. Among the subjects covered are: (1) tri-service/NASA data base, (2) wing-body interference, (3) nonlinear controls, (4) hypersonic transition, (5) vortex interference, (6) airbreathers, supersonic inlets, (7) store separation problems, (8) correlation of missile data, (9) CFD codes for complete configurations, (10) engineering prediction methods, and (11) future configurations. Suggestions are made for future research and development to advance the state of the art of missile aerodynamics. Author

N88-29774*# National Aeronautics and Space Administration. Ames Research Center, Moffett Field, Calif.

THE COMPUTATION OF FLOW PAST AN OBLIQUE WING USING THE THIN-LAYER NAVIER-STOKES EQUATIONS

Unmeel Mehta Jun. 1986 12 p Presented at the 10th International Conference on Numerical Methods in Fluid Mechanics, Beijing, China, 23-27 Jun. 1986 Original contains color illustrations
(NASA-TM-88317; A-86295; NAS 1.15:88317) Avail: NTIS HC A03/MF A01 CSCL 01A

Essential aspects are presented for computing flow past an oblique wing with the thin-layer Navier-Stokes equations. A new method is developed for generating a grid system around a realistic wing. This method utilizes a series of conformal transformations. The thin-shear-layer approximation and an algebraic eddy-viscosity turbulence model are used to simplify the Reynolds-averaged Navier-Stokes equations. An implicit, factored numerical scheme and the concept of pencil data structure are utilized. For the first time, some flow fields caused by the oblique wing in a supersonic free stream are discussed, emphasizing the separated vortex flows associated with such a wing. Author

N88-29775*# New York Univ., New York. Inst. of Mathematical Sciences.

COMPUTATIONAL METHODS FOR THE PROBLEMS OF THE TIP VORTEX Final Technical Report, 1 Apr. 1985 - 31 Aug. 1988

Paul R. Garabedian 6 Sep. 1988 5 p
(Grant NAG2-345)
(NASA-CR-181438; NAS 1.26:181438) Avail: NTIS HC A02/MF A01 CSCL 01A

The tip vortex problem for helicopter rotors in transonic flow was studied. The first model was that of potential flow past a

single blade in parallel transonic flow. The incidence on the wing of a vortex sheet trailing from a blade in front was studied by modeling the incident sheet by a single vortex filament. A 3-D potential flow code was written to incorporate the usual boundary conditions at infinity together with the model of such a vortex filament and to analyze the resulting flow over the wing. The code was used to study the effect of the vortex filament on the production of shocks at the tip of the wing. Another problem studied within the framework of potential flow theory was the rollup of the vortex sheet behind the wing. A comparison was made of flow models described by the potential equation, by the Euler equations for steady flow, and by the Navier-Stokes equations. The question was also studied as to whether there is an advantage in solving the Navier-Stokes equations rather than the Euler equations for steady flow. Author

N88-29776*# National Aeronautics and Space Administration. Langley Research Center, Hampton, Va.
PRESSURE DISTRIBUTIONS FROM SUBSONIC TESTS OF AN ADVANCED LAMINAR-FLOW-CONTROL WING WITH LEADING- AND TRAILING-EDGE FLAPS
Zachary T. Applin and Garl L. Gentry, Jr. Jul. 1988 339 p
(NASA-TM-4040-Pt-2; L-16405; NAS 1.15:4040-Pt-2) Avail: NTIS HC A15/MF A01 CSCL 01A

An unswept, semispan wing model equipped with full-span leading- and trailing-edge flaps was tested in the Langley 14- by 22-Foot Subsonic Tunnel to determine the effect of high-lift components on the aerodynamics of an advanced laminar-flow-control (LFC) airfoil section. Chordwise pressure distributions near the midsemispan were measured for four configurations: cruise, trailing-edge flap only, and trailing-edge flap with a leading-edge Krueger flap of either 0.10 or 0.12 chord. Part 1 of this report (under separate cover) presents a representative sample of the plotted pressure distribution data for each configuration tested. Part 2 presents the entire set of plotted and tabulated pressure distribution data. The data are presented without analysis. Author

N88-29777# Rensselaer Polytechnic Inst., Troy, N.Y.
THEORETICAL AERODYNAMICS, TRANSONIC FLOW Final Report, 1 Jul. 1982 - 31 Oct. 1987
Julian D. Cole 12 Feb. 1988 5 p
(Grant AF-AFOSR-0155-82)
(AD-A196247; AFOSR-88-0656TR) Avail: NTIS HC A02/MF A01 CSCL 20D

A substantial body of work on transonic aerodynamics and problems using related applied mathematical techniques was carried out on this AFOSR grant. A listing of the main publications produced with the support of this grant is given. GRA

N88-29778*# National Aeronautics and Space Administration. Langley Research Center, Hampton, Va.
RECENT ADVANCES IN TRANSONIC COMPUTATIONAL AEROELASTICITY
John T. Batina, Robert M. Bennett, David A. Seidel, Herbert J. Cunningham, and Samuel R. Bland Sep. 1988 28 p Presented at the Symposium on Advances and Trends in Computational Structural Mechanics and Fluid Dynamics, Washington, D.C., 17-19 Oct. 1988
(NASA-TM-100663; NAS 1.15:100663) Avail: NTIS HC A03/MF A01 CSCL 01A

A transonic unsteady aerodynamic and aeroelasticity code called CAP-TSD was developed for application to realistic aircraft configurations. The code permits the calculation of steady and unsteady flows about complete aircraft configurations for aeroelastic analysis in the flutter critical transonic speed range. The CAP-TSD code uses a time accurate approximate factorization algorithm for solution of the unsteady transonic small disturbance potential equation. An overview is given of the CAP-TSD code development effort and results are presented which demonstrate various capabilities of the code. Calculations are presented for several configurations including the General Dynamics 1/9 scale F-16 aircraft model and the ONERA M6 wing. Calculations are also presented from a flutter analysis of a 45 deg sweptback wing which agrees well with the experimental data. Descriptions are presented of the CAP-TSD code and algorithm details along with results and comparisons which demonstrate these recent developments in transonic computational aeroelasticity. Author

N88-29779# Naval Ship Research and Development Center, Bethesda, Md. Aviation Dept.
ANALYSIS OF A FIXED-PITCH X-WING ROTOR EMPLOYING LOWER SURFACE BLOWING Final Report, Apr. 1985 - Sep. 1985
Alan W. Schwartz and Ernest O. Rogers Nov. 1987 27 p Presented at the Circulation Control Workshop, Moffett Field, Calif., 19-21 Feb. 1986 Previously announced as N88-17602 Submitted for publication
(AD-A187379; DTRC-87/045) Avail: NTIS HC A03/MF A01 CSCL 01A

Lower surface blowing (LSB) is investigated as an alternative to the variable blade pitch requirement for the X-wing Circulation Control (CC) rotor concept. Additional trailing edge blowing slots on the lower surfaces of CC airfoils provide a bidirectional lift capability that effectively doubles the control range. The operational requirements of this rotor system are detailed and compared to the projected performance attributes of LSB airfoils. Analysis shows that, aerodynamically, LSB supplies a fixed pitch rotor system with the equivalent lift efficiency and rotor control of present CC rotor designs that employ variable blade pitch. Aerodynamic demands of bidirectional lift production are predicted to be within the capabilities of current CC airfoil design methodology. Emphasis in this analysis is given to the high speed rotary wing flight regime unique to stoppable rotor aircraft. The impact of a fixed pitch restriction in hover and low speeed flight is briefly discussed. Author

N88-29780*# National Aeronautics and Space Administration. Lewis Research Center, Cleveland, Ohio.
AN UNCONDITIONALLY STABLE RUNGE-KUTTA METHOD FOR UNSTEADY FLOWS
Philip C. E. Jorgenson and Rodrick V. Chima [1988] 14 p Prepared for presentation at the 27th Aerospace Sciences Meeting, Reno, Nev., 9-12 Jan. 1989; sponsored in part by AIAA
(NASA-TM-101347; E-4373; NAS 1.15:101347; AIAA-89-0205) Avail: NTIS HC A03/MF A01 CSCL 01A

A quasi-three dimensional analysis was developed for unsteady rotor-stator interaction in turbomachinery. The analysis solves the unsteady Euler or thin-layer Navier-Stokes equations in a body fitted coordinate system. It accounts for the effects of rotation, radius change, and stream surface thickness. The Baldwin-Lomax eddy viscosity model is used for turbulent flows. The equations are integrated in time using a four stage Runge-Kutta scheme with a constant time step. Implicit residual smoothing was employed to accelerate the solution of the time accurate computations. The scheme is described and accuracy analyses are given. Results are shown for a supersonic through-flow fan designed for NASA Lewis. The rotor:stator blade ratio was taken as 1:1. Results are also shown for the first stage of the Space Shuttle Main Engine high pressure fuel turbopump. Here the blade ratio is 2:3. Implicit residual smoothing was used to increase the time step limit of the unsmoothed scheme by a factor of six with negligible differences in the unsteady results. It is felt that the implicitly smoothed Runge-Kutta scheme is easily competitive with implicit schemes for unsteady flows while retaining the simplicity of an explicit scheme. Author

N88-29781# National Aeronautical Establishment, Ottawa (Ontario).
THE USE OF HOT-FILM TECHNIQUE FOR BOUNDARY LAYER STUDIES ON A 21 PERCENT THICK AIRFOIL
M. Khalid May 1987 54 p
(NAE-AN-45; NRC-27892) Avail: NTIS HC A04/MF A01

A heat transfer method of studying boundary layer flows over airfoils at transonic test conditions was investigated. The method employs very thin DISA hot-film gauges housing Constant

Temperature Anemometer probes. Provided that the thickness dimension of the films remains less than the critical disturbances height for inducing transition of the laminar boundary layer, the heat transfer response from the films, positioned carefully on the model surface, can be studied to determine the boundary layer characteristics. Results from an application study on a 21 percent thick laminar flow airfoil model are presented and dissussed.
Author

N88-29782*# National Aeronautics and Space Administration, Washington, D.C.
CALCULATION OF NON-STATIONARY AERODYNAMIC FORCES IN THE NEAR SONIC RANGE
I. Teipel Aug. 1988 29 p Transl. into ENGLISH from Die Berechnung Instationaerer Luftkraefte im Schallnahen Bereich, Journal de Mecanique (Fed. Republic of Germany), v. 4, no. 3, Sep. 1965 p 335-360 Transl. by SCITRAN, Inc., Santa Barbara, Calif. Original document was prepared by Inst. fuer Theoretische Gasdynamik der Deutschen Versuchsanstalt fuer Luft und Raumfahrt, Aachen, Fed. Republic of Germany
(Contract NAsw-4307)
(NASA-TT-20310; NAS 1.77:20310) Avail: NTIS HC A03/MF A01 CSCL 01A

The development of a mathematical method for calculating nonstationary supersonic flow in the near-sonic range is described. A perturbation formula is derived based on the exact stationary values; it is applicable to the equation for potential. The problem can thus be divided into stationary and nonstationary fields. The pressure distribution in an oscillating profile is determined, based on hyperbolic differential equations. It is shown that there are important corollaries concerning the application of linear theory. With suitable extrapolations, linear theory can be used up to about Mach 0.8. Linear theory is not applicable, however, when determining the moment coefficients; for this case, a special technique is described. Author

N88-29731# National Aeronautical Establishment, Ottawa (Ontario). Unsteady Aerodynamics Lab.
AIRCRAFT DYNAMICS: AERODYNAMIC ASPECTS AND WIND TUNNEL TECHNIQUES
K. J. Orlik-Rueckemann *In* AGARD, The Flight of Flexible Aircraft in Turbulence: State-of-the-Art in the Description and Modelling of Atmospheric Turbulence Dec. 1987 14 p Previously announced as N88-13320 (For primary document see N88-29725 24-01)
Copyright Avail: NTIS HC A09/MF A01

03 AIR TRANSPORTATION AND SAFETY

Includes passenger and cargo air transport operations; and aircraft accidents.

For related information see also *16 Space Transportation* and *85 Urban Technology and Transportation.*

N88-29783# Loughborough Univ. of Technology (England). Dept. of Transport Technology.
AN ANALYSIS OF TIME AND SPACE REQUIREMENTS FOR AIRCRAFT TURNROUNDS
Robert E. Caves Aug. 1987 41 p
(TT-8705) Avail: NTIS HC A03/MF A01

By their very nature, airport aprons occupy the space between the runway system and the terminal buildings. Most attempts to increase runway capacity, by the use of parallel taxiways or larger aircraft, reduce the available apron space. Similarly, the growth of piers and satellites to provide extra gates also restricts the apron. The situation is worsened further when more space is required for passenger processing, due to the rate of increase of processing efficiency not keeping pace with traffic growth, yet there is no room for landsite expansion. Discussed is the influence of aircraft technology on apron capacity. Author

N88-29784# Federal Aviation Administration, Washington, D.C. Office of Civil Aviation Security.
REPORT TO CONGRESS ON THE EFFECTIVENESS OF THE CIVIL AVIATION SECURITY PROGRAM Semiannual Report, 1 Jul. - 31 Dec. 1987
31 Dec. 1987 42 p
(AD-A195282; DOT/FAA/ACS-88-1(27)) Avail: NTIS HC A03/MF A01 CSCL 01B

The report includes an analysis of the current threat against civil aviation along with information regarding hijacking attempts, security incidents, bomb threats, and passenger screening activity. It also summarizes ongoing activities to assure adequate protection of civil air commerce against hijacking/sabotage and related crimes, and other aspects of the Civil Aviation Security Program. GRA

N88-29785# Army Aviation Engineering Flight Activity, Edwards AFB, Calif.
JUH-1H REDESIGNED PNEUMATIC BOOT DEICING SYSTEM FLIGHT TEST EVALUATION Final Report, 15 Nov. 1983 - 7 Mar. 1986
Matthew S. Graham, Loran A. Haworth, and Jack L. Kimberly Aug. 1987 144 p
(AD-A194918; USAAEFA-83-13) Avail: NTIS HC A07/MF A01 CSCL 08L

The U.S. Army Aviation Engineering Flight Activity conducted an evaluation of the Pneumatic Boot Deicing System (PBDS) with two pneumatic deicer boot designs, referred to as second and third generation. The objective of the test was to conduct feasibility testing of the pneumatic system concept for deicing helicopter rotor blades in forward flight, and to assess any changes to aircraft performance and handling qualities. Phase 1 consisted of a ground and inflight structural loads survey which established an operational envelope. Phase 2 consisted of forward flight testing in artificial and natural icing conditions of the second generation design only. Phase 3 consisted of limited artificial rain erosion tests of the second generation design. Phase 4 consisted of performance and handling qualities evaluation of the second generation design. Hover and level flight performance were greatly improved over the first generation, but a significant performance penalty still exists. Handling qualities were essentially unchanged from the standard UH-1H. Two unsatisfactory and six undesirable reliability and maintainability characteristics were identified. GRA

N88-29786# Air Command and Staff Coll., Maxwell AFB, Ala.
CENTRALIZED CLASS A FLIGHT MISHAP INVESTIGATION
James R. McDonald Apr. 1988 32 p
(AD-A194397; ACSC-88-1735) Avail: NTIS HC A03/MF A01 CSCL 01B

Although investigation of aircraft mishaps is a vital part of the U.S. Air Force mishap prevention program, these investigations are usually conducted by individuals with little or no experience in this field. This leads to errors in the investigations and the mishap reports. This report looks at two alternative systems in use today: the first used by the Federal Armed Forces, FRG, and the second used by the U.S. Army. A centralized program for the U.S. Air Force is suggested. This program is based at the MAJCOM and is designed to meet Air Force needs and requirements. Recommendations for test program are also included. GRA

04 AIRCRAFT COMMUNICATIONS AND NAVIGATION

Includes digital and voice communication with aircraft; air navigation systems (satellite and ground based); and air traffic control.

For related information see also *17 Space Communications, Spacecraft Communications, Command and Tracking* and *Communications and Radar.*

N88-29787# Naval Postgraduate School, Monterey, Calif.
ACCURACY OF SATELLITE DATA NAVIGATION M.S. Thesis

William J. Bethke Mar. 1988 97 p
(AD-A195877) Avail: NTIS HC A05/MF A01 CSCL 17G

Image navigation is critical to the effective use of digital imagery for meteorological and oceanographic studies. This thesis reviews various methods used to navigate imagery to the earth and investigates the accuracy of the Naval Postgraduate School (NPS) model. An explanation of how the NPS navigation process works is included for completeness. Results from 22 separate runs of the NPS model are studied. The following points are discussed in Chapters 6 and 7: (1) abilities of user affects accuracy, (2) apparent upper bound for navigation landmarks, (3) centrally oriented navigation landmarks enhance accuracy, and (4) evenly distributed navigation landmarks enhance accuracy. The thesis concludes with observations and suggestions to stimulate further research into the effective usw of the NPS image navigation system. GRA

N88-29788 Eurocontrol Experimental Centre, Bretigny (France).
OBSERVED TRACK-KEEPING PERFORMANCE OF DC10 AIRCRAFT EQUIPPED WITH THE COLLINS AINS-70 AREA NAVIGATION SYSTEM: KARLSRUHE AND MASSTRICHT UACs (UPPER AREA CONTROL CENTRES) Report, Mar. 1982 - Oct. 1984
L. Clarke, H. David, and W. Oenema Feb. 1987 92 p
(EEC-202) Avail: NTIS HC E05/MF E05; copy not available from STI Facility CSCL 17G

The results are described which were obtained from data on 964 flights by DC10 aircraft equipped with the Collins AINS-70 Area Navigation System which is based on automatic double DME updating of inertial sensors. Author

05 AIRCRAFT DESIGN, TESTING AND PERFORMANCE

Includes aircraft simulation technology.

For related information see also *18 Spacecraft Design, Testing and Performance* and *39 Structural Mechanics*.For land transportation vehicles see *85 Urban Technology and Transportation.*

N88-29789*# National Aeronautics and Space Administration. Langley Research Center, Hampton, Va.
COMPRESSION PYLON Patent Application
James C. Patterson, Jr., inventor (to NASA) 23 Jun. 1988 14 p
(NASA-Case-LAR-13777-1; NAS 1.71:LAR-13777-1; US-Patent-Appl-SN-210480) Avail: NTIS HC A03/MF A01 CSCL 01C

A compression pylon for an aircraft with a wing-mounted engine, that does not cause supersonic airflow to occur within the fuselage-wing-pylon-nacelle channel is presented. The chord length of the pylon is greater than the local chord length of the wing to which it is attached. The maximum thickness of the pylon occurs at a point corresponding to the local trailing edge of the wing. As a result, the airflow through the channel never reaches supersonic velocities. NASA

N88-29790*# Draper (Charles Stark) Lab., Inc., Cambridge, Mass.
INTELLIGENT FAULT DIAGNOSIS AND FAILURE MANAGEMENT OF FLIGHT CONTROL ACTUATION SYSTEMS Final Report, May 1986 - Mar. 1988
William F. Bonnice and Walter Baker May 1988 90 p
(Contract NAS2-12404)
(NASA-CR-177481; NAS 1.26:177481; CSDL-R-2055) Avail: NTIS HC A05/MF A01 CSCL 01C

The real-time fault diagnosis and failure management (FDFM) of current operational and experimental dual tandem aircraft flight control system actuators was investigated. Dual tandem actuators were studied because of the active FDFM capability required to manage the redundancy of these actuators. The FDFM methods used on current dual tandem actuators were determined by examining six specific actuators. The FDFM capability on these six actuators was also evaluated. One approach for improving the FDFM capability on dual tandem actuators may be through the application of artificial intelligence (AI) technology. Existing AI approaches and applications of FDFM were examined and evaluated. Based on the general survey of AI FDFM approaches, the potential role of AI technology for real-time actuator FDFM was determined. Finally, FDFM and maintainability improvements for dual tandem actuators were recommended. Author

N88-29791# Air Command and Staff Coll., Maxwell AFB, Ala.
THE SOVIET STEALTH FIGHTER: CHECK OR CHECKMATE
Stanley P. Siefke Apr. 1988 42 p
(AD-A195200; ACSC-88-2405) Avail: NTIS HC A03/MF A01 CSCL 01C

Stealth technology is a complex science requiring the reduction of characteristic vehicle signatures in the acoustical, optical, infrared, and radar environments. The use of this technology has far reaching impacts on the defenses an opponent must develop the detect such a vehicle. The Soviets have the doctrine that can use vehicles with this technology. It amplifies their firm commitment to offensive capabilities using elements such as surprise, deception, firepower, and maneuver. They have shown understanding of the basic principles involved in the design of this type of vehicle. They also have a strong background in the electromagnetic research and development fields capable of producing radar absorption materials. If all else fails, they definitely have the proven capability to steal it. This study concludes that the Soviet Union will probably deploy their own version of the Advanced Tactical Fighter near the turn of the century. The quality of the vehicle is still suspect, but the U.S. must be prepared to handle such an eventuality. GRA

N88-29792# Anamet Labs., Inc., Hayward, Calif.
COMPUTER PROGRAMS FOR GENERATION OF NASTRAN AND VIBRA-6 AIRCRAFT MODELS Final Report, Dec. 1985 - Dec. 1986
Steven G. Harrison Apr. 1988 94 p
(Contract F33615-84-C-3216)
(AD-A195467; Rept-1286-1A; AFWL-TR-87-21) Avail: NTIS HC A05/MF A01 CSCL 12E

This report describes a series of computer programs designed to aid the analyst in preparing input data for aircraft models to be analyzed using NASTRAN and/or VIBRA-6. The programs permit creation of either beam or plate-type models of aircraft, subsequent postprocessing of NASTRAN OUTPUT2 files, and creation of VIBRA-6 AERO, IMOD and LOAD fixed data decks. In addition, the analyst may specify use of either the Ritz procedure or standard NASTRAN eigensolvers to derive normal modes of the aircraft for use in the VIBRA-6 vulnerability assessment. A command procedure is provided to orchestrate the execution of the various programs, to keep track of file assignments and to maintain a history of program use. GRA

N88-29793# Army Aviation Engineering Flight Activity, Edwards AFB, Calif.
PRELIMINARY AIRWORTHINESS EVALUATION OF THE UH-60A/ESSS (EXTERNAL STORES SUPPORT SYSTEM) WITH HELLFIRE LAUNCHER INSTALLED Final Report, 21 May - 3 Jun. 1987
Daumants Belte, Thomas P. Walsh, Thomas L. Reynolds, Paul W. Losier, and Randall W. Cason Oct. 1987 110 p
(AD-A196187; USAAEFA-86-25) Avail: NTIS HC A06/MF A01 CSCL 01C

The airworthiness evaluation of the UH-60A helicopter configured with the External Stores Support System (ESSS) and 16 HELLFIRE (4 HMMS) missiles installed was conducted at the Sikorsky flight test facility at West Palm Beach, Florida (elevation 28 feet). A total of 16.2 productive hours during 18 flights were flown between 21 May and 3 June 1987. Tests were conducted to determine handling qualities and performance of the UH-60A in the 16 HELLFIRE (4 HMMS) missile system configuration at an average mission gross weight of 17,000 pounds. The handling qualities of the UH-60A with the 16 HELLFIRE (4 HMMS) missile

system installed were essentially unchanged from those previously reported for the UH-60A in the normal utility configuration. The equivalent flat plate area of the 16 HELLFIRE (4 HMMS) missile system was determined to be 11 square feet over that of the UH-60A in the ESSS only configuration. One miscellaneous observation was made regarding the initial installation and fit of the production ESSS fairings. GRA

N88-29794# Iowa Univ., Iowa City. Center for Computer Aided Design.
DYNAMICS OF ARTICULATED AEROSPACE STRUCTURES Final Report, 1 Dec. 1985 - 30 Nov. 1987
Edward J. Haug 22 Apr. 1988 9 p
(Grant AF-AFOSR-0082-86)
(AD-A195685; AFOSR-88-0670TR) Avail: NTIS HC A02/MF A01 CSCL 20K

A unified variational approach to dynamics of flexible multibody systems has been developed and demonstrated on several test problems, including a deployable space structure, flexible manipulators with feedback control, spinning blades, impacting elastic bodies, and variety of mechanisms. A new recursive formulation was developed for dynamics of flexible multibody systems. This new formulation demonstrated in excess of an order of magnitude speed up in computation, compared to the Cartesian coordinate approach, with comparable accuracy and improved stability. A substructuring formulation that accounts for geometrically nonlinear deformation effects in spinning blades and large space structures was developed and demonstrated, using both the Cartesian coordinate and recursive relative coordinate formulations. The substructure technique was further extended to account for contact-impact effects between structural components. A new formulation of translational joints between flexible bodies was developed, to account for deformation due to sliding contacts. GRA

N88-29795# RAND Corp., Santa Monica, Calif.
AIRCRAFT AIRFRAME COST ESTIMATING RELATIONSHIPS: STUDY APPROACH AND CONCLUSIONS
R. W. Hess and H. P. Romanoff Dec. 1987 107 p
(Contract F49620-86-C-0008)
(R-3255-AF; LC-87-28382; ISBN-0-8330-0810-2) Avail: NTIS HC A06/MF A01

Generalized equations are presented for estimating the development and production costs of aircraft airframes. Provided are separate cost estimating relationships (CERs) for engineering, tooling, manufacturing labor, and quality-control hours; manufacturing material, development support, and flight-test cost; and total program cost. The CERs, expressed in the form of exponential equations, were derived by multiple least-squares regression analysis. They were derived from a data base consisting of 34 military aircraft with first flight dates ranging from 1948 to 1978. Most of the aircraft technical data were obtained from either original engineering documents such as manufacturers' performance substantiation reports, or from official Air Force and Navy documents. The cost data were obtained from the airframe manufacturers, either directly from their records or indirectly through standard DoD reports such as Contractor Cost Data Reporting system. Author

N88-29796# RAND Corp., Santa Monica, Calif.
THE COST AND PERFORMANCE IMPLICATIONS OF RELIABILITY IMPROVEMENTS IN THE F-16A/B Interim Report
John B. Abell, Thomas F. Kirkwood, Robert L. Petruschell, and Giles K. Smith Mar. 1988 90 p
(Contract F49620-86-C-0008)
(AD-A195096; RAND/N-2499-AF) Avail: NTIS HC A05/MF A01 CSCL 01C

This Note suggests the magnitude of the effects of policies and strategies to enhance reliability of Air Force aircraft weapon systems. Using the F-16A/B fighter aircraft program as a case study, the authors found that the benefits of improved reliability include: (1) a reduction in base-level maintenance manpower requirements, (2) increased capability to generate sorties, (3) lowered costs for procurement and repair of engines and spare parts, and (4) reductions in the resources (both equipment and manpower) required to deploy a combat unit to an overseas site. GRA

N88-29720# National Aerospace Lab., Emmeloord (Netherlands).
MATCHING P.S.D.: DESIGN LOADS
R. Noback *In* AGARD, The Flight of Flexible Aircraft in Turbulence: State-of-the-Art in the Description and Modelling of Atmospheric Turbulence Jun. 1988 12 p Sponsored by the Netherlands Agency for Aerospace Programs (For primary document see N88-29717 24-01)
Copyright Avail: NTIS HC A06/MF A01

N88-29721# Lockheed Aeronautical Systems Co., Burbank, Calif. Dynamic Loads Div.
A SUMMARY OF METHODS FOR ESTABLISHING AIRFRAME DESIGN LOADS FROM CONTINUOUS GUST DESIGN CRITERIA
Richard N. Moon *In* AGARD, The Flight of Flexible Aircraft in Turbulence: State-of-the-Art in the Description and Modelling of Atmospheric Turbulence Jun. 1988 40 p (For primary document see N88-29717 24-01)
Copyright Avail: NTIS HC A06/MF A01

N88-29722# Messerschmitt-Boelkow-Blohm G.m.b.H., Hamburg (West Germany). Civil and Transport Aircraft Div.
COMPARISON OF THE INFLUENCE OF DIFFERENT GUST MODELS ON STRUCTURAL DESIGN
Manfred Molzow *In* AGARD, The Flight of Flexible Aircraft in Turbulence: State-of-the-Art in the Description and Modelling of Atmospheric Turbulence Jun. 1988 17 p (For primary document see N88-29717 24-01)
Copyright Avail: NTIS HC A06/MF A01

N88-29738# National Aerospace Lab., Amsterdam (Netherlands).
LOW-SPEED LONGITUDINAL FLYING QUALITIES OF MODERN TRANSPORT AIRCRAFT
H. A. Mooij *In* AGARD, Advances in Flying Qualities May 1988 16 p (For primary document see N88-29735 24-01)
Copyright Avail: NTIS HC A09/MF A01

N88-29739# Systems Technology, Inc., Hawthorne, Calif.
ADVANCES IN FLYING QUALITIES: CONCEPTS AND CRITERIA FOR A MISSION ORIENTED FLYING QUALITIES SPECIFICATION
Roger H. Hoh *In* AGARD, Advances in Flying Qualities May 1988 28 p (For primary document see N88-29735 24-01)
Copyright Avail: NTIS HC A09/MF A01

N88-29740# Air Force Wright Aeronautical Labs., Wright-Patterson AFB, Ohio.
A SECOND LOOK AT MIL PRIME FLYING QUALITIES REQUIREMENTS
Robert J. Woodcock *In* AGARD, Advances in Flying Qualities May 1988 15 p (For primary document see N88-29735 24-01)
Copyright Avail: NTIS HC A09/MF A01

06 AIRCRAFT INSTRUMENTATION

Includes cockpit and cabin display devices; and flight instruments.

For related information see also *19 Spacecraft Instrumentation* and *35 Instrumentation and Photography.*

N88-29797# Essex Corp., Alexandria, Va.
USE OF COLOR CRTs (CATHODE RAY TUBES) IN AIRCRAFT COCKPIT: A LITERATURE SEARCH, REVISION B Final Report
Steven L. Hale and Hanns J. Billmayer Apr. 1988 24 p

(Contract DAAA15-88-C-0005; DA Proj. 1L1-62716-A-700) (AD-A195062; EFR-014-Rev-B; HEL-TN-3-88-Rev-B) Avail: NTIS HC A02/MF A01 CSCL 09E

A literature search was conducted to assess the utility and feasibility of incorporating color cathode ray tubes (CRTs) in military aircraft cockpits and is presented in annotated bibliography format. The advantages and disadvantages of color CRTs are reviewed. It is concluded that the incorporation of color on aircraft CRTs will prove beneficial and that potential problems associated with the use of color displays can be eliminated with proper display design and the advancement of technology. GRA

N88-29798# Air Command and Staff Coll., Maxwell AFB, Ala.
THE OFP (OPERATIONAL FLIGHT PROGRAM) UPDATE CYCLE NEEDS YOU
Gregory S. Zaniewski Apr. 1988 35 p
(AD-A194910; ACSC-88-2830) Avail: NTIS HC A03/MF A01 CSCL 12E

The operational flight program (OFP) update cycle provides tactical air-crews (users) the capability to periodically update embedded avionic computer software. This capability allows the users to improve operational effectiveness in response to a change in operational mission, threat, or modifications to current equipment. Unfortunately, the specifics involved to utilize the cycle are embedded in multi-layered regulations and manuals. This article, written for publication in the Tactical Air Command's Fighter Weapons Review quarterly magazine intends to inform the reader about the OFP update cycle. The article identifies potential bottlenecks in the system and suggests methods for increasing users participation in the cycle. Potentially, increased user participation may increase the weapon system operational effectiveness and suitability. GRA

N88-29799# Air Command and Staff Coll., Maxwell AFB, Ala.
INTEGRATION OF LANTIRN (LOW ALTITUDE NAVIGATION AND TARGETING INFRARED FOR NIGHT) INTO OPERATIONAL FIGHTER TRAINING
Andrew M. Gecelosky Apr. 1988 41 p
(AD-A194906; ACSC-88-1015) Avail: NTIS HC A03/MF A01 CSCL 05I

The introduction of the Low Altitude Navigation and Targeting Infrared for Night (LANTIRN) system on the F-15E and F-16C/D aircraft will result in increased night flying. Quality of life issues and safety concerns have been raised in response to an increase of night training. The study proposes seven tenets that, when applied with effective scheduling, enhance quality of life and flight safety at LANTIRN designated bases. The study concludes that LANTIRN can be successfully integrated into the Tactical Air Forces. GRA

N88-29800# Air Force Wright Aeronautical Labs., Wright-Patterson AFB, Ohio.
A MULTIPROCESSOR AVIONICS SYSTEM FOR AN UNMANNED RESEARCH VEHICLE Final Report, 1 Jan. - 15 Dec. 1987
Daniel B. Thompson Mar. 1988 197 p
(AD-A194806; AFWAL-TR-88-3003) Avail: NTIS HC A09/MF A01 CSCL 12F

AFWAL/FIGL is developing a new Unmanned Research Vehicle (URV) testbed system for low cost flight testing of advanced flight control concepts. This new system will incorporate a modular/reconfigurable airframe, will possess greater aerodynamic capabilities, and will utilize an advanced avionics/control system to allow embedded computation of flight test applications. AFWAL/FIGL has utilized its in-house experience in multiprocessor systems technologies to develop a first phase prototype system comprised of multiple microprocessors and a parallel backplane bus. A multiprocessor software operating system and interprocessor communications protocol have been developed and tested. To demonstrate the capabilities of the system and the development of parallel software, an applications set of parallel software tasks have been developed and demonstrated. The hardware and software architecture, approach taken in the development, and results achieved are described in this report. GRA

N88-29801# Management Consulting and Research, Inc., Falls Church, Va.
AIRCRAFT AVIONICS AND MISSILE SYSTEM INSTALLATION COST STUDY. VOLUME 2: APPENDICES F AND G Final Report, Apr. 1987 - Feb. 1988
Kirsten M. Pehrsson and George R. Kreisel 12 Feb. 1988 128 p
(Contract N00600-84-D-4171)
(AD-A195372; MCR-TR-8711/12-1-Vol-2) Avail: NTIS HC A07/MF A01 CSCL 05C

This volume contains appendices F and G, the raw data extracted from Technical Directive Status Accounting System (TDSA), and the TDSA installation manhour normalizations to unit 100, respectively. The TDSA is an automated accounting system designed to store, maintain, and disseminate information concerning the status of TDs. The system provides the incorporation/nonincorporation status of the TDs as they apply to each equipment item (airframe, engine, support equipment, avionics, etc.). It also provides projected and actual man-hour reporting, configuration status of equipment items, change-kits material accounting, and summary reporting for overall management and budgeting. On-line access is provided to each Naval Aviation Rework Facility (NARF) and to the Naval Air Maintenance Organization (NAMO) management. Detailed reports are distributed quarterly at the organizational level. Appendix F contains the data extracted from the TDSA system. The data was obtained from queries to the TDSA at NAMO, Patuxent River. Queries were made for each OSIP for kit costs and then for manhours. The data from both queries was combined in Lotus 1-2-3 files. Appendix G contains the TDSA Installation Manhour Normalizations to Unit 100. The data was normalized using the learning curves as discussed in Volume 1, Section 2, Data Collection/Sources/Normalization. GRA

N88-29719# Technische Univ., Brunswick (West Germany). Inst. for Guidance and Control.
FLIGHT TEST EQUIPMENT FOR THE ON-BOARD MEASUREMENT OF WIND TURBULENCE
G. Schaenzer, M. Swolinsky, and P. Voersmann (Aerodata Flugmesstechnik G.m.b.H., Brunswick, West Germany) *In* AGARD, The Flight of Flexible Aircraft in Turbulence: State-of-the-Art in the Description and Modelling of Atmospheric Turbulence Jun. 1988 11 p (For primary document see N88-29717 24-01)
Copyright Avail: NTIS HC A06/MF A01

N88-29730# National Aeronautical Establishment, Ottawa (Ontario). Flight Research Lab.
THE NAE ATMOSPHERIC RESEARCH AIRCRAFT
J. I. MacPherson and S. W. Baillie *In* AGARD, The Flight of Flexible Aircraft in Turbulence: State-of-the-Art in the Description and Modelling of Atmospheric Turbulence Dec. 1987 19 p (For primary document see N88-29725 24-01)
Copyright Avail: NTIS HC A09/MF A01

07 AIRCRAFT PROPULSION AND POWER

Includes prime propulsion systems and systems components, e.g., gas turbine engines and compressors; and onboard auxilliary power plants for aircraft.

For related information see also *20 Spacecraft Propulsion and Power, 28 Propellants and Fuels,* and *44 Energy Production and Conversion.*

N88-29802# Societe Nationale d'Etude et de Construction de Moteurs d'Aviation, Paris (France).
EVALUATION OF THE ADVANCED AIR BREATHING PROPULSION CONCEPTS, EXECUTIVE SUMMARY

Paris, France ESA Sep. 1987 22 p Original contains color illustrations
(Contract ESA-6823/86-HEW(SC))
(ESA-CR(P)-2540; ETN-88-92765) Avail: NTIS HC A03/MF A01

Air breathing engine concepts to: operate from takeoff to low Earth orbit; provide a high level of specific impulse during air breathing operation; have a high thrust-to-weight ratio; generate a thrust in the range 500 to 1000 kN for the entire propulsion system; have a high thrust per unit of frontal area in the air breathing mode; have a high reliability; allow engine static test and rig test without complex and expensive flight simulation test facilities; and allow a reasonable confidence in performance prediction during the early design phase were assessed. Turborocket without and with inlet air cooler, ramrocket, and tuborocket-ramrocket were considered. The ramrocket is a simple engine. To extend air breathing propulsion beyond Mach 7, supersonic combustion must be evaluated. The use of a rocket for takeoff seems to be penalizing (Isp = 370s) but should be confirmed through a vehicle/engine integration system study. The turborocket-rocket is limited in Mach number below 5 to 6 in the air breathing mode. To extend it, an intake air cooler is necessary but looks very heavy. The turborocket-ramrocket represents a good compromise between ramjet and turborocket (performance/weight). The air breathing mode is limited to Mach 7 as for the ramjet. The extension of this mode is also related to the evaluation of supersonic combustion. ESA

N88-29803# Rolls-Royce Ltd., Derby (England).
V2500 ENGINE COLLABORATION
G. E. Kirk and M. Itoh 26 Oct. 1987 6 p Presented at the 1987 Tokyo International Gas Turbine Conference, Tokyo, Japan, 26-30 Oct. 1987
(PNR90423; ETN-88-92668) Copyright Avail: NTIS HC A02/MF A01

International collaboration in developing the V2500 gas turbine engine is described. The engine configuration and parts are outlined. Engineering management and communication are discussed. ESA

N88-29804*# United Technologies Corp., East Hartford, Conn.
THE EFFECTS OF INLET TURBULENCE AND ROTOR/STATOR INTERACTIONS ON THE AERODYNAMICS AND HEAT TRANSFER OF A LARGE-SCALE ROTATING TURBINE MODEL. VOLUME 2: HEAT TRANSFER DATA TABULATION. 15 PERCENT AXIAL SPACING Final Report
R. P. Dring, M. F. Blair, and H. D. Joslyn Washington, D.C. May 1986 242 p
(Contract NAS3-23717)
(NASA-CR-179467; NAS 1.26:179467; UTRC-R86-956480-Vol-2) Avail: NTIS HC A11/MF A01 CSCL 21E

A combined experimental and analytical program was conducted to examine the effects of inlet turbulence on airfoil heat transfer. The experimental portion of the study was conducted in a large-scale (approx 5X engine), ambient temperature, rotating turbine model configured in both single stage and stage-and-a-half arrangements. Heat transfer measurements were obtained using low-conductivity airfoils with miniature thermcouples welded to a thin, electrically heated surface skin. Heat transfer data were acquired for various combinations of low or high inlet turbulence intensity, flow coefficient, first-stator/rotor axial spacing, Reynolds number and relative circumferential position of the first and second stators. Aerodynamic measurements obtained as part of the program include distributions of the mean and fluctuating velocities at the turbine inlet and, for each airfoil row, midspan airfoil surface pressures and circumferential distributions of the downstream steady state pressures and fluctuating velocities. Analytical results include airfoil heat transfer predictions produced using existing 2-D boundary layer computation schemes and an examination of solutions of the unsteady boundary layer equations. The results are reported in four separate volumes, of which this is Volume 2: Heat Transfer Data Tabulation; 15 Percent Axial Spacing. Author

N88-29805# Minnesota Univ., Minneapolis. Dept. of Mechanical Engineering.
STUDIES OF GAS TURBINE HEAT TRANSFER AIRFOIL SURFACE AND END-WALL COOLING EFFECTS Annual Report, Mar. 1987 - Mar. 1988
E. R. Eckert, R. J. Goldstein, S. V. Patankar, and T. W. Simon Mar. 1988 58 p
(Contract F49620-85-C-0049)
(AD-A195165; A4-TR-88-0546) Avail: NTIS HC A04/MF A01 CSCL 20M

Research results on curved surface heat transfer, airfoil heat transfer, film cooling and end-wall heat transfer are presented. These studies focus on the recovery process of a turbulent boundary layer from curvature, heat transfer measurements and numerical prediction techniques of film-cooling on an adiabatic flat plate by injection through a single row of holes. GRA

N88-29806# Rolls-Royce Ltd., Bristol (England).
EVALUATION OF ADVANCED AIR BREATHING CONCEPTS. VOLUME 1: EXECUTIVE SUMMARY Final Report
H. Grallert and F. A. Hewitt Paris, France ESA 31 Jul. 1987 12 p Prepared in cooperation with Messerschmitt-Boelkow G.m.b.H., Munich, Fed. Republic of Germany
(Contract ESA-6822/86-F-HEW(SC))
(ESA-CR(P)-2539; ETN-88-92764) Avail: NTIS HC A03/MF A01

Air breathing propulsion concepts for winged, reuseable, space launch vehicles were evaluated. Turboramjet, precooled turbojet, ejector ramjet (or ram rocket)/ramjet, air-turborocket/ramjet, and hydrogen expansion engine/ramjet were considered. For single stage to orbit, a variable geometry ejector ramjet (or ram rocket)/ramjet is recommended; for two stages, a turboramjet with gas turbine core. However, the scoring and ranking scheme does not lead to a clear preference for just one propulsion concept for each vehicle. Two other concepts are nominated for consideration to ensure that major opportunities are not missed: precooled turbojet, and turboramjet (turborocket core). ESA

N88-29807*# National Aeronautics and Space Administration. Lewis Research Center, Cleveland, Ohio.
AEROELASTIC RESPONSE OF METALLIC AND COMPOSITE PROPFAN MODELS IN YAWED FLOW
Krishna Rao V. Kaza, Marc H. Williams, Oral Mehmed, and G. V. Narayanan (Sverdrup Technology, Inc., Cleveland, Ohio.) 1988 26 p Presented at the 24th Joint Propulsion Conference, Boston, Mass., 11-13 Jul. 1988; sponsored in part by AIAA, ASEE, ASME and SAE
(NASA-TM-100964; E-4229; NAS 1.15:100964; AIAA-88-3154)
Avail: NTIS HC A03/MF A01 CSCL 21E

An analytical investigation of aeroelastic response of metallic and composite propfan models in yawed flow was performed. The analytical model is based on the normal modes of a rotating blade and the three dimensional unsteady lifting surface aerodynamic theory including blade mistuning. The calculated blade stresses or strains are compared with published wind tunnel data on two metallic and three composite propfan wind tunnel models. The comparison shows a good agreement between theory and experiment. Additional parametric results indicate that blade response is very sensitive to the blade stiffness and also to blade frequency and mode shape mistuning. From these findings, it is concluded that both frequency and mode shape mistuning should be included in aeroelastic response analysis. Furthermore, both calculated and measured strains show that combined blade frequency and mode shape mistuning has beneficial effects on response due to yawed flow. Author

N88-29808# National Aerospace Lab., Amsterdam (Netherlands). Structures and Materials Div.
FAILURE ANALYSIS FOR GAS TURBINES
A. J. A. Mom 18 Apr. 1987 36 p In DUTCH; ENGLISH summary Presented at the Symposium van de Bond voor Materialenkennis Schade in Constructies voor Gebruik bij Hoge

Temperature, Wageningen, The Netherlands, 16 Oct. 1986
(NLR-MP-87037-U; B8803805; ETN-88-92612) Avail: NTIS HC A03/MF A01

A number of failures in gas turbines are discussed, including methods of preventing similar failures, in order to illustrate the diversity of failure analysis. The significance of failure analysis is explained, and the potential benefits of failure analysis for gas turbine users are mentioned. The background, reasons, and materials investigation of the F-16 crash in Lauwersmeer (Netherlands) are described. For the fracture of first-stage turbine blades of a jet motor, the damage analysis and the lifetime analysis are outlined. Damage due to crack formation in compressor drive shafts is treated. ESA

N88-29809# Rolls-Royce Ltd., Derby (England).
DEVELOPING THE ROLLS-ROYCE TAY
N. J. Wilson 30 Jun. 1988 14 p Presented at the 33rd ASME Gas Turbine Conference, Amsterdam, The Netherlands, Jun. 1988
(PNR90447; ETN-88-92680) Copyright Avail: NTIS HC A03/MF A01

The evolution of the Tay engine, launched in response to the requirement for an engine suitable for powering a FAR Part 36 Stage 3 noise compliant aircraft in the 70 to 100 seat range is reviewed. The engine, which is derived from the Spey (RB183) Mk 555 installed in the Fokker F28 aircraft, incorporates latest technology features which are already in service in large turbofan engines. Modularity and maintainability in the design of the engine are discussed in regard to operation in service. ESA

N88-29810# General Electric Co., Cincinnati, Ohio. Advanced Technology Operation.
EMPIRICAL FLUTTER PREDICTION METHOD Final Report, Sep. 1984 - Sep. 1987
J. K. Casey 5 Mar. 1988 358 p
(Contract F33615-84-C-2457)
(AD-A195699; R87AEG; AFWAL-TR-87-2087) Avail: NTIS HC A16/MF A01 CSCL 20D

Design of advanced technology engines is often limited by compressor blade instability or flutter. Test points from the annular cascade data base were analyzed, to predict from aeromechanical data which of 14 types of stability or instability would result. The basic approach was to identify for each pair of stability regions, linear combinations (hyperplanes) of the aeromechanical variables, whose numerical value would be above a critical level for all test points in one stability region and would be below the critical level for test points in the other stability region. It was found that 76 pct of the pairs of stability regions allowed a hyperplane to discriminate between the two regions, but for 24 pct a curved surface or nonlinear combination variables would be needed. Review of 85 pct of the 891 test points used to construct the hyperplanes revealed that the hyperplanes correctly identify the stability condition of 59 pct of the points in a literal sense, but are correct in a broader practical sense for 79 pct of the points. When the hyperplanes were applied to 51 validation test points taken from several actual engine/rig test data, they gave virtually no correct results, which was not immediately explainable. GRA

N88-29811*# Southwest Research Inst., San Antonio, Tex. Dept. of Materials Sciences.
CONSTITUTIVE MODELING FOR ISOTROPIC MATERIALS Final Report
K. S. Chan, U. S. Lindholm, and S. R. Bodner Jun. 1988 155 p
(Contract NAS3-23925; SwRI Proj. 06-7576)
(NASA-CR-182132; NAS 1.26:182132) Avail: NTIS HC A08/MF A01 CSCL 21E

The third and fourth years of a 4-year research program, part of the NASA HOST Program, are described. The program goals were: (1) to develop and validate unified constitutive models for isotropic materials, and (2) to demonstrate their usefulness for structural analysis of hot section components of gas turbine engines. The unified models selected for development and evaluation were those of Bodner-Partom and of Walker. The unified approach for elastic-viscoplastic constitutive equations is a viable method for representing and predicting material response characteristics in the range where strain rate and temperature dependent inelastic deformations are experienced. This conclusion is reached by extensive comparison of model calculations against the experimental results of a test program of two high temperature Ni-base alloys, B1900+Hf and Mar-M247, over a wide temperature range for a variety of deformation and thermal histories including uniaxial, multiaxial, and thermomechanical loading paths. The applicability of the Bodner-Partom and the Walker models for structural applications has been demonstrated by implementing these models into the MARC finite element code and by performing a number of analyses including thermomechanical histories on components of hot sections of gas turbine engines and benchmark notch tensile specimens. The results of the 4-year program have been published in four annual reports. The results of the base program are summarized in this report. The tasks covered include: (1) development of material test procedures, (2) thermal history effects, and (3) verification of the constitutive model for an alternative material. Author

N88-29812# Rockwell International Corp., Thousand Oaks, Calif. Science Center.
A NEW COMPUTATIONAL CAPABILITY FOR RAMJET PROJECTILES Final Report, May 1986 - Apr. 1987
S. R. Chakravarthy Sep. 1987 37 p
(Grant DAAA15-86-C-0053)
(AD-A196061; SC5462.FR; BRL-CR-595) Avail: NTIS HC A03/MF A01 CSCL 21B

A state-of-the-art computer code has been applied to calculate internal and external flows for a ramjet projectile under turbulent, supersonic conditions. A multizone computational approach was used, and its advantages are demonstrated. Two turbulence modeling approaches were tried: (1) the Baldwin-Lomax model applied throughout the flow field; and (2) the Baldwin-Lomax model applied outside the backflow regions and a dedicated algebraic k-epsilon backflow model applied within these regions. Comparisons with experimental data show a significant improvement in the code's predictional capability when the latter approach is used. GRA

N88-29813# Research Inst. of National Defence, Stockholm (Sweden).
REVIEW OF RESEARCH CONCERNING SOLID FUEL RAMJET (SOFRAM) AT THE RESEARCH INSTITUTE OF NATIONAL DEFENCE (FOA) 2
Ralf Eliasson May 1988 21 p In SWEDISH; ENGLISH summary
(FOA-C-20714-2.1; ISSN-0347-3694; ETN-88-93058) Avail: NTIS HC A03/MF A01

An airbreathing engine for velocities over Mach 1.8 is described. A tube-formed propellant of an outer diameter 72 mm was studied. Results show that to reach the optimum length of the motor it is necessary to use a propellant with a higher burning rate than HTPB. Ten different compositions of HTPB propellants were tested: 10 percent ammonium perchlorate increases combustion velocity by 40 percent, but a higher amount can lead to pressure vibrations in the combustion area; the addition of 5 percent lampblack reduces the velocity by 20 percent. Computed figures are given for artillery ammunition of 155 mm driven by SOFRAM. A secondary air intake (a by-pass) was also investigated. Stable combustion is achieved with 42 percent of the air by-passed, the mechanical output being 7 or 8 percent higher, but the combustion chamber must be modified to avoid vibrations. ESA

N88-29911# Pratt and Whitney Aircraft, West Palm Beach, Fla. Engineering Div.
FUEL PROPERTY EFFECTS ON THE US NAVY'S TF30 ENGINE
S. A. Mosier and P. A. Karpovich (Naval Air Propulsion Test Center, Trenton, N.J.) *In* AGARD, Combustion and Fuels in Gas Turbine

Engines Jun. 1988 15 p (For primary document see N88-29910 24-25)
Copyright Avail: NTIS HC A22/MF A01

08 AIRCRAFT STABILITY AND CONTROL

Includes aircraft handling qualities; piloting; flight controls; and autopilots.

For related information see also *05 Aircraft Design, Testing and Performance.*

N88-29814# Air Force Inst. of Tech., Wright-Patterson AFB, Ohio. School of Engineering.
AN ANALYSIS OF LATERAL-DIRECTIONAL HANDLING QUALITIES AND EIGENSTRUCTURE OF HIGH PERFORMANCE AIRCRAFT M.S. Thesis
Michael J. Costigan Jun. 1988 218 p
(AD-A194874; AFIT/GAE/AA/88J-1) Avail: NTIS HC A10/MF A01 CSCL 01A

The relationship between an aircraft's lateral-directional handling qualities and its corresponding eigenstructure is examined. Intuition and simple methematical models were used to develop desirable eigenvectors. For conventional aircraft, the dutch roll eigenvector was shown to a function of the roll to sideslip (phi/beta) ratio. Flight control laws to produce the desired eigenstructures were derived using eigenstructure assignment with output feedback. The control laws were based on a twelfth order linear model of the lateral-directional dynamics of the YA-7D DIGITAC, and varied the dutch roll phi/beta ratio. The handling qualities of the YA-7D were examined. The flight testing consisted of both open loop tasks, and closed loop tasks in which Cooper-Harper ratings were assigned. GRA

N88-29815*# Lockheed-Georgia Co., Marietta.
N-VERSION SOFTWARE DEMONSTRATION FOR DIGITAL FLIGHT CONTROLS Final Report
Dennis B. Mulcare and Lynn A. Barton Apr. 1987 152 p
(Contract NAS2-11853)
(NASA-CR-181483; NAS 1.26:181483; AD-A189864; DOT/FAA/CT-86/33) Avail: NTIS HC A08/MF A01 CSCL 01D

This report illustrates how four independently developed versions of digital flight controls applications software might be used in quadruplex system architecture. This approach to software fault tolerance is called N-version software. Here each computer channel has distinct versions of Ada programming units performing the same functions concurrently. Since intermediate software results are voted to detect and isolate discrepant computations, cross-channel synchronization occurs at each voting plane. The demonstration of this system was based on a high-level software design, English language specifications, and associated Ada program unit specifications parts. The demonstration was performed in non-realtime on a single VAX 8600 computer using an Ada multitasking test harness to effect voting plane synchronization and test case application and analyses. GRA

N88-29816*# Odetics, Inc., Anaheim, Calif.
THREAT EXPERT SYSTEM TECHNOLOGY ADVISOR
E. R. Kurrasch and L. R. Tripp Aug. 1987 101 p
(Contract NAS2-12558)
(NASA-CR-177479; NAS 1.26:177479) Avail: NTIS HC A06/MF A01 CSCL 01C

A prototype expert system was developed to determine the feasibility of using expert system technology to enhance the performance and survivability of helicopter pilots in a combat threat environment while flying NOE (Nap of the Earth) missions. The basis for the concept is the potential of using an Expert System Advisor to reduce the extreme overloading of the pilot who flies NOE mission below treetop level at approximately 40 knots while performing several other functions. The ultimate goal is to develop a Threat Expert System Advisor which provides threat information and advice that are better than even a highly experienced copilot. The results clearly show that the NOE pilot needs all the help in decision aiding and threat situation awareness that he can get. It clearly shows that heuristics are important and that an expert system for combat NOE helicopter missions can be of great help to the pilot in complex threat situations and in making decisions. Author

N88-29817*# Draper (Charles Stark) Lab., Inc., Cambridge, Mass.
DEVELOPMENT AND DEMONSTRATION OF AN ON-BOARD MISSION PLANNER FOR HELICOPTERS
Owen L. Deutsch and Mukund Desai May 1988 126 p
(Contract NAS2-12419)
(NASA-CR-177482; NAS 1.26:177482; CSDL-R-2056) Avail: NTIS HC A07/MF A01 CSCL 01C

Mission management tasks can be distributed within a planning hierarchy, where each level of the hierarchy addresses a scope of action, and associated time scale or planning horizon, and requirements for plan generation response time. The current work is focused on the far-field planning subproblem, with a scope and planning horizon encompassing the entire mission and with a response time required to be about two minutes. The far-feld planning problem is posed as a constrained optimization problem and algorithms and structural organizations are proposed for the solution. Algorithms are implemented in a developmental environment, and performance is assessed with respect to optimality and feasibility for the intended application and in comparison with alternative algorithms. This is done for the three major components of far-field planning: goal planning, waypoint path planning, and timeline management. It appears feasible to meet performance requirements on a 10 Mips flyable processor (dedicated to far-field planning) using a heuristically-guided simulated annealing technique for the goal planner, a modified A* search for the waypoint path planner, and a speed scheduling technique developed for this project. Author

N88-29818# Texas A&I Univ., Kingsville.
A FIBER OPTIC COLLECTIVE FLIGHT CONTROL SYSTEM FOR HELICOPTERS M.S. Thesis
Ellis Wayne Golson May 1988 62 p
(AD-A195406) Avail: NTIS HC A04/MF A01 CSCL 20F

The objective of this thesis is to design a fiber optic transmission system to replace the present collective flight control system for helicopters. A discussion of the present collective control system is presented as well as fiber optic system components necessary to provide positive collective control of the aircraft. Computer simulation has been utilized where possible to verify modulation and receiver circuitry. The fiber optic system provides advantages in weight, survivability, and cockpit organization. GRA

N88-29819*# Manudyne Systems, Inc., Los Altos, Calif.
MINIMUM-COMPLEXITY HELICOPTER SIMULATION MATH MODEL Final Contractor Report, Jul. 1985 - Jul. 1987
Robert K. Heffley and Marc A. Mnich Apr. 1988 102 p Prepared for Army Research and Technology Labs., Moffett Field, Calif.
(Contract NAS2-11665)
(NASA-CR-177476; NAS 1.26:177476; USAAVSCOM-TR-87-A-7)
Avail: NTIS HC A06/MF A01 CSCL 01C

An example of a minimal complexity simulation helicopter math model is presented. Motivating factors are the computational delays, cost, and inflexibility of the very sophisticated math models now in common use. A helicopter model form is given which addresses each of these factors and provides better engineering understanding of the specific handling qualities features which are apparent to the simulator pilot. The technical approach begins with specification of features which are to be modeled, followed by a build up of individual vehicle components and definition of equations. Model matching and estimation procedures are given which enable the modeling of specific helicopters from basic data sources such as flight manuals. Checkout procedures are given which provide for total model validation. A number of possible

model extensions and refinement are discussed. Math model computer programs are defined and listed. Author

N88-29718# Federal Aviation Administration, Seattle, Wash.
CURRENT AND PROPOSED GUST CRITERIA AND ANALYSIS METHODS: AN FAA OVERVIEW
Terence J. Barnes *In* AGARD, The Flight of Flexible Aircraft in Turbulence: State-of-the-Art in the Description and Modelling of Atmospheric Turbulence Jun. 1988 12 p (For primary document see N88-29717 24-01)
Copyright Avail: NTIS HC A06/MF A01

N88-29723# Office National d'Etudes et de Recherches Aeronautiques, Paris (France).
MEASURED AND PREDICTED RESPONSES OF THE NORD 260 AIRCRAFT TO THE LOW ALTITUDE ATMOSPHERIC TURBULENCE
J. L. Meurzec and F. Poirion *In* AGARD, The Flight of Flexible Aircraft in Turbulence: State-of-the-Art in the Description and Modelling of Atmospheric Turbulence Jun. 1988 9 p (For primary document see N88-29717 24-01)
Copyright Avail: NTIS HC A06/MF A01

N88-29724# Civil Aviation Authority, Redhill (England). Airworthiness Div.
A REVIEW OF MEASURED GUST RESPONSES IN THE LIGHT OF MODERN ANALYSIS METHODS
V. Card *In* AGARD, The Flight of Flexible Aircraft in Turbulence: State-of-the-Art in the Description and Modelling of Atmospheric Turbulence Jun. 1988 14 p (For primary document see N88-29717 24-01)
Copyright Avail: NTIS HC A06/MF A01

N88-29726*# National Aeronautics and Space Administration. Langley Research Center, Hampton, Va.
STATUS REVIEW OF ATMOSPHERE TURBULENCE AND AIRCRAFT RESPONSE
J. C. Houbolt *In* AGARD, The Flight of Flexible Aircraft in Turbulence: State-of-the-Art in the Description and Modelling at Atmospheric Turbulence Dec. 1987 11 p (For primary document see N88-29725 24-01)
Copyright Avail: NTIS HC A09/MF A01 CSCL 01C

N88-29729# Taylor (J.), Camberley (England).
AN INTERIM COMPARISON OF OPERATIONAL CG RECORDS IN TURBULENCE ON SMALL AND LARGE CIVIL AIRCRAFT
J. Taylor *In* AGARD, The Flight of Flexible Aircraft in Turbulence: State-of-the-Art in the Description and Modelling of Atmospheric Turbulence Dec. 1987 31 p (For primary document see N88-29725 24-01)
Copyright Avail: NTIS HC A09/MF A01

N88-29732# British Aerospace Aircraft Group, Weybridge (England). Military Aircraft Div.
RE-ASSESSMENT OF GUST STATISTICS USING CAADRP DATA
B. W. Payne, A. E. Dudman, and K. C. Griffiths *In* AGARD, The Flight of Flexible Aircraft in Turbulence: State-of-the-Art in the Description and Modelling of Atmospheric Turbulence Dec. 1987 22 p (For primary document see N88-29725 24-01)
Copyright Avail: NTIS HC A09/MF A01

09 RESEARCH AND SUPPORT FACILITIES (AIR)

Includes airports, hangars and runways; aircraft repair and overhaul facilities; wind tunnels; shock tubes; and aircraft engine test stands.

For related information see also *14 Ground Support Systems and Facilities (Space).*

N88-29820*# National Aeronautics and Space Administration. Langley Research Center, Hampton, Va.
COMPUTER PROGRAMS FOR CALCULATION OF STING PITCH AND ROLL ANGLES REQUIRED TO OBTAIN ANGLES OF ATTACK AND SIDESLIP ON WIND TUNNEL MODELS
John B. Peterson, Jr. Jul. 1988 47 p
(NASA-TM-100659; NAS 1.15:100659) Avail: NTIS HC A03/MF A01 CSCL 14B

Two programs have been developed to calculate the pitch and roll angles of a wind-tunnel sting drive system that will position a model at the desired angle of attack and and angle of sideslip in the wind tunnel. These programs account for the effects of sting offset angles, sting bending angles and wind-tunnel stream flow angles. In addition, the second program incorporates inputs from on-board accelerometers that measure model pitch and roll with respect to gravity. The programs are presented in the report and a description of the numerical operation of the programs with a definition of the variables used in the programs is given. Author

N88-29821*# Stanford Univ., Calif. Dept. of Aeronautics and Astronautics.
AN EXPERIMENTAL STUDY OF AN ADAPTIVE-WALL WIND TUNNEL
Zeki Celik and Leonard Roberts Aug. 1988 155 p
(Contract NCC2-77)
(NASA-CR-183152; NAS 1.26:183152; JIAA-TR-87) Avail: NTIS HC A08/MF A01 CSCL 14B

A series of adaptive wall ventilated wind tunnel experiments was carried out to demonstrate the feasibility of using the side wall pressure distribution as the flow variable for the assessment of compatibility with free air conditions. Iterative and one step convergence methods were applied using the streamwise velocity component, the side wall pressure distribution and the normal velocity component in order to investigate their relative merits. The advantage of using the side wall pressure as the flow variable is to reduce the data taking time which is one the major contributors to the total testing time. In ventilated adaptive wall wind tunnel testing, side wall pressure measurements require simple instrumentation as opposed to the Laser Doppler Velocimetry used to measure the velocity components. In ventilated adaptive wall tunnel testing, influence coefficients are required to determine the pressure corrections in the plenum compartment. Experiments were carried out to evaluate the influence coefficients from side wall pressure distributions, and from streamwise and normal velocity distributions at two control levels. Velocity measurements were made using a two component Laser Doppler Velocimeter system. Author

N88-29822# AeroVironment, Inc., Monrovia, Calif.
DEVELOPMENT AND DESIGN OF WINDTUNNEL AND TEST FACILITY FOR RPV (REMOTE PILOTED VEHICLE) ENHANCEMENT DEVICES Final Report, 15 Sep. 1987 - 15 Apr. 1988
Bart D. Hibbs, Herman M. Drees, and Peter B. Lissaman 15 Apr. 1988 59 p
(Contract DAAH01-87-C-1049; ARPA Order 5916)
(AD-A194842; AV-FR-88/807) Avail: NTIS HC A04/MF A01 CSCL 14B

Viscous drag represent a significant power demand on flight vehicles. Reductions of this requirement could result in higher speeds and altitudes, longer endurance and heavier payloads. General streamlining by shape control is highly developed so that the viscous drag of most vehicles consists mainly of turbulent

skin friction. Recent work in surface (riblets, etc.) and near-surface (vortex generator, etc.) devices has indicated that even this drag level can be further reduced by modifying the turbulent process near the surface. Drag reductions of about seven percent have been claimed for riblets and have been generally supported by various experiments. Engineering applications of these devices shows great potential, but to date have not been extensively pursued because of lack of definitive data. Remote Piloted Vehicles (RPV's) would benefit from these devices, but operate over a Reynolds number range such that much standard aeronautical research is inapplicable. A new facility is required to test and develop new devices appropriate for RPV's. This facility should be capable of testing, with and without pressure gradients, over the necessary range of scales and speeds with sufficient accuracy that engineering design decisions can be made about existing devices and improved, advanced units to be developed. A special purpose closed-return wind tunnel has been designed with a 26 foot long, 4 foot by 4 foot working cross-section driven by a 40 HP motor and operating at speeds up to 120 ft/sec. GRA

N88-29823# Air Force Inst. of Tech., Wright-Patterson AFB, Ohio.
CONTROLLED DEGRADATION OF RESOLUTION OF HIGH-QUALITY FLIGHT SIMULATOR IMAGES FOR TRAINING EFFECTIVENESS EVALUATION M.S. Thesis
Dennis D. Kaip 1988 66 p
(AD-A196189; AFIT/CI/NR-88-46) Avail: NTIS HC A04/MF A01 CSCL 05I

A flight simulator is a device used to train pilots and air crews without the use of an actual aircraft. The use of flight simulators for training is widespread in both the military and civilian sector. The use of flight simulators has significant advantages over the operation of the actual aircraft. In addition, pilots and air crews can practice complex and/or dangerous maneuvers in a flight simulator without risking loss of life or aircraft. As described by Schachter 6, sophisticated flight simulators recreate most of the aspects of flying: aircraft instruments, motion of the aircraft, gravitational forces, radar, and out-the-window views. Most modern flight simulators use computer generated imagery (CGI) to produce the out-the-window views in real-time in response to inputs from flight controls. The imagery can be displayed in a variety of ways: on large CRTs, projected onto the inside of a dome, or through helmet-mounted displays. Different training tasks are presumed to have different requirements with respect to brightness, contrast, and resolution. The goal for visual display flight training simulators in general, is not realism, but training effectiveness. Therefore, the design requirements for flight simulators should take into consideration the desired training task. GRA

N88-29824# Deutsche Forschungs- und Versuchsanstalt fuer Luft- und Raumfahrt, Goettingen (West Germany).
SUPERSONIC WALL ADAPTATION IN THE RUBBER TUBE TEST SECTION OF THE DFVLR GOETTINGEN
A. Hendergott, E. Stanewsky, and E. Wedemeyer Apr. 1987 15 p
(IB-222-87-A-08) Avail: NTIS HC A03/MF A01

Wind tunnel tests in the rubber tube test section have been performed in order to investigate the possibility of reducing supersonic wall interferences by adaptation of the rubber walls. Although the spacing of the jack positions is not sufficiently close for the supersonic wall adaptation, encouraging results were obtained for a cone-cylinder model. Author

N88-29825*# Southwest Research Inst., San Antonio, Tex.
SPRAY AUTOMATED BALANCING OF ROTORS: METHODS AND MATERIALS Final Report
Anthony J. Smalley, Richard M. Baldwin, and Wilbur R. Schick Aug. 1988 122 p
(Contract NAS3-25069; DA Proj. 1L1-62209-AH-76)
(NASA-CR-182151; NAS 1.26:182151; AVSCOM-TR-88-C-018)
Avail: NTIS HC A06/MF A01 CSCL 14B

The work described consists of two parts. In the first part, a survey is performed to assess the state of the art in rotor balancing technology as it applies to Army gas turbine engines and associated power transmission hardware. The second part evaluates thermal spray processes for balancing weight addition in an automated balancing procedure. The industry survey reveals that: (1) computerized balancing equipment is valuable to reduce errors, improve balance quality, and provide documentation; (2) slow-speed balancing is used exclusively, with no forseeable need for production high-speed balancing; (3) automated procedures are desired; and (4) thermal spray balancing is viewed with cautious optimism whereas laser balancing is viewed with concern for flight propulsion hardware. The FARE method (Fuel/Air Repetitive Explosion) was selected for experimental evaluation of bond strength and fatigue strength. Material combinations tested were tungsten carbide on stainless steel (17-4), Inconel 718 on Inconel 718, and Triballoy 800 on Inconel 718. Bond strengths were entirely adequate for use in balancing. Material combinations have been identified for use in hot and cold sections of an engine, with fatigue strengths equivalent to those for hand-ground materials. Author

N88-29826# Air Command and Staff Coll., Maxwell AFB, Ala.
LANTIRN SIMULATOR TRAINING IN THE F-16C
Michael L. Hauser Apr. 1988 51 p
(AD-A195201; ACSC-88-1175) Avail: NTIS HC A04/MF A01 CSCL 05F

The cover of darkness and weather have traditionally had a severe impact on the abilities of air forces to wage war. Although past conflicts have seen the limited use of air power at night and in the weather, the modern high threat battlefield has driven air power into the low altitude structure where night or poor weather operations are extremely hazardous. Modern, capable air defense weapons have given the enemy the ability to use darkness and poor weather as valuable counters to the great capabilities of modern fighter aircraft. The ability to move troops and supplies without danger of air attack is a tremendous advantage on the battlefield, requiring the United States to take steps to equip its fighter and attack aircraft with systems that will allow effective air operations in the low altitude environment at night or under the weather. One of these systems is LANTIRN, Low Altitude Navigation and Targeting Infrared System for Night. LANTIRN is designed to be used on the F-15E and F-16C. GRA

N88-29742# British Aerospace Public Ltd. Co., Preston (England).
THE ROLE OF SIMULATION IN FLYING QUALITIES AND FLIGHT CONTROL SYSTEM RELATED DEVELOPMENT
A. G. Barnes *In* AGARD, Advances in Flying Qualities May 1988 21 p (For primary document see N88-29735 24-01)
Copyright Avail: NTIS HC A09/MF A01

12 ASTRONAUTICS (GENERAL)

For extraterrestrial exploration see *91 Lunar and Planetary Exploration.*

N88-29827# Erno Raumfahrttechnik G.m.b.H., Bremen (West Germany).
STUDY ON LONG-TERM EVOLUTION TOWARDS EUROPEAN MANNED SPACEFLIGHT. VOLUME 1: EXECUTIVE SUMMARY Final Report
J. Ewald, ed., L. Basile, R. Longstaff, and C. Cougnet (MATRA Espace, Toulouse, France) Paris, France ESA Mar. 1988 51 p
(Contract ESA-6669/86-NL-PP(SC))
(ERNO-OX1-002/88-Vol-1; ESA-CR(P)-2627-Vol-1; ETN-88-92799)
Avail: NTIS HC A04/MF A01

Safety aspects of a manned European space station were studied. An escape vehicle, a habitation module, and interconnecting elements were examined. Crew sizing analysis was performed. Orbital parameters were analyzed. ESA

N88-29828# European Space Agency, Paris (France).
BEYOND THE VISIBLE: A DECADE OF OBSERVATIONS WITH THE INTERNATIONAL ULTRAVIOLET EXPLORER (IUE)
Norman Longdon, ed. Apr. 1988 24 p Original contains color illustrations
(ESA-F09; ISSN-1010-5301; ETN-88-93048) Copyright Avail: NTIS HC A03/MF A01

The IUE spacecraft, its mission, and instrumentation are presented. Studies of novae and supernovae (particularly SN 1987A), the solar system, interacting binaries, and hot stars are described. ESA

13 ASTRODYNAMICS

Includes powered and free-flight trajectories; and orbital and launching dynamics.

N88-29829# Air Force Inst. of Tech., Wright-Patterson AFB, Ohio. School of Engineering.
INVESTIGATION OF THE VALIDITY OF THE NON-ROTATING PLANET ASSUMPTION FOR THREE-DIMENSIONAL EARTH ATMOSPHERIC ENTRY M.S. Thesis
Harry A. Karasopoulos Jun. 1988 222 p
(AD-A194877; AFIT/GA/AA/88J-1) Avail: NTIS HC A10/MF A01 CSCL 22C

The assumption of a non-rotating planet, common in most analytical entry trajectory analyses, has been shown to produce significant errors in some solutions for the lifting atmospheric entry to the earth. This thesis investigates the validity of the non-rotating planet assumption for general three-dimensional Earth atmospheric entry. First, the three-dimensional equations of motion for lifting atmospheric entry are expanded to include a rotating planet model. A strictly exponential atmosphere, rotating at the same rate as the planet, is assumed with density as a function of radial distance from the planet's surface. Solutions are developed for the non-rotating Earth equations of motion and for one of the rotating Earth equations of motion using the method of matched asymptotic expansions. It is shown that the non-rotating Earth assumption produces incorrect entry trajectory results for entry orbital inclination angles between 0.5 and 75.0 deg and vehicle speeds ranging from circular orbital velocities to low supersonic speeds. However, a variety of realistic trajectory states exist where some of the non-rotating Earth equations of motion are found to be valid for the same entry trajectory states. GRA

N88-29830# Naval Postgraduate School, Monterey, Calif.
A STANDARD LIBRARY FOR MODELING SATELLITE ORBITS ON A MICROCOMPUTER M.S. Thesis
Kenneth L. Beutel Mar. 1988 239 p
(AD-A195759) Avail: NTIS HC A11/MF A01 CSCL 12E

Introductory students of astrodynamics and the space environment are required to have a fundamental understanding of the kinematic behavior of satellite orbits. This thesis develops a standard library that contains the basic formulas for modeling earth orbiting satellites. This library is used as a basis for implementing a satellite motion simulator that can be used to demonstrate orbital phenomena in the classroom. Surveyed are the equations of orbital elements, coordinate systems and analytic formulas, which are made into a standard method for modeling earth orbiting satellites. The standard library is written in the C programming language and is designed to be highly portable between a variety of computer environments. The simulation draws heavily on the standards established by the library to produce a graphics-based orbit simulation program written for the Apple Macintosh computer. The simulation demonstrates the utility of the standard library functions but, because of its extensive use of the Macintosh user interface, is not portable to other operating systems. GRA

N88-29831# Centre National d'Etudes Spatiales, Toulouse (France).
SPECIFICATIONS AND PERFORMANCE OF ULTRASTABLE OSCILLATORS IN THE DORIS ORBITOGRAPHY AND POSITIONING SYSTEM
J. B. Laporte 1988 20 p Presented at the 2nd European Frequency and Time Forum, Neuchatel, Switzerland, 16-18 Mar. 1988
(ETN-88-92761) Avail: NTIS HC A03/MF A01

A space project whose objective is the precise determination of satellite positions and accurate location of beacons on the ground (project DORIS) for TOPEX is outlined. Ultrastable oscillators used in onboard and ground equipment are assessed. The QAS and BVA technologies in quartz improve short and long-term performance. However, the gains achieved are offset by effects of the environment, particularly temperature, magnetism, and pressure. ESA

N88-30501# Joint Publications Research Service, Arlington, Va.
RELATIONSHIP BETWEEN CHARACTERISTICS OF LOW-ENERGY ELECTRONS AND GEOMAGNETIC DISTURBANCE IN GEOSTATIONARY ORBIT Abstract Only
O. S. Grafodatskiy, V. I. Degtyarev, A. G. Kozlov, V. I. Lazarev, O. I. Platonov, G. V. Popov, and M. V. Teltsov *In its* JPRS Report: Science and Technology. USSR: Space 26 Feb. 1988 p 12-13 Transl. into ENGLISH from Geomagnetizm i Aeronomiya (Moscow, USSR), v. 27, no. 3, May - Jun. 1987 p 494-496 (For primary document see N88-30498 24-88)
Avail: NTIS HC A04/MF A01

N88-30506# Joint Publications Research Service, Arlington, Va.
ORBITAL EVOLUTION OF DISTANT ARTIFICIAL EARTH SATELLITES Abstract Only
M. A. Vashkovyak *In its* JPRS Report: Science and Technology. USSR: Space 26 Feb. 1988 p 14-15 Transl. into ENGLISH from Kosmicheskiye Issledovaniya (Moscow, USSR), v. 25, no. 3, May - Jun. 1987 p 339-355 (For primary document see N88-30498 24-88)
Avail: NTIS HC A04/MF A01

N88-30508# Joint Publications Research Service, Arlington, Va.
FAMILIES OF PERIODIC SOLUTIONS IN PROBLEM OF SOLID BODY ROTATION AT TRIANGULAR LIBRATION POINT IN RESTRICTED THREE-BODY PROBLEM Abstract Only
S. N. Lelyavin *In its* JPRS Report: Science and Technology. USSR: Space 26 Feb. 1988 p 15 Transl. into ENGLISH from Kosmicheskiye Issledovaniya (Moscow, USSR), v. 25, no. 3, May - Jun. 1987 p 362-369 (For primary document see N88-30498 24-88)
Avail: NTIS HC A04/MF A01

N88-30510# Joint Publications Research Service, Arlington, Va.
RESONANCE EFFECTS ACCOMPANYING MOTION WITH LOW THRUST IN EARTH-MOON SYSTEM Abstract Only
A. Yu. Kogan and V. A. Kotin *In its* JPRS Report: Science and Technology. USSR: Space 26 Feb. 1988 p 16 Transl. into ENGLISH from Kosmicheskiye Issledovaniya (Moscow, USSR), v. 25, no. 3, May - Jun. 1987 p 374-383 (For primary document see N88-30498 24-88)
Avail: NTIS HC A04/MF A01

N88-30511# Joint Publications Research Service, Arlington, Va.
INCREASING ACCURACY IN EVALUATING VECTOR OF STATE UNDER CONDITIONS OF INCOMPLETE OBSERVABILITY OF EXPANDED SYSTEM Abstract Only
M. P. Igonin and A. L. Katkov *In its* JPRS Report: Science and Technology. USSR: Space 26 Feb. 1988 p 16 Transl. into ENGLISH from Kosmicheskiye Issledovaniya (Moscow, USSR), v. 25, no. 3, May - Jun. 1987 p 384-392 Original language document was announced in IAA as A87-47556 (For primary document see N88-30498 24-88)
Avail: NTIS HC A04/MF A01

N88-30512# Joint Publications Research Service, Arlington, Va.
CANONICAL VARIABLES AND CANONICAL INTEGRALS FOR MOTION IN NEAR-CIRCULAR ORBITS Abstract Only
A. B. Nayshul *In its* JPRS Report: Science and Technology. USSR: Space 26 Feb. 1988 p 16-17 Transl. into ENGLISH from Kosmicheskiye Issledovaniya (Moscow, USSR), v. 25, no. 3, May - Jun. 1987 p 393-399 Original language document was announced in IAA as A87-47557 (For primary document see N88-30498 24-88)
Avail: NTIS HC A04/MF A01

14 GROUND SUPPORT SYSTEMS AND FACILITIES (SPACE)

Includes launch complexes, research and production facilities; ground support equipment, e.g., mobile transporters; and simulators.

For related information see also *09 Research and Support Facilities (Air).*

N88-29832*# National Aeronautics and Space Administration. Marshall Space Flight Center, Huntsville, Ala.
NASA MARSHALL SPACE FLIGHT CENTER SOLAR OBSERVATORY Report, Jan. - Mar. 1988
James E. Smith Aug. 1988 82 p
(NASA-TM-100339; NAS 1.15:100339) Avail: NTIS HC A05/MF A01 CSCL 14B

A description is provided of the NASA Marshall Space Flight Center's Solar Vector Magnetograph Facility and a summary is given of its observations and data reduction during Jan. to Mar. 1988. The systems that make up the facility are a magnetograph telescope, an H-alpha telescope, a Questar telescope, and a computer center. The data are represented by longitudinal contours with azimuth plots. Author

15 LAUNCH VEHICLES AND SPACE VEHICLES

Includes boosters; operating problems of launch/space vehicle systems; and reusable vehicles.

For related information see also *20 Spacecraft Propulsion and Power.*

N88-29833*# National Aeronautics and Space Administration. Lewis Research Center, Cleveland, Ohio.
THE EFFECT OF THE NEAR EARTH MICROMETEOROID ENVIRONMENT ON A HIGHLY REFLECTIVE MIRROR SURFACE
Michael J. Mirtich, Herman Mark, and William R. Kerslake 1988 40 p Presented at the 26th Aerospace Sciences Meeting, Reno, Nev., 11-14 Jan. 1988; sponsored by AIAA
(NASA-TM-101307; E-4233; NAS 1.15:101307) Avail: NTIS HC A03/MF A01 CSCL 22B

A resurgence of interest in placing large solar concentrator solar dynamic systems in space for power generation has brought up again a concern for maintaining the integrity of the optical properties of highly specular reflecting surfaces in the near earth space environment. One of the environmental hazards needing evaluation is the micrometeoroid environment. It has been shown that highly reflective polished metals and thin film coatings degrade when exposed to simulated micrometeoroids in the lab. At NASA-Lewis, a shock tube was used to simulate the phenomenon of micrometeoroid impact by accelerating micron sized particles to hypervelocities. Any changes in the optical properties of surfaces exposed to this impact were then evaluated. The degradation of optical properties of polished metals and thin metallic films after exposure to simulated micrometeoroids was determined as a function of impacting kinetic energy area of the particles. A calibrated sensor was developed to not only detect the micrometeoroid environment, but also to evaluate the degradation of the optical properties of thin aluminum films in space. Results of the simulation are presented and discussed. Author

N88-29834# Air Command and Staff Coll., Maxwell AFB, Ala.
REDUCED FLEXIBILITY IN PROCESSING TITAN 4 SPACE LAUNCH VEHICLES AT CAPE CANAVERAL AIR FORCE STATION
Michael G. Woolley Apr. 1988 50 p
(AD-A194908; ACSC-88-2805) Avail: NTIS HC A03/MF A01 CSCL 22D

In the recent past DOD has made decisions which reduced the flexibility in processing Titan expendable launch vehicles. This study explores the history of those decisions and their effects. It identifies the throughput capacities of Titan 4 Processing facilities. It evaluates the Cape's ability to meet the Titan 4 Mission Model. The study concludes that the mission model can not be achieved by doing business as usual. Changes must be made to the work schedules (double shifts, extended work weeks, etc.) and more technicians are required. The study recommends several facility modifications which can reestablish the flexibility in processing Titan 4 vehicles for launch. It also suggests further studies which may be useful in this area. GRA

N88-29835*# General Dynamics Corp., San Diego, Calif.
CENTAUR OPERATIONS AT THE SPACE STATION: COST AND TRANSPORTATION ANALYSIS Final Report
10 Aug. 1988 241 p
(Contract NAS3-24900)
(NASA-CR-182128; NAS 1.26:182128; GDSS-SP-88-006) Avail: NTIS HC A11/MF A01 CSCL 22B

A study was conducted to expand on the results of an initial study entitled Centaur Operations at the Space Station. The previous study developed technology demonstration missions (TDMs) that utilized the Centaur G-prime upper stage to advance OTV technologies required for accomodations and operations at the Space Station. An initial evaluation was performed of the cost to NASA for TDM implementation. Due to the potential for commercial communication satellite operation utilizing the TDM hardware, an evaluation of the Centaur's transportation potential was also performed. Author

16 SPACE TRANSPORTATION

Includes passenger and cargo space transportation, e.g., shuttle operations; and space rescue techniques.

For related information see also *03 Air Transportation and Safety* and *18 Spacecraft Design, Testing and Performance.* For space suits see *54 Man/System Technology and Life Support.*

N88-29836*# Eagle Engineering, Inc., Houston, Tex.
SPACECRAFT MASS ESTIMATION, RELATIONSHIPS AND ENGINE DATA: TASK 1.1 OF THE LUNAR BASE SYSTEMS STUDY Report, Oct. 1987 - May 1988
6 Apr. 1988 85 p
(Contracts NAS9-17878; TO-87-57)
(NASA-CR-172061; NAS 1.26:172061; EEI-87-171) Avail: NTIS HC A05/MF A01 CSCL 22B

A collection of scaling equations, weight statements, scaling factors, etc., useful for doing conceptual designs of spacecraft are given. Rules of thumb and methods of calculating quantities of interest are provided. Basic relationships for conventional, and several non-conventional, propulsion systems (nuclear, solar electric and solar thermal) are included. The equations and other data were taken from a number of sources and are not at all consistent with each other in level of detail or method, but provide useful references for early estimation purposes. Author

N88-29837*# Eagle Engineering, Inc., Houston, Tex.
MAINTENANCE AND SUPPLY OPTIONS
May 1988 59 p

(Contract NAS9-17878)
(NASA-CR-172062; NAS 1.26:172062; EEI-87-173) Avail: NTIS HC A04/MF A01 CSCL 22B

The object of the Maintenance and Supply Option was to develop a high level operational philosophy related to maintenance and supply operations and incorporate these concepts into the Lunar Base Study. Specific products to be generated during this task were three trade studies and a conceptual design of the Logistic Supply Module. The crew size study was performed to evaluate crew sizes from the baseline size of four to a crew size of eight and determine the preferred crew size. The second trade study was to determine the impact of extending surface stay times and recommend a preferred duration of stay time as a function of crew, consumables, and equipment support capabilities. The third trade study was an evaluation of packaging and storage methods to determine the preferred logistics approach to support the lunar base. A modified scenario was developed and served as the basis of the individual trade studies. Assumptions and guidelines were also developed from experience with Apollo programs, Space Shuttle operations, and Space Station studies. With this information, the trade studies were performed and a conceptual design for the Logistic Supply Module was developed. Author

17 SPACE COMM., SPACECRAFT COMM., COMMAND & TRACKING

Includes telemetry; space communications networks; astronavigation and guidance; and radio blackout.

For related information see also *04 Aircraft Communications and Navigation* and *32 Communications and Radar.*

N88-30345*# Jet Propulsion Lab., California Inst. of Tech., Pasadena.
MISSION TELEMETRY SYSTEM MONITOR: A REAL-TIME KNOWLEDGE-BASED SYSTEM
Samih A. Mouneimne *In* NASA, Goddard Space Flight Center, The 1988 Goddard Conference on Space Applications of Artificial Intelligence Aug. 1988 p 207-212 (For primary document see N88-30330 24-63)
Avail: NTIS HC A19/MF A01 CSCL 09B

18 SPACECRAFT DESIGN, TESTING AND PERFORMANCE

Includes satellites; space platforms; space stations; spacecraft systems and components such as thermal and environmental controls; and attitude controls.

For life support systems see *54 Man/System Technology and Life Support.* For related information see also *05 Aircraft Design, Testing and Performance, 39 Structural Mechanics,* and *16 Space Transportation.*

N88-29838# National Aerospace Lab., Amsterdam (Netherlands). Space Div.
ERS-1: A SATELLITE WITH AN OCEANOGRAPHIC MISSION
R. W. vanSwol Jul. 1986 17 p In DUTCH; ENGLISH summary Submitted for publication
(NLR-MP-86072-U; B8803806; ETN-88-92606) Avail: NTIS HC A03/MF A01

The ERS-1 program of ESA is outlined. The objectives of the ERS-1 mission and the satellite capabilities are summarized. The payload and orbit characteristics are described, including active microwave instrumentation, radar altimeter, along-track scanning radiometer/microwave sounder, precise range and range rate equipment, and laser retroreflectors. The ground segment and the concept chosen in order to meet the important requirement that data are to be delivered to the users within 3 hr are discussed. ESA

N88-29839# Erno Raumfahrttechnik G.m.b.H., Bremen (West Germany).
STUDY OF ROBOTICS SPACECRAFT SERVICING AND ASSEMBLY IN SPACE. VOLUME 1: EXECUTIVE SUMMARY Final Report
Paris, France ESA Feb. 1988 94 p Prepared in cooperation with Sener S.A., Madrid, Spain; Aeritalia S.p.A., Turin, Italy; Fraunhofer Inst. fuer Productionstechnik und Konstruktionstechnik, Berlin, Fed. Republic of Germany and Spar Aerospace Ltd., Ste-Anne-de-Bellevue, Quebec
(Contract ESA-6837/86-NL-PP(SC))
(ESA-CR(P)-2612-Vol-1; ETN-88-93147) Copyright Avail: NTIS HC A05/MF A01

The robotics, servicing, and assembly requirements of a microgravity mission and an orbital assembly mission were defined. The microgravity mission is based on the Man-Tended Free Flyer (MTFF) enhanced by additional elements, like an airlock, a multiberthing node, and an unpressurized payload area. The in-orbit assembly mission deals with the buildup of this enhanced version of the MTFF towards a European autonomous Space Station. For the micro-g mission the central transportation robot and a rack-dedicated manipulator are outlined as elements of an overall automation concept for the MTFF operation, while the in-orbit assembly mission identifies a moveable assembly manipulator for handling of modules and large structures. ESA

N88-29840# MATRA Espace, Toulouse (France).
PSDE/SAT 2: PRELIMINARY SPACECRAFT CONFIGURATION STUDY, EXECUTIVE SUMMARY
Paris, France ESA 1988 42 p Prepared in cooperation with British Aerospace Ltd, Bristol, England and ANT Nachrichtentechnik, Backnang, Fed. Republic of Germany
(Contract ESA-7190/87)
(ESA-CR(P)-2618; ETN-88-93041) Avail: NTIS HC A03/MF A01

The objectives, candidate payloads, system outputs, platform subsystems, launch, transfer, on-station control, system budgets, and development plan for the SAT 2 communications satellite are summarized. The platform is derived from the Eurostar concept and is designed for data relay, radionavigation and communication, and technology experiment payloads. ESA

N88-29841# Societe Nationale Industrielle Aerospatiale, Cannes (France). Etude Systemes Satellites.
STUDY ON CONCEPTUAL DESIGN OF SPACECRAFT USING COMPUTER AIDED ENGINEERING (CAE)
Paris, France ESA 1988 114 p
(Contract ESA-6885/86)
(SNIAS-920-CA/TS; ESA-CR(P)-2565; ETN-88-93016) Copyright Avail: NTIS HC A06/MF A01

The utility of computer techniques for design of ESA spececraft was assessed. It is concluded that spacecraft design cannot be automated, but could be facilitated by an Assistant Designer Expert System (ADES). Human and sociological issues should not be overlooked if such a project is undertaken: early determination of precise users is a necessary step for a successful introduction of design expert systems. A stepwise approach is recommended, with a first block of the ADES project on a subject to be chosen by ESA. This subject should possess a stable and limited domain knowledge; existing and recognized expertise; interested future users; combinatorial complexity with mixed numeric and symbolic decisions to be made; and choices should be made on the project hardware and software that take into account performance, availability, and possible specific modifications. ESA

N88-29842# Air Command and Staff Coll., Maxwell AFB, Ala.
SENSOR AND ACTUATOR SELECTION FOR LARGE SPACE STRUCTURE CONTROL
Michael L. Delorenzo Apr. 1988 41 p
(AD-A194912; ACSC-88-0725) Avail: NTIS HC A03/MF A01 CSCL 22B

This paper presents an algorithm which aids the controls engineer in specifying a sensor and actuator configuration for

regulation of large scale, linear, stochastic systems such as a Large Space Structure (LSS). The algorithm uses a Linear Quadratic Gaussian (LQG) controller, an efficient weight selection technique based upon successive approximation, and a measure of sensor and actuator effectiveness to provide a final sensor and actuator configuration. This configuration enables the closed-loop system to meet output specifications with minimal input power. The algorithm involves no complex gradient calculations and has proven numerically tractable for large linear models. Additionally, the algorithm provides the controls engineer information on the important design issues of actuator sizing, reliability, redundancy, and optimal number. GRA

N88-29843# Northeastern Univ., Boston, Mass. Electronics Research Lab.
AEROSPACE PAYLOAD SUPPORT SYSTEMS Final Report, 16 Feb. 1981 - 5 May 1987
Richard L. Morin and Lawrence J. OConnor Jul. 1987 69 p
(Contract F19628-81-C-0029; AF Proj. 7659)
(AFGL-TR-87-0241) Avail: NTIS HC A04/MF A01 CSCL 22B

An engineering support system developed for sounding rocket and shuttle payloads is described. Efforts include the mechanical and electrical design, fabrication, integration, testing and launch support of a variety of payloads and related ground support equipment. Specific work areas include: payload structures, component packaging, deployment and eject mechanisms, diagnostic instrumentation, inflight sequencing, power systems and control consoles. Author

N88-29844# Institut fuer Raumfahrtelektronik, Berlin (West Germany).
LOW COST SATELLITE
Udo Renner Paris, France ESA 10 Dec. 1987 97 p
(Contract ESTEC-7153/87-NL-DG)
(ESA-CR(P)-2560; ETN-88-93014) Avail: NTIS HC A05/MF A01

The feasibility of using a low cost design approach for satellite navigation missions was examined, including the analysis of a small cost-effective satellite bus for highly elliptical Earth orbits. Since satellite-based navigation systems require many satellites, the use of low-cost spacecraft in such systems results in considerable cost savings, and improves the overall system feasibility. Ariane, H1, Delta 6925, and AMROC launch; gravity gradient, dual spin, and three axis; launch and orbit strategy; attach fitting; attitude and orbit control; reaction control; and thermal control are considered. ESA

N88-29845*# National Aeronautics and Space Administration. Lewis Research Center, Cleveland, Ohio.
TECHNOLOGY REQUIREMENTS FOR AN ORBITING FUEL DEPOT: A NECESSARY ELEMENT OF A SPACE INFRASTRUCTURE
R. M. Stubbs, R. R. Corban, and A. J. Willoughby (Analex Corp., Cleveland, Ohio.) 1988 10 p Presented at the 39th Annual Astronautical Congress of the International Astronautical Federation, Bangalore, India, 8-15 Oct. 1988
(NASA-TM-101370; E-4414; NAS 1.15:101370) Avail: NTIS HC A02/MF A01 CSCL 22B

Advanced planning within NASA has identified several bold space exploration initiatives. The successful implementation of these missions will require a supporting space infrastructure which would include a fuel depot, an orbiting facility to store, transfer and process large quantities of cryogenic fluids. In order to adequately plan the technology development programs required to enable the construction and operation of a fuel depot, a multidisciplinary workshop was convened to assess critical technologies and their state of maturity. Since technology requirements depend strongly on the depot design assumptions, several depot concepts are presented with their effect on criticality ratings. Over 70 depot-related technology areas are addressed. Author

N88-29846*# Draper (Charles Stark) Lab., Inc., Cambridge, Mass.
ASCENT GUIDANCE FOR A WINGED BOOST VEHICLE M.S. Thesis
Michael Alexander Corvin Aug. 1988 110 p
(Contract NAS9-17560)
(NASA-CR-172083; NAS 1.26:172083; CSDL-T-1002) Avail: NTIS HC A06/MF A01 CSCL 22B

The objective of the advanced ascent guidance study was to investigate guidance concepts which could contribute to increased autonomy during ascent operations in a winged boost vehicle such as the proposed Shuttle II. The guidance scheme was required to yield near a full-optimal ascent in the presence of vehicle system and environmental dispersions. The study included consideration of trajectory shaping issues, trajectory design, closed loop and predictive adaptive guidance techniques and control of dynamic pressure by throttling. An extensive ascent vehicle simulation capability was developed for use in the study. Author

N88-29847# MATRA Espace, Toulouse (France).
STUDY OF THE ASSEMBLY, INTEGRATION AND VERIFICATION PROGRAMS OF TELECOMMUNICATION SATELLITES APPLICABLE TO OTHER SATELLITE PROGRAMS Final Report [ETUDE DES PROGRAMMES D'ASSEMBLAGE, D'INTEGRATION ET DE VERIFICATION DE SATELLITES DE TELECOMMUNICATIONS APPLICABLES A D'AUTRES PROGRAMMES DE SATELLITES]
F. Perrenot, J. P. Vechambre, and C. Chanoine Paris, France ESA 8 Dec. 1987 100 p In FRENCH
(Contract ESTEC-6598/86-NL-MA(SC))
(Matra-100/CC/MLG/031/87; ESA-CR(P)-2593; ETN-88-93032)
Copyright Avail: NTIS HC A05/MF A01

Experience gained in the assembly, integration, and verification (AIV) phases of the ECS program on the ground and in orbit was analyzed to optimize the techniques, planning, and costs of future satellite programs. The actual AIV processes were compared with plans and incidents/failures occurring on the ground and in orbit were examined. The results of the analyses were used to derive recommendations as to testing, quality and product assurance, design and manufacture, and ground mechanical and electrical facilities. ESA

N88-29848*# Alabama Univ., Huntsville. Dept. of Mechanical Engineering.
COORDINATED STUDY OF SOLAR-TERRESTRIAL OBSERVATORY (STO) PAYLOADS ON SPACE STATION Report, 10 Jul. 1984 - 15 Jul. 1988
S. T. Wu Jul. 1988 65 p
(Grant NAG8-488)
(NASA-CR-183142; NAS 1.26:183142) Avail: NTIS HC A04/MF A01 CSCL 22B

Since the publication of the final report of the science study group in October 1984 on the Solar Terrestrial Observatory (STO), its science goals and objectives have been clearly defined and a conceptual design and analysis was carried out by MSFC/NASA. Plans for the possible placing of the STO aboard the Space Station were made. A series of meetings for the STO science study group were held to review the instruments to be placed on the initial STO at Space Station IOC, and the placement of these instruments on the manned space station, polar platform, and the co-orbiting platform. A summary of these initial STO instruments is presented in Section 2. A brief description of the initial plan for the placement of STO instruments is included in Section 3. Finally, in Section 4, the scenario for the operation of the STO is discussed. These results were obtained from the report of the Solar Terrestrial Observatory mini-workshop held at MSFC on 6 June 1985. F.M.R.

N88-29849# Societe Nationale Industrielle Aerospatiale, Les Mureaux (France).
INTERIM FLIGHT OPPORTUNITY (IFO). VOLUME 1: EXECUTIVE SUMMARY Final Report
M. H. Aenishanslin Paris, France ESA 16 Dec. 1987 65 p

Prepared in cooperation with Construcciones Aeronauticas S.A., Madrid, Spain, Saab Space A.B., Goeteborg, Sweden, Erno Raumfahrttechnik G.m.b.H., Bremen, West Germany, Norsk Forsvarsteknologi A/S, Norway, Sener S.A., Madrid, Spain, and Fokker B.V.
(Contract ESA-6272/85-NL-AB)
(SE/LS/AP-36-818/CN-Vol-1; ESA-CR(P)-2583-Vol-1; COL-TN-AS-0059-Vol-1; ETN-88-93028) Avail: NTIS HC A04/MF A01

A space platform for a wide variety of missions prior to Columbus space station availability is proposed. It can be launched as spare capacity or as main payload on different launchers into a variety of orbits, where it circles for a limited time and then a subset or the whole reenters in a controlled way for recovery on ground. The general configuration is composed of two separable elements: an expendable part, the bus, and a reentry vehicle (REV). Maximum diameter for the bus is 2 m to have an easy and feasible accommodation on a wide variety of launchers. The REV is dimensioned to be able to provide a payload dedicated volume greater than 0.2 cum and the global mass of the platform is not greater than 1500 kg. The BUS is conceived for two alternatives: a battery powered baseline for a ten-day mission, and an option with solar arrays for a 1-month mission. Subsystems are: structure, thermal control, electrical power, attitude control, data handling, communication, and mechanisms. The REV is composed of separable units: a propulsion module and a reentry capsule. The subsystem list is similar to the bus with propulsion and recovery systems added. ESA

N88-29850*# National Aeronautics and Space Administration. Langley Research Center, Hampton, Va.
SPACE STRUCTURE (DYNAMICS AND CONTROL) THEME DEVELOPMENT
Richard A. Russell and Richard M. Gates (Boeing Aerospace Co., Seattle, Wash.) Aug. 1988 32 p
(NASA-TM-100597; NAS 1.15:100597) Avail: NTIS HC A03/MF A01 CSCL 22B

A study was made to define the long-range technical objectives and goals for the Space Structure (Dynamics and Control) theme area. The approach was to evaluate ongoing and proposed technology activities such that the technology gaps and voids could be identified. After the technology needs were identified, a set of recommended experimental activities was defined including the technical objectives of each and their relationship. Author

N88-29851# California Univ., Los Angeles.
THEORY OF FILTERING AND CONTROL WITH APPLICATION TO CONTROL OF LARGE SPACE STRUCTURES Final Report, 1 Sep. 1983 - 31 Aug. 1987
A. V. Balakrishnan 30 Mar. 1988 8 p
(Grant AF-AFOSR-0318-83)
(AD-A195500; AFOSR-88-0666TR) Avail: NTIS HC A02/MF A01 CSCL 22B

This report summarizes accomplishments under a grant to study modeling. Identification, and control of flexible structures and to study random fields with applications to laser beam distortion in a turbulent field. Research in flexible structures focused on deriving continuum models base upon partial differential equations and derived methods for the solution of the resulting boundary control problems. A robust controller for stabilization based upon the abstract Hilbert-space semigroup formulation was derived as was a stochastic control theory for partial differential equations. A white noise theory for random fields was derived which has applications to laser beam propagation in the atmosphere; in particular, it is used to model the turbulent field. GRA

N88-29852# Dornier-Werke G.m.b.H., Friedrichshafen (West Germany).
PROCEDURES FOR UPDATING DYNAMIC MATHEMATICAL MODELS, TEST PHASE Final Report
B. Caesar, E. Erben, H. Hueners, M. Link, J. Moreno-Barragan, A. Schumann-Luck, F. Vogel, and M. Weiland (Kassel Univ., West Germany) Paris, France ESA Jun. 1987 413 p
(Contract ESTEC-6262/85-NL-PH)
(MEBS-38/87; ESA-CR(P)-2606; ETN-88-93036) Avail: NTIS HC A18/MF A01

Procedures for updating and identification of dynamic mathematical models were applied to real hardware problems. Small size (spring-mass, beam) structures, a medium size test structure, a spacecraft antenna module, and a whole spacecraft (MAROTS) were investigated. The small and medium size structures were manufactured, and tested with different test methods to get the modal parameters. The test data of the antenna module and the spacecraft were obtained from the relevant projects. The application of modal parameter identification with procedures working in the time domain and in the frequency domain (ISSPA) and the correlation of results from different tests indicates the quality of test results in general. The general applicability of ISSPA is demonstrated. A highly formulized update procedure was applied to improve the mathematical models of the tested structures on the basis of modal test data. The advantages and drawbacks of such a method are described. The applicability to standard size spacecraft problems is demonstrated. ESA

N88-29853# Naval Postgraduate School, Monterey, Calif.
ION GUN GENERATED ELECTROMAGNETIC INTERFERENCE ON THE SCATHA SATELLITE M.S. Thesis
Leonard Earl Weddle Dec. 1987 73 p
(AD-A195179) Avail: NTIS HC A04/MF A01 CSCL 22B

Spacecraft charging at geosynchronous orbit can cause satellite anomalies and failure. Experiments in charge control were conducted on the joint Air Force/NASA P78-2 (SCATHA) satellite using both electron and positive ion emission systems. These experiments were monitored by a variety of plasma wave and particle detectors. Plasma wave data show that arcing was taking place during non-neutralized ion beam emission. The arcing was seen to cease when either the beam was neutralized or the beam acceleration voltage was turned off. Evidence exists which indicate that the arcing is due to differential charging on the satellite surface. A possible effect of non-neutral, non-accelerated ion beam emission is the shielding of the electric field antenna from ion gun generated plasma waves. The effect of shielding these signals is an increase in the sensitivity of the electric field receiver to natural signals. GRA

N88-29854*# Eagle Engineering, Inc., Houston, Tex.
LUNAR LANDER CONCEPTUAL DESIGN: LUNAR BASE SYSTEMS STUDY TASK 2.2 Report, Dec. 1987 - Mar. 1988
30 Mar. 1988 145 p
(Contract NAS9-17878)
(NASA-CR-172051; NAS 1.26:172051; EEI-88-181) Avail: NTIS HC A07/MF A01 CSCL 22B

This study is a first look at the problem of building a lunar lander to support a small lunar surface base. One lander, which can land 25 metric tons, one way, or take a 6 metric ton crew capsule up and down is desired. A series of trade studies are used to narrow the choices and provide some general guidelines. Given a rough baseline, the systems are then reviewed. A conceptual design is then produced. The process was only carried through one iteration. Many more iterations are needed. Assumptions and groundrules are considered. B.G.

N88-29855# BSO/Aerospace, Amsterdam (Netherlands).
MANIP Final Report
Paris, France ESA 1 Oct. 1987 51 p
(Contract ESA-5286/82-NL)
(MANIP-217A; ESA-CR(P)-2544; ETN-88-92771) Avail: NTIS HC A04/MF A01

The MANIP program was conceived as a solution to the user-hostile thermal modeling and simulation environment comprising principally the programs VWHEAT and SINDA. The program MINIP was built to demonstrate the desirability of an interactive and user-friendly interface especially in the 3D graphics area. The MANIP was to present modeling in user terms, not programming terms, constructing geometric models by interactive graphics, and adding active models by use of a simulation language

(not FORTRAN). The user would also have full control of the simulation (calculation) process, and be able to interactively experiment and analyze results. It is shown that MANIP is feasible, but conflict arises from the fact that user-friendliness costs performance, while orders of magnitude better performance is desired. The solution to this lies in the combination of better hardware and concessions in the pure concept. ESA

N88-29856*# National Aeronautics and Space Administration. Langley Research Center, Hampton, Va.
DEFINITION OF COMMON SUPPORT EQUIPMENT AND SPACE STATION INTERFACE REQUIREMENTS FOR IOC MODEL TECHNOLOGY EXPERIMENTS
Richard A. Russell and Richard D. Waiss (Boeing Aerospace Co., Seattle, Wash.) Aug. 1988 163 p
(NASA-TM-100656; NAS 1.15:100656) Avail: NTIS HC A08/MF A01 CSCL 22B

A study was conducted to identify the common support equipment and Space Station interface requirements for the IOC (initial operating capabilities) model technology experiments. In particular, each principal investigator for the proposed model technology experiment was contacted and visited for technical understanding and support for the generation of the detailed technical backup data required for completion of this study. Based on the data generated, a strong case can be made for a dedicated technology experiment command and control work station consisting of a command keyboard, cathode ray tube, data processing and storage, and an alert/annunciator panel located in the pressurized laboratory. Author

N88-30509# Joint Publications Research Service, Arlington, Va.
ROTATIONAL EVOLUTION OF DYNAMICALLY SYMMETRIC GYROSTAT WITH INTERNAL FRICTION Abstract Only
M. L. Pivovarov *In its* JPRS Report: Science and Technology. USSR: Space 26 Feb. 1988 p 15 Transl. into ENGLISH from Kosmicheskiye Issledovaniya (Moscow, USSR), v. 25, no. 3, May - Jun. 1987 p 370-373 (For primary document see N88-30498 24-88)
Avail: NTIS HC A04/MF A01

19 SPACECRAFT INSTRUMENTATION

For related information see also *06 Aircraft Instrumentation* and *35 Instrumentation and Photography.*

N88-29857# Dornier-Werke G.m.b.H., Friedrichshafen (West Germany).
BIOSAMPLE: PRESERVATION, HANDLING AND OBSERVATION SYSTEM SYNTHESIS AND BREADBOARDING
Paris, France ESA Dec. 1987 65 p
(Contract ESTEC-6377/85-NL-PR(SC))
(ESA-CR(P)-2609; ETN-88-93037) Avail: NTIS HC A04/MF A01

A breadboard to perform fully automated handling, observation, and processing of biological samples, e.g., plants, insects, or organisms in liquid culture on Spacelab was built. The infrastructure consists of: transfer system to move the individual sample containers, thermal conditioned areas; life support system (gas supply, illumination); reference centrifuge; vision systems (low and high resolution); and sample containers adapted to special specimens requirements. The real sample processing takes place in the workstation area equipped with plant cutting workstation, chemical workstation, insect counting workstation, and automated syringes for plant cutting and liquid handling. An autofixation device for handling of toxic fixatives, and a microchemistry device to perform automated chemical assays were also developed. ESA

20 SPACECRAFT PROPULSION AND POWER

Includes main propulsion systems and components, e.g., rocket engines; and spacecraft auxilliary power sources.

For related information see also *07 Aircraft Propulsion and Power, 28 Propellants and Fuels, 44 Energy Production and Conversion,* and *15 Launch Vehicles and Space Vehicles.*

N88-29858*# Aerojet TechSystems Co., Sacramento, Calif.
ORBITAL TRANSFER VEHICLE 3000 LBF THRUST CHAMBER ASSEMBLY HOT FIRE TEST PROGRAM Interim Report
Judy Schneider and Warren R. Hayden Sep. 1988 235 p
(Contract NAS3-23772)
(NASA-CR-182145; NAS 1.26:182145) Avail: NTIS HC A11/MF A01 CSCL 21H

The Aerojet Orbital Transfer Vehicle (OTV) Thrust Chamber Assembly (TCA) concept consists of a hydrogen cooled chamber, and annular injector, and an oxygen cooled centerbody. The hot fire testing of a heat sink version of the chamber with only the throat section using hydrogen cooling is documented. Hydraulic performance of the injector and cooled throat were verified by water flow testing prior to TCA assembly. The cooled throat was proof tested to 3000 psia to verify the integrity of the codeposited EF nickel-cobalt closeout. The first set of hot fire tests were conducted with a heat sink throat to obtain heat flux information. After demonstration of acceptable heat fluxes, the heat sink throat was replaced with the LH2 cooled throat section. Fourteen tests were conducted with a heat sink chamber and throat at chamber pressures of 85 to 359 psia. The injector face was modified at this time to add more face coolant flow. Ten tests were then conducted at chamber pressures of 197 to 620 psia. Actual heat fluxes at the higher chamber pressure range were 23 percent higher than the average of 10 Btu/in 2 predicted. Author

N88-29859*# National Aeronautics and Space Administration, Washington, D.C.
THE NASA ELECTRIC PROPULSION PROGRAM
James R. Stone, David C. Byers, and David Q. King (Jet Propulsion Lab., California Inst. of Tech., Pasadena.) 1988 20 p Presented at the 20th International Electric Propulsion Conference, Garmisch-Partenkirchen, Fed. Republic of Germany, 3-6 Oct. 1988; sponsored by DGLR, AIAA and JSASS
(NASA-TM-101324; E-4330; NAS 1.15:101324; IEPC-88-002)
Avail: NTIS HC A03/MF A01 CSCL 21H

The NASA OAST Propulsion, Power, and Energy Division supports an electric propulsion program aimed at providing benefits to a broad class of missions. Concepts which have the potential to enable or significantly benefit space exploration and exploitation are identified and advanced toward application in the near and far term. This paper summarizes recent program progress in mission/system analysis; in electrothermal, electrostatic, and electromagnetic propulsion technologies; and in propulsion/spacecraft integration. Author

N88-29860*# National Aeronautics and Space Administration. Lewis Research Center, Cleveland, Ohio.
PERFORMANCE AND LIFETIME ASSESSMENT OF MPD ARC THRUSTER TECHNOLOGY
James S. Sovey and Maris A. Mantenieks 1988 35 p Presented at the 24th Joint Propulsion Conference, Boston, Mass., 11-13 Jul. 1988; sponsored by AIAA, ASME, SAE and ASEE
(NASA-TM-101293; E-4274; NAS 1.15:101293; AIAA-88-3211)
Avail: NTIS HC A03/MF A01 CSCL 21H

A summary of performance and lifetime characteristics of pulsed and steady-state magnetoplasmadynamic (MPD) thrusters is presented. The technical focus is on cargo vehicle propulsion for exploration-class missions to the Moon and Mars. Relatively high MPD thruster efficiencies of 0.43 and 0.69 have been reported at about 5000 s specific impulse using hydrogen and lithium, respectively. Efficiencies of 0.10 to 0.35 in the 1000 to 4500 s specific impulse range have been obtained with other propellants

(e.g., Ar, NH3, N2). Thermal efficiency data in excess of 0.80 at MW power levels using pulsed thrusters indicate the potential of high MPD thruster performance. Extended tests of pulsed and steady-state MPD thrusters yield total impulses at least two to three orders of magnitude below that necessary for cargo vehicle propulsion. Performance tests and diagnostics for life-limiting mechanisms of megawatt-class thrusters will require high fidelity test stands which handle in excess of 10 kA and a vacuum facility whose operational pressure is less than 3 x 10 to the -4 torr.
Author

N88-29861# Illinois Univ., Urbana. Dept. of Mechanical and Industrial Engineering.
ENERGY CONVERSION MEASUREMENTS IN LASER-SUSTAINED ARGON PLASMAS FOR APPLICATION TO ROCKET PROPULSION Final Technical Report, 18 Feb. 1987 - 17 Feb. 1988
Herman Krier, Jyoti Mazumder, David K. Zerkle, Ayhan Mertogul, and Scott Schwartz 15 Apr. 1988 86 p
(Grant AF-AFOSR-0169-87)
(AD-A194931; UILU-ENG-88-4006; AFOSR-88-0541TR) Avail: NTIS HC A05/MF A01 CSCL 21H

Laser Propulsion is the production of high specific impulse rocket thrust using a high power laser as a remote energy source. Specific impulses in excess of 1000 seconds are achievable because propellant temperatures are very high and low molecular weight gases can be used. This report focuses on the energy conversion mechanisms of laser-sustained plasmas in flowing argon. The status of experiments to determine thermal efficiency and global absorption is detailed. An improved testing facility has allowed plasma operating conditions never before possible. The results indicate that nearly all of the input laser power can be absorbed by a plasma. Plasmas at elevated gas pressure have been tested, and preliminary results presented. Optimal operating conditions have yet to be determined for the available laser powers and gas pressures. Further experimentation at very high argon gas velocities (greater than 20 m/s) must be performed in order to completely characterize plasma behavior. GRA

N88-29862# Deutsche Forschungs- und Versuchsanstalt fuer Luft- und Raumfahrt, Goettingen (West Germany). Inst. for Experimental Fluid Mechanics.
STUDIES ON ROCKET EXHAUST PLUMES AND IMPINGEMENT EFFECTS RELATED TO THE COLUMBUS SPACE STATION PROGRAM: EXECUTIVE SUMMARY
R.-D. Boettcher, C. Dankert, G. Dettleff, and H. Legge Paris, France ESA Feb. 1988 82 p
(Contract ESA-6829/86-NL-PH(SC))
(DFVLR-IB-222-88-A-12; ESA-CR(P)-2614; ETN-88-93148) Avail: NTIS HC A05/MF A01

Using a plume impingement computer code, possible proximity impingement situations in the Columbus space station were analyzed. Experiments investigated the plume flow immediately downstream of the nozzle. The impingement effects (shear stress and pressure) were measured on a plate inclined with respect to the plume axis up to perpendicular impingement. This situation is considered as typical during rendezvous and docking maneuvers.
ESA

N88-29863*# Sundstrand Energy Systems, Rockford, Ill.
STUDY OF TOLUENE STABILITY FOR AN ORGANIC RANKINE CYCLE (ORC) SPACE-BASED POWER SYSTEM Final Report
Vance Havens and Dana Ragaller Jul. 1988 292 p
(Contract NAS3-24663)
(NASA-CR-180884; NAS 1.26:180884) Avail: NTIS HC A13/MF A01 CSCL 21H

The design, fabrication, assembly, and endurance operation of a dynamic test loop, built to evaluate the thermal stability of a proposed Organic Rankine Cycle (ORC) working fluid, is discussed. The test fluid, toluene, was circulated through a heater, simulated turbine, regenerator, condenser and pump to duplicate an actual ORC system. The maximum nominal fluid temperature, 750 F, was at the turbine simulator inlet. Samples of noncondensible gases and liquid toluene were taken periodically during the test. The samples were analyzed to identify the degradation products formed and the quantity of these products. From these data it was possible to determine the degradation rate of the working fluid and the generation rate of noncondensible gases. A further goal of this work was to relate the degradation observed in the dynamic operating loop to degradation obtained in isothermal capsule tests. This relationship was the basis for estimating the power loop degradation in the Space Station Organic Rankine Cycle system.
Author

N88-29864# Naval Postgraduate School, Monterey, Calif.
AUTOMATIC DATA RETRIEVAL FROM ROCKET MOTOR HOLOGRAMS M.S. Thesis
Emin S. Orguc Dec. 1987 56 p
(AD-A195586) Avail: NTIS HC A04/MF A01 CSCL 21I

A technique for obtaining particle size information from holograms of combustion products is described. These data are needed to improve predictive capabilities of propellant performance, to provide input related to ammonium perchlorate (AP), aluminum interactions for steady-state combustion models and to provide in motor particle size distributions to allow more accurate predictions of damping in stability analysis and two phase flow and exhaust plume signature. This study describes the use of Itex/PC software for the filtering and processing of the hologram images to reduce speckle and also improves a FORTRAN program which had been written before to extract the particle feature size data from the modified image. The final step shows the statistical particle feature data exhibition by using the STATGRAPHICS (Statistical Graphics System) software.
GRA

N88-29865# Research Inst. of National Defence, Stockholm (Sweden).
IGNITION AND EXTINGUISHING OF A SOLID FUEL RAMJET (SOFRAM) Status Report
Ralf Eliasson May 1988 24 p In SWEDISH; ENGLISH summary
(FOA-C-20713-2.1; ISSN-0347-3694; ETN-88-93057) Avail: NTIS HC A03/MF A01

Ignition of a tubeformed propellant by means of powder charge is described. Good results are obtained with an ignition strip 10 mm large and 5 mm thick, near the air intake, and composed of 75 percent ammonium perchlorate, 10 percent aluminum powder, and 15 percent carboxyl terminated polybutadiene. A starting squib of 0.3 g BKN03 was used. The ignition lasts for less than 2 sec. The mechanical device for the extinguishing at a suitable point or time is shown. The ignition and extinguishing methods were both tested in a chamber with a circular air intake.
ESA

N88-29866# Messerschmitt-Boelkow-Blohm G.m.b.H., Ottobrunn (West Germany). Space Div.
HERMES: STUDY OF PROPULSION SYSTEM FOR REUSABLE MAN-RATED SPACECRAFT
H. Immich et al. Paris, France ESA 18 Aug. 1987 59 p
(Contract ESTEC-6828/86-NL-PH(SC))
(PSRM-TN-0000-00-04A; ESA-CR(P)-2610; ETN-88-93038)
Avail: NTIS HC A04/MF A01

The impact of man rating and reliability requirements on the design, manufacture, validation, operation, and serviceability of the propulsion system for Hermes, together with the technology developments relating to the propulsion system were investigated. Propulsion system requirements; a design specification for the propulsion system; a flow scheme for the propulsion system; selection of candidate equipment and potential suppliers; failure mode, effects, and criticality analysis (FMECA), reliability and hazards analysis; identification of problem areas and technology developments; and a development plan, schedule, and costs are outlined.
ESA

N88-29867*# Pratt and Whitney Aircraft, West Palm Beach, Fla. Government Engine Business.
BREADBOARD RL10-2B LOW-THRUST OPERATING MODE (SECOND ITERATION) TEST REPORT Topical Report, Dec. 1987 - Jan. 1988
Paul G. Kanic, Raymond B. Kaldor, and Pia M. Watkins Aug. 1988 51 p
(Contract NAS3-25052)
(NASA-CR-182160; NAS 1.26:182160; FR-20311-1) Avail: NTIS HC A04/MF A01 CSCL 21H

Cryogenic rocket engines requiring a cooling process to thermally condition the engine to operating temperature can be made more efficient if cooling propellants can be burned. Tank head idle and pumped idle modes can be used to burn propellants employed for cooling, thereby providing useful thrust. Such idle modes required the use of a heat exchanger to vaporize oxygen prior to injection into the combustion chamber. During December 1988, Pratt and Whitney conducted a series of engine hot firing demonstrating the operation of two new, previously untested oxidizer heat exchanger designs. The program was a second iteration of previous low thrust testing conducted in 1984, during which a first-generation heat exchanger design was used. Although operation was demonstrated at tank head idle and pumped idle, the engine experienced instability when propellants could not be supplied to the heat exchanger at design conditions. Author

N88-29868*# National Aeronautics and Space Administration. Lewis Research Center, Cleveland, Ohio.
EXPERIMENTAL EVALUATION OF RESISTOJET THRUSTER PLUME SHIELDS
Lynnette M. Carney and Allan B. Bailey (Calspan Corp., Arnold AFS, Tenn.) 1988 27 p Presented at the 20th International Electric Propulsion Conference, Garmisch-Partenkirchen, Fed. Republic of Germany, 3-6 Oct. 1988; sponsored by DGLR, AIAA and JSASS
(NASA-TM-101363; E-4356; NAS 1.15:101363; IEPC-88-091)
Avail: NTIS HC A03/MF A01 CSCL 21H

The exhaust of an engineering model resistojet has been investigated using rotary pitot probes and a rotary quartz crystal microbalance. The resistojet operated on CO2 propellant at a mass flow rate of 0.29 g/sec in both heated and unheated flows. Measurements of local flow angles in the near field of a conical plume shield indicated that the shield was not wholly effective in confining the flow to the region upstream of its exit plane. However, the absolute levels of the measured mass flux into the backflow region were very low, on the order of 7 x 10 to the -7 power g/sqcm/sec or less. The use of a circualr disk at the exit plane of the existing conical shield showed some benefit in decreasing the amount of backflow by a factor of two. Lastly, a detached shield placed upstream of the resistojet exit plane demonstrated a small degree of local shielding for the region directly behind it. Author

N88-29869*# National Aeronautics and Space Administration. Lewis Research Center, Cleveland, Ohio.
THE dc POWER CONTROL FOR A LIQUID-FED RESISTOJET
Robert P. Gruber [1988] 12 p Prepared for presentation at the 20th International Electric Propulsion Conference, Garmisch-Partenkirchen, (Fed. Republic of Germany), 3-6 Oct. 1988; sponsored in part by DGLR, AIAA and JSASS
(NASA-TM-101326; E-4337; NAS 1.15:101326; IEPC-88-045)
Avail: NTIS HC A03/MF A01 CSCL 21H

A simple breadboard power controller was designed and demonstrated for a new liquid-fed water resistojet. The 1-piece laboratory model thruster has an integrated vaporizer/superheater using a single heating element. Heater temperature was maintained at or near a preset reference value with the closed loop controller providing pulse width modulated (PWM) dc power into the thruster heater. A combined thruster, temperature readout, PWM transfer function was experimentally determined. This transfer function was used to design a proportional plus integral controller that demonstrated zero steady state error, conservative stability margins and adequate transient response to step changes in propellant flow rate, input voltage and temperature reference. Initial turn-on temperature overshoot from room temperature to a 650 C setpoint was 80 C. In addition, EMI was alleviated by reducing heater dI/dt and dV/dt using a simple diode-inductor-capacitor network. Based on limited initial tests, thruster preheat with no propellant flow was necessary to achieve stable system operation during startup. Breadboard power efficiency was 99 percent at 1 kW, and component mass was 0.4 kg excluding the power loss and mass of an input filter required for spacecraft integration. Author

N88-29870# R and D Associates, Alexandria, Va. Research Lab.
UNIFIED STUDY OF PLASMA/SURFACE INTERACTIONS FOR SPACE POWER AND PROPULSION Final Report, 15 Jul. 1987 - 29 Feb. 1988
29 Feb. 1988 66 p
(Contract F49620-86-C-0069)
(AD-A195971; AFOSR-88-0600TR) Avail: NTIS HC A04/MF A01 CSCL 20I

High specific impulse, high specific power devices, such as magnetoplasmadynamic arcjets, laser or microwave propulsion channels, and MHD generators, involve the flow of modest temperature (0.5 to 5 eV) partially ionized gases at speeds of 5 to 20 km per sec. The interactions of such flows with solid surfaces containing, channeling or penetrating the flow provides a principal source of concern for the efficiency and lifetime of high specific power systems. The present report describes a basic research effort that examines the plasma/surface interaction experimentally in an arrangement providing diagnostic access usually unavailable in mission-oriented, device-development projects. GRA

N88-29871# Technische Univ., Berlin (West Germany). Inst. fuer Luft- und Raumfahrt.
POSSIBILITIES OF ECONOMICAL IMPROVEMENTS FOR MOON BASED ROCKET PROPULSION USING LUNAR PROPELLANTS [MOEGLICHKEITEN DER VERBESSERUNG DER WIRTSCHAFTLICHKEIT VON ANTRIEBEN FUER MONDRAKETEN MITTELS LUNARER TREIBSTOFFE]
D. Goericke and H. H. Koelle 1 Mar. 1988 26 p In GERMAN; ENGLISH summary
(ILR-Mitt-196; ETN-88-93116) Avail: NTIS HC A03/MF A01

Design to cost analysis of adding Al to the fuel of an H2/O2 Moon rocket is examined. The idea is to decrease the H2 part which must be imported from Earth, while Al and O2 are produced on Moon for assumed 5 to 10 $/kg. Specific transportation costs were calculated for a 300 Mg ferry for lunar surface missions by different payloads per year and various fuel costs. These costs are based on estimated mass relationships and cost models. An engine with 60 percent Al and MR = 6.0 is selected to optimize 3 ferries (mo = 100/300/500 Mg) for the given missions. The specific transportation costs were estimated. ESA

N88-29872*# Sundstrand Energy Systems, Rockford, Ill.
STUDY OF TOLUENE ROTARY FLUID MANAGEMENT DEVICE AND SHEAR FLOW CONDENSER PERFORMANCE FOR A SPACE-BASED ORGANIC RANKINE POWER SYSTEM Final Report
Vance Havens and Dana Ragaller Jul. 1988 103 p
(Contract NAS3-24663)
(NASA-CR-180885; NAS 1.26:180885) Avail: NTIS HC A06/MF A01 CSCL 10B

Management of two-phase fluid and control of the heat transfer process in microgravity is a technical challenge that must be addressed for an orbital Organic Rankine Cycle (ORC) application. A test program was performed in 1-g that satisfactorily demonstrated the two-phase management capability of the rotating fluid management device (RFMD) and shear-flow condenser. Operational tests of the RFMD and shear flow condenser in adverse gravity orientations, confirmed that the centrifugal forces in the RFMD and the shear forces in the condenser were capable of overcoming gravity forces. In a microgravity environment, these same forces would not have to compete against gravity and would therefore be dominant. The specific test program covered the

required operating range of the Space Station Solar Dynamic Rankine Cycle power system. Review of the test data verified that: fluid was pumped from the RFMD in all attitudes; subcooled states in the condenser were achieved; condensate was pushed uphill against gravity; and noncondensible gases were swept through the condenser. Author

N88-29873*# National Aeronautics and Space Administration. Lewis Research Center, Cleveland, Ohio.
SUCCESSFUL COMPLETION OF A CYCLIC GROUND TEST OF A MERCURY ION AUXILIARY PROPULSION SYSTEM
David R. Francisco, Charles A. Low, Jr., and John L. Power [1988] 13 p Prepared for presentation at the 20th International Electric Propulsion Conference, Garmisch-Partenkirchen, (Fed. Republic of Germany), 3-6 Oct. 1988; sponsored in part by DGLR, AIAA and JSASS
(NASA-TM-101351; E-4378; NAS 1.15:101351; IEPC-88-035) Avail: NTIS HC A03/MF A01 CSCL 21H

An engineering model Ion Auxiliary Propulsion System (IAPS) 8-cm thruster (S/N 905) has completed a life test at NASA Lewis Research Center. The mercury ion thruster successfully completed and exceeded the test goals of 2557 on/off cycles and 7057 hr of operation at full thrust. The final 1200 cycles and 3600 hr of the life test were conducted using an engineering model of the IAPS power electronics unit (PEU) and breadboard digital controller and interface unit (DCIU). This portion of the test is described in this paper with a charted history of thruster operating parameters and off-normal events. Performance and operating characteristics were constant throughout the test with only minor variations. The engineering model power electronics unit operated without malfunction; the flight software in the digital controller and interface unit was exercised and verified. Post-test inspection of the thruster revealed facility enhanced accelerator grid erosion but overall the thruster was in good condition. It was concluded that the thruster performance was not drastically degraded by time or cycles. Additional cyclic testing is currently under consideration. Author

N88-29874*# National Aeronautics and Space Administration. Lewis Research Center, Cleveland, Ohio.
IRIDIUM-COATED RHENIUM THRUSTERS BY CVD
John T. Harding, John M. Kazaroff, and Marshall A. Appel (Jet Propulsion Lab., California Inst. of Tech., Pasadena.) 1988 12 p Presented at the 2nd International Conference on Surface Modification Technologies, Chicago, Ill., 25-29 Sep. 1988; sponsored by AIME and ASM
(NASA-TM-101309; E-4304; NAS 1.15:101309) Avail: NTIS HC A03/MF A01 CSCL 21H

Operation of spacecraft thrusters at increased temperature reduces propellant requirements. Inasmuch as propellant comprises the bulk of a satellite's mass, even a small percentage reduction makes possible a significant enhancement of the mission in terms of increased payload. Because of its excellent high temperature strength, rhenium is often the structural material of choice. It can be fabricated into free-standing shapes by chemical vapor deposition (CVD) onto an expendable mandrel. What rhenium lacks is oxidation resistance, but this can be provided by a coating of iridium, also by CVD. This paper describes the process used by Ultramet to fabricate 22-N (5-lbf) and, more recently, 445-N (100-lbf) Ir/Re thrusters; characterizes the CVD-deposited materials; and summarizes the materials effects of firing these thrusters. Optimal propellant mixture ratios can be employed because the materials withstand an oxidizing environment up to the meltimg temperature of iridium, 2400 C (4350 F). Author

N88-29875# Societe Europeenne de Propulsion, Vernon (France).
SIMULATION OF VULCAIN ENGINE OPERATION AT LOW INLET PRESSURE
A. Dubebout and B. Thiard 1988 7 p
(ETN-88-93083) Avail: NTIS HC A02/MF A01

The numerical models developed for the Vulcain program were used to simulate engine operation at low inlet pressure. Static and the transient models were used (and adapted when necessary) to look into the turbopump behavior then into the whole engine system stability. Effect of pump cavitation on turbopump stability was studied, either for LH2 or for LOX turbopump, and engine dynamic response was drawn. Trade-off analyses regarding main model hypothesis were performed, but show only minor influence on engine response. Stability margins with regard to operation at low inlet pressure and limits under which no stability could be achieved are identified. This allows a better prediction of engine in-flight performance but also allows to define more accurately the necessary engine monitoring during ground testing. ESA

N88-29876*# Pratt and Whitney Aircraft, West Palm Beach, Fla. Government Engine Business.
OXIDIZER HEAT EXCHANGER COMPONENT TEST Final Report
P. G. Kanic Sep. 1988 120 p
(Contract NAS3-24738)
(NASA-CR-182159; NAS 1.26:182159; PW-FR-19602) Avail: NTIS HC A06/MF A01 CSCL 21H

The RL10-IIB engine, is capable of multimode thrust operation. The engine operates at two low-thrust levels: tank head idle (THI), approximately 1 to 2 percent of full thrust; and pumped idle, 10 percent of full thrust. Operation at THI provides vehicle propellant settling thrust and efficient thermal conditioning; PI operation provides vehicle tank prepressurization and maneuver thrust for low-g deployment. Stable combustion of the RL10-IIB engine during the low-thrust operating modes can be accomplished by using a heat exchanger to supply gaseous oxygen to the propellant injector. The oxidized heat exchanger (OHE) vaporizes the liquid oxygen using hydrogen as the energy source. This report summarizes the test activity and post-test data analysis for two possible heat exchangers, each of which employs a completely different design philosophy. One design makes use of a low-heat transfer (PHT) approach in combination with a volume to attenuate pressure and flow oscillations. The test data showed that the LHT unit satisfied the oxygen exit quality of 0.95 or greater in both the THI and PI modes while maintaining stability. The HHT unit fulfilled all PI requirements; data for THI satisfactory operation is implied from experimental data that straddle the exact THI operating point. Author

23 CHEMISTRY AND MATERIALS (GENERAL)

No abstracts in this category.

24 COMPOSITE MATERIALS

Includes physical, chemical, and mechanical properties of laminates and other composite materials.

For ceramic materials see *27 Nonmetallic Materials*.

N88-29877# Technische Univ., Berlin (West Germany). Inst. fuer Luft- und Raumfahrt.
INVESTIGATIONS ON THE MODIFICATION OF STRUCTURAL RELIABILITY BY SUBSTITUTION OF ALUMINUM BY CARBON FIBER REINFORCED PLASTICS IN AIRCRAFT CONSTRUCTION [UNTERSUCHUNGEN ZUR VERAENDERUNG DER STRUKTURZUVERLAESSIGKEIT BEI SUBSTITUTION VON ALUMINIUM DURCH KOHLEFASERKUNSTSTOFF IN FLUGZEUGKONSTRUKTIONEN]
Bernd Ziegler 1988 188 p In GERMAN
(ILR-Mitt-195; ETN-88-93115) Avail: NTIS HC A09/MF A01

Reliability theory for elementary components is outlined in the case of serial and parallel connected systems and the obtained redundancy is analyzed. Investigations for the determination of

material strength distribution and reliability properties of aluminum alloy and carbon reinforced plastics are described. Tensile strength and elongation are measured for AlCuMg alloy components in serial and parallel systems and their reliability is evaluated. For carbon reinforced plastics variation of fiber angles effects is studied on tensile strength and reliability of aircraft components. ESA

N88-29878# California Univ., Los Angeles. Dept. of Materials Science and Engineering.
CREEP OF CARBON YARN AND CARBON-CARBON COMPOSITES AT HIGH TEMPERATURES AND HIGH STRESSES
George Sines, Zheng Yang, and Brian D. Vickers May 1988 60 p
(Contract N00014-85-K-0667)
(AD-A195224; UCLA-ENG-88-8) Avail: NTIS HC A04/MF A01 CSCL 11B

To better understand the creep-behavior of carbon yarn and carbon-carbon composites, creep experiments were developed that permitted testing at high temperatures (up to 2500 C) and at high stresses (up to 850 MPa) on specially prepared, uniaxial specimens that had a known gage length. Using a Dorn-type power law relation to model steady-state creep the apparent activation energy for the carbon yarn and carbon composite specimens was determined to be 1082 kj/mol. This value represents a single thermally activated process, vacancy diffusion, that compares favorably with the various types of graphitizable carbon. The value determined for the stress exponent was 7.5. It too was found to be independent of the carbon matrix's presence and independent of the specimens' loading history. Values of the pre-exponential constant for the carbon yarn and carbon composites were also calculated. The carbon matrix greatly improves the creep resistance of the carbon composite. This improvement was attributed to the matrix's microstructure. It distributes applied loads more evenly and it may also impose a triaxial stress state in the yarns's filaments. It is proposed that such a stress state may inhibit the flux of vacancies thus accounting in part for this increase in creep resistance. GRA

N88-29879*# National Aeronautics and Space Administration. Langley Research Center, Hampton, Va.
AN IMPROVED BOUNDARY FORCE METHOD FOR ANALYZING CRACKED ANISOTROPIC MATERIALS
Paul W. Tan (Analytical Services and Materials, Inc., Hampton, Va.) and Catherine A. Bigelow Sep. 1988 39 p
(NASA-TM-101495; NAS 1.15:101495) Avail: NTIS HC A03/MF A01 CSCL 11D

The Boundary Force Method (BFM), a form of indirect boundary element method, is used to analyze composite laminates with cracks. The BFM uses the orthotropic elasticity solution for a concentrated horizontal and vertical force and a moment applied at a point in a cracked, infinite sheet as the fundamental solution. The necessary stress functions for this fundamental solution were formulated using the complex variable theory of orthotropic elasticity. The current method is an improvement over a previous method using only forces and no moment. The improved method was verified by comparing it to accepted solutions for a finite-width, center-crack specimen subjected to uniaxial tension. Four graphite/epoxy laminates were used: (0 + or - 45/90)sub s, (0), (+ or - 45)sub s, and (+ or - 30)sub s. The BFM results agreed well with accepted solutions. Convergence studies showed that with the addition of the moment in the fundamental solution, the number of boundary elements required for a converged solution was significantly reduced. Parametric studies were done for two configurations for which no orthotropic solutions are currently available; a single edge crack and an inclined single edge crack. Author

N88-29880*# Utah Univ., Salt Lake City. Dept. of Materials Science and Engineering.
A TEST FOR INTERFACIAL EFFECTS AND STRESS TRANSFER IN CERAMIC MATRIX COMPOSITES Final Report
Willard D. Bascom and Ilzoo Lee 1 Aug. 1988 17 p
(Grant NAG2-444)
(NASA-CR-182873; NAS 1.26:182873) Avail: NTIS HC A03/MF A01 CSCL 11D

The efforts to fabricate single embedded filament specimens of carbon and SiC fibers were unsuccessful largely due to the thermal stresses resulting from differences in thermal coefficient of expansion. Other factors appear to have been involved including embrittlement of the metal substrate by the H2 gas in the chemical vapor deposition flow stream and reaction layers formed between the silicon carbide and the metal substrate. The carbon fiber may have been attacked by the CVD reactant. It is concluded that these differential stresses are so large as to make the embedded fiber test impractical for the study of interphase effects and stress transfer in fiber ceramic matrix systems. Author

N88-29881# United Technologies Research Center, East Hartford, Conn.
A STUDY OF THE CRITICAL FACTORS CONTROLLING THE SYNTHESIS OF CERAMIC MATRIX COMPOSITES FROM PRECERAMIC POLYMERS Semiannual Report
J. R. Strife, C. M. Brunette, R. A. Pike, H. H. Streckert, and J. E. Sheehan 15 Apr. 1988 5 p
(Contract F49620-87-C-0093; DARPA Order 6153)
(AD-A195405; AFOSR-88-0529TR) Avail: NTIS HC A02/MF A01 CSCL 11D

Several DOD technology efforts such as the Integrated High Performance Integrated Turbine Engine Technology Program and the National Aerospace Plane depend on the development of high temperature low density materials. The development of fiber reinforced ceramics is projected to play a major role in this endeavor because of their high temperature capacity and superior mechanical properties on a density normalized basis at elevated temperature. Fiber reinforced ceramics have been processed to date primarily by hot pressing tape materials or by the chemical vapor infiltration of fibrous preforms. GRA

N88-29882# Metal Matrix Composites Information Analysis Center, Santa Barbara, Calif.
SOME THEORETICAL CONSIDERATIONS OF THE SURFACE TENSION OF LIQUID METALS FOR METAL MATRIX COMPOSITES
Jacques E. Schoutens May 1988 27 p
(Contract DLA900-85-C-4100)
(AD-A195999; MMCIAC-000701) Avail: NTIS HC A03/MF A01 CSCL 11D

This paper presents a model for calculating the surface tension of pure metals and their alloys. It is based upon the theory of Eyring et al., which uses classical statistical physics to describe the thermodynamic properties of metals in the liquid state. Calculations show the surface tension of pure aluminum to be nearly 9 percent greater than that measured for pure aluminum having a monolayer of Aluminum Oxide (Al sub 2 O sub 3) is within about 10 percent of measured values for Al-xMg and Al-xCu, where x is the weight percent of the alloying element. The model was also used to calculate the temperature coefficient. For pure aluminum the calculated values fall within experimental measurements, and exhibit a slight temperature dependence. Cast metal composite (MMC) materials reinforced with unidirectional fibers will turn out to be a low cost alternative to MMC fabrication by diffusion bonding, cold and hot compaction, and other methods. GRA

N88-29883# Air Force Inst. of Tech., Wright-Patterson AFB, Ohio. School of Engineering.
DAMAGE INITIATION IN THE SHORT BEAM SHEAR TEST OF COMPOSITE MATERIALS USING STIFFNESS REDUCTION M.S. Thesis
Dean T. Dupont Jun. 1988 102 p
(AD-A194880; AFIT/GAE/AA/87D-5) Avail: NTIS HC A06/MF A01 CSCL 11D

The purpose of this study was to analyze damage initiation in the short beam shear test for composite materials. This thesis proposes a means of predicting damage initiation in a composite

beam using finite element techniques and a continuum mechanics failure criteria. The first objective was to accurately determine the stress field. The second objective was to employ a damage criteria based on the elemental stress field. The final objective was to evaluate the effectiveness of using an elemental stiffness reduction to study damage initiation and progression. The finite element code used was NOSAPM. GRA

N88-29884*# Virginia Polytechnic Inst. and State Univ., Blacksburg. Dept. of Engineering Science and Mechanics.
ANALYTICAL STUDY OF GRAPHITE-EPOXY TUBE RESPONSE TO THERMAL LOADS
Tamara W. Knott and M. W. Hyer Sep. 1988 85 p
(Grant NAG1-343)
(NASA-CR-183215; NAS 1.26:183215; CCMS-88-16; VPI-E-88-25)
Avail: NTIS HC A05/MF A01 CSCL 11D

The thermally-induced stresses and deformations in graphite-epoxy tubes with aluminum foil bonded to both inner and outer surfaces, and to the outer surface only are computed. Tubes fabricated from three material systems, T300/934, P75s/934, and P75s/BP907, and having a 1 inch inner radius and a lamination sequence of (+15/0 + or - 10/0)sub s are studied. Radial, axial, and circumferential stresses in the various layers of the tube, in the foil, and in the adhesive bonding the foil to the tubes are computed using an elasticity solution. The results indicate that the coatings have no detrimental effect on the stress state in the tube, particularly those stresses that lead to microcracking. The addition of the aluminum foil does, however, significantly influence the axial expansion of the T300/934 tube, the tube with the softer graphite fibers. The addition of foil can change the sign of the axial coefficient of thermal expansion. Twist tendencies of the tubes are only slightly affected by the addition of the coatings, but are of second order compared to the axial response. Author

N88-29885# Southwest Research Inst., San Antonio, Tex.
EVALUATION OF BOND TESTING EQUIPMENT FOR INSPECTION OF ARMY ADVANCED COMPOSITE AIRFRAME STRUCTURES Final Report, 1 Jul. 1987 - 12 Feb. 1988
Hegeon Kwun and David G. Alcazar 12 Feb. 1988 45 p
(Contract DLA900-84-C-0910)
(AD-A195795) Avail: NTIS HC A03/MF A01 CSCL 01C

Forty-one ultrasonic bond testing instruments for nondestructive inspection of composite airframe structures were evaluated based on information available in the literature. In addition, three of these instruments, the Fokker Bondtester Model 80-L, the BondaScope 2100, and the Sonatest UFD-S, were evaluated in the laboratory using ten specimens of composite airframe structures supplied by the Army. All the specimens had unknown flaw conditions. Both the Fokker Bondtester and the BondaScope required only a few hours of operator training in calibration and operation. Both instruments require a liquid couplant and are used for spot checking. The UFD-S instrument was difficult to set up and calibrate without reference samples of known characteristics. Also, extensive operator training is required to calibrate and operate the UFD-S instrument. The UFD-S uses a wheel probe which does not require a liquid couplant and allows continuous scanning of the specimen. The inspection speed of the UFD-S was therefore much greater than that of the other two instruments. Surface roughness, surface curvature, and variations in paint thickness were observed to limit the applicability of the instruments. GRA

N88-29886# British Petroleum Co. Ltd., London (England).
THERMAL STRESS ANALYSIS IN PMR-15 CARBON FIBRE LAMINATES
D. A. Elmes and D. G. Gilbert 1988 11 p Presented at the 3rd International Conference on Fiber Reinforced Composites '88, Liverpool, England23-25 Mar. 1988
(ETN-88-93123) Avail: NTIS HC A03/MF A01

The mechanical property data and analysis required to assess accurately thermal stresses in PMR-15/carbon fiber laminates are studied. The analysis is applied to explain the considerable reductions in microcracking that can be achieved by lowering the processing temperature. Significant errors can be introduced by not considering the temperature dependance of the properties used in the calculations. Stresses approaching the transverse tensile strength of a unidirectional laminate are present at room temperature in PMR-15 composites cured at the conventional temperature of 330 C. The small changes seen in resin chemistry and mechanical properties do not alter significantly the laminate thermal stresses. The considerable reduction in thermal microcracking achieved by lowering the cure temperature from 330 to 280 to 290 C is mainly due to the direct effect of lowering the lock-on temperature. This is achieved without the loss of acceptable mechanical properties at both room and elevated temperatures. ESA

N88-29887# Aeronautical Research Labs., Melbourne (Australia).
CRITERIA FOR MATRIX DOMINATED FAILURE
L. Molent, J. J. Paul, and R. Jones Feb. 1988 21 p
(AD-A196263; ARL/STRUC-R-432; DODA-AR-004-597) Avail: NTIS HC A03/MF A01 CSCL 11D

This paper discusses methods for characterizing the matrix controlled strength of composite materials, fracture of adhesives and the failure of adhesively bonded repairs. Attention is focused on the Tsai-Wu, point stress, energy density and energy release rate approaches and the relationship between these various failure theories. GRA

N88-29888*# National Aeronautics and Space Administration. Lewis Research Center, Cleveland, Ohio.
BROMINATED GRAPHITE FIBERS AND METHOD OF PRODUCING THE SAME Patent Application
Ching-Cheh Hung, inventor (to NASA) 14 Jul. 1988 9 p
(NASA-Case-LEW-14698-1; NAS 1.71:LEW-14698-1; US-Patent-Appl-SN-219016) Avail: NTIS HC A02/MF A01 CSCL 11D

Highly graphitized as well as commercially available less graphitized fibers are brominated in a relatively low temperature range. For liquid bromination, this range is between the melting point of bromine and room temperature. For vaporous bromination, this range is between -15 C and 0 C. The brominated fibers are then reacted with fluorine. NASA

N88-29889# Dayton Univ., Ohio.
FATIGUE CRACK GROWTH CHARACTERISTICS OF ARALL (TRADEMARK)-1 Interim Report, Aug. 1987 - Jan. 1988
John J. Ruschau May 1988 34 p
(Contract F33615-84-C-5130)
(AD-A196185; UDR-TR-88-21; AFWAL-TR-88-4075) Avail: NTIS HC A03/MF A01 CSCL 11D

Constant amplitude and spectrum fatigue crack growth rate properties were evaluated for ARALL-1 aluminum laminate. Testing was performed on M(T) specimens under both lab air and high humidity conditions. Crack length monitoring was performed on each aluminum ply utilizing electrical-potential drop techniques to gain a better insight into the fatigue cracking process. Results indicate an outstanding superiority of ARALL-1 in terms of fatigue crack growth resistance over conventionally produced 7000 series aluminum. Fatigue cracking in each of the aluminum plies was fairly uniform, with no large discrepancies in total crack length or growth rates observed between the various plies. For samples tested under a fighter-type load history, the effect of high humidity was actually beneficial, with fatigue crack growth rates typically one-half of those developed under lab air conditions. Explanations based on increased delamination regions are offered to explain this behavior. GRA

N88-29890# Rensselaer Polytechnic Inst., Troy, N.Y.
PROCESSING TECHNOLOGY RESEARCH IN COMPOSITES Final Report, 1 Oct. 1986 - 30 Sep. 1987
Russell J. Diefendorf 31 Dec. 1987 6 p
(Grant AF-AFOSR-0053-87)
(AD-A195693; AFOSR-88-0669TR) Avail: NTIS HC A02/MF A01 CSCL 11D

Chemical vapor deposition has been used for over fifteen years

for depositing carbon matrices in carbon/carbon composites used for reentry nose-tips, rocket nozzle throat inserts, and aircraft brakes. The same technology is appropriate for depositing silicon carbide or other matrices in ceramic-ceramic composites, or ceramic/carbon composites. Furthermore, chemical vapor deposition is a powerful technique for applying the graded oxidation resistant coatings required for carbon/carbon composites in long time oxidizing environments. Modern instrumentation allows many variations in properties to be made which had been impossible in the past. It is for these reasons that we proposed the acquisition of a state-of-the-art Low Pressure Chemical Vapor Deposition Apparatus. GRA

N88-29891# Aerospace Corp., El Segundo, Calif. Materials Sciences Lab.
TRANSVERSE EXPANSION OF INDIVIDUAL CARBON AND GRAPHITE FILAMENTS
Patrick M. Sheaffer 22 Apr. 1988 24 p
(Contract F04701-85-C-0086)
(AD-A195073; TR-0086A(2935-06)-2; SD-TR-88-51) Avail: NTIS HC A03/MF A01 CSCL 11B

The laser diffraction technique for measuring the diameter of fine filaments has been adapted for measuring the transverse coefficient of thermal expansion (CTE) of individual carbon and graphite filaments. CTE was measured on three types of polyacrylonitrile (PAN)-derived filaments and one type of pitch-derived filament that had already been heat-treated to 2600 C. The measurements are unique because the filaments were in a surface-traction-free environment; the data are therefore inherently more accurate than those obtained by conventional methods. Significant variations in the transverse CTE of pitch-based filaments were observed; they have been attributed to local differences in the (transverse) preferred orientation of the graphite layer planes in those filaments. Individual pitch-based filaments were found to twist about their axis when constrained at both ends and heated; the center of the filament presumably undergoes maximum deflection. GRA

N88-29892# Societe Nationale Industrielle Aerospatiale, Les Mureaux (France).
RUPTURE OF CARBON FIBER REINFORCED PLASTICS (T300-914) COMPOSITE MATERIALS: INFLUENCE OF INITIAL FIRST PLY FAILURES ON THE FATIGUE BEHAVIOR
M. Renault, D. Valentian (Ecole Nationale Superieure des Mines, Evry, France), and F. Pereze 1988 12 p Prepared in cooperation with Ecole Nationale Superieure des Mines, Evry, France
(SNIAS-881-422-103; ETN-88-92847) Avail: NTIS HC A03/MF A01

First ply failure consequence on fatigue behavior are experimentally studied for (0, 90)s, (0, 90, + or - 45)s and (03, 90, + or - 45) lay-ups by comparison of undamaged specimens and specimens with initial damage either in the 90 deg plies or in the 0 deg plies. Initial presence of ply failures in the 90 deg plies influences damage evolution and makes the stiffness reduction faster; stress concentrations due to these cracks may also create more fiber breakings; lifetime is equal or longer and this may be explained by modifications of the 0 deg plies properties. If there is initial damage in the 0 deg plies, Poisson's ratio becomes smaller, initial stiffness reduction is similar, and life time is very shorter. ESA

25 INORGANIC AND PHYSICAL CHEMISTRY

Includes chemical analysis, e.g., chromatography; combustion theory; electrochemistry; and photochemistry.

For related information see also *77 Thermodynamics and Statistical Physics.*.

N88-29893*# Eloret Corp., Sunnyvale, Calif.
COMPUTED POTENTIAL ENERGY SURFACES FOR CHEMICAL REACTIONS Semiannual Report, 1 Jan. - 30 Jun. 1988
Stephen P. Walch 6 Sep. 1988 42 p
(Contract NCC2-478)
(NASA-CR-183168; NAS 1.26:183168) Avail: NTIS HC A03/MF A01 CSCL 07D

The minimum energy path for the addition of a hydrogen atom to N2 is characterized in CASSCF/CCI calculations using the (4s3p2d1f/3s2p1d) basis set, with additional single point calculations at the stationary points of the potential energy surface using the (5s4p3d2f/4s3p2d) basis set. These calculations represent the most extensive set of ab initio calculations completed to date, yielding a zero point corrected barrier for HN2 dissociation of approx. 8.5 kcal mol/1. The lifetime of the HN2 species is estimated from the calculated geometries and energetics using both conventional Transition State Theory and a method which utilizes an Eckart barrier to compute one dimensional quantum mechanical tunneling effects. It is concluded that the lifetime of the HN2 species is very short, greatly limiting its role in both termolecular recombination reactions and combustion processes. Author

N88-29894# Aerodyne Products Corp., Billerica, Mass. Center for Chemical and Environmental Physics.
MOLECULAR LINE SHAPE EFFECTS ON ATMOSPHERIC WINDOW ABSORPTION Final Report, 5 Dec. 1985 - 4 Mar. 1988
J. Wormhoudt and R. C. Brown Mar. 1988 74 p
(Contract F19628-85-C-0183)
(AD-A196316; ARI-RR-644.1; AFGL-TR-88-0108) Avail: NTIS HC A04/MF A01 CSCL 07D

Two theoretical approaches have been followed to calculate far wing absorption of collision reduced absorption in the infrared. The first approach was a standard time dependent perturbation theory. Two methods of this kind were pursued, using different limits. A second approach was investigated called the Recursive Residue Generation Method. The first approach was applied to water self-broadening. Results are given in 10 micro m region. The second approach was investigated for feasibility and examined in the context of the HCl-Ar wings. GRA

N88-29895# Ballistic Research Labs., Aberdeen Proving Ground, Md.
COMBUSTION DIAGNOSTICS OF PROPELLANT WITH NEW GRAIN GEOMETRIES
R. E. Tompkins, K. J. White, and A. A. Juhasz Mar. 1988 37 p
(AD-A194944; BRL-TR-2899) Avail: NTIS HC A03/MF A01 CSCL 21I

High progressivity/density (HPD) propellants are under consideration at the Ballistic Research Laboratory (BRL) for a variety of enhanced ballistic applications. The HPD concept involves the tailoring of the mass generation rate to match the increasing chamber volume as the projectile moves down the gun tube. This can be accomplished physically by designing a grain which will increase in surface area at a designated point in the ballistic cycle. It can also be done chemically by formulating grains with compositions that vary throughout the grain. As these layers burn through, the burn rate can be tailored to change at specific points in the ballistic cycle. GRA

N88-29896# Advanced Fuel Research, Inc., East Hartford, Conn.
EXPERIMENTS AND MODELING OF MULTI-COMPONENT FUEL BEHAVIOR IN COMBUSTION Final Report, Sep. 1984 - Nov. 1987
Peter R. Solomon, David G. Hamblen, Michael A. Serio, Kenneth S. Tarantul, and James R. Markam Mar. 1988 306 p
(Contract F33615-84-C-2478)
(AD-A195011; AFWAL-TR-87-2097) Avail: NTIS HC A14/MF A01 CSCL 21D

A computer model was developed to relate pyrolysis and soot formation to fuel properties. A Fourier Transform-Infrared Spectrometer (FT-IR) was used to characterize the effect of temperature, pressure, reaction time, and hydrogen and oxygen concentration of fuels undergoing pyrolysis. The problem of how to identify and measure the hydrogen available for release during pyrolysis was investigated. A detailed data base of a variety of fuels undergoing pyrolysis was developed. The data base conditions included: temperature 800 to 1500 C; pressure 1 to 15 atm; and reaction time from 100ms to 1 sec. Experimental data results show that fuels decompose to form small hydrocarbon species prior to the onset of soot formation. A hydrocarbon model was extended to include Rice-Kossiakoff-Herzfeld mechanism to predict the decomposition of long chain aliphatics to small molecules. A free radical soot model was developed to predict the growth of soot precursors from the small molecules. GRA

N88-29897 Institut d'Aeronomie Spatiale de Belgique, Brussels.
AERONOMIC PROBLEMS OF THE MOLECULAR OXYGEN PHOTODISSOCIATION. PART 3: SOLAR SPECTRAL IRRADIANCES IN THE REGION OF THE O2 HERZBERG CONTINUUM, SCHUMANN-RUNGE BANDS AND CONTINUUM
Marcel Nicolet and Robert Kennes 1988 29 p Submitted for publication Sponsored in cooperation with the Commission of the European Communities and Pennsylvania State University, University Park, Pa.
(Contract N000-14-86-K-0265)
(Aeronomica-Acta-A-332-1988; ISSN-0065-3713; ETN-88-93072) Avail: Institut d'Aeronomie Spatiale de Belgique, 3 Avenue Circulaire, B-1180 Brussels, Belgium

Evaluation of spectral irradiances obtained during 10 years at wavelengths relevant to the photodissociation of molecular oxygen provides an indication of the accuracy and precision of the information. In the spectral region of wavelengths less than 175 nm corresponding to the O2 Schumann-Runge continuum absorbed in the thermosphere, all the observational results are not reliable since the global accuracy is of the order of 50 percent. In the spectral region 175 to 200 nm of the Schumann-Runge bands, mainly absorbed in the mesosphere, the uncertainties of all available data are not less than 20 to 30 percent and make it impossible to determine the exact solar activity effect on the O2 photodissociation rate. Measurements for the spectral region associated with the O2 Herzberg continuum, 200 to 240 nm, relevant to the stratosphere have typical uncertainty limits reaching 10 percent with additional random errors of 10 percent for 1 nm intervals. The general accuracy is not sufficient to infer the exact part in the irradiance changes associated with solar variability. A consistent reference spectrum for a better assessment must be adopted to describe the complex behavior displayed by the spectral solar irradiances in the spectral ranges of the phtodissociation of O2. ESA

N88-29898# Lawrence Livermore National Lab., Calif.
DETERMINATION OF RELATIVE FLAMMABILITY OF MATERIALS BY PYROLYSIS AND GAS-CHROMATOGRAPHIC LIGHT HYDROCARBON ANALYSIS
S. J. Priante 1 Jun. 1988 4 p
(Contract W-7405-eng-48)
(DE88-012449; UCID-21410) Avail: NTIS HC A02/MF A01

A series of tests was performed to study the production of extremely flammable light hydrocarbon gases produced early in the degradation phase of many materials. The tests consisted of three steps: to perform thermogravimetric analysis on a representative sample to determine its thermal history, to pyrolyze a sample portion of the material to collect the resulting degradation smoke, and then to perform gas chromatographic analysis on the gases collected in the trap. We found that if a material produces a high concentration of methane, propane, and acetylene, and has a high ratio of acetylene to both methane and propane, the material has a relatively high flammability. DOE

N88-29899*# National Aeronautics and Space Administration, Washington, D.C.
DESIGN CRITERIA FOR EXTRACTION WITH CHEMICAL REACTION AND LIQUID MEMBRANE PERMEATION
H. J. Bart, A. Bauer, D. Lorbach, and R. Marr Sep. 1988 37 p Transl. into ENGLISH from Chem. Ing. Tech. (Fed. Republic of Germany), v. 60, no. 3 p 169-179 Transl. by Scientific Translation Service, Santa Barbara, Calif.
(Contract NASw-4307)
(NASA-TT-20352; NAS 1.77:20352) Avail: NTIS HC A03/MF A01 CSCL 07D

The design criteria for heterogeneous chemical reactions in liquid/liquid systems formally correspond to those of classical physical extraction. More complex models are presented which describe the material exchange at the individual droplets in an extraction with chemical reaction and in liquid membrane permeation. Author

N88-29900# Chemical Research and Development Center, Aberdeen Proving Ground, Md.
DEVELOPMENT OF COMPUTER-CONTROLLED THERMOGRAVIMETRIC INSTRUMENTATION FOR MEASUREMENT OF ENVIRONMENTAL AND HIGH TEMPERATURE VOLATILIZATION AND DESORPTION OF CONTAMINANTS FROM POLYMERIC MATERIALS Technical Report, Oct. 1983 - Mar. 1986
Wendel J. Shuely, Vincent M. McHugh, and Brian S. Ince Apr. 1988 28 p
(AD-A195934; CRDEC-TR-88054) Avail: NTIS HC A03/MF A01 CSCL 07D

A conventional thermogravimetric analyzer was modified and computerized to provide an environmental chamber adequate for comparative measurement of diffusion and evaporation of liquids from polymers. The computer-instrument system supplements complex and expensive environmental wind tunnel research for preliminary measurements of relative rates of processes at both environmental and high temperatures and under atmospheric conditions. The diffusion and evaporation transport properties of liquid-state chloroesters, diesters, organophosphates, and ether-acetates were measured in or on urethane, polyester, and methacrylate polymers. The results obtained that are of general interest to computer-oriented chemists demonstrate the enhancement of instrument performance by the computer system; the important system components are signal analysis software, kinetic computations, graphic display of rate data, and data base generation. GRA

N88-29901# Rensselaer Polytechnic Inst., Troy, N.Y. Dept. of Chemistry.
EFFECT OF INTERFACIAL PHENOMENA ON CONTACT LINE HEAT TRANSFER-3 Final Report, 1 Oct. 1984 - 30 Sep. 1987
Peter C. Wayner, Jr. 20 Oct. 1987 10 p
(Grant AF-AFOSR-0306-84)
(AD-A194941; AFOSR-88-0046TR) Avail: NTIS HC A02/MF A01 CSCL 07B

The heat transfer characteristics of the contact line region of an evaporating thin liquid film were studied experimentally and theoretically. The effects of composition and temperature gradients on surface shear were analyzed and the results were successfully compared with previously reported experimental trends. The use of a constant vapor pressure boundary condition allowed the relative effects of surface tension, composition and temperature on fluid flow to be mapped. A small heat transfer cell was designed, built and used on the scanning stage of a scanning

microphotometer. The unique use of a microphotometer allows the microscopic details to be measured. GRA

N88-29902# Ballistic Research Labs., Aberdeen Proving Ground, Md.
GAS PHASE COMBUSTION CHEMISTRY OF NITRAMINE PROPELLANTS Final Report, Jun. 1985 - Jun. 1986
Andrzej W. Miziolek, Carl F. Melius, Larry R. Thorne, Paul J. Dagdigian, and Millard H. Alexander Mar. 1988 29 p Prepared in cooperation with Sandia National Labs., Johns Hopkins Univ., and Univ. of Maryland
(AD-A195082; BRL-TR-2906) Avail: NTIS HC A03/MF A01 CSCL 19A

The details of the chemical processes which occur during propellant combustion are generally not known, yet, they directly affect such important propellant combustion characteristics as ignition and burn rate. Recently, a collaboration has been set up to study these details in a coordinated and comprehensive way. This study is concentrating on nitramine-based propellants since their ignition and burn rate properties are of great current interest and importance. This report presents initial results of a long-term study in which both theoretical and experimental efforts are being pursued. Major results in theory include the calculation of thermochemical properties of a number of nitramine decomposition products and combustion intermediates, as well as specifying pathways for the formation of the reactive species HCN, H2CO, NO2 and N2O. Also, quantum chemical models for the interaction of nitrogen-type oxidizers with H atoms have been developed. GRA

N88-29903# Technische Univ., Berlin (West Germany). Fachbereich fuer Physik.
THE OPTICAL SPECTROSCOPY OF COPPER-BLUE LUMINESCENCE IN ZINC SULFIDE CRYSTALS. ZERO-PHONON LINE SPECTRA UNDER THE INFLUENCE OF MAGNETIC FIELD, TEMPERATURE AND EXCITATION INTENSITY Ph.D. Thesis
Adnan M. O. Ismail 1988 112 p Sponsored by the DAAD
(ETN-88-93122) Avail: NTIS HC A06/MF A01

In the copper blue emission band of ZnS:Cu crystals, two zero-phonon lines at 2.965 eV as well as a broad phonon side band are investigated in the helium temperature range by Zeeman spectroscopy. Only the higher energy line was observed in the excitation spectrum of the blue luminescence. The emission and excitation spectra of the zero-phonon lines are studied as a function of temperature, excitation, intensity, and external magnetic field up to 15 Tesla. The oscillator strength ratio of the high energy line to the low energy line is seven. At temperatures higher than 35K, the emission and the excitation lines disappear. Both lines grow parallel to each other with increasing excitation intensity. This behavior indicates that the two lines originate from the same center. ESA

N88-29904# California Univ., Irvine. Dept. of Chemistry.
THE EFFECT OF ORIENTED DEFECTS ON LONG-RANGE ORDERING OF HYDROCARBON FILMS: AZULENE ON Pt(111) Interim Report
Cynthia R. Flores and John C. Hemminger 8 Jun. 1988 7 p
(Contract N00014-87-K-0257)
(AD-A196089; TR-21) Avail: NTIS HC A02/MF A01 CSCL 07B

Low energy electron diffraction has been used to investigate the effect of ion bombardment-induced defects on the long-range ordering of azulene molecules absorbed on Pt(111). Such defects can lead to preferred directional ordering of the organic film. This is demonstrated by the stabilization of certain domains over others which are energetically equivalent on the defect-free surface. GRA

N88-29905# International Business Machines Corp., San Jose, Calif.
NONCONTACT PHOTO-THERMAL SENSING Final Report
Andrew C. Tam May 1988 40 p
(Contract N00014-83-C-0170)
(AD-A195450) Avail: NTIS HC A03/MF A01 CSCL 17E

This Final Report summarizes the research efforts and achievements of the research program which was concerned with the development of noncontact photo-thermal sensing techniques, useful for chemical and physical identification of distant samples. The goals of our research efforts include the exploration of various chemical and physical applications of noncontact photo-thermal sensing, understanding the basic physics and applications of pulsed photo-thermal and photo-acoustic generation, and the understanding of the capabilities of a typical photo-thermal LIDAR (Light Detection And Ranging). GRA

N88-29906*# National Aeronautics and Space Administration, Washington, D.C.
DECOMPOSITION OF HYDRAZINE BY HIGH FREQUENCY GLOW ELECTRICAL DISCHARGES
M. Suzuki, M. Miyazaki, and S. Takahashi Aug. 1988 32 p Transl. into ENGLISH from Nippon Kagaku Zasshi (Japan), no. 88, 1956 p 873-877 Transl. by Scientific Translation Service, Santa Barbara, Calif.
(Contract NASw-4307)
(NASA-TT-20240; NAS 1.77:20240) Avail: NTIS HC A03/MF A01 CSCL 07D

Originally, de Groot et al. examined electrical conductivity phenomena in terms of the thermodynamics of irreversible processes. They considered the system to be discontinuous and calculated only the differences between the opposing ends of the process. Thus these theories are phenomenological. In the present work, thermodynamics is developed as a continuous system based on hydrodynamics and the entropy production for a thin capillary. It is shown that electroconductivity can be interpreted without difficulty. For the electric double layer, the effects of electrolytes and surface conductivity and the gap width were calculated for the Gouy model. Author

N88-29907 Institut d'Aeronomie Spatiale de Belgique, Brussels.
AERONOMIC PROBLEMS OF MOLECULAR OXYGEN PHOTODISSOCIATION. PART 2: THEORETICAL ABSORPTION CROSS SECTIONS OF THE SCHUMANN-RUNGE BANDS AT 79 K
Marcel Nicolet, Stanislas Cieslik, and Robert Kennes 1988 45 p Submitted for publication Sponsored in cooperation with the Commission of the European Communities and Pennsylvania State Univ, University Park, Pa.
(Contracts N000-14-86-K-0265; FC-85-563)
(Aeronomica-Acta-A-331-1988; ISSN-0065-3713; ETN-88-93071)
Avail: Institut d'Aeronomie Spatiale de Belgique, 3 Avenue Circulaire, B-1180 Brussels, Belgium

Theoretical spectra corresponding to the domain of the rotational lines of the 2-0 to 12-0 bands of the Schumann-Runge system of O2 at 79 K are presented. Calculated absorption cross sections are compared with laboratory measurements made at the same temperature. The calculations were based on theoretical determinations at 300 K established after a comparison with results of laboratory measurements made at the same temperature. Such an analysis in which the band oscillator strengths are associated with averaged linewidths of the rotation lines for each band, and with their underlying continuum, gives consistent values for the spectroscopic parameters of the O2 Schumann-Runge bands. ESA

N88-29908# Utah Univ., Salt Lake City. Dept. of Chemistry.
ATTENUATED TOTAL REFLECTANCE FT-IR SPECTROSCOPY TO MEASURE INTERFACIAL REACTION KINETICS AT SILICA SURFACES Technical Report No. 5, Sep. 1987 - Jul. 1988
D. B. Parry and J. M. Harris 15 Jul. 1988 15 p
(Contract N00014-85-K-0712)
(AD-A196330) Avail: NTIS HC A03/MF A01 CSCL 07D

Attenuated total reflection (ATR) FT-IR spectroscopy has been adapted to measure the rates of chemical modification reactions at silica surfaces. In this method, a silicon ATR crystal is oxidized

at 1000C under dry O2 to produce a silicon dioxide layer on the crystal surface, the thickness of which can be measured using ellipsometry. The oxidized silicon layer is then used as a model silica surface in measurements of the rates chemical modification. A flow cell is filled with a solution of a surface active reagent. ATR infrared spectra are obtained at regular time intervals, where confinement of the intensity of the interface by total internal reflection provides a measure of local changes in concentration of species which adsorb or bind to the surface. The effect of the silicon dioxide layer on the sensitivity of measuring absorbance at the silica-solution interface is investigated. A model reaction study is carried out to determine the binding kinetics diphenylchlorosilane to silica from carbon tetrachloride solution. The technique yields both in situ kinetic and structural information about the reaction of this reagent with silica surfaces; ATR spectroscopy, infrared spectroscopy, and liquid/solid interfaces. GRA

N88-29909*# National Aeronautics and Space Administration, Washington, D.C.

ACTIVE SITES AND ROLES OF SOLID ACID BASE CATALYSTS

T. Iizuka Aug. 1988 23 p Transl. into ENGLISH from Kotai San Enki Shokubai no Kasseiten to sono Hataraki, Shokubai 26 (Japan), no. 3, 1984 p 171-176 Transl. by SCITRAN, Inc., Santa Barbara, Calif.

(Contract NASw-4307)

(NASA-TT-20333; NAS 1.77:20333) Avail: NTIS HC A03/MF A01 CSCL 07D

A review on both acid and base catalyst with 42 references is presented. Isomerization of butene, H2-D2 exchange reaction, and hydrogenation reactions are discussed. Author

N88-29910# Advisory Group for Aerospace Research and Development, Neuilly-Sur-Seine (France). Propulsion and Energetics Panel.

COMBUSTION AND FUELS IN GAS TURBINE ENGINES

Jun. 1988 515 p In ENGLISH and FRENCH Symposium held in Chania, Greece, 19-23 Oct. 1987

(AGARD-CP-422; ISBN-92-835-0465-8) Copyright Avail: NTIS HC A22/MF A01

The attention of combustor designers and researchers has focused upon two main factors: the identification of the significance of fuel degradation upon combustion design and performance, and the potential prizes to be gained by the development of better design techniques. The aim of the conference was to review progress made in these areas under four main subject headings: namely, alternative fuels and fuel injection, combustor development, soot and radiation, and the development of mathematical models for the design of gas turbine combustors. For individual titles, see N88-29911 through N88-29951.

N88-29911# Pratt and Whitney Aircraft, West Palm Beach, Fla. Engineering Div.

FUEL PROPERTY EFFECTS ON THE US NAVY'S TF30 ENGINE c07

S. A. Mosier and P. A. Karpovich (Naval Air Propulsion Test Center, Trenton, N.J.) *In* AGARD, Combustion and Fuels in Gas Turbine Engines Jun. 1988 15 p (For primary document see N88-29910 24-25)

Copyright Avail: NTIS HC A22/MF A01

The TF30 engine was introduced into Navy service in 1972 and is scheduled to continue to power the carrier based F14 for some time. Although the engine was designed and developed to operate on specification grade JP-5 fuel, it is conceivable that during its lifetime, the TF30 might have to operate on out-of-spec or broadened-spec fuels. This contingency could arise should the availability of high grade petroleum crude oil used for aircraft fuel production be decreased. Therefore, a program of experimentation and analysis was conducted to evaluate the effects of broadened-spec petroleum fuels on the performance, durability and operability of the TF30-P-414A engine. As fuel quality deteriorated, some reductions in engine performance characteristics were observed. However, based upon limited time testing, the TF30-P-414A engine was shown to be capable of operating on liquid petroleum fuels having a wide range of properties. Author

N88-29912# Illinois Univ., Urbana-Champaign. Dept. of Mechanical and Industrial Engineering.

ALTERNATIVE FUEL SPRAY BEHAVIOR

J. P. Asheim and J. E. Peters *In* AGARD, Combustion and Fuels in Gas Turbine Engines Jun. 1988 16 p (For primary document see N88-29910 24-25)

Copyright Avail: NTIS HC A22/MF A01

The effects of alternative fuels on the combustion characteristics of a liquid fuel sprays were examined. Fuel properties were systematically varied and the effects of these variations on the structure of the spray flames were calculated. In addition, a comparison was made of the differences in two spray flames fueled by the standard NATO F-40 fuel and a proposed alternative fuel, the AGARD Research Fuel. The calculations were performed using a reacting, two phase, two-dimensional flow code which utilizes a Lagrangian calculation of droplet trajectories and an Eulerian approach for the gas phase flow field. Interactions between the drops and the gas phase were accomplished through the particle in cell technique with exchange of mass, momentum and energy between the two phases. A global reaction scheme was used with the reaction rate determined by the minimum of either an Arrhenius rate or mixing rate. Fuel property changes which affect droplet size and volatility were shown to have significant effects on droplet trajectory patterns. However, for the flow field examined, these trajectory changes only moderately modify the fuel vaporization pattern within the spray. Author

N88-29913# Purdue Univ., West Lafayette, Ind. School of Mechanical Engineering.

ATOMIZATION OF ALTERNATIVE FUELS

Arthur H. Lefebvre *In* AGARD, Combustion and Fuels in Gas Turbine Engines Jun. 1988 14 p (For primary document see N88-29910 24-25)

Copyright Avail: NTIS HC A22/MF A01

The influence of atomization quality on several key aspects of combustion performance is reviewed. The performance parameters considered include combustion efficiency, lean blowout, and lean lightup, and also the pollutant emissions of carbon monoxide, unburned hydrocarbons, oxides of nitrogen, and smoke. The fuel properties of importance are described and equations are presented for estimating the effects of changes in fuel properties on spray characteristics for the main types of fuel nozzle employed in aero gas turbines, namely plain orifice, pressure swirl, and airblast atomizers. The anticipated effects on atomization of changes from conventional to alternative fuels is discussed. Author

N88-29914# Centre d'Etudes et de Recherches, Toulouse (France).

SIMULATION STUDY OF SPRAYING, STREAMING AND VAPORIZATION PHENOMENA ASSOCIATED WITH FUEL INJECTION [ETUDE PAR SIMULATION DES PHENOMENES DE PULVERISATION, DE RUISSELEMENT ET DE VAPORISATION LIES A L'INJECTION DE CARBURANT]

P. Hebrard and G. Lavergne *In* AGARD, Combustion and Fuels in Gas Turbine Engines Jun. 1988 13 p In FRENCH (For primary document see N88-29910 24-25)

Copyright Avail: NTIS HC A22/MF A01

Combustion modeling requires a knowledge of the limit conditions and the physical models that can often be provided only through experience. Such an experimentally-based approach for studying injection-associated phenomena, involving simulation starting from experimental measurements, is presented. An evaluation of the performances of the different types of injectors used in the combustion chambers is carried out through particle size analysis: local distribution of size, the Sauter mean diameter, and measurements of drop concentration. Models describing the phenomena of evaporation, acceleration and impact of drops on a hot wall were tested experimentally. The modeling of premixed

fuel injection with a prevaporization type injector is discussed as an example of a modeling approach using experimental results.
Author

N88-29915# Karlsruhe Univ. (West Germany). Lehrstuhl und Inst. fuer Thermische Stroemungsmaschinen.
TURBULENCE EFFECTS ON THE DROPLET DISTRIBUTION BEHIND AIRBLAST ATOMIZERS
S. Wittig, W. Klausmann, and B. Noll *In* AGARD, Combustion and Fuels in Gas Turbine Engines Jun. 1988 13 p Sponsored in part by the Forschunbsvereinigung Verbrennungskraftmaschinen, e.V., and German National Science Foundation, Fed. Republic of Germany (For primary document see N88-29910 24-25)
Copyright Avail: NTIS HC A22/MF A01

Turbulent fluctuations of the airflow in gas turbine combustion chambers have decisive influence on the mixing of fuel droplets and air both in premixing regions and primary zones. Detailed measurements in a recirculating, droplet charged airflow in a combustor model are conducted with an optical diffraction type particle sizer. These investigations yield information about the local fuel concentrations as well as the local concentration weighted diameter distributions under cold and hot airflow conditions. The spray is produced by a prefilming airblast nozzle, which is built into the combustor model. The calculation of the above mentioned quantities using a new computational model shows that in considering turbulence fluctuations significant improvement of the results is obtained and excellent agreement between predicted and measured values is achieved. Therefore, the results indicate that turbulence can be one of the major influencing parameters on droplet distribution.
Author

N88-29916# United Technologies Research Center, East Hartford, Conn.
NOZZLE AIRFLOW INFLUENCES ON FUEL PATTERNATION
T. J. Rosfjord and W. A. Eckerle (Clarkson Univ., Potsdam, N.Y.) *In* AGARD, Combustion and Fuels in Gas Turbine Engines Jun. 1988 12 p Previously announced in IAA as A88-44765 (For primary document see N88-29910 24-25)
(Contract F33615-85-C-2515)
Copyright Avail: NTIS HC A22/MF A01

The velocity and turbulence levels downstream of eight variations of a model gas turbine, aerating, fuel nozzle were measured. The nozzle configurations were assemblies which purposefully altered the airflow in a swirler or contouring swirl vane trailing edges. Data were acquired by a traversing, two component laser velocimeter in planes 0.060 in. or 2.50 in. downstream from the nozzle exit. Analyses of these data indicated that very symmetric flow fields can be produced. Such control was easier to achieve for the airflow than the fuel, supporting the position that nozzle patternation quality was more dependent on the fuel distribution in the nozzle. The presence of swirler wakes could always be discerned at the nozzle exit; the extreme variations imposed by coarse swirlers could dominate the flow. Such airflow influences were not apparent in the velocity profiles at downstream locations. However, their influence in convecting a higher fuel mass flux persisted from the nozzle exit and produced extreme variations in the spray pattern.
Author

N88-29917# National Research Council of Canada, Ottawa (Ontario). Div. of Mechanical Engineering.
MULTIPLE SCATTERING EFFECTS IN DROP SIZING OF DENSE FUEL SPRAYS BY LASER DIFFRACTION
Oemer L. Guelder *In* AGARD, Combustion and Fuels in Gas Turbine Engines Jun. 1988 15 p (For primary document see N88-29910 24-25)
Copyright Avail: NTIS HC A22/MF A01

Practical schemes to correct the effect of multiple scattering in a dense drop field on the measured distribution parameters by laser light scattering based spray sizing techniques are presented. An experimental study, involving multi-modal distributions and drop field which can not be adequately described by single mode two parameter distribution, is described. Data from the experimental program were employed to develop empirical expressions to correct the measured spray parameters at high obscuration levels. Accuracies of the proposed expressions are acceptable for engineering applications, and comparable to the accuracies involved in conversion of light scattering data to drop size information.
Author

N88-29918# Deutsche Forschungs- und Versuchsanstalt fuer Luft- und Raumfahrt, Cologne (West Germany). Inst. fuer Antriebstechnik.
INFLUENCE OF OPERATING CONDITIONS ON THE ATOMIZATION AND DISTRIBUTION OF FUEL BY AIR BLAST ATOMIZERS
M. Cao, H. Eickhoff, F. Joos, and B. Simon (Technische Univ., Munich, West Germany) *In* AGARD, Combustion and Fuels in Gas Turbine Engines Jun. 1988 8 p Sponsored by the Federal German Ministry of Research and Technology, Berlin (For primary document see N88-29910 24-25)
Copyright Avail: NTIS HC A22/MF A01

The performance of a gas turbine combustion chamber depends essentially on the distribution of the fuel in the primary zone. Ignition, stability of combustion, wall temperatures, and smoke and pollutant emission are all affected. Maintaining a fixed geometry, the droplet size and spray angle under variation of the air pressure drop at constant temperature were measured using two test liquids in an air blast atomizer system. Correlation equations were provided for both variables. Known correlations were confirmed for the droplet size. The spray angle is pressure related, increasing very rapidly with increasing pressure.
Author

N88-29919# Cranfield Inst. of Tech., Bedford (England). School of Mechanical Engineering.
SPRAY PERFORMANCE OF A VAPORIZING FUEL INJECTOR
A. K. Jasuja and H. C. Low (Rolls-Royce Ltd., Bristol, England) *In* AGARD, Combustion and Fuels in Gas Turbine Engines Jun. 1988 13 p (For primary document see N88-29910 24-25)
Copyright Avail: NTIS HC A22/MF A01

The spray performance of a vaporizer fuel injector of a type that has accumulated extensive service experience in sub- and super-sonic commercial and military aircraft applications is examined. Spray performance data covers a wide range of operating conditions including the effects of fuel quality as well as the atomizing air temperature. The objective is to further not only the current level of understanding regarding the fundamental functional aspects of vaporizer technology but also the data base for future designs.
Author

N88-29920# Laval Univ. (Quebec). Dept. du Genie Mecanique.
THE CHARACTERIZATIN OF COMBUSTION BY FUEL COMPOSITION: MEASUREMENTS IN A SMALL CONVENTIONAL COMBUSTOR
D. Kretschmer and J. Odgers *In* AGARD, Combustion and Fuels in Gas Turbine Engines Jun. 1988 10 p Sponsored by National Defence Canada (For primary document see N88-29910 24-25)
Copyright Avail: NTIS HC A22/MF A01

In a continuing program on the effects of fuel properties on combustion, some 20 pure hydrocarbons and synthesized fuels were tested at atmospheric conditions in a one third scale version of an aircraft type combustor. This combustor used a Simplex type pressure jet atomizer. Each fuel was burned over a range of air-fuel ratios, and at each condition, a full exhaust gas analysis was done, exhaust temperature distribution was measured, as also weak extinction. The results and their implications are discussed.
Author

N88-29921# Office National d'Etudes et de Recherches Aerospatiales, Palaiseau (France).
FLAME STABILIZATION IN A REHEAT COMBUSTOR
A. Cadiou *In* AGARD, Combustion and Fuels in Gas Turbine Engines Jun. 1988 10 p In FRENCH; ENGLISH summary (For primary document see N88-29910 24-25)
Copyright Avail: NTIS HC A22/MF A01

In a reheat burner, combustion is stabilized with flameholders.

The stabilization depenJs on the following parameters: Mach number, temperature, pressure and equivalence ratio of the flow, flameholder geometry. Many experimental measurements have allowed the calculation of a correlating parameter including the Mach number and the temperature. For the geometry, studies on linear stabilizers in two-dimensional flows have shown that the height of the stabilizer is a convenient parameter. An accurate experimental study of the recirculation zone downstream annular flameholders in a axisymmetric flow have pointed out the effect of another geometrical parameter, the diameter of the flameholder. The experimental results have improved the knowledge of the flame stabilization mechanism downstream annular flameholders. Author

N88-29922# Rolls-Royce Ltd., Bristol (England).
HIGH PERFORMANCE TURBOFAN AFTERBURNER SYSTEMS
A. Sotheran *In* AGARD, Combustion and Fuels in Gas Turbine Engines Jun. 1988 10 p (For primary document see N88-29910 24-25)
Copyright Avail: NTIS HC A22/MF A01

The modern turbofan afterburner is characterized by its high boost and efficiency and by its compact geometry which is achieved by locating the flameholding baffles immediately downstream of the turbine exhaust plane of the engine core and bypass gas stream. At the confluence, the stream divider may be a simple cylinder or it may be of lobed configuration to encourage mixing between the two gas streams in the downstream jet pipe in order to improve the unboosted thrust of the engine. The geometry of the afterburner hardware must be adapted to suit the choice of mixed or unmixed configurations. In flight, selection of the afterburner must be fast and reliable under all flight conditions with times to full thrust of the order of only a second or two. Both the light up and the subsequent acceleration to full thrust are expected to be smooth with no excessive initial thrust jump. Synchronization and matching of the afterburner fuel with the variable final nozzle must be accurate at all times to maintain the engine turbomachinery on its required running lines. The afterburner must always be free of combustion driven pressure oscillations which can occur either in cross stream modes or in longitudinal modes, both of which can be mechanically damaging and, in some cases, cause fan surge and other intolerable effects in the engine. The afterburner must incorporate appropriate measures to avoid various potential thermal problems including fuel boiling and gumming in the supply manifolds and excessive heat transfer to the jet pipe and aircraft engine bay. Author

N88-29923# Technische Univ., Munich (West Germany). MTU Motoren- und Turbinen-Union.
COMPARISON OF THE PERFORMANCE OF A REVERSE FLOW ANNULAR COMBUSTION CHAMBER UNDER LOW AND HIGH PRESSURE CONDITIONS
F. Joos and B. Simon *In* AGARD, Combustion and Fuels in Gas Turbine Engines Jun. 1988 10 p Sponsored by the Federal German Ministry of Research and Development, Berlin (For primary document see N88-29910 24-25)
Copyright Avail: NTIS HC A22/MF A01

Combustor development testing is usually carried out under different pressure conditions; low pressure burning test for the optimization of the fuel distribution inside the combustor and high pressure tests for demonstrating the desired performance. Comparison of the results under these two test conditions often reveal discrepancies, especially in wall temperatures and exit temperature patterns, which cannot be attributed simply to the greater flame radiation and heat release rate associated with the tests at high pressure. Another cause, in particular, lies in differences in the fuel distribution in the primary zone as a function of pressure conditions. This phenomenon is demonstrated by measurements and 3-D 2-phase flow field calculations. Author

N88-29924# Imperial Coll. of Science and Technology, London (England). Fluids Section.
FLOW CHARACTERISTICS OF A MODEL ANNULAR COMBUSTOR
A. F. Bicen, D. Tse, and J. H. Whitelaw *In* AGARD, Combustion and Fuels in Gas Turbine Engines Jun. 1988 13 p Sponsored by Rolls Royce Plc and the Ministry of Defence, United Kingdom (For primary document see N88-29910 24-25)
Copyright Avail: NTIS HC A22/MF A01

Measurements are reported of the velocity and passive scalar characteristics of the isothermal flow in a model combustor which comprises a T-vaporizer and two rectangular sectors of an annular combustor similar to one used in small gas turbine engines. Mean temperatures were also obtained in a reacting flow with an overall equivalence ratio similar to that of takeoff conditions. The results were obtained with a combination of laser velocimetry, thermocouples and probe techniques and quantify the effects of flow asymmetries in the vaporizer fuel arrangement and of different alignments of the primary holes with respect to the vaporizer position. Flow visualization results are also included to indicate the general features of the combustor flow. Author

N88-29925# Southwest Research Inst., San Antonio, Tex.
FUEL EFFECTS ON FLAME RADIATION AND HOT-SECTION DURABILITY
C. A. Moses and P. A. Karpovich (Naval Air Propulsion Test Center, Trenton, N.J.) *In* AGARD, Combustion and Fuels in Gas Turbine Engines Jun. 1988 16 p (For primary document see N88-29910 24-25)
Copyright Avail: NTIS HC A22/MF A01

The results of combustor experiments relating to fuel effects on combustor durability are summarized and analyzed with respect to Navy aircraft operations and maintenance. By combining life ratio models with data on mission profiles, models were developed that predict the impact of flying an aircraft on a fuel of reduced hydrogen content in terms of the combustor life lost in flying a typical mission. To determine the effect of decreasing hydrogen content on maintenance requirements, the life ratio models were combined with data obtained from maintenance depots on combustor life along with information on the importance of combustor life in determining engine overhaul schedules. From this, it was possible to identify which engines or aircraft would be most affected by decreases in hydrogen content, and at what point increases in maintenance requirements are likety to be realized. Author

N88-29926# California Univ., Irvine. Combustion Lab.
THE PERFORMANCE OF A SURROGATE BLEND IN SIMULATING JP-4 IN A SPRAY-FUELED COMBUSTOR
G. S. Samuelsen and C. P. Wood *In* AGARD, Combustion and Fuels in Gas Turbine Engines Jun. 1988 6 p Sponsored in part by the Naval Air Propulsion Center (For primary document see N88-29910 24-25)
(Contract F08635-86-C-0309)
Copyright Avail: NTIS HC A22/MF A01

A surrogate fuel was developed to simulate the atomization and combustor performance of a practical distillate JP-4. The surrogate is comprised of 14 pure hydrocarbons and formulated based on the distillation curve and compound of the distillate parent. In previous work, the atomization performance (evaluated in terms of the atomization quality in an isothermal chamber), and the combustor performance (evaluated in terms of the velocity and thermal fields in a spray fueled combustor) were found to be equivalent for the parent and surrogate JP-4. The sooting performance of the two fuels is addressed, as well as two reference fuels (a JP-5 and isooctane) of purposefully disparate properties. The sooting performance of the parent and surrogate JP-4 are nearly identical, and distinctly different from that of either the JP-5 or the isooctane. The surrogate represents, as a result, an attractive fuel blend for the study of fuel compositional effects on the sooting performance of petroleum fuels in spray fueled combustor. Author

N88-29927# Michigan Univ., Ann Arbor. Dept. of Aerospace Engineering.
RADIATION FROM SOOT-CONTAINING FLAMES
G. M. Faeth, J. P. Gore, and Y. R. Sivathanu *In* AGARD,

Combustion and Fuels in Gas Turbine Engines Jun. 1988 12 p (For primary document see N88-29910 24-25)
(Grant NBS-60-NAN-135D-0576)
Copyright Avail: NTIS HC A22/MF A01

The thermal radiation properties of turbulent soot containing diffusion flames are considered, treating: scalar structure, excluding soot; soot properties; and turbulence/radiation interactions. The laminar flamelet concept, implying universal correlations of scalar properties as a function of mixture fraction appears to be effective for estimates of scalar structure needed for analysis of flame radiation. Extension of the laminar flamelet concept to soot volume fractions was also encouraging; however, universality is cruder than for gas properties due to effects of finite rate chemistry. Turbulence/radiation interactions were studied by comparing radiation perdictions based on statistical simulation of scalar properties along a radiation path (stochastic analysis) with conventional results using time averaged properties along the path. Stochastic predictions of spectral radiation intensities are found to be 40 to 100 percent higher than mean property predictions in luminous turbulent diffusion flames, suggesting significant effects of turbulence/radiation interactions. Author

N88-29928# Cranfield Inst. of Tech., Bedford (England). School of Mechanical Engineering.
FLAMELET CHEMISTRY MODELLING OF SOOT FORMATION FOR RADIATION
J. B. Moss, C. D. Stewart, and K. J. Syed *In* AGARD, Combustion and Fuels in Gas Turbine Engines Jun. 1988 12 p Sponsored in part by Ministry of Defence, Pyestock, United Kingdom, Science and Engineering Research Council and British Gas, United Kingdom (For primary document see N88-29910 24-25)
Copyright Avail: NTIS HC A22/MF A01

The development of generalized models for radiative heat transfer in the gas turbine requires the detailed prediction of the turbulent scalar fields, most notably for temperature, the principal gaseous species and particulate soot. Mixing limited descriptions of the turbulent combustion process have proved quite successful in modeling the effects of heat release on the flow field. However, the chemical aspects of the problem, fuel specific features and the multi component composition, are poorly reproduced. Laminar flamelet modeling currently offers the best prospect for incorporating realistic complex chemistry into the computations. A strategy is described to extend laminar flamelet modeling of turbulent non-premixed hydrocarbon combustion to include a simplified mechanism for soot formation. In the abscence of a widely applicable multistep kinetic mechanism the formation rate must be inferred from detailed measurement but comparatively comprehensive flow field modeling is necessary to distinguish fluid mechanic and chemical kinetic effects and hence interpret the observations in model terms. Author

N88-29929# Instituto Superior Tecnico, Lisbon (Portugal). Dept. of mechanical Engineering.
RADIATION TRANSFER IN GAS TURBINE COMBUSTORS
M. G. Carvalho and P. J. M. Coelho *In* AGARD, Combustion and Fuels in Gas Turbine Engines Jun. 1988 22 p Sponsored by Instituto Nacional de Investigacao Cientifica, Lisbon, Portugal (For primary document see N88-29910 24-25)
Copyright Avail: NTIS HC A22/MF A01

The prediction of the local flow, heat transfer and combustion processes inside a three-dimensional can combustor chamber of a gas turbine is presented. A 3-D numerical solution technique is used to solve the governing time averaged partial differential equations and the physical modeling for the turbulence, combustion and thermal radiation. The heat transfer modeling is emphasized. A method to calculate the distribution of temperature, radiative heat flux and total heat flux of the liner is described. The implications of neglecting radiative heat transfer in gas turbine combustion chamber calculations are discussed. The influence of working pressure on the radiative heat transfer is investigated comparing the radiative heat flux and the temperature distribution of the liner for three different working pressures: 5, 15 and 25 bar. Author

N88-29930# Royal Aircraft Establishment, Farnborough (England). Propulsion Dept.
GAS TURBINE SMOKE MEASUREMENT: A SMOKE GENERATOR FOR THE ASSESSMENT OF CURRENT AND FUTURE TECHNIQUES
S. P. Girling *In* AGARD, Combustion and Fuels in Gas Turbine Engines Jun. 1988 10 p (For primary document see N88-29910 24-25)
Copyright Avail: NTIS HC A22/MF A01

Smoke measurement from gas turbine engines is one instrumentation technique that remains, literally, a black art. Current methods are inaccurate, slow, insensitive and unable to detect transients. A smoke generator was developed capable of generating by pyrolysis of aviation kerosene, stable levels of smoke for prolonged periods, representative of that from engines. Particle size measurements have enabled the comparison of smokes from different sources and provided a greater understanding of the problems of representative sampling using currently approved methods. Several alternative measurement techniques were evaluated using the smoke generator, precluding the need for expensive engine testing. This has promoted research into instrumentation that will give a truer indication of particulate criteria of interest to the engine designer and customer, for example truer visibility and erosiveness. Author

N88-29931# Karlsruhe Univ. (West Germany). Lehrstuhl und Inst. fuer Thermische Stroemungsmaschinen.
PARTICLE SIZE MEASUREMENTS IN SOOTING COMBUSTION SYSTEMS
S. Wittign and H.-J. Feld *In* AGARD, Combustion and Fuels in Gas Turbine Engines Jun. 1988 11 p Sponsored in part by Stiftung Volkswagen AG, Fed. Republic of Germany (For primary document see N88-29910 24-25)
Copyright Avail: NTIS HC A22/MF A01

Radiation effects caused by the presence of soot particles are of dominant influence in gas turbine combustors, especially on the stress distribution in the flame tube. In studying the two-phase flow within and after the combustor experimentally, a wide spectrum of soot particle and fuel droplet sizes is to be considered. Two optical measuring techniques were used throughout. First, the dispersion quotient (DQ) technique was applied to determing the size of the early soot particles, i.e., in the small-diameter range. The second method, the well established Multiple-Ratio-Single-Particle Counter (MRSPC), was used to measure the larger particle sizes, i.e., fuel droplets and soot. Furthermore, attention was focused on data acquisition- and analysis-techniques. Experimental results were obtained from measurements in a combustor with high concentration of soot particles and in the exhaust gas of a gas turbine. Author

N88-29932# Technische Hochschule, Darmstadt (West Germany). Inst. fuer Physikalische Chemie.
LARGE IONIC SPECIES IN SOOTING ACETYLENE AND BENZENE FLAMES
Ph. Gerhardt, K. H. Homann, S. Loeffler, and H. Wolf *In* AGARD, Combustion and Fuels in Gas Turbine Engines Jun. 1988 11 p Sponsored by Deutsche Forshcungagemeinschaft and Fonde der Chemischen Industrie, Fed. Republic of Germany (For primary document see N88-29910 24-25)
Copyright Avail: NTIS HC A22/MF A01

Ionic species with masses from 24 to 10,000 u were studied in premixed, fuel-rich, low-pressure acetylene and benzene flames by means of a time-of-flight mass spectrometer. Total positive and negative ion concentrations in the flame were also determined by sampling ions from a beam. The mass spectrum of positive poly-yne ions corresponds to two different Poisson distributions for the groups C sub 2nH sub 3(+) and C sub 2n + 1H sub 3(+) respectively. THese ions are not related to soot formation. The growth of polycyclic aromatic hydrocarbon ions, however, could be followed up to a mass of about 2000 u where coagulation started resulting in ions of about 4000 u which then grew further. The relative volume fractions of charged and neutral soot was determined using a method of soot deposition in vacuum. The

results can be interpreted by a partial-equilibrium model. Polyhedral carbon ions were detected as a completely new class of flame ions similar to those found in the laser-evaporation of graphite. The C sub 60(+) is the dominant positive ion of this group, while C sub 50(+) and a broad distribution of C sub 2n(-) with 2n up to about 210 are characteristic for the negative polyhedral ions.
Author

N88-29933# Leeds Univ. (England). Dept. of Fuel and Energy.
RATES OF FORMATION OF SOOT FROM HYDROCARBON FLAMES AND ITS DESTRUCTION
J. Mullins, B. Simmons, and A. Williams *In* AGARD, Combustion and Fuels in Gas Turbine Engines Jun. 1988 14 p Sponsored by IEA, Lucas-CAV Ltd, British Gas Plc and SERC, United Kingdom (For primary document see N88-29910 24-25)
Copyright Avail: NTIS HC A22/MF A01

The equations that were proposed in the literature to describe the rate of soot formation in hydrocarbon flames are surveyed. Recent work using a shock tube to measure soot formation rates is outlined and the correlation equation proposed compared with that of other workers. Data on the rate of combustion of soot particles are also outlined and combined with recent measurements to give an overall soot oxidation rate expression. The two equations are combined to give an expression suitable to describe soot formation and burn out for gas turbines and tested to a limited degree.
Author

N88-29934# Goettingen Univ. (West Germany). Inst. fuer Physikalische Chemie.
THE INFLUENCE OF PRESSURE ON SOOT FORMATION
H. Gg. Wagner *In* AGARD, Combustion and Fuels in Gas Turbine Engines Jun. 1988 11 p (For primary document see N88-29910 24-25)
Copyright Avail: NTIS HC A22/MF A01

The influence of pressure on soot formation was investigated for pyrolysis, premixed flames, and diffusion flames. Detailed kinetic studies are available for the first two. It is shown that the essential steps: particle inception, induction time (tau), coagulation, and surface growth remain similar for different pressures, also the influence of temperature on the maximum amount of soot formed. Tau for pyrolysis depends on the carbon density, strongly on temperature, and only slightly on pressure. The coagulation rate constant decreases slightly towards higher pressures. The amount (f sub v) of soot formed per cubic cm for a given fuel-air mixture increases with pressure P like P sup n, n was found for C(sub 2)H(sub 4)-air up to 3, for other fuels near one, it depends on pressure. Larger (f sub v) means larger soot particles, larger radiation losses and longer oxidation time at a given temperature and therefore higher chance for smoke emission.
Author

N88-29935# General Electric Co., Cincinnati, Ohio. Aircraft Engines.
NUMERICAL MODELS FOR ANALYTICAL PREDICTIONS OF COMBUSTOR AEROTHERMAL PERFORMANCE CHARACTERISTICS
D. L. Burrus, W. Shyy, and M. E. Braaten (General Electric Co., Schenectady, N.Y.) *In* AGARD, Combustion and Fuels in Gas Turbine Engines Jun. 1988 25 p (For primary document see N88-29910 24-25)
Copyright Avail: NTIS HC A22/MF A01

An overview of the work performed at GE Aircraft Engines under an ongoing program to develop and improve the sophisticated analytical models for the design and analysis of aircraft turbine engine combustors is presented. This effort has focused on the full three-dimensional (3-D) elliptic combustor internal flow model. The objectives of the program are reviewed. The progress made in the past five years is discussed starting with the initial application and assessment of first generation 3-D combustor models based on cartesian grids, progressing to the development and recent application of an improved second generation 3-D combustor model based on a body fitted generalized curvilinear grid. Finally, a brief review of planned future modeling activities to be conducted under this program will be discussed.
Author

N88-29936# General Motors Corp., Indianapolis, Ind. Gas Turbine Div.
GAS TURBINE COMBUSTION MODELING Status Report
Hukam C. Mongia *In* AGARD, Combustion and Fuels in Gas Turbine Engines Jun. 1988 14 p (For primary document see N88-29910 24-25)
Copyright Avail: NTIS HC A22/MF A01

To effectively use multidimensional models for gas tubine combustor design and development activities, a method is presented to compute aerothermal performance parameters including CO, unburned hydrocarbon, NOx and smoke emissions; lean blowout and ignition fuel/air ratios, and pattern factor. To further improve modeling accuracy, advances are required in numerics and physical submodels of turbulence and spray transport processes. A status report is presented on the ongoing Allison modeling activities.
Author

N88-29937# Sheffield Univ. (England). Dept. of Chemical Engineering and Fuel Technology.
THREE-DIMENSIONAL GAS TURBINE COMBUSTOR MODELLING
P. N. Wild, F. Boysan, J. Swithenbank, and X. Lu *In* AGARD, Combustion and Fuels in Gas Turbine Engines Jun. 1988 14 p (For primary document see N88-29910 24-25)
Copyright Avail: NTIS HC A22/MF A01

A mathematical model of the finite difference type is employed to predict the three-dimensional reacting flows within realistic combustor geometries. Both algebraic stress and k-epsilon submodels were employed for turbulence, together with combustion models of the Magnussen type and a detailed fuel spray model. A Lagrangian type model for the calculation of residence time distribution has also proved useful in validating the predicted flow fields. Modeling is carried out for a cylindrical combustor can and for a sector of an annular gas turbine burner. Both of these possess swirl stabilized primary zones. Experimental measurements of gas velocity, combustor resistence time distribution, composition and temperature were employed for model validation and results obtained to date were encouraging.
Author

N88-29938# Karlsruhe Univ. (West Germany). Lehrstuhl und Inst. fuer Thermische Stroemungsmaschinen.
ON THE APPLICATION OF FINITE-DIFFERENCE TECHNIQUES FOR THE COMPUTATION OF THE FLOW FIELD IN GAS TURBINE COMBUSTORS WITH COMPLEX GEOMETRIES
S. Wittig, H.-J. Bauer, and B. Noll *In* AGARD, Combustion and Fuels in Gas Turbine Engines Jun. 1988 14 p Sponsored by German National Science Foundation, Fed. Republic of Germany (For primary document see N88-29910 24-25)
Copyright Avail: NTIS HC A22/MF A01

A finite-volume method is presented for solving the time-averaged two-dimensional Navier-Stokes equations in non-orthogonal curvilinear coordinates. In contrast to most existing codes, a non-staggered grid is employed for the discretization of the momentum equations avoiding the onset of pressure and velocity ocsillations by additional steps. In a first step, turbulent transport is taken into account by the standard k, -model. As a test-case, the turbulent flow through a model combustor with variable cross-sectional area and dilution air jets is considered. The results of the computations are compared with measurements as well as with finite-difference calculations of other available codes utilizing orthogonal coordinates especially adapted for this geometry. The advantages of the new non-orthogonal approach are demonstrated. It is shown that the proposed mathematical model serves as a powerful tool for the computation of turbulent separated flows in ducts with complex geometries pertinent to modern gas turbine combustors, especailly those of the reverse-flow type.
Author

N88-29939# Politecnico di Milano (Italy). Dipt. di Energetica.
NUMERICAL MODELING OF COMBUSTION PROCESSES IN GAS TURBINES
L. Galfetti, M. Belli, and C. Bruno (Consiglio Nazionale delle Ricerche, Peschiera Borromeo, Italy) *In* AGARD, Combustion and Fuels in Gas Turbine Engines Jun. 1988 14 p Prepared in cooperation with National Center for Energetics and Propulsion, Peschiera Borromeo, Italy (For primary document see N88-29910 24-25)
Copyright Avail: NTIS HC A22/MF A01

The indications coming from fundamental turbulence research were incorporated in combustor modeling without a systematic analysis of their effect on predictions. Comparisons are presented between finite rate (overall) kinetics and equilibrium in their influence on the structure of the recirculation region attached to a disk flame-holder. The effect of including density gradient terms in the k-epsilon turbulence model is also examined. The results indicate that the fluid dynamic field may determine whether equilibrium or kinetics produces higher temperatures, and that the temperature difference predicted with the two approaches tends to become small with increasing pressure. The effect of introducing density gradients has a moderate effect on temperature. Author

N88-29940# Imperial Coll. of Science and Technology, London (England). Fluids Section.
THREE-DIMENSIONAL COMBUSTOR PREDICTORS: A COMPARISON OF EQUILIBRIUM AND LAMINAR FLAMELET CHEMISTRY MODELS
J. J. McGuirk *In* AGARD, Combustion and Fuels in Gas Turbine Engines Jun. 1988 11 p (For primary document see N88-29910 24-25)
Copyright Avail: NTIS HC A22/MF A01

Numerical calculations are reported for the three-dimensional reacting flow inside a can-type combustor geometry. Several flow features found in current combustor designs are included, a swirl driven primary zone and a single row of radially inward dilution air jets. The particular aspect of the mathematical formulation given special attention concerns the mode for the chemical reaction. Alternative descriptions of the instantaneous thermochemistry are adopted which correspond to either full chemical equilibrium or the laminar flamelet approach. In the latter case the flamelet structure is taken over from published calculations of laminar propane-air diffusion flames. All other aspects of the mathematical model such as numerical discretization and solution algorithm, turbulence model and turbulence/chemistry interaction are common in the predictions obtained (the two k-epsilon model and a beta-probability density function (pdf) were used). The results obtained indicate that the predicted flow patterns are essentially the same for both chemistry models, even though differences of almost 100 percent are observed for the density field. The predictions with both models indicate, however, a deficiency in the representation of CO burn out and it is probable this will require an alternative chemistry description. Finally, although the calculations have used an unstrained laminar flame description, predictions of the mean scalar dissipation rate are presented to assess the likelihood of local quenching due to flame stretching. Author

N88-29941# National Technical Univ., Athens (Greece). Thermal Engineering Section.
THE EFFECT OF PARTICLE PROPERTIES ON RADIATIVE HEAT TRANSFER
Em. Kakaras, M. Founti, and N. Papageorgiou *In* AGARD, Combustion and Fuels in Gas Turbine Engines Jun. 1988 7 p (For primary document see N88-29910 24-25)
Copyright Avail: NTIS HC A22/MF A01

Radiative heat transfer in combustion chambers is strongly influenced by the presence among the gaseous combustion products of solid particles of various size and chemical composition such as soot, char, and fly-ash. The particle parameters of these products are of great importance for the calculation of radiative heat transfer and insufficient knowledge of their magnitude can often lead to erroneous simplifications. The importance of absorption or scattering phenomena in radiative transfer is also sometimes misinterpreted. It is the aim of this work to provide computational data in order to demonstrate and explain the importance of solid particles, present in the combustion products, on absorption and scattering phenomena occurring in the radiative heat transfer. Author

N88-29942# Centre National de la Recherche Scientifique, Chatenay-Malabry (France).
FLAMELET MODELING OF TURBULENT PREMIXED FLAMES
N. Darabiha, V. Giovangigli, A. Trouve, S. M. Candel, and E. Esposito *In* AGARD, Combustion and Fuels in Gas Turbine Engines Jun. 1988 17 p Sponsored by Societe Nationale d'Etude et de Construction de Moteurs d'Aviation and DRET, France Prepared in cooperation with Ecole Centrale des Arts et Manufactures, France (For primary document see N88-29910 24-25)
Copyright Avail: NTIS HC A22/MF A01

Some aspects of the effort to analyze turbulent combustion on the basis of an extension of the coherent flame model initially proposed by Marble and Broadwell are described. At this stage the model comprises a local description (flamelets) and a global representation of the turbulent flow-field including a balance equation for the mean flame area per unit volume. The flamelets are non-adiabatic premixed strained flames, a model suggested by Libby, Linan, and Williams. Complex chemistry calculations were carried out for a large number of propane-air flames and a large data-vase of flamelets is being constructed. These calculations provide consumption rates, extinction, and ignition characteristics which are used in the global turbulent calculation to model the mean reaction terms. Numerical results obtained for turbulent premixed flames stabilized in a duct are discussed. Experiments performed on a model combustor provide distributions of the mean heat release rate. These distributions are compared with those determined numerically. This comparison indicates that the coherent flame description accounts for important features found in this experiment. Author

N88-29943# Centre d'Etudes et de Recherches, Toulouse (France).
MODELING THE STABILITY OF A TURBULENT PREMIXED FLAME, DOWNSTREAM FROM A STEP BY A LAGRANGIAN METHOD [MODELISATION DE LA STABILISATION D'UNE FLAMME TURBULENTE PREMELANGEE, EN AVAL D'UNE MARCHE PAR UNE METHODE LAGRANGIENNE]
A. Giovannini *In* AGARD, Combustion and Fuels in Gas Turbine Engines Jun. 1988 11 p In FRENCH (For primary document see N88-29910 24-25)
Copyright Avail: NTIS HC A22/MF A01

Calculations are carried out for a backward facing step, by solving numerically the Navier-Stokes equations utilizing a Lagrangian method of singularity type. The combustion of premixed gas is modeled by utilizing the concept of a thin flame separating burning and mixing gases (treated as incompressible). The exothermicity of the reaction is represented with the aid of volumetric sources positioned in front of the flame. The advancement of the later is realized through advection, and normally with the combustion velocity as a function, not only of the thermodynamic mixing state, but also of the local curve of the front and of the front in its entirety. Thus, the combustion aerodynamics can be discussed from the point of view of coherent structures, and the velocities compared with the work of Pitz and Daily with and without chemical reaction. Author

N88-29944# Institut National de Recherche d'Informatique et d'Automatique, Valbonne (France).
NUMERICAL MODELLING OF PREMIXED FLAMES IN GASEOUS MEDIA
B. Larrouturou *In* AGARD, Combustion and Fuels in Gas Turbine Engines Jun. 1988 13 p (For primary document see N88-29910 24-25)
Copyright Avail: NTIS HC A22/MF A01

Numerical methods and numerical results for the propagation

of premixed flame fronts in a two-dimensional gaseous flow are presented. The study is restricted to simple rectangular geometries, and considers both open and closed vessels. The methods use essentially finite-element approximations and adaptive gridding procedures. The results include curved flame propagation, cellular front instabilities and quenching phenomena due to non-adiabatic walls. Author

N88-29945# Centre National de la Recherche Scientifique, Poitiers (France).
GASEOUS PREMIXED FLAMES IN NON-UNIFORM FLOWS
P. Cambray, B. Deshales, and G. Joulin *In* AGARD, Combustion and Fuels in Gas Turbine Engines Jun. 1988 6 p Prepared in cooperation with Ecole Nationale Superieure de Mecanique et d'Aerotechnique, Poitiers, France (For primary document see N88-29910 24-25)
(Contract DRET-85/130)
Copyright Avail: NTIS HC A22/MF A01

A theoretical analysis led to an evolution law for a flame front propagating in a nonuniform flow when the scales of the nonuniformity of the flow are much larger than the flame thickness. This law gives the local burning velocity of the flame front as a function of the flame stretch which can be split in two parts, one accounting for the geometry of the front and the other for the nonuniformity of the flow. In such a law, all the physio-chemical properties of the mixture are lumped in only two scale factors. A theoretical determination of one of these two scale factors (i.e., the so-called Markstein length) is developed. An experimental test of the evolution law is presented in different flame and flow configurations, which leads to experimental values for the two scale factors in the case of lean propane-oxygen-nitrogen mixtures. Finally experimental and theoretical values are compared. Author

N88-29946# Centre National de la Recherche Scientifique, Poitiers (France). Lab. d'Energetique et de Detonique.
MODELING AND EXPERIMENTAL STUDY OF A REACTIVE FLOW CONFINED WITH WELL INJECTION [MODELISATION ET ETUDE EXPERIMENTALE D'UN ECOULEMENT REACTIF CONFINE AVEC INJECTION PARIETALE]
P. Bruel, M. Champion, M. Boutouili, and J. C. Bellet *In* AGARD, Combustion and Fuels in Gas Turbine Engines Jun. 1988 9 p In FRENCH Prepared in cooperation with Ecole Nationale Superieure de Mecanique et d'Aerotechnique, Poitiers, France (For primary document see N88-29910 24-25)
Copyright Avail: NTIS HC A22/MF A01

The combustion of premixed fuel injected into a two-dimensional channel is studied numerically and experimentally. In the case of a high injection rate, a model of turbulent combustion with second-order closure for mass and energy transport is developed taking into account prior results obtained in the case of reactive shear flows in a simpler structure. The corresponding code is tested by comparing one part with the exact solution from the case of a Couette flow, and the other part with the experimental results obtained from the velocity fields in a two-dimensional channel. Author

N88-29947# Racal Defence Electronics (Radar) Ltd., Walton-on-Thames (England).
MODELLING OF CO OXIDATION IN DILUTION JET FLOWS
P. V. Chleboun, K. P. Hubbert, and C. G. W. Sheppard (Leeds Univ., England) *In* AGARD, Combustion and Fuels in Gas Turbine Engines Jun. 1988 11 p Sponsored in part by Rolls-Royce Plc, United Kingdom (For primary document see N88-29910 24-25)
Copyright Avail: NTIS HC A22/MF A01

Existing equilibrium chemistry and laminar flamelet computer codes are inadequate for calculation of post-flame carbon monoxide burn-up in gas turbine combustion chamber dilution zones. The amount of reaction occurring in such zones is small, but significant in terms of CO emissions, especially under low power conditions. A method was developed, based on a small departure from equilibrium concept, which shows promise in modeling dilution zone carbon monoxide oxidation rate. The procedure, when incorporated into the Rolls-Royce PACE program, still only requires specification of a one-dimensional probability function and entails just one extra conservation equation. Output data were compared with those measured experimentally in an idealized dilution zone. Author

N88-29948# Office National d'Etudes et de Recherches Aerospatiales, Paris (France).
INFLUENCE OF THE CONVECTION ON EVAPORATION AND COMBUSTION OF A FUEL DROPLET
Dominique Scherrer *In* AGARD, Combustion and Fuels in Gas Turbine Engines Jun. 1988 8 p In FRENCH; ENGLISH summary (For primary document see N88-29910 24-25)
Copyright Avail: NTIS HC A22/MF A01

A numerical model is presented for the combustion of a droplet in a gaseous flow. The method is based on the integration of the unsteady balance equations in the two phases. It uses a finite volumes implicit scheme. The results for the vaporization law are compared with the empirical law of Ranz-Marshall: a good agreement is found only in the case of pure vaporizaton (without combustion) at a sufficient Reynolds number. The other results are the following: the data of the droplet is decreased by the vaporization; the unsteady effects in the gaseous phase become negligible with convection (except those due to finite rate reaction which are not studied here); and the velocities inside the droplet are not sufficient to neglect the unsteady effects due to heat tranfer in the liquid phase. Author

N88-29949# Deutsche Forschungs- und Versuchsanstalt fuer Luft- und Raumfahrt, Cologne (West Germany). Inst. fuer Antriebstechnik.
ANALYSIS OF THE FLOW THROUGH DOUBLE SWIRL AIRBLAST ATOMIZERS
E. Bluemcke, H. Eickhoff, C. Hassa, and J. Koopman *In* AGARD, Combustion and Fuels in Gas Turbine Engines Jun. 1988 13 p (For primary document see N88-29910 24-25)
Copyright Avail: NTIS HC A22/MF A01

The flow field resulting from a counterswirl airblast atomizer was investigated numerically and experimentally. The flow pattern shows the typical features of a swirling flow with an inner recirculation zone. Comparison of calculated results with experimental data shows that general features of the flow can be predicted with reasonable accuracy. The propagation of the spray downstream from the atomizer was investigated theoretically using a deterministic flow model for the liquid phase. The predictions demonstrate the influence of operating conditions on the spray characteristics. Author

N88-29950# Laval Univ. (Quebec). Dept. du Genie Mecanique.
THE BEHAVIOUR OF SYNTHETIC FUELS IN A SMALL TRANSPARENT COMBUSTOR
J. Odgers and D. Kretschmer *In* AGARD, Combustion and Fuels in Gas Turbine Engines Jun. 1988 11 p Sponsored by Canadian National Defence and Canadian National Science and Engineering Research Council (For primary document see N88-29910 24-25)
Copyright Avail: NTIS HC A22/MF A01

In a continuing program on the effects of fuel properties on combustion, some 20 pure hydrocarbons and synthesized fuels were tested at atmospheric conditions in a small transparent combustor. This combustor used a very efficient air assist atomizer, such that droplet size was nearly constant. Each fuel was burned over a range of air/fuel rations, and at each condition, a full exhaust gas analysis was done, exhaust temperature distribution was measured, as also flame radiation and weak extinction. The results and their implications are discussed. Author

N88-29951# KHD Luftfahrttechnik G.m.b.H., Oberursel (West Germany).
A SMALL ANNULAR COMBUSTOR OF HIGH POWER DENSITY, WIDE OPERATING RANGE AND LOW MANUFACTURING COST
K. H. Collin *In* AGARD, Combustion and Fuels in Gas Turbine

Engines Jun. 1988 12 p (For primary document see N88-29910 24-25)
Copyright Avail: NTIS HC A22/MF A01

A short description will be given of the design and manufacturing philosophy, testing, and optimization of a combustion chamber. The features and design layout of the burner are characterized by the requirements for a low cost propulsion system for an unmanned flight vehicle, such as RPV and drones. Rig test results for the ignition and the performance over a wide operating range will be discussed. Ignition by hot gas from a cartridge as well as experience with testing this combustor in the demonstrator turbojet engine will be described. Author

N88-29952*# National Aeronautics and Space Administration. Lewis Research Center, Cleveland, Ohio.
ELECTROCATALYTIC REDUCTION OF OXYGEN ON MODIFIED OXIDE SURFACES M.S. Thesis
Scott A. Chaffins, Vakula S. Srinivasan (Bowling Green State Univ., Ohio.), and Joseph Singer Sep. 1988 84 p
(Grant NGT-36-002-800)
(NASA-TM-101333; E-4345; NAS 1.15:101333) Avail: NTIS HC A05/MF A01 CSCL 07D

A first step which frequently occurs in the reduction of dioxygen, e.g., at the cathode of the alkaline fuel cell, is the two-electron reduction to the peroxyl ion, HO bar 2. For the efficiency of the fuel cell, this ion must be further reduced, or decomposed, to OH(-). Rate constants for HO bar 2 decomposition have been determined in 31 percent KOH at 25 C for the following catalysts in the form of suspended powders and Teflon-bonded electrodes: Pt, Au, cobalt tetrametoxyl phenyl porphyrin (CoTMPP), and La sub 0.5Pb sub 0.5MnO3. Rates were normalized to unit surface area measured by several methods as suitable. Where possible, four methods were used to measure rate constants: gasometric, oxygen probe, rotating disk electrode, and open-circuit potential decay. Steady-state polarization was also tried but was not as satisfactory. Comparisons are given for the methods in regard to reliability, applicability to the material, and convenience. Author

N88-29953# Aerospace Corp., El Segundo, Calif. Aerophysics Lab.
PARTICLE SIZING IN COMBUSTION SYSTEMS, USING SCATTERED LASER LIGHT
Jay M. Bernard 25 May 1988 30 p
(Contract F04701-85-C-0086)
(AD-A196231; TR0086A(2060)-3; SD-TR-88-37) Avail: NTIS HC A03/MF A01 CSCL 21B

Light scattering techniques for particle sizing are reviewed, with emphasis on their use in combustion diagnostics. Submicron soot-particle sizing in flames, using the diffusion-broadened spectrum of scattered light, is discussed in detail, beginning with the pioneering work of S.S. Penner and coworkers. Recent developments in the inversion of scattering data to yield soot number densities and size distributions are then reviewed. Two imaging techniques for measuring particle sizes greater than 1 micro meter are mentioned: a holographic technique and a method using laser light emitted by the particle itself. GRA

N88-29954# American Science and Engineering, Inc., Cambridge, Mass.
ZT IMAGING SYSTEM FOR LAYERED THIN WALL STRUCTURES Final Report, Jun. - Dec. 1987
P. J. Bjorkholm Mar. 1988 79 p
(Contract F04611-87-C-0049)
(AD-A195466; ASE-5343; AFAL-TR-88-011) Avail: NTIS HC A05/MF A01 CSCL 14B

Phase 1 demonstrated the feasibility of using a one-sided X-ray backscatter imaging technique called ZT to display very small delaminations, cracks, porosity, and chemical species differences in a variety of objects. Using both supplied carbon composites materials, some with known defects, and custom built phantoms, experiments were performed to measure the sensitivity limits of the ZT technique to the various anomalies. During the execution of the program, we modified both the focussing collimator, the detectors and the X-ray beam scanning mechanism to observe the differences in image quality caused by parametric changes in these items. Delaminations as small as 127 microns (0.005 in.) deep and 0.05 in. in diameter were imaged with the laboratory system. In the porosity phantom, holes as small as 787 microns in diameter were visualized. Our density investigations showed the ability to detect density differences as small as 2 percent. Also uncovered during the density experiments was the sensitivity of ZT to chemical species variations. A math model is constructed which accurately predicts total system performance, including the backscatter process and the human detection probability. Author

N88-29955 Institut d'Aeronomie Spatiale de Belgique, Brussels.
AERONOMIC PROBLEMS OF MOLECULAR OXYGEN PHOTODISSOCIATION. PART 4: THE VARIOUS PARAMETERS FOR THE HERZBERG CONTINUUM
Marcel Nicolet and Robert Kennes 1988 28 p Submitted for publication Sponsored in cooperation with Pennsylvania State University, University Park, Pa. and the Commission of the European Communities
(Contract N000-14-86-K-0265)
(Aeronomica-Acta-A-333-1988; ISSN-0065-3713; ETN-88-93073)
Avail: Institut d'Aeronomie Spatiale de Belgique, 3 Avenue Circulaire, B-1180 Brussels, Belgium

Stratospheric conditions of direct photodissociation of molecular oxygen by solar radiation in the 202 to 242 nm wavelength range were determined after introduction of solar irradiances of SUSIM from Spacelab 2, O2 absorption cross sections, molecular scattering cross sections, and O2 absorption cross sections. The O2 photodissociation frequency has a maximum of 5.8 times 10 to the minus 10th power/sec, becomes 5.3 times 10 to the minus 10th power/sec at the stratopause and reaches an isophotolytic level at 5 times 10 to the minus 12th power/sec for any variation in the adopted O2 absorption cross section. The accuracy of the O3 absorption cross section should be better than 2.5 percent particularly in the 202 to 220 nm wavelength range to reduce the errors in the O2 photodissociation rates at low stratospheric levels to less than 10 percent. ESA

N88-29956# Ballistic Research Labs., Aberdeen Proving Ground, Md.
FLAMESPREADING PROCESSES IN OBLIQUELY LOADED STICK PROPELLANT BEDS Technical Report, Oct. 1985 - Sep. 1986
Thomas C. Minor Mar. 1988 30 p
(AD-A195081; BRL-TR-2894) Avail: NTIS HC A03/MF A01 CSCL 19A

Stick propellants have seen increasing use in recent years, in part because the small resistance to the flow of ignition and early combustion gases presented by the packed stick bundle allows the use of simplified, base ignition systems. The resistance to gas flow along the axial dimension is approximately two orders of magnitude lower for a stick propellant bed than for a granular one. However, in the real world of propellant charges, conditions arise in which the flow of gases might attack the stick bundle obliquely rather than along its axis. Such situations might include propellants contained in cases in a manner that the sticks can become shifted or twisted to some degree of obliquity either during the loading process or during handling prior to firing. A similar situation might arise with a central primer venting into a stick bed, in which case the flow might be perpendicular to the axis of the sticks. Clearly, to varying degrees the picture of nearly resistanceless flow within the bed does not apply in these cases. GRA

N88-29957# Technische Univ., Berlin (West Germany). Fachbereich fuer Physik.
EXPERIMENTAL AND THEORETICAL INVESTIGATIONS OF ISOTOPE SHIFT AND HYPERFINE STRUCTURE ON 5d ELEMENTS (ESPECIALLY PLATINUM, IRIDIUM AND RHENIUM) Ph.D. Thesis [EXPERIMENTELLE UND THEORETISCHE UNTERSUCHUNGEN DER ISOTOPIEVERSCHIEBUNG UND HYPERFEINSTRUKTUR AN 5D-ELEMENTEN (INSBESONDERE PLATIN, IRIDIUM UND RHENIUM)]
Guenter Sawatzky 1988 141 p In GERMAN
(ETN-88-93121) Avail: NTIS HC A07/MF A01

Interference optical investigations on isotope shifts and hyperfine structure of 5d elements iridium and platinum are presented. Experimental isotope shift studies are carried out for rhenium and values are determined. Using the parameters and the hyperfine structure parameters, the nuclei charge sizes are obtained. ESA

26 METALLIC MATERIALS

Includes physical, chemical, and mechanical properties of metals, e.g., corrosion; and metallurgy.

N88-29958# Illinois Univ., Urbana. Dept. of Materials Science and Engineering.
HYDROGEN EMBRITTLEMENT OF IRON-NICKEL ALLOYS
W. Y. Chu and H. K. Birnbaum Apr. 1988 23 p
(Contract N00014-83-K-0468)
(AD-A195909) Avail: NTIS HC A03/MF A01 CSCL 11F

In many alloy systems, hydrogen embrittlement under relatively high fugacity conditions occurs by intergranular fracture. One of these is the iron nickel alloy system which exhibits intergranular hydrogen related fracture when tested with a high supersaturation of solute hydrogen or while being cathodically charged with hydrogen. The results obtained on this alloy system indicate that the hydrogen embrittlement susceptibility decreases as the iron concentration of the alloy increased. These early measurements contained no information about the grain boundary chemistry and it is known that the effects of hydrogen are generally sensitive to the concentrations of other elements at grain boundaries. One particular element, sulphur, is known to increase the susceptibility of nickel alloys and Fe alloys to hydrogen embrittlement although the mechanism of this increased susceptibility is not known. GRA

N88-29959# Auburn Univ., Ala. Dept. of Mechanical Engineering.
CRYSTAL STRUCTURES OF ORDERED CARBON METAL ALLOYS Final Report, 1 Sep. 1986 - 29 Feb. 1988
Bryan A. Chin 1988 5 p
(Grant AF-AFOSR-0233-86)
(AD-A195597; AFOSR-88-0532TR) Avail: NTIS HC A02/MF A01 CSCL 11F

This scientific instrumentation grant was awarded to Auburn University for the examination of crystal structures of the various ordered carbon metal alloy systems. The major instrument purchased was a high-temperature X-ray diffractometer for in-situ phase identifications. The following instruments were purchased under this grant: X-ray powder diffractometer, high precision ion mill, high precision dimple system for sample preparation. GRA

N88-29960# Army Armament Research and Development Command, Watervliet, N. Y.
ADDITIONAL FRACTURE AND STRENGTH TEST RESULTS FOR A723 STEEL AND 38644 TITANIUM Final Report
J. H. Underwood, M. H. Kamdar, and R. R. Fujczak Apr. 1988 21 p
(AD-A196329; ARCCB-TR-88018) Avail: NTIS HC A02/MF A01 CSCL 11F

Four types of additional mechanical test results are described for high strength steel and titanium alloys, as a continuation of previous work: (1) The effects of elevated temperature on the circumferential orientation tensile properties of titanium and steel cylinders are described. (2) A comparison is presented of strength and fracture toughness results from two titanium ingots. (3) The fatigue lives of notched bend specimens of titanium are measured and compared with calculated fatigue lives for steel. (4) The effects of elevated temperature cycles and plasma spraying process on the strength of steel are presented. GRA

N88-29961*# Cincinnati Univ., Ohio. Dept. of Aerospace Engineering and Engineering Mechanics.
ANISOTROPIC CONSTITUTIVE MODELING FOR NICKEL-BASE SINGLE CRYSTAL SUPERALLOYS Ph.D. Thesis
Michael Y. Sheh 1988 190 p
(Grant NAG3-511)
(NASA-CR-182157; NAS 1.26:182157) Avail: NTIS HC A09/MF A01 CSCL 11F

An anisotropic constitutive model was developed based on crystallographic slip theory for nickel base single crystal superalloys. The constitutive equations developed utilizes drag stress and back stress state variables to model the local inelastic flow. Specially designed experiments were conducted to evaluate the existence of back stress in single crystal superalloy Rene N4 at 982 C. The results suggest that: (1) the back stress is orientation dependent; and (2) the back stress state variable is required for the current model to predict material anelastic recovery behavior. The model was evaluated for its predictive capability on single crystal material behavior including orientation dependent stress-strain response, tension/compression asymmetry, strain rate sensitivity, anelastic recovery behavior, cyclic hardening and softening, stress relaxation, creep and associated crystal lattice rotation. Limitation and future development needs are discussed. Author

N88-29962# Aptech Engineering Services, Inc., Sunnyvale, Calif.
STRESS INTENSITY FACTORS FOR CRACKED METALLIC STRUCTURES UNDER RAPID THERMAL LOADING Final Report, Aug. 1986 - May 1987
Russell C. Cipolla and Kimble J. Clark Oct. 1987 74 p
(Contract F33615-86-C-3217; AF Proj. 3005)
(AES-8609709F-1; AFWAL-TR-87-3059) Avail: NTIS HC A04/MF A01 CSCL 11F

High intensity heating of aircraft structures can challenge the structural integrity of critical aircraft components, especially when they may contain flaws. The evaluation of flawed components requires the application of fracture mechanics wherein crack tip stress intensity factors are used to provide a quantitative means of assessing structural integrity. The primary objectives were to develop an analysis method for computing stress intensity factors for severe thermal loadings of interest to the Air Force and to demonstrate the applicability of the method to microcomputers. A methodology was developed based on influence functions to determine stress intensity factors for structures exposed to intense thermal heating. A demonstration of the method is given and results detailed. Author

N88-29963# Army Belvoir Research and Development Center, Fort Belvoir, Va.
MULTI-METALLIC GALVANIC CORROSION Final Report, Mar. 1987 - Feb. 1988
Lisa R. Whiting, Chris Miller, and Dario A. Emeric May 1988 19 p
(AD-A195995; BRDEC-2466) Avail: NTIS HC A03/MF A01 CSCL 11F

In the past, there have been a number of material failures in the Army's equipment. Many of these failures have been caused by some form of corrosion. One type of corrosion involved is galvanic corrosion. This happens when dissimilar metals come in contact in an electrolyte. The electrolyte could be a marine or even a humid environment. When this occurs, the less noble metal (anode) corrodes in order to protect the more noble metal (cathode). By exposing multi-metallic galvanic couples of high

strength materials in aggressive environments, the number of failures in bridges and other military equipment could be reduced. GRA

N88-29964# Technical Research Centre of Finland, Espoo. Metallurgy Lab.
STATE VARIABLE APPROACH TO DEFORMATION PHENOMENA IN FACE CENTERED CUBIC (FCC) METALS Ph.D. Thesis - Helsinki University of Technology
Simo-Pekka Hannula Jan. 1988 117 p Sponsored by DOE; NSF; the Outokumpu Oy, Tapiola, Finland; and the Technical Research Center of Finland, Espoo, Finland
(VTT-44; ISBN-9-51-383058-6; ISSN-0358-5069; ETN-88-92650)
Copyright Avail: NTIS HC A06/MF A01; Technical Research Center of Finland (VTT), Vuorimiehentie 5, SF-02150 Espoo 15, Finland 95 Finnish marks

Phenomenological deformation theories for plastic deformation are surveyed, emphasizing the state variable model of Hart (1970). Work hardening behavior of face centered cubic metals is explained in terms of Hart's model and a work hardening correlation based on the separation of athermal and thermal contributions to the work hardening coefficient is proposed. The effects of strain aging on the state variable treatment of plastic deformation in stainless steel are determined and a treatment based on the evolution of drag stress is suggested. The analysis of strain aging experiments on a variety of materials shows that in addition to the hardness parameter, another state variable, i.e., the rate parameter, is generally needed if strain aging is to be accounted for. It is shown that an indentation load relaxation experiment may be used to obtain pertinent material information for deformation models. ESA

N88-29965# Army Belvoir Research and Development Center, Fort Belvoir, Va.
SOME EFFECTS OF NITRATES ON THE TENSILE PROPERTIES OF Al 7075-T7351 Final Technical Report, Aug. 1985 - Oct. 1986
Donovan Harris, Chris Miller, and Dario Emeric Mar. 1988 159 p
(AD-A195118; BRDEC-2461) Avail: NTIS HC A08/MF A01 CSCL 11F

This report is the first of three related to the effects of nitrates on the chloride corrosion of Al 7075-T7351 alloy. Laboratory work was performed from March 1983 through February 1987 at the Belvoir RD and E Center. This report highlights research performed between August 1985 and October 1986. It details experimental testing efforts and results of a study on the effects of nitrates on the mechanical and physical properties of aluminum alloy Al 7075-T73751 when exposed in a chloride environment. The results show that changes in the tensile properties of unstressed Al 7075-T7351 followed exposure to a nitrate-chloride environment in four instances. GRA

27 NONMETALLIC MATERIALS

Includes physical, chemical, and mechanical properties of plastics, elastomers, lubricants, polymers, textiles, adhesives, and ceramic materials.

For composite materials see *24 Composite Materials.*

N88-29966# Naval Civil Engineering Lab., Port Hueneme, Calif.
PERFORMANCE PREDICTION FOR COATINGS. PROCEEDINGS OF A WORKSHOP
Peter J. Herst Oct. 1987 91 p Workshop held in Port Hueneme, Calif., 15 Sep. 1986
(AD-A188973) Avail: NTIS HC A05/MF A01 CSCL 11C

Emerging technologies that might be applied to rapid performance prediction for coatings are discussed. Ultrasonic detection, coating degradation, corrosion prevention, polymeric coatings, prediction techniques, electrical impedance measurements and spectroscopic techniques are among the topics discussed. For individual titles, see N88-29967 through N88-29979.

N88-29967# Kent State Univ., Ohio. Rheology and Coatings Lab.
ULTRASONIC DETECTION OF DIFFUSION AND ADHESION LOSS
Carl J. Knauss *In* Naval Civil Engineering Lab., Performance Prediction for Coatings. Proceedings of a Workshop Oct. 1987 p 3-10 (For primary document see N88-29966 24-27)
Avail: NTIS HC A05/MF A01 CSCL 11C

Three techniques are described which can monitor the performance of coatings for prediction of early failure. The two techniques, ultrasonic impedometry and the strip delay line method, can measure the rate of diffusion of water and solvents and detect when materials begin to lose adhesion to metals and begin to corrode. The third method uses Lamb waves to detect incipient adhesion loss of a coating to metal sheets. These instruments, in conjunction with additional accelerated test methods, can aid in coating performance predictions. Author

N88-29968# North Dakota State Univ., Fargo. Dept. of Polymers and Coatings.
PHOTOACOUSTIC FOURIER TRANSFORM INFRARED SPECTROSCOPY. AN EARLY DETECTION TECHNIQUE FOR COATINGS DEGRADATION
Marek W. Urban *In* Naval Civil Engineering Lab., Performance Prediction for Coatings. Proceedings of a Workshop Oct. 1987 p 11-18 (For primary document see N88-29966 24-27)
Avail: NTIS HC A05/MF A01 CSCL 11C

A new spectroscopic tool, photoacoustic Fourier transform infrared spectroscopy as a method to characterize coatings and interfaces, is described. It is a novel technique that allows characterization of surfaces at various depths and provides information on the molecular level. Because of its nondestructive nature, it can be used as an early detection method of detecting weathering processes, kinetics of UV curing and to determine substrate-coating interactions. Major advantages and applications of the technique are described. Author

N88-29969# Naval Civil Engineering Lab., Port Hueneme, Calif.
DEGRADATION OF PROTECTIVE COATINGS ON STEEL IN CORROSIVE ENVIRONMENTS
T. Nguyen, E. Byrd, and D. Bentz *In its* Performance Prediction for Coatings. Proceedings of a Workshop Oct. 1987 p 19-28 (For primary document see N88-29966 24-27)
Avail: NTIS HC A05/MF A01 CSCL 11C

Thermal wave electron microscopy was successfully applied to: (1) image corrosion products of approx. 5 microns in size on the sufaces of both bare steel and steel protected by clear or opaque organic coatings; (2) image the microstructure of steel both inside and outside corroded areas, as well as under a thin organic film; (3) estimate thicknesses of corrosion product layers; and (4) determine, through the use of computer image analysis procedures, the shape and area, and the percentage of the total corroded area. The method has potential as a technique for rapidly screening the effectiveness of corrosion inhibitors and protective coatings, and for developing data on fundamental degradation processes which are needed in the development of test procedures to aid in service life prediction of protective coatings. Author

N88-29970# Sherwin-Williams Co., Chicago, Ill.
PREDICTION OF DEGRADATION OF POLYMERIC COATING MATERIALS
T. K. Rehfeldt *In* Naval Civil Engineering Lab., Performance Prediction for Coatings. Proceedings of a Workshop Oct. 1987 p 29-34 (For primary document see N88-29966 24-27)
Avail: NTIS HC A05/MF A01 CSCL 11C

A program was undertaken to develop methods to characterize coating degradation during service and to find means to predict lifetimes of current polymeric coating systems. Research was primarily concerned with the photooxidation of urethane based aircraft coatings meeting MIL-C-83286. A large number of coating

samples were prepared for accelerated and real time exterior exposure. Standard physical paint tests were made on all coatings. An objective of this investigation was to try to use these tests as a measure of coating degradation and to find test that would be representative of the changes in the polymer and which would correlate with standard paint tests. Author

N88-29971# National Bureau of Standards, Gaithersburg, Md.
A RELIABILITY-BASED PROGRAM FOR PREDICTING THE SERVICE LIFE OF ORGANIC COATING SYSTEMS
Jonathan W. Martin, Mary E. McKnight, and Tinh Nguyen *In* Naval Civil Engineering Lab., Performance Prediction for Coatings. Proceedings of a Workshop Oct. 1987 p 35-40 (For primary document see N88-29966 24-27)
Avail: NTIS HC A05/MF A01 CSCL 11C

The main objective of this reliability based program is to quantitatively predict the service life of an organic coating system which is subjected to its intended operating and service environment. Service life is defined in terms of the probability that a coating system will perform its intended function. Author

N88-29972# Case Western Reserve Univ., Cleveland, Ohio. Dept. of Physics.
PREDICTING THE DURABILITY OF ADHESIVES AND COATINGS BY REMOTE DETECTION OF HIDDEN DEFECTS AND COATING-THICKNESS IRREGULARITIES: A THEORETICAL AND NUMERICAL STUDY
V. K. Pinus and Philip L. Taylor *In* Naval Civil Engineering Lab., Performance Prediction for Coatings. Proceedings of a Workshop Oct. 1987 p 41-45 (For primary document see N88-29966 24-27)
Avail: NTIS HC A05/MF A01 CSCL 11C

The goal is the production of a theory capable of giving both realistic reconstruction of defects from their thermal images and the establishment of values of laser wavelength and intensity and of sample thickness for which a method can be applied. Researchers derived a basic set of equations that describe the development of the temperature field in both coating and substrate layers for any arbitrarily given laser flux density as a function of time. By solving these equations, one can determine the temperature fields for any given laser flux density. From this, one may determine the infrared radiation field. After that, one can calculate such experimentally measured quantities dependent on the infrared radiation field as the spectral surface luminosity, the brightness temperature, the color temperature, and the emittance of the body. In this way, it should be possible to determine which quantities are more sensitive and more appropriate for thermal wave imaging. Author

N88-29973# Naval Ship Research and Development Center, Bethesda, Md.
ELECTRICAL DETECTION OF COATING DETERIORATION
G. Loeb and J. Mihm *In* Naval Civil Engineering Lab., Performance Prediction for Coatings. Proceedings of a Workshop Oct. 1987 p 47-50 (For primary document see N88-29966 24-27)
Avail: NTIS HC A05/MF A01 CSCL 11C

Electrical impedance measurements of epoxy coated steel panels at 95 percent relative humidity using two electrodes were performed for two reasons: to complement other studies performed when the panels were immersed in sea water using the three electrode method, and to ascertain whether significant predictive capabilities were achievable with this method. The data obtained to date are fragmentary, but an example is given of a matched pair of panels to illustrate the type of data obtained. Author

N88-29974# Rockwell International Science Center, Thousand Oaks, Calif.
ELECTROCHEMICAL EVALUATION OF THE LONG TERM CORROSION RESISTANCE OF POLYMER COATED STEEL
Martin W. Kendig *In* Naval Civil Engineering Lab., Performance Prediction for Coatings. Proceedings of a Workshop Oct. 1987 p 51-56 (For primary document see N88-29966 24-27)
Avail: NTIS HC A05/MF A01 CSCL 11C

A number of painted phosphated steel coupons of known salt spray behavior were evaluated using electrochemical impedance spectroscopy (EIS) and potentiostatic cathodic disbonding (PCD), which allowed evaluation of the water uptake and cathodic debonding efficiency. A combined function of cathodic bonding efficiency measured over a 72 hour period and water uptake measured after 24 hours correlated well with 900 hour salt spray tests. Hence, the electrochemical methods provide a rapid quantitative means for classifying coatings according to their corrosion resistance. Author

N88-29975# Rockwell International Science Center, Thousand Oaks, Calif.
AN ELECTROCHEMICAL IMPEDANCE SPECTROSCOPY STUDY OF REACTIONS AT THE METAL/COATING INTERFACE Abstract Only
F. Mansfeld, S. L. Jeanjaquet, and M. W. Kendig *In* Naval Civil Engineering Lab., Performance Prediction for Coatings. Proceedings of a Workshop Oct. 1987 p 5 (For primary document see N88-29966 24-27)
Avail: NTIS HC A05/MF A01 CSCL 11C

A segmented two-electrode system was used to obtain impedance spectra under a polymer coating. These spectra have been compared with those obtained across the coating between the short-circuited steel electrodes and a counter electrode. Similar experiments were carried out for Cu/steel and Zn/steel with a 20 micron epoxy coating. For these electrode systems, the galvanic current between the two dissimilar metals was recorded continuously as a function of exposure time to NaCl. A transmission line model was added to obtain estimates for the delaminated volume and the polarization resistance of the steel electrodes. Author

N88-29976# Naval Ship Research and Development Center, Bethesda, Md. Marine Corrosion Branch.
EVALUATION OF ORGANIC COATING DETERIORATION AND SUBSTRATE CORROSION IN SEAWATER USING ELECTROCHEMICAL IMPEDANCE MEASUREMENTS
John R. Scully *In* Naval Civil Engineering Lab., Performance Prediction for Coatings. Proceedings of a Workshop Oct. 1987 p 59-64 (For primary document see N88-29966 24-27)
Avail: NTIS HC A05/MF A01 CSCL 11C

The specific objective of this research was to demonstrate the feasibility of monitoring, evaluating and quantifying the nature and degree of coating deterioration and underfilm corrosion of HY-80 steel in seawater, using electrochemical AC impedance techniques. Results of coating deterioration, substrate corrosion, area effects, and mass transfer effects are given. Author

N88-29977# Nevada Univ., Reno. Dept. of Chemical and Metallurgical Engineering.
ALTERNATIVE IMMERSION ACCELERATED TESTING OF COATING SYSTEMS FOR NAVAL SHORELINE FACILITIES
Denny A. Jones *In* Naval Civil Engineering Lab., Performance Prediction for Coatings. Proceedings of a Workshop Oct. 1987 p 65-70 (For primary document see N88-29966 24-27)
Avail: NTIS HC A05/MF A01 CSCL 11C

Alternative immersion accelerated testing of coating systems for naval shoreline facilities are discussed. It was found that continuous immersion at room temperature caused no blistering, because only a colloidal corrosion product was formed which did not undercut the coating. Alternate immersion in 3 percent NaCl at room temperature caused blistering on latex and vinyl coatings. Alternate immersion at 50 C in 3 percent NaCl generally accelerated the attack on the susceptible coatings in the same environment at room temperature. Alternate immersion in sulfate at room temperature produced heavy deposits but was less aggressive in causing blisters. Author

N88-29978# Missouri Univ., Rolla.
ZINC FILLED COATINGS
J. O. Stoffer and John Montle (Carboline Co., Saint Louis, Mo.) *In* Naval Civil Engineering Lab., Performance Prediction for

Coatings. Proceedings of a Workshop Oct. 1987 p 71-80 (For primary document see N88-29966 24-27)
Avail: NTIS HC A05/MF A01 CSCL 11C

The use of zinc-filled coatings to prevent corrosion of metal surfaces is briefly discussed. Methods of preparation, atmospheric exposure effects, the characteristics of ethyl silicate zinc rich primers, and the importance of porosity are among the topics covered. Author

N88-29979# Steel Structures Painting Council, Pittsburgh, Pa.
REDUCED TIME FRAME FOR PREDICTING COATING PERFORMANCE
Bernard R. Appleman *In* Naval Civil Engineering Lab., Performance Prediction for Coatings. Proceedings of a Workshop Oct. 1987 p 81-86 (For primary document see N88-29966 24-27)
Avail: NTIS HC A05/MF A01 CSCL 11C

Early macroscopic examination was applied to a set of U.S. Navy data on 5-year exposures of painted metal at a severe marine site. The major parameters evaluated were degree of rusting on a logarithmic scale of 1 to 10, distance of undercutting from the scribe in 1/32 in., and general protection, including a compilation of all defects rated on a logarithmic scale of 1 to 10. Author

N88-29980# Bendix Corp., Kansas City, Mo.
PRIMERLESS RTV SILICONES Final Report
J. S. Tira Nov. 1987 24 p
(Contract DE-AC04-76-DP-00613)
(BDX-613-3807) Avail: NTIS HC A03/MF A01

A survey and evaluation of 6 one- and two-part primerless room temperature vulcanizing silicone adhesives, sealants, and encapsulation materials were conducted to gain working experience with these materials. A table of physical properties of each material was compiled; also, testing was performed and data reported for the following material properties: Shore A hardness, lap shear strength, dielectric strength, coefficient of thermal expansion, adhesion 180 deg peel with various plastic and metal materials, adhesion to silicone and rubber materials, and contact corrosion. Author

N88-29981# Purdue Univ., West Lafayette, Ind. Dept. of Physics.
STORING BITS ON A DNA POLYMER CHAIN Annual Report, 15 May 1987 - 15 May 1988
Lonnie L. VanZandt 10 Apr. 1988 6 p
(Contract N00014-87-K-0162; RR0-4108)
(AD-A195701) Avail: NTIS HC A02/MF A01 CSCL 06B

The DNA polymer in dilute aqueous solution responds to external illumination. Because it is a charged system surrounded by another charged system, counterions, it interacts strongly electromagnetically. We find that a normal mode may exist in the form of a one-dimensional plasmon, analogous to the three-dimensional plasmons well known in metal physics and the two-dimensional surface plasmons of surface physics of conductors. The DNA plasmon frequency is proportional to the excitation wave number, i.e., the first power, in contrast with the one/half power for surface plasmons and the zero power for bulk metallic plasmons. GRA

N88-29982# Army Belvoir Research and Development Center, Fort Belvoir, Va.
STRESSED FABRIC ABRASION TEST PROCEDURE FOR URETHANE COATED FABRIC FUEL TANKS Final Report, Apr. 1987 - Apr. 1988
Pat Butler and Dave Flanagan Jun. 1988 15 p
(AD-A196327; BRDEC-2469) Avail: NTIS HC A03/MF A01 CSCL 21D

This report details investigations conducted and results obtained in efforts to develop a test procedure for measuring the effects of abrasion under stress in urethane-coated fabric tanks. The Rubber and Coated Fabrics Research Group, Materials, Fuels and Lubricants Directorate, Belvoir Research, Development and Engineering Center, prepared all samples from material submitted by coated fabric suppliers, performed all tests, and documented results. Four different urethane materials were tested on the Taber Abrader which was modified to test the fabric under stress. The urethanes showed a marked decline in the ability to withstand abrasion while under stress. GRA

N88-29983# University Coll. of North Wales, Bangor. School of Electronic Engineering Science.
POLYMER-CERAMIC COMPOSITES Periodic Report No. 4
Dilip K. Das-Gupta Apr. 1988 9 p
(Contract DAJA45-86-C-0034)
(AD-A195789) Avail: NTIS HC A02/MF A01 CSCL 11D

Composites of Lead Zirconate Titanate (PZT) and polyvinylidene fluoride (PVDF) were prepared and the electrical and dielectric behaviors were analyzed. PZT phase has been suggested to have a significant contribution on the electrical conduction and low frequency dielectric loss at high temperatures. The pyroelectric behavior obtained from composites of different materials may suggest that the elastic stiffness and thermal expansion of the polymer matrix were among the factors contributing to the measured pyroelectric activity. A higher pyroelectric figure of merit as compared to PZT has been achieved in one of the PZT/PVDF composites. GRA

N88-29984*# National Aeronautics and Space Administration. Lewis Research Center, Cleveland, Ohio.
NOVEL LADDER POLYMERS FOR USE AS HIGH TEMPERATURE STABLE RESINS OR COATINGS Patent Application
Mary Ann Meador, inventor (to NASA) 11 Aug. 1988 21 p
(NASA-Case-LEW-14203-1; NAS 1.71:LEW-14203-1; US-Patent-Appl-SN-231026) Avail: NTIS HC A03/MF A01 CSCL 11C

An object of the invention is to synthesize a new class of ladder and partial ladder polymers. In accordance with the invention, the new class of ladder and partial ladder polymers are synthesized by polymerizing a bis-dienophile with a bis-diene. Another object of the invention is to provide a fabricated, electrically conducting, void free composite comprising the new class of the ladder and partial ladder polymers described above. The novelty of the invention relates to a new class of ladder and partial ladder polymers and a process for synthesizing these polymers. These polymers are soluble in common organic solvents and are characterized with a unique dehydration property at temperatures of 300 to 400 C to provide thermo-oxidatively stable pentiptycene units along the polymeric backbone. These polymers are further characterized with high softening points and good thermo-oxidative stability properties. Thus these polymers have potential as processable, matrix resins for high temperature composite applications. NASA

28 PROPELLANTS AND FUELS

Includes rocket propellants, igniters, and oxidizers; their storage and handling procedures; and aircraft fuels.

For related information see also *07 Aircraft Propulsion and Power, 20 Spacecraft Propulsion and Power,* and *44 Energy Production and Conversion.*

N88-29985# Air Force Astronautics Lab., Edwards AFB, Calif.
DESCRIPTIVE CHARACTERIZATION OF PROPELLANT PARTICLES Final Report, Oct. 1984 - Oct. 1987
Kurt G. Chandler Apr. 1988 28 p
(AD-A195176; AFAL-TR-88-042) Avail: NTIS HC A03/MF A01 CSCL 21I

Particle characterization is used for burn rate and rheology predictions for solid rocket propellants. This report compares the burn rate of solid rocket propellants to various measurement techniques to determine the best routine characterization parameter for burn rate predictions. These measurement techniques include surface area measurements, diameter measurements from ensemble light scattering, light blocking, sieving techniques, and a

new particle solvolysis technique. The diameter techniques also provided data for surface area calculations. Propellants containing HMX, AP, and AN were burned in a window bomb at pressures ranging from 500 psig to 2000 psig. The results indicate a volume dependent process for HMX burning, a surface area dependent process for AN, and a surface area dependent process affected by the particle distribution for AP. For burn rate prediction, routine measurements of weight median diameters are recommended for HMX, surface area measurements or ensemble light scattering weight median diameters are recommended for AP, and surface area measurements are recommended for AN. GRA

N88-29986# Erno Raumfahrttechnik G.m.b.H., Bremen (West Germany).
DESIGN AND DEVELOPMENT OF A REFUELING TEST BED Summary Report
J. Kowalek Paris, France ESA Jan. 1988 94 p
(Contract ESA-6827/86-NL-PH(SC))
(FTMS-RP-ER-011; ESA-CR(P)-2623; ETN-88-93150) Avail: NTIS HC A05/MF A01

The specification, design, procurement, and manufacturing of a test bed for ground based studies of in orbit refueling are described. The test bed is mainly built from available commercial standard materials and components. Fluid valves are of flight standard design. The integration and acceptance tests of the various hardware levels are explained. Development tests were performed with the test bed in order to verify the refueling process and to consider specific engineering problems in this area. Propellant gaging methods were also studied. ESA

N88-29987# Argonne National Lab., Ill. Components Technology Div.
PRELIMINARY INVESTIGATION OF FLOW MODELING DURING SOLID PROPELLANT PROCESSING Interim Report, May 1986 - Sep. 1987
H. M. Domanus, W. T. Sha, and S. L. Soo (Illinois Univ., Urbana-Champaign.) 19 Feb. 1988 36 p Prepared in cooperation with Illinois Univ. at Urbana, Dept. of Mechanical and Industrial Engineering
(Grant W-31-109-ENG-38)
(AD-A196168; AD-E951137; AMSMI/CR-RD-PR-88-1) Avail: NTIS HC A03/MF A01 CSCL 21I

The results of preliminary modeling of a solid propellant flow as would occur during propellant casting is presented. Both single and multiple velocity field models were investigated. Results with the single velocity field model produced solid particle segregation that was in qualitative agreement with experience. It is the objective of this work to understand and ultimately predict the composition gradients that result during solid propellant processing. GRA

N88-29988# Research Inst. of National Defence, Stockholm (Sweden).
THERMOMECHANICAL COMPUTATIONS FOR GAP, A HIGH ENERGY BINDER FOR COMPOSITE PROPELLANTS
Torsten Liljegren and Roger Lundgren Jun. 1988 15 p In SWEDISH; ENGLISH summary
(FOA-C-20718-2.1; ISSN-0347-3694; ETN-88-93059) Avail: NTIS HC A03/MF A01

Computations for propellants for rocket motors, airbreathing engines, and low vulnerability ammunition powder for guns are discussed. Rocket propellants with GAP show a considerably lower power specific impulse than HTPB based composites, while the volume specific impulse is only slightly lower, due to the higher density of GAP. Nitramine as oxidizer gives a propellant where the smoke is reduced to a minimum with comparable performance as double base propellants. In a solid propellant ramjet engine, the burning rate can be at least as important as the specific impulse; HTPB has a low burning rate. Therefore GAP can be an interesting alternative. ESA

N88-29989# Army Armament Research, Development and Engineering Center, Picatinny Arsenal, N.J. Armament Engineering Directorate.
DISCOVERY OF A LOW TEMPERATURE FORM OF TAGN (TRIAMINOGUANIDINIUM NITRATE)
A. J. Bracuti and J. K. Salo Jul. 1988 20 p
(AD-A196059; ARAED-TR-88009) Avail: NTIS HC A03/MF A01 CSCL 19A

Triaminoguanidinium nitrate (TAGN) has been frequently added to cyclic nitramine (RDX) propellant formulations in an effort to increase the burning rates of these propellants. This is particularly important in LOVA propellants formulated for high performance artillery or tank gun applications where faster burning rates are necessary. Although this property of TAGN was known for quite some time, no satisfactory explanation for this phenomenon presently exists. In an effort to understand this compound and its properties more completely, a room temperature single crystal X-ray diffraction study was initiated. A low temperature polymorph of triaminoguanidinium nitrate (TAGN) was discovered during the course of a rigid-body motion study of the nitrate ion. Differential scanning calorimetry (DSC) measurements made at several different heating rates over a temperature range of -100 degrees C to room temperature yielded a small reversible endotherm with a reproducible onset temperature and reproducible heat capacity values. X-ray diffraction measurements also were carried out over a similar temperature range to determine the relationships among reflection intensity, lattice parameters (unit-cell volume), and temperature. Details of the experimental procedures, results, and implications are presented. GRA

N88-29990# Ballistic Research Labs., Aberdeen Proving Ground, Md.
TITRIMETRIC ANALYSIS OF HAN-BASED LIQUID PROPELLANTS
M. M. Decker, E. Freedman, N. Klein, C. S. Leveritt, and J. Q. Wojciechowski Mar. 1988 31 p
(AD-A196225; BRL-TR-2907) Avail: NTIS HC A03/MF A01 CSCL 21I

Liquid propellants that are aqueous mixtures of hydroxylammonium nitrate (HAN) and triethanolammonium nitrate (TEAN) are analyzed using a combination of acid-base and Karl Fischer titrimetry, procedures that quantitatively determine the three major propellant components. The method developed converts HAN to acetoxime and nitric acid by reaction with acetone and then uses either tetrabutylammonium hydroxide or n-butylamine in ethanol or aqueous sodium hydroxide as titrant for both HAN and TEAN. Water is determined by Karl Fischer titration using the proprietary reagent Hydranal. Each major propellant component is, therefore, determined separately. GRA

N88-29991# Coordinating Research Council, Inc., Atlanta, Ga. Hydroperoxide Potential of Jet Fuels Panel.
DETERMINATION OF THE HYDROPEROXIDE POTENTIAL OF JET FUELS
Apr. 1988 111 p
(AD-A195975; CRC-559) Avail: NTIS HC A06/MF A01 CSCL 21D

In 1963 and in 1976, peroxide attack on certain engine rubber parts was found with the use of some Far Eastern fuels. The problem was corrected by requiring oxidation inhibitor be added to fuels meeting Specifications DERD 2494 and MIL-T-5624. Because the majority of commercial aviation turbine fuel had not shown significant peroxide formation, CRC was requested to develop a technique which would identify the hydroperoxide-forming tendencies of jet fuels. Heating the fuel at 65 C for four weeks and measuring the peroxide number is concluded to be an adequate Go/No Go test. GRA

29 MATERIALS PROCESSING

Includes space-based development of products and processes for commercial applications.
For biological materials see *55 Space Biology*.

N88-29992# Aeritalia S.p.A., Naples (Italy). Gruppo Sistemi Spaziali.
FLUID PHYSICS DOUBLE RACK Summary Report
Rosalinda Bianchi Paris, France ESA 4 Jul. 1986 99 p
(Contract ESA-6521/85)
(SD-TN-AI-012; ESA-CR(P)-2548-Vol-1; ETN-88-92767) Avail: NTIS HC A05/MF A01

The fluid physics double rack standard Spacelab double rack is described. It contains three different fluid physic/dynamic facilities: an autonomous fluid physics facility (AFPF), a bubble drop and particle unit, (BDPU), and a critical point facility (CPF). The AFPF is a multiuser instrument to support investigations into column stability, free convection, drop coalescence, surface and interfacial forces, and floating zone analyses under microgravity conditions. The BPDU is designed for experiments concerning the dynamics of bubbles, drops, and particles within optically transparent liquid matrices. The CPF is a multiuser instrument designed to investigate critical phenomena at a given temperature and in a microgravitational environment. Materials studied are simple fluids and optically transparent mixtures. ESA

N88-29993# Levy (Salomon), Inc., Campbell, Calif.
EXPERIMENTAL AND ANALYTICAL STUDY OF TWO-PHASE FLOW IN ZERO GRAVITY Final Report, Sep. 1985 - Oct. 1987
Davood Abdollahian, Ralph Grief, Van P. Carey, and Wang Li-Ping Mar. 1988 147 p
(Contract F33615-85-C-3418)
(AD-A195223; SLI-8707; AFWAL-TR-87-3102) Avail: NTIS HC A07/MF A01 CSCL 20D

More effective and efficient thermal transport techniques will be needed for heat rejection from equipment on satellites. Circulating two-phase fluid loops have been suggested and laboratory tested for possible application in the above areas. In comparison to a single-phase loop, the two-phase system operates at considerably smaller flow rates and maintains a tighter temperature control with higher heat transfer coefficients. However, the two-phase fluid flow regimes, pressure gradients and heat transfer coefficients must be evaluated for application in the weightless environment of an orbiting satellite. This projecting studies two-phase flow behavior under zero gravity conditions. The overall objectives of this study were to generate a data base for two-phase pressure drop and the void-quality relationship under simulated zero gravity conditions and to develop analytical models to predict these parameters for bubbly and annular flow. The simulation of zero gravity two-phase flow was achieved by using two immiscible liquids with equal densities to eliminate the buoyancy component. Although this approach does not eliminate the gravity effects, it provides a representation for void distribution in the absence of gravity. The modeling effort is limited to developing relations for the two-phase friction multiplier and void-quality relation under bubbly and annular flow conditions. The bubbly flow model is based on the assumption of local homogeneous conditions between the phases GRA

N88-29994# Aeritalia S.p.A., Naples (Italy). Gruppo Sistemi Spaziale.
ACCOMMODATION CONCEPT FOR FLUID PHYSICS FACILITIES, VOLUME 2 Final Report
Paris, France ESA 1 Dec. 1986 466 p
(Contract ESA-6521/85)
(SG-TN-AI-027-Vol-2; ESA-CR(P)-2548-Vol-2; ETN-88-92768)
Avail: NTIS HC A20/MF A01

The Spacelab fluid physics double rack design study and definition; central service facilities design; mission support equipment design; and preliminary operations planning are presented. ESA

31 ENGINEERING (GENERAL)

Includes vacuum technology; control engineering; display engineering; cryogenics; and fire prevention.

N88-29995*# SatCon Technology Corp., Cambridge, Mass.
SYNCHRONOUS RESPONSE MODELLING AND CONTROL OF AN ANNULAR MOMENTUM CONTROL DEVICE Final Report
Richard Hockney, Bruce G. Johnson, and Kathleen Misovec Washington NASA Aug. 1988 146 p
(Contract NAS1-18322)
(NASA-CR-4166; NAS 1.26:4166) Avail: NTIS HC A07/MF A01 CSCL 13I

Research on the synchronous response modelling and control of an advanced Annular Momentun Control Device (AMCD) used to control the attitude of a spacecraft is described. For the flexible rotor AMCD, two sources of synchronous vibrations were identified. One source, which corresponds to the mass unbalance problem of rigid rotors suspended in conventional bearings, is caused by measurement errors of the rotor center of mass position. The other sources of synchronous vibrations is misalignment between the hub and flywheel masses of the AMCD. Four different control algorithms were examined. These were lead-lag compensators that mimic conventional bearing dynamics, tracking notch filters used in the feedback loop, tracking differential-notch filters, and model-based compensators. The tracking differential-notch filters were shown to have a number of advantages over more conventional approaches for both rigid-body rotor applications and flexible rotor applications such as the AMCD. Hardware implementation schemes for the tracking differential-notch filter were investigated. A simple design was developed that can be implemented with analog multipliers and low bandwidth, digital hardware. Author

N88-29996# Army Natick Research and Development Command, Mass.
CONTROL SYSTEMS FOR PLATFORM LANDINGS CUSHIONED BY AIR BAGS Final Technical Report, Jul. - Aug. 1985
Edward W. Ross Jul. 1987 40 p
(AD-A196154; NATICK/TR-88/021) Avail: NTIS HC A03/MF A01 CSCL 15E

This report presents an exploratory mathematical study of control systems for airdrop platform landings cushioned by airbags. The basic theory of airbags is reviewed and solutions to special cases are noted. A computer program is presented, which calculates the time-dependence of the principal variables during a landing under the action of various control systems. Two existing control systems of open-loop type are compared with a conceptual feedback (closed-loop) system for a fairly typical set of landing conditions. The feedback controller is shown to have performance much superior to tho other systems. The feedback system undergoes an interesting oscillation not present in the other systems, the source of which is investigated. Recommendations for future work are included. GRA

N88-29997*# National Aeronautics and Space Administration. Lewis Research Center, Cleveland, Ohio.
OPTICAL MEASUREMENTS OF SOOT AND TEMPERATURE PROFILES IN PREMIXED PROPANE-OXYGEN FLAMES
Valerie J. Lyons and Patrick J. Pagni (California Univ., Berkeley.) 1988 20 p Proposed for presentation at the Winter Annual Meeting of the American Society of Mechanical Engineers, Chicago, Ill., 28 Nov. - 2 Dec. 1988
(NASA-TM-101343; E-4363; NAS 1.15:101343) Avail: NTIS HC A03/MF A01 CSCL 13B

Two laser diagnostic techniques were used to measure soot volume fractions, number densities and soot particle radii in premixed propane/oxygen flat flames. The two techniques used were two wavelength extinction, using 514.5 nm to 632.8 nm and 457.9 nm to 632.8 nm wavelength combinations, and extinction/scattering using 514.5 nm light. The flames wre fuel-rich (equivalence ratios from 2.1 to 2.8) and had cold gas velocities varying from 3.4 to 5.5 cm/s. Measurements were made at various

heights above the sintered-bronze, water-cooled flat flame burner with the equivalence ratio and cold gas velocity fixed. Also, measurements were made at a fixed height above the burner and fixed cold gas velocity while varying the equivalence ratio. Both laser techniques are based on the same underlying assumptions of particle size distribution and soot optical properties. Full Mie theory was used to determine the extinction coefficients K sub ext, and the scattering efficiencies, Q sub vv. Temperature measurements in the flames were made using infrared radiometry. Good agreement between the two techniques in terms of soot particle radii, number density and volume fraction was found for intensity ratios (I/I sub o) between 0.1 and 0.8. For intensity ratios higher or lower than this range, the differences in extinction coefficients at the wavelengths chosen for the two-wavelength method are too small to give accurate results for comparing particle radii and number densities. However, when comparing only soot volume fractions, the agreement between the two techniques continued to be good for intensity ratios up to 0.95. Author

N88-29998# Naval Postgraduate School, Monterey, Calif.
NUMERICAL FIELD MODEL SIMULATION OF FULL SCALE FIRE TESTS IN A CLOSED SPHERICAL/CYLINDRICAL VESSEL M.S. Thesis
Janet K. Raycraft Dec. 1987 241 p
(AD-A195067) Avail: NTIS HC A11/MF A01 CSCL 13L

Most of the casualties incurred during a fire are due to the smoke generated. An understanding of the way smoke and fire spread during a fire would provide a valuable tool to save lives and minimize damage. The Naval Research Laboratory maintains a full scale test facility called Fire-1. The computer model developed in this thesis is based on the actual geometry of Fire-1 and uses field modeling. It is a three dimensional, finite difference model using primitive variables. The model includes local and global pressure corrections, surface radiation, turbulence, strong buoyancy, and conjugate boundary conditions. Given heat input data, the computer code produces pressure, temperature, density, and velocity fields. Experimental fire tests conducted in Fire-1 are used to validate the computer code. Reasonable agreement in the results has been found. Because of the model's ability to account for pressure, temperature and smoke buildup, its envisioned use is to predict fires aboard ships and submarines. GRA

32 COMMUNICATIONS AND RADAR

Includes radar; land and global communications; communications theory; and optical communications.

For related information see also *04 Aircraft Communications and Navigation* and *17 Space Communications, Spacecraft Communications, Command and Tracking.* For search and rescue see *03 Air Transportation and Safety,* and *16 Space Transportation.*

N88-29999# California Inst. of Tech., Pasadena. Dept. of Electrical Engineering.
ACOUSTOOPTIC PROCESSING OF TWO-DIMENSIONAL SIGNALS USING TEMPORAL AND SPATIAL INTEGRATION Annual Report, 1 Mar. 1987 - 28 Feb. 1988
Demetri Psaltis, Dave Brady, Scott Hudson, Fai Mok, and Jeff Yu 28 Feb. 1988 41 p
(Grant AF-AFOSR-0332-85)
(AD-A194803; AFOSR-88-0410TR) Avail: NTIS HC A03/MF A01 CSCL 17I

The goal of this project is the development of optical signal processing architectures and techniques that are suitable for processing information in two dimensions. We have applied our methods to synthetic aperture radar (SAR), image recognition, two-dimensional spectrum analysis of one-dimensional signals and adaptive phased arrays. In previous years we have developed several specific acoustooptic architectures in each category. In this report we describe our recent results in the areas of radar imaging, image correlation, and integrated optical signal processing. GRA

N88-30000# TICRA A/s, Copenhagen (Denmark).
DEVELOPMENT OF A GENERAL SOFTWARE PACKAGE FOR THE ANALYSIS AND SYNTHESIS OF PLANAR ANTENNA ARRAYS FOR SPACE APPLICATIONS Final Report
P. Balling and J. Mosig Paris, France ESA Apr. 1987 181 p
(Contract ESTEC-6567/85-NL-IW(SC))
(S-247-02; ESA-CR(P)-2582; ETN-88-93027) Avail: NTIS HC A09/MF A01

A computer program for synthesis and analysis of planar array space antennas meeting complex service requirements is described. State of the art array element excitation optimization procedures are presented. The synthesis of the beam-forming network is less well developed and depends on the technology chosen. A simple BFN synthesis procedure is implemented in the program. Far fields and near fields may be calculated. The analysis does not include mutual coupling and interactions with the BFN. Random BFN component errors and quantization effects may be modeled. A microstrip patch radiator data base was set up using a state of the art microstrip patch analysis program. The data base contains many pattern and network data for rectangular and circular patch radiators for single elements and for small clusters of elements. ESA

N88-30001*# National Aeronautics and Space Administration. Pasadena Office, Calif.
DOPPLER-CORRECTED DIFFERENTIAL DETECTION SYSTEM Patent Application
Marvin K. Simon, inventor (to NASA) and Dariush Divsalar, inventor (to NASA) (Jet Propulsion Lab., California Inst. of Tech., Pasadena.) 31 May 1988 55 p
(Contract NAS7-918)
(NASA-Case-NPO-16987-1-CU; NAS 1.71:NPO-16987-1-CU; US-Patent-Appl-SN-203376) Avail: NTIS HC A04/MF A01 CSCL 20N

Doppler in a communication system operating with a multiple differential phase-shift-keyed format (MDPSK) creates an adverse phase shift in an incoming signal. An open loop frequency estimation is derived from a Doppler-contaminated incoming signal. Based upon the recognition that, whereas the change in phase of the received signal over a full symbol contains both the differentially encoded data and the Doppler induced phase shift, the same change in phase over half a symbol (within a given symbol interval) contains only the Doppler induced phase shift, and the Doppler effect can be estimated and removed from the incoming signal. Doppler correction occurs prior to the receiver's final output of decoded data. A multiphase system can operate with two samplings per symbol interval at no penalty in signal-to-noise ratio provided that an ideal low pass pre-detection filter is employed, and two samples, at 1/4 and 3/4 of the symbol interval T sub s, are taken and summed together prior to incoming signal data detection. NASA

N88-30002# Naples Univ. (Italy). Lab. di Onde Elettromagnetische.
APPLICATION OF SAMPLING TECHNIQUES TO NEAR-FIELD FAR-FIELD TRANSFORMATION Final Report
Ovidio M. Bucci, Giorgio Franceschetti, Giuseppe Delia, Claudio Gennarelli, Giovanni Leone, Giuseppe Mazzarella, Rocco Pierri, and Gilda Schirinzi Paris, France ESA Dec. 1986 170 p
(Contract ESTEC-5709/83-NL-GH)
(ESA-CR(P)-2546; ETN-88-92769) Avail: NTIS HC A08/MF A01

The application of sampling techniques to improve near field to far field (NF/FF) transformation for antenna measurements is described. A technique for redundancy elimination is considered, thus minimizing the required number of measurements while preserving the efficiency of the usual approach. This technique was implemented in a computer program. A more effective computational algorithm for the spherical wave technique was developed and implemented in a computer program. The possibility

of avoiding the use of spherical wave expansion, in order to improve the efficiency of the transformation in the case of focusing antennas, is exploited. Techniques based on the use of the sampling-like approach, which are not redundant and are independent of the geometry of the scanning surface are presented. This flexibility is appealing in order to deal with positioning errors. Problems related to phase retrieval are reviewed. ESA

N88-30003# Naval Postgraduate School, Monterey, Calif.
LONG HAUL COMMUNICATIONS IN THE HF SPECTRUM UTILIZING HIGH SPEED MODEMS M.S. Thesis
Robert H. Ellis Mar. 1988 74 p
(AD-A194683; AD-E801635) Avail: NTIS HC A04/MF A01 CSCL 09A

In the past ten years reliable high-speed satellite systems have pushed slower less reliable communication systems to the bottom of the list for development programs. Concern over reduced budgets, vulnerability of expensive satellite systems, and recent advances in HF technology are creating new interest in upgrading existing HF communication systems. Nondevelopment Items (NDI) are defined as the use of off-the-shelf commercial items instead of costly, time-consuming conventional research and development programs. The Navy Department's current policies are designed to insure the maximum use of NDI to fulfill Navy requirements. The speed of HF systems can be improved using current signaling and modulation techniques, and reliability can be increased by error-correcting codes or error detection used in conjunction with automatic repeat request (ARQ) schemes. Improved HF systems not only provide survivable back-up capability, but increased capacity for present communication needs. GRA

N88-30004# BDM Corp., McLean, Va.
OPTICS AND SYMBOLIC COMPUTING Semiannual Report, 14 Aug. 1987 - 31 Mar. 1988
R. Athale 31 Mar. 1988 64 p
(Contract F49620-86-C-0030; ARPA Order 4952)
(AD-A195119; BDM/MCL-88-0182-TR; AFOSR-88-0478TR)
Avail: NTIS HC A04/MF A01 CSCL 12F

Sorting is central to the solution of many knowledge-based and switching problems in advance computation and communication systems. Parallel-pipelined sorting algorithms are appropriate for applications that demand high throughput, low delay and many data channels. One such algorithm, the bitonic sor, can be implemented with passive perfect shuffle interconnects between active stages of compare-and-exchange elements. This paper focuses on optical hardware to implement the C and E operation and show that by taking advantage of a distinctive feature of optical logic, namely bistability, comparison circuits of remarkable simplicity are attainable. Described are implementations of C and E in a variety of optical device technologies capable of performing latching and nonlatching logic. Based on the device characteristics potential application areas for each technology are outlined. GRA

N88-30005# Massachusetts Inst. of Tech., Lexington. Lincoln Lab.
AN IMPROVED SPHERICAL EARTH DIFFRACTION ALGORITHM FOR SEKE
Michael P. Shatz and George H. Polychronopoulos 15 Apr. 1988 48 p
(Contract F19628-85-C-0002)
(AD-A195847; CMT-111; ESD-TR-88-122) Avail: NTIS HC A03/MF A01 CSCL 20N

The spherical earth diffraction subroutine SPH35 in the radar propagation code SEKE has been known to cause errors in propagation loss computations for a range of combinations of antenna and target heights. In this report an efficient method to evaluate the Airy function in the complex plane is presented. This method uses the power series expansion near the origin and an integral representation elsewhere. It is more accurate and as fast as the method employed in the spherical earth diffraction subroutine SPH35 that evaluates every Airy function of Fock's series by a fourth-order polynomial fit to its logarithm. The algorithm presented was incorporated in a new spherical earth diffraction subroutine (SPH35N). It was found that, if SEKE uses this subroutine, no problems arise for normalized heights of up to 5000 (i.e., about 350 km at VHF or 17 km at Ku-band). The subroutine SPH35N, described in this report, has been used in the versions of SEKE running at Lincoln Laboratory, and is in the version of SEKE currently being supplied to other users. GRA

N88-30006# Air Force Weapons Lab., Kirtland AFB, N. Mex.
EMPTAC (ELECTROMAGNETIC PULSE TEST AIRCRAFT) USER'S GUIDE Final Report, Oct. 1984 - Dec. 1986
Dale R. Cleaveland and Avery Burkhard Apr. 1988 56 p
(AD-A195072; AFWL-TR-88-28) Avail: NTIS HC A04/MF A01 CSCL 20N

This guide was established to give test managers a way to familiarize themselves with the Air Force Weapons Laboratory's electromagnetic pulse (EMP) test aircraft program located at Kirtland Air Force Base (KAFB), New Mexico. Brief descriptions of the available EMP test facilities at KAFB are also included. This guide should give prospective customers (users) adequate information to scope the magnitude of their test effort and to accomplish general planning without extensive involvement in test execution details. GRA

N88-30007# Naval Research Lab., Washington, D.C.
TRACK PERFORMANCE CONSIDERATIONS FOR MONOPULSE RADARS
Ching-Tai Lin and Dean D. Howard 8 Jun. 1988 26 p
(AD-A196232; NRL-9119) Avail: NTIS HC A03/MF A01 CSCL 17I

A generic monopulse radar simulation model is being developed to assess the effectiveness of counter-measures and counter-countermeasures in selectable tactical scenarios. In this report, track performance consideration for monopulse radars is analyzed in detail. The radar tracking stability and sensitivity are analyzed in terms of the open-loop gain crossover, open-loop phase margin, and the closed-loop bandwidth and damping ration. Track loops are synthesized through filter pole/zero placement with consideration of the overall loop gain. An analytical solution is derived as a function of radar parameters that describes the angle and range tracking responses. This eliminates time-consuming computer simulations and provides detailed insight into how basic radar characteristics affect monopulse radar track. GRA

N88-30008# Catholic Univ. of America, Washington, D.C.
TRANSIENT INTERACTION OF ELECTROMAGNETIC PULSES IN DIELECTRICS AND MICROWAVE BIOPHYSICS Final Report, 15 Feb. 1985 - 30 Sep. 1987
Theodore C. Guo and Wendy W. Guo 12 May 1988 23 p
(Contract MIPR-85-MM-5507; DA Proj. 3M1-61102-BS-10)
(AD-A195687) Avail: NTIS HC A03/MF A01 CSCL 06G

This research includes the following three subjects: (1) pressure waves generated by microwave pulses; a thorough formulation on microwave electrostrictive effects is developed. It is shown that pressure waves may be generated via two physical mechanisms, one by thermoelastic process and another by electrostrictive force. On the thermoelastic process, pressure waves are generated by microwave pulses if there are thermal, mechanical, or electrical discontinuities in dielectrics, (2) transient dielectric response; a non-steady state model of dielectric relaxation is developed to analyze dielectric response to short microwave pulses in the transient regime, and (3) microwave dosimetry and microwave imaging; two non-invasive microwave dosimetry techniques are developed, which are also applied to develop three-dimensional microwave imaging algorithms of arbitrary inhomogeneous dielectric bodies. GRA

N88-30009# Syracuse Univ., N. Y. Dept. of Electrical and Computer Engineering.
ON ADAPTIVE CELL-AVERAGING CFAR (CONSTANT FALSE-ALARM RATE) RADAR SIGNAL DETECTION Final Technical Report, Jun. 1984 - Dec. 1986
Mourad Barkat and Pramod K. Varshney Oct. 1987 170 p

(Contract F30602-81-C-0169)
(AD-A196286; RADC-TR-87-160) Avail: NTIS HC A08/MF A01 CSCL 17I

In radar signal detection, the problem is to automatically detect a target in a nonstationary noise and clutter background while maintaining a constant probability of false alarm. Classical detection using a matched filter receiver and a fixed threshold is not applicable due to the nonstationary nature of the background noise. Therefore, adaptive threshold techniques are needed to maintain a constant false-alarm rate (CFAR). One approach to adaptive detection in nonstationary noise and clutter background is to compare the processed target signal to an adaptive threshold. In the cell-averaging CFAR processing, an estimate of the background noise from the leading and the lagging reference windows is used to set the adaptive threshold. A threshold multiplier (or scaling factor) is used to scale the threshold to achieve the desired probability of false alarm. In the first part of this report, we have proposed two modified cell-averaging detectors for multiple target situations. The first one is a weighted cell-averaging CFAR detector, WCA-CFAR, where weighted leading and lagging reference windows are used to obtain the adaptive threshold. The second is a cell-censored, cell averaging CFAR processor where a predetermined fixed threshold is used to eliminate those cells that may contain interference. GRA

N88-30010# Massachusetts Inst. of Tech., Cambridge. Microsystems Research Center.
PERFORMANCE ANALYSIS OF k-ary n-CUBE INTERCONNECTION NETWORKS
William J. Dally Nov. 1987 28 p
(Contracts N00014-80-C-0622; N00014-85-K-0124)
(AD-A195542; VLSI-Memo-87-424) Avail: NTIS HC A03/MF A01 CSCL 25C

VLSI communication networks are wire limited. The cost of a network is not a function of the number of switches required, but rather a function of the wiring density required to construct the network. This paper analyzes communication networks of varying dimension under the assumption of constant wire bisection. Expressions for the latency, average case throughput, and hot-spot throughput of k-ary n-cube networks with constant bisection are derived that agree closely with experimental measurements. It is shown that low-dimensional networks (e.g., tori) have lower latency and higher hot-spot throughput than high-dimensional networks (e.g., binary n-cubes) with the same bisection width. GRA

N88-30011# Texas Univ., Austin. Dept. of Electrical and Computer Engineering.
CONFIRMATION OF SLOW-WAVES IN A CROSSTIE OVERLAY COPLANAR WAVEGUIDE AND ITS APPLICATION TO BAND-REJECT GRATINGS AND REFLECTORS
Te-Hui Wang and Tatsuo Itoh Mar. 1988 168 p
(Contract DAAL03-88-K-0005)
(AD-A194981; ARO-25045.1-EL) Avail: NTIS HC A08/MF A01 CSCL 09A

The slow-wave propagation along a new crosstie overlay slow-wave coplanar waveguide has been investigated both theoretically and experimentally. A slow-wave factor observed agrees reasonably well with the theoretical prediction. This structure is used for construction of a frequency-selective distributed Bragg reflectors (DBR's) with a compact size. The effect of conductor loss is considered. A doubly-periodic band-reject grating has been created from the DBR's and the band-reject phenomenon was observed as predicted. To improve passband characteristics of the grating, a monolithic slow-wave Chebyshev reflector was designed and fabricated. Agreement between theory and preliminary experiment has been confirmed. Based on this theory, a new slow-wave reflector with improved characteristics is proposed and examined. A respectable slow-wave factor and a drastic reduction of conductor loss have been obtained. GRA

N88-30012# Universidad Autonoma de Madrid, Cantoblanco (Spain). Dept. of Applied Physics.
STUDY OF SECONDARY EMISSION PROPERTIES OF MATERIALS USED FOR HIGH POWER RF COMPONENTS IN SPACE Final Report
L. Galan, C. Moranti, F. Rueda, and J. M. Sanz Paris, France ESA 1988 86 p
(Contract ESTEC-6577/85-NL-PB)
(ESA-CR(P)-2587; ETN-88-93031) Avail: NTIS HC A05/MF A01

Secondary electron emission (SEE) properties of materials used for high power waveguide components in space, particularly on surfaces for space hardware were studied, including Alodine surfaces before and after power conditioning. Surface treatments to aid multipactor suppression for these materials, including methods for surface protection and handling, were examined. If only true SEE is considered, Alodine coatings have better characteristics than TiN, TiC, Cr2O3, and C. The rugosity of Alodine may explain its good properties. No clear correlation between SEE characteristic values and multipactor threshold power is found; smaller SEE is not determinant for obtaining higher multipactor threshold power. ESA

N88-30013# British Aerospace Public Ltd. Co., Stevenage (England). Space and Communications Div.
OPTICAL MULTIPLE ACCESS INTERSATELLITE LINKS Final Report
M. A. Grant, comp., N. F. Matthews, comp., and D. Robson, comp. Paris, France ESA Mar. 1988 122 p
(Contract ESTEC-7211/87-NL-DG)
(BAe-TP-8502; ESA-CR(P)-2619; ETN-88-93042) Copyright Avail: NTIS HC A06/MF A01

The feasibility of an optical implementation of a multiple access medium data rate data relay service on the timescale of Euro-DRS was assessed. The service requirements for the feasibility study are based on the service which, in existing or planned systems, is implemented at S band. The system should communicate simultaneously with up to 8 LEO users in orbits of radii up to 7400 km providing 8 independently agile links. On each link, it should communicate at up to 2Mb/sec, at bit error rates of 10 to the minus 6th power in the return direction (LEO to GEO). A design concept for the GEO central node was produced. Mass and power estimates were evaluated and a preliminary spacecraft accommodation study performed. The system weighs 130 kg and has a power consumption of 300 W. The optical subsystem occupies a 75 x 75 x 30 cm volume on the top floor of the spacecraft. A number of trade-offs were identified and performed in reaching the final system configuration. The system should have 1 telescope system per user, a periscope mirror configuration for coarse pointing, a single telescope for both transmit and receive, and the use of both 0.8 micron for the LEO-GEO link and 1.3 micron for GEO-LEO. ESA

N88-30014# Massachusetts Inst. of Tech., Cambridge. Artificial Intelligence Lab.
DESIGN OF A SELF-TIMED VLSI MULTICOMPUTER COMMUNICATION CONTROLLER
William J. Dally and Paul Song Nov. 1987 7 p
(Contracts N00014-80-C-0622; N00014-85-K-0124)
(AD-A194567; VLSI-Memo-87-423) Avail: NTIS HC A02/MF A01 CSCL 12G

We describe the design of the network design frame, (NDF), a self-timed routing chip for a message-passing concurrent computer. The NDF uses a partitioned data path, low-voltage output drivers, and a distributed token-passing arbiter to provide a bandwidth of 450 Mbits/sec into the network. Wormhole routing and bidirectional virtual channels are used to provide low latency communications, less than micro seconds latency to deliver a 216 bit message across the diameter of a 1K node machine. To support concurrent software systems, the NDF provides two logical networks, one for user messages and one for system messages, that share the same set of physical wires. To facilitate the development of network

nodes, the NDF is a design frame. The NDF circuitry is integrated into the pad frame of a chip leaving the center of the chip uncommitted. GRA

N88-30015 Eurocontrol Experimental Centre, Bretigny (France).
EVALUATION OF LISBON TAR SSR RADAR Report, Sep. 1986 - Apr. 1987
I. Fuller Apr. 1987 186 p
(EEC/NOTE-5/87) Avail: NTIS HC E09/MF E09; copy not available from STI Facility CSCL 17I

The evaluation was carried out to investigate the TAR SSR performance with various combinations of antenna tilt, transmitter power and PRF in order to determine an optimum solution for TMA and long range detection performance with minimum false alarm rate. The evaluation was carried out in two stages: (1) on site visual evaluation of individual targets on the TAR SSR for each configuration, concurrently recordings were made of plots and local track data for TAR, MONTE JUNTO and FOIA, and (2) evaluation of the recordings using LAURENCE chain of program at EEC for probability of detection, plot reliability. The EEC note presents the results of both stages of the evaluation for selected configurations of the TAR SSR. Author

N88-30016# Polytechnic Inst. of New York, Farmingdale. Research Inst.
MILLIMETER WAVE GENERATION BY RELATIVISTIC ELECTRON BEAMS Final Report, 1 Nov. 1986 - 31 Oct. 1987
Spencer P. Kuo Oct. 1987 8 p
(Grant AF-AFOSR-0040-87)
(AD-A195683; AFOSR-88-0675TR) Avail: NTIS HC A02/MF A01 CSCL 20C

Under the support of this equipment grant, the facilities of the Plasma laboratory of the Institute used for an on-going research program funded by the AFOSR have been upgraded. Our research program bears the scientific goal to develop a high power, compact microwave device carrying good output efficiency. A cusptron device is thus designed to fit the requirements. This device utilizes the negative mass instability for the resonant interaction between an axis-encircling electron beam and the modes of a slotted cylindrical waveguide. This beam configuration is produced by passing an electron beam through cusp magnetic field and maximizes the finite Larmour radius effect for harmonic cyclotron resonance interaction. Further, the slotted boundary introducing a periodic fringe field near the orbits of the electron beam, thus, enriches the resonant harmonic contents of the RF fields as experienced by the gyrating electrons. GRA

N88-30017# Ohio State Univ., Columbus.
ROLE OF ORDINARY TO EXTRAORDINARY MODE WAVE COUPLING IN IONOSPHERIC HEATING EXPERIMENTS Final Report, Jul. 1983 - Aug. 1985
B. Abali, T. A. Seliga, and K. Aydin Mar. 1988 147 p
(Contract F19628-83-K-0005)
(AD-A195335; AS-S-121; RADC-TR-88-22) Avail: NTIS HC A07/MF A01 CSCL 12C

Electromagnetic wave propagation in a plane stratified ionospheric plasma and its possible applications to high power, high frequency (HF) experiments are investigated. A theoretical and computational examination of ordinary to extraordinary mode wave coupling is made. This coupling occurs when the propagation is in the magnetic meridian, near the critical angle of incidence. The importance of the mode coupling phenomenon in ionospheric heating experiments is discussed and demonstrated with numerical full wave solutions of the generalized differential equations governing radiowave propagation in a stratified ionosphere. Computational results indicate that mode coupling leads to intense absorption of radiowave energy near the plasma resonance level. The angular shape of the coupling window, in which the coupling is most effective, is found to be approximately circular with its width being a function of the gradient of the electron density. GRA

N88-30018# Lowell Univ., Mass. Center for Atmospheric Research.
THE EFFECT OF EQUATORIAL IONOSPHERIC IRREGULARITIES ON THE PERFORMANCE OF A SOUTH-LOOKING OTH-B (OVER-THE-HORIZON-BACKSCATTER) RADAR Scientific Report No. 6
Gary S. Sales Oct. 1987 21 p Prepared in cooperation with Northwest Research Associates, Inc., Bellevue, Wash.
(Contract F19628-87-C-0003)
(AD-A195090; AFGL-TR-87-0332) Avail: NTIS HC A03/MF A01 CSCL 17I

Mid and high latitude ionospheric irregularities are a known source of wideband clutter for Over-the-Horizon Backscatter (OTH-B) radars that operate with a northern boresight component. For northerly boresighted radars, specular scatter (Sales, 1987) was shown to possess characteristics closely related to the spatial occurrence of wideband, ionospheric clutter. This report summarizes a study to investigate specular scatter as a potential source of clutter for south-looking OTH-B radars. The results of this study show that over the azimuths of 120 to 240 degrees (clockwise from north), and for the cases considered, that clutter should not impact south-looking OTH-B radar performance. GRA

N88-30019# Naval Postgraduate School, Monterey, Calif.
COMPARATIVE ANALYSIS OF PASSIVE COMMUNICATIONS SATELLITES EMPLOYING THE SHF AND HF SPECTRUM FOR USE IN A STRATEGIC ROLE M.S. Thesis
Giuseppe Donadio Mar. 1988 82 p
(AD-A194682; AD-E801635) Avail: NTIS HC A05/MF A01 CSCL 22B

Passive communications satellites were instrumental in the evolution of today's satellite communications networks. However, ever since the successful deployment of the first geostationary satellite, research and development into passive communications satellites has almost come to a halt. In addition to examining the characteristics of the historic passive satellites, this thesis will evaluate the capabilities of a new design approach for a passive system. The passive backscatter array, which was initially proposed by Joseph Yater, was intended to provide an effective communications satellite with a large radar cross section. Primary emphasis is placed upon this system's survivability within a nuclear stressed environment. The effects of a nuclear burst upon the propagation of an electromagnetic signal are evaluated so as to assess systems survivability. GRA

N88-30020# Massachusetts Inst. of Tech., Lexington.
CORNER EXTRACTION FROM RADAR IMAGES
T. Peli 1988 5 p Repr. from Proceedings of ICASSP-International Conference, Acoustics, Speech, and Signal Processing, 1988 p 1216-1219 Submitted for publication
(Contract F19628-85-C-0002)
(AD-A194857; MS-7681; ESD-TR-88-156) Avail: NTIS HC A02/MF A01 CSCL 17I

The 3D structure of a moving object such as a satellite may be estimated from a sequence of radar images using machine intelligence techniques. In this paper we explore a region growing approach for the extraction of features such as the corner of a panel. The grown regions are seeded by strong radar returns. Since the extracted regions are fragmented and do not lead to an outline as would be perceived by a human observer, and adaptive nonlinear algorithm was designed to obtain an improved estimate of the outlines. Corners were detected by a method based on the polygon approximation of the outlines. The proposed corner detector was compared to a number of other corner detectors and was found to be superior. GRA

N88-30021# Illinois Univ., Urbana. Coordinated Science Lab.
PERFORMANCE OF DS/SSMA COMMUNICATIONS IN IMPULSIVE CHANNELS. PART 1: CORRELATION RECEIVERS
B. Aazhang and H. V. Poor Nov. 1987 12 p
(Contract DAAL03-86-K-0093)

(AD-A195712; ARO-23026.1-EL) Avail: NTIS HC A03/MF A01 CSCL 12I

The performance of digital linear correlation receivers is studied in a multiuser environment. There are assumed to be two types of sources interfering with data transmission: multiple-access interference, and additive channel noise which is attributed to impulsive noise sources in the environment. The contribution of multiple-access interference is examined by considering K asynchronous users transmitting simultaneously over a linear channel using the binary PSK direct-sequency spread-spectrum multiple-access (DS/SSMA) technique. Alternatively, the effects of the non-Gaussian impulsive channel in such a system are studied by modeling the samples of noise after front-end filtering. Error-probability performance under these conditions is compared to that for additive white Gaussian noise (AWGN) channels. Due to computational complexity, exact analysis is limited here to systems utilizing short spreading sequences. Computationally simple methods are proposed for approximating the average error probability when the length of the signature sequences is large. Furthermore, some asymptotic results are obtained for the case of infinitely long sequences. In all cases, performance variation is examined as the shape of the noise density varies with SNR held constant. The results of this analysis indicate that the presence of impulsive noise can cause significant performance degradation over that predicted from an AWGN model, even when the total noise power does not increase. GRA

N88-30022# Marconi Space and Defence Systems Ltd., Portsmouth (England).

DEVELOPMENT OF PROCEDURES FOR PERFORMING END-TO-END TESTS ON THE ERS-1 RADAR ALTIMETER AND AMI USING A COMPACT ANTENNA TEST RANGE Final Report

P. R. Miller Paris, France ESA Aug. 1987 36 p (Contract ESA-3991-00786-FR)
(ESA-CR(P)-2558; ETN-88-93013) Copyright Avail: NTIS HC A03/MF A01

Performing end-to-end tests on the ERS-1 radar altimeter and AMI using a Compact Antenna Test Range (CATR), using the CATR as a plane wave interface to a return signal processor was studied. Consideration of the procedures and error budgets shows that, with care, very good accuracy can be achieved in the measurement of all the major parameters. The proposed design for the return signal simulators is to use analog delay and attenuation only and to provide any target simulation by post-detection processing. The possibility of providing the target simulation within the return signal processor was rejected due to the lack of speed of most digital processors (the A/D requirement is 12 bit encoding at a 35 MHz sampling frequency). However, this situation is changing and clutter simulators offering 16 + J16 bit resolution at 2 MHz FM chirp bandwidth are available. ESA

N88-30023# International Scientific Radio Union, Brussels (Belgium).

REVIEW OF RADIO SCIENCE, 1984-1986

Geoffrey Hyde, ed. (Communications Satellite Corp., Clarksburg, Md.) 1987 185 p
Avail: NTIS HC A09/MF A01

Radio science is the underpinning of a communication information revolution that is fueled by telephone, television and radio navigation, and explosively developed by satellite communication, space exploration, fiber optics, and computers maturing to deal with information as well as arithmetic. The state of the science in 1987 is presented. The summaries by area and the extensive list of references are valuable tools for students of radio science. For individual titles, see N88-30024 through N88-30032.

N88-30024# International Scientific Radio Union, Brussels (Belgium).

ELECTROMAGNETIC METROLOGY

R. Kaarls, ed., G. deJong, ed., J. deVreede, ed., and C. Harmans, ed. *In its* Review of Radio Science, 1984-1986 1987 27 p (For primary document see N88-30023 24-32)
Avail: NTIS HC A09/MF A01

A survey is presented of progress in electrical and electromagnetic metrology. Included in the survey is literature on: impedance and reflection coefficient; voltage, power, attenuation, and noise; electromagnetic fields; bioeffects by EM fields; material properties; optical power and fiber metrology; frequency standards; time scale formation and comparisons; and the electrical SI units, their associated standards and the role of quantum metrology. Numerous references are included. E.R.

N88-30025# International Scientific Radio Union, Brussels (Belgium).

FIELDS AND WAVES

E. V. Jull, ed., I. M. Besieris, W. D. Burnside, D. G. Dudley, K. J. Langenberg, E. Lueneberg, E. K. Miller, A. D. Olver, and E. Yamashita *In its* Review of Radio Science, 1984-1986 1987 20 p (For primary document see N88-30023 24-32)
Avail: NTIS HC A09/MF A01

A survey is presented of progress in fields and waves. Growing activity in fields and waves is evident, not only in journals and books, but also in the growth and proliferation of conferences. The overall direction of development in fields and waves is in part a continuation of trends evident in previous reviews. Areas of interest included in the survey are general scattering and diffraction; high frequency techniques; transient fields; computational techniques; propagation in random, inhomogeneous, and nonlinear media; inverse scattering; guided waves; and antennas. E.R.

N88-30026# International Scientific Radio Union, Brussels (Belgium).

SIGNALS AND SYSTEMS

K. Geher, ed., G. Barany, ed., L. Gyoerfi, ed., J. Solymosi, ed., and Cs. Szabo, ed. (Technical Univ. of Budapest, Hungary) *In its* Review of Radio Science, 1984-1986 1987 10 p (For primary document see N88-30023 24-32)
Avail: NTIS HC A09/MF A01

Advances in signal processing, information theory, circuit theory, telecommunication, satellite communication, mobile radio, computer networks, and optical communication are reported. In addition to the prevailing national projects, new international projects involving electronic and telecommuncation research have begun. Optical and digital signal processing is surveyed along with optical fiber communications. Author

N88-30027# International Scientific Radio Union, Brussels (Belgium).

ELECTRONIC AND OPTICAL DEVICES AND APPLICATIONS

c33

Jeannine Henaff *In its* Review of Radio Science, 1984-1986 1987 16 p (For primary document see N88-30023 24-32)
Avail: NTIS HC A09/MF A01

This survey was made to mark the progress in research and development on electronic and optoelectronic devices which may later affect other areas. For more than 10 years, information processing and its storage, transmission, and control have been achieved with electrons, as well as photons and phonons, as demonstrated by the devices and applications reviewed in this survey. Electronic devices, microwave circuits, semiconductor physics, surface acoustic waves and optical fibers are areas included. E.R.

N88-30028# International Scientific Radio Union, Brussels (Belgium).

ELECTROMAGNETIC NOISE AND INTERFERENCE

H. Kikuchi *In its* Review of Radio Science, 1984-1986 1987 13 p (For primary document see N88-30023 24-32)
Avail: NTIS HC A09/MF A01

A survey of progress for the past three years in the field of electromagnetic noise and interference is presented. Areas of concern are terrestrial and planetary noise of natural and man made origin, the composite noise environment, the effects of noise

on system performance, the lasting effects of transients on equipment performance, the scientific basis of noise and interference control and spectrum utilization. E.R.

N88-30029# International Scientific Radio Union, Brussels (Belgium).
WAVE PROPAGATION AND REMOTE SENSING **c43**
R. K. Crane, comp. *In its* Review of Radio Science, 1984-1986 1987 12 p (For primary document see N88-30023 24-32)
Avail: NTIS HC A09/MF A01

This survey, abstracted from a list of 924 references cited in the national contributions, summarizes the work in wave propagation through nonionized media and the remote sensing of the properties of such media published from 1983 to 1986. The review is divided into three major sections: wave propagation theory, applications in remote sensing, and applications in communications. Author

N88-30030# International Scientific Radio Union, Brussels (Belgium).
IONOSPHERIC RADIO AND PROPAGATION: WAVES IN PLASMAS
R. F. Benson, K. Davies, V. I. Aksenov, ed., S. Ananthakrishnan, ed., L. W. Barclay, ed., Sa. Basu, ed., Su. Basu, ed., S. J. Bauer, ed., T. F. Bell, ed., and G. Belmont, ed. et al. *In its* Review of Radio Science, 1984-1986 1987 40 p (For primary document see N88-30023 24-32)
Avail: NTIS HC A09/MF A01

A survey is presented of literature concerning the ionospheric radio and propagation of waves in plasma. Specific areas are: incoherent scatter; coherent scatter and other sounding methods; probing of the ionosphere and magnetosphere by means of EM waves; basic wave processes in plasma; ionospheric plasma instabilities; ionospheric modifications; magnetospheric plasma instabilities; influence of the ionosphere on radio systems; composition, ionization and chemistry of the D region; ionospheric dynamics; models of the ionosphere; and stratosphere, mesosphere, ionosphere interactions. E.R.

N88-30031# International Scientific Radio Union, Brussels (Belgium).
RADIO ASTRONOMY **c89**
R. Wielebinski, ed. *In its* Review of Radio Science, 1984-1986 1987 16 p (For primary document see N88-30023 24-32)
Avail: NTIS HC A09/MF A01

A survey of literature concerning radio astronomy is presented. A survey covers recent developments during 1983 to 1986. Subject areas are: new instrumentation; computing and new methods; VLBI instrumentation; solar radio astronomy; solar system radio astronomy; galactic research; extragalactic radio astronomy; and new fields of research. E.R.

N88-30032# International Scientific Radio Union, Brussels (Belgium).
BIOEFFECTS OF ELECTROMAGNETIC WAVES **c52**
C. Romero-Sierra *In its* Review of Radio Science, 1984-1986 1987 20 p (For primary document see N88-30023 24-32)
Avail: NTIS HC A09/MF A01

The scientific literature of these years, 1984 to 1986, on the bioeffects of electromagnetic (EM) waves includes many articles with not only the finest scientific methodology but also discriminating critical analysis and data interpretation. A better understanding of the basic interactive mechanisms was gained in recognizing that they depend on three groups of variables: the EM field, the living systems and their components, and their coupling efficiency, i.e., dosimetry and window phenomena. Although most areas of this scientific field have developed steadily during these years, some of them have attracted particular attention, e.g., dosimetry, cellular and subcellular effects, diagnostic and therapeutic applications, and pulsed EM fields. Author

N88-30033# Naval Research Lab., Washington, D.C. High Power Electromagnetic Radiation Branch.
A SUBMILLIMETER WAVELENGTH SPACE-BASED IMAGING RADAR Interim Report
Wallace M. Manheimer 31 May 1988 26 p
(AD-A195846; NRL-9111) Avail: NTIS HC A03/MF A01 CSCL 17I

This report considers the use of a submillimeter wavelength space-based imaging radar. The main application envisioned is midcourse decoy discrimination for strategic defense, for which it would have the capability of producing a series of images, in real time, at strategic ranges, with less than meter scale resolution and with modest power requirements. Undoubtedly, there are other applications. The requirements for a SAR and ISAR imaging radar at submillimeter wavelength are determined, and the prospect for the development of RF sources to power the radar is examined. GRA

N88-30034# Naval Postgraduate School, Monterey, Calif.
SCATTERING IMPULSE RESPONSE SYNTHESIS USING RANDOM NOISE ILLUMINATION: INITIAL CONCEPT EVALUATION M.S. Thesis
Dong Il Lee Mar. 1988 119 p
(AD-A195086) Avail: NTIS HC A06/MF A01 CSCL 17I

This thesis investigates the synthesis of smoothed impulse responses using sampled data of the input and output of random noise driven electromagnetic systems. Special interactive software was developed for the Naval Postgraduate School's time domain electromagnetic scattering laboratory. The system performs signal acquisition, synthesizes time and frequency domain scattering responses using broad band random noise and provides results as easily evaluated graphic displays. Attempted validations of the system are made by comparing synthesized impulse responses for microwave filters and transient scatterers to alternate experimental and computational data. GRA

N88-30035# Environmental Research Inst. of Michigan, Ann Arbor. Radar Science Lab.
MIZEX (MARGINAL ICE ZONE EXPERIMENT) 1987 SAR (SYNTHETIC APERTURE RADAR) DATA SUMMARY
R. A. Shuchman, L. L. Sutherland, and B. A. Burns Feb. 1988 137 p
(Contracts N00014-87-C-0418; N00014-81-C-0195)
(AD-A195560; ERIM-154600-34-T) Avail: NTIS HC A07/MF A01 CSCL 08L

The 1987 Winter MIZEX in the Greenland and Barents Seas, combined observation systems from both remote sensing and in situ data collection to provide an integrated approach to the study of winter marginal ice zone conditions. Favorable weather permitted 18 consecutive days of SAR coverage and field operations with real-time imagery downlinked to the ships in the field. Two INTERA SAR equipped aircraft were deployed to collect ice edge imagery. Throughout the experiment, real-time data was reviewed by scientists at Svalbard and on board the M/V POLAR CIRCLE. Observations made from this imagery enabled them to select areas of special interest for intensive study and sea truthing, and to plan successive SAR missions. Preliminary analysis indicates SAR imagery: (1) permits differentiation between first year ice, multi-year ice, and many stages of young ice; (2) can be used to detect surface expressions of eddies both in the open ocean and within the ice pack; (3) permits the tracking of ocean waves both outside and propagating approximately 100 km into the ice pack; (4) shows internal wave features beneath the ice pack; and (5) mapped an ocean polar front in the Barents Sea. GRA

N88-30036# Naval Research Lab., Washington, D.C.
MEASUREMENT AND INTERPRETATION OF NORTH ATLANTIC OCEAN MARINE RADAR SEA SCATTER Interim Report, Jan. 1985 - Jun. 1987
Dennis B. Trizna 31 May 1988 54 p
(AD-A196239; NRL-9099) Avail: NTIS HC A04/MF A01 CSCL 17I

Results are presented for experiments conducted with a

noncoherent, high-resolution marine navigation radar aboard the NOAA ship Researcher in the North Atlantic Ocean. High-resolution radar backscatter data were collected under wind-wave equilibrium conditions, i.e., both fetch and time requirements for fully developed seas were satisfied for the wind speeds reported. Cumulative distributions of normalized radar cross section (NRCS) of the sea surface are calculated and found to follow two Weibull distributions. Based on their characteristics, the distributions may be ascribed to two different scattering mechanisms: one due to scatterers evenly distributed over the surface, such as Bragg scatter; one due to localized scattering features, such as wave crests. The percentage occurrence of the localized scattering events (often called sea spikes) behaves with wind speed in a manner much like that found for whitecaps. Other characteristics of the two distributions also appear to correlate with wind speed, with a weak dependence on air-sea surface temperature difference. For very low grazing angles, many of these characteristics vary sharply near the 2 deg depression angle, which is a critical angle in several scattering models. An additional scattering model is proposed here to explain this behavior. GRA

N88-30037# Alcatel Thomson Espace, Toulouse (France).
A 30/20 GHz MULTIBEAM ARRAY ANTENNA SUITABLE FOR FUTURE HIGH RATE TDMA EUROPEAN SATELLITE NETWORKS
R. Lenormand, J. P. Marre, and D. Rene 1987 4 p Presented at the IEEE APS-URSI Meeting, Va., 1987
(ETN-88-93079) Avail: NTIS HC A02/MF A01

A satellite multibeam phased array antenna for 30/20 GHz transmit/receive high rate time division multiple access (TDMA) links was designed to match high gain, beam to beam isolation, and double polarization requirements. The proposed design also takes into account the mechanical and thermal constraints of the European OLYMPUS platform. It exploits the scanning capability of phased arrays without great mechanical constraints; in the wideband satellite case, 3 spots are simultaneously steered down to 3 Earth station at 500 Mb/sec. It has good polarization purity due to the use of a direct radiating array; such a design provides the suitable beam to beam isolation for two adjacent cross polarized spot beams. It shows suitable gain performance with a reasonable number of elements; less than 290 elements result in a minimum gain of 45.4 dB at 30 GHz over any point of the service zone. ESA

N88-30038# Air Force Inst. of Tech., Wright-Patterson AFB, Ohio.
MODELING AND PERFORMANCE OF HF/OTH (HIGH-FREQUENCY/OVER-THE-HORIZON) RADAR TARGET IDENTIFICATION SYSTEMS M.S. Thesis
Donald J. Strausberger 1988 156 p
(AD-A196287; AD-E951149; AFIT/CI/NR-88-87) Avail: NTIS HC A08/MF A01 CSCL 17I

Several Radar Target Identification (RTI) techniques have been developed at The Ohio State University in recent years. Using the ElectroScience Laboratory compact range a large database of coherent RCS measurement has been constructed for several types of targets (aircraft, ships, and ground vehicles) at a variety of polarizations, aspect angles, and frequency bands. This extensive database has been used to analyze the performance of several different classification algorithms through the use of computer simulations. In order to optimize classification performance, it was concluded that the radar frequency range should lie in the Rayleigh-resonance frequency range, where the wavelength is on the order of or larger than the target size. For aircraft and ships with general dimensions on the order of 10 meters to 100 meters it is apparent that the High Frequency (HF) band provides optimal classification performance. Since existing HF radars are currently being used for detection and tracking or aircraft and ships of these dimensions, it is natural to further investigate the possibility of using these existing radars as the measurement devices in a radar target classification system. GRA

N88-30039*# National Aeronautics and Space Administration. Goddard Space Flight Center, Greenbelt, Md.
THE FOCAL PLANE RECEPTION PATTERN CALCULATION FOR A PARABOLOIDAL ANTENNA WITH A NEARBY FENCE
Richard F. Schmidt, Hwai-Soon Cheng, and Michael W. Kao (Science Applications Research, Lanham, Md.) 1987 56 p
(NASA-TM-100691; NAS 1.15:100691) Avail: NTIS HC A04/MF A01 CSCL 20N

A computer simulation program is described which is used to estimate the effects of a proximate diffraction fence on the performance of paraboloid antennas. The computer program is written in FORTRAN. The physical problem, mathematical formulation and coordinate references are described. The main control structure of the program and the function of the individual subroutines are discussed. The Job Control Language set-up and program instruction are provided in the user's instruction to help users execute the present program. A sample problem with an appropriate output listing is made available as an illustration of the usage of the program. Author

N88-30040 Technische Hogeschool, Delft (Netherlands). Afd. der Elektrotechniek.
TIME-DOMAIN FAR-FIELD SCATTERING OF PLANE ELECTROMAGNETIC WAVES BY A PENETRABLE OBJECT IN THE BORN APPROXIMATION
D. Quak and A. T. deHoop Aug. 1986 7 p
(PB87-176129; Rept-1986-20) Avail: NTIS HC E03/MF E01; copy not available from STI Facility CSCL 20N

The Born approximation is applied to time domain scattering of a plane electromagnetic wave by a penetrable object of bounded extent, embedded in an isotropic and homogeneous medium. Closed form analytical expressions are obtained for the spherical wave far field scattering amplitude related to homogeneous objects of the following shapes: an ellipsoid, and elliptic cone of finite height, and a tetrahedron. Relaxation effects and anisotropy of the scattering object are included. The results are, among others, useful as test cases for time domain inverse scattering algorithms. Author

N88-30486*# Massachusetts Inst. of Tech., Westford. Haystack Observatory.
HIGH-RESOLUTION (30 m) LUNAR RADAR IMAGES
Stanley H. Zisk *In* Lunar and Planetary Inst., Nineteenth Lunar and Planetary Science Conference. Press abstracts 1988 p 34-36 (For primary document see N88-30473 24-88)
Avail: NTIS HC A03/MF A01 CSCL 17I

33 ELECTRONICS AND ELECTRICAL ENGINEERING

Includes test equipment and maintainability; components, e.g., tunnel diodes and transistors; microminiaturization; and integrated circuitry.

For related information see also *60 Computer Operations and Hardware* and *76 Solid-State Physics.*

N88-30041# California Univ., Berkeley. Coll. of Engineering.
PIERCE DIODE WITH EXTERNAL CIRCUIT. PART 3: CHAOTIC BEHAVIOR
William S. Lawson 28 Oct. 1987 38 p
(Contract N00014-85-K-0809)
(AD-A194837; UCB/ERL-M87/74) Avail: NTIS HC A03/MF A01 CSCL 12I

The existence of the strange attractor discovered by Godfrey in the neighborhood of alpha=3pi for the Pierce Diode is verified, and his numerical results are refined. The evolution of this attractor is then followed as an external capacitance is introduced. The Pierce diode is perhaps the simplest realistic theoretical model for a bounded one-dimensional plasma system. It is comprised of two parallel electrodes with electrons injected at one of the electrodes with velocity vo. Ions are considered to be infinitely massive, and in a uniform background which neutralizes the charge

density of the electrons at the electrode from which the electrons are injected. The electrodes are also held at the same potential, i.e., short-circuited. This short circuit allows feedback, and leads to a wealth of interesting behavior. GRA

N88-30042# Texas Univ., Arlington.
DIELECTRIC MILLIMETER WAVEGUIDES: A FEASIBILITY STUDY FOR A NOVEL DIELECTRIC MILLIMETER WAVEGUIDE Final Technical Report, Mar. 1986 - Feb. 1987
Charles V. Smith, Jr. and Jonathan S. Bagby Mar. 1988 57 p
(Contract F30602-81-C-0206)
(AD-A195104; RADC-TR-88-32-Vol-2) Avail: NTIS HC A04/MF A01 CSCL 09A

This is a final report of an initial research to theoretically access engineering feasibility of manufacturing low cost, low loss millimeter (10mm to 1mm) waveguide systems using methods from fiber optics research developed for production of glass fiber lightguides. The research completed as of this reporting indicates the following: (1) There exist low loss, approximately 10 percent of center frequency bandwidth TE propagation modes for the guides as proposed. (2) The structures tend to be excessively large in transverse dimensions at the longer wavelengths; however, as expected, the structures appear to be of a very desirable size at the short wavelengths. (3) The materials data is difficult to obtain and substantiate because of the proprietary nature associated with material development and the technical difficulty in making measurements at the proposed frequencies. GRA

N88-30043# Air Force Wright Aeronautical Labs., Wright-Patterson AFB, Ohio.
PRECISION MEASUREMENT OF THE FRESNEL DRAG COEFFICIENT USING A RING LASER Final Report, Jan. 1985 - Sep. 1986
James G. Grote May 1988 96 p
(AD-A196025; AFWAL-TR-88-1050) Avail: NTIS HC A05/MF A01 CSCL 09C

An attempt is made to improve the accuracy of the measurement of the Fresnel drag coefficient in a ring laser gyroscope. Fresnel drag is a change in the speed of light passing through a transparent moving medium. This change in velocity is proportional to the refractive index and velocity of the medium. The ring laser gyroscope used for this experiment was designed to test the performance characteristics of ring laser gyro mirrors. By inserting a transparent moving medium into the laser cavity, with a known index of refraction and accurately controlling its velocity, one can introduce an artificial gyro rotation rate since the output beat frequency of the ring laser gyro will be proportional to the rotation rate of the medium. Improvement in the accuracy of the drag coefficient was necessary to test the performance of these laser gyro mirrors. To accomplish this, the measurement techniques for most of the parameters used to determine the drag coefficient were modified. Higher accuracy, better quality components and equipment were utilized. This resulted in accuracies in the measurements of most of the parameters exceeding or equalling those observed in the two previous experiments. The experimental apparatus were controlled and the data recorded using a computer. This provided simultaneous recording of the outputs and minimized the contribution of human error. GRA

N88-30044# Polytechnic Inst. of New York, Farmingdale. Dept. of Chemistry.
STRUCTURE AND DYNAMICS OF SOLUTIONS OF LITHIUM SALTS RELEVANT TO BATTERY CONSTRUCTION Final Report, Mar. 1985 - Mar. 1988
1988 45 p
(Contract DAAG29-85-K-0051)
(AD-A195399; ARO-21758.12-CH) Avail: NTIS HC A03/MF A01 CSCL 07D

Solutions of lithium salts in media of low permittivity without or with addition of macrocycles have been characterized in their structural and dynamical behavior using various methods as infrared spectra, audio frequency electrical conductivity, microwave dielectric relaxation and ultrasonic relaxation techniques. The above electrolyte solutions and the criteria of their choice are highly relevant topics for the construction of secondary lithium batteries, the optimization of their use and of their recycling. GRA

N88-30045# Massachusetts Inst. of Tech., Cambridge. Microsystems Research Center.
REDUCING THE PARALLEL SOLUTION TIME OF SPARSE CIRCUIT MATRICES USING REORDERED GAUSSIAN ELIMINATION AND RELAXATION
David Smart and Jacob White Mar. 1988 14 p
(Contract N00014-85-K-0825)
(AD-A195152; VLSI-Memo-88-440) Avail: NTIS HC A03/MF A01 CSCL 09A

Using parallel processors to reduce the execution times of classical circuit simulation programs like SPICE and ASTAP has been the focus of much current research. In these efforts, good parallel speed increases were achieved for linearized system construction, but it has been difficult to get good parallel speed increases for sparse matrix solution. In this paper we examine two approaches for reducing parallel sparse matrix solution time; the first based on pivot ordering algorithms for Gaussian elimination, and the second based on relaxation algorithms. In the section on Gaussian elimination sparse matrix solution, we present a pivot ordering algorithm which increases the parallelism of Gaussian elimination compared to the commonly used Markowitz method. The performance of the new algorithm is compared to other suggested ordering algorithms for a collection of circuit examples. The minimum number of parallel steps for the solution of a tridiagonal matrix is derived, and it is shown that this optimum is nearly achieved by the ordering heuristics which attempt to maximize parallelism. In the section on relaxation, we present an optimality result about Gauss-Jacobi over Gauss-Seidel relaxation on parallel processors. GRA

N88-30046# Massachusetts Inst. of Tech., Cambridge. Microsystems Research Center.
CIRCUIT DESIGN CRITERIA FOR STABLE LATERAL INHIBITION NEURAL NETWORKS
J. L. Wyatt, Jr. and D. L. Standley Mar. 1988 6 p
(Contracts N00014-80-C-0622; N00014-87-K-0825)
(AD-A195066; VLSI-Memo-88-0622) Avail: NTIS HC A02/MF A01 CSCL 09A

In the analog VLSI implementation of neural systems, it is sometimes convenient to build lateral inhibition networks by using a locally connected on-chip resistive grid. A serious problem of unwanted spontaneous oscillation often arises with these circuits and renders them unusable in practice. This paper reports a design approach that guarantees such a system will be stable, even though the values of designed elements in the resistive grid may be imprecise and the location and values of parasitic elements may be unknown. The method is based on a rigorous, somewhat novel mathematical analysis using Tellegen's theorem and the idea of Popov multipliers from control theory. It is thoroughly practical because the criteria are local in the sense that no overall analysis of the interconnected system is required, empirical in the sense that they involve only measurable frequency response data on the individual cells, and robust in the sense that unmodelled parasitic resistances and capacitances in the interconnect network cannot affect the analysis. GRA

N88-30047# Technische Univ., Berlin (West Germany). Fachbereich fuer Elektrotechnik.
VOLTAGE DIRECTIVE DRIVE WITH CLAW POLE MOTOR AND CONTROL WITHOUT ROTOR POSITION INDICATOR Ph.D. Thesis [EIN SPANNUNGSRICHTERANTRIEB MIT KLAUENPOLMASCHINE UND LAGEGEBERLOSER REGELUNG]
Volker Ewald Stroenisch 1988 191 p In GERMAN
(ETN-88-93120) Avail: NTIS HC A09/MF A01

Design and testing of a voltage directive drive for synchronous variable speed claw pole motor and control without rotor position indicator is described. Economic analysis of the designed regulation

is performed. Computations of stationary and dynamic behavior are given and experimental operational behavior is determined. The motors can be used for electric transportation vehicles, diesel motors, and electric railway engines. ESA

N88-30048*# National Aeronautics and Space Administration. Lewis Research Center, Cleveland, Ohio.
HIGH FREQUENCY GaAlAs MODULATOR AND PHOTODETECTOR FOR PHASED ARRAY ANTENNA APPLICATIONS
P. C. Claspy, C. M. Chorey, S. M. Hill (Case Western Reserve Univ., Cleveland, Ohio.), and K. B. Bhasin Sep. 1988 12 p Presented at the International Symposium and Exhibition on Fiber Optics, Optoelectronics, and Laser Applications, Boston, Mass., 6-9 Sep. 1988; sponsored in part by Society of Photo-Optical Instrumentation Engineers
(NASA-TM-101328; E-4339; NAS 1.15:101328) Avail: NTIS HC A03/MF A01 CSCL 09C

A waveguide Mach-Zehnder electro-optic modulator and an interdigitated photoconductive detector designed to operate at 820 nm, fabricated on different GaAlAs/GaAs heterostructure materials, are being investigated for use in optical interconnects in phased array antenna systems. Measured optical attenuation effects in the modulator are discussed and the observed modulation performance up to 1 GHz is presented. Measurements of detector frequency response are described and results presented. Author

N88-30049# Air Force Astronautics Lab., Edwards AFB, Calif.
IN-HOUSE CAPACITOR TECHNOLOGY PROGRAM Final Report, Jul. 1977 - Feb. 1987
Denis Cote, Rudolph J. Hausauer, and Alcus G. Cromartie Feb. 1988 30 p
(AD-A194804; AFAL-TR-88-002) Avail: NTIS HC A03/MF A01 CSCL 09A

This report presents the results of a technology program directed towards the development of a long-life high energy density capacitor for applications in space. The desired high energy density of the capacitors manufactured was 40 joules/pound. Life curve data was taken in order to validate the total number of capacitor discharges while operating at a rated voltage of 2.5Kv. The capacitors tested were paper free and were composed primarily of K-film (polyvinylidene fluoridc), aluminum foil and an impregnant material. Of the several candidate impregnant materials (TCP, DAP, MIPB, and Silicone Oil), the silicone oil impregnant proved to be most successful for test purposes. Subsequently, various tests were conducted on the high energy density capacitors under various temperatures and vacuum conditions. GRA

N88-30050# Aerospace Corp., El Segundo, Calif. Chemistry and Physics Lab.
MICROCIRCUIT TRACE CUTTING WITH FOCUSED ION BEAMS
G. W. Stupian and M. S. Leung 20 Jun. 1988 14 p
(Contract F04701-85-C-0086)
(AD-A196030; TR-0086(6945-02)-2; SD-TR-88-70) Avail: NTIS HC A03/MF A01 CSCL 09A

When a failed microelectronic device is examined in a scanning electron microscope (SEM), several possible failure sites are often visible, but positive identification of the primary failure site based on micrographs alone is difficult. Several other SEM imaging modes, e.g., electron beam induced current (EBIC) and voltage contrast imaging, have been shown to be very helpful in identifying failure sites or clarifying failure mechanisms. These methods involve collecting current or supplying voltage signals through external leads to the failed device. However, application of these techniques is precluded if shorting of device elements (traces) has occurred as a result of catastrophic failure. Failure analysis is facilitated if trace metallizations can be cut selectively to isolate the electrically shorted portions of the device. This report describes the disadvantages of current trace cutting techniques and introduces a new method without these disadvantages - focused ion beam cutting. GRA

N88-30051# Argonne National Lab., Ill. Materials Science, Chemistry and Chemical Technology Div.
IMPURITY ANALYSIS IN SIMOX SAMPLES BY HIGH-EFFICIENCY RESONANCE IONIZATION TIME-OF-FLIGHT MASS SPECTROMETRY
C. E. Young, M. J. Pellin, W. F. Calaway, J. W. Burnett, D. M. Gruen, H. J. Stein, and S. S. Tsao (Sandia National Labs., Albuquerque, N. Mex.) 1988 3 p Presented at the 4th International Symposium on Resonance Ionization Spectroscopy and its Applications, Gaithersburg, Md., 10 Apr. 1988 Prepared in cooperation with Sandia National Labs., Albuquerque, New Mexico
(Contracts W-31-109-eng-38; DE-AC04-76DP-00789)
(DE88-012061; CONF-880435-21) Avail: NTIS HC A02/MF A01

The SIMOX process provides a means for the fabrication of integrated circuitry in a thin silicon layer isolated from the bulk wafer. The benefits derived from this procedure include reduced parasitic interaction of closely-spaced transistor devices and substantially increased resistance to radiation damage. These advantages can be nullified, however, by trace quantities of deep level trap impurities such as Fe in the thin silicon surface layer. The SARISA (Surface Analysis by Resonance Ionization of Sputtered Atoms) technology utilizes isochronous refocusing time-of-flight mass spectrometry optimized for the parameter useful yield: atoms detected/atoms removed from the sample. Monolayer resolution in the surface region and suppression of isobaric interferences are important instrument characteristics for the presented application. DOE

N88-30052# Energy Research Corp., Danbury, Conn.
AIRCRAFT BATTERY STATE OF CHARGE AND CHARGE CONTROL SYSTEM Final Report, Jul. 1984 - Jun. 1987
Sivaswamy Viswanathan and Allen Charkey Jan. 1988 184 p
(Contract F33615-84-C-2435)
(AD-A194979; AFWAL-TR-87-2088) Avail: NTIS HC A09/MF A01 CSCL 10B

This Final Report describes work done by Energy Research Corporation (ERC) in developing an aircraft battery state-of-charge indicator and charge control system. The basis for this system, developed by ERC, is a nickel-oxygen (NiO2) pilot cell (0.374 Ah). This pilot cell is cycled in tandem with nickel-cadmium battery. The oxygen pressure of the pilot cell is used to determine and control the state-of-charge of the nickel-cadmium battery. Nickel-cadmium batteries from different manufacturers were cycled using this pilot cell charge indication and control system. GRA

N88-30053# Naval Research Lab., Washington, D.C.
NONLINEAR DYNAMICS OF COUPLED OSCILLATOR ARRAYS
David Mosher 18 Mar. 1988 17 p
(AD-A194888; NRL-MR-6144) Avail: NTIS HC A03/MF A01 CSCL 09A

The phase-locked dynamics of large oscillator arrays is currently of interest because of possible microwave directed energy applications. Straight-forward integration of the coupled dynamical equations for such arrays is computationally costly for the associated multidimensional parameter space, long integration times, various initial conditions and system configurations. Finite difference analogs of the nonlinear differential equations can reproduce their complex dynamical behavior with a 2 to 3 order-of-magnitude improvement in computational time. Here, the applicability of the finite difference technique is demonstrated by solutions of the dynamical equations for 2 coupled oscillators and rings of larger numbers. Parameter studies for these configurations suggest the values of the coupler length and coupling strength required to provide robust phase-locked operation. The finite difference technique can be extended to model large oscillator arrays with other coupling geometries, amplifier arrays, and additional physical phenomena. GRA

N88-30054# Minnesota Univ., Minneapolis. Corrosion Research Center.
MORPHOLOGICAL CHANGES IN POLYMER ELECTROLYTE CELLS Technical Report, 15 Jul. 1985 - 30 May 1988
M. Z. Munshi and B. B. Owens May 1988 24 p Sponsored by ONR, Washington, D.C.
(AD-A195821; ONR-TR-18) Avail: NTIS HC A03/MF A01 CSCL 10C

Rechargeable solid state batteries utilizing lithium anodes, V sub 6 O sub 13 composite cathodes and polymer electrolytes made from polyethylene oxide - LiCF sub 3 SO sub 3 complex were investigated at 100 C. The cells exhibited good cycling and reversibility. Optical and scanning electron microscopy were used the morphological changes taking place at the electrodes and electrolyte as a function of cycle number. Post-mortem examination of the cell material indicated that the structures of lithium, electrolyte and cathode become finer grained and hence smoother. In addition the structures were more coherent. The cathode appeared to undergo a re-healing process during the early stage of cycling. The results indicate that the structures are consistent with one another and that long cycle life can be obtained with these types of cells. GRA

N88-30055*# Case Western Reserve Univ., Cleveland, Ohio.
OPTOELECTRONIC GAIN CONTROL OF A MICROWAVE SINGLE STAGE GaAs MESFET AMPLIFIER Final Report
Rainee N. Simons Sep. 1988 12 p
(Grant NAG3-816)
(NASA-CR-182201; E-3963; NAS 1.26:182201) Avail: NTIS HC A03/MF A01 CSCL 09A

Gain control of a single stage GaAs MESFET amplifier is demonstrated by the use of optical illumination of photon energy greater than the GaAs bandgap. The optical illumination is supplied by a semiconductor laser diode and is coupled to the Schottky gate of the MESFET by an optical fiber. The increase in gain is observed to be as much as 5.15 dB when the MESFET is biased close to pinchoff, that is, V(sub gs) equals -1.5 V and with optical illumination of 1.5 mW. The computed maximum available gain (MAG) and current gain (bar h sub 21 bar) from the de-embedded s-parameters show that MAG is unaffected by optical illumination, however, bar h(sub 21)bar increases by more than 2 dB under optical illumination of 1.5 mW. The maximum frequency of oscillation (F sub max) and the unity current gain cut-off frequency (F sub t) obtained by extrapolating the MAG and bar h(sub 21)bar curves, respectively, show that the F(sub max) is insensitive to optical illumination but F(sub t) increases by 5 GHz. Author

N88-30056# Cornell Univ., Ithaca, N.Y. School of Chemical Engineering.
REACTIVE PLASTICIZERS IN NEGATIVE E-BEAM RESISTS Technical Report No. 7
Y. M. Namaste, S. K. Obendorf, and R. Rodriguez 16 May 1988 25 p Presented at the 32nd International Symposium on Electron, Ion, and Photon Beams, Fort Lauderdale, Fla., 31 May - 3 Jun. 1988
(Contract N00014-85-K-0474)
(AD-A195161) Avail: NTIS HC A03/MF A01 CSCL 07C

Negative electron resists generally exhibit excellent sensitivity, but suffer from swelling during development which results in poor resolution. A new approach to this problem is presented, in which reactive monomers are blended with host polymers to provide sensitive negative resists with improved resolution. Polychloromethylstyrene (PCMS) and VMCH (A terpolymer containing 86 percent vinyl chloride, 13 percent vinyl acetate and 1 percent maleic acid) were both found to be compatible with two reactive monomers, trimethylolpropanetrimethacrylate (TMPTMA) and dipentaerythritolpentaacrylate (DPEPA). Addition of 20 percent (w/w) of either monomer to PCMs or VMCH resulted in approximately tenfold increases in sensitivity. GRA

N88-30027# International Scientific Radio Union, Brussels (Belgium).
ELECTRONIC AND OPTICAL DEVICES AND APPLICATIONS
Jeannine Henaff *In its* Review of Radio Science, 1984-1986 1987 16 p (For primary document see N88-30023 24-32)
Avail: NTIS HC A09/MF A01

34 FLUID MECHANICS AND HEAT TRANSFER

Includes boundary layers; hydrodynamics; fluidics; mass transfer; and ablation cooling.

For related information see also *02 Aerodynamics* and *77 Thermodynamics and Statistical Physics.*

N88-30057# Stanford Univ., Calif. Applied Mathematics Group.
MATHEMATICAL PROBLEMS OF NONLINEAR WAVE PROPAGATION AND OF WAVES IN HETEROGENEOUS MEDIA Final Report, 1 Oct. 1986 - 30 Sep. 1987
Joseph B. Keller 31 Mar. 1988 9 p
(Grant AF-AFOSR-0007-87)
(AD-A195970; AFOSR-88-0652TR) Avail: NTIS HC A02/MF A01 CSCL 20D

The asymptotic behavior of weakly nonlinear waves at caustics is determined for nonlinear wave propagation. A theory is developed for the propagation of short waves of any strength. A method is found for analyzing the stability of a large class of nonlinear waves. The theory of acoustoelasticity is reduced by considering nonlinear effects on waves in granular material. The theory of waves in heterogeneous media analyzed scattering by slender bodies. The pass and stop bands are determined for waves in stratified periodic media. The same is done for an acoustic medium containing rigid spheres arranged in a simple cubic lattice. The amplitude equations are determined for resonantly-interacting water waves in water of nonuniform depth. GRA

N88-30058*# National Aeronautics and Space Administration. Langley Research Center, Hampton, Va.
TRANSITION AT HYPERSONIC SPEEDS Final Report
Mark V. Morkovin May 1987 27 p
(Contract NAS1-18107)
(NASA-CR-178315; ICASE-IR-1; NAS 1.26:178315) Avail: NTIS HC A03/MF A01 CSCL 20D

Certain conjectures on the physics of instabilities in high-speed flows are discussed and the state of knowledge of hypersonic transition summarized. The case is made for an unpressured systematic research program in this area consisting of controlled microscopic experiments, theory, and numerical simulations. Author

N88-30059# Ballistic Research Labs., Aberdeen Proving Ground, Md.
NUMERICAL CALCULATIONS OF THE RESPONSE OF A SPINNING SPHEROIDAL PAYLOAD TO CONING MOTION
Gene R. Cooper Mar. 1988 17 p
(AD-A195890; BRL-MR-3661) Avail: NTIS HC A03/MF A01 CSCL 19J

A method for numerically evaluating a particular type of singular integral coupled with a complex eigenvalue problem is presented here. This presentation provides the information needed to carry out the numerical calculation found in the cited Murphy report. This technique has proved useful for calculating the moment exerted by a low-viscosity spinning liquid in a coning spheroidal container. GRA

N88-30060# Air Force Inst. of Tech., Wright-Patterson AFB, Ohio.
THE EFFECTS OF INCOMING BOUNDARY LAYER THICKNESS ON UNSTEADY SHOCK-INDUCED TURBULENT SEPARATIONS INDUCED BY CYLINDERS M.S. Thesis
Douglas R. Smith Dec. 1987 118 p
(AD-A196190; AFIT/CI/NR-88-44) Avail: NTIS HC A06/MF A01 CSCL 20D

Wall pressure fluctuations were measured under the unsteady

separation shock/turbulent boundary layer interaction induced by unswept circular cylinders to determine the role of the incoming turbulent boundary layer thickness on the shock motion. Measurements were taken in a high Reynolds number, Mach 5 flow in the turbulent boundary layer developed on the wind tunnel floor. The wall temperature was adiabatic. High frequency response, miniature pressure transducers were mounted flush with the tunnel floor to measure the pressure fluctuations caused by the shock motion. A conditional sampling algorithm was used to separate the pressure fluctuations due to the shock motion from those fluctuations associated with the incoming and downstream turbulent boundary layer. Standard time series analysis techniques were used to analyze the data. Results show that the turbulent boundary layer has only second order effects on the frequency of the separation shock. Shock frequencies are at least one order of magnitude less than the large eddy frequency of the turbulent boundary layer. The low frequency pressure fluctuations of the separated region are within the same frequency range as the shock frequencies. These pressure fluctuations are a possible cause of the shock motion and warrant further investigation. GRA

N88-30061# Physical Sciences, Inc., Andover, Mass.
VOLUMETRIC MEASUREMENT OF VORTICITY VECTORS BY OPTICAL PROBE Final Report, Sep. 1987 - Mar. 1988
R. D. Ferguson and Michael B. Frish 27 May 1988 79 p
(Contract N00014-87-C-0865)
(AD-A195997; PSI-1048/TR-795) Avail: NTIS HC A05/MF A01 CSCL 14B

The general goal of the program was to demonstrate that the fluid flow measurement technique known as the Vorticity Optical Probe (VOP) could be used to measure the vorticity vectors within a volume of a flow field at many distinguishable locations simultaneously. The spatial resolution of the measurements would be small enough for them to be sensitive to the fine-scale fluctuations of the flow, yet the overall sampling volume large enough to enable study of the interactions between fine-scale features and large-scale structures. The specific objectives of the program were to demonstrate that: (1) The VOP provides sufficient information to allow rapid measurement of all three components of the vorticity vector at a single well-defined point within the flow field; (2) The vorticity vectors at several spatially distinct but unknown positions can be measured concurrently; and (3) A method could be developed for determining where in the sampling volume the vorticity is being measured. These three specific goals have been met using simulations of both the VOP and rotational flow. A data analysis technique has been developed which demonstrates the three-component measurement capability and indicates the inherent limits on its precision. GRA

N88-30062# Von Karman Inst. for Fluid Dynamics, Rhode-Saint-Genese (Belgium).
ANALYSIS OF A FEED DEVICE FOR THE PNEUMATIC TRANSPORT OF NONCOHESIVE PARTICLES [ANALYSE D'UN DISPOSITIF D'ALIMENTATION POUR LE TRANSPORT PNEUMATIQUE DE PARTICULES NON-COHESIVES]
Y. Tomita and M. L. Riethmuller Aug. 1987 16 p In FRENCH
(VKI-TM-44; ETN-88-92718) Avail: NTIS HC A03/MF A01

A device which pumps gas into a pile of particles to enable them to be transported pneumatically as a fluid was developed. A dimensional analysis of mass flow in the system was compared with results of tests using glass beads of 480 micron diameter and volume mass when heaped of 1300 kg/cu m. It is shown that mass flow of the particles remains constant if total gas mass flow and another parameter remain constant, even though the level of particles in the container decreases. This proves that mass flow of the particles through the opening is independent of the weight of particles in the container. ESA

N88-30063*# United Technologies Research Center, East Hartford, Conn.
USER'S MANUAL FOR THREE DIMENSIONAL BOUNDARY LAYER (BL3-D) CODE Final Report
O. L. Anderson and B. Caplin 29 Aug. 1985 143 p
(Contract NAS3-23716)
(NASA-CR-174899; NAS 1.26:174899; R85-956834-1) Avail: NTIS HC A07/MF A01 CSCL 20D

An assessment has been made of the applicability of a 3-D boundary layer analysis to the calculation of heat transfer, total pressure losses, and streamline flow patterns on the surface of both stationary and rotating turbine passages. In support of this effort, an analysis has been developed to calculate a general nonorthogonal surface coordinate system for arbitrary 3-D surfaces and also to calculate the boundary layer edge conditions for compressible flow using the surface Euler equations and experimental data to calibrate the method, calculations are presented for the pressure endwall, and suction surfaces of a stationary cascade and for the pressure surface of a rotating turbine blade. The results strongly indicate that the 3-D boundary layer analysis can give good predictions of the flow field, loss, and heat transfer on the pressure, suction, and endwall surface of a gas turbine passage. Author

N88-30064# Rutgers - The State Univ., New Brunswick, N. J. Dept. of Mechanical and Aerospace Engineering.
NUMERICAL SIMULATION OF NOZZLE FLOWS Final Report, May 1984 - Aug. 1987
Doyle D. Knight and Datta V. Gaitonde 18 Feb. 1988 91 p
(Contract F33615-84-K-3009)
(AD-A195144; RU-TR-169-MAE-F; AFWAL-TR-87-3110) Avail: NTIS HC A05/MF A01 CSCL 20D

A three-dimensional grid generation code implementing the multisurface technique is developed with major emphasis on the use of color computer graphics. A precise control method is employed to permit grid point control. A significant departure from existing approaches is the extension of user interaction to all phases of grid generation. This facilitates easy and rapid developments of grids especially for 3-D applications. The code is employed to generate grids for a 3-D axisymmetric nozzle and an aircraft type section. The flow is a non-axisymmetric nozzle, computed under the assumptions of horizontal and vertical symmetry. The Mach number of external flow is 1.2. The results are validated by comparison with experiment. Overall good agreement is observed with static pressure comparisons. Preliminary flow analysis indicates the existence of a number of interesting flow structures including shocks, pressure wave systems and regions of flow separation. Viscous-inviscid interactions, Computational fluid dynamics, Navier-stokes equations, Turbulence. GRA

N88-30065# Air Force Inst. of Tech., Wright-Patterson AFB, Ohio.
THE ASPECT RATIO DEPENDENCE OF THE ATTRACTOR DIMENSION IN TAYLOR-COUETTE FLOW Ph.D. Thesis
Donald A. Hirst 1988 202 p
(AD-A196297; AD-E951149; AFIT/CI/NR-88-140) Avail: NTIS HC A10/MF A01 CSCL 20D

An investigation of the aspect ratio dependence of the attractor dimension in flow between concentric cylinders (Taylor-Couette flow) was performed with the inner cylinder rotating and the outer cylinder at rest. Phase space attractors were reconstructed from experimental velocity data by time delay methods and the attractor dimension calculated by both the Grassberger-Procaccia and Badii-Politi algorithms. The aspect ratio was varied between 19.9 and 34.48 and the inner cylinder Reynolds numbers ranged between R/R sub c=11 and R/R sub c=15, where R sub c is the critical Reynolds number for the primary instability. No aspect ratio dependence of the attractor dimension was found in this study in the parameter space explored. A second area explored was the bifurcation from Couette flow to secondary flow for counter-rotating cylinders. The bifurcation boundaries were located to an accuracy of 0.3 percent for outer cylinder Reynolds numbers ranging from 0 to -250. The locations of the codimension-2 points and the wavespeeds and axial wavelengths measured at the transition boundaries compared well with a recent linear stability analysis of Golubitsky and Langford. No hysteresis was found in

the primary bifurcation boundary, but hysteresis of at least 3 percent of the outer cylinder Reynolds number was found in the secondary bifurcation boundary at the first codimension-2 point. No new states arising from mode competition were observed around the codimension-2 points. GRA

N88-30066*# United Technologies Research Center, East Hartford, Conn.
ASSESSMENT OF A 3-D BOUNDARY LAYER ANALYSIS TO PREDICT HEAT TRANSFER AND FLOW FIELD IN A TURBINE PASSAGE Final Analysis Report
O. L. Anderson 29 Aug. 1985 93 p
(Contract NAS3-23716)
(NASA-CR-174894; NAS 1.26:174894; R85-956834) Avail: NTIS HC A05/MF A01 CSCL 20D

An assessment was made of the applicability of a three dimensional boundary layer analysis of heat transfer, total pressure losses, and streamline flow patterns on the surfaces of both stationary and rotating turbine passages. In support of this effort, an analysis was developed to calculate a general nonorthogonal surface coordinate system for arbitrary three dimensional surfaces and also to calculate the boundary layer edge conditions for compressible flow using the surface Euler equations and experimental pressure distributions. Calculations are presented for the pressure, endwall, and suction surfaces of a stationary cascade and for the pressure surface of a rotating turbine blade. The results strongly indicate that the three dimensional boundary layer analysis can give good predictions of the flow field, loss, and heat transfer on the pressure, suction, and endwall surface of a gas turbine passage. Author

N88-30067# European Space Agency, Paris (France).
THE VISCOUS FLOW ON SURFACES WITH STREAMLINE RIBLETS
Manfred Bartenwerfer and Dietrich W. Bechert Jun. 1988 105 p Transl. into ENGLISH of Die Viskose Stroemung Ueber Oberflaechen mit Laengsrippen, Berlin, Fed. Republic of Germany (DFVLR) Original language document was announced as N88-16961
(ESA-TT-1091; DFVLR-FB-87-21; ETN-88-93053) Avail: NTIS HC A06/MF A01; original German version available from DFVLR, VB-PL-DO, 90 60 58, 5000 Cologne, Fed. Republic of Germany 27 deutsche marks

The viscous sublayer of a turbulent boundary layer on a surface with riblets was calculated. Only the mean flow constituent was considered: using conformal mapping viscous flow on various riblet configurations was determined, including sawtooth profiles and U-shaped groove configurations. The decreased turbulent drag of riblet surfaces is caused by hampering the fluctuating cross flow. The efficiency of the riblets depends on their protrusion height. However, the protrusion height cannot be increased beyond 22 percent of the lateral rib spacing, which limits the drag reduction potential of riblet surfaces. ESA

N88-30068*# National Aeronautics and Space Administration, Washington, D.C.
STUDIES ON PRESSURE RESPONSE OF GAS BUBBLES CONTRIBUTIONS OF CONDENSED DROPLETS IN BUBBLES GENERATED BY A UNIFORM NUCLEATION
Y. Matsumoto Aug. 1988 32 p Transl. into ENGLISH from Nippon Kikai Gakkai Ronbunshu (B), (Japan), v. 50, no. 455, 1984 p 1649 Presented at the 61st National Meeting, 10 Oct. 1983 Transl. by SCITRAN, Inc., Santa Barbara, Calif. Original document was prepared by Tokyo Univ., Japan
(NASA-TT-20343; NAS 1.77:20343) Avail: NTIS HC A03/MF A01 CSCL 20D

The response of a tiny gas bubble under reduced pressure is investigated in its relation to cavitation. Equations of motion are formulated for gas mixtures inside the bubble and numerical calculations performed for several examples. The conclusions are as follows: (1) at the onset of bubble growth, the gas mixture inside it adiabatically expands and the temperature decreases. Condensed droplets appear inside the gas mixture due to a uniform nucleation and the temperature recovers, thus the motion of the bubble is apparently isothermal; (2) the evaporation and condensation coefficient largely affects bubble motions (maximum radius, period and rate of attenuation of the bubble oscillation) including the uniform contraction; (3) the oscillation period of the bubble is longer as the equilibrium bubble radius is larger when the surrounding pressure decreases stepwise. In this circumstance the temperature inside the bubble is kept constant due to condensation evaporation phenomena and is nearly isothermal; and (4) when the surrounding pressure decreases in a stepwise fashion, the critical pressure bubble radius relation becomes closer to that for the isothermal process if the bubble radius is larger than 8 microns. F.M.R.

N88-30069# Tennessee Univ., Tullahoma.
CONTAMINATION AND DISTORTION OF STEADY FLOW FIELD INDUCED BY DISCRETE FREQUENCY DISTURBANCES IN AIRCRAFT GAS ENGINES Final Report, Jan. - Dec. 1987
M. Kurosaka Apr. 1988 5 p
(Grant AF-AFOSR-0049-83)
(AD-A195440; AFOSR-88-0640TR) Avail: NTIS HC A02/MF A01 CSCL 20D

The main objective of this program was to acquire fundamental understanding of two aerodynamic effects induced by vortices shed by blades of aircraft gas turbines: (1) the instantaneous separation of total temperature and pressure around vortices in the wake shed and its time averaged effect; and (2) the issue of over 100 percent efficiency measured near the hub section of an advanced turbofan design of the Air Force Aeropropulsion Laboratory. Through the combination of experimental and theoretical investigations, the mechanisms of the two phenomena have been identified. GRA

N88-30070*# Institut d'Aeronomie Spatiale de Belgique, Brussels.
GENERAL EQUATIONS FOR THE MOTIONS OF ICE CRYSTALS AND WATER DROPS IN GRAVITATIONAL AND ELECTRIC FIELDS
John S. Nisbet 1988 63 p Submitted for publication
(Grant NGL-39-009-003)
(NASA-CR-183229; NAS 1.26:183229;
Aeronomica-Acta-A-330-1988; ETN-88-92725) Avail: NTIS HC A04/MF A01 CSCL 20D

General equations for the Reynolds number of a variety of types of ice crystals and water drops are given in terms of the Davies, Bond, and Knudsen numbers. The equations are in terms of the basic physical parameters of the system and are valid for calculating velocities in gravitational and electric fields over a very wide range of sizes and atmospheric conditions. The equations are asymptotically matched at the bottom and top of the size spectrum, useful when checking large computer codes. A numerical system for specifying the dimensional properties of ice crystals is introduced. Within the limits imposed by such variables as particle density, which have large deviations, the accuracy of velocities appears to be within 10 percent over the entire range of sizes of interest. ESA

N88-30071*# Sterling Software, Palo Alto, Calif.
AN ANALYSIS OF FINITE-DIFFERENCE AND FINITE-VOLUME FORMULATIONS OF CONSERVATION LAWS Final Technical Report
Marcel Vinokur Jun. 1986 60 p Submitted for publication
(Contract NAS2-11555)
(NASA-CR-177416; NAS 1.26:177416) Avail: NTIS HC A04/MF A01 CSCL 20D

Finite-difference and finite-volume formulations are analyzed in order to clear up the confusion concerning their application to the numerical solution of conservation laws. A new coordinate-free formulation of systems of conservation laws is developed, which clearly distinguishes the role of physical vectors from that of algebraic vectors which characterize the system. The analysis considers general types of equations--potential, Euler, and Navier-Stokes. Three-dimensional unsteady flows with time-varying

grids are described using a single, consistent nomeclature for both formulations. Grid motion due to a non-inertial reference frame as well as flow adaptation is covered. In comparing the two formulations, it is found useful to distinguish between differences in numerical methods and differences in grid definition. The former plays a role for non-Cartesian grids, and results in only cosmetic differences in the manner in which geometric terms are handled. The differences in grid definition for the two formulations is found to be more important, since it affects the manner in which boundary conditions, zonal procedures, and grid singularities are handled at computational boundaries. The proper interpretation of strong and weak conservation-law forms for quasi-one-dimensional and axisymmetric flows is brought out. Author

N88-30072*# National Aeronautics and Space Administration. Lewis Research Center, Cleveland, Ohio.
CONTAINMENT OF A SILICONE FLUID FREE SURFACE IN REDUCED GRAVITY USING BARRIER COATINGS
Alexander D. Pline (Case Western Reserve Univ., Cleveland, Ohio.) and Thomas P. Jacobson 1988 15 p Presented at the 117th TMS-AIME Annual Meeting, Phoenix, Ariz., 25-29 Jan. 1988; sponsored by ASM
(NASA-TM-101314; E-4309; NAS 1.15:101314) Avail: NTIS HC A03/MF A01 CSCL 20D

In support of the Surface Tension Driven Convection Experiment planned for flight aboard the Space Shuttle, tests were conducted under reduced gravity in the 2.2-sec Drop Tower and the 5.0-sec Zero-G facility at the NASA Lewis Research Center. The dynamics of controlling the test fluid, a 10-cSt viscosity silicone fluid in a low gravity environment were investigated using different container designs and barrier coatings. Three container edge designs were tested without a barrier coating; a square edge, a sharp edge with a 45-deg slope, and a sawtooth edge. All three edge designs were successful in containing the fluid below the edge. G-jitter experiments were made in scaled down containers subjected to horizontal accelerations. The data showed that a barrier coating is effective in containing silicone fluid under g-levels up to 10 sup -1 sub g sub 0. In addition, a second barrier coating was found which has similar anti-wetting characteristics and is also more durable. Author

N88-30073# Ballistic Research Labs., Aberdeen Proving Ground, Md.
NUMERICAL SIMULATION OF UNSTEADY INCOMPRESSIBLE FLOW IN A PARTIALLY-FILLED ROTATING CYLINDER
Michael J. Nusca Jun. 1988 58 p
(AD-A196001; BRL-TR-2915) Avail: NTIS HC A04/MF A01 CSCL 20D

The liquid flowfield in a full or partially-filled right circular cylinder in rapid axial rotation is investigated numerically. The governing equations are the axisymmetric, unsteady, viscous, incompressible Navier-Stokes equations. These equations are written in stream function-vorticity form for a cylindrical coordinate system in a nonrotating reference frame. The governing equations are discretized using second-order finite-differences for time and space on a nonuniform grid employing logarithmic stretching in regions where high flow gradients are anticipated. Time dependent solutions for Reynolds numbers between 1,000 and 100,000 have been obtained using a Gauss-Seidel relaxation procedure. For partially filled cases the free surface is assumed to be cylindrical and located at a constant radius from the axis of spin. Numerical solutions for full cylinders are consistent with previous solutions and experimental data. Numerical solutions for a partially-filled cylinder are consistent with experimental data for a liquid centrifuge except at the free surface. Computations of the roll moment exerted on the cylinder by the contained liquid shows a smaller moment for the partially-filled compared with the full cylinder results. GRA

N88-30074# United Kingdom Atomic Energy Authority, Abingdon (England).
THE USE OF UPWIND SCHEMES AT HIGH REYNOLDS NUMBER: A CAUTIONARY NOTE
Wayne Arter Jan. 1988 11 p
(AD-A196227; CLM-P-835) Avail: NTIS HC A03/MF A01 CSCL 20D

Simple upwind schemes are the basis of many codes of practical importance for design studies in heat transfer and fluid flow applications, e.g., the FLOW3D code. With care, it is possible to produce codes that can give bounded answers regardless of mesh spacing or time step size. This note highlights a rather disturbing inaccuracy that can arise if the mesh spacing is taken too large. GRA

N88-30075# European Space Agency, Paris (France).
NUMERICAL SIMULATION OF THE INTERACTION OF PRESSURE WAVES WITH LAMINAR AND TURBULENT BOUNDARY LAYERS
Heinrich Reister Jun. 1988 110 p Transl. into ENGLISH of Numerische Simulation der Wechselwirkung von Druckwellen mit Laminaren und Turbulenten Grenzschichten, Gottingen, Federal Rep. of West Germany (DFVLR) Original language document was announced as N88-16960
(ESA-TT-1089; DFVLR-FB-87-18; ETN-88-92910) Avail: NTIS HC A06/MF A01; original German version available from DFVLR, VB-PL-DO, 90 60 58, 5000 Cologne, Fed. Republic of Germany 33.50 deutsche marks

The interaction of upstream moving pressure waves with laminar and turbulent boundary layers was investigated. The unsteady, compressible Navier-Stokes equations were solved using a Runge-Kutta finite volume method. The numerical solutions for simplified physical models, e.g., the formation of an acoustic boundary layer and the steepening of linear waves to a sawtooth pattern, were compared with analytical solutions, showing good agreement. The numerical solution of the pressure-wave boundary-layer interaction demonstrates under which conditions reversed flow areas occur in the boundary layer and what their structure is. ESA

N88-30076*# Garrett Engine Co., Phoenix, Ariz.
TRANSITION MIXING STUDY EMPIRICAL MODEL REPORT
Report, Sep. 1986 - Jan. 1988
R. Srinivasan and C. White Feb. 1988 126 p
(Contract NAS3-24340)
(NASA-CR-182139; NAS 1.26:182139; GARRETT-21-6689)
Avail: NTIS HC A07/MF A01 CSCL 20D

The empirical model developed in the NASA Dilution Jet Mixing Program has been extended to include the curvature effects of transition liners. This extension is based on the results of a 3-D numerical model generated under this contract. The empirical model results agree well with the numerical model results for all tests cases evaluated. The empirical model shows faster mixing rates compared to the numerical model. Both models show drift of jets toward the inner wall of a turning duct. The structure of the jets from the inner wall does not exhibit the familiar kidney-shaped structures observed for the outer wall jets or for jets injected in rectangular ducts. Author

N88-30077# Naval Research Lab., Washington, D.C.
APPROXIMATION OF VISCOELASTIC STRESSES FROM NEWTONIAN TURBULENT KINEMATICS
John V. Lawler 1988 58 p
(AD-A194317) Avail: NTIS HC A04/MF A01 CSCL 20D

Small amounts of high molecular weight polymers (a few parts per million by weight) dissolved in a solvent can reduce the turbulent flow frictional resistance of that solution by 75 percent. Since the viscosity of a polymer/solvent mix is increased over that of the solvent alone, the fact that viscous drag is decreased is somewhat surprising. Study has been made of drag reducing, non-Newtonian fluid flows. The examination by fluid dynamicists of the turbulent flow properties of thermodynamically dilute solutions of long chain high-molecular weight polymers has generated literally hundreds of publications, of which a majority are experimental investigations. This preponderance of experimental studies is no doubt due to the difficult theoretical nature of the problem, which includes not only turbulence but the interaction of a viscoelastic fluid with

turbulence. The study of viscoelastic fluids as they relate to drag reduction is itself an area of investigation among rheologists. This paper is in two sections. The first section, reviews the rheological properties of dilute polymer solutions. The second section presents a method for approximating viscoelastic stresses in a turbulent flow. GRA

N88-30078*# National Aeronautics and Space Administration. Lewis Research Center, Cleveland, Ohio.
THREE-DIMENSIONAL ELLIPTIC GRID GENERATION TECHNIQUE WITH APPLICATION TO TURBOMACHINERY CASCADES
S. C. Chen (Sverdrup Technology, Inc., Cleveland, Ohio.) and J. R. Schwab Aug. 1988 20 p
(NASA-TM-101330; E-4342; NAS 1.15:101330) Avail: NTIS HC A03/MF A01 CSCL 20D

Described is a numerical method for generating 3-D grids for turbomachinery computational fluid dynamic codes. The basic method is general and involves the solution of a quasi-linear elliptic partial differential equation via pointwise relaxation with a local relaxation factor. It allows specification of the grid point distribution on the boundary surfaces, the grid spacing off the boundary surfaces, and the grid orthogonality at the boundary surfaces. A geometry preprocessor constructs the grid point distributions on the boundary surfaces for general turbomachinery cascades. Representative results are shown for a C-grid and an H-grid for a turbine rotor. Two appendices serve as user's manuals for the basic solver and the geometry preprocessor. Author

N88-30079*# National Aeronautics and Space Administration. Langley Research Center, Hampton, Va.
RECENT INSIGHTS INTO INSTABILITY AND TRANSITION TO TURBULENCE IN OPEN-FLOW SYSTEMS Final Report
Mark V. Morkovin (Illinois Inst. of Tech., Chicago.) Aug. 1988 84 p Submitted for publication
(Contracts NAS1-18107; NAS1-18605)
(NASA-CR-181693; ICASE-88-44; NAS 1.26:181693) Avail: NTIS HC A05/MF A01 CSCL 20D

Roads to turbulence in open-flow shear layers are interpreted as sequences of often competing instabilities. These correspond to primary and higher order restructurings of vorticity distributions which culminate in convected spatial disorder (with some spatial coherence on the scale of the shear layer) traditionally called turbulence. Attempts are made to interpret these phenomena in terms of concepts of convective and global instabilities on one hand, and of chaos and strange attractors on the other. The first is fruitful, and together with a review of mechanisms of receptivity provides a unifying approach to understanding and estimating transition to turbulence. In contrast, current evidence indicates that concepts of chaos are unlikely to help in predicting transition in open-flow systems. Furthermore, a distinction should apparently be made between temporal chaos and the convected spatial disorder of turbulence past Reynolds numbers where boundary layers and separated shear layers are formed. Author

N88-30080# European Space Agency, Paris (France).
INVESTIGATION OF LARGE-SCALE STRUCTURES IN THE NEAR WAKE OF A PARALLEL FLAT PLATE
Volker Strunck (Deutsche Forschungs- und Versuchsanstalt fuer Luft- und Raumfahrt, Goettingen, West Germany) Jun. 1988 100 p Transl. into ENGLISH of Untersuchung Grossraeumigen Strukturen im Nachlauf einer Laengsangestroemten ebenen Platte, Gottingen, Federal Rep. of West Germany (DFVLR) Original language document was announced as N88-16967
(ESA-TT-1100; DFVLR-FB-87-31; ETN-88-92912) Avail: NTIS HC A05/MF A01; original German version available from DFVLR, VB-PL-DO, 90 60 58, 5000 Cologne, Fed. Republic of Germany 29 deutsche marks

The near wake behind a flat plate was investigated using the conditional sampling method and laser Doppler velocimetry. The conditional sampling technique provided information about the development of the separation of the vorticity layers and the development of turbulence. The created vortices form the configuration of a Karman vortex street at Reynolds numbers 1 million, 1.5 million and 3 million. It is found that nearly half of the separated vorticity leaving the trailing edge is convected downstream for the production of vortices, and that the vortex energy increases proportional to the turbulent energy. ESA

N88-30081# International Centre for Theoretical Physics, Trieste (Italy).
RADIATIVE HEAT TRANSFER TO STEADY FLOW OF A CHEMICALLY REACTING FLUID IN A HORIZONTAL POROUS CHANNEL WITH VARIABLE WALL TEMPERATURE
A. R. Bestman Sep. 1987 14 p
(DE88-702704; IC-87/304) Avail: NTIS (US Sales Only) HC A03/MF A01

Fluid motion in a horizontal channel at very high temperatures is studied when the radiative heat flux is expressible in general differential form. On the assumption that the fluid is chemically reacting while the temperatures of the channel walls vary linearly with axial distance, the problem is reduced to a set of coupled nonlinear ordinary integro-differential equations when only linear terms in the axial distance are retained. An iterative sequence is established in which the eventual linear equations are discretized by employing finite differences for derivatives and trapezium rule for integrals. The effect of the chemical rate constant and the radiative parameters on the flow are discussed. DOE

N88-30082# Michigan State Univ., East Lansing. Turbulence Structure Lab.
EXPERIMENTAL DETERMINATION OF DRAG MODIFICATIONS DUE TO ELASTIC COMPLIANT SURFACES USING QUANTITATIVE VISUAL TECHNIQUES Final Technical Report, 1982 - 1985
R. E. Falco and C. C. Chu 27 Apr. 1988 36 p
(Contract N00014-82-K-0348)
(AD-A194785; TSL-88-2) Avail: NTIS HC A03/MF A01 CSCL 20D

Direct measurements of the wall shear stress have been made at a point on three thicknesses of an elastic compliant surface. Approximately 8 percent C sub f reduction was measured on each surface. Observations of the surfaces' motion showed that they responded to the microscale turbulent eddies. At higher forcing the onset of various surface wave phenomena were observed. GRA

N88-30083# Von Karman Inst. for Fluid Dynamics, Rhode-Saint-Genese (Belgium).
LASER DOPPLER VELOCIMETER (LDV) AND PRESSURE MEASUREMENTS OF GAS PARTICLE FLOWS IN BENDS
M. L. Riethmuller and Y. Tomita Oct. 1987 42 p
(VKI-TN-163; ETN-88-92719) Avail: NTIS HC A03/MF A01

Particle velocity in a circular 90 deg bend of several bend configurations was measured using a laser Doppler velocimeter. The radius and inside diameter of the bend were 132 and 44 mm. Superficial air velocity was changed between 5 and 20 m/sec and the maximum solid loading ratio was 14.6. Glass beads of 480 microns and plastic particles of 3.25 mm mean diameters were used for the test particles. The streamwise velocity profiles for the particles were obtained at the bend inlet, outlet, and 45 deg angular position. Static pressure at the bend inlet and outlet was measured. The ratio of this pressure difference to that of gas alone is uniquely correlated with the solid loading ratio. ESA

N88-30084*# National Aeronautics and Space Administration. Lewis Research Center, Cleveland, Ohio.
EXPERIMENTAL AND NUMERICAL INVESTIGATION OF THE EFFECT OF DISTRIBUTED SUCTION ON OBLIQUE SHOCK WAVE/TURBULENT BOUNDARY LAYER INTERACTION Ph.D. Thesis
Driss Benhachmi, Isaac Greber (Case Western Reserve Univ., Cleveland, Ohio.), and Warren R. Hingst Aug. 1988 192 p
(Grant NAG3-61)
(NASA-TM-101334; E-4349; NAS 1.15:101334) Avail: NTIS HC A09/MF A01 CSCL 20D

A combined experimental and numerical study of the interaction of an incident oblique shock wave with a turbulent boundary layer on a rough plate and on a porous plate with suction is presented. The experimental phase involved the acquisition of mean data upstream of, within, and downstream of the interaction region at Mach numbers 2.5 and 3.0. Data were taken at unit Reynolds numbers of 1.66 E7 and 1.85 E7 m respectively, and for flow deflection angles of 0, 4, 6 and 8 degs. Measured data include wall static pressure, pitot pressure profiles, and local bleed distributions on the porous plate. On the rough plate, with no suction, the boundary layer profiles were modified near the wall, but not separated for the 4 deg flow deflection angle. For the higher deflection angles of 6 and 8 degs, the boundary layer was separated. Suction increases the strength of the incident shock required to separate the turbulent boundary layer; for all shock strengths tested, separation is completely eliminated. The pitot pressure profiles are affected throughout the whole boundary layer; they are fuller than the ones obtained on the rough plate. It is also found that the combination of suction and roughness introduces spatial perturbations. Author

N88-30085*# National Aeronautics and Space Administration. Ames Research Center, Moffett Field, Calif.
NUMERICAL SIMULATION OF UNSTEADY INCOMPRESSIBLE VISCOUS FLOWS IN GENERALIZED COORDINATE SYSTEMS
Moshe Rosenfeld and Dochan Kwak Jul. 1988 12 p Presented at the 11th International Conference on Numerical Methods in Fluid Dynamics, Williamsburg, Va., 27 Jun. - 1 Jul. 1988
(NASA-TM-101016; A-88254; NAS 1.15:101016) Avail: NTIS HC A03/MF A01 CSCL 20D

Several numerical solutions of the three dimensional unsteady incompressible Navier-Stokes equations in generalized coordinate systems are presented. The governing equations are discretized by finite volumes with special care to the accurate approximation of the geometric quantities. The unknowns are the pressure and the volume fluxes over the computational cell faces. This formulation results in a robust fractional step solution method for solving discrete equations. Although this method is formulated for the three dimensional case, only two dimensional unsteady results are given. Results are presented for a lid driven two dimensional cavity flow at Reynolds number of 10,000, and for the flow over a circular cylinder with vortex shedding for several Reynolds numbers in the range 100 less than Re less than 1000. Author

N88-30086# Johns Hopkins Univ., Baltimore, Md.
BOLTZMANN EQUATION APPROACH TO TWO-PHASE FLOW TURBULENCE Technical Report, Apr. 1986 - May 1987
G. Domokos, S. Kovesi-Domokos, and C. K. Zoltani Mar. 1988 24 p
(DA Proj. 1L1-61102-AH-43)
(AD-A196153; BRL-TR-2893) Avail: NTIS HC A03/MF A01 CSCL 20D

A description of the turbulent flow of a two phase system is given in terms of a coupled system of Boltzmann and Navier-Stokes equations. The use of a Boltzmann equation for the particle phase makes the description valid for low concentrations. The Boltzmann equation is appropriately modified to account for a velocity dependent interphase interaction. Within the framework of Chapman Enskog expansion, moment equations are derived for the particle phase. The coupled system of moment equations is cast into a form suitable for a statistical description of the turbulent flow. GRA

N88-30087*# National Aeronautics and Space Administration, Washington, D.C.
DETERMINATION OF THE SPECIFIC AREA OF LIQUID GAS AND THE VELOCITY OF WEAK PRESSURE WAVES IN AQUEOUS FOAMS
Jean Saint-Cloud, Claude Guerraud, Michel Moreau, and Numa Manson Aug. 1988 7 p Transl. into ENGLISH from C. R. Acad. Sci., Ser. 2 (France), no. 292 p 825-828 Transl. by Scientific Translation Service, Santa Barbara, Calif.
(Contract NASw-4307)
(NASA-TT-20347; NAS 1.77:20347) Avail: NTIS HC A02/MF A01 CSCL 20D

The specific area of an aqueous foam contained in a tube is obtained by determining the fraction of the quantity of light emitted by a source and diffused by the specific area of the column of the foam. The velocity of the waves of weak pressure (which propagate in the air with the velocity of sound) is measured by noticing the moment when the wave penetrates the column and the moment when, having reached the opposite side, it determines a variation of the light diffused by the area of the latter. Author

N88-30088*# National Aeronautics and Space Administration, Washington, D.C.
ANALYSIS METHOD FOR THE PRODUCTION OF REYNOLDS STRESSES IN COMPRESSIBLE TURBULENT FLOW (FLUID MECHANICS)
Jean Francois Debieve Sep. 1988 9 p Transl. into ENGLISH from Comptes Rendus, Serie A-Science Mathematiques (France), v. 286, no. 16, 24 Apr. 1978 p 705-708 Transl. by Scientific Translation Service, Santa Barbara, Calif.
(Contract NASw-4307)
(NASA-TT-20330; NAS 1.77:20330) Avail: NTIS HC A02/MF A01 CSCL 20D

A geometrical interpretation of the grouping and variation rate terms of Reynolds stresses in compressible turbulent flow is presented. Examples of applications of the method are also given. Author

N88-30089# International Centre for Theoretical Physics, Trieste (Italy).
NONEQUILIBRIUM FLOW OF A DISSOCIATING GAS IN A HORIZONTAL CHANNEL WITH AXIAL TEMPERATURE VARIATION
A. R. Bestman May 1987 17 p
(DE88-702536; IC-87/101) Avail: NTIS (US Sales Only) HC A03/MF A01

Flow of a rarified high temperature ideal dissociating gas in a horizontal channel is studied under a general differential approximation for radiative heat flux. On the assumption that there is a small but linear axial wall temperature variation, the problem is tackled by an iterative algorithm involving nonlinear integral equations. The higher approximation which is linear is solved by a finite difference scheme. Consequences of the effect of relaxation on the heat transfer are discussed quantitatively. DOE

N88-30090*# National Aeronautics and Space Administration. Lewis Research Center, Cleveland, Ohio.
OPTICAL MEASUREMENTS OF SOOT IN PREMIXED FLAMES Ph.D. Thesis - California Univ.
Valerie J. Lyons Aug. 1988 180 p
(NASA-TM-101305; E-4295; NAS 1.15:101305) Avail: NTIS HC A09/MF A01 CSCL 20D

Two laser diagnostic techniques were used to measure soot volume fractions, number densities and soot particle radii in premixed propane/oxygen flat flames. The two techniques were two wavelength extinction, using 514.5 to 632.8 nm and 457.9 to 632.8 nm wavelength combinations, and extinction/scattering using 514.5 nm light. The flames were fuel rich and had cold gas velocities varying from 3.4 to 5.5 cm/s. Measurements were made at various heights above the sintered bronze, water colored flat flame burner with the equivalence ratio and cold gas velocity fixed. Also, measurements were made at a fixed height above the burner and fixed cold gas velocity while varying the equivalence ratio. Both laser techniques are based on the same underlying assumptions of particle size distribution and soot optical properties. Full Mie theory was used to determine the extinction coefficients and the scattering efficiencies. Temperature measurements in the flame were made using infrared radiometry and fine wire thermocouples. Good agreement between the two techniques in terms of soot particle radii, number density and volume fraction was found for intensity ratios between 0.1 and 0.8. Author

N88-30091# Rolls-Royce Ltd., Derby (England).
POSITRON EMISSION TOMOGRAPHY: A NEW TECHNIQUE FOR OBSERVING FLUID BEHAVIOR IN ENGINEERING SYSTEMS
P. A. E. Stewart, J. D. Rogers, R. T. Skelton, P. Salter, M. Allen, R. Parker, P. Davis, P. Fowles, M. R. Hawkesworth, and M. A. Odwyer et al. 17 Sep. 1988 27 p Presented at the EWD NDT Conference, London, United Kingdom, 13-17 Sep. 1987 Sponsored by the United Kingdom Science and Engineering Research Council
(PNR90471; ETN-88-92698) Copyright Avail: NTIS HC A03/MF A01

Positron emission tomography for flow tracing and measurement within metal structures in general and operating engines in particular is introduced. The principles involved are outlined, and a mobile positron camera system is described. Examples of the camera's capability drawn from its use to study annular oil volumes simulated by positron line sources in a power turbine shaft and in a small helicopter engine are presented. ESA

N88-30092# Sheffield Univ. (England).
DEVELOPMENT OF A MORE GENERAL REYNOLDS STRESS CLOSURE FOR SWIRLING FLOW Final Report
S. B. Chin and J. Swithenbank Mar. 1988 16 p
(Grant AF-AFOSR-0248-85)
(AD-A195121; HIC466) Avail: NTIS HC A03/MF A01 CSCL 20D

This paper is concerned with the modelling of the return to isotropy part of the pressure strain term in homogeneous anisotropic turbulent flows. Analytical solutions of the transport equations of the invariants of the anisotropy tensor as well as that of turbulent kinetic energy as a function of the natural time of decay are provided and discussed. Principal components of the Reynolds stresses are obtained from the solution of a cubic equation which involves the invariants. It is shown that current models based on Rotta's hypothesis are subject to a constraint which is only satisfied by axisymmetric homogeneous turbulence, and the constraint can be eliminated by non-linear modelling. A physical picture of energy transfer among the Reynolds stress components which takes into account the influence of the third invariant on the process of return to isotropy is presented. GRA

N88-30093*# National Aeronautics and Space Administration. Hugh L. Dryden Flight Research Facility, Edwards, Calif.
TECHNIQUES USED IN THE F-14 VARIABLE-SWEEP TRANSITION FLIGHT EXPERIMENT
Bianca Trujillo Anderson, Robert R. Meyer, Jr., and Harry R. Chiles Jul. 1988 25 p Presented at the 4th AIAA Flight Test Conference, San Diego, Calif., 18-20 May 1988
(NASA-TM-100444; H-1461; NAS 1.15:100444; AIAA-88-2110)
Avail: NTIS HC A03/MF A01 CSCL 20D

This paper discusses and evaluates the test measurement techniques used to determine the laminar-to-turbulent boundary layer transition location in the F-14 variable-sweep transition flight experiment (VSTFE). The main objective of the VSTFE was to determine the effects of wing sweep on the laminar-to-turbulent transition location at conditions representative of transport aircraft. Four methods were used to determine the transition location: (1) a hot-film anemometer system; (2) two boundary-layer rakes; (3) surface pitot tubes; and (4) liquid crystals for flow visualization. Of the four methods, the hot-film anemometer system was the most reliable indicator of transition. Author

N88-30094*# National Aeronautics and Space Administration. Lewis Research Center, Cleveland, Ohio.
IMPACT OF ETO PROPELLANTS ON THE AEROTHERMODYNAMIC ANALYSES OF PROPULSION COMPONENTS
K. C. Civinskas, R. J. Boyle, and H. V. McConnaughey 1988 26 p Presented at the 24th Joint Propulsion Conference, Boston, Mass., 11-13 Jul. 1988; sponsored in part by AIAA, ASME, SAE and ASEE Prepared in cooperation with NASA, Marshall Space Flight Center, Huntsville, Ala.; and Army Aviation Systems Command, Cleveland, Ohio
(NASA-TM-101303; E-4262; NAS 1.15:101303; AIAA-88-3091; AVSCOM-TP-88-C-001) Avail: NTIS HC A03/MF A01 CSCL 20D

The operating conditions and the propellant transport properties used in Earth-to-Orbit (ETO) applications affect the aerothermodynamic design of ETO turbomachinery in a number of ways. Some aerodynamic and heat transfer implications of the low molecular weight fluids and high Reynolds number operating conditions on future ETO turbomachinery are discussed. Using the current SSME high pressure fuel turbine as a baseline, the aerothermodynamic comparisons are made for two alternate fuel turbine geometries. The first is a revised first stage rotor blade designed to reduce peak heat transfer. This alternate design resulted in a 23 percent reduction in peak heat transfer. The second design concept was a single stage rotor to yield the same power output as the baseline two stage rotor. Since the rotor tip speed was held constant, the turbine work factor doubled. In this alternate design, the peak heat transfer remained the same as the baseline. While the efficiency of the single stage design was 3.1 points less than the baseline two stage turbine, the design was aerothermodynamically feasible, and may be structurally desirable. Author

N88-30095# Naval Postgraduate School, Monterey, Calif.
THE THERMAL BEHAVIOR OF FILM COOLED TURBULENT BOUNDARY LAYERS AS AFFECTED BY LONGITUDINAL VORTICES M.S. Thesis
Alfredo Ortiz Sep. 1987 208 p
(AD-A195155) Avail: NTIS HC A10/MF A01 CSCL 20M

Heat transfer effects of longitudinal vortices embedded within film-cooled turbulent boundary layers on a flat plate were examined for freestream velocities of 10 m/s and 15 m/s, and for blowing ratios ranging from 0.47 to 1.26. Moderate strength vortices were employed having circulation to freestream velocity ratios of about 1.6 cm. Spatially resolved heat transfer measurements from a constant heat flux surface and mean temperature distributions in spanwise planes show that local heat transfer is significantly affected by spanwise vortex position, and blowing ration. Of particular significance are boundary layer and vortex structural changes which occur at high blowing ratios. GRA

35 INSTRUMENTATION AND PHOTOGRAPHY

Includes remote sensors; measuring instruments and gages; detectors; cameras and photographic supplies; and holography.

For aerial photography see *43 Earth Resources and Remote Sensing*. For related information see also *06 Aircraft Instrumentation*, and *19 Spacecraft Instrumentation*.

N88-30096# Pennsylvania State Univ., University Park. Materials Research Lab.
PIEZOELECTRIC AND ELECTROSTRICTIVE MATERIALS FOR TRANSDUCER APPLICATIONS, VOLUME 1 Annual Report, 1 Jan. - 31 Dec. 1987
L. E. Cross, R. E. Newnham, G. R. Barsch, and J. V. Biggers Mar. 1988 235 p
(Contract N00014-82-K-0339)
(AD-A194957) Avail: NTIS HC A11/MF A01 CSCL 20C

The topics covered under the program are reported under three major topic areas: Piezoelectric and Related Composites, Electrostriction, Phenomenology and Properties of Conventional Ceramic, and Piezoelectrics. A brief report is also given of related studies required to support and supplement work on the three major areas, under the title Associated Programs. The year has seen major personnel changes at the Post-Doctoral and Graduate Assistant levels as befits a university based program and new personnel are now in place. The summer apprentice program under ONR sponsorship on this program has again given research

opportunity to four upward bound high school students who joined Universities in Science and Engineering programs in the fall of 1987. GRA

N88-30097# Aeronautical Research Labs., Melbourne (Australia).
EXPERIMENTAL ASPECTS OF USING TIME-AVERAGED HOLOGRAPHIC INTERFEROMETRY TO DETECT BARELY VISIBLE IMPACT DAMAGE IN A GRAPHITE/EPOXY COMPOSITE PLATE
S. J. Rumble 25 Aug. 1987 36 p
(AD-A194418; ARL/STRUC-TM-467; DODA-AR-004-549) Avail: NTIS HC A03/MF A01 CSCL 11D

Time-averaged holographic interferometry has been used to detect barely visible impact damage in a graphite/epoxy plate. Details are given of both the experimental and theoretical aspects of time-averaged holographic interferometry, including temporal modulation of the laser light. Double exposure holographic interferometry has also been used to detect barely visible impact damage. GRA

N88-30098# Rolls-Royce Ltd., Derby (England). Advanced Research Lab.
USE OF HOLOGRAPHY IN VIBRATION AND FLUTTER STUDY OF FANS
R. J. Parker 4 Feb. 1988 43 p Presented at the Von Karmen Institute for Fluid Dynamics Lecture Series No. 3: Transonic Compressors, Rhode Saint Genese, Belgium, 1-4 Feb. 1988 Sponsored by the United Kingdom Ministry of Defence, London
(PNR90458; ETN-88-92688) Copyright Avail: NTIS HC A03/MF A01

Use of holography to investigate mechanical behavior of individual vibrating blades and fan assemblies is reviewed. Holograms taken through an optical derotator allow vibration modes of the rotating fan to be mapped during resonance or flutter. Of equal interest to the techniques themselves are the problems encountered and overcome in applying these techniques in a demanding, at times hostile, industrial environment away from the laboratory. Examples of the use of this technique to study vibration characteristics of individual blades and bladed disk assemblies are given. Other examples demonstrate the use on rotating components at rotational speeds up to and in excess of 10,000 rpm. Holography provides valuable information used to verify numerical modeling of the fan vibration. ESA

N88-30099*# National Aeronautics and Space Administration. Lewis Research Center, Cleveland, Ohio.
MEASUREMENT OF LOCAL HIGH-LEVEL, TRANSIENT SURFACE HEAT FLUX
Curt H. Liebert Sep. 1988 9 p Sponsored by NASA, Washington, D.C.
(NASA-TP-2840; E-4200; NAS 1.60:2840) Avail: NTIS HC A02/MF A01 CSCL 14B

This study is part of a continuing investigation to develop methods for measuring local transient surface heat flux. A method is presented for simultaneous measurements of dual heat fluxes at a surface location by considering the heat flux as a separate function of heat stored and heat conducted within a heat flux gage. Surface heat flux information is obtained from transient temperature measurements taken at points within the gage. Heat flux was determined over a range of 4 to 22 MW/sq m. It was concluded that the method is feasible. Possible applications are for heat flux measurements on the turbine blade surfaces of space shuttle main engine turbopumps and on the component surfaces of rocket and advanced gas turbine engines and for testing sensors in heat flux gage calibrators. Author

N88-30100*# Aerojet Electrosystems Co., Azusa, Calif.
DEVELOPMENT OF A UNIT CELL FOR A Ge:Ga DETECTOR ARRAY Final Contractor Report, Jun. 1984 - Sep. 1986
Aug. 1988 93 p
(Contract NAS2-11927)
(NASA-CR-177445; NAS 1.26:177445) Avail: NTIS HC A05/MF A01 CSCL 14B

Two modules of gallium-doped germanium (Ge:Ga) infrared detectors with integrated multiplexing readouts and supporting drive electronics were designed and tested. This development investigated the feasibility of producing two-dimensional Ge:Ga arrays by stacking linear modules in a housing capable of providing uniaxial stress for enhanced long-wavelength response. Each module includes 8 detectors (1x1x2 mm) mounted to a sapphire board. The element spacing is 12 microns. The back faces of the detector elements are beveled with an 18 deg angle, which was proved to significantly enhance optical absorption. Each module includes a different silicon metal-oxide semiconductor field effect transistor (MOSFET) readout. The first circuit was built from discrete MOSFET components; the second incorporated devices taken from low-temperature integrated circuit multiplexers. The latter circuit exhibited much lower stray capacitance and improved stability. Using these switched-FET circuits, it was demonstrated that burst readout, with multiplexer active only during the readout period, could successfully be implemented at approximately 3.5 K. Author

N88-30101# Oulu Univ. (Finland). Dept. of Physics.
FIVE CHANNEL AURORAL PHOTOMETER
Kari Kaila, Reijo Rasinkangas, Esko Herrala, and Pekka Tanskanen Sep. 1987 74 p Sponsored in part by the Finnish Cultural Foundation
(Rept-112; ISBN-9-51-422421-3; ISSN-0356-1852; ETN-88-92431) Avail: NTIS HC A04/MF A01

A computer controlled scanning photometer with five different phototubes, each operating at a fixed wavelength is described. The background radiation can be measured in each channel at desired intervals. The light from the sky enters the phototubes through a mirror, which can be either looking at a chosen point in the sky, or scanning within a chosen angle in the south-north direction, i.e., at right angles to the most commonly occurring auroral arcs. Mirror speed can be chosen. Together with the measurement time this speed determines the spatial resolution of the device. The measurement time, i.e., the time over which the phototubes are integrating the photons, can be set as short as 0.1 sec. Parallel to the photometer measurements, a low light level TV-camera is operated to record auroral activity also on video tape. It is possible to calibrate videopictures by using the corresponding photometer data, thus obtaining intensity data from a large portion of the sky. ESA

N88-30102# British Aerospace Public Ltd. Co., Bristol (England). Space and Communications Div.
MICROWAVE INSTRUMENT FOR PLANETARY MISSION (TITAN/CASSINI MISSION ORBITER SPACECRAFT) Final Report
P. J. L. Wildman, R. Durrant, S. Madsen, and N. Skou Paris, France ESA Nov. 1987 262 p
(Contract ESA-6917/86-NL-JG(SC))
(BAe-CS/TP-8359; ESA-CR(P)-2616; ETN-88-93040) Copyright Avail: NTIS HC A12/MF

A microwave altimeter/imager for the investigation of Titan from the CASSINI mission Saturn orbiter was designed. Performance goals are 5 km imaging resolution with a 400 km swath width and an altimetric resolution of 50 m. It is concluded that atmospheric absorption is negligible for frequencies below 40 GHz. The baseline uses a 30 GHz carrier frequency and a dedicated imaging radar antenna. By using a time-multiplex scheme it is possible to obtain simultaneous, continuous, altimeter profiles, real aperture medium resolution images, and synthetic aperture high resolution images. The baseline uses the probe relay dish antenna for altimetry and a 3 m by 0.2 m antenna panel for imaging radar. From a block diagram level design of the complete system including RF hardware, high-power amplifier, waveform generator, and digital processing subsystems, mass and power budgets and critical components were defined. The principal mission constraint is limited coverage from Titan flybys to no closer than 1000 km. The

accommodation of the 3 m x 0.2 m imager antenna and its pointing requirements are the principal spacecraft constraints. ESA

N88-30103# Scientific Research Associates, Inc., Glastonbury, Conn.
NUMERICAL SIMULATION OF THE FUNCTION OF SCIENTIFIC INSTRUMENTATION FOR MEASURING THE SPEED OF ELECTRON DEVICES Final Report, 1 Aug. 1987 - 31 Jan. 1988
M. A. Osman, H. L. Grubin, and B. J. Morrison 30 Mar. 1988 67 p
(Contract F49620-87-C-0070)
(AD-A194969; SRA-R87-910024-F; AFOSR-88-0449TR) Avail: NTIS HC A04/MF A01 CSCL 14B

The feasibility of using numerical simulation to assess the function of scientific instrumentation for measuring the speed of electron devices has been demonstrated by obtaining: (1) the dc characteristics of the VHEMT and PHEMT, (2) transient response of the PHEMT to picosecond voltage pulses superimposed on the gate. The drift and diffusion and Poisson's equations were solved in two dimensions. The HEMT and PHEMT demonstrated transconductance of 94 and 375 mS/mm, respectively. The transient response is strongly dependent on the pulse shape and duration. GRA

N88-30104# Pennsylvania State Univ., University Park. Materials Research Lab.
PIEZOELECTRIC AND ELECTROSTRICTIVE MATERIALS FOR TRANSDUCER APPLICATIONS, VOLUME 2 Annual Report, 1 Jan. - 31 Dec. 1987
L. E. Cross, R. E. Newnham, G. R. Barsch, and J. V. Biggers Mar. 1988 196 p
(Contract N00014-82-K-0339)
(AD-A194956) Avail: NTIS HC A09/MF A01 CSCL 20C

A modified Michelson interferometer is used to study the strain properties of piezoelectric and electrostrictive materials. For small displacement, a feedback loop is introduced to stabilize the system against the low frequency optical path-length drifting and the system is capable of resolving displacements of the order of .001 A. For the strain induced by domain switching, a dual-channel signal detection scheme is used which automatically reads out the displacement of the sample. The effect on the measurement of the sample bonding to a substrate and other related problems are discussed. GRA

N88-30105*# National Aeronautics and Space Administration. Langley Research Center, Hampton, Va.
QUANTITATIVE SURFACE TEMPERATURE MEASUREMENT USING TWO-COLOR THERMOGRAPHIC PHOSPHORS AND VIDEO EQUIPMENT Patent Application
Gregory M. Buck, inventor (to NASA) 13 Jun. 1988 14 p
(NASA-Case-LAR-13740-1; NAS 1.71:LAR-13740-1; US-Patent-Appl-SN-205900) Avail: NTIS HC A03/MF A01 CSCL 14B

A thermal imaging system provides quantitative temperature information and is particularly useful in hypersonic wind tunnel applications. An object to be measured is prepared by coating with a two-color, ultraviolet-activated, thermographic phosphor. The colors emitted by the phosphor are detected by a conventional color video camera. A phosphor emitting blue and green light with a ratio that varies depending on temperature is used so that the intensity of light in the blue and green wavelengths detected by the blue and green tubes in the video camera can be compared. Signals representing the intensity of blue and green light at points on the surface of the model in a hypersonic wind tunnel are used to calculate a ratio of blue to green light intensity which provides quantitative temperature information for the surface of the model. NASA

N88-30106*# Northwestern Univ., Evanston, Ill. Technological Inst.
ELECTRICAL PROPERTIES OF MATERIALS FOR ELEVATED TEMPERATURE RESISTANCE STRAIN GAGE APPLICATION Ph.D. Thesis
Jih-Fen Lei Jun. 1987 276 p
(Grant NAG3-501)
(NASA-CR-182214; NAS 1.26:182214) Avail: NTIS HC A13/MF A01 CSCL 14B

The objective was to study the electrical resistances of materials that are potentially useful as resistance strain gages at 1000 C. Transition metal carbides and nitrides, boron carbide and silicon carbide were selected for the experimental phase of this research. Due to their low temperature coefficient of resistance and good stability, TiC, ZrC, B sub 4 C and beta-SiC are suggested as good candidates for high temperature resistance strain gage applications. Author

N88-30107# Aeronautical Research Labs., Melbourne (Australia).
DEVELOPMENT AND INSTALLATION OF AN INSTRUMENTATION PACKAGE FOR GE F404 INVESTIGATIVE TESTING
D. K. Streatfeild Jan. 1988 36 p
(AD-A196265; ARL/AERO-PROP-TM-446; DODA-AR-004-584)
Avail: NTIS HC A03/MF A01 CSCL 21E

The development and installation of an Instrumentation Package for GE F404 Investigative Testing is described. The package is used in conjunction with the ARL MOBILE (Transient) Data Acquisition System (MODAS) and can be used on the F404 engine at both Fixed or Mobile Engine Test locations. GRA

N88-30108* National Aeronautics and Space Administration. Langley Research Center, Hampton, Va.
METHOD OF ATTACHING STRAIN GAUGES TO VARIOUS MATERIALS Patent
Timothy D. Schott, inventor (to NASA), Robert L. Fox, inventor (to NASA), and John D. Buckley, inventor (to NASA) 30 Aug. 1988 7 p Continuation-in-part of US-Patent-Appl-SN-831372, filed 20 Feb. 1986, abandoned
(NASA-Case-LAR-13797-1; US-Patent-4,767,484; US-Patent-Appl-SN-074792; US-Patent-Class-156-233; US-Patent-Class-156-247; US-Patent-Class-156-272.4; US-Patent-Class-156-274.8; US-Patent-Class-156-275.5; US-Patent-Class-156-307.7; US-Patent-Appl-SN-831372) Avail: US Patent and Trademark Office CSCL 14B

A method is provided to bond strain gauges to various materials. First, a tape with an adhesive backing is placed across the inside of the fixture frame. The strain gauge is flatly placed against the adhesive backing and coated with a thin, uniform layer of adhesive. The tape is then removed from the fixture frame and placed, strain gauge side down, on the material to be tested. If the material is a high reluctance material, the induction heating source is placed on the tape. If the material is a low reluctance material, a plate with a ferric side and a rubber side is placed, ferric side down, onto the tape. The induction heating source is then placed upon the rubber side. If the material is an insulator material, a ferric plate is placed on the tape. The induction heating source is then placed on the ferric plate. The inductive heating source then generates frequenty from 60 to 70 kilocycles to inductively heat either low reluctance material, ferric side, of ferric plate and provides incidental pressure of approximately five pounds per square inch to the tape for two minutes, thoroughly curing the adhesive. The induction heating source, and, if necessary, the plate or ferric plate, are then removed from the tape after one minute. The tape is then removed from the bonded strain gauge. Official Gazette of the U.S. Patent and Trademark Office

N88-30109# National Bureau of Standards, Gaithersburg, Md. Center for Radiation Research.
NBS (NATIONAL BUREAU OF STANDARDS) MEASUREMENT SERVICES: THE NBS PHOTODETECTOR SPECTRAL RESPONSE CALIBRATION TRANSFER PROGRAM Final Report
E. F. Zalewski Mar. 1988 66 p
(PB88-201595; NBS-SP-250-17) Avail: NTIS HC A04/MF A01 CSCL 14B

A silicon-photodiode-based radiometer is supplied to transfer

the calibration of absolute spectral response in units of A/W (Amperes/Watts) and A sq cm/W in the 250 to 1064 nm region of the spectrum. The radiometer is also characterized for linearity over the four decade range of the amplifier gain settings. Also included with the radiometer are components and a procedure for measuring error diagnosis. The methods for obtaining and using this calibrated radiometer are described, as well as the calibration and characterization procedures used at NBS. Author

N88-30110# Army Missile Command, Redstone Arsenal, Ala.
EVALUATION OF MULTI-FOCUS HOLOGRAPHIC LENSES Final Technical Report
Don A. Gregory and James F. Hawk 24 May 1988 23 p
(AD-A196167; AD-E951148; AMSMI/TR-RD-RE-88-2) Avail: NTIS HC A03/MF A01 CSCL 14A

The properties of two, 7 x 7 dichromated gelatin hololenses were measured and compared with the specifications under which they were procured. The intended use for these lenses is a coherent optical correlator. The 49 memory locations would exceed the previously achieved 25 locations and expand the usefulness of the correlator. Several preliminary hololenses were also evaluated which had been made from a new photopolymer from Polaroid, designated DMP-128. Results obtained include the overall diffraction efficiency and the uniformity of the arrays. GRA

N88-30111# Royal Signals and Radar Establishment, Malvern (England).
AUTOMATIC PROBER FOR THE dc CHARACTERISATION OF GALLIUM ARSENIDE DEVICES. PART 2: THE DATA SORTING AND DISPLAY FACILITY
B. T. Hughes and B. E. Avery Jul. 1987 53 p
(AD-A195408; RSRE-Memo-4066-Pt-2; DRIC-BR-105535-Pt-2)
Avail: NTIS HC A04/MF A01 CSCL 20L

The Automatic Device Probing System used in the Microwave Devices Division (DP2) comprises separate measurement and data handling facilities. The measurement facility is described in RSRE Memorandum 4065 and the data sorting and display facility forms the subject of this memorandum. The facility described is designed to assist in analyzing the large quantity of measured data obtained from device wafers and allows general trends as well as individual device parameters to be investigated. Programs have been written to produce maps which allow parameter variations across wafers to be assessed and additional routines are available which present the data in histogram form. These options allow the numeric as well as the geographic distribution of the data to be investigated. Three main types of map display are available, these display the variation in magnitude of a device parameter across a wafer, the location and nature of the failure of any failed devices and the location of devices with a specified combination of parameters. GRA

N88-30112# Pennsylvania State Univ., University Park. Materials Research Lab.
PIEZOELECTRIC AND ELECTROSTRICTIVE MATERIALS FOR TRANSDUCER APPLICATIONS, VOLUME 3 Annual Report, 1 Jan. - 31 Dec. 1987
L. E. Cross, R. E. Newnham, G. R. Barsch, and J. V. Biggers Mar. 1988 81 p
(Contract N00014-82-K-0339)
(AD-A194949) Avail: NTIS HC A05/MF A01 CSCL 20C

In the course of the development of a phenomenological model for the whole lead zirconate-titanate (PZT) solid solution system, it was found that some of the required experimental information was missing. To permit these required measurements, pure homogeneous ceramic samples of specific PZT compositions were fabricated from sol-gel derived powders. This paper describes the preparation and characterization of these required compositions. GRA

36 LASERS AND MASERS

Includes parametric amplifiers.
For related information see also *76 Solid-State Physics.*

N88-30113*# Oklahoma State Univ., Stillwater. Dept. of Physics.
GROWTH AND CHARACTERIZATION OF MATERIALS FOR TUNABLE LASERS IN THE NEAR INFRARED SPECTRAL REGION Semiannual Progress Report, 1 Feb. - 31 Jul. 1988
Richard C. Powell and Joel J. Martin Jul. 1988 25 p
(Grant NAG1-694)
(NASA-CR-183132; NAS 1.26:183132) Avail: NTIS HC A03/MF A01 CSCL 20E

During this reporting period, work proceeded in two directions. The first was the development of crystal growth procedures for rare earth doped LiYF4 crystals. The procedures for growth and pre-growth treatment of starting materials for undoped LiYF4 crystals were established and good optical quality materials were grown. A significant amount of time was spent trying to establish the optimum growth parameters for Yb(3+)-doped crystals. Unfortunately, it has proven difficult to obtain large size boules of high optical quality crystals of LiYF4 with doping concentrations of Yb(3+) of several percent. Because of these problems, this research is to be changed to attempt doping with other trivalent rare earth ions such as Ho, Er, and Tm. The second research area was investigating the potential of LiNbO3:Mg,Cr and LiNbO3:Mg,Cr,Yb as possible laser materials. The results are summarized. Author

N88-30114# Colorado Univ., Boulder.
SPONTANEOUS FORCE OPTICAL TRAPS Annual Report, Jun. 1987 - Jun. 1988
D. Sesko, C. G. Fan, and Carl F. Wieman 1 Jun. 1988 16 p
Sponsored in part by NSF and Navy
(Contract N00014-87-K-0396)
(AD-A196103; CU-153-1200) Avail: NTIS HC A03/MF A01 CSCL 20M

Very well controlled diode laser systems are constructed and used to produce laser cooled atoms. Very low pressures are required to study very cold atoms and a high vacuum chamber is constructed to achieve the necessary pressure. The behavior of laser trapped and cooled atoms is studied and found, not to agree with present theoretical predictions. GRA

N88-30115# Berkeley Research Associates, Inc., Calif.
RESEARCH ON A TWO-STAGE FREE ELECTRON LASER OSCILLATOR Final Report
Mar. 1988 98 p
(Contract N00014-86-C-2342)
(AD-A195991; BRA-88-W032R) Avail: NTIS HC A05/MF A01 CSCL 09C

The research involved the theoretical and numerical analysis of the physics of free electron lasers using relativistic particle beams. The major emphasis of the research was to obtain design criteria for the development of a two-stage FEL oscillator operating in the trapped particle mode. The present work was centered on the development of a fully relativistic, nonlinear analysis of the spatial and temporal evolution of multiple modes within a free electron laser oscillator and of a large amplitude, nonlinearly saturated state characteristic of trapped particle mode operation. The equations solved are the Maxwell equations of electrodynamics coupled with the collisionless Boltzmann equation that describes collisionless particles under influence of the electromagnetic fields. The electromagnetic fields include the radiation fields from the FEL and the self-electric fields from the longitudinal potential due to the space charge, i.e., the dominant component of the interparticle Coulomb forces. The particle dynamics transverse to the magnetic axis are included, but gradients in the radiation fields are ignored. The electron beam equilibrium is assumed to be spatially uniform and temporally stationary. Justification and probable impact of further approximations are discussed in the technical section of this report. The approximations employed are

consistent with the purpose of obtaining experimentally implementable design criteria for the FEL oscillator. GRA

N88-30116# Defense Intelligence Agency, Washington, D.C. Directorate for Scientific and Technical Intelligence.
BIBLIOGRAPHY OF SOVIET LASER DEVELOPMENTS, NUMBER 88, MARCH - APRIL 1987
3 Mar. 1988 172 p
(AD-A195978; DIA-DST-2700Z-002-88) Avail: NTIS HC A08/MF A01 CSCL 09C

This is the Soviet Laser Bibliography for March-April 1987, and is No. 88 in a continuing series on Soviet laser developments. The coverage includes basic research on solid state, liquid, gas, and chemical laser components; nonlinear optics; spectroscopy of laser materials; ultrashort pulse generation; theoretical aspects of advanced lasers; and general laser theory. Laser applications are listed under biological effects; communications systems; beam propagation; adaptive optics; computer technology; holography; laser-induced chemical reactions; measurement of laser parameters; laser measurement applications laser-excited optical effects; laser spectroscopy; beam-target interaction; and plasma generation and diagnostics. GRA

N88-30117# Air Force Systems Command, Wright-Patterson AFB, Ohio. Foreign Technology Div.
MODE LOCKING OF SEMICONDUCTOR LASER WITH EXTERNAL CAVITY
Xiaorong Qin, Tao Fang, Hansheng Zeng, and Yizhi Gao 10 May 1988 13 p Transl. into ENGLISH from Yingyong Jiguang (People's Republic of China), v. 6, no. 6, 1986 p 250-252
(AD-A196018; FTD-ID(RS)T-0147-88) Avail: NTIS HC A03/MF A01 CSCL 09C

Mode locking of a semiconductor laser with external cavity has been observed by optoelectronic feedback. The noticeable narrowing of the microwave spectrum explains the mode locking phenomenon which occurs when the optoelectronic feedback is sufficiently strong. A second order harmonic relating method or a strip camera can be used to measure the pulse width in order to positively identify the locking condition. After testing several semiconductor lasers, the results show that most of these possess a relatively string induced self-pulsing at 1 GHz. A better result can be achieved if a 1 GHz amplifier is used and its magnifying power is increased. The experiment shows that an induced self-pulsing can be obtained from the LD, which originally has no self-pulsing, after an external cavity reaches the passive locking mode, an active-passive self-adjusting locking mode, which occurs owing to the automatic matching between the adjusting frequency and cavity length, can be achieved after the optoelectronic feedback. GRA

N88-30118# Battelle Inst., Frankfurt am Main (West Germany).
SPACEBORNE LIDAR: DEVELOPMENT OF A LABORATORY TEST SYSTEM Final Report
M. Endemann, V. Klein, H.-J. Hoeffgen, C. Malvichini, G. Mombrini, and E. Nava Paris, France ESA Feb. 1988 159 p
(Contract ESTEC-5966/84-NL-PR(SC))
(BF-R-66.090-1; ESA-CR(P)-2605; ETN-88-93035) Avail: NTIS HC A08/MF A01

The design, realization, and testing of a functional backscatter lidar intended to validate the overall system design concept of operational spaceborne lidar instruments, and to aid in the development and optimization of the lidar components are described. It is a compact lidar that allows easy modification of components to verify their performance in the overall system. It performs atmospheric measurements through the window of a laboratory and thus is not optimized with respect to size, mass, and power consumption. A fiber optics coupler connects the scanning receiving telescope with the detector package. Thus the positioning of the detectors becomes uncritical for the instrument alignment, allowing use of a particularly simple and light structure that still warrants high alignment stability of the components. This scanner arrangement performs well in tests and is recommended as baseline design for the spaceborne lidar. A frequency-doubled Nd:YAG transmitter laser is suggested. ESA

N88-30119# Air Force Systems Command, Wright-Patterson AFB, Ohio. Foreign Technology Div.
TRANSVERSE CO2 LASER TWO-DIMENSIONAL GAIN DISTRIBUTIONS
Liyin Chen, Zexiang Chu, and Haitao Chen 24 Jun. 1988 22 p Transl. into ENGLISH from Jiguang (Peoples Republic of China), v. 11, no. 5, 1984 p 257-262
(AD-A196240; FTD-ID(RS)T-0265-88) Avail: NTIS HC A03/MF A01 CSCL 07D

Using one-dimensional gas flows and quasi-two-dimensional electrical discharge models, we calculated the two-dimensional gain curve contour lines for equal values on perpendicular electrode planes. We studied the electrical discharge area gas flow speeds and electrical discharge parameters as well as gas constituents and similar items and their effects on the rules or patterns of changes along the direction of the gas flow. As far as each gas pressure is concerned, they had flow speed ranges which corresponded to optimum gain curves. We took calculation results and experimental results and carried out a comparison. GRA

N88-30120# Aerospace Corp., El Segundo, Calif. Electronics Research Lab.
TOLERANCES FOR PHASE LOCKING OF SEMICONDUCTOR LASER ARRAYS
Elsa M. Garmire 18 Apr. 1988 25 p
(Contract F04701-85-C-0086)
(AD-A195974; TR-0086(6925-04)-1; SD-TR-88-55) Avail: NTIS HC A03/MF A01 CSCL 09C

The fabrication and operating conditions for semiconductor laser arrays to be phase-locked are described. The analysis is based on a linear theory of the locking of coupled oscillators. Results show that the refractive index of adjacent lasers must be the same to approx. 0.0001. This puts close tolerances on fabrication if phase-locking is to be maintained. The average aluminum concentration in adjacent stripes must be the same to within approx. 0.0001, while the average epilayer thickness must be the same to within 0.2 pct, or a tolerance of 3 A on the active layer. Changes in refractive index due to free carrier injection provide an additional tolerance condition, which translates to a requirement that the stripe width and contact resistance be uniform to within a few percent. In addition, because thermal profiles may be detrimental, careful heat-sinking is required. These fabricational tolerances support the fact that high quality epilayers such as grown by molecular-beam epitaxy (MBE) and metal-organic chemical vapor deposition (MOCVD) are usually required for phase-locked laser arrays, and that photoresist processing and bonding must be done carefully. GRA

N88-30121# Vanderbilt Univ., Nashville, Tenn. Dept. of Physics and Astronomy.
VANDERBILT FREE ELECTRON LASER PROJECT IN BIOMEDICAL AND MATERIALS RESEARCH Annual Report, 1 Feb. 1987 - 31 Jan. 1988
Richard F. Haglund and N. H. Tolk Jun. 1988 17 p
(Contract N00014-87-C-0146)
(AD-A195961) Avail: NTIS HC A03/MF A01 CSCL 06G

The Medical Free Electron Laser Program was awarded to develop, construct and operate a free-electron laser facility dedicated to biomedical and materials studies, with particular emphases on: fundamental studies of absorption and localization of electromagnetic energy on and near material surfaces, especially through electronic and other selective, non-statistical processes; non-thermal photon-materials interactions (e.g., electronic bond-breaking or vibrational energy transfer) in physical and biological materials as well as in long-wavelength biopolymer dynamics; development of FEL-based methods to study drug action and to characterize biomolecular properties and metabolic processes in biomembranes; clinical applications in otolaryngology, neurosurgery, ophthalmology and radiology stressing the use of

the laser for selective laser-tissue, laser-cellular and laser-molecule interactions in both therapeutic and diagnostic modalities. GRA

N88-30122# Army Missile Command, Redstone Arsenal, Ala. Advanced Sensors Directorate.
NONLINEAR OPTICAL PHASE CONJUGATION TECHNIQUES TO REDUCE THE PHYSICAL SIZE OF LASERS Final Technical Report, May - Jul. 1987
H. L. Pratt Sep. 1987 22 p
(AD-A196170; AD-E951144; AMSMI/TR-RD-AS-87-19) Avail: NTIS HC A03/MF A01 CSCL 02F

Optical phase conjugation involves the use of various techniques to reverse the wavefront of an optical beam. Nonlinear optical interactions within various media may be used to generate phase conjugation. This report reviews the most promising techniques for nonlinear optical phase conjugation and postulates how phase conjugation might be used to reduce the physical size of laser systems. A number of examples from literature are cited.
Author (GRA)

N88-30123# Naval Research Lab., Washington, D.C. Plasma Physics Div.
AUTOIONIZATION FOR LOWER LEVEL DETRAPPING IN X-RAY LASERS Interim Report
R. C. Elton 9 May 1988 23 p
(AD-A195845; NRL-9103) Avail: NTIS HC A03/MF A01 CSCL 09C

A novel type of X-ray laser is analyzed in which the population of the lower level is depleted by autoionization instead of by spontaneous decay. The intention is to decrease radiative trapping effects that quench the gain and require microscopic plasmas. Proof-of-principle atomic-physics experiments and numerical modeling are needed to verify predicted feasibility, fluorescence, and lasing. GRA

N88-30124# State Univ. of New York, Albany. Research Foundation.
LASER SENSING FOR IDENTIFICATION AND CONTROL OF DISTRIBUTED PARAMETER SYSTEMS Final Report, 1 Dec. 1986 - 30 Nov. 1987
Daniel J. Inman 1 May 1988 17 p
(Grant AF-AFOSR-0099-87)
(AD-A195886; AFOSR-88-0654TR) Avail: NTIS HC A03/MF A01 CSCL 14B

This instrumentation award funded the purchase of a laser vibrometer system, mass computer data storage and data acquisition equipment. This equipment used in conjunction with existing vibration testing and control facilities provides a sophisticated low frequency velocity measurement system for use in identifying the coefficients in partial differential equation models of distributed mass structures. In addition, the vibrometer system provides straightforward and direct velocity feedback for such systems. These flexible structures characteristically have very low natural frequencies which cannot be detected by accelerometers. This system has and is being used to perform tests on models and sub-assemblies of large space structures for the purpose of evaluating existing identification and control strategies as well as to stimulate new research in the area of control, observers (estimators) and identification. Several intense experiments using the laser vibrometer were performed to measure the response of a quasi isotropic cantilevered beam with a removable tip mass excited by an impulse at various locations. This data was collected, stored, and sent to AFOSR researchers at Brown University transmitted using BITNET. The data was analyzed using a spline based estimation procedure, starting with a partial differential equation model of the structure. A clear advantage over modal methods based on a finite dimensional model of the same system was observed. GRA

N88-30125# Technische Univ., Berlin (West Germany). Fachbereich fuer Elektrotechnik.
SPECTRAL PROPERTIES OF SEMICONDUCTOR LASERS WITH EXTERNAL RESONATORS Ph.D. Thesis [SPEKTRALE EIGENSCHAFTEN VON HALBLEITERLASERN MIT EXTERNEN RESONATOREN]
Gerhard Wenke 1988 153 p In GERMAN
(ETN-88-93119) Avail: NTIS HC A08/MF A01

Mode partition noise limitation in laser transmission systems is studied. Noise sources are investigated in the case of two different emission modules. For the transmission of 2.24 Gbit/sec a dispersive single mode laser with external optical resonator was developed and analyzed. A transmission system at 560 Mbit/sec with external phase modulation and optical transfer reception or direct reception is also considered. In both systems spectral behavior of semiconductor lasers is specified and various laser-fiber couplings are envisaged. ESA

N88-30126# Princeton Univ., N. J. Dept. of Electrical Engineering and Computer Science.
ULTRAFAST PROCESSES AND SPECTROSCOPY WITH FREE ELECTRON LASERS Annual Report, 1 Jun. 1987 - 31 May 1988
Philippe M. Fauchet Apr. 1988 4 p
(Contract N00014-86-K-0711)
(AD-A195248) Avail: NTIS HC A02/MF A01 CSCL 20E

Femtosecond laser spectroscopy has been used to study carrier relaxation times in amorphous silicon. We find a relaxation time of 1 picosecond above the mobility edge and a relaxation time of 10 picoseconds in the bandtail states, after which temperature effects dominate the optical properties. Theoretical modeling of femtosecond spectroscopic measurements has also helped define what is measurable and what is not. Picosecond time-resolved reflectivity measurements have been performed during laser-induced phase transitions. The dielectric function of molten Si has been measured and superheating in the liquid phase has been observed to last at least 10 picoseconds. Work continues in both areas. We expect to expand the experimental program to other wavelengths thanks to the free electron laser. GRA

37 MECHANICAL ENGINEERING

Includes auxiliary systems (nonpower); machine elements and processes; and mechanical equipment.

N88-30127# Technische Univ., Berlin (West Germany). Inst. fuer Luft- und Raumfahrt.
STABILITY OF STICK-SLIP PHENOMENON BY USING CONSTITUTIVE FRICTION LAWS OF DIETRICH AND RUINA [STABILITAET EINES REIBSCHWINGERS UNTER VERWENDUNG EINES KONSTITUTIVEN REIBGESETZES NACH DIETRICH UND RUINA]
Marcel Bunge, Jingyun Chu, Arnold Gross-Thebing, and Klaus Knothe Apr. 1988 105 p In GERMAN
(ILR-Mitt-197; ETN-88-93117) Avail: NTIS HC A06/MF A01

The friction laws established by Dietrich and Ruina are examined and the constitutive equations verified and applied to rolling contact. Stability investigation is carried out for the linear differential equations systems in presence of structure damping. Nonlinear friction oscillations are outlined by using the constitutive sliding friction equations. Numerical results and computational procedure are presented for different rigidity and damping values, surface properties, and initial velocities. ESA

N88-30128*# National Aeronautics and Space Administration. Lewis Research Center, Cleveland, Ohio.
HELICOPTER TRANSMISSION RESEARCH AT NASA LEWIS RESEARCH CENTER
John J. Coy, Dennis P. Townsend, David G. Lewicki (Army Aviation Systems Command, Cleveland, Ohio.), and Harold H. Coe [1988] 19 p Prepared for presentation at the International Conference on Gearing, Zhengzhou, Peoples Republic of China,

5-10 Nov. 1988; sponsored in part by the Chinese Mechanical Engineering Society
(DA Proj. 1L1-62209-A-47-A)
(NASA-TM-100962; E-4181; AVSCOM-TM-88-C-003; NAS 1.15:100962) Avail: NTIS HC A03/MF A01 CSCL 13I

A joint helicopter transmission research program between NASA Lewis Research Center and the U.S. Army Aviation Systems Command has existed since 1970. Program goals are to reduce weight and noise and to increase life and reliability. Reviewed are significant advances in technology for gears and transmissions and the experimental facilities at NASA Lewis for helicopter transmission testing are described. A description of each of the rigs is presented along with some significant results from the experiments. Author

N88-30129# Ecole Nationale Superieure de l'Aeronautique et de l'Espace, Toulouse (France).
STUDIES OF UNSTEADY AXIAL-COMPRESSOR FUNCTIONING
A. Carrere 1986 55 p In FRENCH Sponsored by Direction des Recherches, Etudes et Techniques, Paris, France
Avail: NTIS HC E04/MF E04; copy not available from STI Facility

Unsteady functioning of axial flow compressors are studied just before a surge. The ENSAE compressor test bench, consisting of two transonic axial compressor stages, is specially designed to record steady and unsteady measurements at a number of points. Axisymmetric flow in this compressor was first studied and described using experimental methods (study of distribution at the inlet and diagram of the compressor field in the steady mode), then compared to axisymmetric flow calculated by the SNECMA calculation flow and stability code program. A whole series of unsteady measurements were carried out in order to describe the machine's functioning around surge point. Author

N88-30130*# National Aeronautics and Space Administration. Langley Research Center, Hampton, Va.
CLEVIS JOINT FOR DEPLOYABLE SPACE STRUCTURES Patent Application
Marvin D. Rhodes, inventor (to NASA) 28 Jul. 1988 13 p
(NASA-Case-LAR-13898-1; NAS 1.71:LAR-13898-1; US-Patent-Appl-SN-225427) Avail: NTIS HC A03/MF A01 CSCL 13K

This invention relates generally to pin clevis joints, and more particularly, to zero play pin clevis joints for connecting structural members of a deployable space structure. A joint includes a pin, a tang, and a shackle. The pin is tapered at the same angle as the bores extending through the projections of the shackle and the tang. A spring washer biases the tang onto the tapered sidewall of the pin. The invention solves the free play problem associated with deployable space structures by using a tapered pin which is held in tapered holes by the spring washers. NASA

N88-30131* National Aeronautics and Space Administration. Lyndon B. Johnson Space Center, Houston, Tex.
ARC LENGTH CONTROL FOR PLASMA WELDING Patent
William F. Iceland, inventor (to NASA) (Rockwell International Corp., Canoga Park, Calif.) 23 Aug. 1988 8 p
(NASA-Case-MSC-20900-1; US-Patent-4,766,286; US-Patent-Appl-SN-079317; US-Patent-Class-219-121.57; US-Patent-Class-219-124.02; US-Patent-Class-219-130.4; US-Patent-Class-219-121.54; US-Patent-Class-219-121.56) Avail: U.S. Patent and Trademark Office CSCL 13H

A control system to be used with a plasma arc welding apparatus is disclosed. The plasma arc welding apparatus includes a plasma arc power supply, a contactor, and an electrode assembly for moving the electrode relative to a work piece. The electrode assembly is raised or lowered by a drive motor. The present apparatus includes a plasma arc adapter connected across the power supply to measure the voltage across the plasma arc. The plasma arc adapter forms a dc output signal input to a differential amplifier. A second input is defined by an adjustable resistor connected to a dc voltage supply to permit operator control. The differential amplifier forms an output difference signal provided to an adder circuit. The adder circuit then connects with a power amplifier which forms the driving signal for the motor. In addition, the motor connects to a tachometor which forms a feedback signal delivered to the adder to provide damping, therby avoiding servo loop overshoot.
Official Gazette of the U.S. Patent and Trademark Office

N88-30132# Massachusetts Inst. of Tech., Cambridge. Artificial Intelligence Lab.
MODELING ROBOT FLEXIBILITY FOR ENDPOINT FORCE CONTROL
Steven D. Eppinger and Warren P. Seering May 1988 17 p
(Contract N00014-85-K-0124)
(AD-A195923; AI-M-1046) Avail: NTIS HC A03/MF A01 CSCL 12I

Dynamic models have been developed in an attempt to match the response of a robot arm. The experimental data show rigid-body and five resonant modes. The frequency response and pole-zero arrays for various models of structural flexibility are compared with the data to evaluate the characteristics of the models, and to provide insight into the nature of the flexibility in the robot. Certain models are better able to depict transmission flexibility while others describe types of structural flexibility. GRA

N88-30133# Amsterdam Univ. (Netherlands). Dept. of Computer Science.
PATH PLANNING AND PATH FOLLOWING FOR THE AMSTERDAM AUTONOMOUS CART
H. Muller Oct. 1986 35 p
(FVI-86-22) Avail: NTIS HC E03/MF E01; copy not available from STI Facility

At the University of Amsterdam, an autonomous cart was developed for research on intelligent multisensor systems. The main design criteria for the cart were the following: The vehicle must be capable of finding its way through a simple environment. To find its way, it has to have: knowledge about the environment in the form of a two dimensional map with the position of walls, doors and obstacles; the command, go to a position, can be executed; the cart must be autonomous, everything is onboard (computer power and power supply); and, a real time performance with a speed of + or - 0.5 m/s. To perform its task (drive from A to B), the cart is equipped with the following hardware: two driven wheels, at the right and left back side of the cart which have a continuous motor regulation and one castor front wheel; shaft encoders for dead reckoning; eight sonar distance meters, used for detection of walls and obstacles; and onboard MC68020 microprocessor board with floating point coprocessor and 1 Mb ram. Author

N88-30134*# Catholic Univ. of America, Washington, D.C. Dept. of Electrical Engineering.
ROBUST DESIGN OF DISTRIBUTED CONTROLLERS FOR LARGE FLEXIBLE SPACE STRUCTURES Final Technical Report
Charles C. Nguyen Sep. 1988 33 p
(Grant NAG5-949)
(NASA-CR-183202; NAS 1.26:183202) Avail: NTIS HC A03/MF A01 CSCL 13I

Independent Modal Space Control (IMSC) method avoids control spillover generated by conventional control schemes such as Coupled Modal Control by decoupling the large flexible space structure into independent subsystems of second order and controlling each mode independently. The IMSC implementation requires that the number of actuators be equal to that of modeled modes, which is in general very huge. Consequently the number of required actuators is unrealizable. Two methods are proposed for the implementation of IMSC with reduced number of actuators. In the first method, the first m modes are optimized, leaving the last (n-m) modes unchanged. In the second method, generalized inverse matrices are employed to design the feedback controller so that the control scheme is suboptimal with respect to IMSC. The performance of the proposed methods is tested by performing

computer simulation on a simply support beam. Simulation results are presented and discussed. Author

N88-30135# Institut Franco-Allemand de Recherches, St. Louis (France).
INTERACTION OF HIGH POWER LASER RADIATION WITH METALS IN LASER WELDING
M. Schellhorn and G. Spindler (Deutsche Forschungs- und Versuchsanstalt fuer Luft- und Raumfahrt, Stuttgart, West Germany) 1987 7 p Presented at the Conference on Laser and Electro-Optic Techniques, Baltimore, Md., 26 Apr. - 1 May 1987
(ISL-PU-304/87; ETN-88-92020) Avail: NTIS HC A02/MF A01

Interaction of high power laser radiation with metals during welding; and transient absorption behavior of metals during laser welding are discussed. ESA

N88-30136# European Space Tribology Lab., Risley (England).
THE LUBRICATING PROPERTIES OF MAGNETRON SPUTTERED MoS2
E. W. Roberts Paris, France ESA Oct. 1987 64 p
(Contract ESA-5615/83-NL-PP)
(ESA-ESTL-76; ESA-CR(P)-2624; ETN-88-93151) Avail: NTIS HC A04/MF A01

It is shown that the tribological quality of MoS2 lubricant films formed by magnetron sputtering is determined by the choice of sputtering conditions. By selecting the appropriate conditions, films of extremely low friction coefficient and high endurance (in vacuum) are obtained. Such MoS2 films, when applied to precision ball bearings, give the lowest torques (for the given test conditions) observed with dry lubricants. It is shown that bearing endurance (in vacuum) depends on cage type and that long endurances are possible when PTFE composite cages are employed with sputter coated raceways and balls. While high perforance obtains in vacuum, tests in air show a marked deterioration in lubricating qualities, due to the adsorption of water vapor on MoS2 surfaces. This occurs in two stages and corresponds to adsorption at two types of surface site. Friction is speed-dependent and load-dependent. Film quality is determined by its chemical composition, which is a function of deposition rate. ESA

38 QUALITY ASSURANCE AND RELIABILITY

Includes product sampling procedures and techniques; and quality control.

N88-30137# Polytechnic Univ., Brooklyn, N.Y.
IN SITU FAULT DETECTION BY THE HYBRID RAY MODE METHOD Annual Technical Report, 1 Mar. 1987 - 29 Feb. 1988
L. B. Felsen 29 Feb. 1988 25 p
(Grant AF-AFOSR-0318-86)
(AD-A195226; AFOSR-88-0545TR) Avail: NTIS HC A03/MF A01 CSCL 17A

The objective of this research has been to develop algorithms for in situ location, by ultrasound, of flaws in plates or laminated layered materials. Achieving this objective requires detailed knowledge of the excitation, propagation, scattering and detection of high frequency sound waves in the flawed environment. Based on an understanding of these fundamental wave phenomena, one may then attempt to construct analytical models with accompanying algorithms, so as to parametrize the Nonlinear Differential Equation problem in terms of good observables. GRA

N88-30138# Stanford Univ., Calif. Lab. of Physics.
APPLICATION OF NONDESTRUCTIVE TESTING TECHNIQUES TO MATERIALS TESTING Final Report, 1 Jan. 1984 - 30 Nov. 1987
G. S. Kino Dec. 1987 66 p
(Grant AF-AFOSR-0063-84)
(AD-A195716; AFOSR-88-0667TR) Avail: NTIS HC A04/MF A01 CSCL 14B

A set of new techniques in scanning acoustic and optical microscopy is described. Starting with an acoustic microscope that can directly measure both phase and amplitude, similar techniques have been developed for the scanning optical microscope. These make it possible to measure range to a thousandth of a wavelength. Other techniques involving scanning optical microscopy have been demonstrated which make it possible to carry out profiling of semiconductor circuits. Developments of these methods are now being actively pursued for use in the semiconductor industry. Developments of acoustic technology pioneered on this program have proved extremely important for measuring internal defects in composites and surface cracks on ceramics. GRA

N88-30139# Intespace, Toulouse (France).
QUALIFICATION TEST LEVELS FOR UNITS TO BE DERIVED FROM MECHANICAL TEST DATA ANALYSIS Final Report
A. Girard, H. Defosse, and M. Pawlowski Paris, France ESA 19 Oct. 1987 192 p
(Contract ESTEC-6892/86-NL-MA(SC))
(Rept-87-158-EI/ET/AG; ESA-CR(P)-2547; ETN-88-92770) Avail: NTIS HC A09/MF A01

An environment requirement specification for space equipment (unit level test verification) was derived from mechanical test data evaluation. Standard mechanical test specifications for space units to be launched on Ariane-4 or on the shuttle are needed to realize program cost savings. European specifications for sine and random testing at unit level based on a statistical analysis using test data obtained from sine, random, and acoustic testing at system level were improved and completed, using data from OLYMPUS and HIPPARCOS for more reliable statistics and better understanding of the results. Improved data processing was performed to give better results for sine levels near the satellite first resonant frequency and to derive specifications for random testing in the form of continuous functions of mass providing an extrapolation for heavy equipment items. The specifications are proposed to update the ESA standard. An extrapolation to Ariane-5 qualification levels was derived. ESA

N88-30140# Industrial Quality, Inc., Gaithersburg, Md.
DEVELOPMENT OF GRADED REFERENCE RADIOGRAPHS FOR ALUMINUM WELDS, PHASE 1 Final Report, 7 Jul. 1987 - 7 Mar. 1988
Daniel Polansky, Edward Criscuolo, Harold Berger, and Thomas S. Jones 7 Mar. 1988 33 p
(Contract DAAK70-87-C-0027)
(AD-A195594) Avail: NTIS HC A03/MF A01 CSCL 11F

The purpose of this Small Business Innovation Research Phase 1 project was to develop a data bank for graded sets of reference radiographs of aluminum welds. Reference radiographic documents of this type are extremely valuable for procurements related to ships, aircraft, other vehicles, construction and similar projects that include aluminum welds. The reference radiographs serve as a recognized way of acceptance or rejection of welds. There are no recognized standards for graded reference radiographs of aluminum welds. The only alternative at present is to use graded sets of reference radiographs for steel welds such as ASTM standard E-390. This is not a technically acceptable alternative because the radiographic contrasts and general appearance are different for steel welds as compared to aluminum welds. During this Phase 1 project, a data bank of production radiographs of aluminum welds was collected. Several thousand radiographs are presently in the data bank. From this data bank, a set of proposed reference radiographs has been assembled. These include five grades of reference radiographs for three types of porosity, fine scattered porosity, coarse scattered porosity and linear porosity. The suggested reference radiograph document also includes three grades of clustered porosity, two illustrations of inadequate penetration, two illustrations of tungsten inclusions, and examples of longitudinal and transverse cracks, lack of fusion and undercut. GRA

39 STRUCTURAL MECHANICS

Includes structural element design and weight analysis; fatigue; and thermal stress.

For applications see *05 Aircraft Design, Testing and Performance* and *18 Spacecraft Design, Testing and Performance.*

N88-30141# Queensland Univ., Brisbane (Australia). Dept. of Civil Engineering.
GEOMETRIC AND MATERIAL NONLINEAR ANALYSIS OF STRUCTURES COMPRISING RECTANGULAR HOLLOW SECTIONS
S. Kitipornchai, F. G. A. Al-Bermani, and S. L. Chan Jan. 1987 42 p
(CE-79) Avail: NTIS HC A03/MF A01

A nonlinear finite element analysis is presented of structures comprising thin walled rectangular hollow sections. Nonlinearities due to both the change of geometry and material yielding are included, incorporating also the effects of strain unloading. The geometry and the stiffness of the elements are modified and used to update the structure tangent stiffness matrix. An iterative procedure combining the arc length and the work methods is employed for the solution of the incremental equation of equilibrium. The method was applied successfully to predict the nonlinear load deflection behavior of isolated cold formed square hollow section (SHS) columns, fabricated rectangular hollow section parabolic fixed end arches, and double chord SHS trusses having different joint configurations. Author

N88-30142# California Univ., Berkeley. Dept. of Materials Science and Mineral Engineering.
MODELING OF MICROMECHANISMS OF FATIGUE AND FRACTURE IN HYBRID MATERIALS Annual Report No. 1, 15 Apr. 1987 - 14 Apr. 1988
R. O. Ritchie, W. Yu, and S. C. Siu May 1988 59 p
(Grant AF-AFOSR-0158-87)
(AD-A195604; UCB/R/88/A1053) Avail: NTIS HC A04/MF A01 CSCL 11D

The obvious benefits of the design of aerospace structures using lighter materials with high specific strengths and stiffness has led in recent years to the development of numerous reinforced composite materials, which have become serious commercial competitors to traditional monolithic metallic alloys. While significant advances in processing technology have made the fabrication of such hybrid materials more of an economic reality, their widespread use in airframes or other critical structures has in general been limited by serious deficiencies in particular mechanical properties, such as ductility, toughness and fatigue. This problem is often compounded by the lack of fundamental studies which provide a rational basis for the underlying sources of crack-propagation resistance in these materials, and in particular which define the critical role of composite microstructure. Accordingly, the current program is aimed at studying the physics and micromechanisms of fracture toughness and particularly the fatigue-crack growth resistance in laminate, discontinuously-reinforced and continuously-reinforced metal-matrix composites, with special reference to the role of microstructure. GRA

N88-30143# Grumman Aerospace Corp., Bethpage, N.Y.
AUTOMATED EARLY FATIGUE DAMAGE SENSING SYSTEM Final Report, 5 Dec. 1983 - 6 Sep. 1987
Alan Hencken and Michael Horn Mar. 1988 93 p
(Contract F33615-83-C-3225)
(AD-A195717; AFWAL-TR-88-3008) Avail: NTIS HC A05/MF A01 CSCL 11F

Structural fatigue testing plays a vital role in assuring the long term integrity of aerospace vehicles and components. However, substantial uncertainty involving large-scale complex structural tests does exist due to their inherent one shot nature. Crack propagation not revealed by a catastrophic failure during a single test can cause structural problems later in production aircraft. The overall objective of this program was to develop a reliable nondestructive testing system for the detection of initiating cracks generated during structural fatigue testing. The goals were to: (1) detect cracks as small as 0.050 in. in complex structures, and (2) develop a detection system that could be operated by technician-level personnel typically assigned to structural test areas. GRA

N88-30144# Naval Postgraduate School, Monterey, Calif.
ANALYTICAL AND EXPERIMENTAL STUDIES OF BEAM WAVEGUIDE ABSORBERS FOR STRUCTURAL DAMPING M.S. Thesis
Gi Gon Lee Mar. 1988 123 p
(AD-A195085) Avail: NTIS HC A06/MF A01 CSCL 13J

The reduction of structural vibrations in ships and submarines is a long standing concern of the Navy. Waveguide absorbers are very effective devices which can be applied to this problem. This study evaluates the increase in vibration damping of a plate structure across a broad frequency range using light weight beam waveguide absorbers. Viscoelastic and constrained layer beam waveguide absorbers were studied both theoretically and experimentally. Impedances of the waveguide absorbers at the attachment point were predicted using both Bernoulli-Euler and Timoshenko beam theory for the viscoelastic beam and using sixth order beam theory for the constrained layer beam. The theoretically predicted impedances were compared with the experimental measurements. Results from random vibration tests of a plate structure showed significant increases in damping over a broad frequency range (100 Hz to 2 KHz) when the waveguide absorbers were attached on the plate. GRA

N88-30145# Wisconsin Univ., Madison. Center for Mathematical Sciences.
INITIAL VALUE PROBLEMS IN VISCOELASTICITY Technical Summary Report
W. J. Hrusa, J. A. Nohel, and M. Renardy (Virginia Polytechnic Inst. and State Univ., Blacksburg.) Mar. 1988 30 p
(Contract DAAL03-87-K-0036; Grants AF-AFOSR-0307-85; AF-AFOSR-0191-87; NSF DMS-86-20303; NSF DMS-87-96241; NSF DMS-87-12058)
(AD-A196052; CMS-TSR-88-27) Avail: NTIS HC A03/MF A01 CSCL 20K

This document reviews some recent mathematical results concerning integrodifferential equations that model the motion of one-dimensional nonlinear viscoelastic materials. In particular, the authors discuss global (in time) existence and long-time behavior of classical solutions, as well as the formation of singularities in finite time from smooth initial data. Although the mathematical theory is comparatively incomplete, some remarks concern more the existence of weak solutions (i.e., solutions with shocks). Some relevant results from linear wave propagation are also discussed. GRA

N88-30146# Centre de Recherches Scientifiques et Techniques de l'Industrie des Fabrications Metalliques, Brussels (Belgium). Afdeling Ketelbouw.
STRESSES IN CYLINDRICAL SHELLS WITH TANGENTIAL NOZZLES SUBMITTED TO EXTERNAL LOADS AND INTERNAL PRESSURE
J. Decock Feb. 1988 55 p Sponsored by the Institut pour l'Encouragement de la Recherche Scientifique dans l'Industrie et l'Agriculture, Belgium
(CRIF-MT-172; ETN-88-92652) Avail: NTIS HC A04/MF A01

Elastic stress analyses under internal pressure and different external loads applied to a tangential nozzle are discussed. Not much data about tangential nozzles was available and consequently the design of such nozzles is not clear. The different behavior of tangential and radial nozzles is shown. For a restricted number of geometries, a method by which the highest local stresses can be obtained is presented. ESA

N88-30147# Army Armament Research and Development Command, Watervliet, N. Y.
WIDE RANGE STRESS INTENSITY FACTOR EXPRESSION FOR AN EDGE-CRACKED ROUND BAR BEND SPECIMEN Final Technical Report

J. H. Underwood and R. L. Woodward May 1988 20 p Presented at the ASTM Committee E-24 on Fracture, Sparks, Nev., 25-28 Apr. 1988
(AD-A196285; ARCCB-TR-88022) Avail: NTIS HC A03/MF A01 CSCL 20K

An edge-cracked round bar was analyzed for use as a fracture mechanics test specimen. Shallow and deep crack limit solutions were developed and combined with experimental and numerical results to obtain K expressions which apply for all crack depths. Specimen and loading geometries were suggested for standardized fracture mechanics tests using a round bar. GRA

N88-30148*# National Academy of Sciences - National Research Council, Washington, D. C. Science and Engineering Directorate.
FREE VIBRATION OF RECTANGULAR PLATES WITH A SMALL INITIAL CURVATURE Final Report
A. A. Adeniji-Fashola and A. A. Oyediran (Lagos State Univ., Ojo, Nigeria) Aug. 1988 53 p
(Contract NASw-3458)
(NASA-CR-179370; NAS 1.26:179370) Avail: NTIS HC A04/MF A01 CSCL 20K

The method of matched asymptotic expansions is used to solve the transverse free vibration of a slightly curved, thin rectangular plate. Analytical results for natural frequencies and mode shapes are presented in the limit when the dimensionless bending rigidity, epsilon, is small compared with in-plane forces. Results for different boundary conditions are obtained when the initial deflection is: (1) a polynomial in both directions, and (2) the product of a polynomial and a trigonometric function, and arbitrary. For the arbitrary initial deflection case, the Fourier series technique is used to define the initial deflection. The results obtained show that the natural frequencies of vibration of slightly curved plates are coincident with those of perfectly flat, prestressed rectangular plates. However, the eigenmodes are very different from those of initially flat prestressed rectangular plates. The total deflection is found to be the sum of the initial deflection, the deflection resulting from the solution of the flat plate problem, and the deflection resulting from the static problem. Author

N88-30149# Oak Ridge National Lab., Tenn. Engineering Technology Div.
DETERMINATION OF MULTIAXIAL FLOW SURFACES AT ELEVATED TEMPERATURES USING THE CONCEPT OF DISSIPATION POTENTIAL
J. A. Clinard and C. Lacombe (Tennessee Univ., Knoxville.) Apr. 1988 89 p
(Contract DE-AC05-84OR-21400)
(ORNL/TM-10787) Avail: NTIS HC A05/MF A01

Multiaxial flow surfaces were measured using tubular specimens of type 316 stainless steel. Tests were isothermal at 650 C. Flow surface determination was conducted after certain torsional preloadings and was composed of a series of 16 probes at 16 distinct axial/torsional stress rate ratios. These probes sufficiently characterized the flow surfaces in the stress subspace. Previous analytical efforts reduced the experimental data for determination of surfaces of constant inelastic strain rate. Current efforts remove assumptions concerning the inelastic strain state (for the multiaxial response) and reuse the experimental data to cast flow surfaces in the form of surfaces of constant dissipation potential (SCDP). Some 43 SCDP flow surface families are determined from the high temperature experimental data base. Details of the analytical techniques are provided. Resulting preliminary assessments are presented and discussed concerning various theoretical subjects such as normality of strain rate vectors and goodness-of-fit of candidate stress functions composed of second and third stress invariants. Author

N88-30150# Texas Instruments, Inc., Dallas. Semiconductor Group.
STRESS RELATED FAILURES CAUSING OPEN METALLIZATION Final Report, Jun. 1985 - Jul. 1987
Steven K. Groothuis Jan. 1988 66 p
(Contract F30602-85-C-0093)
(AD-A195061; RADC-TR-88-8) Avail: NTIS HC A04/MF A01 CSCL 11C

Non-linear Finite Element Analysis has been used to model stresses and infer stress induced void formation in narrow Al-Si metal lines. Observed failures correlate well with calculated stresses determined by varying intrinsic stress of the passivation, topography, line width and silicon nodule size. GRA

N88-30151*# Purdue Univ., West Lafayette, Ind. School of Mechanical Engineering.
VIBRATIONAL POWER FLOW ANALYSIS OF RODS AND BEAMS Thesis
James Christopher Wohlever and R. J. Bernhard Aug. 1988 179 p
(Grant NAG1-58)
(NASA-CR-183166; NAS 1.26:183166; Rept-0353-12; HL-88-24; PRF-520-1288-0353) Avail: NTIS HC A09/MF A01 CSCL 20K

A new method to model vibrational power flow and predict the resulting energy density levels in uniform rods and beams is investigated. This method models the flow of vibrational power in a manner analogous to the flow of thermal power in a heat conduction problem. The classical displacement solutions for harmonically excited, hysteretically damped rods and beams are used to derive expressions for the vibrational power flow and energy density in the rod and beam. Under certain conditions, the power flow in these two structural elements will be shown to be proportional to the energy density gradient. Using the relationship between power flow and energy density, an energy balance on differential control volumes in the rod and beam leads to a Poisson's equation which models the energy density distribution in the rod and beam. Coupling the energy density and power flow solutions for rods and beams is also discussed. It is shown that the resonant behavior of finite structures complicates the coupling of solutions, especially when the excitations are single frequency inputs. Two coupling formulations are discussed, the first based on the receptance method, and the second on the travelling wave approach used in Statistical Energy Analysis. The receptance method is the more computationally intensive but is capable of analyzing single frequency excitation cases. The traveling wave approach gives a good approximation of the frequency average of energy density and power flow in coupled systems, and thus, is an efficient technique for use with broadband frequency excitation. Author

N88-30152# Queensland Univ., St. Lucia (Australia). Dept. of Civil Engineering.
A PARAMETRIC STUDY OF EMBEDDED CANTILEVER RETAINING WALLS: THE RESULTS OF A FINITE ELEMENT STUDY
A. B. Fourie and D. M. Potts Aug. 1987 40 p
(RR-CE83; ISBN-0-86776-251-9) Avail: NTIS HC A03/MF A01

The design of cantilever retaining walls is based on approximate limit equilibrium calculations which assume a point of zero movement occurs at some depth near the toe of the wall. The results of a finite element study to check the validity of this technique are presented. The accuracy of the calculated embedment is checked, and the influence of parameters such as initial soil stress and construction procedure is evaluated. The analysis is restricted to fully drained, effective stress soil parameters in order to facilitate comparison with limit equilibrium results. An elasto-plastic constitutive law is used to model the soil behavior. The results indicate that the limit equilibrium method gives a very reasonable estimate of the embedment depth required to ensure stability. The maximum bending moment calculated using the limit equilibrium technique was found to be greater than the corresponding values from the finite element analyses, irrespective of the initial soil stresses. The results indicate that some reduction in bending moment as calculated by the limit equilibrium method may therefore be warranted. Author

N88-30153# Sener S.A., Las Arenas (Spain). Tecnica Industrial y Naval.
OBTAINING STRESS INTENSITY FACTORS ON CRACKS, BY MEANS OF FITTING TECHNIQUES ON NUMERICAL RESULTS CALCULATED WITH THE FINITE ELEMENT METHOD [OBTENCION DE FACTORES DE INTENSIDAD DE TENSION EN GRIETAS, MEDIANTE TECNICAS DE AJUSTE SOBRE RESULTADOS NUMERICOS CALCULADOS CON EL METODO DE LOS ELEMENTOS FINITOS]
Isidoro Miranda 1988 14 p In SPANISH Presented at the 13th Annual Meeting of the Spanish Nuclear Society, La Toja, Spain, 7-9 Oct. 1987
Avail: NTIS HC A03/MF A01

The use of isoparametric elements of distortion geometry permits the inclusion of singular stress analogs at the existence in the neighborhood of the crack edge depending on the fracture mechanics. The numerical information obtained by means of the finite element method (FEM) analysis can be utilized for calculation of fracture intensity stress by means of fitting by the least squares method in theoretical and numerical displacements. The calculation of K (sub I) by means of the indicated fitting makes an alternative front by the method based on the obtaining of G and J, notably more complex. With the advantage of that, the displayed methodology is evenly applicable to the cases of thermal loads. Author

N88-30154# Queensland Univ., Brisbane (Australia). Dept. of Civil Engineering.
IMPACT FORCE AS A PART OF THE TOTAL BREAKING WAVE FORCE ON A VERTICAL CYLINDER
C. J. Apelt and J. Piorewicz Jan. 1987 35 p
(RR-CE78) Avail: NTIS HC A03/MF A01

The total breaking wave force can be considered as the sum of the slowly varying wave force and the impact force that occurs when a pile is struck by the vertical or nearly vertical portion of the breaking wave. For the range of experimental data, H sub o/L sub o less than 0.05 and D/H sub o less than 2.5, the empirical relation between impact force and total force was obtained. The experiments indicate that up to 30 percent of the height of the wave crest should be considered as the impact region. Since the impact force has very short duration, its large magnitude is important in consideration of the fatigue life of the structure. Author

N88-30155# Ohio State Univ., Columbus.
FATIGUE CRACK PROPAGATION: PROBABILISTIC MODELING AND STATISTICAL ANALYSIS Final Report, 1 Jul. 1984 - 30 Jun. 1987
Saul Blumenthal and Prem Goel 23 Mar. 1988 9 p
(Grant AF-AFOSR-0162-84)
(AD-A195885; AFOSR-88-0653TR) Avail: NTIS HC A02/MF A01 CSCL 20K

This is the final report for a research grant to study probability models with application to fatigue crack propagation. Research problems considered included estimation with truncated data, burn-in reliability problems, and accelerated life testing. GRA

N88-30156# Army Lab. Command, Watertown, Mass. Material Technology Lab.
THE EFFECT OF NOTCH ROOT RADIUS ON THE DETERMINATION OF TOUGHNESS IN ULTRAHIGH STRENGTH STEEL FRICTION WELDS Final Report
William S. Ricci and Eric B. Kula Jun. 1988 11 p
(AD-A195952; MTL-TR-88-21) Avail: NTIS HC A02/MF A01 CSCL 11F

The plain strain fracture toughness and Charpy impact energy of friction welds in ultrahigh strength AISI 4340 steel were determined. Fracture toughness values for the weld zone were found to exceed those of the base metal. This is believed to be due to the larger prior austenite grain size in the weld zone resultant from the weld thermal cycle. Charpy impact energy data for the weld zone, however, were approximately 50 percent lower than those of the base metal. This was due to the adverse reorientation of sulfide inclusions in the weld zone resulting from the forging stage of the welding cycle. Discrepancies between fracture toughness and Charpy impact test data can be attributed to notch root radius effects. The use of both sharp notch and rounded notch toughness tests are recommended for the determination of weld joint ductility in ultrahigh strength steels. GRA

N88-30157# Aeronautical Research Inst. of Sweden, Stockholm. Structures Dept.
STANDARD FATIGUE SPECIMENS FOR FASTENER EVALUATION
Bjorn Palmberg and Lars Jarfall (Saab-Scania, Goteberg, Sweden) Oct. 1987 51 p
(Contract FMV-FFL-82250-85-076-73-001)
(FFA-TN-1987-68; ETN-88-93062) Avail: NTIS HC A04/MF A01

Spectrum fatigue testing was carried out using single shear joints with U-channel splice plates and four different fastener systems. Single column, double row joints were used. The joints frequently developed splice plate failures making the completion of the testing program not worthwhile. Studies of secondary bending, amount of load transfer and fastener flexibility were performed successfully. The base plate material in the joints was 5 mm thick aluminum alloy 7050-T73651. The four different fastener systems included Hi-lok and Hi-tigue fasteners mounted in plain holes, interference fit holes, and cold worked holes. Bending ratio depends slightly on the fastener system used and having a magnitude in the range 0.27 to 0.41. Midpoint supporting increases secondary bending. Load transfer is 49 percent for the single specimen tested with an adequate strain gaging. A large difference in fastener flexibility between Hi-lok and Hi-tigue fasteners is observed. Flexibility ranges from 5.9 to 19.5 mm/MN. ESA

N88-30158# Air Force Inst. of Tech., Wright-Patterson AFB, Ohio. School of Engineering.
LARGE DISPLACEMENT AND ROTATIONAL FORMULATION FOR LAMINATED CYLINDRICAL SHELLS INCLUDING PARABOLIC TRANSVERSE SHEAR Ph.D. Thesis
Scott T. Dennis May 1988 374 p
(AD-A194871; AFIT/DS/AA/88-1) Avail: NTIS HC A16/MF A01 CSCL 11D

A 2-D geometrically nonlinear shell theory applicable to arbitrary geometries that can be described by orthogonal curvilinear coordinates and encompassing large displacements and rotations for small strain situations has been developed. Additionally, the theory includes a parabolic transverse shear stress distribution through the thickness. Flat plate and cylindrical shell solutions do not shear lock based upon exact elemental integrations. Transverse shear deformation was found to be significant for linear thick pinched cylinders and clamped pressure vessels. Orthotropic pressure vessels where the longitudinal stiffness is greater than the circumferential experience much more transverse shear deformation than do those where the circumferential stiffness is greater than the longitudinal. Middle surface inextensibility is often assumed in the closed form solutions used for comparison with the present approach. The consequences of this assumption is examined for both linear and nonlinear problems. The present formulation is applied to axially compressed quasi-isotropic cylindrical panels. GRA

N88-30159# Ballistic Research Labs., Aberdeen Proving Ground, Md.
NONLINEAR STRESS-STRAIN AND INELASTIC REBOUND WITH EXPONENTIAL STIFFNESS
James T. Dehn Jul. 1988 54 p
(AD-A195667; BRL-TR-2925) Avail: NTIS HC A04/MF A01 CSCL 20K

Bilinear or power-law presentations are often used to describe the application and release of tension or compression. Here a new nonlinear equation of motion with exact solutions is developed which can describe not only a tension or compression half-cycle, but the entire hysteretic loop. Solutions of the same equation can be used to describe impact phenomena which are important in a

number of areas from package cushioning to stopping a fragment or bullet. Oscillatory solutions can also be applied to a variety of mechanical and electrical phenomena. Specific examples are given to some two-segment limit cycles which are special cases of more general solutions. Methods of generalizing the approach used to many other cases are also indicated. GRA

N88-30160*# National Aeronautics and Space Administration. Langley Research Center, Hampton, Va.
ULTRASONIC METHOD AND APPARATUS FOR DETERMINING CRACK OPENING LOAD Patent Application
William T. Yost, inventor (to NASA) 23 Jun. 1988 15 p
(NASA-Case-LAR-13889-1; NAS 1.71:LAR-13889-1; US-Patent-Appl-SN-210277) Avail: NTIS HC A03/MF A01 CSCL 20K

This invention relates generally to materials testing, and more particularly, to an ultrasonic apparatus for determining crack opening load in a specimen having a crack. A specimen having a crack is provided with a transmit transducer and a receive transmitter. An ultrasonic signal passing between the two transducers is mechanically rectified by the crack to produce a second harmonic of the input signal. By measuring the peak harmonic amplitude while increasing the tension load on the specimen, a crack opening is determined. NASA

N88-30161# Aeronautical Research Labs., Melbourne (Australia).
REPORT ON AN OVERSEAS VISIT TO USA RELATING TO THE THERMOELASTIC MEASUREMENT OF STRESSES, 16-21 AUGUST 1987
A. K. Wong Feb. 1988 15 p
(AD-A195313; ARL/STRUC-TM-481; DODA-AR-004-590) Avail: NTIS HC A03/MF A01 CSCL 20K

This report describes a short overseas visit made by the author to the United States in 1987. The purpose of the visit was to attend the 31st Annual International Technical Symposium on Optical and Optoelectronic Applied Science and Engineering, and to present an invited paper. GRA

N88-30162# Defence Research Establishment Atlantic, Dartmouth (Nova Scotia).
RESPONSE OF SMA (SHIELDED METAL ARC) AND NARROW GAP HY80 WELDMENTS TO EXPLOSIVE SHOCK LOADING
J. F. Porter, D. O. Morehouse, and J. R. Matthews Mar. 1988 39 p
(AD-A195994; DREA-TM-88/206) Avail: NTIS HC A03/MF A01 CSCL 11F

The performance of high yield strength steel plate and weldments, subjected to high levels of dynamic plastic deformation from explosive shock, is an important aspect in the study of materials used in submarine pressure hull construction. This report describes the development of an explosive shock test procedure and its application to study the behavior of HY80 plate, several shielded metal arc weldments of HY80, and several metal inert gas narrow gap HY80 weldments. An integral part of the submarine materials technology program at Defense Research Establishment Atlantic's Dockyard Laboratory (DREA/DL) is the evaluation of submarine pressure hull weldment response to explosive shock. The ability of the weldment structure to withstand significant plastic deformation prior to the formation and propagation of a crack is an important requirement for modern submarine steels and weldments. GRA

N88-30163# Air Force Inst. of Tech., Wright-Patterson AFB, Ohio. School of Engineering.
AN INVESTIGATION OF CONSTITUTIVE MODELS FOR PREDICTING VISCOPLASTIC RESPONSE DURING CYCLIC LOADING M.S. Thesis
David A. Shaffer Jun. 1988 95 p
(AD-A194875; AFIT/GAE/AA/87D-21) Avail: NTIS HC A05/MF A01 CSCL 20K

The Air Force's Engine Structural Integrity Program (ENSIP) (Ref 1) requires determination of damage tolerance for jet engine components in order to allow more economical rejection criteria to be adopted. To this end, means have been developed for predicting fatigue crack growth in jet engine components such as turbine disks made of nickel-based superalloys and operating at elevated temperatures. The presence of time-dependent plastic deformation greatly affects crack propagation rates, particularly at elevated temperatures and thus must be accounted for when modelling crack growth in turbine materials. The purpose of this thesis was to investigate the frequency response aspects of the Bodner-Partom constitutive law's behavior and to compare its results with those of other models and to cyclic and non-cyclic uniaxial tensile test data. GRA

N88-30164*# Akron Univ., Ohio. Dept. of Civil Engineering.
AN EXPERIMENTAL STUDY OF BIAXIAL YIELD IN MODIFIED 9Cr-1Mo STEEL AT ROOM TEMPERATURE Final Report
J. R. Ellis Nov. 1985 16 p Presented at the 8th International Conference on Structural Mechanics in Reactor Technology, Brussels, Belgium, 19-23 Aug. 1985 Sponsored in cooperation with DOE and Union Carbide Corp.
(Grant NAG3-379)
(NASA-CR-175012; E-2776; NAS 1.26:175012) Avail: NTIS HC A03/MF A01 CSCL 20K

Described are two biaxial experiments which investigated yield, hardening, and flow behavior in modified 9Cr-1Mo steel at room temperature. The aim of these experiments was to determine whether the procedures recommended in NE Standard F9-5T for inelastic design analysis are applicable for this material in normalized and tempered condition. The first experiment investigated small offset yield behavior subsequent to radial preloads (sq rt of 3 sub sigma 12 = sub sigma 11) in tension-torsion stress space. The second experiment investigated yield behavior subsequent to nonradial preloads and also the time-dependent flow occurring during 0.5 hour periods at constant stress. The results of these experiments were qualitatively similar to those obtained earlier for types 304 and 316 stainless steel. Specifically, the von Mises yield criterion was found to provide a reasonable approximation of initial yield behavior. Although the subsequent yield surfaces suffered considerable distortion from their near-circular form after both radial and nonradial preloads, the hardening behavior was to the first order kinematic in nature. The strain-time data obtained during the 0.5 hr hold periods showed characteristics typical of creep curves. As in the case of earlier experiments, the high initial flow rates diminished more rapidly than would be estimated from elevated temperature data.
Author

42 GEOSCIENCES (GENERAL)

No abstracts in this category.

43 EARTH RESOURCES AND REMOTE SENSING

Includes remote sensing of earth resources by aircraft and spacecraft; photogrammetry; and aerial photography.
For instrumentation see *35 Instrumentation and Photography.*

N88-30165# Instituto de Pesquisas Espaciais, Sao Jose dos Campos (Brazil).
TM/LANDSAT-5 DATA TO EVALUATE WHEAT AND BEAN PERCENT SOIL COVER AND LEAF AREA INDEX
Jose Carlos NevesEpiphanio and Antonio Roberto Formaggio Jun. 1988 11 p Presented at the 16th Congress of International

Society for Photogrammetry and Remote Sensing, Kyoto, Japan, 1-10 Jul. 1988 Submitted for publication
(INPE-4609-PRE/1332) Avail: NTIS HC A03/MF A01

The correlations are described between two crop parameters (green leaf area index and percent soil cover) and eighteen TM/LANDSAT-5 parameters (six bands and twelve band ratios). The TM/LANDSAT-5 data used were the digital numbers extracted from CCT's and corrected for minimizing atmospheric effects. It was used for three overpasses during wheat and bean vegetative cycles. The percent soil cover was estimated using 35 mm photographs taken perpendicular to the ground. The results showed that the correlation between remote sensing data and crop parameters is dependent on the level of expression of the crop parameters (crop stages). When the crop vegetative parameters are at their maximum expression there are poor correlations with remote sensing data. So, the more significant values of correlations were obtained in the pre-flowering stage. The most useful TM bands were TM4 and TM3, but their usefulness varied in function of the date of overpass, the crop family, and the crop parameter. Ratios were useful in cases where the single bands showed poor correlations, but no single ratio could be identified with good correlations in all situations. Finally, it was concluded that the knowledge of general development condition of crops is necessary in the selection of the most appropriate remote sensing parameter for correlation to the crop parameters considered in this study. Author

N88-30166# Army Engineer Topographic Labs., Fort Belvoir, Va.
INTEGRATING MULTISPECTRAL IMAGERY AND GROUND LEVEL HYPERSPECTRAL SIGNATURE DATA
Melvin B. Satterwhite 8 Apr. 1988 48 p
(AD-A195976; ETL-R-145) Avail: NTIS HC A03/MF A01
CSCL 17E

Present day state-of-the-art digital image processing hardware and software can provide the image analyst the opportunity to use multispectral imagery (MSI) and, in the future, hyper-spectral imagery (HSI) for evaluating and monitoring terrain and target features. However, the lack of training in the spectral signatures of terrain features can inhibit the analyst's interpretation of the multispectral false color composite image, prevent him from selecting the proper bands to achieve highest discrimination between the background and the target, and be a hinderance when he orders or displays a false color composite image. Training our analysts in the spectral signatures of terrain features should result in better exploitation of the pretty pictures. This training is equally as important as learning the operation of the digital image processing equipment. Without it the analyst uses the MSI/HSI image as a mpa or as a photograph. He seldom or rarely uses the multispectral information within the image as part of his image analysis. GRA

N88-30167*# European Centre for Medium-Range Weather Forecasts, Reading (England).
A STUDY OF THE FEASIBILITY OF USING SEA AND WIND INFORMATION FROM THE ERS-1 SATELLITE. PART 1: WIND SCATTEROMETER DATA
D. Anderson, A. Hollingsworth, S. Uppala, and P. Woiceshyn (Jet Propulsion Lab., California Inst. of Tech., Pasadena.) Paris, France ESA Jun. 1987 127 p
(Contract ESRIN-6297/86-HGE-I(SC))
(NASA-CR-182833; NAS 1.26:182833; ESA-CR(P)-2604-Pt-1; ETN-88-93033) Copyright Avail: NTIS HC A07/MF A01
CSCL 04A

The use of scatterometer and altimeter data in wind and wave assimilation, and the benefits this offers for quality assurance and validation of ERS-1 data were examined. Real time use of ERS-1 data was simulated through assimilation of Seasat scatterometer data. The potential for quality assurance and validation is demonstrated by documenting a series of substantial problems with the scatterometer data, which are known but took years to establish, or are new. A data impact study, and an analysis of the performance of ambiguity removal algorithms on real and simulated data were conducted. The impact of the data on analyses and forecasts is large in the Southern Hemisphere, generally small in the Northern Hemisphere, and occasionally large in the Tropics. Tests with simulated data give more optimistic results than tests with real data. Errors in ambiguity removal results occur in clusters. The probabilities which can be calculated for the ambiguous wind directions on ERS-1 contain more information than is given by a simple ranking of the directions. ESA

N88-30168# Instituto de Pesquisas Espaciais, Sao Jose dos Campos (Brazil).
EVALUATION OF LANDSAT-TM DATA FOR GEOMORPHOLOGICAL MAPPING
Teresa GallottiFlorenzano and Hermann Johann Heinr Kux Jun. 1988 9 p Presented at the 16th Congress of International Society for Photogrammetry and Remote Sensing, Kyoto, Japan, 1-10 Jul. 1988 Submitted for publication
(INPE-4593-PRE/1324) Avail: NTIS HC A02/MF A01

The objective of this study is to evaluate LANDSAT/TM data to perform geomorphological mapping in a semiarid environment. The tests site is located at the Rio Parnaiba Valley (Piaui and Maranhao states), NE, Brazil. Data sets of TM (bands 3, 4, 5, and 7) were digitally analyzed using the following algorithms: linear contrast stretch, principal components and IHS transformations. Different color composites were obtained. Finally a discussion is made on the usefulness of digital processing techniques using TM data to discriminate geomorphological units. Author

N88-30169# Societe Nationale Industrielle Aerospatiale, Cannes (France).
IMAGING INSTRUMENT OF THE VEGETATION PAYLOAD (SPOT 4)
R. Krawczyk and G. Cerutti-Maori 25 Mar. 1988 8 p
(SNIAS-881-440-107; ETN-88-92876) Avail: NTIS HC A02/MF A01

A SPOT 4 payload for an operational world-scale survey of the evolution of vegetation (forecasting of agricultural yields and environmental studies), and observation of oceanic areas is described. Field of view is + or - 50.5 deg (2000 km on ground), with observation frequency of less than 2 days at equator. The system, equipped with its own telemetry channels and on-board computers, sends coded data according 2 types of observation : world wide observation recording, then time-tagged transmission, with a nadir resolution of 1.165 km x 1.165 km or 4.66 km x 4.66 km (agglomeration of 16 pixels); and regional observation real-time transmission, with a nadir resolution of 1.165 km. It has a pushbroom CCD focal plane array with an imager consisting of five lenses (one for each band). ESA

N88-30170# Instituto de Pesquisas Espaciais, Sao Jose dos Campos (Brazil).
THE USE OF ORBITAL REMOTE SENSING DATA FOR LOW COST GROUND-WATER SURVEY
Tomoyuki Ohara, Roberto PereiradaCunha, and Marx PrestesBarbosa Jun. 1988 8 p Presented at the 16th Congress of International Society for Photogrammetry and Remote Sensing, Kyoto, Japan, 1-10 Jul. 1988
(INPE-4587-PRE/1318) Avail: NTIS HC A02/MF A01

A remote sensing survey of alluvial areas in the state of Pernambuco (Brazil) for water resource purposes is presented. Photointerpretation maps of alluvial occurrences (scale 1:100,000), show information obtained from LANDSAT/TM photographic images, including: identification of alluvial areas as a contribution to underground water research. Additional information includes: updating of road systems, agricultural activities, nucleus and/or rural properties, and maps containing the localization of existing water wells. Based on the information acquired through orbital remote sensing, the government may establish, in short time, emergency plans for water supply needs of the local population. Author

N88-30171# Alcatel Thomson Espace, Toulouse (France).
MICROWAVE REMOTE SENSING IN THE FRENCH INDUSTRIES
Norbert Lannelongue 1987 10 p Presented at the French Aeronautical and Space Exhibition and Conference, Washington D.C., 20-23 Jan. 1987
(ETN-88-93081) Avail: NTIS HC A02/MF A01
French participation in the ERS-1, TOPEX/POSEIDON, VARAN-S, and passive radiometry projects is sketched. ESA

N88-30172# Instituto de Pesquisas Espaciais, Sao Jose dos Campos (Brazil).
REFLECTANCE PATTERN AND THE PHYSICAL AND CHEMICAL CHARACTERISTICS OF THREE BRAZILIAN OXISOLS
Antonio Roberto Formaggio and Jose Carlos NevesEpiphanio Jun. 1988 11 p Presented at the 16th Congress of International Society for Photogrammetry and Remote Sensing, Kyoto, Japan, 1-10 Jul. 1988 Submitted for publication
(INPE-4590-PRE/1320) Avail: NTIS HC A03/MF A01
Spectral data were obtained in three data collection levels: laboratory (400 to 1100 nm), field (400 to 1050 nm), and satellite (MSS and TM/LANDSAT) in two areas with different parent materials. The soil physical and chemical parameters were highly correlated with the spectral reflectance pattern of the three studied Oxisols. The results showed the importance of parent material and texture as influencing parameters of the soils spectral pattern. Also, for the soild originated from eruptive basic rocks, clear indications were found that the inferences of soil properties relaged with iron oxides are possible due to the strong absorption that occurs in the spectra of these soils. Author

N88-30173# Instituto de Pesquisas Espaciais, Sao Jose dos Campos (Brazil).
USE OF DIGITAL IMAGES AS A MINERAL PROSPECTING TOOL IN THE TIN PROVINCE OF GOIAS, BRAZIL
Raimundo AlmeidaFilho May 1988 12 p Presented at the 16th Congress for Photogrammetry and Remote Sensing, Kyoto, Japan, 1-10 Jul. 1988 Submitted for publication
(INPE-4537-PRE/1284) Avail: NTIS HC A03/MF A01
The application of LANDSAT-TM images is discussed as an auxiliary tool for mineral prospecting in the tin province of Goias, Central Brazil. Six granitoid massifs were studied through multispectral/multiseasonal analysis of digitally enhanced images. The presence of locally specific geobotanical association has permitted the discrimination of albitized/greisenized facies of these granitoids. These metasomatically altered facies are important as lithological control of significant tin (cassiterite) mineralization in the region. Field check has indicated the occurrence of cassiterite in most of the target areas identified by the study. This fact has allowed production of accurate maps which show potential mineralized areas for each granitoid. Prospection for primary tin deposits in the region should be directed to specific target areas, which represent less than 5 percent of the total surface of the granitoids, resulting in substantial savings in time and cost.
Author

N88-30174# Instituto de Pesquisas Espaciais, Sao Jose dos Campos (Brazil).
STUDY OF THE SPECTRAL RESPONSE OF SOYBEANS
Getulio TeixeiraBatista and Bernardo Rudorff, F. T. Jun. 1988 11 p Presented at the 16th Congress of International Society for Photogrammetry and Remote Sensing, Kyoto, Japan, 1-10 Jul. 1988 Submitted for publication
(INPE-4592-PRE/1322) Avail: NTIS HC A03/MF A01
The spectral responses of two soybean varieties planted monthly (in a period of three months) and their relationship to percent ground cover, biomass, and yield were investigated. The bidirectional reflectance factor was measured throughout the growing period (five campaigns at approximately 20-day intervals) of six experimental plots of 5 x 10 m size (three plots of each variety planted at one month intervals) using a 17 band (visible and NIR) portable radiometer. In each campaign, six measurements per plot were taken in order to obtain a representative estimate of the plot reflectance factor. Plant height and development stage were estimated concomitant to the radiometric measurements; biomass estimates were samples three times per plot during specific development stages (flowering, grain filling, and maturation), and total plot production was measured at-harvest. The percent ground cover was estimated through photographs taken simultaneously with the radiometric measurements. Results indicated that differences in reflectance between the two varieties correspond to differences in their biomass. However, in the visible peak at 550 nm, there is a slight difference between the two varieties. Preliminary analysis of spectral trajectory plots and vegetation indices indicated that the reflectance measures are related to the studied agronomic variables. Author

N88-30175# Army Engineer Topographic Labs., Fort Belvoir, Va.
DATATRAN: DATUM TRANSFORMATION SOFTWARE
Anthony R. Niles 14 Jan. 1988 10 p
(AD-A195723; ETL-R-143) Avail: NTIS HC A02/MF A01
CSCL 08E
The North American Datum of 1927 (NAD27) has become unsuitable for present-day surveys. Satellite surveys and accuracy requirements of conventional surveys have dictated the need for a more accurate earth-centered datum. Thus, the North American Datum of 1983 (NAD83) is replacing the NAD27. In anticipation of this transition, The National Geodetic Survey developed a computer program to convert survey data from NAD27 to NAD83, or vice-versa. This program, called LEFTI, converts geodetic positions (latitude/longitude) using a least squares adjustment. Since Corps of Engineers' Districts often use state plane coordinates, two other programs were developed to convert between geodetic positions and state plane coordinates on either datum. Thus, if a user desired to convert between NAD27 and NAD83 using state plane coordinates, two or more program runs were required. The output from one program was used as the input to the next program. In order to simplify this process, USAETL combined all three programs into one software package, called DATATRAN. This report concentrates on the program capabilities and procedures for use with only brief and general mention of conversion technique. GRA

N88-30176# European Centre for Medium-Range Weather Forecasts, Reading (England).
A STUDY OF THE FEASIBILITY OF USING SEA AND WIND INFORMATION FROM THE ERS-1 SATELLITE. PART 2: USE OF SCATTEROMETER AND ALTIMETER DATA IN WAVE MODELING AND ASSIMILATION
Peter A. E. M. Janssen, Piero Lionello (Consiglio Nazionale delle Ricerche, Venice, Italy), Magnar Reistad, and Anthony Hollingsworth Paris, France ESA Jun. 1987 113 p
(Contract ESRIN-6297/86-HGE-I(SC))
(ESA-CR(P)-2604-Pt-2; ETN-88-93034) Copyright Avail: NTIS HC A06/MF A01
A third generation wave-model and a global wave assimilation system were used to study the sensitivity of waves to scatterometer winds, and to simulate real time use of ERS-1 altimeter data through assimilation of Seasat altimeter data. The assimilation of altimeter wave data demonstrates the potential of a coupled real-time wind/wave assimilation for quality assurance and validation of scatterometer and altimeter data. The two-dimensional wave spectrum from a third-generation wave model can be used in interpretation and validation of the synthetic aperture radar image spectrum. ESA

N88-30177# Instituto de Pesquisas Espaciais, Sao Jose dos Campos (Brazil).
LANDSAT-TM DATA TO MAP FLOODED AREAS
Sergio dosAnjosFerreiraPinto and Teresa GallottiFlorenzano Jun. 1988 9 p Presented at the 16th Congress of International Society for Photogrammetry and Remote Sensing, Kyoto, Japan, 1-10 Jul. 1988 Submitted for publication
(INPE-4594-PRE/1324) Avail: NTIS HC A02/MF A01

The objective of this study is to identify flooded areas using digital LANDSAT-TM data. The test site is a section along the Parnaiba river (NE of Brazil). By means of a digital processing, the spectral separability of the classes, which are characterized by the presence of water surface with different intensities of a pixel in the near infrared band, are analyzed. A density slicing algorithm is applied for this purpose. The multitemporal analysis of the data is accomplished through the merging of the band 4 images corresponding to normal and flood periods. After this procedure, a maximum likelihood algorithm is applied in both images. The Density Slicing is also applied in multitemporal difference of the image (band 4 normal minus band 4 flood). A comparative analysis of the digital processing techniques using TM data to study flooded areas is presented. Author

N88-30178# Instituto de Pesquisas Espaciais, Sao Jose dos Campos (Brazil).
MICROWAVE REMOTE SENSING AT INPE (INSTITUTE FOR SPACE RESEARCH) BRAZIL: CONCEPTS AND FUTURE PROSPECTS OF SOIL MOISTURE STUDIES
Hermann J. H. Kux and Joao VianeiSoares May 1988 6 p Presented at the International Geoscience and Remote Sensing Symposium, Edinburgh, Scotland, 12-16 Sep. 1988
(INPE-4569-PRE/1310) Avail: NTIS HC A02/MF A01

The experiences obtained by INPE at microwave remote sensing, applied specifically to soil moisture studies, presenting the main concepts and prospects for future research, are described. In the approach proposed, information derived from ground truth, airborne and orbital data, as well as meteorological data, are important inputs. Author

N88-30179# Instituto de Pesquisas Espaciais, Sao Jose dos Campos (Brazil).
RELIEF EFFECT CORRECTION ON LANDSAT IMAGERY FOR FOREST APPLICATIONS USING DIGITAL TERRAIN MODELS
Luiz Alberto VieiraDias, Eni AlvimdeOliveira, and Flavio Jorge Ponzoni Jun. 1988 12 p Presented at the 16th Congress of International Society of Photogrammetry and Remote Sensing, Kyoto, Japan, 1-10 Jul. 1988
(INPE-4611-PRE/1334) Avail: NTIS HC A03/MF A01

Many times forests are planted on mountainous terrain. In this case the remotely sensed radiation at the LANDSAT sensor is highly dependent on the terrain slope, rendering difficult an accurate classification of the multispectral data. With a slope map derived from a digital terrain model (DTM), and information about the position of the sun, and the satellite sensor, it is possible to correct the image for the relief effect, by means of an illumination model. This work studies quantitatively the effect of this correction on the image classification, for an Eucalyptus ssp. forest near Jambeiro, SP, Brazil. Author

N88-30180# Instituto de Pesquisas Espaciais, Sao Jose dos Campos (Brazil).
LANDSAT TM AND AGROMETEOROLOGICAL DATA FOR WHEAT YIELD ESTIMATION AT THE FARM LEVEL
Bernardo F. T. Rudorff and Getulio TeixeiraBatista Jun. 1988 12 p Presented at the 16th Congress of International Society for Photogrammetry and Remote Sensing, Kyoto, Japan, 1-10 Jul. 1988 Submitted for publication
(INPE-4591-PRE/1321) Avail: NTIS HC A03/MF A01

Wheat plays an important role in the Brazilian commodity production. Therefore, objective and reliable methods for yield estimation are needed specially at the farm level where several management actions have to be taken. The LANDSAT TM and agrometeorological data were integrated in order to obtain a model for wheat yield estimation at the farm level for a test site in the south of Sao Paulo State. The LANDSAT data for the crop years of 1986 (three acquisitions) and 1987 (two acquisitions), agronomic and meteorological data were related to yield estimates at the field level (approximately 200 fields). Results have shown that vegetative index derived from LANDSAT TM explained 60 and 40 percent of wheat yield variability for the crop years analyzed. The joint use of both vegetative index and agrometeorological data in a single model improved significantly the results as compared to either vegetation index or agrometeorological data separately. The proposed model is to be validated for future crop seasons nevertheless it provided objective and accurate results for wheat estimation on the two crop seasons analyzed. Author

N88-30029# International Scientific Radio Union, Brussels (Belgium).
WAVE PROPAGATION AND REMOTE SENSING
R. K. Crane, comp. *In its* Review of Radio Science, 1984-1986 1987 12 p (For primary document see N88-30023 24-32)
Avail: NTIS HC A09/MF A01

N88-30524# Joint Publications Research Service, Arlington, Va.
DETERMINING NEAR-WATER WIND SPEED USING RADAR DATA FROM COSMOS-1500 ARTIFICIAL EARTH SATELLITE Abstract Only
G. V. Volpyan and Yu. G. Spiridonov *In its* JPRS Report: Science and Technology. USSR: Space 26 Feb. 1988 p 22 Transl. into ENGLISH from Issledovaniye Zemli iz Kosmosa (Moscow, USSR), no. 3, May - Jun. 1987 p 3-11 (For primary document see N88-30498 24-88)
Avail: NTIS HC A04/MF A01

N88-30527# Joint Publications Research Service, Arlington, Va.
ANALYTICAL METHOD FOR APPROXIMATE GEODETIC REFERENCING OF SCANNER IMAGES OF METEOROLOGICAL ARTIFICIAL EARTH SATELLITES USING CONTROL POINTS Abstract Only
M. V. Ivanchik and V. A. Krovotyntsev *In its* JPRS Report: Science and Technology. USSR: Space 26 Feb. 1988 p 23 Transl. into ENGLISH from Issledovaniye Zemli iz Kosmosa (Moscow, USSR), no. 3, May - Jun. 1987 p 109-115 Original language document was announced in IAA as A88-10923 (For primary document see N88-30498 24-88)
Avail: NTIS HC A04/MF A01

N88-30530# Joint Publications Research Service, Arlington, Va.
STRUCTURE OF EASTERN TURKESTAN RIDGE BASED ON SPACE PHOTOGRAPHS Abstract Only
I. G. Tsukornik, A. V. Alekseyenko, A. V. Berezanskiy, and I. I. Soloshenko *In its* JPRS Report: Science and Technology. USSR: Space 26 Feb. 1988 p 24 Transl. into ENGLISH from Issledovaniye Zemli iz Kosmosa (Moscow, USSR), no. 4, Jul. - Aug. 1987 p 47-52 Original language document was announced in IAA as A88-19566 (For primary document see N88-30498 24-88)
Avail: NTIS HC A04/MF A01

N88-30531# Joint Publications Research Service, Arlington, Va.
DETERMINING THE SPATIAL STRUCTURE OF FIELDS OF PRECIPITATION FROM SPACE RADAR IMAGES IN TWO ORTHOGONAL POLARIZATIONS Abstract Only
A. P. Pichugin, Yu. G. Spridonov, and A. B. Fetisov *In its* JPRS Report: Science and Technology. USSR: Space 26 Feb. 1988 p 24 Transl. into ENGLISH from Issledovaniye Zemli iz Kosmosa (Moscow, USSR), no. 4, Jul. - Aug. 1987 p 70-77 (For primary document see N88-30498 24-88)
Avail: NTIS HC A04/MF A01

N88-30532# Joint Publications Research Service, Arlington, Va.
ESTIMATION OF SOIL TEMPERATURE PROFILE FROM REMOTE MICROWAVE AND IR MEASUREMENTS Abstract Only
Ye. A. Reutov and A. M. Shutko *In its* JPRS Report: Science and Technology. USSR: Space 26 Feb. 1988 p 24 Transl. into ENGLISH from Issledovaniye Zemli iz Kosmosa (Moscow, USSR), no. 4, Jul. - Aug. 1987 p 78-85 (For primary document see N88-30498 24-88)
Avail: NTIS HC A04/MF A01

N88-30533# Joint Publications Research Service, Arlington, Va.
MONTE-CARLO ESTIMATION OF THE INFLUENCE OF PLANT ARCHITECTURE PARAMETERS ON SPECTRAL BRIGHTNESS Abstract Only
Yu. K. Ross and A. L. Marshak *In its* JPRS Report: Science and Technology. USSR: Space 26 Feb. 1988 p 24-25 Transl. into ENGLISH from Issledovaniye Zemli iz Kosmosa (Moscow, USSR), no. 4, Jul. - Aug. 1987 p 86-93 (For primary document see N88-30498 24-88)
Avail: NTIS HC A04/MF A01

44 ENERGY PRODUCTION AND CONVERSION

Includes specific energy conversion systems, e.g., fuel cells; global sources of energy; geophysical conversion; and windpower.

For related information see also *07 Aircraft Propulsion and Power, 20 Spacecraft Propulsion and Power,* and *28 Propellants and Fuels.*

N88-30181*# Lockheed Missiles and Space Co., Sunnyvale, Calif.
ADVANCED PLANAR ARRAY DEVELOPMENT FOR SPACE STATION Final Report, 1 Jun. 1985 - 1 Jun. 1987
Jun. 1987 101 p
(Contract NAS8-36419)
(NASA-CR-179373; NAS 1.26:179373; LMSC-F115808) Avail: NTIS HC A05/MF A01 CSCL 10B

The results of the Advanced Planar Array Development for the Space Station contract are presented. The original objectives of the contract were: (1) to develop a process for manufacturing superstrate assemblies, (2) to demonstrate superstrate technology through fabrication and test, (3) to develop and analyze a preliminary solar array wing design, and (4) to fabricate a wing segment based on wing design. The primary tasks completed were designing test modules, fabricating, and testing them. LMSC performed three tasks which included thermal cycle testing for 2000 thermal cycles, thermal balance testing at the Boeing Environmental Test Lab in Kent, Washington, and acceptance testing a 15 ft x 50 in panel segment for 100 thermal cycles. The superstrate modules performed well during both thermal cycle testing and thermal balance testing. The successful completion of these tests demonstrate the technical feasibility of a solar array power system utilizing superstrate technology. This final report describes the major elements of this contract including the manufacturing process used to fabricate modules, the tests performed, and the results and conclusions of the tests. Author

N88-30182# AEG-Telefunken, Wedel (West Germany). Space and New Technologies Subdivision.
ALTERNATIVE MODULE CONFIGURATIONS FOR ADVANCED SOLAR ARRAYS ON LOW ORBIT AND EXTENDED LIFETIME MISSIONS (AMOC 2) Final Report
D. Gringel, U. Hoffmann, J. Koch, F. Reissmann, and W. Schmitz Paris, France ESA 15 Dec. 1987 116 p
(Contract ESTEC-5508/83-NL-PB(SC))
(ESA-CR(P)-2581; ETN-88-93026) Avail: NTIS HC A06/MF A01

The applicability of the bifacial solar cell for generators operating in the low earth orbit and having extended life time mission was studied. Two candidate module concepts for flexible roll out and/or fold out solar generator systems were defined. One module concept is characterized by a continuous light transparent substrate and uses a transparent adhesive to glue the solar cells onto the substrate. The other module concept uses a nontransparent substrate with cutouts (windows) in the solar cell area of the substrate so that only small rearside areas of the individual solar cells are covered. The design and the bifacial solar cell technology were improved with regard to their applicability for larger assemblies. A thermal vacuum cycling test on a foldable ATOX resistant window type solar panel assembly confirms design feasibility. ESA

N88-30183# Dornier-Werke G.m.b.H., Friedrichshafen (West Germany).
FUEL CELLS FOR SPACE USE Final Report
U. Knoebel Paris, France ESA 4 Aug. 1987 222 p
(Contract ESA-6787/86-NL-IW(SC))
(FCP-TR-DOS-SY-026; ESA-CR(P)-2563; ETN-88-93015) Avail: NTIS HC A10/MF A01

Hermes fuel cell requirements were analyzed, and the state of the art in Europe was reviewed. A computerized mathematical model for system simulation was established, and mobile and immobile KOH systems and SPE systems were analyzed. A system decision is not possible. A development plan is proposed. ESA

N88-30184*# United Technologies Corp., South Windsor, Conn. Power Systems Div.
REGENERATIVE FUEL CELL ENERGY STORAGE SYSTEM FOR A LOW EARTH ORBIT SPACE STATION
R. E. Martin, J. Garow, and K. B. Michaels 1988 139 p
(Contract NAS3-22234)
(NASA-CR-174802; FCR-6128; NAS 1.26:174802) Avail: NTIS HC A07/MF A01 CSCL 10C

A study was conducted to define characteristics of a Regenerative Fuel Cell System (RFCS) for low earth orbit Space Station missions. The RFCS's were defined and characterized based on both an alkaline electrolyte fuel cell integrated with an alkaline electrolyte water electrolyzer and an alkaline electrolyte fuel cell integrated with an acid solid polymer electrolyte (SPE) water electrolyzer. The study defined the operating characteristics of the systems including system weight, volume, and efficiency. A maintenance philosophy was defined and the implications of system reliability requirements and modularization were determined. Finally, an Engineering Model System was defined and a program to develop and demonstrate the EMS and pacing technology items that should be developed in parallel with the EMS were identified. The specific weight of an optimized RFCS operating at 140 F was defined as a function of system efficiency for a range of module sizes. An EMS operating at a nominal temperature of 180 F and capable of delivery of 10 kW at an overall efficiency of 55.4 percent is described. A program to develop the EMS is described including a technology development effort for pacing technology items. Author

45 ENVIRONMENT POLLUTION

Includes atmospheric, noise, thermal, and water pollution.

N88-30185# Instituto de Pesquisas Espaciais, Sao Jose dos Campos (Brazil).
RECENT MEASUREMENTS OF OZONE IN THE AMAZON FORESTS [RECENTES MEDIDAS DE OZONIO EM FLORESTA AMAZONICA]
V. W. J. H. Kirchhoff and I. M. O. daSilva May 1988 20 p In PORTUGESE Presented at the 2nd Regional Meeting on Geophysics, Salvador-BA (Brazil), 25-27 Nov. 1987
(Contract FINEP-537/CT)
(INPE-4494-PRE/1258) Avail: NTIS HC A03/MF A01

The gas ozone is measured in the middle Amazon forest, in the Ducke forest reservation, INDA ownership, located 30 km north of Manaus (3 deg S, 60 deg W). Surface ozone data and its temporal variations, as well as ozone profile, in the troposphere and stratosphere, were obtained by balloon sounding. The measurements were obtained between 4/8 and 5/11, 1987, representative period of the rainy cycle. This was the second experiment called GTE/ABLE-2B, in collaboration with NASA, the first occurred during the dry cycle. Ozone in the troposphere of the Amazon region was investigated presenting decreasing concentrations. Comparative measurements were done beneath the crown of the trees and in the glade, as well as in different

altitudes above the surface, for determining the concentration of ozone, which is more numerously accented in the Amazon region. Author

N88-30186# Instituto de Pesquisas Espaciais, Sao Jose dos Campos (Brazil).
RECENT OBSERVATIONS OF CARBON MONOXIDE IN THE AMAZON RAIN FOREST [RECENTES OBSERVACOES DE MONOXIDO DE CARBONO EM FLORESTA AMAZONICA]
V. W. J. H. Kirchhoff and E. V. A. Marinho Feb. 1988 21 p In PORTUGESE Presented at the 2nd Regional Meeting of Geophysics, Salvador B. A., 25-27 Nov. 1987
(Contract FINEP-537/CT)
(INPE-4478-PRE/1245) Avail: NTIS HC A03/MF A01

Concentrations of carbon monoxide were measured in air samples gathered approximate to the surface, during participation in the scientific GTE/ABLE-2B to the Amazon. The presence of a large quantity of organic mass concentrated under the vegetative canopy in the very humid and hot atmosphere facilitates a series of chemical reactions and the development of microorganisms and bacteria which through their metabolic processes can liberate gases to the atmosphere. The objective of the measurements is to obtain a better knowledge of the influence of the Amazon Rain Forest concerning the composition of the middle atmosphere, in terms of carbon monoxide, CO, a precursor of ozone. Author

N88-30187# European Space Agency, Paris (France).
INVESTIGATION OF THE LARGE-SCALE IMPACT OF AIR POLLUTION COMPONENTS ON FOREST ECOSYSTEMS IN BAVARIA
Dieter Paffrath (Deutsche Forschungs- und Versuchsanstalt fuer Luft- und Raumfahrt, Oberpfaffenhofen, West Germany) and Wolfgang Peters Jun. 1987 191 p Transl. into ENGLISH of Untersuchung Grossraeumiger Luftschadstoffbelastungen im Zusammenhang mit den Waldschaeden in Bayern, Oberpfaffenhofen, Fed. Republic of Germany (DFVLR) Original language document was announced as N88-10434
(ESA-TT-1087; DFVLR-FB-87-17; ETN-88-92909) Avail: NTIS HC A09/MF A01; original German version available from DFVLR, VB-PL-DO, 90 60 58, 5000 Cologne, Fed. Republic of Germany 47.50 deutsche marks

Typical mean distributions of pollutant concentrations were obtained on the basis of large-scale distributions of concentrations of SO2, NOx, ozone, and of acid-forming paticles over Bavarian forest damage areas measured by aircraft and vehicle. The impact of polluted fog on the forests in the Fichtelgebirge was investigated. The results show that no direct damaging effects of the SO2 and NOx gases can be detected. However, serious forest damage exists in the areas having the highest mean ozone concentration levels. It is not possible to establish a clear correlation between polluted fog and forest damage. ESA

N88-30188 Institut d'Aeronomie Spatiale de Belgique, Brussels.
CHANGES IN STRATOSPHERIC OZONE: OBSERVATIONS AND THEORIES
Guy Brasseur and Paul C. Simon 1988 41 p Presented at the Deutsche Gesellschaft fuer Chemisches Apparatewesem, Chemische Technik und Biotechnologie e.V Conference, Frankfurt, Fed. Republic of Germany, Dec. 1987 and the Conf. on Air Pollution and its Effects on the Environ., Padua, Italy Submitted for publication
(Aeronomica-Acta-A-334-1988; ISSN-0065-3713; ETN-88-93074)
Avail: Institut d'Aeronomie Spatiale de Belgique, 3 Avenue Circulaire, B-1180 Brussels, Belgium

Observations used to derive a possible ozone trend over the last decade, and model simulations of ozone changes are reviewed. Theories to explain ozone depletion over Antarctica especially during springtime are presented. Recent observations show unambiguously that elevated amounts of ClO are present over Antarctica in the lower stratosphere during springtime. It is believed that the release of active chlorine is activated by the presence of polar stratospheric clouds. ESA

N88-30189# Department of Energy, Las Vegas, Nev.
THE DYNAMICS OF TRANSURANICS AND OTHER RADIONUCLIDES IN NATURAL ENVIRONMENTS, DECEMBER 1985
W. A. Howard, ed. and R. G. Fuller, ed. Sep. 1987 579 p
(DE87-014456; NVO-272) Avail: NTIS HC A25/MF A01

The GALILEO area is the first region of the Nevada Test Site to be surveyed by the Radionuclide Inventory and Distribution Program (RIDP). This report describes in detail the use of soil sampling and in situ spectrometry to estimate radionuclide activities at selected sampling locations; the descriptions of these methods will be used as a reference for future RIDP reports. The data collected at GALILEO were analyzed by kriging and the polygons of influence method to estimate the total inventory and the distribution of the six man-made radionuclides. The results of the different statistical methods agree fairly well, although the data did not give very good estimates of the variogram for kriging, and further study showed the results of kriging to be highly dependent on the variogram parameters. The results also showed that in situ spectrometry gives better estimates of radionuclide activity than soil sampling, which tends to miss highly radioactive particles associated with vegetation. Author

N88-30484*# City Univ. of New York, Brooklyn. Seismological Lab.
DID THE GREENHOUSE EFFECT KILL THE DINOSAURS
John D. OKeefe and Thomas J. Ahrens *In* Lunar and Planetary Inst., Nineteenth Lunar and Planetary Science Conference. Press abstracts 1988 p 28-30 (For primary document see N88-30473 24-88)
Avail: NTIS HC A03/MF A01 CSCL 13B

46 GEOPHYSICS

Includes aeronomy; upper and lower atmosphere studies; ionospheric and magnetospheric physics; and geomagnetism.

For space radiation see *93 Space Radiation.*

N88-30190# Air Force Geophysics Lab., Hanscom AFB, Mass.
PARTICLE TRAJECTORIES AND POTENTIALS IN A PLANE SHEATH MOVING IN A MAGNETOPLASMA
Charles W. Dubs and David L. Cooke 15 Jul. 1987 40 p
(AD-A196228; AFGL-TR-87-0225; AFGL-ERP-980) Avail: NTIS HC A03/MF A01 CSCL 04A

A plane sheath moving in the direction of its normal across the magnetic field through a magnetoplasma is analyzed. The self consistent analytic solution for solution for electric field and trajectories of univelocity attracted particles as a function of sheath edge entry angle is derived. For simplicity, the sheath edge is assumed to be sharp. The solution is similar to that for a planar magnetron found much earlier. A quantity q, the square of the ratio of plasma frequency to gyrofrequency, is found to be critical in the behavior of the attracted species. If it is more than a limiting (cutoff) value, am, that depends only on entry angle and Mach number, M, the particles penetrate the whole sheath, some or all of the particles return to the sheath edge. In the frame of the object plane, for M is dominated by 1, q sub m is 1.2(2M) at vertical and infinity at grazing incidence; for M=1, q sub m = 1; for M dominates 1, q sub m is 1.2. So the effect of magnetic field can increase greatly for drift velocity much less than thermal speed. The range of entry angles is derived. For typical low earth orbit conditions, electrons enter between grazing incidence and 45 deg, and have a value of q less than a third of q sub m , whereas 0+ ions enter within 7 deg of vertical incidence and have a value of q over 10 to the 5th power times larger than q sub m. So the magnetic field effects the electrons greatly but the ions only very slightly. GRA

N88-30191# Teledyne Geotechnical, Alexandria, Va.
MAXIMUM-LIKELIHOOD MULTICHANNEL DECONVOLUTION OF P WAVES AT SEISMIC ARRAYS Final Report, 1 Oct. 1985 - 1 Oct. 1986
Z. A. Der, A. C. Lees, W. W. Chan, R. H. Shumway, and K. L. McLaughlin Nov. 1987 176 p
(Contract F08606-86-C-0006; ARPA Order 4511)
(AD-A194990; TGAL-87-3) Avail: NTIS HC A09/MF A01 CSCL 17J

The results of maximum-likelihood multichannel deconvolution applied to array recordings and three component station networks for teleseismic P waves, are presented and interpreted in terms of possible surface reflections and other arrivals from explosions conducted at many of the world's major nuclear test sites. The deconvolution method utilizes the fact that P wave spectra can be decomposed into source and receiver spectral factors. The source functions obtained in the deconvolution process provide a better picture of the nature of explosion source time functions, and in particular of the presence or lack of secondary arrivals following the P wave such as pP or spall. The presence of such secondary arrivals and their effects on the first cycle of the P wave are very important in yield estimation. Significant variations in the deconvolved source time function between test sites may be associated with topography and testing practices. All of the source functions show complexity in addition to the initial P arrival and pP arrival, if present. There is also a great deal of variation between source time functions for events at the same test site. Often, events occurring near each other look particularly similar. The site functions are also complex in most cases and azimuthal variations are significant in both source and receiver regions.
GRA

N88-30192# Stockholm Univ. (Sweden). Dept. of Meteorology.
GLOBAL VERTICAL MASS TRANSPORT BY CLOUDS: A TWO-DIMENSIONAL MODEL STUDY
Mats Olofsson May 1988 42 p Sponsored by the Swedish Air Force
(CM-74; ISSN-0280-445X; ETN-88-93061) Avail: NTIS HC A03/MF A01

A two-dimensional global dispersion model, where vertical transport in the troposphere carried out by convective as well as by frontal cloud systems is explicitly treated, is developed from an existing diffusion model. A parameterization scheme for the cloud transport, based on global cloud statistics, is presented. The model was tested by using Kr-85, Rn-222, and SO2 as tracers, and also with model results without the cloud transport, using eddy diffusion as the primary means of vertical transport. The model results indicate that for trace species with a turnover time of days to weeks, the introduction of cloud-transport gives much more realistic simulations of their vertical distribution. A combination of vertical transport by convective and frontal cloud systems is shown to improve the model simulations, compared to limiting it to convective transport only. The scavenging processes for SO2 are parameterized without the introduction of detailed chemistry.
ESA

N88-30193# Aeronautical Research Labs., Melbourne (Australia).
IMPLEMENTATION OF THE NCAR (NATIONAL CENTRE FOR ATMOSPHERIC RESEARCH) GRAPHICS PACKAGE AT ARL (AERONAUTICAL RESEARCH LABORATORY)
B. D. Fairlie Jan. 1988 138 p
(AD-A195163; ARL/AERO-TM-394; DODA-AR-004-593) Avail: NTIS HC A07/MF A01 CSCL 12E

The NCAR graphics package consists of several graphics utilities and their supporting routines which are designed to provide a wide range of high-level graphics functions. Its capabilities range from simple contouring, labelling and smoothing of lines, plus vector and velocity field plotting and a mapping facility for any part of the Earth. This document describes the philosophy used in implementing the package at ARL, the mechanisms for using the package, and the capabilities of the routines currently implemented. It represents the current status of the package as of August 1987.
GRA

N88-30194# Air Force Inst. of Tech., Wright-Patterson AFB, Ohio.
ATMOSPHERIC CORRECTIONS FOR IN-FLIGHT SATELLITE RADIOMETRIC CALIBRATION M.S. Thesis
Richard J. Bartell 1988 113 p
(AD-A196124; AFIT/CI/NR-88-86) Avail: NTIS HC A06/MF A01 CSCL 04A

Accurate determination of atmospheric effects is crucial to earth-based in-flight radiometric calibration of existing satellite systems. Such calibration work relies on computer codes which compute atmospheric transmittance due to both scattering and absorption processes. Two programs evaluated in this paper are 5S, the Simulation of the Satellite Signal in the Solar Spectrum, and LOWTRAN 6. Two solar radiometers of differing designs were used for atmospheric data collection. The collected data were used to compute total optical depths. Results obtained from the two instruments in the visible are compared. Modifications made to the autotracking instrument are discussed. The accuracy of existing methods for determining the amounts of key constituents actually present in the atmosphere at satellite overpass time is examined. The computation of integrated water vapor content based on solar radiometer data is discussed. Calculations to account for the effects of gaseous absorption in the near infrared spectral bands of a solar radiometer are outlined. Such corrections will facilitate calibration of these spectral bands. In conclusion, the effects on radiance at the satellite level of the uncertainties in the current determination of crucial atmospheric parameters such as the extent of gaseous absorption and the aerosol characterization are examined.
GRA

N88-30195# Johns Hopkins Univ., Laurel, Md. Applied Physics Lab.
INVESTIGATIONS OF MAGNETOSPHERE-IONOSPHERE COUPLING RELEVANT TO OPERATIONAL SYSTEMS Final Scientific Report, 1984 - 1987
C. I. Meng and P. T. Newell Feb. 1988 105 p
(Grant AF-AFOSR-0049-84)
(AD-A195972; AFOSR-88-0622TR) Avail: NTIS HC A06/MF A01 CSCL 04A

Important advances were made in understanding the dynamics of the magnetosphere and its coupling to the ionosphere. Significant progress was made in the areas of polar cusp precipitation and dynamics; dayside auroral morphology and auroral boundary dynamics; polar rain; the quiescent polar cap; the physics of impulsive injection phenomena; and problems of global magnetospheric plasma transport.
GRA

N88-30196# Analytic Sciences Corp., Reading, Mass.
ESTIMATION OF SHORT-WAVELENGTH GRAVITY ON A DENSE GRID USING DIGITAL TERRAIN ELEVATION DATA Scientific Report No. 1, May 1986 - May 1987
J. D. Goldstein, J. V. White, R. P. Commer, and W. G. Heller Oct. 1987 41 p
(Contract F19628-86-C-0077)
(AD-A196325; ANSER-TR-5362-1; AFGL-TR-0280) Avail: NTIS HC A03/MF A01 CSCL 08E

The precise determination of the gravity field at or near the earth's surface is required for compensating navigation/guidance systems and for testing gravity gradiometers. With conventional gravimeters it is usually impractical to measure the gravity field over an extended area at very short wavelengths (e.g., wavelengths less than 10 km). Since very short-wavelength gravitational perturbations at the surface are caused largely by near-surface mass variations in the local area, and since digital terrain elevation data (DTED) are available on dense grids (e.g., three arc second spacing) for selected regions, the very short-wavelength components of gravity can be estimated without a gravity survey by using the DTED and the assumption of constant mass density. This report presents an approach to computing the short-wavelength, terrain-induced gravity field at a prescribed rms

accuracy. For a relatively flat test area in Oklahoma, the rms effect of terrain elevation on the gravity field at mean elevation for wavelengths shorter than 10 km varies between 0.6 mgal and 2.2 mgal. The largest point value of the high-frequency terrain effect is 18.0 mgal. GRA

N88-30197# Air Force Geophysics Lab., Hanscom AFB, Mass.
ON FORMULATING A SIMPLE D-REGION MODEL
William Swider 28 Oct. 1987 19 p
(AD-A195841; AFGL-TR-87-0308; AFGL-ERP-987) Avail: NTIS HC A03/MF A01 CSCL 04A

This report focuses on a body of work that suggests that the effective recombination coefficients in the daytime D-Region are fairly invariant and thus lead to a rather simple solution for the electron concentrations. In addition, a quadratic expression is available for the estimation of electron concentrations at night. The ionization production rate q must be known and incorporated into the chemistry of the D region to determine electron concentrations (e) as a function of altitude. There is some D region research which supports a simple way to determine (e) once q is known. Thus, the daytime effective recombination coefficient, Psi, appears to be relatively insensitive to q and can provide for the determination of (e), (e) = sq rt(q/Psi) under steady-state conditions. For steady-state conditions at night, an equation exists which yields (e) with reasonable accuracy. GRA

N88-30198# Montana Univ., Missoula.
RELATIONSHIPS AMONG EARTH'S GRAVITY FIELD, MAGNETIC FIELD, CRUSTAL STRUCTURE AND THE MAGNETIC CHARACTER OF CRUSTAL ROCKS Final Report, 1 Oct. 1986 - 30 Sep. 1987
Steven D. Sheriff 3 Dec. 1987 3 p
(Grant AF-AFOSR-0025-87)
(AD-A195539; AFOSR-88-0549TR) Avail: NTIS HC A02/MF A01 CSCL 08D

The equipment has been purchased and received. It is currently in a phase of beta-testing with a research project on the edge of the Idaho Batholith in western Montana. The equipment includes: (1) Sun Microsystems 3/110 workstation with supporting software and manuals. This includes a floating point accelerator, modem and 0.25 inch tape drive; Compatible Sun Laserwriter and Hewlett Packard color-dot printer; (2) Summagraphics 42 x 60 inch Microgrid II digitizing table and microcomputer interface; (3) Schonstedt SSM-2A spinner magnetometer; Advance Magnetics magnetic shield assemblies; Schonstedt DM-2220 digital magnetometer; (4) 10 kiloGauss alpha Scientific electromagnet including the matched reversible power supply; and (5) Bartington Instruments digital magnetic susceptibility meter. GRA

N88-30199# Naval Environmental Prediction Research Facility, Monterey, Calif.
THE SURFACE EVAPORATIVE DUCT HEIGHT PRODUCT: AN EVALUATION Final Report, 1 Oct. 1986 - 30 Sep. 1987
William T. Thompson Dec. 1987 56 p
(AD-A195918; NEPRF-TR-87-05) Avail: NTIS HC A04/MF A01 CSCL 17I

The existence of a surface evaporative duct has many serious operational implications. One of the most serious and obvious implications is that the extended range of the radar will allow distant hostile units to detect the radar (and to be detected by the radar). Thus, the existence of a surface evaporative duct is an important component of the decision on whether or not to radiate. Another consequence of the duct is that a radar hole will exist between the top of the duct and the base of the lobes unaffected by the duct (see figure 1). Hostile aircraft or missiles will thus be able to approach the radar undetected. Conversely, knowledge of the refractivity profile in the vicinity of enemy radars can be turned to tactical advantage. GRA

N88-30200*# Universities Space Research Association, Huntsville, Ala.
AN IMPROVEMENT IN THE NUMERICAL INTEGRATION PROCEDURE USED IN THE NASA MARSHALL ENGINEERING THERMOSPHERE MODEL Interim Report
Michael Philip Hickey Aug. 1988 53 p
(Contract NAS8-36639)
(NASA-CR-179389; NAS 1.26:179389) Avail: NTIS HC A04/MF A01 CSCL 04A

A proposed replacement scheme for the integration of the barometric and diffusion equations in the NASA Marshall Engineering Thermosphere (MET) model is presented. This proposed integration scheme is based on Gaussian Quadrature. Extensive numerical testing reveals it to be faster, more accurate and more reliable than the present integration scheme (a modified form of Simpson's Rule) used in the MET model. Numerous graphical examples are provided, along with a listing of a modified form of the MET model in which subroutine INTEGRATE (using Simpson's Rule) is replaced by subroutine GAUSS (which uses Gaussian Quadrature). It is recommended that the Gaussian Quadrature integration scheme, as used here, be used in the MET model. Author

N88-30201*# Lunar and Planetary Inst., Houston, Tex.
WORKSHOP ON THE GROWTH OF CONTINENTAL CRUST
Lewis D. Ashwal, ed. 1988 174 p Workshop held in Oxford, England, 13-16 Jul. 1987
(Contract NASw-4066)
(NASA-CR-183073; NAS 1.26:183073; LPI-TR-88-02) Avail: NTIS HC A08/MF A01 CSCL 08G

Constraints and observations were discussed on a fundamental unsolved problem of global scale relating to the growth of planetary crusts. All of the terrestrial planets were considered, but emphasis was placed on the Earth's continental crust. The title of each session is: (1) Extraterrestrial crustal growth and destruction; (2) Constraints for observations and measurements of terrestrial rocks; (3) Models of crustal growth and destruction; and (4) Process of crustal growth and destruction. For individual titles, see N88-30202 through N88-30255.

N88-30202*# Lamont-Doherty Geological Observatory, Palisades, N.Y.
CONSTRAINTS ON CONTINENTAL ACCRETION FROM SEDIMENTATION
Dallas Abbott *In* Lunar and Planetary Inst., Workshop on the Growth of Continental Crust 1988 p 29-30 (For primary document see N88-30201 24-46)
Avail: NTIS HC A08/MF A01 CSCL 08G

Heat loss in the ancient Earth was discussed assuming that classical sea floor spreading was the only mechanism. This may be expressed as faster spreading or longer total ridge length. These have important implications as to the size and number of cratonic plates in the distant past, the degree to which they are flooded, the kinds of sediments and volcanics that would be expected, and the amount of recycling of continental material taking place. The higher proportion of marine sedimentary rocks and oceanic volcanics in the Archean, and the relative paucity of evaporites and continental volcanics may in part be due to smaller cratonic blocks. A model was developed of the percentage of continental flooding which utilizes round continents and a constant width of the zone of flooding. This model produces a reasonable good fit to the percentage of flooding on the present day continents. E.R.

N88-30203*# Centre National de la Recherche Scientifique, Vandoeure (France).
Nd ISOTOPES AND CRUSTAL GROWTH RATE
F. Albarede *In* Lunar and Planetary Inst., Workshop on the Growth of Continental Crust 1988 p 33-34 (For primary document see N88-30201 24-46)
Avail: NTIS HC A08/MF A01 CSCL 08G

Sm/Nd isotopic constraints on crustal growth is discussed. In order to constrain Sm/Nd fractionation between continental crust

and depleted mantle, an extensive data base of isotopic measurements (assumed to be adequately representative of continental crust) was compiled. The results imply that the evolution of depleted mantles was roughly linear, with no major discontinuities over the course of geologic time. This is different from other determinations of depleting mantle evolution, which show nonlinear behavior. The Sm/Nd evolution lines for continental crust and depleted mantle intersect between 3.8 to 4.0 Ga, which may indicate that the onset of continental growth was later than 4.5 Ga. A mathematical model is described, the results of which imply that time integrated crustal additions from the mantle are about 1.8 to 2.5 cu km/a, whereas crustal subtractions by sediment recycling are about 0.6 to 1.5 cu km/a. This results in a net time integrated crustal growth rate of about 1 cu km/a, which is similar to present day rates determined, for example, by Reymer and Schubert. E.R.

N88-30204*# Max-Planck-Inst. fuer Chemie, Mainz (West Germany).
RECYCLING OF LOWER CONTINENTAL CRUST THROUGH FOUNDERING OF CUMULATES FROM CONTAMINATED MAFIC INTRUSIONS
Nicholas T. Arndt and Steven L. Goldstein *In* Lunar and Planetary Inst., Workshop on the Growth of Continental Crust 1988 p 35-37 (For primary document see N88-30201 24-46)
Avail: NTIS HC A08/MF A01 CSCL 08G

A mechanism is presented for recycling of lower continental material back into the mantle. Picritic magmas, possible parental to volumious continental volcanics such as the Karoo and Deccan, became trapped at the Moho, where they interacted with and become contaminated by lower crustal materials. Upon crystallization, the magmas differentiated into lower ultramafic cumulate zones and upper gabbroic-anorthositic zones. The ultramafic cumulates are denser than underlying mantle and sink, carrying lower crustal components as trapped liquid, as xenoliths or rafts, and as constituents of cumulate minerals. This model provides a potentially significant crust-mantle differentiation mechanism, and may also represent a contributing factor in crustal recycling, possibly important in producing some OIB reservoirs. E.R.

N88-30205*# Max-Planck-Inst. fuer Chemie, Mainz (West Germany).
GROWTH OF CONTINENTAL CRUST: CLUES FROM Nd ISOTOPES AND Nb-Th RELATIONSHIPS IN MANTLE-DERIVED MAGMAS
N. T. Arndt, C. Chauvel, K.-P. Jochum, G. Gruau, and A. W. Hofmann *In* Lunar and Planetary Inst., Workshop on the Growth of Continental Crust 1988 p 38-39 (For primary document see N88-30201 24-46)
Avail: NTIS HC A08/MF A01 CSCL 08G

Isotope and trace element geochemistry of Precambrian mantle derived rocks and implications for the formation of the continental crust is discussed. Epsilon Nd values of Archean komatiites are variable, but range up to at least +5, suggesting that the Archean mantle was heterogeneous and, in part, very depleted as far back as 3.4 to 3.5 Ga. This may be taken as evidence for separation of continental crust very early in Earth history. If these komatiite sources were allowed to evolve in a closed system, they would produce modern day reservoirs with much higher epsilon Nd values than is observed. This implies recycling of some sort of enriched material, perhaps subducted sediments, although other possibilities exist. Archean volcanics show lower Nb/Th than modern volcanics, suggesting a more primitive mantle source than that observed nowadays. However, Cretaceous komatiites from Gorgona island have similar Nb/Th to Archean volcanics, indicating either the Archean mantle source was indeed more primitive, or Archean magmas were derived from a deep ocean island source like that proposed for Gorgona. E.R.

N88-30206*# Colorado School of Mines, Golden. Dept. of Geology and Geological Engineering.
PLUTON EMPLACEMENT AND MAGMATIC ARC CONSTRUCTION: A MODEL FROM THE PATAGONIAN BATHOLITH
Robert Bruce, Eric Nelson, and Stephen Weaver *In* Lunar and Planetary Inst., Workshop on the Growth of Continental Crust 1988 p 40-41 (For primary document see N88-30201 24-46)
Avail: NTIS HC A08/MF A01 CSCL 08G

A model of batholithic construction in Andean arcs and its applicability to possibly similar environments in the past is described. Age and compositional data from the Patagonian batholith of southern Chile show a long history of magmatism in any given area (total age range is 15 to 157 Ma), but different regions appear to have different magmatic starting ages. Furthermore, mafic rocks seem to be the oldest components of any given region. An assembly line model involving semicontinuous magmatism and uplift was outlined, which has implications for other terranes: uplift rates will be proportional to observed ranges in age, and total uplift will be proportional to the age of the oldest pluton in any given area. It is suggested that misleading results would be obtained if only small areas of similar terranes in the Archean were available for study. E.R.

N88-30207*# Lunar and Planetary Inst., Houston, Tex.
AN ILLUSTRATION OF THE COMPLEXITY OF CONTINENT FORMATION
Kevin Burke *In its* Workshop on the Growth of Continental Crust 1988 p 42-44 (For primary document see N88-30201 24-46)
Avail: NTIS HC A08/MF A01 CSCL 08G

It was pointed out that a consensus may be emerging in crustal growth models, considering the clustering of most growth curves and their uncertainties. Curves most distant from this clustering represent models involving extensive recycling of continental material back into the mantle, but the author wondered if geochemical signatures for this would be recognizable considering the lack of evidence from seismic tomography for discrete mantle reservoirs, and the likelihood of core-mantle interaction based on recent high pressure experiments. Unreactivated Archean rocks represent only 2 percent of present continental area, and the author was uncomfortable about basing inferences on what the early Earth was like on such a small amount of information. He feels that the hypothesis of continental assembly that needs testing is that of banging together of island arcs, such as in Indonesia today. As an example of how complex this process can be, the author described the geology of the Caribbean arc system, which shows evidence for reversals of subduction polarity, numerous collisional events, and substantial strike-slip movements. It seemed unlikely to the author that Archean examples would have been less complicated. E.R.

N88-30208*# North Carolina Univ., Chapel Hill.
THE KERALA KHONDALITE BELT (KKB) OF SOUTHERN INDIA: AN ENSIALIC MOBILE BELT
Thomas Chacko, James K. Meen, G. R. Ravindra Kumar (Centre for Earth Science Studies, Trivandrum, India), and John J. W. Rogers *In* Lunar and Planetary Inst., Workshop on the Growth of Continental Crust 1988 p 45-47 (For primary document see N88-30201 24-46)
Avail: NTIS HC A08/MF A01 CSCL 08G

The Proterozoic Kerala Khondalite belt of the Southern Indian Shield is described, a belt dominated by granulite grade (750 C, 5 to 6 kbar) supracrustal rocks whose protoliths included arkoses and shales with cratonic provenances. Rare earth elements and other geochemical signatures suggest a granitic source for these metasediments, possibly the spatially associated charnockite massifs. The presence of intercalated mafic gneisses, interpreted as basalts, implies a cratonic rift basin rather than a foreland basin setting. It was argued that the Kerala, as well as other early Proterozoic mobile belts formed during abortive continental rifting without major additions of new crust. E.R.

N88-30209*# Cambridge Univ. (England). Dept. of Earth Sciences.
THE TIMING AND MECHANISM OF DEPLETION IN LEWISIAN GRANULITES Abstract Only
A. S. Cohen, R. K. ONions, and M. J. OHara (University Coll. of Wales, Aberystwyth.) *In* Lunar and Planetary Inst., Workshop on the Growth of Continental Crust 1988 p 48 (For primary document see N88-30201 24-46)
Avail: NTIS HC A08/MF A01 CSCL 08G

Large Ion Lithophile (LIL) depletion in Lewisian granulites is discussed. Severe depletions in U, Th, and other LIL have been well documented in Lewisan mafic and felsic gneisses, but new Pb isotopic analyses show little or no depletion in lithologies with high solidus temperatures, such as peridotite. This suggests that LIL transport in this terrane took place by removal of partial melts rather than by pervasive flooding with externally derived CO2. The Pb and Nd isotopic data gathered on these rocks show that the depletion and granulite metamorphism are distinct events about 250 Ma apart. Both fluid inclusions and cation exchange geothermometers date from the later metamorphic event and therefore have little bearing on the depletion event, suggesting a note of caution for interpretations of other granulite terranes. E.R.

N88-30210*# MacQuarie Univ., North Ryde (Australia). School of Earth Sciences.
GENESIS OF ARCHEAN GRANITOIDS IN THE PILBARA BLOCK AND IMPLICATIONS FOR CRUSTAL GROWTH
W. J. Collins *In* Lunar and Planetary Inst., Workshop on the Growth of Continental Crust 1988 p 49-50 (For primary document see N88-30201 24-46)
Avail: NTIS HC A08/MF A01 CSCL 08G

The origin of the Mount Edgar Batholith of the Pilbara Block in Western Australia is discussed, along with other Archean granitoids that show relatively primitive isotopic characteristics but more evolved bulk geochemistry. Geochemical evidence is presented in support of a multistage process of crustal ripening, involving partial melting of a thick basaltic crust to produce the tonalitic and dacitic sources of the more evolved granitoids. These events must produce stable continental crust in less than 200 Ma and are different geologically and geochemically from those which produced Phanerozoic granitoids in Andean margin settings. E.R.

N88-30211*# Australian National Univ., Canberra. Res. School Earth Sci.
ROLE OF ZIRCON IN TRACING CRUSTAL GROWTH AND RECYCLING
W. Compston, I. S. Williams, R. A. Armstrong, J. C. Claoue-Long, P. D. Kinny, J. J. Foster, A. Kroener, R. T. Pidgeon, and J. S. Myers (Western Australian Inst. of Tech., Bentley.) *In* Lunar and Planetary Inst., Workshop on the Growth of Continental Crust 1988 p 51-54 (For primary document see N88-30201 24-46)
Avail: NTIS HC A08/MF A01 CSCL 08G

Single crystal ion probe ages of zircons is discussed, which allow much better time resolution compared to other geochronological methods, although the technique is not without problems. Rocks from two areas that contain composite zircon populations, including true magmatic zircons as well as a variety of xenocrystic types are described. It is often difficult to distinguish these; xenocrystic zircons, for example, cannot always be identified on the basis of morphology alone. Additional evidence is needed before making age interpretations. Evidence is also presented of zircon growth long after the original time of crystallization, in some cases apparently at temperatures less than 300 C. The spectacular discovery of 4.1 to 4.2 Ga detrital zircons in metaquartzites from the Mount Narryer area of Western Australia is described. Similar zircons with ages as old as 4276 Ma have been found in the nearby Jack Hills area. The source areas or parent lithologies of these zircons have not yet been determined, but the author expects that they may be unrecognized or buried antecedents of the K rich Narryer gneisses. U or Th concentrations of zircon cannot be used to discriminate between felsic and mafic source rocks. E.R.

N88-30212*# National Aeronautics and Space Administration. Lyndon B. Johnson Space Center, Houston, Tex.
CHRONOLOGY OF EARLY LUNAR CRUST
E. J. Dasch, L. E. Nyquist, and G. Ryder *In* Lunar and Planetary Inst., Workshop on the Growth of Continental Crust 1988 p 54-56 Prepared in cooperation with Oregon State Univ., Corvallis (For primary document see N88-30201 24-46)
Avail: NTIS HC A08/MF A01 CSCL 08G

The chronology of lunar rocks is summarized. The oldest pristine (i.e., lacking meteoritic contamination of admixed components) lunar rock, recently dated with Sm-Nd by Lugmair, is a ferroan anorthosite, with an age of 4.44 + 0.02 Ga. Ages of Mg-suite rocks (4.1 to 4.5 Ga) have large uncertainties, so that age differences between lunar plutonic rock suites cannot yet be resolved. Most mare basalts crystallized between 3.1 and 3.9 Ga. The vast bulk of the lunar crust, therefore, formed before the oldest preserved terrestrial rocks. If the Moon accreted at 4.56 Ga, then 120 Ma may have elapsed before lunar crust was formed. E.R.

N88-30213*# California Univ., Los Angeles. Dept. of Earth and Space Sciences.
CONSTRUCTION OF MASS-AGE CURVES FOR THE CONTINENTAL CRUST: AN EMPIRICAL MODEL AND AN EXAMPLE FROM THE WESTERN US
D. J. DePaolo, G. S. Schubert, and Ann Linn *In* Lunar and Planetary Inst., Workshop on the Growth of Continental Crust 1988 p 57-58 (For primary document see N88-30201 24-46)
Avail: NTIS HC A08/MF A01 CSCL 08G

The methodology of determining crustal mass-age curves is discussed. Problems in doing this include determination of model ages and accounting for mixing of materials of different ages during crust forming processes. These difficulties can be overcome with some reasonable assumptions and estimates of rock volumes based on areal proportions. This technique was used to construct a reasonably well constrained mass-age curve for the southwestern U.S. based on isotopic measurements on over 100 samples. The results imply that the crust in this area grew episodically at 2.8, 1.8, and 0.1 Ga. It is estimated that it would take on the order of 10000 to 100000 individual Sm-Nd isotopic measurements to carry out a similar exercise for continental crust world wide. E.R.

N88-30214*# Oxford Univ. (England). Dept. of Earth Sciences.
DOES SUBDUCTION ZONE MAGMATISM PRODUCE AVERAGE CONTINENTAL CRUST
R. M. Ellam and C. J. Hawkesworth (Open Univ., Milton, England) *In* Lunar and Planetary Inst., Workshop on the Growth of Continental Crust 1988 p 59-61 (For primary document see N88-30201 24-46)
Avail: NTIS HC A08/MF A01 CSCL 08G

The question of whether present day subduction zone magmatism produces material of average continental crust composition, which perhaps most would agree is andesitic, is addressed. It was argued that modern andesitic to dacitic rocks in Andean-type settings are produced by plagioclase fractionation of mantle derived basalts, leaving a complementary residue with low Rb/Sr and a positive Eu anomaly. This residue must be removed, for example by delamination, if the average crust produced in these settings is andesitic. The author argued against this, pointing out the absence of evidence for such a signature in the mantle. Either the average crust is not andesitic, a conclusion the author was not entirely comfortable with, or other crust forming processes must be sought. One possibility is that during the Archean, direct slab melting of basaltic or eclogitic oceanic crust produced felsic melts, which together with about 65 percent mafic material, yielded an average crust of andesitic composition. E.R.

N88-30215*# Scripps Institution of Oceanography, La Jolla, Calif.
Pb ISOTOPE CONSTAINTS ON THE EXTENT OF CRUSTAL RECYCLING INTO A STEADY STATE MANTLE
S. J. G. Galer, S. L. Goldstein, and R. K. ONions (Cambridge Univ., England) *In* Lunar and Planetary Inst., Workshop on the

Growth of Continental Crust 1988 p 62-64 (For primary document see N88-30201 24-46)
Avail: NTIS HC A08/MF A01 CSCL 08G

Isotopic and geochemical evidence was discussed against recycling of continental crust into the mantle. Element ratios such as Sm/Nd, Th/Sc, and U/Pb in sedimentary masses have remained relatively constant throughout Earth history, and this can only be reconciled with steady state recycling models if new crustal materials added from the mantle have had similar ratios. Such recycling models would also require shorter processing times for U, Th, and Pb through the mantle than are geodynamically reasonable. Models favoring subduction of pelagic sediments as the only recycling mechanism fail to account for the Pb isotopic signature of the mantle. Recycling of bulk crust with Pb isotopic compositions similar to those expected for primitive mantle would be permissable with available data, but there appear to be no plausible tectonic mechanisms to carry this out. E.R.

N88-30216*# Max-Planck-Inst. fuer Chemie, Mainz (West Germany).
DECOUPLED Rb-Sr AND Sm-Nd ISOTOPIC EVOLUTION OF THE CONTINENTAL CRUST
S. L. Goldstein *In* Lunar and Planetary Inst., Workshop on the Growth of Continental Crust 1988 p 65-67 (For primary document see N88-30201 24-46)
Avail: NTIS HC A08/MF A01 CSCL 08G

Evidence was presented that the Rb-Sr and Sm-Nd isotopic systems are decoupled in crust-mantle evolution. Rare earth element (including Sm and Nd) residue principally in silicates, and are resistant to mobilization by weathering and metamorphism. In contrast, Rb and Sr are easily fractionated by crustal processes and residue in carbonates as well as in silicates. As a result, continental Sr, but not Nd, can be recycled into the mantle by exchange of seawater with basalt at spreading ridges and by subduction of carbonates associated with ridge processes. These effects result in mean Rb-Sr ages of the continental crust and of the upper mantle that are too young. Crustal growth curves based largely on Rb-Sr data, such that of Hurley and Rand, are therefore incorrect. E.R.

N88-30217*# Massachusetts Univ., Amherst. Dept. of Geology.
CRUSTAL EVOLUTION AND THE ECLOGITE TO GRANULITE PHASE TRANSITION IN XENOLITHS FROM THE WEST AFRICAN CRATON
S. E. Haggerty, D. V. Hills, and P. B. Toft *In* Lunar and Planetary Inst., Workshop on the Growth of Continental Crust 1988 p 68-70 (For primary document see N88-30201 24-46)
Avail: NTIS HC A08/MF A01 CSCL 08G

A suite of eclogite and granulite facies xenoliths from kimberlite pipes in the Archean Man Shield of West Africa is described. The xenoliths include lithologies ranging in composition from komatiite to anorthosite and appear to be geochemically, petrologically, and geophysically related. The suite may represent fractionation of felsic material separated from ancient mantle and added to early Archean crust. The samples can be used to define a xenolith geotherm, which may represent an ancient episode of high heat flow. The samples also imply that the crust-mantle boundary is a gradational and possibly interlayered geochemical, mineralogical, and seismic transition. It is speculated that the depleted subcontinental mantle required by diamond bearing coalescence of smaller depletion cells formed by extraction of ancient crustal components. These depleted zones are surrounded by fertile asthenospheric mantle, which may have given rise to later flood basalts such as the Karroo and Parana Provinces. E.R.

N88-30218*# Oxford Univ. (England).
METAMORPHIC P-T PATHS AND PRECAMBRIAN CRUSTAL GROWTH IN EAST ANTARCTICA
S. L. Harley *In* Lunar and Planetary Inst., Workshop on the Growth of Continental Crust 1988 p 71-73 (For primary document see N88-30201 24-46)
Avail: NTIS HC A08/MF A01 CSCL 08G

The metamorphic constraints on crustal thicknesses in Archean and post-Archean terranes are summarized along with possible implications for tectonic processes. It is important to recognize that P-T estimates represent perturbed conditions and should not be used to estimate steady state geothermal gradients or crustal thicknesses. The example is cited of the Dora Maira complex in the French Alps, where crustal rocks record conditions of 35 kbar and 800 C, implying their subduction to depths of 100 km or more, followed by subsequent uplift to the surface. Therefore such P-T estimates tell more about processes than crustal thicknesses. More importantly, according to the author, are determinations of P-T paths, particularly coupled with age measurements, because these may provide constraints on how and when perturbed conditions relax back to steady state conditions. P-T paths are illustrated that should be expected from specific tectonic processes, including Tibetan style collision, with and without subsequent extension, rifting of thin or thickened crust, and magmatic accretion. Growth of new crust, associated with magmatic accretion, for example, could possibly be monitored with these P-T paths. E.R.

N88-30219*# Planetary Science Inst., Tucson, Ariz.
EARLY INTENSE CRATERING: EFFECTS ON GROWTH OF EARTH'S CRUST
William K. Hartmann *In* Lunar and Planetary Inst., Workshop on the Growth of Continental Crust 1988 p 74-76 (For primary document see N88-30201 24-46)
Avail: NTIS HC A08/MF A01 CSCL 08G

The disrupting effects of early intense meteorite bombardment on Earth's protocrustal evolution is discussed. The author emphasized that one should not consider the Earth's impact history as a discrete phase separate from an early crust forming event, and also that the end of the impacts was not a singular event that destroyed all previously formed crust. E.R.

N88-30220*# Geological Survey, Menlo Park, Calif.
THE GROWTH OF CONTINENTS AND SOME CONSEQUENCES SINCE 1.5 Ga
David G. Howell *In* Lunar and Planetary Inst., Workshop on the Growth of Continental Crust 1988 p 77-78 (For primary document see N88-30201 24-46)
Avail: NTIS HC A08/MF A01 CSCL 08G

The budget of Earth's oceanic sediment masses was discussed in terms of crustal growth and recycling. Based on estimates of the volume of oceanic sediments and the average age of oceanic crust, a continental denudation rate of 1.65 cu km/yr was computed. This crudely balances estimated crustal production rates of about 1 cu km/yr, but the efficiency of sediment loss via subduction, for example, must be considered. It was argued, on the basis of earthquake focal solutions, imagery of subduction zones, and plate kinematic reconstructions that little, if any, sediment was lost in this way. This yields a present day crustal growth rate of about 1 cu km/yr. The volume of continents to 1.5 Ga ago was discussed, assuming constant continental thickness and freeboard, and a constant hydrosphere volume. It was concluded that ocean ridge length was a factor of about 1.75 greater 1.5 Ga ago, but a major uncertainty is the average spreading rate in the past. E.R.

N88-30221*# Australian National Univ., Canberra. Research School of Earth Sciences.
THE EARLY ARCHAEAN CRUSTAL HISTORY OF WEST GREENLAND AS RECORDED BY DETRITAL ZIRCONS
P. D. Kinny, W. Compston, and V. R. McGregor (Atammik, Sukkertoppen, Greenland) *In* Lunar and Planetary Inst., Workshop on the Growth of Continental Crust 1988 p 79-81 (For primary document see N88-30201 24-46)
Avail: NTIS HC A08/MF A01 CSCL 08G

The isotope systematics of some of the oldest samples on Earth from both Greenland and Australia was discussed. The antiquity was confirmed of the 4.1 to 4.2 Ga zircons from Western Australia; the model Lu-Hf age of these zircons, as measured with the ANU ion probe is 4.14 + or - 0.24 Ga, although the oldest preserved rock units there are anorthosites with a Lu-Hf model age of about 3.73 Ga. U-Pb ion probe ages of detrital

zircons ranging between 2.87 and 3.89 Ga from an Akilia association quartzite was reported, whose age of deposition is probably around 3.8 Ga. It was argued that the younger age in this range are discordant because of late Pb-loss, probably associated with a high grade metamorphic event at about 3.6 Ga. It was also argued that the earliest crust in West Greenland and elsewhere is about 3.9 Ga, but in some places, such as Western Australia, crustal evolution took place much earlier, perhaps starting as far back as 4.3 Ga. This would account for the presence in that terrane of abundant K rich granitoid, the paucity of tonalitic and trondhjemitic materials, and the existence of Eu anomalies in early Archean sediments. E.R.

N88-30222*# British Institutions' Reflection Profiling Syndicate, Cambridge (England).
DEEP SEISMIC REFLECTION PROFILING AND CONTINENTAL GROWTH CURVES
Simon L. Klemperer *In* Lunar and Planetary Inst., Workshop on the Growth of Continental Crust 1988 p 82-84 (For primary document see N88-30201 24-46)
Avail: NTIS HC A08/MF A01 CSCL 08G

The results of deep seismic reflection profiling is discussed which shows that the lower crust is prominently layered, in many continental areas, regardless of the age of the surface rocks. The seismic Moho is commonly shallower than the petrological Moho, leading to the question of the nature and origin of this prominent reflector in the deep crust. The lower crust is much less well defined in Phanerozoic and Proterozoic accreted terranes, suggesting possible differences in types of lower crusts. E.R.

N88-30223*# Mainz Univ. (West Germany).
GROWTH OF EARLY ARCHAEAN CRUST IN THE ANCIENT GNEISS COMPLEX OF SWAZILAND AND ADJACENT BARBERTON GREENSTONE BELT, SOUTHERN AFRICA
A. Kroener, W. Compston, A. Tegtmeyer, C. Milisenda, and T. C. Liew (Max-Planck-Inst. fuer Chemie, Mainz, West Germany) *In* Lunar and Planetary Inst., Workshop on the Growth of Continental Crust 1988 p 85-87 (For primary document see N88-30201 24-46)
Avail: NTIS HC A08/MF A01 CSCL 08G

The relationship between early Archean greenstones and high grade gneisses in the Ancient Gneiss Complex of Swaziland and the neighboring Barberton greenstone belt in Southern Africa is discussed. New high precision zircon analyses reveal a complex history in individual zircons from tonalitic orthogneisses, with ages as old as 3644 + 4 Ma. This suggests the presence of continental crust prior to the formation of the supracrustal rocks of the Barberton greenstone belt, which have been previously considered the earliest rocks in the area. The author suggested that these data are incompatible with the intraoceanic settings that have been widely accepted for this terrane, and favors either a marginal basin or rift environment. By using the detailed age information obtained from zircons in combination with Ar-40 and Ar-39 and paleomagnetic measurements, the author estimated that plate velocities for this part of Africa craton were about 10 to 70 mm/yr, during the period 3.4 to 2.5 Ga. This is not incompatible with the idea that Archean plate velocities may have been similiar to those of today. E.R.

N88-30224*# National Inst. of Oceanography, Haifa (Israel).
DIAPIRS OF THE MEDITERRANEAN RIDGE: THE TECTONIC REGIME OF AN INCIPIENT ACCRETED TERRANE
Y. Mart *In* Lunar and Planetary Inst., Workshop on the Growth of Continental Crust 1988 p 88-89 (For primary document see N88-30201 24-46)
Avail: NTIS HC A08/MF A01 CSCL 08G

The occurrence of diapirs in the Mediterranean ridge stems mostly from the massive deposition of salt and gypsum in the Mediterranean basin during the late Miocean. The diapiric emplacement of the evaporitic sequence is not obvious, because the mobilization of the salt beds and the initiation of the diapiric upward flow are constrained by the relatively shallow thickness of the Plio-Pleistocene sedimentary overburden and by the low heat flow that prevails in the eastern Mediterranean. The diapirs consist also of early Cretaceous shales as well as other gravitationally metastable strata which are less mobile than salt. Studies of subduction trenches and their surroundings show that shallow ridges occur seaward of the trenches in many places. The collisional motion between the African and the Eurasian plates would further enhance accretion of sediments in the Mediterranean ridge, which would attain subaerial exposure, and eventually would become a mountain range accreted to southern Europe. The numerous diapirs of salt and shales that occur in the ridge would be common features in the future accreted terrane, indicating an intermediate extensional phase in the tectonic history of the development of crustal growth. Author

N88-30225*# National Inst. of Oceanography, Haifa (Israel).
THE TECTONIC SETTING OF THE SEYCHELLES, MASCARENE AND AMIRANTE PLATEAUS IN THE WESTERN EQUATORIAL INDIAN OCEAN
Y. Mart *In* Lunar and Planetary Inst., Workshop on the Growth of Continental Crust 1988 p 90-91 (For primary document see N88-30201 24-46)
Avail: NTIS HC A08/MF A01 CSCL 08G

A system of marine plateaus occurs in the western equatorial Indian Ocean, forming an arcuate series of wide and shallow banks with small islands in places. The oceanic basins that surround the Seychelles - Amirante region are of various ages and reflect a complex seafloor spreading pattern. The structural analysis of the Seychelle - Amirante - Mascarene region reflects the tectonic evolution of the western equatorial Indian Ocean. It is suggested that due to the seafloor spreading during a tectonic stage, the Seychelles continental block drifted southwestwards to collide with the oceanic crust of the Mascarene Basin, forming an elongated folded structure at first, and then a subduction zone. The morphological similarity, the lithological variability and the different origin of the Seychelles Bank, the Mascarene Plateau and the Amirante Arc emphasizes the significant convergent effects of various plate tectonic processes on the development of marine plateaus. Author

N88-30226*# Washington Univ., Seattle.
EVIDENCE FOR CRUSTAL RECYCLING DURING THE ARCHEAN: THE PARENTAL MAGMAS OF THE STILLWATER COMPLEX
I. S. McCallum *In* Lunar and Planetary Inst., Workshop on the Growth of Continental Crust 1988 p 92-94 (For primary document see N88-30201 24-46)
Avail: NTIS HC A08/MF A01 CSCL 08G

The petrology and geochemistry of the Stillwater Complex, an Archean (2.7 Ga) layered mafic intrusion in the Beartooth Mountains of Montana is discussed. Efforts to reconstruct the compositions of possible parental magmas and thereby place some constraints on the composition and history of their mantle source regions was studied. A high-Mg andesite or boninite magma best matches the crystallization sequences and mineral compositions of Stillwater cumulates, and represents either a primary magma composition or a secondary magma formed, for example, by assimilation of crustal material by a very Mg-rich melt such as komatiite. Isotopic data do not support the extensive amounts of assimilation required by the komatiite parent hypothesis, and it is argued that the Stillwater magma was generated from a mantle source that had been enriched by recycling and homogenization of older crustal material over a large area. E.R.

N88-30227*# Open Univ., Milton (England). Dept. of Earth Sciences.
CHANGING STYLES OF CRUSTAL GROWTH IN SOUTHERN AFRICA: CONSTRAINTS FROM GEOCHEMICAL AND Sr-Nd ISOTOPE STUDIES IN ARCHAEAN TO PAN AFRICAN TERRAINS
F. McDermott, C. J. Hawkesworth, and N. B. W. Harris *In* Lunar and Planetary Inst., Workshop on the Growth of Continental Crust 1988 p 95-97 (For primary document see N88-30201 24-46)
Avail: NTIS HC A08/MF A01 CSCL 08G

Nd isotopic data was presented for southern Africa in support of episodic crustal growth. Over 50 percent of the continental crust there had formed before 2.5 Ga, and less than 10 percent was produced after about 1.0 Ga. The data imply a mean crustal age of about 2.4 Ga for southern Africa, and a higher rate of crustal growth than that derived from Australian shale data, particularly during the Proterozoic. Isotopic data from Damara metasediments imply that there is no need to invoke decoupling of the Rb-Sr and Sm-Nd systems in the continental crust. E.R.

N88-30228*# Massachusetts Univ., Amherst. Dept. of Geology and Geography.
STRUCTURE OF SOUTHWESTERN MICHIPICOTEN GREENSTONE BELT, ONTARIO: EVIDENCE FOR ARCHEAN ACCRETION
George E. McGill and Catherine H. Shrady *In* Lunar and Planetary Inst., Workshop on the Growth of Continental Crust 1988 p 98-100 (For primary document see N88-30201 24-46)
Avail: NTIS HC A08/MF A01 CSCL 08G

The results of detailed mapping of a well exposed (by a large fume kill) Archean Michipicoten greenstone belt of Ontario is discussed. Numerous structural features are described including soft sediment deformation, thrust faults, isoclinal folds, and sill intrusion, which apparently formed prior to the earliest flattening cleavage. It was inferred that all of these events may have taken place before the rocks were completely lithified, and the question was raised as to whether early soft sediment and tectonic deformation were coeval. If so, the overall picture would permit (but not compel) recognition of a convergent oceanic environment such as an accretionary wedge or forearc basin. E.R.

N88-30229*# Colgate Univ., Hamilton, N.Y. Dept. of Geology.
MID TO LATE PROTEROZOIC MAGMATISM WITHIN NORTHEASTERN NORTH AMERICA AND ITS IPLICATIONS FOR THE GROWTH OF THE CONTINENTAL CRUST
J. M. McLelland *In* Lunar and Planetary Inst., Workshop on the Growth of Continental Crust 1988 p 101-102 (For primary document see N88-30201 24-46)
Avail: NTIS HC A08/MF A01 CSCL 08G

Recent studies of the mangerite-charnockite-alaskite suite exposed in the Adirondack Highlands strongly suggest that these rocks were emplaced under anorogenic, or mildly extensional, conditions. The characteristic signatures of the rocks are high (FeO/FeO+MgO) and (FeO/Fe2O3); mildly alkaline to subalkaline and metaluminous trends; high Ga/Al2O3; and within plate concentrations of Nb vs Y, Ta vs Yb, Rb vs (Y+Nb), and Rb vs (Yb+Ta). Evolved members of the series are low in CaO and MgO and high in alkalies and halogens. All of these properties are consistent with anorogenic magmatism comprising acidic crustal melts and mantle derived mafic additions to the crust. Major and minor element trends, as well as field evidence, strongly suggest that the anorogenic acidic suite is coeval, but not comagmatic, with closely associated anorthositic massifs. Present outcrop configurations are consistent with the evolution of the acidic and anorthositic rocks in zoned, bimodal magma chambers cored by the mafic constituents and overlain by explosive, caldera-type volcanism. Age determinations indicate that the emplacement of the anorthosite-charnockite suite extended over approximately 500 Ma in the Grenville and adjacent Nain, Provinces. Author

N88-30230*# Lunar and Planetary Inst., Houston, Tex.
THERMAL MODELS PERTAINING TO CONTINENTAL GROWTH
Paul Morgan (University of Northern Arizona, Flagstaff.) and Lew Ashwal *In its* Workshop on the Growth of Continental Crust 1988 p 103-105 (For primary document see N88-30201 24-46)
Avail: NTIS HC A08/MF A01 CSCL 08G

Thermal models are important to understanding continental growth as the genesis, stabilization, and possible recycling of continental crust are closely related to the tectonic processes of the earth which are driven primarily by heat. The thermal energy budget of the earth was slowly decreasing since core formation, and thus the energy driving the terrestrial tectonic engine was decreasing. This fundamental observation was used to develop a logic tree defining the options for continental growth throughout earth history. Author

N88-30231*# National Aeronautics and Space Administration. Lyndon B. Johnson Space Center, Houston, Tex.
THE TECTONIC SETTING OF ARCHEAN ANORTHOSITES
Abstract Only
D. A. Morrison, W. C. Phinney, and D. E. Maczuga (Lockheed Engineering and Management Services Co., Inc., Houston, Tex.) *In* Lunar and Planetary Inst., Workshop on the Growth of Continental Crust 1988 p 106 (For primary document see N88-30201 24-46)
Avail: NTIS HC A08/MF A01 CSCL 08G

Archean anorthosites, anorthositic gabbros, and related rocks form intrusive complexes in every Archean craton. These complexes are characterized by the presence of equidimensional plagioclase megacrysts of typically uniform and calcic (An80-90) composition. Many, if not all, such complexes developed in greenstone belt terrains and appear to be genetically linked to contemporary volcanics. The petrogenesis of Archean anorthosites appears to argue for development in oceanic settings and implies intensive magmatic activity. Author

N88-30232*# Tennessee Univ., Knoxville. Dept. of Geological Sciences.
THE PETROGENESIS OF OCEANIC KIMBERLITES AND INCLUDED MANTLE MEGACRYSTS: THE MALAITAN ALNOITE
Clive R. Neal *In* Lunar and Planetary Inst., Workshop on the Growth of Continental Crust 1988 p 107-109 (For primary document see N88-30201 24-46)
Avail: NTIS HC A08/MF A01 CSCL 08G

The study of unambiguous suboceanic mantle was facilitated by the occurrence of anomalous kimberlite-type intrusives on Malaita in the Solomon Islands. The pseudo-kimberlites were termed alnoites, and are basically mica lamprophyres with melilite in the ground mass. Alnoitic magmas were explosively intruded into the Ontong Java Plateau (OJP) 34 Ma ago. The OJP is a vastly overthickened portion of the Pacific plate which now abuts the Indo-Australian plate. Malaita is considered to be the obducted leading edge of the OJP. Initial diapiric upwelling beneath the OJP produced the proto-alnoite magma. After impingement on the rigid lithosphere, megacrysts fractionation occurred, with augites precipitating first, representing the parental magma. Sea water-altered oceanic crust, which underplated the OJP, was assimilated by the proto-alnoite magma during megacrysts fractionation (AFC). Author

N88-30233*# Colorado School of Mines, Golden.
RIDGE-TRENCH COLLISION IN ARCHEAN AND POST-ARCHEAN CRUSTAL GROWTH: EVIDENCE FROM SOUTHERN CHILE
E. P. Nelson and R. D. Forsythe (Rutgers - The State Univ., New Brunswick, N. J.) *In* Lunar and Planetary Inst., Workshop on the Growth of Continental Crust 1988 p 110-111 (For primary document see N88-30201 24-46)
Avail: NTIS HC A08/MF A01 CSCL 08G

The growth of continental crust at convergent plate margins involves both continuous and episodic processes. Ridge-trench collision is one episodic process that can cause significant magmatic and tectonic effects on convergent plate margins. Because the sites of ridge collision (ridge-trench triple junctions) generally migrate along convergent plate boundaries, the effects of ridge collision will be highly diachronous in Andean-type orogenic belts and may not be adequately recognized in the geologic record. The Chile margin triple junction (CMTJ, 46 deg S), where the actively spreading Chile rise is colliding with the sediment-filled Peru-Chile trench, is geometrically and kinematically the simplest modern example of ridge collision. The south Chile margin illustrates the importance of the ridge-collision tectonic setting in crustal evolution at convergent margins. Similarities between ridge-collision features in southern Chile and features of Archean greenstone

belts raise the question of the importance of ridge collision in Archean crustal growth. Archean plate tectonic processes were probably different than today; these differences may have affected the nature and importance of ridge collision during Archean crustal growth. In conclusion, it is suggested that smaller plates, greater ridge length, and/or faster spreading all point to the likelihood that ridge collision played a greater role in crustal growth and development of the greenstone-granite terranes during the Archean. However, the effects of modern ridge collision, and the processes involved, are not well enough known to develop specific models for the Archean ridge collison. Author

N88-30234*# Memorial Univ. of Newfoundland, St. Johns. Dept. of Earth Sciences.
REAPPRAISAL OF THE GEOLOGY OF KANGIMUT SAMMISOQ, AMERALIK FJORD, SOUTHERN WEST GREENLAND: CRUSTAL STRUCTURE AND INTERPRETATION OF ISOTOPIC DATA
Allen P. Nutman, Clark R. L. Friend, and Vic R. McGregor (Atammik, Sukkertoppen, Greenland) *In* Lunar and Planetary Inst., Workshop on the Growth of Continental Crust 1988 p 112-115 (For primary document see N88-30201 24-46)
Avail: NTIS HC A08/MF A01 CSCL 08G

In Godthabsfjord, in the North Atlantic Archean Craton, early Archean Amitsoq gneisses are found in association with the mid to late Archean Nuk gneisses. The Amitsoq gneisses contain the Ameralik dykes, now subconcordant strips of amphibolite. The Nuk and Amitsoq gneisses have amphibolite facies polymetamorphic assemblages. To the southeast of Godthabsfjord, there is an extensive region affected by granulite facies metamorphism at 2800 Ma. Early models of crustal evolution for Godthabsfjord and the region to the SE are discussed. Recent detailed mapping combined with U-Pb zircon dating is examined. Author

N88-30235*# Peking Univ. (China). Dept. of Geology.
ARCHEAN CRUSTAL EVOLUTION OF THE NORTHERN NORTH CHINA CRATON
Xianglin Qian, Yaping Chen, and Jinzhong Liu *In* Lunar and Planetary Inst., Workshop on the Growth of Continental Crust 1988 p 116-118 (For primary document see N88-30201 24-46)
Avail: NTIS HC A08/MF A01 CSCL 08G

The Archean granultie facies rocks of the North China (Sino-Korean) Craton mostly occur inside the northern boundary forming a unique and spectacular granulite belt trending roughly E-W from eastern Hebei, North China in the east to Mt. Daqinchan, western Inner Mongolia in the west, ranging about 1,000 km long. Over the years in the middle portion of this Archean high-grade metamorphic belt a stratigraphic unconformity between the khondalite rock assemblage and the medium in composition granulite assemblage in Datong-Xinghe area is determined. The geological structural properties of the North China Craton are discussed. Author

N88-30236*# Australian National Univ., Canberra. School of Earth Sciences.
GROWTH OF THE LOWER CONTINENTAL CRUST
Roberta L. Rudnick *In* Lunar and Planetary Inst., Workshop on the Growth of Continental Crust 1988 p 119-121 (For primary document see N88-30201 24-46)
Avail: NTIS HC A08/MF A01 CSCL 08G

One of the largest uncertainties in crustal composition and growth models is the nature of the lower continental crust. Specifically, by what processes is it formed and modified, and when is it formed, particularly in reference to the upper crust? The main reason for this lack of information is the scarcity of lower crustal rock samples. These are restricted to two types: rocks which outcrop in granulite facies terrains and granulite facies xenoliths which are transported to the earth's surface by young volcanics. The important conclusions arising from the xenolith studies are: the majority of mafic lower crustal xenoliths formed through cumulate process, resitic xenoliths are rare; and formation and metamorphism of the deep crust is intimately linked to igneous activity and/or orogeny which are manifest in one form or another at the earth's surface. Therefore, estimates of crustal growth based on surface exposures is representative, although the proportion of remobilized pre-existing crust may be significantly greater at the surface than in the deep crust. Author

N88-30237*# National Aeronautics and Space Administration. Lyndon B. Johnson Space Center, Houston, Tex.
THE COMPLEXITY, DEPTH, AND RAPIDITY OF PROCESSES THAT FORMED THE LUNAR CRUST **c91**
Graham Ryder (Lunar and Planetary Inst., Houston, Tex.) and Julius Dasch *In* Lunar and Planetary Inst., Workshop on the Growth of Continental Crust 1988 p 122-124 Prepared in cooperation with Oregon State Univ., Corvallis (For primary document see N88-30201 24-46)
Avail: NTIS HC A08/MF A01 CSCL 03B

From its birth the moon had a large-scale, complex magma system. The evidence is the massive differentiation of the moon that was partially preserved. The system might be a magma ocean or a magmasphere; even in the former case it was superposed by smaller but also very complex magma systems. The main episode produced a plagioclase-rich crust including genuine anorthosites; it was over by about 4.35 b.y. ago, although magmatism continues. The processes of crust-building remain in serious dispute. Lunar crusts; massive differentiation; crustal material composition; processes which produced crustal materials; and differences from earth are briefly discussed. Author

N88-30238*# Leicester Univ. (England). Dept. of Geology.
CONTINENTAL CRUSTAL FORMATION AND RECYCLING: EVIDENCE FROM OCEANIC BASALTS
A. D. Saunders, J. Tarney, and M. J. Norry *In* Lunar and Planetary Inst., Workshop on the Growth of Continental Crust 1988 p 125-126 (For primary document see N88-30201 24-46)
Avail: NTIS HC A08/MF A01 CSCL 08G

Despite the wealth of geochemical data for subduction-related magma types, and the clear importance of such magmas in the creation of continental crust, there is still no concensus about the relative magnitudes of crustal creation versus crustal destruction (i.e., recycling of crust into the mantle). The role of subducted sediment in the formation of the arc magmas is now well documented; but what proportion of sediment is taken into the deeper mantle? Integrated isotopic and trace element studies of magmas erupted far from presently active subduction zones, in particular basaltic rocks erupted in the ocean basins, are providing important information about the role of crustal recycling. By identifying potential chemical tracers, it is impossible to monitor the effects of crustal recycling, and produce models predicting the mass of material recycled into the mantle throughout long periods of geological time. Author

N88-30239*# Quebec Univ., Montreal.
GEOCHRONOLOGICAL AND LEAD-ISOTOPE EVIDENCES FOR RAPID CRUST FORMATION IN MIDDLE-PROTEROZOIC TIME: THE LABRADOR EXAMPLE
Urs Schaerer *In* Lunar and Planetary Inst., Workshop on the Growth of Continental Crust 1988 p 127-130 (For primary document see N88-30201 24-46)
Avail: NTIS HC A08/MF A01 CSCL 08G

Extensive U-Pb geochronological studies in the Grenville and Makkovik provinces have shown that eastern Labrador is underlain by two distinct crustal blocks. In order to substantiate the juvenile character of the middle-Proterozoic crustal block, the isotopic compositon of lead in leached k-feldspars from the same rocks were analyzed. The results of the analysis are briefly discussed. Author

N88-30240*# California Univ., Los Angeles. Dept. of Earth and Space Sciences.
PHYSICAL PROCESSES IN THE GROWTH OF THE CONTINENTAL CRUST
G. Schubert *In* Lunar and Planetary Inst., Workshop on the

Growth of Continental Crust 1988 p 131-132 (For primary document see N88-30201 24-46)
Avail: NTIS HC A08/MF A01 CSCL 08G

Major mechanisms of crustal addition are volcanism and plutonism at plate boundaries and within plate interiors. One approach to deciding if island arc magmatism dominated ancient crustal growth is to assess the rate at which the process has operated in the recent past. The localized addition rates were found to be comparable to present day global rates. One physical observable that was used to constrain models of crustal growth is sea level. A simple physical model was developed to explore the consequences of constant freeboard (the height of the continents above sea level). Global geoid and sea floor topography data were used to identify and study oceanic plateaus and swells that have either continental crustal roots or anomalously thick ocean crusts. Author

N88-30241*# National Geophysical Research Inst., Hyderabad (India).
EVOLUTION OF THE DHARWAR CRATON: A TERRAIN OF EARLY ARCHEAN CRUSTAL STABILITY, LONG TERM OROGENIC CYCLES AND LARGE SCALE PALAEOBIOLOGICAL ACTIVITY
R. Srinivasan and S. M. Naqvi *In* Lunar and Planetary Inst., Workshop on the Growth of Continental Crust 1988 p 133-135 (For primary document see N88-30201 24-46)
Avail: NTIS HC A08/MF A01 CSCL 08G

Traceable history of the Dharwar Craton goes back to approximately 3400 m.y. old tonalitic to trondhjemitic fundamental gneiss whose REE composition indicates its derivation from a preexisting basalt which apparently had very short time of crustal residence. The fundamental gneiss is preserved only as rare relicts in the vast gneissic complex of the Indian Peninsula (the Peninsular Gneiss), and as pebbles in the conglomerates of the Archean Dharwar sequence. Study of these relicts, shows evidence of a deformation episode prior to the deposition of the high- and low-grade Dharwar supracrustal sequence. The Dharwar supracrustal sequence is briefly described. Geochemistry of the volcanic and sedimentary rocks of the Dharwar supracrustal belts are examined. Author

N88-30242*# Max-Planck-Inst. fuer Chemie, Mainz (West Germany).
LITHOSPHERIC EVOLUTION OF THE NORTHERN ARABIAN SHIELD: CHEMICAL AND ISOTOPIC EVIDENCE FROM BASALTS, XENOLITHS AND GRANITES
M. Stein *In* Lunar and Planetary Inst., Workshop on the Growth of Continental Crust 1988 p 136-138 Prepared in cooperation with Hebrew Univ., Jerusalem (Israel) (For primary document see N88-30201 24-46)
Avail: NTIS HC A08/MF A01 CSCL 08G

The evolution of the upper-mantle and the lower-crust (the conteinental lithosphere), is the area of Israel and Sinai was studied, using the chemical composition and the Nd-Sr isotopic systematics from mantle and crustal nodules, their host basalts, and granites. The magmatism and the metasomatism making the lithosphere are related to uprise of mantle diapirs in the uppermost mantle of the area. These diapirs heated the base of the lithosphere, eroded, and replaced it with new hot material. It caused a domal uplift of the lithosphere (and the crust). The doming resulted in tensional stresses that in turn might develop transport channels for the basalt. Author

N88-30243*# Leicester Univ. (England).
TRACE ELEMENT DIFFERENCES BETWEEN ARCHEAN, PROTEROZOIC AND PHANEROZOIC CRUSTAL COMPONENTS: IMPLICATIONS FOR CRUSTAL GROWTH PROCESSES
J. Tarney, L. E. A. Wyborn, J. W. Sheraton, and D. Wyborn (Bureau of Mineral Resources, Geology and Geophysics, Canberra, Australia) *In* Lunar and Planetry Inst., Workshop on the Growth of Continental Crust 1988 p 139-140 (For primary document see N88-30201 24-46)
Avail: NTIS HC A08/MF A01 CSCL 08G

Critical to models for continental crust growth and recycling are the processes through which crustal growth takes place. In particular, it is important to know whether these processes have changed fundamentally with time in response to the earth's thermal evolution, and whether the crustal compositions generated are compatible with crustal remobilization, crustal recycling, or represent primary additions. There are some significant and consistent differences in the major and trace element compositions of crustal components with time which have important implications for crustal growth processes. These will be illustrated with reference to Archean rocks from a number of shield areas, Proterozoic granitoids from Australia and elsewhere, Palaeozoic granitoids from Australia and Scotland, and Mesozoic - recent granitoids from present continental margin belts. Surprisingly some rather simple and consistent patterns energy using this technique. There are then significant differences in compositions of granitoid crustal additions throughout geological time, with a particular type of granitoid apparently dominating a particular time period. This implies that the tectonic processes giving rise to granite generation have changed in response to the earth's thermal evolution. Author

N88-30244*# Tennessee Univ., Knoxville. Dept. of Geology.
CONTINENTAL GROWTH THROUGH TIME BY UNDERPLATING OF SUBDUCTED OCEANIC CRUST: EVIDENCE FROM KIMBERLITES IN SOUTH AFRICA AND SW PACIFIC
Lawrence A. Taylor and Clive R. Neal *In* Lunar and Planetary Inst., Workshop on the Growth of Continental Crust 1988 p 141-143 (For primary document see N88-30201 24-46)
Avail: NTIS HC A08/MF A01 CSCL 08G

In the dynamic model of plate tectonics, it is evident that crustal components are returned to the mantle by subduction. Chemical signatures of these subducted components were identified in ocean island volcanics and in island arc volcanics. Indeed, an origin involving a subducted protolith was postulated for certain types of xenoliths in kimberlite, including diamonds. Recent studies of eclogite xenoliths in kimberlite from southern Africa and megacrysts form the Malaitan alnoite, Solomon islands, indicate that lithospheric underplating by subducted oceanic crust has occurred in these two contrasting areas. The results of new eclogite studies from the Bellsbank kimberlite, South Africa, and isotopic data from the Malaitan alnoite megacryst suite. This forms the basis for discerning the role of lithospheric underplating in the growth of cratons and in the evolution of mantle-derived magma. Author

N88-30245*# Oxford Univ. (England). Dept. of Earth Sciences.
THE GROWTH OF THE CONTINENTAL CRUST: CONSTRAINTS FROM RADIOGENIC ISOTOPE GEOCHEMISTRY
Paul N. Taylor *In* Lunar and Planetary Inst., Workshop on the Growth of Continental Crust 1988 p 144-146 (For primary document see N88-30201 24-46)
Avail: NTIS HC A08/MF A01 CSCL 08G

Most models for evolution of continental crust are expressed in the form of a diagram illustrating the cumulative crustal mass (normalized relative to the present crustal mass) as a function of time. Thus, geochronological data inevitably play a major role in either constructing or testing crustal growth models. For all models, determining the start-time for effective crustal accretion is of vital importance. To this end, the continuing search for, and reliable characterization of, the most ancient crustal rock-units remains a worthy enterprise. Another important role for geochronology and radiogenic isotope geochemistry is to assess the status of major geological events as period either of new crust generation or of reworking of earlier formed continental crust. For age characterization of major geological provinces, using the critieria outined, the mass (or volume) of crust surviving to the present day should be determinable as a function of crust formation age. More recent developments, however, appear to set severe limitations on recycling of crust, at least by the process of sediment subduction. In modeling crustal growth without recycling, valuable

constaints on growth rate variations through time can be provided if variations in the average age of the continental crust can be monitored through geological history. The question of the average age of the exposed continental crust was addressed by determining Sm-Nd crustal residence model ages (T-CR) for fine-grained sediment loads of many of the world's major rivers. Author

N88-30246*# Australian National Univ., Canberra. Research School of Earth Sciences.
CRUSTAL GROWTH IN THE ARCHEAN: THE GEOCHEMICAL EVIDENCE
Stuart Ross Taylor *In* Lunar and Planetary Inst., Workshop on the Growth of Continental Crust 1988 p 147-149 (For primary document see N88-30201 24-46)
Avail: NTIS HC A08/MF A01 CSCL 08G

Differences between Archean and post-Archean crusts; growth models; Archean high-grade terrains; tectonic significance; and Archean crustal growth are examined briefly. B.G.

N88-30247*# Australian National Univ., Canberra. Research School of Earth Sciences.
GROWTH OF PLANETARY CRUSTS
Stuart Ross Taylor *In* Lunar and Planetary Inst., Workshop on the Growth of Continental Crust 1988 p 150-152 (For primary document see N88-30201 24-46)
Avail: NTIS HC A08/MF A01 CSCL 08G

The solid planets and satellites mostly have crusts which differ markedly in composition both from their interior, and from primordial solar nebula composition. Primary crusts, mercury, icy crusts, early intense cratering, Mars, Venus, Ganymede, and tertiary crusts are discussed. B.G.

N88-30248*# Lunar and Planetary Inst., Houston, Tex.
GRAVITY ANOMALIES, PLATE TECTONICS AND THE LATERAL GROWTH OF PRECAMBRIAN NORTH AMERICA
M. D. Thomas, R. A. F. Grieve (Geological Survey of Canada, Ottawa, Ontario), and V. L. Sharpton *In its* Workshop on the Growth of Continental Crust 1988 p 153-155 (For primary document see N88-30201 24-46)
Avail: NTIS HC A08/MF A01 CSCL 08G

The widespread gravity coverage of North America provides a picture of the gross structural fabric of the continent via the trends of gravity anomalies. The structural picture so obtained reveals a mosaic of gravity trend domains, many of which correlate closely with structural provinces and orogenic terranes. The gravity trend map, interpreted in the light of plate-tectonic theory, thus provides a new perspective for examining the mode of assembly and growth of North America. Suture zones, palaeosubduction directions, and perhaps, contrasting tectonic histories may be identified using gravity patterns. Author

N88-30249*# Hebrew Univ., Jerusalem (Israel). Inst. of Earth Sciences.
SOLID EARTH AS A RECYCLING SYSTEMS AND THE LATERAL GROWTH OF PRECAMBRIAN NORTH AMERICA
Abstract Only
Jan Veizer *In* Lunar and Planetary Inst., Workshop on the Growth of Continental Crust 1988 p 156 (For primary document see N88-30201 24-46)
Avail: NTIS HC A08/MF A01 CSCL 08G

If plotted on mass vs time diagrams, geologic entities (for example, continental and oceanic crust, sediments, and mineral resources) display an exponential (power law) relationship, with entity per unit time increasing toward the present. This relationship is consistent with the concept of recycling and can be simulated mathematically. The approach is based on the plate tectonic theory and considers area-age or mass-age distributions of crystalline basement and sediments for major global tectonic realms. Each tectonic realm is characterized by a specific lifespan, which is an inverse function of its recycling rate. The estimated average half-area of half-mass ages are given. The corresponding parameters for continental crust are 690 Ma for K/Ar, and approximately 1200 Ma for Rb/St and U-Th/Pb dating pairs. Tectonic diversity preserved in the geologic record is therefore a function of time, with oceanic tectonic realms, because of their rapid recycling, underrepresented in the rocks older than approximately 300 Ma. The Sm/Nd isotopic systematic of sediments suggest that, for a near steady-state post-Archean sedimentary mass, recycling is approximately 90 + or - 5 percent cannibalistic. This yields an estimated upper limit on crust-mantle exchange via sediment subduction of approximately 1.1 + or - 0.5 x 10 g a(sup -1) considerably less than demanded by isotopic constraints. The discrepancy may indicate the existence of additional loci, such as orogenic belts, for significant crust-mantle interaction. Author

N88-30250*# Ottawa Univ. (Ontario). Dept. of Geology.
MINERALIZATION THROUGH GEOLOGIC TIME: EVOLUTION OF CONTINENTAL CRUST
Jan Veizer, Peter Laznicka, and S. L. Jansen (Carleton Univ., Ottawa, Ontario) *In* Lunar and Planetary Inst., Workshop on the Growth of Continental Crust 1988 p 157-158 (For primary document see N88-30201 24-46)
Avail: NTIS HC A08/MF A01 CSCL 08G

In analogy to living systems, geologic entities (e.g., rocks, mineral deposits, tectonic realms and domains) are involved in the process of perpetual generation and destruction (birth/death cycles). This results in time distribution patterns akin to age structures in living populations and the systematics is amenable to treatment by the concepts of population dynamics. Utilizing this theoretical approach, the survivorship patterns for major realms of the plate tectonic system, for consitutent rocks, and for the entombed mineral resources are predicted. The present inventory encompasses global economic accumulations of metals by geologic age. The deposits of these metals were assigned to nine broad genetic categories, with an attempt to relate each category to tectonic setting within the framework of global plate tectonics. Author

N88-30251*# California Univ., Los Angeles. Inst. of Geophysics.
GROWTH OF THE CONTINENTAL CRUST: A PLANETARY-MANTLE PERSPECTIVE
Paul H. Warren *In* Lunar and Planetary Inst., Workshop on the Growth of Continental Crust 1988 p 159-161 (For primary document see N88-30201 24-46)
Avail: NTIS HC A08/MF A01 CSCL 08G

The lack of earth rocks older than about 3.8 Ga is frequently interpreted as evidence that the earth formed little or no subduction-resistant continental crust during the first 700 My of its history. Such models obviously imply that the pre-3.8 Ga earth was covered entirely or almost entirely by smoothly subducting oceanic crust. On the other hand, the thermal regime of the early earth probably tended to cause the oceanic crust at this time to be comparatively thin and comparatively mafic. The present earth is covered by about 50 percent oceanic crust, averaging about 7 km in thickness, and 41 percent continental crust, averaging roughly 40 km in thickness. Thus continentless-early-earth models would seem to imply a total mass of crust less than 1/3 that of the present day earth. Possible explanations are examined. Author

N88-30252*# Geological Survey, St. Paul, Minn.
CRUSTAL UNDERPLATING IN THE NORTH AMERICAN CRATON: EVIDENCE FROM THE PETROGENESIS OF ANORTHOSITIC ROCKS IN THE MIDDLE PROTEROZOIC MIDCONTINENT RIFT SYSTEM
P. W. Weiblen and J. D. Miller, Jr. *In* Lunar and Planetary Inst., Workshop on the Growth of Continental Crust 1988 p 162-164 (For primary document see N88-30201 24-46)
Avail: NTIS HC A08/MF A01 CSCL 08G

Circumstantial evidence for underplating as a significant mechanism for the growth of continental crust continues to accumulate, particularly from considerations of thermal, seismic, and density contraints on the lower crust and upper mantle. Compelling geochemical and petrological arguments were made that in continental flood basalt provinces, the volume of underplated

cumulates may be at least as large as the expression of surface lavas. Geological, petrological, and geochemical data are presented on anorthositic rocks in the Duluth Complex, which indicates that underplating processes similar to those postulated by Cox played a significant role in their origin. The interpretations may be applicable to the origin of anorthositic rocks in general. Author

N88-30253*# Oxford Univ. (England). Dept. of Earth Sciences.
LATE-ARCHAEAN CRUSTAL GROWTH IN THE LEWISIAN COMPLEX OF NORTHWEST SCOTLAND: DIACHRONEITY IN MAGMATIC ACCRETION AND IMPLICATIONS FOR MODELS OF CRUSTAL GROWTH
M. J. Whitehouse *In* Lunar and Planetary Inst., Workshop on the Growth of Continental Crust 1988 p 165-167 (For primary document see N88-30201 24-46)
Avail: NTIS HC A08/MF A01 CSCL 08G

The Lewisian Complex of northwestern Scotland is an Archaean basement terrain that was reworked during the Proterozoic. Previous geochronological studies have established that the complex represents an entirely new crustal addition during late-Archaean times, and the difference between a Sm-Nd accretion date of 2920 + or - 50 Ma and a Pb/Pb metamorphic date of 2680 + or - 70 Ma was interpreted as indicating a crustal accretion-differentiation superevent (CADS) lasting 240 + or - 110 Ma. A combined Rb-Sr, Pb/Pb, and Sm-Nd isotopic study reported was applied to the Lewisian CADS to attempt to address the problem of whether this comprised a short regional scale magmatic accretion event followed approximately 200 Ma later by regional high-grade metamorphism, or a long period of episodic or semi-continuous magmatic accretion prior to high-grade metamorphism. Author

N88-30254*# Strathclyde Univ., Glasgow (Scotland). Dept. of Applied Geology.
THE EFFECT OF THICKER OCEANIC CRUST IN THE ARCHAEAN ON THE GROWTH OF CONTINENTAL CRUST THROUGH TIME Abstract Only
M. E. Wilks *In* Lunar and Planetary Inst., Workshop on the Growth of Continental Crust 1988 p 168 (For primary document see N88-30201 24-46)
Avail: NTIS HC A08/MF A01 CSCL 08G

Present crustal evolution models fail to account for the generation of the large volume of continental crust in the required time intervals. All Archaean plate tectonic models, whether invoking faster spreading rates, similar to today's spreading rates, or longer ridge lengths, essentially propose that continental crust has grown by island arc accretion due to the subduction of oceanic crust. The petrological differences that characterize the Archaean from later terrains result from the subduction of hotter oceanic crust into a hotter mantle. If the oceanic crust was appreciably thicker in the Archaean, as geothermal models would indicate, this thicker crust is surely going to have an effect on tectonic processes. A more valid approach is to compare the possible styles of convergence of thick oceanic crust with modern convergence zones. The best modern analog occurs where thick continental crust is colliding with thick continental crust. Oceanic crustal collision on the scale of the present-day Himalayan continental collision zone may have been a frequent occurrence in the Archaean, resulting in extensive partial melting of the hydrous underthrust oceanic crust to produce voluminous tonalite melts, leaving a depleted stabilized basic residuum. Present-day island arc accretion may not have been the dominant mechanism for the growth of the early Archaean crust. Author

N88-30255*# National Aeronautics and Space Administration. Lyndon B. Johnson Space Center, Houston, Tex.
VOLCANIC CONTRIBUTION TO CRUSTAL GROWTH IN THE CENTRAL ANDES: A NEW ESTIMATE AND A DISCUSSION OF UNCERTAINTIES
C. A. Wood and P. Francis (Lunar and Planetary Inst., Houston, Tex.) *In* Lunar and Planetary Inst., Workshop on the Growth of Continental Crust 1988 p 169-171 (For primary document see N88-30201 24-46)
Avail: NTIS HC A08/MF A01 CSCL 08G

Volcanism above subduction zones is a major mechanism for crustal growth and compared to some other proposed processes calculation of growth rates is relatively easy given accurate volumes and ages of volcanic material. Francis and Rundie (1976) first used this approach in a small region of the Central Andes, and extrapolated their result to the entire Central Andean arc. The derived rate of 3 to 4.2 x 10 to the minus 6th cubic km yr/km of arc length is compared with an independent estimate based upon a reconnaissance census of all major volcanoes in the Central Andes. Author

N88-30256# Lowell Univ., Mass. Center for Atmospheric Research.
IONOSONDE STUDIES OF FIELD-ALIGNED IRREGULARITIES DURING HIGH-POWER HF HEATING AT ARECIBO
Leo F. McNamara, Bodo W. Reinisch, and Jurgen Buchau Feb. 1988 46 p
(Contract F19628-83-C-0092)
(AD-A195848; ULRF-433/CAR; AFGL-TR-86-0168; SR-4) Avail: NTIS HC A03/MF A01 CSCL 04A

Backscatter ionograms recorded by an airborne digital ionosonde during the September 1981 ionospheric HF heating campaign at Arecibo have been simulated using simplified ionospheric models and analytic raytracing techniques. The simulations indicate that irregularities were created at all altitudes from the interaction height (where the plasma frequency was equal to the heater frequency) down to the base of the F layer, but with a preferred altitude near the interaction height. There was no evidence for the existence of irregularities at altitudes much above the interaction height. THe horizontal east/west extent of the irregularity patch was approximately 100 to 150 km, shifted towards the west with respect to the Arecibo magnetic meridian (asymmetry 25 km to the east/125 km to the west). GRA

N88-30257# Sierra Geophysics, Inc., Kirkland, Wash.
DISCRIMINATION STUDIES USING SHORT-PERIOD P WAVES AT UPPER MANTLE DISTANCES Annual Report, Jan. 1986 - Jan. 1987
J. W. Given, S. M. Ihnen, G. R. Mellman, and W. C. Tucker Jan. 1988 82 p
(Contract F08606-86-C-0014)
(AD-A195468; SGI-R-88-136) Avail: NTIS HC A05/MF A01 CSCL 08K

This report reviews the properties of seismograms recorded at upper mantle distances in a stable continental region such as northwest Eurasia in order to examine how well current models predict the general behavior of the observations and to see how much unmodeled energy, or noise, is present. In general the proposed models for the region predict the major arrivals observed in the data. For explosions, there are few distinct arrivals that are not associated with some predicted upper mantle phase. However, noise levels (or code amplitudes), are large, since each arrival has a code associated with it that adds constructively at the receiver. Predicted coda amplitudes are used in a Pearce algorithm to discriminate on the basis of focal mechanism. Given good azimuthal coverage of an event (e.g., 3 of 4 quadrants), the observed complexity of the explosion seismograms is incompatible with that predicted for earthquakes at depth using simple models for the reflection of the depth phases pP and sP. These results are similar to previous findings that considered teleseismic data. GRA

N88-30258*# Lunar and Planetary Inst., Houston, Tex.
A COMPILATION OF INFORMATION AND DATA ON THE MANSON IMPACT STRUCTURE
Jack B. Hartung and Raymond R. Anderson 1988 37 p
(Contract NASw-4066)
(NASA-CR-183169; NAS 1.26:183169; LPI-TR-88-08) Avail: NTIS HC A03/MF A01 CSCL 08G

A problem for the impact hypothesis for the Cretaceous-Tertiary (K-T) mass extinction is the apparent absence of an identifiable

impact site. The Manson Impact Structure is a candidate because it is the largest recognized in the U.S.; it is relatively close to the largest and most abundant shocked quartz grains found at the K-T boundary; and its age is indistinguishable from that of the K-T boundary based on paleontological evidence, fission track dates, and preliminary Ar-40/Ar-39 measurements. The region of northwest central Iowa containing the Manson Impact Structure is covered by Quaternary glacial deposits underlain by Phanerozoic sedimentary rocks (mostly flat-lying carbonates) and Proterozoic red clastic, metamorphic, volcanic, and plutonic rocks. In a circular area about 22 miles (35 km) in diameter around Manson, Iowa, this normal sequence is absent or disturbed and near the center of the disturbed area granitic basement rocks have been uplifted some 20,000 ft (6000m). Attention was drawn to Manson initially by the unusual quality of the groundwater there. Within the structure three roughly concentric zones of rock associations have been identified: (1) displaced strata; (2) completely disrupted strata, and igneous and metamorphic rocks. Manson was established as an impact structure based on its circular shape, its central uplift, and the presence of shocked quartz within the granitic central uplift. A gravity survey identified locations of low-density brecciated rocks and high-density uplifted crystalline rocks, but the outer boundary of the structure could not be established. Aeromagnetic and ground magnetic surveys showed locations and depths of shallowly buried crystalline rock and the locations of faults. A refraction seismic survey identified the crystalline central uplift, determined that the average elevation of bedrock is 70 ft (20 m) higher outside the structure than within, and was used to map the bedrock topography within the structure. A connection between the Manson impact and the K-T boundary may be established or refuted through study of the impact energy, the impact time, and composition of host rock, possible impactors, and impact melts. Author

N88-30259# Teledyne Geotechnical, Alexandria, Va.
FINITE-DIFFERENCE SIMULATIONS OF RAYLEIGH-WAVE SCATTERING BY SHALLOW HETEROGENEITY Scientific Report No. 1, Feb. 1986 - Feb. 1988
Keith L. McLaughlin and Rong-Song Jih Nov. 1987 114 p
(Contract F19628-86-C-0054)
(AD-A194961; TGAL-87-02; AFGL-TR-87-0322) Avail: NTIS HC A06/MF A01 CSCL 08K

Rayleigh waves normally incident upon 2-D shallow heterogeneity are simulated by the linear finite-difference method to study attenuation, transmission, and reflection of Rayleigh waves and to measure the Rayleigh-to-P and -SV body wave conversion. Transmission, reflection, and scattering depend on the depth, average scale size of the heterogeneity and the amplitude of the spatial fluctuation of velocity. As expected, larger spatial variation in velocity attenuates Rayleigh waves more than smooth media and the attenuation is roughly proportional to the variance of the velocity fluctuation. The attenuation and scattering due to shallow heterogeneity is weaker than attenuation due to moderately rough topography. GRA

N88-30260*# Stanford Univ., Calif. Space, Telecommunications and Radioscience Lab.
SPECTRAL ANALYSIS OF THE ELATINA VARVE SERIES
R. N. Bracewell Feb. 1988 25 p
(Grant NGL-05-020-272)
(NASA-CR-183085; NAS 1.26:183085; CSSA-ASTRO-88-13)
Avail: NTIS HC A03/MF A01 CSCL 08G

The Elatina formation in South America, which provides a rich fossil record of presumptive solar activity in the late Precambrian, is of great potential significance for the physics of the sun because it contains luminae grouped in cycles of about 12, an appearance suggestive of the solar cycle. Here, the laminae are treated as varves laid down yearly and modulated in thickness in accordance with the late Precambrian sunspot activity for the year of deposition. The purpose is to present a simple structure, or intrinsic spectrum, that will be uncovered by appropriate data analysis. Author

N88-30488*# Arizona State Univ., Tempe. Dept. of Geology.
ERUPTIVE VISCOSITY AND VOLCANO MORPHOLOGY
Seth B. Posin and Ronald Greeley *In* Lunar and Planetary Inst., NASA MEVTV Program Working Group Meeting: Volcanism on Mars 1988 p 1-3 (For primary document see N88-30487 24-88)
Avail: NTIS HC A03/MF A01 CSCL 08K

N88-30490*# Naples Univ. (Italy).
LAVA THICKNESSES: IMPLICATIONS FOR RHEOLOGICAL AND CRUSTAL DEVELOPMENT
C. R. J. Kilburn and R. M. C. Lopes (London Univ. Observatory, England) *In* Lunar and Planetary Inst., NASA MEVTV Program Working Group Meeting: Volcanism on Mars 1988 p 9-11 Prepared in cooperation with Consiglio Nazionale delle Ricerche, Naples, Italy, and Old Royal Observatory, London, England (For primary document see N88-30487 24-88)
Avail: NTIS HC A03/MF A01 CSCL 08G

N88-30494*# Hawaii Univ., Honolulu. Inst. of Geophysics.
RIFTS OF DEEPLY ERODED HAWAIIAN BASALTIC SHIELDS: A STRUCTURAL ANALOG FOR LARGE MARTIAN VOLCANOES
Michael D. Knight, G. P. L. Walker, P. J. Mouginis-Mark, and Scott K. Rowland (Geological Survey, Menlo Park, Calif.) *In* Lunar and Planetary Inst., NASA MEVTV Program Working Group Meeting: Volcanism on Mars 1988 p 23-25 (For primary document see N88-30487 24-88)
Avail: NTIS HC A03/MF A01 CSCL 08G

N88-30496*# Jet Propulsion Lab., California Inst. of Tech., Pasadena.
SMALL-SCALE VOLCANIC LANDFORMS INDICATIVE OF DISTRIBUTARY TUBE SYSTEMS
E. Theilig *In* Lunar and Planetary Inst., NASA MEVTV Program Working Group Meeting: Volcanism on Mars 1988 p 31-32 (For primary document see N88-30487 24-88)
Avail: NTIS HC A03/MF A01 CSCL 08G

N88-30499# Joint Publications Research Service, Arlington, Va.
PHOTOCHEMISTRY OF IONOSPHERIC D-REGION WITH INJECTION OF NITROGEN OXIDES Abstract Only
S. I. Kozlov *In its* JPRS Report: Science and Technology. USSR: Space 26 Feb. 1988 p 12 Transl. into ENGLISH from Geomagnetizm i Aeronomiya (Moscow, USSR), v. 27, no. 3, May-Jun. 1987 p 383-387 Original language document was announced in IAA as A88-24681 (For primary document see N88-30498 24-88)
Avail: NTIS HC A04/MF A01

N88-30500# Joint Publications Research Service, Arlington, Va.
STRUCTURAL DYNAMICS OF HIGH-LATITUDE MAGNETOSPHERE DETERMINED FROM SOLAR ELECTRON DATA Abstract Only
V. A. Sergeyev, S. N. Kuznetsov, and Yu. V. Gotselyuk *In its* JPRS Report: Science and Technology. USSR: Space 26 Feb. 1988 p 12 Transl. into ENGLISH from Geomagnetizm i Aeronomiya (Moscow, USSR), v. 27, no. 3, May - Jun. 1987 p 440-447 (For primary document see N88-30498 24-88)
Avail: NTIS HC A04/MF A01

N88-30502# Joint Publications Research Service, Arlington, Va.
USING NONSTATIONARY MODELS OF THE ATMOSPHERE TO DESCRIBE SATELLITE DRAG Abstract Only
O. A. Malkin and V. A. Lupovka *In its* JPRS Report: Science and Technology. USSR: Space 26 Feb. 1988 p 13 Transl. into ENGLISH from Izvestiya Vysshikh Uchebnykh Zavedeniy: Geodeziya i Aerofotosyemka (Moscow, USSR), no. 2, Mar. - Apr. 1987 p 59-69 Original language document was announced in IAA as A88-10906 (For primary document see N88-30498 24-88)
Avail: NTIS HC A04/MF A01

N88-30503# Joint Publications Research Service, Arlington, Va.
APPROXIMATION OF ATMOSPHERIC DENSITY BY CHEBYSHEV POLYNOMIALS IN PREDICTING MOTION OF LOW ARTIFICIAL EARTH SATELLITES Abstract Only
V. A. Lupovka *In its* JPRS Report: Science and Technology. USSR: Space 26 Feb. 1988 p 13-14 Transl. into ENGLISH from Izvesitya Vysshikh Uchebnykh Zavedeniy: Geodeziya i Aerofotosyemka (Moscow, USSR), no. 3, May - Jun. 1987 p 70-75 Original language document was announced in IAA as A88-13668 (For primary document see N88-30498 24-88)
Avail: NTIS HC A04/MF A01

N88-30513# Joint Publications Research Service, Arlington, Va.
MODEL REPRESENTATION OF ELECTRON CONCENTRATION DISTRIBUTION IN OUTER MIDDLE-LATITUDE IONOSPHERE USING DATA FROM INTERCOSMOS-19 ARTIFICIAL EARTH SATELLITE Abstract Only
N. P. Benkova, A. D. Legenka, N. A. Kochenova, M. N. Fatkullin, and M. D. Fligel *In its* JPRS Report: Science and Technology. USSR: Space 26 Feb. 1988 p 17 Transl. into ENGLISH from Kosmicheskiye Issledovaniya (Moscow, USSR), v. 25, no. 3, May - Jun. 1987 p 410-420 (For primary document see N88-30498 24-88)
Avail: NTIS HC A04/MF A01

N88-30514# Joint Publications Research Service, Arlington, Va.
RING CURRENT ROLE IN DYNAMICS OF FLUCTUATING ELECTRON AND ION FLUXES IN LOW-LATITUDE MAGNETOSPHERE Abstract Only
N. M. Shyutte and N. I. Izhovkina *In its* JPRS Report: Science and Technology. USSR: Space 26 Feb. 1988 p 17 Transl. into ENGLISH from Kosmicheskiye Issledovaniya (Moscow, USSR), v. 25, no. 3, May - Jun. 1987 p 421-425 (For primary document see N88-30498 24-88)
Avail: NTIS HC A04/MF A01

N88-30515# Joint Publications Research Service, Arlington, Va.
PLASMA OF EARTH'S MAGNETOSPHERE RING CURRENTS. MODEL COMPARED WITH RESULTS OF AMPTE/CCE EXPERIMENT Abstract Only
V. V. Temnyy *In its* JPRS Report: Science and Technology. USSR: Space 26 Feb. 1988 p 17-18 Transl. into ENGLISH from Kosmicheskiye Issledovaniya (Moscow, USSR), v. 25, no. 3, May - Jun. 1987 p 426-438 (For primary document see N88-30498 24-88)
Avail: NTIS HC A04/MF A01

N88-30516# Joint Publications Research Service, Arlington, Va.
EXPERIMENTAL PROOF OF QUASILONGITUDINAL PROPAGATION OF LOW-FREQUENCY WAVES IN MIDDLE LATITUDES IN UPPER IONOSPHERE Abstract Only
V. I. Altyntseva, V. F. Gubskiy, and V. I. Larkina *In its* JPRS Report: Science and Technology. USSR: Space 26 Feb. 1988 p 18 Transl. into ENGLISH from Kosmicheskiye Issledovaniya (Moscow, USSR), v. 25, no. 3, May - Jun. 1987 p 464-465 Original language document was announced in IAA as A87-47565 (For primary document see N88-30498 24-88)
Avail: NTIS HC A04/MF A01

N88-30517# Joint Publications Research Service, Arlington, Va.
ONE EQUATORIAL ANOMALY IN NIGHTTIME IONOSPHERIC F REGION Abstract Only
G. V. Givishvili, N. A. Kochenova, L. N. Leshchenko, and M. D. Fligel *In its* JPRS Report: Science and Technology. USSR: Space 26 Feb. 1988 p 18 Transl. into ENGLISH from Kosmicheskiye Issledovaniya (Moscow, USSR), v. 25, no. 3, May - Jun. 1987 p 466-467 Original language document was announced in IAA as A87-47566 (For primary document see N88-30498 24-88)
Avail: NTIS HC A04/MF A01

N88-30526# Joint Publications Research Service, Arlington, Va.
POSSIBILITIES OF DETERMINING VERTICAL PROFILES OF MICROPHYSICAL CHARACTERISTICS OF STRATOSPHERIC AEROSOL USING SPACE MEASUREMENTS OF TRANSPARENCY AND SOLAR HALO Abstract Only
P. Yu. Romanov, V. V. Rozanov, and Yu. M. Timofeyev *In its* JPRS Report: Science and Technology. USSR: Space 26 Feb. 1988 p 22-23 Transl. into ENGLISH from Issledovaniye Zemli iz Kosmosa (Moscow, USSR), no. 3, May - Jun. 1987 p 54-63 (For primary document see N88-30498 24-88)
Avail: NTIS HC A04/MF A01

47 METEOROLOGY AND CLIMATOLOGY

Includes weather forecasting and modification.

N88-30261# Air Force Inst. of Tech., Wright-Patterson AFB, Ohio.
DOPPLER RADAR ANALYSIS OF COASTAL MARINE ATMOSPHERIC BOUNDARY LAYER STRUCTURE DURING A COLD AIR OUTBREAK M.S. Thesis
Michael N. Jones 1988 131 p
(AD-A196023; AFIT/CI/NR-88-1) Avail: NTIS HC A07/MF A01 CSCL 17I

This study documents and interprets the spatial and temporal variation of Marine Atmospheric Boundary Layer (MABL) structure during the latter stages of a Cold Air Outbreak (CAO) along the Outer Banks of North Carolina, 8 March 1986. Two C-band pulsed Doppler radars, one at Ocracoke and the other at Cape Hatteras, were used to collect reflectivity and radial velocity data in the chaff-filled MABL. The single Doppler analysis technique known as Velocity Azimuth Display, henceforth VAD (Browning and Wexler, 1968), was used to attain numerical values for a variety of kinematic properties. Time-height plots of horizontal wind spread, vertical velocity, horizontal divergence and deformation were constructed to depict the temporal variation of the MABL. Horizontal wind speed and direction versus altitude were plotted for each VAD analysis in order that anomalies in the MABL wind profiles may be identified and explained. The VAD analysis radius was varied between 5 and 15 kilometers so that spatial distribution of the wind field could also be observed. Chaff was dispersed by aircraft at a distance equivalent to 40 minutes travel distance upwind from the radar network. GRA

N88-30262# Presbyterian-St. Lukes Hospital, Chicago, Ill. Dept. of Pathology.
TEMPERATURE PROFILE CONSTRUCTION METHODS: AN EVALUATION Final Report, 1 Oct. 1986 - 30 Sep. 1987
William T. Thompson Dec. 1987 64 p Sponsored by Navy
(AD-A195919; NEPRF-TR-87-04) Avail: NTIS HC A04/MF A01 CSCL 04B

This report evaluates two different methods for construction of vertical temperature profiles from analysis fields of numerical weather prediction models. Ship observations are sparse and satellite-derived profiles lack sufficient vertical resolution and accuracy near the surface. An alternative method involves extracting temperature values from numerical weather prediction (NWP) model analysis fields at standard levels. The locations of the weather station ships used in the evaluation are shown in Figure 51. In Table 1, the cases are categorized in terms of the ship used, the date time group, which pseudo-sounding was most representative of the ship sounding, and whether the boundary layer was stably or unstably stratified. GRA

N88-30263# Instituto de Pesquisas Espaciais, Sao Jose dos Campos (Brazil).
SOME RESULTS FROM THE AMAZON FOREST MICROMETEOROLOGICAL EXPERIMENT
Y. Viswanadham, V. P. SilvaFilho, L. D. A. Sa, A. O. Manzi, L. C. B. Molion, R. G. B. Andre, and J. L. M. Nogueira Aug. 1988 7 p Presented at the International Conference on Tropical

Micrometeorology and Air-Pollution, New Delhi, India, Feb. 1988 (INPE-4631-PRE/1346) Avail: NTIS HC A02/MF A01

This extended abstract presents some information about the radiation and energy balance parameters, and the Deacon numbers as a function of the Richardson gradient number. Author

N88-30264# Naval Research Lab., Washington, D.C. Radar Propagation Staff.

ANALYSIS OF ENVIRONMENTAL PARAMETERS FROM THE PANAMA CITY TOWER RADAR EXPERIMENT Interim Report, Jan. 1986 - Jun. 1987

Lee U. Martin and Dennis B. Trizna 12 Apr. 1988 31 p (AD-A194994; NRL-MR-6100) Avail: NTIS HC A03/MF A01 CSCL 17I

Wind and wave data have been analyzed for the Panama City Tower Radar Experiment performed by Keller, Plant and Weissmann (1985), for comparison with radar data. Time series of wave height records were analyzed for a variety of definitions of wave height, with the resultant RMS heights calibrated against spectrum analysis results. As a result of the consideration of the wave spectra and wind history, the data are sorted into three types: equilibrium, fetch limited, and transient in time. Tracking the series of cross section-wind speed pairs for each data set over a few hour period indicates a well defined but different sequential development from one set to the next. While plotting of all the data produces the broad scatter previously reported, little scatter occurs about each individual track. This indicates that the specific sea surface characterization is primarily responsible for determining magnitudes of RCS, and that wind speed is only an implicit variable. Flow distortion effects are suggested as responsible for unusually high radar cross sections (RCS) previously reported for northerly winds, rather than atmospheric stability effects which were suggested originally. GRA

N88-30265# World Meteorological Organization, Geneva (Switzerland).

[ACTIVITIES REPORT OF THE WORLD METEOROLOGICAL ORGANIZATION] Annual Report, 1987

1988 223 p

(WMO-689; ISBN-9-26-310689-4; ETN-88-92716) Copyright Avail: NTIS MD A01; print copy available at World Meteorological Organization, Case Postale no. 5, CH-1211 Geneva 20, Switzerland

The status of the World Meteorological Organization's World Weather Watch, World Climate, research and development, applications of meteorology, hydrology and water resources, education and training, technical cooperation, and regional programs is summarized. ESA

N88-30266*# National Aeronautics and Space Administration, Washington, D.C.

A DIGITAL SIMULATION TECHNIQUE FOR THE DRYDEN ATMOSPHERIC MODEL

Zhenyan Zhao, Yelun Xiao, and Yijian Shi Aug. 1988 20 p Transl. into ENGLISH from Acta Aeronautica et Astronautica Sinica (Peoples Republic of China), v. 7, no. 5, Oct. 1986 p 433-443 Original language document was announced in IAA as A87-24715 Transl. by SCITRAN, Inc., Santa Barbara, Calif. Original document was prepared by Beijing Inst. of Aeronautics and Astronautics (Peoples Republic of China)

(Contract NASw-4307)

(NASA-TT-20342; NAS 1.77:20342) Avail: NTIS HC A03/MF A01 CSCL 04B

The Dryden model is usually used in studying the response of flight vehicles to atmospheric turbulence. For a modern flight simulator, it is necessary to generate random winds (in Dryden model or sometimes others) with a digital computer. A theoretically strict new method to meet this purpose is proposed. By this method, a three dimensional atmospheric turbulence can be obtained which contains three components of wind velocity and three components of wind velocity gradient. The reliability of this method is checked by comparing the theoretical autocorrelation value. A numerical example has shown a satisfactory result. Finally, some proposals concerning the use of this mathematical model in a flight simulator are given. Author

N88-30267# Washington Univ., Seattle. Dept. of Atmospheric Sciences.

PASSIVE MICROWAVE MEASUREMENTS OF WATER VAPOR FIELDS AND RAIN FOR LOCATING FRONTS IN CYCLONIC STORMS Final Report, 1 Jul. 1986 - 31 Aug. 1987

Kristina B. Katsaros, Iftekhar A. Bhatti, Lynn A. McMurdie, and Grant W. Petty Mar. 1988 50 p

(Contract N00014-86-K-0453; R35-82)

(AD-A195632; NEPRF-CR-88-01) Avail: NTIS HC A03/MF A01 CSCL 04B

This report describes some basic research techniques and algorithms developed to diagnose fronts in cyclonic storms over the ocean with passive microwave data. The need for this research stems from the limited availability of reliable weather reports over the ocean, and the occasional disruption of weather map transmissions. In earlier work it was found that strong gradients in integrated atmospheric water vapor are good indicators of surface locations of fronts in midlatitude cyclones over the oceans. A second significant indicator of frontal activity is precipitation. Therefore, methods have been developed for flagging strong gradients in integrated atmospheric water vapor (WVG-flag) and the presence of rain by using data from the Scanning Multichannel Microwave Radiometer (SMMR) aboard polar-orbiting SEASAT and Nimbus-7 satellites. The data were not received in real time, but were analyzed from archived tapes. Examination of 65 frontal systems showed the water vapor gradient flag to catch 86 pct of the fronts while the precipitation flagged 90 pct. Each flag emphasizes different portions of the cyclone and are therefore complimentary. Ultimately these techniques are intended for operational use with data from the Special Sensor Microwave Imager (SSM/I) which was launched in June 1987 on a satellite in the Defense Meteorological Satellite Program (DMSP). Such data can be received in real time directly by ships at sea. GRA

N88-30268# Army Missile Command, Redstone Arsenal, Ala.

ENERGY BUDGET AND GROUND TEMPERATURES IN HOT REGIONS Technical Report, for Period Ending Feb. 1988

Dorathy Anne Stewart Jun. 1988 44 p

(AD-A196298; AD-E951149; AMSMI/TR-RD-RE-88-1) Avail: NTIS HC A03/MF A01 CSCL 04B

This report discusses characteristics of the atmospheric energy balance which contribute to the production of high surface air temperatures and high ground temperatures. This discussion is followed by climatological information. The hottest regions are in northwestern Africa, the Arabian Peninsula, part of Pakistan, and a small part of the southwestern United States. Author (GRA)

N88-30269# Colorado State Univ., Fort Collins. Dept. of Atmospheric Science.

CLOUD/MESOSCALE MODEL DEVELOPMENT AND APPLICATION STUDIES Final Report, 11 Oct. 1983 - 20 Jun. 1987

William R. Cotton and Gregory J. Tripoli 30 Sep. 1987 150 p

(Contract F19628-84-C-0005; AF Proj. 6670)

(AFGL-TR-87-0219) Avail: NTIS HC A07/MF A01 CSCL 04B

A two dimensional and/or three dimensional model study to define potential for aircraft icing was performed. A one dimensional version of the turbulence closure model and development of a cirrus cloud model is presented. The forecasting and diagnosis of extreme wind shear and turbulence associated with thunderstorms was also studied. A summary is presented of the CSU Regional Atmospheric Modeling System. Author

N88-30270# Wisconsin Univ., Madison. Space Science and Engineering Center.

VALIDATE ALGORITHMS FOR THE DETERMINATION OF RAINFALL RATES FROM SSM/I MICROWAVE SATELLITE IMAGERY Progress Report, Feb. - Mar. 1988

William S. Olson 5 May 1988 7 p
(Contract N00014-86-K-2001)
(AD-A195428) Avail: NTIS HC A02/MF A01 CSCL 17I

Having completed all software necessary for the validation, we are performing the validation of the Hughes rain retrieval algorithm utilizing validation sites from which we have received comparative radar data. So far we have received radar data from sites in the United Kingdom; Marshall, Colorado; and Cape Canaveral, Florida covering the summer and some of the fall months of 1987. Based on the recommendations of Dr. Gene Poe of NRL, and auxiliary information from James Peirce of Hughes Aircraft Co., we have made long-and cross-track shifts of the SSM/I data and derived products (EDR's) to account for data earth-location errors. Our own investigations have shown that without such adjustments, rain signatures in the satellite data do not correlate with regions of precipitation, which often are relatively small scale. Earth-location errors have been observed to be as great as 25 km downtrack and 12.5 km cross-track (in the direction of scan motion) in the U.K. region on ascending passes, based on comparisons with coastline geography. GRA

N88-30271# Control Data Corp., Minneapolis, Minn. Meteorology Research Center.
UTILIZATION OF A SINGLE CLEAR-AIR DOPPLER RADAR BEAM TO MEASURE VERTICAL DIVERGENCE
W. L. Clark, G. D. Nastrom, K. S. Gage, J. L. Green, and R. G. Strauch 23 Mar. 1988 3 p
(Contract F49620-86-C-0027; Grant NSF ATM-85-12513)
(AD-A195543; AFOSR-88-0496TR) Avail: NTIS HC A02/MF A01 CSCL 17I

Clear-air Doppler radars, also called wind profilers, have the almost unique capability to profile the vertical air motion over the radar on a nearly continuous basis. Clark et al., (1986) point out that partial of w with respect to z, the vertical divergence component, may easily be obtained from these measurements through simple height differencing. This technique is sensitive to all scales of motion and should be complimentary to values of horizontal velocity divergence determined from the NWS rawinsonde network or those obtained from the future clear-air Doppler radar networks (see Chadwick and Hassel, 1987), using techniques similar to those of Zamora et al., (1987). GRA

N88-29727*# National Aeronautics and Space Administration. Langley Research Center, Hampton, Va.
A SUMMARY OF ATMOSPHERIC TURBULENCE MEASUREMENTS WITH SPECIALLY-EQUIPPED AIRCRAFT IN THE US
H. N. Murrow *In* AGARD, The Flight of Flexible Aircraft in Turbulence: State-of the Art in the Description and Modelling of Atmospheric Turbulence Dec. 1987 11 p (For primary document see N88-29725 24-01)
Copyright Avail: NTIS HC A09/MF A01 CSCL 04B

N88-29728# Royal Aircraft Establishment, Bedford (England).
MEASUREMENT AND ANALYSIS OF LOW ALTITUDE ATMOSPHERIC TURBULENCE OBTAINED USING A SPECIALLY INSTRUMENTED GNAT AIRCRAFT
G. W. Foster and J. G. Jones *In* AGARD, The Flight of Flexible Aircraft in Turbulence: State-of-the Art in the Description and Modelling of Atmospheric Turbulence Dec. 1987 45 p (For primary document see N88-29725 24-01)
Copyright Avail: NTIS HC A09/MF A01

N88-29733# National Aerospace Lab., Amsterdam (Netherlands).
ACQUISITION OF GUST STATISTICS FROM AIDS-RECORDED DATA
J. B. deJonge, A. J. P. vanderWekken, and R. Noback *In* AGARD, The Flight of Flexible Aircraft in Turbulence: State-of-the-Art in the Description and Modelling of Atmospheric Turbulence Dec. 1987 14 p Previously announced as N88-14586 (For primary document see N88-29725 24-01)
Copyright Avail: NTIS HC A09/MF A01

N88-29734# Office National d'Etudes et de Recherches Aerospatiales, Paris (France).
EXTREME GUSTS DISTRIBUTION
Gabriel Coupry *In* AGARD, The Flight of Flexible Aircraft in Turbulence: State-of-the-Art in the Description and Modelling of Atmospheric Turbulence Dec. 1987 9 p In FRENCH; ENGLISH summary Original language document was announced in IAA as A87-44328 (For primary document see N88-29725 24-01)
Copyright Avail: NTIS HC A09/MF A01

48 OCEANOGRAPHY

Includes biological, dynamic, and physical oceanography; and marine resources.

For related information see also *43 Earth Resources and Remote Sensing.*

N88-30272# Naval Postgraduate School, Monterey, Calif.
AN ANALYSIS OF RESULTS OF A HIGH-RESOLUTION WORLD OCEAN CIRCULATION MODEL M.S. Thesis
Wesley A. Barton Mar. 1988 163 p
(AD-A195760) Avail: NTIS HC A08/MF A01 CSCL 08C

Results of a highly vectorized and multitasked model of the world ocean circulation were analyzed. This model which uses realistic physics, geometry, and forcing on a high-resolution grid, was run on the NCAR Cray X-MP/48 using a robust-diagnostic strategy. Twenty years of model integration using one-half degree horizontal resolution and 20 levels of vertical resolution were accomplished after 200 wall-clock hours at a maximum FORTRAN performance speed of 450 megaflops. Seven key regions of the world ocean were analyzed using an ocean model processor. A representation of the global ocean circulation emerged that compared well with observations and that included strong advective features, fronts, and subtropical meanders. A diagnostic analysis program was developed to analyze meridional heat and volume transports. The results in all basins appear to be reasonable when compared to the results of other studies. For example, an anomalous northward heat transport of 3.8 x 10 to the 14th power W at 30 deg in the South Atlantic compares favorably with the estimate of 4.2 x 10 to the 14th power at 32 deg S by Bennet (1978) using hydrographic data. The results of simulations conducted in this study can be compared and contrasted against the results of future eddy-resolving simulations. GRA

N88-30273 Exeter Univ. (England).
ROSSBY WAVES IN MID-LATITUDE OCEANS Ph.D. Thesis
Rosemary Grace Wood 1987 163 p
Avail: Univ. Microfilms Order No. BRDX81111

This work is concerned with the generation and propagation of Rossby waves at mid-latitudes. It comprises three main areas of study. The first investigates the generation of linear, baroclinic Rossby waves by an imposed current distribution, in a reduced gravity ocean, both with and without an eastern coast. In the next study, the generation of linear baroclinic Rossby waves which either translates at a constant speed or oscillates sinusoidally in latitudinal position is examined. Finally, open boundary conditions are discussed in relation to outgoing Rossby waves incident at the edge of a numerical model. Dissert. Abstr.

N88-30525# Joint Publications Research Service, Arlington, Va.
EVOLUTION OF THERMAL STRUCTURE OF BENGUELA UPSWELLING SYSTEM ACCORDING TO SATELLITE AND SHIPBOARD DATA Abstract Only
A. S. Kazmin, R. Legeckis, and K. N. Fedorov *In its* JPRS Report: Science and Technology. USSR: Space 26 Feb. 1988 p 22 Transl. into ENGLISH from Issledovaniye Zemli iz Kosmosa (Moscow, USSR), no. 3, May - Jun. 1987 p 26-37 (For primary document see N88-30498 24-88)
Avail: NTIS HC A04/MF A01

N88-30534# Joint Publications Research Service, Arlington, Va.
KOSPAS-SARSAT SATELLITES USED FOR OCEAN CURRENT STUDY Abstract Only
Yu. Kolesnikov *In its* JPRS Report: Science and Technology. USSR: Space 26 Feb. 1988 p 26 Transl. into ENGLISH from Sotsialisticheskaya Industriya (Moscow, USSR), 2 Dec. 1987 p 4
(For primary document see N88-30498 24-88)
Avail: NTIS HC A04/MF A01

51 LIFE SCIENCES (GENERAL)

N88-30274*# California State Univ., Northridge.
SEMI-MICRODROPLET ASSAY FOR CELL ADHESION MOLECULES M.S. Thesis
Lawrence Shinzo Tawa Aug. 1988 9 p
(Grant NAG2-499)
(NASA-CR-183139; NAS 1.26:183139) Avail: NTIS HC A02/MF A01 CSCL 06C

A new cell-to-cell adhesion assay was devised. Using dissociated embryos of the sea urchin, this procedure involves rotating a 0.100 ml suspension of single cells with 0.100 ml of the solution to be tested in the bulb portion of a transfer pipet with the tip removed. After 1 hour of rotation at 60 rpm at 15 C, the contents of each bulb were transferred into individual wells of a 96 well flat bottom plate. After the plate was incubated for 1 hour at 15 C, black and white photographs were taken with a 35 mm camera attached to an inverted photomicroscope. Examining a proof sheet of the negatives directly allowed a rapid evaluation of suspected cell adhesion promoting factors. A ranking system was used to evaluate all samples. The assay was tested by examining the effect of specific solutions on the aggregation of single cells obtained from dissociated 23 hour embryos. Author

N88-30275*# California State Univ., Northridge.
SCANNING ELECTRON MICROSCOPY STUDY OF ADHESION IN SEA URCHIN BLASTULAE M.S. Thesis
Susan D. Crowther May 1988 5 p
(Grant NAG2-499)
(NASA-CR-183136; NAS 1.26:183136) Avail: NTIS HC A02/MF A01 CSCL 06C

The dissociation supernatant (DS) isolated by disaggregating Strongylocentrotus purpuratus blastulae in calcium- and magnesium-free seawater specifically promotes reaggregation of S. purpuratus blastula cells. The purpose of this study was to use scanning electron microscopy to examine the gross morphology of aggregates formed in the presence of DS to see if it resembles adhesion in partially dissociated blastulae. A new reaggregation procedure developed here, using large volumes of cell suspension and a large diameter of rotation, was utilized to obtain sufficient quantities of aggregates for scanning electron microscopy. The results indicate that aggregates formed in the presence of DS resemble partially dissociated intact embryos in terms of the direct cell-cell adhesion observed. DS did not cause aggregation to form as a result of the entrapment of cells in masses of extracellular material. These studies provide the groundwork for further studies using transmission electron microscopy to more precisely define the adhesive contacts made by cells in the presence of the putative adhesion molecules present in DS. Author

N88-30276*# California State Univ., Northridge.
IMMUNOFLUORESCENCE LOCALIZATION OF DISSOCIATION SUPERNATANT AND EXTRACELLULAR MATRIX COMPONENTS IN LYTECHINUS PICTUS SECTIONED EMBRYOS M.S. Thesis
Ana Leticia GarciaFlack May 1988 5 p
(Grant NAG2-499)
(NASA-CR-183137; NAS 1.26:183137) Avail: NTIS HC A02/MF A01 CSCL 06C

Indirect immunofluorescence was used to localize specific extracellular components in embryos of the sea urchin Lytechinus pictus. Hyalin and S2 (a group of components found in the disaggregation supernatant from Strongylocentrotus purpuratus blastulae) were uniformly present at all stages (unfertilized up to 32 hr) except hyalin could not be detected at the 12 hour early blastula stage. Laminin was found in 16 cell, 32 cell, 6 hour, 18 hour, 24 hour, and 32 hour stages, with especially bright fluorescence at 18 hours. Collagen I was present at all stages (freshly fertilized up to 32 hour) except little was detected at 12 hours. Fibronectin was uniformly present in blastocoelar fibers stained with anto-collagen I and anti-fibronectin. These results were compared with those for S. purpuratus to produce an overview of the localization of specific extracellular matrix components during development of two species of sea urchins. The results set the stage for future studies that will examine the function of these components at the various developmental stages. Author

N88-30277# Kansas Univ., Lawrence. Dept. of Chemistry.
CYTOCHROME ELECTRON TRANSFER AND BIOMOLECULAR ELECTRONICS Annual Report, Nov. 1987 - Jun. 1988
George S. Wilson and Michael A. Cusanovich 22 Jun. 1988 6 p
(Contract N00014-88-K-0055; Proj. RR0-4108)
(AD-A195482) Avail: NTIS HC A02/MF A01 CSCL 06A

This research pursues the previous observation that films of cytochrome c3 deposited on a gold substrate undergo a change in resistivity of ten orders of magnitude when this tetraheme protein passes from a fully oxidized to a fully reduced state. This unusual behavior appears to be attributable to the ability of the four hemes to communicate through intramolecular as well as intermolecular electron transfer. To understand this phenomenon in more detail, four cytochromes c3 with differing physical properties have been selected: (1) D. vulgaris (Miyazaki); (2) D. vulgaris (Hildenborough); (3) D. sulfuricans (Norway); and (4) D. gigas. The macroscopic redox potentials for each of the hemes in the four proteins have been determined. Electrostatic field maps based on the X-ray structures of the Norway and Miyazaki proteins have been prepared to assist in the design of homogeneous and heterogeneous electron transfer experiments. In the next year, the electrical properties of cytochrome films will be evaluated through Hall effect measurements in particular to establish whether the conductivity is ionic or electronic. GRA

52 AEROSPACE MEDICINE

Includes physiological factors; biological effects of radiation; and effects of weightlessness on man and animals.

N88-30278# Army Research Inst. of Environmental Medicine, Natick, Mass.
ACCIDENTAL HYPOTHERMIA
Daniel F. Danzl, Robert S. Pozos, and Murray P. Hamlet 3 Mar. 1988 113 p
(AD-A194967) Avail: NTIS HC A06/MF A01 CSCL 06E

Hypothermia has played a major role in the medical statistics from many armies deploying in a cold environment. The loss of body heat, either from the decreased heat production, increased heat loss, or alterations in thermoregulation are important in the epidemiology of this injury. Cold appears to protect various portions of the body from the decreasing cardiovascular capability of delivering nutrients and oxygen. Recognition of these patients as they are severely hypothermic is the key to survival. Emergency Department of Management involves fluid resuscitation, respiratory support, active core rewarming and management of electrolytes. Cardiovascular support is critical to long-term management and a successful outcome. Prevention is the key to individuals exposed to a high threat environment. GRA

N88-30279# Naval Submarine Medical Center, Groton, Conn.
VISUAL SENSITIVITIES UNDER REDUCED OXYGEN Interim Report
S. M. Luria and Nancy Morris 27 Jan. 1988 19 p

(AD-A195628; NSMRL-1108) Avail: NTIS HC A03/MF A01 CSCL 06D

Thirteen subjects were confined in a hypobaric chamber for 15 days, and their scotopic sensitivity and field-of-view were measured twice a day. The oxygen concentration in the nitrogen-oxygen atmosphere was changed every three days in this sequence: 21 pct, 17 pct, 21 pct, 13 pct, and 21 pct. The barometric pressure was always equivalent to sea-level, except for the final 7 hours of exposure to 17 pct oxygen when it was reduced to 576 torr. The atmosphere was contaminated with 0.9 pct carbon-dioxide throughout the confinement. Neither visual function was degraded by the lowered oxygen levels. GRA

N88-30280# School of Aerospace Medicine, Brooks AFB, Tex.
CENTRAL SEROUS CHORIORETINOPATHY IN USAF AVIATORS: A REVIEW Final Report, Dec. 1986 - Dec. 1987
Robert P. Green, Jr., Dean W. Carlson, J. P. Dieckert, and Thomas J. Tredici Mar. 1988 20 p
(AD-A195697; USAFSAM-TR-87-34) Avail: NTIS HC A03/MF A01 CSCL 06E

Idiopathic central serous chorioretinopathy (ICSC) is an uncommon disease with the potential to cause loss of visual acuity, decreased color vision, and decreased depth perception. These visual changes may become permanent and require removal of aviators from flight status. This study reviews 55 eyes of 47 USAF aviators with ICSC examined at the United States Air Force School of Aerospace Medicine (USAFSAM), Brooks Air Force Base, Texas. Clinical and aeromedical findings, both on initial and on follow-up ophthalmic examination were studied. Ninety-seven percent of aviators otherwise medically qualified were ultimately returned to flight status. Overall, 51 percent had recurrent episodes, 17 percent had bilateral disease, and 13 percent underwent laser photocoagulation. Visual acuity correlated with active disease, and there was a trend toward poor stereopsis and diminished color vision with worsening visual acuity. Eighty-six percent attained a final visual acuity of 20/20 or better. On final examination, 90 percent had normal stereopsis, 87 percent had normal color vision, and 49 percent had a normal central visual field. Eyes with recurrent disease tended to have degraded final visual acuity, stereopsis, color vision, and central visual field. GRA

N88-30281* National Aeronautics and Space Administration, Washington, D.C.
AEROSPACE MEDICINE AND BIOLOGY: A CONTINUING BIBLIOGRAPHY WITH INDEXES (SUPPLEMENT 315)
Oct. 1988 71 p
(NASA-SP-7011(315); NAS 1.21:7011(315)) Avail: NTIS HC A04; NTIS standing order as PB88-912300. $9.00 domestic, $18.00 foreign CSCL 06E

This bibliography lists 211 reports, articles and other documents introduced into the NASA scientific and technical information system in September, 1988. Author

N88-30282# Air Force Inst. of Tech., Wright-Patterson AFB, Ohio.
COMPARISON OF MORNING WITH AFTERNOON NITROGEN ELIMINATION IN RESTING SUBJECTS BREATHING 100 PERCENT OXYGEN M.S. Thesis
Grant A. Brown 1988 49 p
(AD-A196191; AFIT/CI/NR-88-23) Avail: NTIS HC A03/MF A01 CSCL 06D

The purpose of this study was to compare morning with afternoon nitrogen elimination rates in subjects breathing 100 percent oxygen. Less nitrogen elimination during the morning could possibly account for the higher incidence of altitude-induced decompression sickness reported during the morning. No difference was noted between the volume of nitrogen eliminated in the morning or afternoon sessions. However, significant correlations were noted between nitrogen elimination and physiological parameters associated with stress (e.g., increased heart rate and increased carbon dioxide elimination) implying that psychological and metabolic factors may influence the rate of nitrogen elimination. These data suggest that there is no diurnal variation in the effectiveness of breathing 100 percent oxygen as a means of denitrogenation. The increased incidence of DCS during the morning hours must therefore be due to other factors. GRA

N88-30283# Technion - Israel Inst. of Tech., Haifa.
MODELS OF CEREBRAL-BODY PERFUSION AND CEREBRAL CHEMICAL TRANSPORT Annual Report, Oct. 1986 - Oct. 1987
S. Sorek, J. Bear, and M. Feinsod Mar. 1988 71 p
(Grants AF-AFOSR-0320-86; AF-AFOSR-0233-85)
(AD-A194945; SR-3) Avail: NTIS HC A04/MF A01 CSCL 06D

In this research, a sequence of models is constructed to simulate the movement of fluids and chemicals in the cerebrovascular system. One model simulates the nonsteady response to perfusion in various sections of the brain. In a second model certain relevant parts of the body are added to form a single brain-body model. A third model simulates the transport of selected chemical components through the cerebrovascular system. Predictions derived from the brain model were shown to be well within the range of available clinical observations. The brain-body model describes the interaction between the cerebral, the cardiovascular and the respiration systems. It is excited by expiration/inspiration fluxes and accounts for the effects of hydrostatic, environmental pressures, flight maneuvers with excessive (head to bottom) gravity acceleration and resuscitation procedures. In simulating chemical processes in the brain, the model accounts for carbon dioxide, bicarbonate, and hydrogen, as they are transport by perfusion and diffusion in the presence of chemical reactions. This model also focuses on the flow control between brain arteries and capillaries, due to changes in CO2 concentration. GRA

N88-30284# Louvain Univ. (Belgium).
CENTRAL ADRENERGIC RECEPTORS AS MEDIATORS OF CENTRAL RESPONSE TO STRESS: STUDY WITH POSITRON EMISSION TOMOGRAPHY (PET) Final Scientific Report, 30 Sep. 1986 - 29 Sep. 1987
Andre M. Goffinet 19 Feb. 1988 9 p
(AD-A194947) Avail: NTIS HC A02/MF A01 CSCL 06D

This report describes initial studies designed to investigate the effects of a high degree of neurological alertness on brain metabolism. Positron emission tomography (PET) was used to quantitate brain metabolism using fluorodeoxyglucose (FDG) as an indicator of glucose uptake during mental stimulation provided by playing a video game (Mooncrash) for 30 minutes. Brain metabolism in 22 regions during neurological alertness was compared with the resting state. In most subjects there was a marked increase in brain metabolism with stimulation, however there was tremendous variability in brain metabolism in the eight subjects. Consistent patterns of activation were found with maximal activation in primary visual cortex, followed by parieto-occipital cortex, cerebellum and thalamus. GRA

N88-30285# School of Aerospace Medicine, Brooks AFB, Tex.
A FIELD STUDY ON SOFT CONTACT LENS WEAR IN USAF MILITARY TRANSPORT AIRCRAFT Progress Report, May 1985 - Jan. 1987
Richard J. Dennis, William J. Flynn, Carolyn J. Oakley, and Thomas J. Tredici Apr. 1988 24 p
(AD-A195962; USAFSAM-TR-88-4) Avail: NTIS HC A03/MF A01 CSCL 06J

Contact lens wear as an alternative to spectacles for the correction of refractive errors in USAF aircrew members remains a controversial issue. Military transport aircrew must contend with reduced oxygen levels (typical cabin pressures of 5,000 to 8,000 ft), low relative humidity (10 to 15 percent), cigarette smoke, and fatigue and stress on long missions. Ten subjects wearing soft contact lenses and 6 control subjects not wearing contact lenses were evaluated visually and with a slit lamp onboard a C-5 aircraft on a routine mission to PACAF. Soft contact lens wearers noted no significant loss of visual acuity or contrast sensitivity during the flights. Some measures of corneal physiological stress (conjunctival injection, tear debris, etc.) were evaluated in both

contact lens wearers and controls. Lens dehydration from the low relative humidity may have been the primary cause of the corneal physiological stress in the contact lens wearers. The results indicate that although there are increased physiological stresses on the cornea in the aircraft environment, there was not sufficient degradation in visual performance or lens comfort to preclude soft contact lens wear in military transport aircraft. GRA

N88-30286# North Carolina Univ., Chapel Hill.
EVALUATION OF THE POTENTIAL HEALTH HAZARDS ASSOCIATED WITH THE MACHINING OF CARBON FIBER COMPOSITES M.S. Thesis Final Report
Michael A. Zustra 1987 79 p
(AD-A194835) Avail: NTIS HC A05/MF A01 CSCL 06I

Industrial hygiene surveys were conducted to assess personnel exposures to carbon fibers and carbon/epoxy composite dust during carbon composite airframe sanding operations. The operation is currently performed every two to three weeks for eight hours at a time. The nature and frequency of operation performance is expected to change as more composite aircraft are put into service. The health implications of carbon composite particulate exposure are not well understood. Good industrial hygiene practices, however, suggest that exposure levels be kept to a minimum. Recommendations for reducing personnel exposure have been made. To characterize the composite debris, a particle size distribution and fiber dimension analyses were done. Additionally, several organizational standards relating to carbon composite particulates were evaluated. A recommendation for reducing the applicable Coast Guard standards has been made. Other potential hazards identified were exposure to solvents during lay-up procedures, and to primer dust during sanding work. Both require further evaluation to determine the extent of the exposure. GRA

N88-30287# Ohio Wesleyan Univ., Delaware. Dept. of Psychology.
FUNCTIONAL ASSESSMENT OF LASER IRRADIATION Annual Report, Mar. 1984 - Feb. 1985
David O. Robbins Mar. 1988 44 p
(Contract DAMD17-81-C-1065; DA Proj. 3E1-62777-A-878)
(AD-A195735) Avail: NTIS HC A03/MF A01 CSCL 06G

Exposure of the retina to intense spots of coherent light produces immediate changes in the ability of the animal to perform a visual discrimination task. Relatively large shifts in visual acuity occur during laser irradiation and recovery is somewhat rapid following termination of relatively low-energy, long duration exposures. With more intense energies, recovery is slower and permanent shifts in postexposure spectral sensitivity often accompany these types of exposure conditions. GRA

N88-30032# International Scientific Radio Union, Brussels (Belgium).
BIOEFFECTS OF ELECTROMAGNETIC WAVES
C. Romero-Sierra *In its* Review of Radio Science, 1984-1986 1987 20 p (For primary document see N88-30023 24-32)
Avail: NTIS HC A09/MF A01

53 BEHAVIORAL SCIENCES

Includes psychological factors; individual and group behavior; crew training and evaluation; and psychiatric research.

N88-30288# Naval Ocean Systems Center, San Diego, Calif.
MULTILEVEL COMPUTATIONAL THEORY OF STEREOSCOPIC VISUAL IMAGE PROCESSING Final Report, 15 Jun. 1985 - 31 Dec. 1987
William R. Uttal Mar. 1988 19 p
(AD-A195331; NOSC/TR-1216) Avail: NTIS HC A03/MF A01 CSCL 05H

This is the final report of a research program that explored the perception of visual forms. The project consisted of psycho-physical studies in which stereoscopically generated, three-dimensional forms were studied in terms of their detectability, discriminability, recognizability, and reconstructability. The project produced a book and 11 articles, all of which spoke to the problem of how humans see forms in space. Two more articles are in progress. This report summarizes the findings of the extensive series of experiments carried out during the program. Results of this study are applicable to a wide range of U.S. Navy interests including computer vision, autonomous vehicles, remotely controlled devices (teleoperators), and displays. GRA

N88-30289# Tennessee Univ., Knoxville. Dept. of Psychology.
ADVANCEMENT OF LATENT TRAIT THEORY Final Report, 1981 - 1987
Fumiko Samejima Feb. 1988 153 p
(Contract N00014-81-C-0569; Proj. RR0-4204)
(AD-A194302) Avail: NTIS HC A08/MF A01 CSCL 05H

There were six main objectives in the original research proposal, and they can be summarized as follows: (1) Investigation of theory and method for estimating the operating characteristics of discrete item responses, which include the plausibility functions of the distractors of the multiple-choice test item, as well as the graded item responses of the free-response test item, without assuming any specific mathematical forms, and without using too many examinees in the whole procedure; (2) Investigation of the various characteristics of the new family of models for the multiple-choice test item, both in theory and in practice; (3) Production and revision of a set of systematic procedures for applying some combinations of a method and an approach for estimating the operating characteristics of discrete item responses, by modifying and reorganizing all the computer programs written for this purpose; (4) Development of latent trait theory further, and include more varieties of situations; (5) Investigation of ways of bridging across mathematical psychology and cognitive psychology, through latent trait theory; and (6) Systematizing theories and methods to eventually lead to a good introductory book on latent trait theory and other publications. GRA

N88-30290# Retina Foundation, Boston, Mass. Eye Research Inst.
EYE MOVEMENTS AND SPATIAL PATTERN VISION Annual Report, 1 Mar. 1987 - 29 Feb. 1988
Lawrence E. Arend 31 Mar. 1988 19 p
(Grant AF-AFOSR-0128-86)
(AD-A195496; AFOSR-88-0547TR) Avail: NTIS HC A03/MF A01 CSCL 06D

Models of lightness and color perception must take account of human color constancy, a tendency for apparent surface color to be relatively independent of the color and intensity of the illuminating light source. Observers matched the lightnesses and brightnesses of regions in simple and complex achromatic spatial patterns. The data showed that the observers' knowledge of the surface reflectances (revealed by lightness matches) was unaffected by changing brightness of the same surfaces (revealed by brightness matches). In the analogous chromatic experiments, observers matched the hue and saturation of patches or the patches' apparent surface colors. The observers' knowledge of the surface colors was not as reliable as in the achromatic case. Patches' hues and saturations matched when their chromaticities were approximately the same. Shifts of hue attributable to simultaneous color contrast were in the correct direction but too small to produce hue constancy. GRA

N88-30291# Dayton Univ., Ohio. Research Inst.
COMPARATIVE ASPECTS OF MULTIPLE PROCESSES OF ATTENTION Final Report, Aug. 1986 - Sep. 1987
MaryLou Cheal May 1988 27 p
(Contract F3615-84-C-0066)
(AD-A195805; AFHRL-TR-87-53) Avail: NTIS HC A03/MF A01 CSCL 05H

In this paper, first, there are examples of human and animal research in which attention is separated into various components. Terms used to designate various aspects or subcomponents of

attention are compared from different research paradigms. Secondly, four experiments on the time course of human attentional effects on discrimination of different stimuli are discussed in relationship to other research in the literature. For these experiments, a precue was used to move attention to the target location. Accuracy in discrimination of the target as a function of the time between precue and target was measured. In three of these experiments, targets differed as to line arrangement or line orientation. It was suggested that line arrangement discrimination requires focused attention whereas line orientation discrimination may not. The data were related to some of the dichotomous terms used to describe processes that differ in the need for focused attention. In a fourth experiment, eccentricity of the target was varied. These data provided evidence of time invariant attention movement for distance less than ten degrees. GRA

54 MAN/SYSTEM TECHNOLOGY AND LIFE SUPPORT

Includes human engineering; biotechnology; and space suits and protective clothing.

For related information see also *16 Space Transportation.*

N88-30292# Air Force Inst. of Tech., Wright-Patterson AFB, Ohio.

A DETECTION THEORY ANALYSIS OF VISUAL DISPLAY PERFORMANCE M.S. Thesis

Thomas R. Mabry 1988 65 p

(AD-A196291; AD-E951149; AFIT/CI/NR-88-126) Avail: NTIS HC A04/MF A01 CSCL 17K

This study investigated how information is processed from graphic vs. alphanumeric multi-element visual displays using principles derived from the Theory of Signal Detection (TSD). A diagnostic decision task was used in an evaluation of four different display formats: (1) a numerical display composed of n two-digit numbers arranged in a linear horizontal format; (2) a similar numerical display in which the display elements were arranged in a square matrix array; (3) an analog gauge display composed of n vertical line gauges also organized in a square matrix array; and (4) a similar analog gauge display in which the display elements were arranged in a linear horizontal format. Performance was evaluated for 1,2,4,9, and 16 element displays and over a range of display durations. Detection performance, as measured by d', increased as the number of display elements was increased up to an asymptotic value that was dependent on display type, arrangement and display duration. Performance was best with analog display elements arranged in a horizontal line. The relative influence of particular spatial element and the total number of elements that influence a subject's response appears to be highly dependent on display type and arrangement. GRA

N88-30293# Selskapet for Industriell og Teknisk Forskning, Trondheim (Norway). Div. of Medical Technology

STUDY OF HUMAN FACTORS ENGINEERING CRITERIA FOR EXTRA VEHICULAR ACTIVITY (EVA) SYSTEMS, VOLUME 2 Final Report

E. Myrseth, A. Pasche, B. Holand, and G. Bolstad et al. Paris, France ESA 8 Dec. 1987 47 p Sponsored in part by the Royal Norwegian Council for Scientific and Industrial Research, Trondheim, Norway

(Contract ESTEC-7016/87-NL-PP(SC))

(STF23-F87025-Vol-2; ESA-CR(P)-2572-Vol-2; ETN-88-93021) Avail: NTIS HC A03/MF A01

Effects of thermal conditions on manual and cognitive performance for support divers in a neutral buoyancy facility training situation were assessed in three dives. The only variable significantly different from one dive to another is thermal comfort. Neither manual nor cognitive performance show any significant changes in the 18 to 19 C water compared to the 32 to 33 C water for either of 2 suits used in the colder water. A dive with a thin neoprene suit is rated as cold by the divers after 1 hr in the water, and as very cold after 2 hr. When diving with 6.5 mm neoprene wet-suits all 6 subjects rate their thermal condition as comfortable until 2 hr, and as slightly cold to cold after 3 hr. The dive with water temperature of 32 to 33 C is rated as very comfortable to too warm. ESA

N88-30294# Human Engineering Labs., Aberdeen Proving Ground, Md.

FOUR-AXIS SIDE-ARM FLIGHT CONTROL SIMULATOR INVESTIGATION Final Report

William B. DeBellis May 1988 32 p

(AD-A196026; HEL-TM-4-88) Avail: NTIS HC A03/MF A01 CSCL 01D

This report presents the results of the second in a series of investigations to compile a data base on multiaxis side-arm flight controls. This second investigation focused on the effects that wearing a large and relatively bulky chemical and biological protective glove had on the pilots' flight control. Pilots were allowed to adjust the position of the armrest and the controller for individual comfort. A multivariate analysis of variance (MANOVA) was performed using three different arrangements of controller and armrest and two levels of clothing. In general, the root-mean-square deviation measure was not able to detect a consistent statistically significant difference between the three levels of controller/armrest arrangement or the two levels of clothing across all flight phases at the 5 percent level. This was true for both aircraft performance measures and pilot input measures. There were also no statistically significant interactions detected between these dependent measures. Additional data analysis showed that there were statistically significant differences on individual pilot performances and pilot to dependent measure interaction. GRA

N88-30295# Carnegie-Mellon Univ., Pittsburgh, Pa. Dept. of Psychology.

CONTRIBUTIONS TO ENGINEERING MODELS OF HUMAN-COMPUTER INTERACTION, VOLUME 1 Ph.D. Thesis

Bonnie E. John 6 May 1988 124 p

(Contract N00014-87-K-0432; RR0-4209)

(AD-A195590; Rept-1-51206A-Vol-1) Avail: NTIS HC A06/MF A01 CSCL 12H

This dissertation presents two engineering models of behavior at the human-computer interface; a model of immediate behavior stimulus-response compatibility and a model of transcription typing. Formulated within the architecture of the Model Human Processor of Card, Moran and Newell, these models are able to make zero-parameter, quantitative predictions of human response time in their respective domains. They are also completely integrated, making good predictions about performance on a dual reaction-time/typing task. Parameters of the models are set using response time data from an abbreviation recall experiment. These parameters are then used to make predictions about response time in another abbreviation recall experiment, three classic stimulus-response experiments, and over 29 experiments that reflect robust phenomena associated with transcription typing. These models are the first to make successful predictions across domain boundaries, both within tasks exhibiting stimulus-response compatibility and outside that paradigm to transcription typing. GRA

N88-30296# Virginia Polytechnic Inst. and State Univ., Blacksburg. Human Factors Engineering Center.

HUMAN FACTORS REPORT ON INFORMATION MANAGEMENT REQUIREMENTS FOR NEXT-GENERATION MANNED BOMBERS Final Report, Jun. 1986 - Oct. 1987

Douglas B. Beaudet, Dennis L. Price, Gilbert G. Kuperman, and Denise L. Wilson Dec. 1987 529 p

(Contract F33615-85-D-0514)

(AD-A195870; AAMRL-TR-87-042) Avail: NTIS HC A23/MF A01 CSCL 12A

A technology-free mission scenario was analyzed to determine crew information and system information management requirements. Criteria for technology insertion were developed and

applied. Information sets were identified and display formats were prototyped. GRA

N88-30297*# California Univ., Davis. Dept. of Mechanical Engineering.
PREDICTION AND MEASUREMENT OF HUMAN PILOT DYNAMIC CHARACTERISTICS IN A MANNED ROTORCRAFT SIMULATION
Ronald A. Hess and James T. Reedy 7 Oct. 1988 44 p
(Contract NCC2-241)
(NASA-CR-183246; NAS 1.26:183246) Avail: NTIS HC A03/MF A01 CSCL 05H

An analytical and experimental study of the human pilot control strategies in a manned rotorcraft simulation is described. The task simulated involves a low-speed, constant-altitude maneuvering task in which a head-down display is utilized to allow the pilot to track a moving hover point. The efficacy of the display law driving an acceleration symbol is determined and the manner in which the prediction and measurement of pilot/vehicle dynamics can be made part of man/machine system evaluations is demonstrated. Author

N88-30298# Selskapet for Industriell og Teknisk Forskning, Trondheim (Norway). Div. of Medical Technology.
STUDY OF HUMAN FACTORS ENGINEERING CRITERIA FOR EXTRAVEHICULAR ACTIVITY (EVA) SYSTEMS, VOLUME 1 Final Report
A. O. Brubakk, B. Holand, G. Bolstad, A. Pasche, T. Syversen, O. Bjorseth, H. Ryvarden, H. Fathi, B. Brekke, and O. I. Molvaer et al. Paris, France ESA 8 Dec. 1987 333 p Sponsored in part by the Royal Norwegian Council for Scientific and Industrial Research, Trondheim, Norway
(Contract ESTEC-7016/87-NL-PP(SC))
(STF23-F87025-Vol-1; ESA-CR(P)-2572-Vol-1; ETN-88-93020)
Avail: NTIS HC A15/MF A01

Human factors engineering for EVA: anthropometry; physiological and biochemical parameters at 1g conditions; physiological effects of the space environment; structural considerations; procedures; EVA suit design recommendations; EVA airborne support equipment; and EVA operational support equipment was reviewed. Design guidelines for man-machine interfaces for EVA systems are presented. Guidelines for astronaut training for EVA are suggested. Simulation techniques for EVA development studies and training are considered. Training systems; neutral buoyancy facilities; and water tanks and diver test systems are discussed. ESA

N88-30299# California Univ., Santa Barbara. Community and Organization Research Inst.
HAPTIC EXPLORATION IN HUMANS AND MACHINES: ATTRIBUTE INTEGRATION AND MACHINE RECOGNITION/IMPLEMENTATION Technical Report, 1 May 1987 - 30 Apr. 1988
Susan J. Lederman, Roberta L. Klatzky, Catherine Reed, R. Bajcsy, and S. A. Stansfield 30 Apr. 1988 57 p
(Contract N00014-86-K-0232)
(AD-A193692; TR-88-01) Avail: NTIS HC A04/MF A01 CSCL 23B

This technical report comprises three documents. The first describes the integration of haptic attributes during object categorization. The second describes a machine object recognition system with haptic as well as visual sensors. The third describes the development of a novel end effector of medium complexity. GRA

N88-30300# Crew Systems Consultants, Yellow Springs, Ohio.
IMPROVEMENT OF HEAD-UP DISPLAY STANDARDS. VOLUME 3: AN EVALUATION OF HEAD-UP DISPLAY SAFETY Final Report, Oct. 1984 - Jun. 1987
Richard L. Newman Sep. 1987 36 p
(Contract F33615-85-C-3602)
(AD-A195787; AFWAL-TR-87-3055-Vol-3) Avail: NTIS HC A03/MF A01 CSCL 01D

A review of the safety aspects of head-up displays (HUDs) is presented. Because of the widespread concern about the use of HUDs during unusual attitudes, particular attention was paid to spatial disorientation and the implications of flying by reference to the HUD during unusual attitude recoveries. It is concluded that the HUD is not inherently unsafe during instrument meterological conditions and is quite suitable for use as a primary flight display. It is clear, however, that current military training for pilots in the use of the HUD is inadequate both in terms of initial pilot training and recurrent training. Any problem with head-up displays is exacerbated by the lack of adequate training. The use of a generic HUD procedures trainer is highly recommended. GRA

N88-30301*# National Aeronautics and Space Administration. Ames Research Center, Moffett Field, Calif.
SPACE STATION PROXIMITY OPERATIONS WINDOWS: HUMAN FACTORS DESIGN GUIDELINES
Richard F. Haines Mar. 1987 109 p
(NASA-TM-88233; A-86185; NAS 1.15:88233) Avail: NTIS HC A06/MF A01 CSCL 06K

Proximity operations refers to all activities outside the Space Station which take place within a 1-km radius. Since there will be a large number of different operations involving manned and unmanned vehicles, single- and multiperson crews, automated and manually controlled flight, a wide variety of cargo, and construction/repair activities, accurate and continuous human monitoring of these operations from a specially designed control station on Space Station will be required. Total situational awareness will be required. This paper presents numerous human factors design guidelines and related background information for control windows which will support proximity operations. Separate sections deal with natural and artificial illumination geometry; all basic rendezvous vector approaches; window field-of-view requirements; window size; shape and placement criteria; window optical characteristics as they relate to human perception; maintenance and protection issues; and a comprehensive review of windows installed on U.S. and U.S.S.R. manned vehicles. Author

N88-29736# Systems Technology, Inc., Hawthorne, Calif.
PILOT MODELING
Duane T. McRuer *In* AGARD, Advances in Flying Qualities May 1988 30 p (For primary document see N88-29735 24-01) Copyright Avail: NTIS HC A09/MF A01

N88-29737# Systems Technology, Inc., Hawthorne, Calif.
PILOT MODELING APPLICATIONS
Irving L. Ashkenas *In* AGARD, Advances in Flying Qualities May 1988 38 p (For primary document see N88-29735 24-01) Copyright Avail: NTIS HC A09/MF A01

N88-29741# Pisa Univ. (Italy). Dipartimento di Ingegneria Aerospaziale.
THE OPTIMAL CONTROL PILOT MODEL AND APPLICATIONS
Mario Innocenti *In* AGARD, Advances in Flying Qualities May 1988 17 p (For primary document see N88-29735 24-01) Copyright Avail: NTIS HC A09/MF A01

N88-30346*# National Bureau of Standards, Gaithersburg, Md.
LOW LEVEL IMAGE PROCESSING TECHNIQUES USING THE PIPELINE IMAGE PROCESSING ENGINE IN THE FLIGHT TELEROBOTIC SERVICER
Marilyn Nashman and Karen J. Chaconas *In* NASA, Goddard Space Flight Center, The 1988 Goddard Conference on Space Applications of Artificial Intelligence Aug. 1988 p 215-229 (For primary document see N88-30330 24-63)
Avail: NTIS HC A19/MF A01 CSCL 09B

N88-30357*# Jet Propulsion Lab., California Inst. of Tech., Pasadena.
THE SPACE STATION ASSEMBLY PHASE: SYSTEM DESIGN TRADE-OFFS FOR THE FLIGHT TELEROBOTIC SERVICER
Jeffrey H. Smith, Max Gyamfi, Kent Volkmer, and Wayne Zimmerman *In* NASA, Goddard Space Flight Center, The 1988

Goddard Conference on Space Applications of Artificial Intelligence Aug. 1988 p 381-396 (For primary document see N88-30330 24-63)
(Contract NAS7-918)
Avail: NTIS HC A19/MF A01 CSCL 05H

55 SPACE BIOLOGY

Includes exobiology; planetary biology; and extraterrestrial life.

No abstracts in this category.

59 MATHEMATICAL AND COMPUTER SCIENCES (GENERAL)

No abstracts in this category.

60 COMPUTER OPERATIONS AND HARDWARE

Includes hardware for computer graphics, firmware, and data processing.

For components see *33 Electronics and Electrical Engineering.*

N88-30302# Washington Univ., Seattle. Dept. of Computer Science.
A MODEL FOR ARCHITECTURAL COMPARISON
Sam Ho and Larry Snyder Apr. 1988 17 p
(Contract MDA903-85-K-0072)
(AD-A195993; TR-88-04-01) Avail: NTIS HC A03/MF A01 CSCL 12F

Recently, architectures for sequential computers have become a topic of much discussion and controversy. At the center of this storm is the Reduced Instruction Set Computer, or RISC, first described at Berkeley in 1980. While the merits of the RISC architecture cannot be ignored, its opponents have tried to do just that, while its proponents have expanded and frequently exaggerated them, a situation which persists. This paper attempts not to settle the controversy, since indeed there likely is no one answer, but to provide a quantitative framework for a rational discussion of the issues. The model presented takes an architecture and a computation. It has the following features to: (1) quantitatively measure an architecture; (2) examines an architecture working on a computation; (3) separate the overall computation into logical pieces; (4) determine from the architecture how long each piece takes; (5) consider how much parallelism is available; and (6) compare the results with other architectures. GRA

N88-30303# Naval Postgraduate School, Monterey, Calif.
THE DESIGN OF AN INTELLIGENT MULTIDISK CONTROL MODULE FOR VME BUS BASED SYSTEMS M.S. Thesis
Steven L. Brooks Dec. 1987 91 p
(AD-A195587) Avail: NTIS HC A05/MF A01 CSCL 12F

The design of an intelligent multidisk control module for VME bus based systems is presented. The control module is designed to support concurrent disk operations on up to four flexible disk drives with multiple VME bus MASTERS. The design is presented for a UNIX compatible operating system but the operating system interface is kept simple enough that the multidisk control module can be used with most modern operating systems with minimal changes required. GRA

61 COMPUTER PROGRAMMING AND SOFTWARE

Includes computer programs, routines, alogorithms, and specific applications, e.g., CAD/CAM.

N88-30304*# SRI International Corp., Menlo Park, Calif.
QUALITY MEASURES AND ASSURANCE FOR AI (ARTIFICIAL INTELLIGENCE) SOFTWARE Final Report
John Rushby Washington NASA Oct. 1988 139 p
(Contract NAS1-17067)
(NASA-CR-4187; NAS 1.26:4187; SRI-4616) Avail: NTIS HC A07/MF A01 CSCL 09B

This report is concerned with the application of software quality and evaluation measures to AI software and, more broadly, with the question of quality assurance for AI software. Considered are not only the metrics that attempt to measure some aspect of software quality, but also the methodologies and techniques (such as systematic testing) that attempt to improve some dimension of quality, without necessarily quantifying the extent of the improvement. The report is divided into three parts Part 1 reviews existing software quality measures, i.e., those that have been developed for, and applied to, conventional software. Part 2 considers the characteristics of AI software, the applicability and potential utility of measures and techniques identified in the first part, and reviews those few methods developed specifically for AI software. Part 3 presents an assessment and recommendations for the further exploration of this important area. Author

N88-30305# Stanford Univ., Calif. Center for Large Scale Scientific Computation.
ALGORITHMS FOR NONLINEAR LEAST-SQUARES PROBLEMS
Christina Fraley May 1988 45 p
(Contract N00014-82-K-0335)
(AD-A196071; CLASSIC-88-22) Avail: NTIS HC A03/MF A01 CSCL 12C

This paper addresses a nonlinear least-squares problem which arises most often in data fitting applications. Much research has focused on the development of specialized algorithms that attempt to exploit the structure of the nonlinear least-squares objective. We survey methods developed for problems in which sparsity in the derivatives of function is not taken into account in formulating algorithms. GRA

N88-30306# Oak Ridge National Lab., Tenn. Instrumentation and Controls Div.
CONVERSION OF PRODUCTIONS IN OPS5 TO THEIR EQUIVALENT ENGLISH
S. J. Wertheimer, B. B. Baird, and N. B. Gove Oct. 1987 54 p
(Contract DE-AC05-84OR-21400)
(ORNL/TM-10246) Avail: NTIS HC A04/MF A01

A computer program has been written to provide English language versions of reactor analysis logic in OPS5. The present version, written in Prolog (a computer language designed for logic and language parsing), produces an English narrative translation of an individual OPS5 production rule. The translation is in two steps and involves an intermediate format consisting of Prolog-readable data statements. Translation to other languages or to other forms of English would not, therefore, require changing the first step. Samples are shown for OPS5 production rules related to the High Flux Isotope Reactor Intelligent Advisor Project. The Prolog programs are also shown. Author

N88-30307# Army Engineer Waterways Experiment Station, Vicksburg, Miss. Information Technology Lab.
COMPUTER-AIDED STRUCTURAL ENGINEERING (CASE) PROJECT. DEVELOPMENT OF DESIGN FORMULAS FOR RIBBED MAT FOUNDATIONS ON EXPANSIVE SOILS Final Technical Report
Joseph P. Hartman and B. H. James Apr. 1988 67 p
(AD-A194807; WES-TR-ITL-88-1) Avail: NTIS HC A04/MF A01 CSCL 13M

Background information and procedures for the analysis and structural design of ribbed mat foundations on expansive soils are the basis for this report. Within the text are the basic rules and requirements for the design according to soil behavior. Different design methods are compared and the design formulas and construction details are presented with an objective for simplicity, accuracy, rationality, and flexibility. The Tulsa District -- Structural Section conducted computer parametric studies on which a new design procedure was based and developed. GRA

N88-30308*# Sterling Software, Palo Alto, Calif.
SUPERMAP FOR CRAY FORTRAN: A USER'S GUIDE
Clayton J. Guest Feb. 1986 54 p
(Contract NAS2-11555)
(NASA-CR-177410; NAS 1.26:177410; TN86-7104-101-23) Avail: NTIS HC A04/MF A01 CSCL 09B

This program produces a map giving an overall view of all components and attributes of a FORTRAN program unit run by Cray. Unlike the maps produced by the Cray FORTRAN compiler which relates only to a single module, this map relates to the entire program. It maps the usage of all variable and all commons used. Author

N88-30309*# National Aeronautics and Space Administration. Ames Research Center, Moffett Field, Calif.
TELESCIENCE TESTBED PILOT PROGRAM Interim Report
Barry M. Leiner Feb. 1988 20 p
(Contract NASw-4234)
(NASA-CR-183207; RIACS-TR-88.6; NAS 1.26:183207) Avail: NTIS HC A03/MF A01 CSCL 09B

The Universities Space Research Association (USRA), under sponsorship from the NASA Office of Space Science and Applications, is conducting a Telescience Testbed Pilot Program. Fifteen universities, under subcontract to USRA, are conducting a variety of scientific experiments using advanced technology to determine the requirements and evaluate the tradeoffs for the information system of the Space Station era. An interim set of recommendations based on the experiences of the first six months of the pilot program is presented. Author

N88-30310# Instituto de Pesquisas Espaciais, Sao Jose dos Campos (Brazil).
USING PRIMAL SKETCH PRIMITIVES AS THE BASIS FOR THE HOUGH TRANSFORM
Flavio Roberto DiasVelasco, Antonio Miguel VieiraMonteiro, and Leonardo SantAnnaBins May 1988 11 p Presented at the 2nd International Conference on Computer Vision, Florida, 5-8 Dec. 1988 Submitted for publication
(INPE-4564-PRE/1305) Avail: NTIS HC A03/MF A01

The Hough transform was proposed originally as an efficient way to detect straight lines in images. It was generalized to detect lines and arbitrary shapes. This generalization made the Hough transform a kind of universal tool for object detection. The use of primal sketch primitives as defined by Marr, is proposed as the basic element upon which the transform is constructed (instead of simple edge elements). The advantages of using the primitives are a better discrimination and less computational effort. Author

N88-30311# Massachusetts Inst. of Tech., Cambridge. Artificial Intelligence Lab.
SYNTACTIC CLOSURES
Alan Bawden and Jonathan Rees Jun. 1988 29 p
(Contracts N00014-85-K-0124; N00014-86-K-0180)
(AD-A195921; AI-M-1049) Avail: NTIS HC A03/MF A01 CSCL 05B

This paper describes syntactic closures. Syntactic closures address the scoping problems that arise when writing macros. Some issues raised by introducing syntactic closures into the macro expansion interface are discussed and syntactic closures are compared with other approaches. Included is a complete implementation. GRA

N88-30312*# Stanford Univ., Calif. Computer Systems Lab.
PERFORMANCE PREDICTION OF CONCURRENT SYSTEMS
Victor W. K. Mak Dec. 1987 160 p
(Grants NAG2-248; NAGw-419)
(NASA-CR-183175; NAS 1.26:183175; CSL-TR-87-344)
Copyright Avail: NTIS HC A08/MF A01 CSCL 09B

Concurrent systems are computers that use multiple processors to solve a single problem. A means to predict the application performance on these systems is a useful tool in many areas of concurrent system research. A computationally efficient and accurate method to predict performance for a class of parallel computations on concurrent systems is described. A parallel computation is modeled as a task system with precedence relationships expressed as a series parallel directed acyclic graph. Resources in concurrent systems are modeled as service centers in queueing network models. Using these two models as inputs, the method outputs predictions of both the time to complete the computation and the concurrent system utilization. The algorithm used is based on the approximate Mean Value Analysis in queueing network modeling with extensions to model concurrency in the computation. The new algorithm was validated against both detailed simulation and actual execution on a commercial multiprocessor. Author

N88-30313# Colorado Univ., Boulder. Dept. of Computer Science.
NEW METHODS FOR NONLINEAR OPTIMIZATION Final Report, 1 Aug. 1984 - 31 Dec. 1987
Robert B. Schnabel and Richard H. Byrd 11 May 1988 8 p
(Contract DAAG29-84-K-0140)
(AD-A195982; ARO-21453.12-MA) Avail: NTIS HC A02/MF A01 CSCL 12D

This research project has investigated topics in unconstrained and constrained optimization, solving systems of nonlinear equations, nonlinear least squares, and parallel optimization. We have continued our development of tensor methods for nonlinear equations and extended these methods to unconstrained optimization and nonlinear least squares. In all cases, the tensor methods appear to provide significant practical improvements over the best currently known methods, on both singular and nonsingular problems. We have developed new trust region methods for equality constrained optimization problems that have strong convergence properties, and have begun to implement these methods. We have also developed new analysis techniques that provide local convergence results for constrained optimization problems. We have developed and analyzed an efficient method for orthogonal distance regression, intended for problems where there are errors in independent as well as dependent variables, and have developed a robust code that implements this method. Finally, we have developed, implemented, and analyzed parallel methods for global optimization and for unconstrained optimization. GRA

N88-30314*# National Aeronautics and Space Administration. Ames Research Center, Moffett Field, Calif.
KNOWLEDGE-BASED FLOW FIELD ZONING
Alison E. Andrews Aug. 1988 13 p Prepared for presentation at the 2nd International Conference on Numerical Grid Generation in CFD, Miami Beach, Fla., 5-8 Dec. 1988
(NASA-TM-101023; A-88274; NAS 1.15:101023) Avail: NTIS HC A03/MF A01 CSCL 09B

Automation flow field zoning in two dimensions is an important step towards easing the three-dimensional grid generation bottleneck in computational fluid dynamics. A knowledge based approach works well, but certain aspects of flow field zoning make

the use of such an approach challenging. A knowledge based flow field zoner, called EZGrid, was implemented and tested on representative two-dimensional aerodynamic configurations. Results are shown which illustrate the way in which EZGrid incorporates the effects of physics, shape description, position, and user bias in a flow field zoning. Author

N88-30315# Instituto de Pesquisas Espaciais, Sao Jose dos Campos (Brazil).
METHOD FOR COMBINED IMAGE INTERPOLATION-RESTORATION THROUGH A FIR FILTER DESIGN TECHNIQUE
Leila Maria GarciaFonseca and Nelson DelfinodAvilaMascarenhas May 1988 12 p Presented at the 16th Congress of International Society for Photogrammetry and Remote Sensing, Kyoto, Japan, 1-10 Jul. 1988 Submitted for publication
(INPE-4561-PRE/1302) Avail: NTIS HC A03/MF A01

In digital image processing there is often a need to interpolate an image. Examples occur in scale magnification, image registration, and geometric correction. On the other hand, this image can be subjected to several sources of resolution degradation and an improvement of this resolution may be necessary. Therefore, the problem of combining the interpolation and the restoration in a single operation, thereby reducing the computational effort is addressed. This is done by means of a 2D, separable, FIR filter. The ideal low-pass FIR filter for interpolation is modified to account for the restoration process. The Modified Inverse Filter (MIF) is used for this purpose. The proposed method is applied to the interpolation-restoration of LANDSAT-5 Thematic Mapper data. The later process takes into account the degradation due to optics, detector, and electronic filtering. A comparison with the parametric cubic convolution interpolation technique is made. Author

N88-30316# Instituto de Pesquisas Espaciais, Sao Jose dos Campos (Brazil).
A DIGITAL TERRAIN MODEL SYSTEM FOR A MICROCOMPUTER
Carlos Alberto Felgueiras, Guaraci Jose Erthal, and Luiz Alberto VieiraDias Jun. 1988 10 p Presented at the 16th Congress of International Society for Photogrammetry and Remote Sensing, Kyoto, Japan, 1-10 Jul. 1988
(INPE-4610-PRE/1333) Avail: NTIS HC A02/MF A01

The objective of this work is to describe the development and the implementation of a Digital Terrain Model (DTM), in a 16 bits microcomputer IBM-PC, under a MS-DOS Operational System. The model was developed at the Image Processing Department, Institute for Space Research (INPE), Brazil, and is integrated into a Geological Information System that allows the combination of DTM data with other information images and thematic maps. Author

N88-30317# Army Engineer Waterways Experiment Station, Vicksburg, Miss. Information Technology Lab.
COMPUTER-AIDED STRUCTURAL ENGINEERING (CASE) PROJECT. COMPUTER PROGRAM FOR ANALYSIS OF PLANAR GRID STRUCTURES (CGRID), USER'S GUIDE Final Report
William P. Dawkins Apr. 1988 69 p
(AD-A195977; WES/IR/ITL-88-1) Avail: NTIS HC A04/MF A01 CSCL 12E

The computer program CGRID, described in this user's guide, performs an analysis of planar grid structures using conventional matrix analysis techniques based on the assumptions of linearly elastic structural response to infinitesimally small displacements. The program is limited to structures with no more than 100 joints and 180 members. All members are assumed to be prismatic, possessing straight centroidal axes and composed of a linearly elastic, homogeneous material. Output consists of joint displacements, reactions, and member forces. The output may be printed at the user's terminal or directed to a file. Graphical output of the results is also available. GRA

N88-30318# Massachusetts Inst. of Tech., Cambridge. Lab. for Information and Decision Systems.
THE BOUNDED RATIONALITY CONSTRAINT: EXPERIMENTAL AND ANALYTICAL RESULTS M.S. Thesis
Anne-Claire A. Louvet Jun. 1988 151 p
(Contracts N00014-85-K-0329; N00014-85-K-0782)
(AD-A195897; LIDS-TH-1771) Avail: NTIS HC A08/MF A01 CSCL 12D

The bounded rationality constraint sets and upper limit on the rate with which decisionmakers can process information satisfactorily. This rate is studied both experimentally and analytically. A simple computer game for a single decisionmaker was used in which subjects were asked to find the smallest of a set of ratios present on the screen for a limited amount of time. Both the amount of time (twelve values) and the number of ratios (two values) were varied. A Gompertz curve is used to model the experimental results and establish the existence of a time threshold beyond which performance decreased significantly. An information theoretic model of the cognitive workload is used to estimate the workload associated with the tasks. The time threshold T* and the cognitive workload lead to a value for the bounded rationality constraint for each subject and each number of ratios. The distribution of the bounded rationality constraint across subjects for each number of ratios is found to be normal. Also, the bounded rationality of each subject as the number of ratios is changed does not vary significantly. These results may be used in the design of multiperson experiments and eventually in the methodology for organization design. GRA

N88-30319# Massachusetts Inst. of Tech., Cambridge. Artificial Intelligence Lab.
SCHEME86: A SYSTEM FOR INTERPRETING SCHEME
Andrew Berlin and Henry Wu Apr. 1988 24 p
(Contract N00014-86-K-0180)
(AD-A195931; AI-M-1040) Avail: NTIS HC A03/MF A01 CSCL 12E

Scheme86 is a computer system designed to interpret programs written in the SCHEME dialect of LISP. A specialized architecture, coupled with new techniques for optimizing register management in the interpreter, allow Scheme86 to execute interpreted SCHEME at a speed comparable to that of compiled LISP on conventional workstations. The Scheme86 design is based on the observation that sequences of chronologically dependent memory references are often the factor limiting the execution speed of LISP programs. To attack the dependent reference problem, the architecture is optimized to reduce the latency of memory-processor-memory operations. Parallel execution units allow multiple operations to occur during each machine cycle, making effective use of a low-latency memory system. GRA

N88-30320*# Old Dominion Univ., Norfolk, Va. Dept. of Computer Science.
GEOMETRIC MODELING FOR COMPUTER AIDED DESIGN Progress Report, period ending 15 Dec. 1987
James L. Schwing Aug. 1988 47 p
(Contract NCC1-99)
(NASA-CR-183161; NAS 1.26:183161) Avail: NTIS HC A03/MF A01 CSCL 09B

Research focused on two major areas. The first effort addressed the design and implementation of a technique that allows for the visualization of the real time variation of physical properties. The second effort focused on the design and implementation of an on-line help system with components designed for both authors and users of help information. Author

N88-30321*# National Aeronautics and Space Administration. Ames Research Center, Moffett Field, Calif.
PERFORMANCE ANALYSIS OF FDDI
Marjory J. Johnson Apr. 1988 20 p
(Contract NCC2-387)
(NASA-CR-183206; NAS 1.26:183206; RIACS-TR-88.11) Avail: NTIS HC A03/MF A01 CSCL 09B

The Fiber Distributed Data Interface (FDDI) is an imerging ANSI

and ISO standard for a 100 megabit per second fiber optic token ring. The performance of the FDDI media access control protocol is analyzed using a simulation developed at NASA Ames. Both analyses using standard measures of performance (including average delay for asynchronous traffic, channel utilization, and transmission queue length) and analyses of characteristics of ring behavior which can be attributed to constraints imposed by the timed token protocol on token holding time (including bounded token rotation time, support for synchronous traffic, and fairness of channel access for nodes transmitting asynchronous traffic) are included. Author

N88-30322# Naval Postgraduate School, Monterey, Calif.
A STATIC SCHEDULER FOR THE COMPUTER AIDED PROTOTYPING SYSTEM: AN IMPLEMENTATION GUIDE M.S. Thesis
Dorothy M. Janson Mar. 1988 125 p
(AD-A194340) Avail: NTIS HC A06/MF A01 CSCL 12F

As demand for hard real-time and embedded computer systems increases, a new approach to software development is critical. Software engineers and users would benefit from an automated methodology allowing validation of design specifications or functional requirements early in the development life cycle. A fast, efficient, easy-to-use tool would increase productivity and would enhance user confidence that software would be delivered at less cost and on schedule. The Computer Aided Prototyping System (CAPS) is a conceptualized tool providing these capabilities. This thesis represents a pioneering effort to develop a Static Scheduler for the CAPS Execution Support System using the Ada programming language. The Static Scheduler initially extracts critical operators, timing constraints and precedence relationships from a high-level prototype source program. The Static Scheduler then creates a static schedule for run-time execution, using worst case scenarios, guaranteeing that timing constraints are met. The primary goal of this thesis is to provide the scheduling algorithms and implementation guidelines for the Static Scheduler. Secondary goals are to demonstrate the significance of continued research to telecommunications applications and to demonstrate the feasibility of Ada as the implementation language. GRA

N88-30323# National Aerospace Lab., Amsterdam (Netherlands). Informatics/Space Div.
COMPRESSION AND DECOMPRESSION OF IMAGING SENSOR SIGNALS (CADISS): A MULTIPROCESSOR SYSTEM FOR IMAGE COMPRESSION/DECOMPRESSION ON BOARD SCIENTIFIC SATELLITES
H. F. A. Roefs and A. Monkel Paris, France ESA 9 Jun. 1987 116 p Original contains color illustrations
(Contracts ESA-5047/82-NL-HP; NIVR-1987)
(NLR-TR-87076-I; ESA-CR(P)-2578; ETN-88-93023) Avail: NTIS HC A06/MF A01

A low-power (micro) programmable multiprocessor for compression and decompression of image-type signals, generated by imaging sensors on board spacecraft or satellites (CADISS) is described. The CADISS enables an efficient use of the on-board mass memory and the satellite/ground downlink. It can accommodate various digital data-sensor signals: mono/multi-spectral (visible, infrared), multiframe (TV), and the like. The CADISS can be applied in various configurations, for instance to compress image data on-line before they are transmitted to the ground station, which enhances the downlink telemetry channel efficiency considerably; if needed, the compressed data can be stored temporarily in the satellite mass memory for postponed transmission. It can also decompress previously compressed and stored data, which allows an efficient use of the on-board mass memory, while the data structure transparency is maintained. The CADISS algorithms, technology, and testing are outlined. ESA

N88-30324# Washington Univ., Seattle. Dept. of Computer Science.
THE TRIANGLE: A MULTIPROCESSOR ARCHITECTURE FOR FAST CURVE AND SURFACE GENERATION
Thomas J. Holman and Tony DeRose Aug. 1987 38 p
(Contract N00014-86-K-0264)
(AD-A195882; TR-87-08-07) Avail: NTIS HC A03/MF A01 CSCL 12F

Described are the architecture and operation of the Triangle, a pipelined, parallel multiprocessor architecture for the computation and rendering of line segments, conic sections, spline curves, triangular patch surfaces, and tensor product surfaces. Based on a generalization of deCasteljau's algorithm for computing points on Bezier curves, the Triangle can be used as an accelerator to dramatically enhance the performance of standard graphics workstations. Although there is a wide spectrum of possible implementations, we estimate that a custom VLSI implementation that is currently being designed will be capable of peak rates well in excess of one million points of evaluation per second. Assuming a Motorola 68020 host, such a processor should be capable of completely recomputing 65 bicubic patches in real-time, at a density of 1,000 points per patch. GRA

N88-30325# Aeritalia S.p.A., Turin (Italy). Space Systems Group.
IMPROVEMENTS OF DCAP 1, PHASE 2-3/A Final Report
Paris, France ESA Nov. 1987 25 p
(Contract ESA-6451/85)
(D2-RP-AI-106; ESA-CR(P)-2580; ETN-88-93025) Avail: NTIS AC A03/MF A01

The user friendliness and the computational capabilities of the DCAP 1 program were improved. User friendliness was improved by the definition of an interactive preprocessor which assists the user in the definition of the input data required by the program, and by the development of subroutines which allow the user to avoid the burden of coding a number of user defined subroutines as required by previous DCAP releases. An alternative solution scheme based on the singular value decomposition was identified and implemented to allow the analysis of a wider range of constrained systems. A modular structure of the software system was identified, and for each module the functional requirements and the interfaces were defined. ESA

N88-30326# Massachusetts Inst. of Tech., Cambridge. Artificial Intelligence Lab.
REIFICATION WITHOUT EVALUATION
Alan Bawden Jun. 1988 28 p
(Contract N00014-85-K-0-0124)
(AD-A195928; AI-M-946) Avail: NTIS HC A03/MF A01 CSCL 12E

Constructing self-referential systems, such as Brian Smith's 3-LISP language, is actually more straightforward than you think. Anyone can build an infinite tower of processors (where each processor implements the processor at the next level below) by employing some common sense and one simple trick. In particular, it is not necessary to re-design quotation, take a stand on the relative merits of evaluation vs. normalization, or treat continuations as meta-level objects. This paper presents a simple programming language interpreter that illustrates how this can be done. By keeping its expression evaluator entirely separate from the mechanisms that implement its infinite tower, this interpreter avoids many troublesome aspects of previous self-referential programming languages. Given these basically straightforward techniques, processor towers might be easily constructed for a wide variety of systems to enable them to manipulate and reason about themselves. GRA

N88-30327*# Sterling Software, Palo Alto, Calif.
THE elvaN: A FORWARD-LOOKING INTERACTIVE ORBITAL TRAJECTORY PLOTTING TOOL FOR USE WITH PROXIMITY OPERATIONS (PROX OPS) AND OTHER MANEUVERS: DESCRIPTION AND USER'S MANUAL
Adam R. Brody Jun. 1988 12 p
(Contract NAS2-11555)
(NASA-CR-177490; NAS 1.26:177490) Avail: NTIS HC A03/MF A01 CSCL 09B

The results of vehicle burns on-orbit are very difficult to anticipate because of nonlinearities in the equations of motion

governing orbiting bodies. This confusion was noticed firsthand in prior experimentation. Out of plane motion is relatively simple as it is uncoupled from the other two degrees of freedom. However, in plane thrusts are more complex because the motions resulting from these inputs are coupled. An interactive planning device, eivaN, was developed to plot resulting trajectories, to provide a better comprehension of orbital mechanics effects, and to help the user to develop heuristics for on-orbit mission planning. The eivaN runs with Microsoft Excel on a Macintosh computer. It provides a forward looking display: burn parameters in the three orthogonal axes in addition to time inputted, and the resultant trajectory is then plotted. Position and velocity components for any burn at any user specified time are readily available. A new area of research related to the human factors of real time, on-orbit mission planning was identified and is currently being investigated. Author

62 COMPUTER SYSTEMS

Includes computer networks and special application computer systems.

N88-30328# Selenia Spazio S.p.A., Rome (Italy).
THE LTPP COMMUNICATION PROCESSOR Final Report
A. Francia, F. Cantini, A. Morando, A. Sbardellati, D. Galindo, D. Bulliat, and M. Lellouch Paris, France ESA Dec. 1987 96 p Prepared in cooperation with MATRA Espace, Toulouse, France
(Contract ESTEC-6950/86-NL-IW(SC))
(CL/CP/SES/FR/004; ESA-CR(P)-2579; ETN-88-93024) Avail: NTIS HC A05/MF A01

A spaceborne communication processor to support communications services allowing interconnection between the on board data transport means and external communication facilities (either radiofrequency links or communication means of a docked vehicle) for Hermes and Columbus was defined. The processor is one node of a more global communication system, composed of subnetworks, interconnected with each other, permitting data exchange between users, interfacing with remote and heterogeneous subnetworks. The communication processor requirements are defined by the communication scenarios of the vehicles, and, in particular, for each mission phase by: the end to end transmission scenario, i.e., the definition of the routes used to disseminate data from data generating end users to destination end users, the characteristics, performances, and protocols of the subnetworks crossed by the data; data characteristics; and interfaces. The design specification, problem areas, and recommendations for product development are outlined. ESA

N88-30329*# PRC Systems Services Co., Hampton, Va.
AN OPERATIONS MANUAL FOR THE DIGITAL DATA SYSTEM
Michael G. Jones Aug. 1988 34 p
(Contract NAS1-18000)
(NASA-CR-181688; NAS 1.26:181688) Avail: NTIS HC A03/MF A01 CSCL 09B

The Digital Data System (DDS) was designed to incorporate the analog-to-digital conversion process into the initial data acquisition stage and to store the data in a digital format. This conversion is done as part of the acquisition process. Consequently, the data are ready to be analyzed as soon as the test is completed. This capability permits the researcher to alter test parameters during the course of the experiment based on the information acquired in a prior portion of the test. The DDS is currently able to simultaneously acquire up to 10 channels of data. The purpose of this document is fourfold: (1) to describe the capabilities of the hardware in sufficient detail to allow the reader to determine whether the DDS is the optimum system for a particular experiment; (2) to present some of the more significant software developed to provide analyses within a short time of the completion of data acquisition; (3) to provide the reader with sample runs of major software routines to demonstrate their convenience and simple usage; and (4) a portion of the document is used to describe software which uses an FFT-box to provide a means of comparison against which the DDS can be checked. Author

63 CYBERNETICS

Includes feedback and control theory, artificial intelligence, robotics and expert systems.

For related information see also *54 Man/System Technology and Life Support.*

N88-30330*# National Aeronautics and Space Administration. Goddard Space Flight Center, Greenbelt, Md.
THE 1988 GODDARD CONFERENCE ON SPACE APPLICATIONS OF ARTIFICIAL INTELLIGENCE
James Rash, ed. and Peter Hughes, ed. Aug. 1988 437 p Conference held in Greenbelt, Md., 24 May 1988 Sponsored by NASA, Washington, D.C.
(NASA-CP-3009; Rept-88B0212; NAS 1.55:3009) Avail: NTIS HC A19/MF A01 CSCL 09B

This publication comprises the papers presented at the 1988 Goddard Conference on Space Applications of Artificial Intelligence held at the NASA/Goddard Space Flight Center, Greenbelt, Maryland on May 24, 1988. The purpose of this annual conference is to provide a forum in which current research and development directed at space applications of artificial intelligence can be presented and discussed. The papers in these proceedings fall into the following areas: mission operations support, planning and scheduling; fault isolation/diagnosis; image processing and machine vision; data management; modeling and simulation; and development tools/methodologies. For individual titles, see N88-30331 through N88-30362.

N88-30331*# National Aeronautics and Space Administration. Lyndon B. Johnson Space Center, Houston, Tex.
AN INTELLIGENT TRAINING SYSTEM FOR SPACE SHUTTLE FLIGHT CONTROLLERS
R. Bowen Loftin, Lui Wang, Paul Baffes, and Grace Hua (Computer Sciences Corp., Houston, Tex.) *In* NASA, Goddard Space Flight Center, The 1988 Goddard Conference on Space Applications of Artificial Intelligence Aug. 1988 p 3-15 (For primary document see N88-30330 24-63)
Avail: NTIS HC A19/MF A01 CSCL 09B

An autonomous intelligent training system which integrates expert system technology with training/teaching methodologies is described. The system was designed to train Mission Control Center (MCC) Flight Dynamics Officers (FDOs) to deploy a certain type of satellite from the Space Shuttle. The Payload-assist module Deploys/Intelligent Computer-Aided Training (PD/ICAT) system consists of five components: a user interface, a domain expert, a training session manager, a trainee model, and a training scenario generator. The interface provides the trainee with information of the characteristics of the current training session and with on-line help. The domain expert (DeplEx for Deploy Expert) contains the rules and procedural knowledge needed by the FDO to carry out the satellite deploy. The DeplEx also contains mal-rules which permit the identification and diagnosis of common errors made by the trainee. The training session manager (TSM) examines the actions of the trainee and compares them with the actions of DeplEx in order to determine appropriate responses. A trainee model is developed for each individual using the system. The model includes a history of the trainee's interactions with the training system and provides evaluative data on the trainee's current skill level. A training scenario generator (TSG) designs appropriate training exercises for each trainee based on the trainee model and the training goals. All of the expert system components of PD/ICAT communicate via a common blackboard. The PD/ICAT is currently being tested. Ultimately, this project will serve as a vehicle for developing a general architecture for intelligent training systems together with a software environment for creating such systems. Author

N88-30332*# National Aeronautics and Space Administration. Goddard Space Flight Center, Greenbelt, Md.
ARTIFICIAL INTELLIGENCE COSTS, BENEFITS, RISKS FOR SELECTED SPACECRAFT GROUND SYSTEM AUTOMATION SCENARIOS
Walter F. Truszkowski, Barry G. Silverman, Martha Kahn, and Henry Hexmoor (Intellitek, Inc., Rockville, Md.) *In its* The 1988 Goddard Conference on Space Applications of Artificial Intelligence Aug. 1988 p 17-31 (For primary document see N88-30330 24-63)
Avail: NTIS HC A19/MF A01 CSCL 09B

In response to a number of high-level strategy studies in the early 1980s, expert systems and artificial intelligence (AI/ES) efforts for spacecraft ground systems have proliferated in the past several years primarily as individual small to medium scale applications. It is useful to stop and assess the impact of this technology in view of lessons learned to date, and hopefully, to determine if the overall strategies of some of the earlier studies both are being followed and still seem relevant. To achieve that end four idealized ground system automation scenarios and their attendant AI architecture are postulated and benefits, risks, and lessons learned are examined and compared. These architectures encompass: (1) no AI (baseline), (2) standalone expert systems, (3) standardized, reusable knowledge base management systems (KBMS), and (4) a futuristic unattended automation scenario. The resulting artificial intelligence lessons learned, benefits, and risks for spacecraft ground system automation scenarios are described. Author

N88-30333*# National Aeronautics and Space Administration. Ames Research Center, Moffett Field, Calif.
A SHARED-WORLD CONCEPTUAL MODEL FOR INTEGRATING SPACE STATION LIFE SCIENCES TELESCIENCE OPERATIONS
Vicki Johnson and John Bosley (Bionetics Corp., Moffett Field, Calif.) *In* NASA, Goddard Space Flight Center, The 1988 Goddard Conference on Space Applications of Artificial Intelligence Aug. 1988 p 33-44 (For primary document see N88-30330 24-63)
Avail: NTIS HC A19/MF A01 CSCL 09B

Mental models of the Space Station and its ancillary facilities will be employed by users of the Space Station as they draw upon past experiences, perform tasks, and collectively plan for future activities. The operational environment of the Space Station will incorporate telescience, a new set of operational modes. To investigate properties of the operational environment, distributed users, and the mental models they employ to manipulate resources while conducting telescience, an integrating shared-world conceptual model of Space Station telescience is proposed. The model comprises distributed users and resources (active elements); agents who mediate interactions among these elements on the basis of intelligent processing of shared information; and telescience protocols which structure the interactions of agents as they engage in cooperative, responsive interactions on behalf of users and resources distributed in space and time. Examples from the life sciences are used to instantiate and refine the model's principles. Implications for transaction management and autonomy are discussed. Experiments employing the model are described which the authors intend to conduct using the Space Station Life Sciences Telescience Testbed currently under development at Ames Research Center. Author

N88-30334*# Jet Propulsion Lab., California Inst. of Tech., Pasadena.
ARTIFICIAL INTELLIGENCE IN A MISSION OPERATIONS AND SATELLITE TEST ENVIRONMENT
Carl Busse *In* NASA, Goddard Space Flight Center, The 1988 Goddard Conference on Space Applications of Artificial Intelligence Aug. 1988 p 45-57 (For primary document see N88-30330 24-63)
Avail: NTIS HC A19/MF A01 CSCL 09B

A Generic Mission Operations System using Expert System technology to demonstrate the potential of Artificial Intelligence (AI) automated monitor and control functions in a Mission Operations and Satellite Test environment will be developed at the National Aeronautics and Space Administration (NASA) Jet Propulsion Laboratory (JPL). Expert system techniques in a real time operation environment are being studied and applied to science and engineering data processing. Advanced decommutation schemes and intelligent display technology will be examined to develop imaginative improvements in rapid interpretation and distribution of information. The Generic Payload Operations Control Center (GPOCC) will demonstrate improved data handling accuracy, flexibility, and responsiveness in a complex mission environment. The ultimate goal is to automate repetitious mission operations, instrument, and satellite test functions by the applications of expert system technology and artificial intelligence resources and to enhance the level of man-machine sophistication. Author

N88-30335*# National Aeronautics and Space Administration. Lyndon B. Johnson Space Center, Houston, Tex.
AUTOMATED SPACE VEHICLE CONTROL FOR RENDEZVOUS PROXIMITY OPERATIONS
Robert N. Lea *In* NASA, Goddard Space Flight Center, The 1988 Goddard Conference on Space Applications of Artificial Intelligence Aug. 1988 p 59-66 (For primary document see N88-30330 24-63)
Avail: NTIS HC A19/MF A01 CSCL 09B

Rendezvous during the unmanned space exploration missions, such as a Mars Rover/Sample Return will require a completely automatic system from liftoff to docking. A conceptual design of an automated rendezvous, proximity operations, and docking system is being implemented and validated at the Johnson Space Center (JSC). The emphasis is on the progress of the development and testing of a prototype system for control of the rendezvous vehicle during proximity operations that is currently being developed at JSC. Fuzzy sets are used to model the human capability of common sense reasoning in decision making tasks and such models are integrated with the expert systems and engineering control system technology to create a system that performs comparably to a manned system. Author

N88-30336*# Ford Aerospace and Communications Corp., Seabrook, Md.
AUTOMATED SATELLITE CONTROL IN Ada
Allan Jaworski and J. T. Thompson *In* NASA, Goddard Space Flight Center, The 1988 Goddard Conference on Space Applications of Artificial Intelligence Aug. 1988 p 67-75 (For primary document see N88-30330 24-63)
Avail: NTIS HC A19/MF A01 CSCL 09B

The Advanced Ground Segment, a prototype satellite/payload operations control center workstation, which represents an evolutionary effort to improve the automation of control centers while improving software practices and supporting distributed control center functions, is described. Multiple levels of automation are supported through a rule-based control strategy. The architecture provides the necessary interfaces and modularity for future inclusion of more sophisticated control strategies. Author

N88-30337*# Martin Marietta Corp., Denver, Colo. Information and Communication Systems.
CONTINGENCY RESCHEDULING OF SPACECRAFT OPERATIONS
Daniel L. Britt, Amy L. Geoffroy, and John R. Gohring *In* NASA, Goddard Space Flight Center, The 1988 Goddard Conference on Space Applications of Artificial Intelligence Aug. 1988 p 79-90 (For primary document see N88-30330 24-63)
Avail: NTIS HC A19/MF A01 CSCL 09B

Spacecraft activity scheduling was a focus of attention in artificial intelligence recently. Several scheduling systems were devised which more-or-less successfully address various aspects of the activity scheduling problem, though most of these are not yet mature, with the notable expection of NASA's ESP. Few current scheduling systems, however, make any attempt to deal fully with the problem of modifying a schedule in near-real-time in the event of contingencies which may arise during schedule execution. These contingencies can include resources becoming unavailable unpredictably, a change in spacecraft conditions or environment,

or the need to perform an activity not scheduled. In these cases it becomes necessary to repair an existing schedule, disrupting ongoing operations as little as possible. Normal scheduling is just a part of that which must be accomplished during contingency rescheduling. A prototype system named MAESTRO was developed for spacecraft activity scheduling. MAESTRO is briefly described with a focus on recent work in the area of real-time contingency handling. Included is a discussion of some of the complexities of the scheduling problem and how they affect contingency rescheduling, such as temporal constraints between activities, activities which may be interrupted and continued in any of several ways, and different ways to choose a resource complement which will allow continuation of an activity. Various heuristics used in MAESTRO for contingency rescheduling is discussed, as are operational concerns such as interaction of the scheduler with spacecraft subsystems controllers. Author

N88-30338*# Computer Sciences Corp., Baltimore, Md. Astronomy Programs.

KNOWLEDGE BASED TOOLS FOR HUBBLE SPACE TELESCOPE PLANNING AND SCHEDULING: CONSTRAINTS AND STRATEGIES

Glenn Miller, Mark Johnston, Shon Vick, Jeff Sponsler (Space Telescope Science Inst., Baltimore, Md.), and Kelly Lindenmayer *In* NASA, Goddard Space Flight Center, The 1988 Goddard Conference on Space Applications of Artificial Intelligence Aug. 1988 p 91-106 (For primary document see N88-30330 24-63)

Avail: NTIS HC A19/MF A01 CSCL 09B

The Hubble Space Telescope (HST) presents an especially challenging scheduling problem since a year's observing program encompasses tens of thousands of exposures facing numerous coupled constraints. Recent progress in the development of planning and scheduling tools is discussed which augment the existing HST ground system. General methods for representing activities, constraints, and constraint satisfaction, and time segmentation were implemented in a scheduling testbed. The testbed permits planners to evaluate optimal scheduling time intervals, calculate resource usage, and to generate long and medium range plans. Graphical displays of activities, constraints, and plans are an important feature of the system. High-level scheduling strategies using rule based and neural net approaches were implemented. Author

N88-30339*# Computer Sciences Corp., Baltimore, Md. Astronomy Programs.

THE PROPOSAL ENTRY PROCESSOR: TELESCIENCE APPLICATIONS FOR HUBBLE SPACE TELESCOPE SCIENCE OPERATIONS

Robert Jackson, Mark Johnston, Glenn Miller, Kelly Lindenmayer, Patricia Monger, Shon Vick, Robin Lerner, and Joel Richon (Space Telescope Science Inst., Baltimore, Md.) *In* NASA, Goddard Space Flight Center, The 1988 Goddard Conference on Space Applications of Artificial Intelligence Aug. 1988 p 107-123 (For primary document see N88-30330 24-63)

Avail: NTIS HC A19/MF A01 CSCL 09B

The Proposal Entry Processor (PEP) System supports the submission, entry, technical evaluation review, selection and implementation of Hubble Space Telescope (HST) observing proposals. The PEP system is described concentrating on features which illustrate principles of telescience as applied to the HST. These principles are applicable to other observatories, both space and ground based. The PEP proposal forms allow a scientist to specify scientific objectives without becoming needlessly involved in implementation details. The Remote Proposal Submission System (RPSS) allows proposers to submit proposals electronically via Telenet, SPAN, and other networks. The RPSS performs syntax and sematic checks on proposals. The PEP uses a fourth generation database system to store proposal information and to allow general queries and reports. The Transformation subsystem uses an expert system written in OPS5 to cast a scientific description of an observing program into parameters used by the planning and scheduling system. The TACOS system is a natural language database which supports the proposal selection process. Technical evaluations for resource usage and duplicate science are performed using rulebased systems. Author

N88-30340*# Computer Sciences Corp., Beltsville, Md.

CANDIDATE FUNCTIONS FOR ADVANCED TECHNOLOGY IMPLEMENTATION IN THE COLUMBUS MISSION PLANNING ENVIRONMENT

Audrey Loomis and Albrecht Kellner (Messerschmitt-Boelkow-Blohm G.m.b.H., Bremen, West Germany) *In* NASA, Goddard Space Flight Center, The 1988 Goddard Conference on Space Applications of Artificial Intelligence Aug. 1988 p 125-139 Prepared in cooperation with Entwicklungsring Nord, Bremen, Fed. Republic of Germany (For primary document see N88-30330 24-63)

Avail: NTIS HC A19/MF A01 CSCL 09B

The Columbus Project is the European Space Agency's contribution to the International Space Station program. Columbus is planned to consist of three elements (a laboratory module attached to the Space Station base, a man-tended freeflyer orbiting with the Space Station base, and a platform in polar orbit). System definition and requirements analysis for Columbus are underway, scheduled for completion in mid-1990. An overview of the Columbus mission planning environment and operations concept as currently defined is given, and some of the challenges presented to software maintainers and ground segment personnel during mission operators are identified. The use of advanced technologies in system implementation is being explored. Both advantages of such solutions and potential problems they present are discussed, and the next steps to be taken by Columbus before targeting any functions for advanced technology implementation are summarized. Several functions in the mission planning process were identified as candidates for advanced technology implementation. These range from expert interaction with Columbus' data bases through activity scheduling and near-real-time response to departures from the planned timeline. Each function is described, and its potential for advanced technology implementation briefly assessed. Author

N88-30341*# National Aeronautics and Space Administration. Goddard Space Flight Center, Greenbelt, Md.

A RULE-BASED SYSTEMS APPROACH TO SPACECRAFT COMMUNICATIONS CONFIGURATION OPTIMIZATION

James L. Rash, Yen F. Wong, and James J. Cieplak *In its* The 1988 Goddard Conference on Space Applications of Artificial Intelligence Aug. 1988 p 141-153 (For primary document see N88-30330 24-63)

Avail: NTIS HC A19/MF A01 CSCL 09B

An experimental rule-based system for optimizing user spacecraft communications configurations was developed at NASA to support mission planning for spacecraft that obtain telecommunications services through NASA's Tracking and Data Relay Satellite System. Designated Expert for Communications Configuration Optimization (ECCO), and implemented in the OPS5 production system language, the system has shown the validity of a rule-based systems approach to this optimization problem. The development of ECCO and the incremental optimization method on which it is based are discussed. A test case using hypothetical mission data is included to demonstrate the optimization concept. Author

N88-30342*# Ford Aerospace and Communications Corp., College Park, Md.

INTEGRATED RESOURCE SCHEDULING IN A DISTRIBUTED SCHEDULING ENVIRONMENT

David Zoch and Gardiner Hall *In* NASA, Goddard Space Flight Center, The 1988 Goddard Conference on Space Applications of Artificial Intelligence Aug. 1988 p 155-172 (For primary document see N88-30330 24-63)

Avail: NTIS HC A19/MF A01 CSCL 09B

The Space Station era presents a highly-complex multi-mission planning and scheduling environment exercised over a highly distributed system. In order to automate the scheduling process,

customers require a mechanism for communicating their scheduling requirements to NASA. A request language that a remotely-located customer can use to specify his scheduling requirements to a NASA scheduler, thus automating the customer-scheduler interface, is described. This notation, Flexible Envelope-Request Notation (FERN), allows the user to completely specify his scheduling requirements such as resource usage, temporal constraints, and scheduling preferences and options. The FERN also contains mechanisms for representing schedule and resource availability information, which are used in the inter-scheduler inconsistency resolution process. Additionally, a scheduler is described that can accept these requests, process them, generate schedules, and return schedule and resource availability information to the requester. The Request-Oriented Scheduling Engine (ROSE) was designed to function either as an independent scheduler or as a scheduling element in a network of schedulers. When used in a network of schedulers, each ROSE communicates schedule and resource usage information to other schedulers via the FERN notation, enabling inconsistencies to be resolved between schedulers. Individual ROSE schedules are created by viewing the problem as a constraint satisfaction problem with a heuristically guided search strategy. Author

N88-30343*# Westinghouse Electric Corp., Seabrook, Md.
MOORE: A PROTOTYPE EXPERT SYSTEM FOR DIAGNOSING SPACECRAFT PROBLEMS
Katherine Howlin, Jerry Weissert, and Kerry Krantz *In* NASA, Goddard Space Flight Center, The 1988 Goddard Conference on Space Applications of Artificial Intelligence Aug. 1988 p 175-190 (For primary document see N88-30330 24-63)
Avail: NTIS HC A19/MF A01 CSCL 09B

MOORE is a rule-based, prototype expert system that assists in diagnosing operational Tracking and Data Relay Satellite (TDRS) problems. It is intended to assist spacecraft engineers at the TDRS ground terminal in trouble shooting problems that are not readily solved with routine procedures, and without expert counsel. An additional goal of the prototype system is to develop in-house expert system and knowledge engineering skills. The prototype system diagnoses antenna pointing and earth pointing problems that may occur within the TDRS Attitude Control System (ACS). Plans include expansion to fault isolation of problems in the most critical subsystems of the TDRS spacecraft. Long term benefits are anticipated with use of an expert system during future TDRS programs with increased mission support time, reduced problem solving time, and retained expert knowledge and experience. Phase 2 of the project is intended to provide NASA the necessary expertise and capability to define requirements, evaluate proposals, and monitor the development progress of a highly competent expert system for NASA's Tracking Data Relay Satellite. Phase 2 also envisions addressing two unexplored applications for expert systems, spacecraft integration and tests (I and T) and support to launch activities. The concept, goals, domain, tools, knowledge acquisition, developmental approach, and design of the expert system. It will explain how NASA obtained the knowledge and capability to develop the system in-house without assistance from outside consultants. Future plans will also be presented. Author

N88-30344*# National Aeronautics and Space Administration. Goddard Space Flight Center, Greenbelt, Md.
ACHIEVING REAL-TIME PERFORMANCE IN FIESTA
William Wilkinson, Nadine Happell, Steve Miksell, Robert Quillin (Stanford Telecommunications, Inc., Reston, Va.), and Candace Carlisle *In its* The 1988 Goddard Conference on Space Applications of Artificial Intelligence Aug. 1988 p 191-205 (For primary document see N88-30330 24-63)
(Contract NAS5-31500)
Avail: NTIS HC A19/MF A01 CSCL 09B

The Fault Isolation Expert System for TDRSS Applications (FIESTA) is targeted for operation in a real-time online environment. Initial stages of the prototype development concentrated on acquisition and representation of the knowledge necessary to isolate faults in the TDRSS Network. Recent efforts focused on achieving real-time performance including: a discussion of the meaning of FIESTA real-time requirements, determination of performance levels (benchmarking) and techniques for optimization. Optimization techniques presented include redesign of critical relations, filtering of redundant data and optimization of patterns used in rules. Results are summarized. Author

N88-30345*# Jet Propulsion Lab., California Inst. of Tech., Pasadena.
MISSION TELEMETRY SYSTEM MONITOR: A REAL-TIME KNOWLEDGE-BASED SYSTEM **c17**
Samih A. Mouneimne *In* NASA, Goddard Space Flight Center, The 1988 Goddard Conference on Space Applications of Artificial Intelligence Aug. 1988 p 207-212 (For primary document see N88-30330 24-63)
Avail: NTIS HC A19/MF A01 CSCL 09B

The Galileo Mission Telemetry System (MTS) has a cluster of computer subsystems configured as a star network. The MTS handles the real-time processing of spacecraft telemetry and ground monitor data. Large volumes of status and fault messages are generated as a result of changes in the system environment. These messages are triggered by the conditions that exist on any one particular subsystem or device. The order of message generation is in time sequence and does not always correlate to the function sequence of active processes. A significant number of messages provide context with varying degrees of uncertainty. As such, highly skilled telemetry controllers are required to regularly go through high volumes of messages generated by the MTS to identify, diagnose, and isolate faults. A knowledge-based system prototype is being developed to monitor the Galileo Mission Telemetry System performance. The system design approach features temporal reasoning, uncertainty management, and intelligent graphic user interfaces. Author

N88-30346*# National Bureau of Standards, Gaithersburg, Md.
LOW LEVEL IMAGE PROCESSING TECHNIQUES USING THE PIPELINE IMAGE PROCESSING ENGINE IN THE FLIGHT TELEROBOTIC SERVICER **c54**
Marilyn Nashman and Karen J. Chaconas *In* NASA, Goddard Space Flight Center, The 1988 Goddard Conference on Space Applications of Artificial Intelligence Aug. 1988 p 215-229 (For primary document see N88-30330 24-63)
Avail: NTIS HC A19/MF A01 CSCL 09B

The sensory processing system for the NASA/NBS Standard Reference Model (NASREM) for telerobotic control is described. This control system architecture was adopted by NASA of the Flight Telerobotic Servicer. The control system is hierarchically designed and consists of three parallel systems: task decomposition, world modeling, and sensory processing. The Sensory Processing System is examined, and in particular the image processing hardware and software used to extract features at low levels of sensory processing for tasks representative of those envisioned for the Space Station such as assembly and maintenance are described. Author

N88-30347*# Jet Propulsion Lab., California Inst. of Tech., Pasadena.
AUTONOMOUS IMAGE DATA REDUCTION BY ANALYSIS AND INTERPRETATION
Susan Eberlein, Gigi Yates, and Niles Ritter *In* NASA, Goddard Space Flight Center, The 1988 Goddard Conference on Space Applications of Artificial Intelligence Aug. 1988 p 231-242 (For primary document see N88-30330 24-63)
Avail: NTIS HC A19/MF A01 CSCL 09B

Image data is a critical component of the scientific information acquired by space missions. Compression of image data is required due to the limited bandwidth of the data transmission channel and limited memory space on the acquisition vehicle. This need becomes more pressing when dealing with multispectral data where each pixel may comprise 300 or more bytes. An autonomous, real time, on-board image analysis system for an exploratory vehicle such as a Mars Rover is developed. The completed system will be capable of interpreting image data to produce reduced representations of the image, and of making decisions regarding

the importance of data based on current scientific goals. Data from multiple sources, including stereo images, color images, and multispectral data, are fused into single image representations. Analysis techniques emphasize artificial neural networks. Clusters are described by their outlines and class values. These analysis and compression techniques are coupled with decision making capacity for determining importance of each image region. Areas determined to be noise or uninteresting can be discarded in favor of more important areas. Thus limited resources for data storage and transmission are allocated to the most significant images.
Author

N88-30348*# Maryland Univ., College Park. Robotics Lab.
AN AUTOMATED COMPUTERIZED VISION TECHNIQUE FOR DETERMINATION OF THREE-DIMENSIONAL OBJECT GEOMETRY
Pen-Tai Chiang, Jackson C. S. Yang, and V. Pavlin *In* NASA, Goddard Space Flight Center, The 1988 Goddard Conference on Space Applications of Artificial Intelligence Aug. 1988 p 243-257 (For primary document see N88-30330 24-63)
(Grant NSF MSM-86-15187)
Avail: NTIS HC A19/MF A01 CSCL 09B

It is very important to determine three dimensional geometry of objects quickly in various military, space, construction, and industrial applications. An automatic scheme to obtain three dimensional geometry of objects by employing only one camera is presented. At present, this technique is applicable to a limited category of objects, satisfying the following constraints: they are flat-surfaces, and all the vertex points have to be recognized as corner points of the two dimensional image. The scheme consists of corner detection, data communication, camera calibration techniques and point searching and matching, edge cancelation, and creation procedures. An L shaped model is chosen as a test object. Experimental results demonstrated the reconstruction of this object geometry within 5 mm discrepancy. This scheme is quite convenient, efficient to use and can be applied to a wide range of problems in the real world.
Author

N88-30349*# National Aeronautics and Space Administration. Goddard Space Flight Center, Greenbelt, Md.
AN INTERACTIVE TESTBED FOR DEVELOPMENT OF EXPERT TOOLS FOR PATTERN RECOGNITION
Stephen W. Wharton *In its* The 1988 Goddard Conference on Space Applications of Artificial Intelligence Aug. 1988 p 259-273 (For primary document see N88-30330 24-63)
Avail: NTIS HC A19/MF A01 CSCL 09B

The initial implementation of an interactive testbed for development of expert system applications in image processing, i.e., a toolbox of procedures designed to facilitate the capture of expert knowledge for region grouping and analysis is described. The user can elect to interactively enter commands (via a command interpreter) for region manipulation to, in effect, simulate the actions of a hypothetical expert system. The user can then incorporate any rules and procedures as derived from interactive experimentation into customized region processing procedures using the library of utility functions. An iterative technique based on image pyramids is used to compute the initial region segmentation without the use of process parameters. These regions can then be interactively examined and manipulated using the command interpreter.
Author

N88-30350*# George Mason Univ., Fairfax, Va. Dept. of Computer Science.
PARALLEL AND DISTRIBUTED COMPUTATION FOR FAULT-TOLERANT OBJECT RECOGNITION
Harry Wechsler *In* NASA, Goddard Space Flight Center, The 1988 Goddard Conference on Space Applications of Artificial Intelligence Aug. 1988 p 275-293 (For primary document see N88-30330 24-63)
Avail: NTIS HC A19/MF A01 CSCL 09B

The distributed associative memory (DAM) model is suggested for distributed and fault-tolerant computation as it relates to object recognition tasks. The fault-tolerance is with respect to geometrical distortions (scale and rotation), noisy inputs, occulsion/overlap, and memory faults. An experimental system was developed for fault-tolerant structure recognition which shows the feasibility of such an approach. The approach is futher extended to the problem of multisensory data integration and applied successfully to the recognition of colored polyhedral objects.
Author

N88-30351*# Wayne State Univ., Detroit, Mich.
RANGE DATA DESCRIPTION BASED ON MULTIPLE CHARACTERISTICS c82
Ezzet Al-Hujazi and Arun Sood (George Mason Univ., Fairfax, Va.) *In* NASA, Goddard Space Flight Center, The 1988 Goddard Conference on Space Applications of Artificial Intelligence Aug. 1988 p 295-309 (For primary document see N88-30330 24-63)
Avail: NTIS HC A19/MF A01 CSCL 05B

An algorithm for describing range images based on Mean curvature (H) and Gaussian curvature (K) is presented. Range images are unique in that they directly approximate the physical surfaces of a real world 3-D scene. The curvature parameters are derived from the fundamental theorems of differential geometry and provides visible invariant pixel labels that can be used to characterize the scene. The sign of H and K can be used to classify each pixel into one of eight possible surface types. Due to the sensitivity of these parameters to noise the resulting HK-sing map does not directly identify surfaces in the range images and must be further processed. A region growing algorithm based on modeling the scene points with a Markov Random Field (MRF) of variable neighborhood size and edge models is suggested. This approach allows the integration of information from multiple characteristics in an efficient way. The performance of the proposed algorithm on a number of synthetic and real range images is discussed.
Author

N88-30352*# National Aeronautics and Space Administration. Goddard Space Flight Center, Greenbelt, Md.
THE SECOND GENERATION INTELLIGENT USER INTERFACE FOR THE CRUSTAL DYNAMICS DATA INFORMATION SYSTEM c82
Nicholas Short, Jr. and Scott L. Wattawa (Science Applications Research, Greenbelt, Md.) *In its* The 1988 Goddard Conference on Space Applications of Artificial Intelligence Aug. 1988 p 313-327 (For primary document see N88-30330 24-63)
Avail: NTIS HC A19/MF A01 CSCL 05B

For the past decade, operations and research projects that support a major portion of NASA's overall mission have experienced a dramatic increase in the volume of generated data and resultant information that is unparalleled in the history of the agency. The effect of such an increase is that most of the science and engineering disciplines are undergoing an information glut, which has occurred, not only because of the amount, but also because of the type of data being collected. This information glut is growing exponentially and is expected to grow for the foreseeable future. Consequently, it is becoming physically and intellectually impossible to identify, access, modify, and analyze the most suitable information. Thus, the dilemma arises that the amount and complexity of information has exceeded and will continue to exceed, using present information systems, the ability of all the scientists and engineers to understand and take advantage of this information. As a result of this information problem, NASA has initiated the Intelligent Data Management (IDM) project to design and develop Advanced Information Management Systems (AIMS). The first effort of the Project was the prototyping of an Intelligent User Interface (IUI) to an operational scientific database using expert systems, natural language processing, and graphics technologies. An overview of the IUI formulation and development for the second phase is presented.
Author

N88-30353*# National Aeronautics and Space Administration. Goddard Space Flight Center, Greenbelt, Md.
SPACELAB DATA PROCESSING FACILITY (SLDPF) QUALITY ASSURANCE (QA)/DATA ACCOUNTING (DA) EXPERT SYSTEMS: TRANSITION FROM PROTOTYPES TO OPERATIONAL SYSTEMS **c82**
Lisa Basile *In its* The 1988 Goddard Conference on Space Applications of Artificial Intelligence Aug. 1988 p 329-341 (For primary document see N88-30330 24-63)
Avail: NTIS HC A19/MF A01 CSCL 05B

The SLDPF is responsible for the capture, quality monitoring processing, accounting, and shipment of Spacelab and/or Attached Shuttle Payloads (ASP) telemetry data to various user facilities. Expert systems will aid in the performance of the quality assurance and data accounting functions of the two SLDPF functional elements: the Spacelab Input Processing System (SIPS) and the Spacelab Output Processing System (SOPS). Prototypes were developed for each as independent efforts. The SIPS Knowledge System Prototype (KSP) used the commercial shell OPS5+ on an IBM PC/AT; the SOPS Expert System Prototype used the expert system shell CLIPS implemented on a Macintosh personal computer. Both prototypes emulate the duties of the respective QA/DA analysts based upon analyst input and predetermined mission criteria parameters, and recommended instructions and decisions governing the reprocessing, release, or holding for further analysis of data. These prototypes demonstrated feasibility and high potential for operational systems. Increase in productivity, decrease of tedium, consistency, concise historial records, and a training tool for new analyses were the principal advantages. An operational configuration, taking advantage of the SLDPF network capabilities, is under development with the expert systems being installed on SUN workstations. This new configuration in conjunction with the potential of the expert systems will enhance the efficiency, in both time and quality, of the SLDPF's release of Spacelab/AST data products. Author

N88-30354*# National Aeronautics and Space Administration. Goddard Space Flight Center, Greenbelt, Md.
AUTOMATED CATALOGING AND CHARACTERIZATION OF SPACE-DERIVED DATA **c82**
William J. Campbell, Larry Roelofs, and Michael Goldberg (Mitre Corp., McLean, Va.) *In its* The 1988 Goddard Conference on Space Applications of Artificial Intelligence Aug. 1988 p 343-354 (For primary document see N88-30330 24-63)
Avail: NTIS HC A19/MF A01 CSCL 05B

One of the most significant technical issues that NASA must address and resolve is the problem of managing the enormous amounts of scientific and engineering data that will be generated by the next generation of remote sensing systems such as the Hubble Space Telescope (HST) and the Earth Observing System (EOS). The amount of data these sensors are expected to produce will be orders of magnitude greater than NASA has ever experienced. Consequently new solutions must be developed for managing, accessing, and automatically inputting the data into a database in some expressive fashion that will provide a meaningful understanding and effective utilization of this data in a multidisciplinary environment. Presently, scientific data provided by satellites and other sources are processed, cataloged, and archived according to narrow mission or project-specific requirements with little regard to the semantics of the overall research. Scientists therefore lack knowledge of or access to potentially valuable data outside their own field. What is needed is an innovative approach that will allow collected data to be automatically cataloged, characterized, and managed in a domain-community. A concept and design approach that employs expert system-based knowledge controllers combined with advanced spatial database systems and graphical data structures is discussed. Author

N88-30355*# LNK Corp., Riverdale, Md.
A DESIGN FOR A GROUND-BASED DATA MANAGEMENT SYSTEM **c82**
Barbara A. Lambird and David Lavine *In* NASA, Goddard Space Flight Center, The 1988 Goddard Conference on Space Applications of Artificial Intelligence Aug. 1988 p 355-369 (For primary document see N88-30330 24-63)
Avail: NTIS HC A19/MF A01 CSCL 05B

An initial design for a ground-based data management system which includes intelligent data abstraction and cataloging is described. The large quantity of data on some current and future NASA missions leads to significant problems in providing scientists with quick access to relevant data. Human screening of data for potential relevance to a particular study is time-consuming and costly. Intelligent databases can provide automatic screening when given relevent scientific parameters and constraints. The data management system would provide, at a minimum, information of availability of the range of data, the type available, specific time periods covered together with data quality information, and related sources of data. The system would inform the user about the primary types of screening, analysis, and methods of presentation available to the user. The system would then aid the user with performing the desired tasks, in such a way that the user need only specify the scientific parameters and objectives, and not worry about specific details for running a particular program. The design contains modules for data abstraction, catalog plan abstraction, a user-friendly interface, and expert systems for data handling, data evaluation, and application analysis. The emphasis is on developing general facilities for data representation, description, analysis, and presentation that will be easily used by scientists directly, thus bypassing the knowledge acquisition bottleneck. Expert system technology is used for many different aspects of the data management system, including the direct user interface, the interface to the data analysis routines, and the analysis of instrument status. Author

N88-30356*# National Aeronautics and Space Administration. Marshall Space Flight Center, Huntsville, Ala.
AUTOMATIC MATHEMATICAL MODELING FOR REAL TIME SIMULATION SYSTEM
Caroline Wang and Steve Purinton *In* NASA, Goddard Space Flight Center, The 1988 Goddard Conference on Space Applications of Artificial Intelligence Aug. 1988 p 373-380 (For primary document see N88-30330 24-63)
Avail: NTIS HC A19/MF A01 CSCL 09B

A methodology for automatic mathematical modeling and generating simulation models is described. The models will be verified by running in a test environment using standard profiles with the results compared against known results. The major objective is to create a user friendly environment for engineers to design, maintain, and verify their model and also automatically convert the mathematical model into conventional code for conventional computation. A demonstration program was designed for modeling the Space Shuttle Main Engine Simulation. It is written in LISP and MACSYMA and runs on a Symbolic 3670 Lisp Machine. The program provides a very friendly and well organized environment for engineers to build a knowledge base for base equations and general information. It contains an initial set of component process elements for the Space Shuttle Main Engine Simulation and a questionnaire that allows the engineer to answer a set of questions to specify a particular model. The system is then able to automatically generate the model and FORTRAN code. The future goal which is under construction is to download the FORTRAN code to VAX/VMS system for conventional computation. The SSME mathematical model will be verified in a test environment and the solution compared with the real data profile. The use of artificial intelligence techniques has shown that the process of the simulation modeling can be simplified. Author

N88-30357*# Jet Propulsion Lab., California Inst. of Tech., Pasadena.
THE SPACE STATION ASSEMBLY PHASE: SYSTEM DESIGN TRADE-OFFS FOR THE FLIGHT TELEROBOTIC SERVICER **c54**
Jeffrey H. Smith, Max Gyamfi, Kent Volkmer, and Wayne Zimmerman *In* NASA, Goddard Space Flight Center, The 1988 Goddard Conference on Space Applications of Artificial Intelligence Aug. 1988 p 381-396 (For primary document

see N88-30330 24-63)
(Contract NAS7-918)
Avail: NTIS HC A19/MF A01 CSCL 05H

The effects of a recent study aimed at identifying key issues and trade-offs associated with using a Flight Telerobotic Servicer (FTS) to aid in Space Station assembly-phase tasks is described. The use of automation and robotic (A and R) technologies for large space systems often involves a substitution of automation capabilities for human EVA or IVA activities. A methodology is presented that incorporates assessment of candidate assembly-phase tasks, telerobotic performance capabilities, development costs, and effects of operational constaints. Changes in the region of cost-effectiveness are examined under a variety of system design assumptions. A discussion of issues is presented with focus on three roles the FTS might serve: as a research-oriented test bed to learn more about space usage of telerobotics; as a research based test bed having an experimental demonstration orientation with limited assembly and servicing applications; or as an operational system to augment EVA and to aid construction of the Space Station and to reduce the program (schedule) risk by increasing the flexibility of mission operations.
Author

N88-30358*# Ford Aerospace and Communications Corp., Seabrook, Md.
A SIMULATION ENGINE: COMBINING AN EXPERT SYSTEM WITH A SIMULATION LANGUAGE
James R. Spiegel and David B. LaVallee *In* NASA, Goddard Space Flight Center, The 1988 Goddard Conference on Space Applications of Artificial Intelligence Aug. 1988 p 397-406 (For primary document see N88-30330 24-63)
Avail: NTIS HC A19/MF A01 CSCL 09B

Expert systems were applied in a number of ways to the field of simulation. One of these is the application of an expert system to drive a simulation, by making run-time decisions which effect the simulation. This approach was successful for a number of specific simulation models. The simulation engine extends this capability by supporting this type of interaction in a general purpose setting. A general purpose simulation language is provided for building models, and an inference engine is provided for knowledge processing. This combination results in a mechanism which allows general purpose models to be simulated in concert with interactive knowledge bases.
Author

N88-30359*# Science Applications Research, Greenbelt, Md. National Space Science Data Center.
THE ADVICE TAKER/INQUIRER: A SYSTEM FOR HIGH-LEVEL ACQUISITION OF EXPERT KNOWLEDGE
Robert F. Cromp *In* NASA, Goddard Space Flight Center, The 1988 Goddard Conference on Space Applications of Artificial Intelligence Aug. 1988 p 409-423 (For primary document see N88-30330 24-63)
Avail: NTIS HC A19/MF A01 CSCL 09B

The Advice Taker/Inquirer (AT/I) is a domain-independent program that is used to construct, monitor, and improve an expert system. In the learning phase, an expert teaches a strategy to the AT/I by providing it with declarative and procedural knowledge, expressed in the expert's domain-specific vocabulary. The expert can modify any advice given to the system earlier, and any advice dependent on the altered advice is reviewed automatically for syntatic and sematic soundness. Knowledge acquisition and methods for ensuring the integrity of the knowledge base in an expert system is discussed.
Author

N88-30360*# Space Telescope Science Inst., Baltimore, Md.
LISP OBJECT STATE SAVER (LOSS): A FACILITY USED TO SAVE PARTIAL SCHEDULES OF THE HUBBLE SPACE TELESCOPE
Jeffrey L. Sponsler *In* NASA, Goddard Space Flight Center, The 1988 Goddard Conference on Space Applications of Artificial Intelligence Aug. 1988 p 425-433 (For primary document see N88-30330 24-63)
Avail: NTIS HC A19/MF A01 CSCL 09B

Current research in the area of long term scheduling of the Hubble Space Telescope is being done using Common Lisp and Flavors on Lisp Machines. The planning tools manipulate memory-resident data structures which represent the many entities and relationships that represent planning states. The Lisp Object State Saver (LOSS), a general purpose utility, was constructed which allows one to take a snapshot of memory by storing a representation of the structures in a text file. This text file can later be loaded thus restoring the pre-existing and logically equivalent planning state. A LOSS template must be created for each datatype to be stored and a simple grammar governs the creation of such templates.
Author

N88-30361*# Space Telescope Science Inst., Baltimore, Md.
VERIFICATION AND VALIDATION OF RULEBASED SYSTEMS FOR HUBBLE SPACE TELESCOPE GROUND SUPPORT
Shon Vick and Kelly Lindenmayer (Computer Sciences Corp., Baltimore, Md.) *In* NASA, Goddard Space Flight Center, The 1988 Goddard Conference on Space Applications of Artificial Intelligence Aug. 1988 p 435-448 (For primary document see N88-30330 24-63)
Avail: NTIS HC A19/MF A01 CSCL 09B

As rulebase systems become more widely used in operational environments, the focus is on the problems and concerns of maintaining expert systems. In the conventional software model, the verification and validation of a system have two separate and distinct meanings. To validate a system means to demonstrate that the system does what is advertised. The verification process refers to investigating the actual code to identify inconsistencies and redundancies within the logic path. In current literature regarding maintaining rulebased systems, little distinction is made between these two terms. In fact, often the two terms are used interchangeably. Verification and validation of rulebased systems are discussed as separate but equally important aspects of the maintenance phase. Also described are some of the tools and methods that were developed at the Space Telescope Science Institute to aid in the maintenance of the rulebased system.
Author

N88-30362*# Computer Sciences Corp., Beltsville, Md. System Sciences Div.
THE NEED FOR A COMPREHENSIVE EXPERT SYSTEM DEVELOPMENT METHODOLOGY
John Baumert, Anna Critchfield, and Karen Leavitt *In* NASA, Goddard Space Flight Center, The 1988 Goddard Conference on Space Applications of Artificial Intelligence Aug. 1988 p 449-460 (For primary document see N88-30330 24-63)
Avail: NTIS HC A19/MF A01 CSCL 09B

In a traditional software development environment, the introduction of standardized approaches has led to higher quality, maintainable products on the technic. / side and greater visibility into the status of the effort on the management side. This study examined expert system development to determine whether it differed enough from traditional systems to warrant a reevaluation of current software development methodologies. Its purpose was to identify areas of similarity with traditional software development and areas requiring tailoring to the unique needs of expert systems. A second purpose was to determine whether existing expert system development methodologies meet the needs of expert system development, management, and maintenance personnel. The study consisted of a literature search and personal interviews. It was determined that existing methodologies and approaches to developing expert systems are not comprehensive nor are they easily applied, especially to cradle to grave system development. As a result, requirements were derived for an expert system development methodology and an initial annotated outline derived for such a methodology.
Author

N88-30363# Johns Hopkins Univ., Baltimore, Md. Dept. of Electrical Engineering and Computer Science.
K(SUP th)-ORDER EXTENDED LINEARIZATION Report, 1 Mar. 1987 - 29 Feb. 1988
Jianliang Wang and Wilson J. Rugh 1 Mar. 1988 7 p

(Grant AF-AFOSR-0101-87)
(AD-A194786; AFOSR-88-0435TR) Avail: NTIS HC A02/MF A01 CSCL 12D

For a given nonlinear system, consider the design of a nonlinear control law such that the following properties hold. First, as in the extended linearization method, linearizations of the closed-loop system about constant operating points of the closed-loop system achieve specified, linear design objectives. Second, the Taylor series expansion of the closed-loop state equation about any constant operating point is such that terms of order 2, 3..., k are zero. or at least are minimized in a certain sense. Conditions under which this can be achieved, while simple to state, are restrictive. GRA

N88-30364# Massachusetts Inst. of Tech., Cambridge. Artificial Intelligence Lab.
THE COMBINATORICS OF OBJECT RECOGNITION IN CLUTTERED ENVIRONMENTS USING CONSTRAINED SEARCH
W. E. Grimson Feb. 1988 40 p
(Contracts N00014-85-K-0124; DACA76-85-C-0010)
(AD-A196224) Avail: NTIS HC A03/MF A01 CSCL 12I

The problem of recognizing rigid objects from noisy sensory data has been successfully attacked in previous work by using a constrained search approach. Empirical investigations have shown the method to be very effective when recognizing and localizing isolated objects, but less effective when dealing with occluded objects where much of the sensory data arises from objects other than the one of interest. When clustering techniques such as the Hough transform are used to isolate likely subspaces of the search space, empirical performance in cluttered scenes improves considorably. This note establishes formal bounds on the combinatorics of this approach. Under some simple assumptions, the expected complexity of recognizing isolated objects is quadratic in the number of model and sensory fragments, but the expected complexity of recognizing objects in cluttered environments is exponential in the size of the correct interpretation. Formal bounds are provided on the efficacy of using the Hough transform to preselect likely subspaces, showing that problem remains exponential, but that in practical terms, the size of the problem is significantly decreased. GRA

N88-30365# LABEN Space Instrumentation and Systems, Milan (Italy).
STUDY OF SOFTWARE REQUIREMENTS AND ARTIFICIAL INTELLIGENCE TECHNIQUES FOR ROBOTICS Final Report
P. Donzelli Paris, France ESA Jan. 1988 93 p
(Contract ESA-6029/84-NL-PP(SC))
(TL-3333; ESA-CR(P)-2577; ETN-88-93022) Avail: NTIS HC A05/MF A01

Software requirements to be applied on space service manipulator systems (SMS) were determined. An architectural design for the higher levels of the SMS control software organization was defined. The proposed architecture makes wide use of AI paradigms and provides indications on implementation aspects. Programming languages and development environments suitable for the implementation of the proposed architecture were studied, for robotics and general purpose languages. Ada is the preferred option in combination with AI languages. The state of the art of AI techniques and concepts applied to robotic problems to be experimented and verified in the frame of the SMS control as outlined in the software architecture was reviewed. ESA

N88-30366# Massachusetts Inst. of Tech., Cambridge. Artificial Intelligence Lab.
DYNAMICAL SYSTEMS AND MOTION VISION
Joachim Heel Apr. 1988 56 p
(Contract N00014-85-K-0124)
(AD-A195932; AI-M-1037) Avail: NTIS HC A04/MF A01 CSCL 12I

This paper shows how the theory of dynamical systems can be employed to solve problems in motion vision. It develops algorithms for recovery of dense depth maps and motion parameters using state space observers or filters. Start with a review of previous, related work followed by an overview of relevant aspects of the theory of dynamical systems. Three dynamical models of the imaging situation are presented: The first model assumes that motion is known and a reflectance model for the surface is given. Depth is recovered directly from brightness measurements with a nonlinear Kalman filter. The second model assumes that a planar surface is being reviewed. Motion and depth are recovered with a nonlinear observer. The third model makes no explicit assumptions about motion or surface. It is embedded in a system that iteratively improves an estimate for both the motion parameters and a dense depth map using Kalman filters. No feature-matching preprocessor is required. Solutions to other motion vision problems (tracking, camera parameter estimation) using dynamical systems theory are suggested. GRA

N88-30367# Naval Postgraduate School, Monterey, Calif.
ADAPTIVE CONTROL IN POSITIONING A RIGID-FLEXIBLE ROBOT ARM M.S. Thesis
Constantinos Mardas Mar. 1988 168 p
(AD-A195194) Avail: NTIS HC A08/MF A01 CSCL 13H

The feasibility of controlling a rigid-flexible, two links planar robot arm with an adaptive computer simulation model is investigated. The velocity curve following method was used as the adaptive control scheme. The motors acting at each joint were driven by the adaptive model. The adaptive algorithm update the states and the gain parameter of the ideal motor used in the computer model. This adaptation procedure was accomplished using only the measured angular position of the arm. The mathematical model for the proposed manipulator was derived using the Lagrangian dynamics approach. Simulation results were obtained with the manipulator performing under various conditions, by changing the load of the arm and the forces included in the environment. GRA

N88-30368# Army Military Personnel Center, Alexandria, Va.
SIMULATION OF A TWO LINK ROBOT MANIPULATOR WITH ELASTIC MEMBERS Final Report, 1 Sep. - 6 May 1988
John C. Hinds 6 May 1988 124 p
(AD-A196014) Avail: NTIS HC A06/MF A01 CSCL 13H

This study considers the dynamic effects of elastic link displacements in a two-link robot manipulator as simulated by a hierarchy of models. In all, five separate system models are developed. The last model, TFTFEL, allows both manipulator links to bend in a single plane and to twist. Therefore, the effects of bending-torsion vibrations in each link may be observed when the manipulator attempts motion with an inertially asymmetric payload grasped in its end-effector. This elasto-dynamic behavior is simulated, and results indicate a definite disturbance of the joint angle trajectories. The use of structural damping to eliminate these high frequency vibrations and increase the manipulator's accuracy is evaluated. GRA

N88-30369*# Applied Research Lab., State College, Pa.
AN APPROACH TO CMG STEERING USING FEEDBACK LINEARIZATION
John Dzielski, Edward Bergmann, Joseph Paradiso, Derek Rowell, and David Wormley (Massachusetts Inst. of Tech., Cambridge.) 1988 35 p
(Contract NAS9-17560)
(NASA-CR-183172; NAS 1.26:183172) Avail: NTIS HC A03/MF A01 CSCL 09B

This paper presents an approach for controlling spacecraft equipped with control moment gyroscopes. A technique from feedback linearization theory is used to transform the original nonlinear problem to an equivalent linear form without approximating assumptions. In this form, the spacecraft dynamics appear linearly, and are decoupled from redundancy in the system of gyroscopes. A general approach to distributing control effort among the available actuators is described which includes provisions for redistribution of rotors, explicit bounds in gimbal rates, and guaranteed operation at or near singular configurations.

A particular algorithm is developed for systems of double-gimbal devices, and demonstrated in two examples for which existing approaches fail to give adequate performance. Author

N88-30370# SRI International Corp., Menlo Park, Calif. Artificial Intelligence Center.
RESEARCH ON PROBLEM-SOLVING SYSTEMS Final Report, 1 Oct. 1984 - 14 Feb. 1988
David E. Wilkins Feb. 1988 164 p
(Contract F49620-85-K-0001)
(AD-A195154; AFOSR-88-0563TR) Avail: NTIS HC A08/MF A01 CSCL 12I

This is the final report for a research project which focused on artificial intelligence planning systems. The research investigated methods for representing, generating, and executing hierarchical plans that contain parallel actions. Reasoning about actions is critical to many important areas including automatic planning systems, expert consultation systems, and real-time control of robotic systems. This report describes progress in planning, including efficient techniques for generating hierarchical and parallel plans in certain domains. This work was performed using SIPE (System for Interactive Planning and Execution Monitoring) which was developed in part under this contract. GRA

N88-30371# Massachusetts Inst. of Tech., Cambridge. Artificial Intelligence Lab.
A STANDARD ARCHITECTURE FOR CONTROLLING ROBOTS
Sundar Narasimhan, David M. Siegel, and John M. Hollerbach Jul. 1988 25 p
(Contracts N00014-86-K-0685; N00014-85-K-0124)
(AD-A195929; AI-M-977) Avail: NTIS HC A03/MF A01 CSCL 12F

This paper describes a fully implemented computational architecture that controls the Utah-MIT dextrous hand and other complex robots. Robots like the Utah-MIT hand are characterized by large numbers of actuators and sensors, and require high servo rates. Consequently, powerful and flexible computer architectures are needed to control them. The robotic architecture described in this paper derives its power from the highly efficient real-time environment provided for its control processors, coupled with a development host that enables flexible program development. By mapping the memory of a dedicated group of processors into the address space of a host computer, efficient sharing of system resources between them is possible. The software is characterized by a few simple design concepts but provides the facilities out of which more powerful utilities like a multi-processor pseudo-terminal emulator, a transparent and fast file server, and a flexible symbolic debugger could be constructed. GRA

N88-30372# Carnegie-Mellon Univ., Pittsburgh, Pa. Robotics Inst.
KNOWLEDGE BASED SIMULATION: AN ARTIFICIAL INTELLIGENCE APPROACH TO SYSTEM MODELING AND AUTOMATING THE SIMULATION LIFE CYCLE Interim Technical Report
Mark S. Fox, Nizwer Husain, Malcolm McRoberts, and Y. V. Reddy 13 Apr. 1988 46 p Sponsored in part by Digital Equipment Corp. and Eestinghouse Electric Corp.
(AD-A195838; CMI-RI-TR-88-5) Avail: NTIS HC A03/MF A01 CSCL 12I

This paper summarizes the past eight years of research in the application of Artificial Intelligence (AI) to Simulation. Our focus has been in two areas: the use of AI knowledge representation techniques for the modeling of complex systems, and the codification of simulation expertise so that it can be used to manage the simulation life cycle. The Knowledge Based Simulation system is an embodiment of this research. It provides a complete simulation decision support environment for the modeling, validation, simulation and analysis of complex systems. KBS has been applied to a variety of problems including factory and distribution system analysis. By using a frame language to represent domain concepts, such as object structure, and goals, there is a one to one correspondence between the domain and the simulation model 2. Secondly, by using rules to represent object behavior, the specification and modification of the behaviors become easier. Lastly, explanation techniques developed around rule based systems provide the basis for explaining event behaviors. GRA

N88-30373*# National Aeronautics and Space Administration. Ames Research Center, Moffett Field, Calif.
NESTED NEURAL NETWORKS
Yoram Baram Aug. 1988 26 p
(NASA-TM-101032; A-88288; NAS 1.15:101032) Avail: NTIS HC A03/MF A01 CSCL 09B

Nested neural networks, consisting of small interconnected subnetworks, allow for the storage and retrieval of neural state patterns of different sizes. The subnetworks are naturally categorized by layers of corresponding to spatial frequencies in the pattern field. The storage capacity and the error correction capability of the subnetworks generally increase with the degree of connectivity between layers (the nesting degree). Storage of only few subpatterns in each subnetworks results in a vast storage capacity of patterns and subpatterns in the nested network, maintaining high stability and error correction capability. Author

N88-30374# Massachusetts Inst. of Tech., Cambridge. Artificial Intelligence Lab.
SYMBOLIC CONSTRUCTION OF A 2D SCALE-SPACE IMAGE
Eric Saund Apr. 1988 61 p
(Contract N00014-85-K-0124)
(AD-A195926; AI-M-1028) Avail: NTIS HC A04/MF A01 CSCL 23C

The shapes of naturally occurring objects characteristically involve spatial events occurring at many scales. It is important to make explicit the multiscale structure of a shape object in order to effectively perform shape recognition or to engage in other forms of reasoning about shape. Currently available techniques for multiscale shape analysis include image blurring and contour smoothing; each of these techniques involves uniform application of a smoothing operator to the entire image array or contour. This paper offers a new, symbolic, approach to constructing a primitive shape description across scales for 2D binary (silhouette) shape images. Under this approach, grouping operations are performed over collections of tokens residing on a Scale-Space Blackboard. Two types of grouping operations are identified that, respectively: (1) aggregate edge primitives at one scale into edge primitives at a coarser scale, and (2) group edge primitives into partial-region assertions, including curved-contours, primitive-corners, and bars. Algorithms to perform these computations are presented. GRA

N88-30375# Massachusetts Inst. of Tech., Cambridge. Artificial Intelligence Lab.
EXPLOITING LEXICAL REGULARITIES IN DESIGNING NATURAL LANGUAGE SYSTEMS
Boris Katz and Beth Levin Apr. 1988 25 p
(Contract N00014-85-K-0124)
(AD-A195922; AI-M-1041) Avail: NTIS HC A03/MF A01 CSCL 05G

This paper presents the lexical component of the START Question Answering system developed at the MIT Artificial Intelligence Lab. START is able to interpret correctly a wide range of semantic relationships associated with alternate expressions of the arguments of verbs. The design of the system takes advantage of the results of recent linguistic research into the structure of the lexicon, allowing START to attain a broader range of coverage than many existing systems. It is concluded that the addition of a component that explicitly encodes verb classes and their characteristic properties, enables the START system to handle a wide range of phenomena reflecting semantic-syntactic correspondences that are characteristic of English verbs. By factoring properties that belong to whole classes of verbs out of the entries of individual verbs and letting these entries simply designate the verb's class membership, we do more than merely simplify entries. We facilitate the addition of new words to the

lexicon and make it easier to extend the system's coverage of linguistic phenomena. GRA

64 NUMERICAL ANALYSIS

Includes iteration, difference equations, and numerical approximation.

N88-30376# California Univ., Irvine. Dept. of Electrical Engineering.
STATISTICAL ANALYSIS OF THE LMS (LAST MEAN SQUARES) AND MODIFIED STOCHASTIC GRADIENT Final Report, 15 Mar. 1987 - 14 Apr. 1988
Bershad 7 Apr. 1988 6 p
(Grant AF-AFOSR-0093-86)
(AD-A195497; AFOSR-88-0588TR) Avail: NTIS HC A02/MF A01 CSCL 12C

Research on the stochastic behavior of the last mean squares (LMS) and related algorithms has yielded results in four majors. Significant progress has been made in determining the joint transient and steady state probability density functions of the time domain LMS weights for Gaussian jammers. The effects of non-linearities on the time domain LMS algorithm have been analyzed. GRA

N88-30377*# National Aeronautics and Space Administration. Lewis Research Center, Cleveland, Ohio.
CONVERGENCE ACCELERATION FOR VECTOR SEQUENCES AND APPLICATIONS TO COMPUTATIONAL FLUID DYNAMICS
Avram Sidi and Mark L. Celestina (Sverdrup Technology, Inc., Cleveland, Ohio.) Aug. 1988 25 p
(NASA-TM-101327; E-4338; ICOMP-88-17; NAS 1.15:101327)
Avail: NTIS HC A03/MF A01 CSCL 12A

Some recent developments in acceleration of convergence methods for vector sequences are reviewed. The methods considered are the minimal polynomial extrapolation, the reduced rank extrapolation, and the modified minimal polynomial extrapolation. The vector sequences to be accelerated are those that are obtained from the iterative solution of linear or nonlinear systems of equations. The convergence and stability properties of these methods as well as different ways of numerical implementation are discussed in detail. Based on the convergence and stability results, strategies that are useful in practical applications are suggested. Two applications to computational fluid mechanics involving the three dimensional Euler equations for ducted and external flows are considered. The numerical results demonstrate the usefulness of the methods in accelerating the convergence of the time marching techniques in the solution of steady state problems. Author

N88-30378# Mississippi State Univ., Mississippi State. Dept. of Aerophsyics and Aerospace Engineering.
GENERATION OF SURFACE GRIDS THROUGH ELLIPTIC PARTIAL DIFFERENTIAL EQUATIONS FOR AIRCRAFT AND MISSILE CONFIGURATIONS Final Report, Jun. 1987 - Mar. 1988
Z. U. Warsi 16 May 1988 27 p
(Grant AF-AFOSR-0143-85)
(AD-A195639; ASE-88-6; AFOSR-88-0636TR) Avail: NTIS HC A03/MF A01 CSCL 12A

The main aim of the project was to develop a set of partial differential equations which are the most optimum for the generation of grid lines in arbitrary surfaces. Equations have been developed on the basis of differential-geometric concepts which are elliptic in character and look to be the most optimum among the class of equations which can be used to generate the surface coordinates. The developed equations require a specification of the forcing function which depends on the geometry of the given surface. The surface in which the coordinates are to be introduced is usually given in discrete data form. Methods have been developed which fit a function over the given data to evaluate the forcing function for complicated shapes, e.g., an airplane, the functional fit and the eventual grid generation for the fuselage and wings are done separately and then integrated to obtain the grid lines on the surface. GRA

N88-30379# Massachusetts Inst. of Tech., Cambridge. Artificial Intelligence Lab.
AUTOMATIC QUALITATIVE ANALYSIS OF ORDINARY DIFFERENTIAL EQUATIONS USING PIECEWISE LINEAR APPROXIMATIONS Ph.D. Thesis
Elisha Peretz Sacks Mar. 1988 97 p
(Contracts N00014-85-K-0124; N00014-86-K-0180)
(AD-A196310; AI-TR-1031) Avail: NTIS HC A05/MF A01 CSCL 12E

This thesis explores automating the qualitative analysis of physical systems. Scientists and engineers model many physical systems with ordinary differential equations. They deduce the behavior of the systems by analyzing the equations. Most realistic models are nonlinear, hence difficult or impossible to solve explicitly. Analysts must resort to approximations or to sophisticated mathematical techniques. The author describes a computer program, called PLR (for Piecewise Linear Reasoner), that formalizes an analysis strategy employed by experts. PLR takes parametrized ordinary differential equations as input and produces a qualitative description of the solution for all initial values. It approximates intractable nonlinear systems with piecewise linear ones, analyzes the approximations, and draws conclusions about the original systems. It chooses approximations that are accurate enough to reproduce the essential properties of their nonlinear prototypes, yet simple enough to be analyzed completely and efficiently. GRA

N88-30380# Carnegie-Mellon Univ., Pittsburgh, Pa. Robotics Inst.
KALMAN FILTER-BASED ALGORITHMS FOR ESTIMATING DEPTH FROM IMAGE SEQUENCES
Larry Matthies, Richard Szeliski, and Takeo Kanade Jan. 1988 55 p
(Contract F33615-87-C-1499)
(AD-A195818; CMU-RI-TR-88-1) Avail: NTIS HC A04/MF A01 CSCL 12E

Using known camera motion to estimate depth from image sequences is important in robotics applications such as navigation and manipulation. For many applications, having an on-line, incremental estimate of depth is important. To permit the blending of new measurements with old estimates, it is essential that the representation include not only the current depth estimate, but also an estimate of the current uncertainty. Kalman filtering provides the needed framework to integrate new measurements and reduce the uncertainty over time. Previous applications of Kalman filtering to depth from motion have been limited to the estimation of depth at the location of a sparse set of features. In this paper, we introduce a new pixel-based (iconic) algorithm that estimates depth from an image sequence and incrementally refines its estimate over time. We also present a feature-based version of the algorithm which is used for comparison. We compare the performance of both approaches mathematically, with quantitative experiments using images of a flat scene, and with qualitative experiments using images of a realistic outdoor scene model. The results show that the method is an effective way to extract depth from lateral camera translations. GRA

N88-30381# Wisconsin Univ., Madison. Center for Mathematical Sciences.
ON THE NASH POINT EQUILIBRIA IN THE CALCULUS OF VARIATIONS Technical Summary Report
Kung-Ching Chang Nov. 1987 22 p
(Contract DAAL03-87-K-0043)
(AD-A194959; CMS-TSR-88-16) Avail: NTIS HC A03/MF A01 CSCL 12B

The existence and partial regularity of the Nash point equilibria for a pair of multiple integrals are studied. The conditions as well as the results are similar to those for local minima obtained by Acerbi, Fusco and Giaquinta, Guisti. GRA

N88-30382# Air Force Inst. of Tech., Wright-Patterson AFB, Ohio. School of Engineering.
ROBUST FINITE-DIMENSIONAL LQG (LINEAR QUADRIC GAUSSIAN)-BASED CONTROLLERS FOR A CLASS OF DISTRIBUTED PARAMETER SYSTEMS Ph.D. Thesis
Randall N. Paschall Jun. 1988 163 p
(AD-A194872; AFIT/DS/ENG/88J-1) Avail: NTIS HC A08/MF A01 CSCL 12D

The problem of robustly stabilizing infinite-dimensional systems using finite-dimensional controllers is considered. The controllers are assumed to be linear quadratic Gaussian (LQG) based controllers. This research uses a direct approach to demonstrate the existence of finite-dimensional LQG-based controllers that stabilize the nominal system. Once existence is proven, the research focuses on ways to analyze the robustness of the controller. Several types of perturbations are considered, including bounded, relatively bounded, additive, and multiplicative. Several approaches to analyzing robustness are developed. Direct analysis using results from functional analysis is accomplished, followed by an approach called the optimal projection equation approach, and then H-infinity techniques are used to develop a sufficient condition for robustness in the presence of multiplicative perturbations of the plant transfer function. A new interpretation of the linear quadratic Gaussian/loop transfer recovery technique (LQG/LTR) is made for the case of reduced order controllers. GRA

N88-30383# Massachusetts Inst. of Tech., Cambridge. Research Lab. of Electronics.
RECONSTRUCTION OF MULTIDIMENSIONAL SIGNALS FROM MULTIPLE LEVEL THRESHOLD CROSSINGS Ph.D. Thesis
Avideh Zakhor Jan. 1988 187 p
(Contract N00014-81-K-0742; Grant NSF ECS-84-07285)
(AD-A195561; TR-534) Avail: NTIS HC A09/MF A01 CSCL 12A

The first approach extended new theoretical results in multivariate polynomial interpolation theory, in order to define a variety of semi-implicit sampling strategies. These strategies, which provide sufficient conditions for recovery of multidimensional signals from nonuniform samples on lines of rational slope, are ultimately applied to the problem of reconstruction from multiple-level crossings. Although these semi-implicit results are general enough to be used for recovery from signal crossings with arbitrary functions, they do not provide conditions for reconstruction of signals from an arbitrarily small number of thresholds. To circumvent this difficulty, a second approach which is implicit, uses algebraic geometric concepts to find conditions under which a signal is almost always reconstructable from its multi-level threshold crossings. A problem distinct from that of uniquely specifying signals with level crossings is that of developing specific algorithms for recovering them from level crossing information, once it is known that the signals satisfy the appropriate constraints. A variety of reconstruction algorithms are proposed for each of our two approaches, and results for several images demonstrated. GRA

N88-30384*# Sterling Federal Systems, Inc., Palo Alto, Calif.
NONEQUILIBRIUM FLOW COMPUTATIONS. 1: AN ANALYSIS OF NUMERICAL FORMULATIONS OF CONSERVATION LAWS
Yen Liu and Marcel Vinokur Jun. 1988 29 p
(Contract NAS2-11555)
(NASA-CR-177489; NAS 1.26:177489) Avail: NTIS HC A03/MF A01 CSCL 12A

Modern numerical techniques employing properties of flux Jacobian matrices are extended to general, nonequilibrium flows. Generalizations of the Beam-Warming scheme, Steger-Warming and van Leer Flux-vector splittings, and Roe's approximate Riemann solver are presented for 3-D, time-varying grids. The analysis is based on a thermodynamic model that includes the most general thermal and chemical nonequilibrium flow of an arbitrary gas. Various special cases are also discussed. Author

N88-30385# Massachusetts Inst. of Tech., Cambridge. Lab. for Information and Decision Systems.
STABILITY, STOCHASTIC STATIONARITY AND GENERALIZED LYAPUNOV EQUATIONS FOR TWO-POINT BOUNDARY-VALUE DESCRIPTOR SYSTEMS
Ramine Nikoukhah, Bernard C. Levy, and Alan S. Willsky 3 Mar. 1988 52 p Prepared in cooperation with California Univ., Davis
(Contract AF-AFOSR-0032-88; Grants AF AFOSR-0032-88; NSF ECS-87-00903)
(AD-A195645; LIDS-P-1758; AFOSR-88-0630TR) Avail: NTIS HC A04/MF A01 CSCL 12B

This paper introduces the concept of internal stability for two-point boundary-value descriptor systems (TPBVDSs). Since TPBVDSs are defined only over a finite interval, the concept of stability is not easy to formulate for these systems. The definition which is used here consists in requiring that as the length of the interval of definition increases, the effect of boundary conditions on states located close to the center of the interval should go to zero. Stochastic TPBVDSs are studied, and the property of stochastic stationarity is characterized in terms of a generalized Lyapunov equation satisfied by the state variance of a stochastically stationary TPBVDS is also introduced, and the existence and uniqueness of positive definite solutions to this equation is then used to characterize the property of internal stability. GRA

N88-30386*# National Aeronautics and Space Administration. Langley Research Center, Hampton, Va.
CONVERGENCE OF GALERKIN APPROXIMATIONS FOR OPERATOR RICCATI EQUATIONS: A NONLINEAR EVOLUTION EQUATION APPROACH Final Report
I. G. Rosen (California Univ., Los Angeles.) Aug. 1988 30 p Submitted for publication
(Contract NAS1-18107)
(NASA-CR-181706; ICASE-88-49; NAS 1.26:181706) Avail: NTIS HC A03/MF A01 CSCL 12A

An approximation and convergence theory was developed for Galerkin approximations to infinite dimensional operator Riccati differential equations formulated in the space of Hilbert-Schmidt operators on a separable Hilbert space. The Riccati equation was treated as a nonlinear evolution equation with dynamics described by a nonlinear monotone perturbation of a strongly coercive linear operator. A generic approximation result was proven for quasi-autonomous nonlinear evolution system involving accretive operators which was then used to demonstrate the Hilbert-Schmidt norm convergence of Galerkin approximations to the solution of the Riccati equation. The application of the results was illustrated in the context of a linear quadratic optimal control problem for a one dimensional heat equation. Author

N88-30387# Maryland Univ., College Park. Dept. of Mathematics.
REGULARITY AND NUMERICAL SOLUTION OF EIGENVALUE PROBLEMS WITH PIECEWISE ANALYTIC DATA
I. Babuska, B. Q. Guo, and J. E. Osborn Jan. 1988 62 p
(Contract N00014-85-K-0169; Grants NSF DMS-16191-85; NSF DMS-10324-84)
(AD-A194993; MD87-50-IB-BQC-JEO; TR-87-50; BN-1073) Avail: NTIS HC A04/MF A01 CSCL 12A

This paper discusses the regularity of the eigenfunctions of eigenvalue problems with piecewise analytic data and the approximation of the eigenvalues and eigenfunctions of such problems. A detailed and systematic numerical study of these approximations is presented, together with an analysis of the numerical results in light of the theoretical results. The specific aim is to assess the reliability of the theoretical results (of an asymptotic nature) as a guide to practical computations, which may take place in the preasymptotic phase, and to look for characteristic features of the numerical results which are not completely explained by known theoretical results. GRA

N88-30388# Systems Engineering Labs., Inc., Greenbelt, Md.
ANALYTICAL METHODS IN STOCHASTIC CONTROL AND NONLINEAR FILTERING Final Report, 1 Jun. 1986 - 30 Aug. 1987
J. S. Baras and G. L. Blankenship 31 Dec. 1987 120 p
(Contract DAAL03-86-C-0014)
(AD-A194272; SEI-TR-87-13; ARO-23344.7-MA-S) Avail: NTIS HC A06/MF A01 CSCL 12C

The focus of this report is on advanced tools for the analysis of nonlinear stochastic control and filtering systems. In Sections 1 and 2, we present a series of results on the analysis of certain classes of nonlinear filtering problems using comparatively simple bounding techniques. We consider both problems with small noise (large signal to noise ratios) and weakly nonlinear systems. We show that the optimal nonlinear filters can be well approximated by linear filters which are very easy to implement. Moreover, we provide sharp estimates of the degree of suboptimality involved in using the linear approximating filters. In Section 3, we consider the problem of managing the estimation of (nonlinear) diffusion process by a system employing several sensors. The essential problem is to schedule the use of the sensor to optimize the estimate of a function of the state of the diffusion process. The solution is obtained in terms of a system of quasi-variational inequalities in the space of solutions of certain Zakai equations. In Section 4, we provide a new proof of the minimum principle in stochastic optimal control theory for systems of partially observed diffusions. In Section 5, we provide a concise analysis of the conditional adjoint process arising in the stochastic minimum principle for partially observed diffusion processes. GRA

N88-30389# Wisconsin Univ., Madison. Center for Mathematical Sciences.
MULTIPLE SOLUTIONS AND BIFURCATION FOR A CLASS OF NONLINEAR STURM-LIOUVILLE EIGENVALUE PROBLEMS ON AN UNBOUNDED DOMAIN Technical Summary Report
Chao-Nien Chen Apr. 1988 129 p
(Contracts DAAL03-87-K-0043; N00014-88-K-0134; Grant AF-AFOSR-0202-87)
(AD-A195954; CMS-TSR-88-30) Avail: NTIS HC A07/MF A01 CSCL 12B

A class of nonlinear Sturm-Liouville problems is considered. These problems admit zero as a trivial solution and the nonlinear operator linearized about zero has a purely continuous spectrum (0, infinity). Variational methods and approximation arguments are used to obtain the existence of nontrivial solutions with any prescribed number of nodes, and for some nonlinearities it is shown that this solution is unique. Moreover, the lowest point of the continuous spectrum is bifurcation point; infinitely many continua of solutions, which are distinguished by nodal properties, bifurcate from the line of trivial solutions at this point. Results are also obtained in higher dimensions via investigation of the set of radial solutions of appropriate partial differential equations. GRA

65 STATISTICS AND PROBABILITY

Includes data sampling and smoothing; Monte Carlo method; and stochastic processes.

N88-30390# Illinois Univ., Urbana. Dept. of Statistics.
INSTRUMENTATION FOR COMPUTATIONAL STATISTICAL RESEARCH Final Report, 15 Jul. - 15 Nov. 1987
Jerome Sacks 15 Nov. 1987 4 p
(Grant AF-AFOSR-0041-87)
(AD-A195887; AFOSR-88-0657TR) Avail: NTIS HC A02/MF A01 CSCL 12F

This is the final report of a grant issued under the University Research Instrumentation Program. Computing equipment was purchased to establish a network of 14 Sun work-stations. This network made a variety of research efforts in the area of design and analysis of computational experiments. This report details purchases and related publications. GRA

N88-30391# Chicago Univ., Ill. Center for Decision Research.
VENTURE THEORY: A MODEL OF DECISION WEIGHTS
Robin M. Hogarth and Hillel J. Einhorn Jan. 1988 49 p
(Contract N00014-84-C-0018)
(AD-A194809; TR-21) Avail: NTIS HC A03/MF A01 CSCL 12D

Several theories suggest that people replace probabilities by decision weights when evaluating risky outcomes. This paper proposes a model, called venture theory, of how people assess decision weights. It is assumed that people first anchor on a stated probability and then adjust this by mentally simulating other possible values. The amount of mental simulation is affected both by the extent to which the anchor deviates from the extremes of 0 and 1 (i.e., where there is no uncertainty) and the level of perceived ambiguity concerning the relevant probability. The net effect of the adjustment (i.e., up or down relative to the anchor) reflects the relative weight given in imagination to values above as opposed to below the anchor. This, in turn, is taken to be a function of both individual and situational variables, and in particular, the sign and size of payoffs. Cognitive and motivational factors therefore both play important roles in determining decision weights. Assuming that people evaluate outcomes by a prospect theory value function (Kahneman and Tversky, 1979) and are cautious in the face of risk, predictions are derived concerning attitudes toward risk and ambiguity as functions of different levels of payoffs and probabilities. The results of two experiments are reported. GRA

N88-30392# Missouri Univ., Columbia. Dept. of Statistics.
DIRICHLET PRIOR IN BAYESIAN ESTIMATION OF ITEM RESPONSE CURVES Technical Report No. 143, Jan. 1987 - Apr. 1988
Robert K. Tsutakawa May 1988 44 p
(Contract N00014-85-K-0113; Proj. RR0-4204)
(AD-A195311) Avail: NTIS HC A03/MF A01 CSCL 12C

This article examines the use of the ordered Dirichlet prior for binary logistic item response models. This prior is based on the investigator's prior information about the probabilities of correct response to items from examinees at several ability levels. The effect of the prior is examined in terms of the posterior mode of item parameters computed via the EM algorithm. An illustration describes the application of a 1981 ACT math test to form a prior which is used on a similar 1987 test. Detailed computational expressions for the three-parameter logistic model are summarized in an appendix. GRA

66 SYSTEMS ANALYSIS

Includes mathematical modeling; network analysis; and operations research.

N88-30393# Strategic Defense Initiative Organization, Washington, D.C.
REPORT TO CONGRESS ON THE STRATEGIC DEFENSE SYSTEM ARCHITECTURE
Jan. 1988 38 p
(AD-A195476) Avail: NTIS HC A03/MF A01 CSCL 15C

The Services and SDIO are running parallel, complementary studies to evaluate sensor combinations for cost effective operation in midcourse defense SDIO in a national-level midcourse sensor study, which is looking in depth at the possible contribution of the potential sensor platforms as a function of their configuration, location, and quantities. The Army is looking in detail at the contribution of GSTS (Ground Surveillance Tracking System) probes to the Phase 1 system. The results of these studies are due at the end of 1987 and will be analyzed and merged so that an informed decision can be made in early 1988. The SDIO Architecture contractors are doing in-depth analysis of the characteristics and performance of the baseline Phase 1 architecture with specific assumptions regarding its elements. The purpose of their work is to refine the operational requirements of the system and get more definition of the BM/C3. They are using

both conventional and process description methodologies in their analyses and the tools they are developing will be passed on to the NTB Test Bed. The Architecture contractors are also supporting the SDIO midcourse sensor study. GRA

N88-30394# Army War Coll., Carlisle Barracks, Pa.
LOOKING BEYOND THE STRATEGIC DEFENSE INITIATIVE
Dean H. Nichols 30 Mar. 1988 48 p
(AD-A195079) Avail: NTIS HC A03/MF A01 CSCL 15C

On 23 March 1983, President Reagan announced a new proposal. This study looks at the Strategic Defense Initiative (SDI) and how it will achieve the objectives President Reagan envisioned in his speech. It examines a scenario in which deterrence has failed and the time for Presidential decision making is severely compressed. It then looks at Presidential decision making during such a crisis and examines his options. Next, it looks at how the SDI is envisioned to work and contribute to the ultimate goal of eliminating the threat posed by nuclear ballistic missiles. Last, it examines the possibility that SDI may create a world we do not want; a dangerous world in which conventional wars between the two superpowers would become possible, maybe even probable. It does this by examining its impact on NATO, particularly in light of the proposed Intermediate-Range Nuclear Forces treaty. GRA

N88-30395# Massachusetts Inst. of Tech., Cambridge. Artificial Intelligence Lab.
THEORIES OF COMPARATIVE ANALYSIS Ph.D. Thesis
Daniel S. Weld May 1988 185 p
(Contract N00014-85-K-0124)
(AD-A196328; AI-TR-1035) Avail: NTIS HC A09/MF A01 CSCL 12I

Comparative analysis is the problem of predicting how a system will react to perturbations in its parameters, and why. For example, comparative analysis could be asked to explain why the period of an oscillating spring/block system would increase if the mass of the block were larger. This thesis formalizes the task of comparative analysis and presents two solution techniques: differential qualitative (DQ) analysis and exaggeration. Both techniques solve many comparative analysis problems, providing explanations suitable for use by design systems, automated diagnosis, intelligent tutoring systems, and explanation based generalization. This thesis explains the theoretical basis for each technique, describes how they are implemented, and discusses the difference between the two. DQ analysis is sound; it never generates an incorrect answer to a comparative analysis question. Although exaggeration does occasionally produce misleading answers, it solves a larger class of problems than DQ analysis and frequently results in simpler explanations. GRA

N88-30396# Air Command and Staff Coll., Maxwell AFB, Ala.
ANTISATELLITE WEAPONS AND SATELLITE DEPLOYMENT STRATEGIES
Randall W. Chapman Apr. 1988 35 p
(AD-A195014; ACSC-88-0510) Avail: NTIS HC A03/MF A01 CSCL 15C

Space is becoming a more and more likely arena for future combat. The strength of future U.S. antisatellite capabilities and the survivability of U.S. satellites will determine if space power supports U.S. national security. The study evaluates the oft stated conclusion that ASATs destabilize superpower relations. The study concludes that the actual sources of instability are the weaknesses in current U.S. military space strategy. These weaknesses are: (1) failure to deploy ASAT systems, and (2) continued reliance on a small number of highly vulnerable, complex, multipurpose satellites. Deployment of a U.S. ASAT and a move to a more survivable satellite deployment strategy--suggestive of current Soviet practices--will be stabilizing influences in superpower relations. GRA

67 THEORETICAL MATHEMATICS

Includes topology and number theory.

No abstracts in this category.

70 PHYSICS (GENERAL)

For precision time and time interval (PTTI) see *35 Instrumentation and Photography;* for geophysics, astrophysics or solar physics see *46 Geophysics, 90 Astrophysics,* or *92 Solar Physics.*

N88-30397# Massachusetts Inst. of Tech., Cambridge. Artificial Intelligence Lab.
UTILIZING DYNAMIC STABILITY OF ORIENT PARTS
Neil C. Singer and Warren P. Seering Feb. 1988 16 p
(Contracts N00014-85-K-0494; N00014-85-K-0124)
(AD-A195730; AI-M-1013) Avail: NTIS HC A03/MF A01 CSCL 13H

The intent of this research is to study the dynamic behavior of a solid body resting on a moving surface. Results of the study are then used to propose methods for controlling the orientation of parts in preparation for automatic assembly. Two dynamic models are discussed in detail. The first examines the use of oscillatory motion to selectively reorient parts. This study demonstrates that the dynamic behaviors of solid bodies, under the conditions mentioned above, vary considerably with small changes in geometry or orientation. Conventionally, parts are oriented by bowl feeders. The machines vibrate and thereby convey parts through a series of filters which reject all but a particular orientation. Rejected parts are returned to storage. Many researchers have examined the implementation of programmable or adjustable filter stages. These techniques are often successful for limited classes of parts. The scope of this paper is to present theoretical results which may be useful in feeder designs. It is hoped that a more detailed understanding of the dynamic behavior of bodies resting on a moving surface will facilitate the design of new types of programmable parts feeders. GRA

71 ACOUSTICS

Includes sound generation, transmission and attenuation. For noise pollution see *45 Environmental Pollution.*

N88-30398# Aeronautical Research Labs., Melbourne (Australia).
THE DEVELOPMENT OF ACOUSTIC EMISSION FOR STRUCTURAL INTEGRITY MONITORING OF AIRCRAFT
C. M. Scala, S. J. Bowles, and L. G. Scott Jan. 1988 35 p
(AD-A196264; ARL/MAT-R-120; DODA-AR-004-585) Avail: NTIS HC A03/MF A01 CSCL 14B

This paper reviews procedures for distinguishing between acoustic emission (AE) from fatigue crack propagation and from spurious sources in aircraft applications. Particular emphasis is placed on the development of procedures applicable during AE monitoring of complex-shaped components. First, procedures to eliminate extraneous sources are evaluated, including the use of guard sensors and source location systems. The capabilities of additional signal-processing (which in principle can range from adaptive to non-adaptive) for identifying and locating AE from fatigue crack propagation are then evaluated. The problems in applying adaptive processing are illustrated by AE results from a Macchi aircraft in-flight and Mirage aircraft during full-scale fatigue testing. The ARL development of semi-adaptive processing based on background research on AE sources, sensors, calibration and other techniques is described. Successful application of this processing to the Mirage test above is then detailed, and the

value of using reduced adaptation in processing is demonstrated. GRA

N88-30399*# Planning Research Corp., Hampton, Va. System Services.
AIRCRAFT NOISE PREDICTION PROGRAM PROPELLER ANALYSIS SYSTEM IBM-PC VERSION USER'S MANUAL VERSION 2.0
Sandra K. Nolan Aug. 1988 236 p
(Contract NAS1-18000)
(NASA-CR-181689; NAS 1.26:181689) Avail: NTIS HC A11/MF A01 CSCL 20A

The IBM-PC version of the Aircraft Noise Prediction Program (ANOPP) Propeller Analysis System (PAS) is a set of computational programs for predicting the aerodynamics, performance, and noise of propellers. The ANOPP-PAS is a subset of a larger version of ANOPP which can be executed on CDC or VAX computers. This manual provides a description of the IBM-PC version of the ANOPP-PAS and its prediction capabilities, and instructions on how to use the system on an IBM-XT or IBM-AT personal computer. Sections within the manual document installation, system design, ANOPP-PAS usage, data entry preprocessors, and ANOPP-PAS functional modules and procedures. Appendices to the manual include a glossary of ANOPP terms and information on error diagnostics and recovery techniques. Author

72 ATOMIC AND MOLECULAR PHYSICS

Includes atomic structure, electron properties, and molecular spectra.

N88-30400# Harvard Univ., Cambridge, Mass. Div. of Applied Sciences.
INTRAMOLECULAR DYNAMICS: A STUDY OF MOLECULES AT HIGH LEVELS OF VIBRATIONAL EXCITATION Final Report
Eric Mazur 27 May 1988 92 p
(Contract DAAG29-85-K-0060)
(AD-A195285; ARO-22416.8-PH) Avail: NTIS HC A05/MF A01 CSCL 07D

The intramolecular vibrational energy distribution of infrared multiphoton-excited molecules is studied with time-resolved spontaneous Raman spectroscopy. For several molecules highly nonthermal energy distributions are observed, indicating high selectivity below the dissociation threshold. GRA

N88-30401# United Kingdom Atomic Energy Authority, Harwell (England). Radiation Effects and Applications Centre.
THE EFFECTS OF TOTAL DOSE ON THE SEU SENSITIVITY OF CMOS STATIC RAMS Final Report
T. K. Sanderson, D. Mapper, J. H. Stephen, and J. Farren Paris, France ESA Jul. 1987 77 p
(Contract ESTEC-5313/83-NL-HP)
(AERE-R-12779; ESA-CR(P)-2551; ISBN-0-70-581286-3; ETN-88-92774) Copyright Avail: NTIS HC A05/MF A01; Her Majesty's Stationary Office, P.O. Box 276, London SW8 5DT, United Kingdom 5 pounds

The effects of accumulated total dose on single event upset (SEU) sensitivity of 4Kx1 CMOS static random access memories (RAMs) were studied by making SEU measurements using the fission particles produced by a Cf252 source, while total dose was accumulated by a continuous low dose rate irradiation with Co60 gamma rays, lasting 8 months. The saturation cross section for SEU in the 4Kx1 CMOS static RAMs shows no significant change with increasing total dose from a low dose-rate Co60 source. However, in even more complex devices possessing a critical charge that is already small, any process such as total dose accumulation, that greatly reduces this critical charge, is important. In this situation, the large fluxes in space of low atomic number particles such as helium ions, start to contribute to the upset rate. Changes in the switching characteristics of a MOS static RAM cell can occur, associated with shifts in the threshold voltages of the n and p channel MOSFETs in the circuit. ESA

73 NUCLEAR AND HIGH-ENERGY PHYSICS

Includes elementary and nuclear particles; and reactor theory.
For space radiation see *93 Space Radiation.*

N88-30402*# National Aeronautics and Space Administration. Langley Research Center, Hampton, Va.
EIKONAL SOLUTIONS TO OPTICAL MODEL COUPLED-CHANNEL EQUATIONS
Francis A. Cucinotta, Govind S. Khandelwal, Khin M. Maung (Old Dominion Univ., Norfolk, Va.), Lawrence W. Townsend, and John W. Wilson Nov. 1988 30 p
(NASA-TP-2830; L-16462; NAS 1.60:2830) Avail: NTIS HC A03/MF A01 CSCL 20H

Methods of solution are presented for the Eikonal form of the nucleus-nucleus coupled-channel scattering amplitudes. Analytic solutions are obtained for the second-order optical potential for elastic scattering. A numerical comparison is made between the first and second order optical model solutions for elastic and inelastic scattering of H-1 and He-4 on C-12. The effects of bound-state excitations on total and reaction cross sections are also estimated. Author

N88-30403# Helsinki Univ. of Technology, Espoo (Finland). Dept. of Technical Physics.
PHASE MODULATION OF RECOILESS GAMMA RADIATION IN MOSSBAUER SPECTROSCOPY Ph.D. Thesis
Erkki Ikonen 1987 36 p Sponsored by the Academy of Finland; the Finnish Cultural Foundation; and the Emil Aaltonen Foundation, Finland
(ETN-88-92648) Avail: NTIS HC A03/MF A01

Measurement of subatomic displacements for Mossbauer spectroscopy; coherent transient effects in Mossbauer spectroscopy; coherent transient effects due to phase modulation of recoilless gamma radiation; enhanced transient effects due to saturated absorption of recoilless gamma radiation; magnetic phase modulation of recoilless gamma radiation by nuclear Zeeman effect; influence of alternating magnetic fields on Zn67 Mossbauer resonance in ZnO; and failure of the classical field model of Mossbauer spectroscopy are discussed. ESA

74 OPTICS

Includes light phenomena; and optical devices.
For lasers see *36 Lasers and Masers.*

N88-30404# Naval Ocean Systems Center, San Diego, Calif.
A FIBER OPTIC BEAMFORMING PROCESSOR FOR WIDEBAND DIRECTION FINDING Professional Paper, Mar. 1988
Stephen A. Pappert Apr. 1988 3 p Presented at the Dept. of Defense Fiber Optics Conference, McLean, Va., 22-25 Mar. 1988
(AD-A194862) Avail: NTIS HC A02/MF A01 CSCL 17K

This paper describes a wideband electro-optic direction finding (DF) processor employing an array of laser diodes, an array of photo-detectors, and a network of fiber optic delay lines. This DF filter offers a potential operational bandwidth in excess of 10 GHz and allows for multiple, simultaneous beam angular responses with peaks which are independent of frequency. Two eight-laser, two-beam laboratory test model DF devices, one utilizing multimode optical fiber and the other single-mode fiber, were constructed. These experimental optical beamforming filters are operable in the 100 to 2000 MHz frequency range and can simultaneously monitor two angles of arrival. Experiments were performed to determine the two systems' sensitivity, dynamic range, angular resolution, and frequency response. GRA

N88-30405# Technical Research Centre of Finland, Espoo. Semiconductor Lab.
ION EXCHANGE PROCESSES FOR FABRICATION OF INTEGRATED OPTICAL WAVEGUIDE STRUCTURES INTO GLASS SUBSTRATES Ph.D. Thesis - Helsinki University of Technology
Seppo Honkanen Feb. 1988 67 p
(VTT-46; ISBN-9-51-383085-3; ISBN-0358-5069; ETN-88-92651)
Copyright Avail: NTIS HC A04/MF A01; Technical Research Institute of Finland (VTT), Vuorimiehentie 5, SF-02150 Espoo 15, Finland 70 Finnish marks

The fabrication of multimode waveguides by an Ag(+)-Na(+) exchange with Ag thin film ion sources was analyzed. The process was applied to the fabrication of multimode components. Using Ag thin film ion sources channel waveguides were fabricated directly into the integrated circuit lithography mask plates, patterned with high accuracy by the mask manufacturer. The method is especially promising for single-mode applications, where the accuracy of the patterning is of great importance. For single-mode applications an ionic masking method, which utilizes molten salt ion sources, was also studied. The method was applied to the fabrication of narrow channel waveguides and to the control of birefringence in waveguides. ESA

N88-30406# Colorado Univ., Boulder.
OPTICAL SYMBOLIC COMPUTING Annual Report, May 1987 - Apr. 1988
W. T. Cathey and Rodney A. Schmidt 30 Apr. 1988 21 p
(Grant AF-AFOSR-0189-86)
(AD-A195690; CU-1536935; AFOSR-88-0661TR) Avail: NTIS HC A03/MF A01 CSCL 20F

This report describes the results of the work on optical symbolic computing that was performed on grant AFOSR-86-0189 during the second year of the three year program. The detail of the research is in the appended papers. This section of the report is to summarize the motivation for the work, the reasons for the approach taken, and the results. First, a rationale is given for the use of optics in A.I., and then the approach taken is described. The results of the research are then given. GRA

N88-30407# Research Inst. of National Defence, Linkoeping (Sweden).
A SYSTEM STUDY WITH AN INFRARED SENSITIVE MICROELECTRONIC IMAGE SENSOR
Sven-Tuve Persson and Olof Engstroem Feb. 1988 32 p In SWEDISH; ENGLISH summary
(FOA-C-30481-3.1; ISSN-0347-3708; ETN-88-93060) Avail: NTIS HC A03/MF A01; Research Institute of National Defence, Box 1165, S-581 11 Linkoeping, Sweden 50 Swedish crowns

An image sensor was fabricated using a standard CMOS process with infrared sensitive elements consisting of palladium silicide Schottky diodes. The target tracker model consists of a sensor mounted in a cryostat connected to a microprocessor based control unit with an xy-recorder. The target was simulated by a heating coil with controlled temperature. The location of the target was determined by calculating the center of gravity. The image sensor linearity and angular sensitivity were investigated. ESA

N88-30408# Army Lab. Command, Watertown, Mass. Material Technology Lab.
PRINCIPLES OF THE OPTICAL DIFFERENTIAL THERMAL ANALYSIS Final Report
Jaroslav L. Caslavsky Apr. 1988 15 p
(AD-A195951; MTL-TR-88-11) Avail: NTIS HC A03/MF A01 CSCL 20F

Optical differential thermal analysis (ODTA) can operate in the 490 to 3600 C range, using infrared pyrometers for the temperature detection of both the Black-Body and the sample. Hence, the method is called optical. Infrared detection of any phase transition is a result of two cooperative effects: Delta H and the emissivity change. Such cooperation leads to a high sensitivity thereby permitting ODTA measurements at temperature rates as low as 0.1 C/min. Hence, phase transitions can be studied at almost equilibrium conditions. In order to detect emissivity changes, single color pyrometers have to be used. Problems associated with simultaneous use of the Black-Body as a temperature reference source and a heater are discussed. Use of the ODTA at high temperatures is demonstrated on a study of the melting behavior of a sapphire single crystal. The feasibility of computing emissivities as a function of temperature from the gathered data is indicated. GRA

N88-30409# Tacan Aerospace Corp., Carlsbad, Calif.
SPECTROSCOPIC STUDIES WITH MULTIPLE QUANTUM WELL MATERIALS WITH APPLICATIONS TO OPTICAL SIGNAL PROCESSING AT ROOM TEMPERATURE Final Report, 17 Sep. 1986 - 17 Sep. 1987
Michael M. Salour 17 Nov. 1987 55 p
(Contract DAAG29-84-C-0021)
(AD-A194171; ARO-21436.9-EL-S) Avail: NTIS HC A04/MF A01 CSCL 09A

This program investigated the variety of laser induced optical processes in multiple quantum well (MQW) and other nonlinear waveguide materials. These studies combined both theory and experiment. This work demonstrated the first optically pumped mode-locked Al0.3Ga0.7As/GaAs multiple quantum well (MQW) laser in external cavity. The MQW structure with a total thickness of 5 micrometers was grown by molecular beam epitaxy on a Si-doped GaAs substrate and was synchronously pumped by a mode-locked Kr+ laser (82 MGz) at 647.1 nm. The MQW laser emitted 10 ps pulses at 8085A with peak powers as high as 6W. The demonstrated MQW laser combines desirable properties of quantum wells with advantages of an external cavity, such as specific band-gap design with high beam quality and the possibility of intracavity tailoring of the laser beam. We also demonstrated the first mode-locked Si-doped bulk GaAs laser tunable over 300A range. Several experiments to measure the third order nonlinear optical susceptibility of MQW and other novel nonlinear materials were successfully completed. The first measurement of the third order nonlinear optical susceptibility of transpolyacetylene by third harmonic generation in third films is reported. GRA

N88-30410# Carnegie-Mellon Univ., Pittsburgh, Pa. Robotics Inst.
IMAGE FOCUSING IN SPACE AND TIME Interim Technical Report
M. W. Siegel Feb. 1988 16 p
(AD-A195839; CMI-RI-TR-88-2) Avail: NTIS HC A03/MF A01 CSCL 12I

The integral form of the instrument transmission function for a one-dimensional pixel in a two-dimensional optical system is presented. The integral is solved explicitly in the paraxial ray approximation for a single spatial Fourier component of a Lambertian object. The difference between signals from adjacent pixels is derived. It is shown to have zero derivative with respect to focusing error when the focusing error is zero, i.e., it is a weak source of range-from-focus information. Describing the instantaneous focusing error as the sum of a fixed offset and a time-domain sinusoidal dither, the power spectrum of the signal from each individual pixel is shown to large first and second harmonic terms for physically reasonable values of the parameters. The first harmonic signal is proportional to the product of the dither amplitude and the offset. The second harmonic signal is proportional to the square of the dither amplitude and is independent of offset. The two coefficients are identical except for an integral numerical factor. It is suggested that the ratio of second harmonic to first harmonic signals is thus potentially a powerful measure of offset, i.e., of focusing error in the limit of zero dither, and thus of range-from-focus pixel-by-pixel. Extending the model to three dimensions, removing the approximations, extending the model to natural scenes, and verifying and implementing the results experimentally are outlined briefly. GRA

N88-30411# Rochester Univ., N. Y. Inst. of Optics.
CENTER FOR OPTO-ELECTRONIC SYSTEMS RESEARCH Progress Report, 1 Oct. 1986 - 31 Dec. 1987

Nicholas George 1 Feb. 1988 65 p
(Contract DAAL03-86-K-0173)
(AD-A195159; ARO-24626.33-PH) Avail: NTIS HC A04/MF A01 CSCL 09E

The primary goal of the Center is to contribute fundamental scientific knowledge which is relevant to opto-electronic systems with an emphasis on key technology areas common to these systems, e.g., lasers, modulation, optical systems design, propagation and coherence, detection theory, signal processing, digital methods, and display. Progress for the year (1987) described in this report is grouped into three main sectors: Sources and Sensors; Signal Processing and Image Understanding; and Optical Systems Design. GRA

N88-30412*# National Aeronautics and Space Administration. Marshall Space Flight Center, Huntsville, Ala.
A REVIEW OF MELT AND VAPOR GROWTH TECHNIQUES FOR POLYDIACETYLENE THIN FILMS FOR NONLINEAR OPTICAL APPLICATIONS
B. G. Penn, A. Shields, and D. O. Frazier Sep. 1988 12 p
(NASA-TM-100340; NAS 1.15:100340) Avail: NTIS HC A03/MF A01 CSCL 20F

Methods for the growth of polydiacetylene thin films by melt and vapor growth and their subsequent polymerization are summarized. Films with random orientations were obtained when glass or quartz were used as substrates in the vapor growth process. Oriented polydiacetylene films were fabricated by the vapor deposition of diacetylene monomer onto oriented polydiacetylene on a glass substrate and its subsequent polymerization by UV light. A method for the growth of oriented thin films by a melt-shear growth process as well as a method of film growth by seeded recrstallization from the melt between glass plates, that may be applied to the growth of polydiacetylene films, are described. Moreover, a method is presented for the fabrication of single crystal thin films of polyacetylenes by irradiation of the surface of diacetylene single crystals to a depth between 100 and 2000 angstroms. Author

N88-30413# Naval Ocean Systems Center, San Diego, Calif.
ULTRA-WIDEBAND DIRECTION FINDING USING A FIBER OPTIC BEAMFORMING PROCESSOR Professional Paper, Jan. 1988
Stephen A. Pappert Apr. 1988 9 p Presented at the SPIE's O-E Lase, Los Angeles, Calif., 13 Jan. 1988
(AD-A194861) Avail: NTIS HC A02/MF A01 CSCL 17K

Described is a wideband electro-optic direction finding (DF) processor employing an array of laser diodes, an array of photodetectors, and a network of fiber optic delay lines. This DF filter offers a potential operational bandwidth in excess of 10 GHz and allows for multiple, simultaneous beam angular responses with peaks which are independent of frequency. Two eight-laser, two-beam laboratory test model DF devices, one utilizing multimode optical fiber and the other single-mode fiber, were constructed. These experimental optical beamforming filters are operable in the 100 to 2000 MHz frequency range and can simultaneously monitor two angles of arrival. Experiments were performed to determine the two systems' sensitivity, dynamic range, angular resolution, and frequency response. It is concluded from theoretical and experimental results obtained that the multimode DF device is slightly superior in performance to the single-mode system due to the higher throughput optical power levels possible with multimode systems. Further, it is concluded that this fiber optic beamforming processor can be a useful device for ultra-wideband DF. GRA

N88-30414# Pennsylvania State Univ., University Park. Dept. of Chemistry.
AN ORGANOMETALLIC ROUTE TO MICRON-SIZED WHISKERS OF ZINC SULFIDE
C. L. Czekaj, M. S. Rau, G. L. Geoffroy, T. A. Guiton, and C. G. Pantano 22 Jun. 1988 12 p Submitted for publication
(Contract N00014-86-K-0191)
(AD-A195889; TR-1) Avail: NTIS HC A03/MF A01 CSCL 20F

A number of technologies require the development of high performance optical materials that also meet stringent specifications of optical transparency and thermal, chemical, and mechanical properties. For example, an infrared transmitting window material should have low thermal expansion, high melting and decomposition temperatures, chemical inertness to hydrolysis and oxidation, and high fracture toughness. One of the most attractive materials for many infrared optical applications is Zinc sulfide, but this material, as presently fabricated, does not process the required mechanical properties. One approach to improving the mechanical properties of a material is to form a self-similar composite, in this case, ZnS whiskers in polycrystalline ZnS matrix. To fabricate IR transmitting ZnS/ZnS composites, it would be necessary to use micron-sized whiskers of ZnS that have length to width ratios (aspect ratios) greater than 10. No present methodology exists for the convenient, large-scale preparation of such whiskers, although larger single crystals and whiskers of ZnS have been made by a variety of high temperature (less than 900 C), generally vapor-phase, routes. GRA

N88-30415# Center for Night Vision and Electro-Optics, Fort Belvoir, Va.
COMMON MODULES: A SUCCESS STORY Final Report, 1971 - 1986
Walter B. Morrow, Jr. Jun. 1988 21 p
(AD-A195937; AMSEL-NV-TR-0068) Avail: NTIS HC A03/MF A01 CSCL 17E

During the late 1960s and early 1970s, the U.S. military found far-infrared or thermal imaging systems very useful as night vision devices because of ready application as troop-carried, combat vehicle-mounted, and aircraft-mounted systems. The rapid proliferation of applications posed a serious financial problem, yet clearly solved critical needs. The development and acquisition process for each system's development, purchase, and maintenance was both lengthy and expensive. Therefore, an investigative committee was formed in 1971 within the Center for Night Vision and Electro-Optics to analyze the problems and develop the design concept for Common Modules. This report focuses on the detector modules and develops cost benefits accrued to date and expected to accrue in the Army's future as a result of common module development and implementation. GRA

N88-30416# Rutgers - The State Univ., New Brunswick, N. J. Lab. for Computer Science Research.
ARCHITECTURE FOR OPTICAL DIGITAL COMPUTERS Annual Report
Saul Y. Levy, J. S. Hall, and Miles J. Murdocca 31 Aug. 1987 18 p
(Grant AF-AFOSR-0294-86)
(AD-A195477; AFOSR-88-0531TR) Avail: NTIS HC A03/MF A01 CSCL 20F

A Content Addressable Memory architecture for a digital optical computer is investigated. This investigation is being funded by AFOSR, and is being carried out in conjunction with work on digital optical computing devices at Bell Laboratories in Holmdel, N.J. Because of the massive parallelism inherent in the CAM organization it is an ideal candidate to help construct the types of optical components being investigated at the Labs. GRA

N88-30417# California Univ., Santa Barbara. Dept. of Electrical and Computer Engineering.
USE OF DEPLETION EDGE TRANSLATION FOR HIGH-SPEED MODULATION AND SWITCHING OF LIGHTWAVES Annual Report, 1 Mar. 1987 - 29 Feb. 1988
L. A. Coldren, J. G. Mendoza, T. R. Hausken, K. W. Lee, and R. J. Simes May 1988 18 p
(Grant AF-AFOSR-0323-85)
(AD-A195611; CU-ECE-88-06; AFOSR-88-0612TR) Avail: NTIS HC A03/MF A01 CSCL 09E

The main objective continues to be the achievement of large

index shifts at low voltages for applications in modulators and switches for optical processing, the device area of application has shifted from the in-plane guided wave modulator vehicle to a surface-normal modulator configuration more appropriate for spatial light modulator arrays, optical logic gates and reconfigurable optical interconnection. However, in the course of building up the surface-normal effort in the early portion of this reporting period, we also were wrapping up some important in-plane results. Thus, since these results were not previously reported, they are briefly summarized here. GRA

75 PLASMA PHYSICS

Includes magnetohydrodynamics and plasma fusion.

For ionospheric plasmas see *46 Geophysics*. For space plasmas see *90 Astrophysics*.

N88-30418# Swedish Inst. of Space Physics, Uppsala.
CHARACTERISTICS OF SOLITARY WAVES AND WEAK DOUBLE LAYERS IN THE MAGNETOSPHERIC PLASMA
R. Bostrom, G. Gustafsson, B. Holback, G. Holmgren, Hannu Koskinen, and Paul Kintner Feb. 1988 11 p
(IRF-Preprint-105; ISSN-0284-1711; ETN-88-92701) Avail: NTIS HC A03/MF A01

The wave experiment of the Swedish Viking satellite frequently detected dynamic small scale (approx 100 m), large amplitude rarefactive (delta n/n less than or = 50 percent) solitary waves of negative potential (phi less than or = 2 V) moving upwards along the magnetic field lines (v = 5 to 50 km/sec). The structures which resemble ion holes often have an upward directed net potential drop (less than or = 1 volt) and are interpreted as weak double layers. ESA

N88-30419# Sydney Univ. (Australia). Dept. of Wills Plasma Physics.
[THE STUDY OF HYDROMAGNETIC WAVES AND RF HEATING USING THE TORTUS TOKAMAK, THE DEVELOPMENT OF DIAGNOSTIC TECHNIQUES BASED ON SUBMILLIMETER LASERS AND THE GYROTRON, AND GAS DISCHARGE]
1986 41 p
Avail: NTIS HC A03/MF A01

This experimental research program has three major directions: (1) the study of hydromagnetic waves and RF heating using the TORTUS tokamak; (2) the development of diagnostic techniques particulary those based on submillimeter lasers and the gyrotron; and (3) gas discharge studies. Results are summarized. Author

N88-30420# Instituto de Pesquisas Espaciais, Sao Jose dos Campos (Brazil).
RFP (REVISED FIELD PINCH) PLASMA EXPERIMENT AT INPE
Mario Ueda and Yoshiyuki Aso Jun. 1988 10 p Presented at the 6th Japan-Brazil Workshop on Science and Technology, Sao Paulo, Brazil, 11-12 Aug. 1988
(INPE-4613-PRE/1336) Avail: NTIS HC A02/MF A01

Plasma experiments in CECI, a small Reversed Field Pinch (RFP) apparatus, is described. Preliminary measurements in this device have shown the production of a plasma with peak current of 1.2 kA and discharge duration of nearly 80 microsec, when a toroidal DC field of 100 G was used. A loop voltage of 40 V was measured and a maximum electron temperature of 3 eV was estimated for these discharges. Experimental points in the F-theta diagram for CECI indicate that its plasma is approaching the RFP configuration as the discharge is optimized. The probe data also show that the plasma column expands outward. Furthermore, numerical results indicate that leakage fields have to be reduced below 5 G to form appropriate magnetic surfaces. These two effects seem to be limiting the plasma current. Hence a compensating vertical field coil is under preparation. Author

N88-30421# Berkeley Research Associates, Inc., Calif.
CONSIDERATION OF PLASMA OPENING SWITCHES FROM A WAVE PROPAGATION PERSPECTIVE Technical Report, 10 Sep. 1986 - 22 Oct. 1987
Stephen H. Brecht and Robert J. Kares 22 Oct. 1987 61 p
(Contract DNA001-86-C-0174)
(AD-A195681; BRA-87-320R; DNA-TR-87-280) Avail: NTIS HC A04/MF A01 CSCL 20I

In this report we have considered the dynamics of the plasma opening switch from the perspective of an electromagnetic wave propagating in a coaxial waveguide. It is found that switches with plasma densities in the 10 to the 12th power range or lower will allow energy to couple to normal modes in the plasma and propagate through the switch. The energy propagates at the Alfven speed or higher. At densities above 10 to the 13th power the picture changes to one where the dissipative properties of the plasma prevent direct electromagnetic energy propagation. The energy must penetrate the plasma by diffusion. This report addresses the microinstabilities that lead to this diffusion picture. Consistent with this picture several suggestions are made for enhancing the conduction time of the plasma opening switch. GRA

N88-30422# Swedish Inst. of Space Physics, Umea.
RECONSTRUCTION OF WAVE DISTRIBUTION FUNCTIONS IN WARM PLASMAS
T. E. Oscarsson and K. G. Ronnmark Jan. 1988 28 p
(IRF-Preprint-104; ISSN-0284-1711; ETN-88-92700) Avail: NTIS HC A03/MF A01

For reconstructing the wave distribution function in warm plasmas from observed frequency spectra, a method which does not rely on cold plasma theory is developed. Numerical methods solve the dispersion relation for waves in a warm, homogeneous, anisotropic, and multicomponent plasma. This allows treatment of almost any linear wave mode and also to handle a large variety of plasma models, also including warm plasma. Doppler effects are taken into account, and reconstruction is performed over a wide frequency range simultaneously. To define a unique solution to the inverse underdetermined problem occurring in the reconstruction, the maximum-entropy method is used. As a test a model problem with simulated data was solved. ESA

N88-30423# Air Force Inst. of Tech., Wright-Patterson AFB, Ohio.
ION KINETICS IN SILANE PLASMAS M.S. Thesis
Peter D. Haaland Feb. 1988 244 p
(AD-A196202; AFIT/CI/NR-88-101) Avail: NTIS HC A11/MF A01 CSCL 07C

The kinetics of ion formation by electron impact and subsequent reaction in silane:noble-gas mixtures have been examined using pulsed ion cyclotron resonance (ICR) mass spectrometry with the objective of discerning the role played by ions in plasma reactors which deposit amorphous silicon films. Cross-sections for ionization of the noble-gases and silane as well as dissociative attachment of electrons to silane are presented. GRA

N88-30424# Naval Research Lab., Washington, D.C.
STRUCTURING PROCESSES IN EXPANDING LASER-PRODUCED PLASMAS Interim Report
B. H. Ripin, J. Grun, T. N. Lee, C. K. Manka, and E. A. McLean 30 Mar. 1988 23 p
(AD-A195249; NRL-MR-6154) Avail: NTIS HC A03/MF A01 CSCL 09C

A plasma expanding into a magnetic field and/or another plasma can undergo several instabilities which will cause spatial nonuniformities and large scale structure to develop. Potential structure forming instabilities include: various forms of the Rayleigh-Taylor or interchange instability, Kelvin-Helmholtz instabilities. In addition, experimental geometric factors can also affect expansion uniformity. The phenomena reported here should be of interest to a broad range of disciplines GRA

N88-30425# California Univ., Berkeley. Coll. of Engineering.
VORTEX FORMATION AND PARTICLE TRANSPORT IN A CROSS-FIELD PLASMA SHEATH
K. Theilhaber 20 Mar. 1988 101 p
(Contract N00014-80-C-0507)
(AD-A194838; UCB/ERL-M88/21) Avail: NTIS HC A06/MF A01 CSCL 20I

The time-dependent behavior of a transversely magnetized, two-dimensional plasma wall sheath has been studied through particle simulations, with the aim of modelling plasma behavior in the vicinity of the limiters and walls of magnetized plasma devices. The simulations have shown that the cross field sheath between a wall and a plasma is a turbulent boundary layer, with strong potential fluctuations and anomalous particle transport. The driving mechanism for this turbulence is the Kelvin-Helmholtz instability, which arises from the sheared particle drifts created near the wall. Provided it is replenished by an internal flux of particles, the sheath maintains itself in a dynamic equilibrium, in which the linear edge instability, the nonlinear dynamics of the particles and the outward particle diffusion all balance each other. The sheath maintains large, long-lived vortices, with amplitudes which drift parallel to the wall at roughly half the ion thermal velocity. The sheath also maintains a large, spatially-averaged potential drop from the wall to the plasma in sharp distinction with the unmagnetized sheath, where the plasma potential is higher than at the wall. Accompanying the long-wavelength vortices is a spectrum of shorter-wavelength fluctuations, which induce an anomalous cross field transport. GRA

N88-30426# Miami Univ., Coral Gables, Fla.
THEORETICAL MODELING OF ACCELERATING ARC PLASMAS Final Report, 31 Jul. 1984 - 31 Jul. 1987
Manuel A. Huerta 22 Apr. 1988 33 p
(Grant AF-AFOSR-0116-84)
(AD-A195606; AFOSR-88-0576TR) Avail: NTIS HC A03/MF A01 CSCL 20C

The researchers present a calculation in a simplified geometry for the current distribution in the rails, taking into account the motion of the armature and the time variation of the current. Closed form, asymptotic, results for the current density are obtained for arbitrary time dependent electrical conductivity of the rails, and upsilon is the speed of the armature. Because of eddy current effects the rail current may reverse in portions of the rails when the total current decreases. The current is used as a source of Joule heating to find the temperature distribution in the rails. The heat diffusivity is negligible and give numerical results concerning melting. GRA

N88-30518# Joint Publications Research Service, Arlington, Va.
INFLUENCE OF PLASMA PARAMETERS ON VLF RADIATION IN NEAR-ROCKET REGION Abstract Only
N. I. Izhovkina, S. A. Pulinets, and Ye. P. Trushkina *In its* JPRS Report: Science and Technology. USSR: Space 26 Feb. 1988 p 18-19 Transl. into ENGLISH from Kosmicheskiye Issledovaniya (Moscow, USSR), v. 25, no. 3, May - Jun. 1987 p 467-470 Original language document was announced in IAA as A87-47567 (For primary document see N88-30498 24-88)
Avail: NTIS HC A04/MF A01

76 SOLID-STATE PHYSICS

Includes superconductivity.

For related information, see also *33 Electronics and Electrical Engineering* and *36 Lasers and Masers.*

N88-30427*# National Bureau of Standards, Gaithersburg, Md.
X-RAY DIFFRACTION IMAGING (TOPOGRAPHY) OF ELECTROOPTICCRYSTALS BY SYNCHROTRON RADIATION
Bruce Steiner, Masao Kuriyama, Ronald C. Dobbyn, and Uri Laor 1988 16 p
(Grant NAGw-976)
(NASA-CR-183266; NAS 1.26:183266) Avail: NTIS HC A03/MF A01 CSCL 20L

Information of special interest to crystal growers and device physicists now available from monochromatic synchrotron diffraction imaging (topography) is reviewed. Illustrations are taken from a variety of electro-optic crystals. Aspects of the detailed understanding of crystal growth processes obtainable from carefully selected samples are described. Finally, new experimental opportunities now available for exploitation are indicated. Author

N88-30428# California Univ., Los Angeles. Dept. of Electrical Engineering.
LIGHT-MILLIMETER WAVE INTERACTIONS IN SEMICONDUCTOR DEVICES Semiannual Report, 1 Jan. - 31 Dec. 1987
Fetterman 31 Dec. 1987 3 p
(Contract F49620-86-K-0007)
(AD-A195898; AFOSR-88-0528TR) Avail: NTIS HC A02/MF A01 CSCL 20L

Techniques of Optical Control of millimeter wave devices have been explored using both mixing techniques and short pico-second optical pulses. The devices under test include the fastest GaAlAs HEMT Structures as well as new high frequency bipolar heterojunction devices. GRA

N88-30429# Massachusetts Inst. of Tech., Cambridge.
WAVEFORM RELAXATION APPLIED TO TRANSIENT DEVICE SIMULATION
M. Reichelt, J. White, J. Allen, and F. Odeh Mar. 1988 14 p
Prepared in cooperation with IBM Thomas J. Watson Research Center, Yorktown Heights, N.Y.
(Contract N00014-87-K-0825; Grant AF-AFOSR-0164-86)
(AD-A194992) Avail: NTIS HC A03/MF A01 CSCL 09A

This paper investigates the possibility of accelerating the transient simulation of Metal Oxide Semiconductor devices by using waveform relaxation. Standard spatial discretization techniques are used to generate a large, sparsely-connected system of algebraic and ordinary differential equations in time. The waveform relaxation (WR) algorithm for solving such a system is described, and several theoretical results that characterize the convergence of WR for device simulation are given. In addition, one-dimensional experimental results are presented. GRA

N88-30430# Technical Univ. of Istanbul (Turkey). Faculty of Aeronautics and Astronautics.
A DYNAMIC ANALYSIS OF PIEZOELECTRIC STRAINED ELEMENTS Periodic Report No. 4, Nov. 1987 - May 1988
M. C. Dokmeci May 1988 6 p
(Contract DAJA45-86-C-0005)
(AD-A196079) Avail: NTIS HC A02/MF A01 CSCL 20C

In the fourth part of this study, the review article concerned with the dynamic applications of piezoelectric crystals is reviewed and published with its 233 references. Then, an updated review of the open literature is prepared which deals with waves and vibrations in piezoelectric elements and especially in those elements subjected to residual stresses and strains. This survey article summarizes the advances and trends on the subject, and it will be written up for publication. To reproduce some or all the fundamental equations of nonlinear piezoelectricity in variational form, certain integral and differential types of variational principles are deduced from Hamilton's principle by augmenting it through the dislocation potentials and Lagrange undetermined multipliers. This work is checked, minor revisions are made, and then it is accepted for publication. The variational principles lead, as their Euler-Lagrange equations, to the fundamental equations of electroelastic solid with small piezoelectric coupling and those of piezoelectric solid subjected to initial stress. Similar variational principles are formulated for a thermopiezoelectric solid with or without initial stress. The generalized variational principles are extracted from the principle of conservation of energy by augmenting it again through Friedrichs' transformation. GRA

N88-30431*# National Bureau of Standards, Gaithersburg, Md.
DIFFRACTION IMAGING (TOPOGRAPHY) WITH MONOCHROMATIC SYNCHROTRON RADIATION
Bruce Steiner, Masao Kuriyama, Ronald C. Dobbyn, and Uri Laor 1988 50 p
(Grant NAGw-976)
(NASA-CR-183264; NAS 1.26:183264) Avail: NTIS HC A03/MF A01 CSCL 20L

Structural information of special interest to crystal growers and device physicists is now available from high resolution monochromatic synchrotron diffraction imaging (topography). In the review, the importance of superior resolution in momentum transfer and in space is described, and illustrations are taken from a variety of crystals: gallium arsenide, cadmium telluride, mercuric iodide, bismuth silicon oxide, and lithium niobate. The identification and understanding of local variations in crystal growth processes are shown. Finally, new experimental opportunities now available for exploitation are indicated. Author

N88-30432# Princeton Univ., N. J. Dept. of Physics.
THEORY OF SUPERCONDUCTIVITY IN OXIDES Final Technical Report
P. W. Anderson 18 May 1988 4 p
(Grant AF-AFOSR-0392-87)
(AD-A195647; AFOSR-88-0633TR) Avail: NTIS HC A02/MF A01 CSCL 20C

We made our greatest progress towards a final theory of high T sub c superconductivity. The key elements are the work on normal state properties, and the actual mechanism for T sub c. With the understanding (ZA) of the large anisotropy and other transport properties in the normal state, the model is uniquely determined: one must have one version or another of a holon-spinon quantum fluid state, which is not a normal fermi liquid. And with the recognition (HWA) of the large repulsion holon-holon interactions, we have the first way of thinking quantitatively about the superconducting state. Work on the pure Heisenberg system, which is related but not necessarily crucial to understanding the superconducting properties is described. GRA

N88-30433# Illinois Univ., Urbana. Coordinated Science Lab.
ELECTRONIC MATERIALS AND DEVICES PREPARED BY MOLECULAR BEAM EPITAXY Final Report, Nov. 1986 - Sep. 1987
Hadis Morkoc 27 Apr. 1988 6 p
(Grant AF-AFOSR-0093-87)
(AD-A195694; AFOSR-88-0683TR) Avail: NTIS HC A02/MF A01 CSCL 20B

Six Perkin Elmer 430P III-V MBE Systems and a PE Si MBE with appropriate transfer tubes for a totally interconnected MBE Complex has been purchased and installation has begun. The complex is located in the Coordinated Science Laboratory in Room 200 with the majority of administrative role being played by MRL. In this complex, two III-V MBE systems and a transfer tube (13 feet long) and the associated assortment of equipment has been paid for by funds obtained from AFOSR. These growth chambers have been termed as Growth Reactors A and B, with the transfer tube being called 1 Tube. The systems are presently in CSL Room 200 which has been remodeled for this purpose and we are in the process of installing them. GRA

N88-30434# International Centre for Theoretical Physics, Trieste (Italy).
BEHAVIOUR AND HYSTERESIS LOSSES OF IRREVERSIBLE TYPE-2 SUPERCONDUCTING CYLINDRICAL SHELL
A. G. Saif Sep. 1987 10 p
(DE88-702708; IC-87/309) Avail: NTIS (US Sales Only) HC A02/MF A01

The internal magnetic field distribution in a type-2 superconducting cylindrical shell is determined. The superheating - and the supercooling - fields are developed. We have shown the effect of a transport current on the creation and annihilating of the potential barrier for high H-cylindrical shell. The ac losses are studied in the frame of the general critical state theory. For high T(sub c) superconducting sample, we get a smaller superheating - and supercooling - fields than that for conventional superconductors. DOE

N88-30435# Crystal Systems, Inc., Salem, Mass.
GROWTH OF GaAs CRYSTALS BY THE HEAT EXCHANGER METHOD FOR MICROWAVE DEVICE APPLICATIONS Final Report, Jul. - Dec. 1987
Chandra P. Khattak and Frederick Schmid Mar. 1988 51 p
(Contract F33615-87-C-5291)
(AD-A196028; CSI-R1027; AFWAL-TR-88-4043) Avail: NTIS HC A04/MF A01 CSCL 17B

Large GaAs crystals with uniform properties and low defect density are required for microwave devices. The variable quality of the available GaAs, wafer-to-wafer, intra-wafer, boule-to-boule, and intra-boule is unsatisfactory for high yield device processing. It has been shown that undoped (100) semi-insulating GaAs crystals can be grown using the Heat Exchanger Method (HEMTM) with remarkably uniform electronic properties. It has also been demonstrated that undoped dislocation free GaAs crystals can be grown by HEM. The present effort was to understand the cause of lineage and twinning observed in the structure of 3-inch-diameter GaAs boules. GRA

N88-30436# Naval Ocean Systems Center, San Diego, Calif.
POWER MISFETs ON OnP Report, 18 - 23 Oct. 1987
L. J. Messick Apr. 1988 19 p
(AD-A195242) Avail: NTIS HC A03/MF A01 CSCL 20L

Mesa expitaxial and planar implanted InP power MISFET's have been fabricated. At 9.7 GHz CW mesa devices demonstrated 4.5W output with 4 dB gain at 46 percent power-added efficiency with a power density of 4.5W/mm, over three times the highest value ever reported for GaAs FET's. Power output is stable with 2 percent over 167h continuous operation. Planar implanted devices exhibited 3.5W output with 5.4 dB gain, 40 percent power-added efficiency and 3.5W/mm power density at 9.7 GHz. GRA

N88-30437*# National Bureau of Standards, Gaithersburg, Md. Inst. for Materials Science and Engineering.
STREAKING IMAGES THAT APPEAR ONLY IN THE PLANE OF DIFFRACTION IN UNDOPED GaAs SINGLE CRYSTALS: DIFFRACTION IMAGING (TOPOGRAPHY) BY MONOCHROMATIC SYNCHROTRON RADIATION
Masao Kuriyama, Bruce Steiner, Ronald C. Dobbyn, Uri Laor, David Larson, and Margaret Brown (Grumman Aerospace Corp., Bethpage, N.Y.) 1988 20 p
(Grant NAGw-976)
(NASA-CR-183267; NAS 1.26:183267) Avail: NTIS HC A03/MF A01 CSCL 20L

Streaking images restricted to the direction of the diffraction (scattering) vector have been observed on transmission through undoped GaAs. These disruption images (caused by the reduction of diffraction in the direction of observation) appear both in the forward and in Bragg diffracted directions in monochromatic synchrontron radiation diffraction imaging. This previously unobserved phenomenon can be explained in terms of planar defects (interfaces) or platelets which affects the absorption coefficient in anomalous transmission. Such regions of the crystal look perfect despite the presence of imperfections when the scattering vector is not perpendicular to the normal of the platelets. The observed crystallographic orientation of these interfaces strongly indicates that they are antiphase boundaries. Author

N88-30438# Illinois Univ., Urbana. Coordinated Science Lab.
ON 3-5 HETEROJUNCTION STRUCTURES AND HIGH SPEED DEVICES Annual Progress Report, 1 Feb. 1987 - 31 Jan. 1988
Hadis Morkoc 8 Mar. 1988 41 p
(Grant AF-AFOSR-0111-86)
(AD-A195464; AFOSR-88-0530TR) Avail: NTIS HC A03/MF A01 CSCL 20L

A systematic investigation of the InyGa1-yAs/Al0.15Ga0.85 As pseudomorphic MODFET has revealed an optimum InAs mole fraction of 0.15 less than or = y less than or = 0.20. Meanwhile,

continuing studies of the InGaAs/GaAs strained layer MQW by optical transmission and photoreflectance have displayed sharp spectral features, revealing the excellent optical quality of the samples. With good agreement between the measured spectra and our band structure model, an increased understanding of the InGa/GaAs MQW structures into p-i-n optical modulators, large 27 percent changes in transmission have been reported. Operating this MQW electroabsorption optical modulator as a Self-Electrooptic Effect Device, we have reported the first demonstration of this device in the InGaAs material system. GRA

N88-30439# California Univ., Berkeley. Electronics Research Lab.
JOINT SERVICES ELECTRONICS PROGRAM Annual Progress Report, 1 May - 31 Dec. 1987
W. G. Oldham 29 Feb. 1988 99 p
(Contract F49620-87-C-0041)
(AD-A195731; UCB/ERL-87/1; AFOSR-88-0569TR) Avail: NTIS HC A05/MF A01 CSCL 20L

As part of a project to construct, model and compare very high performances Si and GaAs devices, deep-submicron Si MOSFETs have been investigated. Using a novel optical lithography process, these extremely high-gain MOSFETs with varying oxide thicknesses and channel lengths have been fabricated. Figure 1 shows a Scanning Electron Microscope (SEM) picture of a transistor cross-section with an effective channel length 0.2 micron, an oxide thickness of 86 A, and junction depth of 0.2 micron. Devices with effective channel lengths as small as 0.15 micron and oxide thickness as thin as 36 A have been successfully fabricated and operated. GRA

N88-30440*# National Bureau of Standards, Gaithersburg, Md. Inst. for Materials Science and Engineering.
APPLICATIONS OF SYNCHROTRON RADIATION TO MATERIALS SCIENCE: DIFFRACTION IMAGING (TOPOGRAPHY) AND MICRORADIOGRAPHY
Masao Kuriyama 1988 15 p Transl. into ENGLISH from Advanced Techniques for Microstructure Characterization, Aedermannsdorf, Switzerland, 1988 Sponsored in part by DOE
(Grants NAGw-976; NSF DMR-84-12465)
(NASA-CR-183265; NAS 1.26:183265) Avail: NTIS HC A03/MF A01 CSCL 20L

Synchrotron radiation sources are now available throughout the world. The use of hard X-ray radiation from these sources for materials science is described with emphasis on diffraction imaging for material characterization. With the availability of synchrotron radiation, real-time in situ measurements of dynamic microstructural phenomena have been started. This is a new area where traditional application of X-rays has been superseded. Examples are chosen from limited areas and are by no means exhaustive. The new emerging information will, no doubt, have great impact on materials science and engineering. Author

N88-30441# International Centre for Theoretical Physics, Trieste (Italy).
THEORETICAL MODEL OF HIGH TEMPERATURE SUPERCONDUCTORS
A. G. Saif Sep. 1987 7 p
(DE88-702707; IC-87/308) Avail: NTIS (US Sales Only) HC A02/MF A01

A theoretical model related to the mechanism of the interaction between superconductivity and the antiferromagnetism is developed. The critical temperature and the Neel temperature of doping systems are formulated as a function of that for undoped systems. This model is used to describe the behavior of T(sub c) in La(sub 2-x)Ba(sub x)Cu O(sub 4-y). DOE

N88-30442# General Electric Co., Princeton, N.J. Astrospace Div.
HEAVY ION AND PROTON TESTS FOR SUBSYSTEM UPSET Final Report
G. J. Brucker, P. Oey, J. Patella, J. Boross, and M. Xapsos 21 Mar. 1988 10 p
(Contract N00014-85-C-2530)
(AD-A195267) Avail: NTIS HC A02/MF A01 CSCL 18F

This report describes the results of heavy ion and proton tests for upset in a CMOS/SOS subsystem ALU (Arithmetic Logic Unit) which is part of a spacecraft computer. Provided are an iron spectrum with a maximum LET of 83 MeV-cm2/mg at normal incidence. Protons of 180-MeV energy and 10-microsec pulsewidths were obtained at the Brookhaven REF facility. Peak proton dose rates of 7.9E9 rad/s were delivered by micropulses of 1-ns width and with a period of 5 ns. Results showed that the ALU operated without upset during both heavy ion tests. However, functional failure of microprocessor devices occurred during proton irradiations; whereas RAM and MXR (Microprogram Controller and Sequencer) parts were not upset. A single pulse of 119 krads (Si) caused upset of the microprocessor, but multiple pulse doses of 19 to 60 megarads did not upset the RAM and MXR, respectively. GRA

N88-30443# Hughes Research Labs., Malibu, Calif.
CLUSTER BEAM STUDIES Final Report, 1 Aug. 1985 - 31 Oct. 1987
W. Knauer and R. L. Poeschel Apr. 1988 69 p
(Contract F49620-85-C-0125)
(AD-A195182; AFOSR-88-0544TR) Avail: NTIS HC A04/MF A01 CSCL 13H

Cluster beams offer a means of depositing high-quality thin films at low substrate temperature for microelectronics fabrication. The advantage of cluster beam depositions is the ability to optimize the energy of the impacting particles, either directly in clustered vapors of nonvolatile materials or indirectly by bombarding the film during deposition with clusters of inert gases. When a cluster beam is ionized and accelerated through several thousand volts, clusters that contain 1000 or more atoms strike the surface with several electron volt energy per atom. The suprathermal energy of the depositing atoms is thought to produce unique thin films (either in quality, or in the ability to be deposited at all). This report describes the general effort on cluster beam formation methods, on cluster ionization by electron bombardment in a gridded ionization cell, on electrostatic mass separation, and on electrostatic acceleration to a predetermined velocity. Detailed results are given on the improvements in performance of ionization cells for clusters beams of nonvolatile and gaseous materials. GRA

N88-30444*# National Aeronautics and Space Administration, Washington, D.C.
A METHOD FOR THE QUANTITATIVE DETERMINATION OF CRYSTALLINE PHASES BY X-RAY
I. Petzenhauser and P. Jaeger Sep. 1988 14 p Transl. into ENGLISH from Ber. Dtsch. Keram. Ges. (Fed. Republic of Germany), v. 45, 1968 3 p Transl. by Scientific Translation Service, Santa Barbara, Calif.
(Contract NASw-4307)
(NASA-TT-20324; NAS 1.77:20324) Avail: NTIS HC A03/MF A01 CSCL 20L

A mineral analysis method is described for rapid quantitative determination of crystalline substances in those cases in which the sample is present in pure form or in a mixture of known composition. With this method there is no need for prior chemical analysis. Author

77 THERMODYNAMICS AND STATISTICAL PHYSICS

Includes quantum mechanics; theoretical physics; and Bose and Fermi statistics.

For related information see also *25 Inorganic and Physical Chemistry* and *34 Fluid Mechanics and Heat Transfer.*

N88-30445# International Centre for Theoretical Physics, Trieste (Italy).
INTRODUCTION TO STRING THEORY
S. Randjbar-Daemi and J. Strathdee Oct. 1987 44 p
(DE88-702706; IC-87/307) Avail: NTIS (US Sales Only) HC A03/MF A01

These notes are based on a set of six introductory lectures given jointly by the authors. After developing the canonical methods we discuss the covariant quantization of the bosonic as well as the fermionic string. Conformal field theory methods are also introduced and used to calculate the anomaly coefficient (c), as well as the critical dimensions for bosonic and superstrings. We briefly sketch the BRS quantization and then offer an elementary derivation of the anomaly in the ghost number current. Finally, we address the one-loop partition function of the bosonic string and the question of SL(2,Z) invariance. DOE

80 SOCIAL SCIENCES (GENERAL)

Includes educational matters.

No abstracts in this category.

81 ADMINISTRATION AND MANAGEMENT

Includes management planning and research.

N88-30446# Erno Raumfahrttechnik G.m.b.H., Bremen (West Germany).
STUDY ON INDUSTRIAL ORGANIZATION FOR EUROPEAN GROUND SUPPORT EQUIPMENT (EGSE) TO SUPPORT EUROPEAN SPACE PROGRAMS. VOLUME 1: TECHNICAL REPORTS Final Report
H. Michaelis, L. Battocchio, H. Uchard, R. Comerford, and H. Just Paris, France ESA Sep. 1988 592 p Prepared in cooperation with Aeritalia S.p.A., Turin, Italy, MATRA Espace, Toulouse, France and Marconi Space Systems Ltd., Portsmouth, United Kingdom
(Contract ESTEC-7025/87-NL-IW(SC))
(SD-RP-AI-009-Vol-1; ESA-CR(P)-2569-Vol-1; ETN-88-93018)
Avail: NTIS HC A25/MF A01

A technical and programmatical approach towards the ground based end-to-end operation and verification infrastructure (GEOVI) was identified. An industrial organization relative to future GEOVI requirements with the capability to develop, supply, maintain, and operate the ground infrastructure is proposed. The specification for a reference example, the Payload Integration and Verification Center, permitting the mapping of the organization, was established. Other objectives were to define and categorize the GEOVI functions, analyze and identify commonalities within/between categories and establish a commonality matrix; and propose initial activities as a first step towards implementation of GEOVI to demonstrate the feasibility of common developments. ESA

N88-30447# European Space Agency, Paris (France).
WITH AN EYE TO THE FUTURE: ESA GENERAL STUDIES PROGRAM 1988
Norman Londdon, ed. and Brigitte Kaldeich, ed. Apr. 1988 38 p Original contains color illustrations
(ESA-SP-1100; ISSN-0250-1589; ETN-88-93047) Copyright
Avail: NTIS HC A03/MF A01

The ESA programs concerning end-to-end telematics architecture; long-term evolution of telecommunications services and systems; long-term evolution of Earth observation; microgravity utilization; autonomous orbital capability architecture; in-orbit assembly, servicing, and tending; long-term evolution of space transportation systems; and European ground infrastructure are presented. ESA

N88-30448# Erno Raumfahrttechnik G.m.b.H., Bremen (West Germany).
STUDY ON INDUSTRIAL ORGANIZATION FOR EUROPEAN GROUND SUPPORT EQUIPMENT (EGSE) TO SUPPORT EUROPEAN SPACE PROGRAMS. VOLUME 2: TECHNICAL REPORTS Final Report
H. Michaelis, L. Battocchio, H. Uchard, R. Comerford, and H. Just Paris, France ESA Sep. 1988 674 p Prepared in cooperation with Aeritalia S.p.A., Turin, Italy, MATRA Espace, Toulouse, France and Marconi Space Systems Ltd., Portsmouth, United Kingdom
(Contract ESTEC-7025/87-NL-IW(SC))
(SD-RP-AI-009-Vol-2; ESA-CR(P)-2569-Vol-2; ETN-88-93019)
Avail: NTIS HC A99/MF A01

A technical and programmatical approach towards the ground based end-to-end operation and verification infrastructure (GEOVI) was identified. An industrial organization relative to future GEOVI requirements with the capability to develop, supply, maintain and operate the ground infrastructure is proposed. The specification for a reference example, the Payload Integration and Verification Center, permitting the mapping of the organization, was established. Other objectives were to define and categorize the GEOVI functions, analyze and identify commonalities within/between categories and establish a commonality matrix; and propose initial activities as a first step towards implementation of GEOVI to demonstrate the feasibility of common developments. ESA

N88-30466# Glasgow Univ. (Scotland). Business School.
TECHNICAL CHANGE NEEDS ORGANIZATIONAL CHANGE
David Boddy *In* AGARD, Barriers to Information Transfer and Approaches Toward Their Reduction Mar. 1988 5 p (For primary document see N88-30458 24-82)
Copyright Avail: NTIS HC A06/MF A01

82 DOCUMENTATION AND INFORMATION SCIENCE

Includes information management; information storage and retrieval technology; technical writing; graphic arts; and micrography.

For computer documentation see *61 Computer Programming and Software.*

N88-30449# Massachusetts Inst. of Tech., Cambridge.
KNOWLEDGE-BASED INTEGRATED INFORMATION SYSTEMS ENGINEERING: HIGHLIGHTS AND BIBLIOGRAPHY. KNOWLEDGE-BASED INTEGRATED INFORMATION SYSTEMS ENGINEERING (KBIISE) PROJECT, VOLUME 1 Final Report, Sep. 1986 - Jan. 1988
Amar Gupta, ed. and Stuart Madnick, ed. Dec. 1987 134 p Sponsored in part by the Department of the Air Force, Washington, D.C.
(Contract DTRS57-85-C-00083)
(AD-A195850; AD-E500978; MIT-KBIISE-1) Avail: NTIS HC A07/MF A01 CSCL 12G

This volume presents the highlights of the Knowledge-Based Integrated Information Systems Engineering (KBIISE) project, an effort that focuses on identifying and understanding the key issues involved in the intelligent integration of large-scale distributed information systems. Underlying trends in the information technology area have led to a situation where most organizations depend on a portfolio of systems, ranging from mainframes to minicomputers, and from general purpose workstations to

sophisticated CAD/CAM systems, to support their computational requirements. The large size of individual systems and the high degree of diversity between systems make the task of integrating islands of disparate information systems very formidable. The integration of existing system involves surmounting major technical and non-technical barriers which are described in the first part of this volume. The significance of these barriers is analyzed, and approaches for mitigating key problems are developed. Apart from the major issues of concurrency control and recovery in a heterogeneous computing environment, the technical analysis focuses on the subjects of logical connectivity and the use of expert systems technology to draw meaningful inferences in situations characterized by incomplete or conflicting information. The second part of this volume contains a comprehensive annotated bibliography of published papers and technical reports that relate to Knowledge-Based Integrated Information Systems. GRA

N88-30450# Naval Postgraduate School, Monterey, Calif.
THE P-3 SCHEDULING SUPPORT SYSTEM (P-3 S3) M.S. Thesis
William B. Anderson Mar. 1988 146 p
(AD-A194824) Avail: NTIS HC A07/MF A01 CSCL 01C

A P-3 Scheduling Support System (P-3 S3) is a Management Information System (MIS) that was designed using structured techniques. Structured analysis was used to determine the functionality and data requirements. Computer Assisted Systems Engineering (CASE) tools were used to document the analysis and design. The system was designed to be implemented in dBase III Plus, a data base management tool developed by Ashton Tate. P-3 S3 is designed to run on a microcomputer with the MS-DOS operating system. It provides real-time access to historical data and provides suggested personnel assignments to the user. The design provides for faster flight schedule generation and prevention of conflicting schedule events. GRA

N88-30451# North Carolina Univ., Chapel Hill. Dept. of Computer Science.
PARTITIONED STORAGE FOR TEMPORAL DATABASES
Ilsoo Ahn and Richard Snodgrass 20 Jan. 1988 32 p
(Contract N00014-86-K-0680)
(AD-A195093; UNC-TEMPIS-19) Avail: NTIS HC A03/MF A01 CSCL 12F

Efficiently maintaining history data on line together with current data is difficult. This paper discusses one promising approach, the temporally partitioned store. The current store contains current data and possibly some history data, while the history store holds the rest of the data. The two stores can utilize different storage formats, and even different storage media, depending on the individual data characteristics. We discuss various issues on the temporally partitioned store, investigate several formats for the history store, and evaluate their performance on a set of sample queries. GRA

N88-30452# Massachusetts Inst. of Tech., Cambridge.
INTEGRATING IMAGES, APPLICATIONS, AND COMMUNICATIONS NETWORKS, VOLUME 5 Final Report, Sep. 1986 - Jan. 1988
Amar Gupta and Stuart Madnick Dec. 1987 342 p
(Contract DTRS57-85-C-00083)
(AD-A195854; AD-E500978; MIT-KBIISE-5) Avail: NTIS HC A15/MF A01 CSCL 05B

This volume presents practical ideas and prototype systems for integrating existing information and communications resources. It is divided into four parts. The first part, Knowledge-Based Pictorial Information Systems, describes a prototype system that enables users to manage all types of information, especially pictorial information. The Image Database Management System (IDBM) provides an integrated standard that can be used to specify the information to be retrieved, in a format acceptable to all participating computers. The second part, Storage and Retrieval of Pictorial Information in Heterogeneous Computing Systems, studies existing techniques for storing pictorial images, such as bit-mapped mechanisms, vector-based techniques, and quadtree and pyramid-oriented approaches. Recent advances in compression techniques are also discussed. The third part, An Expert System for Accessing and Integrating Design Analysis Knowledge, presents an approach for integrating information from multiple design environments. Mechanical design packages such as CADAM and CATIA, thermal design packages such as ITAM and PHOENIS, and other specialized packages can be linked together through a common expert system. The fourth part highlights a number of critical connectivity issues in the context of data communication networks maintained by two large organizations. GRA

N88-30453*# Jet Propulsion Lab., California Inst. of Tech., Pasadena.
PUBLICATIONS OF THE JET PROPULSION LABORATORY 1987
15 Aug. 1988 32 p
(NASA-CR-181198; JPL-Bibl-39-29; NAS 1.26:181198) Avail: NTIS HC A03/MF A01 CSCL 05B

A bibliography is presented which describes and indexes by author the externally distributed technical reporting, released during the calender year 1987, that resulted from scientific and engineering work performed, or managed, by the Jet Propulsion Lab. Three classes of publications are included: (1) JPL publications in which the information is complete for a specific accomplishment; (2) Articles from the quarterly Telecommunications and Data Acquisition Progress Report; and (3) Articles published in the open literature. E.R.

N88-30454# Massachusetts Inst. of Tech., Cambridge.
TECHNICAL OPINIONS REGARDING KNOWLEDGE-BASED INTEGRATED INFORMATION SYSTEMS ENGINEERING, VOLUME 8 Final Report, Sep. 1986 - Jan. 1988
Amar Gupta and Stuart Madnick Dec. 1987 339 p Sponsored in part by DOT, DOD, and AF
(Contract DTRS57-85-C-00083)
(AD-A195857; AD-E500978; MIT-KBIISE-8) Avail: NTIS HC A15/MF A01 CSCL 12G

This volume encapsulates the views of a panel of experts drawn from government, industry and academia. It is divided into three parts. The first part, Record of discussions held at the first meeting of Technical Advisory Panel on February 17, 1987, highlights the most significant dimensions of Knowledge-Based Integrated Information Systems Engineering. The second part, Record of discussions held at the second meeting of Technical Advisory Panel on May 21, and 22, 1987, presents opinions in the areas of: Organization, Strategy, and Management; Distributed Database Technology; Knowledge and Semantics; and Information Modeling and Mapping. A framework for tackling the problems in these areas is also presented. The third part, Contributions by members of the Technical Advisory Panel (TAP), contains ten outstanding papers contributed by members of the TAP. The first set of three papers focuses on distributed databases. The second set of three papers concentrates on information modeling alternatives. The final set of four papers examines a range of auxiliary issues in the context of large scale, distributed, heterogeneous information systems. GRA

N88-30455# Massachusetts Inst. of Tech., Cambridge.
KNOWLEDGE-BASED INTEGRATED INFORMATION SYSTEMS DEVELOPMENT METHODOLOGIES PLAN.
KNOWLEDGE-BASED INTEGRATED INFORMATION SYSTEMS ENGINEERING (KBIISE) REPORT, VOLUME 2 Final Report, Sep. 1986 - Jan. 1988
Amar Gupta, ed. and Stuart Madnick, ed. Dec. 1987 350 p Sponsored in part by the Department of the Air Force, Washington, D.C.
(Contract DTRS57-85-C-00083)
(AD-A195851; AD-E500978; MIT-KBIISE-2) Avail: NTIS HC A15/MF A01 CSCL 12G

This volume describes the Integrated System Evolution Environment (IISEE) which is structured approach for the strategic planning, tactical planning, requirements definition, design,

construction, implementation, and maintenance of large scale distributed, heterogeneous integrated information systems. This approach is designed to enable system developers in the Air Force and its contractor community to evolve their current systems into a unified framework. The overall goal of the IISEE thrust is to establish a structured systems development approach consisting of methodologies, methods, tools, techniques, and practices which can improve productivity of participants, and reduce cost and time required for integrated information systems development. The IISEE strategy has been designed keeping in view the objectives of the Integrated Design Support System (IDS) Program of the Air Force. The latter program encompasses all issues relating to capture, management, and communication of product technical data from its initial creation in design, through realization in manufacture, to logistics operations. GRA

N88-30456# Air Force Inst. of Tech., Wright-Patterson AFB, Ohio.
DESIGN AND PERFORMANCE ANALYSIS OF A RELATIONAL REPLICATED DATABASE SYSTEM Ph.D. Thesis
Jon G. Hanson 1988 434 p
(AD-A196290; AD-E951149; AFIT/CI/NR-88-89) Avail: NTIS HC A19/MF A01 CSCL 12G

The hardware organization and software structure of a new database system are presented. This system, the relational replicated database system (RRDS), is based on a set of replicated processors operating on a partitioned database. Performance improvements and capacity growth can be obtained by adding more processors to the configuration. Based on design goals a set of hardware and software design questions were developed. The system then evolved according to a five-phase process, based on simulation and analysis, which addressed and resolved the design questions. Strategies and algorithms were developed for data access, data placement, and directory management for the hardware organization. A predictive performance analysis was conducted to determine the extent to which original design goals were satisfied. The predictive performance results, along with an analytical comparison with three other relational multi-backend systems, provided information about the strengths and weaknesses of our design as well as a basis for future research. GRA

N88-30457# Massachusetts Inst. of Tech., Cambridge.
STRATEGIC, ORGANIZATIONAL AND STANDARDIZATION ASPECTS OF INTEGRATED INFORMATION SYSTEMS, VOLUME 6 Final Report, Sep. 1986 - Jan. 1988
Amar Gupta and Stuart Madnick Dec. 1987 259 p Sponsored in part by DOT, DOD and AF
(Contract DTRS57-85-C-00083)
(AD-A195855; AD-E500978; MIT-KBIISE-6) Avail: NTIS HC A12/MF A01 CSCL 12G

This volume highlights key strategic and organizational issues involved in integrating heterogeneous information systems. It is divided into four parts. The first part, Towards a CIS Model for Strategic Applications, explores the nature of strategic goals underlying composite information systems (CIS) and ways to increase the likelihood of success. These aspects are analyzed using an example in which the relationship between the constituents is loosely-coupled and inter-dependent. The second part, Interorganizational Information Systems Via Information Technology: A Network Perspective, deals with the evolution of organizational theory and the importance of inter-organizational information networks. By effective establishment and use of these networks, participating organizations can realize competitive advantages in the marketplace. The third part, The Use of Standard Data Definitions in Composite Information Systems, describes the problems involved in establishing common standards. The fourth part describes a methodology for the development of standards for data exchange in an integrated environment. GRA

N88-30458# Advisory Group for Aerospace Research and Development, Neuilly-Sur-Seine (France). Technical Information Panel.
BARRIERS TO INFORMATION TRANSFER AND APPROACHES TOWARD THEIR REDUCTION
Mar. 1988 110 p In ENGLISH and FRENCH Meeting held in Washington, D.C., 23-24 Sep. 1987
(AGARD-CP-430; ISBN-92-835-0449-6) Copyright Avail: NTIS HC A06/MF A01

Topics addressed include: an overview of the barriers to the international transfer of information, particularly in aerospace and defence; linguistic, political, and economic barriers; the use of technology to overcome these and other barriers, e.g., machine translation, links between disparate databases and teleconferencing; the importance of standards; and the need to change organizations when introducing or changing technology to prevent internal barriers reducing the acceptance and the use of the new technology. For individual titles, see N88-30459 through N88-30467.

N88-30459# Commissariat a l'Energie Atomique, Gif-sur-Yvette (France).
LINGUISTIC AND CULTURAL BARRIERS TO THE TRANSFER OF INFORMATION
Roland Larue *In* AGARD, Barriers to Information Transfer and Approaches Toward Their Reduction Mar. 1988 7 p (For primary document see N88-30458 24-82)
Copyright Avail: NTIS HC A06/MF A01

The relative importance of languages in the world in 1987 is described showing that the world population makes use of about ten languages, each of which covers an area of the globe. The trends are revealed by an analysis of population density and socio-economic balances. The use of language is studied in the field of science and technology, according to the type of communication (written or spoken) and the contents (from mathematics to technology) and the tendencies are shown. The attempts which were made to overcome the linguistic barrier - such as the introduction of a single common language (esperanto or English) or the development of the study of foreign languages are examined. The detailed analysis of the cultural barrier is carried out by several approaches (sociological, psychosociological, psychoanalytic, and psycholinguistic) in order to reveal the genuine individual and collective stakes. Future trends, such as the working of the Commission of the European Communities with its nine official languages are discussed, and some predictions are put forward on the linguistic state of the world at the beginning of the 21st century. Author

N88-30460# Congressional Research Service, Washington, D.C. Science Policy Research Div.
POLITICAL AND ECONOMIC BARRIERS TO INFORMATION TRANSFER
Jane Bortnick *In* AGARD, Barriers to Information Transfer and Approaches Toward Their Reduction Mar. 1988 4 p (For primary document see N88-30458 24-82)
Copyright Avail: NTIS HC A06/MF A01

As international computer/communications networks proliferate, the issue of limits to information transfer becomes more critical. Individual businesses and even entire industries depend upon the ability to transfer information on a global basis in a timely and cost-effective basis. Additionally, international cooperation in science and technology involves greater international collaboration and joint efforts. Barriers that threaten this capability ultimately reduce the growth of markets and limit innovation. For this reason, efforts are underway in bilateral and multinational negotiations to reduce barriers and establish consensus guidelines in areas ranging from privacy to trade. Some of the specific limitations to information transfer, including privacy, trade restrictions, national security, and telecommunications regulations are focused on. It also highlights international efforts to reduce these barriers and establish common approaches to facilitate information transfer. Author

N88-30461# Saarland Univ., Saarbrucken (West Germany).
LINGUISTIC-TECHNICAL ASPECTS OF MACHINE TRANSLATION
Harald H. Zimmermann *In* AGARD, Barriers to Information Transfer and Approaches Toward Their Reduction Mar. 1988 7 p (For primary document see N88-30458 24-82)
Copyright Avail: NTIS HC A06/MF A01

To allow comparison of computer aided translation (CAT) and machine translation (MT) systems, essential criteria and typical exponents of the various concepts are presented. Among the most important criteria of differentiation are the following: translation of complete texts (including titles, abstracts) vs lexical aid for translation; all-round translation vs translation of specialized fields and texts; bilingual translation vs multilingual translation; user-oriented vs administrator-oriented expansion of dictionaries and systems; and portability. Included essential critieria for evaluation are: quality of the raw (also called informative) translation, advantages/disadvantages as opposed to human translation; embedding in a user environment (data bases, indexing and retrieval, word processing, electronic publishing); user friendliness; costs of development and installation; and running costs and effects of realization. Author

N88-30462# Defense Technical Information Center, Alexandria, Va.
INFORMATION RETRIEVAL SYSTEMS EVOLVE-ADVANCES FOR EASIER AND MORE SUCCESSFUL USE
Gladys Cotter *In* AGARD, Barriers to Information Transfer and Approaches Toward Their Reduction Mar. 1988 14 p (For primary document see N88-30458 24-82)
Copyright Avail: NTIS HC A06/MF A01

The advances which are being made in information retrieval systems to assist end-users and information specialists to overcome the critical barriers which make it difficult for them to exploit the power of these systems are described. Technology which is being applied to allow users to interact with information retrieval systems with greater ease and more successful results is identified. To illustrate this process, the efforts of the U.S. Defense Technical Information Center to develop and implement an integrated, functional scientific and technical information network are described. This network was purposefully designed to incorporate both end-users and their information management intermediaries in a complementary manner making them resolute partners in the work and its rewards. The uses of technology modules (artificial intelligence, expert systems, gateways, user-friendly interfaces) to overcome user barriers are described. Author

N88-30463# Atlantic Refining Co., Philadelphia, Pa. ARCOvision Services.
INFORMATION TECHNOLOGY TO FACILITATE GROUP INTERACTION
Cynthia A. Savage *In* AGARD, Barriers to Information Transfer and Approaches Toward Their Reduction Mar. 1988 3 p (For primary document see N88-30458 24-82)
Copyright Avail: NTIS HC A06/MF A01

Atlantic Richfield has successfully operated an interactive, full-motion video teleconferencing system since September of 1983. The system, named ARCOvision, is for internal use only and consists of six locations in the United States including Alaska. The implementation, capabilities, equipment, and costs related to the ARCOvision system will be discussed. Author

N88-30464# Department of the Secretary of State, Ottawa (Ontario).
WORDS: KEYS OR BARRIERS TO INFORMATION TRANSFER
Suzanne Richer *In* AGARD, Barriers to Information Transfer and Approaches Toward Their Reduction Mar. 1988 4 p (For primary document see N88-30458 24-82)
Copyright Avail: NTIS HC A06/MF A01

Terms can create or resolve barriers in the processes pertaining to the transfer of knowledge and the access to information. Selecting words to organize, process, and retrieve data leads to the establishment of hierarchies. The building of thesauri provides for tools enabling the organization of concepts. National and international guidelines were developed for the establishment of monolingual and multilingual thesauri. New words find their way in solid hierarchies. The introduction mechanisms for new words rely on cross-referencing to already established and recognized terms. Manual and machine indexing provide the same basic tools, machine indexing being, in many cases, more feasible. Standardized terms are compiled in special listings such as the glossaries prepared and published by NATO. The linguistic quality norms of standardized terminologies are limited to the specialized objectives of such terminologies. Terminological barriers are costly and should therefore be reduced in order not to hinder the transfer of knowledge and access to information data. Author

N88-30465# National Scientific and Technical Documentation Center, Brussels (Belgium). Belgian Translation Centre.
LINGUISTIC BARRIERS: TRANSLATION PROBLEMS
I. Clemens *In* AGARD, Barriers to Information Transfer and Approaches Toward Their Reduction Mar. 1988 6 p (For primary document see N88-30458 24-82)
Copyright Avail: NTIS HC A06/MF A01

Linguistic problems are in close connection with information problems. They therefore are examined jointly in order to solve the terminological problems and to reach the documentary mass. The problems of comprehension of the texts by the specialist are examined as well as the difficulty raised by the translator. Linguistic problems are examined according to characteristics of the unilingual and multilingual countries and according to the groups of languages. The existing means to reduce linguistic barrier and implied institutions are considered from the point of view of the user, and of the translator. The translator is the keyman to overcome linguistic barrier. The translator is confronted with the problems of scientific and technical text comprehension, of search for information and technical terms sources, of adaptation to the modern work methods. The use of data processing provides him some help and multiple possibilities of the translation process. Among the known method of translation, computer-assisted translation seems currently the most performing: use of a PC for translation processes as such, use of computerized dictionaries and bibliographical data bases as multilingual terminology sources reliable and up-to-date. The whole of raised measures makes it possible to reduce linguistic difficulties of the information user and to ensure an effective help to the transfer. Author

N88-30466# Glasgow Univ. (Scotland). Business School.
TECHNICAL CHANGE NEEDS ORGANIZATIONAL CHANGE **c81**
David Boddy *In* AGARD, Barriers to Information Transfer and Approaches Toward Their Reduction Mar. 1988 5 p (For primary document see N88-30458 24-82)
Copyright Avail: NTIS HC A06/MF A01

It is shown that effective performance cannot be assured simply by installing expensive, state of the art technology. The studies of many applications of computing and information technology have included both successful and unsuccessful examples. The clear practical lesson from this work is that the successful cases were usually those where technical change was accompanied by appropriate organizational change. The less successful ones were generally those where project were dominated by technical considerations, with little of no thought given to organizational ones. These lessons seem as relevant to defence installations as to the civilian ones in which the research was conducted. The common characteristic is that all organizations are confronted by technical developments, which are intended to help them meet their objectives. For them to succeed in that task, it appears that management needs to ensure that three big hurdles are successfully crossed. These are: managing the project, setting the right objectives; and changing the organization. Each of these hurdles will be outlined in turn, and some proposals on how they can be overcome are suggested. Author

N88-30467# National Library of Canada, Ottawa (Ontario).
USING STANDARDS TO BREAK DOWN INFORMATION TRANSFER BARRIERS
Cynthia J. Durance *In* AGARD, Barriers to Information Transfer and Approaches Toward Their Reduction Mar. 1988 5 p (For primary document see N88-30458 24-82)
Copyright Avail: NTIS HC A06/MF A01

Standards for representing and encoding data as well as standards for the interconnection of systems having different hardware and software are both essential for effective electronic information transfer. To date, although major strides were made internationally on standards in both the data and telecommunications areas, much remains to be done before effective electronic information transfer can take place either nationally or internationally. The difficulties in achieving approved standards internationally are addressed, and some new standard that potentially will have a positive impact on information transfer such as those pertaining to an electronic publishing. It also addresses the Open Systems Interconnection Reference Model, a suite of telecommunications standards which hold great promise for the interconnection of systems with different hardware and software. Finally, the work that was done to date to implement these standards for library and information applications and challenges for the future are discussed. Author

N88-30468# Massachusetts Inst. of Tech., Cambridge.
INTEGRATING INFORMATION SYSTEMS IN A MAJOR DECENTRALIZED INTERNATIONAL ORGANIZATION, VOLUME 7 Final Report, Sep. 1986 - Jan. 1988
Amar Gupta and Stuart Madnick Dec. 1987 289 p Sponsored in part by DOT, DOD and AF
(Contract DTRS57-85-C-00083)
(AD-A195856; AD-E500978; MIT-KBIISE-7) Avail: NTIS HC A13/MF A01 CSCL 12G

This volume examines the problems involved in integrating information systems currently in use in a large decentralized international organization. It is divided into three parts. The first part, A Conceptual Model for Integrated Autonomous Processing, highlights the fact that the technical strategy was modulated by three key conflicting organizational forces - autonomy, integration, and evolution. A conceptual system architecture has been developed to provide a technological message-oriented and data-oriented response to meet the organizational needs. The second part, Gaining Strategic Advantage Through Composite Information Systems, identified critical success factors for the successful deployment of Composite Information Systems (CIS) ideas and techniques. For this environment, a data-driven strategy offers the best chances for successful development of a modular and flexible infrastructure suited to the decentralized and highly autonomous structure of the organization. The third part, Integrating Systems for Financial Institutions Services Using Composite Information Systems, analyzes the three key organizational forces in greater detail. Autonomy, for example, is examined in terms of hardware control, operational control, transaction control, software control, data control, and management control. The forces of integration and evolution are also decomposed in a similar vein. The case study reveals that the operations of the organization can be improved by more foresight. GRA

N88-30351*# Wayne State Univ., Detroit, Mich.
RANGE DATA DESCRIPTION BASED ON MULTIPLE CHARACTERISTICS
Ezzet Al-Hujazi and Arun Sood (George Mason Univ., Fairfax, Va.) *In* NASA, Goddard Space Flight Center, The 1988 Goddard Conference on Space Applications of Artificial Intelligence Aug. 1988 p 295-309 (For primary document see N88-30330 24-63)
Avail: NTIS HC A19/MF A01 CSCL 05B

N88-30352*# National Aeronautics and Space Administration. Goddard Space Flight Center, Greenbelt, Md.
THE SECOND GENERATION INTELLIGENT USER INTERFACE FOR THE CRUSTAL DYNAMICS DATA INFORMATION SYSTEM
Nicholas Short, Jr. and Scott L. Wattawa (Science Applications Research, Greenbelt, Md.) *In its* The 1988 Goddard Conference on Space Applications of Artificial Intelligence Aug. 1988 p 313-327 (For primary document see N88-30330 24-63)
Avail: NTIS HC A19/MF A01 CSCL 05B

N88-30353*# National Aeronautics and Space Administration. Goddard Space Flight Center, Greenbelt, Md.
SPACELAB DATA PROCESSING FACILITY (SLDPF) QUALITY ASSURANCE (QA)/DATA ACCOUNTING (DA) EXPERT SYSTEMS: TRANSITION FROM PROTOTYPES TO OPERATIONAL SYSTEMS
Lisa Basile *In its* The 1988 Goddard Conference on Space Applications of Artificial Intelligence Aug. 1988 p 329-341 (For primary document see N88-30330 24-63)
Avail: NTIS HC A19/MF A01 CSCL 05B

N88-30354*# National Aeronautics and Space Administration. Goddard Space Flight Center, Greenbelt, Md.
AUTOMATED CATALOGING AND CHARACTERIZATION OF SPACE-DERIVED DATA
William J. Campbell, Larry Roelofs, and Michael Goldberg (Mitre Corp., McLean, Va.) *In its* The 1988 Goddard Conference on Space Applications of Artificial Intelligence Aug. 1988 p 343-354 (For primary document see N88-30330 24-63)
Avail: NTIS HC A19/MF A01 CSCL 05B

N88-30355*# LNK Corp., Riverdale, Md.
A DESIGN FOR A GROUND-BASED DATA MANAGEMENT SYSTEM
Barbara A. Lambird and David Lavine *In* NASA, Goddard Space Flight Center, The 1988 Goddard Conference on Space Applications of Artificial Intelligence Aug. 1988 p 355-369 (For primary document see N88-30330 24-63)
Avail: NTIS HC A19/MF A01 CSCL 05B

83 ECONOMICS AND COST ANALYSIS

Includes cost effectiveness studies.

N88-30469# Martin Marietta Corp., Denver, Colo. Astronautics Group.
SPACE SYSTEMS COST STUDY Final Report, Sep. 1987 - Feb. 1988
Doug Dilts and Craig Mogensen Mar. 1988 195 p
(Contract MDA972-87-C-0005)
(AD-A196024; MCR-88-511) Avail: NTIS HC A09/MF A01 CSCL 22B

The objective was to develop a methodology and automated database/model that would enable DARPA to evaluate low cost satellite programs and appropriate cost reduction approaches. The methodology and results are based on a point conceptual design. For the government to see the appropriate time phased impact, the parametric group recommends that when LIGHTSAT is awarded, an actual characterization be generated and the characterization live with the design and build life cycle. Real-time adjustments and decisions (cost and schedule) can be implemented from DARPASS data to arrive at the lowest possible program cost. GRA

N88-30470# Stanford Univ., Calif. Systems Optimization Lab.
FORMULATION AND SOLUTION OF ECONOMIC EQUILIBRIUM PROBLEMS
John C. Stone Apr. 1988 83 p
(Contract N00014-85-K-0343; Grant NSF DMS-84-20623)
(AD-A196034; SU-SOL-88-7) Avail: NTIS HC A05/MF A01 CSCL 12D

A number of equivalent mathematical formulations of the

general equilibrium problem in economics are developed and assessed. It begins with the traditional representation as a nonlinear complementarity problem and develops alternative representations as nonlinear optimization problems. All of the formulations depart from previous approaches by including an explicit linear equality for price normalization and a matched artificial variable which must be zero at any equilibrium solution. This structure has the theoretical and computational advantage that any linearization of the equilibrium problem has a feasible complementary solution. Moreover, under a reasonable rank condition, a basic complementary solution exists which can be successfully computed by Lemke's almost-complementary pivoting method. It describes five general-purpose methods which can be applied to solving the equilibrium problem. The common feature of these methods is solving a sequence of linearized problems. It establishes a number of equivalences between the methods, when applied to the equilibrium problem, and assesses their local and global convergence properties in that context. An important new tool in this analysis is another problem formulation based on a differentiable exact penalty function. This formulation provides, perhaps for the first time, a rigorous means of evaluating the progress of a sequential method for computing an equilibrium solution. GRA

84 LAW, POLITICAL SCIENCE AND SPACE POLICY

Includes NASA appropriation hearings; aviation law; space law and policy; international law; international cooperation; and patent policy.

No abstracts in this category.

85 URBAN TECHNOLOGY AND TRANSPORTATION

Includes applications of space technology to urban problems; technology transfer; technology assessment; and surface and mass transportation.

For related information see also *03 Air Transportation and Safety, 16 Space Transportation,* and *44 Energy Production and Conversion.*

N88-30471# Army War Coll., Carlisle Barracks, Pa.
CHINA'S ACQUISITION AND USE OF FOREIGN AVIATION TECHNOLOGY
Mary VonBriesen 30 Mar. 1988 26 p
(AD-A194827) Avail: NTIS HC A03/MF A01 CSCL 05D

Following the establishment of diplomatic relations between the United States and the People's Republic of China in 1979, many people in both countries looked forward to the rapid transfer of technology between the two countries. On the Chinese side, the hopes were to modernize rapidly, leapfrogging the slow development process followed by most other nations. For their part, many Americans saw not only a potential market of over one billion but also a chance to play the China card against the Soviet Union. This study focuses on China's acquisition and use of foreign technology in the aviation industry, pointing out the patterns of Chinese behavior in these transactions. GRA

N88-30472*# National Aeronautics and Space Administration. Lewis Research Center, Cleveland, Ohio.
TESTING OF A VARIABLE-STROKE STIRLING ENGINE Final Report
Lanny G. Thieme and David J. Allen (Sverdrup Technology, Inc., Cleveland, Ohio.) 1986 31 p Presented at the 21st Intersociety Energy Conversion Engineering Conference (IECEC), San Diego, Calif., 25-29 Aug. 1986; sponsored by ACS, SAE, ANS, ASME, IEEE, AIAA and AIChE Previously announced in IAA as A87-18036
(NASA-TM-100899; DOE/NASA/50112-75; E-3056; NAS 1.15:100899) Avail: NTIS HC A03/MF A01 CSCL 10B

Testing of a variable-stroke Stirling engine at NASA Lewis has been completed. In support of the DOE Stirling Engine Highway Vehicle Systems Program, the engine was tested for about 70 hours total with both He and H2 as working fluids over a range of pressures and strokes. A direct comparison was made of part-load efficiencies obtained with variable-stroke (VS) and variable-pressure operation. Two failures with the variable-angle swash-plate drive system limited testing to low power levels. These failures are not thought to be caused by problems inherent with the VS concept but do emphasize the need for careful design in the area of the crossheads. Author

88 SPACE SCIENCES (GENERAL)

N88-30473*# Lunar and Planetary Inst., Houston, Tex.
NINETEENTH LUNAR AND PLANETARY SCIENCE CONFERENCE. PRESS ABSTRACTS
1988 41 p Conference held in Houston, Tex., 14-19 Mar. 1978
(Contract NASw-4066)
(NASA-CR-183037; NAS 1.26:183037; LPI-Contrib-650) Avail: NTIS HC A03/MF A01 CSCL 03B

Topics addressed include: origin of the moon; mineralogy of rocks; CO2 well gases; ureilites; antarctic meteorites; Al-26 decay in a Semarkona chondrule; meteorite impacts on early earth; crystal structure and density of helium; Murchison carbonaceous chondrite composition; greenhouse effect and dinosaurs; Simud-Tiu outflow system of Mars; and lunar radar images. For individual titles, see N88-30474 through N88-30486.

N88-30474*# Harvard-Smithsonian Center for Astrophysics, Cambridge, Mass.
THE ORIGIN OF THE MOON: FURTHER STUDIES OF THE GIANT IMPACT **c91**
W. Benz, A. G. W. Cameron, and H. J. Melosh (Arizona Univ., Tucson.) *In* Lunar and Planetary Inst., Nineteenth Lunar and Planetary Science Conference. Press abstracts 1988 p 1-4
(For primary document see N88-30473 24-88)
Avail: NTIS HC A03/MF A01 CSCL 03B

A number of technical improvements in the calculations which simulate the most violent event that has occurred to the earth during its history: its collision with the next largest body which was present in its region of accumulation in the early solar system, are discussed. This body was a planet in its own right, an object a little more massive than the planet Mars. The collision created a disk of molten and gaseous debris in orbit around the protoearth, and it is believed that the dissipation of this disk resulted in the formation of the moon. Also discussed is the serendipitous discovery that has emerged from the simulations: the role played by a huge, hot, rotating bar of rock and iron, which is formed immediately after the collision, in transferring angular momentum to much of the rock that is put into orbit, and in robbing the iron of angular momentum so that it falls promptly into the protoearth. Author

N88-30475*# Louisiana State Univ., Baton Rouge.
EXOTIC MINERALS IN 3,500 MILLION YEAR OLD ROCKS: EVIDENCE FOR LARGE METEORITE IMPACTS **c90**
G. R. Byerly, D. R. Lowe, and F. Asaro (California Univ., Berkeley.) *In* Lunar and Planetary Inst., Nineteenth Lunar and Planetary Science Conference. Press abstracts 1988 p 5-7
(For primary document see N88-30473 24-88)
Avail: NTIS HC A03/MF A01 CSCL 03B

A relatively small area of mountainous terrain in southern Africa provides scientists from all over the world a look at what the surface of the earth was like three and a half billion years ago.

The Barberton Mountains lie astride the borders of the Republic of South Africa, Mozambique, and the Kingdom of Swaziland. The discovery of several widely distributed deposits that were likely formed by major terrestrial impacts of large extraterrestrial bodies during this early period of earth's history is reported. The Barberton impact deposits are being studied by electron microscopy. The impact deposits were examined for minerals that show the effects of shock metamorphism or compositions unusual in terrestrial rocks. B.G.

N88-30476*# Lawrence Livermore National Lab., Calif.
NON-ATMOSPHERIC NOBLE GASES FROM CO(SUB 2) WELL GA **c90**
M. W. Caffee, G. B. Hudson, C. Velsko, E. C. Alexander, Jr., G. R. Huss, and A. R. Chivas (Australian National Univ., Canberra.) *In* Lunar and Planetary Inst., Nineteenth Lunar and Planetary Science Conference. Press abstracts 1988 p 8-9 (For primary document see N88-30473 24-88)
Avail: NTIS HC A03/MF A01 CSCL 03B

In recent years a number of studies of both terrestrial and extraterrestrial material has allowed the piecing together of a picture of events occurring in the early solar system (4.5 Gyr ago), including the formation of the earth. However, before this picture can be completed with an appropriate amount of detail it will be necessary to make further advances. One of the areas where knowledge is lacking is the chemical and isotopic composition of the earth as a whole. The lack of knowledge has less to do with the capabilities of modern techniques than with the availability of samples to study. About 99.6 percent of the earth's mass is contained in the mantle and core, leaving less that 1 percent in the crust and atmosphere. Although the crust is derived from the mantle it has undergone extensive changes and it is therefore difficult (although not impossible) to use crustal material to study events occurring 4.5 Gyr ago. More information about the early earth could be obtained from studies of the mantle but it is difficult to obtain mantle material, because the mean thickness of the crust is 17 km, much greater than even the deepest mines or drill shafts. The two types of available mantle samples are discussed. Author

N88-30477*# Chicago Univ., Ill.
UREILITES ARE NOT IGNEOUS DIFFERENTIATES **c91**
Robert N. Clayton and Toshiko K. Mayeda *In* Lunar and Planetary Inst., Nineteenth Lunar and Planetary Science Conference. Press abstracts 1988 p 10-11 (For primary document see N88-30473 24-88)
Avail: NTIS HC A03/MF A01 CSCL 03B

Although most all meteorites are as old as the solar system (4.5 billion years), they can be subdivided into primitive and evolved groups, depending on the extent of their chemical and physical processing. Primitive meteorites, most of which are chondrites, are assemblages of dust and millimeter-sized pellets from the presolar nebula, which were not extensively heated and processed since their assembly. Thus they provide information about the conditions in the nebular cloud. Many of the evolved meteorites are achondrites, which are igneous rocks produced by melting on or within an asteroidal object known as the parent body. A major unsolved problem in solar system studies is identification of the source of heat which led to melting of the achondrites. The role of oxygen isotopes in establishing genetic relationships among meteorites is examined. Author

N88-30478*# Geological Survey, Reston, Va.
NEW TYPE OF PRIMITIVE METEORITE FOUND IN ANTARCITCA **c91**
J. N. Grossman, A. E. Rubin, G. J. MacPherson, E. R. D. Scott, M. K. Weisberg, M. Prinz, and C. E. Nehru (American Museum of Natural History, New York, N.Y.) *In* Lunar and Planetary Inst., Nineteenth Lunar and Planetary Science Conference. Press abstracts 1988 p 12-13 (For primary document see N88-30473 24-88)
Avail: NTIS HC A03/MF A01 CSCL 03B

A stony meteorite found in Antarctica in 1985, recently identified as a type of chondrite, probably represents material from a previously unsampled region of the solar system. Scientists are currently debating how the object formed. Preliminary results on Allan Hills 85085 (ALH85085) were presented. Author

N88-30479*# California Inst. of Tech., Pasadena. Div. of Geology and Planetary Science.
EVIDENCE OF THE IN SITU DECAY OF Al-26 IN A SEMARKONA CHONDRULE **c91**
I. D. Hutcheon, R. Hutchison, and G. J. Wasserburg *In* Lunar and Planetary Inst., Nineteenth Lunar and Planetary Science Conference. Press abstracts 1988 p 14-16 (For primary document see N88-30473 24-88)
Avail: NTIS HC A03/MF A01 CSCL 03B

A long-standing problem in the study of meteorites, with broad implications for the evolution of the solar system, is the source of heat for melting small planets. Meteorites, such as the eucrites, were obviously the result of a melting process on a small planet, yet the decay of the long-lived radionuclides present on the earth, K-40, U-235, U-238, and Th-232, could not have provided nearly enough heat to initiate melting approximately 4.5 aeons ago, even on bodies 1000 km in diameter. This problem addressed by H.C. Urey in 1955, who recognized that the presence of short-lived (and now extinct) radionuclides such as Al-26 (half-life of approximately 720,000 y) in the early solar system would have provided an abundant heat source for melting small asteroid-size bodies. Since any Al-26 initially present in the solar nebula would have completely decayed after only a few tens of millions of years, the problem became one of finding evidence of Al-26, in the form of excess Mg-26, in meteorites. The search for evidence of the Al-26 is briefly examined. Author

N88-30480*# Louisiana State Univ., Baton Rouge.
LSU SCIENTISTS DISCOVER EVIDENCE OF LARGE METEORITE IMPACTS ON THE EARLY EARTH **c90**
Donald R. Lowe and Gary R. Byerly *In* Lunar and Planetary Inst., Nineteenth Lunar and Planetary Science Conference. Press abstracts 1988 p 17-18 (For primary document see N88-30473 24-88)
Avail: NTIS HC A03/MF A01 CSCL 03B

Recent discoveries by scientists at Lousiana State University are examined which may provide a window through which early planetary accretion is viewed and studied and the role of large meteorite impacts on the evolution of life and the earth's surface evaluated. Author

N88-30481*# Carnegie Institution of Washington, D. C. Geophysical Lab.
CRYSTAL STRUCTURE AND DENSITY OF HELIUM TO 232 kbar **c91**
H. K. Mao, Y. Wu, A. P. Jephcoat, R. J. Hemley, P. M. Bell, and W. A. Bassett (Cornell Univ., Ithaca, N.Y.) *In* Lunar and Planetary Inst., Nineteenth Lunar and Planetary Science Conference. Press abstracts 1988 p 19-21 (For primary document see N88-30473 24-88)
Avail: NTIS HC A03/MF A01 CSCL 03B

The properties of helium and hydrogen at high pressure are topics of great interest to the understanding of planetary interiors. These materials constitute 95 percent of the entire solar system. A technique was presented for the measurement of X-ray diffraction from single-crystals of low-Z condenses gases in a diamond-anvil cell at high pressure. The first such single-crystal X-ray diffraction measurements on solid hydrogen to 26.5 GPa were presented. The application of this technique to the problem of the crystal structure, equation of state, and phase diagram of solid helium is reported. Crucial for X-ray diffraction studies of these materials is the use of a synchrotron radiation source which provides high brillance, narrow collimation of the incident and diffracted X-ray beams to reduce the background noise, and energy-dispersive diffraction techniques with polychromatic (white) radiation, which provides high detection efficiency. Author

N88-30482*# National Aeronautics and Space Administration. Lyndon B. Johnson Space Center, Houston, Tex.
LEWIS CLIFF 86010, A UNIQUE ANTARCTIC METEORITE: POSSIBLE NEW CLUES TO THE EARLY HISTORY OF THE SOLAR SYSTEM **c90**
G. A. McKay, G. Crozaz, M. Prinz, C. A. Goodrich, and J. S. Delaney (Rutgers Univ., New Brunswick, N. J.) *In* Lunar and Planetary Inst., Nineteenth Lunar and Planetary Science Conference. Press abstracts 1988 p 22-23 (For primary document see N88-30473 24-88)
Avail: NTIS HC A03/MF A01 CSCL 03B

Results form the Antarctic sample, LEW 86010 indicate that it is an extremely interesting meteorite of clear igneous origin, and is probably closely related to ADOR. Several important questions await further detailed study. The most stringent test of the relationship to ADOR will come from the measurement of the oxygen isotopic composition. One possibility proposed is that LEW 86010 represents a partial or total melt of a mixture of material similar to the white Allende clasts and more ordinary chondritic meteorite material. Several lines of investigation will contribute to resolve this question. Further melting studies will be performed to determine whether LEW 86010 represents molten lava. In addition to test the connection with Allende, isotopic studies will look for anomalous isotopic compositions which are ubiquitous in Allende white inclusions. All of these studies will be performed on a tiny sample which weights only 5 grams, and is smaller than a marble, but which contains important clues to events which occurred during the birth of the solar system. Author

N88-30483*# Chicago Univ., Ill. Dept. of Chemistry.
NOBLE GASES, C,N, AND Si ISOTOPES IN INTERSTELLAR SiC FORM THE MURCHISON CARBONACEOUS CHONDRITE **c90**
Tang Ming, Edward Anders, and Ernst Zinner (Washington Univ., St. Louis, Mo.) *In* Lunar and Planetary Inst., Nineteenth Lunar and Planetary Science Conference. Press abstracts 1988 p 25-27 (For primary document see N88-30473 24-88)
Avail: NTIS HC A03/MF A01 CSCL 03B

Isotopic measurements of presolar interstellar silicon carbide are presented. Silicon carbide was recently identified in a primitive meteorite Murray. There exists strong evidence that the silicon carbide predates the formation of the solar system and originated in the atmospheres of certain stars. Thus, this material provides a link with its stellar sources and gives the opportunity to study processes taking place in distant stars. Author

N88-30484*# City Univ. of New York, Brooklyn. Seismological Lab.
DID THE GREENHOUSE EFFECT KILL THE DINOSAURS **c45**
John D. OKeefe and Thomas J. Ahrens *In* Lunar and Planetary Inst., Nineteenth Lunar and Planetary Science Conference. Press abstracts 1988 p 28-30 (For primary document see N88-30473 24-88)
Avail: NTIS HC A03/MF A01 CSCL 13B

According to a study at the California Institute of Technology, the carbon dioxide (CO2) released by a meteor or comet striking the earth 65 million years ago could have doomed many species of animals and plants by dramatically raising temperatures worldwide. The results of this study will be presented at the 19th Lunar and Planetary Science Conference in Houston, Texas.
Author

N88-30485*# Geological Survey, Flagstaff, Ariz.
DEBRIS FLOWS OF THE SIMUD-TIU OUTFLOW SYSTEM OF MARS **c91**
Kenneth L. Tanaka *In* Lunar and Planetary Inst., Nineteenth Lunar and Planetary Science Conference. Press abstracts 1988 p 31-33 (For primary document see N88-30473 24-88)
Avail: NTIS HC A03/MF A01 CSCL 03B

It is seen that the magnitude of geologic happenings are commonly quite different between the Earth and Mars because of differences in the makeup and breakup of their crusts. By assessing the differences, and the similarities, between planets, the geologic history of Mars can be more fully understood. The identification of debris-flow deposits in channels of Mars, for example, helps to establish which of several competing explanations for the origin of the channels actually occurred. In turn, the Earth is viewed in new, and commonly enlightening perspectives. By the way, it is fortunate that on Earth, thick sequences of impact ejected are not found that could be transformed into the monstrous debris flows that have devastated the Martian surface. Author

N88-30486*# Massachusetts Inst. of Tech., Westford. Haystack Observatory.
HIGH-RESOLUTION (30 m) LUNAR RADAR IMAGES **c32**
Stanley H. Zisk *In* Lunar and Planetary Inst., Nineteenth Lunar and Planetary Science Conference. Press abstracts 1988 p 34-36 (For primary document see N88-30473 24-88)
Avail: NTIS HC A03/MF A01 CSCL 17I

New high-resolution radar images of the lunar surface are being produced using the Haystack Observatory range-Doppler radar system. The goals are to: investigate the decameter-scale properties of the lunar surface, as an aid in the understanding of the geophysical history of the moon; and to improve the understanding of the mechanisms of planetary radar backscattering, to aid in the interpretation of the coarser-resolution images which were and will be obtained from planetary probe missions and other earth-based observations. Author

N88-30487*# Lunar and Planetary Inst., Houston, Tex.
NASA MEVTV PROGRAM WORKING GROUP MEETING: VOLCANISM ON MARS
1988 33 p Meeting held in Oahu, Hawaii, 27-30 Jun. 1988 (Contract NASw-4066)
(NASA-CR-183074; NAS 1.26:183074; LPI-Contrib-660) Avail: NTIS HC A03/MF A01 CSCL 03B

The purpose of this working group meeting is to focus predominantly on volcanism on Mars, prior to considering the more complex issues of interactions between volcanism and tectonism or between volcanism and global or regional volatile evolution. It is also hoped that the topical areas of research identified will aid the planetary geology community in understanding volcanism on Mars and its relationship to other physical processes. For individual titles, see N88-30488 through N88-30497.

N88-30488*# Arizona State Univ., Tempe. Dept. of Geology.
ERUPTIVE VISCOSITY AND VOLCANO MORPHOLOGY **c46**
Seth B. Posin and Ronald Greeley *In* Lunar and Planetary Inst., NASA MEVTV Program Working Group Meeting: Volcanism on Mars 1988 p 1-3 (For primary document see N88-30487 24-88)
Avail: NTIS HC A03/MF A01 CSCL 08K

Terrestrial central volcanoes formed predominantly from lava flows were classified as shields, stratovolcanoes, and domes. Shield volcanoes tend to be large in areal extent, have convex slopes, and are characterized by their resemblance to inverted hellenic war shields. Stratovolcanoes have concave slopes, whereas domes are smaller and have gentle convex slopes near the vent that increase near the perimeter. In addition to these differences in morphology, several other variations were observed. The most important is composition: shield volcanoes tend to be basaltic, stratovolcanoes tend to be andesitic, and domes tend to be dacitic. However, important exceptions include Fuji, Pico, Mayon, Izalco, and Fuego which have stratovolcano morphologies but are composed of basaltic lavas. Similarly, Ribkwo is a Kenyan shield volcano composed of trachyte and Suswa and Kilombe are shields composed of phonolite. These exceptions indicate that eruptive conditions, rather than composition, may be the primary factors that determine volcano morphology. The objective of this study is to determine the relationships, if any, between eruptive conditions (viscosity, erupted volume, and effusion rate) and effusive volcano morphology. Moreover, it is the goal of this study to incorporate these relationships into a model to predict the eruptive conditions of extraterrestrial (Martian) volcanoes based on their morphology.
Author

N88-30489*# Geological Survey, Flagstaff, Ariz.
FAULTING AND ITS RELATION TO VOLCANISM: MARS WESTERN EQUATORIAL REGION **c91**
David H. Scott and James Dohm *In* Lunar and Planetary Inst., NASA MEVTV Program Working Group Meeting: Volcanism on Mars 1988 p 5-7 (For primary document see N88-30487 24-88)
Avail: NTIS HC A03/MF A01 CSCL 03B

Recently completed geologic maps of Mars show the global distribution of lava flows that were emplaced during each of the three Martian time-stratigraphic periods and the faults and ridges that originated during these periods. These data were extracted from the geologic maps to make a series of volcano-tectonic maps for the Noachian, Hesperian, and Amazonian Periods. The map series is being compiled on Viking photomosaics at 1:15,000,000 scale. These maps will provide a basis for assessing the interactive roles of volcanism and tectonism in the crustal evolution of Mars. Author

N88-30490*# Naples Univ. (Italy).
LAVA THICKNESSES: IMPLICATIONS FOR RHEOLOGICAL AND CRUSTAL DEVELOPMENT **c46**
C. R. J. Kilburn and R. M. C. Lopes (London Univ. Observatory, England) *In* Lunar and Planetary Inst., NASA MEVTV Program Working Group Meeting: Volcanism on Mars 1988 p 9-11 Prepared in cooperation with Consiglio Nazionale delle Ricerche, Naples, Italy, and Old Royal Observatory, London, England (For primary document see N88-30487 24-88)
Avail: NTIS HC A03/MF A01 CSCL 08G

The morphology of a lava flow is strongly influenced by its rheological structure. The rheological structure is, in turn, dependent on numerous factors including: (1) bulk composition, (2) crystallingity, (3) vesicularity, and (4) crustal development. Identifying which of the latter factors are most significant, and hence most readily investigated by remote-sensing techniques, is necessary to clarify short-term objectives and expectations from the study of Martian lava flows. Insights into the rheological controls on flow morphology are provided by variations in thickness of undrained lava streams on Etna and Vesuvius, Southern Italy. Both pahoehoe and aa lavas were studied. Author

N88-30491*# Geological Survey, Flagstaff, Ariz.
MARS: VOLCANISM IN THE VALLES MARINERIS OVERLOOKED **c91**
B. K. Lucchitta *In* Lunar and Planetary Inst., NASA MEVTV Program Working Group Meeting: Volcanism on Mars 1988 p 13-14 (For primary document see N88-30487 24-88)
Avail: NTIS HC A03/MF A01 CSCL 03B

Do volcanic rocks exist in the Valles Marineris. This question is pertinent because the Valles Marineris are gigantic grabens, rivaling rift valleys on earth in size and depth. The Valles Marineris were interpreted as extensional tectonic structures, perhaps incipient rifts. On earth, rift valleys commonly contain volcanic deposits. On Mars, deposits inside the Valles Marineris grabens do not have the morphologic signature of such easily identified volcanic features as shield volcanoes or lava flows. Therefore, many researchers have not recognized the deposits inside the Valles Marineris as volcanic. Is Mars, then, different from earth in having formed riftlike grabens unaccompanied by volcanism. Overall, results from the study suggest that volcanism was present in the Valles Marineris; the volcanism was explosive in places; some volcanism was more felsic than that generally assumed elsewhere; and the younger sequence of interior beds was emplaced so late in Martian history that the planet may be considered to be still volcanically active. Author

N88-30492*# Arizona State Univ., Tempe. Dept. of Geology.
THE MARTIAN HIGHLAND PATERAE: EVIDENCE FOR EXPLOSIVE VOLCANISM ON MARS **c91**
David A. Crown and Ronald Greeley *In* Lunar and Planetary Inst., NASA MEVTV Program Working Group Meeting: Volcanism on Mars 1988 p 15-17 (For primary document see N88-30487 24-88)
Avail: NTIS HC A03/MF A01 CSCL 03B

The Martian surface exhibits numerous volcanic landforms displaying great diversity in size, age, and morphology. Most research regarding Martian volcanology has centered around effusive basaltic volcanism, including analyses of individual lava flows, extensive lava plains, and large shield volcanoes. These studies were hindered by a lack of definitive morphologic criteria for the remote identification of ash deposits. Knowledge of the abundances, ages, and geologic settings of explosive volcanic deposits on Mars is essential to a comprehensive understanding of the evolution of the Martian surface, with implications for the evolution of the lithosphere and atmosphere as well as the histories of specific volcanic centers and provinces. Author

N88-30493*# Smithsonian Institution, Washington, D. C. Center for Earth and Planetary Studies.
PHYSICAL PROPERTIES OF SURFACE MATERIALS ON MARTIAN VOLCANOES: DUST-COVERED LAVA AND ASH **c91**
James R. Zimbelman *In* Lunar and Planetary Inst., NASA MEVTV Program Working Group Meeting: Volcanism on Mars 1988 p 19-21 (For primary document see N88-30487 24-88)
Avail: NTIS HC A03/MF A01 CSCL 03B

Remote sensing measurements provide information about the Martian surface at scales smaller than can be inferred from imaging data alone. Measurements of Martian volcanoes obtained at visual, infrared, and radar wavelengths are discussed in order to evaluate the physical properties. A related issue involves identifying possible ash deposits by distinctive or anomalous physical characteristics. Author

N88-30494*# Hawaii Univ., Honolulu. Inst. of Geophysics.
RIFTS OF DEEPLY ERODED HAWAIIAN BASALTIC SHIELDS: A STRUCTURAL ANALOG FOR LARGE MARTIAN VOLCANOES **c46**
Michael D. Knight, G. P. L. Walker, P. J. Mouginis-Mark, and Scott K. Rowland (Geological Survey, Menlo Park, Calif.) *In* Lunar and Planetary Inst., NASA MEVTV Program Working Group Meeting: Volcanism on Mars 1988 p 23-25 (For primary document see N88-30487 24-88)
Avail: NTIS HC A03/MF A01 CSCL 08G

Recently derived morphologic evidence suggests that intrusive events have not only influenced the growth of young shield volcanoes on Mars but also the distribution of volatiles surrounding these volcanoes: in addition to rift zones and flank eruptions on Arsia Mons and Pavonis Mons, melt water channels were identified to the northwest of Hecates Tholus, to the south of Hadriaca Patera, and to the SE of Olympus Mons. Melt water release could be the surface expression of tectonic deformation of the region or, potentially, intrusive events associated with dike emplacement from each of these volcanoes. In this study the structural properties of Hawaiian shield volcanoes were studied where subaerial erosion has removed a sufficient amount of the surface to enable a direct investigation of the internal structure of the volcanoes. The field investigation of dike morphology and magma flow characteristics for several volcanoes in Hawaii is reported. A comprehensive investigation was made of the Koolau dike complex that passes through the summit caldera. A study of two other dissected Hawaiian volcanoes, namely Waianae and East Molokai, was commenced. The goal is not only to understand the emplacement process and magma flow within these terrestrial dikes, but also to explore the possible role that intrusive events may have played in volcano growth and the distribution of melt water release on Mars. Author

N88-30495*# Jet Propulsion Lab., California Inst. of Tech., Pasadena.
SIMULATIONS OF LAVA FLOWS ON MARS **c91**
S. Baloga and J. Crisp *In* Lunar and Planetary Inst., NASA MEVTV Program Working Group Meeting: Volcanism on Mars 1988 p 27-29 (For primary document see N88-30487 24-88)
Avail: NTIS HC A03/MF A01 CSCL 03B

One way to approach the understanding of the lava flows observed in the Viking images is to use well-documented terrestrial flows and to simulate comparable eruptions adjusted for Martian conditions. The detailed documentation available for several episodes of the 1983 to 1984 PuuOo eruption can be used in combination with an extension of the emplacement theory for solitary lobate flows to simulate comparable eruptions on the surface of Mars. For simplicity, the simulation is restricted to differences in the gravity between earth and Mars. Author

N88-30496*# Jet Propulsion Lab., California Inst. of Tech., Pasadena.
SMALL-SCALE VOLCANIC LANDFORMS INDICATIVE OF DISTRIBUTARY TUBE SYSTEMS c46
E. Theilig *In* Lunar and Planetary Inst., NASA MEVTV Program Working Group Meeting: Volcanism on Mars 1988 p 31-32 (For primary document see N88-30487 24-88)
Avail: NTIS HC A03/MF A01 CSCL 08G

Surface features tens to hundreds of meters in size on Martian lava flows are revealed in high resolution Viking Orbiter images. Many of these morphological features form in response to certain flow emplacement mechanisms, eruptive styles, or rheological properties of the lava. Insight into the relationships between lava flow morphology and the emplacement and characteristics of magma is an ongoing areas of research and allows constraints to be placed on interpretation of Martian volcanism. This report focuses on pressure ridges, tumuli, and pressure plateaus which comprise a suite fo features characteristics of compound pahoehoe lava flows. Similar ridges and mounds were identified in the Tharsis region of Mars. Author

N88-30497*# Jet Propulsion Lab., California Inst. of Tech., Pasadena.
VOLCANIC STYLES AT ALBA PATERA, MARS: IMPLICATIONS OF LAVA FLOW MORPHOLOGY TO THE VOLCANIC HISTORY c91
D. M. Schneeberger and D. C. Pieri *In* Lunar and Planetary Inst., NASA MEVTV Program Working Group Meeting: Volcanism on Mars 1988 p 33-35 (For primary document see N88-30487 24-88)
Avail: NTIS HC A03/MF A01 CSCL 03B

Alba Patera presents styles of volcanism that are unique to Mars. Its very low profile, large areal extent, unusually long and voluminous lava flows, and circumferential graben make it among Mars' most interesting volcanic features. Clues to Alba's volcanic history are preserved in its morphology and stratigraphy. Understanding the relationship of lava flow morphology to emplacement processes should enable estimates of viscosity, effusion rate, and gross composition to be made. Lava flows, with dimensions considered enormous by terrestrial standards, account for a major portion of the exposed surface of Alba Patera. These flows exhibit a range of morphologies. While most previous works have focused on the planimetric characteristics, attention was drawn to the important morphological attributes, paying particular attention to what the features suggest about the emplacement process. Author

N88-30498# Joint Publications Research Service, Arlington, Va.
JPRS REPORT: SCIENCE AND TECHNOLOGY. USSR: SPACE
26 Feb. 1988 64 p Transl. into ENGLISH from various Russian articles
(JPRS-USP-88-001) Avail: NTIS HC A04/MF A01

JPRS Report USP-88-001, Science and Technology, USSR: Space, 26 February 1988, contains reports on the following principal subjects: Manned Missions, Space Sciences, Interplanetary Sciences, Space Applications, and Space Policy, Administration. Of special interest in this volume are reports on Earth Atmosphere, Supernova 1987A, Orbital Mechanics, Earth Ionosphere, and Venus Atmosphere. For individual titles, see N88-30499 through N88-30534.

N88-30499# Joint Publications Research Service, Arlington, Va.
PHOTOCHEMISTRY OF IONOSPHERIC D-REGION WITH INJECTION OF NITROGEN OXIDES Abstract Only c46
S. I. Kozlov *In its* JPRS Report: Science and Technology. USSR: Space 26 Feb. 1988 p 12 Transl. into ENGLISH from Geomagnetizm i Aeronomiya (Moscow, USSR), v. 27, no. 3, May-Jun. 1987 p 383-387 Original language document was announced in IAA as A88-24681 (For primary document see N88-30498 24-88)
Avail: NTIS HC A04/MF A01

A theoretical study of D-region photochemistry with artificial injection of NO and NO2 is presented. Numerical calculations are used to determine the main mechanisms responsible for variations of electron density and other components of the atmosphere. A quantitative analysis of the effect of diffusion is presented, and it is shown that this effect can increase substantially due to the appearance of concentration gradients in the perturbed region. Author

N88-30500# Joint Publications Research Service, Arlington, Va.
STRUCTURAL DYNAMICS OF HIGH-LATITUDE MAGNETOSPHERE DETERMINED FROM SOLAR ELECTRON DATA Abstract Only c46
V. A. Sergeyev, S. N. Kuznetsov, and Yu. V. Gotselyuk *In its* JPRS Report: Science and Technology. USSR: Space 26 Feb. 1988 p 12 Transl. into ENGLISH from Geomagnetizm i Aeronomiya (Moscow, USSR), v. 27, no. 3, May - Jun. 1987 p 440-447 (For primary document see N88-30498 24-88)
Avail: NTIS HC A04/MF A01

The characteristics of the auroral peak, a specific structure of injections of high-energy solar electrons on the nighttime side of the polar cap, were investigated. The study was based on data from the Intercosmos-17 satellite, which registered leaking electrons with E greater than 30 keV, and leaking and trapped electrons with E greater than 8 keV. These data were supplemented by measurements of high-energy electrons by the ISEE-1 satellite and information on magnetic variations and auroras registered by an all-sky camera at Kheys station. All the considered data apply to an interval of registry of extremely strong streams of solar cosmic rays observed on 13-14 February 1978. Analysis revealed that the auroral peak is associated with the leakage of solar electrons on closed lines of force, and therefore the boundary of injections of solar electrons on the nighttime side is not the boundary of closed-open tubes of force in the tail of the magnetosphere, as postulated earlier, although this does not hold for the daytime sector. The most probable mechanism of auroral peak formation is nonadiabatic scattering of particles in the current sheet. The breakup region and the polar margin of the auroral cusp are linked to the auroral peak region, which is a projection of the part of the current sheet with a low normal magnetic field component. Author

N88-30501# Joint Publications Research Service, Arlington, Va.
RELATIONSHIP BETWEEN CHARACTERISTICS OF LOW-ENERGY ELECTRONS AND GEOMAGNETIC DISTURBANCE IN GEOSTATIONARY ORBIT Abstract Only c13
O. S. Grafodatskiy, V. I. Degtyarev, A. G. Kozlov, V. I. Lazarev, O. I. Platonov, G. V. Popov, and M. V. Teltsov *In its* JPRS Report: Science and Technology. USSR: Space 26 Feb. 1988 p 12-13 Transl. into ENGLISH from Geomagnetizm i Aeronomiya (Moscow, USSR), v. 27, no. 3, May - Jun. 1987 p 494-496 (For primary document see N88-30498 24-88)
Avail: NTIS HC A04/MF A01

Measurements of low-energy (0.3 to 5.0 keV) electrons made on the Raduga geostationary satellite during a period of low magnetospheric disturbance in April-September 1980 are analyzed. The spectra of particles in the substorm disturbance region differ from Maxwellian and their fluxes are increased as a result of acceleration of plasma sheet particles from the tail of the magnetosphere in the region 6.6 R sub E. The fluxes and spectra of these particles are complexly and strongly dependent on the level of magnetic disturbance and LT. In order to ascertain the

relationship between the observed spectra and the physical processes in the magnetosphere it was assumed that a magnetosphereic distrubance develops in a spatially limited nucleus near the midnight meridian and in its expansion forms the charged particles injection front. The results of measurements of electron fluxes were averaged for fixed hourly LT intervals and the diurnal variations of fluxes of electrons of different energies was determined from these averaged values. The effects of local magnetospheric disturbances and the effects of movements of the plasma sheet edge could be separated. In a particularly quiet magnetosphere there were no regions in the neighborhood of the geostationary orbit where electron acceleration could occur; in the quiet magnetosphere small local disturbances can occur; in a slightly disturbed magnetosphere the frequency and intensity of local disturbances increase. Author

N88-30502# Joint Publications Research Service, Arlington, Va.
USING NONSTATIONARY MODELS OF THE ATMOSPHERE TO DESCRIBE SATELLITE DRAG Abstract Only **c46**
O. A. Malkin and V. A. Lupovka *In its* JPRS Report: Science and Technology. USSR: Space 26 Feb. 1988 p 13 Transl. into ENGLISH from Izvestiya Vysshikh Uchebnykh Zavedeniy: Geodeziya i Aerofotosyemka (Moscow, USSR), no. 2, Mar. - Apr. 1987 p 59-69 Original language document was announced in IAA as A88-10906 (For primary document see N88-30498 24-88)
Avail: NTIS HC A04/MF A01

The use of the following models to describe satellite drag is considered: GOST 22721-77, DTM, CIRA-72, MSIS-77, MSIS-83, and an analytic version of J77A model. The models are compared in terms of total atmospheric density for heights of 250, 400, and 1000 km for medium and near-extremum levels of solar and geomagnetic activity. Semimajor-axis calculations were obtained to assess differences among the models. Author

N88-30503# Joint Publications Research Service, Arlington, Va.
APPROXIMATION OF ATMOSPHERIC DENSITY BY CHEBYSHEV POLYNOMIALS IN PREDICTING MOTION OF LOW ARTIFICIAL EARTH SATELLITES Abstract Only **c46**
V. A. Lupovka *In its* JPRS Report: Science and Technology. USSR: Space 26 Feb. 1988 p 13-14 Transl. into ENGLISH from Izvesitya Vysshikh Uchebnykh Zavedeniy: Geodeziya i Aerofotosyemka (Moscow, USSR), no. 3, May - Jun. 1987 p 70-75 Original language document was announced in IAA as A88-13668 (For primary document see N88-30498 24-88)
Avail: NTIS HC A04/MF A01

The development of an auxiliary upper-atmosphere model for predicting the motion of low-flying satellites is examined. It is shown that model compactness and economy are achieved by representing variations of atmospheric density in the form of Chebyshev multidimensional interpolation forms in geographic, solar-ecliptic, and solar-geomagnetic coordinate systems. Author

N88-30504# Joint Publications Research Service, Arlington, Va.
ASTRON OBSERVATIONS OF SUPERNOVA 1987A IN LARGE MAGELLANIC CLOUD Abstract Only **c89**
A. A. Boyarchuk, R. Ye. Gershberg, A. M. Zvereva, P. P. Petrov, A. B. Severnyy, A. V. Terebizh, C. T. Hua, and A. I. Sheykhet *In its* JPRS Report: Science and Technology. USSR: Space 26 Feb. 1988 p 14 Transl. into ENGLISH from Pisma v Astronomicheskiy Zhurnal (Moscow, USSR), v. 13, no. 9, Sep. 1987 p 739-743 (For primary document see N88-30498 24-88)
Avail: NTIS HC A04/MF A01

The supernova 1987A flared in the Large Magellanic Cloud on 23 February 1987 and rapidly attained a brightness of about 4 sup m. It was decided to observe it from the Astron astrophysical station, but since none of the 15 standard reference stars could be used, Saturn was chosen as a reference object. Four series of observations were made: 4, 6, 9, and 12 March. Observations ended when Saturn was no longer suitable for Astron orientation. During the observations there was an appreciable general attenuation of supernova brightness. On 12 March the radius of the photosphere was 24 a.u., exceeding the orbital radius of Uranus, and the mean rate of increase in photosphere radius from the time of the flare was close to 2400 km/s. Three strong absorptions (gIgI2960, 3150, and 3260A) show up clearly on the registered spectra, but the strong blending caused by the great rate of expansion did not make it possible to draw any conclusions concerning the chemical composition of the emitting envelope. Supernova 1987A flared at the location of a hot star of the spectral class B3I, but no proof was obtained that a B3 supergiant had exploded. Special efforts were made to find traces of such a hot object on the registered spectra, but no evident traces of the spectrum of a hot star were discovered. Author

N88-30505# Joint Publications Research Service, Arlington, Va.
GAMMA RADIATION EXPECTED FROM SUPERNOVA 1987A IN LARGE MAGELLANIC CLOUD **c93**
O. S. Bartunov, S. I. Blinnikov, L. V. Levakhina, and D. K. Nadezhin *In its* JPRS Report: Science and Technology. USSR: Space 26 Feb. 1988 p 14 Transl. into ENGLISH from Pisma v Astonomicheskiy Zhurnal (Moscow, USSR), v. 13, no. 9, Sep. 1987 p 744-750 Original language document was announced in IAA as A88-19582 (For primary document see N88-30498 24-88)
Avail: NTIS HC A04/MF A01

The Monte Carlo method is used to obtain the spectra of photons in the 0.1 to 3.5 MeV range escaping the supernova 1987A envelope: they were generated during Co-56 decay or by the young pulsar. The time dependence of the gamma-flux in energy intervals of 0.1 to 0.2 MeV and 0.8 to 0.9 MeV is analyzed for variants of Co-56 decay. It is shown how differences in the parameters of the expanding envelope appear in the observations. Author

N88-30506# Joint Publications Research Service, Arlington, Va.
ORBITAL EVOLUTION OF DISTANT ARTIFICIAL EARTH SATELLITES Abstract Only **c13**
M. A. Vashkovyak *In its* JPRS Report: Science and Technology. USSR: Space 26 Feb. 1988 p 14-15 Transl. into ENGLISH from Kosmicheskiye Issledovaniya (Moscow, USSR), v. 25, no. 3, May - Jun. 1987 p 339-355 (For primary document see N88-30498 24-88)
Avail: NTIS HC A04/MF A01

A study was made of the main features of orbital evolution of artificial earth satellites (AES) with semimajor axes 100 to 200 thousand kilometers in time intervals of about 10 to 15 years using a numerical analysis method. The greatest difficulty is caused by the rather strong lunar perturbing influence. In the analysis this makes it necessary to use a model of an evolving lunar orbit and in the expansion of the perturbing function to take into account a considerably greater number of terms than in the case of the geostationary AES. Orbits with periods commensurate with a sidereal month are not considered. Slower variables (mean solar longitude, ecliptic longitudes of perigee and ascending node of the lunar orbit), changing the periods of 1.9 and 18.5 years, are retained in the perturbing function. Other slow variables in AES orbits which are taken into account are eccentricity, argument of perigee and longitude of the ascending node. In the averaged problem the semimajor axes of AES orbits are constant values. A geocentric ecliptic coordinate system is used as the main system and the averaged equations are written in canonical form for a second system of Poincare elements. The results are compared with the results of numerical integration of rigorous equations of AES motion with allowance for both lunar and solar perturbations. The ranges of changes of eccentricities and inclinations for initial almost circular AES orbits are determined for a 10-year period. Author

N88-30507# Joint Publications Research Service, Arlington, Va.
PLANE PERIODIC SATELLITE MOTIONS RELATIVE TO CENTER OF MASS IN NEIGHBORHOOD OF COLLINEAR LIBRATION POINT Abstract Only **c90**
N. I. Chirkina *In its* JPRS Report: Science and Technology. USSR: Space 26 Feb. 1988 p 15 Transl. into ENGLISH from Kosmicheskiye Issledovaniya (Moscow, USSR), v. 25, no. 3, May

- Jun. 1987 p 356-361 (For primary document see N88-30498 24-88)
Avail: NTIS HC A04/MF A01

By applying the Lyapunov theorem on a holomorphic integral it can be demonstrated that there are two families of periodic motions of a point of infinitely small mass near the libration point L sub 2. A study was made of one of these families of periodic motions for which the center of satellite mass moves in an orbit lying in the plane of motion of finite masses m sub 1 and m sub 2, the distance between which is used as a unit of length. Such motion is possible with ordinary assumptions concerning the nondependence of the trajectory of the satellite center of mass on its motion relative to the center of mass. Three right-handed coordinate systems are introduced for solution of the problem. The extent of the periodic orbit of satellite center of mass near L sub 2 is considered small in comparison with the distance between the m sub 1 and m sub 2 points, characterized by the small parameter gy. This orbit can be stipulated by series in powers of gy. The equations of satellite motion relative to its center of mass allow solutions corresponding to plane motions for which one of the main central axes of the ellipsoid of satellite inertia during the entire time of motion is perpendicular to the orbital plane. With this taken into account, a study is made of the problem of existence and stability of periodic motions produced by plane rotations and oscillations of an arbitrary amplitude. Author

N88-30508# Joint Publications Research Service, Arlington, Va.
FAMILIES OF PERIODIC SOLUTIONS IN PROBLEM OF SOLID BODY ROTATION AT TRIANGULAR LIBRATION POINT IN RESTRICTED THREE-BODY PROBLEM Abstract Only **c13**
S. N. Lelyavin *In its* JPRS Report: Science and Technology. USSR: Space 26 Feb. 1988 p 15 Transl. into ENGLISH from Kosmicheskiye Issledovaniya (Moscow, USSR), v. 25, no. 3, May - Jun. 1987 p 362-369 (For primary document see N88-30498 24-88)
Avail: NTIS HC A04/MF A01

Satellite rotations at libration points is important due to the development of numerous plans for using libration points of the earth-moon system. By modeling a satellite as a solid body, it is possible to study its rotation around the libration points. Triangular libration points are of the greatest interest because the motion of the center of mass of the solid body at these points is stable. The theory of periodic Poincare solutions was used earlier to study families of periodic solutions for a solid body situated at the triangular libration point of the restricted (circular or elliptical) three-body problem. This article represents a continuation of the aforementioned study and is devoted to periodic regimes of rotational motion of a solid body near the triangular libration point of the restricted three-body problem. A study is also made of new families of periodic solutions. The basis for this research is the theory of periodic Poincare solutions for Hamiltonian systems of the standard type and the equations of rotational motion in normalized canonical variables. Author

N88-30509# Joint Publications Research Service, Arlington, Va.
ROTATIONAL EVOLUTION OF DYNAMICALLY SYMMETRIC GYROSTAT WITH INTERNAL FRICTION Abstract Only **c18**
M. L. Pivovarov *In its* JPRS Report: Science and Technology. USSR: Space 26 Feb. 1988 p 15 Transl. into ENGLISH from Kosmicheskiye Issledovaniya (Moscow, USSR), v. 25, no. 3, May - Jun. 1987 p 370-373 (For primary document see N88-30498 24-88)
Avail: NTIS HC A04/MF A01

The presence of a passive damper of nutational oscillations on a satellite ensuring the evolution into permanent rotation makes it possible not only to preclude stabilization errors, but also to use the simplest and most economical algorithm for the control of motion. Only an impulse is required, for example, to correct the direction of the kinetic moment of the satellite, after which the damper eliminates oscillations of the angle of nutation which arise without changing the position of the kinetic moment in absolute space. A free flywheel dispersing energy due to viscous friction in the bearings is one of the simplest types of dampers of nutational oscillations. The averaging method is used on this study of the rotational evolution of a dynamically symmetric satellite with a damping flywheel on the assumption that the perturbing moment caused by the influence of the damper is small in comparison with the kinetic energy of satellite rotation. A dynamically symmetric gyrostat was investigated; the axis of the free flywheel is orthogonal to the gd-axis and the directions of the gy- and gh-axes are such that the flywheel axis is parallel to the gh-axis. There is viscous friction between the flywheel and the gyrostat body. In this formulation it is shown that the solid body rotation problem is integrable. An analytical dependence between the angle of nutation and time was found and the optimal viscosity ensuring the most rapid decrease in the angle of nutation was determined. Author

N88-30510# Joint Publications Research Service, Arlington, Va.
RESONANCE EFFECTS ACCOMPANYING MOTION WITH LOW THRUST IN EARTH-MOON SYSTEM Abstract Only **c13**
A. Yu. Kogan and V. A. Kotin *In its* JPRS Report: Science and Technology. USSR: Space 26 Feb. 1988 p 16 Transl. into ENGLISH from Kosmicheskiye Issledovaniya (Moscow, USSR), v. 25, no. 3, May - Jun. 1987 p 374-383 (For primary document see N88-30498 24-88)
Avail: NTIS HC A04/MF A01

None of the many studies made of spacecraft motion along spiral trajectories in the earth's gravitational field have considered the perturbing effect of the moon, especially as regards resonance. A study of interorbital resonances was made, but limited to plane motions of the spacecraft and assuming the lunar orbit to be circular. The investigation is made in the framework of the restricted circular three-body problem, complicated by an allowance for jet acceleration. The possibility of capture at resonance is examined. It is shown that sometimes when commensurability is attained between the periods of revolution of the sapcecraft and moon the evolution of the spiral orbit eases because the engine thrust is compensated by the attraction of the moon. Only one of the possible mechanisms of capture at resonance is studied, i.e., the winding of a spiral trajectory into an asymptotically stable periodic orbit. The problem is examined in a uniformly rotating coordinate system in which the earth and moon are at rest. It is shown that under definite conditions the influence of orbital resonances qualitatively changes the character of motion, including the occurrence of capture. An analytical expression for describing these conditions is derived. Examples of asymptotically stable resonance orbits are presented. Author

N88-30511# Joint Publications Research Service, Arlington, Va.
INCREASING ACCURACY IN EVALUATING VECTOR OF STATE UNDER CONDITIONS OF INCOMPLETE OBSERVABILITY OF EXPANDED SYSTEM Abstract Only **c13**
M. P. Igonin and A. L. Katkov *In its* JPRS Report: Science and Technology. USSR: Space 26 Feb. 1988 p 16 Transl. into ENGLISH from Kosmicheskiye Issledovaniya (Moscow, USSR), v. 25, no. 3, May - Jun. 1987 p 384-392 Original language document was announced in IAA as A87-47556 (For primary document see N88-30498 24-88)
Avail: NTIS HC A04/MF A01

Consideration is given to the state-vector estimation of a linear plant under incomplete observability of an extended system describing the dynamics of the plant and the evolution of low-frequency components of external disturbances and measurement errors. Dynamic filtering is used to synthesize an algorithm of state-vector estimation for the optimal control of the plant. The synthesis of a motion control system for a spacecraft is considered as an example. Author

N88-30512# Joint Publications Research Service, Arlington, Va.
CANONICAL VARIABLES AND CANONICAL INTEGRALS FOR MOTION IN NEAR-CIRCULAR ORBITS Abstract Only **c13**
A. B. Nayshul *In its* JPRS Report: Science and Technology. USSR: Space 26 Feb. 1988 p 16-17 Transl. into ENGLISH from Kosmicheskiye Issledovaniya (Moscow, USSR), v. 25, no. 3, May - Jun. 1987 p 393-399 Original language document was

announced in IAA as A87-47557 (For primary document see N88-30498 24-88)
Avail: NTIS HC A04/MF A01

The motion of a spacecraft in a nearly circular orbit is divided into motions in three independent subspaces. These subspaces have their own variables and integrals of motion, which are used for the analytical solution of problems of optimal navigation and orbit correction. Author

N88-30513# Joint Publications Research Service, Arlington, Va.
MODEL REPRESENTATION OF ELECTRON CONCENTRATION DISTRIBUTION IN OUTER MIDDLE-LATITUDE IONOSPHERE USING DATA FROM INTERCOSMOS-19 ARTIFICIAL EARTH SATELLITE Abstract Only **c46**
N. P. Benkova, A. D. Legenka, N. A. Kochenova, M. N. Fatkullin, and M. D. Fligel *In its* JPRS Report: Science and Technology. USSR: Space 26 Feb. 1988 p 17 Transl. into ENGLISH from Kosmicheskiye Issledovaniya (Moscow, USSR), v. 25, no. 3, May - Jun. 1987 p 410-420 (For primary document see N88-30498 24-88)
Avail: NTIS HC A04/MF A01

The outer ionosphere was empirically modeled for daytime summer conditions in the middle latitudes on the basis of data from satellite and surface soundings, representing a refinement of work already published. In that study the zone examined was 40-50SD, with a 120SD breakdown longitudinally (350-50SD and 170-230SD; 230-350SD; 50-170SD). However, the longitudinal differences in the third zone were too great for all the data to be combined into a single model. Moreover, it was found that the first zone had to be divided into two sectors (Europe and Pacific Ocean). Accordingly, the original model has been modified so that it distinguishes five sectors. Much more material has been exploited in comparison with the original scheme, but as before, use was made of ionospheric data only for slightly disturbed magnetic conditions, as is customary in ionospheric modeling. The description of the revised model discusses the data used and the dependence of the parameters of the F region maximum (electron concentration N sub m and altitude h sub m) on solar activity; the dependence of electron concentration N at fixed altitudes on solar activity; normalized electron concentration profiles, analytical representation of models and comparison with other models. The range of solar activities examined was F sub 10.7 = 60 to 300. The model is represented by the exponential formula N/N sub m = ga exp(-gb(h-h sub m)), where the parameters of the maximum N sub m, h sub m are linearly dependent on solar activity. Author

N88-30514# Joint Publications Research Service, Arlington, Va.
RING CURRENT ROLE IN DYNAMICS OF FLUCTUATING ELECTRON AND ION FLUXES IN LOW-LATITUDE MAGNETOSPHERE Abstract Only **c46**
N. M. Shyutte and N. I. Izhovkina *In its* JPRS Report: Science and Technology. USSR: Space 26 Feb. 1988 p 17 Transl. into ENGLISH from Kosmicheskiye Issledovaniya (Moscow, USSR), v. 25, no. 3, May - Jun. 1987 p 421-425 (For primary document see N88-30498 24-88)
Avail: NTIS HC A04/MF A01

Data from the Cosmos-900 satellite revealed the presence of electron and ion fluxes with fluctuating energy spectra in the low-latitude magnetosphere, suggesting an instability of particle fluxes relative to wave generation on the VLF and ELF frequency ranges. These fluxes have the following local structure: the maximum intensities of electron fluxes under quiet and moderately disturbed conditions are approximately two orders of magnitide greater than for ions; the energy spectra for ions are less smooth; the total densities for the electron and ion plasma components (for E = 100 eV to 20 keV) are virtually identical (quasineutrality of plasma is not impaired). There is a dependence of the frequency of appearance of such fluxes for low L-shells on the D sub st index, to a considerable degree characterizing the dynamics of ring currents. With an increase in the absolute D sub st value the frequency of appearance of fluxes with fluctuating energy spectra at low L-shells decreases. Such fluxes are observed most frequently in the zone of the South Atlantic Magnetic Anomaly. This is evidence of a dependence of these fluxes on geomagentic field structure. The diffusion of such fluxes in the middle-latitude magnetosphere is evidently controlled by processes of radial and pitch angle diffusion of particles in the region of capture of VLF and ELF waves in waveguide channels at the plasmasphere boundary. Author

N88-30515# Joint Publications Research Service, Arlington, Va.
PLASMA OF EARTH'S MAGNETOSPHERE RING CURRENTS. MODEL COMPARED WITH RESULTS OF AMPTE/CCE EXPERIMENT Abstract Only **c46**
V. V. Temnyy *In its* JPRS Report: Science and Technology. USSR: Space 26 Feb. 1988 p 17-18 Transl. into ENGLISH from Kosmicheskiye Issledovaniya (Moscow, USSR), v. 25, no. 3, May - Jun. 1987 p 426-438 (For primary document see N88-30498 24-88)
Avail: NTIS HC A04/MF A01

A model of the distribution of ion energy density in the ring current region was developed on the basis of experimental data for 1961 to 1983 in order to demonstrate the stationary filling of this region with plasma having an energy density commensurable with geomagnetic field energy density. Four main features of the quiet ring current were defined on the basis of a comparison of a model of the radial variation of energy density in the quiet ring current in the earth's magnetosphere and the parameters of the energetic ion component of plasma found in the AMPTE/CCE experiment. It was found that the radial variation of modeled ring current energy density, close to the geomagnetic field energy density at L greater than or equal to 4, coincides with the registered radial variation of plasma pressure perpendicular to the magnetic field, varying little during a magnetic storm. A hot component of ring current ions with temperatures of tens of keV, a concentration of more than 1/cu cm and an energy density of about 100 keV cu cm was discriminated when the ion distribution functions obtained using spectra from the AMPTE/CCE experiment were approximated by a Maxwellian approximation. The concentration and energy density of oxygen ions indicate an ionospheric source of ring current hot ions. The transport of ions into the ring current from the ionosphere may occur due to ambipolar diffusion. The drift of ring current ions with the oberved pressure gradient results in formation of a drift ring current with a westerly direction. The direction of the magnetic moment at the center of the quiet ring current coincides with the direction of the geomagnetic dipole. Author

N88-30516# Joint Publications Research Service, Arlington, Va.
EXPERIMENTAL PROOF OF QUASILONGITUDINAL PROPAGATION OF LOW-FREQUENCY WAVES IN MIDDLE LATITUDES IN UPPER IONOSPHERE Abstract Only **c46**
V. I. Altyntseva, V. F. Gubskiy, and V. I. Larkina *In its* JPRS Report: Science and Technology. USSR: Space 26 Feb. 1988 p 18 Transl. into ENGLISH from Kosmicheskiye Issledovaniya (Moscow, USSR), v. 25, no. 3, May - Jun. 1987 p 464-465 Original language document was announced in IAA as A87-47565 (For primary document see N88-30498 24-88)
Avail: NTIS HC A04/MF A01

An analsis of Intercosmos-19 data indicates that, at midlatitides (below 50 deg), waves in the entire ELF range propagate quasi-longitudinally, i.e., low-frequency waves arising in the equatorial region at plasmasphere heights propagate practically along the magnetic field lines. Results indicate that simultaneous measurements of the magnetic and electric components of the LF field can be used to determine plasma concentration at midlatitudes in quiet and moderately perturbed conditions. Author

N88-30517# Joint Publications Research Service, Arlington, Va.
ONE EQUATORIAL ANOMALY IN NIGHTTIME IONOSPHERIC F REGION Abstract Only **c46**
G. V. Givishvili, N. A. Kochenova, L. N. Leshchenko, and M. D. Fligel *In its* JPRS Report: Science and Technology. USSR: Space 26 Feb. 1988 p 18 Transl. into ENGLISH from Kosmicheskiye Issledovaniya (Moscow, USSR), v. 25, no. 3, May

- Jun. 1987 p 466-467 Original language document was announced in IAA as A87-47566 (For primary document see N88-30498 24-88)
Avail: NTIS HC A04/MF A01

Intercosmos-19 vertical sounding data and ship measurements confirm the conclusion of Balev et al., (1976) that at least one local large-scale zone with amomalously low electron density is regularly observed in the near-equatorial nighttime F-region during the winter solstice. At base heights, the decrease can amount to 1 to 2 orders of magnitude; at the layer maximum, the decrease is by 2 to 4 times, this decrease extending from the base to the F2-layer maximum, and possible higher. Author

N88-30518# Joint Publications Research Service, Arlington, Va.
INFLUENCE OF PLASMA PARAMETERS ON VLF RADIATION IN NEAR-ROCKET REGION Abstract Only c75
N. I. Izhovkina, S. A. Pulinets, and Ye. P. Trushkina *In its* JPRS Report: Science and Technology. USSR: Space 26 Feb. 1988 p 18-19 Transl. into ENGLISH from Kosmicheskiye Issledovaniya (Moscow, USSR), v. 25, no. 3, May - Jun. 1987 p 467-470 Original language document was announced in IAA as A87-47567 (For primary document see N88-30498 24-88)
Avail: NTIS HC A04/MF A01

VLF waves in the 0.1 to 5 MHz range were recorded during electron injection in the Araks rocket experiment. The spectral charactieristics of the VLF emission were found to change when the onboard plasma generator was switched on. It is shown that this change was apparently due to the unsteady and nonuniform nature of the external magnetic field near the rocket resulting from variations of plasma conductivity in the near-rocket region and a restructuring of the current system comprising the injection-electron current and rocket neutralization currents.
Author

N88-30519# Joint Publications Research Service, Arlington, Va.
CHARGE COMPOSITION OF PRIMARY COSMIC RAY NUCLEI WITH z GREATER THAN OR EQUAL TO 2 IN ENERGY REGION GREATER THAN OR EQUAL TO 2 TeV Abstract Only c93
I. P. Ivanenko, N. L. Grigorov, V. Ya. Shestoperov, Yu. V. Basina, P. V. Vakulov, Yu. Ya. Vasilyev, R. M. Golynskaya, L. B. Grigoryeva, D. A. Zhuravlev, and V. I. Zatsepin et al. *In its* JPRS Report: Science and Technology. USSR: Space 26 Feb. 1988 p 19 Transl. into ENGLISH from Kosmicheskiye Issledovaniya (Moscow, USSR), v. 25, no. 3, May - Jun. 1987 p 471-473 Original language document was announced in IAA as A87-47568 (For primary document see N88-30498 24-88)
Avail: NTIS HC A04/MF A01

An experiment to study cosmic ray particles with energies approximately 1 TeV or greater was carried out in 1984 using the Sokol instrument carried aboard the Cosmos-1543. Particle energy was measured using an ionization calorimeter and particle charge was measured using Cerenkov detectors situated above it. Protons and alpha particles are reliably separated by DZ-1 detectors. The fraction of alpha particles among the registered protons and the fraction of protons among the alpha particles does not exceed a few percent. The charge distribution of nuclei with z greater than 5 for the energy interval 1 to 10 TeV and the charge distribution of nuclei with z greater than or equal to 2 for an energy greater than or equal to 2 TeV are shown graphically. With transition to energies greater than or equal to 2 TeV the charge composition of primary cosmic ray nuclei with z greater than or equal to 2 does not experience significant changes. Author

N88-30520# Joint Publications Research Service, Arlington, Va.
MEASUREMENT OF GALACTIC RADIO EMISSION AT FREQUENCY 37 GHz FROM ABOARD SPACECRAFT Abstract Only c93
I. A. Strukov and D. P. Skulachev *In its* JPRS Report: Science and Technology. USSR: Space 26 Feb. 1988 p 19 Transl. into ENGLISH from Pisma v Astronomicheskiy Zhurnal (Moscow, USSR), v. 13, no. 6, Jun. 1987 p 469-473 (For primary document see N88-30498 24-88)
Avail: NTIS HC A04/MF A01

It is postulated that the distribution of thermal galactic radio emission is dominated by extended low-density HII regions (ELD regions), with the remaining HII regions accounting for only 16. Until now it has been impossible to measure the parameters of extended sources of thermal radio emission with sufficient accuracy. This can be done by exoatmospheric scanning at relatively high frequencies. Such measurements were made in 1983 and 1984 by Prognoz-9 during the Relikt experiment. Measurements of the celestial sphere were made in the 400 MHz band near the 37 GHz central frequency; the antenna directional diagram had a width of 5SD.5 at half power. Each celestial sphere point near the galactic plane was observed some 5000 times; total observation time for each point was about 1.5 hours. Fifteen million measurements were made, 10 pct near the galactic plane. The IR excess was found to be greater by a factor of 1.5 to 2.5, requiring a modification of the parameters of the previous distribution model and masses of ionized gases. A precise knowledge of the radiation intensity of extended sources in the short wave portion of the radio range is vital for proper interpretation of data for research on the anisotropy of relict radiation. Author

N88-30521# Joint Publications Research Service, Arlington, Va.
BINARY STAR MEASUREMENTS USING DIGITAL SPECKLE INTERFEROMETER OF 6-m TELESCOPE Abstract Only c89
I. I. Balega and Yu. Yu. Balega *In its* JPRS Report: Science and Technology. USSR: Space 26 Feb. 1988 p 19-20 Transl. into ENGLISH from Pisma v Astronomicheskiy Zhurnal (Moscow, USSR), v. 13, no. 6, Jun. 1987 p 508-514 (For primary document see N88-30498 24-88)
Avail: NTIS HC A04/MF A01

New results have been obtained from speckle interferometer studies of binary stars. The work has been done since 1983 using the 6-m telescope at the Special Astrophysical Observatory. The observations are summarized in three tables. The work was done in November 1984 (4 nights) and March 1985 (3 nights). Table 1 gives 98 measurements of 80 binaries; two of these stars, BD+19SD662 and BD+23SD1346, were directly resolved for the first time. The tables give the catalog designation, names, coordinates for epoch 2000, observation dates, position angles and distances. Table 2 gives information on observations of 20 binaries and suspected binaries which were unresolved with the 6-m telescope. Table 3 gives a comparison of position angle and distance measurements and computer values for 35 systems.
Author

N88-30522# Joint Publications Research Service, Arlington, Va.
MICROPHYSICAL PROCESSES IN CLOUD LAYERS OF VENUS Abstract Only c91
D. V. Titov *In its* JPRS Report: Science and Technology. USSR: Space 26 Feb. 1988 p 21 Transl. into ENGLISH from Kosmicheskiye Issledovaniya (Moscow, USSR), v. 25, no. 3, May - Jun. 1987 p 448-455 Original language document was announced in IAA as A87-47563 (For primary document see N88-30498 24-88)
Avail: NTIS HC A04/MF A01

Available space-probe data are used to identify the main microphysical characteristics of aerosol in the Venus cloud layer, including the particle size distribution and the aerosol number density. Attention is given to the evolution of the particle size distribution function at the initial stages of the formation of sulfur-acid clouds. An analysis is made of the role of various microphysical processes (nucleation, condensation, coagulation, sedimentation, and turbulent mixing) in the formation of the observed particle size spectra. Author

N88-30523# Joint Publications Research Service, Arlington, Va.
STABILITY OF VENUSIAN IONOPAUSE Abstract Only c91
A. M. Krymskiy *In its* JPRS Report: Science and Technology. USSR: Space 26 Feb. 1988 p 21 Transl. into ENGLISH from Kosmicheskiye Issledovaniya (Moscow, USSR), v. 25, no. 3, May

- Jun. 1987 p 456-463 (For primary document see N88-30498 24-88)
Avail: NTIS HC A04/MF A01

The Pioneer-Venus spacecraft discovered in 1979 that although Venus does not have its own magnetic field, under conditions of low dynamic pressure of the solar wind, regions with a relatively strong magnetic field with a strength of 50 to 100 gamma could be detected. Characterized by field bursts of several seconds, and therefore having an extent of tens of kilometers, these regions were interpreted as plaits of magnetic lines of force. The nature of this phenomenon has remained unclear. One of the suggested mechanisms is ionopause destruction due to instability caused by a marked change in the velocity of plasma flow near the ionopause with transition from the moving plasma of the solar wind transition region to the at-rest plasma of the ionosphere and the transport of the magnetic plaits forming in the nonlinear stage of instability into the depths of the ionosphere due to plasma convection. Research has shown that Kelvin-Helmholtz instability develops in the region of small zenith angles. During periods of low solar wind dynamic pressure the Venus ionopause is stable relative to perturbations with a characteristic dimension 50 km (size of the magnetic plaits) in the region of zenith angles of 10 deg or less. Author

N88-30524# Joint Publications Research Service, Arlington, Va.
DETERMINING NEAR-WATER WIND SPEED USING RADAR DATA FROM COSMOS-1500 ARTIFICIAL EARTH SATELLITE Abstract Only **c43**
G. V. Volpyan and Yu. G. Spiridonov *In its* JPRS Report: Science and Technology. USSR: Space 26 Feb. 1988 p 22 Transl. into ENGLISH from Issledovaniye Zemli iz Kosmosa (Moscow, USSR), no. 3, May - Jun. 1987 p 3-11 (For primary document see N88-30498 24-88)
Avail: NTIS HC A04/MF A01

The SEASAT satellite carried a two-ray radar apparatus designed to determine speed and direction of the near-water wind in a scanning zone 2 x 475 km. However, it is questionable if the instrument is optimal for solution of problems related to study of the near-water wind with respect to statistical reliability or spatial resolution. The side-looking radar on the Cosmos-1500 with a scanning zone of approximately 470 km has considerably better spatial resolution (about 1 x 2 km) compared to the American scatterometer. This side-looking radar can be used to study the spatial structure of wind fields in rapidly changing synoptic situations, such as along fronts, in hurricanes and squalls, and in some cases to obtain estimates of wind direction for forecasting purposes. The statistical reliability of these estimates is ensured by the possibility of selecting the required window of spatial averaging of radar data for each situation. The method and algorithm used to determine speed of the near-water wind using the physical calibration of side-looking radar relative to the known radar characteristics of multiyear sea ice are described. Author

N88-30525# Joint Publications Research Service, Arlington, Va.
EVOLUTION OF THERMAL STRUCTURE OF BENGUELA UPSWELLING SYSTEM ACCORDING TO SATELLITE AND SHIPBOARD DATA Abstract Only **c48**
A. S. Kazmin, R. Legeckis, and K. N. Fedorov *In its* JPRS Report: Science and Technology. USSR: Space 26 Feb. 1988 p 22 Transl. into ENGLISH from Issledovaniye Zemli iz Kosmosa (Moscow, USSR), no. 3, May - Jun. 1987 p 26-37 (For primary document see N88-30498 24-88)
Avail: NTIS HC A04/MF A01

Hydrophysical research was carried out in the Benguela upwelling region along the Namibian coast in April-June 1985 during the 14th cruise of the Prof. Shtokman. An analysis of shipboard and satellite data was made to determine the structure of ocean surface temperature (OST) and its evolution in the research area. The ship made six runs perpendicular to the coast with a minimum spacing of 15 miles. Infrared photos from the NOAA-NESS satellite were also used. It was possible to trace the full cycle of development of the hydrological situation, which included: a greatly transformed state of the system under conditions of prolonged absence of upwelling of fresh waters, a relatively brief phase of active upwelling associated with wind intensification, followed by relaxation until a new upwelling event occurs. During the observation period active upwelling processes were of moderate intensity, upwelling of waters occurred from realtively shallow depths and the coastal upwellings on the front were much less sharp than on fronts to the south. A study was made of the horizontal and vertical structure of a stationary large-scale anticyclonic eddy on the boundary of the cold coastal waters and its influence on the OST field. Author

N88-30526# Joint Publications Research Service, Arlington, Va.
POSSIBILITIES OF DETERMINING VERTICAL PROFILES OF MICROPHYSICAL CHARACTERISTICS OF STRATOSPHERIC AEROSOL USING SPACE MEASUREMENTS OF TRANSPARENCY AND SOLAR HALO Abstract Only **c46**
P. Yu. Romanov, V. V. Rozanov, and Yu. M. Timofeyev *In its* JPRS Report: Science and Technology. USSR: Space 26 Feb. 1988 p 22-23 Transl. into ENGLISH from Issledovaniye Zemli iz Kosmosa (Moscow, USSR), no. 3, May - Jun. 1987 p 54-63 (For primary document see N88-30498 24-88)
Avail: NTIS HC A04/MF A01

Various space methods for measuring atmospheric transparency and the solar halo were evaluated applicable to determining the microphysical characteristics of aerosol in three stratospheric layers (14 to 20 km, 20 to 30 km, and 30 to 50 km). Parametric and histogram methods can be employed for numerical analysis of possibilities for retrieving the particle-size distribution function. It is found that a considerable quantity of information can be obtained concerning the microstructure of stratospheric aerosol in the particle-size range 0.1 to 10 microns by spectral measurements of transparency and solar halo brightness on slant paths. The spectral transparency or spectral halo methods may be more informative, depending on stratospheric altitude or the particular stratospheric aerosol model used. Simultaneous measurements are preferable to ensure maximum information yield. Definite information on the real part of the refractive index can be obtained using the spectral halo method for a background model of stratospheric aerosol. Optical methods make it possible to refine a priori data on both real and imaginary parts of the refractive index for a model of disturbed atmospheric aerosol. Author

N88-30527# Joint Publications Research Service, Arlington, Va.
ANALYTICAL METHOD FOR APPROXIMATE GEODETIC REFERENCING OF SCANNER IMAGES OF METEOROLOGICAL ARTIFICIAL EARTH SATELLITES USING CONTROL POINTS Abstract Only **c43**
M. V. Ivanchik and V. A. Krovotyntsev *In its* JPRS Report: Science and Technology. USSR: Space 26 Feb. 1988 p 23 Transl. into ENGLISH from Issledovaniye Zemli iz Kosmosa (Moscow, USSR), no. 3, May - Jun. 1987 p 109-115 Original language document was announced in IAA as A88-10923 (For primary document see N88-30498 24-88)
Avail: NTIS HC A04/MF A01

A georeferencing method is proposed which relies on the coordinates of characteristic reference points on space images, the orbital inclinations and the satellite revolution period. The method does not require the satellite trajectory data input, and the algorithms of the procedure are simple and compact, making it possible to program a problem with a small expenditure of the computer time for image processing. The correlating accuracy of the method is + or - 20 to 30 km. Author

N88-30528# Joint Publications Research Service, Arlington, Va.
DETERMINING EARTH'S ROTATION FROM LASER OBSERVATIONS OF LAGEOS ARTIFICIAL EARTH SATELLITE (DURING PERIOD OF MAIN MERIT CAMPAIGN) Abstract Only **c90**
I. M. Tsyupak *In its* JPRS Report: Science and Technology. USSR: Space 26 Feb. 1988 p 23 Transl.into ENGLISH from Izvestiya Vysshikh Uchebnykh Zavedeniy: Geodeziya i Aerofotosyemka (Moscow, USSR), no. 3, May - Jun. 1987 p

75-82 (For primary document see N88-30498 24-88)
Avail: NTIS HC A04/MF A01

An additional contribution is made to determine the parameters of the earth's rotation by laser determinations of the LAGEOS artificial earth satellite as observed during the main campaign of the MERIT program. Ways to solve the many problems involved were outlined in the MERIT standards. However, the traditional algorithm to determine the parameters of the earth's rotation do not take into account the erroneousness or neglecting of parameters of the earth's rotation arising in the numerical integration of the equations of motion of a satellite, although this influence may be significant when making highly precise observations. This article gives the results of a series of determinations of parameters of the earth's rotation obtained during the period 1 September 1983 to 31 October 1984 using a new algorithm which takes this influence into account. A table gives the parameters of the earth's rotation for 89 arcs. Four solutions were obtained by the processing of 49,506 normal points of laser observations distributed in a 14-month interval. An improved method is proposed for more precise determination of sidereal time on the basis of laser observations of artificial earth satellites. Author

N88-30529# Joint Publications Research Service, Arlington, Va.
OBLIGUE METALLOGENIC ZONES RECOGNIZED BY INTERPRETING SPACE PHOTOGRAPHS OF SOUTHERN TIEN SHAN Abstract Only **c89**
N. T. Kochneva, G. A. Tananayeva, and R. A. Belov *In its* JPRS Report: Science and Technology. USSR: Space 26 Feb. 1988 p 23-24 Transl. into ENGLISH from Issledovaniye Zemli iz Kosmosa (Moscow, USSR), no. 4, Jul. - Aug. 1987 p 41-46 Original language document was announced in IAA as A88-19565 (For primary document see N88-30498 24-88)
Avail: NTIS HC A04/MF A01

A new type of poorly discernible oblique metallogenic zone has been identified on satellite remote-sensing imagery. The typical features of these zones are described for different landscapes in the southern Tien-Shan territory. It is found that the oblique zones affect the location of mineral ore deposits. Author

N88-30530# Joint Publications Research Service, Arlington, Va.
STRUCTURE OF EASTERN TURKESTAN RIDGE BASED ON SPACE PHOTOGRAPHS Abstract Only **c43**
I. G. Tsukornik, A. V. Alekseyenko, A. V. Berezanskiy, and I. I. Soloshenko *In its* JPRS Report: Science and Technology. USSR: Space 26 Feb. 1988 p 24 Transl. into ENGLISH from Issledovaniye Zemli iz Kosmosa (Moscow, USSR), no. 4, Jul. - Aug. 1987 p 47-52 Original language document was announced in IAA as A88-19566 (For primary document see N88-30498 24-88)
Avail: NTIS HC A04/MF A01

Lineaments identified on space photos of the eastern Turkestan Range are considered. The observed lineament zones correspond to latitudinally oriented Paleozoic structural-formational zones in the region. Submeridional zones indicating hidden deep-seated faults with an anti-Tien Shen direction are also identified. Author

N88-30531# Joint Publications Research Service, Arlington, Va.
DETERMINING THE SPATIAL STRUCTURE OF FIELDS OF PRECIPITATION FROM SPACE RADAR IMAGES IN TWO ORTHOGONAL POLARIZATIONS Abstract Only **c43**
A. P. Pichugin, Yu. G. Spridonov, and A. B. Fetisov *In its* JPRS Report: Science and Technology. USSR: Space 26 Feb. 1988 p 24 Transl. into ENGLISH from Issledovaniye Zemli iz Kosmosa (Moscow, USSR), no. 4, Jul. - Aug. 1987 p 70-77 (For primary document see N88-30498 24-88)
Avail: NTIS HC A04/MF A01

Based on the analysis of radar images produced with a side-looking radar installed on the Cosmos-1500 spacecraft, a study is made of the effective scattering area of precipitation as a function of the characteristics of precipitation fields in the 3-cm band. Use of a dual-polarization method allows study of the 3-D structure of precipitation fields over broad areas over the ocean, determining the spatial distribution of precipitation intensity and more precise measurements of the specific effective scattering area of the ocean surface when precipitation is present. This is important in determining the natural wind velocity field and other hydrophysical parameters. Author

N88-30532# Joint Publications Research Service, Arlington, Va.
ESTIMATION OF SOIL TEMPERATURE PROFILE FROM REMOTE MICROWAVE AND IR MEASUREMENTS Abstract Only **c43**
Ye. A. Reutov and A. M. Shutko *In its* JPRS Report: Science and Technology. USSR: Space 26 Feb. 1988 p 24 Transl. into ENGLISH from Issledovaniye Zemli iz Kosmosa (Moscow, USSR), no. 4, Jul. - Aug. 1987 p 78-85 (For primary document see N88-30498 24-88)
Avail: NTIS HC A04/MF A01

A study is made of a method for estimating the soil temperature profile based on remote microwave and IR radiometric measurements. This article presents a broader interpretation of earlier results and does not assume constant moisture content with depth. All heat transfer processes in the soil are reduced to conduction, convection, radiation, and moisture transfer. The method is suitable for estimation of soil temperature down to 100 cm depth with a maximum absolute error of not over 5.0 to 5.5 C and a mean square error of 3 C. Author

N88-30533# Joint Publications Research Service, Arlington, Va.
MONTE-CARLO ESTIMATION OF THE INFLUENCE OF PLANT ARCHITECTURE PARAMETERS ON SPECTRAL BRIGHTNESS Abstract Only **c43**
Yu. K. Ross and A. L. Marshak *In its* JPRS Report: Science and Technology. USSR: Space 26 Feb. 1988 p 24-25 Transl. into ENGLISH from Issledovaniye Zemli iz Kosmosa (Moscow, USSR), no. 4, Jul. - Aug. 1987 p 86-93 (For primary document see N88-30498 24-88)
Avail: NTIS HC A04/MF A01

A previous work stated the problem of calculating the reflection of radiation from a soil-plant system, constructed and demonstrated an algorithm based on the Monte Carlo method and described a plant cover model. This article turns primary attention to the study of the influence of the plant canopy architecture on the index of reflection. Factors analyzed include canopy height, distance between leaves, leaf size, canopy structure, leaf shape, genetic spiral angle of rotation and stems. The architecture is found to influence the index of reflection primarily in the area of reverse shine in the direction opposite to the direction of the incident sunlight and in the area around the nadir. Increasing the diameter of a circular leaf or decreasing the height of the canopy increases the spectral brightness coefficient. Increasing ellipticity of leaf shape decreases brightness. Near the nadir, the index of reflection depends on the contrast of spectral brightness between leaves and soil and the genetic spiral rotation angle. Increasing the fraction of vertical stems causes an increase in asymmetry of spectral brightness relative to the nadir direction. Author

N88-30534# Joint Publications Research Service, Arlington, Va.
KOSPAS-SARSAT SATELLITES USED FOR OCEAN CURRENT STUDY Abstract Only **c48**
Yu. Kolesnikov *In its* JPRS Report: Science and Technology. USSR: Space 26 Feb. 1988 p 26 Transl. into ENGLISH from Sotsialisticheskaya Industriya (Moscow, USSR), 2 Dec. 1987 p 4 (For primary document see N88-30498 24-88)
Avail: NTIS HC A04/MF A01

KOSPAS-SARSAT satellites receive distress signals from special buoys. Scientists of the Ukrainian Academy of Sciences' Marine Hydrophysics Instsiute and the Lvov Polytechnical Institute thought: why not use these satellites to study ocean currents? They developed methods and equipment for a suitable experiment, which was conducted in the tropical zone of the Atlantic Ocean near the coasts of Surinam, Guyana and Brazil. The space rescue system ensured communication with the oceanologists' buoys for as many as five to seven times a day. Whenever one of the satellites passed over these drifting radio transmitters, it registered

its position. The spacecraft recorded this information in its memory and transmitted it to earth while flying over receiving stations. The information was then relayed to the laboratories of the oceanologists. Another advantage of the new method is that long searches for buoys after storm and fog will no longer be necessary. The equipment can be set adrift by practically any vessel whose route passes through a starting point designated by the scientists. Author

N88-30535# European Southern Observatory, Garching (West Germany).
[ACTIVITIES REPORT IN ASTRONOMY] Annual Report, 1987
L. Woltjer Apr. 1988 97 p In ENGLISH; FRENCH; and GERMAN Original contains color illustrations
(ISSN-0531-4496; ETN-88-93114) Avail: NTIS HC A05/MF A01

The 16 m Very Large Telescope project was approved including four 8m telescopes with thin (15 to 20 cm) meniscus shaped mirrors supported by 300 motorized supports and controlled by a computer on the basis of continuous monitoring of the image quality. The 15m Swedish ESO Submillimeter Telescope was completed, tested, and observed. The 3.5 m New Technology Telescope was assembled and tested. The IR photometers and the wobbing secondary were installed at the 2.2 m telescope. The appearance of the supernova in the Large Magellanic Cloud (SN 1987A) led to a large change in observing programs. In sky survey, plates were taken for all 606 fields of the ESO-R survey. ESA

N88-30536*# Lunar and Planetary Inst., Houston, Tex.
WORKSHOP ON THE ORIGINS OF SOLAR SYSTEMS
Joseph A. Nuth, ed. and Paul Sylvester, ed. 1988 107 p Workshop held in Queenstown, Md., 15-18 Dec. 1986 and 14-17 Dec. 1987
(Contract NASw-4066)
(NASA-CR-183025; NAS 1.26:183025; LPI-TR-88-04) Avail: NTIS HC A06/MF A01 CSCL 03B

Topics addressed include: interstellar chemistry and primitive bodies; astronomical measurements and nebula models; solar nebula models and meteorite; and planetary accumulation and evolution. For individual titles, see N88-30537 through N88-30544.

N88-30537*# National Aeronautics and Space Administration. Ames Research Center, Moffett Field, Calif.
STAR FORMATION AND MOLECULAR CLOUDS **c90**
A. G. G. M. Tielens *In* Lunar and Planetary Inst., Workshop on the Origins of Solar Systems 1988 p 5-21 Prepared in cooperation with California Univ., Berkeley (For primary document see N88-30536 24-88)
Avail: NTIS HC A06/MF A01 CSCL 03B

Several differnt stages can be discerned within the star formation process. Star formation can be considered to start when a molecular cloud fragments into many clumps. Many different physical processes are likely to play an important role in star formation, including self-gravity, magnetic fields, rotation, winds, and radiation transport. The current knowledge on some of these processes are reviewed. Author

N88-30538*# California Univ., Berkeley. Radio Astronomy Lab.
OBSERVATIONS OF STAR FORMATION **c89**
William J. Welch *In* Lunar and Planetary Inst., Workshop on the Origins of Solar Systems 1988 p 23-29 (For primary document see N88-30536 24-88)
Avail: NTIS HC A06/MF A01 CSCL 03A

The present observational status of objects that have some bearing on star formation are reviewed: giant molecular clouds, cloud cores and T-Tauri stars, outflows, infall, disks, and interstellar chemistry. Prospects for the future are summarized. Author

N88-30539*# Planetary Science Inst., Pasadena, Calif.
COMPARISONS OF SOLAR NEBULA MODELS **c90**
S. J. Weidenschilling *In* Lunar and Planetary Inst., Workshop on the Origins of Solar Systems 1988 p 31-37 (For primary document see N88-30536 24-88)
Avail: NTIS HC A06/MF A01 CSCL 03B

The relationship between meteorites and solar nebulae is examined. Turbulent models of the solar nebulae are compared and discussed. B.G.

N88-30540*# Harvard Univ., Cambridge, Mass. Center for Astrophysics.
PHYSICAL PROCESSES AND TIMESCALES IN PLANET AND SMALL-BODY ACCRETION **c91**
John A. Wood *In* Lunar and Planetary Inst., Workshop on the Origins of Solar Systems 1988 p 39-43 (For primary document see N88-30536 24-88)
Avail: NTIS HC A06/MF A01 CSCL 03B

A series of processes in the solar nebula transforms infallen interstellar grains into planets. Somewhat surprisingly, samples of planetary material from the very first stages of this processing and aggregration were preserved, and are accessible for study in the terrestrial laboratory. These are the chondritic meteoroids, which passed the last 4.5 Gyr safely stored in asteroids. Thermal processing of interstellar grains, sticky agglomeration of chondrules, Goldreich-Ward instability, and gravitational accretion of planetesimals into planets are discussed. B.G.

N88-30541*# California Univ., Los Angeles. Inst. of Geophysics and Planetary Physics.
NEBULAR PROCESSES RECORDED IN CHONDRITIC METEORITES **c90**
John T. Wasson *In* Lunar and Planetary Inst., Workshop on the Origins of Solar Systems 1988 p 45-49 (For primary document see N88-30536 24-88)
Avail: NTIS HC A06/MF A01 CSCL 03B

The key fact concerning the chondritic meteorites is that they consist of grains that were present in the solar nebulae. The most primitive (least altered) of them have preserved in their chemical compositions and in their structures evidence concerning processes that occurred in the nebulae 4.5 Ga ago. The chondrites that were not metamorphosed, however, preserve much information about the earliest history of the nebula and are worthy of intense, long-term study. By studying them we can attempt to infer the times and places at which the various chondrite group formed and the conditions present at each of these places. Author

N88-30542*# Massachusetts Inst. of Tech., Cambridge. Dept. of Earth, Atmospheric and Planetary Sciences.
COSMOCHEMICAL TRENDS OF VOLATILE ELEMENTS IN THE SOLAR SYSTEM **c90**
Bruce Fegley, Jr. *In* Lunar and Planetary Inst., Workshop on the Origins of Solar Systems 1988 p 51-59 (For primary document see N88-30536 24-88)
(Grants NAGw-821; NAG9-108)
Avail: NTIS HC A06/MF A01 CSCL 03B

Chemical interactions between gases and grains in the solar nebula played a central role in establishing the presently observed volatile element inventories of the planets, their satellites, and the other bodies in the solar system. Kinetic constraints relevant to gas-grain chemical interactions in the solar nebula are reviewed. The abundant, chemically active volatiles H, O, C, N, and S are emphasized; however, less abundant volatiles such as P, Cl, and F are discussed where appropriate. B.G.

N88-30543*# Carnegie Institution of Washington, D. C. Dept. of Terrestrial Magnetism.
TERRESTRIAL VERSUS GIANT PLANET FORMATION **c91**
Alan P. Boss *In* Lunar and Planetary Inst., Workshop on the Origins of Solar Systems 1988 p 61-68 (For primary document see N88-30536 24-88)
(Grant NAGw-398)
Avail: NTIS HC A06/MF A01 CSCL 03B

Given a solar nebular surrounding the early protosun, containing dust grains that have already undergone growth through collisions to about centimeter-size, the question of the formation of the

terrestrial and giant planets is considered. In contrast to the usual approach of emphasizing how well a problem is understood, the uncertainties and areas where more work needs to be done will be accentuated. Also, the emphasis will be on the dynamics of planetary formation, because profound problems still exist in this area, and because it seems most logical to concentrate first on the dynamical questions involved with assembling the planets before putting too much effort into the detailed chemical and geological consequences of certain formation mechanisms.
Author

N88-30544*# National Aeronautics and Space Administration. Langley Research Center, Hampton, Va.
THE ATMOSPHERES OF THE EARTH AND THE OTHER PLANETS: ORIGIN, EVOLUTION AND COMPOSITION c91
Joel S. Levine *In* Lunar and Planetary Inst., Workshop on the Origins of Solar Systems 1988 p 69-79 (For primary document see N88-30536 24-88)
Avail: NTIS HC A06/MF A01 CSCL 03B

The current understanding of the composition, chemistry, and structure of the atmospheres of the other planets and the origin, early history, and evolution of the earth's atmosphere is reviewed. The information on the atmospheres of the other planets is based on the successful Mariner, Viking, Pioneer, and Voyager missions to these planets. The information on the origin, early history, and evolution of the atmosphere, which is somewhat speculative, is largely based on numerical studies with geochemical and photochemical models.
Author

89 ASTRONOMY

Includes radio, gamma-ray, and infrared astronomy, and astrometry.

N88-30545*# National Aeronautics and Space Administration. Goddard Space Flight Center, Greenbelt, Md.
FAR INFRARED SUPPLEMENT: CATALOG OF INFRARED OBSERVATIONS, SECOND EDITION
Daniel Y. Gezari, Marion Schmitz (Computer Sciences Corp., Beltsville, Md.), and Jaylee M. Mead Aug. 1988 233 p
(NASA-RP-1205; Rept-88B-121; NAS 1.61:1205) Avail: NTIS HC A11/MF A01 CSCL 03A

The Far Infrared Supplement: Catalog of Infrared Observations summarizes all infrared astronomical observations at far infrared wavelengths (5 to 1000 microns) published in the scientific literature from 1965 through 1986. The Supplement list contain 25 percent of the observations in the full Catalog of Infrared Observations (CIO), and essentially eliminates most visible stars from the listings. The Supplement is thus more compact than the main catalog, and is intended for easy reference during astronomical observations. The Far Infrared Supplement (2nd Edition) includes the Index of Infrared Source Positions and the Bibliography of Infrared Astronomy for the subset of far infrared observations listed.
Author

N88-30546# Geneva Observatory (Switzerland).
A NEW DETERMINATION OF THE GENEVA PHOTOMETRIC PASSBANDS AND THEIR ABSOLUTE CALIBRATION
F. Rufener and B. Nicolet 1988 26 p Submitted for publication
(Ser-C-Prepubl-Fasc-26; ETN-88-93068) Avail: NTIS HC A03/MF A01

The consensus regarding the absolute calibrations of the spectra of alpha Lyr and subdwarfs provoked a revision of the calibration of the Geneva photometric system passbands. The alterations made to the earlier version by Rufener and Maeder (1971) are smaller than plus or minus -5 percent. The new response functions are presented in tabular form for an equiphotonic flux. An absolute spectrophotometric adjustment allows to obtain for each entry of the Geneva catalog (28,000 stars) a corresponding spectrophotometric description in SI units. The definition and the means of computing the necessary quasi-isophotal frequencies or wavelengths are given. The coherence of the Geneva catalog with several sets of absolute spectrophotometric data is examined. A correction for the entire Gunn and Stryker (1983) catalog is proposed.
ESA

N88-30547*# Space Telescope Science Inst., Baltimore, Md.
THE GUIDE STAR CATALOG
Barry M. Lasker, Helmut Jenkner, and Jane L. Russell Jul. 1987 15 p Sponsored by NASA
(Grant NAG8-697)
(NASA-CR-183253; NAS 1.26:183253; PPS-187) Avail: NTIS HC A03/MF A01 CSCL 03A

Part 1 of the catalog presents an astronomical overview of the Guide Star Catalog, together with its history, the properties of its current implementation, and the prospects for enhancement. Part 2 presents the algorithms used in photometric and astrometric calibration of the catalog, as well as the analyses of the related errors. Part 3 presents the current structure and content, as well as future enhancements in this area. An overview of the forthcoming publications is given, both with regard to scientific papers and electronic media.
Author

N88-30548# Stuttgart Univ. (West Germany).
STUDY OF MODERN INSTRUMENTATION AND METHODS FOR ASTRONOMIC POSITIONING IN THE FIELD Technical Report No. 2
Mar. 1988 17 p
(Contract DAJA45-84-C-0043)
(AD-A196173; R/D-4618-EN-01) Avail: NTIS HC A03/MF A01 CSCL 03A

The First Technical Report contained a detailed simulation study about the possible accuracy of astronomic positioning in the field. The simulation study was based on the assumption that the objects of field observations, the stars, are perfectly known, including also the various astronomic reductions such as proper motion, aberration, parallax etc. Here one allows for some uncertainty of the star position: a detailed analysis of how to proceed is presented once only dispersive prior information about star positions is available. The nonlinear condition equations are linearized by a two-step Taylor series expansion accounting for stochastic information alpha, delta of right ascension and declination, the parameters of star positions. A numerical analysis will be presented in the Final Report.
GRA

N88-30549*# Space Telescope Science Inst., Baltimore, Md.
STARBURSTS AND THEIR DYNAMICS
Colin Norman Aug. 1987 10 p Sponsored by NASA
(NASA-CR-180227; NAS 1.26:180227; PPS-190) Avail: NTIS HC A02/MF A01 CSCL 03A

Detailed mechanisms associated with dynamical process occurring in starburst galaxies are considered including the role of bars, waves, mergers, sinking satellites, self gravitating gas and bulge heating. The current understanding of starburst galaxies both observational and theoretical is placed in the context of theories of galaxy formations, Hubble sequence evolution, starbursts and activity, and the nature of quasar absorption lines.
Author

N88-30550*# Space Telescope Science Inst., Baltimore, Md.
EVOLUTIONARY HELIUM AND CNO ANOMALIES IN THE ATMOSPHERES AND WINDS OF MASSIVE HOT STARS
Nolan R. Walborn Sep. 1987 13 p Sponsored by NASA
(Grant NAG8-697)
(NASA-CR-183254; NAS 1.26:183254; PPS-202) Avail: NTIS HC A03/MF A01 CSCL 03A

The ubiquitous evidence for processed materials in the atmospheres, winds, and circumstellar ejecta of massive stars is reviewed. A broad array of normal and peculiar evolutionary stages is considered, up to and including Type II supernova progenitors. The quantitative analysis of these spectra is difficult, and until recently for the most part only qualitative or approximate results have been available. However, several important current programs promise reliable abundance calculations. A significant emerging result is that the morphologically normal majority of both hot and

cold supergiants may already display an admixture of CNO-cycle products in their atmospheres. It may become possible in this way to identify blue supergiants returning from the red supergiant region, as appears to have been the case for the SN 1987A progenitor. Author

N88-30551# Instituto de Pesquisas Espaciais, Sao Jose dos Campos (Brazil). Dept. of Astrophysics.
A CODED MASK TELESCOPE FOR OBSERVATIONS OF X AND GAMMA RAY SOURCES IN THE SOUTHERN SKY
T. Villela, U. B. Jayanthi, J. A. C. F. Neri, J. Braga, C. A. W. Souza, and N. FigueredoFilho Jun. 1988 7 p Presented at the 6th Simposio Nipo-Brasileiro de Ciencia e Tecnologia, Sao Jose dos Campos, Brazil
(INPE-4580-PRE/1314) Avail: NTIS HC A02/MF A01

An X- and gamma-ray telescope employing a coded aperture imaging technique is being developed to observe southern sky sources in the energy range of 40 KeV to 8 MeV with an angular resolution of approximately 20 arc min. The payload to be flown at 40 km altitude on board a stratospheric balloon will utilize a stabilized platform. The technical and scientific aspects of the experiment are discussed. Author

N88-30552# Contraves Corp., Zurich (Switzerland). Space Dept.
FAR INFRARED SPECTROSCOPY TELESCOPE (FIRST) INFLATABLE THERMAL SHIELD, PHASE 1 Final Report
S. Kose Paris, France ESA Jun. 1987 197 p
(Contract ESA-6324/85-NL-PB(SC))
(SR/FIS/108(87)CZ; ESA-CR(P)-2568; ETN-88-93017) Copyright
Avail: NTIS HC A09/MF A01

Inflatable space rigidized structures (ISRS) were assessed for the FIRST satellite thermal shield. The baseline shield configuration, the so called obliquely cut cylindrical shield configuration, has a diameter of 10 m, a maximum height of 10 m, and a cut angle of 30 deg. This shield consists of an ISRS skeleton of tubes of diameter 0.45 m carrying the thermal control layers. The stringent requirements on the thermal control can be met by a 6-layer multilayer insulation, consisting of 2 layers of SAK (1 Mil) and 4-layers of DAM (0.25 Mil). Using the BF3 catalyst, the ISRS structure can be cured in 3 preselected positions with respect to Sun within 9 hr. Curing without catalyst is also possible, but in this case a 90 deg tilt of the satellite and longer cure times (24 hr) must be faced. The first eigenfrequency of the baseline thermal shield in deployed configuration is 2.15 Hz, thus the stiffness requirement is fulfilled. The thermal shield can survive the thermal stresses introduced during the worst operational case. The total mass lies comfortably within the specified limit of 220 kg. The shield can be well stowed in the allowable volume of the Ariane 4 shroud. ESA

N88-30553# Texas Univ., Austin.
THE ULTRASHORT PERIOD DWARF NOVA SW URSAE MAJORIS
A. W. Shafter, J. A. Hill, E. L. Robinson, P. Szkody, J. R. Thorstensen (Dartmouth Coll., Hanover, N.H.), and M. A. Wood [1988] 2 p
Avail: NTIS HC A02/MF A01

SW UMa is an unusual dwarf nova in several respects. Recent observations by Robinson et al. have established that SW UMa is a SU UMa system, while Shafter, Szkody, and Thorstensen have presented evidence suggesting that SW UMa may be a DQ Her system as well. If the DQ Her classification is confirmed, then SW UMa will be the only system to have this dual classification. Finally, time resolved spectroscopy of SW UMa has revealed the presence of an S wave component in the H-alpha emission which has an unexpected phasing relative to the line wings. Author

N88-30554*# Jet Propulsion Lab., California Inst. of Tech., Pasadena.
THE DEEP SPACE NETWORK: AN INSTRUMENT FOR RADIO ASTRONOMY RESEARCH
N. A. Renzetti, G. S. Levy, T. B. H. Kuiper, P. R. Walken, and R. C. Chandlee 1 Sep. 1988 63 p Sponsored by NASA, Washington, D.C.
(NASA-CR-183219; JPL-Publ-82-68-Rev-1; NAS 1.26:183219)
Avail: NTIS HC A04/MF A01 CSCL 03A

The NASA Deep Space Network operates and maintains the Earth-based two-way communications link for unmanned spacecraft exploring the solar system. It is NASA's policy to also make the Network's facilities available for radioastronomy observations. The Network's microwave communication systems and facilities are being continually upgraded. This revised document, first published in 1982, describes the Network's current radioastronomy capabilities and future capabilities that will be made available by the ongoing Network upgrade. The Bibliography, which includes published papers and articles resulting from radioastronomy observations conducted with Network facilities, has been updated to include papers to May 1987. Author

N88-30555*# Space Telescope Science Inst., Baltimore, Md.
OBSERVATIONS OF FAINT FIELD GALAXIES
David C. Koo Sep. 1987 9 p Sponsored by NASA
(Grant NAG8-697)
(NASA-CR-183251; NAS 1.26:183251; PPS-205) Avail: NTIS HC A02/MF A01 CSCL 03A

Number counts, colors, and angular correlations of field galaxies fainter than 20th mag are summarized. Resulting conclusions regarding the presence and nature of luminosity, spectral, and clustering evolution remain contraversial. Preliminary analysis of two major spectroscopic surveys near completion suggests that by z approximately 0.5, larger numbers of very blue galaxies of moderate luminosities are found than today. The skewer-like surveys also provide new probes of galaxy clustering on scales previously unexplored (larger than 200 Mpc) and over lookback times of several billion years. Author

N88-30556# European Space Agency, Paris (France). Space Science Dept.
ESA REPORT TO THE 27TH COSPAR MEETING
V. Domingo, U. O. Fisk, R. Grard, P. Jakobsen, M. F. Kessler, J.-P. Lebreton, R. Marsden, A. Peacock, A. Pederson, and M. A. C. Perryman et al. Jun. 1988 148 p Meeting held in Helskinki, Finland, Jul. 1988 Original contains color illustrations
(ESA-SP-1098; ISSN-0379-6566; ETN-88-93046) Copyright
Avail: NTIS HC A07/MF A01

The ISEE, IUE, EXOSAT, and Giotto missions are described. The status of the Ulysses, Hubble Space Telescope, HIPPARCOS, ISO, and solar-terrestrial science programs is discussed. The high throughput X-ray spectroscopy mission, submillimeter spectroscopy mission, and the comet nucleus sample return mission are presented. The CASSINI, GRASP, Lyman, Quasat, Vesta, and Giotto extended missions are introduced. The EURECA and Columbus space station programs are reviewed. ESA

N88-30557# European Space Agency, Paris (France).
THE HIGH-THROUGHPUT X-RAY SPECTROSCOPY MISSION: THE MISSION-SCIENCE REPORT
Bruce Battrick, ed. Mar. 1988 84 p Original contains color illustrations
(ESA-SP-1097; ISSN-0379-6566; ETN-88-93045) Copyright
Avail: NTIS HC A05/MF A01; ESA Publications Division, Noordwijk, The Netherlands 40 Dutch guilders

The high throughput X-ray spectroscopy mission (XMM) of ESA and the astrophysics problems it addresses are described. The spaceborne XMM observatory offers spatial resolution within 30 arcsec (half energy width); effective area 6000 sq cm at 2 keV and 300 sq cm at 7 keV; Broadband (0.1 to 10 keV) spectroscopy with a resolving power (FWHM) between 5 and 60; medium-resolution spectroscopy between 0.1 to 3 keV with a resolving power of over 250 at 0.5 keV; and simultaneous optical monitoring between 2000 and 6000 A to a limiting magnitude of 24.5. Topics studied include large/medium scale structure of hot matter in the Universe; accretion-powered radiation sources; supernova remnants; the interstellar medium; and stellar atmospheres. ESA

N88-30558*# Space Telescope Science Inst., Baltimore, Md.
A DEEP REDSHIFT SURVEY OF FIELD GALAXIES. COMMENTS ON THE REALITY OF THE BUTCHER-OEMLER EFFECT
David C. Koo and Richard G. Kron Sep. 1987 16 p Sponsored by NASA
(Grant NAG8-697)
(NASA-CR-183255; NAS 1.26:183255; PPS-204) Avail: NTIS HC A03/MF A01 CSCL 03A

A spectroscopic survey of over 400 field galaxies has been completed in three fields for which we have deep UBVI photographic photometry. The galaxies typically range from B=20 to 22 and possess redshifts z from 0.1 to 0.5 that are often quite spiky in distribution. Little, if any, luminosity evolution is observed up to redshifts z approx 0.5. By such redshifts, however, an unexpectedly large fraction of luminous galaxies has very blue intrinsic colors that suggest extensive star formation; in contrast, the reddest galaxies still have colors that match those of present-day ellipticals. Author

N88-30559# Instituto de Pesquisas Espaciais, Sao Jose dos Campos (Brazil).
INTERMEDIATE POLARS OBSERVED IN BRAZIL IN THE LAST EIGHT YEARS
F. J. Jablonski May 1988 10 p Presented at the Symposium Commemorative to the 25th Anniversary of the Cerro Tololo Inter-American Observatory (Chile), and at the 6th Simposio Nipo-Brasileiro de Ciencia e Tecnologia, San Jose dos Campos, Brazil
(INPE-4567-PRE/1308) Avail: NTIS HC A02/MF A01

The results of a photometric program performed at the Laboratorio Nacional de Astrofisica in Brazil, on cataclysmic varibles of the intermediate polar sub-type, along a time base that covers the last eight observational seasons. The spin stories of the compact object in four systems, namely, EX Hya, V1223 Sgr, FO Aqr, and AO Psc are presented and discussed. Author

N88-30031# International Scientific Radio Union, Brussels (Belgium).
RADIO ASTRONOMY
R. Wielebinski, ed. *In its* Review of Radio Science, 1984-1986 1987 16 p (For primary document see N88-30023 24-32)
Avail: NTIS HC A09/MF A01

N88-30504# Joint Publications Research Service, Arlington, Va.
ASTRON OBSERVATIONS OF SUPERNOVA 1987A IN LARGE MAGELLANIC CLOUD Abstract Only
A. A. Boyarchuk, R. Ye. Gershberg, A. M. Zvereva, P. P. Petrov, A. B. Severnyy, A. V. Terebizh, C. T. Hua, and A. I. Sheykhet *In its* JPRS Report: Science and Technology. USSR: Space 26 Feb. 1988 p 14 Transl. into ENGLISH from Pisma v Astronomicheskiy Zhurnal (Moscow, USSR), v. 13, no. 9, Sep. 1987 p 739-743 (For primary document see N88-30498 24-88)
Avail: NTIS HC A04/MF A01

N88-30521# Joint Publications Research Service, Arlington, Va.
BINARY STAR MEASUREMENTS USING DIGITAL SPECKLE INTERFEROMETER OF 6-m TELESCOPE Abstract Only
I. I. Balega and Yu. Yu. Balega *In its* JPRS Report: Science and Technology. USSR: Space 26 Feb. 1988 p 19-20 Transl. into ENGLISH from Pisma v Astronomicheskiy Zhurnal (Moscow, USSR), v. 13, no. 6, Jun. 1987 p 508-514 (For primary document see N88-30498 24-88)
Avail: NTIS HC A04/MF A01

N88-30529# Joint Publications Research Service, Arlington, Va.
OBLIGUE METALLOGENIC ZONES RECOGNIZED BY INTERPRETING SPACE PHOTOGRAPHS OF SOUTHERN TIEN SHAN Abstract Only
N. T. Kochneva, G. A. Tananayeva, and R. A. Belov *In its* JPRS Report: Science and Technology. USSR: Space 26 Feb. 1988 p 23-24 Transl. into ENGLISH from Issledovaniye Zemli iz Kosmosa (Moscow, USSR), no. 4, Jul. - Aug. 1987 p 41-46 Original language document was announced in IAA as A88-19565 (For primary document see N88-30498 24-88)
Avail: NTIS HC A04/MF A01

N88-30538*# California Univ., Berkeley. Radio Astronomy Lab.
OBSERVATIONS OF STAR FORMATION
William J. Welch *In* Lunar and Planetary Inst., Workshop on the Origins of Solar Systems 1988 p 23-29 (For primary document see N88-30536 24-88)
Avail: NTIS HC A06/MF A01 CSCL 03A

90 ASTROPHYSICS

Includes cosmology; celestial mechanics; space plasmas; and interstellar and interplanetary gases and dust.
For related information see also *75 Plasma Physics.*

N88-30560# Geneva Observatory (Switzerland).
THE KINEMATICS OF LATE-TYPE SUPERGIANTS
P. Dubath, M. Mayor, and G. Burki 1988 21 p Submitted for publication Sponsored in part by the Swiss National Science Foundation, Berne, Switzerland
(Ser-C-Prepubl-Fasc-28; ETN-88-93070) Avail: NTIS HC A03/MF A01

Using a radial velocity survey with the CORAVEL spectrometer, the kinematics of late spectral-type supergiants was investigated. On a distance range of 3 kpc, the best set of galactic rotation constants obtained is: A = 16 + or - 1.5 kms/sec/kpc; Uo = -9.7 + or - 1.3 km/sec; Vo = 13.0 + or - 1.1 km/sec. A review of similar work shows that the agreement for the value of A is very good, if the results are corrected for the bias introduced by the random errors on the distances. The value of A depends on the distance range considered. The local value of A is very large and decreases when the domain of investigation in the galactic plane is increased. Thus, the value of A on a very large scale can be in good agreement with a roughly flat rotation curve, but the high local value of A reveals a sharp dip on the rotation curve in the neighborhood of the Sun. Methods for determining the solar motion are reviewed: the mean motion of all stars in the solar neighborhood; extrapolation of the asymmetric drift relation; kinematical analysis applied to young subpopulations (or the gaseous component); and the imposed symmetry of south and north galactic rotation curves. For each method, the internal agreement between determinations is good. However, discrepancies from one method to another are very large. ESA

N88-30561# Geneva Observatory (Switzerland).
DUPLICITY IN THE SOLAR NEIGHBORHOOD: PART 4: SPECTROSCOPIC ORBITS FOR FOUR DWARF M STARS
A. Duquennoy and M. Mayor 1988 15 p Submitted for publication Sponsored by the Swiss National Foundation for Scientific Research, Meikirch, Switzerland
(Ser-C-Prepubl-Fasc-21; ETN-88-93063) Avail: NTIS HC A03/MF A01

Orbital elements for four dwarf M stars in the Gliese catalog were derived: Gl 319, Gl 570B, Gl 735 and Gl 815. All except Gl 319 are members of chromospherically active systems. Values of vsini were determined. Gliese 319 appears as a quadruple system and may contain the a nonactive dM binary star, with an orbital period as low as 21 days; Gl 570A is also the bright star HR 5568 whose visual secondary appears double-lined with a mass ratio of 0.71 + or - 0.02, and which could be resolved with speckle interferometry; Gl 735 is a double-lined spectroscopic binary, whose previously observed photometric variations should be reinvestigated in order to compare their periodicity with the orbital period of 10.3 d; Gl 815 is resolved into a triple-lined spectroscopic binary, which permits the determination of preliminary elements for the outer astrometric orbit with P = 29.3 yr. Two other outer systems (Gl 319 AC and Gl 570 AB) claimed to be unbound with hyperbolic orbits are found to be very likely bound. ESA

N88-30562# Geneva Observatory (Switzerland).
DUPLICITY IN THE SOLAR NEIGHBORHOOD: PART 5: SPECTROSCOPIC ORBIT FOR THE NEARBY DOUBLE-LINED SOLAR-TYPE STAR HR 8581
A. Duquennoy, M. Mayor, R. F. Griffin, W. I. Beavers, and J. J. Eitter (Iowa State Univ. of Science and Technology, Ames.) 1988 9 p Submitted for publication Sponsored in part by the Swiss National Foundation for Scientific Research, Meikirch, Switzerland
(Grants NSF AST-82-05956-A02; NSF AST-86-04324)
(Ser-C-Prepubl-Fasc-23; ETN-88-93065) Avail: NTIS HC A02/MF A01

The nearby solar-type star HR 8581 is found to be a double-lined spectroscopic binary with an orbital period of 632.5 days. The mass ratio of the two components is 0.55, with a blue magnitude difference of 2.5 mag, suggesting a model consisting of a F8V + K4V pair of stars. Speckle interferometric measurements are suggested to complete the determination of the elements and of the stellar masses. ESA

N88-30563# Academy of Sciences of the Armenian SSR, Erivan.
LAGRANGIAN OF THE SELF-DUALITY EQUATION AND d = 10, N = 2b SUPERGRAVITY
A. R. Kavalov and R. L. Mkrtchyan 1986 18 p
(DE88-701554; EFI-938(89)-86) Avail: NTIS (US Sales Only) HC A03/MF A01

An invariant (supersymmetric, Lorentz-invariant) Langrangian of a ten-dimensional chiral extended supergravity is constructed up to bilinear over the Fermi fields terms inclusively. A new element is the introduction of a Lagrangian multiplier Theta sub alpha 1 - alpha 5/beta 1 - beta 5, the variation over which yields an equation equivalent to that of the self duality of the supercovariant strength tensor of the physical field A sub nm/upsilon/lambda/rho. The field Theta sub alpha 1 - alpha 5/beta 5 - beta 5 is a gauge field of a gauge symmetry, nontrivially acting only off the mass shell, which closes the formerly open supersymmetry algebra on all the boson fields. DOE

N88-30564# Geneva Observatory (Switzerland).
RADIAL VELOCITY MEASUREMENTS OF A SAMPLE OF NORTHERN METAL-DEFICIENT STARS
G. Jasniewicz (Observatoire de Strasbourg, France) and M. Mayor 1988 27 p Submitted for publication
(Ser-C-Prepubl-Fasc-25; ETN-88-93067) Avail: NTIS HC A03/MF A01

A sample of 41 northern metal-deficient stars composed of 14 stars with Fe/H less than -1.1, 11 stars with -1.1 less than or equal to Fe/H less than -0.6 and 16 stars with -0.6 less than or equal to Fe/H less than -0.3 was observed with the radial velocity scanner CORAVEL. Seven stars were discovered as certain or possible spectroscopic binaries (SBs). The measurements are in fair agreement with those of Carney and Latham (1987), but in disagreement with those of Stryker et al (1985). Spectroscopic orbits are determined for HD 108754 (period: 26d) and HD 153847 (period: 5d). The distribution of SBs as a function of period between this sample of metal-deficient stars and a sample of metal-rich G-type stars (Fe/H greater than or equal to -0.3) is proved to be statistically similar. For high-velocity and/or metal-deficient SBs, the distribution of orbital eccentricities versus logarithm of period is discussed in terms of tidal circularization. ESA

N88-30565# Geneva Observatory (Switzerland).
THE STABILITY OF DISK GALAXIES AND CONSTRAINTS ON THEIR MASS-LUMINOSITY RATIO
L. Martinet 1988 11 p Submitted for publication
(Ser-C-Prepubl-Fasc-27; ETN-88-93069) Avail: NTIS HC A03/MF A01

The stability parameter Q behavior in disk galaxies is discussed. The influence of various factors on its radial variations is considered. A range of possible values of Q as a consequence of dynamical properties connected with the morphology of these galaxies is suggested. Applications for NGC 891, NGC 4244, and NGC 5907 are proposed. ESA

N88-30566*# California Inst. of Tech., Pasadena.
RESEARCH IN PARTICLE AND GAMMA-RAY ASTROPHYSICS Semiannual Status Report, 1 Apr. 1987 - 31 Mar. 1988
E. C. Stone, L. Davis, Jr., R. A. Mewaldt, and T. A. Prince 16 Aug. 1988 26 p
(Grant NGR-05-002-160)
(NASA-CR-183126; NAS 1.26:183126) Avail: NTIS HC A03/MF A01 CSCL 03B

Research activities in cosmic rays, gamma rays, and astrophysical plasmas are covered. Each activity is described, followed by a bibliography. The research program is directed toward the investigation of the astrophysical aspects of cosmic rays and gamma rays and of the radiation and electromagnetic field environment of the earth and other planets. These investigations were performed by means of energetic particle and photon detector systems flown on spacecraft and balloons. B.G.

N88-30567# Geneva Observatory (Switzerland).
THE DYNAMICS OF SBO GALAXIES. PART 1: THE DATA
B. J. Jarvis, P. Dubath, L. Martinet, and R. Bacon 18 Mar. 1988 20 p Submitted for publication Sponsored in part by the Swiss National Science Foundation, Berne, Switzerland
(Ser-C-Prepubl-Fasc-22; ETN-88-93064) Avail: NTIS HC A03/MF A01

Two-dimensional surface photometry in the Gunn-Thuan photometric system of 5 mostly face-on southern early type barred galaxies, NGC's 1291, 1543, 1574, 4477, and 4754 is presented. The rotation velocity and velocity dispersion profiles along the principal axes of these galaxies are shown. ESA

N88-30568# Massachusetts Inst. of Tech., Cambridge. Artificial Intelligence Lab.
NUMERICAL EVIDENCE THAT THE MOTION OF PLUTO IS CHAOTIC
Gerald J. Sussman and Jack Wisdom 27 Apr. 1988 20 p
(Contract N00014-86-K-0180)
(AD-A195920; AI-M-1039) Avail: NTIS HC A03/MF A01 CSCL 03C

The Digital Orrery has been used to perform an integration of the motion of the outer planets for 845 million years. This integration indicates that the long-term motion of the planet Pluto is chaotic. Nearby trajectories diverge exponentially with an e-folding time of only about 20 million years. GRA

N88-30569# Geneva Observatory (Switzerland).
ORBITAL STABILITY IN ROTATING TRIAXIAL STELLAR SYSTEMS
L. Martinet and T. deZeeuw (Institute for Advanced Study, Princeton, N.J.) 1988 19 p Submitted for publication Sponsored in part by the Swiss National Science Foundation, Berne, Switzerland; and RCA
(Ser-C-Prepubl-Fasc-24; ETN-88-93066) Avail: NTIS HC A03/MF A01

The stability of simple periodic orbits in rotating triaxial potentials that correspond to Ferrers' density law was analyzed. Different values of the axial ratios, and of the rotation frequency were considered. Calculations for rotating logarithmic potentials are presented. The connection of the anomalous orbits, inclined with respect to the (y, z) and (x, z) planes with the equatorial retrograde family and the z-axis family is clarified. When rotation frequency increases, the sequence of bifurcation of the latter family is modified. Beyond a critical value it becomes complex unstable, and the stable anomalous orbit no longer bifurcates from it. This behavior is expected to be general, and is confirmed in other potentials. Constraints inferred from these facts for the construction of self-gravitating equilibrium models are discussed. Apart from the z-axis family, complex instability seems to play a negligible role in the dynamics of one-component triaxial systems because it appears only on the edge of the systems. ESA

N88-30570# Instituto de Pesquisas Espaciais, Sao Jose dos Campos (Brazil).
ACTIVITIES IN ASTROPHYSICS
Hugo V. Capelato Jun. 1988 9 p Presented at the 6th Simposio Nipo-Brasileiro de Ciencia e Tecnologia, Sao Jose dos Campos, Brazil
(INPE-4582-PRE/1316) Avail: NTIS HC A02/MF A01
A brief description of the scientific activities in the field of astrophysics, which are presently being carried out at the Department of Astrophysics of INPE is given. Author

N88-30475*# Louisiana State Univ., Baton Rouge.
EXOTIC MINERALS IN 3,500 MILLION YEAR OLD ROCKS: EVIDENCE FOR LARGE METEORITE IMPACTS
G. R. Byerly, D. R. Lowe, and F. Asaro (California Univ., Berkeley.) *In* Lunar and Planetary Inst., Nineteenth Lunar and Planetary Science Conference. Press abstracts 1988 p 5-7 (For primary document see N88-30473 24-88)
Avail: NTIS HC A03/MF A01 CSCL 03B

N88-30476*# Lawrence Livermore National Lab., Calif.
NON-ATMOSPHERIC NOBLE GASES FROM CO(SUB 2) WELL GA
M. W. Caffee, G. B. Hudson, C. Velsko, E. C. Alexander, Jr., G. R. Huss, and A. R. Chivas (Australian National Univ., Canberra.) *In* Lunar and Planetary Inst., Nineteenth Lunar and Planetary Science Conference. Press abstracts 1988 p 8-9 (For primary document see N88-30473 24-88)
Avail: NTIS HC A03/MF A01 CSCL 03B

N88-30480*# Louisiana State Univ., Baton Rouge.
LSU SCIENTISTS DISCOVER EVIDENCE OF LARGE METEORITE IMPACTS ON THE EARLY EARTH
Donald R. Lowe and Gary R. Byerly *In* Lunar and Planetary Inst., Nineteenth Lunar and Planetary Science Conference. Press abstracts 1988 p 17-18 (For primary document see N88-30473 24-88)
Avail: NTIS HC A03/MF A01 CSCL 03B

N88-30482*# National Aeronautics and Space Administration. Lyndon B. Johnson Space Center, Houston, Tex.
LEWIS CLIFF 86010, A UNIQUE ANTARCTIC METEORITE: POSSIBLE NEW CLUES TO THE EARLY HISTORY OF THE SOLAR SYSTEM
G. A. McKay, G. Crozaz, M. Prinz, C. A. Goodrich, and J. S. Delaney (Rutgers Univ., New Brunswick, N. J.) *In* Lunar and Planetary Inst., Nineteenth Lunar and Planetary Science Conference. Press abstracts 1988 p 22-23 (For primary document see N88-30473 24-88)
Avail: NTIS HC A03/MF A01 CSCL 03B

N88-30483*# Chicago Univ., Ill. Dept. of Chemistry.
NOBLE GASES, C,N, AND Si ISOTOPES IN INTERSTELLAR SIC FORM THE MURCHISON CARBONACEOUS CHONDRITE
Tang Ming, Edward Anders, and Ernst Zinner (Washington Univ., St. Louis, Mo.) *In* Lunar and Planetary Inst., Nineteenth Lunar and Planeta.y Science Conference. Press abstracts 1988 p 25-27 (For primary document see N88-30473 24-88)
Avail: NTIS HC A03/MF A01 CSCL 03B

N88-30507# Joint Publications Research Service, Arlington, Va.
PLANE PERIODIC SATELLITE MOTIONS RELATIVE TO CENTER OF MASS IN NEIGHBORHOOD OF COLLINEAR LIBRATION POINT Abstract Only
N. I. Chirkina *In its* JPRS Report: Science and Technology. USSR: Space 26 Feb. 1988 p 15 Transl. into ENGLISH from Kosmicheskiye Issledovaniya (Moscow, USSR), v. 25, no. 3, May - Jun. 1987 p 356-361 (For primary document see N88-30498 24-88)
Avail: NTIS HC A04/MF A01

N88-30528# Joint Publications Research Service, Arlington, Va.
DETERMINING EARTH'S ROTATION FROM LASER OBSERVATIONS OF LAGEOS ARTIFICIAL EARTH SATELLITE (DURING PERIOD OF MAIN MERIT CAMPAIGN) Abstract Only
I. M. Tsyupak *In its* JPRS Report: Science and Technology. USSR: Space 26 Feb. 1988 p 23 Transl.into ENGLISH from Izvestiya Vysshikh Uchebnykh Zavedeniy: Geodeziya i Aerofotosyemka (Moscow, USSR), no. 3, May - Jun. 1987 p 75-82 (For primary document see N88-30498 24-88)
Avail: NTIS HC A04/MF A01

N88-30537*# National Aeronautics and Space Administration. Ames Research Center, Moffett Field, Calif.
STAR FORMATION AND MOLECULAR CLOUDS
A. G. G. M. Tielens *In* Lunar and Planetary Inst., Workshop on the Origins of Solar Systems 1988 p 5-21 Prepared in cooperation with California Univ., Berkeley (For primary document see N88-30536 24-88)
Avail: NTIS HC A06/MF A01 CSCL 03B

N88-30539*# Planetary Science Inst., Pasadena, Calif.
COMPARISONS OF SOLAR NEBULA MODELS
S. J. Weidenschilling *In* Lunar and Planetary Inst., Workshop on the Origins of Solar Systems 1988 p 31-37 (For primary document see N88-30536 24-88)
Avail: NTIS HC A06/MF A01 CSCL 03B

N88-30541*# California Univ., Los Angeles. Inst. of Geophysics and Planetary Physics.
NEBULAR PROCESSES RECORDED IN CHONDRITIC METEORITES
John T. Wasson *In* Lunar and Planetary Inst., Workshop on the Origins of Solar Systems 1988 p 45-49 (For primary document see N88-30536 24-88)
Avail: NTIS HC A06/MF A01 CSCL 03B

N88-30542*# Massachusetts Inst. of Tech., Cambridge. Dept. of Earth, Atmospheric and Planetary Sciences.
COSMOCHEMICAL TRENDS OF VOLATILE ELEMENTS IN THE SOLAR SYSTEM
Bruce Fegley, Jr. *In* Lunar and Planetary Inst., Workshop on the Origins of Solar Systems 1988 p 51-59 (For primary document see N88-30536 24-88)
(Grants NAGw-821; NAG9-108)
Avail: NTIS HC A06/MF A01 CSCL 03B

91 LUNAR AND PLANETARY EXPLORATION

Includes planetology; and manned and unmanned flights.
For spacecraft design or space stations see *18 Spacecraft Design, Testing and Performance.*

N88-30571*# Colorado Univ., Boulder. Lab. for Atmospheric and Space Physics.
VOLATILES ON MARS Semiannual Report
Bruce M. Jakosky 9 Aug. 1988 10 p
(Grant NAGw-552)
(NASA-CR-183113; NAS 1.26:183113) Avail: NTIS HC A02/MF A01 CSCL 03B
The long-term evolution of both the atmosphere and the surface of Mars can be understood by examining the history of volatiles in the Mars atmosphere, their non-atmospheric reservoirs, and the processes of exchange between the two. Clearly, the present state of both the surface and the atmosphere can only be seen, so that any inferences about the evolution of the climate system are just that, inferences. The processes which control the atmosphere and surface on a seasonal basis, however, are the same processes which can act on longer timescales; only the specific solar and atmospheric forcing will differ. Once the ability of each process to affect the seasonal behavior is understood, the long-timescale forcing may be applied to the various processes

in order to clearly identify the ability of the processes to act over the entire history of Mars. The areas of surface-atmospheric interaction of Mars are addressed in the ongoing research. The climate system on Mars is controlled by processes involving the exchange between the surface and atmosphere, so it is important to understand the current behavior of those processes. This is especially so in light of the current interest in understanding Mars; the upcoming Mars Observer mission, and the potential for a future sample-return or human-exploration mission will focus emphasis on this area of Mars science. Author

N88-30572*# Atmospheric and Environmental Research, Inc., Cambridge, Mass.
EXTENDED ATMOSPHERES OF OUTER PLANET SATELLITES AND COMETS Final Report, 1 Aug. 1984 - 31 Aug. 1988
William H. Smyth and Michael R. Combi Aug. 1988 28 p (Contract NASw-3966)
(NASA-CR-183157; NAS 1.26:183157) Avail: NTIS HC A03/MF A01 CSCL 03B

In the third year of this 3-year project, research accomplishments are discussed and related to the overall objective. In the area of the distribution of hydrogen in the Saturn system, new Voyager UVS data have been discovered and are discussed. The data suggest that both Titan's hydrogen torus and Saturn's hydrogen corona play a major role in the circumplanetary gas source. Modeling analysis of this new data establishes a strong basis for continuing studies to be undertaken in a new NASA-sponsored project. In the area of the cometary atmospheres, observational data for H, O, C, and OH acquired with the Pioneer Venus Orbiter are evaluated and preliminary modeling analysis for some of the hydrogen Lyman-alpha data is presented. In addition, the importance of collisional thermalization in spatial properties and structure of the inner and extended comae of comets has been demonstrated using the recently developed particle trajectory model. The successful simulation by this model of the hydrogen Lyman-alpha image for Comet Kohoutec near perihelion, an extreme case for collisional thermalization, is particularly noteworthy. Author

N88-30573*# National Aeronautics and Space Administration. Lyndon B. Johnson Space Center, Houston, Tex.
ANTARCTIC METEORITE NEWSLETTER, VOLUME 11, NUMBER 2, AUGUST 1988
Aug. 1988 38 p
(NASA-TM-89801; NAS 1.15:89801) Avail: NTIS HC A03/MF A01 CSCL 03B

Presented are classifications and descriptions of a large number of meteorites which include the last samples from the 1984 collection and the first samples from the 1987 collection. There is a particularly good selection of meteorites of special petrologic type in the 1987 collection. The achondrites include aubrites, ureilites, howardites, eucrites, and a diogenite. The howardites are particularly notable because of their size and previous scarcity in the Antarctic collection. Noteworthy among the 7 irons and 3 mesosiderities are 2 anamolous irons and 2 large mesosiderites. The carbonaceous chondrites include good suites of C2 and C4 meteorites, and 2 highly equilibrated carbonaceous chondrites tentatively identified as C5 and C6 meteorites. Also included are surveys of numerous meteorites for Al-26 and thermoluminescence. These studies provide information on the thermal and radiation histories of the meteorites and can be used as measures of their terrestrial ages. Author

N88-30237*# National Aeronautics and Space Administration. Lyndon B. Johnson Space Center, Houston, Tex.
THE COMPLEXITY, DEPTH, AND RAPIDITY OF PROCESSES THAT FORMED THE LUNAR CRUST
Graham Ryder (Lunar and Planetary Inst., Houston, Tex.) and Julius Dasch *In* Lunar and Planetary Inst., Workshop on the Growth of Continental Crust 1988 p 122-124 Prepared in cooperation with Oregon State Univ., Corvallis (For primary document see N88-30201 24-46)
Avail: NTIS HC A08/MF A01 CSCL 03B

N88-30474*# Harvard-Smithsonian Center for Astrophysics, Cambridge, Mass.
THE ORIGIN OF THE MOON: FURTHER STUDIES OF THE GIANT IMPACT
W. Benz, A. G. W. Cameron, and H. J. Melosh (Arizona Univ., Tucson.) *In* Lunar and Planetary Inst., Nineteenth Lunar and Planetary Science Conference. Press abstracts 1988 p 1-4 (For primary document see N88-30473 24-88)
Avail: NTIS HC A03/MF A01 CSCL 03B

N88-30477*# Chicago Univ., Ill.
UREILITES ARE NOT IGNEOUS DIFFERENTIATES
Robert N. Clayton and Toshiko K. Mayeda *In* Lunar and Planetary Inst., Nineteenth Lunar and Planetary Science Conference. Press abstracts 1988 p 10-11 (For primary document see N88-30473 24-88)
Avail: NTIS HC A03/MF A01 CSCL 03B

N88-30478*# Geological Survey, Reston, Va.
NEW TYPE OF PRIMITIVE METEORITE FOUND IN ANTARCITCA
J. N. Grossman, A. E. Rubin, G. J. MacPherson, E. R. D. Scott, M. K. Weisberg, M. Prinz, and C. E. Nehru (American Museum of Natural History, New York, N.Y.) *In* Lunar and Planetary Inst., Nineteenth Lunar and Planetary Science Conference. Press abstracts 1988 p 12-13 (For primary document see N88-30473 24-88)
Avail: NTIS HC A03/MF A01 CSCL 03B

N88-30479*# California Inst. of Tech., Pasadena. Div. of Geology and Planetary Science.
EVIDENCE OF THE IN SITU DECAY OF Al-26 IN A SEMARKONA CHONDRULE
I. D. Hutcheon, R. Hutchison, and G. J. Wasserburg *In* Lunar and Planetary Inst., Nineteenth Lunar and Planetary Science Conference. Press abstracts 1988 p 14-16 (For primary document see N88-30473 24-88)
Avail: NTIS HC A03/MF A01 CSCL 03B

N88-30481*# Carnegie Institution of Washington, D. C. Geophysical Lab.
CRYSTAL STRUCTURE AND DENSITY OF HELIUM TO 232 kbar
H. K. Mao, Y. Wu, A. P. Jephcoat, R. J. Hemley, P. M. Bell, and W. A. Bassett (Cornell Univ., Ithaca, N.Y.) *In* Lunar and Planetary Inst., Nineteenth Lunar and Planetary Science Conference. Press abstracts 1988 p 19-21 (For primary document see N88-30473 24-88)
Avail: NTIS HC A03/MF A01 CSCL 03B

N88-30485*# Geological Survey, Flagstaff, Ariz.
DEBRIS FLOWS OF THE SIMUD-TIU OUTFLOW SYSTEM OF MARS
Kenneth L. Tanaka *In* Lunar and Planetary Inst., Nineteenth Lunar and Planetary Science Conference. Press abstracts 1988 p 31-33 (For primary document see N88-30473 24-88)
Avail: NTIS HC A03/MF A01 CSCL 03B

N88-30489*# Geological Survey, Flagstaff, Ariz.
FAULTING AND ITS RELATION TO VOLCANISM: MARS WESTERN EQUATORIAL REGION
David H. Scott and James Dohm *In* Lunar and Planetary Inst., NASA MEVTV Program Working Group Meeting: Volcanism on Mars 1988 p 5-7 (For primary document see N88-30487 24-88)
Avail: NTIS HC A03/MF A01 CSCL 03B

N88-30491*# Geological Survey, Flagstaff, Ariz.
MARS: VOLCANISM IN THE VALLES MARINERIS OVERLOOKED
B. K. Lucchitta *In* Lunar and Planetary Inst., NASA MEVTV Program Working Group Meeting: Volcanism on Mars 1988 p 13-14 (For primary document see N88-30487 24-88)
Avail: NTIS HC A03/MF A01 CSCL 03B

N88-30492*# Arizona State Univ., Tempe. Dept. of Geology.
THE MARTIAN HIGHLAND PATERAE: EVIDENCE FOR EXPLOSIVE VOLCANISM ON MARS
David A. Crown and Ronald Greeley *In* Lunar and Planetary Inst., NASA MEVTV Program Working Group Meeting: Volcanism on Mars 1988 p 15-17 (For primary document see N88-30487 24-88)
Avail: NTIS HC A03/MF A01 CSCL 03B

N88-30493*# Smithsonian Institution, Washington, D. C. Center for Earth and Planetary Studies.
PHYSICAL PROPERTIES OF SURFACE MATERIALS ON MARTIAN VOLCANOES: DUST-COVERED LAVA AND ASH
James R. Zimbelman *In* Lunar and Planetary Inst., NASA MEVTV Program Working Group Meeting: Volcanism on Mars 1988 p 19-21 (For primary document see N88-30487 24-88)
Avail: NTIS HC A03/MF A01 CSCL 03B

N88-30495*# Jet Propulsion Lab., California Inst. of Tech., Pasadena.
SIMULATIONS OF LAVA FLOWS ON MARS
S. Baloga and J. Crisp *In* Lunar and Planetary Inst., NASA MEVTV Program Working Group Meeting: Volcanism on Mars 1988 p 27-29 (For primary document see N88-30487 24-88)
Avail: NTIS HC A03/MF A01 CSCL 03B

N88-30497*# Jet Propulsion Lab., California Inst. of Tech., Pasadena.
VOLCANIC STYLES AT ALBA PATERA, MARS: IMPLICATIONS OF LAVA FLOW MORPHOLOGY TO THE VOLCANIC HISTORY
D. M. Schneeberger and D. C. Pieri *In* Lunar and Planetary Inst., NASA MEVTV Program Working Group Meeting: Volcanism on Mars 1988 p 33-35 (For primary document see N88-30487 24-88)
Avail: NTIS HC A03/MF A01 CSCL 03B

N88-30522# Joint Publications Research Service, Arlington, Va.
MICROPHYSICAL PROCESSES IN CLOUD LAYERS OF VENUS Abstract Only
D. V. Titov *In its* JPRS Report: Science and Technology. USSR: Space 26 Feb. 1988 p 21 Transl. into ENGLISH from Kosmicheskiye Issledovaniya (Moscow, USSR), v. 25, no. 3, May - Jun. 1987 p 448-455 Original language document was announced in IAA as A87-47563 (For primary document see N88-30498 24-88)
Avail: NTIS HC A04/MF A01

N88-30523# Joint Publications Research Service, Arlington, Va.
STABILITY OF VENUSIAN IONOPAUSE Abstract Only
A. M. Krymskiy *In its* JPRS Report: Science and Technology. USSR: Space 26 Feb. 1988 p 21 Transl. into ENGLISH from Kosmicheskiye Issledovaniya (Moscow, USSR), v. 25, no. 3, May - Jun. 1987 p 456-463 (For primary document see N88-30498 24-88)
Avail: NTIS HC A04/MF A01

N88-30540*# Harvard Univ., Cambridge, Mass. Center for Astrophysics.
PHYSICAL PROCESSES AND TIMESCALES IN PLANET AND SMALL-BODY ACCRETION
John A. Wood *In* Lunar and Planetary Inst., Workshop on the Origins of Solar Systems 1988 p 39-43 (For primary document see N88-30536 24-88)
Avail: NTIS HC A06/MF A01 CSCL 03B

N88-30543*# Carnegie Institution of Washington, D. C. Dept. of Terrestrial Magnetism.
TERRESTRIAL VERSUS GIANT PLANET FORMATION
Alan P. Boss *In* Lunar and Planetary Inst., Workshop on the Origins of Solar Systems 1988 p 61-68 (For primary document see N88-30536 24-88)
(Grant NAGw-398)
Avail: NTIS HC A06/MF A01 CSCL 03B

N88-30544*# National Aeronautics and Space Administration. Langley Research Center, Hampton, Va.
THE ATMOSPHERES OF THE EARTH AND THE OTHER PLANETS: ORIGIN, EVOLUTION AND COMPOSITION
Joel S. Levine *In* Lunar and Planetary Inst., Workshop on the Origins of Solar Systems 1988 p 69-79 (For primary document see N88-30536 24-88)
Avail: NTIS HC A06/MF A01 CSCL 03B

92 SOLAR PHYSICS

Includes solar activity, solar flares, solar radiation and sunspots.

For related information see *93 Space Radiation.*

N88-30574# National Geophysical Data Center, Boulder, Colo.
SOLAR-GEOPHYSICAL DATA NUMBER 523, MARCH 1988. PART 1: (PROMPT REPORTS). DATA FOR FEBRUARY 1988, JANUARY 1988 AND LATE DATA
Helen E. Coffey, ed. and John A. McKinnon, ed. Mar. 1988 114 p
(Contract N00014-86-F-0049)
(PB88-212766; SGD-523-Pt-1; ISSN-0038-0911; LC-79-640375)
Avail: NTIS HC A06/MF A01 CSCL 03B

Data is presented for February 1988. It includes IUWDS alert periods (advance and worldwide); solar activity indices; solar flares; solar radio emission; Stanford mean solar magnetic field; and VOSTOK inferred interplanetary magnetic field. E.R.

N88-30575# Jet Propulsion Lab., California Inst. of Tech., Pasadena.
CORONA-SOLAR WIND COUPLING REVIEW Final Report, Apr. 1985 - Jun. 1987
J. Feynman Jun. 1987 96 p
(AF Proj. 2311)
(AFGL-TR-87-0203) Avail: NTIS HC A05/MF A01 CSCL 03B

The prediction and forecasting of the particle and field environment within the magnetosphere is of importance to the Air Force. Conditions within the magnetosphere are linked to conditions within the solar corona by the following chain: the coupling between the corona and the solar wind in the vicinity of the sun, the propagation of the solar wind from the vicinity of the sun to the vicinity of the earth, and the coupling of the solar wind at 1 AU to the magnetosphere. A review is presented of the present knowledge of the coronal-solar wind coupling along with a brief description of problems that remain for the development of an enhanced capability to predict the level of geomagnetic disturbances. Recommendations for a 3 year and a 10 year research plan to address these problems is also included.

Author

N88-30576# National Geophysical Data Center, Boulder, Colo.
SOLAR-GEOPHYSICAL DATA NUMBER 523, MARCH 1988. PART 2: (COMPREHENSIVE REPORTS). DATA FOR SEPTEMBER 1987 AND MISCELLANEA
Helen E. Coffey, ed. and John A. McKinnon, ed. Mar. 1988 64 p
(Contract N00014-86-F-0049)
(PB88-212774; SGD-523-Pt-2; ISSN-0038-0911; LC-79-640375)
Avail: NTIS HC A04/MF A01 CSCL 03B

Solar geophysical data is presented for September 1987. The data includes: Meudon Carte synoptique; solar flares; solar radio bursts at fixed frequencies; solar X-ray radiation from GOES satellite (graphs); mass ejections from the sun; and active prominences and filaments. E.R.

93 SPACE RADIATION

Includes cosmic radiation; and inner and outer earth's radiation belts.

For biological effects of radiation see *52 Aerospace Medicine.* For theory see *73 Nuclear and High-Energy Physics.*

N88-30577# Instituto de Pesquisas Espaciais, Sao Jose dos Campos (Brazil).
AGN (OIII) EMISSION LINE PROFILES: DEPENDENCIES ON GALAXY INCLINATION AND BALMER DECREMENT
Ivo C. Busko Jun. 1988 12 p Presented at the Symposium Commerative to the 25th Anniversary of the Cerro Tolalo Inter-American Observatory (Chile)
(INPE-4596-PRE/1324) Avail: NTIS HC A03/MF A01

Analysis of a sample of high resolution narrow (O III) emission line profiles from Seyfert galaxies showed that: (1) emission line width correlates with galaxy disk inclination to the line of sight, indicating a planar nature of the emitting region; and (2) emission line shape correlates with dust content, indicating that there is dust inside the emitting region, situated mainly in low-velocity clouds. Author

N88-30578# Instituto de Pesquisas Espaciais, Sao Jose dos Campos (Brazil).
X- AND GAMMA-RAY BACKGROUND OBSERVATIONS IN ANTARCTIC
U. B. Jayanthi Jun. 1988 14 p Presented at the 1st Seminario Sobre Ciencias Atmosfericas e Espaciais do Programa Antartico Brasileiro, Sao Jose dos Campos, Brazil
(INPE-4583-PRE/1317) Avail: NTIS HC A03/MF A01

Atmospheric X- and gamma-rays are products of complex electromagnetic interactions between charged particles and atmospheric constituents. The latitudinal dependence of the cosmic ray secondaries, auroral and South Atlantic Anomaly phenomena produce flux variations especially the later temporal flux variations. These variations are discussed in relevance to balloon flight observations of X- and gamma-ray atmospheric background at polar latitudes. Author

N88-30579*# Space Telescope Science Inst., Baltimore, Md.
RADIO AND INFRARED PROPERTIES OF YOUNG STARS
Nino Panagia Sep. 1987 29 p Prepared in cooperation with Catania Univ. (Italy) Sponsored by NASA
(Grant NAG8-697)
(NASA-CR-183252; NAS 1.26:183252; PPS-203) Avail: NTIS HC A03/MF A01 CSCL 03B

Observing young stars, or more appropriately, pre-main-sequence (PMS) stars, in the infrared and at radio frequencies has the advantage over optical observation in that the heavy extinction associated with a star forming region is only a minor problem, so that the whole region can be studied thoroughly. Therefore, it means being able to: (1) search for stars and do statistical studies on the rate of star formation; (2) determine their luminosity, hence, to study luminosity functions and initial mass functions down to low masses; and (3) to study their spectra and, thus, to determine the prevailing conditions at and near the surface of a newly born star and its relations with the surrounding environment. The third point is of principal interest. The report limits itself to a consideration of the observations concerning the processes of outflows from, and accretion onto, PMS stars and the theory necessary to interpret them. Section 2 discusses the radiative processes relevant in stellar outflows. The main observational results are presented in Section 3. A discussion of the statistical properties of stellar winds from PMS stars are given in Section 4. Author

N88-30580# United Kingdom Atomic Energy Authority, Harwell (England). Radiation Effects and Applications Centre.
THE SINGLE EVENT UPSET (SEU) TEST FACILITY ON THE HARDWELL TANDEM GENERATOR FOR COSMIC RAY SIMULATION Final Report
T. K. Sanderson, D. Mapper, J. H. Stephen, and J. Farren Paris, France ESA Nov. 1987 59 p
(Contract ESTEC-5635/86-NL-MA)
(AERE-R-12896; ESA-CR(P)-2613; ETN-88-93039) Copyright Avail: NTIS HC A04/MF A01

The design, commissioning, and use of a dedicated beam line for single event testing are described. Correlation of the results with those obtained elsewhere indicates the suitability of the ion beams available and the accuracy of the beam dosimetry. The facility was used to examine the single event upset sensitivity of 64K static RAMs and the Inmos T414 Transputer. Results show that the dosimetry system provides reliable information and that the facility can be used for characterizing the cosmic ray sensitivity of VLSI devices with confidence. Ion beams can be steered and focused in the new beam line with particular ease. These characteristics are beneficial in the setting up of beams and in maintaining a steady flux. ESA

N88-30505# Joint Publications Research Service, Arlington, Va.
GAMMA RADIATION EXPECTED FROM SUPERNOVA 1987A IN LARGE MAGELLANIC CLOUD
O. S. Bartunov, S. I. Blinnikov, L. V. Levakhina, and D. K. Nadezhin *In its* JPRS Report: Science and Technology. USSR: Space 26 Feb. 1988 p 14 Transl. into ENGLISH from Pisma v Astonomicheskiy Zhurnal (Moscow, USSR), v. 13, no. 9, Sep. 1987 p 744-750 Original language document was announced in IAA as A88-19582 (For primary document see N88-30498 24-88)
Avail: NTIS HC A04/MF A01

N88-30519# Joint Publications Research Service, Arlington, Va.
CHARGE COMPOSITION OF PRIMARY COSMIC RAY NUCLEI WITH z GREATER THAN OR EQUAL TO 2 IN ENERGY REGION GREATER THAN OR EQUAL TO 2 TeV Abstract Only
I. P. Ivanenko, N. L. Grigorov, V. Ya. Shestoperov, Yu. V. Basina, P. V. Vakulov, Yu. Ya. Vasilyev, R. M. Golynskaya, L. B. Grigoryeva, D. A. Zhuravlev, and V. I. Zatsepin et al. *In its* JPRS Report: Science and Technology. USSR: Space 26 Feb. 1988 p 19 Transl. into ENGLISH from Kosmicheskiye Issledovaniya (Moscow, USSR), v. 25, no. 3, May - Jun. 1987 p 471-473 Original language document was announced in IAA as A87-47568 (For primary document see N88-30498 24-88)
Avail: NTIS HC A04/MF A01

N88-30520# Joint Publications Research Service, Arlington, Va.
MEASUREMENT OF GALACTIC RADIO EMISSION AT FREQUENCY 37 GHz FROM ABOARD SPACECRAFT Abstract Only
I. A. Strukov and D. P. Skulachev *In its* JPRS Report: Science and Technology. USSR: Space 26 Feb. 1988 p 19 Transl. into ENGLISH from Pisma v Astronomicheskiy Zhurnal (Moscow, USSR), v. 13, no. 6, Jun. 1987 p 469-473 (For primary document see N88-30498 24-88)
Avail: NTIS HC A04/MF A01

99 GENERAL

N88-30581*# National Aeronautics and Space Administration, Washington, D.C.
SCIENCE AT NASA FIELD CENTERS: FINDINGS AND RECOMMENDATIONS ON THE SCOPE, STRENGTH AND INTERACTIONS OF SCIENCE AND SCIENCE-RELATED TECHNOLOGY PROGRAMS
May 1988 92 p
(Grant NAGw-1090)
(NASA-TM-101188; NAS 1.15:101188) Avail: NTIS HC A05/MF A01 CSCL 05A

Great achievements by NASA and other space agencies have shown us what opportunities lie in the opening of the space frontier. A broad and vigorous science program in NASA is vital to full U.S. exploitation of these new opportunities. Today, science in

NASA Centers is characterized by its breadth, relevance, and excellence. The NASA in-house science program and its links to university programs constitute a vitally important national resource. Maintaining excellence as a foundation for the future is a fundamental responsibility of NASA, one that requires constant attention and effort. This report by the NASA Center Science Assessment Team documents the current state of science within NASA and recommends actions to maintain a healthy program. NASA scientists have always played key roles in planning, guiding, and conducting national programs in space science. The review of Center science programs is intended to ensure that both NASA and the nation can depend on their continuing contribution in these roles. Author

N88-30582# Politecnico di Torino (Italy). Dept. of Aerospace Engineering.
[ACTIVITIES REPORT OF THE DEPARTMENT OF AEROSPACE ENGINEERING] Annual Report, 1986
Dec. 1987 37 p
(ETN-88-91607) Avail: NTIS HC A03/MF A01

Research in aeronautics and astronautics; fluid dynamics and propulsion; structures and materials; and systems engineering and management is summarized. ESA

N88-30583*# National Aeronautics and Space Administration. Lyndon B. Johnson Space Center, Houston, Tex.
RESEARCH AND TECHNOLOGY OF THE LYNDON B. JOHNSON SPACE CENTER Annual Report, 1987
Feb. 1988 98 p
(NASA-TM-100463; S-575; NAS 1.15:100463) Avail: NTIS HC A05/MF A01 CSCL 05D

Johnson Space Center accomplishments in new and advanced concepts during 1987 are highlighted. Included are research projects funded by the Office of Aeronautics and Space Technology, Solar System Exploration and Life Sciences research funded by the Office of Space Sciences and Applications, and advanced Programs tasks funded by the Office of Space Flight. Summary sections describing the role of the Johnson Space Center in each program are followed by descriptions of significant projects. Descriptions are suitable for external consumption, free of technical jargon, and illustrated to increase ease of comprehension.
Author

Typical Subject Index Listing

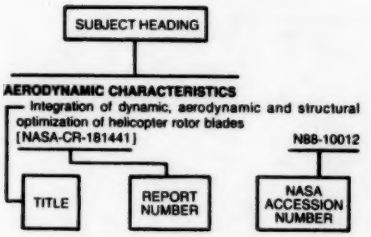

The subject heading is the key to the subject content of the document. Titles, report numbers, and accession numbers of pertinent documents are provided under each subject heading. When the title is insufficiently descriptive of the document content, a title extension has been added, separated from the title by three hyphens. The report number helps to indicate the type of document cited (e.g., NASA report, NASA translation, NASA contractor report). The NASA accession number is the number by which the document abstracts are arranged in this journal and by which the document is sold or requested. The titles, with title extensions if present, are arranged under each subject heading in ascending accession number order. The subject headings have been selected from the latest revision of the *NASA Thesaurus* (NASA SP-7053).

A

ABRASION
Stressed fabric abrasion test procedure for urethane coated fabric fuel tanks
[AD-A196327] N88-29982

ABSORPTION CROSS SECTIONS
Aeronomic problems of molecular oxygen photodissociation. Part 2: Theoretical absorption cross sections of the Schumann-Runge bands at 79 K
[AERONOMICA-ACTA-A-331-1988] N88-29907

ABSORPTIVITY
The effect of particle properties on radiative heat transfer N88-29941

ABSTRACTS
Nineteenth Lunar and Planetary Science Conference. Press abstracts
[NASA-CR-183037] N88-30473

ACCELERATED LIFE TESTS
Performance Prediction for Coatings. Proceedings of a Workshop
[AD-A188973] N88-29966
Prediction of degradation of polymeric coating materials N88-29970
Alternative immersion accelerated testing of coating systems for Naval shoreline facilities N88-29977

ACCELERATION (PHYSICS)
Models of cerebral-body perfusion and cerebral chemical transport
[AD-A194945] N88-30283

ACCESS CONTROL
Performance analysis of FDDI
[NASA-CR-183206] N88-30321

ACCOUNTING
Aircraft avionics and missile system installation cost study. Volume 2: Appendices F and G
[AD-A195372] N88-29801

ACCURACY
Accuracy of satellite data navigation
[AD-A195877] N88-29787
Precision measurement of the Fresnel drag coefficient using a ring laser
[AD-A196025] N88-30043
Increasing accuracy in evaluating vector of state under conditions of incomplete observability of expanded system N88-30511

ACETYLENE
Large ionic species in sooting acetylene and benzene flames N88-29932

ACHONDRITES
Ureilites are not igneous differentiates N88-30477

ACIDS
Active sites and roles of solid acid base catalysts
[NASA-TT-20333] N88-29909

ACOUSTIC EMISSION
The development of acoustic emission for structural integrity monitoring of aircraft
[AD-A196264] N88-30398

ACOUSTIC MICROSCOPES
Application of nondestructive testing techniques to materials testing
[AD-A195716] N88-30138

ACOUSTIC VELOCITY
Calculation of non-stationary aerodynamic forces in the near sonic range
[NASA-TT-20310] N88-29782

ACOUSTO-OPTICS
Acoustooptic processing of two-dimensional signals using temporal and spatial integration
[AD-A194803] N88-29999

ACQUISITION
Scattering impulse response synthesis using random noise illumination: Initial concept evaluation
[AD-A195086] N88-30034

ACTIVE GALACTIC NUCLEI
Activities in astrophysics
[INPE-4582-PRE/1316] N88-30570

ACTUATORS
Sensor and actuator selection for large space structure control
[AD-A194912] N88-29842
A standard architecture for controlling robots
[AD-A195929] N88-30371

ADAPTATION
On adaptive cell-averaging CFAR (Constant False-Alarm Rate) radar signal detection
[AD-A196286] N88-30009

ADAPTIVE CONTROL
Adaptive mesh generation for viscous flows using Delaunay triangulation
[NASA-CR-181699] N88-29749
Supersonic wall adaptation in the rubber tube test section of the DFVLR Goettingen
[IB-222-87-A-06] N88-29824
Adaptive control in positioning a rigid-flexible robot arm
[AD-A195194] N88-30367

ADHESION
Ultrasonic detection of diffusion and adhesion loss N88-29967
Semi-microdroplet assay for cell adhesion molecules
[NASA-CR-183139] N88-30274
Scanning electron microscopy study of adhesion in sea urchin blastulae
[NASA-CR-183136] N88-30275

ADHESION TESTS
Semi-microdroplet assay for cell adhesion molecules
[NASA-CR-183139] N88-30274

ADHESIVE BONDING
Criteria for matrix dominated failure
[AD-A196263] N88-29887
Method of attaching strain gauges to various materials
[NASA-CASE-LAR-13797-1] N88-30108

ADHESIVES
Criteria for matrix dominated failure
[AD-A196263] N88-29887
Predicting the durability of adhesives and coatings by remote detection of hidden defects and coating-thickness irregularities: A theoretical and numerical study N88-29972
Primerless RTV silicones
[BDX-613-3807] N88-29980

AERODYNAMIC CHARACTERISTICS
Aircraft dynamics: Aerodynamic aspects and wind tunnel techniques N88-29731
Survey on nonlinear effects N88-29757
Semi-empirical methods for conventional and unconventional missiles N88-29758
Air intake aerodynamics N88-29762
A new computational capability for ramjet projectiles
[AD-A196061] N88-29812

AERODYNAMIC COEFFICIENTS
A preliminary investigation of drag reduction and mechanism for a blunt body of revolution with slanted base
[NASA-TT-20349] N88-29753
Accuracy criteria for evaluating supersonic aerodynamic coefficient predictions N88-29756
Computational aerodynamic analysis for a range-limited 25mm training round
[AD-A185270] N88-29772

AERODYNAMIC CONFIGURATIONS
Space shuttle phase B wind tunnel model and test information. Volume 3: Launch configuration
[NASA-CR-178416-VOL-3-PT-2] N88-29744
Space shuttle phase B wind tunnel model and test information. Volume 1: Booster configuration
[NASA-CR-178414-VOL-1-PT-1] N88-29745
Special Course on Missile Aerodynamics
[AGARD-R-754] N88-29755
Prediction of dynamic derivatives N88-29761
Next generation missile design N88-29766

AERODYNAMIC DRAG
A preliminary investigation of drag reduction and mechanism for a blunt body of revolution with slanted base
[NASA-TT-20349] N88-29753

AERODYNAMIC FORCES
Contamination and distortion of steady flow field induced by discrete frequency disturbances in aircraft gas engines
[AD-A195440] N88-30069

AERODYNAMIC HEATING
Aerodynamic heating of missiles N88-29764

AERODYNAMIC INTERFERENCE
The present status and the future of missile aerodynamics
[NASA-TM-100063] N88-29773

AERODYNAMIC LOADS
Matching P.S.D.: Design loads N88-29720
A summary of methods for establishing airframe design loads from continuous gust design criteria N88-29721
Status review of atmosphere turbulence and aircraft response N88-29726
A summary of atmospheric turbulence measurements with specially-equipped aircraft in the US N88-29727
Calculation of non-stationary aerodynamic forces in the near sonic range
[NASA-TT-20310] N88-29782
Empirical flutter prediction method
[AD-A195699] N88-29810

AERODYNAMIC STABILITY
The present status and the future of missile aerodynamics
[NASA-TM-100063] N88-29773

AERODYNAMICS
Theoretical aerodynamics, transonic flow
[AD-A196247] N88-29777

AEROELASTICITY
Application of unsteady aerodynamic methods for transonic aeroelastic analysis
[NASA-TM-100685] N88-29754
History of aeroelasticity in Germany from the beginning to 1945
[ESA-TT-1082] N88-29767
Recent advances in transonic computational aeroelasticity
[NASA-TM-100063] N88-29778
Aeroelastic response of metallic and composite propfan models in yawed flow
[NASA-TM-100964] N88-29807

AERONAUTICAL ENGINEERING
Development and design of windtunnel and test facility for RPV (Remote Piloted Vehicle) enhancement devices
[AD-A194842] N88-29822
AERONAUTICS
Activities report of the Department of Aerospace Engineering
[ETN-88-91607] N88-30582
AERONOMY
Aeronomic problems of the molecular oxygen photodissociation. Part 3: Solar spectral irradiances in the region of the O2 Herzberg continuum, Schumann-Runge bands and continuum
[AERONOMICA-ACTA-A-332-1988] N88-29897
Aeronomic problems of molecular oxygen photodissociation. Part 2: Theoretical absorption cross sections of the Schumann-Runge bands at 79 K
[AERONOMICA-ACTA-A-331-1988] N88-29907
Aeronomic problems of molecular oxygen photodissociation. Part 4: The various parameters for the Herzberg continuum
[AERONOMICA-ACTA-A-333-1988] N88-29955
AEROSOLS
Microphysical processes in cloud layers of Venus N88-30522
Possibilities of determining vertical profiles of microphysical characteristics of stratospheric aerosol using space measurements of transparency and solar halo N88-30526
Volatiles on Mars
[NASA-CR-183113] N88-30571
AEROSPACE ENGINEERING
The 1988 Goddard Conference on Space Applications of Artificial Intelligence
[NASA-CP-3009] N88-30330
Activities report of the Department of Aerospace Engineering
[ETN-88-91607] N88-30582
AEROSPACE INDUSTRY
Aircraft airframe cost estimating relationships: Study approach and conclusions
[R-3255-AF] N88-29795
Study on industrial organization for European Ground Support Equipment (EGSE) to support European space programs. Volume 1: Technical reports
[SD-RP-AI-009-VOL-1] N88-30446
Study on industrial organization for European Ground Support Equipment (EGSE) to support European space programs. Volume 2: Technical reports
[SD-RP-AI-009-VOL-2] N88-30448
AEROSPACE MEDICINE
Central serous chorioretinopathy in USAF aviators: A review
[AD-A195697] N88-30280
Aerospace medicine and biology: A continuing bibliography with indexes (supplement 315)
[NASA-SP-7011(315)] N88-30281
AEROSPACE PLANES
Ascent guidance for a winged boost vehicle
[NASA-CR-172083] N88-29846
A study of the critical factors controlling the synthesis of ceramic matrix composites from preceramic polymers
[AD-A195405] N88-29881
AEROSPACE SCIENCES
JPRS report: Science and technology. USSR: Space
[JPRS-USP-88-001] N88-30498
AEROSPACE SYSTEMS
Sensor and actuator selection for large space structure control
[AD-A194912] N88-29842
AEROSPACE VEHICLES
Dynamics of articulated aerospace structures
[AD-A195685] N88-29794
Automated early fatigue damage sensing system
[AD-A195717] N88-30143
AEROTHERMODYNAMICS
Numerical models for analytical predictions of combustor aerothermal performance characteristics N88-29935
Impact of ETO propellants on the aerothermodynamic analyses of propulsion components
[NASA-TM-101303] N88-30094
AFTERBURNING
High performance turbofan afterburner systems N88-29922
AGRICULTURE
Study of the spectral response of soybeans
[INPE-4592-PRE/1322] N88-30174
AGROMETEOROLOGY
LANDSAT TM and agrometeorological data for wheat yield estimation at the farm level
[INPE-4591-PRE/1321] N88-30180
AH-64 HELICOPTER
Test of an 0.6-scale model of the AH-64 Apache in the NASA Langley full-scale wind tunnel
[AD-A196129] N88-29768
AIR DEFENSE
Integration of LANTIRN (Low Altitude Navigation and Targeting Infrared for Night) into operational fighter training
[AD-A194906] N88-29799
LANTIRN simulator training in the F-16C
[AD-A195201] N88-29826
AIR DROP OPERATIONS
Control systems for platform landings cushioned by air bags
[AD-A196154] N88-29996
AIR FLOW
Nozzle airflow influences on fuel patternation N88-29916
AIR MASSES
Energy budget and ground temperatures in hot regions
[AD-A196298] N88-30268
AIR NAVIGATION
Observed track-keeping performance of DC10 aircraft equipped with the Collins AINS-70 area navigation system: Karlsruhe and Maastricht UACs (Upper Area Control centres)
[EEC-202] N88-29788
Integration of LANTIRN (Low Altitude Navigation and Targeting Infrared for Night) into operational fighter training
[AD-A194906] N88-29799
AIR POLLUTION
Investigation of the large-scale impact of air pollution components on forest ecosystems in Bavaria
[ESA-TT-1087] N88-30187
AIR WATER INTERACTIONS
Doppler radar analysis of coastal marine atmospheric boundary layer structure during a cold air outbreak
[AD-A196023] N88-30261
Analysis of environmental parameters from the Panama City tower radar experiment
[AD-A194994] N88-30264
AIRBORNE/SPACEBORNE COMPUTERS
Development and demonstration of an on-board mission planner for helicopters
[NASA-CR-177482] N88-29817
AIRCRAFT ACCIDENT INVESTIGATION
Centralized class A flight mishap investigation
[AD-A194397] N88-29786
AIRCRAFT ACCIDENTS
Failure analysis for gas turbines
[NLR-MP-87037-U] N88-29808
AIRCRAFT COMPARTMENTS
A field study on soft contact lens wear in USAF military transport aircraft
[AD-A195962] N88-30285
AIRCRAFT CONFIGURATIONS
Recent advances in transonic computational aeroelasticity
[NASA-TM-100663] N88-29778
Generation of surface grids through elliptic partial differential equations for aircraft and missile configurations
[AD-A195639] N88-30378
AIRCRAFT CONTROL
Comparison of the influence of different gust models on structural design N88-29722
Pilot modeling N88-29736
Pilot modeling applications N88-29737
Advances in flying qualities: Concepts and criteria for a mission oriented flying qualities specification N88-29739
A second look at MIL prime flying qualities requirements N88-29740
The role of simulation in flying qualities and flight control system related development N88-29742
Angle of attack and sideslip estimation using an inertial reference platform
[AD-A194876] N88-29769
A fiber optic collective flight control system for helicopters
[AD-A195406] N88-29818
Controlled degradation of resolution of high-quality flight simulator images for training effectiveness evaluation
[AD-A196189] N88-29823
Numerical simulation of nozzle flows
[AD-A195144] N88-30064
Four-axis side-arm flight control simulator investigation
[AD-A196026] N88-30294
Prediction and measurement of human pilot dynamic characteristics in a manned rotorcraft simulation
[NASA-CR-183246] N88-30297
AIRCRAFT DESIGN
The Flight of Flexible Aircraft in Turbulence: State-of-the-Art in the Description and Modelling of Atmospheric Turbulence
[AGARD-R-734-ADD] N88-29717
Current and proposed gust criteria and analysis methods: An FAA overview N88-29718
Matching P.S.D.: Design loads N88-29720
A summary of methods for establishing airframe design loads from continuous gust design criteria N88-29721
Comparison of the influence of different gust models on structural design N88-29722
Measured and predicted responses of the Nord 260 aircraft to the low altitude atmospheric turbulence N88-29723
A review of measured gust responses in the light of modern analysis methods N88-29724
Aircraft dynamics: Aerodynamic aspects and wind tunnel techniques N88-29731
Compression pylon
[NASA-CASE-LAR-13777-1] N88-29789
AIRCRAFT ENGINES
Developing the Rolls-Royce Tay
[PNR90447] N88-29809
Fuel effects on flame radiation and hot-section durability N88-29925
Contamination and distortion of steady flow field induced by discrete frequency disturbances in aircraft gas engines
[AD-A195440] N88-30069
AIRCRAFT EQUIPMENT
The Flight of Flexible Aircraft in Turbulence: State-of-the-Art in the Description and Modelling of Atmospheric Turbulence
[AGARD-R-734] N88-29725
A summary of atmospheric turbulence measurements with specially-equipped aircraft in the US N88-29727
Standard fatigue specimens for fastener evaluation — aircraft components
[FFA-TN-1987-68] N88-30157
AIRCRAFT FUELS
Combustion and fuels in gas turbine engines
[AGARD-CP-422] N88-29910
AIRCRAFT HAZARDS
Extreme gusts distribution N88-29734
AIRCRAFT INDUSTRY
China's acquisition and use of foreign aviation technology
[AD-A194827] N88-30471
AIRCRAFT MANEUVERS
An interim comparison of operational CG records in turbulence on small and large civil aircraft N88-29729
AIRCRAFT MODELS
Computer programs for generation of NASTRAN and VIBRA-6 aircraft models
[AD-A195467] N88-29792
AIRCRAFT NOISE
Aircraft noise prediction program propeller analysis system IBM-PC version user's manual version 2.0
[NASA-CR-181689] N88-30399
AIRCRAFT PERFORMANCE
Measured and predicted responses of the Nord 260 aircraft to the low altitude atmospheric turbulence N88-29723
Status review of atmosphere turbulence and aircraft response N88-29726
Aircraft dynamics: Aerodynamic aspects and wind tunnel techniques N88-29731
AIRCRAFT PILOTS
Central serous chorioretinopathy in USAF aviators: A review
[AD-A195697] N88-30280
AIRCRAFT RELIABILITY
The Flight of Flexible Aircraft in Turbulence: State-of-the-Art in the Description and Modelling of Atmospheric Turbulence
[AGARD-R-734-ADD] N88-29717
Current and proposed gust criteria and analysis methods: An FAA overview N88-29718
Re-assessment of gust statistics using CAADRP data N88-29732
Acquisition of gust statistics from AIDS-recorded data N88-29733
Preliminary airworthiness evaluation of the UH-60A/ESSS (External Stores Support System) with HELLFIRE launcher installed
[AD-A196187] N88-29793
The development of acoustic emission for structural integrity monitoring of aircraft
[AD-A196264] N88-30398
AIRCRAFT SAFETY
The Flight of Flexible Aircraft in Turbulence: State-of-the-Art in the Description and Modelling of Atmospheric Turbulence
[AGARD-R-734-ADD] N88-29717
AIRCRAFT STABILITY
A second look at MIL prime flying qualities requirements N88-29740
AIRCRAFT STRUCTURES
Dynamics of articulated aerospace structures
[AD-A195685] N88-29794

Aircraft airframe cost estimating relationships: Study approach and conclusions
[R-3255-AF] N88-29795

AIRCRAFT SURVIVABILITY
Threat expert system technology advisor
[NASA-CR-177479] N88-29816

AIRDROPS
Control systems for platform landings cushioned by air bags
[AD-A196154] N88-29996

AIRFOILS
The use of hot-film technique for boundary layer studies on a 21 percent thick airfoil
[NAE-AN-45] N88-29781
The effects of inlet turbulence and rotor/stator interactions on the aerodynamics and heat transfer of a large-scale rotating turbine model. Volume 2: Heat transfer data tabulation. 15 percent axial spacing
[NASA-CR-179467] N88-29804
Studies of gas turbine heat transfer airfoil surface and end-wall cooling effects
[AD-A195165] N88-29805

AIRFRAMES
A summary of methods for establishing airframe design loads from continuous gust design criteria N88-29721
Aircraft airframe cost estimating relationships: Study approach and conclusions
[R-3255-AF] N88-29795
Evaluation of bond testing equipment for inspection of Army advanced composite airframe structures
[AD-A195795] N88-29885

AIRPORTS
An analysis of time and space requirements for aircraft turnrounds
[TT-8705] N88-29783

ALBEDO
Energy budget and ground temperatures in hot regions
[AD-A196298] N88-30268

ALGORITHMS
A streamwise upwind algorithm for the Euler and Navier-Stokes equations applied to transonic flows
[NASA-TM-101019] N88-29751
An improved spherical earth diffraction algorithm for SEKE
[AD-A195847] N88-30005
Transient interaction of electromagnetic pulses in dielectrics and microwave biophysics
[AD-A195687] N88-30008
Reducing the parallel solution time of sparse circuit matrices using reordered Gaussian elimination and relaxation
[AD-A195152] N88-30045
LANDSAT-TM data to map flooded areas
[INPE-4594-PRE/1324] N88-30177
Validate algorithms for the determination of rainfall rates from SSM/I microwave satellite imagery
[AD-A195428] N88-30270
Algorithms for nonlinear least-squares problems
[AD-A196071] N88-30305
Range data description based on multiple characteristics N88-30351
Statistical analysis of the LMS (Last Mean Squares) and modified stochastic gradient
[AD-A195497] N88-30376
Kalman filter-based algorithms for estimating depth from image sequences
[AD-A195818] N88-30380
Reconstruction of multidimensional signals from multiple level threshold crossings
[AD-A195561] N88-30383
Design and performance analysis of a relational replicated database system
[AD-A196290] N88-30456
The guide star catalog
[NASA-CR-183253] N88-30547

ALKALINE BATTERIES
Regenerative fuel cell energy storage system for a low earth orbit space station
[NASA-CR-174802] N88-30184

ALUMINUM
Fatigue crack growth characteristics of ARALL (trademark)-1
[AD-A196185] N88-29889
High frequency GaAlAs modulator and photodetector for phased array antenna applications
[NASA-TM-101328] N88-30048
Development of graded reference radiographs for aluminum welds, phase 1
[AD-A195594] N88-30140

ALUMINUM ALLOYS
Some effects of nitrates on the tensile properties of Al 7075-T7351
[AD-A195118] N88-29965

ALUMINUM GALLIUM ARSENIDES
Spectroscopic studies with multiple quantum well materials with applications to optical signal processing at room temperature
[AD-A194171] N88-30409

AMAZON REGION (SOUTH AMERICA)
Recent measurements of ozone in the Amazon forests
[INPE-4494-PRE/1258] N88-30185

AMMONIUM NITRATES
Titrimetric analysis of HAN-based liquid propellants
[AD-A196225] N88-29990

AMMONIUM PERCHLORATES
Descriptive characterization of propellant particles
[AD-A195176] N88-29985

AMORPHOUS SEMICONDUCTORS
Ultrafast processes and spectroscopy with free electron lasers
[AD-A195248] N88-30126

AMPHIBOLES
Reappraisal of the geology of Kangimut Sammisoq, Ameralik Fjord, Southern West Greenland: Crustal structure and interpretation of isotopic data N88-30234

AMPLIFICATION
Optoelectronic gain control of a microwave single stage GaAs MESFET amplifier
[NASA-CR-182201] N88-30055

AMPTE (SATELLITES)
Plasma of earth's magnetosphere ring currents. Model compared with results of AMPTE/CCE experiment N88-30515

ANALOGS
Rifts of deeply eroded Hawaiian basaltic shields: A structural analog for large Martian volcanoes N88-30494

ANALYSIS (MATHEMATICS)
Theoretical aerodynamics, transonic flow
[AD-A196247] N88-29777

ANALYTIC FUNCTIONS
Track performance considerations for monopulse radars
[AD-A196232] N88-30007

ANDESITE
Does subduction zone magmatism produce average continental crust N88-30214

ANGLE OF ATTACK
Angle of attack and sideslip estimation using an inertial reference platform
[AD-A194876] N88-29769
Computer programs for calculation of sting pitch and roll angles required to obtain angles of attack and sideslip on wind tunnel models
[NASA-TM-100659] N88-29820

ANISOTROPIC MEDIA
An improved boundary force method for analyzing cracked anisotropic materials
[NASA-TM-101495] N88-29879

ANISOTROPY
Anisotropic constitutive modeling for nickel-base single crystal superalloys
[NASA-CR-182157] N88-29961

ANNULAR SUSPENSION AND POINTING SYSTEM
Synchronous response modelling and control of an annular momentum control device
[NASA-CR-4166] N88-29995

ANOMALIES
One equatorial anomaly in nighttime ionospheric F region N88-30517
Evolutionary helium and CNO anomalies in the atmospheres and winds of massive hot stars
[NASA-CR-183254] N88-30550

ANORTHOSITE
The tectonic setting of Archean anorthosites N88-30231
Crustal underplating in the North American Craton: Evidence from the Petrogenesis of anorthositic rocks in the Middle Proterozoic Midcontinent Rift System N88-30252

ANTARCTIC REGIONS
Changes in stratospheric ozone: Observations and theories
[AERONOMICA-ACTA-A-334-1988] N88-30188
Antarctic Meteorite Newsletter, Volume 11, Number 2, August 1988
[NASA-TM-89801] N88-30573

ANTENNA ARRAYS
Development of a general software package for the analysis and synthesis of planar antenna arrays for space applications
[S-247-02] N88-30000
High frequency GaAlAs modulator and photodetector for phased array antenna applications
[NASA-TM-101328] N88-30048

ANTENNA DESIGN
Development of a general software package for the analysis and synthesis of planar antenna arrays for space applications
[S-247-02] N88-30000
Fields and waves N88-30025
A 30/20 GHz multibeam array antenna suitable for future high rate TDMA European satellite networks
[ETN-88-93079] N88-30037

ANTENNA RADIATION PATTERNS
Application of sampling techniques to near-field far-field transformation
[ESA-CR(P)-2546] N88-30002
The focal plane reception pattern calculation for a paraboloidal antenna with a nearby fence
[NASA-TM-100691] N88-30039

ANTICLINES
Diapirs of the Mediterranean ridge: The tectonic regime of an incipient accreted terrane N88-30224

ANTIFERROMAGNETISM
Theory of superconductivity in oxides
[AD-A195647] N88-30432
Theoretical model of high temperature superconductors
[DE88-702707] N88-30441

ANTIMISSILE DEFENSE
Report to congress on the strategic defense system architecture
[AD-A195476] N88-30393

ANTIMISSILE MISSILES
Looking beyond the strategic defense initiative
[AD-A195079] N88-30394

APPROXIMATION
Numerical modelling of premixed flames in gaseous media N88-29944
Approximation of viscoelastic stresses from Newtonian turbulent kinematics
[AD-A194317] N88-30077
Automatic qualitative analysis of ordinary differential equations using piecewise linear approximations
[AD-A196310] N88-30379
Convergence of Galerkin approximations for operator Riccati equations: A nonlinear evolution equation approach
[NASA-CR-181706] N88-30386
Image focusing in space and time
[AD-A195839] N88-30410

ARC JET ENGINES
Performance and lifetime assessment of MPD arc thruster technology
[NASA-TM-101293] N88-29860
Unified study of plasma/surface interactions for space power and propulsion
[AD-A195971] N88-29870

ARC WELDING
ARC length control for plasma welding
[NASA-CASE-MSC-20900-1] N88-30131

ARCHITECTURE
The triangle: A multiprocessor architecture for fast curve and surface generation
[AD-A195882] N88-30324
Report to congress on the strategic defense system architecture
[AD-A195476] N88-30393
Monte-Carlo estimation of the influence of plant architecture parameters on spectral brightness N88-30533

ARCHITECTURE (COMPUTERS)
A multiprocessor avionics system for an unmanned research vehicle
[AD-A194806] N88-29800
N-version software demonstration for digital flight controls
[NASA-CR-181483] N88-29815
Acoustooptic processing of two-dimensional signals using temporal and spatial integration
[AD-A194803] N88-29999
A model for architectural comparison
[AD-A195993] N88-30302
The design of an intelligent multidisk control module for VME bus based systems
[AD-A195587] N88-30303
Scheme86: A system for interpreting SCHEME
[AD-A195931] N88-30319
Automated satellite control in Ada N88-30336
MOORE: A prototype expert system for diagnosing spacecraft problems N88-30343
A standard architecture for controlling robots
[AD-A195829] N88-30371
Architecture for optical digital computers
[AD-A195477] N88-30416
Integrating information systems in a major decentralized international organization, volume 7
[AD-A195856] N88-30488

AREA
Determination of the specific area of liquid gas and the velocity of weak pressure waves in aqueous foams
[NASA-TT-20347] N88-30087
AREA NAVIGATION
Observed track-keeping performance of DC10 aircraft equipped with the Collins AINS-70 area navigation system: Karlsruhe and Maastricht UACs (Upper Area Control centres)
[EEC-202] N88-29788
ARGON PLASMA
Energy conversion measurements in laser-sustained argon plasmas for application to rocket propulsion
[AD-A194931] N88-29661
ARIANE LAUNCH VEHICLE
Simulation of Vulcain engine operation at low inlet pressure
[ETN-88-93083] N88-29875
ARMED FORCES (UNITED STATES)
Centralized class A flight mishap investigation
[AD-A194397] N88-29786
ARRAYS
Nonlinear dynamics of coupled oscillator arrays
[AD-A194886] N88-30053
Development of a unit cell for a GeGa detector array
[NASA-CR-177445] N88-30100
Tolerances for phase locking of semiconductor laser arrays
[AD-A195974] N88-30120
ARTERIES
Models of cerebral-body perfusion and cerebral chemical transport
[AD-A194945] N88-30283
ARTIFICIAL INTELLIGENCE
Corner extraction from radar images
[AD-A194857] N88-30020
Path planning and path following for the Amsterdam autonomous cart
[FVI-86-22] N88-30133
The design of an intelligent multidisk control module for VME bus based systems
[AD-A195587] N88-30303
Quality measures and assurance for AI (Artificial Intelligence) software
[NASA-CR-4187] N88-30304
Reification without evaluation
[AD-A195928] N88-30326
The 1988 Goddard Conference on Space Applications of Artificial Intelligence
[NASA-CP-3009] N88-30330
An intelligent training system for space shuttle flight controllers N88-30331
Artificial intelligence costs, benefits, risks for selected spacecraft ground system automation scenarios N88-30332
A shared-world conceptual model for integrating space station life sciences telescience operations N88-30333
Artificial intelligence in a mission operations and satellite test environment N88-30334
Automated satellite control in Ada N88-30336
Contingency rescheduling of spacecraft operations N88-30337
Knowledge based tools for Hubble Space Telescope planning and scheduling: Constraints and strategies N88-30338
The proposal entry processor: Telescience applications for Hubble Space Telescope science operations N88-30339
Candidate functions for advanced technology implementation in the Columbus mission planning environment N88-30340
A rule-based systems approach to spacecraft communications configuration optimization N88-30341
MOORE: A prototype expert system for diagnosing spacecraft problems N88-30343
Low level image processing techniques using the pipeline image processing engine in the flight telerobotic servicer N88-30346
Autonomous image data reduction by analysis and interpretation N88-30347
Parallel and distributed computation for fault-tolerant object recognition N88-30350
The second generation intelligent user interface for the crustal dynamics data information system N88-30352
Spacelab data processing facility (SLDPF) Quality Assurance (QA)/Data Accounting (DA) expert systems: Transition from prototypes to operational systems N88-30353
Automated cataloging and characterization of space-derived data N88-30354
A design for a ground-based data management system N88-30355
Automatic mathematical modeling for real time simulation system N88-30356
A simulation engine: Combining an expert system with a simulation language N88-30358
Verification and validation of rulebased systems for Hubble Space Telescope ground support N88-30361
The need for a comprehensive expert system development methodology N88-30362
The combinatorics of object recognition in cluttered environments using constrained search
[AD-A196224] N88-30364
Study of software requirements and artificial intelligence techniques for robotics
[TL-3333] N88-30365
Research on problem-solving systems
[AD-A195154] N88-30370
Knowledge based simulation: An artificial intelligence approach to system modeling and automating the simulation life cycle
[AD-A195838] N88-30372
Theories of comparative analysis
[AD-A196328] N88-30395
Optical symbolic computing
[AD-A195690] N88-30406
Information retrieval systems evolve-advances for easier and more successful use N88-30462
ARTIFICIAL SATELLITES
Long haul communications in the HF spectrum utilizing high speed modems
[AD-A194683] N88-30003
DATATRAN: Datum transformation software
[AD-A195723] N88-30175
Space systems cost study
[AD-A196024] N88-30469
Orbital evolution of distant artificial earth satellites N88-30506
Families of periodic solutions in problem of solid body rotation at triangular libration point in restricted three-body problem N88-30508
ASCENT PROPULSION SYSTEMS
Ascent guidance for a winged boost vehicle
[NASA-CR-172083] N88-29846
ASCENT TRAJECTORIES
Ascent guidance for a winged boost vehicle
[NASA-CR-172083] N88-29846
ASPECT RATIO
The aspect ratio dependence of the attractor dimension in Taylor-Couette flow
[AD-A196297] N88-30065
ASSEMBLING
Study of the assembly, integration and verification programs of telecommunication satellites applicable to other satellite programs
[MATRA-100/CC/MLG/031/87] N88-29847
ASTRODYNAMICS
The kinematics of late-type supergiants
[SER-C-PREPUBL-FASC-28] N88-30560
ASTRONAUTICS
Activities report of the Department of Aerospace Engineering
[ETN-88-91607] N88-30582
ASTRONOMICAL CATALOGS
Far infrared supplement: Catalog of infrared observations, second edition
[NASA-RP-1205] N88-30545
A new determination of the Geneva photometric passbands and their absolute calibration
[SER-C-PREPUBL-FASC-26] N88-30546
The guide star catalog
[NASA-CR-183253] N88-30547
ASTRONOMICAL MAPS
The guide star catalog
[NASA-CR-183253] N88-30547
ASTRONOMICAL MODELS
Workshop on the Origins of Solar Systems
[NASA-CR-183025] N88-30536
Comparisons of solar nebula models N88-30539
The atmospheres of the earth and the other planets: Origin, evolution and composition N88-30544
ASTRONOMICAL SATELLITES
Far infrared spectroscopy telescope (FIRST) inflatable thermal shield, phase 1
[SR/FIS/108(87)CZ] N88-30552
ASTRONOMICAL SPECTROSCOPY
The high-throughput X-ray spectroscopy mission: The mission-science report
[ESA-SP-1097] N88-30557
ASTRONOMY
Activities report in astronomy
[ISSN-0531-4496] N88-30535
Workshop on the Origins of Solar Systems
[NASA-CR-183025] N88-30536
ASTROPHYSICS
A coded mask telescope for observations of X and gamma ray sources in the southern sky
[INPE-4580-PRE/1314] N88-30551
Research in particle and gamma-ray astrophysics
[NASA-CR-183126] N88-30566
Activities in astrophysics
[INPE-4582-PRE/1316] N88-30570
ASYMPTOTIC SERIES
Mathematical problems of nonlinear wave propagation and of waves in heterogeneous media
[AD-A195970] N88-30057
ATMOSPHERIC BOUNDARY LAYER
The surface evaporative duct height product: An evaluation
[AD-A195918] N88-30199
Doppler radar analysis of coastal marine atmospheric boundary layer structure during a cold air outbreak
[AD-A196023] N88-30261
ATMOSPHERIC CHEMISTRY
Photochemistry of ionospheric D-region with injection of nitrogen oxides N88-30499
ATMOSPHERIC COMPOSITION
Recent measurements of ozone in the Amazon forests
[INPE-4494-PRE/1258] N88-30185
Recent observations of carbon monoxide in the Amazon Rain Forest
[INPE-4478-PRE/1245] N88-30186
ATMOSPHERIC CORRECTION
Atmospheric corrections for in-flight satellite radiometric calibration
[AD-A196124] N88-30194
ATMOSPHERIC DENSITY
Approximation of atmospheric density by Chebyshev polynomials in predicting motion of low artificial earth satellites N88-30503
ATMOSPHERIC DIFFUSION
Global vertical mass transport by clouds: A two-dimensional model study
[CM-74] N88-30192
ATMOSPHERIC ENTRY
Investigation of the validity of the non-rotating planet assumption for three-dimensional earth atmospheric entry
[AD-A194877] N88-29829
ATMOSPHERIC HEATING
Ionosonde studies of field-aligned irregularities during high-power HF heating at Arecibo
[AD-A195848] N88-30256
ATMOSPHERIC MODELS
Global vertical mass transport by clouds: A two-dimensional model study
[CM-74] N88-30192
Ionosonde studies of field-aligned irregularities during high-power HF heating at Arecibo
[AD-A195848] N88-30256
Cloud/mesoscale model development and application studies
[AFGL-TR-87-0219] N88-30269
Using nonstationary models of the atmosphere to describe satellite drag N88-30502
Model representation of electron concentration distribution in outer middle-latitude ionosphere using data from Intercosmos-19 artificial earth satellite N88-30513
ATMOSPHERIC PHYSICS
Investigations of magnetosphere-ionosphere coupling relevant to operational systems
[AD-A195972] N88-30195
ATMOSPHERIC SOUNDING
Microwave instrument for planetary mission (Titan/CASSINI mission orbiter spacecraft)
[BAE-CS/TP-8359] N88-30102
Spaceborne lidar: Development of a laboratory test system
[BF-R-86.090-1] N88-30118
Possibilities of determining vertical profiles of microphysical characteristics of stratospheric aerosol using space measurements of transparency and solar halo N88-30526
ATMOSPHERIC TEMPERATURE
Energy budget and ground temperatures in hot regions
[AD-A196298] N88-30268
ATMOSPHERIC TURBULENCE
The Flight of Flexible Aircraft in Turbulence: State-of-the-Art in the Description and Modelling of Atmospheric Turbulence
[AGARD-R-734-ADD] N88-29717
Current and proposed gust criteria and analysis methods: An FAA overview N88-29718
Flight test equipment for the on-board measurement of wind turbulence N88-29719
Measured and predicted responses of the Nord 260 aircraft to the low altitude atmospheric turbulence N88-29723
The Flight of Flexible Aircraft in Turbulence: State-of-the-Art in the Description and Modelling of Atmospheric Turbulence
[AGARD-R-734] N88-29725
Status review of atmosphere turbulence and aircraft response N88-29726
A summary of atmospheric turbulence measurements with specially-equipped aircraft in the US N88-29727

The NAE atmospheric research aircraft N88-29730
Extreme gusts distribution N88-29734
A digital simulation technique for the Dryden atmospheric model
[NASA-TT-20342] N88-30266
Microphysical processes in cloud layers of Venus N88-30522

ATMOSPHERIC WINDOWS
Molecular line shape effects on atmospheric window absorption
[AD-A196316] N88-29894

ATOMIZERS
Analysis of the flow through double swirl airblast atomizers N88-29949

ATOMS
Cluster beam studies
[AD-A195182] N88-30443

ATTACKING (ASSAULTING)
Determination of the hydroperoxide potential of jet fuels
[AD-A195975] N88-29991

ATTENTION
Central adrenergic receptors as mediators of central response to stress: Study with Positron Emission Tomography (PET)
[AD-A194947] N88-30284
Comparative aspects of multiple processes of attention
[AD-A195805] N88-30291

ATTENUATION
Finite-difference simulations of Rayleigh-wave scattering by shallow heterogeneity
[AD-A194961] N88-30259

ATTITUDE CONTROL
Angle of attack and sideslip estimation using an inertial reference platform
[AD-A194876] N88-29769
Synchronous response modelling and control of an annular momentum control device
[NASA-CR-4166] N88-29995
Robust design of distributed controllers for large flexible space structures
[NASA-CR-183202] N88-30134
MOORE: A prototype expert system for diagnosing spacecraft problems N88-30343

AURORAS
Five channel auroral photometer
[REPT-112] N88-30101
Structural dynamics of high-latitude magnetosphere determined from solar electron data N88-30500
X- and gamma-ray background observations in Antarctic
[INPE-4583-PRE/1317] N88-30578

AUTOIONIZATION
Autoionization for lower level detrapping in X-ray lasers
[AD-A195845] N88-30123

AUTOMATIC CONTROL
Spray automated balancing of rotors: Methods and materials
[NASA-CR-182151] N88-29825
Artificial intelligence costs, benefits, risks for selected spacecraft ground system automation scenarios N88-30332
Automated space vehicle control for rendezvous proximity operations N88-30335
An automated computerized vision technique for determination of three-dimensional object geometry N88-30348

AUTOMOBILE ENGINES
Testing of a variable-stroke Stirling engine
[NASA-TM-100899] N88-30472

AUTONOMY
Path planning and path following for the Amsterdam autonomous cart
[FVI-86-22] N88-30133
Integrating information systems in a major decentralized international organization, volume 7
[AD-A195856] N88-30468

AUXILIARY PROPULSION
Successful completion of a cyclic ground test of a mercury ion auxiliary propulsion system
[NASA-TM-101351] N88-29873

AVIONICS
The OFP (Operational Flight Program) update cycle needs you
[AD-A194910] N88-29798
Aircraft avionics and missile system installation cost study. Volume 2: Appendices F and G
[AD-A195372] N88-29801

AXIAL FLOW
Studies of unsteady axial-compressor functioning N88-30129

AXIAL LOADS
Determination of multiaxial flow surfaces at elevated temperatures using the concept of dissipation potential
[ORNL/TM-10787] N88-30149

AZULENE
The effect of oriented defects on long-range ordering of hydrocarbon films: Azulene on Pt(111)
[AD-A196089] N88-29904

B

BACKSCATTERING
ZT imaging system for layered thin wall structures
[AD-A195466] N88-29954
The effect of equatorial ionospheric irregularities on the performance of a south-looking OTH-B (Over-The-Horizon-Backscatter) radar
[AD-A195090] N88-30018
Measurement and interpretation of North Atlantic Ocean marine radar sea scatter
[AD-A196239] N88-30036
Spaceborne lidar: Development of a laboratory test system
[BF-R-86.090-1] N88-30118

BACKWARD FACING STEPS
Modeling the stability of a turbulent premixed flame, downstream from a step by a Lagrangian method N88-29943

BALANCING
Spray automated balancing of rotors: Methods and materials
[NASA-CR-182151] N88-29825

BALLISTICS
Combustion diagnostics of propellant with new grain geometries
[AD-A194944] N88-29895

BANDSTOP FILTERS
Confirmation of slow-waves in a crosstie overlay coplanar waveguide and its application to band-reject gratings and reflectors
[AD-A194981] N88-30011

BANDWIDTH
A fiber optic beamforming processor for wideband direction finding
[AD-A194862] N88-30404
Ultra-wideband direction finding using a fiber optic beamforming processor
[AD-A194861] N88-30413

BAROCLINIC WAVES
Rossby waves in mid-latitude oceans N88-30273

BARRIER LAYERS
Containment of a silicone fluid free surface in reduced gravity using barrier coatings
[NASA-TM-101314] N88-30072

BARS
Wide range stress intensity factor expression for an edge-cracked round bar bend specimen
[AD-A196285] N88-30147

BASES
Active sites and roles of solid acid base catalysts
[NASA-TT-20333] N88-29909

BATHOLITHS
Pluton emplacement and magmatic arc construction: A model from the Patagonian batholith N88-30206
Genesis of archean granitoids in the Pilbara block and implications for crustal growth N88-30210

BATTERY CHARGERS
Aircraft battery state of charge and charge control system
[AD-A194979] N88-30052

BAYES THEOREM
Dirichlet prior in Bayesian estimation of item response curves
[AD-A195311] N88-30392

BEADS
Analysis of a feed device for the pneumatic transport of noncohesive particles
[VKI-TM-44] N88-30062

BEAM WAVEGUIDES
Analytical and experimental studies of beam waveguide absorbers for structural damping
[AD-A195085] N88-30144

BEAMS (SUPPORTS)
Damage initiation in the short beam shear test of composite materials using stiffness reduction
[AD-A194880] N88-29883
Vibrational power flow analysis of rods and beams
[NASA-CR-183166] N88-30151

BEDROCK
Structure of Southwestern Michipicoten Greenstone Belt, Ontario: Evidence for Archean accretion N88-30228

BENZENE
Large ionic species in sooting acetylene and benzene flames N88-29932

BIBLIOGRAPHIES
Bibliography of Soviet laser developments, number 88, March - April 1987
[AD-A195978] N88-30116
Aerospace medicine and biology: A continuing bibliography with indexes (supplement 315)
[NASA-SP-7011(315)] N88-30281
Publications of the Jet Propulsion Laboratory 1987
[NASA-CR-181198] N88-30453

BINARY STARS
Binary star measurements using digital speckle interferometer of 6-m telescope N88-30521
Duplicity in the solar neighborhood: Part 4: Spectroscopic orbits for four dwarf M stars
[SER-C-PREPUBL-FASC-21] N88-30561
Duplicity in the solar neighborhood: Part 5: Spectroscopic orbit for the nearby double-lined solar-type star HR 8581
[SER-C-PREPUBL-FASC-23] N88-30562
Activities in astrophysics
[INPE-4582-PRE/1316] N88-30570

BIOELECTRICITY
Cytochrome electron transfer and biomolecular electronics
[AD-A195482] N88-30277

BIOLOGICAL EFFECTS
Bioeffects of electromagnetic waves N88-30032
Aerospace medicine and biology: A continuing bibliography with indexes (supplement 315)
[NASA-SP-7011(315)] N88-30281

BIOLOGICAL EVOLUTION
LSU scientists discover evidence of large meteorite impacts on the early earth N88-30480

BIOMASS
Study of the spectral response of soybeans
[INPE-4592-PRE/1322] N88-30174

BIOPHYSICS
Transient interaction of electromagnetic pulses in dielectrics and microwave biophysics
[AD-A195687] N88-30008

BIOTITE
The petrogenesis of oceanic kimberlites and included mantle megacrysts: The Malaitan alnoite N88-30232

BLADE TIPS
Computational methods for the problems of the tip vortex
[NASA-CR-181438] N88-29775

BLUNT BODIES
A preliminary investigation of drag reduction and mechanism for a blunt body of revolution with slanted base
[NASA-TT-20349] N88-29753

BODIES OF REVOLUTION
A preliminary investigation of drag reduction and mechanism for a blunt body of revolution with slanted base
[NASA-TT-20349] N88-29753

BOLTED JOINTS
Clevis joint for deployable space structures
[NASA-CASE-LAR-13898-1] N88-30130

BOLTZMANN DISTRIBUTION
Boltzmann equation approach to two-phase flow turbulence
[AD-A196153] N88-30086

BOMBER AIRCRAFT
The Soviet Stealth fighter: Check or checkmate
[AD-A195200] N88-29791
Human factors report on information management requirements for next-generation manned bombers
[AD-A195870] N88-30296

BOMBS (ORDNANCE)
Descriptive characterization of propellant particles
[AD-A195176] N88-29985

BONDING
Evaluation of bond testing equipment for inspection of Army advanced composite airframe structures
[AD-A195795] N88-29885

BORN APPROXIMATION
Time-domain far-field scattering of plane electromagnetic waves by a penetrable object in the Born approximation
[PB87-176129] N88-30040

BORON CARBIDES
Electrical properties of materials for elevated temperature resistance strain gage application
[NASA-CR-182214] N88-30106

BOUNDARY ELEMENT METHOD
An improved boundary force method for analyzing cracked anisotropic materials
[NASA-TM-101495] N88-29879

BOUNDARY LAYER CONTROL
Pressure distributions from subsonic tests of an advanced laminar-flow-control wing with leading- and trailing-edge flaps
[NASA-TM-4040-PT-2] N88-29776

BOUNDARY LAYER FLOW
The use of hot-film technique for boundary layer studies on a 21 percent thick airfoil
[NAE-AN-45] N88-29781
BOUNDARY LAYER SEPARATION
A study of the effect of random input motion on low Reynolds number flows
[AD-A195559] N88-29747
The effects of incoming boundary layer thickness on unsteady shock-induced turbulent separations induced by cylinders
[AD-A196190] N88-30060
BOUNDARY LAYER TRANSITION
On the generation of mean flows by the interaction of Goertler vortices and Tollmien-Schlichting waves in curved channel flows
[NASA-CR-181690] N88-29743
Techniques used in the F-14 variable-sweep transition flight experiment
[NASA-TM-100444] N88-30093
BOUNDARY LAYERS
Temperature profile construction methods: An evaluation
[AD-A195919] N88-30262
BOUNDARY VALUE PROBLEMS
Theory of filtering and control with application to control of large space structures
[AD-A195500] N88-29851
Initial value problems in viscoelasticity
[AD-A196052] N88-30145
Stability, stochastic stationarity and generalized Lyapunov equations for two-point boundary-value descriptor systems
[AD-A195645] N88-30385
Multiple solutions and bifurcation for a class of nonlinear Sturm-Liouville eigenvalue problems on an unbounded domain
[AD-A195954] N88-30389
BRAIN
Central adrenergic receptors as mediators of central response to stress: Study with Positron Emission Tomography (PET)
[AD-A194947] N88-30284
BRAIN CIRCULATION
Models of cerebral-body perfusion and cerebral chemical transport
[AD-A194945] N88-30283
BREADBOARD MODELS
Biosample: Preservation, handling and observation system synthesis and breadboarding --- Spacelab
[ESA-CR(P)-2609] N88-29857
Breadboard RL10-2B low-thrust operating mode (second iteration) test report
[NASA-CR-182160] N88-29867
The dc power control for a liquid-fed resistojet
[NASA-TM-101326] N88-29869
BREMSSTRAHLUNG
X- and gamma-ray background observations in Antarctic
[INPE-4583-PRE/1317] N88-30578
BRIDGES (STRUCTURES)
Multi-metallic galvanic corrosion
[AD-A195995] N88-29963
BRIGHTNESS
Astron observations of supernova 1987A in large magellanic cloud N88-30504
BROADBAND
The effect of equatorial ionospheric irregularities on the performance of a south-looking OTH-B (Over-The-Horizon-Backscatter) radar
[AD-A195090] N88-30018
Scattering impulse response synthesis using random noise illumination: Initial concept evaluation
[AD-A195086] N88-30034
A fiber optic beamforming processor for wideband direction finding
[AD-A194862] N88-30404
Ultra-wideband direction finding using a fiber optic beamforming processor
[AD-A194861] N88-30413
BROMINATION
Brominated graphite fibers and method of producing the same
[NASA-CASE-LEW-14698-1] N88-29888
BUBBLES
Fluid physics double rack --- Spacelab
[SD-TN-AI-012] N88-29992
Studies on pressure response of gas bubbles contributions of condensed droplets in bubbles generated by a uniform nucleation
[NASA-TT-20343] N88-30068
BUOYS
KOSPAS-SARSAT satellites used for ocean current study N88-30534
BURNERS
Flame stabilization in a reheat combustor N88-29921
BURNING RATE
Combustion diagnostics of propellant with new grain geometries
[AD-A194944] N88-29895
Descriptive characterization of propellant particles
[AD-A195178] N88-29985
Discovery of a low temperature form of TAGN (Triaminoguanidinium Nitrate)
[AD-A196059] N88-29989

C

CALCULUS OF VARIATIONS
On the Nash point equilibria in the calculus of variations
[AD-A194959] N88-30381
CALIBRATING
NBS (National Bureau of Standards) measurement services: The NBS photodetector spectral response calibration transfer program
[PB88-201595] N88-30109
Atmospheric corrections for in-flight satellite radiometric calibration
[AD-A196124] N88-30194
A new determination of the Geneva photometric passbands and their absolute calibration
[SER-C-PREPUBL-FASC-26] N88-30546
CAMERAS
Kalman filter-based algorithms for estimating depth from image sequences
[AD-A195818] N88-30380
CANONICAL FORMS
Canonical variables and canonical integrals for motion in near-circular orbits N88-30512
CANTILEVER MEMBERS
A parametric study of embedded cantilever retaining walls: The results of a finite element study
[RR-CE83] N88-30152
CAPACITORS
In-house capacitor technology program
[AD-A194804] N88-30049
CAPILLARIES (ANATOMY)
Models of cerebral-body perfusion and cerebral chemical transport
[AD-A194945] N88-30283
CARBON DIOXIDE CONCENTRATION
Visual sensitivities under reduced oxygen
[AD-A195628] N88-30279
CARBON DIOXIDE LASERS
Transverse CO2 laser two-dimensional gain distributions
[AD-A196240] N88-30119
CARBON FIBER REINFORCED PLASTICS
Investigations on the modification of structural reliability by substitution of aluminum by carbon fiber reinforced plastics in aircraft construction
[ILR-MITT-195] N88-29877
Thermal stress analysis in PMR-15 carbon fibre laminates
[ETN-88-93123] N88-29886
Rupture of carbon fiber reinforced plastics (T300-914) composite materials: Influence of initial first ply failures on the fatigue behavior
[SNIAS-881-422-103] N88-29892
Evaluation of the potential health hazards associated with the machining of carbon fiber composites
[AD-A194835] N88-30286
CARBON FIBERS
A test for interfacial effects and stress transfer in ceramic matrix composites
[NASA-CR-182873] N88-29880
Brominated graphite fibers and method of producing the same
[NASA-CASE-LEW-14698-1] N88-29888
Transverse expansion of individual carbon and graphite filaments
[AD-A195073] N88-29891
Evaluation of the potential health hazards associated with the machining of carbon fiber composites
[AD-A194835] N88-30286
CARBON MONOXIDE
Modelling of CO oxidation in dilution jet flows N88-29947
Recent observations of carbon monoxide in the Amazon Rain Forest
[INPE-4478-PRE/1245] N88-30186
CARBON STEELS
Multi-metallic galvanic corrosion
[AD-A195995] N88-29963
CARBON-CARBON COMPOSITES
Creep of carbon yarn and carbon-carbon composites at high temperatures and high stresses
[AD-A195224] N88-29878
CARBONACEOUS CHONDRITES
Noble gases, C,N, and Si isotopes in interstellar SiC form the Murchison carbonaceous chondrite N88-30483
CARDIOVASCULAR SYSTEM
Models of cerebral-body perfusion and cerebral chemical transport
[AD-A194945] N88-30283
CASCADE FLOW
Numerical solutions of unsteady inviscid transonic turbine cascade flows
[AD-A196111] N88-29748
Aerodynamics in ground effect and predicted landing ground roll of a fighter configuration with a secondary-nozzle thrust reverser
[NASA-TP-2834] N88-29752
Three-dimensional elliptic grid generation technique with application to turbomachinery cascades
[NASA-TM-101330] N88-30078
CASTING
Preliminary investigation of flow modeling during solid propellant processing
[AD-A196168] N88-29987
CATACLYSMIC VARIABLES
Intermediate polars observed in Brazil in the last eight years
[INPE-4567-PRE/1308] N88-30559
Activities in astrophysics
[INPE-4582-PRE/1316] N88-30570
CATALYSTS
Active sites and roles of solid acid base catalysts
[NASA-TT-20333] N88-29909
CATHODE RAY TUBES
Use of color CRTs (Cathode Ray Tubes) in aircraft cockpit: A literature search, revision B
[AD-A195062] N88-29797
CATHODES
Electrocatalytic reduction of oxygen on modified oxide surfaces
[NASA-TM-101333] N88-29952
CAVITATION FLOW
Studies on pressure response of gas bubbles contributions of condensed droplets in bubbles generated by a uniform nucleation
[NASA-TT-20343] N88-30068
CAVITIES
Studies on pressure response of gas bubbles contributions of condensed droplets in bubbles generated by a uniform nucleation
[NASA-TT-20343] N88-30068
CELESTIAL GEODESY
Study of modern instrumentation and methods for astronomic positioning in the field
[AD-A196173] N88-30548
CELESTIAL MECHANICS
A standard library for modeling satellite orbits on a microcomputer
[AD-A195759] N88-29830
CELL ANODES
Morphological changes in polymer electrolyte cells
[AD-A195821] N88-30054
CENTAUR LAUNCH VEHICLE
Centaur operations at the space station: Cost and transportation analysis
[NASA-CR-182128] N88-29835
CENTRAL PROCESSING UNITS
The LTPP communication processor --- Columbus and Hermes
[CL/CP/SES/FR/004] N88-30328
CERAMIC MATRIX COMPOSITES
A test for interfacial effects and stress transfer in ceramic matrix composites
[NASA-CR-182873] N88-29880
A study of the critical factors controlling the synthesis of ceramic matrix composites from preceramic polymers
[AD-A195405] N88-29881
Processing technology research in composites
[AD-A195693] N88-29890
CERAMICS
A study of the critical factors controlling the synthesis of ceramic matrix composites from preceramic polymers
[AD-A195405] N88-29881
Processing technology research in composites
[AD-A195693] N88-29890
Polymer-ceramic composites
[AD-A195789] N88-29983
Piezoelectric and electrostrictive materials for transducer applications, volume 1
[AD-A194957] N88-30096
CEREBRUM
Models of cerebral-body perfusion and cerebral chemical transport
[AD-A194945] N88-30283

CHANNEL FLOW
The strong nonlinear interaction of Tollmien-Schlichting waves and Taylor-Goertler vortices in curved channel flow
[NASA-CR-181697] N88-29716
On the generation of mean flows by the interaction of Goertler vortices and Tollmien-Schlichting waves in curved channel flows
[NASA-CR-181690] N88-29743
CHANNELS (DATA TRANSMISSION)
Optics and symbolic computing
[AD-A195119] N88-30004
Performance of DS/SSMA communications in impulsive channels. Part 1: Correlation receivers
[AD-A195712] N88-30021
CHAOS
Pierce diode with external circuit. Part 3: Chaotic behavior
[AD-A194837] N88-30041
CHARGE DISTRIBUTION
Charge composition of primary cosmic ray nuclei with z greater than or equal to 2 in energy region greater than or equal to 2 TeV N88-30519
CHARPY IMPACT TEST
The effect of notch root radius on the determination of toughness in ultrahigh strength steel friction welds
[AD-A195952] N88-30156
CHEBYSHEV APPROXIMATION
Approximation of atmospheric density by Chebyshev polynomials in predicting motion of low artificial earth satellites N88-30503
CHEMICAL ANALYSIS
Noncontact photo-thermal sensing
[AD-A195450] N88-29905
Geochronological and lead-isotope evidences for rapid crust formation in middle-proterozoic time: The Labrador example N88-30239
Lithospheric evolution of the Northern Arabian Shield: Chemical and isotopic evidence from basalts, xenoliths and granites N88-30242
Evidence of the in situ decay of Al-26 in a Semarkona chondrule N88-30479
CHEMICAL COMPOSITION
The characterizatin of combustion by fuel composition: Measurements in a small conventional combustor N88-29920
The performance of a surrogate blend in simulating JP-4 in a spray-fueled combustor N88-29926
The effect of particle properties on radiative heat transfer N88-29941
Bibliography of Soviet laser developments, number 88, March - April 1987
[AD-A195978] N88-30116
Archean crustal evolution of the northern North China Craton N88-30235
The complexity, depth, and rapidity of processes that formed the lunar crust N88-30237
Lithospheric evolution of the Northern Arabian Shield: Chemical and isotopic evidence from basalts, xenoliths and granites N88-30242
Growth of planetary crusts N88-30247
Non-atmospheric noble gases from CO(sub 2) well ga N88-30476
Star formation and molecular clouds N88-30537
CHEMICAL LASERS
Bibliography of Soviet laser developments, number 88, March - April 1987
[AD-A195978] N88-30116
CHEMICAL PROPERTIES
Attenuated total reflectance FT-IR spectroscopy to measure interfacial reaction kinetics at silica surfaces
[AD-A196330] N88-29908
CHEMICAL REACTIONS
Computed potential energy surfaces for chemical reactions
[NASA-CR-183168] N88-29893
Design criteria for extraction with chemical reaction and liquid membrane permeation
[NASA-TT-20352] N88-29899
Gas phase combustion chemistry of nitramine propellants
[AD-A195082] N88-29902
Attenuated total reflectance FT-IR spectroscopy to measure interfacial reaction kinetics at silica surfaces
[AD-A196330] N88-29908
Recent observations of carbon monoxide in the Amazon Rain Forest
[INPE-4478-PRE/1245] N88-30186
CHEMICAL WARFARE
Four-axis side-arm flight control simulator investigation
[AD-A196026] N88-30294
CHEMORECEPTORS
Central adrenergic receptors as mediators of central response to stress: Study with Positron Emission Tomography (PET)
[AD-A194947] N88-30284
CHINA
Archean crustal evolution of the northern North China Craton N88-30235
CHIPS (ELECTRONICS)
Design of a self-timed VLSI multicomputer communication controller
[AD-A194567] N88-30014
Circuit design criteria for stable lateral inhibition neural networks
[AD-A195066] N88-30046
CHLORIDES
Some effects of nitrates on the tensile properties of Al 7075-T7351
[AD-A195118] N88-29965
CHONDRITES
New type of primitive meteorite found in Antarcitca N88-30478
Nebular processes recorded in chondritic meteorites N88-30541
CHONDRULE
Evidence of the in situ decay of Al-26 in a Semarkona chondrule N88-30479
Physical processes and timescales in planet and small-body accretion N88-30540
CHROMIUM
An experimental study of biaxial yield in modified 9Cr-1Mo steel at room temperature
[NASA-CR-175012] N88-30164
CHRONOLOGY
Chronology of early lunar crust N88-30212
Lewis Cliff 86010, a unique Antarctic meteorite: Possible new clues to the early history of the solar system N88-30482
CIRCUITS
Confirmation of slow-waves in a crosstie overlay coplanar waveguide and its application to band-reject gratings and reflectors
[AD-A194981] N88-30011
Reducing the parallel solution time of sparse circuit matrices using reordered Gaussian elimination and relaxation
[AD-A195152] N88-30045
CIRCULAR CYLINDERS
The effects of incoming boundary layer thickness on unsteady shock-induced turbulent separations induced by cylinders
[AD-A196190] N88-30060
CIRCULAR ORBITS
Canonical variables and canonical integrals for motion in near-circular orbits N88-30512
CIRCULATION
Experimental and analytical study of two-phase flow in zero gravity
[AD-A195223] N88-29993
An analysis of results of a high-resolution world ocean circulation model
[AD-A195760] N88-30272
CIRCULATION CONTROL ROTORS
Analysis of a fixed-pitch X-wing rotor employing lower surface blowing
[AD-A187379] N88-29779
CIRRUS CLOUDS
Cloud/mesoscale model development and application studies
[AFGL-TR-87-0219] N88-30269
CIVIL AVIATION
An interim comparison of operational CG records in turbulence on small and large civil aircraft N88-29729
Re-assessment of gust statistics using CAADRP data N88-29732
An analysis of time and space requirements for aircraft turnrounds
[TT-8705] N88-29783
Report to Congress on the effectiveness of the Civil Aviation Security Program
[AD-A195282] N88-29784
CLASSIFICATIONS
Relief effect correction on LANDSAT imagery for forest applications using digital terrain models
[INPE-4611-PRE/1334] N88-30179
Lava thicknesses: Implications for rheological and crustal development N88-30490
CLEAR AIR TURBULENCE
Utilization of a single clear-air Doppler radar beam to measure vertical divergence
[AD-A195543] N88-30271
CLIMATE
Activities report of the World Meteorological Organization
[WMO-689] N88-30265
CLIMATOLOGY
Energy budget and ground temperatures in hot regions
[AD-A196298] N88-30268
CLINICAL MEDICINE
Vanderbilt free electron laser project in biomedical and materials research
[AD-A195961] N88-30121
CLOSURES
Development of a more general Reynolds stress closure for swirling flow
[AD-A195121] N88-30092
Syntactic closures
[AD-A195921] N88-30311
CLOUD PHYSICS
Global vertical mass transport by clouds: A two-dimensional model study
[CM-74] N88-30192
Microphysical processes in cloud layers of Venus N88-30522
CLUTTER
The effect of equatorial ionospheric irregularities on the performance of a south-looking OTH-B (Over-The-Horizon-Backscatter) radar
[AD-A195090] N88-30018
CMOS
The effects of total dose on the SEU sensitivity of CMOS static RAMS — single event upset (SEU), satellite components
[AERE-R-12779] N88-30401
A system study with an infrared sensitive microelectronic image sensor
[FOA-C-30481-3.1] N88-30407
COASTS
Doppler radar analysis of coastal marine atmospheric boundary layer structure during a cold air outbreak
[AD-A196023] N88-30261
COATINGS
Iridium-coated rhenium thrusters by CVD
[NASA-TM-101309] N88-29874
Ultrasonic detection of diffusion and adhesion loss N88-29967
Photoacoustic Fourier transform infrared spectroscopy. An early detection technique for coatings degradation N88-29968
Predicting the durability of adhesives and coatings by remote detection of hidden defects and coating-thickness irregularities: A theoretical and numerical study N88-29972
An electrochemical impedance spectroscopy study of reactions at the metal/coating interface N88-29975
Containment of a silicone fluid free surface in reduced gravity using barrier coatings
[NASA-TM-101314] N88-30072
COCKPITS
Use of color CRTs (Cathode Ray Tubes) in aircraft cockpit: A literature search, revision B
[AD-A195062] N88-29797
COGNITION
Advancement of latent trait theory
[AD-A194302] N88-30289
Contributions to engineering models of human-computer interaction, volume 1
[AD-A195590] N88-30295
The bounded rationality constraint: Experimental and analytical results
[AD-A195897] N88-30318
COHERENT SCATTERING
Ionospheric radio and propagation: Waves in plasmas N88-30030
COLD TRAPS
Spontaneous force optical traps
[AD-A196103] N88-30114
COLLOIDS
Preliminary investigation of flow modeling during solid propellant processing
[AD-A196168] N88-29987
COLOR
Use of color CRTs (Cathode Ray Tubes) in aircraft cockpit: A literature search, revision B
[AD-A195062] N88-29797
COLOR CODING
Use of color CRTs (Cathode Ray Tubes) in aircraft cockpit: A literature search, revision B
[AD-A195062] N88-29797
COLOR VISION
Central serous chorioretinopathy in USAF aviators: A review
[AD-A195697] N88-30280
Eye movements and spatial pattern vision
[AD-A195496] N88-30290
COLUMBUS SPACE STATION
Study on long-term evolution towards European manned spaceflight. Volume 1: Executive summary
[ERNO-OX1-002/88-VOL-1] N88-29827
Studies on rocket exhaust plumes and impingement effects related to the Columbus Space Station program: Executive summary
[DFVLR-IB-222-88-A-12] N88-29862

The LTPP communication processor — Columbus and Hermes
[CL/CP/SES/FR/004] N88-30326
Candidate functions for advanced technology implementation in the Columbus mission planning environment N88-30340
COMBINATORIAL ANALYSIS
The combinatorics of object recognition in cluttered environments using constrained search
[AD-A196224] N88-30364
COMBUSTIBLE FLOW
Modeling and experimental study of a reactive flow confined with well injection N88-29946
COMBUSTION
Particle sizing in combustion systems, using scattered laser light
[AD-A196231] N88-29953
Optical measurements of soot and temperature profiles in premixed propane-oxygen flames
[NASA-TM-101343] N88-29997
COMBUSTION CHAMBERS
Automatic data retrieval from rocket motor holograms
[AD-A195586] N88-29864
Combustion and fuels in gas turbine engines
[AGARD-CP-422] N88-29910
Comparison of the performance of a reverse flow annular combustion chamber under low and high pressure conditions N88-29923
Flow characteristics of a model annular combustor N88-29924
Particle size measurements in sooting combustion systems N88-29931
Numerical models for analytical predictions of combustor aerothermal performance characteristics N88-29935
Gas turbine combustion modeling N88-29936
Three-dimensional gas turbine combustor modelling N88-29937
Numerical modeling of combustion processes in gas turbines N88-29939
Three-dimensional combustor predictors: A comparison of equilibrium and laminar flamelet chemistry models N88-29940
The effect of particle properties on radiative heat transfer N88-29941
Analysis of the flow through double swirl airblast atomizers N88-29949
The behaviour of synthetic fuels in a small transparent combustor N88-29950
A small annular combustor of high power density, wide operating range and low manufacturing cost N88-29951
Transition mixing study empirical model report
[NASA-CR-182139] N88-30076
COMBUSTION CHEMISTRY
Experiments and modeling of multi-component fuel behavior in combustion
[AD-A195011] N88-29896
Gas phase combustion chemistry of nitramine propellants
[AD-A195082] N88-29902
COMBUSTION EFFICIENCY
Atomization of alternative fuels N88-29913
Spray performance of a vaporizing fuel injector N88-29919
The characterizatin of combustion by fuel composition: Measurements in a small conventional combustor N88-29920
High performance turbofan afterburner systems N88-29922
Comparison of the performance of a reverse flow annular combustion chamber under low and high pressure conditions N88-29923
COMBUSTION PHYSICS
Numerical modeling of combustion processes in gas turbines N88-29939
Modeling the stability of a turbulent premixed flame, downstream from a step by a Lagrangian method N88-29943
Modeling and experimental study of a reactive flow confined with well injection N88-29946
COMBUSTION PRODUCTS
Automatic data retrieval from rocket motor holograms
[AD-A195586] N88-29864
Gas turbine smoke measurement: A smoke generator for the assessment of current and future techniques N88-29930
Rates of formation of soot from hydrocarbon flames and its destruction N88-29933
The influence of pressure on soot formation N88-29934
COMBUSTION STABILITY
High performance turbofan afterburner systems N88-29922
COMBUSTION TEMPERATURE
Flow characteristics of a model annular combustor N88-29924
COMETARY ATMOSPHERES
Extended atmospheres of outer planet satellites and comets
[NASA-CR-183157] N88-30572
COMETS
Did the greenhouse effect kill the dinosaurs N88-30484
COMFORT
Study of human factors engineering criteria for Extra Vehicular Activity (EVA) systems, volume 2
[STF23-F87025-VOL-2] N88-30293
COMMAND AND CONTROL
Definition of common support equipment and space station interface requirements for IOC model technology experiments
[NASA-TM-100656] N88-29856
The design of an intelligent multidisk control module for VME bus based systems
[AD-A195587] N88-30303
Automated satellite control in Ada N88-30336
COMMERCIAL AIRCRAFT
Report to Congress on the effectiveness of the Civil Aviation Security Program
[AD-A195282] N88-29784
COMMUNICATION
Barriers to Information Transfer and Approaches Toward Their Reduction
[AGARD-CP-430] N88-30458
Linguistic and cultural barriers to the transfer of information N88-30459
Political and economic barriers to information transfer N88-30460
COMMUNICATION EQUIPMENT
Doppler-corrected differential detection system
[NASA-CASE-NPO-16987-1-CU] N88-30001
COMMUNICATION NETWORKS
Performance analysis of k-ary n-cube interconnection networks
[AD-A195542] N88-30010
Design of a self-timed VLSI multicomputer communication controller
[AD-A194567] N88-30014
Comparative analysis of passive communications satellites employing the SHF and HF spectrum for use in a strategic role
[AD-A194682] N88-30019
Integrating images, applications, and communications networks, volume 5
[AD-A195854] N88-30452
COMMUNICATION SATELLITES
PSDE/SAT 2: Preliminary spacecraft configuration study, executive summary
[ESA-CR(P)-2618] N88-29840
Comparative analysis of passive communications satellites employing the SHF and HF spectrum for use in a strategic role
[AD-A194682] N88-30019
COMPARISON
A model for architectural comparison
[AD-A195993] N88-30302
Design and performance analysis of a relational replicated database system
[AD-A196290] N88-30456
Plasma of earth's magnetosphere ring currents. Model compared with results of AMPTE/CCE experiment N88-30515
COMPOSITE MATERIALS
Creep of carbon yarn and carbon-carbon composites at high temperatures and high stresses
[AD-A195224] N88-29878
An improved boundary force method for analyzing cracked anisotropic materials
[NASA-TM-101495] N88-29879
ZT imaging system for layered thin wall structures
[AD-A195466] N88-29954
Polymer-ceramic composites
[AD-A195789] N88-29983
Piezoelectric and electrostrictive materials for transducer applications, volume 1
[AD-A194957] N88-30096
Experimental aspects of using time-averaged holographic interferometry to detect barely visible impact damage in a graphite/epoxy composite plate
[AD-A194418] N88-30097
Application of nondestructive testing techniques to materials testing
[AD-A195716] N88-30138
An organometallic route to micron-sized whiskers of zinc sulfide
[AD-A195889] N88-30414
COMPOSITE PROPELLANTS
Thermomechanical computations for GAP, a high energy binder for composite propellants
[FOA-C-20718-2.1] N88-29988
COMPOSITE STRUCTURES
Damage initiation in the short beam shear test of composite materials using stiffness reduction
[AD-A194880] N88-29883
Evaluation of bond testing equipment for inspection of Army advanced composite airframe structures
[AD-A195795] N88-29885
Experimental aspects of using time-averaged holographic interferometry to detect barely visible impact damage in a graphite/epoxy composite plate
[AD-A194418] N88-30097
COMPRESSIBILITY
Survey on nonlinear effects N88-29757
Compression pylon
[NASA-CASE-LAR-13777-1] N88-29789
COMPRESSIBLE FLOW
Analysis method for the production of Reynolds stresses in compressible turbulent flow (fluid mechanics)
[NASA-TT-20330] N88-30088
Development of a more general Reynolds stress closure for swirling flow
[AD-A195121] N88-30092
COMPRESSING
Nonlinear stress-strain and inelastic rebound with exponential stiffness
[AD-A195667] N88-30159
COMPRESSOR BLADES
Empirical flutter prediction method
[AD-A195689] N88-29810
COMPUTATION
Calculation of non-stationary aerodynamic forces in the near sonic range
[NASA-TT-20310] N88-29782
A new computational capability for ramjet projectiles
[AD-A196061] N88-29812
Multilevel computational theory of stereoscopic visual image processing
[AD-A195331] N88-30288
A model for architectural comparison
[AD-A195993] N88-30302
Nonequilibrium flow computations. 1: An analysis of numerical formulations of conservation laws
[NASA-CR-177489] N88-30384
Regularity and numerical solution of eigenvalue problems with piecewise analytic data
[AD-A194993] N88-30387
Instrumentation for computational statistical research
[AD-A195887] N88-30390
COMPUTATIONAL FLUID DYNAMICS
The computation of flow past an oblique wing using the thin-layer Navier-Stokes equations
[NASA-TM-88317] N88-29774
Computational methods for the problems of the tip vortex
[NASA-CR-181438] N88-29775
Recent advances in transonic computational aeroelasticity
[NASA-TM-100663] N88-29778
Gas turbine combustion modeling N88-29936
Numerical modeling of combustion processes in gas turbines N88-29939
Numerical simulation of nozzle flows
[AD-A195144] N88-30064
The viscous flow on surfaces with streamline riblets
[ESA-TT-1091] N88-30067
Knowledge-based flow field zoning
[NASA-TM-101023] N88-30314
Convergence acceleration for vector sequences and applications to computational fluid dynamics
[NASA-TM-101327] N88-30377
COMPUTATIONAL GRIDS
The computation of flow past an oblique wing using the thin-layer Navier-Stokes equations
[NASA-TM-88317] N88-29774
Knowledge-based flow field zoning
[NASA-TM-101023] N88-30314
Generation of surface grids through elliptic partial differential equations for aircraft and missile configurations
[AD-A195639] N88-30378
COMPUTER AIDED DESIGN
Special Course on Missile Aerodynamics
[AGARD-R-754] N88-29755
Semiempirical methods for airbreathing missiles N88-29783
Study on conceptual design of spacecraft using Computer Aided Engineering (CAE)
[SNIAS-920-CA/TS] N88-29841
MANIP — spacecraft modeling program
[MANIP-217A] N88-29855
Development of a general software package for the analysis and synthesis of planar antenna arrays for space applications
[S-247-02] N88-30000

Computer-Aided Structural Engineering (CASE) project. Development of design formulas for ribbed mat foundations on expansive soils
[AD-A194807] N88-30307
Computer-Aided Structural Engineering (CASE) project. Computer program for analysis of planar grid structures (CGRID), user's guide
[AD-A195977] N88-30317
Geometric modeling for computer aided design
[NASA-CR-183161] N88-30320
The triangle: A multiprocessor architecture for fast curve and surface generation
[AD-A195882] N88-30324
The P-3 Scheduling Support System (P-3 S3)
[AD-A194824] N88-30450

COMPUTER AIDED MANUFACTURING
Utilizing dynamic stability of orient parts
[AD-A195730] N88-30397

COMPUTER GRAPHICS
Numerical simulation of nozzle flows
[AD-A195144] N88-30064
Implementation of the NCAR (National Centre for Atmospheric Research) graphics package at ARL (Aeronautical Research Laboratory)
[AD-A195163] N88-30193
Geometric modeling for computer aided design
[NASA-CR-183161] N88-30320

COMPUTER NETWORKS
Signals and systems N88-30026
Telescience testbed pilot program
[NASA-CR-183207] N88-30309
Performance analysis of FDDI
[NASA-CR-183206] N88-30321
The LTPP communication processor — Columbus and Hermes
[CL/CP/SES/FR/004] N88-30328
Knowledge-based integrated information systems engineering: Highlights and bibliography. Knowledge-Based Integrated Information Systems Engineering (KBIISE) Project, volume 1
[AD-A195850] N88-30449
Integrating images, applications, and communications networks, volume 5
[AD-A195854] N88-30452
Knowledge-Based Integrated Information Systems Development Methodologies Plan. Knowledge-Based Integrated Information Systems Engineering (KBIISE) report, volume 2
[AD-A195851] N88-30455

COMPUTER PROGRAMMING
A standard library for modeling satellite orbits on a microcomputer
[AD-A195759] N88-29830
Syntactic closures
[AD-A195921] N88-30311

COMPUTER PROGRAMS
Space marching Euler solvers N88-29759
Prediction of dynamic derivatives N88-29761
Prediction of base-flows N88-29765
Computer programs for generation of NASTRAN and VIBRA-6 aircraft models
[AD-A195467] N88-29792
A new computational capability for ramjet projectiles
[AD-A196061] N88-29812
N-version software demonstration for digital flight controls
[NASA-CR-181483] N88-29815
Computer programs for calculation of sting pitch and roll angles required to obtain angles of attack and sideslip on wind tunnel models
[NASA-TM-100659] N88-29820
Development of computer-controlled thermogravimetric instrumentation for measurement of environmental and high temperature volatilization and desorption of contaminants from polymeric materials
[AD-A195934] N88-29900
Scattering impulse response synthesis using random noise illumination: Initial concept evaluation
[AD-A195086] N88-30034
DATATRAN: Datum transformation software
[AD-A195723] N88-30175
Computer-Aided Structural Engineering (CASE) project. Computer program for analysis of planar grid structures (CGRID), user's guide
[AD-A195977] N88-30317
The elvaN: A forward-looking interactive orbital trajectory plotting tool for use with proximity operations (PROX OPS) and other maneuvers: Description and user's manual
[NASA-CR-177490] N88-30327
Automatic qualitative analysis of ordinary differential equations using piecewise linear approximations
[AD-A196310] N88-30379
Linguistic-technical aspects of machine translation N88-30461

COMPUTER STORAGE DEVICES
Laser sensing for identification and control of distributed parameter systems
[AD-A195886] N88-30124

COMPUTER SYSTEMS DESIGN
Telescience testbed pilot program
[NASA-CR-183207] N88-30309
Scheme86: A system for interpreting SCHEME
[AD-A195931] N88-30319
The LTPP communication processor — Columbus and Hermes
[CL/CP/SES/FR/004] N88-30328
The P-3 Scheduling Support System (P-3 S3)
[AD-A194824] N88-30450

COMPUTER SYSTEMS PERFORMANCE
A new computational capability for ramjet projectiles
[AD-A196061] N88-29812
Telescience testbed pilot program
[NASA-CR-183207] N88-30309

COMPUTER SYSTEMS PROGRAMS
N-version software demonstration for digital flight controls
[NASA-CR-181483] N88-29815
Development of a general software package for the analysis and synthesis of planar antenna arrays for space applications
[S-247-02] N88-30000
Improvements of DCAP 1, phase 2-3/A
[D2-RP-AI-106] N88-30325

COMPUTER TECHNIQUES
A static scheduler for the computer aided prototyping system: An implementation guide
[AD-A194340] N88-30322

COMPUTER VISION
Using primal sketch primitives as the basis for the Hough transform
[INPE-4564-PRE/1305] N88-30310
An automated computerized vision technique for determination of three-dimensional object geometry N88-30348

COMPUTERIZED SIMULATION
Numerical methods: Euler time dependent solver N88-29760
A fiber optic collective flight control system for helicopters
[AD-A195406] N88-29818
Minimum-complexity helicopter simulation math model
[NASA-CR-177476] N88-29819
Experiments and modeling of multi-component fuel behavior in combustion
[AD-A195011] N88-29896
Numerical field model simulation of full scale fire tests in a closed spherical/cylindrical vessel
[AD-A195067] N88-29998
Track performance considerations for monopulse radars
[AD-A196232] N88-30007
The focal plane reception pattern calculation for a paraboloidal antenna with a nearby fence
[NASA-TM-100691] N88-30039
The 1988 Goddard Conference on Space Applications of Artificial Intelligence
[NASA-CP-3009] N88-30330
Automatic mathematical modeling for real time simulation system N88-30356
A simulation engine: Combining an expert system with a simulation language N88-30358
Adaptive control in positioning a rigid-flexible robot arm
[AD-A195194] N88-30367
Knowledge based simulation: An artificial intelligence approach to system modeling and automating the simulation life cycle
[AD-A195838] N88-30372
Design and performance analysis of a relational replicated database system
[AD-A196290] N88-30456
The origin of the moon: Further studies of the giant impact N88-30474

COMPUTERS
Heavy ion and proton tests for subsystem upset
[AD-A195267] N88-30442

CONCURRENT PROCESSING
Performance analysis of k-ary n-cube interconnection networks
[AD-A195542] N88-30010
Performance prediction of concurrent systems
[NASA-CR-183175] N88-30312

CONDENSERS
Study of toluene rotary fluid management device and shear flow condenser performance for a space-based organic Rankine power system
[NASA-CR-180685] N88-29872

CONFERENCES
The NASA Electric Propulsion Program
[NASA-TM-101324] N88-29859
Performance Prediction for Coatings. Proceedings of a Workshop
[AD-A188973] N88-29966
The 1988 Goddard Conference on Space Applications of Artificial Intelligence
[NASA-CP-3009] N88-30330
Barriers to Information Transfer and Approaches Toward Their Reduction
[AGARD-CP-430] N88-30458
Information technology to facilitate group interaction N88-30463
NASA MEVTV Program Working Group Meeting: Volcanism on Mars
[NASA-CR-183074] N88-30487
Workshop on the Origins of Solar Systems
[NASA-CR-183025] N88-30536

CONGRESSIONAL REPORTS
Report to Congress on the effectiveness of the Civil Aviation Security Program
[AD-A195282] N88-29784

CONICAL BODIES
Numerical calculations of the response of a spinning spheroidal payload to coning motion
[AD-A195890] N88-30059

CONICAL FLOW
Numerical calculations of the response of a spinning spheroidal payload to coning motion
[AD-A195890] N88-30059

CONSERVATION EQUATIONS
Experimental and analytical study of two-phase flow in zero gravity
[AD-A195223] N88-29993

CONSERVATION LAWS
An analysis of finite-difference and finite-volume formulations of conservation laws
[NASA-CR-177416] N88-30071
Nonequilibrium flow computations. 1: An analysis of numerical formulations of conservation laws
[NASA-CR-177489] N88-30384

CONSTITUTIVE EQUATIONS
Constitutive modeling for isotropic materials
[NASA-CR-182132] N88-29811
Anisotropic constitutive modeling for nickel-base single crystal superalloys
[NASA-CR-182157] N88-29961
Stability of stick-slip phenomenon by using constitutive friction laws of Dietrich and Ruina
[ILR-MITT-197] N88-30127

CONSTRAINTS
The bounded rationality constraint: Experimental and analytical results
[AD-A195897] N88-30318

CONSTRUCTION
Structure and dynamics of solutions of lithium salts relevant to battery construction
[AD-A195399] N88-30044

CONTACT LENSES
A field study on soft contact lens wear in USAF military transport aircraft
[AD-A195962] N88-30285

CONTAMINANTS
Development of computer-controlled thermogravimetric instrumentation for measurement of environmental and high temperature volatilization and desorption of contaminants from polymeric materials
[AD-A195934] N88-29900

CONTAMINATION
Experimental evaluation of resistojet thruster plume shields
[NASA-TM-101363] N88-29868
Contamination and distortion of steady flow field induced by discrete frequency disturbances in aircraft gas engines
[AD-A195440] N88-30069

CONTINENTAL DRIFT
Constraints on continental accretion from sedimentation N88-30202
Metamorphic P-T paths and Precambrian crustal growth in East Antarctica N88-30218

CONTINENTAL SHELVES
Mid to late proterozoic magmatism within Northeastern North America and its iplications for the growth of the continental crust N88-30229

CONTINENTS
Workshop on the Growth of Continental Crust
[NASA-CR-183073] N88-30201
Constraints on continental accretion from sedimentation N88-30202
Recycling of lower continental crust through foundering of cumulates from contaminated mafic intrusions N88-30204
Growth of continental crust: Clues from Nd isotopes and Nb-Th relationships in mantle-derived magmas N88-30205
An illustration of the complexity of continent formation N88-30207

The Kerala Khondalite Belt (KKB) of Southern India: An ensialic mobile belt N88-30208
Genesis of archean granitoids in the Pilbara block and implications for crustal growth N88-30210
Does subduction zone magmatism produce average continental crust N88-30214
Decoupled Rb-Sr and Sm-Nd isotopic evolution of the continental crust N88-30216
The growth of continents and some consequences since 1.5 Ga N88-30220
Thermal models pertaining to continental growth N88-30230
Growth of the lower continental crust N88-30236
Continental crustal formation and recycling: Evidence from oceanic basalts N88-30238
Physical processes in the growth of the continental crust N88-30240
Continental growth through time by underplating of subducted oceanic crust: Evidence from kimberlites in South Africa and SW Pacific N88-30244
The growth of the continental crust: Constraints from radiogenic isotope geochemistry N88-30245
Mineralization through geologic time: Evolution of continental crust N88-30250
Growth of the continental crust: A planetary-mantle perspective N88-30251
The effect of thicker oceanic crust in the Archaean on the growth of continental crust through time N88-30254

CONTINUOUS RADIATION
Aeronomic problems of the molecular oxygen photodissociation. Part 3: Solar spectral irradiances in the region of the O2 Herzberg continuum, Schumann-Runge bands and continuum
[AERONOMICA-ACTA-A-332-1988] N88-29697
Aeronomic problems of molecular oxygen photodissociation. Part 4: The various parameters for the Herzberg continuum
[AERONOMICA-ACTA-A-333-1988] N88-29955

CONTINUUM MECHANICS
Theory of filtering and control with application to control of large space structures
[AD-A195500] N88-29851
Damage initiation in the short beam shear test of composite materials using stiffness reduction
[AD-A194880] N88-29883

CONTOURS
Implementation of the NCAR (National Centre for Atmospheric Research) graphics package at ARL (Aeronautical Research Laboratory)
[AD-A195163] N88-30193
A digital terrain model system for a microcomputer
[INPE-4610-PRE/1333] N88-30316

CONTROL MOMENT GYROSCOPES
An approach to CMG steering using feedback linearization
[NASA-CR-183172] N88-30369

CONTROL SIMULATION
Four-axis side-arm flight control simulator investigation
[AD-A196026] N88-30294

CONTROL SYSTEMS DESIGN
Space structure (dynamics and control) theme development
[NASA-TM-100597] N88-29850
Aircraft battery state of charge and charge control system
[AD-A194979] N88-30052
ARC length control for plasma welding
[NASA-CASE-MSC-20900-1] N88-30131
Robust design of distributed controllers for large flexible space structures
[NASA-CR-183202] N88-30134
The design of an intelligent multidisk control module for VME bus based systems
[AD-A195587] N88-30303
A shared-world conceptual model for integrating space station life sciences telescience operations N88-30333
Artificial intelligence in a mission operations and satellite test environment N88-30334
Automated space vehicle control for rendezvous proximity operations N88-30335
Automated satellite control in Ada N88-30336
Low level image processing techniques using the pipeline image processing engine in the flight telerobotic servicer N88-30346

CONTROL THEORY
Theory of filtering and control with application to control of large space structures
[AD-A195500] N88-29851
K(sup th)-order extended linearization
[AD-A194786] N88-30363
Analytical methods in stochastic control and nonlinear filtering
[AD-A194272] N88-30388

CONTROLLABILITY
Advances in Flying Qualities
[AGARD-LS-157] N88-29735
Advances in flying qualities: Concepts and criteria for a mission oriented flying qualities specification N88-29739
A second look at MIL prime flying qualities requirements N88-29740
The optimal control pilot model and applications N88-29741
The role of simulation in flying qualities and flight control system related development N88-29742
An analysis of lateral-directional handling qualities and Eigenstructure of high performance aircraft
[AD-A194874] N88-29814
Minimum-complexity helicopter simulation math model
[NASA-CR-177476] N88-29819

CONTROLLERS
Robust design of distributed controllers for large flexible space structures
[NASA-CR-183202] N88-30134
An intelligent training system for space shuttle flight controllers N88-30331

CONVECTION
Influence of the convection on evaporation and combustion of a fuel droplet N88-29948

CONVECTIVE HEAT TRANSFER
Impact of ETO propellants on the aerothermodynamic analyses of propulsion components
[NASA-TM-101303] N88-30094

CONVERGENCE
Convergence acceleration for vector sequences and applications to computational fluid dynamics
[NASA-TM-101327] N88-30377
Convergence of Galerkin approximations for operator Riccati equations: A nonlinear evolution equation approach
[NASA-CR-181706] N88-30386

COOLING
Spontaneous force optical traps
[AD-A196103] N88-30114

COORDINATES
DATATRAN: Datum transformation software
[AD-A195723] N88-30175

COPLANARITY
Confirmation of slow-waves in a crosstie overlay coplanar waveguide and its application to band-reject gratings and reflectors
[AD-A194981] N88-30011

COPPER
An electrochemical impedance spectroscopy study of reactions at the metal/coating interface N88-29975

COPPER OXIDES
Theory of superconductivity in oxides
[AD-A195647] N88-30432

CORNEA
A field study on soft contact lens wear in USAF military transport aircraft
[AD-A195962] N88-30285

CORRELATION
Performance of DS/SSMA communications in impulsive channels. Part 1: Correlation receivers
[AD-A195712] N88-30021

CORRELATORS
Evaluation of multi-focus holographic lenses
[AD-A196167] N88-30110

CORROSION
Some effects of nitrates on the tensile properties of Al 7075-T7351
[AD-A195118] N88-29965
Performance Prediction for Coatings. Proceedings of a Workshop
[AD-A188973] N88-29966
Degradation of protective coatings on steel in corrosive environments N88-29969
Evaluation of organic coating deterioration and substrate corrosion in seawater using electrochemical impedance measurements N88-29976
Alternative immersion accelerated testing of coating systems for Naval shoreline facilities N88-29977
Zinc filled coatings N88-29978

CORROSION PREVENTION
Degradation of protective coatings on steel in corrosive environments N88-29969
Reduced time frame for predicting coating performance N88-29979

CORROSION RESISTANCE
Performance Prediction for Coatings. Proceedings of a Workshop
[AD-A188973] N88-29966
Electrochemical evaluation of the long term corrosion resistance of polymer coated steel N88-29974
Zinc filled coatings N88-29978
Reduced time frame for predicting coating performance N88-29979

CORROSION TESTS
Reduced time frame for predicting coating performance N88-29979

COSMIC RAYS
Research in particle and gamma-ray astrophysics
[NASA-CR-183126] N88-30566
The Single Event Upset (SEU) test facility on the Hardwell tandem generator for cosmic ray simulation
[AERE-R-12896] N88-30580

COSMOCHEMISTRY
Workshop on the Origins of Solar Systems
[NASA-CR-183025] N88-30536
Nebular processes recorded in chondritic meteorites N88-30541
Cosmochemical trends of volatile elements in the solar system N88-30542

COSMOLOGY
Activities in astrophysics
[INPE-4582-PRE/1316] N88-30570

COSMOS SATELLITES
Determining near-water wind speed using radar data from Cosmos-1500 artificial earth satellite N88-30524

COSPAS
KOSPAS-SARSAT satellites used for ocean current study N88-30534

COST ANALYSIS
Aircraft airframe cost estimating relationships: Study approach and conclusions
[R-3255-AF] N88-29795
The cost and performance implications of reliability improvements in the F-16A/B
[AD-A195096] N88-29796
Aircraft avionics and missile system installation cost study. Volume 2: Appendices F and G
[AD-A195372] N88-29801
Centaur operations at the space station: Cost and transportation analysis
[NASA-CR-182128] N88-29835
Space systems cost study
[AD-A196024] N88-30469

COST EFFECTIVENESS
Report to congress on the strategic defense system architecture
[AD-A195476] N88-30393

COST ESTIMATES
Aircraft avionics and missile system installation cost study. Volume 2: Appendices F and G
[AD-A195372] N88-29801

COST REDUCTION
Space systems cost study
[AD-A196024] N88-30469

COSTS
Artificial intelligence costs, benefits, risks for selected spacecraft ground system automation scenarios N88-30332
Information technology to facilitate group interaction N88-30463

COUETTE FLOW
The aspect ratio dependence of the attractor dimension in Taylor-Couette flow
[AD-A196297] N88-30065

COUPLED MODES
Role of ordinary to extraordinary mode wave coupling in ionospheric heating experiments
[AD-A195335] N88-30017

COUPLINGS
Multi-metallic galvanic corrosion
[AD-A195995] N88-29963

CRACK GEOMETRY
Wide range stress intensity factor expression for an edge-cracked round bar bend specimen
[AD-A196285] N88-30147

CRACK INITIATION
Thermal stress analysis in PMR-15 carbon fibre laminates
[ETN-88-93123] N88-29886

CRACK OPENING DISPLACEMENT
Ultrasonic method and apparatus for determining crack opening load
[NASA-CASE-LAR-13889-1] N88-30160

CRACK PROPAGATION
Fatigue crack growth characteristics of ARALL (trademark)-1
[AD-A196185] N88-29889
Stress intensity factors for cracked metallic structures under rapid thermal loading
[AES-8609709F-1] N88-29962
Modeling of micromechanisms of fatigue and fracture in hybrid materials
[AD-A195604] N88-30142
Automated early fatigue damage sensing system
[AD-A195717] N88-30143
Fatigue crack propagation: Probabilistic modeling and statistical analysis
[AD-A195885] N88-30155

The development of acoustic emission for structural integrity monitoring of aircraft
[AD-A196264] N88-30396

CRACKING (FRACTURING)
An improved boundary force method for analyzing cracked anisotropic materials
[NASA-TM-101495] N88-29879

CRACKS
Obtaining stress intensity factors on cracks, by means of fitting techniques on numerical results calculated with the finite element method N88-30153

CRASHES
Centralized class A flight mishap investigation
[AD-A194397] N88-29786

CRATERING
Early intense cratering: Effects on growth of earth's crust N88-30219

CRATONS
Archean crustal evolution of the northern North China Craton N88-30235
Evolution of the Dharwar Craton: A terrain of early Archean crustal stability, long term orogenic cycles and large scale paleobiological activity N88-30241
Crustal underplating in the North American Craton: Evidence from the Petrogenesis of anorthositic rocks in the Middle Proterozoic Midcontinent Rift System N88-30252

CRAY COMPUTERS
Supermap for Cray FORTRAN: A user's guide
[NASA-CR-177410] N88-30308

CREWS
Human factors report on information management requirements for next-generation manned bombers
[AD-A195870] N88-30296

CRITERIA
Accuracy criteria for evaluating supersonic aerodynamic coefficient predictions N88-29756

CRITICAL POINT
Fluid physics double rack --- Spacelab
[SD-TN-AI-012] N88-29992

CROP GROWTH
LANDSAT TM and agrometeorological data for wheat yield estimation at the farm level
[INPE-4591-PRE/1321] N88-30180

CROSSED FIELDS
Vortex formation and particle transport in a cross-field plasma sheath
[AD-A194838] N88-30425

CRYOGENIC COOLING
Development of a unit cell for a Ge:Ga detector array
[NASA-CR-177445] N88-30100

CRYOGENIC FLUID STORAGE
Technology requirements for an orbiting fuel depot: A necessary element of a space infrastructure
[NASA-TM-101370] N88-29845

CRYOGENIC ROCKET PROPELLANTS
Breadboard RL10-2B low-thrust operating mode (second iteration) test report
[NASA-CR-182160] N88-29867

CRYSTAL DEFECTS
Streaking images that appear only in the plane of diffraction in undoped GaAs single crystals: Diffraction imaging (topography) by monochromatic synchrotron radiation
[NASA-CR-183267] N88-30437

CRYSTAL GROWTH
Growth and characterization of materials for tunable lasers in the near infrared spectral region
[NASA-CR-183132] N88-30113
Growth of GaAs crystals by the Heat Exchanger Method for microwave device applications
[AD-A196028] N88-30435

CRYSTAL OSCILLATORS
Specifications and performance of ultrastable oscillators in the DORIS orbitography and positioning system
[ETN-88-92761] N88-29831

CRYSTAL RECTIFIERS
Pierce diode with external circuit. Part 3: Chaotic behavior
[AD-A194837] N88-30041

CRYSTAL STRUCTURE
Crystal structures of ordered carbon metal alloys
[AD-A195597] N88-29959
Discovery of a low temperature form of TAGN (Triaminoguanidinium Nitrate)
[AD-A196059] N88-29989
Crystal structure and density of helium to 232 kbar N88-30481

CRYSTAL SURFACES
Attenuated total reflectance FT-IR spectroscopy to measure interfacial reaction kinetics at silica surfaces
[AD-A196330] N88-29908

CRYSTALLINITY
A method for the quantitative determination of crystalline phases by X-ray
[NASA-TT-20324] N88-30444

CRYSTALS
General equations for the motions of ice crystals and water drops in gravitational and electric fields
[NASA-CR-183229] N88-30070

CULTURE (SOCIAL SCIENCES)
Linguistic and cultural barriers to the transfer of information N88-30459

CURVES
The triangle: A multiprocessor architecture for fast curve and surface generation
[AD-A195882] N88-30324

CUTTING
Microcircuit trace cutting with focused ion beams
[AD-A196030] N88-30050

CYCLES
The OFP (Operational Flight Program) update cycle needs you
[AD-A194910] N88-29798

CYCLIC LOADS
An investigation of constitutive models for predicting viscoplastic response during cyclic loading
[AD-A194875] N88-30163

CYCLONES
Passive microwave measurements of water vapor fields and rain for locating fronts in cyclonic storms
[AD-A195632] N88-30267

CYCLOTRON RESONANCE
Ion kinetics in silane plasmas
[AD-A196202] N88-30423

CYCLOTRON RESONANCE DEVICES
The study of hydromagnetic waves and RF heating using the TORTUS tokamak, the development of diagnostic techniques based on submillimeter lasers and the gyrotron, and gas discharge N88-30419

CYLINDRICAL BODIES
Additional fracture and strength test results for A723 steel and 38644 titanium
[AD-A196329] N88-29960
The aspect ratio dependence of the attractor dimension in Taylor-Couette flow
[AD-A196297] N88-30065

CYLINDRICAL SHELLS
Stresses in cylindrical shells with tangential nozzles submitted to external loads and internal pressure
[CRIF-MT-172] N88-30146
Large displacement and rotational formulation for laminated cylindrical shells including parabolic transverse shear
[AD-A194871] N88-30158
Behaviour and hysteresis losses of irreversible type-2 superconducting cylindrical shell
[DE88-702708] N88-30434

CYTOCHROMES
Cytochrome electron transfer and biomolecular electronics
[AD-A195482] N88-30277

D

D REGION
On formulating a simple D-region model
[AD-A195841] N88-30197
Photochemistry of ionospheric D-region with injection of nitrogen oxides N88-30499

DAMAGE
Damage initiation in the short beam shear test of composite materials using stiffness reduction
[AD-A194880] N88-29883
Automated early fatigue damage sensing system
[AD-A195717] N88-30143
An investigation of constitutive models for predicting viscoplastic response during cyclic loading
[AD-A194875] N88-30163

DAMPERS
Rotational evolution of dynamically symmetric gyrostat with internal friction N88-30509

DAMPING
Analytical and experimental studies of beam waveguide absorbers for structural damping
[AD-A195085] N88-30144

DAMPING TESTS
Analytical and experimental studies of beam waveguide absorbers for structural damping
[AD-A195085] N88-30144

DATA ACQUISITION
Acquisition of gust statistics from AIDS-recorded data N88-29733
MIZEX (marginal ice zone experiment) 1987 SAR (Synthetic Aperture Radar) data summary
[AD-A195560] N88-30035
Laser sensing for identification and control of distributed parameter systems
[AD-A195886] N88-30124
Microwave remote sensing at INPE (Institute for Space Research) Brazil: Concepts and future prospects of soil moisture studies
[INPE-4569-PRE/1310] N88-30178
China's acquisition and use of foreign aviation technology
[AD-A194827] N88-30471

DATA BASE MANAGEMENT SYSTEMS
Space shuttle phase B wind tunnel model and test information. Volume 3: Launch configuration
[NASA-CR-178416-VOL-3-PT-2] N88-29744
Space shuttle phase B wind tunnel model and test information. Volume 1: Booster configuration
[NASA-CR-178414-VOL-1-PT-1] N88-29745
Space shuttle phase B wind tunnel model and test information. Volume 1: Booster configuration
[NASA-CR-178414-VOL-1-PT-2] N88-29770
An operations manual for the digital data system
[NASA-CR-181688] N88-30329
The second generation intelligent user interface for the crustal dynamics data information system N88-30352
The P-3 Scheduling Support System (P-3 S3)
[AD-A194824] N88-30450
Integrating images, applications, and communications networks, volume 5
[AD-A195854] N88-30452

DATA BASES
The advice taker/inquirer: A system for high-level acquisition of expert knowledge N88-30359
Partitioned storage for temporal databases
[AD-A195093] N88-30451
Technical opinions regarding knowledge-based integrated information systems engineering, volume 8
[AD-A195857] N88-30454
Design and performance analysis of a relational replicated database system
[AD-A196290] N88-30456

DATA COMPRESSION
Compression and decompression of imaging sensor signals (CADISS): A multiprocessor system for image compression/decompression on board scientific satellites
[NLR-TR-87076-L] N88-30321

DATA LINKS
Optical multiple access intersatellite links
[BAE-TP-8502] N88-30013
The LTPP communication processor --- Columbus and Hermes
[CL/CP/SES/FR/004] N88-30328

DATA MANAGEMENT
Automated cataloging and characterization of space-derived data N88-30354
A design for a ground-based data management system N88-30355
Knowledge-Based Integrated Information Systems Development Methodologies Plan. Knowledge-Based Integrated Information Systems Engineering (KBIISE) report, volume 2
[AD-A195851] N88-30455

DATA PROCESSING
Automatic prober for the dc characterisation of gallium arsenide devices. Part 2: The data sorting and display facility
[AD-A195408] N88-30111
Method for combined image interpolation-restoration through a fir filter design technique
[INPE-4561-PRE/1302] N88-30315
Spacelab data processing facility (SLDPF) Quality Assurance (QA)/Data Accounting (DA) expert systems: Transition from prototypes to operational systems N88-30353
Automated cataloging and characterization of space-derived data N88-30354

DATA REDUCTION
Autonomous image data reduction by analysis and interpretation N88-30347

DATA SAMPLING
Application of sampling techniques to near-field far-field transformation
[ESA-CR(P)-2546] N88-30002

DATA STORAGE
Laser sensing for identification and control of distributed parameter systems
[AD-A195886] N88-30124
Partitioned storage for temporal databases
[AD-A195093] N88-30451

DATA STRUCTURES
Lisp Object State Saver (LOSS): A facility used to save partial schedules of the Hubble Space Telescope N88-30360

DATA TRANSMISSION
Design of a self-timed VLSI multicomputer communication controller
[AD-A194567] N88-30014

Integrating images, applications, and communications networks, volume 5
[AD-A195854] N88-30452

DECEPTION
The Soviet Stealth fighter: Check or checkmate
[AD-A195200] N88-29791

DECISION MAKING
Reduced flexibility in processing Titan 4 space launch vehicles at Cape Canaveral Air Force Station
[AD-A194908] N88-29834
A detection theory analysis of visual display performance
[AD-A196291] N88-30292
The bounded rationality constraint: Experimental and analytical results
[AD-A195897] N88-30318
The advice taker/inquirer: A system for high-level acquisition of expert knowledge N88-30359
Verification and validation of rulebased systems for Hubble Space Telescope ground support N88-30361
Venture theory: A model of decision weights
[AD-A194809] N88-30391
Looking beyond the strategic defense initiative
[AD-A195079] N88-30394
Strategic, organizational and standardization aspects of integrated information systems, volume 6
[AD-A195855] N88-30457
Technical change needs organizational change N88-30466

DECOMPOSITION
Experiments and modeling of multi-component fuel behavior in combustion
[AD-A195011] N88-29896
Decomposition of hydrazine by high frequency glow electrical discharges
[NASA-TT-20240] N88-29906

DEEP SPACE NETWORK
The Deep Space Network: An instrument for radio astronomy research
[NASA-CR-183219] N88-30554

DEFECTS
The effect of oriented defects on long-range ordering of hydrocarbon films: Azulene on Pt(111)
[AD-A196089] N88-29904
Predicting the durability of adhesives and coatings by remote detection of hidden defects and coating-thickness irregularities: A theoretical and numerical study N88-29972

DEFLECTION
Free vibration of rectangular plates with a small initial curvature
[NASA-CR-178370] N88-30148

DEGRADATION
Photoacoustic Fourier transform infrared spectroscopy. An early detection technique for coatings degradation N88-29968
Degradation of protective coatings on steel in corrosive environments N88-29969
Prediction of degradation of polymeric coating materials N88-29970
A reliability-based program for predicting the service life of organic coating systems N88-29971

DEICERS
JUH-1H redesigned pneumatic boot deicing system flight test evaluation
[AD-A194918] N88-29785

DENSITY (NUMBER/VOLUME)
Large ionic species in sooting acetylene and benzene flames N88-29932

DEOXYRIBONUCLEIC ACID
Storing bits on a DNA polymer chain
[AD-A195701] N88-29981

DEPLETION
The timing and mechanism of depletion in Lewisian granulites N88-30209

DEPLOYMENT
Antisatellite weapons and satellite deployment strategies
[AD-A195014] N88-30396

DEPOSITION
Cluster beam studies
[AD-A195182] N88-30443

DEPTH
Kalman filter-based algorithms for estimating depth from image sequences
[AD-A195818] N88-30380

DESCENT TRAJECTORIES
Investigation of the validity of the non-rotating planet assumption for three-dimensional earth atmospheric entry
[AD-A194877] N88-29829

DESIGN ANALYSIS
Euler analysis of a swirl recovery vane design for use with an advanced single-rotation propfan
[NASA-TM-101357] N88-29771

Spacecraft mass estimation, relationships and engine data: Task 1.1 of the lunar base systems study
[NASA-CR-172061] N88-29836
Design criteria for extraction with chemical reaction and liquid membrane permeation
[NASA-TT-20352] N88-29899
Circuit design criteria for stable lateral inhibition neural networks
[AD-A195066] N88-30046
Advanced planar array development for space station
[NASA-CR-179373] N88-30181
Design and performance analysis of a relational replicated database system
[AD-A196290] N88-30456

DESORPTION
Development of computer-controlled thermogravimetric instrumentation for measurement of environmental and high temperature volatilization and desorption of contaminants from polymeric materials
[AD-A195934] N88-29900

DETECTION
Noncontact photo-thermal sensing
[AD-A195450] N88-29905
Performance Prediction for Coatings. Proceedings of a Workshop
[AD-A188973] N88-29966
Ultrasonic detection of diffusion and adhesion loss N88-29967
Photoacoustic Fourier transform infrared spectroscopy. An early detection technique for coatings degradation N88-29968
Predicting the durability of adhesives and coatings by remote detection of hidden defects and coating-thickness irregularities: A theoretical and numerical study N88-29972
Electrical detection of coating deterioration N88-29973
Experimental aspects of using time-averaged holographic interferometry to detect barely visible impact damage in a graphite/epoxy composite plate
[AD-A194418] N88-30097
Laser sensing for identification and control of distributed parameter systems
[AD-A195886] N88-30124
In situ fault detection by the hybrid ray mode method
[AD-A195226] N88-30137
Automated early fatigue damage sensing system
[AD-A195717] N88-30143

DETERIORATION
Electrical detection of coating deterioration N88-29973
Evaluation of organic coating deterioration and substrate corrosion in seawater using electrochemical impedance measurements N88-29978

DIAGNOSIS
Optical measurements of soot and temperature profiles in premixed propane-oxygen flames
[NASA-TM-101343] N88-29997
Stress related failures causing open metallization
[AD-A195061] N88-30150

DIELECTRICS
Polymer-ceramic composites
[AD-A195789] N88-29983
Transient interaction of electromagnetic pulses in dielectrics and microwave biophysics
[AD-A195687] N88-30008
Dielectric millimeter waveguides: A feasibility study for a novel dielectric millimeter waveguide
[AD-A195104] N88-30042

DIFFERENTIAL EQUATIONS
Automatic qualitative analysis of ordinary differential equations using piecewise linear approximations
[AD-A196310] N88-30379

DIFFRACTION
Evaluation of multi-focus holographic lenses
[AD-A196167] N88-30110
Diffraction imaging (topography) with monochromatic synchrotron radiation
[NASA-CR-183264] N88-30431
Streaking images that appear only in the plane of diffraction in undoped GaAs single crystals: Diffraction imaging (topography) by monochromatic synchrotron radiation
[NASA-CR-183267] N88-30437

DIFFRACTION PATTERNS
Multiple scattering effects in drop sizing of dense fuel sprays by laser diffraction N88-29917

DIFFRACTION PROPAGATION
An improved spherical earth diffraction algorithm for SEKE
[AD-A195847] N88-30005

DIFFUSION
Ultrasonic detection of diffusion and adhesion loss N88-29967
Analytical methods in stochastic control and nonlinear filtering
[AD-A194272] N88-30388

DIFFUSION FLAMES
Radiation from soot-containing flames N88-29927
Flamelet chemistry modelling of soot formation for radiation N88-29928
The influence of pressure on soot formation N88-29934
Three-dimensional combustor predictors: A comparison of equilibrium and laminar flamelet chemistry models N88-29940

DIGITAL COMPUTERS
Architecture for optical digital computers
[AD-A195477] N88-30416

DIGITAL DATA
Relief effect correction on LANDSAT imagery for forest applications using digital terrain models
[INPE-4611-PRE/1334] N88-30179
Method for combined image interpolation-restoration through a fir filter design technique
[INPE-4561-PRE/1302] N88-30315
An operations manual for the digital data system
[NASA-CR-181688] N88-30329

DIGITAL NAVIGATION
Accuracy of satellite data navigation
[AD-A195877] N88-29787

DIGITAL SIMULATION
Numerical simulation of unsteady incompressible flow in a partially-filled rotating cylinder
[AD-A196001] N88-30073
Numerical simulation of the interaction of pressure waves with laminar and turbulent boundary layers
[ESA-TT-1089] N88-30075
Numerical simulation of unsteady incompressible viscous flows in generalized coordinate systems
[NASA-TM-101016] N88-30085
A digital simulation technique for the Dryden atmospheric model
[NASA-TT-20342] N88-30266

DIGITAL SYSTEMS
N-version software demonstration for digital flight controls
[NASA-CR-181483] N88-29815
Performance of DS/SSMA communications in impulsive channels. Part 1: Correlation receivers
[AD-A195712] N88-30021
Estimation of short-wavelength gravity on a dense grid using digital terrain elevation data
[AD-A196325] N88-30196
Binary star measurements using digital speckle interferometer of 6-m telescope N88-30521

DIGITAL TECHNIQUES
Evaluation of LANDSAT-TM data for geomorphological mapping
[INPE-4593-PRE/1324] N88-30168
Use of digital images as a mineral prospecting tool in the tin province of Goias, Brazil
[INPE-4537-PRE/1284] N88-30173
LANDSAT-TM data to map flooded areas
[INPE-4594-PRE/1324] N88-30177

DIMENSIONS
Robust finite-dimensional LQG (Linear Quadric Gaussian)-based controllers for a class of distributed parameter systems
[AD-A194872] N88-30382

DIODES
On 3-5 heterojunction structures and high speed devices
[AD-A195464] N88-30436

DIRECT CURRENT
The dc power control for a liquid-fed resistojet
[NASA-TM-101326] N88-29869
Numerical simulation of the function of scientific instrumentation for measuring the speed of electron devices
[AD-A194969] N88-30103
Automatic prober for the dc characterisation of gallium arsenide devices. Part 2: The data sorting and display facility
[AD-A195408] N88-30111

DIRECTION FINDING
A fiber optic beamforming processor for wideband direction finding
[AD-A194862] N88-30404
Ultra-wideband direction finding using a fiber optic beamforming processor
[AD-A194861] N88-30413

DIRECTORIES
Design and performance analysis of a relational replicated database system
[AD-A196290] N88-30456

DIRICHLET PROBLEM
Dirichlet prior in Bayesian estimation of item response curves
[AD-A195311] N88-30392

DISCRIMINATION
Discrimination studies using short-period P waves at upper mantle distances
[AD-A195468] N88-30257
DISEASES
Central serous chorioretinopathy in USAF aviators: A review
[AD-A195697] N88-30280
DISK GALAXIES
The stability of disk galaxies and constraints on their mass-luminosity ratio
[SER-C-PREPUBL-FASC-27] N88-30565
DISPERSING
Particle size measurements in sooting combustion systems N88-29931
DISPLACEMENT
Large displacement and rotational formulation for laminated cylindrical shells including parabolic transverse shear
[AD-A194871] N88-30158
DISPLAY DEVICES
Use of color CRTs (Cathode Ray Tubes) in aircraft cockpit: A literature search, revision B
[AD-A195062] N88-29797
A detection theory analysis of visual display performance
[AD-A196291] N88-30292
DISSIPATION
Determination of multiaxial flow surfaces at elevated temperatures using the concept of dissipation potential
[ORNL/TM-10787] N88-30149
DISSOCIATION
Nonequilibrium flow of a dissociating gas in a horizontal channel with axial temperature variation
[DE88-702536] N88-30089
Ion kinetics in silane plasmas
[AD-A196202] N88-30423
DISTORTION
Theory of filtering and control with application to control of large space structures
[AD-A195500] N88-29851
Contamination and distortion of steady flow field induced by discrete frequency disturbances in aircraft gas engines
[AD-A195440] N88-30069
DISTRIBUTED PARAMETER SYSTEMS
Laser sensing for identification and control of distributed parameter systems
[AD-A195886] N88-30124
Robust finite-dimensional LQG (Linear Quadric Gaussian)-based controllers for a class of distributed parameter systems
[AD-A194872] N88-30382
DISTRIBUTED PROCESSING
Performance analysis of FDDI
[NASA-CR-183206] N88-30321
Parallel and distributed computation for fault-tolerant object recognition N88-30350
Knowledge-based integrated information systems engineering: Highlights and bibliography. Knowledge-Based Integrated Information Systems Engineering (KBIISE) Project, volume 1
[AD-A195850] N88-30449
DIURNAL VARIATIONS
Comparison of morning with afternoon nitrogen elimination in resting subjects breathing 100 percent oxygen
[AD-A196191] N88-30282
DIVERGENCE
Utilization of a single clear-air Doppler radar beam to measure vertical divergence
[AD-A195543] N88-30271
DIVING (UNDERWATER)
Study of human factors engineering criteria for Extra Vehicular Activity (EVA) systems, volume 2
[STF23-F87025-VOL-2] N88-30293
DMSP SATELLITES
Investigations of magnetosphere-ionosphere coupling relevant to operational systems
[AD-A195972] N88-30195
Passive microwave measurements of water vapor fields and rain for locating fronts in cyclonic storms
[AD-A195632] N88-30267
DOCUMENTS
Development of graded reference radiographs for aluminum welds, phase 1
[AD-A195594] N88-30140
DOMAINS
Multiple solutions and bifurcation for a class of nonlinear Sturm-Liouville eigenvalue problems on an unbounded domain
[AD-A195954] N88-30389
DOMES (GEOLOGY)
Diapirs of the Mediterranean ridge: The tectonic regime of an incipient accreted terrane N88-30224
DOPED CRYSTALS
Development of a unit cell for a Ge:Ga detector array
[NASA-CR-177445] N88-30100
Growth and characterization of materials for tunable lasers in the near infrared spectral region
[NASA-CR-183132] N88-30113
DOPPLER EFFECT
Particle sizing in combustion systems, using scattered laser light
[AD-A196231] N88-29953
Doppler-corrected differential detection system
[NASA-CASE-NPO-16987-1-CU] N88-30001
DOPPLER RADAR
The NAE atmospheric research aircraft N88-29730
Doppler radar analysis of coastal marine atmospheric boundary layer structure during a cold air outbreak
[AD-A196023] N88-30261
Utilization of a single clear-air Doppler radar beam to measure vertical divergence
[AD-A195543] N88-30271
DOSAGE
Heavy ion and proton tests for subsystem upset
[AD-A195267] N88-30442
DRAG MEASUREMENT
Precision measurement of the Fresnel drag coefficient using a ring laser
[AD-A196025] N88-30043
Experimental determination of drag modifications due to elastic compliant surfaces using quantitative visual techniques
[AD-A194785] N88-30082
DRAG REDUCTION
A preliminary investigation of drag reduction and mechanism for a blunt body of revolution with slanted base
[NASA-TT-20349] N88-29753
Compression pylon
[NASA-CASE-LAR-13777-1] N88-29789
Development and design of windtunnel and test facility for RPV (Remote Piloted Vehicle) enhancement devices
[AD-A194842] N88-29822
The viscous flow on surfaces with streamline riblets
[ESA-TT-1091] N88-30067
DROP SIZE
Alternative fuel spray behavior N88-29912
Simulation study of spraying, streaming and vaporization phenomena associated with fuel injection N88-29914
Multiple scattering effects in drop sizing of dense fuel sprays by laser diffraction N88-29917
Influence of operating conditions on the atomization and distribution of fuel by air blast atomizers N88-29918
DROPS (LIQUIDS)
Influence of the convection on evaporation and combustion of a fuel droplet N88-29948
General equations for the motions of ice crystals and water drops in gravitational and electric fields
[NASA-CR-183229] N88-30070
DRUMS (CONTAINERS)
Containment of a silicone fluid free surface in reduced gravity using barrier coatings
[NASA-TM-101314] N88-30072
DUALITY THEOREM
Lagrangian of the self-duality equation and d = 10, N = 2b supergravity
[DE88-701554] N88-30563
DUCTILITY
Modeling of micromechanisms of fatigue and fracture in hybrid materials
[AD-A195604] N88-30142
DURABILITY
Predicting the durability of adhesives and coatings by remote detection of hidden defects and coating-thickness irregularities: A theoretical and numerical study N88-29972
DUST
AGN (OIII) emission line profiles: Dependencies on galaxy inclination and Balmer decrement
[INPE-4596-PRE/1324] N88-30577
DWARF NOVAE
The ultrashort period dwarf nova SW Ursae Majoris N88-30553
DWARF STARS
Duplicity in the solar neighborhood: Part 4: Spectroscopic orbits for four dwarf M stars
[SER-C-PREPUBL-FASC-21] N88-30561
DYNAMIC CHARACTERISTICS
A dynamic analysis of piezoelectric strained elements
[AD-A196079] N88-30430
DYNAMIC CONTROL
Dynamics of articulated aerospace structures
[AD-A195685] N88-29794
DYNAMIC LOADS
Ultrasonic method and apparatus for determining crack opening load
[NASA-CASE-LAR-13889-1] N88-30160
DYNAMIC MODELS
Procedures for updating dynamic mathematical models, test phase --- spacecraft hardware
[MEBS-38/87] N88-29852
MANIP --- spacecraft modeling program
[MANIP-217A] N88-29855
Nonlinear dynamics of coupled oscillator arrays
[AD-A194888] N88-30053
Modeling robot flexibility for endpoint force control
[AD-A195923] N88-30132
Continental growth through time by underplating of subducted oceanic crust: Evidence from kimberlites in South Africa and SW Pacific N88-30244
Dynamical systems and motion vision
[AD-A195932] N88-30366
DYNAMIC RESPONSE
The Flight of Flexible Aircraft in Turbulence: State-of-the-Art in the Description and Modelling of Atmospheric Turbulence
[AGARD-R-734] N88-29725
Status review of atmosphere turbulence and aircraft response N88-29726
Aircraft dynamics: Aerodynamic aspects and wind tunnel techniques N88-29731
Acquisition of gust statistics from AIDS-recorded data N88-29733
Analytical study of graphite-epoxy tube response to thermal loads
[NASA-CR-183215] N88-29884
Rotational evolution of dynamically symmetric gyrostat with internal friction N88-30509
DYNAMIC STABILITY
Utilizing dynamic stability of orient parts
[AD-A195730] N88-30397
DYNAMIC STRUCTURAL ANALYSIS
Space structure (dynamics and control) theme development
[NASA-TM-100597] N88-29850
Geometric and material nonlinear analysis of structures comprising rectangular hollow sections
[CE-79] N88-30141
DYNAMICAL SYSTEMS
Studies on pressure response of gas bubbles contributions of condensed droplets in bubbles generated by a uniform nucleation
[NASA-TT-20343] N88-30068
Prediction and measurement of human pilot dynamic characteristics in a manned rotorcraft simulation
[NASA-CR-183246] N88-30297
Dynamical systems and motion vision
[AD-A195932] N88-30366
Intramolecular dynamics: A study of molecules at high levels of vibrational excitation
[AD-A195285] N88-30400
Ring current role in dynamics of fluctuating electron and ion fluxes in low-latitude magnetosphere N88-30514
DYNAMICS
Structural dynamics of high-latitude magnetosphere determined from solar electron data N88-30500

E

EARTH (PLANET)
Spectral analysis of the Elatina varve series
[NASA-CR-183085] N88-30260
Exotic minerals in 3,500 million year old rocks: Evidence for large meteorite impacts N88-30475
LSU scientists discover evidence of large meteorite impacts on the early earth N88-30480
EARTH ATMOSPHERE
Implementation of the NCAR (National Centre for Atmospheric Research) graphics package at ARL (Aeronautical Research Laboratory)
[AD-A195163] N88-30193
Did the greenhouse effect kill the dinosaurs N88-30484
EARTH CORE
An illustration of the complexity of continent formation N88-30207
EARTH CRUST
Relationships among earth's gravity field, magnetic field, crustal structure and the magnetic character of crustal rocks
[AD-A195539] N88-30198
Workshop on the Growth of Continental Crust
[NASA-CR-183073] N88-30201
Constraints on continental accretion from sedimentation N88-30202
Nd isotopes and crustal growth rate N88-30203
Recycling of lower continental crust through foundering of cumulates from contaminated mafic intrusions N88-30204
Growth of continental crust: Clues from Nd isotopes and Nb-Th relationships in mantle-derived magmas N88-30205

Pluton emplacement and magmatic arc construction: A model from the Patagonian batholith N88-30206
The Kerala Khondalite Belt (KKB) of Southern India: An enslalic mobile belt N88-30208
Genesis of archean granitoids in the Pilbara block and implications for crustal growth N88-30210
Role of zircon in tracing crustal growth and recycling N88-30211
Construction of mass-age curves for the continental crust: An empirical model and an example from the western US N88-30213
Does subduction zone magmatism produce average continental crust N88-30214
Pb isotope constaints on the extent of crustal recycling into a steady state mantle N88-30215
Decoupled Rb-Sr and Sm-Nd isotopic evolution of the continental crust N88-30216
Metamorphic P-T paths and Precambrian crustal growth in East Antarctica N88-30218
Early intense cratering: Effects on growth of earth's crust N88-30219
The growth of continents and some consequences since 1.5 Ga N88-30220
The early archaean crustal history of West Greenland as recorded by detrital zircons N88-30221
Deep seismic reflection profiling and continental growth curves N88-30222
Growth of early archaean crust in the ancient Gneiss complex of Swaziland and adjacent Barberton Greenstone Belt, Southern Africa N88-30223
Evidence for crustal recycling during the Archean: The parental magmas of the stillwater complex N88-30226
Changing styles of crustal growth in Southern Africa: Constraints from geochemical and Sr-Nd isotope studies in Archaean to Pan African terrains N88-30227
Structure of Southwestern Michipicoten Greenstone Belt, Ontario: Evidence for Archean accretion N88-30228
Mid to late proterozoic magmatism within Northeastern North America and its iplications for the growth of the continental crust N88-30229
Thermal models pertaining to continental growth N88-30230
Ridge-trench collision in Archean and Post-Archean crustal growth: Evidence from southern Chile N88-30233
Reappraisal of the geology of Kangimut Sammisoq, Ameralik Fjord, Southern West Greenland: Crustal structure and interpretation of isotopic data N88-30234
Archean crustal evolution of the northern North China Craton N88-30235
Growth of the lower continental crust N88-30236
The complexity, depth, and rapidity of processes that formed the lunar crust N88-30237
Continental crustal formation and recycling: Evidence from oceanic basalts N88-30238
Geochronological and lead-isotope evidences for rapid crust formation in middle-proterozoic time: The Labrador example N88-30239
Physical processes in the growth of the continental crust N88-30240
Trace element differences between Archean, Proterozoic and Phanerozoic crustal components: Implications for crustal growth processes N88-30243
The growth of the continental crust: Constraints from radiogenic isotope geochemistry N88-30245
Crustal growth in the Archean: The geochemical evidence N88-30246
Solid earth as a recycling systems and the lateral growth of Precambrian North America N88-30249
Mineralization through geologic time: Evolution of continental crust N88-30250
Growth of the continental crust: A planetary-mantle perspective N88-30251
Crustal underplating in the North American Craton: Evidence from the Petrogenesis of anorthositic rocks in the Middle Proterozoic Midcontinent Rift System N88-30252
Late-Archaean crustal growth in the Lewisian Complex of Northwest Scotland: Diachroneity in magmatic accretion and implications for models of crustal growth N88-30253
The effect of thicker oceanic crust in the Archaean on the growth of continental crust through time N88-30254
Volcanic contribution to crustal growth in the Central Andes: A new estimate and a discussion of uncertainties N88-30255
The second generation intelligent user interface for the crustal dynamics data information system N88-30352
Non-atmospheric noble gases from CO(sub 2) well ga N88-30476
Lava thicknesses: Implications for rheological and crustal development N88-30490

EARTH IONOSPHERE
The effect of equatorial ionospheric irregularities on the performance of a south-looking OTH-B (Over-The-Horizon-Backscatter) radar
[AD-A195090] N88-30018
On formulating a simple D-region model
[AD-A195841] N88-30197
Model representation of electron concentration distribution in outer middle-latitude ionosphere using data from Intercosmos-19 artificial earth satellite N88-30513

EARTH MAGNETOSPHERE
Structural dynamics of high-latitude magnetosphere determined from solar electron data N88-30500
Ring current role in dynamics of fluctuating electron and ion fluxes in low-latitude magnetosphere N88-30514
Plasma of earth's magnetosphere ring currents. Model compared with results of AMPTE/CCE experiment N88-30515

EARTH MANTLE
Workshop on the Growth of Continental Crust
[NASA-CR-183073] N88-30201
Recycling of lower continental crust through foundering of cumulates from contaminated mafic intrusions N88-30204
An illustration of the complexity of continent formation N88-30207
Pb isotope constaints on the extent of crustal recycling into a steady state mantle N88-30215
The petrogenesis of oceanic kimberlites and included mantle megacrysts: The Malaitan alnoite N88-30232
Growth of the continental crust: A planetary-mantle perspective N88-30251
Discrimination studies using short-period P waves at upper mantle distances
[AD-A195468] N88-30257
Non-atmospheric noble gases from CO(sub 2) well ga N88-30476

EARTH OBSERVATIONS (FROM SPACE)
Determining earth's rotation from laser observations of Lageos artificial earth satellite (during period of main merit campaign) N88-30528
Obligue metallogenic zones recognized by interpreting space photographs of southern Tien Shan N88-30529

EARTH ORBITAL ENVIRONMENTS
Relationship between characteristics of low-energy electrons and geomagnetic disturbance in geostationary orbit N88-30501

EARTH ORBITS
A standard library for modeling satellite orbits on a microcomputer
[AD-A195759] N88-29830
Particle trajectories and potentials in a plane sheath moving in a magnetoplasma
[AD-A196228] N88-30190

EARTH PLANETARY STRUCTURE
Deep seismic reflection profiling and continental growth curves N88-30222

EARTH ROTATION
Investigation of the validity of the non-rotating planet assumption for three-dimensional earth atmospheric entry
[AD-A194877] N88-29829
Determining earth's rotation from laser observations of Lageos artificial earth satellite (during period of main merit campaign) N88-30528

EARTH SURFACE
Estimation of short-wavelength gravity on a dense grid using digital terrain elevation data
[AD-A196325] N88-30196

ECLOGITE
Crustal evolution and the eclogite to granulite phase transition in xenoliths from the West African Craton N88-30217

ECONOMIC ANALYSIS
Possibilities of economical improvements for Moon based rocket propulsion using lunar propellants
[ILR-MITT-196] N88-29871

ECONOMICS
Political and economic barriers to information transfer N88-30460
Formulation and solution of economic equilibrium problems
[AD-A196034] N88-30470

ECOSYSTEMS
Investigation of the large-scale impact of air pollution components on forest ecosystems in Bavaria
[ESA-TT-1087] N88-30187

EDUCATION
Integration of LANTIRN (Low Altitude Navigation and Targeting Infrared for Night) into operational fighter training
[AD-A194906] N88-29799

EFFECTIVENESS
Report to Congress on the effectiveness of the Civil Aviation Security Program
[AD-A195282] N88-29784

EFFICIENCY
Experimental and analytical study of two-phase flow in zero gravity
[AD-A195223] N88-29993
A standard architecture for controlling robots
[AD-A195929] N88-30371

EIGENVALUES
Numerical calculations of the response of a spinning spheroidal payload to coning motion
[AD-A195890] N88-30059
Regularity and numerical solution of eigenvalue problems with piecewise analytic data
[AD-A194993] N88-30387
Multiple solutions and bifurcation for a class of nonlinear Sturm-Liouville eigenvalue problems on an unbounded domain
[AD-A195954] N88-30389

EIKONAL EQUATION
Eikonal solutions to optical model coupled-channel equations
[NASA-TP-2830] N88-30402

ELASTIC BODIES
Dynamics of articulated aerospace structures
[AD-A195685] N88-29794

ELASTIC DEFORMATION
Dynamics of articulated aerospace structures
[AD-A195685] N88-29794

ELASTIC PROPERTIES
Experimental determination of drag modifications due to elastic compliant surfaces using quantitative visual techniques
[AD-A194785] N88-30082
A dynamic analysis of piezoelectric strained elements
[AD-A196079] N88-30430

ELASTIC SCATTERING
Eikonal solutions to optical model coupled-channel equations
[NASA-TP-2830] N88-30402

ELASTIC WAVES
Numerical simulation of the interaction of pressure waves with laminar and turbulent boundary layers
[ESA-TT-1089] N88-30075
Determination of the specific area of liquid gas and the velocity of weak pressure waves in aqueous foams
[NASA-TT-20347] N88-30087

ELECTRIC BATTERIES
Structure and dynamics of solutions of lithium salts relevant to battery construction
[AD-A195399] N88-30044
Aircraft battery state of charge and charge control system
[AD-A194979] N88-30052

ELECTRIC CONNECTORS
Circuit design criteria for stable lateral inhibition neural networks
[AD-A195066] N88-30046

ELECTRIC DISCHARGES
In-house capacitor technology program
[AD-A194804] N88-30049
Transverse CO2 laser two-dimensional gain distributions
[AD-A196240] N88-30119

ELECTRIC FIELDS
Ion gun generated electromagnetic interference on the SCATHA satellite
[AD-A195179] N88-29853
Wave propagation and remote sensing N88-30029
General equations for the motions of ice crystals and water drops in gravitational and electric fields
[NASA-CR-183229] N88-30070

ELECTRIC MOTOR VEHICLES
Voltage directive drive with claw pole motor and control without rotor position indicator
[ETN-88-93120] N88-30047

ELECTRIC MOTORS
Voltage directive drive with claw pole motor and control without rotor position indicator
[ETN-88-93120] N88-30047

ELECTRIC PROPULSION
The NASA Electric Propulsion Program
[NASA-TM-101324] N88-29859
Performance and lifetime assessment of MPD arc thruster technology
[NASA-TM-101293] N88-29860
The dc power control for a liquid-fed resistojet
[NASA-TM-101326] N88-29869
Successful completion of a cyclic ground test of a mercury ion auxiliary propulsion system
[NASA-TM-101351] N88-29873

ELECTRICAL ENGINEERING
Statistical analysis of the LMS (Last Mean Squares) and modified stochastic gradient
[AD-A195497] N88-30376

ELECTRICAL IMPEDANCE
Electrical detection of coating deterioration N88-29973

Electrochemical evaluation of the long term corrosion resistance of polymer coated steel N88-29974
An electrochemical impedance spectroscopy study of reactions at the metal/coating interface N88-29975
Evaluation of organic coating deterioration and substrate corrosion in seawater using electrochemical impedance measurements N88-29976
Review of Radio Science, 1984-1986 N88-30023
Electromagnetic metrology N88-30024

ELECTRICAL MEASUREMENT
Electrical detection of coating deterioration N88-29973
Electrochemical evaluation of the long term corrosion resistance of polymer coated steel N88-29974
Evaluation of organic coating deterioration and substrate corrosion in seawater using electrochemical impedance measurements N88-29976

ELECTRICAL PROPERTIES
Cytochrome electron transfer and biomolecular electronics
[AD-A195482] N88-30277
A dynamic analysis of piezoelectric strained elements
[AD-A196079] N88-30430

ELECTRICAL RESISTANCE
Electrical properties of materials for elevated temperature resistance strain gage application
[NASA-CR-182214] N88-30106

ELECTRO-OPTICAL EFFECT
X-ray diffraction imaging (topography) of electrooptic crystals by synchrotron radiation
[NASA-CR-183266] N88-30427

ELECTRO-OPTICS
Electronic and optical devices and applications N88-30027
Mode locking of semiconductor laser with external cavity
[AD-A196018] N88-30117
Report on an overseas visit to USA relating to the thermoelastic measurement of stresses, 16-21 August 1987
[AD-A195313] N88-30161
A fiber optic beamforming processor for wideband direction finding
[AD-A194862] N88-30404
Center for opto-electronic systems research
[AD-A195159] N88-30411
Ultra-wideband direction finding using a fiber optic beamforming processor
[AD-A194861] N88-30413
Common modules: A success story
[AD-A195937] N88-30415
Power MISFETs on OnP
[AD-A195242] N88-30436

ELECTROCATALYSTS
Electrocatalytic reduction of oxygen on modified oxide surfaces
[NASA-TM-101333] N88-29952

ELECTROCHEMICAL CORROSION
Multi-metallic galvanic corrosion
[AD-A195995] N88-29963

ELECTROCHEMISTRY
An electrochemical impedance spectroscopy study of reactions at the metal/coating interface N88-29975
Evaluation of organic coating deterioration and substrate corrosion in seawater using electrochemical impedance measurements N88-29976
Cytochrome electron transfer and biomolecular electronics
[AD-A195482] N88-30277

ELECTRODES
An electrochemical impedance spectroscopy study of reactions at the metal/coating interface N88-29975

ELECTROLYTES
Multi-metallic galvanic corrosion
[AD-A195995] N88-29963
Structure and dynamics of solutions of lithium salts relevant to battery construction
[AD-A195399] N88-30044

ELECTROLYTIC CELLS
Morphological changes in polymer electrolyte cells
[AD-A195821] N88-30054

ELECTROMAGNETIC ABSORPTION
Bioeffects of electromagnetic waves N88-30032

ELECTROMAGNETIC FIELDS
Electromagnetic metrology N88-30024
Bioeffects of electromagnetic waves N88-30032
Research in particle and gamma-ray astrophysics
[NASA-CR-183126] N88-30566

ELECTROMAGNETIC INTERFERENCE
Ion gun generated electromagnetic interference on the SCATHA satellite
[AD-A195179] N88-29853

ELECTROMAGNETIC NOISE
Electromagnetic noise and interference N88-30028

ELECTROMAGNETIC PULSES
EMPTAC (Electromagnetic Pulse Test Aircraft) user's guide
[AD-A195072] N88-30006
Transient interaction of electromagnetic pulses in dielectrics and microwave biophysics
[AD-A195687] N88-30008
Electromagnetic noise and interference N88-30028

ELECTROMAGNETIC RADIATION
Comparative analysis of passive communications satellites employing the SHF and HF spectrum for use in a strategic role
[AD-A194682] N88-30019
Review of Radio Science, 1984-1986 N88-30023
Bioeffects of electromagnetic waves N88-30032
Time-domain far-field scattering of plane electromagnetic waves by a penetrable object in the Born approximation
[PB87-176129] N88-30040
Vanderbilt free electron laser project in biomedical and materials research
[AD-A195961] N88-30121

ELECTROMAGNETIC SCATTERING
Review of Radio Science, 1984-1986 N88-30023
Fields and waves N88-30025
Time-domain far-field scattering of plane electromagnetic waves by a penetrable object in the Born approximation
[PB87-176129] N88-30040

ELECTROMAGNETIC SHIELDING
Electromagnetic noise and interference N88-30028

ELECTROMAGNETIC WAVE TRANSMISSION
Nonlinear optical phase conjugation techniques to reduce the physical size of lasers
[AD-A196170] N88-30122
Consideration of plasma opening switches from a wave propagation perspective
[AD-A195681] N88-30421

ELECTROMAGNETISM
Electromagnetic metrology N88-30024
X- and gamma-ray background observations in Antarctic
[INPE-4583-PRE/1317] N88-30578

ELECTRON ACCELERATION
Relationship between characteristics of low-energy electrons and geomagnetic disturbance in geostationary orbit N88-30501

ELECTRON BEAMS
Microcircuit trace cutting with focused ion beams
[AD-A196030] N88-30050
Reactive plasticizers in negative E-beam resists
[AD-A195161] N88-30056
Influence of plasma parameters on VLF radiation in near-rocket region N88-30518

ELECTRON BOMBARDMENT
The effect of oriented defects on long-range ordering of hydrocarbon films: Azulene on Pt(111)
[AD-A196089] N88-29904

ELECTRON DENSITY (CONCENTRATION)
On formulating a simple D-region model
[AD-A195841] N88-30197
Model representation of electron concentration distribution in outer middle-latitude ionosphere using data from Intercosmos-19 artificial earth satellite N88-30513

ELECTRON DIFFRACTION
The effect of oriented defects on long-range ordering of hydrocarbon films: Azulene on Pt(111)
[AD-A196089] N88-29904

ELECTRON IMPACT
Ion kinetics in silane plasmas
[AD-A196202] N88-30423

ELECTRON MICROSCOPY
Degradation of protective coatings on steel in corrosive environments N88-29969
Scanning electron microscopy study of adhesion in sea urchin blastulae
[NASA-CR-183136] N88-30275

ELECTRON OSCILLATIONS
Research on a two-stage free electron laser oscillator
[AD-A195991] N88-30115

ELECTRON TRANSFER
Cytochrome electron transfer and biomolecular electronics
[AD-A195482] N88-30277

ELECTRONIC CONTROL
The design of an intelligent multidisk control module for VME bus based systems
[AD-A195587] N88-30303

ELECTRONIC COUNTERMEASURES
The surface evaporative duct height product: An evaluation
[AD-A195918] N88-30199

ELECTRONIC EQUIPMENT
Numerical simulation of the function of scientific instrumentation for measuring the speed of electron devices
[AD-A194969] N88-30103
Electronic materials and devices prepared by molecular beam epitaxy
[AD-A195694] N88-30433

ELECTRONS
Particle trajectories and potentials in a plane sheath moving in a magnetoplasma
[AD-A196228] N88-30190
Ring current role in dynamics of fluctuating electron and ion fluxes in low-latitude magnetosphere N88-30514

ELECTROPHOTOMETERS
Five channel auroral photometer
[REPT-112] N88-30101

ELECTROSTRICTION
Piezoelectric and electrostrictive materials for transducer applications, volume 1
[AD-A194957] N88-30096
Piezoelectric and electrostrictive materials for transducer applications, volume 2
[AD-A194956] N88-30104
Piezoelectric and electrostrictive materials for transducer applications, volume 3
[AD-A194949] N88-30112

ELEVATION
Estimation of short-wavelength gravity on a dense grid using digital terrain elevation data
[AD-A196325] N88-30196

ELIMINATION
Comparison of morning with afternoon nitrogen elimination in resting subjects breathing 100 percent oxygen
[AD-A196191] N88-30282

ELLIPTIC DIFFERENTIAL EQUATIONS
Generation of surface grids through elliptic partial differential equations for aircraft and missile configurations
[AD-A195639] N88-30378

ELLIPTIC FUNCTIONS
Three-dimensional elliptic grid generation technique with application to turbomachinery cascades
[NASA-TM-101330] N88-30078

EMBEDDING
A parametric study of embedded cantilever retaining walls: The results of a finite element study
[RR-CE83] N88-30152

EMBRYOS
Semi-microdroplet assay for cell adhesion molecules
[NASA-CR-183139] N88-30274
Immunofluorescence localization of dissociation supernatant and extracellular matrix components in Lytechinus pictus sectioned embryos
[NASA-CR-183137] N88-30276

ENCAPSULATING
Primerless RTV silicones
[BDX-613-3807] N88-29980

ENERGY CONVERSION EFFICIENCY
Energy conversion measurements in laser-sustained argon plasmas for application to rocket propulsion
[AD-A194931] N88-29861

ENERGY STORAGE
Regenerative fuel cell energy storage system for a low earth orbit space station
[NASA-CR-174802] N88-30184

ENERGY TRANSFER
Vanderbilt free electron laser project in biomedical and materials research
[AD-A195961] N88-30121
Energy budget and ground temperatures in hot regions
[AD-A196298] N88-30268

ENGINE DESIGN
V2500 engine collaboration
[PNR90423] N88-29803
Developing the Rolls-Royce Tay
[PNR90447] N88-29809
Combustion and fuels in gas turbine engines
[AGARD-CP-422] N88-29910
Voltage directive drive with claw pole motor and control without rotor position indicator
[ETN-88-93120] N88-30047
Impact of ETO propellants on the aerothermodynamic analyses of propulsion components
[NASA-TM-101303] N88-30094

ENGINE MONITORING INSTRUMENTS
Development and installation of an instrumentation package for GE F404 investigative testing
[AD-A196265] N88-30107

ENGINE PARTS
V2500 engine collaboration
[PNR90423] N88-29803

Determination of the hydroperoxide potential of jet fuels
[AD-A195975] N88-29991
An investigation of constitutive models for predicting viscoplastic respones during cyclic loading
[AD-A194875] N88-30163

ENGINE TESTS
Orbital transfer vehicle 3000 LBF thrust chamber assembly hot fire test program
[NASA-CR-182145] N88-29858
Fuel property effects on the US Navy's TF30 engine N88-29911
Comparison of the performance of a reverse flow annular combustion chamber under low and high pressure conditions N88-29923
Fuel effects on flame radiation and hot-section durability N88-29925
Testing of a variable-stroke Stirling engine
[NASA-TM-100899] N88-30472

ENGINEERING MANAGEMENT
An improvement in the numerical integration procedure used in the NASA Marshall engineering thermosphere model
[NASA-CR-179389] N88-30200

ENGINES
Empirical flutter prediction method
[AD-A195699] N88-29810

ENGLISH LANGUAGE
Conversion of productions in OPS5 to their equivalent English
[ORNL/TM-10246] N88-30306

ENVIRONMENT EFFECTS
Investigation of the large-scale impact of air pollution components on forest ecosystems in Bavaria
[ESA-TT-1087] N88-30187

ENVIRONMENTAL CONTROL
Development of computer-controlled thermogravimetric instrumentation for measurement of environmental and high temperature volatilization and desorption of contaminants from polymeric materials
[AD-A195934] N88-29900

ENVIRONMENTAL TESTS
Qualification test levels for units to be derived from mechanical test data analysis — ESA
[REPT-87-158-EI/ET/AG] N88-30139

ENVIRONMENTS
Multi-metallic galvanic corrosion
[AD-A195995] N88-29963
Analysis of environmental parameters from the Panama City tower radar experiment
[AD-A194994] N88-30264

EPOXY COMPOUNDS
Electrical detection of coating deterioration N88-29973

EPOXY RESINS
Alternative immersion accelerated testing of coating systems for Naval shoreline facilities N88-29977
Experimental aspects of using time-averaged holographic interferometry to detect barely visible impact damage in a graphite/epoxy composite plate
[AD-A194418] N88-30097

EQUATIONS OF MOTION
General equations for the motions of ice crystals and water drops in gravitational and electric fields
[NASA-CR-183229] N88-30070
Nonlinear stress-strain and inelastic rebound with exponential stiffness
[AD-A195667] N88-30159
Canonical variables and canonical integrals for motion in near-circular orbits N88-30512
Lagrangian of the self-duality equation and d = 10, N = 2b supergravity
[DE88-701554] N88-30563

EQUATIONS OF STATE
State variable approach to deformation phenomena in Face Centered Cubic (FCC) metals
[VTT-44] N88-29964

EQUATORIAL ATMOSPHERE
One equatorial anomaly in nighttime ionospheric F region N88-30517

EQUILIBRIUM EQUATIONS
On the Nash point equilibria in the calculus of variations
[AD-A194959] N88-30381
Formulation and solution of economic equilibrium problems
[AD-A196034] N88-30470

EQUILIBRIUM METHODS
A parametric study of embedded cantilever retaining walls: The results of a finite element study
[RR-CE83] N88-30152

ERROR ANALYSIS
NBS (National Bureau of Standards) measurement services: The NBS photodetector spectral response calibration transfer program
[PB88-201595] N88-30109
Performance prediction of concurrent systems
[NASA-CR-183175] N88-30312
Achieving real-time performance in FIESTA N88-30344

ERROR CORRECTING CODES
Long haul communications in the HF spectrum utilizing high speed modems
[AD-A194683] N88-30003

ERROR SIGNALS
Long haul communications in the HF spectrum utilizing high speed modems
[AD-A194683] N88-30003

ERRORS
In situ fault detection by the hybrid ray mode method
[AD-A195226] N88-30137

ERS-1 (ESA SATELLITE)
ERS-1: A satellite with an oceanographic mission
[NLR-MP-86072-U] N88-29838
Development of procedures for performing end-to-end tests on the ERS-1 radar altimeter and AMI using a compact antenna test range — Active Microwave Instrument (AMI)
[ESA-CR(P)-2558] N88-30022
A study of the feasibility of using sea and wind information from the ERS-1 satellite. Part 1: Wind scatterometer data
[NASA-CR-182833] N88-30167
A study of the feasibility of using sea and wind information from the ERS-1 satellite. Part 2: Use of scatterometer and altimeter data in wave modeling and assimilation
[ESA-CR(P)-2604-PT-2] N88-30176

ESA SATELLITES
PSDE/SAT 2: Preliminary spacecraft configuration study, executive summary
[ESA-CR(P)-2618] N88-29840
The high-throughput X-ray spectroscopy mission: The mission-science report
[ESA-SP-1097] N88-30557

ESA SPACECRAFT
Study on conceptual design of spacecraft using Computer Aided Engineering (CAE)
[SNIAS-920-CA/TS] N88-29841

ESTIMATES
Spacecraft mass estimation, relationships and engine data: Task 1.1 of the lunar base systems study
[NASA-CR-172061] N88-29836
Monte-Carlo estimation of the influence of plant architecture parameters on spectral brightness N88-30533

EULER EQUATIONS OF MOTION
A streamwise upwind algorithm for the Euler and Navier-Stokes equations applied to transonic flows
[NASA-TM-101019] N88-29751
Space marching Euler solvers N88-29759
Numerical methods: Euler time dependent solver N88-29760
Euler analysis of a swirl recovery vane design for use with an advanced single-rotation propfan
[NASA-TM-101357] N88-29771

EUROPEAN COMMUNICATIONS SATELLITE
Study of the assembly, integration and verification programs of telecommunication satellites applicable to other satellite programs
[MATRA-100/CC/MLG/031/87] N88-29847

EUROPEAN SPACE AGENCY
Candidate functions for advanced technology implementation in the Columbus mission planning environment N88-30340
With an eye to the future: ESA general studies program 1988
[ESA-SP-1100] N88-30447
ESA report to the 27th COSPAR meeting
[ESA-SP-1098] N88-30556

EUROPEAN SPACE PROGRAMS
Study on long-term evolution towards European manned spaceflight. Volume 1: Executive summary
[ERNO-OX1-002/88-VOL-1] N88-29827
ERS-1: A satellite with an oceanographic mission
[NLR-MP-86072-U] N88-29838
Study of the assembly, integration and verification programs of telecommunication satellites applicable to other satellite programs
[MATRA-100/CC/MLG/031/87] N88-29847
Interim Flight Opportunity (IFO). Volume 1: Executive summary — space platform
[SE/LS/AP-36-818/CN-VOL-1] N88-29849
Qualification test levels for units to be derived from mechanical test data analysis — ESA
[REPT-87-158-EI/ET/AG] N88-30139
Study on industrial organization for European Ground Support Equipment (EGSE) to support European space programs. Volume 1: Technical reports
[SD-RP-AI-009-VOL-1] N88-30446
With an eye to the future: ESA general studies program 1988
[ESA-SP-1100] N88-30447
Study on industrial organization for European Ground Support Equipment (EGSE) to support European space programs. Volume 2: Technical reports
[SD-RP-AI-009-VOL-2] N88-30448
ESA report to the 27th COSPAR meeting
[ESA-SP-1098] N88-30556
The high-throughput X-ray spectroscopy mission: The mission-science report
[ESA-SP-1097] N88-30557

EVALUATION
Quality measures and assurance for AI (Artificial Intelligence) software
[NASA-CR-4187] N88-30304

EVAPORATION
Influence of the convection on evaporation and combustion of a fuel droplet N88-29948

EVAPORATION RATE
Development of computer-controlled thermogravimetric instrumentation for measurement of environmental and high temperature volatilization and desorption of contaminants from polymeric materials
[AD-A195934] N88-29900

EVOLUTION
Rotational evolution of dynamically symmetric gyrostat with internal friction N88-30509
Evolution of thermal structure of Benguela upswelling system according to satellite and shipboard data N88-30525

EVOLUTION (DEVELOPMENT)
Mid to late proterozoic magmatism within Northeastern North America and its iplications for the growth of the continental crust N88-30229
Thermal models pertaining to continental growth N88-30230
Ridge-trench collision in Archean and Post-Archean crustal growth: Evidence from southern Chile N88-30233
Archean crustal evolution of the northern North China Craton N88-30235
Growth of the lower continental crust N88-30236
The complexity, depth, and rapidity of processes that formed the lunar crust N88-30237
Geochronological and lead-isotope evidences for rapid crust formation in middle-proterozoic time: The Labrador example N88-30239
Physical processes in the growth of the continental crust N88-30240
Evolution of the Dharwar Craton: A terrain of early Archean crustal stability, long term orogenic cycles and large scale palaeobiological activity N88-30241
Lithospheric evolution of the Northern Arabian Shield: Chemical and isotopic evidence from basalts, xenoliths and granites N88-30242
Trace element differences between Archean, Proterozoic and Phanerozoic crustal components: Implications for crustal growth processes N88-30243
Continental growth through time by underplating of subducted oceanic crust: Evidence from kimberlites in South Africa and SW Pacific N88-30244
Growth of planetary crusts N88-30247
Mineralization through geologic time: Evolution of continental crust N88-30250
Volcanic contribution to crustal growth in the Central Andes: A new estimate and a discussion of uncertainties N88-30255
A compilation of information and data on the Manson impact structure
[NASA-CR-183169] N88-30258
Noble gases, C,N, and Si isotopes in interstellar SiC form the Murchison carbonaceous chondrite N88-30483
Observations of star formation N88-30538
Nebular processes recorded in chondritic meteorites N88-30541

EXHAUST NOZZLES
Numerical simulation of nozzle flows
[AD-A195144] N88-30064

EXOBIOLOGY
Biosample: Preservation, handling and observation system synthesis and breadboarding — Spacelab
[ESA-CR(P)-2609] N88-29857
Aerospace medicine and biology: A continuing bibliography with indexes (supplement 315)
[NASA-SP-7011(315)] N88-30281

EXPERIMENT DESIGN
Fluid physics double rack — Spacelab
[SD-TN-AI-012] N88-29992
Accommodation concept for fluid physics facilities, volume 2 — Spacelab
[SG-TN-AI-027-VOL-2] N88-29994

EXPERT SYSTEMS
Threat expert system technology advisor
[NASA-CR-177479] N88-29816
The 1988 Goddard Conference on Space Applications of Artificial Intelligence
[NASA-CP-3009] N88-30330

An intelligent training system for space shuttle flight controllers N88-30331
Artificial intelligence costs, benefits, risks for selected spacecraft ground system automation scenarios N88-30332
Artificial intelligence in a mission operations and satellite test environment N88-30334
Automated space vehicle control for rendezvous proximity operations N88-30335
Automated satellite control in Ada N88-30336
Knowledge based tools for Hubble Space Telescope planning and scheduling: Constraints and strategies N88-30338
The proposal entry processor: Telescience applications for Hubble Space Telescope science operations N88-30339
Candidate functions for advanced technology implementation in the Columbus mission planning environment N88-30340
A rule-based systems approach to spacecraft communications configuration optimization N88-30341
MOORE: A prototype expert system for diagnosing spacecraft problems N88-30343
Achieving real-time performance in FIESTA N88-30344
Mission telemetry system monitor: A real-time knowledge-based system N88-30345
Low level image processing techniques using the pipeline image processing engine in the flight telerobotic servicer N88-30346
An interactive testbed for development of expert tools for pattern recognition N88-30349
The second generation intelligent user interface for the crustal dynamics data information system N88-30352
Spacelab data processing facility (SLDPF) Quality Assurance (QA)/Data Accounting (DA) expert systems: Transition from prototypes to operational systems N88-30353
Automated cataloging and characterization of space-derived data N88-30354
A design for a ground-based data management system N88-30355
Automatic mathematical modeling for real time simulation system N88-30356
A simulation engine: Combining an expert system with a simulation language N88-30358
The advice taker/inquirer: A system for high-level acquisition of expert knowledge N88-30359
Verification and validation of rulebased systems for Hubble Space Telescope ground support N88-30361
The need for a comprehensive expert system development methodology N88-30362
Knowledge-based integrated information systems engineering: Highlights and bibliography. Knowledge-Based Integrated Information Systems Engineering (KBIISE) Project, volume 1
[AD-A195850] N88-30449
Technical opinions regarding knowledge-based integrated information systems engineering, volume 8
[AD-A195857] N88-30454
Knowledge-Based Integrated Information Systems Development Methodologies Plan. Knowledge-Based Integrated Information Systems Engineering (KBIISE) report, volume 2
[AD-A195851] N88-30455
Information retrieval systems evolve-advances for easier and more successful use N88-30462

EXPLOSIVES
Response of SMA (Shielded Metal Arc) and narrow gap HY80 weldments to explosive shock loading
[AD-A195994] N88-30162

EXPOSURE
Alternative immersion accelerated testing of coating systems for Naval shoreline facilities N88-29977
Reduced time frame for predicting coating performance N88-29979

EXTERNAL STORE SEPARATION
The present status and the future of missile aerodynamics
[NASA-TM-100083] N88-29773

EXTERNAL STORES
Preliminary airworthiness evaluation of the UH-60A/ESSS (External Stores Support System) with HELLFIRE launcher installed
[AD-A196187] N88-29793

EXTINCTION
Optical measurements of soot in premixed flames
[NASA-TM-101305] N88-30090
A compilation of information and data on the Manson impact structure
[NASA-CR-183169] N88-30258
Intermediate polars observed in Brazil in the last eight years
[INPE-4567-PRE/1308] N88-30559

EXTINGUISHING
Ignition and extinguishing of a Solid Fuel Ramjet (SOFRAM)
[FOA-C-20713-2.1] N88-29865

EXTRACTION
Design criteria for extraction with chemical reaction and liquid membrane permeation
[NASA-TT-20352] N88-29899

EXTRAPOLATION
Application of sampling techniques to near-field far-field transformation
[ESA-CR(P)-2546] N88-30002
Convergence acceleration for vector sequences and applications to computational fluid dynamics
[NASA-TM-101327] N88-30377

EXTRAVEHICULAR ACTIVITY
Maintenance and supply options
[NASA-CR-172062] N88-29837
Study of human factors engineering criteria for extravehicular activity (EVA) systems, volume 1
[STF23-F87025-VOL-1] N88-30298

EXTREMELY LOW FREQUENCIES
Experimental proof of quasilongitudinal propagation of low-frequency waves in middle latitudes in upper ionosphere N88-30516

EXTRUDING
Volcanic contribution to crustal growth in the Central Andes: A new estimate and a discussion of uncertainties N88-30255

EYE (ANATOMY)
Central serous chorioretinopathy in USAF aviators: A review
[AD-A195697] N88-30260

EYE MOVEMENTS
Eye movements and spatial pattern vision
[AD-A195496] N88-30290

F

F REGION
One equatorial anomaly in nighttime ionospheric F region N88-30517

F-14 AIRCRAFT
Techniques used in the F-14 variable-sweep transition flight experiment
[NASA-TM-100444] N88-30093

F-16 AIRCRAFT
The cost and performance implications of reliability improvements in the F-16A/B
[AD-A195096] N88-29796
LANTIRN simulator training in the F-16C
[AD-A195201] N88-29826

FABRICATION
Tolerances for phase locking of semiconductor laser arrays
[AD-A195974] N88-30120
Ion exchange processes for fabrication of integrated optical waveguide structures into glass substrates
[VTT-48] N88-30405
Cluster beam studies
[AD-A195182] N88-30443

FABRICS
Stressed fabric abrasion test procedure for urethane coated fabric fuel tanks
[AD-A196327] N88-29982

FACE CENTERED CUBIC LATTICES
State variable approach to deformation phenomena in Face Centered Cubic (FCC) metals
[VTT-44] N88-29964

FACTOR ANALYSIS
Advancement of latent trait theory
[AD-A194302] N88-30269

FAILURE
Criteria for matrix dominated failure
[AD-A196263] N88-29887
Multi-metallic galvanic corrosion
[AD-A195995] N88-29963
Electrochemical evaluation of the long term corrosion resistance of polymer coated steel N88-29974
Automated early fatigue damage sensing system
[AD-A195717] N88-30143
Stress related failures causing open metallization
[AD-A195061] N88-30150
Heavy ion and proton tests for subsystem upset
[AD-A195267] N88-30442

FAILURE ANALYSIS
Intelligent fault diagnosis and failure management of flight control actuation systems
[NASA-CR-177481] N88-29790
Failure analysis for gas turbines
[NLR-MP-87037-U] N88-29808
Rupture of carbon fiber reinforced plastics (T300-914) composite materials: Influence of initial first ply failures on the fatigue behavior
[SNIAS-881-422-103] N88-29892

FAINT OBJECTS
Observations of faint field galaxies
[NASA-CR-183251] N88-30555

FALSE ALARMS
On adaptive cell-averaging CFAR (Constant False-Alarm Rate) radar signal detection
[AD-A196286] N88-30009
Evaluation of LISBON TAR SSR radar
[EEC/NOTE-5/87] N88-30015

FAR FIELDS
Development and demonstration of an on-board mission planner for helicopters
[NASA-CR-177482] N88-29817
Application of sampling techniques to near-field far-field transformation
[ESA-CR(P)-2546] N88-30002

FAR INFRARED RADIATION
Far infrared supplement: Catalog of infrared observations, second edition
[NASA-RP-1205] N88-30545

FASTENERS
Standard fatigue specimens for fastener evaluation — aircraft components
[FFA-TN-1987-68] N88-30157

FATIGUE (MATERIALS)
Fatigue crack growth characteristics of ARALL (trademark)-1
[AD-A196185] N88-29889
Modeling of micromechanisms of fatigue and fracture in hybrid materials
[AD-A195604] N88-30142
Automated early fatigue damage sensing system
[AD-A195717] N88-30143
Fatigue crack propagation: Probabilistic modeling and statistical analysis
[AD-A195885] N88-30155
An investigation of constitutive models for predicting viscoplastic response during cyclic loading
[AD-A194875] N88-30163
The development of acoustic emission for structural integrity monitoring of aircraft
[AD-A196264] N88-30398

FATIGUE LIFE
Spray automated balancing of rotors: Methods and materials
[NASA-CR-182151] N88-29825
Rupture of carbon fiber reinforced plastics (T300-914) composite materials: Influence of initial first ply failures on the fatigue behavior
[SNIAS-881-422-103] N88-29892

FATIGUE TESTS
Damage initiation in the short beam shear test of composite materials using stiffness reduction
[AD-A194880] N88-29883
Standard fatigue specimens for fastener evaluation — aircraft components
[FFA-TN-1987-68] N88-30157
The development of acoustic emission for structural integrity monitoring of aircraft
[AD-A196264] N88-30398

FAULT TOLERANCE
MOORE: A prototype expert system for diagnosing spacecraft problems N88-30343
Achieving real-time performance in FIESTA N88-30344
Parallel and distributed computation for fault-tolerant object recognition N88-30350

FEASIBILITY ANALYSIS
JUH-1H redesigned pneumatic boot deicing system flight test evaluation
[AD-A194918] N88-29785
Dielectric millimeter waveguides: A feasibility study for a novel dielectric millimeter waveguide
[AD-A195104] N88-30042

FEEDBACK
Mode locking of semiconductor laser with external cavity
[AD-A196018] N88-30117

FEEDBACK CONTROL
Pilot modeling N88-29736
Pilot modeling applications N88-29737
An analysis of lateral-directional handling qualities and Eigenstructure of high performance aircraft
[AD-A194874] N88-29814
Track performance considerations for monopulse radars
[AD-A196232] N88-30007
K(sup th)-order extended linearization
[AD-A194786] N88-30363
An approach to CMG steering using feedback linearization
[NASA-CR-183172] N88-30369

FEEDING (SUPPLYING)
Utilizing dynamic stability of orient parts
[AD-A195730] N88-30397

FIBER COMPOSITES
A test for interfacial effects and stress transfer in ceramic matrix composites
[NASA-CR-182873] N88-29880
A study of the critical factors controlling the synthesis of ceramic matrix composites from preceramic polymers
[AD-A195405] N88-29881
FIBER OPTICS
A fiber optic collective flight control system for helicopters
[AD-A195406] N88-29818
Performance analysis of FDDI
[NASA-CR-183206] N88-30321
A fiber optic beamforming processor for wideband direction finding
[AD-A194862] N88-30404
Ultra-wideband direction finding using a fiber optic beamforming processor
[AD-A194861] N88-30413
FIBER ORIENTATION
Rupture of carbon fiber reinforced plastics (T300-914) composite materials: Influence of initial first ply failures on the fatigue behavior
[SNIAS-881-422-103] N88-29892
FIBER STRENGTH
A test for interfacial effects and stress transfer in ceramic matrix composites
[NASA-CR-182873] N88-29880
Rupture of carbon fiber reinforced plastics (T300-914) composite materials: Influence of initial first ply failures on the fatigue behavior
[SNIAS-881-422-103] N88-29892
FIELD EFFECT TRANSISTORS
Optoelectronic gain control of a microwave single stage GaAs MESFET amplifier
[NASA-CR-182201] N88-30055
Power MISFETs on OnP
[AD-A195242] N88-30436
Joint services electronics program
[AD-A195731] N88-30439
FIELD OF VIEW
Visual sensitivities under reduced oxygen
[AD-A195628] N88-30279
FIELD THEORY (PHYSICS)
Introduction to string theory
[DE88-702706] N88-30445
FIGHTER AIRCRAFT
Aircraft dynamics: Aerodynamic aspects and wind tunnel techniques N88-29731
The Soviet Stealth fighter: Check or checkmate
[AD-A195200] N88-29791
The cost and performance implications of reliability improvements in the F-16A/B
[AD-A195096] N88-29796
Integration of LANTIRN (Low Altitude Navigation and Targeting Infrared for Night) into operational fighter training
[AD-A194906] N88-29799
FILM COOLING
Studies of gas turbine heat transfer airfoil surface and end-wall cooling effects
[AD-A195165] N88-29805
The thermal behavior of film cooled turbulent boundary layers as affected by longitudinal vortices
[AD-A195155] N88-30095
FINITE DIFFERENCE THEORY
Space marching Euler solvers N88-29759
Three-dimensional gas turbine combustor modelling N88-29937
On the application of finite-difference techniques for the computation of the flow field in gas turbine combustors with complex geometries N88-29938
Numerical field model simulation of full scale fire tests in a closed spherical/cylindrical vessel
[AD-A195067] N88-29998
An analysis of finite-difference and finite-volume formulations of conservation laws
[NASA-CR-177416] N88-30071
Finite-difference simulations of Rayleigh-wave scattering by shallow heterogeneity
[AD-A194961] N88-30259
FINITE ELEMENT METHOD
Damage initiation in the short beam shear test of composite materials using stiffness reduction
[AD-A194880] N88-29883
Numerical modelling of premixed flames in gaseous media N88-29944
Geometric and material nonlinear analysis of structures comprising rectangular hollow sections
[CE-79] N88-30141
A parametric study of embedded cantilever retaining walls: The results of a finite element study
[RR-CE83] N88-30152
Obtaining stress intensity factors on cracks, by means of fitting techniques on numerical results calculated with the finite element method N88-30153
FINITE VOLUME METHOD
On the application of finite-difference techniques for the computation of the flow field in gas turbine combustors with complex geometries N88-29938
An analysis of finite-difference and finite-volume formulations of conservation laws
[NASA-CR-177416] N88-30071
Numerical simulation of unsteady incompressible viscous flows in generalized coordinate systems
[NASA-TM-101016] N88-30085
FIRES
Numerical field model simulation of full scale fire tests in a closed spherical/cylindrical vessel
[AD-A195067] N88-29998
FIXED WINGS
Analysis of a fixed-pitch X-wing rotor employing lower surface blowing
[AD-A187379] N88-29779
FLAME HOLDERS
Flame stabilization in a reheat combustor N88-29921
FLAME PROPAGATION
Numerical modelling of premixed flames in gaseous media N88-29944
Gaseous premixed flames in non-uniform flows N88-29945
Flamespreading processes in obliquely loaded stick propellant beds
[AD-A195081] N88-29956
FLAME STABILITY
Flame stabilization in a reheat combustor N88-29921
Modeling the stability of a turbulent premixed flame, downstream from a step by a Lagrangian method N88-29943
FLAMMABILITY
Determination of relative flammability of materials by pyrolysis and gas-chromatographic light hydrocarbon analysis
[DE88-012449] N88-29898
FLAT PLATES
Studies of gas turbine heat transfer airfoil surface and end-wall cooling effects
[AD-A195165] N88-29805
Investigation of large-scale structures in the near wake of a parallel flat plate
[ESA-TT-1100] N88-30080
FLEXIBILITY
Reduced flexibility in processing Titan 4 space launch vehicles at Cape Canaveral Air Force Station
[AD-A194908] N88-29834
Modeling robot flexibility for endpoint force control
[AD-A195923] N88-30132
FLEXIBLE BODIES
Current and proposed gust criteria and analysis methods: An FAA overview N88-29718
Measured and predicted responses of the Nord 260 aircraft to the low altitude atmospheric turbulence N88-29723
Dynamics of articulated aerospace structures
[AD-A195685] N88-29794
Robust design of distributed controllers for large flexible space structures
[NASA-CR-183202] N88-30134
FLIGHT CHARACTERISTICS
Advances in Flying Qualities
[AGARD-LS-157] N88-29735
Advances in flying qualities: Concepts and criteria for a mission oriented flying qualities specification N88-29739
A second look at MIL prime flying qualities requirements N88-29740
The role of simulation in flying qualities and flight control system related development N88-29742
FLIGHT CONTROL
Advances in Flying Qualities
[AGARD-LS-157] N88-29735
Low-speed longitudinal flying qualities of modern transport aircraft N88-29738
Advances in flying qualities: Concepts and criteria for a mission oriented flying qualities specification N88-29739
The role of simulation in flying qualities and flight control system related development N88-29742
Intelligent fault diagnosis and failure management of flight control actuation systems
[NASA-CR-177481] N88-29790
A multiprocessor avionics system for an unmanned research vehicle
[AD-A194806] N88-29800
An analysis of lateral-directional handling qualities and Eigenstructure of high performance aircraft
[AD-A194874] N88-29814
N-version software demonstration for digital flight controls
[NASA-CR-181483] N88-29815
A fiber optic collective flight control system for helicopters
[AD-A195406] N88-29818
Controlled degradation of resolution of high-quality flight simulator images for training effectiveness evaluation
[AD-A196189] N88-29823
Four-axis side-arm flight control simulator investigation
[AD-A196026] N88-30294
Improvement of head-up display standards. Volume 3: An evaluation of head-up display safety
[AD-A195787] N88-30300
Space station proximity operations windows: Human factors design guidelines
[NASA-TM-88233] N88-30301
An intelligent training system for space shuttle flight controllers N88-30331
FLIGHT CREWS
A field study on soft contact lens wear in USAF military transport aircraft
[AD-A195962] N88-30285
FLIGHT INSTRUMENTS
The NAE atmospheric research aircraft N88-29730
Improvement of head-up display standards. Volume 3: An evaluation of head-up display safety
[AD-A195787] N88-30300
FLIGHT OPTIMIZATION
The OFP (Operational Flight Program) update cycle needs you
[AD-A194910] N88-29798
FLIGHT SIMULATION
The role of simulation in flying qualities and flight control system related development N88-29742
Minimum-complexity helicopter simulation math model
[NASA-CR-177476] N88-29819
A digital simulation technique for the Dryden atmospheric model
[NASA-TT-20342] N88-30266
Prediction and measurement of human pilot dynamic characteristics in a manned rotorcraft simulation
[NASA-CR-183246] N88-30297
FLIGHT SIMULATORS
Controlled degradation of resolution of high-quality flight simulator images for training effectiveness evaluation
[AD-A196189] N88-29823
LANTIRN simulator training in the F-16C
[AD-A195201] N88-29826
FLIGHT TESTS
Flight test equipment for the on-board measurement of wind turbulence N88-29719
Angle of attack and sideslip estimation using an inertial reference platform
[AD-A194876] N88-29769
Preliminary airworthiness evaluation of the UH-60A/ESSS (External Stores Support System) with HELLFIRE launcher installed
[AD-A196187] N88-29793
A multiprocessor avionics system for an unmanned research vehicle
[AD-A194806] N88-29800
An analysis of lateral-directional handling qualities and Eigenstructure of high performance aircraft
[AD-A194874] N88-29814
Space structure (dynamics and control) theme development
[NASA-TM-100597] N88-29850
Techniques used in the F-14 variable-sweep transition flight experiment
[NASA-TM-100444] N88-30093
FLIGHT TRAINING
Integration of LANTIRN (Low Altitude Navigation and Targeting Infrared for Night) into operational fighter training
[AD-A194906] N88-29799
FLOODS
LANDSAT-TM data to map flooded areas
[INPE-4594-PRE/1324] N88-30177
Constraints on continental accretion from sedimentation N88-30202
FLOW CHARACTERISTICS
Flow characteristics of a model annular combustor N88-29924
FLOW DISTRIBUTION
Numerical solutions of unsteady inviscid transonic turbine cascade flows
[AD-A196111] N88-29748
A streamwise upwind algorithm for the Euler and Navier-Stokes equations applied to transonic flows
[NASA-TM-101019] N88-29751
Space marching Euler solvers N88-29759
Prediction of base-flows N88-29765
The computation of flow past an oblique wing using the thin-layer Navier-Stokes equations
[NASA-TM-88317] N88-29774
Computational methods for the problems of the tip vortex
[NASA-CR-181438] N88-29775

A new computational capability for ramjet projectiles [AD-A196061] N88-29812
An experimental study of an adaptive-wall wind tunnel [NASA-CR-183152] N88-29821
Alternative fuel spray behavior N88-29912
Flow characteristics of a model annular combustor N88-29924
Flamelet chemistry modelling of soot formation for radiation N88-29926
On the application of finite-difference techniques for the computation of the flow field in gas turbine combustors with complex geometries N88-29938
Analysis of the flow through double swirl airblast atomizers N88-29949
Volumetric measurement of vorticity vectors by optical probe [AD-A195997] N88-30061
User's manual for three dimensional boundary layer (BL3-D) code [NASA-CR-174899] N88-30063
Assessment of a 3-D boundary layer analysis to predict heat transfer and flow field in a turbine passage [NASA-CR-174894] N88-30066
Contamination and distortion of steady flow field induced by discrete frequency disturbances in aircraft gas engines [AD-A195440] N88-30069
Numerical simulation of unsteady incompressible flow in a partially-filled rotating cylinder [AD-A196001] N88-30073
Investigation of large-scale structures in the near wake of a parallel flat plate [ESA-TT-1100] N88-30080
Experimental and numerical investigation of the effect of distributed suction on oblique shock wave/turbulent boundary layer interaction [NASA-TM-101334] N88-30084
Studies of unsteady axial-compressor functioning N88-30129
Determination of multiaxial flow surfaces at elevated temperatures using the concept of dissipation potential [ORNL/TM-10787] N88-30149
Vibrational power flow analysis of rods and beams [NASA-CR-183166] N88-30151
Knowledge-based flow field zoning [NASA-TM-101023] N88-30314

FLOW EQUATIONS
Mathematical problems of nonlinear wave propagation and of waves in heterogeneous media [AD-A195970] N88-30057

FLOW MEASUREMENT
Volumetric measurement of vorticity vectors by optical probe [AD-A195997] N88-30061
Investigation of large-scale structures in the near wake of a parallel flat plate [ESA-TT-1100] N88-30080
Laser Doppler Velocimeter (LDV) and pressure measurements of gas particle flows in bends [VKI-TN-163] N88-30083
Positron emission tomography: A new technique for observing fluid behavior in engineering systems [PNR90471] N88-30091

FLOW STABILITY
Transition at hypersonic speeds [NASA-CR-178315] N88-30058

FLOW VELOCITY
A study of the effect of random input motion on low Reynolds number flows [AD-A195559] N88-29747
Flow characteristics of a model annular combustor N88-29924

FLOW VISUALIZATION
A study of the effect of random input motion on low Reynolds number flows [AD-A195559] N88-29747
Positron emission tomography: A new technique for observing fluid behavior in engineering systems [PNR90471] N88-30091
Use of holography in vibration and flutter study of fans [PNR90458] N88-30098

FLUID DYNAMICS
Accommodation concept for fluid physics facilities, volume 2 — Spacelab [SG-TN-AI-027-VOL-2] N88-29994
Assessment of a 3-D boundary layer analysis to predict heat transfer and flow field in a turbine passage [NASA-CR-174894] N88-30066

FLUID FLOW
Preliminary investigation of flow modeling during solid propellant processing [AD-A196168] N88-29987
Experimental and analytical study of two-phase flow in zero gravity [AD-A195223] N88-29993
The use of upwind schemes at high Reynolds number: A cautionary note [AD-A196227] N88-30074
Approximation of viscoelastic stresses from Newtonian turbulent kinematics [AD-A194317] N88-30077
Simulations of lava flows on Mars N88-30495
Small-scale volcanic landforms indicative of distributary tube systems N88-30496
Volcanic styles at Alba Patera, Mars: Implications of lava flow morphology to the volcanic history N88-30497

FLUID MANAGEMENT
Study of toluene rotary fluid management device and shear flow condenser performance for a space-based organic Rankine power system [NASA-CR-180865] N88-29872

FLUID MECHANICS
Fluid physics double rack — Spacelab [SD-TN-AI-012] N88-29992

FLUORESCENCE
Autoionization for lower level detrapping in X-ray lasers [AD-A195845] N88-30123
Immunofluorescence localization of dissociation supernatant and extracellular matrix components in Lytechinus pictus sectioned embryos [NASA-CR-183137] N88-30276

FLUTTER
Empirical flutter prediction method [AD-A195699] N88-29810

FLUTTER ANALYSIS
A streamwise upwind algorithm for the Euler and Navier-Stokes equations applied to transonic flows [NASA-TM-101019] N88-29751
Application of unsteady aerodynamic methods for transonic aeroelastic analysis [NASA-TM-100665] N88-29754
Recent advances in transonic computational aeroelasticity [NASA-TM-100663] N88-29778
Use of holography in vibration and flutter study of fans [PNR90458] N88-30098

FLUX (RATE)
Ring current role in dynamics of fluctuating electron and ion fluxes in low-latitude magnetosphere N88-30514

FLUX DENSITY
Matching P.S.D.: Design loads N88-29720
In-house capacitor technology program [AD-A194804] N88-30049
Vibrational power flow analysis of rods and beams [NASA-CR-183166] N88-30151

FOAMS
Determination of the specific area of liquid gas and the velocity of weak pressure waves in aqueous foams [NASA-TT-20347] N88-30087

FOCAL PLANE DEVICES
The focal plane reception pattern calculation for a paraboloidal antenna with a nearby fence [NASA-TM-100691] N88-30039
Imaging instrument of the vegetation payload (SPOT 4) [SNIAS-881-440-107] N88-30169

FOCUSING
Image focusing in space and time [AD-A195839] N88-30410

FOLDING STRUCTURES
Alternative module configurations for advanced solar arrays on low orbit and extended lifetime missions (AMOC 2) [ESA-CR(P)-2581] N88-30182

FORCED CONVECTION
Impact of ETO propellants on the aerothermodynamic analyses of propulsion components [NASA-TM-101303] N88-30094

FORESTS
Recent measurements of ozone in the Amazon forests [INPE-4494-PRE/1258] N88-30185
Investigation of the large-scale impact of air pollution components on forest ecosystems in Bavaria [ESA-TT-1087] N88-30187
Some results from the Amazon Forest micrometeorological experiment [INPE-4631-PRE/1346] N88-30263

FORMAT
A detection theory analysis of visual display performance [AD-A196291] N88-30292
Partitioned storage for temporal databases [AD-A195093] N88-30451

FORMULATIONS
Large displacement and rotational formulation for laminated cylindrical shells including parabolic transverse shear [AD-A194871] N88-30158
Formulation and solution of economic equilibrium problems [AD-A196034] N88-30470

FORTRAN
Supermap for Cray FORTRAN: A user's guide [NASA-CR-177410] N88-30308

FOUNDATIONS
Computer-Aided Structural Engineering (CASE) project. Development of design formulas for ribbed mat foundations on expansive soils [AD-A194807] N88-30307

FOURIER TRANSFORMATION
Photoacoustic Fourier transform infrared spectroscopy. An early detection technique for coatings degradation N88-29968

FRACTURE MECHANICS
Additional fracture and strength test results for A723 steel and 38644 titanium [AD-A196329] N88-29960
Stress intensity factors for cracked metallic structures under rapid thermal loading [AES-8609709F-1] N88-29962
Modeling of micromechanisms of fatigue and fracture in hybrid materials [AD-A195604] N88-30142
Obtaining stress intensity factors on cracks, by means of fitting techniques on numerical results calculated with the finite element method N88-30153

FRACTURE STRENGTH
Additional fracture and strength test results for A723 steel and 38644 titanium [AD-A196329] N88-29960
Modeling of micromechanisms of fatigue and fracture in hybrid materials [AD-A195604] N88-30142

FRACTURES (MATERIALS)
Hydrogen embrittlement of iron-nickel alloys [AD-A195909] N88-29958

FREE ELECTRON LASERS
Research on a two-stage free electron laser oscillator [AD-A195991] N88-30115
Bibliography of Soviet laser developments, number 88, March - April 1987 [AD-A195978] N88-30116
Vanderbilt free electron laser project in biomedical and materials research [AD-A195961] N88-30121
Ultrafast processes and spectroscopy with free electron lasers [AD-A195248] N88-30126

FREE FLOW
Containment of a silicone fluid free surface in reduced gravity using barrier coatings [NASA-TM-101314] N88-30072

FREE VIBRATION
Free vibration of rectangular plates with a small initial curvature [NASA-CR-179370] N88-30148

FRENCH SPACE PROGRAMS
Microwave remote sensing in the French industries [ETN-88-93081] N88-30171

FREQUENCIES
Contamination and distortion of steady flow field induced by discrete frequency disturbances in aircraft gas engines [AD-A195440] N88-30069

FREQUENCY STABILITY
The aspect ratio dependence of the attractor dimension in Taylor-Couette flow [AD-A196297] N88-30065

FREQUENCY STANDARDS
Electromagnetic metrology N88-30024

FRESNEL DIFFRACTION
Precision measurement of the Fresnel drag coefficient using a ring laser [AD-A196025] N88-30043

FRICTION WELDING
The effect of notch root radius on the determination of toughness in ultrahigh strength steel friction welds [AD-A195952] N88-30156

FUEL CELLS
Electrocatalytic reduction of oxygen on modified oxide surfaces [NASA-TM-101333] N88-29952
Fuel cells for space use [FCP-TR-DOS-SY-026] N88-30183

FUEL COMBUSTION
Experiments and modeling of multi-component fuel behavior in combustion [AD-A195011] N88-29896
Alternative fuel spray behavior N88-29912
Atomization of alternative fuels N88-29913
Turbulence effects on the droplet distribution behind airblast atomizers N88-29915
Multiple scattering effects in drop sizing of dense fuel sprays by laser diffraction N88-29917

Influence of operating conditions on the atomization and distribution of fuel by air blast atomizers N88-29916
The characterizatin of combustion by fuel composition: Measurements in a small conventional combustor N88-29920
Flame stabilization in a reheat combustor N88-29921
High performance turbofan afterburner systems N88-29922
Comparison of the performance of a reverse flow annular combustion chamber under low and high pressure conditions N88-29923
Radiation transfer in gas turbine combustors N88-29929
Gas turbine smoke measurement: A smoke generator for the assessment of current and future techniques N88-29930
Rates of formation of soot from hydrocarbon flames and its destruction N88-29933
Modeling the stability of a turbulent premixed flame, downstream from a step by a Lagrangian method N88-29943
Gaseous premixed flames in non-uniform flows N88-29945
Modeling and experimental study of a reactive flow confined with well injection N88-29946
Influence of the convection on evaporation and combustion of a fuel droplet N88-29948
A small annular combustor of high power density, wide operating range and low manufacturing cost N88-29951

FUEL CONTAMINATION
Atomization of alternative fuels N88-29913
Fuel effects on flame radiation and hot-section durability N88-29925

FUEL CONTROL
Nozzle airflow influences on fuel patternation N88-29916

FUEL INJECTION
The dc power control for a liquid-fed resistojet [NASA-TM-101326] N88-29869
Combustion and fuels in gas turbine engines [AGARD-CP-422] N88-29910
Simulation study of spraying, streaming and vaporization phenomena associated with fuel injection N88-29914
Spray performance of a vaporizing fuel injector N88-29919
Modeling and experimental study of a reactive flow confined with well injection N88-29946

FUEL SPRAYS
Alternative fuel spray behavior N88-29912
Atomization of alternative fuels N88-29913
Simulation study of spraying, streaming and vaporization phenomena associated with fuel injection N88-29914
Turbulence effects on the droplet distribution behind airblast atomizers N88-29915
Nozzle airflow influences on fuel patternation N88-29916
Multiple scattering effects in drop sizing of dense fuel sprays by laser diffraction N88-29917
Influence of operating conditions on the atomization and distribution of fuel by air blast atomizers N88-29918
Spray performance of a vaporizing fuel injector N88-29919
The characterizatin of combustion by fuel composition: Measurements in a small conventional combustor N88-29920
The performance of a surrogate blend in simulating JP-4 in a spray-fueled combustor N88-29926

FUEL TANKS
Stressed fabric abrasion test procedure for urethane coated fabric fuel tanks [AD-A196327] N88-29962

FUEL TESTS
Fuel property effects on the US Navy's TF30 engine N88-29911

FULL SCALE TESTS
Numerical field model simulation of full scale fire tests in a closed spherical/cylindrical vessel [AD-A195067] N88-29998

FUNCTIONAL ANALYSIS
Robust finite-dimensional LQG (Linear Quadric Gaussian)-based controllers for a class of distributed parameter systems [AD-A194872] N88-30382

FUNCTIONAL DESIGN SPECIFICATIONS
Specifications and performance of ultrastable oscillators in the DORIS orbitography and positioning system [ETN-88-92761] N88-29831
Qualification test levels for units to be derived from mechanical test data analysis — ESA [REPT-37-158-EI/ET/AG] N88-30139
Study of human factors engineering criteria for extravehicular activity (EVA) systems, volume 1 [STF23-F87025-VOL-1] N88-30298

FUNCTIONS (MATHEMATICS)
Algorithms for nonlinear least-squares problems [AD-A196071] N88-30305

FUSELAGES
Test of an 0.8-scale model of the AH-64 Apache in the NASA Langley full-scale wind tunnel [AD-A196129] N88-29768

G

GALACTIC EVOLUTION
Starbursts and their dynamics [NASA-CR-180227] N88-30549
Observations of faint field galaxies [NASA-CR-183251] N88-30555
A deep redshift survey of field galaxies. Comments on the reality of the Butcher-Oemler effect [NASA-CR-183255] N88-30558

GALACTIC RADIATION
Measurement of galactic radio emission at frequency 37 GHz from aboard spacecraft N88-30520

GALACTIC RADIO WAVES
Measurement of galactic radio emission at frequency 37 GHz from aboard spacecraft N88-30520

GALACTIC ROTATION
The kinematics of late-type supergiants [SER-C-PREPUBL-FASC-28] N88-30560
The dynamics of SBO galaxies. Part 1: The data [SER-C-PREPUBL-FASC-22] N88-30567

GALAXIES
Observations of faint field galaxies [NASA-CR-183251] N88-30555
A deep redshift survey of field galaxies. Comments on the reality of the Butcher-Oemler effect [NASA-CR-183255] N88-30558

GALERKIN METHOD
Convergence of Galerkin approximations for operator Riccati equations: A nonlinear evolution equation approach [NASA-CR-181706] N88-30386

GALILEO PROJECT
Mission telemetry system monitor: A real-time knowledge-based system N88-30345

GALLIUM
Development of a unit cell for a Ge:Ga detector array [NASA-CR-177445] N88-30100

GALLIUM ARSENIDES
High frequency GaAlAs modulator and photodetector for phased array antenna applications [NASA-TM-101328] N88-30048
Optoelectronic gain control of a microwave single stage GaAs MESFET amplifier [NASA-CR-182201] N88-30055
Automatic prober for the dc characterisation of gallium arsenide devices. Part 2: The data sorting and display facility [AD-A195408] N88-30111
Growth of GaAs crystals by the Heat Exchanger Method for microwave device applications [AD-A196028] N88-30435
Streaking images that appear only in the plane of diffraction in undoped GaAs single crystals: Diffraction imaging (topography) by monochromatic synchrotron radiation [NASA-CR-183257] N88-30437
Joint services electronics program [AD-A195731] N88-30439

GAMMA RAY ASTRONOMY
Gamma radiation expected from supernova 1987A in large magellanic cloud N88-30505

GAMMA RAYS
Phase modulation of recoilless gamma radiation in Mossbauer spectroscopy [ETN-88-92648] N88-30403
A coded mask telescope for observations of X and gamma ray sources in the southern sky [INPE-4580-PRE/1314] N88-30551
Research in particle and gamma-ray astrophysics [NASA-CR-183126] N88-30566
X- and gamma-ray background observations in Antarctic [INPE-4583-PRE/1317] N88-30578

GAS ANALYSIS
The behaviour of synthetic fuels in a small transparent combustor N88-29950
Energy budget and ground temperatures in hot regions [AD-A196298] N88-30268

GAS CHROMATOGRAPHY
Determination of relative flammability of materials by pyrolysis and gas-chromatographic light hydrocarbon analysis [DE88-012449] N88-29898

GAS COOLING
Studies of gas turbine heat transfer airfoil surface and end-wall cooling effects [AD-A195165] N88-29805

GAS DISCHARGES
The study of hydromagnetic waves and RF heating using the TORTUS tokamak, the development of diagnostic techniques based on submillimeter lasers and the gyrotron, and gas discharge N88-30419

GAS FLOW
Laser Doppler Velocimeter (LDV) and pressure measurements of gas particle flows in bends [VKI-TN-163] N88-30083
Nonequilibrium flow of a dissociating gas in a horizontal channel with axial temperature variation [DE88-702536] N88-30089
Transverse CO2 laser two-dimensional gain distributions [AD-A196240] N88-30119

GAS GIANT PLANETS
Numerical evidence that the motion of Pluto is chaotic [AD-A195920] N88-30568

GAS LASERS
Bibliography of Soviet laser developments, number 88, March - April 1987 [AD-A195978] N88-30116

GAS TEMPERATURE
Nonequilibrium flow of a dissociating gas in a horizontal channel with axial temperature variation [DE88-702536] N88-30089

GAS TURBINE ENGINES
V2500 engine collaboration [PNR90423] N88-29803
Constitutive modeling for isotropic materials [NASA-CR-182132] N88-29811
Spray automated balancing of rotors: Methods and materials [NASA-CR-182151] N88-29825
Radiation transfer in gas turbine combustors N88-29929
Gas turbine smoke measurement: A smoke generator for the assessment of current and future techniques N88-29930
Assessment of a 3-D boundary layer analysis to predict heat transfer and flow field in a turbine passage [NASA-CR-174894] N88-30066

GAS TURBINES
Failure analysis for gas turbines [NLR-MP-87037-U] N88-29808
Gas turbine combustion modeling N88-29936
Three-dimensional gas turbine combustor modelling N88-29937
On the application of finite-difference techniques for the computation of the flow field in gas turbine combustors with complex geometries N88-29938
Numerical modeling of combustion processes in gas turbines N88-29939
Modelling of CO oxidation in dilution jet flows N88-29947
Determination of the hydroperoxide potential of jet fuels [AD-A195975] N88-29991
User's manual for three dimensional boundary layer (BL3-D) code [NASA-CR-174899] N88-30063
Contamination and distortion of steady flow field induced by discrete frequency disturbances in aircraft gas engines [AD-A195440] N88-30069

GASES
Numerical modelling of premixed flames in gaseous media N88-29944

GAUGE THEORY
Lagrangian of the self-duality equation and d = 10, N = 2b supergravity [DE88-701554] N88-30563

GAUSSIAN ELIMINATION
Reducing the parallel solution time of sparse circuit matrices using reordered Gaussian elimination and relaxation [AD-A195152] N88-30045

GEOCHEMISTRY
Pb isotope constaints on the extent of crustal recycling into a steady state mantle N88-30215
Crustal evolution and the eclogite to granulite phase transition in xenoliths from the West African Craton N88-30217
Changing styles of crustal growth in Southern Africa: Constraints from geochemical and Sr-Nd isotope studies in Archaean to Pan African terrains N88-30227
Continental crustal formation and recycling: Evidence from oceanic basalts N88-30238
Evolution of the Dharwar Craton: A terrain of early Archean crustal stability, long term orogenic cycles and large scale palaeobiological activity N88-30241

The growth of the continental crust: Constraints from radiogenic isotope geochemistry N88-30245
Crustal growth in the Archean: The geochemical evidence N88-30246
Crustal underplating in the North American Craton: Evidence from the Petrogenesis of anorthositic rocks in the Middle Proterozoic Midcontinent Rift System N88-30252
Terrestrial versus giant planet formation N88-30543

GEOCHRONOLOGY
Workshop on the Growth of Continental Crust [NASA-CR-183073] N88-30201
Role of zircon in tracing crustal growth and recycling N88-30211
Construction of mass-age curves for the continental crust: An empirical model and an example from the western US N88-30213
Pb isotope constaints on the extent of crustal recycling into a steady state mantle N88-30215
Metamorphic P-T paths and Precambrian crustal growth in East Antarctica N88-30218
The early archaean crustal history of West Greenland as recorded by detrital zircons N88-30221
Growth of early archaean crust in the ancient Gneiss complex of Swaziland and adjacent Barberton Greenstone Belt, Southern Africa N88-30223
Structure of Southwestern Michipicoten Greenstone Belt, Ontario: Evidence for Archean accretion N88-30228
Geochronological and lead-isotope evidences for rapid crust formation in middle-proterozoic time: The Labrador example N88-30239
The growth of the continental crust: Constraints from radiogenic isotope geochemistry N88-30245
Mineralization through geologic time: Evolution of continental crust N88-30250
Late-Archaean crustal growth in the Lewisian Complex of Northwest Scotland: Diachroneity in magmatic accretion and implications for models of crustal growth N88-30253
The effect of thicker oceanic crust in the Archaean on the growth of continental crust through time N88-30254
Spectral analysis of the Elatina varve series [NASA-CR-183085] N88-30260

GEODETIC ACCURACY
Estimation of short-wavelength gravity on a dense grid using digital terrain elevation data [AD-A196325] N88-30196

GEODETIC SURVEYS
DATATRAN: Datum transformation software [AD-A195723] N88-30175
Estimation of short-wavelength gravity on a dense grid using digital terrain elevation data [AD-A196325] N88-30196
Analytical method for approximate geodetic referencing of scanner images of meteorological artificial earth satellites using control points N88-30527

GEOGRAPHIC INFORMATION SYSTEMS
A digital terrain model system for a microcomputer [INPE-4610-PRE/1333] N88-30316

GEOLOGICAL FAULTS
Diapirs of the Mediterranean ridge: The tectonic regime of an incipient accreted terrane N88-30224
Faulting and its relation to volcanism: Mars western equatorial region N88-30489

GEOLOGY
NASA MEVTV Program Working Group Meeting: Volcanism on Mars [NASA-CR-183074] N88-30487

GEOMAGNETIC TAIL
Relationship between characteristics of low-energy electrons and geomagnetic disturbance in geostationary orbit N88-30501

GEOMETRICAL THEORY OF DIFFRACTION
Fields and waves N88-30025

GEOMETRY
Numerical modelling of premixed flames in gaseous media N88-29944
An automated computerized vision technique for determination of three-dimensional object geometry N88-30348

GEOMORPHOLOGY
Evaluation of LANDSAT-TM data for geomorphological mapping [INPE-4593-PRE/1324] N88-30168
Eruptive viscosity and volcano morphology N88-30488
The Martian highland paterae: Evidence for explosive volcanism on Mars N88-30492
Physical properties of surface materials on Martian volcanoes: Dust-covered lava and ash N88-30493
Rifts of deeply eroded Hawaiian basaltic shields: A structural analog for large Martian volcanoes N88-30494
Small-scale volcanic landforms indicative of distributary tube systems N88-30496

GEOPHYSICS
Solar-geophysical data number 523, March 1988. Part 2: (Comprehensive reports). Data for September 1987 and miscellanea [PB88-212774] N88-30576

GEOSYNCHRONOUS ORBITS
Relationship between characteristics of low-energy electrons and geomagnetic disturbance in geostationary orbit N88-30501

GEOTHERMAL ANOMALIES
Metamorphic P-T paths and Precambrian crustal growth in East Antarctica N88-30218

GERMANIUM
Development of a unit cell for a Ge:Ga detector array [NASA-CR-177445] N88-30100

GERMANY
History of aeroelasticity in Germany from the beginning to 1945 [ESA-TT-1082] N88-29767

GET AWAY SPECIALS (STS)
Aerospace payload support systems [AFGL-TR-87-0241] N88-29843

GLASS
Ion exchange processes for fabrication of integrated optical waveguide structures into glass substrates [VTT-46] N88-30405

GLOVES
Four-axis side-arm flight control simulator investigation [AD-A196026] N88-30294

GLOW DISCHARGES
Decomposition of hydrazine by high frequency glow electrical discharges [NASA-TT-20240] N88-29906

GNEISS
The timing and mechanism of depletion in Lewisian granulites N88-30209
Growth of early archaean crust in the ancient Gneiss complex of Swaziland and adjacent Barberton Greenstone Belt, Southern Africa N88-30223
Reappraisal of the geology of Kangimut Sammisoq, Ameralik Fjord, Southern West Greenland: Crustal structure and interpretation of isotopic data N88-30234

GOERTLER INSTABILITY
The strong nonlinear interaction of Tollmien-Schlichting waves and Taylor-Goertler vortices in curved channel flow [NASA-CR-181697] N88-29716
On the generation of mean flows by the interaction of Goertler vortices and Tollmien-Schlichting waves in curved channel flows [NASA-CR-181690] N88-29743

GOVERNMENT PROCUREMENT
The cost and performance implications of reliability improvements in the F-16A/B [AD-A195096] N88-29796

GRAIN BOUNDARIES
Transverse expansion of individual carbon and graphite filaments [AD-A195073] N88-29891

GRANITE
The timing and mechanism of depletion in Lewisian granulites N88-30209
Genesis of archean granitoids in the Pilbara block and implications for crustal growth N88-30210
Crustal evolution and the eclogite to granulite phase transition in xenoliths from the West African Craton N88-30217

GRAPHITE
Transverse expansion of individual carbon and graphite filaments [AD-A195073] N88-29891

GRAPHITE-EPOXY COMPOSITES
Analytical study of graphite-epoxy tube response to thermal loads [NASA-CR-183215] N88-29884
Experimental aspects of using time-averaged holographic interferometry to detect barely visible impact damage in a graphite/epoxy composite plate [AD-A194418] N88-30097

GRAPHITIZATION
Brominated graphite fibers and method of producing the same [NASA-CASE-LEW-14698-1] N88-29888

GRAVITATIONAL EFFECTS
The origin of the moon: Further studies of the giant impact N88-30474

GRAVITATIONAL FIELDS
General equations for the motions of ice crystals and water drops in gravitational and electric fields [NASA-CR-183229] N88-30070
Estimation of short-wavelength gravity on a dense grid using digital terrain elevation data [AD-A196325] N88-30196
Relationships among earth's gravity field, magnetic field, crustal structure and the magnetic character of crustal rocks [AD-A195539] N88-30198
Gravity anomalies, plate tectonics and the lateral growth of Precambrian North America N88-30248
Resonance effects accompanying motion with low thrust in earth-moon system N88-30510

GRAVITY ANOMALIES
Gravity anomalies, plate tectonics and the lateral growth of Precambrian North America N88-30248

GREENHOUSE EFFECT
Nineteenth Lunar and Planetary Science Conference. Press abstracts [NASA-CR-183037] N88-30473
Did the greenhouse effect kill the dinosaurs N88-30484

GRID GENERATION (MATHEMATICS)
Adaptive mesh generation for viscous flows using Delaunay triangulation [NASA-CR-181699] N88-29749
Three-dimensional elliptic grid generation technique with application to turbomachinery cascades [NASA-TM-101330] N88-30078
Knowledge-based flow field zoning [NASA-TM-101023] N88-30314

GROUND EFFECT (AERODYNAMICS)
Aerodynamics in ground effect and predicted landing ground roll of a fighter configuration with a secondary-nozzle thrust reverser [NASA-TP-2834] N88-29752

GROUND SUPPORT EQUIPMENT
Artificial intelligence costs, benefits, risks for selected spacecraft ground system automation scenarios N88-30332
Study on industrial organization for European Ground Support Equipment (EGSE) to support European space programs. Volume 1: Technical reports [SD-RP-AI-009-VOL-1] N88-30446
Study on industrial organization for European Ground Support Equipment (EGSE) to support European space programs. Volume 2: Technical reports [SD-RP-AI-009-VOL-2] N88-30448

GROUND SUPPORT SYSTEMS
Reduced flexibility in processing Titan 4 space launch vehicles at Cape Canaveral Air Force Station [AD-A194908] N88-29834
Aerospace payload support systems [AFGL-TR-87-0241] N88-29843
Study on industrial organization for European Ground Support Equipment (EGSE) to support European space programs. Volume 1: Technical reports [SD-RP-AI-009-VOL-1] N88-30446
Study on industrial organization for European Ground Support Equipment (EGSE) to support European space programs. Volume 2: Technical reports [SD-RP-AI-009-VOL-2] N88-30448

GROUND TESTS
Successful completion of a cyclic ground test of a mercury ion auxiliary propulsion system [NASA-TM-101351] N88-29873

GROUND TRUTH
Integrating multispectral imagery and ground level hyperspectral signature data [AD-A195976] N88-30166

GROWTH
Growth of continental crust: Clues from Nd isotopes and Nb-Th relationships in mantle-derived magmas N88-30205

GUANIDINES
Discovery of a low temperature form of TAGN (Triaminoguanidinium Nitrate) [AD-A196059] N88-29989

GUN PROPELLANTS
Gas phase combustion chemistry of nitramine propellants [AD-A195082] N88-29902
Flamespreading processes in obliquely loaded stick propellant beds [AD-A195081] N88-29956

GUNS (ORDNANCE)
Combustion diagnostics of propellant with new grain geometries [AD-A194944] N88-29895

GUST ALLEVIATORS
The Flight of Flexible Aircraft in Turbulence: State-of-the-Art in the Description and Modelling of Atmospheric Turbulence [AGARD-R-734-ADD] N88-29717
A review of measured gust responses in the light of modern analysis methods N88-29724
Measurement and analysis of low altitude atmospheric turbulence obtained using a specially instrumented Gnat aircraft N88-29728

GUST LOADS
Current and proposed gust criteria and analysis methods: An FAA overview N88-29718
Comparison of the influence of different gust models on structural design N88-29722
A review of measured gust responses in the light of modern analysis methods N88-29724
The Flight of Flexible Aircraft in Turbulence: State-of-the-Art in the Description and Modelling of Atmospheric Turbulence
[AGARD-R-734] N88-29725
An interim comparison of operational CG records in turbulence on small and large civil aircraft N88-29729
Acquisition of gust statistics from AIDS-recorded data N88-29733
Extreme gusts distribution N88-29734

GUSTS
Matching P.S.D.: Design loads N88-29720
A summary of methods for establishing airframe design loads from continuous gust design criteria N88-29721
An interim comparison of operational CG records in turbulence on small and large civil aircraft N88-29729
Re-assessment of gust statistics using CAADRP data N88-29732

H

HAND (ANATOMY)
A standard architecture for controlling robots
[AD-A195929] N88-30371

HEAD-UP DISPLAYS
Improvement of head-up display standards. Volume 3: An evaluation of head-up display safety
[AD-A195787] N88-30300

HEALTH
Evaluation of the potential health hazards associated with the machining of carbon fiber composites
[AD-A194835] N88-30286

HEAT BUDGET
Energy budget and ground temperatures in hot regions
[AD-A196298] N88-30268

HEAT EXCHANGERS
Oxidizer heat exchanger component test
[NASA-CR-182159] N88-29876
Theories of comparative analysis
[AD-A196328] N88-30395
Growth of GaAs crystals by the Heat Exchanger Method for microwave device applications
[AD-A196028] N88-30435

HEAT FLUX
The thermal behavior of film cooled turbulent boundary layers as affected by longitudinal vortices
[AD-A195155] N88-30095
Measurement of local high-level, transient surface heat flux
[NASA-TP-2840] N88-30099

HEAT PIPES
Effect of interfacial phenomena on contact line heat Transfer-3
[AD-A194941] N88-29901

HEAT RESISTANT ALLOYS
Anisotropic constitutive modeling for nickel-base single crystal superalloys
[NASA-CR-182157] N88-29961

HEAT SHIELDING
Far infrared spectroscopy telescope (FIRST) inflatable thermal shield, phase 1
[SRI/FIS/106(87)CZ] N88-30552

HEAT TRANSFER
Aerodynamic heating of missiles N88-29764
The use of hot-film technique for boundary layer studies on a 21 percent thick airfoil
[NAE-AN-45] N88-29781
The effects of inlet turbulence and rotor/stator interactions on the aerodynamics and heat transfer of a large-scale rotating turbine model. Volume 2: Heat transfer data tabulation. 15 percent axial spacing
[NASA-CR-179467] N88-29804
Effect of interfacial phenomena on contact line heat Transfer-3
[AD-A194941] N88-29901
Radiation from soot-containing flames N88-29927
Transition at hypersonic speeds
[NASA-CR-178315] N88-30058
Assessment of a 3-D boundary layer analysis to predict heat transfer and flow field in a turbine passage
[NASA-CR-174894] N88-30066
The use of upwind schemes at high Reynolds number: A cautionary note
[AD-A196227] N88-30074
The thermal behavior of film cooled turbulent boundary layers as affected by longitudinal vortices
[AD-A195155] N88-30095

HEAT TRANSFER COEFFICIENTS
Experimental and analytical study of two-phase flow in zero gravity
[AD-A195223] N88-29993

HEAVY IONS
Eikonal solutions to optical model coupled-channel equations
[NASA-TP-2830] N88-30402

HEAVY NUCLEI
Charge composition of primary cosmic ray nuclei with z greater than or equal to 2 in energy region greater than or equal to 2 TeV N88-30519

HEIGHT
Analysis of environmental parameters from the Panama City tower radar experiment
[AD-A194994] N88-30264

HELICOPTER CONTROL
Minimum-complexity helicopter simulation math model
[NASA-CR-177476] N88-29819

HELICOPTER PERFORMANCE
Preliminary airworthiness evaluation of the UH-60A/ESSS (External Stores Support System) with HELLFIRE launcher installed
[AD-A196187] N88-29793

HELICOPTERS
JUH-1H redesigned pneumatic boot deicing system flight test evaluation
[AD-A194918] N88-29785
Threat expert system technology advisor
[NASA-CR-177479] N88-29816
Development and demonstration of an on-board mission planner for helicopters
[NASA-CR-177482] N88-29817
A fiber optic collective flight control system for helicopters
[AD-A195406] N88-29818

HELIUM
Crystal structure and density of helium to 232 kbar N88-30481
Evolutionary helium and CNO anomalies in the atmospheres and winds of massive hot stars
[NASA-CR-183254] N88-30550

HERMES MANNED SPACEPLANE
Hermes: Study of propulsion system for reusable man-rated spacecraft
[PSRM-TN-0000-00-04A] N88-29866
Fuel cells for space use
[FCP-TR-DOS-SY-026] N88-30183
The LTPP communication processor — Columbus and Hermes
[CL/CP/SES/FR/004] N88-30328

HERZBERG BANDS
Aeronomic problems of the molecular oxygen photodissociation. Part 3: Solar spectral irradiances in the region of the O2 Herzberg continuum, Schumann-Runge bands and continuum
[AERONOMICA-ACTA-A-332-1988] N88-29897
Aeronomic problems of molecular oxygen photodissociation. Part 4: The various parameters for the Herzberg continuum
[AERONOMICA-ACTA-A-333-1988] N88-29955

HETEROGENEITY
Mathematical problems of nonlinear wave propagation and of waves in heterogeneous media
[AD-A195970] N88-30057

HETEROJUNCTION DEVICES
On 3-5 heterojunction structures and high speed devices
[AD-A195464] N88-30438
Joint services electronics program
[AD-A195731] N88-30439

HETEROJUNCTIONS
Spectroscopic studies with multiple quantum well materials with applications to optical signal processing at room temperature
[AD-A194171] N88-30409

HIGH ELECTRON MOBILITY TRANSISTORS
Light-millimeter wave interactions in semiconductor devices
[AD-A195898] N88-30428

HIGH ENERGY INTERACTIONS
A coded mask telescope for observations of X and gamma ray sources in the southern sky
[INPE-4580-PRE/1314] N88-30551

HIGH FREQUENCIES
Decomposition of hydrazine by high frequency glow electrical discharges
[NASA-TT-20240] N88-29906
Long haul communications in the HF spectrum utilizing high speed modems
[AD-A194683] N88-30003
Comparative analysis of passive communications satellites employing the SHF and HF spectrum for use in a strategic role
[AD-A194682] N88-30019
Modeling and performance of HF/OTH (High-Frequency/Over-the-Horizon) radar target identification systems
[AD-A196287] N88-30039
High frequency GaAlAs modulator and photodetector for phased array antenna applications
[NASA-TM-101328] N88-30048
In situ fault detection by the hybrid ray mode method
[AD-A195226] N88-30137

HIGH LEVEL LANGUAGES
Conversion of productions in OPS5 to their equivalent English
[ORNL/TM-10246] N88-30306

HIGH POWER LASERS
Energy conversion measurements in laser-sustained argon plasmas for application to rocket propulsion
[AD-A194931] N88-29861

HIGH RESOLUTION
An analysis of results of a high-resolution world ocean circulation model
[AD-A195760] N88-30272

HIGH REYNOLDS NUMBER
The use of upwind schemes at high Reynolds number: A cautionary note
[AD-A196227] N88-30074

HIGH SPEED
Ultrafast processes and spectroscopy with free electron lasers
[AD-A195248] N88-30126
On 3-5 heterojunction structures and high speed devices
[AD-A195464] N88-30438

HIGH STRENGTH STEELS
Additional fracture and strength test results for A723 steel and 38644 titanium
[AD-A196329] N88-29960

HIGH TEMPERATURE
Creep of carbon yarn and carbon-carbon composites at high temperatures and high stresses
[AD-A195224] N88-29878
A study of the critical factors controlling the synthesis of ceramic matrix composites from preceramic polymers
[AD-A195405] N88-29881
Electrical properties of materials for elevated temperature resistance strain gage application
[NASA-CR-182214] N88-30106

HIGH TEMPERATURE ENVIRONMENTS
Development of computer-controlled thermogravimetric instrumentation for measurement of environmental and high temperature volatilization and desorption of contaminants from polymeric materials
[AD-A195934] N88-29900

HIGH TEMPERATURE SUPERCONDUCTORS
Theory of superconductivity in oxides
[AD-A195647] N88-30432
Theoretical model of high temperature superconductors
[DE88-702707] N88-30441

HIGH TEMPERATURE TESTS
Determination of multiaxial flow surfaces at elevated temperatures using the concept of dissipation potential
[ORNL/TM-10787] N88-30149

HISTORIES
History of aeroelasticity in Germany from the beginning to 1945
[ESA-TT-1082] N88-29767
Analysis of environmental parameters from the Panama City tower radar experiment
[AD-A194994] N88-30264

HMX
Descriptive characterization of propellant particles
[AD-A195176] N88-29985

HOLOGRAPHIC INTERFEROMETRY
Experimental aspects of using time-averaged holographic interferometry to detect barely visible impact damage in a graphite/epoxy composite plate
[AD-A194418] N88-30097
Use of holography in vibration and flutter study of fans
[PNR90458] N88-30098

HOLOGRAPHY
Automatic data retrieval from rocket motor holograms
[AD-A195586] N88-29864
Evaluation of multi-focus holographic lenses
[AD-A196167] N88-30110
High-resolution (30 m) lunar radar images N88-30486

HOMOGENEOUS TURBULENCE
Development of a more general Reynolds stress closure for swirling flow
[AD-A195121] N88-30092

HOT STARS
Evolutionary helium and CNO anomalies in the atmospheres and winds of massive hot stars
[NASA-CR-183254] N88-30550

HOT SURFACES
Constitutive modeling for isotropic materials
[NASA-CR-182132] N88-29811
HOT-FILM ANEMOMETERS
The use of hot-film technique for boundary layer studies on a 21 percent thick airfoil
[NAE-AN-45] N88-29781
HTPB PROPELLANTS
Review of research concerning Solid Fuel Ramjet (SOFRAM) at the Research Institute of National Defence (FOA) 2
[FOA-C-20714-2.1] N88-29813
Thermomechanical computations for GAP, a high energy binder for composite propellants
[FOA-C-20718-2.1] N88-29988
HUBBLE SPACE TELESCOPE
Knowledge based tools for Hubble Space Telescope planning and scheduling: Constraints and strategies N88-30338
The proposal entry processor: Telescience applications for Hubble Space Telescope science operations N88-30339
Lisp Object State Saver (LOSS): A facility used to save partial schedules of the Hubble Space Telescope N88-30360
HULLS (STRUCTURES)
Response of SMA (Shielded Metal Arc) and narrow gap HY80 weldments to explosive shock loading
[AD-A195994] N88-30162
HUMAN BEHAVIOR
Contributions to engineering models of human-computer interaction, volume 1
[AD-A195590] N88-30295
HUMAN BEINGS
Multilevel computational theory of stereoscopic visual image processing
[AD-A195331] N88-30288
Eye movements and spatial pattern vision
[AD-A195496] N88-30290
Haptic exploration in humans and machines: Attribute integration and machine recognition/implementation
[AD-A193692] N88-30299
HUMAN FACTORS ENGINEERING
Advances in Flying Qualities
[AGARD-LS-157] N88-29735
Pilot modeling N88-29736
Human factors report on information management requirements for next-generation manned bombers
[AD-A195870] N88-30296
Study of human factors engineering criteria for extravehicular activity (EVA) systems, volume 1
[STF23-F87025-VOL-1] N88-30298
Haptic exploration in humans and machines: Attribute integration and machine recognition/implementation
[AD-A193692] N88-30299
Space station proximity operations windows: Human factors design guidelines
[NASA-TM-88233] N88-30301
HUMIDITY
Fatigue crack growth characteristics of ARALL (trademark)-1
[AD-A196185] N88-29889
HYDRAZINES
Decomposition of hydrazine by high frequency glow electrical discharges
[NASA-TT-20240] N88-29906
HYDROCARBON FUELS
Experiments and modeling of multi-component fuel behavior in combustion
[AD-A195011] N88-29896
HYDROCARBONS
Determination of relative flammability of materials by pyrolysis and gas-chromatographic light hydrocarbon analysis
[DE88-012449] N88-29898
Rates of formation of soot from hydrocarbon flames and its destruction N88-29933
HYDRODYNAMICS
Gaseous premixed flames in non-uniform flows N88-29945
HYDROGEN
Extended atmospheres of outer planet satellites and comets
[NASA-CR-183157] N88-30572
HYDROGEN ATOMS
Computed potential energy surfaces for chemical reactions
[NASA-CR-183168] N88-29893
HYDROGEN EMBRITTLEMENT
Hydrogen embrittlement of iron-nickel alloys
[AD-A195909] N88-29958
HYDROGEN OXYGEN FUEL CELLS
Regenerative fuel cell energy storage system for a low earth orbit space station
[NASA-CR-174802] N88-30184
HYDROGRAPHY
An analysis of results of a high-resolution world ocean circulation model
[AD-A195760] N88-30272
HYPERFINE STRUCTURE
Experimental and theoretical investigations of isotope shift and hyperfine structure on 5d elements (especially platinum, iridium and rhenium)
[ETN-88-93121] N88-29957
HYPERSONIC BOUNDARY LAYER
The effects of incoming boundary layer thickness on unsteady shock-induced turbulent separations induced by cylinders
[AD-A196190] N88-30060
HYPERSONIC SPEED
Transition at hypersonic speeds
[NASA-CR-178315] N88-30058
HYPERSONIC WIND TUNNELS
Quantitative surface temperature measurement using two-color thermographic phosphors and video equipment
[NASA-CASE-LAR-13740-1] N88-30105
HYPERVELOCITY IMPACT
The effect of the near earth micrometeoroid environment on a highly reflective mirror surface
[NASA-TM-101307] N88-29833
HYPOBARIC ATMOSPHERES
Visual sensitivities under reduced oxygen
[AD-A195628] N88-30279
HYPOTHERMIA
Accidental hypothermia
[AD-A194967] N88-30278
HYPOXIA
Visual sensitivities under reduced oxygen
[AD-A195628] N88-30279
HYSTERESIS
The aspect ratio dependence of the attractor dimension in Taylor-Couette flow
[AD-A196297] N88-30065
Nonlinear stress-strain and inelastic rebound with exponential stiffness
[AD-A195667] N88-30159
Behaviour and hysteresis losses of irreversible type-2 superconducting cylindrical shell
[DE88-702708] N88-30434

I

IBM COMPUTERS
Aircraft noise prediction program propeller analysis system IBM-PC version user's manual version 2.0
[NASA-CR-181689] N88-30399
ICE
General equations for the motions of ice crystals and water drops in gravitational and electric fields
[NASA-CR-183229] N88-30070
ICE FORMATION
JUH-1H redesigned pneumatic boot deicing system flight test evaluation
[AD-A194918] N88-29785
Cloud/mesoscale model development and application studies
[AFGL-TR-87-0219] N88-30269
IDENTIFYING
Modeling and performance of HF/OTH (High-Frequency/Over-the-Horizon) radar target identification systems
[AD-A196287] N88-30038
IGNEOUS ROCKS
Pluton emplacement and magmatic arc construction: A model from the Patagonian batholith N88-30206
IGNITION
Ignition and extinguishing of a Solid Fuel Ramjet (SOFRAM)
[FOA-C-20713-2.1] N88-29885
Gas phase combustion chemistry of nitramine propellants
[AD-A195082] N88-29902
Flamespreading processes in obliquely loaded stick propellant beds
[AD-A195081] N88-29956
IGNITION SYSTEMS
Flamespreading processes in obliquely loaded stick propellant beds
[AD-A195081] N88-29956
ILLUSIONS
Eye movements and spatial pattern vision
[AD-A195496] N88-30290
IMAGE ANALYSIS
Evaluation of LANDSAT-TM data for geomorphological mapping
[INPE-4593-PRE/1324] N88-30168
Autonomous image data reduction by analysis and interpretation N88-30347
IMAGE PROCESSING
Accuracy of satellite data navigation
[AD-A195877] N88-29787
Automatic data retrieval from rocket motor holograms
[AD-A195586] N88-29864
Degradation of protective coatings on steel in corrosive environments N88-29989
Integrating multispectral imagery and ground level hyperspectral signature data
[AD-A195976] N88-30166
LANDSAT-TM data to map flooded areas
[INPE-4594-PRE/1324] N88-30177
Multilevel computational theory of stereoscopic visual image processing
[AD-A195331] N88-30288
Using primal sketch primitives as the basis for the Hough transform
[INPE-4564-PRE/1305] N88-30310
A digital terrain model system for a microcomputer
[INPE-4610-PRE/1333] N88-30316
Compression and decompression of imaging sensor signals (CADISS): A multiprocessor system for image compression/decompression on board scientific satellites
[NLR-TR-87076-L] N88-30323
The 1988 Goddard Conference on Space Applications of Artificial Intelligence
[NASA-CP-3009] N88-30330
Low level image processing techniques using the pipeline image processing engine in the flight telerobotic servicer N88-30346
An interactive testbed for development of expert tools for pattern recognition N88-30349
The combinatorics of object recognition in cluttered environments using constrained search
[AD-A196224] N88-30364
Symbolic construction of a 2D scale-space image
[AD-A195926] N88-30374
Image focusing in space and time
[AD-A195839] N88-30410
Activities in astrophysics
[INPE-4582-PRE/1316] N88-30570
IMAGE RECONSTRUCTION
Reconstruction of multidimensional signals from multiple level threshold crossings
[AD-A195581] N88-30383
IMAGERY
Microcircuit trace cutting with focused ion beams
[AD-A196030] N88-30050
Integrating multispectral imagery and ground level hyperspectral signature data
[AD-A195976] N88-30166
Symbolic construction of a 2D scale-space image
[AD-A195926] N88-30374
Kalman filter-based algorithms for estimating depth from image sequences
[AD-A195818] N88-30380
Diffraction imaging (topography) with monochromatic synchrotron radiation
[NASA-CR-183264] N88-30431
Applications of synchrotron radiation to materials science: Diffraction imaging (topography) and microradiography
[NASA-CR-183265] N88-30440
IMAGES
Particle sizing in combustion systems, using scattered laser light
[AD-A196231] N88-29953
Comparative aspects of multiple processes of attention
[AD-A195805] N88-30291
Dynamical systems and motion vision
[AD-A195932] N88-30366
Symbolic construction of a 2D scale-space image
[AD-A195926] N88-30374
Kalman filter-based algorithms for estimating depth from image sequences
[AD-A195818] N88-30380
Streaking images that appear only in the plane of diffraction in undoped GaAs single crystals: Diffraction imaging (topography) by monochromatic synchrotron radiation
[NASA-CR-183267] N88-30437
IMAGING RADAR
A submillimeter wavelength space-based imaging radar
[AD-A195846] N88-30033
IMAGING TECHNIQUES
ZT imaging system for layered thin wall structures
[AD-A195468] N88-29954
Quantitative surface temperature measurement using two-color thermographic phosphors and video equipment
[NASA-CASE-LAR-13740-1] N88-30105

Method for combined image interpolation-restoration through a fir filter design technique
[INPE-4561-PRE/1302] N88-30315
A coded mask telescope for observations of X and gamma ray sources in the southern sky
[INPE-4580-PRE/1314] N88-30551

IMMUNE SYSTEMS
Immunofluorescence localization of dissociation supernatant and extracellular matrix components in Lytechinus pictus sectioned embryos
[NASA-CR-183137] N88-30276

IMMUNOLOGY
Bioeffects of electromagnetic waves N88-30032

IMPACT
Nineteenth Lunar and Planetary Science Conference. Press abstracts
[NASA-CR-183037] N88-30473
Exotic minerals in 3,500 million year old rocks: Evidence for large meteorite impacts N88-30475
LSU scientists discover evidence of large meteorite impacts on the early earth N88-30480

IMPACT DAMAGE
Experimental aspects of using time-averaged holographic interferometry to detect barely visible impact damage in a graphite/epoxy composite plate
[AD-A194418] N88-30097
A compilation of information and data on the Manson impact structure
[NASA-CR-183169] N88-30258

IMPACT LOADS
Control systems for platform landings cushioned by air bags
[AD-A196154] N88-29996
Impact force as a part of the total breaking wave force on a vertical cylinder
[RR-CE78] N88-30154

IMPACT TESTS
Experimental aspects of using time-averaged holographic interferometry to detect barely visible impact damage in a graphite/epoxy composite plate
[AD-A194418] N88-30097

IMPEDANCE MEASUREMENT
Ultrasonic detection of diffusion and adhesion loss N88-29967

IMPINGEMENT
Studies on rocket exhaust plumes and impingement effects related to the Columbus Space Station program: Executive summary
[DFVLR-IB-222-88-A-12] N88-29862

IMPLICATION
The cost and performance implications of reliability improvements in the F-15A/B
[AD-A195096] N88-29796

IMPURITIES
Impurity analysis in SIMOX samples by high-efficiency resonance ionization time-of-flight mass spectrometry
[DE88-012061] N88-30051

IN-FLIGHT MONITORING
Acquisition of gust statistics from AIDS-recorded data N88-29733
The development of acoustic emission for structural integrity monitoring of aircraft
[AD-A196264] N88-30398

INCOHERENT SCATTERING
Ionospheric radio and propagation: Waves in plasmas N88-30030

INCOMPRESSIBLE BOUNDARY LAYER
Nonlinear Tollmien-Schlichting/vortex interaction in boundary layers
[NASA-CR-181698] N88-29715

INCOMPRESSIBLE FLOW
Numerical simulation of unsteady incompressible flow in a partially-filled rotating cylinder
[AD-A196001] N88-30073
Numerical simulation of unsteady incompressible viscous flows in generalized coordinate systems
[NASA-TM-101016] N88-30085

INDEPENDENT VARIABLES
Canonical variables and canonical integrals for motion in near-circular orbits N88-30512

INDEXES (DOCUMENTATION)
A design for a ground-based data management system N88-30355

INDIUM PHOSPHATES
Power MISFETs on OnP
[AD-A195242] N88-30436

INDUSTRIAL SAFETY
Evaluation of the potential health hazards associated with the machining of carbon fiber composites
[AD-A194835] N88-30286

INELASTIC SCATTERING
Eikonal solutions to optical model coupled-channel equations
[NASA-TP-2830] N88-30402

INELASTIC STRESS
An experimental study of biaxial yield in modified 9Cr-1Mo steel at room temperature
[NASA-CR-175012] N88-30164

INERTIAL NAVIGATION
Angle of attack and sideslip estimation using an inertial reference platform
[AD-A194876] N88-29769
Observed track-keeping performance of DC10 aircraft equipped with the Collins AINS-70 area navigation system: Karlsruhe and Maastricht UACs (Upper Area Control centres)
[EEC-202] N88-29788
Estimation of short-wavelength gravity on a dense grid using digital terrain elevation data
[AD-A196325] N88-30196

INERTIAL PLATFORMS
Angle of attack and sideslip estimation using an inertial reference platform
[AD-A194876] N88-29769

INFERENCE
Theories of comparative analysis
[AD-A196328] N88-30395

INFLATABLE STRUCTURES
Far infrared spectroscopy telescope (FIRST) inflatable thermal shield, phase 1
[SR/FIS/108(87)CZ] N88-30552

INFLUENCE COEFFICIENT
Comparison of the influence of different gust models on structural design N88-29722
An experimental study of an adaptive-wall wind tunnel
[NASA-CR-183152] N88-29821

INFORMATION DISSEMINATION
Barriers to Information Transfer and Approaches Toward Their Reduction
[AGARD-CP-430] N88-30458
Linguistic and cultural barriers to the transfer of information N88-30459

INFORMATION MANAGEMENT
Information retrieval systems evolve-advances for easier and more successful use N88-30462

INFORMATION PROCESSING (BIOLOGY)
Nested neural networks
[NASA-TM-101032] N88-30373

INFORMATION RETRIEVAL
Information retrieval systems evolve-advances for easier and more successful use N88-30462

INFORMATION SYSTEMS
EMPTAC (Electromagnetic Pulse Test Aircraft) user's guide
[AD-A195072] N88-30006
Human factors report on information management requirements for next-generation manned bombers
[AD-A195870] N88-30296
Telescience testbed pilot program
[NASA-CR-183207] N88-30309
A shared-world conceptual model for integrating space station life sciences telescience operations N88-30333
The second generation intelligent user interface for the crustal dynamics data information system N88-30352
Knowledge-based integrated information systems engineering: Highlights and bibliography. Knowledge-Based Integrated Information Systems Engineering (KBIISE) Project, volume 1
[AD-A195850] N88-30449
Technical opinions regarding knowledge-based integrated information systems engineering, volume 8
[AD-A195857] N88-30454
Knowledge-Based Integrated Information Systems Development Methodologies Plan. Knowledge-Based Integrated Information Systems Engineering (KBIISE) report, volume 2
[AD-A195851] N88-30455
Strategic, organizational and standardization aspects of integrated information systems, volume 6
[AD-A195855] N88-30457
Integrating information systems in a major decentralized international organization, volume 7
[AD-A195856] N88-30468

INFORMATION THEORY
Signals and systems N88-30026
The bounded rationality constraint: Experimental and analytical results
[AD-A195897] N88-30318

INFORMATION TRANSFER
Barriers to Information Transfer and Approaches Toward Their Reduction
[AGARD-CP-430] N88-30458
Linguistic and cultural barriers to the transfer of information N88-30459
Political and economic barriers to information transfer N88-30460
Information retrieval systems evolve-advances for easier and more successful use N88-30462
Words: Keys or barriers to information transfer N88-30464
Technical change needs organizational change N88-30466
Using standards to break down information transfer barriers N88-30467

INFRARED ASTRONOMY
Far infrared supplement: Catalog of infrared observations, second edition
[NASA-RP-1205] N88-30545

INFRARED DETECTORS
Integration of LANTIRN (Low Altitude Navigation and Targeting Infrared for Night) into operational fighter training
[AD-A194906] N88-29799
Development of a unit cell for a Ge:Ga detector array
[NASA-CR-177445] N88-30100
A system study with an infrared sensitive microelectronic image sensor
[FOA-C-30481-3.1] N88-30407
Principles of the optical differential thermal analysis
[AD-A195951] N88-30408
Estimation of soil temperature profile from remote microwave and IR measurements N88-30532

INFRARED IMAGERY
A system study with an infrared sensitive microelectronic image sensor
[FOA-C-30481-3.1] N88-30407
Common modules: A success story
[AD-A195937] N88-30415

INFRARED INSTRUMENTS
Common modules: A success story
[AD-A195937] N88-30415

INFRARED LASERS
Predicting the durability of adhesives and coatings by remote detection of hidden defects and coating-thickness irregularities: A theoretical and numerical study N88-29972

INFRARED RADIATION
Principles of the optical differential thermal analysis
[AD-A195951] N88-30408
Radio and infrared properties of young stars
[NASA-CR-183252] N88-30579

INFRARED SOURCES (ASTRONOMY)
Far infrared supplement: Catalog of infrared observations, second edition
[NASA-RP-1205] N88-30545

INFRARED SPECTROSCOPY
Attenuated total reflectance FT-IR spectroscopy to measure interfacial reaction kinetics at silica surfaces
[AD-A196330] N88-29908
Photoacoustic Fourier transform infrared spectroscopy. An early detection technique for coatings degradation N88-29968

INFRARED TELESCOPES
Far infrared spectroscopy telescope (FIRST) inflatable thermal shield, phase 1
[SR/FIS/108(87)CZ] N88-30552

INFRARED WINDOWS
An organometallic route to micron-sized whiskers of zinc sulfide
[AD-A195889] N88-30414

INJECTION
Influence of plasma parameters on VLF radiation in near-rocket region N88-30518

INLET FLOW
The effects of inlet turbulence and rotor/stator interactions on the aerodynamics and heat transfer of a large-scale rotating turbine model. Volume 2: Heat transfer data tabulation. 15 percent axial spacing
[NASA-CR-179467] N88-29804

INLET PRESSURE
Simulation of Vulcain engine operation at low inlet pressure
[ETN-88-93083] N88-29875

INPUT
A study of the effect of random input motion on low Reynolds number flows
[AD-A195559] N88-29747

INSPECTION
Evaluation of bond testing equipment for inspection of Army advanced composite airframe structures
[AD-A195795] N88-29885

INSTALLING
Aircraft avionics and missile system installation cost study. Volume 2: Appendices F and G
[AD-A195372] N88-29801
Electronic materials and devices prepared by molecular beam epitaxy
[AD-A195694] N88-30433

INSTRUMENT FLIGHT RULES
Improvement of head-up display standards. Volume 3: An evaluation of head-up display safety
[AD-A195787] N88-30300

INTAKE SYSTEMS
Air intake aerodynamics N88-29762

INTEGRAL EQUATIONS
Initial value problems in viscoelasticity
[AD-A196052] N88-30145
INTEGRALS
Numerical calculations of the response of a spinning spheroidal payload to coning motion
[AD-A195890] N88-30059
On the Nash point equilibria in the calculus of variations
[AD-A194959] N88-30381
Canonical variables and canonical integrals for motion in near-circular orbits N88-30512
INTEGRATED CIRCUITS
Signals and systems N88-30026
Electronic and optical devices and applications N88-30027
Circuit design criteria for stable lateral inhibition neural networks
[AD-A195066] N88-30046
Impurity analysis in SIMOX samples by high-efficiency resonance ionization time-of-flight mass spectrometry
[DE88-012061] N88-30051
Stress related failures causing open metallization
[AD-A195061] N88-30150
INTEGRATED OPTICS
Ion exchange processes for fabrication of integrated optical waveguide structures into glass substrates
[VTT-46] N88-30405
INTERACTIONAL AERODYNAMICS
Three-dimensional Navier-Stokes simulations of turbine rotor-stator interaction
[NASA-TM-100081] N88-29750
Experimental and numerical investigation of the effect of distributed suction on oblique shock wave/turbulent boundary layer interaction
[NASA-TM-101334] N88-30084
INTERACTIVE CONTROL
Numerical simulation of nozzle flows
[AD-A195144] N88-30064
INTERFACES
Definition of common support equipment and space station interface requirements for IOC model technology experiments
[NASA-TM-100656] N88-29856
INTERFACIAL TENSION
A test for interfacial effects and stress transfer in ceramic matrix composites
[NASA-CR-182873] N88-29880
Some theoretical considerations of the surface tension of liquid metals for metal matrix composites
[AD-A195999] N88-29882
Effect of interfacial phenomena on contact line heat Transfer-3
[AD-A194941] N88-29901
INTERGRANULAR CORROSION
Hydrogen embrittlement of iron-nickel alloys
[AD-A195909] N88-29958
INTERIOR BALLISTICS
Flamespreading processes in obliquely loaded stick propellant beds
[AD-A195081] N88-29956
INTERNATIONAL COOPERATION
Using standards to break down information transfer barriers N88-30467
INTERPLANETARY FLIGHT
JPRS report: Science and technology. USSR: Space
[JPRS-USP-88-001] N88-30498
INTERPLANETARY GAS
Extended atmospheres of outer planet satellites and comets
[NASA-CR-183157] N88-30572
INTERPOLATION
Method for combined image interpolation-restoration through a fir filter design technique
[INPE-4581-PRE/1302] N88-30315
Reconstruction of multidimensional signals from multiple level threshold crossings
[AD-A195561] N88-30383
INTERPROCESSOR COMMUNICATION
Design of a self-timed VLSI multicomputer communication controller
[AD-A194567] N88-30014
INTERSTELLAR CHEMISTRY
Observations of star formation N88-30538
INTRAMOLECULAR STRUCTURES
Intramolecular dynamics: A study of molecules at high levels of vibrational excitation
[AD-A195285] N88-30400
INTRUSION
Volcanic contribution to crustal growth in the Central Andes: A new estimate and a discussion of uncertainties N88-30255
INVENTORIES
The dynamics of transuranics and other radionuclides in natural environments, December 1985
[DE87-014456] N88-30189
INVERSE SCATTERING
Fields and waves N88-30025
INVISCID FLOW
Numerical solutions of unsteady inviscid transonic turbine cascade flows
[AD-A196111] N88-29748
ION BEAMS
Ion gun generated electromagnetic interference on the SCATHA satellite
[AD-A195179] N88-29853
Microcircuit trace cutting with focused ion beams
[AD-A196030] N88-30050
The Single Event Upset (SEU) test facility on the Hardwell tandem generator for cosmic ray simulation
[AERE-R-12896] N88-30580
ION EMISSION
Ion gun generated electromagnetic interference on the SCATHA satellite
[AD-A195179] N88-29853
ION ENGINES
The NASA Electric Propulsion Program
[NASA-TM-101324] N88-29859
ION EXCHANGING
Ion exchange processes for fabrication of integrated optical waveguide structures into glass substrates
[VTT-46] N88-30405
ION PROBES
Role of zircon in tracing crustal growth and recycling N88-30211
ION PRODUCTION RATES
On formulating a simple D-region model
[AD-A195841] N88-30197
IONIC COLLISIONS
Eikonal solutions to optical model coupled-channel equations
[NASA-TP-2830] N88-30402
IONIZATION
Impurity analysis in SIMOX samples by high-efficiency resonance ionization time-of-flight mass spectrometry
[DE88-012061] N88-30051
Cluster beam studies
[AD-A195182] N88-30443
IONIZATION COEFFICIENTS
On formulating a simple D-region model
[AD-A195841] N88-30197
IONOSONDES
Ionosonde studies of field-aligned irregularities during high-power HF heating at Arecibo
[AD-A195848] N88-30256
IONOSPHERIC COMPOSITION
Photochemistry of ionospheric D-region with injection of nitrogen oxides N88-30499
IONOSPHERIC DISTURBANCES
The effect of equatorial ionospheric irregularities on the performance of a south-looking OTH-B (Over-The-Horizon-Backscatter) radar
[AD-A195090] N88-30018
IONOSPHERIC ELECTRON DENSITY
One equatorial anomaly in nighttime ionospheric F region N88-30517
IONOSPHERIC HEATING
Role of ordinary to extraordinary mode wave coupling in ionospheric heating experiments
[AD-A195335] N88-30017
IONOSPHERIC PROPAGATION
Role of ordinary to extraordinary mode wave coupling in ionospheric heating experiments
[AD-A195335] N88-30017
Review of Radio Science, 1984-1986 N88-30023
Ionospheric radio and propagation: Waves in plasmas N88-30030
IONOSPHERIC SOUNDING
Ionospheric radio and propagation: Waves in plasmas N88-30030
IONS
Large ionic species in sooting acetylene and benzene flames N88-29932
Particle trajectories and potentials in a plane sheath moving in a magnetoplasma
[AD-A196228] N88-30190
Ion kinetics in silane plasmas
[AD-A196202] N88-30423
Ring current role in dynamics of fluctuating electron and ion fluxes in low-latitude magnetosphere N88-30514
IRIDIUM
Iridium-coated rhenium thrusters by CVD
[NASA-TM-101309] N88-29874
IRIDIUM ISOTOPES
Experimental and theoretical investigations of isotope shift and hyperfine structure on 5d elements (especially platinum, iridium and rhenium)
[ETN-88-93121] N88-29957
IRON
Radial velocity measurements of a sample of northern metal-deficient stars
[SER-C-PREPUBL-FASC-25] N88-30564
IRON ALLOYS
Hydrogen embrittlement of iron-nickel alloys
[AD-A195909] N88-29958
IRON OXIDES
Reflectance pattern and the physical and chemical characteristics of three Brazilian Oxisols
[INPE-4590-PRE/1320] N88-30172
IRRADIANCE
Aeronomic problems of the molecular oxygen photodissociation. Part 3: Solar spectral irradiances in the region of the O2 Herzberg continuum, Schumann-Runge bands and continuum
[AERONOMICA-ACTA-A-332-1988] N88-29897
IRRADIATION
Functional assessment of laser irradiation
[AD-A195735] N88-30267
IRREVERSIBLE PROCESSES
Behaviour and hysteresis losses of irreversible type-2 superconducting cylindrical shell
[DE88-702708] N88-30434
ISLAND ARCS
Pluton emplacement and magmatic arc construction: A model from the Patagonian batholith N88-30206
An illustration of the complexity of continent formation N88-30207
ISOMERIZATION
Active sites and roles of solid acid base catalysts
[NASA-TT-20333] N88-29909
ISOTOPE EFFECT
Experimental and theoretical investigations of isotope shift and hyperfine structure on 5d elements (especially platinum, iridium and rhenium)
[ETN-88-93121] N88-29957
ISOTOPES
Lithospheric evolution of the Northern Arabian Shield: Chemical and isotopic evidence from basalts, xenoliths and granites N88-30242
The growth of the continental crust: Constraints from radiogenic isotope geochemistry N88-30245
Noble gases, C,N, and Si isotopes in interstellar SiC form the Murchison carbonaceous chondrite N88-30483
ISOTOPIC LABELING
The timing and mechanism of depletion in Lewisian granulites N88-30209
Genesis of archean granitoids in the Pilbara block and implications for crustal growth N88-30210
Decoupled Rb-Sr and Sm-Nd isotopic evolution of the continental crust N88-30216
The early archaean crustal history of West Greenland as recorded by detrital zircons N88-30221
ISOTROPIC MEDIA
Constitutive modeling for isotropic materials
[NASA-CR-182132] N88-29811
ITERATIVE SOLUTION
Convergence acceleration for vector sequences and applications to computational fluid dynamics
[NASA-TM-101327] N88-30377
IUE
Beyond the visible: A decade of observations with the International Ultraviolet Explorer (IUE)
[ESA-F09] N88-29828

J

JET AIRCRAFT
Integration of LANTIRN (Low Altitude Navigation and Targeting Infrared for Night) into operational fighter training
[AD-A194906] N88-29799
JET ENGINE FUELS
Fuel property effects on the US Navy's TF30 engine N88-29911
Determination of the hydroperoxide potential of jet fuels
[AD-A195975] N88-29991
JET ENGINES
An investigation of constitutive models for predicting viscoplastic response during cyclic loading
[AD-A194875] N88-30163
JET FLOW
Modelling of CO oxidation in dilution jet flows N88-29947
JOINTS (JUNCTIONS)
Criteria for matrix dominated failure
[AD-A196263] N88-29887
JP-4 JET FUEL
The performance of a surrogate blend in simulating JP-4 in a spray-fueled combustor N88-29926

K

K-EPSILON TURBULENCE MODEL
Three-dimensional gas turbine combustor modelling N88-29937
Numerical modeling of combustion processes in gas turbines N88-29939
Three-dimensional combustor predictors: A comparison of equilibrium and laminar flamelet chemistry models N88-29940
Analysis of the flow through double swirl airblast atomizers N88-29949

KALMAN FILTERS
Dynamical systems and motion vision
[AD-A195932] N88-30366
Kalman filter-based algorithms for estimating depth from image sequences
[AD-A195818] N88-30380

KELVIN-HELMHOLTZ INSTABILITY
Vortex formation and particle transport in a cross-field plasma sheath
[AD-A194838] N88-30425

KINEMATICS
Approximation of viscoelastic stresses from Newtonian turbulent kinematics
[AD-A194317] N88-30077
The kinematics of late-type supergiants
[SER-C-PREPUBL-FASC-28] N88-30560

KINETICS
Ion kinetics in silane plasmas
[AD-A196202] N88-30423

KNOWLEDGE REPRESENTATION
Knowledge-based flow field zoning
[NASA-TM-101023] N88-30314
Knowledge based simulation: An artificial intelligence approach to system modeling and automating the simulation life cycle
[AD-A195836] N88-30372

L

L-SAT
A 30/20 GHz multibeam array antenna suitable for future high rate TDMA European satellite networks
[ETN-88-93079] N88-30037

LABORATORIES
Center for opto-electronic systems research
[AD-A195159] N88-30411
Electronic materials and devices prepared by molecular beam epitaxy
[AD-A195694] N88-30433

LABORATORY EQUIPMENT
Biosample: Preservation, handling and observation system synthesis and breadboarding --- Spacelab
[ESA-CR(P)-2609] N88-29857
Crystal structures of ordered carbon metal alloys
[AD-A195597] N88-29959
Accommodation concept for fluid physics facilities, volume 2 --- Spacelab
[SG-TN-AI-027-VOL-2] N88-29994

LAGEOS (SATELLITE)
Determining earth's rotation from laser observations of Lageos artificial earth satellite (during period of main merit campaign) N88-30528

LAGRANGE MULTIPLIERS
Lagrangian of the self-duality equation and d = 10, N = 2b supergravity
[DE88-701554] N88-30563

LAMINAR BOUNDARY LAYER
Numerical simulation of the interaction of pressure waves with laminar and turbulent boundary layers
[ESA-TT-1089] N88-30075

LAMINAR FLOW
Pressure distributions from subsonic tests of an advanced laminar-flow-control wing with leading- and trailing-edge flaps
[NASA-TM-4040-PT-2] N88-29776
Radiation from soot-containing flames N88-29927
Techniques used in the F-14 variable-sweep transition flight experiment
[NASA-TM-100444] N88-30093

LAMINATES
Thermal stress analysis in PMR-15 carbon fibre laminates
[ETN-88-93123] N88-29886
ZT imaging system for layered thin wall structures
[AD-A195468] N88-29954
Modeling of micromechanisms of fatigue and fracture in hybrid materials
[AD-A195604] N88-30142
Large displacement and rotational formulation for laminated cylindrical shells including parabolic transverse shear
[AD-A194871] N88-30158

LAND USE
An analysis of time and space requirements for aircraft turnrounds
[TT-8705] N88-29783

LANDING AIDS
Control systems for platform landings cushioned by air bags
[AD-A196154] N88-29996

LANDING LOADS
Control systems for platform landings cushioned by air bags
[AD-A196154] N88-29996

LANGUAGES
Linguistic-technical aspects of machine translation N88-30461
Linguistic barriers: Translation problems N88-30465

LANTHANUM OXIDES
Theory of superconductivity in oxides
[AD-A195647] N88-30432

LARGE SPACE STRUCTURES
Sensor and actuator selection for large space structure control
[AD-A194912] N88-29842
Space structure (dynamics and control) theme development
[NASA-TM-100597] N88-29850
Theory of filtering and control with application to control of large space structures
[AD-A195500] N88-29851
Clevis joint for deployable space structures
[NASA-CASE-LAR-13898-1] N88-30130
Robust design of distributed controllers for large flexible space structures
[NASA-CR-183202] N88-30134

LASER APPLICATIONS
Optical measurements of soot and temperature profiles in premixed propane-oxygen flames
[NASA-TM-101343] N88-29997
Optical measurements of soot in premixed flames
[NASA-TM-101305] N88-30090
Spontaneous force optical traps
[AD-A196103] N88-30114
Bibliography of Soviet laser developments, number 88, March - April 1987
[AD-A195978] N88-30116
Laser sensing for identification and control of distributed parameter systems
[AD-A195886] N88-30124

LASER CAVITIES
Mode locking of semiconductor laser with external cavity
[AD-A196018] N88-30117

LASER DAMAGE
Functional assessment of laser irradiation
[AD-A195735] N88-30287

LASER DOPPLER VELOCIMETERS
Laser Doppler Velocimeter (LDV) and pressure measurements of gas particle flows in bends
[VKI-TN-163] N88-30083

LASER GYROSCOPES
Precision measurement of the Fresnel drag coefficient using a ring laser
[AD-A196025] N88-30043

LASER MATERIALS
Growth and characterization of materials for tunable lasers in the near infrared spectral region
[NASA-CR-183132] N88-30113
Bibliography of Soviet laser developments, number 88, March - April 1987
[AD-A195978] N88-30116

LASER MODES
Spectral properties of semiconductor lasers with external resonators
[ETN-88-93119] N88-30125

LASER OUTPUTS
Theory of filtering and control with application to control of large space structures
[AD-A195500] N88-29851
Bibliography of Soviet laser developments, number 88, March - April 1987
[AD-A195978] N88-30116
Transverse CO2 laser two-dimensional gain distributions
[AD-A196240] N88-30119
Nonlinear optical phase conjugation techniques to reduce the physical size of lasers
[AD-A196170] N88-30122
Functional assessment of laser irradiation
[AD-A195735] N88-30287
Spectroscopic studies with multiple quantum well materials with applications to optical signal processing at room temperature
[AD-A194171] N88-30409

LASER PLASMA INTERACTIONS
Unified study of plasma/surface interactions for space power and propulsion
[AD-A195971] N88-29870

LASER PLASMAS
Energy conversion measurements in laser-sustained argon plasmas for application to rocket propulsion
[AD-A194931] N88-29861
Bibliography of Soviet laser developments, number 88, March - April 1987
[AD-A195978] N88-30116
Structuring processes in expanding laser-produced plasmas
[AD-A195249] N88-30424

LASER PUMPING
Spectroscopic studies with multiple quantum well materials with applications to optical signal processing at room temperature
[AD-A194171] N88-30409

LASER RANGE FINDERS
Determining earth's rotation from laser observations of Lageos artificial earth satellite (during period of main merit campaign) N88-30528

LASER SPECTROSCOPY
Particle sizing in combustion systems, using scattered laser light
[AD-A196231] N88-29953

LASER TARGET INTERACTIONS
Interaction of high power laser radiation with metals in laser welding
[ISL-PU-304/87] N88-30135

LASER WEAPONS
Looking beyond the strategic defense initiative
[AD-A195079] N88-30394

LASER WELDING
Interaction of high power laser radiation with metals in laser welding
[ISL-PU-304/87] N88-30135

LASERS
Tolerances for phase locking of semiconductor laser arrays
[AD-A195974] N88-30120
Nonlinear optical phase conjugation techniques to reduce the physical size of lasers
[AD-A196170] N88-30122
The study of hydromagnetic waves and RF heating using the TORTUS tokamak, the development of diagnostic techniques based on submillimeter lasers and the gyrotron, and gas discharge N88-30419

LATE STARS
The kinematics of late-type supergiants
[SER-C-PREPUBL-FASC-28] N88-30560

LAUNCH VEHICLES
Reduced flexibility in processing Titan 4 space launch vehicles at Cape Canaveral Air Force Station
[AD-A194908] N88-29834

LAVA
Lava thicknesses: Implications for rheological and crustal development N88-30490
Simulations of lava flows on Mars N88-30495
Small-scale volcanic landforms indicative of distributary tube systems N88-30496
Volcanic styles at Alba Patera, Mars: Implications of lava flow morphology to the volcanic history N88-30497

LEAD ISOTOPES
Pb isotope constaints on the extent of crustal recycling into a steady state mantle N88-30215
Geochronological and lead-isotope evidences for rapid crust formation in middle-proterozoic time: The Labrador example N88-30239

LEADING EDGE FLAPS
Pressure distributions from subsonic tests of an advanced laminar-flow-control wing with leading- and trailing-edge flaps
[NASA-TM-4040-PT-2] N88-29776

LEAST SQUARES METHOD
Obtaining stress intensity factors on cracks, by means of fitting techniques on numerical results calculated with the finite element method N88-30153
Algorithms for nonlinear least-squares problems
[AD-A196071] N88-30305
New methods for nonlinear optimization
[AD-A195982] N88-30313

LEGUMINOUS PLANTS
TM/LANDSAT-5 data to evaluate wheat and bean percent soil cover and leaf area index
[INPE-4609-PRE/1332] N88-30165

LENSES
Evaluation of multi-focus holographic lenses
[AD-A196167] N88-30110

LEVEL (QUANTITY)
Validate algorithms for the determination of rainfall rates from SSM/I microwave satellite imagery
[AD-A195428] N88-30270

LIAPUNOV FUNCTIONS
Stability, stochastic stationarity and generalized Lyapunov equations for two-point boundary-value descriptor systems
[AD-A195645] N88-30385
LIBRARIES
A standard library for modeling satellite orbits on a microcomputer
[AD-A195759] N88-29830
LIBRATION
Plane periodic satellite motions relative to center of mass in neighborhood of collinear libration point N88-30507
LIBRATIONAL MOTION
Families of periodic solutions in problem of solid body rotation at triangular libration point in restricted three-body problem N88-30508
LIFE (DURABILITY)
Performance and lifetime assessment of MPD arc thruster technology
[NASA-TM-101293] N88-29860
Successful completion of a cyclic ground test of a mercury ion auxiliary propulsion system
[NASA-TM-101351] N88-29873
Morphological changes in polymer electrolyte cells
[AD-A195821] N88-30054
A static scheduler for the computer aided prototyping system: An implementation guide
[AD-A194340] N88-30322
Knowledge based simulation: An artificial intelligence approach to system modeling and automating the simulation life cycle
[AD-A195838] N88-30372
Space systems cost study
[AD-A196024] N88-30469
LIFE SCIENCES
A shared-world conceptual model for integrating space station life sciences telescience operations N88-30333
LIFE SUPPORT SYSTEMS
Maintenance and supply options
[NASA-CR-172062] N88-29837
LIFT AUGMENTATION
Analysis of a fixed-pitch X-wing rotor employing lower surface blowing
[AD-A187379] N88-29779
LIGHT (VISIBLE RADIATION)
Precision measurement of the Fresnel drag coefficient using a ring laser
[AD-A196025] N88-30043
LIGHT AIRCRAFT
An interim comparison of operational CG records in turbulence on small and large civil aircraft N88-29729
LIGHT AMPLIFIERS
Nonlinear optical phase conjugation techniques to reduce the physical size of lasers
[AD-A196170] N88-30122
LIGHT CURVE
The ultrashort period dwarf nova SW Ursae Majoris N88-30553
LIGHT MODULATION
Use of depletion edge translation for high-speed modulation and switching of lightwaves
[AD-A195611] N88-30417
LIGHT SCATTERING
Particle sizing in combustion systems, using scattered laser light
[AD-A196231] N88-29953
LIGHT SOURCES
Eye movements and spatial pattern vision
[AD-A195496] N88-30290
LINE SHAPE
Molecular line shape effects on atmospheric window absorption
[AD-A196316] N88-29894
LINE SPECTRA
The optical spectroscopy of copper-blue luminescence in zinc sulfide crystals. Zero-phonon line spectra under the influence of magnetic field, temperature and excitation intensity
[ETN-88-93122] N88-29903
LINEAR FILTERS
Analytical methods in stochastic control and nonlinear filtering
[AD-A194272] N88-30388
LINEAR QUADRATIC GAUSSIAN CONTROL
Robust finite-dimensional LQG (Linear Quadric Gaussian)-based controllers for a class of distributed parameter systems
[AD-A194872] N88-30382
LINEAR SYSTEMS
Performance of DS/SSMA communications in impulsive channels. Part 1: Correlation receivers
[AD-A195712] N88-30021
Increasing accuracy in evaluating vector of state under conditions of incomplete observability of expanded system N88-30511
LINEARITY
Formulation and solution of economic equilibrium problems
[AD-A196034] N88-30470
LINEARIZATION
An approach to CMG steering using feedback linearization
[NASA-CR-183172] N88-30369
LINGUISTICS
Linguistic and cultural barriers to the transfer of information N88-30459
Linguistic-technical aspects of machine translation N88-30461
Linguistic barriers: Translation problems N88-30465
LIQUID ATOMIZATION
Atomization of alternative fuels N88-29913
Turbulence effects on the droplet distribution behind airblast atomizers N88-29915
Influence of operating conditions on the atomization and distribution of fuel by air blast atomizers N88-29918
Spray performance of a vaporizing fuel injector N88-29919
The characterizatin of combustion by fuel composition: Measurements in a small conventional combustor N88-29920
The performance of a surrogate blend in simulating JP-4 in a spray-fueled combustor N88-29926
LIQUID FILLED SHELLS
Numerical calculations of the response of a spinning spheroidal payload to coning motion
[AD-A195890] N88-30059
LIQUID LASERS
Bibliography of Soviet laser developments, number 88, March - April 1987
[AD-A195978] N88-30116
LIQUID METALS
Some theoretical considerations of the surface tension of liquid metals for metal matrix composites
[AD-A195999] N88-29882
LIQUID PROPELLANT ROCKET ENGINES
Breadboard RL10-2B low-thrust operating mode (second iteration) test report
[NASA-CR-182160] N88-29867
Oxidizer heat exchanger component test
[NASA-CR-182159] N88-29876
LIQUID SURFACES
Development of computer-controlled thermogravimetric instrumentation for measurement of environmental and high temperature volatilization and desorption of contaminants from polymeric materials
[AD-A195934] N88-29900
Effect of interfacial phenomena on contact line heat Transfer-3
[AD-A194941] N88-29901
LIQUID-SOLID INTERFACES
Attenuated total reflectance FT-IR spectroscopy to measure interfacial reaction kinetics at silica surfaces
[AD-A196330] N88-29908
LIQUIDS
The dc power control for a liquid-fed resistojet
[NASA-TM-101326] N88-29869
Design criteria for extraction with chemical reaction and liquid membrane permeation
[NASA-TT-20352] N88-29899
Titrimetric analysis of HAN-based liquid propellants
[AD-A196225] N88-29990
LISP (PROGRAMMING LANGUAGE)
Scheme86: A system for interpreting SCHEME
[AD-A195931] N88-30319
Lisp Object State Saver (LOSS): A facility used to save partial schedules of the Hubble Space Telescope N88-30360
LITERATURE
Publications of the Jet Propulsion Laboratory 1987
[NASA-CR-181198] N88-30453
LITHIUM
Morphological changes in polymer electrolyte cells
[AD-A195821] N88-30054
LITHIUM COMPOUNDS
Structure and dynamics of solutions of lithium salts relevant to battery construction
[AD-A195399] N88-30044
LITHOGRAPHY
The Kerala Khondalite Belt (KKB) of Southern India: An ensialic mobile belt N88-30208
The timing and mechanism of depletion in Lewisian granulites N88-30209
LITHOSPHERE
Lithospheric evolution of the Northern Arabian Shield: Chemical and isotopic evidence from basalts, xenoliths and granites N88-30242
LOADING RATE
An investigation of constitutive models for predicting viscoplastic response during cyclic loading
[AD-A194875] N88-30163
LOCAL GROUP (ASTRONOMY)
Duplicity in the solar neighborhood: Part 4: Spectroscopic orbits for four dwarf M stars
[SER-C-PREPUBL-FASC-21] N88-30561
Duplicity in the solar neighborhood: Part 5: Spectroscopic orbit for the nearby double-lined solar-type star HR 8581
[SER-C-PREPUBL-FASC-23] N88-30562
LOCKING
Mode locking of semiconductor laser with external cavity
[AD-A196018] N88-30117
LOGIC CIRCUITS
Use of depletion edge translation for high-speed modulation and switching of lightwaves
[AD-A195611] N88-30417
LOGISTICS
Dirichlet prior in Bayesian estimation of item response curves
[AD-A195311] N88-30392
LONGITUDINAL CONTROL
Low-speed longitudinal flying qualities of modern transport aircraft N88-29738
LONGITUDINAL WAVES
Experimental proof of quasilongitudinal propagation of low-frequency waves in middle latitudes in upper ionosphere N88-30516
LOSSES
Behaviour and hysteresis losses of irreversible type-2 superconducting cylindrical shell
[DE88-702708] N88-30434
LOW ALTITUDE
Integration of LANTIRN (Low Altitude Navigation and Targeting Infrared for Night) into operational fighter training
[AD-A194906] N88-29799
LOW COST
A multiprocessor avionics system for an unmanned research vehicle
[AD-A194806] N88-29800
Low cost satellite
[ESA-CR(P)-2560] N88-29844
Interim Flight Opportunity (IFO). Volume 1: Executive summary --- space platform
[SE/LS/AP-36-818/CN-VOL-1] N88-29849
Space systems cost study
[AD-A196024] N88-30469
LOW LEVEL TURBULENCE
Measurement and analysis of low altitude atmospheric turbulence obtained using a specially instrumented Gnat aircraft N88-29726
LOW PRESSURE
Simulation of Vulcain engine operation at low inlet pressure
[ETN-88-93083] N88-29875
LOW REYNOLDS NUMBER
A study of the effect of random input motion on low Reynolds number flows
[AD-A195559] N88-29747
LOW SPEED STABILITY
Low-speed longitudinal flying qualities of modern transport aircraft N88-29738
LOW TEMPERATURE
Discovery of a low temperature form of TAGN (Triaminoguanidinium Nitrate)
[AD-A196059] N88-29989
LOW TEMPERATURE ENVIRONMENTS
Accidental hypothermia
[AD-A194967] N88-30278
LOW THRUST
Breadboard RL10-2B low-thrust operating mode (second iteration) test report
[NASA-CR-182160] N88-29867
LUBRICANT TESTS
The lubricating properties of magnetron sputtered MoS2
[ESA-ESTL-76] N88-30136
LUMINESCENCE
The optical spectroscopy of copper-blue luminescence in zinc sulfide crystals. Zero-phonon line spectra under the influence of magnetic field, temperature and excitation intensity
[ETN-88-93122] N88-29903
LUMINOSITY
The stability of disk galaxies and constraints on their mass-luminosity ratio
[SER-C-PREPUBL-FASC-27] N88-30565
LUNAR BASES
Maintenance and supply options
[NASA-CR-172062] N88-29837
LUNAR CRUST
Chronology of early lunar crust N88-30212
The complexity, depth, and rapidity of processes that formed the lunar crust N88-30237

LUNAR EFFECTS
Orbital evolution of distant artificial earth satellites N88-30506
LUNAR EVOLUTION
Chronology of early lunar crust N88-30212
Nineteenth Lunar and Planetary Science Conference. Press abstracts
[NASA-CR-183037] N88-30473
The origin of the moon: Further studies of the giant impact N88-30474
LUNAR GRAVITATION
Resonance effects accompanying motion with low thrust in earth-moon system N88-30510
LUNAR LANDING MODULES
Lunar lander conceptual design: Lunar base systems study task 2.2
[NASA-CR-172051] N88-29854
LUNAR LOGISTICS
Maintenance and supply options
[NASA-CR-172062] N88-29837
LUNAR ROCKS
Chronology of early lunar crust N88-30212
LUNAR SPACECRAFT
Possibilities of economical improvements for Moon based rocket propulsion using lunar propellants
[ILR-MITT-196] N88-29871
LUNAR SURFACE
Growth of planetary crusts N88-30247
High-resolution (30 m) lunar radar images N88-30486

M

M STARS
Duplicity in the solar neighborhood: Part 4: Spectroscopic orbits for four dwarf M stars
[SER-C-PREPUBL-FASC-21] N88-30561
MACHINE TRANSLATION
Linguistic-technical aspects of machine translation N88-30461
Linguistic barriers: Translation problems N88-30465
MACHINING
Evaluation of the potential health hazards associated with the machining of carbon fiber composites
[AD-A194835] N88-30286
MAGELLANIC CLOUDS
Astron observations of supernova 1987A in large magellanic cloud N88-30504
Gamma radiation expected from supernova 1987A in large magellanic cloud N88-30505
MAGMA
Growth of continental crust: Clues from Nd isotopes and Nb-Th relationships in mantle-derived magmas N88-30205
Pluton emplacement and magmatic arc construction: A model from the Patagonian batholith N88-30206
Does subduction zone magmatism produce average continental crust N88-30214
Evidence for crustal recycling during the Archean: The parental magmas of the stillwater complex N88-30226
Mid to late proterozoic magmatism within Northeastern North America and its iplications for the growth of the continental crust N88-30229
Late-Archaean crustal growth in the Lewisian Complex of Northwest Scotland: Diachronelty in magmatic accretion and implications for models of crustal growth N88-30253
Volcanic contribution to crustal growth in the Central Andes: A new estimate and a discussion of uncertainties N88-30255
MAGNETIC DISTURBANCES
Relationship between characteristics of low-energy electrons and geomagnetic disturbance in geostationary orbit N88-30501
MAGNETIC FIELD CONFIGURATIONS
Millimeter wave generation by relativistic electron beams
[AD-A195683] N88-30016
MAGNETIC FIELDS
NASA Marshall Space Flight Center solar observatory
[NASA-TM-100339] N88-29832
Relationships among earth's gravity field, magnetic field, crustal structure and the magnetic character of crustal rocks
[AD-A195539] N88-30196
Structuring processes in expanding laser-produced plasmas
[AD-A196249] N88-30424
Stability of Venusian ionopause N88-30522
MAGNETIC PROPERTIES
Particle trajectories and potentials in a plane sheath moving in a magnetoplasma
[AD-A196228] N88-30190
MAGNETIC STORMS
Corona-solar wind coupling review
[AFGL-TR-87-0203] N88-30575
MAGNETOHYDRODYNAMIC GENERATORS
Unified study of plasma/surface interactions for space power and propulsion
[AD-A195971] N88-29870
MAGNETOHYDRODYNAMIC WAVES
The study of hydromagnetic waves and RF heating using the TORTUS tokamak, the development of diagnostic techniques based on submillimeter lasers and the gyrotron, and gas discharge N88-30419
MAGNETOHYDRODYNAMICS
Theoretical modeling of accelerating arc plasmas
[AD-A195606] N88-30426
MAGNETOPLASMADYNAMICS
Performance and lifetime assessment of MPD arc thruster technology
[NASA-TM-101293] N88-29860
MAGNETOSPHERE-IONOSPHERE COUPLING
Investigations of magnetosphere-ionosphere coupling relevant to operational systems
[AD-A195972] N88-30195
Corona-solar wind coupling review
[AFGL-TR-87-0203] N88-30575
MAGNETOSPHERES
Characteristics of solitary waves and weak double layers in the magnetospheric plasma
[IRF-PREPRINT-105] N88-30418
MAGNETRON SPUTTERING
The lubricating properties of magnetron sputtered MoS2
[ESA-ESTL-76] N88-30136
MAINTENANCE
Maintenance and supply options
[NASA-CR-172062] N88-29837
Fuel effects on flame radiation and hot-section durability N88-29925
MAN MACHINE SYSTEMS
Prediction and measurement of human pilot dynamic characteristics in a manned rotorcraft simulation
[NASA-CR-183246] N88-30297
Haptic exploration in humans and machines: Attribute integration and machine recognition/implementation
[AD-A193692] N88-30299
Artificial intelligence in a mission operations and satellite test environment N88-30334
Integrated resource scheduling in a distributed scheduling environment N88-30342
Barriers to Information Transfer and Approaches Toward Their Reduction
[AGARD-CP-430] N88-30458
MAN-COMPUTER INTERFACE
MANIP — spacecraft modeling program
[MANIP-217A] N88-29855
Contributions to engineering models of human-computer interaction, volume 1
[AD-A195590] N88-30295
MANAGEMENT INFORMATION SYSTEMS
The P-3 Scheduling Support System (P-3 S3)
[AD-A194824] N88-30450
MANAGEMENT METHODS
Technical change needs organizational change N88-30466
MANAGEMENT PLANNING
Development and demonstration of an on-board mission planner for helicopters
[NASA-CR-177482] N88-29817
Reduced flexibility in processing Titan 4 space launch vehicles at Cape Canaveral Air Force Station
[AD-A194908] N88-29834
MANEUVERABILITY
A second look at MIL prime flying qualities requirements N88-29740
MANIPULATORS
Low-speed longitudinal flying qualities of modern transport aircraft N88-29738
Modeling robot flexibility for endpoint force control
[AD-A195923] N88-30132
Adaptive control in positioning a rigid-flexible robot arm
[AD-A195194] N88-30367
Simulation of a two link robot manipulator with elastic members
[AD-A196014] N88-30368
A standard architecture for controlling robots
[AD-A195929] N88-30371
MANNED SPACE FLIGHT
Study on long-term evolution towards European manned spaceflight. Volume 1: Executive summary
[ERNO-OX1-002/88-VOL-1] N88-29827
JPRS report: Science and technology. USSR: Space
[JPRS-USP-88-001] N88-30498
MANUAL CONTROL
The optimal control pilot model and applications N88-29741
MANUFACTURING
A small annular combustor of high power density, wide operating range and low manufacturing cost N88-29951
Advanced planar array development for space station
[NASA-CR-179373] N88-30181
MAPPING
Evaluation of LANDSAT-TM data for geomorphological mapping
[INPE-4593-PRE/1324] N88-30168
The use of orbital remote sensing data for low cost ground-water survey
[INPE-4587-PRE/1318] N88-30170
Use of digital images as a mineral prospecting tool in the tin province of Goias, Brazil
[INPE-4537-PRE/1284] N88-30173
Implementation of the NCAR (National Centre for Atmospheric Research) graphics package at ARL (Aeronautical Research Laboratory)
[AD-A195163] N88-30193
Structure of Southwestern Michipicoten Greenstone Belt, Ontario: Evidence for Archean accretion N88-30228
Supermap for Cray FORTRAN: A user's guide
[NASA-CR-177410] N88-30308
A digital terrain model system for a microcomputer
[INPE-4610-PRE/1333] N88-30316
Faulting and its relation to volcanism: Mars western equatorial region N88-30489
MARINE ENVIRONMENTS
Doppler radar analysis of coastal marine atmospheric boundary layer structure during a cold air outbreak
[AD-A196023] N88-30261
MARKOV PROCESSES
Range data description based on multiple characteristics N88-30351
MARS (PLANET)
Nineteenth Lunar and Planetary Science Conference. Press abstracts
[NASA-CR-183037] N88-30473
MARS ATMOSPHERE
Volatiles on Mars
[NASA-CR-183113] N88-30571
MARS SURFACE
Debris flows of the Simud-Tiu outflow system of Mars N88-30485
Faulting and its relation to volcanism: Mars western equatorial region N88-30489
Physical properties of surface materials on Martian volcanoes: Dust-covered lava and ash N88-30493
Simulations of lava flows on Mars N88-30495
Volatiles on Mars
[NASA-CR-183113] N88-30571
MARS VOLCANOES
NASA MEVTV Program Working Group Meeting: Volcanism on Mars
[NASA-CR-183074] N88-30487
Mars: Volcanism in the Valles Marineris overlooked N88-30491
The Martian highland paterae: Evidence for explosive volcanism on Mars N88-30492
Physical properties of surface materials on Martian volcanoes: Dust-covered lava and ash N88-30493
Rifts of deeply eroded Hawaiian basaltic shields: A structural analog for large Martian volcanoes N88-30494
Simulations of lava flows on Mars N88-30495
Small-scale volcanic landforms indicative of distributary tube systems N88-30496
Volcanic styles at Alba Patera, Mars: Implications of lava flow morphology to the volcanic history N88-30497
MASS
Spacecraft mass estimation, relationships and engine data: Task 1.1 of the lunar base systems study
[NASA-CR-172061] N88-29836
The stability of disk galaxies and constraints on their mass-luminosity ratio
[SER-C-PREPUBL-FASC-27] N88-30565
MASS DISTRIBUTION
Laser sensing for identification and control of distributed parameter systems
[AD-A195888] N88-30124
MASS FLOW FACTORS
Analysis of a feed device for the pneumatic transport of noncohesive particles
[VKI-TM-44] N88-30062
MASS SPECTROSCOPY
Impurity analysis in SIMOX samples by high-efficiency resonance ionization time-of-flight mass spectrometry
[DE88-012061] N88-30051
Ion kinetics in silane plasmas
[AD-A196202] N88-30423
MASS TRANSFER
Global vertical mass transport by clouds: A two-dimensional model study
[CM-74] N88-30192

MATERIALS HANDLING
Vanderbilt free electron laser project in biomedical and materials research
[AD-A195961] N88-30121
Applications of synchrotron radiation to materials science: Diffraction imaging (topography) and microradiography
[NASA-CR-183265] N88-30440
MATHEMATICAL MODELS
Status review of atmosphere turbulence and aircraft response N88-29726
Extreme gusts distribution N88-29734
Advances in Flying Qualities
[AGARD-LS-157] N88-29735
Pilot modeling N88-29736
Pilot modeling applications N88-29737
Advances in flying qualities: Concepts and criteria for a mission oriented flying qualities specification N88-29739
The optimal control pilot model and applications N88-29741
Prediction of dynamic derivatives N88-29761
Prediction of base-flows N88-29765
Computational methods for the problems of the tip vortex
[NASA-CR-181438] N88-29775
Minimum-complexity helicopter simulation math model
[NASA-CR-177476] N88-29819
Procedures for updating dynamic mathematical models, test phase --- spacecraft hardware
[MEBS-38/87] N88-29852
Some theoretical considerations of the surface tension of liquid metals for metal matrix composites
[AD-A195999] N88-29882
Combustion and fuels in gas turbine engines
[AGARD-CP-422] N88-29910
Flamelet chemistry modelling of soot formation for radiation N88-29928
Numerical models for analytical predictions of combustor aerothermal performance characteristics N88-29935
Gas turbine combustion modeling N88-29936
Three-dimensional gas turbine combustor modelling N88-29937
Flamelet modeling of turbulent premixed flames N88-29942
Numerical modelling of premixed flames in gaseous media N88-29944
Modelling of CO oxidation in dilution jet flows N88-29947
Influence of the convection on evaporation and combustion of a fuel droplet N88-29948
Numerical field model simulation of full scale fire tests in a closed spherical/cylindrical vessel
[AD-A195067] N88-29998
The use of upwind schemes at high Reynolds number: A cautionary note
[AD-A196227] N88-30074
Transition mixing study empirical model report
[NASA-CR-182139] N88-30076
Numerical simulation of the function of scientific instrumentation for measuring the speed of electron devices
[AD-A194969] N88-30103
Fatigue crack propagation: Probabilistic modeling and statistical analysis
[AD-A195885] N88-30155
Relief effect correction on LANDSAT imagery for forest applications using digital terrain models
[INPE-4611-PRE/1334] N88-30179
LANDSAT TM and agrometeorological data for wheat yield estimation at the farm level
[INPE-4591-PRE/1321] N88-30180
Nd isotopes and crustal growth rate N88-30203
Construction of mass-age curves for the continental crust: An empirical model and an example from the western US N88-30213
Temperature profile construction methods: An evaluation
[AD-A195919] N88-30262
Some results from the Amazon Forest micrometeorological experiment
[INPE-4631-PRE/1346] N88-30263
Cloud/mesoscale model development and application studies
[AFGL-TR-87-0219] N88-30269
A digital terrain model system for a microcomputer
[INPE-4610-PRE/1333] N88-30316
Range data description based on multiple characteristics N88-30351
Automatic mathematical modeling for real time simulation system N88-30356
Adaptive control in positioning a rigid-flexible robot arm
[AD-A195194] N88-30367
Nested neural networks
[NASA-TM-101032] N88-30373
Generation of surface grids through elliptic partial differential equations for aircraft and missile configurations
[AD-A195639] N88-30378
Dirichlet prior in Bayesian estimation of item response curves
[AD-A195311] N88-30392
Theoretical modeling of accelerating arc plasmas
[AD-A195606] N88-30426
The origin of the moon: Further studies of the giant impact N88-30474
Volatiles on Mars
[NASA-CR-183113] N88-30571
MATRICES (CIRCUITS)
Reducing the parallel solution time of sparse circuit matrices using reordered Gaussian elimination and relaxation
[AD-A195152] N88-30045
MATRIX MATERIALS
Creep of carbon yarn and carbon-carbon composites at high temperatures and high stresses
[AD-A195224] N88-29878
Criteria for matrix dominated failure
[AD-A196263] N88-29887
MAXIMA
Structural dynamics of high-latitude magnetosphere determined from solar electron data N88-30500
MAXIMUM LIKELIHOOD ESTIMATES
Maximum-likelihood multichannel deconvolution of P waves at seismic arrays
[AD-A194990] N88-30191
Advancement of latent trait theory
[AD-A194302] N88-30289
MAXWELL EQUATION
Research on a two-stage free electron laser oscillator
[AD-A195991] N88-30115
MAZE LEARNING
Path planning and path following for the Amsterdam autonomous cart
[FVI-86-22] N88-30133
MECHANICAL PROPERTIES
Fatigue crack growth characteristics of ARALL (trademark)-1
[AD-A196185] N88-29889
Attenuated total reflectance FT-IR spectroscopy to measure interfacial reaction kinetics at silica surfaces
[AD-A196330] N88-29908
Additional fracture and strength test results for A723 steel and 38644 titanium
[AD-A196329] N88-29960
Initial value problems in viscoelasticity
[AD-A196052] N88-30145
MEDIA
Mathematical problems of nonlinear wave propagation and of waves in heterogeneous media
[AD-A195970] N88-30057
MEDICAL PERSONNEL
Central serous chorioretinopathy in USAF aviators: A review
[AD-A195697] N88-30280
MEDICAL SCIENCE
Vanderbilt free electron laser project in biomedical and materials research
[AD-A195961] N88-30121
MELTING
Evidence of the in situ decay of Al-26 in a Semarkona chondrule N88-30479
MELTS (CRYSTAL GROWTH)
A review of melt and vapor growth techniques for polydiacetylene thin films for nonlinear optical applications
[NASA-TM-100340] N88-30412
MEMBRANES
Design criteria for extraction with chemical reaction and liquid membrane permeation
[NASA-TT-20352] N88-29899
MEMORY
Nested neural networks
[NASA-TM-101032] N88-30373
MENTAL PERFORMANCE
Pilot modeling applications N88-29737
Central adrenergic receptors as mediators of central response to stress: Study with Positron Emission Tomography (PET)
[AD-A194947] N88-30284
Venture theory: A model of decision weights
[AD-A194809] N88-30391
MERCURY ION ENGINES
Successful completion of a cyclic ground test of a mercury ion auxiliary propulsion system
[NASA-TM-101351] N88-29873
MESSAGE PROCESSING
Performance analysis of k-ary n-cube interconnection networks
[AD-A195542] N88-30010
Integrated resource scheduling in a distributed scheduling environment N88-30342
Integrating information systems in a major decentralized international organization, volume 7
[AD-A195856] N88-30468
METAL COATINGS
Zinc filled coatings N88-29978
METAL FILMS
The lubricating properties of magnetron sputtered MoS2
[ESA-ESTL-76] N88-30136
METAL IONS
Storing bits on a DNA polymer chain
[AD-A195701] N88-29981
METAL MATRIX COMPOSITES
Some theoretical considerations of the surface tension of liquid metals for metal matrix composites
[AD-A195999] N88-29882
METAL OXIDE SEMICONDUCTORS
Waveform relaxation applied to transient device simulation
[AD-A194992] N88-30429
Joint services electronics program
[AD-A195731] N88-30439
METAL PROPELLANTS
Possibilities of economical improvements for Moon based rocket propulsion using lunar propellants
[ILR-MITT-196] N88-29871
METAL SHEETS
Ultrasonic detection of diffusion and adhesion loss N88-29967
METAL SURFACES
Storing bits on a DNA polymer chain
[AD-A195701] N88-29981
METALLIZING
Stress related failures causing open metallization
[AD-A195061] N88-30150
METAMORPHISM (GEOLOGY)
The timing and mechanism of depletion in Lewisian granulites N88-30209
Decoupled Rb-Sr and Sm-Nd isotopic evolution of the continental crust N88-30216
Metamorphic P-T paths and Precambrian crustal growth in East Antarctica N88-30218
The early archaean crustal history of West Greenland as recorded by detrital zircons N88-30221
Reappraisal of the geology of Kangimut Sammisoq, Ameralik Fjord, Southern West Greenland: Crustal structure and interpretation of isotopic data N88-30234
Growth of the lower continental crust N88-30236
Late-Archaean crustal growth in the Lewisian Complex of Northwest Scotland: Diachroneity in magmatic accretion and implications for models of crustal growth N88-30253
METEORITE CRATERS
Early intense cratering: Effects on growth of earth's crust N88-30219
A compilation of information and data on the Manson impact structure
[NASA-CR-183169] N88-30258
METEORITES
Nineteenth Lunar and Planetary Science Conference. Press abstracts
[NASA-CR-183037] N88-30473
Exotic minerals in 3,500 million year old rocks: Evidence for large meteorite impacts N88-30475
Evidence of the in situ decay of Al-26 in a Semarkona chondrule N88-30479
LSU scientists discover evidence of large meteorite impacts on the early earth N88-30480
Lewis Cliff 86010, a unique Antarctic meteorite: Possible new clues to the early history of the solar system N88-30482
Did the greenhouse effect kill the dinosaurs N88-30484
Antarctic Meteorite Newsletter, Volume 11, Number 2, August 1988
[NASA-TM-89801] N88-30573
METEORITIC COMPOSITION
Nineteenth Lunar and Planetary Science Conference. Press abstracts
[NASA-CR-183037] N88-30473
Ureilites are not igneous differentiates N88-30477
New type of primitive meteorite found in Antarcitca N88-30478
Physical processes and timescales in planet and small-body accretion N88-30540
Nebular processes recorded in chondritic meteorites N88-30541
METEORITIC DAMAGE
The effect of the near earth micrometeoroid environment on a highly reflective mirror surface
[NASA-TM-101307] N88-29833

METEOROLOGICAL PARAMETERS
Microwave remote sensing at INPE (Institute for Space Research) Brazil: Concepts and future prospects of soil moisture studies
[INPE-4589-PRE/1310] N88-30178
METEOROLOGICAL RADAR
Utilization of a single clear-air Doppler radar beam to measure vertical divergence
[AD-A195543] N88-30271
METEOROLOGICAL SATELLITES
Investigations of magnetosphere-ionosphere coupling relevant to operational systems
[AD-A195972] N88-30195
Passive microwave measurements of water vapor fields and rain for locating fronts in cyclonic storms
[AD-A195632] N88-30267
Analytical method for approximate geodetic referencing of scanner images of meteorological artificial earth satellites using control points N88-30527
METEOROLOGY
Activities report of the World Meteorological Organization
[WMO-689] N88-30265
METHOD OF CHARACTERISTICS
Analysis and optimization of truncated scarf nozzles subject to external flow conditions
[NASA-TM-100955] N88-29746
METROLOGY
Electromagnetic metrology N88-30024
MICHELSON INTERFEROMETERS
Piezoelectric and electrostrictive materials for transducer applications, volume 2
[AD-A194956] N88-30104
MICROCOMPUTERS
A standard library for modeling satellite orbits on a microcomputer
[AD-A195759] N88-29830
MICROELECTRONICS
Electronic and optical devices and applications N88-30027
Microcircuit trace cutting with focused ion beams
[AD-A196030] N88-30050
A system study with an infrared sensitive microelectronic image sensor
[FOA-C-30481-3.1] N88-30407
MICROMECHANICS
Modeling of micromechanisms of fatigue and fracture in hybrid materials
[AD-A195604] N88-30142
MICROMETEOROIDS
The effect of the near earth micrometeoroid environment on a highly reflective mirror surface
[NASA-TM-101307] N88-29833
MICROMETEOROLOGY
Some results from the Amazon Forest micrometeorological experiment
[INPE-4631-PRE/1346] N88-30263
Microphysical processes in cloud layers of Venus N88-30522
MICROPROCESSORS
Heavy ion and proton tests for subsystem upset
[AD-A195267] N88-30442
MICROSTRUCTURE
Creep of carbon yarn and carbon-carbon composites at high temperatures and high stresses
[AD-A195224] N88-29878
Modeling of micromechanisms of fatigue and fracture in hybrid materials
[AD-A195604] N88-30142
MICROWAVE CIRCUITS
Electronic and optical devices and applications N88-30027
MICROWAVE COUPLING
Nonlinear dynamics of coupled oscillator arrays
[AD-A194886] N88-30053
MICROWAVE EQUIPMENT
Millimeter wave generation by relativistic electron beams
[AD-A195683] N88-30016
Growth of GaAs crystals by the Heat Exchanger Method for microwave device applications
[AD-A196028] N88-30435
Estimation of soil temperature profile from remote microwave and IR measurements N88-30532
The Deep Space Network: An instrument for radio astronomy research
[NASA-CR-183219] N88-30554
MICROWAVE FREQUENCIES
Microwave remote sensing in the French industries
[ETN-88-93081] N88-30171
MICROWAVE IMAGERY
Validate algorithms for the determination of rainfall rates from SSM/I microwave satellite imagery
[AD-A195428] N88-30270
MICROWAVE RADIOMETERS
Passive microwave measurements of water vapor fields and rain for locating fronts in cyclonic storms
[AD-A195632] N88-30267
MICROWAVE SCATTERING
Transient interaction of electromagnetic pulses in dielectrics and microwave biophysics
[AD-A195687] N88-30008
MICROWAVE SENSORS
Microwave instrument for planetary mission (Titan/CASSINI mission orbiter spacecraft)
[BAE-CS/TP-8359] N88-30102
MICROWAVE SPECTRA
Mode locking of semiconductor laser with external cavity
[AD-A196018] N88-30117
MICROWAVES
The surface evaporative duct height product: An evaluation
[AD-A195918] N88-30199
MIDCOURSE GUIDANCE
Report to congress on the strategic defense system architecture
[AD-A195476] N88-30393
MIDLATITUDE ATMOSPHERE
Experimental proof of quasilongitudinal propagation of low-frequency waves in middle latitudes in upper ionosphere N88-30516
MILITARY AIR FACILITIES
Reduced flexibility in processing Titan 4 space launch vehicles at Cape Canaveral Air Force Station
[AD-A194908] N88-29834
EMPTAC (Electromagnetic Pulse Test Aircraft) user's guide
[AD-A195072] N88-30006
MILITARY HELICOPTERS
Helicopter transmission research at NASA Lewis Research Center
[NASA-TM-100962] N88-30128
MILITARY OPERATIONS
Centralized class A flight mishap investigation
[AD-A194397] N88-29786
Integration of LANTIRN (Low Altitude Navigation and Targeting Infrared for Night) into operational fighter training
[AD-A194906] N88-29799
Long haul communications in the HF spectrum utilizing high speed modems
[AD-A194683] N88-30003
Looking beyond the strategic defense initiative
[AD-A195079] N88-30394
Antisatellite weapons and satellite deployment strategies
[AD-A195014] N88-30396
MILITARY SPACECRAFT
Antisatellite weapons and satellite deployment strategies
[AD-A195014] N88-30396
MILLIMETER WAVES
Millimeter wave generation by relativistic electron beams
[AD-A195683] N88-30016
Dielectric millimeter waveguides: A feasibility study for a novel dielectric millimeter waveguide
[AD-A195104] N88-30042
Light-millimeter wave interactions in semiconductor devices
[AD-A195898] N88-30428
MINERAL EXPLORATION
Use of digital images as a mineral prospecting tool in the tin province of Goias, Brazil
[INPE-4537-PRE/1284] N88-30173
Oblique metallogenic zones recognized by interpreting space photographs of southern Tien Shan N88-30529
MINERALOGY
Nineteenth Lunar and Planetary Science Conference. Press abstracts
[NASA-CR-183037] N88-30473
Exotic minerals in 3,500 million year old rocks: Evidence for large meteorite impacts N88-30475
MINERALS
Mineralization through geologic time: Evolution of continental crust N88-30250
MINIATURE ELECTRONIC EQUIPMENT
The effects of incoming boundary layer thickness on unsteady shock-induced turbulent separations induced by cylinders
[AD-A196190] N88-30060
MIRRORS
The effect of the near earth micrometeoroid environment on a highly reflective mirror surface
[NASA-TM-101307] N88-29833
MISSILE CONFIGURATIONS
Prediction of dynamic derivatives N88-29761
Semiempirical methods for airbreathing missiles N88-29763
Aerodynamic heating of missiles N88-29764
Next generation missile design N88-29766
Generation of surface grids through elliptic partial differential equations for aircraft and missile configurations
[AD-A195639] N88-30378
MISSILE CONTROL
Special Course on Missile Aerodynamics
[AGARD-R-754] N88-29755
The present status and the future of missile aerodynamics
[NASA-TM-100063] N88-29773
MISSILE DESIGN
Special Course on Missile Aerodynamics
[AGARD-R-754] N88-29755
Accuracy criteria for evaluating supersonic aerodynamic coefficient predictions N88-29756
Survey on nonlinear effects N88-29757
Semi-empirical methods for conventional and unconventional missiles N88-29758
Space marching Euler solvers N88-29759
Numerical methods: Euler time dependent solver N88-29760
Semiempirical methods for airbreathing missiles N88-29763
Aerodynamic heating of missiles N88-29764
Next generation missile design N88-29766
MISSILE LAUNCHERS
Preliminary airworthiness evaluation of the UH-60A/ESSS (External Stores Support System) with HELLFIRE launcher installed
[AD-A196187] N88-29793
MISSILE SYSTEMS
Aircraft avionics and missile system installation cost study. Volume 2: Appendices F and G
[AD-A195372] N88-29801
MISSILES
Air intake aerodynamics N88-29762
Prediction of base-flows N88-29765
MISSION PLANNING
Development and demonstration of an on-board mission planner for helicopters
[NASA-CR-177482] N88-29817
Definition of common support equipment and space station interface requirements for IOC model technology experiments
[NASA-TM-100656] N88-29856
The 1988 Goddard Conference on Space Applications of Artificial Intelligence
[NASA-CP-3009] N88-30330
Contingency rescheduling of spacecraft operations N88-30337
Knowledge based tools for Hubble Space Telescope planning and scheduling: Constraints and strategies N88-30338
Candidate functions for advanced technology implementation in the Columbus mission planning environment N88-30340
A rule-based systems approach to spacecraft communications configuration optimization N88-30341
Integrated resource scheduling in a distributed scheduling environment N88-30342
MODELS
Constitutive modeling for isotropic materials
[NASA-CR-182132] N88-29811
Gas phase combustion chemistry of nitramine propellants
[AD-A195082] N88-29902
Attenuated total reflectance FT-IR spectroscopy to measure interfacial reaction kinetics at silica surfaces
[AD-A196330] N88-29908
Synchronous response modelling and control of an annular momentum control device
[NASA-CR-4166] N88-29995
Track performance considerations for monopulse radars
[AD-A196232] N88-30007
Measurement and interpretation of North Atlantic Ocean marine radar sea scatter
[AD-A196239] N88-30036
An improvement in the numerical integration procedure used in the NASA Marshall engineering thermosphere model
[NASA-CR-179389] N88-30200
Thermal models pertaining to continental growth N88-30230
Continental crustal formation and recycling: Evidence from oceanic basalts N88-30238
Physical processes in the growth of the continental crust N88-30240
Trace element differences between Archean, Proterozoic and Phanerozoic crustal components: Implications for crustal growth processes N88-30243
The growth of the continental crust: Constraints from radiogenic isotope geochemistry N88-30245

Crustal growth in the Archean: The geochemical evidence N88-30246
Growth of the continental crust: A planetary-mantle perspective N88-30251
Late-Archaean crustal growth in the Lewisian Complex of Northwest Scotland: Diachronsity in magmatic accretion and implications for models of crustal growth N88-30253
The effect of thicker oceanic crust in the Archaean on the growth of continental crust through time N88-30254
An analysis of results of a high-resolution world ocean circulation model [AD-A195760] N88-30272
Contributions to engineering models of human-computer interaction, volume 1 [AD-A195590] N88-30295
A model for architectural comparison [AD-A195993] N88-30302
A shared-world conceptual model for integrating space station life sciences telescience operations N88-30333
Automatic qualitative analysis of ordinary differential equations using piecewise linear approximations [AD-A196310] N88-30379
Orbital evolution of distant artificial earth satellites N88-30506

MODULATION
Long haul communications in the HF spectrum utilizing high speed modems [AD-A194683] N88-30003

MODULATORS
High frequency GaAlAs modulator and photodetector for phased array antenna applications [NASA-TM-101328] N88-30048

MODULES
EMPTAC (Electromagnetic Pulse Test Aircraft) user's guide [AD-A195072] N88-30006
Advanced planar array development for space station [NASA-CR-179373] N88-30181
The design of an intelligent multidisk control module for VME bus based systems [AD-A195587] N88-30303

MOLECULAR ABSORPTION
Molecular line shape effects on atmospheric window absorption [AD-A196316] N88-29894

MOLECULAR BEAM EPITAXY
Spectroscopic studies with multiple quantum well materials with applications to optical signal processing at room temperature [AD-A194171] N88-30409
Electronic materials and devices prepared by molecular beam epitaxy [AD-A195694] N88-30433

MOLECULAR CHAINS
Storing bits on a DNA polymer chain [AD-A195701] N88-29981
Novel ladder polymers for use as high temperature stable resins or coatings [NASA-CASE-LEW-14203-1] N88-29984

MOLECULAR CLOUDS
Star formation and molecular clouds N88-30537
Observations of star formation N88-30538
Comparisons of solar nebula models N88-30539

MOLECULAR EXCITATION
Intramolecular dynamics: A study of molecules at high levels of vibrational excitation [AD-A195285] N88-30400

MOLECULAR INTERACTIONS
Cytochrome electron transfer and biomolecular electronics [AD-A195482] N88-30277

MOLECULAR STRUCTURE
Discovery of a low temperature form of TAGN (Triaminoguanidinium Nitrate) [AD-A196059] N88-29989

MOLECULES
Semi-microdroplet assay for cell adhesion molecules [NASA-CR-183139] N88-30274

MOLYBDENUM
An experimental study of biaxial yield in modified 9Cr-1Mo steel at room temperature [NASA-CR-175012] N88-30164

MOLYBDENUM DISULFIDES
The lubricating properties of magnetron sputtered MoS2 [ESA-ESTL-76] N88-30136

MOMENTUM TRANSFER
Development of a more general Reynolds stress closure for swirling flow [AD-A195121] N88-30092

MONOCHROMATIC RADIATION
Diffraction imaging (topography) with monochromatic synchrotron radiation [NASA-CR-183264] N88-30431
Streaking images that appear only in the plane of diffraction in undoped GaAs single crystals: Diffraction imaging (topography) by monochromatic synchrotron radiation [NASA-CR-183267] N88-30437

MONOPULSE RADAR
Track performance considerations for monopulse radars [AD-A196232] N88-30007

MONTE CARLO METHOD
Monte-Carlo estimation of the influence of plant architecture parameters on spectral brightness N88-30533

MORPHOLOGY
Morphological changes in polymer electrolyte cells [AD-A195821] N88-30054
Volcanic styles at Alba Patera, Mars: Implications of lava flow morphology to the volcanic history N88-30497

MOSSBAUER EFFECT
Phase modulation of recoilless gamma radiation in Mossbauer spectroscopy [ETN-88-92648] N88-30403

MOTION PERCEPTION
Dynamical systems and motion vision [AD-A195932] N88-30366

MOTION STABILITY
Utilizing dynamic stability of orient parts [AD-A195730] N88-30397
Orbital stability in rotating triaxial stellar systems [SER-C-PREPUBL-FASC-24] N88-30569

MOUNTAINS
Structure of eastern Turkestan Ridge based on space photographs N88-30530

MULTIPLE ACCESS
Optical multiple access intersatellite links [BAE-TP-8502] N88-30013
Performance of DS/SSMA communications in impulsive channels. Part 1: Correlation receivers [AD-A195712] N88-30021

MULTIPROCESSING (COMPUTERS)
Compression and decompression of imaging sensor signals (CADISS): A multiprocessor system for image compression/decompression on board scientific satellites [NLR-TR-87076-L] N88-30323
The triangle: A multiprocessor architecture for fast curve and surface generation [AD-A195882] N88-30324
Reification without evaluation [AD-A195928] N88-30326

MULTISENSOR APPLICATIONS
Path planning and path following for the Amsterdam autonomous cart [FVI-86-22] N88-30133

MULTIVARIATE STATISTICAL ANALYSIS
Reconstruction of multidimensional signals from multiple level threshold crossings [AD-A195561] N88-30383

N

NAMIBIA
Evolution of thermal structure of Benguela upswelling system according to satellite and shipboard data N88-30525

NAP-OF-THE-EARTH NAVIGATION
LANTIRN simulator training in the F-16C [AD-A195201] N88-29826

NASA SPACE PROGRAMS
Science at NASA field centers: Findings and recommendations on the scope, strength and interactions of science and science-related technology programs [NASA-TM-101188] N88-30581
Research and technology of the Lyndon B. Johnson Space Center [NASA-TM-100483] N88-30583

NASTRAN
Computer programs for generation of NASTRAN and VIBRA-6 aircraft models [AD-A195467] N88-29792

NATURAL LANGUAGE (COMPUTERS)
Exploiting lexical regularities in designing natural language systems [AD-A195922] N88-30375

NATURAL SATELLITES
Extended atmospheres of outer planet satellites and comets [NASA-CR-183157] N88-30572

NAVIER-STOKES EQUATION
Three-dimensional Navier-Stokes simulations of turbine rotor-stator interaction [NASA-TM-100081] N88-29750
A streamwise upwind algorithm for the Euler and Navier-Stokes equations applied to transonic flows [NASA-TM-101019] N88-29751
Application of unsteady aerodynamic methods for transonic aeroelastic analysis [NASA-TM-100665] N88-29754
Aerodynamic heating of missiles N88-29764
Computational aerodynamic analysis for a range-limited 25mm training round [AD-A185270] N88-29772
The computation of flow past an oblique wing using the thin-layer Navier-Stokes equations [NASA-TM-88317] N88-29774
On the application of finite-difference techniques for the computation of the flow field in gas turbine combustors with complex geometries N88-29938
Modeling the stability of a turbulent premixed flame, downstream from a step by a Lagrangian method N88-29943
Numerical simulation of unsteady incompressible viscous flows in generalized coordinate systems [NASA-TM-101016] N88-30085

NAVIGATION
Kalman filter-based algorithms for estimating depth from image sequences [AD-A195818] N88-30380

NAVIGATION AIDS
Accuracy of satellite data navigation [AD-A195877] N88-29787
The guide star catalog [NASA-CR-183253] N88-30547

NAVIGATION INSTRUMENTS
Observed track-keeping performance of DC10 aircraft equipped with the Collins AINS-70 area navigation system: Karlsruhe and Maastricht UACs (Upper Area Control centres) [EEC-202] N88-29788

NEAR FIELDS
Application of sampling techniques to near-field far-field transformation [ESA-CR(P)-2546] N88-30002

NEAR INFRARED RADIATION
Growth and characterization of materials for tunable lasers in the near infrared spectral region [NASA-CR-183132] N88-30113

NEAR WAKES
Investigation of large-scale structures in the near wake of a parallel flat plate [ESA-TT-1100] N88-30080

NEBULAE
Comparisons of solar nebula models N88-30539
Physical processes and timescales in planet and small-body accretion N88-30540
Nebular processes recorded in chondritic meteorites N88-30541
Cosmochemical trends of volatile elements in the solar system N88-30542
Terrestrial versus giant planet formation N88-30543

NEODYMIUM ISOTOPES
Nd isotopes and crustal growth rate N88-30203
Growth of continental crust: Clues from Nd isotopes and Nb-Th relationships in mantle-derived magmas N88-30205
Changing styles of crustal growth in Southern Africa: Constraints from geochemical and Sr-Nd isotope studies in Archaean to Pan African terrains N88-30227

NETWORK ANALYSIS
Performance analysis of k-ary n-cube interconnection networks [AD-A195542] N88-30010

NETWORK CONTROL
Design of a self-timed VLSI multicomputer communication controller [AD-A194567] N88-30014

NEURAL NETS
Circuit design criteria for stable lateral inhibition neural networks [AD-A195066] N88-30046
Autonomous image data reduction by analysis and interpretation N88-30347
Parallel and distributed computation for fault-tolerant object recognition N88-30350
Nested neural networks [NASA-TM-101032] N88-30373

NEUROLOGY
Models of cerebral-body perfusion and cerebral chemical transport [AD-A194945] N88-30283
Central adrenergic receptors as mediators of central response to stress: Study with Positron Emission Tomography (PET) [AD-A194947] N88-30284

NEUROPHYSIOLOGY
Comparative aspects of multiple processes of attention [AD-A195805] N88-30291

NEVADA
The dynamics of transuranics and other radionuclides in natural environments, December 1985
[DE87-014456] N88-30189
NICKEL ALLOYS
Hydrogen embrittlement of iron-nickel alloys
[AD-A195909] N88-29958
Anisotropic constitutive modeling for nickel-base single crystal superalloys
[NASA-CR-182157] N88-29961
NICKEL CADMIUM BATTERIES
Aircraft battery state of charge and charge control system
[AD-A194979] N88-30052
NIGHT FLIGHTS (AIRCRAFT)
Integration of LANTIRN (Low Altitude Navigation and Targeting Infrared for Night) into operational fighter training
[AD-A194906] N88-29799
LANTIRN simulator training in the F-16C
[AD-A195201] N88-29826
NIGHT SKY
One equatorial anomaly in nighttime ionospheric F region N88-30517
NIGHT VISION
Visual sensitivities under reduced oxygen
[AD-A195628] N88-30279
Common modules: A success story
[AD-A195937] N88-30415
NITRAMINE PROPELLANTS
Discovery of a low temperature form of TAGN (Triaminoguanidinium Nitrate)
[AD-A196059] N88-29989
NITRATES
Some effects of nitrates on the tensile properties of Al 7075-T7351
[AD-A195118] N88-29965
Discovery of a low temperature form of TAGN (Triaminoguanidinium Nitrate)
[AD-A196059] N88-29989
NITROGEN
Computed potential energy surfaces for chemical reactions
[NASA-CR-183168] N88-29893
NITROGEN METABOLISM
Comparison of morning with afternoon nitrogen elimination in resting subjects breathing 100 percent oxygen
[AD-A196191] N88-30282
NITROGEN OXIDES
Photochemistry of ionospheric D-region with injection of nitrogen oxides N88-30499
NOISE INTENSITY
Discrimination studies using short-period P waves at upper mantle distances
[AD-A195468] N88-30257
NOISE PREDICTION
Aircraft noise prediction program propeller analysis system IBM-PC version user's manual version 2.0
[NASA-CR-181689] N88-30399
NONDESTRUCTIVE TESTS
Evaluation of bond testing equipment for inspection of Army advanced composite airframe structures
[AD-A195795] N88-29885
In situ fault detection by the hybrid ray mode method
[AD-A195226] N88-30137
Application of nondestructive testing techniques to materials testing
[AD-A195716] N88-30138
Automated early fatigue damage sensing system
[AD-A195717] N88-30143
Report on an overseas visit to USA relating to the thermoelastic measurement of stresses, 16-21 August 1987
[AD-A195313] N88-30161
NONEQUILIBRIUM FLOW
Nonequilibrium flow of a dissociating gas in a horizontal channel with axial temperature variation
[DE88-702536] N88-30089
Nonequilibrium flow computations. 1: An analysis of numerical formulations of conservation laws
[NASA-CR-177489] N88-30384
NONLINEAR EQUATIONS
New methods for nonlinear optimization
[AD-A195982] N88-30313
Convergence acceleration for vector sequences and applications to computational fluid dynamics
[NASA-TM-101327] N88-30377
Convergence of Galerkin approximations for operator Riccati equations: A nonlinear evolution equation approach
[NASA-CR-181706] N88-30386
NONLINEAR FILTERS
Analytical methods in stochastic control and nonlinear filtering
[AD-A194272] N88-30388
NONLINEAR OPTICS
Nonlinear optical phase conjugation techniques to reduce the physical size of lasers
[AD-A196170] N88-30122
A review of melt and vapor growth techniques for polydiacetylene thin films for nonlinear optical applications
[NASA-TM-100340] N88-30412
NONLINEAR SYSTEMS
Nonlinear Tollmien-Schlichting/vortex interaction in boundary layers
[NASA-CR-181698] N88-29715
The strong nonlinear interaction of Tollmien-Schlichting waves and Taylor-Goertler vortices in curved channel flow
[NASA-CR-181697] N88-29716
Nonlinear dynamics of coupled oscillator arrays
[AD-A194888] N88-30053
Mathematical problems of nonlinear wave propagation and of waves in heterogeneous media
[AD-A195970] N88-30057
Initial value problems in viscoelasticity
[AD-A196052] N88-30145
Algorithms for nonlinear least-squares problems
[AD-A196071] N88-30305
K(sup th)-order extended linearization
[AD-A194786] N88-30363
Automatic qualitative analysis of ordinary differential equations using piecewise linear approximations
[AD-A196310] N88-30379
Multiple solutions and bifurcation for a class of nonlinear Sturm-Liouville eigenvalue problems on an unbounded domain
[AD-A195954] N88-30389
NONLINEARITY
Survey on nonlinear effects N88-29757
Nonlinear optical phase conjugation techniques to reduce the physical size of lasers
[AD-A196170] N88-30122
Geometric and material nonlinear analysis of structures comprising rectangular hollow sections
[CE-79] N88-30141
NONNEWTONIAN FLUIDS
Approximation of viscoelastic stresses from Newtonian turbulent kinematics
[AD-A194317] N88-30077
NONUNIFORM FLOW
Gaseous premixed flames in non-uniform flows N88-29945
NORTH AMERICA
DATATRAN: Datum transformation software
[AD-A195723] N88-30175
Gravity anomalies, plate tectonics and the lateral growth of Precambrian North America N88-30248
NOTCH STRENGTH
The effect of notch root radius on the determination of toughness in ultrahigh strength steel friction welds
[AD-A195952] N88-30156
NOZZLE DESIGN
Analysis and optimization of truncated scarf nozzles subject to external flow conditions
[NASA-TM-100955] N88-29746
Stresses in cylindrical shells with tangential nozzles submitted to external loads and internal pressure
[CRIF-MT-172] N88-30146
NOZZLE EFFICIENCY
Analysis and optimization of truncated scarf nozzles subject to external flow conditions
[NASA-TM-100955] N88-29746
NOZZLE FLOW
Aerodynamics in ground effect and predicted landing ground roll of a fighter configuration with a secondary-nozzle thrust reverser
[NASA-TP-2834] N88-29752
Nozzle airflow influences on fuel patternation N88-29916
Numerical simulation of nozzle flows
[AD-A195144] N88-30064
NUCLEAR EXPLOSIONS
Maximum-likelihood multichannel deconvolution of P waves at seismic arrays
[AD-A194990] N88-30191
NUCLEAR RADIATION SPECTROSCOPY
Phase modulation of recoiless gamma radiation in Mossbauer spectroscopy
[ETN-88-92648] N88-30403
NUCLEAR SCATTERING
Eikonal solutions to optical model coupled-channel equations
[NASA-TP-2830] N88-30402
NUCLEAR WEAPONS
Looking beyond the strategic defense initiative
[AD-A195079] N88-30394
NUMERICAL ANALYSIS
Numerical solutions of unsteady inviscid transonic turbine cascade flows
[AD-A196111] N88-29748
Space marching Euler solvers N88-29759
Simulation of Vulcain engine operation at low inlet pressure
[ETN-88-93083] N88-29875
Analysis of the flow through double swirl airblast atomizers N88-29949
Numerical field model simulation of full scale fire tests in a closed spherical/cylindrical vessel
[AD-A195067] N88-29998
Transition at hypersonic speeds
[NASA-CR-178315] N88-30058
Transition mixing study empirical model report
[NASA-CR-182139] N88-30076
Numerical simulation of the function of scientific instrumentation for measuring the speed of electron devices
[AD-A194969] N88-30103
A detection theory analysis of visual display performance
[AD-A196291] N88-30292
Nonequilibrium flow computations. 1: An analysis of numerical formulations of conservation laws
[NASA-CR-177489] N88-30384
Regularity and numerical solution of eigenvalue problems with piecewise analytic data
[AD-A194993] N88-30387
Orbital evolution of distant artificial earth satellites N88-30506
The atmospheres of the earth and the other planets: Origin, evolution and composition N88-30544
Study of modern instrumentation and methods for astronomic positioning in the field
[AD-A196173] N88-30548
Numerical evidence that the motion of Pluto is chaotic
[AD-A195920] N88-30568
NUMERICAL INTEGRATION
An improvement in the numerical integration procedure used in the NASA Marshall engineering thermosphere model
[NASA-CR-179389] N88-30200
NUMERICAL STABILITY
Stability, stochastic stationarity and generalized Lyapunov equations for two-point boundary-value descriptor systems
[AD-A195645] N88-30385
NUTATION
Rotational evolution of dynamically symmetric gyrostat with internal friction N88-30509

O

OBLIQUE SHOCK WAVES
Experimental and numerical investigation of the effect of distributed suction on oblique shock wave/turbulent boundary layer interaction
[NASA-TM-101334] N88-30084
OBLIQUE WINGS
The computation of flow past an oblique wing using the thin-layer Navier-Stokes equations
[NASA-TM-88317] N88-29774
OBSERVABILITY (SYSTEMS)
Increasing accuracy in evaluating vector of state under conditions of incomplete observability of expanded system N88-30511
OCEAN BOTTOM
The growth of continents and some consequences since 1.5 Ga N88-30220
The tectonic setting of the Seychelles, Mascarene and Amirante Plateaus in the Western Equatorial Indian Ocean N88-30225
The petrogenesis of oceanic kimberlites and included mantle megacrysts: The Malaitan alnoite N88-30232
Continental crustal formation and recycling: Evidence from oceanic basalts N88-30238
Solid earth as a recycling systems and the lateral growth of Precambrian North America N88-30249
The effect of thicker oceanic crust in the Archaean on the growth of continental crust through time N88-30254
OCEAN CURRENTS
An analysis of results of a high-resolution world ocean circulation model
[AD-A195760] N88-30272
KOSPAS-SARSAT satellites used for ocean current study N88-30534
OCEAN MODELS
An analysis of results of a high-resolution world ocean circulation model
[AD-A195760] N88-30272

OCEAN SURFACE
Measurement and interpretation of North Atlantic Ocean marine radar sea scatter
[AD-A196239] N88-30036
Analysis of environmental parameters from the Panama City tower radar experiment
[AD-A194994] N88-30264
Determining near-water wind speed using radar data from Cosmos-1500 artificial earth satellite N88-30524
OCEANOGRAPHIC PARAMETERS
A study of the feasibility of using sea and wind information from the ERS-1 satellite. Part 1: Wind scatterometer data
[NASA-CR-182833] N88-30167
A study of the feasibility of using sea and wind information from the ERS-1 satellite. Part 2: Use of scatterometer and altimeter data in wave modeling and assimilation
[ESA-CR(P)-2604-PT-2] N88-30176
OCEANOGRAPHY
ERS-1: A satellite with an oceanographic mission
[NLR-MP-86072-U] N88-29838
OCEANS
MIZEX (marginal ice zone experiment) 1987 SAR (Synthetic Aperture Radar) data summary
[AD-A195560] N88-30035
Rossby waves in mid-latitude oceans N88-30273
ON-LINE SYSTEMS
Geometric modeling for computer aided design
[NASA-CR-183161] N88-30320
ONBOARD DATA PROCESSING
Compression and decompression of imaging sensor signals (CADISS): A multiprocessor system for image compression/decompression on board scientific satellites
[NLR-TR-87076-L] N88-30323
ONBOARD EQUIPMENT
Flight test equipment for the on-board measurement of wind turbulence N88-29719
OPEN CHANNEL FLOW
Recent insights into instability and transition to turbulence in open-flow systems
[NASA-CR-181693] N88-30079
OPERATING SYSTEMS (COMPUTERS)
A rule-based systems approach to spacecraft communications configuration optimization N88-30341
OPTICAL COMMUNICATION
Optical multiple access intersatellite links
[BAE-TP-8502] N88-30013
OPTICAL COMPUTERS
Architecture for optical digital computers
[AD-A195477] N88-30416
OPTICAL DATA PROCESSING
Optical symbolic computing
[AD-A195690] N88-30406
Spectroscopic studies with multiple quantum well materials with applications to optical signal processing at room temperature
[AD-A194171] N88-30409
Use of depletion edge translation for high-speed modulation and switching of lightwaves
[AD-A195611] N88-30417
OPTICAL DATA STORAGE MATERIALS
Evaluation of multi-focus holographic lenses
[AD-A196167] N88-30110
OPTICAL EMISSION SPECTROSCOPY
The optical spectroscopy of copper-blue luminescence in zinc sulfide crystals. Zero-phonon line spectra under the influence of magnetic field, temperature and excitation intensity
[ETN-88-93122] N88-29903
OPTICAL EQUIPMENT
A fiber optic collective flight control system for helicopters
[AD-A195406] N88-29818
Optoelectronic gain control of a microwave single stage GaAs MESFET amplifier
[NASA-CR-182201] N88-30055
Application of nondestructive testing techniques to materials testing
[AD-A195716] N88-30138
OPTICAL MEASUREMENT
Volumetric measurement of vorticity vectors by optical probe
[AD-A195997] N88-30061
Optical measurements of soot in premixed flames
[NASA-TM-101305] N88-30090
OPTICAL MEMORY (DATA STORAGE)
Evaluation of multi-focus holographic lenses
[AD-A196167] N88-30110
OPTICAL PROPERTIES
Growth and characterization of materials for tunable lasers in the near infrared spectral region
[NASA-CR-183132] N88-30113
Spontaneous force optical traps
[AD-A196103] N88-30114
Bibliography of Soviet laser developments, number 88, March - April 1987
[AD-A195978] N88-30116
Atmospheric corrections for in-flight satellite radiometric calibration
[AD-A196124] N88-30194
An organometallic route to micron-sized whiskers of zinc sulfide
[AD-A195889] N88-30414
On 3-5 heterojunction structures and high speed devices
[AD-A195464] N88-30438
OPTICAL RADAR
Spaceborne lidar: Development of a laboratory test system
[BF-R-66.090-1] N88-30118
OPTICAL RESONATORS
Spectral properties of semiconductor lasers with external resonators
[ETN-88-93119] N88-30125
OPTICAL SCANNERS
Five channel auroral photometer
[REPT-112] N88-30101
Application of nondestructive testing techniques to materials testing
[AD-A195716] N88-30138
OPTICAL WAVEGUIDES
Ion exchange processes for fabrication of integrated optical waveguide structures into glass substrates
[VTT-46] N88-30405
Use of depletion edge translation for high-speed modulation and switching of lightwaves
[AD-A195611] N88-30417
OPTICS
Optics and symbolic computing
[AD-A195119] N88-30004
OPTIMAL CONTROL
The optimal control pilot model and applications N88-29741
Sensor and actuator selection for large space structure control
[AD-A194912] N88-29842
Theory of filtering and control with application to control of large space structures
[AD-A195500] N88-29851
Analytical methods in stochastic control and nonlinear filtering
[AD-A194272] N88-30388
Increasing accuracy in evaluating vector of state under conditions of incomplete observability of expanded system N88-30511
OPTIMIZATION
Analysis and optimization of truncated scarf nozzles subject to external flow conditions
[NASA-TM-100955] N88-29746
New methods for nonlinear optimization
[AD-A195982] N88-30313
A rule-based systems approach to spacecraft communications configuration optimization N88-30341
Formulation and solution of economic equilibrium problems
[AD-A196034] N88-30470
OPTOELECTRONIC DEVICES
Electronic and optical devices and applications N88-30027
Optoelectronic gain control of a microwave single stage GaAs MESFET amplifier
[NASA-CR-182201] N88-30055
ORBIT TRANSFER VEHICLES
Centaur operations at the space station: Cost and transportation analysis
[NASA-CR-182128] N88-29835
Orbital transfer vehicle 3000 LBF thrust chamber assembly hot fire test program
[NASA-CR-182145] N88-29858
ORBITAL ASSEMBLY
Centaur operations at the space station: Cost and transportation analysis
[NASA-CR-182128] N88-29835
Study of robotics spacecraft servicing and assembly in space. Volume 1: Executive summary
[ESA-CR(P)-2612-VOL-1] N88-29839
ORBITAL ELEMENTS
Duplicity in the solar neighborhood: Part 4: Spectroscopic orbits for four dwarf M stars
[SER-C-PREPUBL-FASC-21] N88-30561
ORBITAL MANEUVERS
The eivaN: A forward-looking interactive orbital trajectory plotting tool for use with proximity operations (PROX OPS) and other maneuvers: Description and user's manual
[NASA-CR-177490] N88-30327
ORBITAL MECHANICS
Investigation of the validity of the non-rotating planet assumption for three-dimensional earth atmospheric entry
[AD-A194877] N88-29829
Orbital evolution of distant artificial earth satellites N88-30506
Plane periodic satellite motions relative to center of mass in neighborhood of collinear libration point N88-30507
Orbital stability in rotating triaxial stellar systems
[SER-C-PREPUBL-FASC-24] N88-30569
ORBITAL POSITION ESTIMATION
Approximation of atmospheric density by Chebyshev polynomials in predicting motion of low artificial earth satellites N88-30503
ORBITAL SERVICING
Centaur operations at the space station: Cost and transportation analysis
[NASA-CR-182128] N88-29835
Study of robotics spacecraft servicing and assembly in space. Volume 1: Executive summary
[ESA-CR(P)-2612-VOL-1] N88-29839
Technology requirements for an orbiting fuel depot: A necessary element of a space infrastructure
[NASA-TM-101370] N88-29845
Design and development of a refueling test bed
[FTMS-RP-ER-011] N88-29986
ORGANIC MATERIALS
Evaluation of organic coating deterioration and substrate corrosion in seawater using electrochemical impedance measurements N88-29978
ORGANIZATIONS
Strategic, organizational and standardization aspects of integrated information systems, volume 6
[AD-A195855] N88-30457
Technical change needs organizational change N88-30486
ORTHOGONAL FUNCTIONS
Determining the spatial structure of fields of precipitation from space radar images in two orthogonal polarizations N88-30531
OSCILLATIONS
Prediction of dynamic derivatives N88-29761
Theories of comparative analysis
[AD-A196328] N88-30395
Intermediate polars observed in Brazil in the last eight years
[INPE-4567-PRE/1308] N88-30559
OSCILLATORS
Nonlinear dynamics of coupled oscillator arrays
[AD-A194888] N88-30053
Research on a two-stage free electron laser oscillator
[AD-A195991] N88-30115
OVER-THE-HORIZON RADAR
The effect of equatorial ionospheric irregularities on the performance of a south-looking OTH-B (Over-The-Horizon-Backscatter) radar
[AD-A195090] N88-30018
Modeling and performance of HF/OTH (High-Frequency/Over-the-Horizon) radar target identification systems
[AD-A196287] N88-30038
OXIDATION
Modelling of CO oxidation in dilution jet flows N88-29947
OXIDATION RESISTANCE
Processing technology research in composites
[AD-A195693] N88-29890
OXIDATION-REDUCTION REACTIONS
Electrocatalytic reduction of oxygen on modified oxide surfaces
[NASA-TM-101333] N88-29952
OXIDIZERS
Oxidizer heat exchanger component test
[NASA-CR-182159] N88-29876
OXYGEN
Aeronomic problems of the molecular oxygen photodissociation. Part 3: Solar spectral irradiances in the region of the O2 Herzberg continuum, Schumann-Runge bands and continuum
[AERONOMICA-ACTA-A-332-1988] N88-29897
Aeronomic problems of molecular oxygen photodissociation. Part 2: Theoretical absorption cross sections of the Schumann-Runge bands at 79 K
[AERONOMICA-ACTA-A-331-1988] N88-29907
Aeronomic problems of molecular oxygen photodissociation. Part 4: The various parameters for the Herzberg continuum
[AERONOMICA-ACTA-A-333-1988] N88-29955
OZONE
Recent measurements of ozone in the Amazon forests
[INPE-4494-PRE/1258] N88-30185
Changes in stratospheric ozone: Observations and theories
[AERONOMICA-ACTA-A-334-1988] N88-30188
OZONE DEPLETION
Changes in stratospheric ozone: Observations and theories
[AERONOMICA-ACTA-A-334-1988] N88-30188

OZONOMETRY
Changes in stratospheric ozone: Observations and theories
[AERONOMICA-ACTA-A-334-1988] N88-30188

P

P WAVES
Maximum-likelihood multichannel deconvolution of P waves at seismic arrays
[AD-A194990] N88-30191
Discrimination studies using short-period P waves at upper mantle distances
[AD-A195468] N88-30257
PAINTS
Prediction of degradation of polymeric coating materials N88-29970
Electrochemical evaluation of the long term corrosion resistance of polymer coated steel N88-29974
Reduced time frame for predicting coating performance N88-29979
PARABOLAS
Large displacement and rotational formulation for laminated cylindrical shells including parabolic transverse shear
[AD-A194871] N88-30158
PARABOLIC ANTENNAS
The focal plane reception pattern calculation for a paraboloidal antenna with a nearby fence
[NASA-TM-100691] N88-30039
PARALLEL PROCESSING (COMPUTERS)
Performance analysis of k-ary n-cube interconnection networks
[AD-A195542] N88-30010
Reducing the parallel solution time of sparse circuit matrices using reordered Gaussian elimination and relaxation
[AD-A195152] N88-30045
Performance prediction of concurrent systems
[NASA-CR-183175] N88-30312
Parallel and distributed computation for fault-tolerant object recognition N88-30350
PARAMETER IDENTIFICATION
Procedures for updating dynamic mathematical models, test phase — spacecraft hardware
[MEBS-38/87] N88-29852
PARTIAL DIFFERENTIAL EQUATIONS
Laser sensing for identification and control of distributed parameter systems
[AD-A195666] N88-30124
Multiple solutions and bifurcation for a class of nonlinear Sturm-Liouville eigenvalue problems on an unbounded domain
[AD-A195954] N88-30389
PARTICLE BEAMS
Cluster beam studies
[AD-A195182] N88-30443
PARTICLE DENSITY (CONCENTRATION)
Optical measurements of soot in premixed flames
[NASA-TM-101305] N88-30090
PARTICLE EMISSION
Positron emission tomography: A new technique for observing fluid behavior in engineering systems
[PNR90471] N88-30091
PARTICLE SIZE DISTRIBUTION
Automatic data retrieval from rocket motor holograms
[AD-A195586] N88-29864
Simulation study of spraying, streaming and vaporization phenomena associated with fuel injection N88-29914
Turbulence effects on the droplet distribution behind airblast atomizers N88-29915
Multiple scattering effects in drop sizing of dense fuel sprays by laser diffraction N88-29917
Influence of operating conditions on the atomization and distribution of fuel by air blast atomizers N88-29918
Particle size measurements in sooting combustion systems N88-29931
Particle sizing in combustion systems, using scattered laser light
[AD-A196231] N88-29953
Optical measurements of soot and temperature profiles in premixed propane-oxygen flames
[NASA-TM-101343] N88-29997
Optical measurements of soot in premixed flames
[NASA-TM-101305] N88-30090
Evaluation of the potential health hazards associated with the machining of carbon fiber composites
[AD-A194835] N88-30286
PARTICLE TRAJECTORIES
Particle trajectories and potentials in a plane sheath moving in a magnetoplasma
[AD-A196228] N88-30190
PASSIVE SATELLITES
Comparative analysis of passive communications satellites employing the SHF and HF spectrum for use in a strategic role
[AD-A194682] N88-30019
PATENT APPLICATIONS
Ultrasonic method and apparatus for determining crack opening load
[NASA-CASE-LAR-13889-1] N88-30160
PATTERN RECOGNITION
Corner extraction from radar images
[AD-A194857] N88-30020
Path planning and path following for the Amsterdam autonomous cart
[FVI-86-22] N88-30133
Eye movements and spatial pattern vision
[AD-A195496] N88-30290
An interactive testbed for development of expert tools for pattern recognition N88-30349
Parallel and distributed computation for fault-tolerant object recognition N88-30350
Nested neural networks
[NASA-TM-101032] N88-30373
PATTERN REGISTRATION
Method for combined image interpolation-restoration through a fir filter design technique
[INPE-4561-PRE/1302] N88-30315
PAYLOAD CONTROL
Aerospace payload support systems
[AFGL-TR-87-0241] N88-29843
PERCEPTION
Advancement of latent trait theory
[AD-A194302] N88-30289
PERFORMANCE PREDICTION
Measured and predicted responses of the Nord 260 aircraft to the low altitude atmospheric turbulence N88-29723
Semi-empirical methods for conventional and unconventional missiles N88-29758
Space marching Euler solvers N88-29759
Numerical models for analytical predictions of combustor aerothermal performance characteristics N88-29935
Three-dimensional gas turbine combustor modelling N88-29937
Numerical modeling of combustion processes in gas turbines N88-29939
Performance Prediction for Coatings. Proceedings of a Workshop
[AD-A188973] N88-29966
Ultrasonic detection of diffusion and adhesion loss N88-29967
Performance prediction of concurrent systems
[NASA-CR-183175] N88-30312
Theories of comparative analysis
[AD-A196328] N88-30395
PERFORMANCE TESTS
Controlled degradation of resolution of high-quality flight simulator images for training effectiveness evaluation
[AD-A196189] N88-29823
Performance and lifetime assessment of MPD arc thruster technology
[NASA-TM-101293] N88-29860
A small annular combustor of high power density, wide operating range and low manufacturing cost N88-29951
Additional fracture and strength test results for A723 steel and 38644 titanium
[AD-A196329] N88-29960
EMPTAC (Electromagnetic Pulse Test Aircraft) user's guide
[AD-A195072] N88-30006
Qualification test levels for units to be derived from mechanical test data analysis — ESA
[REPT-87-158-EI/ET/AG] N88-30139
PERIDOTITE
The petrogenesis of oceanic kimberlites and included mantle megacrysts: The Malaitan ainoite N88-30232
PERIODIC VARIATIONS
Plane periodic satellite motions relative to center of mass in neighborhood of collinear libration point N88-30507
PERMEATING
Design criteria for extraction with chemical reaction and liquid membrane permeation
[NASA-TT-20352] N88-29899
PEROXIDES
Electrocatalytic reduction of oxygen on modified oxide surfaces
[NASA-TM-101333] N88-29952
Determination of the hydroperoxide potential of jet fuels
[AD-A195975] N88-29991
PERSONAL COMPUTERS
Aircraft noise prediction program propeller analysis system IBM-PC version user's manual version 2.0
[NASA-CR-181689] N88-30399
PERTURBATION
Theories of comparative analysis
[AD-A196328] N88-30395
PERTURBATION THEORY
Free vibration of rectangular plates with a small initial curvature
[NASA-CR-179370] N88-30148
PETROLOGY
Evidence for crustal recycling during the Archean: The parental magmas of the stillwater complex N88-30226
The tectonic setting of Archean anorthosites N88-30231
The petrogenesis of oceanic kimberlites and included mantle megacrysts: The Malaitan ainoite N88-30232
Growth of the continental crust: A planetary-mantle perspective N88-30251
Crustal underplating in the North American Craton: Evidence from the Petrogenesis of anorthositic rocks in the Middle Proterozoic Midcontinent Rift System N88-30252
PHASE CONJUGATION
Nonlinear optical phase conjugation techniques to reduce the physical size of lasers
[AD-A196170] N88-30122
PHASE LOCKED SYSTEMS
Tolerances for phase locking of semiconductor laser arrays
[AD-A195974] N88-30120
PHASE MODULATION
Phase modulation of recoiless gamma radiation in Mossbauer spectroscopy
[ETN-88-92648] N88-30403
PHASE SHIFT KEYING
Doppler-corrected differential detection system
[NASA-CASE-NPO-16987-1-CU] N88-30001
PHASE TRANSFORMATIONS
Crustal evolution and the eclogite to granulite phase transition in xenoliths from the West African Craton N88-30217
A method for the quantitative determination of crystalline phases by X-ray
[NASA-TT-20324] N88-30444
PHASED ARRAYS
High frequency GaAlAs modulator and photodetector for phased array antenna applications
[NASA-TM-101328] N88-30048
Maximum-likelihood multichannel deconvolution of P waves at seismic arrays
[AD-A194990] N88-30191
PHENOMENOLOGY
State variable approach to deformation phenomena in Face Centered Cubic (FCC) metals
[VTT-44] N88-29964
PHOTOACOUSTIC SPECTROSCOPY
Photoacoustic Fourier transform infrared spectroscopy. An early detection technique for coatings degradation N88-29968
PHOTOCHEMICAL REACTIONS
Photochemistry of ionospheric D-region with injection of nitrogen oxides N88-30499
PHOTODISSOCIATION
Aeronomic problems of the molecular oxygen photodissociation. Part 3: Solar spectral irradiances in the region of the O2 Herzberg continuum, Schumann-Runge bands and continuum
[AERONOMICA-ACTA-A-332-1988] N88-29897
Aeronomic problems of molecular oxygen photodissociation. Part 2: Theoretical absorption cross sections of the Schumann-Runge bands at 79 K
[AERONOMICA-ACTA-A-331-1988] N88-29907
Aeronomic problems of molecular oxygen photodissociation. Part 4: The various parameters for the Herzberg continuum
[AERONOMICA-ACTA-A-333-1988] N88-29955
PHOTOELECTRIC EFFECT
NBS (National Bureau of Standards) measurement services: The NBS photodetector spectral response calibration transfer program
[PB88-201595] N88-30109
PHOTOINTERPRETATION
The use of orbital remote sensing data for low cost ground-water survey
[INPE-4587-PRE/1318] N88-30170
Reflectance pattern and the physical and chemical characteristics of three Brazilian Oxisols
[INPE-4590-PRE/1320] N88-30172
PHOTOMAPPING
Integrating multispectral imagery and ground level hyperspectral signature data
[AD-A195976] N88-30166
PHOTOMETERS
Effect of interfacial phenomena on contact line heat Transfer-3
[AD-A194941] N88-29901

High frequency GaAlAs modulator and photodetector for phased array antenna applications
[NASA-TM-101328] N88-30048

PHOTONS
Intramolecular dynamics: A study of molecules at high levels of vibrational excitation
[AD-A195285] N88-30400

PHOTOTHERMAL CONVERSION
Noncontact photo-thermal sensing
[AD-A195450] N88-29905

PHYSIOLOGICAL RESPONSES
Central adrenergic receptors as mediators of central response to stress: Study with Positron Emission Tomography (PET)
[AD-A194947] N88-30284

PHYSIOLOGY
Comparison of morning with afternoon nitrogen elimination in resting subjects breathing 100 percent oxygen
[AD-A196191] N88-30282

PIEZOELECTRIC CERAMICS
Piezoelectric and electrostrictive materials for transducer applications, volume 3
[AD-A194949] N88-30112

PIEZOELECTRIC CRYSTALS
A dynamic analysis of piezoelectric strained elements
[AD-A196079] N88-30430

PIEZOELECTRICITY
Piezoelectric and electrostrictive materials for transducer applications, volume 1
[AD-A194957] N88-30096
Piezoelectric and electrostrictive materials for transducer applications, volume 2
[AD-A194956] N88-30104
Piezoelectric and electrostrictive materials for transducer applications, volume 3
[AD-A194949] N88-30112

PILOT PERFORMANCE
Advances in Flying Qualities
[AGARD-LS-157] N88-29735
Pilot modeling N88-29736
Pilot modeling applications N88-29737
Low-speed longitudinal flying qualities of modern transport aircraft N88-29738
The optimal control pilot model and applications N88-29741
Threat expert system technology advisor
[NASA-CR-177479] N88-29816
Prediction and measurement of human pilot dynamic characteristics in a manned rotorcraft simulation
[NASA-CR-183246] N88-30297

PILOT TRAINING
Controlled degradation of resolution of high-quality flight simulator images for training effectiveness evaluation
[AD-A196189] N88-29823

PIPE FLOW
Laser Doppler Velocimeter (LDV) and pressure measurements of gas particle flows in bends
[VKI-TN-163] N88-30083

PIPES (TUBES)
Analytical study of graphite-epoxy tube response to thermal loads
[NASA-CR-183215] N88-29884

PIXELS
Image focusing in space and time
[AD-A195839] N88-30410

PLANAR STRUCTURES
Development of a general software package for the analysis and synthesis of planar antenna arrays for space applications
[S-247-02] N88-30000
Advanced planar array development for space station
[NASA-CR-179373] N88-30181
Particle trajectories and potentials in a plane sheath moving in a magnetoplasma
[AD-A196228] N88-30190
Computer-Aided Structural Engineering (CASE) project. Computer program for analysis of planar grid structures (CGRID), user's guide
[AD-A195977] N88-30317

PLANE WAVES
Time-domain far-field scattering of plane electromagnetic waves by a penetrable object in the Born approximation
[PB87-176129] N88-30040
Mathematical problems of nonlinear wave propagation and of waves in heterogeneous media
[AD-A195970] N88-30057

PLANETARY ATMOSPHERES
Workshop on the Origins of Solar Systems
[NASA-CR-183025] N88-30536
The atmospheres of the earth and the other planets: Origin, evolution and composition N88-30544

PLANETARY COMPOSITION
Growth of continental crust: Clues from Nd isotopes and Nb-Th relationships in mantle-derived magmas N88-30205
The Kerala Khondalite Belt (KKB) of Southern India: An ensialic mobile belt N88-30208
Does subduction zone magmatism produce average continental crust N88-30214

PLANETARY CRUSTS
Growth of planetary crusts N88-30247
Debris flows of the Simud-Tiu outflow system of Mars N88-30485

PLANETARY EVOLUTION
Workshop on the Growth of Continental Crust
[NASA-CR-183073] N88-30201
Nd isotopes and crustal growth rate N88-30203
An illustration of the complexity of continent formation N88-30207
The Kerala Khondalite Belt (KKB) of Southern India: An ensialic mobile belt N88-30208
The timing and mechanism of depletion in Lewisian granulites N88-30209
Construction of mass-age curves for the continental crust: An empirical model and an example from the western US N88-30213
Pb isotope constaints on the extent of crustal recycling into a steady state mantle N88-30215
Decoupled Rb-Sr and Sm-Nd isotopic evolution of the continental crust N88-30216
Early intense cratering: Effects on growth of earth's crust N88-30219
The growth of continents and some consequences since 1.5 Ga N88-30220
Growth of early archaean crust in the ancient Gneiss complex of Swaziland and adjacent Barberton Greenstone Belt, Southern Africa N88-30223
Diapirs of the Mediterranean ridge: The tectonic regime of an incipient accreted terrane N88-30224
Changing styles of crustal growth in Southern Africa: Constraints from geochemical and Sr-Nd isotope studies in Archaean to Pan African terrains N88-30227
Growth of the continental crust: A planetary-mantle perspective N88-30251
Exotic minerals in 3,500 million year old rocks: Evidence for large meteorite impacts N88-30475
Lewis Cliff 86010, a unique Antarctic meteorite: Possible new clues to the early history of the solar system N88-30482
Workshop on the Origins of Solar Systems
[NASA-CR-183025] N88-30536
Physical processes and timescales in planet and small-body accretion N88-30540
Terrestrial versus giant planet formation N88-30543
The atmospheres of the earth and the other planets: Origin, evolution and composition N88-30544

PLANETARY MASS
Construction of mass-age curves for the continental crust: An empirical model and an exarnple from the western US N88-30213
The growth of continents and some consequences since 1.5 Ga N88-30220

PLANETARY WAVES
Rossby waves in mid-latitude oceans N88-30273

PLANNING
Lisp Object State Saver (LOSS): A facility used to save partial schedules of the Hubble Space Telescope N88-30360
Research on problem-solving systems
[AD-A195154] N88-30370

PLASMA ARC WELDING
ARC length control for plasma welding
[NASA-CASE-MSC-20900-1] N88-30131

PLASMA CURRENTS
RFP (Revised Field Pinch) plasma experiment at INPE
[INPE-4613-PRE/1336] N88-30420

PLASMA DENSITY
Consideration of plasma opening switches from a wave propagation perspective
[AD-A195681] N88-30421

PLASMA DIAGNOSTICS
Ionospheric radio and propagation: Waves in plasmas N88-30030

PLASMA DIFFUSION
Consideration of plasma opening switches from a wave propagation perspective
[AD-A195681] N88-30421

PLASMA DRIFT
Vortex formation and particle transport in a cross-field plasma sheath
[AD-A194838] N88-30425

PLASMA DYNAMICS
Characteristics of solitary waves and weak double layers in the magnetospheric plasma
[IRF-PREPRINT-105] N88-30418
Consideration of plasma opening switches from a wave propagation perspective
[AD-A195681] N88-30421

PLASMA ELECTRODES
Pierce diode with external circuit. Part 3: Chaotic behavior
[AD-A194837] N88-30041

PLASMA ENGINES
Unified study of plasma/surface interactions for space power and propulsion
[AD-A195971] N88-29870

PLASMA GENERATORS
Bibliography of Soviet laser developments, number 88, March - April 1987
[AD-A195978] N88-30116

PLASMA HEATING
Theoretical modeling of accelerating arc plasmas
[AD-A195606] N88-30426

PLASMA JETS
Theoretical modeling of accelerating arc plasmas
[AD-A195606] N88-30426

PLASMA LAYERS
Characteristics of solitary waves and weak double layers in the magnetospheric plasma
[IRF-PREPRINT-105] N88-30418

PLASMA PHYSICS
Pierce diode with external circuit. Part 3: Chaotic behavior
[AD-A194837] N88-30041
Bibliography of Soviet laser developments, number 88, March - April 1987
[AD-A195978] N88-30116

PLASMA PROPULSION
Performance and lifetime assessment of MPD arc thruster technology
[NASA-TM-101293] N88-29860

PLASMA RESONANCE
Role of ordinary to extraordinary mode wave coupling in ionospheric heating experiments
[AD-A195335] N88-30017

PLASMA SHEATHS
Vortex formation and particle transport in a cross-field plasma sheath
[AD-A194838] N88-30425

PLASMA TEMPERATURE
Energy conversion measurements in laser-sustained argon plasmas for application to rocket propulsion
[AD-A194931] N88-29861

PLASMA WAVES
Ionospheric radio and propagation: Waves in plasmas N88-30030
Characteristics of solitary waves and weak double layers in the magnetospheric plasma
[IRF-PREPRINT-105] N88-30418
Reconstruction of wave distribution functions in warm plasmas
[IRF-PREPRINT-104] N88-30422

PLASMA-ELECTROMAGNETIC INTERACTION
Influence of plasma parameters on VLF radiation in near-rocket region N88-30518

PLASMAS (PHYSICS)
Millimeter wave generation by relativistic electron beams
[AD-A195683] N88-30016
Autoionization for lower level detrapping in X-ray lasers
[AD-A195845] N88-30123
Particle trajectories and potentials in a plane sheath moving in a magnetoplasma
[AD-A196228] N88-30190
Ion kinetics in silane plasmas
[AD-A196202] N88-30423
Ring current role in dynamics of fluctuating electron and ion fluxes in low-latitude magnetosphere N88-30514
Plasma of earth's magnetosphere ring currents. Model compared with results of AMPTE/CCE experiment N88-30515

PLASTIC AIRCRAFT STRUCTURES
Investigations on the modification of structural reliability by substitution of aluminum by carbon fiber reinforced plastics in aircraft construction
[ILR-MITT-195] N88-29877

PLASTIC DEFORMATION
Anisotropic constitutive modeling for nickel-base single crystal superalloys
[NASA-CR-182157] N88-29961
State variable approach to deformation phenomena in Face Centered Cubic (FCC) metals
[VTT-44] N88-29964
Response of SMA (Shielded Metal Arc) and narrow gap HY80 weldments to explosive shock loading
[AD-A195994] N88-30162

PLASTICIZERS
Reactive plasticizers in negative E-beam resists
[AD-A195161] N88-30056

PLATEAUS
The tectonic setting of the Seychelles, Mascarene and Amirante Plateaus in the Western Equatorial Indian Ocean N88-30225
PLATES (TECTONICS)
The tectonic setting of the Seychelles, Mascarene and Amirante Plateaus in the Western Equatorial Indian Ocean N88-30225
Ridge-trench collision in Archean and Post-Archean crustal growth: Evidence from southern Chile N88-30233
Continental growth through time by underplating of subducted oceanic crust: Evidence from kimberlites in South Africa and SW Pacific N88-30244
Gravity anomalies, plate tectonics and the lateral growth of Precambrian North America N88-30248
Solid earth as a recycling systems and the lateral growth of Precambrian North America N88-30249
Crustal underplating in the North American Craton: Evidence from the Petrogenesis of anorthositic rocks in the Middle Proterozoic Midcontinent Rift System N88-30252
PLATINUM
The effect of oriented defects on long-range ordering of hydrocarbon films: Azulene on Pt(111)
[AD-A196089] N88-29904
PLATINUM ISOTOPES
Experimental and theoretical investigations of isotope shift and hyperfine structure on 5d elements (especially platinum, iridium and rhenium)
[ETN-88-93121] N88-29957
PLOTTING
Implementation of the NCAR (National Centre for Atmospheric Research) graphics package at ARL (Aeronautical Research Laboratory)
[AD-A195163] N88-30193
PLUMES
Automatic data retrieval from rocket motor holograms
[AD-A195586] N88-29864
Experimental evaluation of resistojet thruster plume shields
[NASA-TM-101363] N88-29868
PNEUMATIC EQUIPMENT
JUH-1H redesigned pneumatic boot deicing system flight test evaluation
[AD-A194918] N88-29785
Analysis of a feed device for the pneumatic transport of noncohesive particles
[VKI-TM-44] N88-30062
PNEUMATICS
Analysis of a feed device for the pneumatic transport of noncohesive particles
[VKI-TM-44] N88-30062
Laser Doppler Velocimeter (LDV) and pressure measurements of gas particle flows in bends
[VKI-TN-163] N88-30063
POINTS (MATHEMATICS)
On the Nash point equilibria in the calculus of variations
[AD-A194959] N88-30381
POLAR REGIONS
The effect of equatorial ionospheric irregularities on the performance of a south-looking OTH-B (Over-The-Horizon-Backscatter) radar
[AD-A195080] N88-30018
MIZEX (marginal ice zone experiment) 1987 SAR (Synthetic Aperture Radar) data summary
[AD-A195560] N88-30035
POLARIZATION
Determining the spatial structure of fields of precipitation from space radar images in two orthogonal polarizations N88-30531
POLARIZATION (CHARGE SEPARATION)
An electrochemical impedance spectroscopy study of reactions at the metal/coating interface N88-29975
POLITICS
Political and economic barriers to information transfer N88-30460
POLYETHYLENES
Morphological changes in polymer electrolyte cells
[AD-A195821] N88-30054
POLYMER CHEMISTRY
Prediction of degradation of polymeric coating materials N88-29970
Novel ladder polymers for use as high temperature stable resins or coatings
[NASA-CASE-LEW-14203-1] N88-29984
POLYMER PHYSICS
Storing bits on a DNA polymer chain
[AD-A195701] N88-29981
POLYMERIC FILMS
Performance Prediction for Coatings. Proceedings of a Workshop
[AD-A188973] N88-29966
Electrochemical evaluation of the long term corrosion resistance of polymer coated steel N88-29974
An electrochemical impedance spectroscopy study of reactions at the metal/coating interface N88-29975
A review of melt and vapor growth techniques for polydiacetylene thin films for nonlinear optical applications
[NASA-TM-100340] N88-30412
POLYMERIZATION
Novel ladder polymers for use as high temperature stable resins or coatings
[NASA-CASE-LEW-14203-1] N88-29984
A review of melt and vapor growth techniques for polydiacetylene thin films for nonlinear optical applications
[NASA-TM-100340] N88-30412
POROUS WALLS
Radiative heat transfer to steady flow of a chemically reacting fluid in a horizontal porous channel with variable wall temperature
[DE88-702704] N88-30081
POSITION (LOCATION)
DATATRAN: Datum transformation software
[AD-A195723] N88-30175
Passive microwave measurements of water vapor fields and rain for locating fronts in cyclonic storms
[AD-A195632] N88-30267
Adaptive control in positioning a rigid-flexible robot arm
[AD-A195194] N88-30387
Utilizing dynamic stability of orient parts
[AD-A195730] N88-30397
Study of modern instrumentation and methods for astronomic positioning in the field
[AD-A196173] N88-30548
POSITION SENSING
Path planning and path following for the Amsterdam autonomous cart
[FVI-86-22] N88-30133
POSITIONING
Study of modern instrumentation and methods for astronomic positioning in the field
[AD-A196173] N88-30548
POSITRONS
Positron emission tomography: A new technique for observing fluid behavior in engineering systems
[PNR90471] N88-30091
POTENTIAL ENERGY
Computed potential energy surfaces for chemical reactions
[NASA-CR-183168] N88-29893
POWER CONDITIONING
The dc power control for a liquid-fed resistojet
[NASA-TM-101326] N88-29869
POWER SERIES
An improved spherical earth diffraction algorithm for SEKE
[AD-A195847] N88-30005
POWER SPECTRA
Matching P.S.D.: Design loads N88-29720
Performance of DS/SSMA communications in impulsive channels. Part 1: Correlation receivers
[AD-A195712] N88-30021
Vibrational power flow analysis of rods and beams
[NASA-CR-183166] N88-30151
PRE-MAIN SEQUENCE STARS
Radio and infrared properties of young stars
[NASA-CR-183252] N88-30579
PRECAMBRIAN PERIOD
Metamorphic P-T paths and Precambrian crustal growth in East Antarctica N88-30218
PRECIPITATION (METEOROLOGY)
Determining the spatial structure of fields of precipitation from space radar images in two orthogonal polarizations N88-30531
PREDICTION ANALYSIS TECHNIQUES
Special Course on Missile Aerodynamics
[AGARD-R-754] N88-29755
Accuracy criteria for evaluating supersonic aerodynamic coefficient predictions N88-29756
Survey on nonlinear effects N88-29757
Prediction of base-flows N88-29765
Next generation missile design N88-29768
A new computational capability for ramjet projectiles
[AD-A196061] N88-29812
Three-dimensional combustor predictors: A comparison of equilibrium and laminar flamelet chemistry models N88-29940
Preliminary investigation of flow modeling during solid propellant processing
[AD-A196168] N88-29987
PREDICTIONS
Prediction of degradation of polymeric coating materials N88-29970
A reliability-based program for predicting the service life of organic coating systems N88-29971
Predicting the durability of adhesives and coatings by remote detection of hidden defects and coating-thickness irregularities: A theoretical and numerical study N88-29972
Contributions to engineering models of human-computer interaction, volume 1
[AD-A195590] N88-30295
PREMIXED FLAMES
The influence of pressure on soot formation N88-29934
Flamelet modeling of turbulent premixed flames N88-29942
Modeling the stability of a turbulent premixed flame, downstream from a step by a Lagrangian method N88-29943
Numerical modelling of premixed flames in gaseous media N88-29944
Gaseous premixed flames in non-uniform flows N88-29945
Optical measurements of soot and temperature profiles in premixed propane-oxygen flames
[NASA-TM-101343] N88-29997
Optical measurements of soot in premixed flames
[NASA-TM-101305] N88-30090
PRESSURE
Determination of the specific area of liquid gas and the velocity of weak pressure waves in aqueous foams
[NASA-TT-20347] N88-30087
PRESSURE DISTRIBUTION
Pressure distributions from subsonic tests of an advanced laminar-flow-control wing with leading- and trailing-edge flaps
[NASA-TM-4040-PT-2] N88-29776
An experimental study of an adaptive-wall wind tunnel
[NASA-CR-183152] N88-29821
The effects of incoming boundary layer thickness on unsteady shock-induced turbulent separations induced by cylinders
[AD-A196190] N88-30060
Studies on pressure response of gas bubbles contributions of condensed droplets in bubbles generated by a uniform nucleation
[NASA-TT-20343] N88-30068
PRESSURE EFFECTS
Comparison of the performance of a reverse flow annular combustion chamber under low and high pressure conditions N88-29923
PRESSURE GRADIENTS
Experimental and analytical study of two-phase flow in zero gravity
[AD-A195223] N88-29993
PRESSURE ICE
MIZEX (marginal ice zone experiment) 1987 SAR (Synthetic Aperture Radar) data summary
[AD-A195560] N88-30035
PRESSURE MEASUREMENT
Laser Doppler Velocimeter (LDV) and pressure measurements of gas particle flows in bends
[VKI-TN-163] N88-30063
PRESSURE PULSES
Transient interaction of electromagnetic pulses in dielectrics and microwave biophysics
[AD-A195687] N88-30008
PRESTRESSING
Free vibration of rectangular plates with a small initial curvature
[NASA-CR-179370] N88-30148
PRIMARY COSMIC RAYS
Charge composition of primary cosmic ray nuclei with z greater than or equal to 2 in energy region greater than or equal to 2 TeV N88-30519
PRIMERS (COATINGS)
Primerless RTV silicones
[BDX-613-3807] N88-29980
PROBABILITY THEORY
Fatigue crack propagation: Probabilistic modeling and statistical analysis
[AD-A195885] N88-30155
Venture theory: A model of decision weights
[AD-A194809] N88-30391
PROBLEM SOLVING
Reducing the parallel solution time of sparse circuit matrices using reordered Gaussian elimination and relaxation
[AD-A195152] N88-30045
MOORE: A prototype expert system for diagnosing spacecraft problems N88-30343
Research on problem-solving systems
[AD-A195154] N88-30370
Multiple solutions and bifurcation for a class of nonlinear Sturm-Liouville eigenvalue problems on an unbounded domain
[AD-A195954] N88-30389
Barriers to Information Transfer and Approaches Toward Their Reduction
[AGARD-CP-430] N88-30458

Linguistic barriers: Translation problems N88-30465
Formulation and solution of economic equilibrium problems
[AD-A196034] N88-30470

PROCESS CONTROL (INDUSTRY)
Preliminary investigation of flow modeling during solid propellant processing
[AD-A196168] N88-29987

PROCUREMENT POLICY
The cost and performance implications of reliability improvements in the F-16A/B
[AD-A195096] N88-29796

PROFILES
Possibilities of determining vertical profiles of microphysical characteristics of stratospheric aerosol using space measurements of transparency and solar halo N88-30526
Estimation of soil temperature profile from remote microwave and IR measurements N88-30532

PROGNOZ SATELLITES
Measurement of galactic radio emission at frequency 37 GHz from aboard spacecraft N88-30520

PROGRAM VERIFICATION (COMPUTERS)
Verification and validation of rulebased systems for Hubble Space Telescope ground support N88-30361

PROGRAMMING LANGUAGES
Conversion of productions in OPS5 to their equivalent English
[ORNL/TM-10246] N88-30306
Syntactic closures
[AD-A195921] N88-30311
Scheme86: A system for interpreting SCHEME
[AD-A195931] N88-30319
Reification without evaluation
[AD-A195928] N88-30326

PROJECT MANAGEMENT
Activities report of the World Meteorological Organization
[WMO-689] N88-30265

PROJECTILES
Computational aerodynamic analysis for a range-limited 25mm training round
[AD-A185270] N88-29772
A new computational capability for ramjet projectiles
[AD-A196061] N88-29812
Numerical calculations of the response of a spinning spheroidal payload to coning motion
[AD-A195890] N88-30059

PROLOG (PROGRAMMING LANGUAGE)
Conversion of productions in OPS5 to their equivalent English
[ORNL/TM-10246] N88-30306

PROP-FAN TECHNOLOGY
Euler analysis of a swirl recovery vane design for use with an advanced single-rotation propfan
[NASA-TM-101357] N88-29771

PROPAGATION VELOCITY
Determination of the specific area of liquid gas and the velocity of weak pressure waves in aqueous foams
[NASA-TT-20347] N88-30087

PROPELLANT BINDERS
Thermomechanical computations for GAP, a high energy binder for composite propellants
[FOA-C-20718-2.1] N88-29988

PROPELLANT COMBUSTION
Ignition and extinguishing of a Solid Fuel Ramjet (SOFRAM)
[FOA-C-20713-2.1] N88-29865
Combustion diagnostics of propellant with new grain geometries
[AD-A194944] N88-29895
Gas phase combustion chemistry of nitramine propellants
[AD-A195082] N88-29902

PROPELLANT DECOMPOSITION
Gas phase combustion chemistry of nitramine propellants
[AD-A195082] N88-29902

PROPELLANT GRAINS
Combustion diagnostics of propellant with new grain geometries
[AD-A194944] N88-29895
Flamespreading processes in obliquely loaded stick propellant beds
[AD-A195081] N88-29956
Descriptive characterization of propellant particles
[AD-A195176] N88-29985

PROPELLANT PROPERTIES
Fuel property effects on the US Navy's TF30 engine N88-29911
Alternative fuel spray behavior N88-29912
The characterizatin of combustion by fuel composition: Measurements in a small conventional combustor N88-29920

PROPELLANT TRANSFER
Design and development of a refueling test bed
[FTMS-RP-ER-011] N88-29986

PROPELLANTS
Lunar lander conceptual design: Lunar base systems study task 2.2
[NASA-CR-172051] N88-29854
Energy conversion measurements in laser-sustained argon plasmas for application to rocket propulsion
[AD-A194931] N88-29861
Titrimetric analysis of HAN-based liquid propellants
[AD-A196225] N88-29990

PROPELLER EFFICIENCY
Aircraft noise prediction program propeller analysis system IBM-PC version user's manual version 2.0
[NASA-CR-181689] N88-30399

PROPELLER FANS
Aeroelastic response of metallic and composite propfan models in yawed flow
[NASA-TM-100964] N88-29807

PROPELLERS
Euler analysis of a swirl recovery vane design for use with an advanced single-rotation propfan
[NASA-TM-101357] N88-29771

PROPULSION
Special Course on Missile Aerodynamics
[AGARD-R-754] N88-29755
Energy conversion measurements in laser-sustained argon plasmas for application to rocket propulsion
[AD-A194931] N88-29861

PROPULSION SYSTEM CONFIGURATIONS
Evaluation of the advanced air breathing propulsion concepts, executive summary
[ESA-CR(P)-2540] N88-29802
Evaluation of advanced air breathing concepts. Volume 1: Executive summary
[ESA-CR(P)-2539] N88-29806
Spacecraft mass estimation, relationships and engine data: Task 1.1 of the lunar base systems study
[NASA-CR-172061] N88-29836
The NASA Electric Propulsion Program
[NASA-TM-101324] N88-29859
Hermes: Study of propulsion system for reusable man-rated spacecraft
[PSRM-TN-0000-00-04A] N88-29866
Unified study of plasma/surface interactions for space power and propulsion
[AD-A195971] N88-29870

PROPULSION SYSTEM PERFORMANCE
Evaluation of the advanced air breathing propulsion concepts, executive summary
[ESA-CR(P)-2540] N88-29802
Evaluation of advanced air breathing concepts. Volume 1: Executive summary
[ESA-CR(P)-2539] N88-29806
Hermes: Study of propulsion system for reusable man-rated spacecraft
[PSRM-TN-0000-00-04A] N88-29866
Unified study of plasma/surface interactions for space power and propulsion
[AD-A195971] N88-29870
Simulation of Vulcain engine operation at low inlet pressure
[ETN-88-93083] N88-29875

PROTECTIVE CLOTHING
Four-axis side-arm flight control simulator investigation
[AD-A196026] N88-30294

PROTECTIVE COATINGS
Processing technology research in composites
[AD-A195693] N88-29890
Performance Prediction for Coatings. Proceedings of a Workshop
[AD-A188973] N88-29966
Degradation of protective coatings on steel in corrosive environments N88-29969
Prediction of degradation of polymeric coating materials N88-29970
A reliability-based program for predicting the service life of organic coating systems N88-29971
Electrical detection of coating deterioration N88-29973
Electrochemical evaluation of the long term corrosion resistance of polymer coated steel N88-29974
Evaluation of organic coating deterioration and substrate corrosion in seawater using electrochemical impedance measurements N88-29976
Alternative immersion accelerated testing of coating systems for Naval shoreline facilities N88-29977
Stressed fabric abrasion test procedure for urethane coated fabric fuel tanks
[AD-A196327] N88-29982

PROTOCOL (COMPUTERS)
Performance analysis of FDDI
[NASA-CR-183206] N88-30321

PROTON IRRADIATION
Heavy ion and proton tests for subsystem upset
[AD-A195267] N88-30442

PROTOSTARS
Star formation and molecular clouds N88-30537

PROTOTYPES
Contingency rescheduling of spacecraft operations N88-30337
Achieving real-time performance in FIESTA N88-30344

PROVING
Confirmation of slow-waves in a crosstie overlay coplanar waveguide and its application to band-reject gratings and reflectors
[AD-A194981] N88-30011

PSYCHOLOGY
Comparison of morning with afternoon nitrogen elimination in resting subjects breathing 100 percent oxygen
[AD-A196191] N88-30282
Advancement of latent trait theory
[AD-A194302] N88-30289

PSYCHOPHYSIOLOGY
Comparative aspects of multiple processes of attention
[AD-A195805] N88-30291

PULSE COMMUNICATION
Signals and systems N88-30026

PUSHBROOM SENSOR MODES
Imaging instrument of the vegetation payload (SPOT 4)
[SNIAS-881-440-107] N88-30169

PYLONS
Compression pylon
[NASA-CASE-LAR-13777-1] N88-29789

PYROLYSIS
Determination of relative flammability of materials by pyrolysis and gas-chromatographic light hydrocarbon analysis
[DE88-012449] N88-29898
The influence of pressure on soot formation N88-29934

PYROMETERS
Principles of the optical differential thermal analysis
[AD-A195951] N88-30408

Q

QUALITY
An analysis of lateral-directional handling qualities and Eigenstructure of high performance aircraft
[AD-A194874] N88-29814

QUALITY CONTROL
Quality measures and assurance for AI (Artificial Intelligence) software
[NASA-CR-4187] N88-30304

QUANTITATIVE ANALYSIS
A method for the quantitative determination of crystalline phases by X-ray
[NASA-TT-20324] N88-30444

QUANTUM CHEMISTRY
Gas phase combustion chemistry of nitramine propellants
[AD-A195082] N88-29902

QUANTUM ELECTRONICS
Spectroscopic studies with multiple quantum well materials with applications to optical signal processing at room temperature
[AD-A194171] N88-30409

QUANTUM WELLS
Spectroscopic studies with multiple quantum well materials with applications to optical signal processing at room temperature
[AD-A194171] N88-30409

QUEUEING THEORY
Performance prediction of concurrent systems
[NASA-CR-183175] N88-30312

R

RADAR
Scattering impulse response synthesis using random noise illumination: Initial concept evaluation
[AD-A195086] N88-30034
Microwave remote sensing at INPE (Institute for Space Research) Brazil: Concepts and future prospects of soil moisture studies
[INPE-4589-PRE/1310] N88-30178
The surface evaporative duct height product: An evaluation
[AD-A195918] N88-30199
Validate algorithms for the determination of rainfall rates from SSM/I microwave satellite imagery
[AD-A195428] N88-30270

RADAR ABSORBERS
The Soviet Stealth fighter: Check or checkmate
[AD-A195200] N88-29791
RADAR BEAMS
Utilization of a single clear-air Doppler radar beam to measure vertical divergence
[AD-A195543] N88-30271
RADAR CROSS SECTIONS
Comparative analysis of passive communications satellites employing the SHF and HF spectrum for use in a strategic role
[AD-A194682] N88-30019
Measurement and interpretation of North Atlantic Ocean marine radar sea scatter
[AD-A196239] N88-30036
Analysis of environmental parameters from the Panama City tower radar experiment
[AD-A194994] N88-30264
RADAR DATA
A study of the feasibility of using sea and wind information from the ERS-1 satellite. Part 1: Wind scatterometer data
[NASA-CR-182833] N88-30167
A study of the feasibility of using sea and wind information from the ERS-1 satellite. Part 2: Use of scatterometer and altimeter data in wave modeling and assimilation
[ESA-CR(P)-2604-PT-2] N88-30176
RADAR DETECTION
On adaptive cell-averaging CFAR (Constant False-Alarm Rate) radar signal detection
[AD-A196286] N88-30009
Modeling and performance of HF/OTH (High-Frequency/Over-the-Horizon) radar target identification systems
[AD-A196287] N88-30038
The surface evaporative duct height product: An evaluation
[AD-A195918] N88-30199
RADAR ECHOES
Measurement and interpretation of North Atlantic Ocean marine radar sea scatter
[AD-A196239] N88-30036
RADAR IMAGERY
Acoustooptic processing of two-dimensional signals using temporal and spatial integration
[AD-A194803] N88-29999
Corner extraction from radar images
[AD-A194857] N88-30020
MIZEX (marginal ice zone experiment) 1987 SAR (Synthetic Aperture Radar) data summary
[AD-A195560] N88-30035
Range data description based on multiple characteristics N88-30351
High-resolution (30 m) lunar radar images N88-30486
Determining the spatial structure of fields of precipitation from space radar images in two orthogonal polarizations N88-30531
RADAR SCATTERING
Measurement and interpretation of North Atlantic Ocean marine radar sea scatter
[AD-A196239] N88-30036
RADAR SIGNATURES
The Soviet Stealth fighter: Check or checkmate
[AD-A195200] N88-29791
RADAR TARGETS
Evaluation of LISBON TAR SSR radar
[EEC/NOTE-5/87] N88-30015
Modeling and performance of HF/OTH (High-Frequency/Over-the-Horizon) radar target identification systems
[AD-A196287] N88-30038
RADAR TRACKING
Track performance considerations for monopulse radars
[AD-A196232] N88-30007
MIZEX (marginal ice zone experiment) 1987 SAR (Synthetic Aperture Radar) data summary
[AD-A195560] N88-30035
Modeling and performance of HF/OTH (High-Frequency/Over-the-Horizon) radar target identification systems
[AD-A196287] N88-30038
RADAR TRANSMITTERS
Evaluation of LISBON TAR SSR radar
[EEC/NOTE-5/87] N88-30015
RADIAL VELOCITY
Radial velocity measurements of a sample of northern metal-deficient stars
[SER-C-PREPUBL-FASC-25] N88-30564
RADIATION DAMAGE
Heavy ion and proton tests for subsystem upset
[AD-A195267] N88-30442
RADIATION HARDENING
EMPTAC (Electromagnetic Pulse Test Aircraft) user's guide
[AD-A195072] N88-30006
RADIATIVE HEAT TRANSFER
Flamelet chemistry modelling of soot formation for radiation N88-29928
Radiation transfer in gas turbine combustors N88-29929
The effect of particle properties on radiative heat transfer N88-29941
Radiative heat transfer to steady flow of a chemically reacting fluid in a horizontal porous channel with variable wall temperature
[DE88-702704] N88-30061
RADIATIVE LIFETIME
Computed potential energy surfaces for chemical reactions
[NASA-CR-183168] N88-29893
RADIO ALTIMETERS
Development of procedures for performing end-to-end tests on the ERS-1 radar altimeter and AMI using a compact antenna test range — Active Microwave Instrument (AMI)
[ESA-CR(P)-2558] N88-30022
RADIO ANTENNAS
Radio astronomy N88-30031
RADIO ASTRONOMY
Review of Radio Science, 1984-1986 N88-30023
Radio astronomy N88-30031
The Deep Space Network: An instrument for radio astronomy research
[NASA-CR-183219] N88-30554
RADIO COMMUNICATION
Wave propagation and remote sensing N88-30029
RADIO FREQUENCIES
Study of secondary emission properties of materials used for high power RF components in space
[ESA-CR(P)-2587] N88-30012
Electromagnetic noise and interference N88-30028
Radio and infrared properties of young stars
[NASA-CR-183252] N88-30579
RADIO FREQUENCY HEATING
Ionosonde studies of field-aligned irregularities during high-power HF heating at Arecibo
[AD-A195848] N88-30256
The study of hydromagnetic waves and RF heating using the TORTUS tokamak, the development of diagnostic techniques based on submillimeter lasers and the gyrotron, and gas discharge N88-30419
RADIO STARS
Radio astronomy N88-30031
RADIO TELESCOPES
Radio astronomy N88-30031
RADIO TRANSMITTERS
KOSPAS-SARSAT satellites used for ocean current study N88-30534
RADIOACTIVE DECAY
Evidence of the in situ decay of Al-26 in a Semarkona chondrule N88-30479
Lewis Cliff 86010, a unique Antarctic meteorite: Possible new clues to the early history of the solar system N88-30482
RADIOACTIVE ISOTOPES
The dynamics of transuranics and other radionuclides in natural environments, December 1985
[DE87-014456] N88-30189
RADIOGRAPHY
Development of graded reference radiographs for aluminum welds, phase 1
[AD-A195594] N88-30140
RADIOMETERS
NBS (National Bureau of Standards) measurement services: The NBS photodetector spectral response calibration transfer program
[PB88-201595] N88-30109
Atmospheric corrections for in-flight satellite radiometric calibration
[AD-A196124] N88-30194
Principles of the optical differential thermal analysis
[AD-A195951] N88-30408
RAILGUN ACCELERATORS
Theoretical modeling of accelerating arc plasmas
[AD-A195606] N88-30426
RAIN
Validate algorithms for the determination of rainfall rates from SSM/I microwave satellite imagery
[AD-A195428] N88-30270
RAINSTORMS
Passive microwave measurements of water vapor fields and rain for locating fronts in cyclonic storms
[AD-A195632] N88-30267
RAMJET ENGINES
Air intake aerodynamics N88-29762
Semiempirical methods for airbreathing missiles N88-29763
Evaluation of the advanced air breathing propulsion concepts, executive summary
[ESA-CR(P)-2540] N88-29802
Evaluation of advanced air breathing concepts. Volume 1: Executive summary
[ESA-CR(P)-2539] N88-29806
A new computational capability for ramjet projectiles
[AD-A196061] N88-29812
Review of research concerning Solid Fuel Ramjet (SOFRAM) at the Research Institute of National Defence (FOA) 2
[FOA-C-20714-2.1] N88-29813
Ignition and extinguishing of a Solid Fuel Ramjet (SOFRAM)
[FOA-C-20713-2.1] N88-29865
RANDOM ACCESS MEMORY
The effects of total dose on the SEU sensitivity of CMOS static RAMS — single event upset (SEU), satellite components
[AERE-R-12779] N88-30401
RANDOM NOISE
Scattering impulse response synthesis using random noise illumination: Initial concept evaluation
[AD-A195086] N88-30034
RANDOM NUMBERS
A study of the effect of random input motion on low Reynolds number flows
[AD-A195559] N88-29747
RANDOM VIBRATION
Analytical and experimental studies of beam waveguide absorbers for structural damping
[AD-A195085] N88-30144
RANGEFINDING
Range data description based on multiple characteristics N88-30351
RANKINE CYCLE
Study of toluene stability for an Organic Rankine Cycle (ORC) space-based power system
[NASA-CR-180884] N88-29863
Study of toluene rotary fluid management device and shear flow condenser performance for a space-based organic Rankine power system
[NASA-CR-180885] N88-29872
RARE GASES
Non-atmospheric noble gases from CO(sub 2) well ga N88-30476
Noble gases, C,N, and Si isotopes in interstellar SiC form the Murchison carbonaceous chondrite N88-30483
RATES (PER TIME)
Validate algorithms for the determination of rainfall rates from SSM/I microwave satellite imagery
[AD-A195428] N88-30270
RAY TRACING
Ionosonde studies of field-aligned irregularities during high-power HF heating at Arecibo
[AD-A195848] N88-30256
RAYLEIGH WAVES
Finite-difference simulations of Rayleigh-wave scattering by shallow heterogeneity
[AD-A194961] N88-30259
RDX
Discovery of a low temperature form of TAGN (Triaminoguanidinium Nitrate)
[AD-A196059] N88-29989
REACTION KINETICS
Experiments and modeling of multi-component fuel behavior in combustion
[AD-A195011] N88-29896
Flamelet modeling of turbulent premixed flames N88-29942
Cosmochemical trends of volatile elements in the solar system N88-30542
REACTIVITY
Active sites and roles of solid acid base catalysts
[NASA-TT-20333] N88-29909
Reactive plasticizers in negative E-beam resists
[AD-A195161] N88-30056
REAL TIME OPERATION
Intelligent fault diagnosis and failure management of flight control actuation systems
[NASA-CR-177481] N88-29790
MIZEX (marginal ice zone experiment) 1987 SAR (Synthetic Aperture Radar) data summary
[AD-A195560] N88-30035
Geometric modeling for computer aided design
[NASA-CR-183161] N88-30320
A static scheduler for the computer aided prototyping system: An implementation guide
[AD-A194340] N88-30322
Achieving real-time performance in FIESTA N88-30344
Mission telemetry system monitor: A real-time knowledge-based system N88-30345
Autonomous image data reduction by analysis and interpretation N88-30347

Automatic mathematical modeling for real time simulation system N88-30356
A standard architecture for controlling robots [AD-A195929] N88-30371
Applications of synchrotron radiation to materials science: Diffraction imaging (topography) and microradiography [NASA-CR-183265] N88-30440

RECEIVERS
On adaptive cell-averaging CFAR (Constant False-Alarm Rate) radar signal detection [AD-A196286] N88-30009
Performance of DS/SSMA communications in impulsive channels. Part 1: Correlation receivers [AD-A195712] N88-30021

RECOGNITION
Multilevel computational theory of stereoscopic visual image processing [AD-A195331] N88-30288
The combinatorics of object recognition in cluttered environments using constrained search [AD-A196224] N88-30364
Symbolic construction of a 2D scale-space image [AD-A195926] N88-30374

RECOMBINATION REACTIONS
Computed potential energy surfaces for chemical reactions [NASA-CR-183168] N88-29893
On formulating a simple D-region model [AD-A195841] N88-30197

RECORDING
Maximum-likelihood multichannel deconvolution of P waves at seismic arrays [AD-A194990] N88-30191

RECOVERABLE LAUNCH VEHICLES
Space shuttle phase B wind tunnel model and test information. Volume 3: Launch configuration [NASA-CR-178416-VOL-3-PT-2] N88-29744
Space shuttle phase B wind tunnel model and test information. Volume 1: Booster configuration [NASA-CR-178414-VOL-1-PT-1] N88-29745
Space shuttle phase B wind tunnel model and test information. Volume 1: Booster configuration [NASA-CR-178414-VOL-1-PT-2] N88-29770

RECTANGULAR PLATES
Free vibration of rectangular plates with a small initial curvature [NASA-CR-179370] N88-30148

RECYCLING
Evidence for crustal recycling during the Archean: The parental magmas of the stillwater complex N88-30225
Continental crustal formation and recycling: Evidence from oceanic basalts N88-30238
Solid earth as a recycling systems and the lateral growth of Precambrian North America N88-30249

RED SHIFT
A deep redshift survey of field galaxies. Comments on the reality of the Butcher-Oemler effect [NASA-CR-183255] N88-30558

REDUCED GRAVITY
Experimental and analytical study of two-phase flow in zero gravity [AD-A195223] N88-29993
Containment of a silicone fluid free surface in reduced gravity using barrier coatings [NASA-TM-101314] N88-30072

REDUNDANCY
Investigations on the modification of structural reliability by substitution of aluminum by carbon fiber reinforced plastics in aircraft construction [ILR-MITT-195] N88-29877

REFERENCE STARS
Astron observations of supernova 1987A in large magellanic cloud N88-30504
The guide star catalog [NASA-CR-183253] N88-30547

REFLECTANCE
The effect of the near earth micrometeoroid environment on a highly reflective mirror surface [NASA-TM-101307] N88-29833
Electromagnetic metrology N88-30024
TM/LANDSAT-5 data to evaluate wheat and bean percent soil cover and leaf area index [INPE-4609-PRE/1332] N88-30165
Reflectance pattern and the physical and chemical characteristics of three Brazilian Oxisols [INPE-4590-PRE/1320] N88-30172
Study of the spectral response of soybeans [INPE-4592-PRE/1322] N88-30174
Deep seismic reflection profiling and continental growth curves N88-30222
Physical properties of surface materials on Martian volcanoes: Dust-covered lava and ash N88-30493

REFLECTORS
Confirmation of slow-waves in a crosstie overlay coplanar waveguide and its application to band-reject gratings and reflectors [AD-A194981] N88-30011

REFRACTIVITY
Monte-Carlo estimation of the influence of plant architecture parameters on spectral brightness N88-30533

REFUELING
Technology requirements for an orbiting fuel depot: A necessary element of a space infrastructure [NASA-TM-101370] N88-29845
Design and development of a refueling test bed [FTMS-RP-ER-011] N88-29986

REGENERATIVE FUEL CELLS
Regenerative fuel cell energy storage system for a low earth orbit space station [NASA-CR-174802] N88-30184

REGULARITY
Regularity and numerical solution of eigenvalue problems with piecewise analytic data [AD-A194993] N88-30387

REGULATIONS
The OFP (Operational Flight Program) update cycle needs you [AD-A194910] N88-29798

REINFORCING FIBERS
A study of the critical factors controlling the synthesis of ceramic matrix composites from preceramic polymers [AD-A195405] N88-29881
Some theoretical considerations of the surface tension of liquid metals for metal matrix composites [AD-A195999] N88-29882

RELATIVISTIC ELECTRON BEAMS
Millimeter wave generation by relativistic electron beams [AD-A195683] N88-30016
Research on a two-stage free electron laser oscillator [AD-A195991] N88-30115

RELIABILITY
The cost and performance implications of reliability improvements in the F-16A/B [AD-A195096] N88-29796
A reliability-based program for predicting the service life of organic coating systems N88-29971

RELIABILITY ANALYSIS
Investigations on the modification of structural reliability by substitution of aluminum by carbon fiber reinforced plastics in aircraft construction [ILR-MITT-195] N88-29877

RELIABILITY ENGINEERING
Intelligent fault diagnosis and failure management of flight control actuation systems [NASA-CR-177481] N88-29790

REMOTE MANIPULATOR SYSTEM
Study of software requirements and artificial intelligence techniques for robotics [TL-3333] N88-30365

REMOTE SENSING
Wave propagation and remote sensing N88-30029
Microwave remote sensing in the French industries [ETN-88-93081] N88-30171
Structure of eastern Turkestan Ridge based on space photographs N88-30530
Estimation of soil temperature profile from remote microwave and IR measurements N88-30532

REMOTE SENSORS
Development of procedures for performing end-to-end tests on the ERS-1 radar altimeter and AMI using a compact antenna test range — Active Microwave Instrument (AMI) [ESA-CR(P)-2558] N88-30022

REMOTELY PILOTED VEHICLES
Development and design of windtunnel and test facility for RPV (Remote Piloted Vehicle) enhancement devices [AD-A194842] N88-29822

REQUIREMENTS
Centralized class A flight mishap investigation [AD-A194397] N88-29786
Long haul communications in the HF spectrum utilizing high speed modems [AD-A194683] N88-30003
Achieving real-time performance in FIESTA N88-30344

RESCUE OPERATIONS
KOSPAS-SARSAT satellites used for ocean current study N88-30534

RESEARCH
Vanderbilt free electron laser project in biomedical and materials research [AD-A195981] N88-30121
Center for opto-electronic systems research [AD-A195159] N88-30411

RESEARCH AIRCRAFT
The NAE atmospheric research aircraft N88-29730

RESEARCH AND DEVELOPMENT
History of aeroelasticity in Germany from the beginning to 1945 [ESA-TT-1082] N88-29767
With an eye to the future: ESA general studies program 1988 [ESA-SP-1100] N88-30447

RESEARCH FACILITIES
Helicopter transmission research at NASA Lewis Research Center [NASA-TM-100962] N88-30128
An improvement in the numerical integration procedure used in the NASA Marshall engineering thermosphere model [NASA-CR-179389] N88-30200
Science at NASA field centers: Findings and recommendations on the scope, strength and interactions of science and science-related technology programs [NASA-TM-101188] N88-30581
Research and technology of the Lyndon B. Johnson Space Center [NASA-TM-100463] N88-30583

RESEARCH MANAGEMENT
Space shuttle phase B wind tunnel model and test information. Volume 1: Booster configuration [NASA-CR-178414-VOL-1-PT-2] N88-29770
Noncontact photo-thermal sensing [AD-A195450] N88-29905
Helicopter transmission research at NASA Lewis Research Center [NASA-TM-100962] N88-30128
Science at NASA field centers: Findings and recommendations on the scope, strength and interactions of science and science-related technology programs [NASA-TM-101188] N88-30581
Research and technology of the Lyndon B. Johnson Space Center [NASA-TM-100463] N88-30583

RESEARCH VEHICLES
A multiprocessor avionics system for an unmanned research vehicle [AD-A194806] N88-29800

RESIDUAL STRESS
A dynamic analysis of piezoelectric strained elements [AD-A196079] N88-30430

RESIN MATRIX COMPOSITES
Novel ladder polymers for use as high temperature stable resins or coatings [NASA-CASE-LEW-14203-1] N88-29984

RESISTOJET ENGINES
Experimental evaluation of resistojet thruster plume shields [NASA-TM-101363] N88-29868
The dc power control for a liquid-fed resistojet [NASA-TM-101326] N88-29869

RESOLUTION
An analysis of results of a high-resolution world ocean circulation model [AD-A195760] N88-30272

RESONANCE
Storing bits on a DNA polymer chain [AD-A195701] N88-29981
Impurity analysis in SIMOX samples by high-efficiency resonance ionization time-of-flight mass spectrometry [DE88-012061] N88-30051
Resonance effects accompanying motion with low thrust in earth-moon system N88-30510

RESONANT FREQUENCIES
Laser sensing for identification and control of distributed parameter systems [AD-A195886] N88-30124

RESOURCES MANAGEMENT
Study of the spectral response of soybeans [INPE-4592-PRE/1322] N88-30174

RESPIRATORY SYSTEM
Accidental hypothermia [AD-A194967] N88-30278
Models of cerebral-body perfusion and cerebral chemical transport [AD-A194945] N88-30283

RESPONSES
Synchronous response modelling and control of an annular momentum control device [NASA-CR-4166] N88-29995
Numerical simulation of the function of scientific instrumentation for measuring the speed of electron devices [AD-A194989] N88-30103
Dirichlet prior in Bayesian estimation of item response curves [AD-A195311] N88-30392

RESTORATION
Method for combined image interpolation-restoration through a fir filter design technique [INPE-4561-PRE/1302] N88-30315

RESUSCITATION
Accidental hypothermia
[AD-A194967] N88-30278
RETINA
Functional assessment of laser irradiation
[AD-A195735] N88-30287
REUSABLE LAUNCH VEHICLES
Space shuttle phase B wind tunnel model and test information. Volume 3: Launch configuration
[NASA-CR-178416-VOL-3-PT-2] N88-29744
Evaluation of the advanced air breathing propulsion concepts, executive summary
[ESA-CR(P)-2540] N88-29802
Evaluation of advanced air breathing concepts. Volume 1: Executive summary
[ESA-CR(P)-2539] N88-29806
REUSABLE SPACECRAFT
Space shuttle phase B wind tunnel model and test information. Volume 1: Booster configuration
[NASA-CR-178414-VOL-1-PT-1] N88-29745
Space shuttle phase B wind tunnel model and test information. Volume 1: Booster configuration
[NASA-CR-178414-VOL-1-PT-2] N88-29770
Lunar lander conceptual design: Lunar base systems study task 2.2
[NASA-CR-172051] N88-29854
REVERSE FIELD PINCH
RFP (Revised Field Pinch) plasma experiment at INPE
[INPE-4813-PRE/1336] N88-30420
REVERSED FLOW
Comparison of the performance of a reverse flow annular combustion chamber under low and high pressure conditions N88-29923
REYNOLDS STRESS
Analysis method for the production of Reynolds stresses in compressible turbulent flow (fluid mechanics)
[NASA-TT-20330] N88-30088
Development of a more general Reynolds stress closure for swirling flow
[AD-A195121] N88-30092
RHENIUM
Iridium-coated rhenium thrusters by CVD
[NASA-TM-101309] N88-29874
RHENIUM ISOTOPES
Experimental and theoretical investigations of isotope shift and hyperfine structure on 5d elements (especially platinum, iridium and rhenium)
[ETN-88-93121] N88-29957
RHEOLOGY
Ultrasonic detection of diffusion and adhesion loss N88-29967
Lava thicknesses: Implications for rheological and crustal development N88-30490
Small-scale volcanic landforms indicative of distributary tube systems N88-30496
RIBS (SUPPORTS)
The viscous flow on surfaces with streamline riblets
[ESA-TT-1091] N88-30067
RICCATI EQUATION
Convergence of Galerkin approximations for operator Riccati equations: A nonlinear evolution equation approach
[NASA-CR-181706] N88-30386
RICHARDSON NUMBER
Some results from the Amazon Forest micrometeorological experiment
[INPE-4631-PRE/1346] N88-30263
RIGID STRUCTURES
Clevis joint for deployable space structures
[NASA-CASE-LAR-13898-1] N88-30130
RING CURRENTS
Ring current role in dynamics of fluctuating electron and ion fluxes in low-latitude magnetosphere N88-30514
Plasma of earth's magnetosphere ring currents. Model compared with results of AMPTE/CCE experiment N88-30515
RING LASERS
Precision measurement of the Fresnel drag coefficient using a ring laser
[AD-A196025] N88-30043
RISK
Venture theory: A model of decision weights
[AD-A194809] N88-30391
ROBOTICS
Study of robotics spacecraft servicing and assembly in space. Volume 1: Executive summary
[ESA-CR(P)-2612-VOL-1] N88-29839
Low level image processing techniques using the pipeline image processing engine in the flight telerobotic servicer N88-30346
An automated computerized vision technique for determination of three-dimensional object geometry N88-30348
Study of software requirements and artificial intelligence techniques for robotics
[TL-3332] N88-30365
Adaptive control in positioning a rigid-flexible robot arm
[AD-A195194] N88-30367
Research on problem-solving systems
[AD-A195154] N88-30370
A standard architecture for controlling robots
[AD-A195929] N88-30371
Kalman filter-based algorithms for estimating depth from image sequences
[AD-A195818] N88-30380
Utilizing dynamic stability of orient parts
[AD-A195730] N88-30397
ROBOTS
Modeling robot flexibility for endpoint force control
[AD-A195923] N88-30132
Haptic exploration in humans and machines: Attribute integration and machine recognition/implementation
[AD-A193692] N88-30299
Simulation of a two link robot manipulator with elastic members
[AD-A196014] N88-30368
ROCK INTRUSIONS
Recycling of lower continental crust through foundering of cumulates from contaminated mafic intrusions N88-30204
Crustal evolution and the eclogite to granulite phase transition in xenoliths from the West African Craton N88-30217
Evidence for crustal recycling during the Archean: The parental magmas of the stillwater complex N88-30226
ROCKET ENGINES
Energy conversion measurements in laser-sustained argon plasmas for application to rocket propulsion
[AD-A194931] N88-29861
Automatic data retrieval from rocket motor holograms
[AD-A195586] N88-29864
Iridium-coated rhenium thrusters by CVD
[NASA-TM-101309] N88-29874
ROCKET EXHAUST
Studies on rocket exhaust plumes and impingement effects related to the Columbus Space Station program: Executive summary
[DFVLR-IB-222-88-A-12] N88-29862
ROCKET FIRING
Orbital transfer vehicle 3000 LBF thrust chamber assembly hot fire test program
[NASA-CR-182145] N88-29858
ROCKET PROPELLANTS
Possibilities of economical improvements for Moon based rocket propulsion using lunar propellants
[ILR-MITT-196] N88-29871
ROCKS
Relationships among earth's gravity field, magnetic field, crustal structure and the magnetic character of crustal rocks
[AD-A195539] N88-30198
Mid to late proterozoic magmatism within Northeastern North America and its iplications for the growth of the continental crust N88-30229
Growth of the lower continental crust N88-30236
Geochronological and lead-isotope evidences for rapid crust formation in middle-proterozoic time: The Labrador example N88-30239
Trace element differences between Archean, Proterozoic and Phanerozoic crustal components: Implications for crustal growth processes N88-30243
Exotic minerals in 3,500 million year old rocks: Evidence for large meteorite impacts N88-30475
RODS
Vibrational power flow analysis of rods and beams
[NASA-CR-183166] N88-30151
ROLL
Aerodynamics in ground effect and predicted landing ground roll of a fighter configuration with a secondary-nozzle thrust reverser
[NASA-TP-2834] N88-29752
Computer programs for calculation of sting pitch and roll angles required to obtain angles of attack and sideslip on wind tunnel models
[NASA-TM-100659] N88-29820
ROOM TEMPERATURE
Alternative immersion accelerated testing of coating systems for Naval shoreline facilities N88-29977
ROTARY WING AIRCRAFT
Prediction and measurement of human pilot dynamic characteristics in a manned rotorcraft simulation
[NASA-CR-183246] N88-30297
ROTARY WINGS
JUH-1H redesigned pneumatic boot deicing system flight test evaluation
[AD-A194918] N88-29785
ROTATING CYLINDERS
Numerical simulation of unsteady incompressible flow in a partially-filled rotating cylinder
[AD-A196001] N88-30073
ROTATING FLUIDS
Study of toluene rotary fluid management device and shear flow condenser performance for a space-based organic Rankine power system
[NASA-CR-180885] N88-29872
ROTATING LIQUIDS
Numerical calculations of the response of a spinning spheroidal payload to coning motion
[AD-A195890] N88-30059
Numerical simulation of unsteady incompressible flow in a partially-filled rotating cylinder
[AD-A196001] N38-30073
ROTATION
The aspect ratio dependence of the attractor dimension in Taylor-Couette flow
[AD-A196297] N88-30065
ROTORS
Three-dimensional Navier-Stokes simulations of turbine rotor-stator interaction
[NASA-TM-100081] N88-29750
An unconditionally stable Runge-Kutta method for unsteady flows
[NASA-TM-101347] N88-29780
The effects of inlet turbulence and rotor/stator interactions on the aerodynamics and heat transfer of a large-scale rotating turbine model. Volume 2: Heat transfer data tabulation. 15 percent axial spacing
[NASA-CR-179467] N88-29804
Spray automated balancing of rotors: Methods and materials
[NASA-CR-182151] N88-29825
RUBBER
Determination of the hydroperoxide potential of jet fuels
[AD-A195975] N88-29991
RUNGE-KUTTA METHOD
An unconditionally stable Runge-Kutta method for unsteady flows
[NASA-TM-101347] N88-29780
RUNWAYS
An analysis of time and space requirements for aircraft turnrounds
[TT-8705] N88-29783
RUSTING
Reduced time frame for predicting coating performance N88-29979

S

SAFETY
Numerical field model simulation of full scale fire tests in a closed spherical/cylindrical vessel
[AD-A195067] N88-29998
Improvement of head-up display standards. Volume 3: An evaluation of head-up display safety
[AD-A195787] N88-30300
SAFETY FACTORS
Study on long-term evolution towards European manned spaceflight. Volume 1: Executive summary
[ERNO-OX1-002/88-VOL-1] N88-29827
SAMARIUM ISOTOPES
Nd isotopes and crustal growth rate N88-30203
Changing styles of crustal growth in Southern Africa: Constraints from geochemical and Sr-Nd isotope studies in Archaean to Pan African terrains N88-30227
SAMPLING
Recent observations of carbon monoxide in the Amazon Rain Forest
[INPE-4478-PRE/1245] N88-30186
The dynamics of transuranics and other radionuclides in natural environments, December 1985
[DE87-014456] N88-30189
New type of primitive meteorite found in Antarctica N88-30478
SARSAT
KOSPAS-SARSAT satellites used for ocean current study N88-30534
SATELLITE ALTIMETRY
Microwave instrument for planetary mission (Titan/CASSINI mission orbiter spacecraft)
[BAE-CS/TP-8359] N88-30102
A study of the feasibility of using sea and wind information from the ERS-1 satellite. Part 1: Wind scatterometer data
[NASA-CR-182833] N88-30167
A study of the feasibility of using sea and wind information from the ERS-1 satellite. Part 2: Use of scatterometer and altimeter data in wave modeling and assimilation
[ESA-CR(P)-2604-PT-2] N88-30176
SATELLITE ANTENNAS
Development of procedures for performing end-to-end tests on the ERS-1 radar altimeter and AMI using a compact antenna test range --- Active Microwave Instrument (AMI)
[ESA-CR(P)-2558] N88-30022

A 30/20 GHz multibeam array antenna suitable for future high rate TDMA European satellite networks
[ETN-88-93079] N88-30037

SATELLITE ATMOSPHERES
Microwave instrument for planetary mission (Titan/CASSINI mission orbiter spacecraft)
[BAE-CS/TP-8359] N88-30102

SATELLITE COMMUNICATION
Comparative analysis of passive communications satellites employing the SHF and HF spectrum for use in a strategic role
[AD-A194682] N88-30019
Signals and systems N88-30026

SATELLITE CONFIGURATIONS
PSDE/SAT 2: Preliminary spacecraft configuration study, executive summary
[ESA-CR(P)-2618] N88-29840

SATELLITE DESIGN
PSDE/SAT 2: Preliminary spacecraft configuration study, executive summary
[ESA-CR(P)-2618] N88-29840
Low cost satellite
[ESA-CR(P)-2560] N88-29844

SATELLITE DOPPLER POSITIONING
Specifications and performance of ultrastable oscillators in the DORIS orbitography and positioning system
[ETN-88-92761] N88-29831

SATELLITE DRAG
Using nonstationary models of the atmosphere to describe satellite drag N88-30502

SATELLITE IMAGERY
Microwave instrument for planetary mission (Titan/CASSINI mission orbiter spacecraft)
[BAE-CS/TP-8359] N88-30102
TM/LANDSAT-5 data to evaluate wheat and bean percent soil cover and leaf area index
[INPE-4609-PRE/1332] N88-30165
Evaluation of LANDSAT-TM data for geomorphological mapping
[INPE-4593-PRE/1324] N88-30168
Imaging instrument of the vegetation payload (SPOT 4)
[SNIAS-881-440-107] N88-30169
The use of orbital remote sensing data for low cost ground-water survey
[INPE-4587-PRE/1318] N88-30170
Reflectance pattern and the physical and chemical characteristics of three Brazilian Oxisols
[INPE-4590-PRE/1320] N88-30172
Use of digital images as a mineral prospecting tool in the tin province of Goias, Brazil
[INPE-4537-PRE/1284] N88-30173
Relief effect correction on LANDSAT imagery for forest applications using digital terrain models
[INPE-4611-PRE/1334] N88-30179
LANDSAT TM and agrometeorological data for wheat yield estimation at the farm level
[INPE-4591-PRE/1321] N88-30180
Volcanic contribution to crustal growth in the Central Andes: A new estimate and a discussion of uncertainties N88-30255
Validate algorithms for the determination of rainfall rates from SSM/I microwave satellite imagery
[AD-A195428] N88-30270
Compression and decompression of imaging sensor signals (CADISS): A multiprocessor system for image compression/decompression on board scientific satellites
[NLR-TR-87076-L] N88-30323
Analytical method for approximate geodetic referencing of scanner images of meteorological artificial earth satellites using control points N88-30527
Determining the spatial structure of fields of precipitation from space radar images in two orthogonal polarizations N88-30531

SATELLITE NAVIGATION SYSTEMS
Accuracy of satellite data navigation
[AD-A195877] N88-29787
Low cost satellite
[ESA-CR(P)-2560] N88-29844

SATELLITE NETWORKS
Optical multiple access intersatellite links
[BAE-TP-8502] N88-30013

SATELLITE OBSERVATION
Oblique metallogenic zones recognized by interpreting space photographs of southern Tien Shan N88-30529

SATELLITE ORBITS
A standard library for modeling satellite orbits on a microcomputer
[AD-A195759] N88-29830
Experimental and analytical study of two-phase flow in zero gravity
[AD-A195223] N88-29903
Plane periodic satellite motions relative to center of mass in neighborhood of collinear libration point N88-30507
Resonance effects accompanying motion with low thrust in earth-moon system N88-30510

SATELLITE ROTATION
Rotational evolution of dynamically symmetric gyrostat with internal friction N88-30509

SATELLITE SOUNDING
Possibilities of determining vertical profiles of microphysical characteristics of stratospheric aerosol using space measurements of transparency and solar halo N88-30526

SATELLITE TEMPERATURE
Far infrared spectroscopy telescope (FIRST) inflatable thermal shield, phase 1
[SR/FIS/106(87)CZ] N88-30552

SATELLITE TRACKING
Approximation of atmospheric density by Chebyshev polynomials in predicting motion of low artificial earth satellites N88-30503

SATELLITE TRANSMISSION
Atmospheric corrections for in-flight satellite radiometric calibration
[AD-A196124] N88-30194

SATELLITE-BORNE PHOTOGRAPHY
Structure of eastern Turkestan Ridge based on space photographs N88-30530

SATURN
Astron observations of supernova 1987A in large magellanic cloud N88-30504

SATURN ATMOSPHERE
Extended atmospheres of outer planet satellites and comets
[NASA-CR-183157] N88-30572

SCALE MODELS
Test of an 0.8-scale model of the AH-64 Apache in the NASA Langley full-scale wind tunnel
[AD-A196129] N88-29768

SCANNING
Scanning electron microscopy study of adhesion in sea urchin blastulae
[NASA-CR-183136] N88-30275

SCATHA SATELLITE
Ion gun generated electromagnetic interference on the SCATHA satellite
[AD-A195179] N88-29853

SCATTERING
The effect of particle properties on radiative heat transfer N88-29941
Scattering impulse response synthesis using random noise illumination: Initial concept evaluation
[AD-A195086] N88-30034
Finite-difference simulations of Rayleigh-wave scattering by shallow heterogeneity
[AD-A194961] N88-30259

SCATTERING AMPLITUDE
Eikonal solutions to optical model coupled-channel equations
[NASA-TP-2830] N88-30402

SCATTEROMETERS
A study of the feasibility of using sea and wind information from the ERS-1 satellite. Part 1: Wind scatterometer data
[NASA-CR-182833] N88-30167
A study of the feasibility of using sea and wind information from the ERS-1 satellite. Part 2: Use of scatterometer and altimeter data in wave modeling and assimilation
[ESA-CR(P)-2604-PT-2] N88-30176

SCHEDULING
A static scheduler for the computer aided prototyping system: An implementation guide
[AD-A194340] N88-30322
Contingency rescheduling of spacecraft operations N88-30337
Knowledge based tools for Hubble Space Telescope planning and scheduling: Constraints and strategies N88-30338
The proposal entry processor: Telescience applications for Hubble Space Telescope science operations N88-30339
Candidate functions for advanced technology implementation in the Columbus mission planning environment N88-30340
Integrated resource scheduling in a distributed scheduling environment N88-30342
Lisp Object State Saver (LOSS): A facility used to save partial schedules of the Hubble Space Telescope N88-30360
The P-3 Scheduling Support System (P-3 S3)
[AD-A194824] N88-30450

SCHUMANN-RUNGE BANDS
Aeronomic problems of the molecular oxygen photodissociation. Part 3: Solar spectral irradiances in the region of the O2 Herzberg continuum, Schumann-Runge bands and continuum
[AERONOMICA-ACTA-A-332-1988] N88-29897
Aeronomic problems of molecular oxygen photodissociation. Part 2: Theoretical absorption cross sections of the Schumann-Runge bands at 79 K
[AERONOMICA-ACTA-A-331-1988] N88-29907

SEA ICE
MIZEX (marginal ice zone experiment) 1987 SAR (Synthetic Aperture Radar) data summary
[AD-A195560] N88-30035

SEA ROUGHNESS
Impact force as a part of the total breaking wave force on a vertical cylinder
[RR-CE78] N88-30154

SEA URCHINS
Scanning electron microscopy study of adhesion in sea urchin blastulae
[NASA-CR-183136] N88-30275
Immunofluorescence localization of dissociation supernatant and extracellular matrix components in Lytechinus pictus sectioned embryos
[NASA-CR-183137] N88-30276

SEA WATER
Evaluation of organic coating deterioration and substrate corrosion in seawater using electrochemical impedance measurements N88-29976

SEALERS
Primerless RTV silicones
[BDX-613-3807] N88-29980

SECONDARY EMISSION
Study of secondary emission properties of materials used for high power RF components in space
[ESA-CR(P)-2587] N88-30012

SECONDARY FLOW
The aspect ratio dependence of the attractor dimension in Taylor-Couette flow
[AD-A196297] N88-30065

SECURITY
Report to Congress on the effectiveness of the Civil Aviation Security Program
[AD-A195282] N88-29784
Antisatellite weapons and satellite deployment strategies
[AD-A195014] N88-30396

SEDIMENTS
Constraints on continental accretion from sedimentation N88-30202
The growth of continents and some consequences since 1.5 Ga N88-30220
Solid earth as a recycling systems and the lateral growth of Precambrian North America N88-30249
Spectral analysis of the Elatina varve series
[NASA-CR-183085] N88-30260

SEISMIC WAVES
Maximum-likelihood multichannel deconvolution of P waves at seismic arrays
[AD-A194990] N88-30191
Deep seismic reflection profiling and continental growth curves N88-30222
Discrimination studies using short-period P waves at upper mantle distances
[AD-A195468] N88-30257

SEISMOLOGY
Maximum-likelihood multichannel deconvolution of P waves at seismic arrays
[AD-A194990] N88-30191

SELECTION
Sensor and actuator selection for large space structure control
[AD-A194912] N88-29842

SEMANTICS
Exploiting lexical regularities in designing natural language systems
[AD-A195922] N88-30375

SEMICONDUCTOR DEVICES
Electronic and optical devices and applications N88-30027
Automatic prober for the dc characterisation of gallium arsenide devices. Part 2: The data sorting and display facility
[AD-A195408] N88-30111
Tolerances for phase locking of semiconductor laser arrays
[AD-A195974] N88-30120
Application of nondestructive testing techniques to materials testing
[AD-A195716] N88-30138
Light-millimeter wave interactions in semiconductor devices
[AD-A195898] N88-30428
Waveform relaxation applied to transient device simulation
[AD-A194992] N88-30429

SEMICONDUCTOR LASERS
Mode locking of semiconductor laser with external cavity
[AD-A196018] N88-30117

SEMICONDUCTORS (MATERIALS)
Power MISFETs on OnP
[AD-A195242] N88-30436
Joint services electronics program
[AD-A195731] N88-30439
SENSORS
Sensor and actuator selection for large space structure control
[AD-A194912] N88-29842
SEPARATED FLOW
Numerical methods: Euler time dependent solver N88-29760
The effects of incoming boundary layer thickness on unsteady shock-induced turbulent separations induced by cylinders
[AD-A196190] N88-30060
Numerical simulation of nozzle flows
[AD-A195144] N88-30064
SEQUENCING
Performance of DS/SSMA communications in impulsive channels. Part 1: Correlation receivers
[AD-A195712] N88-30021
SEQUENTIAL COMPUTERS
A model for architectural comparison
[AD-A195993] N88-30302
SERIES EXPANSION
An improved spherical earth diffraction algorithm for SEKE
[AD-A195847] N88-30005
SERVICE LIFE
Fuel effects on flame radiation and hot-section durability N88-29925
A reliability-based program for predicting the service life of organic coating systems N88-29971
In-house capacitor technology program
[AD-A194804] N88-30049
SERVOMECHANISMS
A standard architecture for controlling robots
[AD-A195929] N88-30371
SEYFERT GALAXIES
AGN (OIII) emission line profiles: Dependencies on galaxy inclination and Balmer decrement
[INPE-4596-PRE/1324] N88-30577
SHAPE CONTROL
Robust design of distributed controllers for large flexible space structures
[NASA-CR-183202] N88-30134
SHAPES
Using primal sketch primitives as the basis for the Hough transform
[INPE-4564-PRE/1305] N88-30310
Symbolic construction of a 2D scale-space image
[AD-A195926] N88-30374
SHEAR FLOW
Study of toluene rotary fluid management device and shear flow condenser performance for a space-based organic Rankine power system
[NASA-CR-180885] N88-29872
SHEAR PROPERTIES
Large displacement and rotational formulation for laminated cylindrical shells including parabolic transverse shear
[AD-A194871] N88-30158
SHEAR STRESS
Experimental determination of drag modifications due to elastic compliant surfaces using quantitative visual techniques
[AD-A194785] N88-30082
Development of a more general Reynolds stress closure for swirling flow
[AD-A195121] N88-30092
SHELL STABILITY
Computational aerodynamic analysis for a range-limited 25mm training round
[AD-A185270] N88-29772
SHIELDING
Experimental evaluation of resistojet thruster plume shields
[NASA-TM-101363] N88-29868
SHIP HULLS
Numerical field model simulation of full scale fire tests in a closed spherical/cylindrical vessel
[AD-A195067] N88-29998
Response of SMA (Shielded Metal Arc) and narrow gap HY80 weldments to explosive shock loading
[AD-A195994] N88-30162
SHOCK LOADS
The effects of incoming boundary layer thickness on unsteady shock-induced turbulent separations induced by cylinders
[AD-A196190] N88-30060
Response of SMA (Shielded Metal Arc) and narrow gap HY80 weldments to explosive shock loading
[AD-A195994] N88-30162
SHOCK WAVE INTERACTION
Numerical simulation of nozzle flows
[AD-A195144] N88-30064
Experimental and numerical investigation of the effect of distributed suction on oblique shock wave/turbulent boundary layer interaction
[NASA-TM-101334] N88-30084
SHORT CIRCUITS
Pierce diode with external circuit. Part 3: Chaotic behavior
[AD-A194837] N88-30041
SHORT TAKEOFF AIRCRAFT
Aerodynamics in ground effect and predicted landing ground roll of a fighter configuration with a secondary-nozzle thrust reverser
[NASA-TP-2834] N88-29752
SIDESLIP
Angle of attack and sideslip estimation using an inertial reference platform
[AD-A194876] N88-29769
Computer programs for calculation of sting pitch and roll angles required to obtain angles of attack and sideslip on wind tunnel models
[NASA-TM-100659] N88-29820
SIGNAL DETECTION
On adaptive cell-averaging CFAR (Constant False-Alarm Rate) radar signal detection
[AD-A196286] N88-30009
A detection theory analysis of visual display performance
[AD-A196291] N88-30292
SIGNAL DETECTORS
Analytical methods in stochastic control and nonlinear filtering
[AD-A194272] N88-30388
SIGNAL PROCESSING
Acoustooptic processing of two-dimensional signals using temporal and spatial integration
[AD-A194803] N88-29999
Doppler-corrected differential detection system
[NASA-CASE-NPO-16987-1-CU] N88-30001
Review of Radio Science, 1984-1986 N88-30023
Signals and systems N88-30026
Quantitative surface temperature measurement using two-color thermographic phosphors and video equipment
[NASA-CASE-LAR-13740-1] N88-30105
Reconstruction of multidimensional signals from multiple level threshold crossings
[AD-A195561] N88-30383
Spectroscopic studies with multiple quantum well materials with applications to optical signal processing at room temperature
[AD-A194171] N88-30409
SIGNAL RECEPTION
The focal plane reception pattern calculation for a paraboloidal antenna with a nearby fence
[NASA-TM-100691] N88-30039
SIGNAL TO NOISE RATIOS
Analytical methods in stochastic control and nonlinear filtering
[AD-A194272] N88-30388
SILANES
Ion kinetics in silane plasmas
[AD-A196202] N88-30423
SILICATES
Recycling of lower continental crust through foundering of cumulates from contaminated mafic intrusions N88-30204
SILICON
Ultrafast processes and spectroscopy with free electron lasers
[AD-A195248] N88-30126
SILICON CARBIDES
Processing technology research in composites
[AD-A195693] N88-29890
Electrical properties of materials for elevated temperature resistance strain gage application
[NASA-CR-182214] N88-30106
SILICONES
Primerless RTV silicones
[BDX-613-3807] N88-29980
Containment of a silicone fluid free surface in reduced gravity using barrier coatings
[NASA-TM-101314] N88-30072
SIMULATION
Simulation of Vulcain engine operation at low inlet pressure
[ETN-88-93083] N88-29875
Finite-difference simulations of Rayleigh-wave scattering by shallow heterogeneity
[AD-A194961] N88-30259
Simulation of a two link robot manipulator with elastic members
[AD-A196014] N88-30368
Waveform relaxation applied to transient device simulation
[AD-A194992] N88-30429
Simulations of lava flows on Mars N88-30495
SINGLE CRYSTALS
Anisotropic constitutive modeling for nickel-base single crystal superalloys
[NASA-CR-182157] N88-29961
Streaking images that appear only in the plane of diffraction in undoped GaAs single crystals: Diffraction imaging (topography) by monochromatic synchrotron radiation
[NASA-CR-183267] N88-30437
SINGLE EVENT UPSETS
The effects of total dose on the SEU sensitivity of CMOS static RAMS — single event upset (SEU), satellite components
[AERE-R-12779] N88-30401
The Single Event Upset (SEU) test facility on the Hardwell tandem generator for cosmic ray simulation
[AERE-R-12896] N88-30580
SIZE DETERMINATION
Gas turbine smoke measurement: A smoke generator for the assessment of current and future techniques N88-29930
Particle size measurements in sooting combustion systems N88-29931
The effect of particle properties on radiative heat transfer N88-29941
SKIN FRICTION
Development and design of windtunnel and test facility for RPV (Remote Piloted Vehicle) enhancement devices
[AD-A194842] N88-29822
SLENDER BODIES
Semi-empirical methods for conventional and unconventional missiles N88-29758
SLIDING FRICTION
Stability of stick-slip phenomenon by using constitutive friction laws of Dietrich and Ruina
[ILR-MITT-197] N88-30127
SLOPES
A preliminary investigation of drag reduction and mechanism for a blunt body of revolution with slanted base
[NASA-TT-20349] N88-29753
SMOKE
Gas turbine smoke measurement: A smoke generator for the assessment of current and future techniques N88-29930
Numerical field model simulation of full scale fire tests in a closed spherical/cylindrical vessel
[AD-A195067] N88-29998
SODIUM CHLORIDES
Alternative immersion accelerated testing of coating systems for Naval shoreline facilities N88-29977
SODIUM HYDROXIDES
Titrimetric analysis of HAN-based liquid propellants
[AD-A196225] N88-29990
SOFTWARE ENGINEERING
Improvements of DCAP 1, phase 2-3/A
[D2-RP-AI-106] N88-30325
The need for a comprehensive expert system development methodology N88-30362
Study of software requirements and artificial intelligence techniques for robotics
[TL-3333] N88-30365
The P-3 Scheduling Support System (P-3 S3)
[AD-A194824] N88-30450
SOFTWARE TOOLS
Quality measures and assurance for AI (Artificial Intelligence) software
[NASA-CR-4187] N88-30304
An operations manual for the digital data system
[NASA-CR-181688] N88-30329
The proposal entry processor: Telescience applications for Hubble Space Telescope science operations N88-30339
SOIL MECHANICS
A parametric study of embedded cantilever retaining walls: The results of a finite element study
[RR-CE83] N88-30152
Computer-Aided Structural Engineering (CASE) project. Development of design formulas for ribbed mat foundations on expansive soils
[AD-A194807] N88-30307
SOIL MOISTURE
Microwave remote sensing at INPE (Institute for Space Research) Brazil: Concepts and future prospects of soil moisture studies
[INPE-4569-PRE/1310] N88-30178
SOILS
Reflectance pattern and the physical and chemical characteristics of three Brazilian Oxisols
[INPE-4590-PRE/1320] N88-30172

The dynamics of transuranics and other radionuclides in natural environments, December 1985
[DE87-014456] N88-30189
Estimation of soil temperature profile from remote microwave and IR measurements N88-30532
SOLAR ARRAYS
Advanced planar array development for space station
[NASA-CR-179373] N88-30181
Alternative module configurations for advanced solar arrays on low orbit and extended lifetime missions (AMOC 2)
[ESA-CR(P)-2581] N88-30182
SOLAR CELLS
Alternative module configurations for advanced solar arrays on low orbit and extended lifetime missions (AMOC 2)
[ESA-CR(P)-2581] N88-30182
SOLAR COLLECTORS
The effect of the near earth micrometeoroid environment on a highly reflective mirror surface
[NASA-TM-101307] N88-29833
SOLAR CORONA
Corona-solar wind coupling review
[AFGL-TR-87-0203] N88-30575
SOLAR CYCLES
Spectral analysis of the Elatina varve series
[NASA-CR-183085] N88-30260
SOLAR DYNAMIC POWER SYSTEMS
Study of toluene stability for an Organic Rankine Cycle (ORC) space-based power system
[NASA-CR-180884] N88-29863
Study of toluene rotary fluid management device and shear flow condenser performance for a space-based organic Rankine power system
[NASA-CR-180885] N88-29872
SOLAR ELECTRONS
Structural dynamics of high-latitude magnetosphere determined from solar electron data N88-30500
SOLAR FLARES
Solar-geophysical data number 523, March 1988. Part 1: (Prompt reports). Data for February 1988, January 1988 and late data
[PB88-212766] N88-30574
Solar-geophysical data number 523, March 1988. Part 2: (Comprehensive reports). Data for September 1987 and miscellanea
[PB88-212774] N88-30576
SOLAR OBSERVATORIES
NASA Marshall Space Flight Center solar observatory
[NASA-TM-100339] N88-29832
Coordinated study of Solar-Terrestrial Observatory (STO) payloads on space station
[NASA-CR-183142] N88-29848
SOLAR ORBITS
Numerical evidence that the motion of Pluto is chaotic
[AD-A195920] N88-30568
SOLAR PHYSICS
Solar-geophysical data number 523, March 1988. Part 1: (Prompt reports). Data for February 1988, January 1988 and late data
[PB88-212766] N88-30574
Solar-geophysical data number 523, March 1988. Part 2: (Comprehensive reports). Data for September 1987 and miscellanea
[PB88-212774] N88-30576
SOLAR RADIATION
Energy budget and ground temperatures in hot regions
[AD-A196298] N88-30268
SOLAR RADIO BURSTS
Solar-geophysical data number 523, March 1988. Part 2: (Comprehensive reports). Data for September 1987 and miscellanea
[PB88-212774] N88-30576
SOLAR RADIO EMISSION
Solar-geophysical data number 523, March 1988. Part 1: (Prompt reports). Data for February 1988, January 1988 and late data
[PB88-212766] N88-30574
SOLAR SPECTRA
Aeronomic problems of the molecular oxygen photodissociation. Part 3: Solar spectral irradiances in the region of the O2 Herzberg continuum, Schumann-Runge bands and continuum
[AERONOMICA-ACTA-A-332-1988] N88-29897
Atmospheric corrections for in-flight satellite radiometric calibration
[AD-A196124] N88-30194
Spectral analysis of the Elatina varve series
[NASA-CR-183085] N88-30260
SOLAR SYSTEM
Lewis Cliff 86010, a unique Antarctic meteorite: Possible new clues to the early history of the solar system N88-30482
Noble gases, C,N, and Si isotopes in interstellar SiC form the Murchison carbonaceous chondrite N88-30483
Workshop on the Origins of Solar Systems
[NASA-CR-183025] N88-30536
Star formation and molecular clouds N88-30537
Observations of star formation N88-30538
Cosmochemical trends of volatile elements in the solar system N88-30542
Terrestrial versus giant planet formation N88-30543
SOLAR TERRESTRIAL INTERACTIONS
Coordinated study of Solar-Terrestrial Observatory (STO) payloads on space station
[NASA-CR-183142] N88-29848
Corona-solar wind coupling review
[AFGL-TR-87-0203] N88-30575
SOLAR WIND
Stability of Venusian ionopause N88-30523
Corona-solar wind coupling review
[AFGL-TR-87-0203] N88-30575
SOLAR X-RAYS
Solar-geophysical data number 523, March 1988. Part 2: (Comprehensive reports). Data for September 1987 and miscellanea
[PB88-212774] N88-30576
SOLID ROCKET PROPELLANTS
Automatic data retrieval from rocket motor holograms
[AD-A195586] N88-29864
Ignition and extinguishing of a Solid Fuel Ramjet (SOFRAM)
[FOA-C-20713-2.1] N88-29865
Combustion diagnostics of propellant with new grain geometries
[AD-A194944] N88-29895
Descriptive characterization of propellant particles
[AD-A195176] N88-29985
Preliminary investigation of flow modeling during solid propellant processing
[AD-A196168] N88-29987
SOLID STATE LASERS
Spectral properties of semiconductor lasers with external resonators
[ETN-88-93119] N88-30125
SOLITARY WAVES
Characteristics of solitary waves and weak double layers in the magnetospheric plasma
[IRF-PREPRINT-105] N88-30418
SOLUTIONS
Structure and dynamics of solutions of lithium salts relevant to battery construction
[AD-A195399] N88-30044
SOLVOLYSIS
Descriptive characterization of propellant particles
[AD-A195176] N88-29985
SOOT
Combustion and fuels in gas turbine engines
[AGARD-CP-422] N88-29910
The performance of a surrogate blend in simulating JP-4 in a spray-fueled combustor N88-29926
Radiation from soot-containing flames N88-29927
Flamelet chemistry modelling of soot formation for radiation N88-29928
Large ionic species in sooting acetylene and benzene flames N88-29932
Rates of formation of soot from hydrocarbon flames and its destruction N88-29933
The influence of pressure on soot formation N88-29934
Particle sizing in combustion systems, using scattered laser light
[AD-A196231] N88-29953
Optical measurements of soot and temperature profiles in premixed propane-oxygen flames
[NASA-TM-101343] N88-29997
Optical measurements of soot in premixed flames
[NASA-TM-101305] N88-30090
SOUND WAVES
In situ fault detection by the hybrid ray mode method
[AD-A195226] N88-30137
SOUNDING ROCKETS
Aerospace payload support systems
[AFGL-TR-87-0241] N88-29843
SOYBEANS
Study of the spectral response of soybeans
[INPE-4592-PRE/1322] N88-30174
SPACE COMMUNICATION
Telescience testbed pilot program
[NASA-CR-183207] N88-30309
The Deep Space Network: An instrument for radio astronomy research
[NASA-CR-183219] N88-30554
SPACE ENVIRONMENT SIMULATION
The effects of total dose on the SEU sensitivity of CMOS static RAMS — single event upset (SEU), satellite components
[AERE-R-12779] N88-30401

The Single Event Upset (SEU) test facility on the Hardwell tandem generator for cosmic ray simulation
[AERE-R-12896] N88-30582
SPACE ERECTABLE STRUCTURES
Clevis joint for deployable space structures
[NASA-CASE-LAR-13898-1] N88-30133
Far infrared spectroscopy telescope (FIRST) inflatal thermal shield, phase 1
[SR/FIS/108(87)CZ] N88-30555
SPACE EXPLORATION
The NASA Electric Propulsion Program
[NASA-TM-101324] N88-29859
Volatiles on Mars
[NASA-CR-183113] N88-30571
SPACE FLIGHT TRAINING
An intelligent training system for space shuttle flight controllers N88-30331
SPACE LAW
JPRS report: Science and technology. USSR: Space
[JPRS-USP-88-001] N88-30498
SPACE OBSERVATIONS (FROM EARTH)
Activities report in astronomy
[ISSN-0531-4496] N88-30535
SPACE PERCEPTION
Central serous chorioretinopathy in USAF aviators: A review
[AD-A195697] N88-30280
SPACE PLATFORMS
Technology requirements for an orbiting fuel depot: A necessary element of a space infrastructure
[NASA-TM-101370] N88-29845
Interim Flight Opportunity (IFO). Volume 1: Executive summary — space platform
[SE/LS/AP-36-818/CN-VOL-1] N88-29849
SPACE SHUTTLE MAIN ENGINE
Automatic mathematical modeling for real time simulation system N88-30356
SPACE SHUTTLE PAYLOADS
Aerospace payload support systems
[AFGL-TR-87-0241] N88-29843
Containment of a silicone fluid free surface in reduced gravity using barrier coatings
[NASA-TM-101314] N88-30072
Spacelab data processing facility (SLDPF) Quality Assurance (QA)/Data Accounting (DA) expert systems: Transition from prototypes to operational systems N88-30353
SPACE SHUTTLES
Space shuttle phase B wind tunnel model and test information. Volume 3: Launch configuration
[NASA-CR-178416-VOL-3-PT-2] N88-29744
Space shuttle phase B wind tunnel model and test information. Volume 1: Booster configuration
[NASA-CR-178414-VOL-1-PT-1] N88-29745
Space shuttle phase B wind tunnel model and test information. Volume 1: Booster configuration
[NASA-CR-178414-VOL-1-PT-2] N88-29770
Ascent guidance for a winged boost vehicle
[NASA-CR-172083] N88-29846
SPACE STATION PAYLOADS
Coordinated study of Solar-Terrestrial Observatory (STO) payloads on space station
[NASA-CR-183142] N88-29848
SPACE STATION POWER SUPPLIES
Regenerative fuel cell energy storage system for a low earth orbit space station
[NASA-CR-174802] N88-30184
SPACE STATIONS
Definition of common support equipment and space station interface requirements for IOC model technology experiments
[NASA-TM-100656] N88-29856
Study of toluene rotary fluid management device and shear flow condenser performance for a space-based organic Rankine power system
[NASA-CR-180885] N88-29872
Advanced planar array development for space station
[NASA-CR-179373] N88-30181
Space station proximity operations windows: Human factors design guidelines
[NASA-TM-88233] N88-30301
A shared-world conceptual model for integrating space station life sciences telescience operations N88-30333
Integrated resource scheduling in a distributed scheduling environment N88-30342
The space station assembly phase: System design trade-offs for the flight telerobotic servicer N88-30357
SPACE TOOLS
Study of software requirements and artificial intelligence techniques for robotics
[TL-3333] N88-30365
SPACE VEHICLE CHECKOUT PROGRAM
Study of the assembly, integration and verification programs of telecommunication satellites applicable to other satellite programs
[MATRA-100/CC/MLG/031/87] N88-29847

SPACE WEAPONS
A submillimeter wavelength space-based imaging radar
[AD-A195846] N88-30033
Looking beyond the strategic defense initiative
[AD-A195079] N88-30394
Antisatellite weapons and satellite deployment strategies
[AD-A195014] N88-30396
SPACE-TIME FUNCTIONS
Image focusing in space and time
[AD-A195839] N88-30410
SPACEBORNE ASTRONOMY
Beyond the visible: A decade of observations with the International Ultraviolet Explorer (IUE)
[ESA-F09] N88-29828
ESA report to the 27th COSPAR meeting
[ESA-SP-1098] N88-30556
The high-throughput X-ray spectroscopy mission: The mission-science report
[ESA-SP-1097] N88-30557
SPACEBORNE EXPERIMENTS
Experimental proof of quasilongitudinal propagation of low-frequency waves in middle latitudes in upper ionosphere N88-30516
Influence of plasma parameters on VLF radiation in near-rocket region N88-30518
Charge composition of primary cosmic ray nuclei with z greater than or equal to 2 in energy region greater than or equal to 2 TeV N88-30519
SPACEBORNE LASERS
Spaceborne lidar: Development of a laboratory test system
[BF-R-66.090-1] N88-30118
SPACECRAFT ANTENNAS
Development of a general software package for the analysis and synthesis of planar antenna arrays for space applications
[S-247-02] N88-30000
SPACECRAFT CHARGING
Ion gun generated electromagnetic interference on the SCATHA satellite
[AD-A195179] N88-29853
SPACECRAFT COMMUNICATION
Optical multiple access intersatellite links
[BAE-TP-8502] N88-30013
The LTPP communication processor --- Columbus and Hermes
[CL/CP/SES/FR/004] N88-30328
A rule-based systems approach to spacecraft communications configuration optimization N88-30341
SPACECRAFT COMPONENTS
Study of secondary emission properties of materials used for high power RF components in space
[ESA-CR(P)-2587] N88-30012
Heavy ion and proton tests for subsystem upset
[AD-A195267] N88-30442
SPACECRAFT CONSTRUCTION MATERIALS
Study of secondary emission properties of materials used for high power RF components in space
[ESA-CR(P)-2587] N88-30012
SPACECRAFT CONTAMINATION
Studies on rocket exhaust plumes and impingement effects related to the Columbus Space Station program: Executive summary
[DFVLR-IB-222-88-A-12] N88-29862
SPACECRAFT CONTROL
Theory of filtering and control with application to control of large space structures
[AD-A195500] N88-29851
Synchronous response modelling and control of an annular momentum control device
[NASA-CR-4166] N88-29995
Robust design of distributed controllers for large flexible space structures
[NASA-CR-183202] N88-30134
Automated space vehicle control for rendezvous proximity operations N88-30335
An approach to CMG steering using feedback linearization
[NASA-CR-183172] N88-30369
Increasing accuracy in evaluating vector of state under conditions of incomplete observability of expanded system N88-30511
SPACECRAFT DEFENSE
Antisatellite weapons and satellite deployment strategies
[AD-A195014] N88-30396
SPACECRAFT DESIGN
Study on long-term evolution towards European manned spaceflight. Volume 1: Executive summary
[ERNO-OX1-002/88-VOL-1] N88-29827
Spacecraft mass estimation, relationships and engine data: Task 1.1 of the lunar base systems study
[NASA-CR-172061] N88-29836
Maintenance and supply options
[NASA-CR-172062] N88-29837
Study on conceptual design of spacecraft using Computer Aided Engineering (CAE)
[SNIAS-920-CA/TS] N88-29841
Interim Flight Opportunity (IFO). Volume 1: Executive summary --- space platform
[SE/LS/AP-36-816/CN-VOL-1] N88-29849
MANIP --- spacecraft modeling program
[MANIP-217A] N88-29855
SPACECRAFT ELECTRONIC EQUIPMENT
Specifications and performance of ultrastable oscillators in the DORIS orbitography and positioning system
[ETN-88-92761] N88-29831
The effects of total dose on the SEU sensitivity of CMOS static RAMS --- single event upset (SEU), satellite components
[AERE-R-12779] N88-30401
SPACECRAFT EQUIPMENT
Qualification test levels for units to be derived from mechanical test data analysis --- ESA
[REPT-87-158-EI/ET/AG] N88-30139
SPACECRAFT GUIDANCE
Ascent guidance for a winged boost vehicle
[NASA-CR-172063] N88-29846
SPACECRAFT INSTRUMENTS
Measurement of galactic radio emission at frequency 37 GHz from aboard spacecraft N88-30520
SPACECRAFT LAUNCHING
Reduced flexibility in processing Titan 4 space launch vehicles at Cape Canaveral Air Force Station
[AD-A194908] N88-29834
SPACECRAFT MODELS
Procedures for updating dynamic mathematical models, test phase --- spacecraft hardware
[MEBS-38/87] N88-29852
MANIP --- spacecraft modeling program
[MANIP-217A] N88-29855
SPACECRAFT MODULES
Maintenance and supply options
[NASA-CR-172062] N88-29837
Alternative module configurations for advanced solar arrays on low orbit and extended lifetime missions (AMOC 2)
[ESA-CR(P)-2581] N88-30182
SPACECRAFT MOTION
Approximation of atmospheric density by Chebyshev polynomials in predicting motion of low artificial earth satellites N88-30503
SPACECRAFT ORBITS
Canonical variables and canonical integrals for motion in near-circular orbits N88-30512
SPACECRAFT PERFORMANCE
Study of the assembly, integration and verification programs of telecommunication satellites applicable to other satellite programs
[MATRA-100/CC/MLG/031/87] N88-29847
SPACECRAFT POWER SUPPLIES
Possibilities of economical improvements for Moon based rocket propulsion using lunar propellants
[ILR-MITT-196] N88-29871
Alternative module configurations for advanced solar arrays on low orbit and extended lifetime missions (AMOC 2)
[ESA-CR(P)-2581] N88-30182
Fuel cells for space use
[FCP-TR-DOS-SY-026] N88-30183
SPACECRAFT PROPULSION
Spacecraft mass estimation, relationships and engine data: Task 1.1 of the lunar base systems study
[NASA-CR-172061] N88-29836
Possibilities of economical improvements for Moon based rocket propulsion using lunar propellants
[ILR-MITT-196] N88-29871
SPACECRAFT RELIABILITY
Hermes: Study of propulsion system for reusable man-rated spacecraft
[PSRM-TN-0000-00-04A] N88-29866
SPACECRAFT STRUCTURES
Dynamics of articulated aerospace structures
[AD-A195685] N88-29794
Sensor and actuator selection for large space structure control
[AD-A194912] N88-29842
Laser sensing for identification and control of distributed parameter systems
[AD-A195886] N88-30124
SPACECRAFT TEMPERATURE
MANIP --- spacecraft modeling program
[MANIP-217A] N88-29855
SPACELAB
Spacelab data processing facility (SLDPF) Quality Assurance (QA)/Data Accounting (DA) expert systems: Transition from prototypes to operational systems N88-30353
SPACELAB PAYLOADS
Biosample: Preservation, handling and observation system synthesis and breadboarding --- Spacelab
[ESA-CR(P)-2609] N88-29857
Fluid physics double rack --- Spacelab
[SD-TN-AI-012] N88-29992
Accommodation concept for fluid physics facilities, volume 2 --- Spacelab
[SG-TN-AI-027-VOL-2] N88-29994
SPATIAL DISTRIBUTION
Eye movements and spatial pattern vision
[AD-A195496] N88-30290
A detection theory analysis of visual display performance
[AD-A196291] N88-30292
Determining the spatial structure of fields of precipitation from space radar images in two orthogonal polarizations N88-30531
SPECIFIC HEAT
Discovery of a low temperature form of TAGN (Triaminoguanidinium Nitrate)
[AD-A196059] N88-29989
SPECIFIC IMPULSE
Unified study of plasma/surface interactions for space power and propulsion
[AD-A195971] N88-29870
SPECKLE INTERFEROMETRY
Binary star measurements using digital speckle interferometer of 6-m telescope N88-30521
SPECTRAL BANDS
Atmospheric corrections for in-flight satellite radiometric calibration
[AD-A196124] N88-30194
SPECTRAL REFLECTANCE
Monte-Carlo estimation of the influence of plant architecture parameters on spectral brightness N88-30533
SPECTRAL SENSITIVITY
Spectral properties of semiconductor lasers with external resonators
[ETN-88-93119] N88-30125
SPECTRAL SIGNATURES
Integrating multispectral imagery and ground level hyperspectral signature data
[AD-A195976] N88-30166
SPECTROPHOTOMETERS
NBS (National Bureau of Standards) measurement services: The NBS photodetector spectral response calibration transfer program
[PB88-201595] N88-30109
SPECTROPHOTOMETRY
The dynamics of SBO galaxies. Part 1: The data
[SER-C-PREPUBL-FASC-22] N88-30567
SPECTROSCOPY
Electrochemical evaluation of the long term corrosion resistance of polymer coated steel N88-29974
An electrochemical impedance spectroscopy study of reactions at the metal/coating interface N88-29975
Ultrafast processes and spectroscopy with free electron lasers
[AD-A195248] N88-30126
Observations of faint field galaxies
[NASA-CR-183251] N88-30555
A deep redshift survey of field galaxies. Comments on the reality of the Butcher-Oemler effect
[NASA-CR-183255] N88-30558
SPECTRUM ANALYSIS
The optical spectroscopy of copper-blue luminescence in zinc sulfide crystals. Zero-phonon line spectra under the influence of magnetic field, temperature and excitation intensity
[ETN-88-93122] N88-29903
Acoustooptic processing of two-dimensional signals using temporal and spatial integration
[AD-A194803] N88-29999
Spectral analysis of the Elatina varve series
[NASA-CR-183085] N88-30260
SPHERICAL COORDINATES
An improved spherical earth diffraction algorithm for SEKE
[AD-A195847] N88-30005
SPIN STABILIZATION
Computational aerodynamic analysis for a range-limited 25mm training round
[AD-A185270] N88-29772
SPIRAL GALAXIES
The dynamics of SBO galaxies. Part 1: The data
[SER-C-PREPUBL-FASC-22] N88-30567
SPOT (FRENCH SATELLITE)
Imaging instrument of the vegetation payload (SPOT 4)
[SNIAS-881-440-107] N88-30169
SPRAY CHARACTERISTICS
Turbulence effects on the droplet distribution behind airblast atomizers N88-29915

Nozzle airflow influences on fuel patternation N88-29916
Spray performance of a vaporizing fuel injector N88-29919

SPRAYED COATINGS
Spray automated balancing of rotors: Methods and materials
[NASA-CR-182151] N88-29825

SPREAD SPECTRUM TRANSMISSION
Statistical analysis of the LMS (Last Mean Squares) and modified stochastic gradient
[AD-A195497] N88-30376

STABILITY
Study of toluene stability for an Organic Rankine Cycle (ORC) space-based power system
[NASA-CR-180884] N88-29883
Circuit design criteria for stable lateral inhibition neural networks
[AD-A195066] N88-30046
Recent insights into instability and transition to turbulence in open-flow systems
[NASA-CR-181693] N88-30079
Stability of Venusian ionopause N88-30523
The stability of disk galaxies and constraints on their mass-luminosity ratio
[SER-C-PREPUBL-FASC-27] N88-30565

STAINLESS STEELS
State variable approach to deformation phenomena in Face Centered Cubic (FCC) metals
[VTT-44] N88-29964
An experimental study of biaxial yield in modified 9Cr-1Mo steel at room temperature
[NASA-CR-175012] N88-30164

STANDARDIZATION
Improvement of head-up display standards. Volume 3: An evaluation of head-up display safety
[AD-A195787] N88-30300
Strategic, organizational and standardization aspects of integrated information systems, volume 6
[AD-A195855] N88-30457

STANDARDS
Integration of LANTIRN (Low Altitude Navigation and Targeting Infrared for Night) into operational fighter training
[AD-A194906] N88-29799
Using standards to break down information transfer barriers N88-30467

STAR FORMATION
Star formation and molecular clouds N88-30537
Observations of star formation N88-30538
Starbursts and their dynamics
[NASA-CR-180227] N88-30549

STARBURST GALAXIES
Starbursts and their dynamics
[NASA-CR-180227] N88-30549

STARS
Study of modern instrumentation and methods for astronomic positioning in the field
[AD-A196173] N88-30548

STATE ESTIMATION
Increasing accuracy in evaluating vector of state under conditions of incomplete observability of expanded system N88-30511

STATE VECTORS
Increasing accuracy in evaluating vector of state under conditions of incomplete observability of expanded system N88-30511

STATIC STABILITY
Stability of stick-slip phenomenon by using constitutive friction laws of Dietrich and Ruina
[ILR-MITT-197] N88-30127

STATICS
A static scheduler for the computer aided prototyping system: An implementation guide
[AD-A194340] N88-30322

STATISTICAL ANALYSIS
Measurement and analysis of low altitude atmospheric turbulence obtained using a specially instrumented Gnat aircraft N88-29728
Re-assessment of gust statistics using CAADRP data N88-29732
Fatigue crack propagation: Probabilistic modeling and statistical analysis
[AD-A195885] N88-30155
Statistical analysis of the LMS (Last Mean Squares) and modified stochastic gradient
[AD-A195497] N88-30376
Instrumentation for computational statistical research
[AD-A195887] N88-30390

STATISTICAL DISTRIBUTIONS
AGN (OIII) emission line profiles: Dependencies on galaxy inclination and Balmer decrement
[INPE-4596-PRE/1324] N88-30577

STATISTICAL TESTS
Instrumentation for computational statistical research
[AD-A195887] N88-30390

STATOR BLADES
Numerical solutions of unsteady inviscid transonic turbine cascade flows
[AD-A196111] N88-29748

STATORS
Three-dimensional Navier-Stokes simulations of turbine rotor-stator interaction
[NASA-TM-100081] N88-29750
An unconditionally stable Runge-Kutta method for unsteady flows
[NASA-TM-101347] N88-29780
The effects of inlet turbulence and rotor/stator interactions on the aerodynamics and heat transfer of a large-scale rotating turbine model. Volume 2: Heat transfer data tabulation. 15 percent axial spacing
[NASA-CR-179467] N88-29804

STEADY FLOW
Contamination and distortion of steady flow field induced by discrete frequency disturbances in aircraft gas engines
[AD-A195440] N88-30069

STEELS
Damage initiation in the short beam shear test of composite materials using stiffness reduction
[AD-A194880] N88-29883
Crystal structures of ordered carbon metal alloys
[AD-A195597] N88-29959
Performance Prediction for Coatings. Proceedings of a Workshop
[AD-A188973] N88-29966
Degradation of protective coatings on steel in corrosive environments N88-29969
Electrical detection of coating deterioration N88-29973
Electrochemical evaluation of the long term corrosion resistance of polymer coated steel N88-29974
An electrochemical impedance spectroscopy study of reactions at the metal/coating interface N88-29975
Evaluation of organic coating deterioration and substrate corrosion in seawater using electrochemical impedance measurements N88-29976
Alternative immersion accelerated testing of coating systems for Naval shoreline facilities N88-29977
The effect of notch root radius on the determination of toughness in ultrahigh strength steel friction welds
[AD-A195952] N88-30156
Response of SMA (Shielded Metal Arc) and narrow gap HY80 weldments to explosive shock loading
[AD-A195994] N88-30162

STELLAR ACTIVITY
Starbursts and their dynamics
[NASA-CR-180227] N88-30549

STELLAR ATMOSPHERES
Evolutionary helium and CNO anomalies in the atmospheres and winds of massive hot stars
[NASA-CR-183254] N88-30550

STELLAR COMPOSITION
Radial velocity measurements of a sample of northern metal-deficient stars
[SER-C-PREPUBL-FASC-25] N88-30564

STELLAR EVOLUTION
Evolutionary helium and CNO anomalies in the atmospheres and winds of massive hot stars
[NASA-CR-183254] N88-30550
Radio and infrared properties of young stars
[NASA-CR-183252] N88-30579

STELLAR MOTIONS
The kinematics of late-type supergiants
[SER-C-PREPUBL-FASC-28] N88-30560

STELLAR ORBITS
Duplicity in the solar neighborhood: Part 4: Spectroscopic orbits for four dwarf M stars
[SER-C-PREPUBL-FASC-21] N88-30561
Orbital stability in rotating triaxial stellar systems
[SER-C-PREPUBL-FASC-24] N88-30569

STELLAR OSCILLATIONS
The ultrashort period dwarf nova SW Ursae Majoris N88-30553

STELLAR PHYSICS
Activities in astrophysics
[INPE-4582-PRE/1316] N88-30570

STELLAR RADIATION
Radio and infrared properties of young stars
[NASA-CR-183252] N88-30579

STELLAR ROTATION
Orbital stability in rotating triaxial stellar systems
[SER-C-PREPUBL-FASC-24] N88-30569

STELLAR SPECTRA
The ultrashort period dwarf nova SW Ursae Majoris N88-30553
Duplicity in the solar neighborhood: Part 5: Spectroscopic orbit for the nearby double-lined solar-type star HR 8581
[SER-C-PREPUBL-FASC-23] N88-30562

STELLAR SPECTROPHOTOMETRY
A new determination of the Geneva photometric passbands and their absolute calibration
[SER-C-PREPUBL-FASC-26] N88-30548

STELLAR SYSTEMS
Orbital stability in rotating triaxial stellar systems
[SER-C-PREPUBL-FASC-24] N88-30569

STELLAR WINDS
Evolutionary helium and CNO anomalies in the atmospheres and winds of massive hot stars
[NASA-CR-183254] N88-30550

STEREOSCOPIC VISION
Multilevel computational theory of stereoscopic visual image processing
[AD-A195331] N88-30288

STIFFNESS
Damage initiation in the short beam shear test of composite materials using stiffness reduction
[AD-A194880] N88-29883
Nonlinear stress-strain and inelastic rebound with exponential stiffness
[AD-A195667] N88-30159

STIFFNESS MATRIX
Geometric and material nonlinear analysis of structures comprising rectangular hollow sections
[CE-79] N88-30141

STIRLING ENGINES
Testing of a variable-stroke Stirling engine
[NASA-TM-100899] N88-30472

STOCHASTIC PROCESSES
Theory of filtering and control with application to control of large space structures
[AD-A195500] N88-29851
Statistical analysis of the LMS (Last Mean Squares) and modified stochastic gradient
[AD-A195497] N88-30376
Stability, stochastic stationarity and generalized Lyapunov equations for two-point boundary-value descriptor systems
[AD-A195645] N88-30385
Analytical methods in stochastic control and nonlinear filtering
[AD-A194272] N88-30388

STORAGE BATTERIES
Structure and dynamics of solutions of lithium salts relevant to battery construction
[AD-A195399] N88-30044

STORMS
Passive microwave measurements of water vapor fields and rain for locating fronts in cyclonic storms
[AD-A195632] N88-30267

STRAIN GAGES
Electrical properties of materials for elevated temperature resistance strain gage application
[NASA-CR-182214] N88-30106
Method of attaching strain gauges to various materials
[NASA-CASE-LAR-13797-1] N88-30109

STRAIN MEASUREMENT
Piezoelectric and electrostrictive materials for transducer applications, volume 2
[AD-A194956] N88-30104

STRAPDOWN INERTIAL GUIDANCE
The NAE atmospheric research aircraft N88-29730

STRATEGY
The advice taker/inquirer: A system for high-level acquisition of expert knowledge N88-30359
Antisatellite weapons and satellite deployment strategies
[AD-A195014] N88-30396

STRATIFICATION
Role of ordinary to extraordinary mode wave coupling in ionospheric heating experiments
[AD-A195335] N88-30017
Mathematical problems of nonlinear wave propagation and of waves in heterogeneous media
[AD-A195970] N88-30057

STRATIGRAPHY
Deep seismic reflection profiling and continental growth curves N88-30222

STRATOSPHERE
Changes in stratospheric ozone: Observations and theories
[AERONOMICA-ACTA-A-334-1988] N88-30188
Possibilities of determining vertical profiles of microphysical characteristics of stratospheric aerosol using space measurements of transparency and solar halo N88-30526

STRESS (PHYSIOLOGY)
Accidental hypothermia
[AD-A194967] N88-30278

STRESS (PSYCHOLOGY)
Central adrenergic receptors as mediators of central response to stress: Study with Positron Emission Tomography (PET)
[AD-A194947] N88-30284

STRESS ANALYSIS
Aeroelastic response of metallic and composite propfan models in yawed flow
[NASA-TM-100964] N88-29807
Thermal stress analysis in PMR-15 carbon fibre laminates
[ETN-88-93123] N88-29886
Stresses in cylindrical shells with tangential nozzles submitted to external loads and internal pressure
[CRIF-MT-172] N88-30146
Determination of multiaxial flow surfaces at elevated temperatures using the concept of dissipation potential
[ORNL/TM-10787] N88-30149
STRESS DISTRIBUTION
A test for interfacial effects and stress transfer in ceramic matrix composites
[NASA-CR-182873] N88-29880
Particle size measurements in sooting combustion systems N88-29931
STRESS INTENSITY FACTORS
Stress intensity factors for cracked metallic structures under rapid thermal loading
[AES-8609709F-1] N88-29962
Wide range stress intensity factor expression for an edge-cracked round bar bend specimen
[AD-A196285] N88-30147
Obtaining stress intensity factors on cracks, by means of fitting techniques on numerical results calculated with the finite element method N88-30153
STRESS MEASUREMENT
Report on an overseas visit to USA relating to the thermoelastic measurement of stresses, 16-21 August 1987
[AD-A195313] N88-30161
STRESS-STRAIN RELATIONSHIPS
Anisotropic constitutive modeling for nickel-base single crystal superalloys
[NASA-CR-182157] N88-29961
Nonlinear stress-strain and inelastic rebound with exponential stiffness
[AD-A195667] N88-30159
STRESSES
Stress related failures causing open metallization
[AD-A195081] N88-30150
STRING THEORY
Introduction to string theory
[DE88-702706] N88-30445
STRONGLY COUPLED PLASMAS
Role of ordinary to extraordinary mode wave coupling in ionospheric heating experiments
[AD-A195335] N88-30017
STRONTIUM
Lewis Cliff 86010, a unique Antarctic meteorite: Possible new clues to the early history of the solar system N88-30482
STRUCTURAL ANALYSIS
Computer programs for generation of NASTRAN and VIBRA-6 aircraft models
[AD-A195467] N88-29792
Constitutive modeling for isotropic materials
[NASA-CR-182132] N88-29811
Attenuated total reflectance FT-IR spectroscopy to measure interfacial reaction kinetics at silica surfaces
[AD-A196330] N88-29908
Stress intensity factors for cracked metallic structures under rapid thermal loading
[AES-8609709F-1] N88-29962
Analytical and experimental studies of beam waveguide absorbers for structural damping
[AD-A195085] N88-30144
Computer-Aided Structural Engineering (CASE) project. Development of design formulas for ribbed mat foundations on expansive soils
[AD-A194807] N88-30307
Computer-Aided Structural Engineering (CASE) project. Computer program for analysis of planar grid structures (CGRID), user's guide
[AD-A195977] N88-30317
Structuring processes in expanding laser-produced plasmas
[AD-A195249] N88-30424
Structural dynamics of high-latitude magnetosphere determined from solar electron data N88-30500
STRUCTURAL DESIGN
Comparison of the influence of different gust models on structural design N88-29722
Lunar lander conceptual design: Lunar base systems study task 2.2
[NASA-CR-172051] N88-29654
Gas turbine combustion modeling N88-29936
A small annular combustor of high power density, wide operating range and low manufacturing cost N88-29951
Alternative module configurations for advanced solar arrays on low orbit and extended lifetime missions (AMOC 2)
[ESA-CR(P)-2581] N88-30182
The space station assembly phase: System design trade-offs for the flight telerobotic servicer N88-30357
STRUCTURAL ENGINEERING
Computer-Aided Structural Engineering (CASE) project. Development of design formulas for ribbed mat foundations on expansive soils
[AD-A194807] N88-30307
Computer-Aided Structural Engineering (CASE) project. Computer program for analysis of planar grid structures (CGRID), user's guide
[AD-A195977] N88-30317
STRUCTURAL FAILURE
The development of acoustic emission for structural integrity monitoring of aircraft
[AD-A196264] N88-30398
STRUCTURAL MEMBERS
Dynamics of articulated aerospace structures
[AD-A195685] N88-29794
STRUCTURAL PROPERTIES (GEOLOGY)
Diapirs of the Mediterranean ridge: The tectonic regime of an incipient accreted terrane N88-30224
The tectonic setting of the Seychelles, Mascarene and Amirante Plateaus in the Western Equatorial Indian Ocean N88-30225
Ridge-trench collision in Archean and Post-Archean crustal growth: Evidence from southern Chile N88-30233
Reappraisal of the geology of Kangimut Sammisoq, Ameralik Fjord, Southern West Greenland: Crustal structure and interpretation of isotopic data N88-30234
Archean crustal evolution of the northern North China Craton N88-30235
Evolution of the Dharwar Craton: A terrain of early Archean crustal stability, long term orogenic cycles and large scale palaeobiological activity N88-30241
Spectral analysis of the Elatina varve series
[NASA-CR-183085] N88-30260
Debris flows of the Simud-Tiu outflow system of Mars N88-30485
High-resolution (30 m) lunar radar images N88-30486
Mars: Volcanism in the Valles Marineris overlooked N88-30491
The Martian highland paterae: Evidence for explosive volcanism on Mars N88-30492
Physical properties of surface materials on Martian volcanoes: Dust-covered lava and ash N88-30493
Rifts of deeply eroded Hawaiian basaltic shields: A structural analog for large Martian volcanoes N88-30494
Small-scale volcanic landforms indicative of distributary lube systems N88-30496
STRUCTURAL RELIABILITY
Automated early fatigue damage sensing system
[AD-A195717] N88-30143
STRUTS
Test of an 0.8-scale model of the AH-64 Apache in the NASA Langley full-scale wind tunnel
[AD-A196129] N88-29768
SUBDUCTION (GEOLOGY)
Recycling of lower continental crust through foundering of cumulates from contaminated mafic intrusions N88-30204
Pluton emplacement and magmatic arc construction: A model from the Patagonian batholith N88-30206
An illustration of the complexity of continent formation N88-30207
Does subduction zone magmatism produce average continental crust N88-30214
Decoupled Rb-Sr and Sm-Nd isotopic evolution of the continental crust N88-30216
Continental crustal formation and recycling: Evidence from oceanic basalts N88-30238
Continental growth through time by underplating of subducted oceanic crust: Evidence from kimberlites in South Africa and SW Pacific N88-30244
SUBMARINES
Numerical field model simulation of full scale fire tests in a closed spherical/cylindrical vessel
[AD-A195067] N88-29998
Response of SMA (Shielded Metal Arc) and narrow gap HY80 weldments to explosive shock loading
[AD-A195994] N88-30162
SUBMERGING
Alternative immersion accelerated testing of coating systems for Naval shoreline facilities N88-29977
SUBMILLIMETER WAVES
A submillimeter wavelength space-based imaging radar
[AD-A195848] N88-30033
The study of hydromagnetic waves and RF heating using the TORTUS tokamak, the development of diagnostic techniques based on submillimeter lasers and the gyrotron, and gas discharge N88-30419
SUBSONIC SPEED
Pressure distributions from subsonic tests of an advanced laminar-flow-control wing with leading- and trailing-edge flaps
[NASA-TM-4040-PT-2] N88-29776
SUBSTRATES
Evaluation of organic coating deterioration and substrate corrosion in seawater using electrochemical impedance measurements N88-29976
Ion exchange processes for fabrication of integrated optical waveguide structures into glass substrates
[VTT-46] N88-30405
SUCTION
Experimental and numerical investigation of the effect of distributed suction on oblique shock wave/turbulent boundary layer interaction
[NASA-TM-101334] N88-30084
SULFUR
Hydrogen embrittlement of iron-nickel alloys
[AD-A195909] N88-29958
SUNSPOTS
Spectral analysis of the Elatina varve series
[NASA-CR-183085] N88-30260
SUPERCOMPUTERS
Supermap for Cray FORTRAN: A user's guide
[NASA-CR-177410] N88-30308
SUPERCONDUCTIVITY
Theory of superconductivity in oxides
[AD-A195647] N88-30432
Behaviour and hysteresis losses of irreversible type-2 superconducting cylindrical shell
[DE88-702708] N88-30434
SUPERGIANT STARS
Evolutionary helium and CNO anomalies in the atmospheres and winds of massive hot stars
[NASA-CR-183254] N88-30550
The kinematics of late-type supergiants
[SER-C-PREPUBL-FASC-28] N88-30560
SUPERGRAVITY
Lagrangian of the self-duality equation and d = 10, N = 2b supergravity
[DE88-701554] N88-30563
SUPERNOVA 1987A
Astron observations of supernova 1987A in large magellanic cloud N88-30504
SUPERNOVAE
Gamma radiation expected from supernova 1987A in large magellanic cloud N88-30505
Activities report in astronomy
[ISSN-0531-4496] N88-30535
SUPERSONIC AIRCRAFT
An analysis of lateral-directional handling qualities and Eigenstructure of high performance aircraft
[AD-A194874] N88-29814
SUPERSONIC FLOW
Accuracy criteria for evaluating supersonic aerodynamic coefficient predictions N88-29756
Compression pylon
[NASA-CASE-LAR-13777-1] N88-29789
SUPERSONIC TURBINES
Numerical solutions of unsteady inviscid transonic turbine cascade flows
[AD-A196111] N88-29748
SUPERSONIC WIND TUNNELS
Supersonic wall adaptation in the rubber tube test section of the DFVLR Goettingen
[IB-222-87-A-08] N88-29824
SUPERSYMMETRY
Lagrangian of the self-duality equation and d = 10, N = 2b supergravity
[DE88-701554] N88-30563
SUPPLYING
Maintenance and supply options
[NASA-CR-172062] N88-29837
SUPPORT SYSTEMS
Definition of common support equipment and space station interface requirements for IOC model technology experiments
[NASA-TM-100656] N88-29856
SURFACE COOLING
Studies of gas turbine heat transfer airfoil surface and end-wall cooling effects
[AD-A195165] N88-29805
SURFACE NAVIGATION
Measurement and interpretation of North Atlantic Ocean marine radar sea scatter
[AD-A196239] N88-30036
SURFACE PROPERTIES
Experimental determination of drag modifications due to elastic compliant surfaces using quantitative visual techniques
[AD-A194785] N88-30082

SURFACE REACTIONS
Quantitative surface temperature measurement using two-color thermographic phosphors and video equipment
[NASA-CASE-LAR-13740-1] N88-30105
Cosmochemical trends of volatile elements in the solar system N88-30542
SURFACE STABILITY
Empirical flutter prediction method
[AD-A195699] N88-29810
Mathematical problems of nonlinear wave propagation and of waves in heterogeneous media
[AD-A195970] N88-30057
SURFACE TEMPERATURE
Measurement and interpretation of North Atlantic Ocean marine radar sea scatter
[AD-A196239] N88-30036
Measurement of local high-level, transient surface heat flux
[NASA-TP-2840] N88-30099
Energy budget and ground temperatures in hot regions
[AD-A196298] N88-30268
SURFACTANTS
Attenuated total reflectance FT-IR spectroscopy to measure interfacial reaction kinetics at silica surfaces
[AD-A196330] N88-29908
SURVEILLANCE RADAR
Evaluation of LISBON TAR SSR radar
[EEC/NOTE-5/87] N88-30015
SURVEYS
The use of orbital remote sensing data for low cost ground-water survey
[INPE-4587-PRE/1318] N88-30170
A dynamic analysis of piezoelectric strained elements
[AD-A196079] N88-30430
A deep redshift survey of field galaxies. Comments on the reality of the Butcher-Oemler effect
[NASA-CR-183255] N88-30558
Antarctic Meteorite Newsletter, Volume 11, Number 2, August 1988
[NASA-TM-89801] N88-30573
SURVIVAL
Accidental hypothermia
[AD-A194967] N88-30278
SWEPT WINGS
Techniques used in the F-14 variable-sweep transition flight experiment
[NASA-TM-100444] N88-30093
SWIRLING
Euler analysis of a swirl recovery vane design for use with an advanced single-rotation propfan
[NASA-TM-101357] N88-29771
Analysis of the flow through double swirl airblast atomizers N88-29949
Development of a more general Reynolds stress closure for swirling flow
[AD-A195121] N88-30092
SWITCHES
Consideration of plasma opening switches from a wave propagation perspective
[AD-A195681] N88-30421
SWITCHING
Optics and symbolic computing
[AD-A195119] N88-30004
Piezoelectric and electrostrictive materials for transducer applications, volume 2
[AD-A194956] N88-30104
Use of depletion edge translation for high-speed modulation and switching of lightwaves
[AD-A195611] N88-30417
SYMBOLIC PROGRAMMING
Optics and symbolic computing
[AD-A195119] N88-30004
Optical symbolic computing
[AD-A195690] N88-30406
SYNCHRONISM
Synchronous response modelling and control of an annular momentum control device
[NASA-CR-4166] N88-29995
SYNCHRONOUS MOTORS
Voltage directive drive with claw pole motor and control without rotor position indicator
[ETN-88-93120] N88-30047
SYNCHROTRON RADIATION
X-ray diffraction imaging (topography) of electrooptic crystals by synchrotron radiation
[NASA-CR-183266] N88-30427
Diffraction imaging (topography) with monochromatic synchrotron radiation
[NASA-CR-183264] N88-30431
Streaking images that appear only in the plane of diffraction in undoped GaAs single crystals: Diffraction imaging (topography) by monochromatic synchrotron radiation
[NASA-CR-183267] N88-30437
Applications of synchrotron radiation to materials science: Diffraction imaging (topography) and microradiography
[NASA-CR-183265] N88-30440
SYNTAX
Exploiting lexical regularities in designing natural language systems
[AD-A195922] N88-30375
SYNTHESIS (CHEMISTRY)
Novel ladder polymers for use as high temperature stable resins or coatings
[NASA-CASE-LEW-14203-1] N88-29984
SYNTHETIC APERTURE RADAR
Acoustooptic processing of two-dimensional signals using temporal and spatial integration
[AD-A194803] N88-29999
A submillimeter wavelength space-based imaging radar
[AD-A195846] N88-30033
MIZEX (marginal ice zone experiment) 1987 SAR (Synthetic Aperture Radar) data summary
[AD-A195560] N88-30035
SYNTHETIC FUELS
The behaviour of synthetic fuels in a small transparent combustor N88-29950
SYSTEM EFFECTIVENESS
The OFP (Operational Flight Program) update cycle needs you
[AD-A194910] N88-29798
Controlled degradation of resolution of high-quality flight simulator images for training effectiveness evaluation
[AD-A196189] N88-29823
SYSTEMS ANALYSIS
Knowledge based simulation: An artificial intelligence approach to system modeling and automating the simulation life cycle
[AD-A195838] N88-30372
Center for opto-electronic systems research
[AD-A195159] N88-30411
SYSTEMS ENGINEERING
Study of robotics spacecraft servicing and assembly in space. Volume 1: Executive summary
[ESA-CR(P)-2612-VOL-1] N88-29839
Accommodation concept for fluid physics facilities, volume 2 — Spacelab
[SG-TN-AI-027-VOL-2] N88-29994
A detection theory analysis of visual display performance
[AD-A196291] N88-30292
Study of human factors engineering criteria for extravehicular activity (EVA) systems, volume 1
[STF23-F87025-VOL-1] N88-30298
Knowledge-based integrated information systems engineering: Highlights and bibliography. Knowledge-Based Integrated Information Systems Engineering (KBIISE) Project, volume 1
[AD-A195850] N88-30449
Technical opinions regarding knowledge-based integrated information systems engineering, volume 8
[AD-A195857] N88-30454
Knowledge-Based Integrated Information Systems Development Methodologies Plan. Knowledge-Based Integrated Information Systems Engineering (KBIISE) report, volume 2
[AD-A195851] N88-30455
SYSTEMS INTEGRATION
Knowledge-based integrated information systems engineering: Highlights and bibliography. Knowledge-Based Integrated Information Systems Engineering (KBIISE) Project, volume 1
[AD-A195850] N88-30449
Knowledge-Based Integrated Information Systems Development Methodologies Plan. Knowledge-Based Integrated Information Systems Engineering (KBIISE) report, volume 2
[AD-A195851] N88-30455
Integrating information systems in a major decentralized international organization, volume 7
[AD-A195856] N88-30468
SYSTEMS SIMULATION
Design and development of a refueling test bed
[FTMS-RP-ER-011] N88-29986
Improvements of DCAP 1, phase 2-3/A
[D2-RP-AI-106] N88-30325

T

TARGET RECOGNITION
Modeling and performance of HF/OTH (High-Frequency/Over-the-Horizon) radar target identification systems
[AD-A196287] N88-30038
TARGETS
Comparative aspects of multiple processes of attention
[AD-A195805] N88-30291
TDR SATELLITES
Optical multiple access intersatellite links
[BAE-TP-8502] N88-30013
TECHNOLOGY ASSESSMENT
Constitutive modeling for isotropic materials
[NASA-CR-182132] N88-29811
Study on conceptual design of spacecraft using Computer Aided Engineering (CAE)
[SNIAS-920-CA/TS] N88-29841
Study of the assembly, integration and verification programs of telecommunication satellites applicable to other satellite programs
[MATRA-100/CC/MLG/031/87] N88-29847
Space structure (dynamics and control) theme development
[NASA-TM-100597] N88-29850
Definition of common support equipment and space station interface requirements for IOC model technology experiments
[NASA-TM-100656] N88-29856
TECHNOLOGY TRANSFER
China's acquisition and use of foreign aviation technology
[AD-A194827] N88-30471
Research and technology of the Lyndon B. Johnson Space Center
[NASA-TM-100463] N88-30583
TECHNOLOGY UTILIZATION
China's acquisition and use of foreign aviation technology
[AD-A194827] N88-30471
TECTONICS
Workshop on the Growth of Continental Crust
[NASA-CR-183073] N88-30201
Structure of Southwestern Michipicoten Greenstone Belt, Ontario: Evidence for Archean accretion N88-30228
The tectonic setting of Archean anorthosites N88-30231
Crustal growth in the Archean: The geochemical evidence N88-30246
NASA MEVTV Program Working Group Meeting: Volcanism on Mars
[NASA-CR-183074] N88-30487
TELECOMMUNICATION
Long haul communications in the HF spectrum utilizing high speed modems
[AD-A194683] N88-30003
Design of a self-timed VLSI multicomputer communication controller
[AD-A194567] N88-30014
A static scheduler for the computer aided prototyping system: An implementation guide
[AD-A194340] N88-30322
Statistical analysis of the LMS (Last Mean Squares) and modified stochastic gradient
[AD-A195497] N88-30376
Integrating images, applications, and communications networks, volume 5
[AD-A195854] N88-30452
Information technology to facilitate group interaction N88-30463
Using standards to break down information transfer barriers N88-30467
TELEMETRY
Accuracy of satellite data navigation
[AD-A195877] N88-29787
Mission telemetry system monitor: A real-time knowledge-based system N88-30345
Automated cataloging and characterization of space-derived data N88-30354
TELEOPERATORS
Low level image processing techniques using the pipeline image processing engine in the flight telerobotic servicer N88-30346
The space station assembly phase: System design trade-offs for the flight telerobotic servicer N88-30357
TELESCOPES
NASA Marshall Space Flight Center solar observatory
[NASA-TM-100339] N88-29832
Binary star measurements using digital speckle interferometer of 6-m telescope N88-30521
Activities report in astronomy
[ISSN-0531-4496] N88-30535
TEMPERATURE CONTROL
Experimental and analytical study of two-phase flow in zero gravity
[AD-A195223] N88-29993
TEMPERATURE DISTRIBUTION
The thermal behavior of film cooled turbulent boundary layers as affected by longitudinal vortices
[AD-A195155] N88-30095

Theoretical modeling of accelerating arc plasmas
[AD-A195606] N88-30426

TEMPERATURE EFFECTS
Thermal stress analysis in PMR-15 carbon fibre laminates
[ETN-88-93123] N88-29886
Effect of interfacial phenomena on contact line heat Transfer-3
[AD-A194941] N88-29901
The thermal behavior of film cooled turbulent boundary layers as affected by longitudinal vortices
[AD-A195155] N88-30095
Study of human factors engineering criteria for Extra Vehicular Activity (EVA) systems, volume 2
[STF23-F87025-VOL-2] N88-30293

TEMPERATURE MEASUREMENT
Energy conversion measurements in laser-sustained argon plasmas for application to rocket propulsion
[AD-A194931] N88-29861
Measurement of local high-level, transient surface heat flux
[NASA-TP-2840] N88-30099
Quantitative surface temperature measurement using two-color thermographic phosphors and video equipment
[NASA-CASE-LAR-13740-1] N88-30105
Estimation of soil temperature profile from remote microwave and IR measurements N88-30532

TEMPERATURE MEASURING INSTRUMENTS
Measurement of local high-level, transient surface heat flux
[NASA-TP-2840] N88-30099

TEMPERATURE PROFILES
Temperature profile construction methods: An evaluation
[AD-A195919] N88-30262

TEMPORAL DISTRIBUTION
Mineralization through geologic time: Evolution of continental crust N88-30250

TENSILE PROPERTIES
Some effects of nitrates on the tensile properties of Al 7075-T7351
[AD-A195118] N88-29965

TENSILE STRESS
Nonlinear stress-strain and inelastic rebound with exponential stiffness
[AD-A195667] N88-30159

TENSORS
New methods for nonlinear optimization
[AD-A195862] N88-30313
The triangle: A multiprocessor architecture for fast curve and surface generation
[AD-A195882] N88-30324

TERMINAL BALLISTICS
Review of research concerning Solid Fuel Ramjet (SOFRAM) at the Research Institute of National Defence (FOA) 2
[FOA-C-20714-2.1] N88-29813

TERRAIN
Evolution of the Dharwar Craton: A terrain of early Archean crustal stability, long term orogenic cycles and large scale palaeobiological activity N88-30241
Crustal growth in the Archean: The geochemical evidence N88-30246

TERRAIN ANALYSIS
Relief effect correction on LANDSAT imagery for forest applications using digital terrain models
[INPE-4611-PRE/1334] N88-30179
A digital terrain model system for a microcomputer
[INPE-4610-PRE/1333] N88-30316

TERRESTRIAL RADIATION
Energy budget and ground temperatures in hot regions
[AD-A196298] N88-30268

TEST CHAMBERS
Development of computer-controlled thermogravimetric instrumentation for measurement of environmental and high temperature volatilization and desorption of contaminants from polymeric materials
[AD-A195934] N88-29900

TEST FACILITIES
Development and design of windtunnel and test facility for RPV (Remote Piloted Vehicle) enhancement devices
[AD-A194842] N88-29822
Design and development of a refueling test bed
[FTMS-RP-ER-011] N88-29986
Numerical field model simulation of full scale fire tests in a closed spherical/cylindrical vessel
[AD-A195067] N88-29998
Development and installation of an instrumentation package for GE F404 investigative testing
[AD-A196265] N88-30107
The dynamics of transuranics and other radionuclides in natural environments, December 1985
[DE87-014456] N88-30189

Maximum-likelihood multichannel deconvolution of P waves at seismic arrays
[AD-A194990] N88-30191

TEST FIRING
Orbital transfer vehicle 3000 LBF thrust chamber assembly hot fire test program
[NASA-CR-182145] N88-29858

TEST RANGES
Development of procedures for performing end-to-end tests on the ERS-1 radar altimeter and AMI using a compact antenna test range — Active Microwave Instrument (AMI)
[ESA-CR(P)-2558] N88-30022

TF-30 ENGINE
Fuel property effects on the US Navy's TF30 engine N88-29911

THEMATIC MAPPERS (LANDSAT)
TM/LANDSAT-5 data to evaluate wheat and bean percent soil cover and leaf area index
[INPE-4609-PRE/1332] N88-30165
LANDSAT-TM data to map flooded areas
[INPE-4594-PRE/1324] N88-30177

THEORETICAL PHYSICS
Introduction to string theory
[DE88-702706] N88-30445

THERMAL ANALYSIS
Principles of the optical differential thermal analysis
[AD-A195951] N88-30408
Evolution of thermal structure of Bengueia upswelling system according to satellite and shipboard data N88-30525

THERMAL BOUNDARY LAYER
Thermal models pertaining to continental growth N88-30230

THERMAL ENVIRONMENTS
Experimental and analytical study of two-phase flow in zero gravity
[AD-A195223] N88-29993

THERMAL EXPANSION
Transverse expansion of individual carbon and graphite filaments
[AD-A195073] N88-29891

THERMAL PLASMAS
Reconstruction of wave distribution functions in warm plasmas
[IRF-PREPRINT-104] N88-30422

THERMAL RADIATION
Combustion and fuels in gas turbine engines
[AGARD-CP-422] N88-29910
Radiation from soot-containing flames N88-29927
Flamelet chemistry modelling of soot formation for radiation N88-29928
Radiation transfer in gas turbine combustors N88-29929
Degradation of protective coatings on steel in corrosive environments N88-29969

THERMAL STRESSES
Analytical study of graphite-epoxy tube response to thermal loads
[NASA-CR-183215] N88-29884
Thermal stress analysis in PMR-15 carbon fibre laminates
[ETN-88-93123] N88-29886
Transverse expansion of individual carbon and graphite filaments
[AD-A195073] N88-29891
Stress intensity factors for cracked metallic structures under rapid thermal loading
[AES-8609709F-1] N88-29962

THERMISTORS
Effect of interfacial phenomena on contact line heat Transfer-3
[AD-A194941] N88-29901

THERMOCHEMISTRY
Gas phase combustion chemistry of nitramine propellants
[AD-A195082] N88-29902
Three-dimensional combustor predictors: A comparison of equilibrium and laminar flamelet chemistry models N88-29940

THERMODYNAMIC PROPERTIES
Some theoretical considerations of the surface tension of liquid metals for metal matrix composites
[AD-A195999] N88-29882
Thermomechanical computations for GAP, a high energy binder for composite propellants
[FOA-C-20718-2.1] N88-29988
Particle trajectories and potentials in a plane sheath moving in a magnetoplasma
[AD-A196228] N88-30190
The origin of the moon: Further studies of the giant impact N88-30474

THERMODYNAMICS
Experimental and analytical study of two-phase flow in zero gravity
[AD-A195223] N88-29993

THERMOELASTICITY
Report on an overseas visit to USA relating to the thermoelastic measurement of stresses, 16-21 August 1987
[AD-A195313] N88-30161

THERMOGRAVIMETRY
Development of computer-controlled thermogravimetric instrumentation for measurement of environmental and high temperature volatilization and desorption of contaminants from polymeric materials
[AD-A195934] N88-29900

THERMOREGULATION
Accidental hypothermia
[AD-A194967] N88-30278

THERMOSPHERE
An improvement in the numerical integration procedure used in the NASA Marshall engineering thermosphere model
[NASA-CR-179389] N88-30200

THESAURI
Exploiting lexical regularities in designing natural language systems
[AD-A195922] N88-30375

THICKNESS
The use of hot-film technique for boundary layer studies on a 21 percent thick airfoil
[NAE-AN-45] N88-29781
Predicting the durability of adhesives and coatings by remote detection of hidden defects and coating-thickness irregularities: A theoretical and numerical study N88-29972

THIN FILMS
Stress related failures causing open metallization
[AD-A195061] N88-30150
A review of melt and vapor growth techniques for polydiacetylene thin films for nonlinear optical applications
[NASA-TM-100340] N88-30412
Cluster beam studies
[AD-A195182] N88-30443

THIN WALLED SHELLS
Geometric and material nonlinear analysis of structures comprising rectangular hollow sections
[CE-79] N88-30141

THREAT EVALUATION
Threat expert system technology advisor
[NASA-CR-177479] N88-29816

THREE BODY PROBLEM
Families of periodic solutions in problem of solid body rotation at triangular libration point in restricted three-body problem N88-30508

THREE DIMENSIONAL BOUNDARY LAYER
User's manual for three dimensional boundary layer (BL3-D) code
[NASA-CR-174899] N88-30063
Assessment of a 3-D boundary layer analysis to predict heat transfer and flow field in a turbine passage
[NASA-CR-174894] N88-30066

THREE DIMENSIONAL FLOW
Three-dimensional Navier-Stokes simulations of turbine rotor-stator interaction
[NASA-TM-100081] N88-29750
Three-dimensional combustor predictors: A comparison of equilibrium and laminar flamelet chemistry models N88-29940
An analysis of finite-difference and finite-volume formulations of conservation laws
[NASA-CR-177416] N88-30071

THREE DIMENSIONAL MODELS
Three-dimensional elliptic grid generation technique with application to turbomachinery cascades
[NASA-TM-101330] N88-30078
Geometric modeling for computer aided design
[NASA-CR-183161] N88-30320

THRUST
Iridium-coated rhenium thrusters by CVD
[NASA-TM-101309] N88-29874

THRUST CHAMBERS
Orbital transfer vehicle 3000 LBF thrust chamber assembly hot fire test program
[NASA-CR-182145] N88-29858

THRUST PROGRAMMING
The eivaN: A forward-looking interactive orbital trajectory plotting tool for use with proximity operations (PROX OPS) and other maneuvers: Description and user's manual
[NASA-CR-177490] N88-30327

THRUST REVERSAL
Aerodynamics in ground effect and predicted landing ground roll of a fighter configuration with a secondary-nozzle thrust reverser
[NASA-TP-2834] N88-29752

TIME DEPENDENCE
Numerical methods: Euler time dependent solver N88-29760

TIME DISCRIMINATION
Comparative aspects of multiple processes of attention
[AD-A195805] N88-30291
TIME DIVISION MULTIPLE ACCESS
A 30/20 GHz multibeam array antenna suitable for future high rate TDMA European satellite networks
[ETN-88-93079] N88-30037
TIME OF FLIGHT SPECTROMETERS
Impurity analysis in SIMOX samples by high-efficiency resonance ionization time-of-flight mass spectrometry
[DE88-012061] N88-30051
TIMOSHENKO BEAMS
Analytical and experimental studies of beam waveguide absorbers for structural damping
[AD-A195085] N88-30144
TIN
Use of digital images as a mineral prospecting tool in the tin province of Goias, Brazil
[INPE-4537-PRE/1284] N88-30173
TITAN
Microwave instrument for planetary mission (Titan/CASSINI mission orbiter spacecraft)
[BAE-CS/TP-8359] N88-30102
TITAN LAUNCH VEHICLES
Reduced flexibility in processing Titan 4 space launch vehicles at Cape Canaveral Air Force Station
[AD-A194908] N88-29834
TITANIUM
Electrical properties of materials for elevated temperature resistance strain gage application
[NASA-CR-182214] N88-30106
TITRATION
Titrimetric analysis of HAN-based liquid propellants
[AD-A196225] N88-29990
TOKAMAK DEVICES
The study of hydromagnetic waves and RF heating using the TORTUS tokamak, the development of diagnostic techniques based on submillimeter lasers and the gyrotron, and gas discharge N88-30419
TOLERANCES (PHYSIOLOGY)
Evaluation of the potential health hazards associated with the machining of carbon fiber composites
[AD-A194835] N88-30286
TOLLMEIN-SCHLICHTING WAVES
Nonlinear Tollmien-Schlichting/vortex interaction in boundary layers
[NASA-CR-181698] N88-29715
The strong nonlinear interaction of Tollmien-Schlichting waves and Taylor-Goertler vortices in curved channel flow
[NASA-CR-181697] N88-29716
On the generation of mean flows by the interaction of Goertler vortices and Tollmien-Schlichting waves in curved channel flows
[NASA-CR-191690] N88-29743
TOLUENE
Study of toluene stability for an Organic Rankine Cycle (ORC) space-based power system
[NASA-CR-180884] N88-29863
Study of toluene rotary fluid management device and shear flow condenser performance for a space-based organic Rankine power system
[NASA-CR-180885] N88-29872
TOMOGRAPHY
Positron emission tomography: A new technique for observing fluid behavior in engineering systems
[PNR90471] N88-30091
Central adrenergic receptors as mediators of central response to stress: Study with Positron Emission Tomography (PET)
[AD-A194947] N88-30284
TOPEX
Specifications and performance of ultrastable oscillators in the DORIS orbitography and positioning system
[ETN-88-92761] N88-29831
TOPOGRAPHY
Finite-difference simulations of Rayleigh-wave scattering by shallow heterogeneity
[AD-A194961] N88-30259
X-ray diffraction imaging (topography) of electrooptic crystals by synchrotron radiation
[NASA-CR-183266] N88-30427
Streaking images that appear only in the plane of diffraction in undoped GaAs single crystals: Diffraction imaging (topography) by monochromatic synchrotron radiation
[NASA-CR-183267] N88-30437
Physical properties of surface materials on Martian volcanoes: Dust-covered lava and ash N88-30493
Obligue metallogenic zones recognized by interpreting space photographs of southern Tien Shan N88-30529
Structure of eastern Turkestan Ridge based on space photographs N88-30530
TOROIDAL PLASMAS
RFP (Revised Field Pinch) plasma experiment at INPE
[INPE-4613-PRE/1336] N88-30420
TRACE ELEMENTS
Role of zircon in tracing crustal growth and recycling N88-30211
Trace element differences between Archean, Proterozoic and Phanerozoic crustal components: Implications for crustal growth processes N88-30243
TRACKING (POSITION)
Observed track-keeping performance of DC10 aircraft equipped with the Collins AINS-70 area navigation system: Karlsruhe and Maastricht UACs (Upper Area Control centres)
[EEC-202] N88-29788
Analysis of environmental parameters from the Panama City tower radar experiment
[AD-A194994] N88-30264
Dynamical systems and motion vision
[AD-A195932] N88-30366
TRAILING EDGE FLAPS
Pressure distributions from subsonic tests of an advanced laminar-flow-control wing with leading- and trailing-edge flaps
[NASA-TM-4040-PT-2] N88-29776
TRAINING EVALUATION
Controlled degradation of resolution of high-quality flight simulator images for training effectiveness evaluation
[AD-A196189] N88-29823
Improvement of head-up display standards. Volume 3: An evaluation of head-up display safety
[AD-A195787] N88-30300
TRAINING SIMULATORS
Controlled degradation of resolution of high-quality flight simulator images for training effectiveness evaluation
[AD-A196189] N88-29823
LANTIRN simulator training in the F-16C
[AD-A195201] N88-29826
TRAJECTORY ANALYSIS
Computational aerodynamic analysis for a range-limited 25mm training round
[AD-A185270] N88-29772
Ascent guidance for a winged boost vehicle
[NASA-CR-172083] N88-29846
TRAJECTORY CONTROL
The eivaN: A forward-looking interactive orbital trajectory plotting tool for use with proximity operations (PROX OPS) and other maneuvers: Description and user's manual
[NASA-CR-177490] N88-30327
TRAJECTORY OPTIMIZATION
The eivaN: A forward-looking interactive orbital trajectory plotting tool for use with proximity operations (PROX OPS) and other maneuvers: Description and user's manual
[NASA-CR-177490] N88-30327
TRANSDUCERS
Piezoelectric and electrostrictive materials for transducer applications, volume 1
[AD-A194957] N88-30096
Piezoelectric and electrostrictive materials for transducer applications, volume 2
[AD-A194956] N88-30104
Piezoelectric and electrostrictive materials for transducer applications, volume 3
[AD-A194949] N88-30112
TRANSFER ORBITS
Impact of ETO propellants on the aerothermodynamic analyses of propulsion components
[NASA-TM-101303] N88-30094
TRANSFORMATIONS (MATHEMATICS)
DATATRAN: Datum transformation software
[AD-A195723] N88-30175
Using primal sketch primitives as the basis for the Hough transform
[INPE-4564-PRE/1305] N88-30310
Reconstruction of multidimensional signals from multiple level threshold crossings
[AD-A195561] N88-30383
TRANSIENT HEATING
Measurement of local high-level, transient surface heat flux
[NASA-TP-2840] N88-30099
TRANSITION FLOW
Transition at hypersonic speeds
[NASA-CR-178315] N88-30058
Transition mixing study empirical model report
[NASA-CR-182139] N88-30076
Recent insights into instability and transition to turbulence in open-flow systems
[NASA-CR-181693] N88-30079
TRANSITION TEMPERATURE
Theory of superconductivity in oxides
[AD-A195647] N88-30432
Theoretical model of high temperature superconductors
[DE88-702707] N88-30441
TRANSLATING
Conversion of productions in OPS5 to their equivalent English
[ORNL/TM-10246] N88-30306
TRANSMISSION LINES
A fiber optic beamforming processor for wideband direction finding
[AD-A194862] N88-30404
Ultra-wideband direction finding using a fiber optic beamforming processor
[AD-A194861] N88-30413
TRANSMISSIONS (MACHINE ELEMENTS)
Helicopter transmission research at NASA Lewis Research Center
[NASA-TM-100962] N88-30128
TRANSONIC COMPRESSORS
Studies of unsteady axial-compressor functioning N88-30129
TRANSONIC FLOW
A streamwise upwind algorithm for the Euler and Navier-Stokes equations applied to transonic flows
[NASA-TM-101019] N88-29751
Application of unsteady aerodynamic methods for transonic aeroelastic analysis
[NASA-TM-100665] N88-29754
Computational methods for the problems of the tip vortex
[NASA-CR-181436] N88-29775
Theoretical aerodynamics, transonic flow
[AD-A196247] N88-29777
TRANSONIC SPEED
Recent advances in transonic computational aeroelasticity
[NASA-TM-100663] N88-29778
TRANSPARENCE
Precision measurement of the Fresnel drag coefficient using a ring laser
[AD-A196025] N88-30043
TRANSPORT AIRCRAFT
Low-speed longitudinal flying qualities of modern transport aircraft N88-29738
TRANSPORT PROPERTIES
Development of computer-controlled thermogravimetric instrumentation for measurement of environmental and high temperature volatilization and desorption of contaminants from polymeric materials
[AD-A195934] N88-29900
Experimental and analytical study of two-phase flow in zero gravity
[AD-A195223] N88-29993
Models of cerebral-body perfusion and cerebral chemical transport
[AD-A194945] N88-30263
TRAPPED PARTICLES
Spontaneous force optical traps
[AD-A196103] N88-30114
Research on a two-stage free electron laser oscillator
[AD-A195991] N88-30115
TRAPPING
Autoionization for lower level detrapping in X-ray lasers
[AD-A195845] N88-30123
TRIANGLES
The triangle: A multiprocessor architecture for fast curve and surface generation
[AD-A195882] N88-30324
TRIANGULATION
Adaptive mesh generation for viscous flows using Delaunay triangulation
[NASA-CR-181699] N88-29749
TRIAXIAL STRESSES
Creep of carbon yarn and carbon-carbon composites at high temperatures and high stresses
[AD-A195224] N88-29878
TRIBOLOGY
The lubricating properties of magnetron sputtered MoS2
[ESA-ESTL-76] N88-30136
TROPICAL REGIONS
Evolution of thermal structure of Benguela upswelling system according to satellite and shipboard data N88-30525
TROPOSPHERE
Global vertical mass transport by clouds: A two-dimensional model study
[CM-74] N88-30192
TRUSSES
Clevis joint for deployable space structures
[NASA-CASE-LAR-13898-1] N88-30130
TUNABLE LASERS
Growth and characterization of materials for tunable lasers in the near infrared spectral region
[NASA-CR-183132] N88-30113

Spectroscopic studies with multiple quantum well materials with applications to optical signal processing at room temperature
[AD-A194171] N88-30409

TURBINE BLADES
Numerical solutions of unsteady inviscid transonic turbine cascade flows
[AD-A196111] N88-29748
User's manual for three dimensional boundary layer (BL3-D) code
[NASA-CR-174899] N88-30063
Impact of ETO propellants on the aerothermodynamic analyses of propulsion components
[NASA-TM-101303] N88-30094

TURBINES
The effects of inlet turbulence and rotor/stator interactions on the aerodynamics and heat transfer of a large-scale rotating turbine model. Volume 2: Heat transfer data tabulation. 15 percent axial spacing
[NASA-CR-179467] N88-29804
Studies of gas turbine heat transfer airfoil surface and end-wall cooling effects
[AD-A195165] N88-29805
An investigation of constitutive models for predicting viscoplastic response during cyclic loading
[AD-A194875] N88-30163

TURBOFAN ENGINES
Euler analysis of a swirl recovery vane design for use with an advanced single-rotation propfan
[NASA-TM-101357] N88-29771
Developing the Rolls-Royce Tay
[PNR90447] N88-29809
High performance turbofan afterburner systems N88-29822
Contamination and distortion of steady flow field induced by discrete frequency disturbances in aircraft gas engines
[AD-A195440] N88-30069
Development and installation of an instrumentation package for GE F404 investigative testing
[AD-A196265] N88-30107

TURBOJET ENGINES
Air intake aerodynamics N88-29762
Semiempirical methods for airbreathing missiles N88-29763
Evaluation of the advanced air breathing propulsion concepts, executive summary
[ESA-CR(P)-2540] N88-29802
Evaluation of advanced air breathing concepts. Volume 1: Executive summary
[ESA-CR(P)-2539] N88-29806

TURBOMACHINERY
Three-dimensional Navier-Stokes simulations of turbine rotor-stator interaction
[NASA-TM-100081] N88-29750
An unconditionally stable Runge-Kutta method for unsteady flows
[NASA-TM-101347] N88-29780
Three-dimensional elliptic grid generation technique with application to turbomachinery cascades
[NASA-TM-101330] N88-30078

TURBULENCE
The effects of inlet turbulence and rotor/stator interactions on the aerodynamics and heat transfer of a large-scale rotating turbine model. Volume 2: Heat transfer data tabulation. 15 percent axial spacing
[NASA-CR-179467] N88-29804
Recent insights into instability and transition to turbulence in open-flow systems
[NASA-CR-181693] N88-30079
Comparisons of solar nebula models N88-30539

TURBULENCE EFFECTS
Turbulence effects on the droplet distribution behind airblast atomizers N88-29915
Radiation transfer in gas turbine combustors N88-29929

TURBULENCE METERS
Flight test equipment for the on-board measurement of wind turbulence N88-29719
A summary of atmospheric turbulence measurements with specially-equipped aircraft in the US N88-29727
Measurement and analysis of low altitude atmospheric turbulence obtained using a specially instrumented Gnat aircraft N88-29728

TURBULENT BOUNDARY LAYER
Studies of gas turbine heat transfer airfoil surface and end-wall cooling effects
[AD-A195165] N88-29805
The effects of incoming boundary layer thickness on unsteady shock-induced turbulent separations induced by cylinders
[AD-A196190] N88-30060
Numerical simulation of the interaction of pressure waves with laminar and turbulent boundary layers
[ESA-TT-1089] N88-30075
Experimental and numerical investigation of the effect of distributed suction on oblique shock wave/turbulent boundary layer interaction
[NASA-TM-101334] N88-30084
The thermal behavior of film cooled turbulent boundary layers as affected by longitudinal vortices
[AD-A195155] N88-30095
Vortex formation and particle transport in a cross-field plasma sheath
[AD-A194838] N88-30425

TURBULENT FLOW
Aerodynamic heating of missiles N88-29764
Flamelet modeling of turbulent premixed flames N88-29942
Modeling the stability of a turbulent premixed flame, downstream from a step by a Lagrangian method N88-29943
Modeling and experimental study of a reactive flow confined with well injection N88-29948
Approximation of viscoelastic stresses from Newtonian turbulent kinematics
[AD-A194317] N88-30077
Boltzmann equation approach to two-phase flow turbulence
[AD-A196153] N88-30086
Analysis method for the production of Reynolds stresses in compressible turbulent flow (fluid mechanics)
[NASA-TT-20330] N88-30068
Development of a more general Reynolds stress closure for swirling flow
[AD-A195121] N88-30092

TURBULENT HEAT TRANSFER
Studies of gas turbine heat transfer airfoil surface and end-wall cooling effects
[AD-A195165] N88-29805

TURBULENT WAKES
Investigation of large-scale structures in the near wake of a parallel flat plate
[ESA-TT-1100] N88-30080

TWO DIMENSIONAL FLOW
Analysis and optimization of truncated scarf nozzles subject to external flow conditions
[NASA-TM-100955] N88-29746
Numerical modelling of premixed flames in gaseous media N88-29944

TWO PHASE FLOW
Experimental and analytical study of two-phase flow in zero gravity
[AD-A195223] N88-29993
Boltzmann equation approach to two-phase flow turbulence
[AD-A196153] N88-30086

U

U.S.S.R.
Bibliography of Soviet laser developments, number 88, March - April 1987
[AD-A195978] N88-30116

U.S.S.R. SPACE PROGRAM
JPRS report: Science and technology. USSR: Space
[JPRS-USP-88-001] N88-30498

UK SATELLITES
Validate algorithms for the determination of rainfall rates from SSM/I microwave satellite imagery
[AD-A195428] N88-30270

ULTRASONIC FLAW DETECTION
Ultrasonic method and apparatus for determining crack opening load
[NASA-CASE-LAR-13889-1] N88-30160

ULTRASONIC TESTS
Ultrasonic method and apparatus for determining crack opening load
[NASA-CASE-LAR-13889-1] N88-30160

ULTRASONICS
Ultrasonic detection of diffusion and adhesion loss N88-29967
In situ fault detection by the hybrid ray mode method
[AD-A195226] N88-30137

ULTRAVIOLET ASTRONOMY
Beyond the visible: A decade of observations with the International Ultraviolet Explorer (IUE)
[ESA-F09] N88-29828

UNDER SURFACE BLOWING
Analysis of a fixed-pitch X-wing rotor employing lower surface blowing
[AD-A187379] N88-29779

UNDERWATER TESTS
Study of human factors engineering criteria for Extra Vehicular Activity (EVA) systems, volume 2
[STF23-F87025-VOL-2] N88-30293

UNSTEADY AERODYNAMICS
Application of unsteady aerodynamic methods for transonic aeroelastic analysis
[NASA-TM-100665] N88-29754
History of aeroelasticity in Germany from the beginning to 1945
[ESA-TT-1082] N88-29767
Recent advances in transonic computational aeroelasticity
[NASA-TM-100663] N88-29778
Aeroelastic response of metallic and composite propfan models in yawed flow
[NASA-TM-100964] N88-29807

UNSTEADY FLOW
Numerical solutions of unsteady inviscid transonic turbine cascade flows
[AD-A196111] N88-29748
An unconditionally stable Runge-Kutta method for unsteady flows
[NASA-TM-101347] N88-29780
The effects of incoming boundary layer thickness on unsteady shock-induced turbulent separations induced by cylinders
[AD-A196190] N88-30060
An analysis of finite-difference and finite-volume formulations of conservation laws
[NASA-CR-177416] N88-30071
Numerical simulation of unsteady incompressible flow in a partially-filled rotating cylinder
[AD-A196001] N88-30073
Numerical simulation of unsteady incompressible viscous flows in generalized coordinate systems
[NASA-TM-101016] N88-30085
Studies of unsteady axial-compressor functioning N88-30129

UNSTEADY STATE
Aircraft dynamics: Aerodynamic aspects and wind tunnel techniques N88-29731

UPPER ATMOSPHERE
Approximation of atmospheric density by Chebyshev polynomials in predicting motion of low artificial earth satellites N88-30503

UPPER IONOSPHERE
Experimental proof of quasilongitudinal propagation of low-frequency waves in middle latitudes in upper ionosphere N88-30516

UPWELLING WATER
Evolution of thermal structure of Benguela upwelling system according to satellite and shipboard data N88-30525

URETHANES
Stressed fabric abrasion test procedure for urethane coated fabric fuel tanks
[AD-A196327] N88-29982

USER MANUALS (COMPUTER PROGRAMS)
User's manual for three dimensional boundary layer (BL3-D) code
[NASA-CR-174899] N88-30063
Supermap for Cray FORTRAN: A user's guide
[NASA-CR-177410] N88-30308
The eivaN: A forward-looking interactive orbital trajectory plotting tool for use with proximity operations (PROX OPS) and other maneuvers: Description and user's manual
[NASA-CR-177490] N88-30327
An operations manual for the digital data system
[NASA-CR-181688] N88-30329
Aircraft noise prediction program propeller analysis system IBM-PC version user's manual version 2.0
[NASA-CR-181689] N88-30399

USER REQUIREMENTS
MANIP --- spacecraft modeling program
[MANIP-217A] N88-29855
A static scheduler for the computer aided prototyping system: An implementation guide
[AD-A194340] N88-30322
Integrated resource scheduling in a distributed scheduling environment N88-30342

V

VANES
Euler analysis of a swirl recovery vane design for use with an advanced single-rotation propfan
[NASA-TM-101357] N88-29771

VAPOR DEPOSITION
Iridium-coated rhenium thrusters by CVD
[NASA-TM-101309] N88-29874
Processing technology research in composites
[AD-A195693] N88-29890
A review of melt and vapor growth techniques for polydiacetylene thin films for nonlinear optical applications
[NASA-TM-100340] N88-30412

VAPORIZERS
Flow characteristics of a model annular combustor N88-29924

VAPORIZING
Simulation study of spraying, streaming and vaporization phenomena associated with fuel injection N88-29914

VARIABLE GEOMETRY STRUCTURES
Techniques used in the F-14 variable-sweep transition flight experiment
[NASA-TM-100444] N88-30093
VARIABLE STARS
The ultrashort period dwarf nova SW Ursae Majoris N88-30553
VARIATIONS
Nonequilibrium flow of a dissociating gas in a horizontal channel with axial temperature variation
[DE88-702536] N88-30089
VARIOMETERS
NASA Marshall Space Flight Center solar observatory
[NASA-TM-100339] N88-29832
VEGETATION
Imaging instrument of the vegetation payload (SPOT 4)
[SNIAS-681-440-107] N88-30169
Study of the spectral response of soybeans
[INPE-4582-PRE/1322] N88-30174
Relief effect correction on LANDSAT imagery for forest applications using digital terrain models
[INPE-4611-PRE/1334] N88-30179
VEGETATIVE INDEX
TM/LANDSAT-5 data to evaluate wheat and bean percent soil cover and leaf area index
[INPE-4609-PRE/1332] N88-30165
LANDSAT TM and agrometeorological data for wheat yield estimation at the farm level
[INPE-4591-PRE/1321] N88-30180
VELOCITY DISTRIBUTION
The dynamics of SBO galaxies. Part 1: The data
[SER-C-PREPUBL-FASC-22] N88-30567
VELOCITY MEASUREMENT
Radial velocity measurements of a sample of northern metal-deficient stars
[SER-C-PREPUBL-FASC-25] N88-30564
VENUS ATMOSPHERE
Microphysical processes in cloud layers of Venus N88-30522
Stability of Venusian ionopause N88-30523
VERTICAL AIR CURRENTS
Global vertical mass transport by clouds: A two-dimensional model study
[CM-74] N88-30192
VERTICAL MOTION
Utilization of a single clear-air Doppler radar beam to measure vertical divergence
[AD-A195543] N88-30271
VERTICAL ORIENTATION
Possibilities of determining vertical profiles of microphysical characteristics of stratospheric aerosol using space measurements of transparency and solar halo N88-30526
VERY LARGE SCALE INTEGRATION
Performance analysis of k-ary n-cube interconnection networks
[AD-A195542] N88-30010
Design of a self-timed VLSI multicomputer communication controller
[AD-A194567] N88-30014
VERY LOW FREQUENCIES
Influence of plasma parameters on VLF radiation in near-rocket region N88-30518
VIBRATION
Containment of a silicone fluid free surface in reduced gravity using barrier coatings
[NASA-TM-101314] N88-30072
Intramolecular dynamics: A study of molecules at high levels of vibrational excitation
[AD-A195285] N88-30400
VIBRATION MEASUREMENT
Use of holography in vibration and flutter study of fans
[PNR90458] N88-30098
Analytical and experimental studies of beam waveguide absorbers for structural damping
[AD-A195085] N88-30144
Vibrational power flow analysis of rods and beams
[NASA-CR-183166] N88-30151
VIBRATION TESTS
Analytical and experimental studies of beam waveguide absorbers for structural damping
[AD-A195085] N88-30144
VIBRATIONAL SPECTRA
Analytical and experimental studies of beam waveguide absorbers for structural damping
[AD-A195085] N88-30144
VIDEO COMMUNICATION
Information technology to facilitate group interaction N88-30463
VIDEO EQUIPMENT
Information technology to facilitate group interaction N88-30463
VINYL POLYMERS
Alternative immersion accelerated testing of coating systems for Naval shoreline facilities N88-29977
VISCOELASTICITY
Approximation of viscoelastic stresses from Newtonian turbulent kinematics
[AD-A194317] N88-30077
Initial value problems in viscoelasticity
[AD-A196052] N88-30145
VISCOPLASTICITY
Determination of multiaxial flow surfaces at elevated temperatures using the concept of dissipation potential
[ORNL/TM-10787] N88-30149
An investigation of constitutive models for predicting viscoplastic response during cyclic loading
[AD-A194875] N88-30163
VISCOSITY
Eruptive viscosity and volcano morphology N88-30488
VISCOUS DRAG
Development and design of windtunnel and test facility for RPV (Remote Piloted Vehicle) enhancement devices
[AD-A194842] N88-29822
VISCOUS FLOW
Adaptive mesh generation for viscous flows using Delaunay triangulation
[NASA-CR-181699] N88-29749
The viscous flow on surfaces with streamline riblets
[ESA-TT-1091] N88-30067
Numerical simulation of unsteady incompressible viscous flows in generalized coordinate systems
[NASA-TM-101016] N88-30085
VISCOUS FLUIDS
Preliminary investigation of flow modeling during solid propellant processing
[AD-A196168] N88-29987
Approximation of viscoelastic stresses from Newtonian turbulent kinematics
[AD-A194317] N88-30077
VISUAL ACUITY
A field study on soft contact lens wear in USAF military transport aircraft
[AD-A195962] N88-30285
Functional assessment of laser irradiation
[AD-A195735] N88-30287
VISUAL DISCRIMINATION
Functional assessment of laser irradiation
[AD-A195735] N88-30287
VISUAL PERCEPTION
Multilevel computational theory of stereoscopic visual image processing
[AD-A195331] N88-30288
Haptic exploration in humans and machines: Attribute integration and machine recognition/implementation
[AD-A193692] N88-30299
Space station proximity operations windows: Human factors design guidelines
[NASA-TM-88233] N88-30301
Dynamical systems and motion vision
[AD-A195932] N88-30366
VOLCANOLOGY
The tectonic setting of Archean anorthosites N88-30231
Physical processes in the growth of the continental crust N88-30240
Volcanic contribution to crustal growth in the Central Andes: A new estimate and a discussion of uncertainties N88-30255
NASA MEVTV Program Working Group Meeting: Volcanism on Mars
[NASA-CR-183074] N88-30487
Eruptive viscosity and volcano morphology N88-30488
Faulting and its relation to volcanism: Mars western equatorial region N88-30489
Mars: Volcanism in the Valles Marineris overlooked N88-30491
The Martian highland paterae: Evidence for explosive volcanism on Mars N88-30492
VOLTAGE CONVERTERS (AC TO AC)
Voltage directive drive with claw pole motor and control without rotor position indicator
[ETN-88-93120] N88-30047
VOLUMETRIC ANALYSIS
Volumetric measurement of vorticity vectors by optical probe
[AD-A195997] N88-30061
VORTICES
Nonlinear Tollmien-Schlichting/vortex interaction in boundary layers
[NASA-CR-181698] N88-29715
On the generation of mean flows by the interaction of Goertler vortices and Tollmien-Schlichting waves in curved channel flows
[NASA-CR-181690] N88-29743
The present status and the future of missile aerodynamics
[NASA-TM-100063] N88-29773
Computational methods for the problems of the tip vortex
[NASA-CR-181438] N88-29775
The thermal behavior of film cooled turbulent boundary layers as affected by longitudinal vortices
[AD-A195155] N88-30095
Vortex formation and particle transport in a cross-field plasma sheath
[AD-A194838] N88-30425
VORTICITY
Volumetric measurement of vorticity vectors by optical probe
[AD-A195997] N88-30061
VULCANIZING
Primerless RTV silicones
[BDX-613-3807] N88-29980
VULNERABILITY
Comparative analysis of passive communications satellites employing the SHF and HF spectrum for use in a strategic role
[AD-A194682] N88-30019

W

WALL FLOW
Supersonic wall adaptation in the rubber tube test section of the DFVLR Goettingen
[IB-222-87-A-08] N88-29824
WALL JETS
Transition mixing study empirical model report
[NASA-CR-182139] N88-30076
WALL PRESSURE
An experimental study of an adaptive-wall wind tunnel
[NASA-CR-183152] N88-29821
The effects of incoming boundary layer thickness on unsteady shock-induced turbulent separations induced by cylinders
[AD-A196190] N88-30060
WALL TEMPERATURE
Radiative heat transfer to steady flow of a chemically reacting fluid in a horizontal porous channel with variable wall temperature
[DE88-702704] N88-30081
WALLS
Experimental determination of drag modifications due to elastic compliant surfaces using quantitative visual techniques
[AD-A194785] N88-30082
A parametric study of embedded cantilever retaining walls: The results of a finite element study
[RR-CE83] N88-30152
WATER
General equations for the motions of ice crystals and water drops in gravitational and electric fields
[NASA-CR-183229] N88-30070
WATER RESOURCES
The use of orbital remote sensing data for low cost ground-water survey
[INPE-4587-PRE/1318] N88-30170
WATER TEMPERATURE
Study of human factors engineering criteria for Extra Vehicular Activity (EVA) systems, volume 2
[STF23-F87025-VOL-2] N88-30293
WATER WAVES
Mathematical problems of nonlinear wave propagation and of waves in heterogeneous media
[AD-A195970] N88-30057
Impact force as a part of the total breaking wave force on a vertical cylinder
[RR-CE78] N88-30154
A study of the feasibility of using sea and wind information from the ERS-1 satellite. Part 2: Use of scatterometer and altimeter data in wave modeling and assimilation
[ESA-CR(P)-2604-PT-2] N88-30176
Analysis of environmental parameters from the Panama City tower radar experiment
[AD-A194994] N88-30264
WAVE FRONT RECONSTRUCTION
Reconstruction of wave distribution functions in warm plasmas
[IRF-PREPRINT-104] N88-30422
WAVE FRONTS
Nonlinear optical phase conjugation techniques to reduce the physical size of lasers
[AD-A196170] N88-30122
WAVE GENERATION
Millimeter wave generation by relativistic electron beams
[AD-A195683] N88-30016
WAVE INTERACTION
Nonlinear Tollmien-Schlichting/vortex interaction in boundary layers
[NASA-CR-181698] N88-29715

The strong nonlinear interaction of Tollmien-Schlichting waves and Taylor-Goertler vortices in curved channel flow
[NASA-CR-181697] N88-29716
Light-millimeter wave interactions in semiconductor devices
[AD-A195898] N88-30428
WAVE PROPAGATION
Wave propagation and remote sensing N88-30029
Mathematical problems of nonlinear wave propagation and of waves in heterogeneous media
[AD-A195970] N88-30057
Determination of the specific area of liquid gas and the velocity of weak pressure waves in aqueous foams
[NASA-TT-20347] N88-30087
Rosby waves in mid-latitude oceans N88-30273
Consideration of plasma opening switches from a wave propagation perspective
[AD-A195681] N88-30421
Experimental proof of quasilongitudinal propagation of low-frequency waves in middle latitudes in upper ionosphere N88-30516
WAVE SCATTERING
Mathematical problems of nonlinear wave propagation and of waves in heterogeneous media
[AD-A195970] N88-30057
WAVEFORMS
Waveform relaxation applied to transient device simulation
[AD-A194992] N88-30429
WAVEGUIDES
Confirmation of slow-waves in a crosstie overlay coplanar waveguide and its application to band-reject gratings and reflectors
[AD-A194961] N88-30011
Dielectric millimeter waveguides: A feasibility study for a novel dielectric millimeter waveguide
[AD-A195104] N88-30042
Analytical and experimental studies of beam waveguide absorbers for structural damping
[AD-A195085] N88-30144
WEAPONS
The Soviet Stealth fighter: Check or checkmate
[AD-A195200] N88-29791
WEATHER FORECASTING
A study of the feasibility of using sea and wind information from the ERS-1 satellite. Part 1: Wind scatterometer data
[NASA-CR-182833] N88-30167
A study of the feasibility of using sea and wind information from the ERS-1 satellite. Part 2: Use of scatterometer and altimeter data in wave modeling and assimilation
[ESA-CR(P)-2604-PT-2] N88-30176
Temperature profile construction methods: An evaluation
[AD-A195919] N88-30262
WEATHERING
Photoacoustic Fourier transform infrared spectroscopy. An early detection technique for coatings degradation N88-29968
WEIBULL DENSITY FUNCTIONS
Measurement and interpretation of North Atlantic Ocean marine radar sea scatter
[AD-A196239] N88-30036
WEIGHT (MASS)
Spray automated balancing of rotors: Methods and materials
[NASA-CR-182151] N88-29825
WEIGHTLESSNESS SIMULATION
Study of human factors engineering criteria for Extra Vehicular Activity (EVA) systems, volume 2
[STF23-F87025-VOL-2] N88-30293
WELDED JOINTS
Development of graded reference radiographs for aluminum welds, phase 1
[AD-A195594] N88-30140
WELLS
The use of orbital remote sensing data for low cost ground-water survey
[INPE-4587-PRE/1318] N88-30170
WEST GERMANY
Investigation of the large-scale impact of air pollution components on forest ecosystems in Bavaria
[ESA-TT-1087] N88-30187
WHARVES
Impact force as a part of the total breaking wave force on a vertical cylinder
[RR-CE78] N88-30154
WHEAT
TM/LANDSAT-5 data to evaluate wheat and bean percent soil cover and leaf area index
[INPE-4609-PRE/1332] N88-30165
LANDSAT TM and agrometeorological data for wheat yield estimation at the farm level
[INPE-4591-PRE/1321] N88-30180
WHISKERS (CRYSTALS)
An organometallic route to micron-sized whiskers of zinc sulfide
[AD-A195889] N88-30414
WIND (METEOROLOGY)
Doppler radar analysis of coastal marine atmospheric boundary layer structure during a cold air outbreak
[AD-A196023] N88-30261
Analysis of environmental parameters from the Panama City tower radar experiment
[AD-A194994] N88-30264
WIND DIRECTION
Analysis of environmental parameters from the Panama City tower radar experiment
[AD-A194994] N88-30264
WIND MEASUREMENT
A study of the feasibility of using sea and wind information from the ERS-1 satellite. Part 1: Wind scatterometer data
[NASA-CR-182833] N88-30167
A study of the feasibility of using sea and wind information from the ERS-1 satellite. Part 2: Use of scatterometer and altimeter data in wave modeling and assimilation
[ESA-CR(P)-2604-PT-2] N88-30176
Determining near-water wind speed using radar data from Cosmos-1500 artificial earth satellite N88-30524
WIND SHEAR
Cloud/mesoscale model development and application studies
[AFGL-TR-87-0219] N88-30269
WIND TUNNEL APPARATUS
Computer programs for calculation of sting pitch and roll angles required to obtain angles of attack and sideslip on wind tunnel models
[NASA-TM-100659] N88-29820
WIND TUNNEL MODELS
Test of an 0.8-scale model of the AH-64 Apache in the NASA Langley full-scale wind tunnel
[AD-A196129] N88-29768
Computer programs for calculation of sting pitch and roll angles required to obtain angles of attack and sideslip on wind tunnel models
[NASA-TM-100659] N88-29820
WIND TUNNEL TESTS
Space shuttle phase B wind tunnel model and test information. Volume 3: Launch configuration
[NASA-CR-178416-VOL-3-PT-2] N88-29744
Space shuttle phase B wind tunnel model and test information. Volume 1: Booster configuration
[NASA-CR-178414-VOL-1-PT-1] N88-29745
Test of an 0.8-scale model of the AH-64 Apache in the NASA Langley full-scale wind tunnel
[AD-A196129] N88-29768
Space shuttle phase B wind tunnel model and test information. Volume 1: Booster configuration
[NASA-CR-178414-VOL-1-PT-2] N88-29770
Pressure distributions from subsonic tests of an advanced laminar-flow-control wing with leading- and trailing-edge flaps
[NASA-TM-4040-PT-2] N88-29776
An experimental study of an adaptive-wall wind tunnel
[NASA-CR-183152] N88-29821
Supersonic wall adaptation in the rubber tube test section of the DFVLR Goettingen
[IB-222-87-A-08] N88-29824
WIND TUNNEL WALLS
An experimental study of an adaptive-wall wind tunnel
[NASA-CR-183152] N88-29821
WIND TUNNELS
Development and design of windtunnel and test facility for RPV (Remote Piloted Vehicle) enhancement devices
[AD-A194842] N88-29822
WIND VELOCITY
A review of measured gust responses in the light of modern analysis methods N88-29724
A summary of atmospheric turbulence measurements with specially-equipped aircraft in the US N88-29727
Re-assessment of gust statistics using CAADRP data N88-29732
Analysis of environmental parameters from the Panama City tower radar experiment
[AD-A194994] N88-30264
A digital simulation technique for the Dryden atmospheric model
[NASA-TT-20342] N88-30266
Determining near-water wind speed using radar data from Cosmos-1500 artificial earth satellite N88-30524
WINDOWS
Space station proximity operations windows: Human factors design guidelines
[NASA-TM-88233] N88-30301
WING LOADING
A summary of methods for establishing airframe design loads from continuous gust design criteria N88-29721
WINTER
One equatorial anomaly in nighttime ionospheric F region N88-30517
WORDS (LANGUAGE)
Exploiting lexical regularities in designing natural language systems
[AD-A195922] N88-30375
Words: Keys or barriers to information transfer N88-30464
WORKING FLUIDS
Radiative heat transfer to steady flow of a chemically reacting fluid in a horizontal porous channel with variable wall temperature
[DE88-702704] N88-30081
WORKLOADS (PSYCHOPHYSIOLOGY)
Threat expert system technology advisor
[NASA-CR-177479] N88-29816
WORLD METEOROLOGICAL ORGANIZATION
Activities report of the World Meteorological Organization
[WMO-689] N88-30265

X

X RAY ANALYSIS
ZT imaging system for layered thin wall structures
[AD-A195466] N88-29954
A method for the quantitative determination of crystalline phases by X-ray
[NASA-TT-20324] N88-30444
X RAY ASTRONOMY
The high-throughput X-ray spectroscopy mission: The mission-science report
[ESA-SP-1097] N88-30557
X RAY DIFFRACTION
X-ray diffraction imaging (topography) of electrooptiocrystals by synchrotron radiation
[NASA-CR-183266] N88-30427
Applications of synchrotron radiation to materials science: Diffraction imaging (topography) and microradiography
[NASA-CR-183265] N88-30440
Crystal structure and density of helium to 232 kbar N88-30481
X RAY IMAGERY
X-ray diffraction imaging (topography) of electrooptiocrystals by synchrotron radiation
[NASA-CR-183266] N88-30427
X RAY LASERS
Autoionization for lower level detrapping in X-ray lasers
[AD-A195845] N88-30123
X RAY SOURCES
A coded mask telescope for observations of X and gamma ray sources in the southern sky
[INPE-4580-PRE/1314] N88-30551
Activities in astrophysics
[INPE-4582-PRE/1316] N88-30570
X RAY SPECTROSCOPY
The high-throughput X-ray spectroscopy mission: The mission-science report
[ESA-SP-1097] N88-30557
X RAYS
X- and gamma-ray background observations in Antarctic
[INPE-4583-PRE/1317] N88-30578
X WING ROTORS
Analysis of a fixed-pitch X-wing rotor employing lower surface blowing
[AD-A187379] N88-29779

Y

YARNS
Creep of carbon yarn and carbon-carbon composites at high temperatures and high stresses
[AD-A195224] N88-29878
YAW
Aeroelastic response of metallic and composite propfan models in yawed flow
[NASA-TM-100964] N88-29807
YIELD POINT
An experimental study of biaxial yield in modified 9Cr-1Mo steel at room temperature
[NASA-CR-175012] N88-30164
YIELD STRENGTH
Geometric and material nonlinear analysis of structures comprising rectangular hollow sections
[CE-79] N88-30141

Z

ZINC
An electrochemical impedance spectroscopy study of reactions at the metal/coating interface N88-29975
Zinc filled coatings N88-29978
ZINC SULFIDES
The optical spectroscopy of copper-blue luminescence in zinc sulfide crystals. Zero-phonon line spectra under the influence of magnetic field, temperature and excitation intensity
[ETN-88-93122] N88-29903
An organometallic route to micron-sized whiskers of zinc sulfide
[AD-A195889] N88-30414
ZIRCONIUM
Electrical properties of materials for elevated temperature resistance strain gage application
[NASA-CR-182214] N88-30106
ZIRCONIUM COMPOUNDS
Role of zircon in tracing crustal growth and recycling N88-30211
The early archaean crustal history of West Greenland as recorded by detrital zircons N88-30221
Growth of early archaean crust in the ancient Gneiss complex of Swaziland and adjacent Barberton Greenstone Belt, Southern Africa N88-30223

Typical Personal Author Index Listing

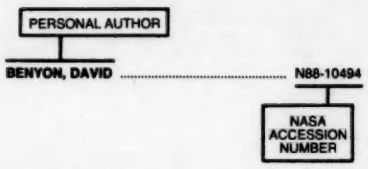

Listings in this index are arranged alphabetically by personal author. The NASA accession number denotes the number by which the citation is identified.

A

AAZHANG, B. N88-30021
ABALI, B. N88-30017
ABBOTT, DALLAS N88-30202
ABDOLLAHIAN, DAVOOD N88-29993
ABELL, JOHN B. N88-29796
ADENIJI-FASHOLA, A. A. N88-30148
AENISHANSLIN, M. H. N88-29849
AHN, ILSOO N88-30451
AHRENS, THOMAS J. N88-30484
AKSENOV, V. I. N88-30030
AL-BERMANI, F. G. A. N88-30141
AL-HUJAZI, EZZET N88-30351
ALBAREDE, F. N88-30203
ALCAZAR, DAVID G. N88-29885
ALEKSEYENKO, A. V. N88-30530
ALEXANDER, E. C., JR. N88-30476
ALEXANDER, MILLARD H. N88-29902
ALLEN, DAVID J. N88-30472
ALLEN, J. N88-30429
ALLEN, M. N88-30091
ALMEIDAFILHO, RAIMUNDO N88-30173
ALTYNTSEVA, V. I. N88-30516
ALVIMDEOLIVEIRA, ENI N88-30179
ANANTHAKRISHNAN, S. N88-30030
ANDERS, EDWARD N88-30483
ANDERSON, BIANCA TRUJILLO N88-30093
ANDERSON, D. N88-30167
ANDERSON, O. L. N88-30063
N88-30066
ANDERSON, P. W. N88-30432
ANDERSON, RAYMOND R. N88-30258
ANDERSON, WILLIAM B. N88-30450
ANDRE, R. G. B. N88-30263
ANDREWS, ALISON E. N88-30314
APELT, C. J. N88-30154
APPEL, MARSHALL A. N88-29874
APPLEMAN, BERNARD R. N88-29979
APPLIN, ZACHARY T. N88-29776
AREND, LAWRENCE E. N88-30290
ARMSTRONG, R. A. N88-30211
ARNDT, N. T. N88-30205
ARNDT, NICHOLAS T. N88-30204
ARTER, WAYNE N88-30074
ASARO, F. N88-30475
ASHEIM, J. P. N88-29912
ASHKENAS, IRVING L. N88-29737
ASHWAL, LEW N88-30230
ASHWAL, LEWIS D. N88-30201
ASO, YOSHIYUKI N88-30420
ATHALE, R. N88-30004
AVERY, B. E. N88-30111
AYDIN, K. N88-30017

B

BABUSKA, I. N88-30387
BACON, R. N88-30567
BAFFES, PAUL N88-30331
BAGBY, JONATHAN S. N88-30042
BAILEY, ALLAN B. N88-29868
BAILLIE, S. W. N88-29730
BAIRD, B. B. N88-30306
BAJCSY, R. N88-30299
BAKER, WALTER N88-29790
BALAKRISHNAN, A. V. N88-29851
BALDWIN, RICHARD M. N88-29825
BALEGA, I. I. N88-30521
BALEGA, YU. YU. N88-30521
BALLING, P. N88-30000
BALOGA, S. N88-30495
BANKS, DANIEL W. N88-29752
BARAM, YORAM N88-30373
BARANY, G. N88-30026
BARAS, J. S. N88-30388
BARCLAY, L. W. N88-30030
BARKAT, MOURAD N88-30009
BARNES, A. G. N88-29742
BARNES, TERENCE J. N88-29718
BARSCH, G. R. N88-30096
N88-30104
N88-30112
BART, H. J. N88-29899
BARTELL, RICHARD J. N88-30194
BARTENWERFER, MANFRED N88-30067
BARTON, LYNN A. N88-29815
BARTON, WESLEY A. N88-30272
BARTUNOV, O. S. N88-30505
BASCOM, WILLARD D. N88-29880
BASILE, L. N88-29827
BASILE, LISA N88-30353
BASINA, YU. V. N88-30519
BASSETT, W. A. N88-30481
BASSOM, ANDREW P. N88-29743
BASU, SA. N88-30030
BASU, SU. N88-30030
BATINA, JOHN T. N88-29778
BATTOCCHIO, L. N88-30446
N88-30448
BATTRICK, BRUCE N88-30557
BAUER, A. N88-29899
BAUER, H.-J. N88-29938
BAUER, S. J. N88-30030
BAUMERT, JOHN N88-30362
BAWDEN, ALAN N88-30311
N88-30326
BEAR, J. N88-30283
BEAUDET, DOUGLAS B. N88-30296
BEAVERS, W. I. N88-30562
BECHERT, DIETRICH W. N88-30067
BELL, P. M. N88-30481
BELL, T. F. N88-30030
BELLET, J. C. N88-29946
BELLI, M. N88-29939
BELMONT, G. N88-30030
BELOV, R. A. N88-30529
BELTE, DAUMANTS N88-29793
BENHACHMI, DRISS N88-30084
BENKOVA, N. P. N88-30513
BENNETT, J. N88-29716
BENNETT, ROBERT M. N88-29778
BENSON, R. F. N88-30030
BENTZ, D. N88-29969
BENZ, W. N88-30474
BEREZANSKIY, A. V. N88-30530
BERGER, HAROLD N88-30140
BERGMANN, EDWARD N88-30369
BERLIN, ANDREW N88-30319
BERNARD, JAY M. N88-29953
BERNHARD, R. J. N88-30151
BERSHAD N88-30376
BESIERIS, I. M. N88-30025
BESTMAN, A. R. N88-30081
N88-30089
BETHKE, WILLIAM J. N88-29787
BEUTEL, KENNETH L. N88-29830
BHASIN, K. B. N88-30048
BHATTI, IFTEKHAR A. N88-30267
BIANCHI, ROSALINDA N88-29992
BICEN, A. F. N88-29924
BIGELOW, CATHERINE A. N88-29879
BIGGERS, J. V. N88-30096
N88-30104
BILLMAYER, HANNS J. N88-29797
BIRNBAUM, H. K. N88-29958
BJORKHOLM, P. J. N88-29954
BJORSETH, O. N88-30298
BLAIR, M. F. N88-29804
BLAND, SAMUEL R. N88-29778
BLANKENSHIP, G. L. N88-30388
BLINNIKOV, S. I. N88-30505
BLUEMCKE, E. N88-29949
BLUMENTHAL, SAUL N88-30155
BODDY, DAVID N88-30468
BODNER, S. R. N88-29811
BOETTCHER, R.-D. N88-29862
BOLSTAD, G. N88-30293
N88-30298
BONNICE, WILLIAM F. N88-29790
BOROSS, J. N88-30442
BORTNICK, JANE N88-30460
BOSLEY, JOHN N88-30333
BOSS, ALAN P. N88-30543
BOSTROM, R. N88-30418
BOUTOUILI, M. N88-29946
BOWLES, S. J. N88-30398
BOYARCHUK, A. A. N88-30504
BOYLE, R. J. N88-30094
BOYSAN, F. N88-29937
BRAATEN, M. E. N88-29935
BRACEWELL, R. N. N88-30260
BRACUTI, A. J. N88-29969
BRADY, DAVE N88-29999
BRAGA, J. N88-30551
BRASSEUR, GUY N88-30188
BRECHT, STEPHEN H. N88-30421
BREKKE, B. N88-30298
BRITT, DANIEL L. N88-30337
BRODY, ADAM R. N88-30327
BROOKS, STEVEN L. N88-30303
BROWN, GRANT A. N88-30282
BROWN, MARGARET N88-30437
BROWN, R. C. N88-29894
BRUBAKK, A. O. N88-30298
BRUCE, ROBERT N88-30206
BRUCKER, G. J. N88-30442
BRUEL, P. N88-29946
BRUNETTE, C. M. N88-29881
BRUNO, C. N88-29939
BUBLITZ, PETER N88-29767
BUCCI, OVIDIO M. N88-30002
BUCHAU, JURGEN N88-30256
BUCK, GREGORY M. N88-30105
BUCKLEY, JOHN D. N88-30108
BULLIAT, D. N88-30328
BUNGE, MARCEL N88-30127
BURKE, KEVIN N88-30207
BURKHARD, AVERY N88-30006
BURKI, G. N88-30560
BURNETT, J. W. N88-30051
BURNS, B. A. N88-30035
BURNSIDE, W. D. N88-30025
BURRUS, D. L. N88-29935
BUSKO, IVO C. N88-30577
BUSSE, CARL N88-30334
BUTLER, PAT N88-29982
BYERLY, G. R. N88-30475
BYERLY, GARY R. N88-30480
BYERS, DAVID C. N88-29859
BYRD, E. N88-29969
BYRD, RICHARD H. N88-30313

C

CADIOU, A. N88-29921
CAESAR, B. N88-29852
CAFFEE, M. W. N88-30476
CALAWAY, W. F. N88-30051
CAMBRAY, P. N88-29945
CAMERON, A. G. W. N88-30474
CAMPBELL, WILLIAM J. N88-30354
CANDEL, S. M. N88-29942
CANTINI, F. N88-30328
CAO, M. N88-29918
CAPELATO, HUGO V. N88-30570

CAPLIN, B. N88-30083
CARD, V. N88-29724
CAREY, VAN P. N88-29993
CARLISLE, CANDACE N88-30344
CARLSON, DEAN W. N88-30280
CARNEY, LYNNETTE M. N88-29868
CARRERE, A. N88-30129
CARVALHO, M. G. N88-29929
CASEY, J. K. N88-29810
CASLAVSKY, JAROSLAV L. N88-30408
CASON, RANDALL W. N88-29793
CATHEY, W. T. N88-30406
CAVES, ROBERT E. N88-29783
CELESTINA, MARK L. N88-30377
CELIK, ZEKI N88-29821
CERUTTI-MAORI, G. N88-30169
CHACKO, THOMAS N88-30208
CHACONAS, KAREN J. N88-30346
CHAFFINS, SCOTT A. N88-29952
CHAKRAVARTHY, S. R. N88-29812
CHAMPION, M. N88-29946
CHAN, K. S. N88-29811
CHAN, S. L. N88-30141
CHAN, W. W. N88-30191
CHANDLEE, R. C. N88-30554
CHANDLER, KURT G. N88-29985
CHANG, KUNG-CHING N88-30381
CHANOINE, C. N88-29847
CHAPMAN, RANDALL W. N88-30396
CHARKEY, ALLEN N88-30052
CHATTOT, J. J. N88-29760
CHAUVEL, C. N88-30205
CHEAL, MARYLOU N88-30291
CHEN, CHAO-NIEN N88-30388
CHEN, HAITAO N88-30119
CHEN, LIYIN N88-30119
CHEN, S. C. N88-30078
CHEN, YAPING N88-30235
CHENG, HWAI-SOON N88-30039
CHIANG, PEN-TAI N88-30348
CHILES, HARRY R. N88-30093
CHIMA, RODRICK V. N88-29780
CHIN, BRYAN A. N88-29959
CHIN, S. B. N88-30092
CHIRKINA, N. I. N88-30507
CHIVAS, A. R. N88-30476
CHLEBOUN, P. V. N88-29947
CHOREY, C. M. N88-30049
CHU, C. C. N88-30082
CHU, JINGYUN N88-30127
CHU, W. Y. N88-29958
CHU, ZEXIANG N88-30119
CIEPLAK, JAMES J. N88-30341
CIESLIK, STANISLAS N88-29907
CIPOLLA, RUSSELL C. N88-29962
CIVINSKAS, K. C. N88-30094
CLAQUE-LONG, J. C. N88-30211
CLARK, KIMBLE J. N88-29962
CLARK, W. L. N88-30271
CLARKE, L. N88-29788
CLASPY, P. C. N88-30048
CLAYTON, ROBERT N. N88-30477
CLEAVELAND, DALE R. N88-30006
CLEMENS, I. N88-30465
CLINARD, J. A. N88-30149
COE, HAROLD H. N88-30128
COELHO, P. J. M. N88-29929
COFFEY, HELEN E. N88-30574
N88-30576
COHEN, A. S. N88-30200
COLDREN, L. A. N88-30417
COLE, JULIAN D. N88-29777
COLLIN, K. H. N88-29951
COLLINS, W. J. N88-30210
COMBI, MICHAEL R. N88-30572
COMERFORD, R. N88-30446
N88-30448
COMMER, R. P. N88-30196
COMPSTON, W. N88-30211
N88-30221
N88-30223
COOKE, DAVID L. N88-30190
COOPER, GENE R. N88-30059
CORBAN, R. R. N88-29845
CORVIN, MICHAEL ALEXANDER N88-29846
COSTIGAN, MICHAEL J. N88-29814
COTE, DENIS N88-30049
COTTER, GLADYS N88-30462
COTTON, WILLIAM R. N88-30269
COUGNET, C. N88-29827
COUPRY, GABRIEL N88-29734
COY, JOHN J. N88-30128
CRANE, R. K. N88-30029
CRISCUOLO, EDWARD N88-30140
CRISP, J. N88-30495
CRITCHFIELD, ANNA N88-30362
CROMARTIE, ALCUS G. N88-30049
CROMP, ROBERT F. N88-30359
CROSS, L. E. N88-30096
N88-30104
N88-30112
CROWN, DAVID A. N88-30492
CROWTHER, SUSAN D. N88-30275
CROZAZ, G. N88-30482
CUCINOTTA, FRANCIS A. N88-30402
CUNNINGHAM, HERBERT J. N88-29778
CUSANOVICH, MICHAEL A. N88-30277
CZEKAJ, C. L. N88-30414

D

DAGDIGIAN, PAUL J. N88-29902
DALLY, WILLIAM J. N88-30010
N88-30014
DANKERT, C. N88-29862
DANZL, DANIEL F. N88-30278
DARABIHA, N. N88-29942
DAS-GUPTA, DILIP K. N88-29983
DASCH, E. J. N88-30212
DASCH, JULIUS N88-30237
DASILVA, I. M. O. N88-30185
DAVID, H. N88-29788
DAVIES, K. N88-30030
DAVIS, L., JR. N88-30566
DAVIS, P. N88-30091
DAWKINS, WILLIAM P. N88-30317
DEBELLIS, WILLIAM B. N88-30294
DEBIEVE, JEAN FRANCOIS N88-30088
DECKER, M. M. N88-29990
DECOCK, J. N88-30146
DEFOSSE, H. N88-30139
DEGTYAREV, V. I. N88-30501
DEHN, JAMES T. N88-30159
DEHOOP, A. T. N88-30040
DEJONG, G. N88-30024
DEJONGE, J. B. N88-29733
DELANEY, J. S. N88-30482
DELERY, J. N88-29765
DELFINODAVILAMASCARENHAS, NELSON N88-30315
DELIA, GIUSEPPE N88-30002
DELORENZO, MICHAEL L. N88-29842
DENNIS, RICHARD J. N88-30285
DENNIS, SCOTT T. N88-30158
DEPAOLO, D. J. N88-30213
DER, Z. A. N88-30191
DEROSE, TONY N88-30324
DESAI, MUKUND N88-29817
DESHALES, B. N88-29945
DETTLEFF, G. N88-29862
DEUTSCH, OWEN L. N88-29817
DEVREEDE, J. N88-30024
DEZEEUW, T. N88-30569
DIASVELASCO, FLAVIO ROBERTO N88-30310
DIECKERT, J. P. N88-30280
DIEFENDORF, RUSSELL J. N88-29890
DILLENIUS, MARNIX F. E. N88-29757
DILTS, DOUG N88-30469
DIVSALAR, DARIUSH N88-30001
DOBBYN, RONALD C. N88-30427
N88-30431
N88-30437
DOHM, JAMES N88-30489
DOKMECI, M. C. N88-30430
DOMANUS, H. M. N88-29987
DOMINGO, V. N88-30556
DOMOKOS, G. N88-30086
DONADIO, GIUSEPPE N88-30019
DONZELLI, P. N88-30365
DOSANJOSFERREIRAPINTO, SERGIO N88-30177
DREES, HERMAN M. N88-29822
DRING, R. P. N88-29804
DUBATH, P. N88-30560
N88-30567
DUBEBOUT, A. N88-29875
DUBS, CHARLES W. N88-30190
DUDLEY, D. G. N88-30025
DUDMAN, A. E. N88-29732
DUPONT, DEAN T. N88-29883
DUQUENNOY, A. N88-30561
N88-30562
DURANCE, CYNTHIA J. N88-30467
DURRANT, R. N88-30102
DZIELSKI, JOHN N88-30369

E

EBERLEIN, SUSAN N88-30347
ECKERLE, W. A. N88-29916
ECKERT, E. R. N88-29805
EICKHOFF, H. N88-29918
N88-29949
EINHORN, HILLEL J. N88-30391
EITTER, J. J. N88-30582
ELIASSON, RALF N88-29813
N88-29885
ELLAM, R. M. N88-30214
ELLIS, J. R. N88-30164
ELLIS, ROBERT H. N88-30003
ELMES, D. A. N88-29886
ELTON, R. C. N88-30123
EMERIC, DARIO N88-29965
EMERIC, DARIO A. N88-29963
ENDEMANN, M. N88-30118
ENGSTROEM, OLOF N88-30407
EPPINGER, STEVEN D. N88-30132
ERBEN, E. N88-29852
ERTHAL, GUARACI JOSE N88-30316
ESPOSITO, E. N88-29942
EWALD, J. N88-29827

F

FAETH, G. M. N88-29927
FAIRLIE, B. D. N88-30193
FALCO, R. E. N88-30082
FAN, C. G. N88-30114
FANG, TAO N88-30117
FARREN, J. N88-30401
N88-30580
FATHI, H. N88-30298
FATKULLIN, M. N. N88-30513
FAUCHET, PHILIPPE M. N88-30126
FEDOROV, K. N. N88-30525
FEGLEY, BRUCE, JR. N88-30542
FEINSOD, M. N88-30283
FELD, H.-J. N88-29931
FELGUEIRAS, CARLOS ALBERTO N88-30316
FELSEN, L. B. N88-30137
FERGUSON, R. D. N88-30061
FETISOV, A. B. N88-30531
FETTERMAN N88-30428
FEYNMAN, J. N88-30575
FIGUEREDOFILHO, N. N88-30551
FISK, U. O. N88-30556
FLANAGAN, DAVE N88-29982
FLIGEL, M. D. N88-30513
N88-30517
FLORES, CYNTHIA R. N88-29904
FLYNN, WILLIAM J. N88-30285
FORMAGGIO, ANTONIO ROBERTO N88-30165
N88-30172
FORSYTHE, R. D. N88-30233
FOSTER, G. W. N88-29728
FOSTER, J. J. N88-30211
FOUNTI, M. N88-29941
FOURIE, A. B. N88-30152
FOWLES, P. N88-30091
FOX, MARK S. N88-30372
FOX, ROBERT L. N88-30108
FRALEY, CHRISTINA N88-30305
FRANCESCHETTI, GIORGIO N88-30002
FRANCIA, A. N88-30328
FRANCIS, P. N88-30255
FRANCISCO, DAVID R. N88-29873
FRAZIER, D. O. N88-30412
FREEDMAN, E. N88-29990
FRIEND, CLARK R. L. N88-30234
FRISH, MICHAEL B. N88-30061
FUCHS, HEINZ N88-29761
FUJCZAK, R. R. N88-29960
FULLER, I. N88-30015
FULLER, R. G. N88-30189

G

GAGE, K. S. N88-30271
GAITONDE, DATTA V. N88-30064
GALAN, L. N88-30012
GALER, S. J. G. N88-30215
GALFETTI, L. N88-29939
GALINDO, D. N88-30328
GALLOTTIFLORENZANO, TERESA N88-30168
N88-30177
GAO, YIZHI N88-30117
GARABEDIAN, PAUL R. N88-29775
GARCIAFLACK, ANA LETICIA N88-30276
GARCIAFONSECA, LEILA MARIA N88-30315
GARMIRE, ELSA M. N88-30120
GAROW, J. N88-30184
GATES, RICHARD M. N88-29850
GECELOSKY, ANDREW M. N88-29799
GEHER, K. N88-30026
GENNARELLI, CLAUDIO N88-30002
GENTRY, GARL L., JR. N88-29776
GEOFFROY, AMY L. N88-30337

GEOFFROY, G. L. N88-30414
GEORGE, NICHOLAS N88-30411
GERHARDT, PH. N88-29932
GERSHBERG, R. YE. N88-30504
GEZARI, DANIEL Y. N88-30545
GILBERT, D. G. N88-29886
GIOVANGIGLI, V. N88-29942
GIOVANNINI, A. N88-29943
GIRARD, A. N88-30139
GIRLING, S. P. N88-29930
GIVEN, J. W. N88-30257
GIVISHVILI, G. V. N88-30517
GLYNN, J. L. N88-29744
N88-29745
N88-29770
GOEL, PREM N88-30155
GOERICKE, D. N88-29671
GOFFINET, ANDRE M. N88-30284
GOHRING, JOHN R. N88-30337
GOLDBERG, MICHAEL N88-30354
GOLDSTEIN, J. D. N88-30196
GOLDSTEIN, R. J. N88-29805
GOLDSTEIN, S. L. N88-30215
N88-30216
GOLDSTEIN, STEVEN L. N88-30204
GOLSON, ELLIS WAYNE N88-29818
GOLYNSKAYA, R. M. N88-30519
GOODRICH, C. A. N88-30482
GOORJIAN, PETER M. N88-29751
GORE, J. P. N88-29927
GOTSELYUK, YU. V. N88-30500
GOVE, N. B. N88-30306
GRAFODATSKIY, O. S. N88-30501
GRAHAM, MATTHEW S. N88-29785
GRALLERT, H. N88-29806
GRANT, M. A. N88-30013
GRARD, R. N88-30556
GREBER, ISAAC N88-30084
GREELEY, RONALD N88-30488
N88-30492
GREEN, J. L. N88-30271
GREEN, ROBERT P., JR. N88-30280
GREGORY, DON A. N88-30110
GRIEF, RALPH N88-29993
GRIEVE, R. A. F. N88-30248
GRIFFIN, R. F. N88-30562
GRIFFITHS, K. C. N88-29732
GRIGOROV, N. L. N88-30519
GRIGORYEVA, L. B. N88-30519
GRIMSON, W. E. N88-30364
GRINGEL, D. N88-30182
GROOTHUIS, STEVEN K. N88-30150
GROSS-THEBING, ARNOLD N88-30127
GROSSMAN, J. N. N88-30478
GROTE, JAMES G. N88-30043
GRUAU, G. N88-30205
GRUBER, ROBERT P. N88-29869
GRUBIN, H. L. N88-30103
GRUEN, D. M. N88-30051
GRUN, J. N88-30424
GUBSKIY, V. F. N88-30516
GUELDER, OEMER L. N88-29917
GUERRAUD, CLAUDE N88-30087
GUEST, CLAYTON J. N88-30308
GUIDOS, BERNARD J. N88-29772
GUITON, T. A. N88-30414
GUO, B. Q. N88-30387
GUO, THEODORE C. N88-30008
GUO, WENDY W. N88-30008
GUPTA, AMAR N88-30449
N88-30452
N88-30454
N88-30455
N88-30457
N88-30468
GUSTAFSSON, G. N88-30418
GYAMFI, MAX N88-30357
GYOERFI, L. N88-30026

H

HAALAND, PETER D. N88-30423
HAGGERTY, S. E. N88-30217
HAGLUND, RICHARD F. N88-30121
HAINES, RICHARD F. N88-30301
HALE, STEVEN L. N88-29797
HALL, GARDINER N88-30342
HALL, J. S. N88-30416
HALL, P. N88-29715
N88-29716
HALL, PHILIP N88-29743
HAMBLEN, DAVID G. N88-29896
HAMLET, MURRAY P. N88-30278
HANNULA, SIMO-PEKKA N88-29964
HANSON, JON G. N88-30456
HAPPELL, NADINE N88-30344
HARDING, JOHN T. N88-29874
HARLEY, S. L. N88-30218
HARMANS, C. N88-30024
HARRIS, DONOVAN N88-29965
HARRIS, J. M. N88-29908
HARRIS, N. B. W. N88-30227
HARRISON, STEVEN G. N88-29792
HARTMAN, JOSEPH P. N88-30307
HARTMANN, WILLIAM K. N88-30219
HARTUNG, JACK B. N88-30258
HASSA, C. N88-29949
HAUG, EDWARD J. N88-29794
HAUSAUER, RUDOLPH J. N88-30049
HAUSER, MICHAEL L. N88-29826
HAUSKEN, T. R. N88-30417
HAVENS, VANCE N88-29863
N88-29872
HAWK, JAMES F. N88-30110
HAWKESWORTH, C. J. N88-30214
N88-30227
HAWKESWORTH, M. R. N88-30091
HAWORTH, LORAN A. N88-29785
HAYDEN, WARREN R. N88-29858
HEBRARD, P. N88-29914
HEEL, JOACHIM N88-30366
HEFFLEY, ROBERT K. N88-29819
HELLER, W. G. N88-30196
HEMLEY, R. J. N88-30481
HEMMINGER, JOHN C. N88-29904
HEMSCH, MICHAEL J. N88-29758
HENAFF, JEANNINE N88-30027
HENCKEN, ALAN N88-30143
HENDERGOTT, A. N88-29824
HERRALA, ESKO N88-30101
HERST, PETER J. N88-29966
HESS, R. W. N88-29795
HESS, RONALD A. N88-30297
HEWITT, F. A. N88-29806
HEXMOOR, HENRY N88-30332
HIBBS, BART D. N88-29822
HICKEY, MICHAEL PHILIP N88-30200
HILL, J. A. N88-30553
HILL, S. M. N88-30048
HILLS, D. V. N88-30217
HINDS, JOHN C. N88-30368
HINGST, WARREN R. N88-30084
HIRST, DONALD A. N88-30065
HO, SAM N88-30302
HOCKNEY, RICHARD N88-29995
HOEFFGEN, H.-J. N88-30118
HOFFMANN, U. N88-30182
HOFMANN, A. W. N88-30205
HOGARTH, ROBIN M. N88-30391
HOH, ROGER H. N88-29739
HOLAND, B. N88-30293
N88-30298
HOLBACK, B. N88-30418
HOLLERBACH, JOHN M. N88-30371
HOLLINGSWORTH, A. N88-30167
HOLLINGSWORTH, ANTHONY N88-30176
HOLMAN, THOMAS J. N88-30324
HOLMGREN, G. N88-30418
HOMANN, K. H. N88-29932
HONKANEN, SEPPO N88-30405
HORN, MICHAEL N88-30143
HOUBOLT, J. C. N88-29726
HOWARD, DEAN D. N88-30007
HOWARD, W. A. N88-30189
HOWELL, DAVID G. N88-30220
HOWLIN, KATHERINE N88-30343
HRUSA, W. J. N88-30145
HUA, C. T. N88-30504
HUA, GRACE N88-30331
HUBBERT, K. P. N88-29947
HUDSON, G. B. N88-30476
HUDSON, SCOTT N88-29999
HUENERS, H. N88-29852
HUERTA, MANUEL A. N88-30426
HUGHES, B. T. N88-30111
HUGHES, PETER N88-30330
HUNG, CHING-CHEH N88-29888
HUSAIN, NIZWER N88-30372
HUSS, G. R. N88-30476
HUTCHEON, I. D. N88-30479
HUTCHISON, R. N88-30479
HYDE, GEOFFREY N88-30023
HYER, M. W. N88-29884

I

ICELAND, WILLIAM F. N88-30131
IGONIN, M. P. N88-30511
IHNEN, S. M. N88-30257
IIZUKA, T. N88-29909
IKONEN, ERKKI N88-30403
IMMICH, H. N88-29868
INCE, BRIAN S. N88-29900
INMAN, DANIEL J. N88-30124
INNOCENTI, MARIO N88-29741
ISMAIL, ADNAN M. O. N88-29903
ITOH, M. N88-29803
ITOH, TATSUO N88-30011
IVANCHIK, M. V. N88-30527
IVANENKO, I. P. N88-30519
IZHOVKINA, N. I. N88-30514
N88-30518

J

JABLONSKI, F. J. N88-30559
JACKSON, ROBERT N88-30339
JACOBSON, THOMAS P. N88-30072
JAEGER, P. N88-30444
JAKOBSEN, P. N88-30556
JAKOSKY, BRUCE M. N88-30571
JAMES, B. H. N88-30307
JANSEN, S. L. N88-30250
JANSON, DOROTHY M. N88-30322
JANSSEN, PETER A. E. M. N88-30176
JARFALL, LARS N88-30157
JARVIS, B. J. N88-30567
JASNIEWICZ, G. N88-30564
JASUJA, A. K. N88-29919
JAWORSKI, ALLAN N88-30336
JAYANTHI, U. B. N88-30551
N88-30578
JEANJAQUET, S. L. N88-29975
JELL, C. S. N88-29762
JENKNER, HELMUT N88-30547
JEPHCOAT, A. P. N88-30481
JIH, RONG-SONG N88-30259
JOCHUM, K.-P. N88-30205
JOHN, BONNIE E. N88-30295
JOHNSON, BRUCE G. N88-29995
JOHNSON, JAMES E. N88-29747
JOHNSON, MARJORY J. N88-30321
JOHNSON, VICKI N88-30333
JOHNSTON, MARK N88-30336
N88-30339
JONES, DENNY A. N88-29977
JONES, J. G. N88-29728
JONES, MICHAEL G. N88-30329
JONES, MICHAEL N. N88-30261
JONES, R. N88-29887
JONES, THOMAS S. N88-30140
JOOS, F. N88-29918
N88-29923
JORGENSON, PHILIP C. E. N88-29780
JOSLYN, H. D. N88-29804
JOULIN, G. N88-29945
JUHASZ, A. A. N88-29895
JULL, E. V. N88-30025
JUST, H. N88-30446
N88-30448

K

KAARLS, R. N88-30024
KAHN, MARTHA N88-30332
KAILA, KARI N88-30101
KAIP, DENNIS D. N88-29823
KAKARAS, EM. N88-29941
KALDEICH, BRIGITTE N88-30447
KALDOR, RAYMOND B. N88-29867
KAMDAR, M. H. N88-29960
KANADE, TAKEO N88-30380
KANIC, P. G. N88-29876
KANIC, PAUL G. N88-29867
KAO, MICHAEL W. N88-30039
KAPP, ROLF N88-29761
N88-29764
KARASOPOULOS, HARRY A. N88-29829
KARES, ROBERT J. N88-30421
KARPOVICH, P. A. N88-29911
N88-29925
KATKOV, A. L. N88-30511
KATSAROS, KRISTINA B. N88-30267
KATZ, BORIS N88-30375
KAVALOV, A. R. N88-30563
KAZA, KRISHNA RAO V. N88-29807
KAZAROFF, JOHN M. N88-29874
KAZMIN, A. S. N88-30525
KELLER, JOSEPH B. N88-30057
KELLNER, ALBRECHT N88-30340
KENDIG, M. W. N88-29975
KENDIG, MARTIN W. N88-29974
KENNES, ROBERT N88-29897
N88-29907
N88-29955

KERSLAKE, WILLIAM R. N88-29833
KESSLER, M. F. N88-30556
KHALID, M. N88-29781
KHANDELWAL, GOVIND S. N88-30402
KHATTAK, CHANDRA P. N88-30435
KIKUCHI, H. N88-30028
KILBURN, C. R. J. N88-30490
KIMBERLY, JACK L. N88-29785
KING, DAVID Q. N88-29659
KINNY, P. D. N88-30211
N88-30221
KINO, G. S. N88-30138
KINTNER, PAUL N88-30418
KIRCHHOFF, V. W. J. H. N88-30185
N88-30186
KIRK, G. E. N88-29803
KIRKWOOD, THOMAS F. N88-29796
KITIPORNCHAI, S. N88-30141
KLATZKY, ROBERTA L. N88-30299
KLAUSMANN, W. N88-29915
KLEIN, N. N88-29990
KLEIN, V. N88-30118
KLEMPERER, SIMON L. N88-30222
KNAUER, W. N88-30443
KNAUSS, CARL J. N88-29967
KNIGHT, DOYLE D. N88-30064
KNIGHT, MICHAEL D. N88-30494
KNOEBEL, U. N88-30183
KNOTHE, KLAUS N88-30127
KNOTT, TAMARA W. N88-29884
KOCH, J. N88-30182
KOCHENOVA, N. A. N88-30513
N88-30517
KOCHNEVA, N. T. N88-30529
KOELLE, H. H. N88-29871
KOGAN, A. YU. N88-30510
KOLESNIKOV, YU. N88-30534
KOO, DAVID C. N88-30555
N88-30558
KOOPMAN, J. N88-29949
KOSE, S. N88-30552
KOSKINEN, HANNU N88-30418
KOTIN, V. A. N88-30510
KOVESI-DOMOKOS, S. N88-30066
KOWALEK, J. N88-29986
KOZLOV, A. G. N88-30501
KOZLOV, S. I. N88-30499
KRANTZ, KERRY N88-30343
KRAWCZYK, R. N88-30169
KREISEL, GEORGE R. N88-29801
KRETSCHMER, D. N88-29920
N88-29950
KRIEGER, R. J. N88-29756
N88-29763
N88-29766
KRIER, HERMAN N88-29861
KROENER, A. N88-30211
N88-30223
KRON, RICHARD G. N88-30558
KROVOTYNTSEV, V. A. N88-30527
KRYMSKIY, A. M. N88-30523
KUIPER, T. B. H. N88-30554
KULA, ERIC B. N88-30156
KUMAR, G. R. RAVINDRA N88-30208
KUO, SPENCER P. N88-30016
KUPERMAN, GILBERT G. N88-30296
KURIYAMA, MASAO N88-30427
N88-30431
N88-30437
N88-30440
KUROSAKA, M. N88-30069
KURRASCH, E. R. N88-29816
KUX, HERMANN J. H. N88-30178
KUX, HERMANN JOHANN HEINRICH N88-30168
KUZNETSOV, S. N. N88-30500
KWAK, DOCHAN N88-30085
KWUN, HEGEON N88-29885

L

LACAU, R. G. N88-29765
LACOMBE, C. N88-30149
LAMBIRD, BARBARA A. N88-30355
LANGENBERG, K. J. N88-30025
LANNELONGUE, NORBERT N88-30171
LAOR, URI N88-30427
N88-30431
N88-30437
LAPORTE, J. B. N88-29831
LARKINA, V. I. N88-30516
LARROUTUROU, B. N88-29944
LARSON, DAVID N88-30437
LARUE, ROLAND N88-30459
LASKER, BARRY M. N88-30547
LAVALLEE, DAVID B. N88-30358
LAVERGNE, G. N88-29914
LAVINE, DAVID N88-30355
LAWLER, JOHN V. N88-30077
LAWSON, WILLIAM S. N88-30041
LAZAREV, V. I. N88-30501
LAZNICKA, PETER N88-30250
LEA, ROBERT N. N88-30335
LEAVITT, KAREN N88-30362
LEBRETON, J.-P. N88-30556
LEDERMAN, SUSAN J. N88-30299
LEE, DONG IL N88-30034
LEE, GI GON N88-30144
LEE, ILZOO N88-29880
LEE, K. W. N88-30417
LEE, T. N. N88-30424
LEES, A. C. N88-30191
LEFEBVRE, ARTHUR H. N88-29913
LEGECKIS, R. N88-30525
LEGENKA, A. D. N88-30513
LEGGE, H. N88-29862
LEI, JIH-FEN N88-30106
LEINER, BARRY M. N88-30309
LELLOUCH, M. N88-30328
LELYAVIN, S. N. N88-30508
LENORMAND, R. N88-30037
LEONE, GIOVANNI N88-30002
LERNER, ROBIN N88-30339
LESHCHENKO, L. N. N88-30517
LEUNG, M. S. N88-30050
LEVAKHINA, L. V. N88-30505
LEVERITT, C. S. N88-29990
LEVIN, BETH N88-30375
LEVINE, JOEL S. N88-30544
LEVY, BERNARD C. N88-30385
LEVY, G. S. N88-30554
LEVY, SAUL Y. N88-30416
LEWICKI, DAVID G. N88-30128
LI-PING, WANG N88-29993
LIEBERT, CURT H. N88-30099
LIEW, T. C. N88-30223
LILJEGREN, TORSTEN N88-29868
LIN, CHING-TAI N88-30007
LINDENMAYER, KELLY N88-30338
N88-30339
N88-30361
LINDHOLM, U. S. N88-29811
LINK, M. N88-29852
LINN, ANN N88-30213
LIONELLO, PIERO N88-30176
LISSAMAN, PETER B. N88-29822
LIU, JINZHONG N88-30235
LIU, YEN N88-30384
LOEB, G. N88-29973
LOEFFLER, S. N88-29932
LOFTIN, R. BOWEN N88-30331
LONDDON, NORMAN N88-30447
LONGDON, NORMAN N88-29828
LONGSTAFF, R. N88-29827
LOOMIS, AUDREY N88-30340
LOPES, R. M. C. N88-30490
LORBACH, D. N88-29899
LOSIER, PAUL W. N88-29793
LOUVET, ANNE-CLAIRE A. N88-30318
LOW, CHARLES A., JR. N88-29873
LOW, H. C. N88-29919
LOWE, D. R. N88-30475
LOWE, DONALD R. N88-30480
LU, X. N88-29937
LUCCHITTA, B. K. N88-30491
LUENEBERG, E. N88-30025
LUNDGREN, ROGER N88-29988
LUPOVKA, V. A. N88-30502
N88-30503
LURIA, S. M. N88-30279
LYONS, VALERIE J. N88-29997
N88-30090

M

MABRY, THOMAS R. N88-30292
MACPHERSON, G. J. N88-30478
MACPHERSON, J. I. N88-29730
MACZUGA, D. E. N88-30231
MADNICK, STUART N88-30449
N88-30452
N88-30454
N88-30455
N88-30457
N88-30468
MADSEN, S. N88-30102
MAK, VICTOR W. K. N88-30312
MALKIN, O. A. N88-30502
MALVICHINI, C. N88-30118
MANHEIMER, WALLACE M. N88-30033
MANKA, C. K. N88-30424
MANSFELD, F. N88-29975
MANSON, NUMA N88-30087
MANTENIEKS, MARIS A. N88-29860
MANZI, A. O. N88-30263
MAO, H. K. N88-30481
MAPPER, D. N88-30401
N88-30580
MARDAS, CONSTANTINOS N88-30367
MARINHO, E. V. A. N88-30186
MARK, HERMAN N88-29833
MARKAM, JAMES R. N88-29896
MARR, R. N88-29899
MARRE, J. P. N88-30037
MARSDEN, R. N88-30556
MARSHAK, A. L. N88-30533
MART, Y. N88-30224
N88-30225
MARTIN, JOEL J. N88-30113
MARTIN, JONATHAN W. N88-29971
MARTIN, LEE U. N88-30264
MARTIN, R. E. N88-30184
MARTINET, L. N88-30565
N88-30567
N88-30569
MATHAUER, H. N88-29764
MATSUMOTO, Y. N88-30068
MATTHEWS, J. R. N88-30162
MATTHEWS, N. F. N88-30013
MATTHIES, LARRY N88-30380
MAUNG, KHIN M. N88-30402
MAVRIPLIS, DIMITRI J. N88-29749
MAYEDA, TOSHIKO K. N88-30477
MAYOR, M. N88-30560
N88-30561
N88-30562
N88-30564
MAZUMDER, JYOTI N88-29861
MAZUR, ERIC N88-30400
MAZZARELLA, GIUSEPPE N88-30002
MCCALLUM, I. S. N88-30226
MCCONNAUGHEY, H. V. N88-30094
MCDERMOTT, F. N88-30227
MCDONALD, JAMES R. N88-29786
MCGILL, GEORGE E. N88-30228
MCGREGOR, V. R. N88-30221
MCGREGOR, VIC R. N88-30234
MCGUIRK, J. J. N88-29940
MCHUGH, VINCENT M. N88-29900
MCKAY, G. A. N88-30482
MCKINNON, JOHN A. N88-30574
N88-30576
MCKNIGHT, MARY E. N88-29971
MCLAUGHLIN, K. L. N88-30191
MCLAUGHLIN, KEITH L. N88-30259
MCLEAN, E. A. N88-30424
MCLELLAND, J. M. N88-30229
MCMURDIE, LYNN A. N88-30267
MCNAMARA, LEO F. N88-30256
MCROBERTS, MALCOLM N88-30372
MCRUER, DUANE T. N88-29736
MEAD, JAYLEE M. N88-30545
MEADOR, MARY ANN N88-29984
MEEN, JAMES K. N88-30208
MEHMED, ORAL N88-29807
MEHTA, UNMEEL N88-29774
MELIUS, CARL F. N88-29902
MELLMAN, G. R. N88-30257
MELOSH, H. J. N88-30474
MENDOZA, J. G. N88-30417
MENG, C. I. N88-30195
MERTOGUL, AYHAN N88-29861
MESSICK, L. J. N88-30436
MEURZEC, J. L. N88-29723
MEWALDT, R. A. N88-30566
MEYER, ROBERT R., JR. N88-30093
MICHAELIS, H. N88-30446
N88-30448
MICHAELS, K. B. N88-30184
MIHM, J. N88-29973
MIKSELL, STEVE N88-30344
MILISENDA, C. N88-30223
MILLER, CHRIS N88-29963
N88-29965
MILLER, CHRISTOPHER J. N88-29771
MILLER, E. K. N88-30025
MILLER, GLENN N88-30338
N88-30339
MILLER, J. D., JR. N88-30252
MILLER, P. R. N88-30022
MING, TANG N88-30483
MINOR, THOMAS C. N88-29956
MIRANDA, ISIDORO N88-30153
MIRTICH, MICHAEL J. N88-29833
MISOVEC, KATHLEEN N88-29995
MIYAZAKI, M. N88-29906
MIZIOLEK, ANDRZEJ W. N88-29902

MKRTCHYAN, R. L. N88-30563
MNICH, MARC A. N88-29819
MOGENSEN, CRAIG N88-30469
MOK, FAI N88-29999
MOLENT, L. N88-29887
MOLION, L. C. B. N88-30263
MOLVAER, O. I. N88-30298
MOLZOW, MANFRED N88-29722
MOM, A. J. A. N88-29808
MOMBRINI, G. N88-30118
MONGER, PATRICIA N88-30339
MONGIA, HUKAM C. N88-29936
MONKEL, A. N88-30323
MONTLE, JOHN N88-29978
MOOIJ, H. A. N88-29738
MOON, RICHARD N. N88-29721
MOORE, RICHARD M. N88-29748
MORANDO, A. N88-30328
MORANTI, C. N88-30012
MOREAU, MICHEL N88-30087
MOREHOUSE, D. O. N88-30162
MORENO-BARRAGAN, J. N88-29852
MORGAN, PAUL N88-30230
MORIN, RICHARD L. N88-29843
MORKOC, HADIS N88-30433
N88-30438
MORKOVIN, MARK V. N88-30058
N88-30079
MORRIS, NANCY N88-30279
MORRISON, B. J. N88-30103
MORRISON, D. A. N88-30231
MORROW, WALTER B., JR. N88-30415
MOSES, C. A. N88-29925
MOSHER, DAVID N88-30053
MOSIER, S. A. N88-29911
MOSIG, J. N88-30000
MOSS, J. B. N88-29928
MOUGINIS-MARK, P. J. N88-30494
MOUNEIMNE, SAMIH A. N88-30345
MULCARE, DENNIS B. N88-29815
MULLER, H. N88-30133
MULLINS, J. N88-29933
MUNSHI, M. Z. N88-30054
MURDOCCA, MILES J. N88-30416
MURROW, H. N. N88-29727
MYERS, J. S. N88-30211
MYRSETH, E. N88-30293

N

NADEZHIN, D. K. N88-30505
NAMASTE, Y. M. N88-30056
NAQVI, S. M. N88-30241
NARASIMHAN, SUNDAR N88-30371
NASHMAN, MARILYN N88-30346
NASTROM, G. D. N88-30271
NAVA, E. N88-30118
NAYSHUL, A. B. N88-30512
NEAL, CLIVE R. N88-30232
N88-30244
NEHRU, C. E. N88-30478
NELSON, E. P. N88-30233
NELSON, ERIC N88-30206
NERAYANAN, G. V. N88-29807
NERI, J. A. C. F. N88-30551
NEVESEPIPHANIO, JOSE CARLOS N88-30165
N88-30172
NEWELL, P. T. N88-30195
NEWMAN, RICHARD L. N88-30300
NEWNHAM, R. E. N88-30096
N88-30104
N88-30112
NGUYEN, CHARLES C. N88-30134
NGUYEN, T. N88-29969
NGUYEN, TINH N88-29971
NICHOLS, DEAN H. N88-30394
NICOLET, B. N88-30546
NICOLET, MARCEL N88-29897
N88-29907
N88-29955
NIELSEN, JACK N. N88-29773
NIKOUKHAH, RAMINE N88-30385
NILES, ANTHONY R. N88-30175
NISBET, JOHN S. N88-30070
NOBACK, R. N88-29720
N88-29733
NOGUEIRA, J. L. M. N88-30263
NOHEL, J. A. N88-30145
NOLAN, SANDRA K. N88-30399
NOLL, B. N88-29915
N88-29938
NORMAN, COLIN N88-30549
NORRY, M. J. N88-30238
NUSCA, MICHAEL J. N88-30073
NUTH, JOSEPH A. N88-30536
NUTMAN, ALLEN P. N88-30234
NYQUIST, L. E. N88-30212

O

OAKLEY, CAROLYN J. N88-30285
OBENDORF, S. K. N88-30056
OCONNOR, LAWRENCE J. N88-29843
ODEH, F. N88-30429
ODGERS, J. N88-29920
N88-29950
ODWYER, M. A. N88-30091
OENEMA, W. N88-29788
OEY, P. N88-30442
OHARA, M. J. N88-30209
OHARA, TOMOYUKI N88-30170
OKEEFE, JOHN D. N88-30484
OLDHAM, W. G. N88-30439
OLOFSSON, MATS N88-30192
OLSON, WILLIAM S. N88-30270
OLVER, A. D. N88-30025
ONIONS, R. K. N88-30209
N88-30215
ORGUC, EMIN S. N88-29864
ORLIK-RUECKEMANN, K. J. N88-29731
ORTIZ, ALFREDO N88-30095
OSBORN, J. E. N88-30387
OSCARSSON, T. E. N88-30422
OSMAN, M. A. N88-30103
OWENS, B. B. N88-30054
OYEDIRAN, A. A. N88-30148

P

PAFFRATH, DIETER N88-30187
PAGNI, PATRICK J. N88-29997
PALMBERG, BJORN N88-30157
PANAGIA, NINO N88-30579
PANTANO, C. G. N88-30414
PAPAGEORGIOU, N. N88-29941
PAPPERT, STEPHEN A. N88-30404
N88-30413
PARADISO, JOSEPH N88-30369
PARK, JOEL T. N88-29747
PARKER, R. N88-30091
PARKER, R. J. N88-30098
PARRY, D. B. N88-29908
PASCHALL, RANDALL N. N88-30382
PASCHE, A. N88-30293
N88-30298
PATANKAR, S. V. N88-29805
PATELLA, J. N88-30442
PATTERSON, JAMES C., JR. N88-29789
PAUL, J. J. N88-29887
PAVLIN, V. N88-30348
PAWLOWSKI, M. N88-30139
PAYNE, B. W. N88-29732
PEACOCK, A. N88-30556
PEDERSON, A. N88-30556
PEHRSSON, KIRSTEN M. N88-29801
PELI, T. N88-30020
PELLIN, M. J. N88-30051
PENN, B. G. N88-30412
PEREIRADACUNHA, ROBERTO N88-30170
PEREZE, F. N88-29892
PERKINS, STANLEY C., JR. N88-29757
PERRENOT, F. N88-29847
PERRYMAN, M. A. C. N88-30556
PERSSON, SVEN-TUVE N88-30407
PETERS, J. E. N88-29912
PETERS, WOLFGANG N88-30187
PETERSON, JOHN B., JR. N88-29820
PETROV, P. P. N88-30504
PETRUSCHELL, ROBERT L. N88-29796
PETTY, GRANT W. N88-30267
PETZENHAUSER, I. N88-30444
PHINNEY, W. C. N88-30231
PICHUGIN, A. P. N88-30531
PIDGEON, R. T. N88-30211
PIERI, D. C. N88-30497
PIERRI, ROCCO N88-30002
PIKE, R. A. N88-29881
PINUS, V. K. N88-29972
PIOREWICZ, J. N88-30154
PIVOVAROV, M. L. N88-30509
PLATONOV, O. I. N88-30501
PLINE, ALEXANDER D. N88-30072
POESCHEL, R. L. N88-30443
POIRION, F. N88-29723
POLANSKY, DANIEL N88-30140
POLYCHRONOPOULOS, GEORGE H. N88-30005
PONZONI, FLAVIO JORGE N88-30179
POOR, H. V. N88-30021
POPOV, G. V. N88-30501
PORTER, J. F. N88-30162
POSIN, SETH B. N88-30488
POTTS, D. M. N88-30152
POUCHER, D. E. N88-29744
N88-29745
N88-29770
POWELL, RICHARD C. N88-30113
POWER, JOHN L. N88-29873
POZOS, ROBERT S. N88-30278
PRATT, H. L. N88-30122
PRESTESBARBOSA, MARX N88-30170
PRIANTE, S. J. N88-29898
PRICE, DENNIS L. N88-30296
PRINCE, T. A. N88-30566
PRINZ, M. N88-30478
N88-30482
PSALTIS, DEMETRI N88-29999
PULINETS, S. A. N88-30518
PURINTON, STEVE N88-30356

Q

QIAN, XIANGLIN N88-30235
QIN, XIAORONG N88-30117
QUAK, D. N88-30040
QUILLIN, ROBERT N88-30344

R

RAGALLER, DANA N88-29863
N88-29872
RAI, MAN MOHAN N88-29750
RAITCH, FREDERICK A. N88-29768
RANDJBAR-DAEMI, S. N88-30445
RASH, JAMES N88-30330
RASH, JAMES L. N88-30341
RASINKANGAS, REIJO N88-30101
RAU, M. S. N88-30414
RAYCRAFT, JANET K. N88-29998
REDDY, Y. V. N88-30372
REED, CATHERINE N88-30299
REEDY, JAMES T. N88-30297
REES, JONATHAN N88-30311
REHFELDT, T. K. N88-29970
REICHELT, M. N88-30429
REINISCH, BODO W. N88-30256
REISSMANN, F. N88-30182
REISTAD, MAGNAR N88-30176
REISTER, HEINRICH N88-30075
RENARDY, M. N88-30145
RENAULT, M. N88-29892
RENE, D. N88-30037
RENNER, UDO N88-29844
RENZETTI, N. A. N88-30554
REUTOV, YE. A. N88-30532
REYNOLDS, THOMAS L. N88-29793
RHODES, MARVIN D. N88-30130
RICCI, WILLIAM S. N88-30156
RICHER, SUZANNE N88-30464
RICHON, JOEL N88-30339
RIEGER, H. N88-29764
RIETHMULLER, M. L. N88-30062
N88-30083
RIPIN, B. H. N88-30424
RITCHIE, R. O. N88-30142
RITTER, NILES N88-30347
ROBBINS, DAVID O. N88-30287
ROBERTS, E. W. N88-30136
ROBERTS, LEONARD N88-29821
ROBINSON, E. L. N88-30553
ROBSON, D. N88-30013
RODRIGUEZ, R. N88-30056
ROEFS, H. F. A. N88-30323
ROELOFS, LARRY N88-30354
ROGERS, ERNEST O. N88-29779
ROGERS, J. D. N88-30091
ROGERS, JOHN J. W. N88-30208
ROMANOFF, H. P. N88-29795
ROMANOV, P. YU. N88-30526
ROMERO-SIERRA, C. N88-30032
RONNMARK, K. G. N88-30422
ROSEN, I. G. N88-30386
ROSENFELD, MOSHE N88-30085
ROSFJORD, T. J. N88-29916
ROSS, EDWARD W. N88-29996
ROSS, YU. K. N88-30533
ROWELL, DEREK N88-30369
ROWLAND, SCOTT K. N88-30494
ROZANOV, V. V. N88-30526
RUBIN, A. E. N88-30478
RUDNICK, ROBERTA L. N88-30236
RUDORFF, BERNARDO F. T. N88-30180
RUDORFF, BERNARDO, F. T. N88-30174
RUEDA, F. N88-30012

RUFENER, F. N88-30546
RUGH, WILSON J. N88-30363
RUMBLE, S. J. N88-30097
RUSCHAU, JOHN J. N88-29889
RUSHBY, JOHN N88-30304
RUSSELL, JANE L. N88-30547
RUSSELL, RICHARD A. N88-29850
N88-29856
RYDER, G. N88-30212
RYDER, GRAHAM N88-30237
RYVARDEN, H. N88-30298

S

SA, L. D. A. N88-30263
SACKS, ELISHA PERETZ N88-30379
SACKS, JEROME N88-30390
SAIF, A. G. N88-30434
N88-30441
SAINT-CLOUD, JEAN N88-30067
SALES, GARY S. N88-30018
SALO, J. K. N88-29989
SALOUR, MICHAEL M. N88-30409
SALTER, P. N88-30091
SAMEJIMA, FUMIKO N88-30289
SAMUELSEN, G. S. N88-29926
SANDERSON, T. K. N88-30401
N88-30580
SANTANNABINS, LEONARDO N88-30310
SANZ, J. M. N88-30012
SATTERWHITE, MELVIN B. N88-30166
SAUND, ERIC N88-30374
SAUNDERS, A. D. N88-30238
SAVAGE, CYNTHIA A. N88-30463
SAWATZKY, GUENTER N88-29957
SBARDELLATI, A. N88-30328
SCALA, C. M. N88-30398
SCHAENZER, G. N88-29719
SCHAERER, URS N88-30239
SCHELLHORN, M. N88-30135
SCHERRER, DOMINIQUE N88-29948
SCHICK, WILBUR R. N88-29825
SCHRINZI, GILDA N88-30002
SCHMID, FREDERICK N88-30435
SCHMIDT, RICHARD F. N88-30039
SCHMIDT, RODNEY A. N88-30406
SCHMITZ, MARION N88-30545
SCHMITZ, W. N88-30182
SCHNABEL, ROBERT B. N88-30313
SCHNEEBERGER, D. M. N88-30497
SCHNEIDER, JUDY N88-29858
SCHOTT, TIMOTHY D. N88-30108
SCHOUTENS, JACQUES E. N88-29882
SCHUBERT, G. N88-30240
SCHUBERT, G. S. N88-30213
SCHUMANN-LUCK, A. N88-29852
SCHWAB, J. R. N88-30078
SCHWARTZ, ALAN W. N88-29779
SCHWARTZ, SCOTT N88-29861
SCHWING, JAMES L. N88-30320
SCOTT, DAVID H. N88-30489
SCOTT, E. R. D. N88-30478
SCOTT, L. G. N88-30398
SCULLY, JOHN R. N88-29976
SEERING, WARREN P. N88-30132
N88-30397
SEIDEL, DAVID A. N88-29778
SELIGA, T. A. N88-30017
SERGEYEV, V. A. N88-30500
SERIO, MICHAEL A. N88-29896
SESKO, D. N88-30114
SEVERNYY, A. B. N88-30504
SHA, W. T. N88-29987
SHAFFER, DAVID A. N88-30163
SHAFTER, A. W. N88-30553
SHARPTON, V. L. N88-30248
SHATZ, MICHAEL P. N88-30005
SHEAFFER, PATRICK M. N88-29891
SHEEHAN, J. E. N88-29881
SHEH, MICHAEL Y. N88-29961
SHEPPARD, C. G. W. N88-29947
SHERATON, J. W. N88-30243
SHERIFF, STEVEN D. N88-30198
SHESTOPEROV, V. YA. N88-30519
SHEYKHET, A. I. N88-30504
SHI, YIJIAN N88-30266
SHIELDS, A. N88-30412
SHORT, NICHOLAS, JR. N88-30352
SHRADY, CATHERINE H. N88-30228
SHUCHMAN, R. A. N88-30035
SHUELY, WENDEL J. N88-29900
SHUMWAY, R. H. N88-30191
SHUTKO, A. M. N88-30532
SHYNE, RICKEY J. N88-29746
SHYUTTE, N. M. N88-30514
SHYY, W. N88-29935
SIDI, AVRAM N88-30377
SIEFKE, STANLEY P. N88-29791
SIEGEL, DAVID M. N88-30371
SIEGEL, M. W. N88-30410
SILVAFILHO, V. P. N88-30263
SILVERMAN, BARRY G. N88-30332
SIMES, R. J. N88-30417
SIMMONS, B. N88-29933
SIMON, B. N88-29918
N88-29923
SIMON, MARVIN K. N88-30001
SIMON, PAUL C. N88-30188
SIMON, T. W. N88-29805
SIMONS, RAINEE N. N88-30055
SINES, GEORGE N88-29878
SINGER, JOSEPH N88-29952
SINGER, NEIL C. N88-30397
SIU, S. C. N88-30142
SIVATHANU, Y. R. N88-29927
SKELTON, R. T. N88-30091
SKOU, N. N88-30102
SKULACHEV, D. P. N88-30520
SMALLEY, ANTHONY J. N88-29825
SMART, DAVID N88-30045
SMITH, CHARLES V., JR. N88-30042
SMITH, DOUGLAS R. N88-30060
SMITH, F. T. N88-29715
N88-29716
SMITH, GILES K. N88-29796
SMITH, JAMES E. N88-29832
SMITH, JEFFREY H. N88-30357
SMYTH, WILLIAM H. N88-30572
SNODGRASS, RICHARD N88-30451
SNYDER, LARRY N88-30302
SOLOMON, PETER R. N88-29896
SOLOSHENKO, I. I. N88-30530
SOLYMOSI, J. N88-30026
SONG, PAUL N88-30014
SOO, S. L. N88-29987
SOOD, ARUN N88-30351
SOREK, S. N88-30283
SOTHERAN, A. N88-29922
SOUZA, C. A. W. N88-30551
SOVEY, JAMES S. N88-29860
SPIEGEL, JAMES R. N88-30358
SPINDLER, G. N88-30135
SPIRIDONOV, YU. G. N88-30524
SPONSLER, JEFF N88-30338
SPONSLER, JEFFREY L. N88-30360
SPRIDONOV, YU. G. N88-30531
SRINIVASAN, R. N88-30076
N88-30241
SRINIVASAN, VAKULA S. N88-29952
STANDLEY, D. L. N88-30046
STANEWSKY, E. N88-29824
STANSFIELD, S. A. N88-30299
STEIN, H. J. N88-30051
STEIN, M. N88-30242
STEINER, BRUCE N88-30427
N88-30431
N88-30437
STEPHEN, J. H. N88-30401
N88-30580
STEWART, C. D. N88-29928
STEWART, DORATHY ANNE N88-30268
STEWART, P. A. E. N88-30091
STOFFER, J. O. N88-29978
STONE, E. C. N88-30566
STONE, JAMES R. N88-29859
STONE, JOHN C. N88-30470
STRATHDEE, J. N88-30445
STRAUCH, R. G. N88-30271
STRAUSBERGER, DONALD J. N88-30038
STREATFEILD, D. K. N88-30107
STRECKERT, H. H. N88-29881
STRIFE, J. R. N88-29881
STROENISCH, VOLKER EWALD N88-30047
STRUKOV, I. A. N88-30520
STRUNCK, VOLKER N88-30080
STUBBS, R. M. N88-29845
STUPIAN, G. W. N88-30050
STUREK, WALTER B. N88-29772
SUSSMAN, GERALD J. N88-30566
SUTHERLAND, L. L. N88-30035
SUZUKI, M. N88-29906
SWIDER, WILLIAM N88-30197
SWITHENBANK, J. N88-29937
N88-30092
SWOLINSKY, M. N88-29719
SYED, K. J. N88-29928
SYLVESTER, PAUL N88-30536
SYVERSEN, T. N88-30298
SZABO, CS. N88-30026
SZELISKI, RICHARD N88-30380
SZKODY, P. N88-30553

T

TAKAHASHI, S. N88-29906
TAM, ANDREW C. N88-29905
TAN, PAUL W. N88-29879
TANAKA, KENNETH L. N88-30485
TANANAYEVA, G. A. N88-30529
TANSKANEN, PEKKA N88-30101
TARANTUL, KENNETH S. N88-29896
TARNEY, J. N88-30238
N88-30243
TAWA, LAWRENCE SHINZO N88-30274
TAYLOR, J. N88-29729
TAYLOR, LAWRENCE A. N88-30244
TAYLOR, PAUL N. N88-30245
TAYLOR, PHILIP L. N88-29972
TAYLOR, STUART ROSS N88-30246
N88-30247
TEGTMEYER, A. N88-30223
TEIPEL, I. N88-29782
TEIXEIRABATISTA, GETULIO N88-30174
N88-30180
TELTSOV, M. V. N88-30501
TEMNYY, V. V. N88-30515
TEREBIZH, A. V. N88-30504
THEILHABER, K. N88-30425
THEILIG, E. N88-30496
THIARD, B. N88-29875
THIEME, LANNY G. N88-30472
THOMAS, M. D. N88-30248
THOMPSON, DANIEL B. N88-29800
THOMPSON, J. T. N88-30336
THOMPSON, WILLIAM T. N88-30199
N88-30262
THORNE, LARRY R. N88-29902
THORSTENSEN, J. R. N88-30553
TIELENS, A. G. G. M. N88-30537
TIMOFEYEV, YU. M. N88-30526
TIRA, J. S. N88-29980
TITOV, D. V. N88-30522
TOFT, P. B. N88-30217
TOLK, N. H. N88-30121
TOMITA, Y. N88-30062
N88-30083
TOMPKINS, R. E. N88-29895
TOWNSEND, DENNIS P. N88-30128
TOWNSEND, LAWRENCE W. N88-30402
TREDICI, THOMAS J. N88-30280
N88-30285
TRIPOLI, GREGORY J. N88-30269
TRIPP, L. R. N88-29816
TRIZNA, DENNIS B. N88-30036
N88-30264
TROUVE, A. N88-29942
TRUSHKINA, YE. P. N88-30518
TRUSZKOWSKI, WALTER F. N88-30332
TSAO, S. S. N88-30051
TSE, D. N88-29924
TSUKORNIK, I. G. N88-30530
TSUTAKAWA, ROBERT K. N88-30392
TSYUPAK, I. M. N88-30528
TUCKER, W. C. N88-30257

U

UCHARD, H. N88-30446
N88-30448
UEDA, MARIO N88-30420
UNDERWOOD, J. H. N88-29960
N88-30147
UNRUH, JAMES F. N88-29747
UPPALA, S. N88-30167
URBAN, MAREK W. N88-29968
UTTAL, WILLIAM R. N88-30288

V

VAKULOV, P. V. N88-30519
VALENTIAN, D. N88-29892
VANDERWEKKEN, A. J. P. N88-29733
VANSWOL, R. W. N88-29838
VANZANDT, LONNIE L. N88-29981
VARSHNEY, PRAMOD K. N88-30009
VASHKOVYAK, M. A. N88-30506
VASILYEV, YU. YA. N88-30519
VECHAMBRE, J. P. N88-29847
VEIZER, JAN N88-30249
N88-30250
VELSKO, C. N88-30476
VIANEISOARES, JOAO N88-30178
VICK, SHON N88-30338
N88-30339
N88-30361

VICKERS, BRIAN D. N88-29878
VIEIRADIAS, LUIZ ALBERTO N88-30179
N88-30316
VIEIRAMONTEIRO, ANTONIO MIGUEL N88-30310
VILLELA, T. N88-30551
VINOKUR, MARCEL N88-30071
N88-30384
VISWANADHAM, Y. N88-30263
VISWANATHAN, SIVASWAMY N88-30052
VOERSMANN, P. N88-29719
VOGEL, F. N88-29852
VOLKMER, KENT N88-30357
VOLPYAN, G. V. N88-30524
VONBRIESEN, MARY N88-30471

W

WAGNER, H. GG. N88-29934
WAISS, RICHARD D. N88-29856
WALBORN, NOLAN R. N88-30550
WALCH, STEPHEN P. N88-29893
WALKEN, P. R. N88-30554
WALKER, G. P. L. N88-30494
WALSH, THOMAS P. N88-29793
WANG, CAROLINE N88-30356
WANG, JIANLIANG N88-30363
WANG, LUI N88-30331
WANG, TE-HUI N88-30011
WARDLAW, ANDREW B., JR. N88-29759
WARREN, PAUL H. N88-30251
WARSI, Z. U. N88-30378
WASSERBURG, G. J. N88-30479
WASSON, JOHN T. N88-30541
WATKINS, PIA M. N88-29867
WATTAWA, SCOTT L. N88-30352
WAYNER, PETER C., JR. N88-29901
WEAVER, STEPHEN N88-30206
WECHSLER, HARRY N88-30350
WEDDLE, LEONARD EARL N88-29853
WEDEMEYER, E. N88-29824
WEIBLEN, P. W. N88-30252
WEIDENSCHILLING, S. J. N88-30539
WEILAND, M. N88-29852
WEISBERG, M. K. N88-30478
WEISSERT, JERRY N88-30343
WELCH, WILLIAM J. N88-30538
WELD, DANIEL S. N88-30395
WENKE, GERHARD N88-30125
WERTHEIMER, S. J. N88-30306
WHARTON, STEPHEN W. N88-30349
WHITE, C. N88-30076
WHITE, J. N88-30429
WHITE, J. V. N88-30196
WHITE, JACOB N88-30045
WHITE, K. J. N88-29895
WHITEHOUSE, M. J. N88-30253
WHITELAW, J. H. N88-29924
WHITING, LISA R. N88-29963
WHITLOW, WOODROW, JR. N88-29754
WIELEBINSKI, R. N88-30031
WIEMAN, CARL F. N88-30114
WILD, P. N. N88-29937
WILDMAN, P. J. L. N88-30102
WILKINS, DAVID E. N88-30370
WILKINSON, WILLIAM N88-30344
WILKS, M. E. N88-30254
WILLIAMS, A. N88-29933
WILLIAMS, I. S. N88-30211
WILLIAMS, J. E. N88-29756
N88-29763
N88-29766
WILLIAMS, MARC H. N88-29807
WILLOUGHBY, A. J. N88-29845
WILLSKY, ALAN S. N88-30385
WILSON, DENISE L. N88-30298
WILSON, GEORGE S. N88-30277
WILSON, JOHN W. N88-30402
WILSON, N J. N88-29809
WISDOM, JACK N88-30568
WITTIG, S. N88-29915
N88-29938
WITTIGN, S. N88-29931
WOHLEVER, JAMES CHRISTOPHER N88-30151
WOICESHYN, P. N88-30167
WOJCIECHOWSKI, J. Q. N88-29990
WOLF, H. N88-29932
WOLTJER, L. N88-30535
WONG, A. K. N88-30161
WONG, YEN F. N88-30341
WOOD, C. A. N88-30255
WOOD, C. P. N88-29926
WOOD, JOHN A. N88-30540
WOOD, M. A. N88-30553
WOOD, ROSEMARY GRACE N88-30273
WOODCOCK, ROBERT J. N88-29740
WOODWARD, R. L. N88-30147
WOOLLEY, MICHAEL G. N88-29834
WORMHOUDT, J. N88-29894
WORMLEY, DAVID N88-30389
WU, HENRY N88-30319
WU, S. T. N88-29848
WU, Y. N88-30481
WYATT, J. L., JR. N88-30046
WYBORN, D. N88-30243
WYBORN, L. E. A. N88-30243

X

XAPSOS, M. N88-30442
XIA, XUEJIAN N88-29753
XIAO, YELUN N88-30266

Y

YAMASHITA, E. N88-30025
YANG, JACKSON C. S. N88-30348
YANG, ZHENG N88-29878
YATES, GIGI N88-30347
YOST, WILLIAM T. N88-30160
YOUNG, C. E. N88-30051
YU, JEFF N88-29999
YU, W. N88-30142
YU, XIAOSHEN N88-29753

Z

ZAKHOR, AVIDEH N88-30383
ZALEWSKI, E. F. N88-30109
ZANIEWSKI, GREGORY S. N88-29798
ZATSEPIN, V. I. N88-30519
ZEIS, JOSEPH E., JR N88-29769
ZENG, HANSHENG N88-30117
ZERKLE, DAVID K. N88-29861
ZHAO, ZHENYAN N88-30266
ZHURAVLEV, D. A. N88-30519
ZIEGLER, BERND N88-29877
ZIMBELMAN, JAMES R. N88-30493
ZIMMERMAN, WAYNE N88-30357
ZIMMERMANN, HARALD H. N88-30461
ZINNER, ERNST N88-30483
ZISK, STANLEY H. N88-30486
ZOCH, DAVID N88-30342
ZOLTANI, C. K. N88-30086
ZUSTRA, MICHAEL A. N88-30286
ZVEREVA, A. M. N88-30504

Typical Corporate Source Index Listing

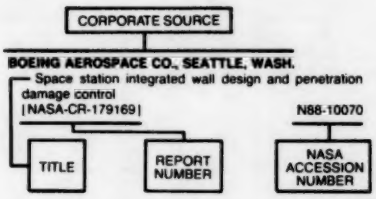

Listings in this index are arranged alphabetically by corporate source. The title of the document provides the user with a brief description of the subject matter. The report number helps to indicate the type of document cited (e.g., NASA report, translation, NASA contractor report). The NASA accession number denotes the number by which the citation is identified. The titles are arranged under each corporate source in ascending accession number order.

A

ACADEMY OF SCIENCES OF THE ARMENIAN SSR, ERIVAN.
Lagrangian of the self-duality equation and d = 10, N = 2b supergravity
[DE88-701554] N88-30563

ADVANCED FUEL RESEARCH, INC., EAST HARTFORD, CONN.
Experiments and modeling of multi-component fuel behavior in combustion
[AD-A195011] N88-29896

ADVISORY GROUP FOR AEROSPACE RESEARCH AND DEVELOPMENT, NEUILLY-SUR-SEINE (FRANCE).
The Flight of Flexible Aircraft in Turbulence: State-of-the-Art in the Description and Modelling of Atmospheric Turbulence
[AGARD-R-734-ADD] N88-29717

The Flight of Flexible Aircraft in Turbulence: State-of-the-Art in the Description and Modelling of Atmospheric Turbulence
[AGARD-R-734] N88-29725

Advances in Flying Qualities
[AGARD-LS-157] N88-29735

Special Course on Missile Aerodynamics
[AGARD-R-754] N88-29755

Combustion and fuels in gas turbine engines
[AGARD-CP-422] N88-29910

Barriers to Information Transfer and Approaches Toward Their Reduction
[AGARD-CP-430] N88-30458

AEG-TELEFUNKEN, WEDEL (WEST GERMANY).
Alternative module configurations for advanced solar arrays on low orbit and extended lifetime missions (AMOC 2)
[ESA-CR(P)-2581] N88-30182

AERITALIA S.P.A., NAPLES (ITALY).
Fluid physics double rack
[SD-TN-AI-012] N88-29992

Accommodation concept for fluid physics facilities, volume 2
[SG-TN-AI-027-VOL-2] N88-29994

AERITALIA S.P.A., TURIN (ITALY).
Study of robotics spacecraft servicing and assembly in space. Volume 1: Executive summary
[ESA-CR(P)-2612-VOL-1] N88-29839

Improvements of DCAP 1, phase 2-3/A
[D2-RP-AI-106] N88-30325

Study on industrial organization for European Ground Support Equipment (EGSE) to support European space programs. Volume 1: Technical reports
[SD-RP-AI-009-VOL-1] N88-30446

Study on industrial organization for European Ground Support Equipment (EGSE) to support European space programs. Volume 2: Technical reports
[SD-RP-AI-009-VOL-2] N88-30448

AERODYNE PRODUCTS CORP., BILLERICA, MASS.
Molecular line shape effects on atmospheric window absorption
[AD-A196316] N88-29894

AEROJET ELECTROSYSTEMS CO., AZUSA, CALIF.
Development of a unit cell for a Ge:Ga detector array
[NASA-CR-177445] N88-30100

AEROJET TECHSYSTEMS CO., SACRAMENTO, CALIF.
Orbital transfer vehicle 3000 LBF thrust chamber assembly hot fire test program
[NASA-CR-182145] N88-29858

AERONAUTICAL RESEARCH INST. OF SWEDEN, STOCKHOLM.
Standard fatigue specimens for fastener evaluation
[FFA-TN-1987-68] N88-30157

AERONAUTICAL RESEARCH LABS., MELBOURNE (AUSTRALIA).
Criteria for matrix dominated failure
[AD-A196263] N88-29887

Experimental aspects of using time-averaged holographic interferometry to detect barely visible impact damage in a graphite/epoxy composite plate
[AD-A194418] N88-30097

Development and installation of an instrumentation package for GE F404 investigative testing
[AD-A196265] N88-30107

Report on an overseas visit to USA relating to the thermoelastic measurement of stresses, 16-21 August 1987
[AD-A195313] N88-30161

Implementation of the NCAR (National Centre for Atmospheric Research) graphics package at ARL (Aeronautical Research Laboratory)
[AD-A195163] N88-30193

The development of acoustic emission for structural integrity monitoring of aircraft
[AD-A196264] N88-30396

AEROSPACE CORP., EL SEGUNDO, CALIF.
Transverse expansion of individual carbon and graphite filaments
[AD-A195073] N88-29891

Particle sizing in combustion systems, using scattered laser light
[AD-A196231] N88-29953

Microcircuit trace cutting with focused ion beams
[AD-A196030] N88-30050

Tolerances for phase locking of semiconductor laser arrays
[AD-A195974] N88-30120

AEROVIRONMENT, INC., MONROVIA, CALIF.
Development and design of windtunnel and test facility for RPV (Remote Piloted Vehicle) enhancement devices
[AD-A194842] N88-29822

AIR COMMAND AND STAFF COLL., MAXWELL AFB, ALA.
Centralized class A flight mishap investigation
[AD-A194397] N88-29786

The Soviet Stealth fighter: Check or checkmate
[AD-A195200] N88-29791

The OFP (Operational Flight Program) update cycle needs you
[AD-A194910] N88-29798

Integration of LANTIRN (Low Altitude Navigation and Targeting Infrared for Night) into operational fighter training
[AD-A194906] N88-29799

LANTIRN simulator training in the F-16C
[AD-A195201] N88-29826

Reduced flexibility in processing Titan 4 space launch vehicles at Cape Canaveral Air Force Station
[AD-A194908] N88-29834

Sensor and actuator selection for large space structure control
[AD-A194912] N88-29842

Antisatellite weapons and satellite deployment strategies
[AD-A195014] N88-30396

AIR FORCE ASTRONAUTICS LAB., EDWARDS AFB, CALIF.
Descriptive characterization of propellant particles
[AD-A195176] N88-29885

In-house capacitor technology program
[AD-A194804] N88-30049

AIR FORCE GEOPHYSICS LAB., HANSCOM AFB, MASS.
Particle trajectories and potentials in a plane sheath moving in a magnetoplasma
[AD-A196228] N88-30190

On formulating a simple D-region model
[AD-A195841] N88-30197

AIR FORCE INST. OF TECH., WRIGHT-PATTERSON AFB, OHIO.
Numerical solutions of unsteady inviscid transonic turbine cascade flows
[AD-A196111] N88-29748

Angle of attack and sideslip estimation using an inertial reference platform
[AD-A194876] N88-29769

An analysis of lateral-directional handling qualities and Eigenstructure of high performance aircraft
[AD-A194874] N88-29814

Controlled degradation of resolution of high-quality flight simulator images for training effectiveness evaluation
[AD-A196189] N88-29823

Investigation of the validity of the non-rotating planet assumption for three-dimensional earth atmospheric entry
[AD-A194877] N88-29829

Damage initiation in the short beam shear test of composite materials using stiffness reduction
[AD-A194880] N88-29883

Modeling and performance of HF/OTH (High-Frequency/Over-the-Horizon) radar target identification systems
[AD-A196287] N88-30036

The effects of incoming boundary layer thickness on unsteady shock-induced turbulent separations induced by cylinders
[AD-A196190] N88-30060

The aspect ratio dependence of the attractor dimension in Taylor-Couette flow
[AD-A196297] N88-30065

Large displacement and rotational formulation for laminated cylindrical shells including parabolic transverse shear
[AD-A194871] N88-30158

An investigation of constitutive models for predicting viscoplastic response during cyclic loading
[AD-A194875] N88-30163

Atmospheric corrections for in-flight satellite radiometric calibration
[AD-A196124] N88-30194

Doppler radar analysis of coastal marine atmospheric boundary layer structure during a cold air outbreak
[AD-A196023] N88-30261

Comparison of morning with afternoon nitrogen elimination in resting subjects breathing 100 percent oxygen
[AD-A196191] N88-30282

A detection theory analysis of visual display performance
[AD-A196291] N88-30292

Robust finite-dimensional LQG (Linear Quadric Gaussian)-based controllers for a class of distributed parameter systems
[AD-A194872] N88-30382

Ion kinetics in silane plasmas
[AD-A196202] N88-30423

Design and performance analysis of a relational replicated database system
[AD-A196290] N88-30456

AIR FORCE SYSTEMS COMMAND, WRIGHT-PATTERSON AFB, OHIO.
Mode locking of semiconductor laser with external cavity
[AD-A196018] N88-30117

Transverse CO2 laser two-dimensional gain distributions
[AD-A196240] N88-30119

AIR FORCE WEAPONS LAB., KIRTLAND AFB, N. MEX.
EMPTAC (Electromagnetic Pulse Test Aircraft) user's guide
[AD-A195072] N88-30006
AIR FORCE WRIGHT AERONAUTICAL LABS., WRIGHT-PATTERSON AFB, OHIO.
A second look at MIL prime flying qualities requirements N88-29740
A multiprocessor avionics system for an unmanned research vehicle
[AD-A194806] N88-29800
Fatigue crack growth characteristics of ARALL (trademark)-1
[AD-A196185] N88-29889
Precision measurement of the Fresnel drag coefficient using a ring laser
[AD-A196025] N88-30043
AKRON UNIV., OHIO.
An experimental study of biaxial yield in modified 9Cr-1Mo steel at room temperature
[NASA-CR-175012] N88-30164
ALABAMA UNIV., HUNTSVILLE.
Coordinated study of Solar-Terrestrial Observatory (STO) payloads on space station
[NASA-CR-183142] N88-29848
ALCATEL THOMSON ESPACE, TOULOUSE (FRANCE).
A 30/20 GHz multibeam array antenna suitable for future high rate TDMA European satellite networks
[ETN-88-93079] N88-30037
Microwave remote sensing in the French industries
[ETN-88-93081] N88-30171
AMERICAN SCIENCE AND ENGINEERING, INC., CAMBRIDGE, MASS.
ZT imaging system for layered thin wall structures
[AD-A195468] N88-29954
AMSTERDAM UNIV. (NETHERLANDS).
Path planning and path following for the Amsterdam autonomous cart
[FVI-86-22] N88-30133
ANALYTIC SCIENCES CORP., READING, MASS.
Estimation of short-wavelength gravity on a dense grid using digital terrain elevation data
[AD-A196325] N88-30196
ANAMET LABS., INC., HAYWARD, CALIF.
Computer programs for generation of NASTRAN and VIBRA-6 aircraft models
[AD-A195467] N88-29792
ANT NACHRICHTENTECHNIK, BACKNANG (WEST GERMANY).
PSDE/SAT 2: Preliminary spacecraft configuration study, executive summary
[ESA-CR(P)-2618] N88-29840
APPLIED RESEARCH LAB., STATE COLLEGE, PA.
An approach to CMG steering using feedback linearization
[NASA-CR-183172] N88-30369
APTECH ENGINEERING SERVICES, INC., SUNNYVALE, CALIF.
Stress intensity factors for cracked metallic structures under rapid thermal loading
[AES-8609709F-1] N88-29962
ARGONNE NATIONAL LAB., ILL.
Preliminary investigation of flow modeling during solid propellant processing
[AD-A196168] N88-29987
Impurity analysis in SIMOX samples by high-efficiency resonance ionization time-of-flight mass spectrometry
[DE88-012061] N88-30051
ARIZONA STATE UNIV., TEMPE.
Eruptive viscosity and volcano morphology N88-30488
The Martian highland paterae: Evidence for explosive volcanism on Mars N88-30492
ARMY ARMAMENT RESEARCH, DEVELOPMENT AND ENGINEERING CENTER, PICATINNY ARSENAL, N.J.
Discovery of a low temperature form of TAGN (Triaminoguanidinium Nitrate)
[AD-A196059] N88-29989
ARMY ARMAMENT RESEARCH AND DEVELOPMENT COMMAND, WATERVLIET, N. Y.
Additional fracture and strength test results for A723 steel and 38644 titanium
[AD-A196329] N88-29960
Wide range stress intensity factor expression for an edge-cracked round bar bend specimen
[AD-A196285] N88-30147
ARMY AVIATION ENGINEERING FLIGHT ACTIVITY, EDWARDS AFB, CALIF.
JUH-1H redesigned pneumatic boot deicing system flight test evaluation
[AD-A194918] N88-29785
Preliminary airworthiness evaluation of the UH-60A/ESSS (External Stores Support System) with HELLFIRE launcher installed
[AD-A196187] N88-29793
ARMY AVIATION SYSTEMS COMMAND, CLEVELAND, OHIO.
Impact of ETO propellants on the aerothermodynamic analyses of propulsion components
[NASA-TM-101303] N88-30094
ARMY AVIATION SYSTEMS COMMAND, ST. LOUIS, MO.
Test of an 0.8-scale model of the AH-64 Apache in the NASA Langley full-scale wind tunnel
[AD-A196129] N88-29766
ARMY BELVOIR RESEARCH AND DEVELOPMENT CENTER, FORT BELVOIR, VA.
Multi-metallic galvanic corrosion
[AD-A195995] N88-29963
Some effects of nitrates on the tensile properties of Al 7075-T7351
[AD-A195118] N88-29965
Stressed fabric abrasion test procedure for urethane coated fabric fuel tanks
[AD-A196327] N88-29982
ARMY ENGINEER TOPOGRAPHIC LABS., FORT BELVOIR, VA.
Integrating multispectral imagery and ground level hyperspectral signature data
[AD-A195976] N88-30166
DATATRAN: Datum transformation software
[AD-A195723] N88-30175
ARMY ENGINEER WATERWAYS EXPERIMENT STATION, VICKSBURG, MISS.
Computer-Aided Structural Engineering (CASE) project. Development of design formulas for ribbed mat foundations on expansive soils
[AD-A194807] N88-30307
Computer-Aided Structural Engineering (CASE) project. Computer program for analysis of planar grid structures (CGRID), user's guide
[AD-A195977] N88-30317
ARMY LAB. COMMAND, WATERTOWN, MASS.
The effect of notch root radius on the determination of toughness in ultrahigh strength steel friction welds
[AD-A195952] N88-30156
Principles of the optical differential thermal analysis
[AD-A195951] N88-30408
ARMY MILITARY PERSONNEL CENTER, ALEXANDRIA, VA.
Simulation of a two link robot manipulator with elastic members
[AD-A196014] N88-30368
ARMY MISSILE COMMAND, REDSTONE ARSENAL, ALA.
Evaluation of multi-focus holographic lenses
[AD-A196167] N88-30110
Nonlinear optical phase conjugation techniques to reduce the physical size of lasers
[AD-A196170] N88-30122
Energy budget and ground temperatures in hot regions
[AD-A196298] N88-30268
ARMY NATICK RESEARCH AND DEVELOPMENT COMMAND, MASS.
Control systems for platform landings cushioned by air bags
[AD-A196154] N88-29996
ARMY RESEARCH AND TECHNOLOGY LABS., MOFFETT FIELD, CALIF.
Minimum-complexity helicopter simulation math model
[NASA-CR-177476] N88-29819
ARMY RESEARCH INST. OF ENVIRONMENTAL MEDICINE, NATICK, MASS.
Accidental hypothermia
[AD-A194967] N88-30278
ARMY WAR COLL., CARLISLE BARRACKS, PA.
Looking beyond the strategic defense initiative
[AD-A195079] N88-30394
China's acquisition and use of foreign aviation technology
[AD-A194827] N88-30471
ATLANTIC REFINING CO., PHILADELPHIA, PA.
Information technology to facilitate group interaction N88-30463
ATMOSPHERIC AND ENVIRONMENTAL RESEARCH, INC., CAMBRIDGE, MASS.
Extended atmospheres of outer planet satellites and comets
[NASA-CR-183157] N88-30572
AUBURN UNIV., ALA.
Crystal structures of ordered carbon metal alloys
[AD-A195597] N88-29959
AUSTRALIAN NATIONAL UNIV., CANBERRA.
Role of zircon in tracing crustal growth and recycling N88-30211
The early archaean crustal history of West Greenland as recorded by detrital zircons N88-30221
Growth of the lower continental crust N88-30236
Crustal growth in the Archean: The geochemical evidence N88-30246
Growth of planetary crusts N88-30247

B

BALLISTIC RESEARCH LABS., ABERDEEN PROVING GROUND, MD.
Computational aerodynamic analysis for a range-limited 25mm training round
[AD-A185270] N88-29772
Combustion diagnostics of propellant with new grain geometries
[AD-A194944] N88-29895
Gas phase combustion chemistry of nitramine propellants
[AD-A195082] N88-29902
Flamespreading processes in obliquely loaded stick propellant beds
[AD-A195081] N88-29956
Titrimetric analysis of HAN-based liquid propellants
[AD-A196225] N88-29990
Numerical calculations of the response of a spinning spheroidal payload to coning motion
[AD-A195890] N88-30059
Numerical simulation of unsteady incompressible flow in a partially-filled rotating cylinder
[AD-A196001] N88-30073
Nonlinear stress-strain and inelastic rebound with exponential stiffness
[AD-A195667] N88-30159
BATTELLE INST., FRANKFURT AM MAIN (WEST GERMANY).
Spaceborne lidar: Development of a laboratory test system
[BF-R-66.090-1] N88-30118
BDM CORP., MCLEAN, VA.
Optics and symbolic computing
[AD-A195119] N88-30004
BENDIX CORP., KANSAS CITY, MO.
Primerless RTV silicones
[BDX-613-3807] N88-29980
BERKELEY RESEARCH ASSOCIATES, INC., CALIF.
Research on a two-stage free electron laser oscillator
[AD-A195991] N88-30115
Consideration of plasma opening switches from a wave propagation perspective
[AD-A195681] N88-30421
BRITISH AEROSPACE AIRCRAFT GROUP, WEYBRIDGE (ENGLAND).
Re-assessment of gust statistics using CAADRP data N88-29732
BRITISH AEROSPACE PUBLIC LTD. CO., BRISTOL (ENGLAND).
Air intake aerodynamics N88-29762
PSDE/SAT 2: Preliminary spacecraft configuration study, executive summary
[ESA-CR(P)-2618] N88-29840
Microwave instrument for planetary mission (Titan/CASSINI mission orbiter spacecraft)
[BAE-CS/TP-8359] N88-30102
BRITISH AEROSPACE PUBLIC LTD. CO., PRESTON (ENGLAND).
The role of simulation in flying qualities and flight control system related development N88-29742
BRITISH AEROSPACE PUBLIC LTD. CO., STEVENAGE (ENGLAND).
Optical multiple access intersatellite links
[BAE-TP-8502] N88-30013
BRITISH INSTITUTIONS' REFLECTION PROFILING SYNDICATE, CAMBRIDGE (ENGLAND).
Deep seismic reflection profiling and continental growth curves N88-30222
BRITISH PETROLEUM CO. LTD., LONDON (ENGLAND).
Thermal stress analysis in PMR-15 carbon fibre laminates
[ETN-88-93123] N88-29886
BSO/AEROSPACE, AMSTERDAM (NETHERLANDS).
MANIP
[MANIP-217A] N88-29855

C

CALIFORNIA INST. OF TECH., PASADENA.
Acoustooptic processing of two-dimensional signals using temporal and spatial integration
[AD-A194803] N88-29999
Evidence of the in situ decay of Al-26 in a Semarkona chondrule N88-30479
Research in particle and gamma-ray astrophysics
[NASA-CR-183126] N88-30566
CALIFORNIA STATE UNIV., NORTHRIDGE.
Semi-microdroplet assay for cell adhesion molecules
[NASA-CR-183139] N88-30274

Scanning electron microscopy study of adhesion in sea urchin blastulae
[NASA-CR-183136] N88-30275
Immunofluorescence localization of dissociation supernatant and extracellular matrix components in Lytechinus pictus sectioned embryos
[NASA-CR-183137] N88-30276

CALIFORNIA UNIV., BERKELEY.
Pierce diode with external circuit. Part 3: Chaotic behavior
[AD-A194837] N88-30041
Modeling of micromechanisms of fatigue and fracture in hybrid materials
[AD-A195604] N88-30142
Vortex formation and particle transport in a cross-field plasma sheath
[AD-A194838] N88-30425
Joint services electronics program
[AD-A195731] N88-30439
Star formation and molecular clouds N88-30537
Observations of star formation N88-30538

CALIFORNIA UNIV., DAVIS.
Prediction and measurement of human pilot dynamic characteristics in a manned rotorcraft simulation
[NASA-CR-183246] N88-30297
Stability, stochastic stationarity and generalized Lyapunov equations for two-point boundary-value descriptor systems
[AD-A195645] N88-30385

CALIFORNIA UNIV., IRVINE.
The effect of oriented defects on long-range ordering of hydrocarbon films: Azulene on Pt(111)
[AD-A196089] N88-29904
The performance of a surrogate blend in simulating JP-4 in a spray-fueled combustor N88-29926
Statistical analysis of the LMS (Last Mean Squares) and modified stochastic gradient
[AD-A195497] N88-30376

CALIFORNIA UNIV., LOS ANGELES.
Theory of filtering and control with application to control of large space structures
[AD-A195500] N88-29851
Creep of carbon yarn and carbon-carbon composites at high temperatures and high stresses
[AD-A195224] N88-29878
Construction of mass-age curves for the continental crust: An empirical model and an example from the western US N88-30213
Physical processes in the growth of the continental crust N88-30240
Growth of the continental crust: A planetary-mantle perspective N88-30251
Light-millimeter wave interactions in semiconductor devices
[AD-A195898] N88-30428
Nebular processes recorded in chondritic meteorites N88-30541

CALIFORNIA UNIV., SANTA BARBARA.
Haptic exploration in humans and machines: Attribute integration and machine recognition/implementation
[AD-A193692] N88-30299
Use of depletion edge translation for high-speed modulation and switching of lightwaves
[AD-A195611] N88-30417

CAMBRIDGE UNIV. (ENGLAND).
The timing and mechanism of depletion in Lewisian granulites N88-30209

CARNEGIE INSTITUTION OF WASHINGTON, D. C.
Crystal structure and density of helium to 232 kbar N88-30481
Terrestrial versus giant planet formation N88-30543

CARNEGIE-MELLON UNIV., PITTSBURGH, PA.
Contributions to engineering models of human-computer interaction, volume 1
[AD-A195590] N88-30295
Knowledge based simulation: An artificial intelligence approach to system modeling and automating the simulation life cycle
[AD-A195838] N88-30372
Kalman filter-based algorithms for estimating depth from image sequences
[AD-A195818] N88-30380
Image focusing in space and time
[AD-A195839] N88-30410

CASE WESTERN RESERVE UNIV., CLEVELAND, OHIO.
Predicting the durability of adhesives and coatings by remote detection of hidden defects and coating-thickness irregularities: A theoretical and numerical study N88-29972
Optoelectronic gain control of a microwave single stage GaAs MESFET amplifier
[NASA-CR-182201] N88-30055

CATANIA UNIV. (ITALY).
Radio and infrared properties of young stars
[NASA-CR-183252] N88-30579

CATHOLIC UNIV. OF AMERICA, WASHINGTON, D.C.
Transient interaction of electromagnetic pulses in dielectrics and microwave biophysics
[AD-A195667] N88-30008
Robust design of distributed controllers for large flexible space structures
[NASA-CR-183202] N88-30134

CENTER FOR NIGHT VISION AND ELECTRO-OPTICS, FORT BELVOIR, VA.
Common modules: A success story
[AD-A195937] N88-30415

CENTRE D'ETUDES ET DE RECHERCHES, TOULOUSE (FRANCE).
Simulation study of spraying, streaming and vaporization phenomena associated with fuel injection N88-29914
Modeling the stability of a turbulent premixed flame, downstream from a step by a Lagrangian method N88-29943

CENTRE DE RECHERCHES SCIENTIFIQUES ET TECHNIQUES DE L'INDUSTRIE DES FABRICATIONS METALLIQUES, BRUSSELS (BELGIUM).
Stresses in cylindrical shells with tangential nozzles submitted to external loads and internal pressure
[CRIF-MT-172] N88-30146

CENTRE NATIONAL D'ETUDES SPATIALES, TOULOUSE (FRANCE).
Specifications and performance of ultrastable oscillators in the DORIS orbitography and positioning system
[ETN-88-92761] N88-29831

CENTRE NATIONAL DE LA RECHERCHE SCIENTIFIQUE, CHATENAY-MALABRY (FRANCE).
Flamelet modeling of turbulent premixed flames N88-29942

CENTRE NATIONAL DE LA RECHERCHE SCIENTIFIQUE, POITIERS (FRANCE).
Gaseous premixed flames in non-uniform flows N88-29945
Modeling and experimental study of a reactive flow confined with well injection N88-29946

CENTRE NATIONAL DE LA RECHERCHE SCIENTIFIQUE, VANDOEURE (FRANCE).
Nd isotopes and crustal growth rate N88-30203

CHEMICAL RESEARCH AND DEVELOPMENT CENTER, ABERDEEN PROVING GROUND, MD.
Development of computer-controlled thermogravimetric instrumentation for measurement of environmental and high temperature volatilization and desorption of contaminants from polymeric materials
[AD-A195934] N88-29900

CHICAGO UNIV., ILL.
Venture theory: A model of decision weights
[AD-A194809] N88-30391
Urelilites are not igneous differentiates N88-30477
Noble gases, C,N, and Si isotopes in interstellar SiC form the Murchison carbonaceous chondrite N88-30483

CHRYSLER CORP., NEW ORLEANS, LA.
Space shuttle phase B wind tunnel model and test information. Volume 3: Launch configuration
[NASA-CR-178416-VOL-3-PT-2] N88-29744
Space shuttle phase B wind tunnel model and test information. Volume 1: Booster configuration
[NASA-CR-178414-VOL-1-PT-1] N88-29745
Space shuttle phase B wind tunnel model and test information. Volume 1: Booster configuration
[NASA-CR-178414-VOL-1-PT-2] N88-29770

CINCINNATI UNIV., OHIO.
Anisotropic constitutive modeling for nickel-base single crystal superalloys
[NASA-CR-182157] N88-29961

CITY UNIV. OF NEW YORK, BROOKLYN.
Did the greenhouse effect kill the dinosaurs N88-30484

CIVIL AVIATION AUTHORITY, REDHILL (ENGLAND).
A review of measured gust responses in the light of modern analysis methods N88-29724

COLGATE UNIV., HAMILTON, N.Y.
Mid to late proterozoic magmatism within Northeastern North America and its iplications for the growth of the continental crust N88-30229

COLORADO SCHOOL OF MINES, GOLDEN.
Pluton emplacement and magmatic arc construction: A model from the Patagonian batholith N88-30206
Ridge-trench collision in Archean and Post-Archean crustal growth: Evidence from southern Chile N88-30233

COLORADO STATE UNIV., FORT COLLINS.
Cloud/mesoscale model development and application studies
[AFGL-TR-87-0219] N88-30269

COLORADO UNIV., BOULDER.
Spontaneous force optical traps
[AD-A196103] N88-30114
New methods for nonlinear optimization
[AD-A195982] N88-30313
Optical symbolic computing
[AD-A195690] N88-30406
Volatiles on Mars
[NASA-CR-183113] N88-30571

COMMISSARIAT A L'ENERGIE ATOMIQUE, GIF-SUR-YVETTE (FRANCE).
Linguistic and cultural barriers to the transfer of information N88-30459

COMPUTER SCIENCES CORP., BALTIMORE, MD.
Knowledge based tools for Hubble Space Telescope planning and scheduling: Constraints and strategies N88-30338
The proposal entry processor: Telescience applications for Hubble Space Telescope science operations N88-30339

COMPUTER SCIENCES CORP., BELTSVILLE, MD.
Candidate functions for advanced technology implementation in the Columbus mission planning environment N88-30340
The need for a comprehensive expert system development methodology N88-30362

CONGRESSIONAL RESEARCH SERVICE, WASHINGTON, D.C.
Political and economic barriers to information transfer N88-30460

CONSIGLIO NAZIONALE DELLE RICERCHE, NAPLES (ITALY).
Lava thicknesses: Implications for rheological and crustal development N88-30490

CONSTRUCCIONES AERONAUTICAS S.A., MADRID (SPAIN).
Interim Flight Opportunity (IFO). Volume 1: Executive summary
[SE/LS/AP-36-818/CN-VOL-1] N88-29849

CONTRAVES CORP., ZURICH (SWITZERLAND).
Far infrared spectroscopy telescope (FIRST) inflatable thermal shield, phase 1
[SR/FIS/108(87)CZ] N88-30552

CONTROL DATA CORP., MINNEAPOLIS, MINN.
Utilization of a single clear-air Doppler radar beam to measure vertical divergence
[AD-A195543] N88-30271

COORDINATING RESEARCH COUNCIL, INC., ATLANTA, GA.
Determination of the hydroperoxide potential of jet fuels
[AD-A195975] N88-29991

CORNELL UNIV., ITHACA, N.Y.
Reactive plasticizers in negative E-beam resists
[AD-A195161] N88-30056

CRANFIELD INST. OF TECH., BEDFORD (ENGLAND).
Spray performance of a vaporizing fuel injector N88-29919
Flamelet chemistry modelling of soot formation for radiation N88-29928

CREW SYSTEMS CONSULTANTS, YELLOW SPRINGS, OHIO.
Improvement of head-up display standards. Volume 3: An evaluation of head-up display safety
[AD-A195787] N88-30300

CRYSTAL SYSTEMS, INC., SALEM, MASS.
Growth of GaAs crystals by the Heat Exchanger Method for microwave device applications
[AD-A196028] N88-30435

D

DAYTON UNIV., OHIO.
Fatigue crack growth characteristics of ARALL (trademark)-1
[AD-A196185] N88-29889
Comparative aspects of multiple processes of attention
[AD-A195805] N88-30291

DEFENCE RESEARCH ESTABLISHMENT ATLANTIC, DARTMOUTH (NOVA SCOTIA).
Response of SMA (Shielded Metal Arc) and narrow gap HY80 weldments to explosive shock loading
[AD-A195994] N88-30162

DEFENSE INTELLIGENCE AGENCY, WASHINGTON, D.C.
Bibliography of Soviet laser developments, number 88, March - April 1987
[AD-A195978] N88-30116

DEFENSE TECHNICAL INFORMATION CENTER, ALEXANDRIA, VA.
Information retrieval systems evolve-advances for easier and more successful use N88-30462

DEPARTMENT OF ENERGY, LAS VEGAS, NEV.
The dynamics of transuranics and other radionuclides in natural environments, December 1985
[DE87-014456] N88-30189

DEPARTMENT OF THE SECRETARY OF STATE, OTTAWA (ONTARIO).
Words: Keys or barriers to information transfer N88-30464

DEUTSCHE FORSCHUNGS- UND VERSUCHSANSTALT FUER LUFT- UND RAUMFAHRT, COLOGNE (WEST GERMANY).
Influence of operating conditions on the atomization and distribution of fuel by air blast atomizers N88-29918
Analysis of the flow through double swirl airblast atomizers N88-29949

DEUTSCHE FORSCHUNGS- UND VERSUCHSANSTALT FUER LUFT- UND RAUMFAHRT, GOETTINGEN (WEST GERMANY).
Supersonic wall adaptation in the rubber tube test section of the DFVLR Goettingen [IB-222-87-A-08] N88-29824
Studies on rocket exhaust plumes and impingement effects related to the Columbus Space Station program: Executive summary [DFVLR-IB-222-88-A-12] N88-29862

DORNIER-WERKE G.M.B.H., FRIEDRICHSHAFEN (WEST GERMANY).
Prediction of dynamic derivatives N88-29761
Aerodynamic heating of missiles N88-29764
Procedures for updating dynamic mathematical models, test phase [MEBS-38/87] N88-29852
Biosample: Preservation, handling and observation system synthesis and breadboarding [ESA-CR(P)-2609] N88-29857
Fuel cells for space use [FCP-TR-DOS-SY-026] N88-30183

DRAPER (CHARLES STARK) LAB., INC., CAMBRIDGE, MASS.
Intelligent fault diagnosis and failure management of flight control actuation systems [NASA-CR-177481] N88-29790
Development and demonstration of an on-board mission planner for helicopters [NASA-CR-177482] N88-29817
Ascent guidance for a winged boost vehicle [NASA-CR-172083] N88-29846

E

EAGLE ENGINEERING, INC., HOUSTON, TEX.
Spacecraft mass estimation, relationships and engine data: Task 1.1 of the lunar base systems study [NASA-CR-172061] N88-29836
Maintenance and supply options [NASA-CR-172062] N88-29837
Lunar lander conceptual design: Lunar base systems study task 2.2 [NASA-CR-172051] N88-29854

ECOLE CENTRALE DES ARTS ET MANUFACTURES, CHATENAY-MALABRY (FRANCE).
Flamelet modeling of turbulent premixed flames N88-29942

ECOLE NATIONALE SUPERIEURE DE L'AERONAUTIQUE ET DE L'ESPACE, TOULOUSE (FRANCE).
Studies of unsteady axial-compressor functioning N88-30129

ECOLE NATIONALE SUPERIEURE DE MECANIQUE ET D'AEROTECHNIQUE, POITIERS (FRANCE).
Gaseous premixed flames in non-uniform flows N88-29945
Modeling and experimental study of a reactive flow confined with well injection N88-29946

ECOLE NATIONALE SUPERIEURE DES MINES, EVRY (FRANCE).
Rupture of carbon fiber reinforced plastics (T300-914) composite materials: Influence of initial first ply failures on the fatigue behavior [SNIAS-881-422-103] N88-29892

ELORET CORP., SUNNYVALE, CALIF.
Computed potential energy surfaces for chemical reactions [NASA-CR-183168] N88-29893

ENERGY RESEARCH CORP., DANBURY, CONN.
Aircraft battery state of charge and charge control system [AD-A194979] N88-30052

ENTWICKLUNGSRING NORD, BREMEN (WEST GERMANY).
Candidate functions for advanced technology implementation in the Columbus mission planning environment N88-30340

ENVIRONMENTAL RESEARCH INST. OF MICHIGAN, ANN ARBOR.
MIZEX (marginal ice zone experiment) 1987 SAR (Synthetic Aperture Radar) data summary [AD-A195560] N88-30035

ERNO RAUMFAHRTTECHNIK G.M.B.H., BREMEN (WEST GERMANY).
Study on long-term evolution towards European manned spaceflight. Volume 1: Executive summary [ERNO-OX1-002/88-VOL-1] N88-29827
Study of robotics spacecraft servicing and assembly in space. Volume 1: Executive summary [ESA-CR(P)-2612-VOL-1] N88-29839
Interim Flight Opportunity (IFO). Volume 1: Executive summary [SE/LS/AP-36-818/CN-VOL-1] N88-29849
Design and development of a refueling test bed [FTMS-RP-ER-011] N88-29986
Study on industrial organization for European Ground Support Equipment (EGSE) to support European space programs. Volume 1: Technical reports [SD-RP-AI-009-VOL-1] N88-30446
Study on industrial organization for European Ground Support Equipment (EGSE) to support European space programs. Volume 2: Technical reports [SD-RP-AI-009-VOL-2] N88-30448

ESSEX CORP., ALEXANDRIA, VA.
Use of color CRTs (Cathode Ray Tubes) in aircraft cockpit: A literature search, revision B [AD-A195062] N88-29797

EUROCONTROL EXPERIMENTAL CENTRE, BRETIGNY (FRANCE).
Observed track-keeping performance of DC10 aircraft equipped with the Collins AINS-70 area navigation system: Karlsruhe and Masstricht UACs (Upper Area Control centres) [EEC-202] N88-29788
Evaluation of LISBON TAR SSR radar [EEC/NOTE-5/87] N88-30015

EUROPEAN CENTRE FOR MEDIUM-RANGE WEATHER FORECASTS, READING (ENGLAND).
A study of the feasibility of using sea and wind information from the ERS-1 satellite. Part 1: Wind scatterometer data [NASA-CR-182833] N88-30167
A study of the feasibility of using sea and wind information from the ERS-1 satellite. Part 2: Use of scatterometer and altimeter data in wave modeling and assimilation [ESA-CR(P)-2604-PT-2] N88-30176

EUROPEAN SOUTHERN OBSERVATORY, GARCHING (WEST GERMANY).
Activities report in astronomy [ISSN-0531-4496] N88-30535

EUROPEAN SPACE AGENCY, PARIS (FRANCE).
History of aeroelasticity in Germany from the beginning to 1945 [ESA-TT-1082] N88-29767
Beyond the visible: A decade of observations with the International Ultraviolet Explorer (IUE) [ESA-F09] N88-29828
The viscous flow on surfaces with streamline riblets [ESA-TT-1091] N88-30067
Numerical simulation of the interaction of pressure waves with laminar and turbulent boundary layers [ESA-TT-1089] N88-30075
Investigation of large-scale structures in the near wake of a parallel flat plate [ESA-TT-1100] N88-30080
Investigation of the large-scale impact of air pollution components on forest ecosystems in Bavaria [ESA-TT-1087] N88-30187
With an eye to the future: ESA general studies program 1988 [ESA-SP-1100] N88-30447
ESA report to the 27th COSPAR meeting [ESA-SP-1098] N88-30556
The high-throughput X-ray spectroscopy mission: The mission-science report [ESA-SP-1097] N88-30557

EUROPEAN SPACE TRIBOLOGY LAB., RISLEY (ENGLAND).
The lubricating properties of magnetron sputtered MoS2 [ESA-ESTL-76] N88-30136

EXETER UNIV. (ENGLAND).
Rossby waves in mid-latitude oceans N88-30273

F

FEDERAL AVIATION ADMINISTRATION, SEATTLE, WASH.
Current and proposed gust criteria and analysis methods: An FAA overview N88-29718

FEDERAL AVIATION ADMINISTRATION, WASHINGTON, D.C.
Report to Congress on the effectiveness of the Civil Aviation Security Program [AD-A195282] N88-29784

FOKKER B.V., AMSTERDAM (NETHERLANDS).
Interim Flight Opportunity (IFO). Volume 1: Executive summary [SE/LS/AP-36-818/CN-VOL-1] N88-29849

FORD AEROSPACE AND COMMUNICATIONS CORP., COLLEGE PARK, MD.
Integrated resource scheduling in a distributed scheduling environment N88-30342

FORD AEROSPACE AND COMMUNICATIONS CORP., SEABROOK, MD.
Automated satellite control in Ada N88-30336
A simulation engine: Combining an expert system with a simulation language N88-30358

FRAUNHOFER-INST. FUER PRODUKTIONSANLAGEN UND KONSTRUKTIONSTECHNIK, BERLIN (WEST GERMANY).
Study of robotics spacecraft servicing and assembly in space. Volume 1: Executive summary [ESA-CR(P)-2612-VOL-1] N88-29839

G

GARRETT ENGINE CO., PHOENIX, ARIZ.
Transition mixing study empirical model report [NASA-CR-182139] N88-30076

GENERAL DYNAMICS CORP., SAN DIEGO, CALIF.
Centaur operations at the space station: Cost and transportation analysis [NASA-CR-182128] N88-29835

GENERAL ELECTRIC CO., CINCINNATI, OHIO.
Empirical flutter prediction method [AD-A195699] N88-29810
Numerical models for analytical predictions of combustor aerothermal performance characteristics N88-29935

GENERAL ELECTRIC CO., PRINCETON, N.J.
Heavy ion and proton tests for subsystem upset [AD-A195267] N88-30442

GENERAL MOTORS CORP., INDIANAPOLIS, IND.
Gas turbine combustion modeling N88-29936

GENEVA OBSERVATORY (SWITZERLAND).
A new determination of the Geneva photometric passbands and their absolute calibration [SER-C-PREPUBL-FASC-26] N88-30546
The kinematics of late-type supergiants [SER-C-PREPUBL-FASC-28] N88-30560
Duplicity in the solar neighborhood: Part 4: Spectroscopic orbits for four dwarf M stars [SER-C-PREPUBL-FASC-21] N88-30561
Duplicity in the solar neighborhood: Part 5: Spectroscopic orbit for the nearby double-lined solar-type star HR 8581 [SER-C-PREPUBL-FASC-23] N88-30562
Radial velocity measurements of a sample of northern metal-deficient stars [SER-C-PREPUBL-FASC-25] N88-30564
The stability of disk galaxies and constraints on their mass-luminosity ratio [SER-C-PREPUBL-FASC-27] N88-30565
The dynamics of SBO galaxies. Part 1: The data [SER-C-PREPUBL-FASC-22] N88-30567
Orbital stability in rotating triaxial stellar systems [SER-C-PREPUBL-FASC-24] N88-30569

GEOLOGICAL SURVEY, FLAGSTAFF, ARIZ.
Debris flows of the Simud-Tiu outflow system of Mars N88-30485
Faulting and its relation to volcanism: Mars western equatorial region N88-30489
Mars: Volcanism in the Valles Marineris overlooked N88-30491

GEOLOGICAL SURVEY, MENLO PARK, CALIF.
The growth of continents and some consequences since 1.5 Ga N88-30220

GEOLOGICAL SURVEY, RESTON, VA.
New type of primitive meteorite found in Antarcitca N88-30478

GEOLOGICAL SURVEY, ST. PAUL, MINN.
Crustal underplating in the North American Craton: Evidence from the Petrogenesis of anorthositic rocks in the Middle Proterozoic Midcontinent Rift System N88-30252

GEORGE MASON UNIV., FAIRFAX, VA.
Parallel and distributed computation for fault-tolerant object recognition N88-30350

GLASGOW UNIV. (SCOTLAND).
Technical change needs organizational change N88-30466

GOETTINGEN UNIV. (WEST GERMANY).
The influence of pressure on soot formation N88-29934

GRUMMAN AEROSPACE CORP., BETHPAGE, N.Y.
Automated early fatigue damage sensing system [AD-A195717] N88-30143

H

HARVARD-SMITHSONIAN CENTER FOR ASTROPHYSICS, CAMBRIDGE, MASS.
The origin of the moon: Further studies of the giant impact N88-30474
HARVARD UNIV., CAMBRIDGE, MASS.
Intramolecular dynamics: A study of molecules at high levels of vibrational excitation
[AD-A195285] N88-30400
Physical processes and timescales in planet and small-body accretion N88-30540
HAWAII UNIV., HONOLULU.
Rifts of deeply eroded Hawaiian basaltic shields: A structural analog for large Martian volcanoes N88-30494
HEBREW UNIV., JERUSALEM (ISRAEL).
Lithospheric evolution of the Northern Arabian Shield: Chemical and isotopic evidence from basalts, xenoliths and granites N88-30242
Solid earth as a recycling systems and the lateral growth of Precambrian North America N88-30249
HELSINKI UNIV. OF TECHNOLOGY, ESPOO (FINLAND).
Phase modulation of recoiless gamma radiation in Mossbauer spectroscopy
[ETN-88-92648] N88-30403
HUGHES RESEARCH LABS., MALIBU, CALIF.
Cluster beam studies
[AD-A195182] N88-30443
HUMAN ENGINEERING LABS., ABERDEEN PROVING GROUND, MD.
Four-axis side-arm flight control simulator investigation
[AD-A196026] N88-30294

I

IBM WATSON RESEARCH CENTER, YORKTOWN HEIGHTS, N.Y.
Waveform relaxation applied to transient device simulation
[AD-A194992] N88-30429
ILLINOIS UNIV., URBANA.
Energy conversion measurements in laser-sustained argon plasmas for application to rocket propulsion
[AD-A194931] N88-29861
Hydrogen embrittlement of iron-nickel alloys
[AD-A195909] N88-29958
Performance of DS/SSMA communications in impulsive channels. Part 1: Correlation receivers
[AD-A195712] N88-30021
Instrumentation for computational statistical research
[AD-A195867] N88-30390
Electronic materials and devices prepared by molecular beam epitaxy
[AD-A195694] N88-30433
On 3-5 heterojunction structures and high speed devices
[AD-A195464] N88-30438
ILLINOIS UNIV., URBANA-CHAMPAIGN.
Alternative fuel spray behavior N88-29912
IMPERIAL COLL. OF SCIENCE AND TECHNOLOGY, LONDON (ENGLAND).
Flow characteristics of a model annular combustor N88-29924
Three-dimensional combustor predictors: A comparison of equilibrium and laminar flamelet chemistry models N88-29940
INDUSTRIAL QUALITY, INC., GAITHERSBURG, MD.
Development of graded reference radiographs for aluminum welds, phase 1
[AD-A195594] N88-30140
INSTITUT D'AERONOMIE SPATIALE DE BELGIQUE, BRUSSELS.
Aeronomic problems of the molecular oxygen photodissociation. Part 3: Solar spectral irradiances in the region of the O2 Herzberg continuum, Schumann-Runge bands and continuum
[AERONOMICA-ACTA-A-332-1988] N88-29897
Aeronomic problems of molecular oxygen photodissociation. Part 2: Theoretical absorption cross sections of the Schumann-Runge bands at 79 K
[AERONOMICA-ACTA-A-331-1988] N88-29907
Aeronomic problems of molecular oxygen photodissociation. Part 4: The various parameters for the Herzberg continuum
[AERONOMICA-ACTA-A-333-1988] N88-29955
General equations for the motions of ice crystals and water drops in gravitational and electric fields
[NASA-CR-183229] N88-30070
Changes in stratospheric ozone: Observations and theories
[AERONOMICA-ACTA-A-334-1988] N88-30188
INSTITUT FRANCO-ALLEMAND DE RECHERCHES, ST. LOUIS (FRANCE).
Interaction of high power laser radiation with metals in laser welding
[ISL-PU-304/87] N88-30135
INSTITUT FUER RAUMFAHRTELEKTRONIK, BERLIN (WEST GERMANY).
Low cost satellite
[ESA-CR(P)-2560] N88-29844
INSTITUT NATIONAL DE RECHERCHE D'INFORMATIQUE ET D'AUTOMATIQUE, VALBONNE (FRANCE).
Numerical modelling of premixed flames in gaseous media N88-29944
INSTITUTO DE PESQUISAS ESPACIAIS, SAO JOSE DOS CAMPOS (BRAZIL).
TM/LANDSAT-5 data to evaluate wheat and bean percent soil cover and leaf area index
[INPE-4609-PRE/1332] N88-30165
Evaluation of LANDSAT-TM data for geomorphological mapping
[INPE-4593-PRE/1324] N88-30168
The use of orbital remote sensing data for low cost ground-water survey
[INPE-4587-PRE/1318] N88-30170
Reflectance pattern and the physical and chemical characteristics of three Brazilian Oxisols
[INPE-4590-PRE/1320] N88-30172
Use of digital images as a mineral prospecting tool in the tin province of Goias, Brazil
[INPE-4537-PRE/1284] N88-30173
Study of the spectral response of soybeans
[INPE-4592-PRE/1322] N88-30174
LANDSAT-TM data to map flooded areas
[INPE-4594-PRE/1324] N88-30177
Microwave remote sensing at INPE (Institute for Space Research) Brazil: Concepts and future prospects of soil moisture studies
[INPE-4569-PRE/1310] N88-30178
Relief effect correction on LANDSAT imagery for forest applications using digital terrain models
[INPE-4611-PRE/1334] N88-30179
LANDSAT TM and agrometeorological data for wheat yield estimation at the farm level
[INPE-4591-PRE/1321] N88-30180
Recent measurements of ozone in the Amazon forests
[INPE-4494-PRE/1258] N88-30185
Recent observations of carbon monoxide in the Amazon Rain Forest
[INPE-4478-PRE/1245] N88-30186
Some results from the Amazon Forest micrometeorological experiment
[INPE-4631-PRE/1346] N88-30263
Using primal sketch primitives as the basis for the Hough transform
[INPE-4564-PRE/1305] N88-30310
Method for combined image interpolation-restoration through a fir filter design technique
[INPE-4561-PRE/1302] N88-30315
A digital terrain model system for a microcomputer
[INPE-4610-PRE/1333] N88-30316
RFP (Revised Field Pinch) plasma experiment at INPE
[INPE-4613-PRE/1336] N88-30420
A coded mask telescope for observations of X and gamma ray sources in the southern sky
[INPE-4580-PRE/1314] N88-30551
Intermediate polars observed in Brazil in the last eight years
[INPE-4567-PRE/1308] N88-30559
Activities in astrophysics
[INPE-4582-PRE/1316] N88-30570
AGN (OIII) emission line profiles: Dependencies on galaxy inclination and Balmer decrement
[INPE-4596-PRE/1324] N88-30577
X- and gamma-ray background observations in Antarctic
[INPE-4583-PRE/1317] N88-30578
INSTITUTO SUPERIOR TECNICO, LISBON (PORTUGAL).
Radiation transfer in gas turbine combustors N88-29929
INTERNATIONAL BUSINESS MACHINES CORP., SAN JOSE, CALIF.
Noncontact photo-thermal sensing
[AD-A195450] N88-29905
INTERNATIONAL CENTRE FOR THEORETICAL PHYSICS, TRIESTE (ITALY).
Radiative heat transfer to steady flow of a chemically reacting fluid in a horizontal porous channel with variable wall temperature
[DE88-702704] N88-30081
Nonequilibrium flow of a dissociating gas in a horizontal channel with axial temperature variation
[DE88-702536] N88-30089
Behaviour and hysteresis losses of irreversible type-2 superconducting cylindrical shell
[DE88-702708] N88-30434
Theoretical model of high temperature superconductors
[DE88-702707] N88-30441
Introduction to string theory
[DE88-702706] N88-30445
INTERNATIONAL SCIENTIFIC RADIO UNION, BRUSSELS (BELGIUM).
Review of Radio Science, 1984-1986 N88-30023
Electromagnetic metrology N88-30024
Fields and waves N88-30025
Signals and systems N88-30026
Electronic and optical devices and applications N88-30027
Electromagnetic noise and interference N88-30028
Wave propagation and remote sensing N88-30029
Ionospheric radio and propagation: Waves in plasmas N88-30030
Radio astronomy N88-30031
Bioeffects of electromagnetic waves N88-30032
INTESPACE, TOULOUSE (FRANCE).
Qualification test levels for units to be derived from mechanical test data analysis
[REPT-87-158-EI/ET/AG] N88-30139
IOWA UNIV., IOWA CITY.
Dynamics of articulated aerospace structures
[AD-A195685] N88-29794

J

JET PROPULSION LAB., CALIFORNIA INST. OF TECH., PASADENA.
Artificial intelligence in a mission operations and satellite test environment N88-30334
Mission telemetry system monitor: A real-time knowledge-based system N88-30345
Autonomous image data reduction by analysis and interpretation N88-30347
The space station assembly phase: System design trade-offs for the flight telerobotic servicer N88-30357
Publications of the Jet Propulsion Laboratory 1987
[NASA-CR-181198] N88-30453
Simulations of lava flows on Mars N88-30495
Small-scale volcanic landforms indicative of distributary tube systems N88-30496
Volcanic styles at Alba Patera, Mars: Implications of lava flow morphology to the volcanic history N88-30497
The Deep Space Network: An instrument for radio astronomy research
[NASA-CR-183219] N88-30554
Corona-solar wind coupling review
[AFGL-TR-87-0203] N88-30575
JOHNS HOPKINS UNIV., BALTIMORE, MD.
Gas phase combustion chemistry of nitramine propellants
[AD-A195082] N88-29902
Boltzmann equation approach to two-phase flow turbulence
[AD-A196153] N88-30086
K(sup th)-order extended linearization
[AD-A194786] N88-30363
JOHNS HOPKINS UNIV., LAUREL, MD.
Investigations of magnetosphere-ionosphere coupling relevant to operational systems
[AD-A195972] N88-30195
JOINT PUBLICATIONS RESEARCH SERVICE, ARLINGTON, VA.
JPRS report: Science and technology. USSR: Space
[JPRS-USP-88-001] N88-30498
Photochemistry of ionospheric D-region with injection of nitrogen oxides N88-30499
Structural dynamics of high-latitude magnetosphere determined from solar electron data N88-30500
Relationship between characteristics of low-energy electrons and geomagnetic disturbance in geostationary orbit N88-30501
Using nonstationary models of the atmosphere to describe satellite drag N88-30502
Approximation of atmospheric density by Chebyshev polynomials in predicting motion of low artificial earth satellites N88-30503
Astron observations of supernova 1987A in large magellanic cloud N88-30504
Gamma radiation expected from supernova 1987A in large magellanic cloud N88-30505
Orbital evolution of distant artificial earth satellites N88-30506
Plane periodic satellite motions relative to center of mass in neighborhood of collinear libration point N88-30507
Families of periodic solutions in problem of solid body rotation at triangular libration point in restricted three-body problem N88-30508

Rotational evolution of dynamically symmetric gyrostat with internal friction N88-30509
Resonance effects accompanying motion with low thrust in earth-moon system N88-30510
Increasing accuracy in evaluating vector of state under conditions of incomplete observability of expanded system N88-30511
Canonical variables and canonical integrals for motion in near-circular orbits N88-30512
Model representation of electron concentration distribution in outer middle-latitude ionosphere using data from Intercosmos-19 artificial earth satellite N88-30513
Ring current role in dynamics of fluctuating electron and ion fluxes in low-latitude magnetosphere N88-30514
Plasma of earth's magnetosphere ring currents. Model compared with results of AMPTE/CCE experiment N88-30515
Experimental proof of quasilongitudinal propagation of low-frequency waves in middle latitudes in upper ionosphere N88-30516
One equatorial anomaly in nighttime ionospheric F region N88-30517
Influence of plasma parameters on VLF radiation in near-rocket region N88-30518
Charge composition of primary cosmic ray nuclei with z greater than or equal to 2 in energy region greater than or equal to 2 TeV N88-30519
Measurement of galactic radio emission at frequency 37 GHz from aboard spacecraft N88-30520
Binary star measurements using digital speckle interferometer of 6-m telescope N88-30521
Microphysical processes in cloud layers of Venus N88-30522
Stability of Venusian ionopause N88-30523
Determining near-water wind speed using radar data from Cosmos-1500 artificial earth satellite N88-30524
Evolution of thermal structure of Benguela upwelling system according to satellite and shipboard data N88-30525
Possibilities of determining vertical profiles of microphysical characteristics of stratospheric aerosol using space measurements of transparency and solar halo N88-30526
Analytical method for approximate geodetic referencing of scanner images of meteorological artificial earth satellites using control points N88-30527
Determining earth's rotation from laser observations of Lageos artificial earth satellite (during period of main merit campaign) N88-30528
Obligue metallogenic zones recognized by interpreting space photographs of southern Tien Shan N88-30529
Structure of eastern Turkestan Ridge based on space photographs N88-30530
Determining the spatial structure of fields of precipitation from space radar images in two orthogonal polarizations N88-30531
Estimation of soil temperature profile from remote microwave and IR measurements N88-30532
Monte-Carlo estimation of the influence of plant architecture parameters on spectral brightness N88-30533
KOSPAS-SARSAT satellites used for ocean current study N88-30534

K

KANSAS UNIV., LAWRENCE.
Cytochrome electron transfer and biomolecular electronics
[AD-A195482] N88-30277
KARLSRUHE UNIV. (WEST GERMANY).
Turbulence effects on the droplet distribution behind airblast atomizers N88-29915
Particle size measurements in sooting combustion systems N88-29931
On the application of finite-difference techniques for the computation of the flow field in gas turbine combustors with complex geometries N88-29938
KENT STATE UNIV., OHIO.
Ultrasonic detection of diffusion and adhesion loss N88-29967
KHD LUFTFAHRTTECHNIK G.M.B.H., OBERURSEL (WEST GERMANY).
A small annular combustor of high power density, wide operating range and low manufacturing cost N88-29951

L

LABEN SPACE INSTRUMENTATION AND SYSTEMS, MILAN (ITALY).
Study of software requirements and artificial intelligence techniques for robotics
[TL-3333] N88-30365
LAMONT-DOHERTY GEOLOGICAL OBSERVATORY, PALISADES, N.Y.
Constraints on continental accretion from sedimentation N88-30202
LAVAL UNIV. (QUEBEC).
The characterizatin of combustion by fuel composition: Measurements in a small conventional combustor N88-29920
The behaviour of synthetic fuels in a small transparent combustor N88-29950
LAWRENCE LIVERMORE NATIONAL LAB., CALIF.
Determination of relative flammability of materials by pyrolysis and gas-chromatographic light hydrocarbon analysis
[DE88-012449] N88-29898
Non-atmospheric noble gases from CO(sub 2) well ga N88-30476
LEEDS UNIV. (ENGLAND).
Rates of formation of soot from hydrocarbon flames and its destruction N88-29933
LEICESTER UNIV. (ENGLAND).
Continental crustal formation and recycling: Evidence from oceanic basalts N88-30238
Trace element differences between Archean, Proterozoic and Phanerozoic crustal components: Implications for crustal growth processes N88-30243
LEVY (SALOMON), INC., CAMPBELL, CALIF.
Experimental and analytical study of two-phase flow in zero gravity
[AD-A195223] N88-29893
LNK CORP., RIVERDALE, MD.
A design for a ground-based data management system N88-30355
LOCKHEED AERONAUTICAL SYSTEMS CO., BURBANK, CALIF.
A summary of methods for establishing airframe design loads from continuous gust design criteria N88-29721
LOCKHEED-GEORGIA CO., MARIETTA.
N-version software demonstration for digital flight controls
[NASA-CR-181483] N88-29815
LOCKHEED MISSILES AND SPACE CO., SUNNYVALE, CALIF.
Advanced planar array development for space station
[NASA-CR-179373] N88-30181
LOUGHBOROUGH UNIV. OF TECHNOLOGY (ENGLAND).
An analysis of time and space requirements for aircraft turnrounds
[TT-8705] N88-29783
LOUISIANA STATE UNIV., BATON ROUGE.
Exotic minerals in 3,500 million year old rocks: Evidence for large meteorite impacts N88-30475
LSU scientists discover evidence of large meteorite impacts on the early earth N88-30480
LOUVAIN UNIV. (BELGIUM).
Central adrenergic receptors as mediators of central response to stress: Study with Positron Emission Tomography (PET)
[AD-A194947] N88-30284
LOWELL UNIV., MASS.
The effect of equatorial ionospheric irregularities on the performance of a south-looking OTH-B (Over-The-Horizon-Backscatter) radar
[AD-A195090] N88-30018
Ionosonde studies of field-aligned irregularities during high-power HF heating at Arecibo
[AD-A195848] N88-30256
LUNAR AND PLANETARY INST., HOUSTON, TEX.
Workshop on the Growth of Continental Crust
[NASA-CR-183073] N88-30201
An illustration of the complexity of continent formation N88-30207
Thermal models pertaining to continental growth N88-30230
Gravity anomalies, plate tectonics and the lateral growth of Precambrian North America N88-30248
A compilation of information and data on the Manson impact structure
[NASA-CR-183169] N88-30258
Nineteenth Lunar and Planetary Science Conference. Press abstracts
[NASA-CR-183037] N88-30473
NASA MEVTV Program Working Group Meeting: Volcanism on Mars
[NASA-CR-183074] N88-30487
Workshop on the Origins of Solar Systems
[NASA-CR-183025] N88-30536

M

MACQUARIE UNIV., NORTH RYDE (AUSTRALIA).
Genesis of archean granitoids in the Pilbara block and implications for crustal growth N88-30210
MAINZ UNIV. (WEST GERMANY).
Growth of early archaean crust in the ancient Gneiss complex of Swaziland and adjacent Barberton Greenstone Belt, Southern Africa N88-30223
MANAGEMENT CONSULTING AND RESEARCH, INC., FALLS CHURCH, VA.
Aircraft avionics and missile system installation cost study. Volume 2: Appendices F and G
[AD-A195372] N88-29801
MANUDYNE SYSTEMS, INC., LOS ALTOS, CALIF.
Minimum-complexity helicopter simulation math model
[NASA-CR-177476] N88-29819
MARCONI SPACE AND DEFENCE SYSTEMS LTD., PORTSMOUTH (ENGLAND).
Development of procedures for performing end-to-end tests on the ERS-1 radar altimeter and AMI using a compact antenna test range
[ESA-CR(P)-2558] N88-30022
MARCONI SPACE SYSTEMS LTD., PORTSMOUTH (ENGLAND).
Study on industrial organization for European Ground Support Equipment (EGSE) to support European space programs. Volume 1: Technical reports
[SD-RP-AI-009-VOL-1] N88-30446
Study on industrial organization for European Ground Support Equipment (EGSE) to support European space programs. Volume 2: Technical reports
[SD-RP-AI-009-VOL-2] N88-30448
MARTIN MARIETTA CORP., DENVER, COLO.
Contingency rescheduling of spacecraft operations N88-30337
Space systems cost study
[AD-A196024] N88-30469
MARYLAND UNIV., COLLEGE PARK.
Gas phase combustion chemistry of nitramine propellants
[AD-A195082] N88-29902
An automated computerized vision technique for determination of three-dimensional object geometry N88-30348
Regularity and numerical solution of eigenvalue problems with piecewise analytic data
[AD-A194993] N88-30387
MASSACHUSETTS INST. OF TECH., CAMBRIDGE.
Performance analysis of k-ary n-cube interconnection networks
[AD-A195542] N88-30010
Design of a self-timed VLSI multicomputer communication controller
[AD-A194567] N88-30014
Reducing the parallel solution time of sparse circuit matrices using reordered Gaussian elimination and relaxation
[AD-A195152] N88-30045
Circuit design criteria for stable lateral inhibition neural networks
[AD-A195066] N88-30046
Modeling robot flexibility for endpoint force control
[AD-A195923] N88-30132
Syntactic closures
[AD-A195921] N88-30311
The bounded rationality constraint: Experimental and analytical results
[AD-A195897] N88-30318
Scheme86: A system for interpreting SCHEME
[AD-A195931] N88-30319
Reification without evaluation
[AD-A195928] N88-30326
The combinatorics of object recognition in cluttered environments using constrained search
[AD-A196224] N88-30364
Dynamical systems and motion vision
[AD-A195932] N88-30366
A standard architecture for controlling robots
[AD-A195929] N88-30371
Symbolic construction of a 2D scale-space image
[AD-A195926] N88-30374
Exploiting lexical regularities in designing natural language systems
[AD-A195922] N88-30375
Automatic qualitative analysis of ordinary differential equations using piecewise linear approximations
[AD-A196310] N88-30379
Reconstruction of multidimensional signals from multiple level threshold crossings
[AD-A195561] N88-30383
Stability, stochastic stationarity and generalized Lyapunov equations for two-point boundary-value descriptor systems
[AD-A195645] N88-30385
Theories of comparative analysis
[AD-A196328] N88-30395
Utilizing dynamic stability of orient parts
[AD-A195730] N88-30397

Waveform relaxation applied to transient device simulation
[AD-A194992] N88-30429
Knowledge-based integrated information systems engineering: Highlights and bibliography. Knowledge-Based Integrated Information Systems Engineering (KBIISE) Project, volume 1
[AD-A195850] N88-30449
Integrating images, applications, and communications networks, volume 5
[AD-A195854] N88-30452
Technical opinions regarding knowledge-based integrated information systems engineering, volume 8
[AD-A195857] N88-30454
Knowledge-Based Integrated Information Systems Development Methodologies Plan. Knowledge-Based Integrated Information Systems Engineering (KBIISE) report, volume 2
[AD-A195851] N88-30455
Strategic, organizational and standardization aspects of integrated information systems, volume 6
[AD-A195855] N88-30457
Integrating information systems in a major decentralized international organization, volume 7
[AD-A195856] N88-30468
Cosmochemical trends of volatile elements in the solar system N88-30542
Numerical evidence that the motion of Pluto is chaotic
[AD-A195920] N88-30568

MASSACHUSETTS INST. OF TECH., LEXINGTON.
An improved spherical earth diffraction algorithm for SEKE
[AD-A195847] N88-30005
Corner extraction from radar images
[AD-A194857] N88-30020

MASSACHUSETTS INST. OF TECH., WESTFORD.
High-resolution (30 m) lunar radar images N88-30486

MASSACHUSETTS UNIV., AMHERST.
Crustal evolution and the eclogite to granulite phase transition in xenoliths from the West African Craton N88-30217
Structure of Southwestern Michipicoten Greenstone Belt, Ontario: Evidence for Archean accretion N88-30228

MATRA ESPACE, TOULOUSE (FRANCE).
PSDE/SAT 2: Preliminary spacecraft configuration study, executive summary
[ESA-CR(P)-2618] N88-29840
Study of the assembly, integration and verification programs of telecommunication satellites applicable to other satellite programs
[MATRA-100/CC/MLG/031/87] N88-29847
The LTPP communication processor
[CL/CP/SES/FR/004] N88-30328
Study on industrial organization for European Ground Support Equipment (EGSE) to support European space programs. Volume 1: Technical reports
[SD-RP-AI-009-VOL-1] N88-30446
Study on industrial organization for European Ground Support Equipment (EGSE) to support European space programs. Volume 2: Technical reports
[SD-RP-AI-009-VOL-2] N88-30448

MATRA SERVICE AERODYNAMIQUE, VELIZY-VILLACOUBLAY (FRANCE).
Numerical methods: Euler time dependent solver N88-29760

MAX-PLANCK-INST. FUER CHEMIE, MAINZ (WEST GERMANY).
Recycling of lower continental crust through foundering of cumulates from contaminated mafic intrusions N88-30204
Growth of continental crust: Clues from Nd isotopes and Nb-Th relationships in mantle-derived magmas N88-30205
Decoupled Rb-Sr and Sm-Nd isotopic evolution of the continental crust N88-30216
Lithospheric evolution of the Northern Arabian Shield: Chemical and isotopic evidence from basalts, xenoliths and granites N88-30242

MCDONNELL-DOUGLAS ASTRONAUTICS CO., ST. LOUIS, MO.
Accuracy criteria for evaluating supersonic aerodynamic coefficient predictions N88-29756
Semiempirical methods for airbreathing missiles N88-29763
Next generation missile design N88-29766

MEMORIAL UNIV. OF NEWFOUNDLAND, ST. JOHNS.
Reappraisal of the geology of Kangimut Sammisoq, Ameralik Fjord, Southern West Greenland: Crustal structure and interpretation of isotopic data N88-30234

MESSERSCHMITT-BOELKOW-BLOHM G.M.B.H., HAMBURG (WEST GERMANY).
Comparison of the influence of different gust models on structural design N88-29722

MESSERSCHMITT-BOELKOW-BLOHM G.M.B.H., MUNICH (WEST GERMANY).
Evaluation of advanced air breathing concepts. Volume 1: Executive summary
[ESA-CR(P)-2539] N88-29806

MESSERSCHMITT-BOELKOW-BLOHM G.M.B.H., OTTOBRUNN (WEST GERMANY).
Hermes: Study of propulsion system for reusable man-rated spacecraft
[PSRM-TN-0000-00-04A] N88-29866

METAL MATRIX COMPOSITES INFORMATION ANALYSIS CENTER, SANTA BARBARA, CALIF.
Some theoretical considerations of the surface tension of liquid metals for metal matrix composites
[AD-A195999] N88-29882

MIAMI UNIV., CORAL GABLES, FLA.
Theoretical modeling of accelerating arc plasmas
[AD-A195606] N88-30426

MICHIGAN STATE UNIV., EAST LANSING.
Experimental determination of drag modifications due to elastic compliant surfaces using quantitative visual techniques
[AD-A194785] N88-30082

MICHIGAN UNIV., ANN ARBOR.
Radiation from soot-containing flames N88-29927

MINNESOTA UNIV., MINNEAPOLIS.
Studies of gas turbine heat transfer airfoil surface and end-wall cooling effects
[AD-A195165] N88-29805
Morphological changes in polymer electrolyte cells
[AD-A195821] N88-30054

MISSISSIPPI STATE UNIV., MISSISSIPPI STATE.
Generation of surface grids through elliptic partial differential equations for aircraft and missile configurations
[AD-A195639] N88-30378

MISSOURI UNIV., COLUMBIA.
Dirichlet prior in Bayesian estimation of item response curves
[AD-A195311] N88-30392

MISSOURI UNIV., ROLLA.
Zinc filled coatings N88-29978

MONTANA UNIV., MISSOULA.
Relationships among earth's gravity field, magnetic field, crustal structure and the magnetic character of crustal rocks
[AD-A195539] N88-30198

N

NAPLES UNIV. (ITALY).
Application of sampling techniques to near-field far-field transformation
[ESA-CR(P)-2546] N88-30002
Lava thicknesses: Implications for rheological and crustal development N88-30490

NATIONAL ACADEMY OF SCIENCES - NATIONAL RESEARCH COUNCIL, WASHINGTON, D. C.
Free vibration of rectangular plates with a small initial curvature
[NASA-CR-179370] N88-30148

NATIONAL AERONAUTICAL ESTABLISHMENT, OTTAWA (ONTARIO).
The NAE atmospheric research aircraft N88-29730
Aircraft dynamics: Aerodynamic aspects and wind tunnel techniques N88-29731
The use of hot-film technique for boundary layer studies on a 21 percent thick airfoil
[NAE-AN-45] N88-29781

NATIONAL AERONAUTICS AND SPACE ADMINISTRATION, WASHINGTON, D.C.
A preliminary investigation of drag reduction and mechanism for a blunt body of revolution with slanted base
[NASA-TT-20349] N88-29753
Calculation of non-stationary aerodynamic forces in the near sonic range
[NASA-TT-20310] N88-29782
The NASA Electric Propulsion Program
[NASA-TM-101324] N88-29859
Design criteria for extraction with chemical reaction and liquid membrane permeation
[NASA-TT-20352] N88-29899
Decomposition of hydrazine by high frequency glow electrical discharges
[NASA-TT-20240] N88-29906
Active sites and roles of solid acid base catalysts
[NASA-TT-20333] N88-29909
Studies on pressure response of gas bubbles contributions of condensed droplets in bubbles generated by a uniform nucleation
[NASA-TT-20343] N88-30068
Determination of the specific area of liquid gas and the velocity of weak pressure waves in aqueous foams
[NASA-TT-20347] N88-30087
Analysis method for the production of Reynolds stresses in compressible turbulent flow (fluid mechanics)
[NASA-TT-20330] N88-30088
A digital simulation technique for the Dryden atmospheric model
[NASA-TT-20342] N88-30266
Aerospace medicine and biology: A continuing bibliography with indexes (supplement 315)
[NASA-SP-7011(315)] N88-30281
A method for the quantitative determination of crystalline phases by X-ray
[NASA-TT-20324] N88-30444
Science at NASA field centers: Findings and recommendations on the scope, strength and interactions of science and science-related technology programs
[NASA-TM-101188] N88-30581

NATIONAL AERONAUTICS AND SPACE ADMINISTRATION. AMES RESEARCH CENTER, MOFFETT FIELD, CALIF.
Three-dimensional Navier-Stokes simulations of turbine rotor-stator interaction
[NASA-TM-100061] N88-29750
A streamwise upwind algorithm for the Euler and Navier-Stokes equations applied to transonic flows
[NASA-TM-101019] N88-29751
The present status and the future of missile aerodynamics
[NASA-TM-100063] N88-29773
The computation of flow past an oblique wing using the thin-layer Navier-Stokes equations
[NASA-TM-88317] N88-29774
Numerical simulation of unsteady incompressible viscous flows in generalized coordinate systems
[NASA-TM-101016] N88-30085
Space station proximity operations windows: Human factors design guidelines
[NASA-TM-88233] N88-30301
Telescience testbed pilot program
[NASA-CR-183207] N88-30309
Knowledge-based flow field zoning
[NASA-TM-101023] N88-30314
Performance analysis of FDDI
[NASA-CR-183206] N88-30321
A shared-world conceptual model for integrating space station life sciences telescience operations N88-30333
Nested neural networks
[NASA-TM-101032] N88-30373
Star formation and molecular clouds N88-30537

NATIONAL AERONAUTICS AND SPACE ADMINISTRATION. GODDARD SPACE FLIGHT CENTER, GREENBELT, MD.
The focal plane reception pattern calculation for a paraboloidal antenna with a nearby fence
[NASA-TM-100691] N88-30039
The 1988 Goddard Conference on Space Applications of Artificial Intelligence
[NASA-CP-3009] N88-30330
Artificial intelligence costs, benefits, risks for selected spacecraft ground system automation scenarios N88-30332
A rule-based systems approach to spacecraft communications configuration optimization N88-30341
Achieving real-time performance in FIESTA N88-30344
An interactive testbed for development of expert tools for pattern recognition N88-30349
The second generation intelligent user interface for the crustal dynamics data information system N88-30352
Spacelab data processing facility (SLDPF) Quality Assurance (QA)/Data Accounting (DA) expert systems: Transition from prototypes to operational systems N88-30353
Automated cataloging and characterization of space-derived data N88-30354
Far infrared supplement: Catalog of infrared observations, second edition
[NASA-RP-1205] N88-30545

NATIONAL AERONAUTICS AND SPACE ADMINISTRATION. HUGH L. DRYDEN FLIGHT RESEARCH FACILITY, EDWARDS, CALIF.
Techniques used in the F-14 variable-sweep transition flight experiment
[NASA-TM-100444] N88-30093

NATIONAL AERONAUTICS AND SPACE ADMINISTRATION. LYNDON B. JOHNSON SPACE CENTER, HOUSTON, TEX.
ARC length control for plasma welding
[NASA-CASE-MSC-20900-1] N88-30131
Chronology of early lunar crust N88-30212
The tectonic setting of Archean anorthosites N88-30231
The complexity, depth, and rapidity of processes that formed the lunar crust N88-30237
Volcanic contribution to crustal growth in the Central Andes: A new estimate and a discussion of uncertainties N88-30255

An intelligent training system for space shuttle flight controllers N88-30331
Automated space vehicle control for rendezvous proximity operations N88-30335
Lewis Cliff 86010, a unique Antarctic meteorite: Possible new clues to the early history of the solar system N88-30482
Antarctic Meteorite Newsletter, Volume 11, Number 2, August 1988
[NASA-TM-89801] N88-30573
Research and technology of the Lyndon B. Johnson Space Center
[NASA-TM-100463] N88-30583

NATIONAL AERONAUTICS AND SPACE ADMINISTRATION. LANGLEY RESEARCH CENTER, HAMPTON, VA.

Nonlinear Tollmien-Schlichting/vortex interaction in boundary layers
[NASA-CR-181698] N88-29715
The strong nonlinear interaction of Tollmien-Schlichting waves and Taylor-Goertler vortices in curved channel flow
[NASA-CR-181697] N88-29716
Status review of atmosphere turbulence and aircraft response N88-29726
A summary of atmospheric turbulence measurements with specially-equipped aircraft in the US N88-29727
On the generation of mean flows by the interaction of Goertler vortices and Tollmien-Schlichting waves in curved channel flows
[NASA-CR-181690] N88-29743
Adaptive mesh generation for viscous flows using Delaunay triangulation
[NASA-CR-181699] N88-29749
Aerodynamics in ground effect and predicted landing ground roll of a fighter configuration with a secondary-nozzle thrust reverser
[NASA-TP-2834] N88-29752
Application of unsteady aerodynamic methods for transonic aeroelastic analysis
[NASA-TM-100665] N88-29754
Pressure distributions from subsonic tests of an advanced laminar-flow-control wing with leading- and trailing-edge flaps
[NASA-TM-4040-PT-2] N88-29776
Recent advances in transonic computational aeroelasticity
[NASA-TM-100663] N88-29778
Compression pylon
[NASA-CASE-LAR-13777-1] N88-29789
Computer programs for calculation of sting pitch and roll angles required to obtain angles of attack and sideslip on wind tunnel models
[NASA-TM-100659] N88-29820
Space structure (dynamics and control) theme development
[NASA-TM-100597] N88-29850
Definition of common support equipment and space station interface requirements for IOC model technology experiments
[NASA-TM-100656] N88-29856
An improved boundary force method for analyzing cracked anisotropic materials
[NASA-TM-101495] N88-29879
Transition at hypersonic speeds
[NASA-CR-178315] N88-30058
Recent insights into instability and transition to turbulence in open-flow systems
[NASA-CR-181693] N88-30079
Quantitative surface temperature measurement using two-color thermographic phosphors and video equipment
[NASA-CASE-LAR-13740-1] N88-30105
Method of attaching strain gauges to various materials
[NASA-CASE-LAR-13797-1] N88-30108
Clevis joint for deployable space structures
[NASA-CASE-LAR-13896-1] N88-30130
Ultrasonic method and apparatus for determining crack opening load
[NASA-CASE-LAR-13889-1] N88-30160
Convergence of Galerkin approximations for operator Riccati equations: A nonlinear evolution equation approach
[NASA-CR-181706] N88-30386
Eikonal solutions to optical model coupled-channel equations
[NASA-TP-2830] N88-30402
The atmospheres of the earth and the other planets: Origin, evolution and composition N88-30544

NATIONAL AERONAUTICS AND SPACE ADMINISTRATION. LEWIS RESEARCH CENTER, CLEVELAND, OHIO.

Analysis and optimization of truncated scarf nozzles subject to external flow conditions
[NASA-TM-100955] N88-29746
Euler analysis of a swirl recovery vane design for use with an advanced single-rotation propfan
[NASA-TM-101357] N88-29771
An unconditionally stable Runge-Kutta method for unsteady flows
[NASA-TM-101347] N88-29780
Aeroelastic response of metallic and composite propfan models in yawed flow
[NASA-TM-100964] N88-29807
The effect of the near earth micrometeoroid environment on a highly reflective mirror surface
[NASA-TM-101307] N88-29833
Technology requirements for an orbiting fuel depot: A necessary element of a space infrastructure
[NASA-TM-101370] N88-29845
Performance and lifetime assessment of MPD arc thruster technology
[NASA-TM-101293] N88-29860
Experimental evaluation of resistojet thruster plume shields
[NASA-TM-101363] N88-29868
The dc power control for a liquid-fed resistojet
[NASA-TM-101326] N88-29869
Successful completion of a cyclic ground test of a mercury ion auxiliary propulsion system
[NASA-TM-101351] N88-29873
Iridium-coated rhenium thrusters by CVD
[NASA-TM-101309] N88-29874
Brominated graphite fibers and method of producing the same
[NASA-CASE-LEW-14696-1] N88-29888
Electrocatalytic reduction of oxygen on modified oxide surfaces
[NASA-TM-101333] N88-29952
Novel ladder polymers for use as high temperature stable resins or coatings
[NASA-CASE-LEW-14203-1] N88-29984
Optical measurements of soot and temperature profiles in premixed propane-oxygen flames
[NASA-TM-101343] N88-29997
High frequency GaAlAs modulator and photodetector for phased array antenna applications
[NASA-TM-101328] N88-30048
Containment of a silicone fluid free surface in reduced gravity using barrier coatings
[NASA-TM-101314] N88-30072
Three-dimensional elliptic grid generation technique with application to turbomachinery cascades
[NASA-TM-101330] N88-30078
Experimental and numerical investigation of the effect of distributed suction on oblique shock wave/turbulent boundary layer interaction
[NASA-TM-101334] N88-30084
Optical measurements of soot in premixed flames
[NASA-TM-101305] N88-30090
Impact of ETO propellants on the aerothermodynamic analyses of propulsion components
[NASA-TM-101303] N88-30094
Measurement of local high-level, transient surface heat flux
[NASA-TP-2840] N88-30099
Helicopter transmission research at NASA Lewis Research Center
[NASA-TM-100962] N88-30128
Convergence acceleration for vector sequences and applications to computational fluid dynamics
[NASA-TM-101327] N88-30377
Testing of a variable-stroke Stirling engine
[NASA-TM-100699] N88-30472

NATIONAL AERONAUTICS AND SPACE ADMINISTRATION. MARSHALL SPACE FLIGHT CENTER, HUNTSVILLE, ALA.

NASA Marshall Space Flight Center solar observatory
[NASA-TM-100339] N88-29832
Impact of ETO propellants on the aerothermodynamic analyses of propulsion components
[NASA-TM-101303] N88-30094
Automatic mathematical modeling for real time simulation system N88-30356
A review of melt and vapor growth techniques for polydiacetylene thin films for nonlinear optical applications
[NASA-TM-100340] N88-30412

NATIONAL AERONAUTICS AND SPACE ADMINISTRATION. PASADENA OFFICE, CALIF.

Doppler-corrected differential detection system
[NASA-CASE-NPO-16967-1-CU] N88-30001

NATIONAL AEROSPACE LAB., AMSTERDAM (NETHERLANDS).

Acquisition of gust statistics from AIDS-recorded data N88-29733
Low-speed longitudinal flying qualities of modern transport aircraft N88-29738
Failure analysis for gas turbines
[NLR-MP-87037-U] N88-29808
ERS-1: A satellite with an oceanographic mission
[NLR-MP-88072-U] N88-29838
Compression and decompression of imaging sensor signals (CADISS): A multiprocessor system for image compression/decompression on board scientific satellites
[NLR-TR-87076-L] N88-30323

NATIONAL AEROSPACE LAB., EMMELOORD (NETHERLANDS).

Matching P.S.D.: Design loads N88-29720

NATIONAL BUREAU OF STANDARDS, GAITHERSBURG, MD.

A reliability-based program for predicting the service life of organic coating systems N88-29971
NBS (National Bureau of Standards) measurement services: The NBS photodetector spectral response calibration transfer program
[PB88-201595] N88-30109
Low level image processing techniques using the pipeline image processing engine in the flight telerobotic servicer N88-30346
X-ray diffraction imaging (topography) of electrooptic crystals by synchrotron radiation
[NASA-CR-183266] N88-30427
Diffraction imaging (topography) with monochromatic synchrotron radiation
[NASA-CR-183264] N88-30431
Streaking images that appear only in the plane of diffraction in undoped GaAs single crystals: Diffraction imaging (topography) by monochromatic synchrotron radiation
[NASA-CR-183267] N88-30437
Applications of synchrotron radiation to materials science: Diffraction imaging (topography) and microradiography
[NASA-CR-183265] N88-30440

NATIONAL CENTER FOR ENERGETICS AND PROPULSION, PESCHIERA BORROMEO (ITALY).

Numerical modeling of combustion processes in gas turbines N88-29939

NATIONAL GEOPHYSICAL DATA CENTER, BOULDER, COLO.

Solar-geophysical data number 523, March 1988. Part 1: (Prompt reports). Data for February 1988, January 1988 and late data
[PB88-212766] N88-30574
Solar-geophysical data number 523, March 1988. Part 2: (Comprehensive reports). Data for September 1987 and miscellanea
[PB88-212774] N88-30576

NATIONAL GEOPHYSICAL RESEARCH INST., HYDERABAD (INDIA).

Evolution of the Dharwar Craton: A terrain of early Archean crustal stability, long term orogenic cycles and large scale palaeobiological activity N88-30241

NATIONAL INST. OF OCEANOGRAPHY, HAIFA (ISRAEL).

Diapirs of the Mediterranean ridge: The tectonic regime of an incipient accreted terrane N88-30224
The tectonic setting of the Seychelles, Mascarene and Amirante Plateaus in the Western Equatorial Indian Ocean N88-30225

NATIONAL LIBRARY OF CANADA, OTTAWA (ONTARIO).

Using standards to break down information transfer barriers N88-30457

NATIONAL RESEARCH COUNCIL OF CANADA, OTTAWA (ONTARIO).

Multiple scattering effects in drop sizing of dense fuel sprays by laser diffraction N88-29917

NATIONAL SCIENTIFIC AND TECHNICAL DOCUMENTATION CENTER, BRUSSELS (BELGIUM).

Linguistic barriers: Translation problems N88-30465

NATIONAL TECHNICAL UNIV., ATHENS (GREECE).

The effect of particle properties on radiative heat transfer N88-29941

NAVAL CIVIL ENGINEERING LAB., PORT HUENEME, CALIF.

Performance Prediction for Coatings. Proceedings of a Workshop
[AD-A188973] N88-29966
Degradation of protective coatings on steel in corrosive environments N88-29969

NAVAL ENVIRONMENTAL PREDICTION RESEARCH FACILITY, MONTEREY, CALIF.

The surface evaporative duct height product: An evaluation
[AD-A195918] N88-30199

NAVAL OCEAN SYSTEMS CENTER, SAN DIEGO, CALIF.

Multilevel computational theory of stereoscopic visual image processing
[AD-A195331] N88-30288
A fiber optic beamforming processor for wideband direction finding
[AD-A194862] N88-30404

Ultra-wideband direction finding using a fiber optic beamforming processor
[AD-A194861] N88-30413
Power MISFETs on OnP
[AD-A195242] N88-30436

NAVAL POSTGRADUATE SCHOOL, MONTEREY, CALIF.
Accuracy of satellite data navigation
[AD-A195877] N88-29787
A standard library for modeling satellite orbits on a microcomputer
[AD-A195759] N88-29830
Ion gun generated electromagnetic interference on the SCATHA satellite
[AD-A195179] N88-29853
Automatic data retrieval from rocket motor holograms
[AD-A195586] N88-29864
Numerical field model simulation of full scale fire tests in a closed spherical/cylindrical vessel
[AD-A195067] N88-29998
Long haul communications in the HF spectrum utilizing high speed modems
[AD-A194883] N88-30003
Comparative analysis of passive communications satellites employing the SHF and HF spectrum for use in a strategic role
[AD-A194682] N88-30019
Scattering impulse response synthesis using random noise illumination: Initial concept evaluation
[AD-A195086] N88-30034
The thermal behavior of film cooled turbulent boundary layers as affected by longitudinal vortices
[AD-A195155] N88-30095
Analytical and experimental studies of beam waveguide absorbers for structural damping
[AD-A195065] N88-30144
An analysis of results of a high-resolution world ocean circulation model
[AD-A195760] N88-30272
The design of an intelligent multidisk control module for VME bus based systems
[AD-A195587] N88-30303
A static scheduler for the computer aided prototyping system: An implementation guide
[AD-A194340] N88-30322
Adaptive control in positioning a rigid-flexible robot arm
[AD-A195194] N88-30367
The P-3 Scheduling Support System (P-3 S3)
[AD-A194824] N88-30450

NAVAL RESEARCH LAB., WASHINGTON, D.C.
Track performance considerations for monopulse radars
[AD-A196232] N88-30007
A submillimeter wavelength space-based imaging radar
[AD-A195846] N88-30033
Measurement and interpretation of North Atlantic Ocean marine radar sea scatter
[AD-A196239] N88-30036
Nonlinear dynamics of coupled oscillator arrays
[AD-A194888] N88-30053
Approximation of viscoelastic stresses from Newtonian turbulent kinematics
[AD-A194317] N88-30077
Autoionization for lower level detrapping in X-ray lasers
[AD-A195845] N88-30123
Analysis of environmental parameters from the Panama City tower radar experiment
[AD-A194994] N88-30264
Structuring processes in expanding laser-produced plasmas
[AD-A195249] N88-30424

NAVAL SHIP RESEARCH AND DEVELOPMENT CENTER, BETHESDA, MD.
Analysis of a fixed-pitch X-wing rotor employing lower surface blowing
[AD-A187379] N88-29779
Electrical detection of coating deterioration N88-29973
Evaluation of organic coating deterioration and substrate corrosion in seawater using electrochemical impedance measurements N88-29976

NAVAL SUBMARINE MEDICAL CENTER, GROTON, CONN.
Visual sensitivities under reduced oxygen
[AD-A195628] N88-30279

NAVAL SURFACE WEAPONS CENTER, SILVER SPRING, MD.
Space marching Euler solvers N88-29759

NEVADA UNIV., RENO.
Alternative immersion accelerated testing of coating systems for Naval shoreline facilities N88-29977

NEW YORK UNIV., NEW YORK.
Computational methods for the problems of the tip vortex
[NASA-CR-181436] N88-29775

NIELSEN ENGINEERING AND RESEARCH, INC., MOUNTAIN VIEW, CALIF.
Survey on nonlinear effects N88-29757

NORSK FORSVARSTEKNOLOGI A/S (NORWAY).
Interim Flight Opportunity (IFO). Volume 1: Executive summary
[SE/LS/AP-36-818/CN-VOL-1] N88-29849

NORTH CAROLINA UNIV., CHAPEL HILL.
The Kerala Khondalite Belt (KKB) of Southern India: An enclalic mobile belt N88-30208
Evaluation of the potential health hazards associated with the machining of carbon fiber composites
[AD-A194835] N88-30286
Partitioned storage for temporal databases
[AD-A195093] N88-30451

NORTH DAKOTA STATE UNIV., FARGO.
Photoacoustic Fourier transform infrared spectroscopy. An early detection technique for coatings degradation N88-29968

NORTHEASTERN UNIV., BOSTON, MASS.
Aerospace payload support systems
[AFGL-TR-87-0241] N88-29843

NORTHWEST RESEARCH ASSOCIATES, INC., BELLEVUE, WASH.
The effect of equatorial ionospheric irregularities on the performance of a south-looking OTH-B (Over-The-Horizon-Backscatter) radar
[AD-A195090] N88-30018

NORTHWESTERN UNIV., EVANSTON, ILL.
Electrical properties of materials for elevated temperature resistance strain gage application
[NASA-CR-182214] N88-30106

O

OAK RIDGE NATIONAL LAB., TENN.
Determination of multiaxial flow surfaces at elevated temperatures using the concept of dissipation potential
[ORNL/TM-10787] N88-30149
Conversion of productions in OPS5 to their equivalent English
[ORNL/TM-10246] N88-30306

ODETICS, INC., ANAHEIM, CALIF.
Threat expert system technology advisor
[NASA-CR-177479] N88-29816

OFFICE NATIONAL D'ETUDES ET DE RECHERCHES AEROSPATIALES, PALAISEAU (FRANCE).
Flame stabilization in a reheat combustor N88-29921

OFFICE NATIONAL D'ETUDES ET DE RECHERCHES AERONAUTIQUES, PARIS (FRANCE).
Measured and predicted responses of the Nord 260 aircraft to the low altitude atmospheric turbulence N88-29723

OFFICE NATIONAL D'ETUDES ET DE RECHERCHES AEROSPATIALES, PARIS (FRANCE).
Extreme gusts distribution N88-29734
Prediction of base-flows N88-29765
Influence of the convection on evaporation and combustion of a fuel droplet N88-29948

OHIO STATE UNIV., COLUMBUS.
Role of ordinary to extraordinary mode wave coupling in ionospheric heating experiments
[AD-A195335] N88-30017
Fatigue crack propagation: Probabilistic modeling and statistical analysis
[AD-A195885] N88-30155

OHIO WESLEYAN UNIV., DELAWARE.
Functional assessment of laser irradiation
[AD-A195735] N88-30287

OKLAHOMA STATE UNIV., STILLWATER.
Growth and characterization of materials for tunable lasers in the near infrared spectral region
[NASA-CR-183132] N88-30113

OLD DOMINION UNIV., NORFOLK, VA.
Geometric modeling for computer aided design
[NASA-CR-183161] N88-30320

OLD ROYAL OBSERVATORY, LONDON (ENGLAND).
Lava thicknesses: Implications for rheological and crustal development N88-30490

OPEN UNIV., MILTON (ENGLAND).
Changing styles of crustal growth in Southern Africa: Constraints from geochemical and Sr-Nd isotope studies in Archaean to Pan African terrains N88-30227

OREGON STATE UNIV., CORVALLIS.
Chronology of early lunar crust N88-30212
The complexity, depth, and rapidity of processes that formed the lunar crust N88-30237

OTTAWA UNIV. (ONTARIO).
Mineralization through geologic time: Evolution of continental crust N88-30250

OULU UNIV. (FINLAND).
Five channel auroral photometer
[REPT-112] N88-30101

OXFORD UNIV. (ENGLAND).
Does subduction zone magmatism produce average continental crust N88-30214
Metamorphic P-T paths and Precambrian crustal growth in East Antarctica N88-30218
The growth of the continental crust: Constraints from radiogenic isotope geochemistry N88-30245
Late-Archaean crustal growth in the Lewisian Complex of Northwest Scotland: Diachroneity in magmatic accretion and implications for models of crustal growth N88-30253

P

PEKING UNIV. (CHINA).
Archean crustal evolution of the northern North China Craton N88-30235

PENNSYLVANIA STATE UNIV., UNIVERSITY PARK.
Piezoelectric and electrostrictive materials for transducer applications, volume 1
[AD-A194957] N88-30096
Piezoelectric and electrostrictive materials for transducer applications, volume 2
[AD-A194956] N88-30104
Piezoelectric and electrostrictive materials for transducer applications, volume 3
[AD-A194949] N88-30112
An organometallic route to micron-sized whiskers of zinc sulfide
[AD-A195889] N88-30414

PHYSICAL SCIENCES, INC., ANDOVER, MASS.
Volumetric measurement of vorticity vectors by optical probe
[AD-A195997] N88-30061

PISA UNIV. (ITALY).
The optimal control pilot model and applications N88-29741

PLANETARY SCIENCE INST., PASADENA, CALIF.
Comparisons of solar nebula models N88-30539

PLANETARY SCIENCE INST., TUCSON, ARIZ.
Early intense cratering: Effects on growth of earth's crust N88-30219

PLANNING RESEARCH CORP., HAMPTON, VA.
Aircraft noise prediction program propeller analysis system IBM-PC version user's manual version 2.0
[NASA-CR-181689] N88-30399

POLITECNICO DI MILANO (ITALY).
Numerical modeling of combustion processes in gas turbines N88-29939

POLITECNICO DI TORINO (ITALY).
Activities report of the Department of Aerospace Engineering
[ETN-88-91607] N88-30582

POLYTECHNIC INST. OF NEW YORK, FARMINGDALE.
Millimeter wave generation by relativistic electron beams
[AD-A195683] N88-30016
Structure and dynamics of solutions of lithium salts relevant to battery construction
[AD-A195399] N88-30044

POLYTECHNIC UNIV., BROOKLYN, N.Y.
In situ fault detection by the hybrid ray mode method
[AD-A195226] N88-30137

PRATT AND WHITNEY AIRCRAFT, WEST PALM BEACH, FLA.
Breadboard RL10-2B low-thrust operating mode (second iteration) test report
[NASA-CR-182160] N88-29867
Oxidizer heat exchanger component test
[NASA-CR-182159] N88-29876
Fuel property effects on the US Navy's TF30 engine N88-29911

PRC KENTRON, INC., HAMPTON, VA.
Semi-empirical methods for conventional and unconventional missiles N88-29758

PRC SYSTEMS SERVICES CO., HAMPTON, VA.
An operations manual for the digital data system
[NASA-CR-181688] N88-30329

PRESBYTERIAN-ST. LUKES HOSPITAL, CHICAGO, ILL.
Temperature profile construction methods: An evaluation
[AD-A195919] N88-30262

PRINCETON UNIV., N. J.
Ultrafast processes and spectroscopy with free electron lasers
[AD-A195248] N88-30126
Theory of superconductivity in oxides
[AD-A195647] N88-30432

PURDUE UNIV., WEST LAFAYETTE, IND.
Atomization of alternative fuels N88-29913
Storing bits on a DNA polymer chain
[AD-A195701] N88-29981

Vibrational power flow analysis of rods and beams
[NASA-CR-183166] N88-30151

Q

QUEBEC UNIV., MONTREAL.
Geochronological and lead-isotope evidences for rapid crust formation in middle-proterozoic time: The Labrador example N88-30239
QUEENSLAND UNIV., BRISBANE (AUSTRALIA).
Geometric and material nonlinear analysis of structures comprising rectangular hollow sections
[CE-79] N88-30141
Impact force as a part of the total breaking wave force on a vertical cylinder
[RR-CE78] N88-30154
QUEENSLAND UNIV., ST. LUCIA (AUSTRALIA).
A parametric study of embedded cantilever retaining walls: The results of a finite element study
[RR-CE83] N88-30152

R

R AND D ASSOCIATES, ALEXANDRIA, VA.
Unified study of plasma/surface interactions for space power and propulsion
[AD-A195971] N88-29870
RACAL DEFENCE ELECTRONICS (RADAR) LTD., WALTON-ON-THAMES (ENGLAND).
Modelling of CO oxidation in dilution jet flows N88-29947
RAND CORP., SANTA MONICA, CALIF.
Aircraft airframe cost estimating relationships: Study approach and conclusions
[R-3255-AF] N88-29795
The cost and performance implications of reliability improvements in the F-16A/B
[AD-A195096] N88-29796
RENSSELAER POLYTECHNIC INST., TROY, N.Y.
Theoretical aerodynamics, transonic flow
[AD-A196247] N88-29777
Processing technology research in composites
[AD-A195693] N88-29890
Effect of interfacial phenomena on contact line heat Transfer-3
[AD-A194941] N88-29901
RESEARCH INST. OF NATIONAL DEFENCE, LINKOEPING (SWEDEN).
A system study with an infrared sensitive microelectronic image sensor
[FOA-C-30481-3.1] N88-30407
RESEARCH INST. OF NATIONAL DEFENCE, STOCKHOLM (SWEDEN).
Review of research concerning Solid Fuel Ramjet (SOFRAM) at the Research Institute of National Defence (FOA) 2
[FOA-C-20714-2.1] N88-29813
Ignition and extinguishing of a Solid Fuel Ramjet (SOFRAM)
[FOA-C-20713-2.1] N88-29865
Thermomechanical computations for GAP, a high energy binder for composite propellants
[FOA-C-20718-2.1] N88-29866
RETINA FOUNDATION, BOSTON, MASS.
Eye movements and spatial pattern vision
[AD-A195496] N88-30290
ROCHESTER UNIV., N. Y.
Center for opto-electronic systems research
[AD-A195159] N88-30411
ROCKWELL INTERNATIONAL CORP., THOUSAND OAKS, CALIF.
A new computational capability for ramjet projectiles
[AD-A196061] N88-29812
ROCKWELL INTERNATIONAL SCIENCE CENTER, THOUSAND OAKS, CALIF.
Electrochemical evaluation of the long term corrosion resistance of polymer coated steel N88-29974
An electrochemical impedance spectroscopy study of reactions at the metal/coating interface N88-29975
ROLLS-ROYCE LTD., BRISTOL (ENGLAND).
Evaluation of advanced air breathing concepts. Volume 1: Executive summary
[ESA-CR(P)-2539] N88-29806
High performance turbofan afterburner systems N88-29922
ROLLS-ROYCE LTD., DERBY (ENGLAND).
V2500 engine collaboration
[PNR90423] N88-29803
Developing the Rolls-Royce Tay
[PNR90447] N88-29809
Positron emission tomography: A new technique for observing fluid behavior in engineering systems
[PNR90471] N88-30091
Use of holography in vibration and flutter study of fans
[PNR90458] N88-30098
ROYAL AIRCRAFT ESTABLISHMENT, BEDFORD (ENGLAND).
Measurement and analysis of low altitude atmospheric turbulence obtained using a specially instrumented Gnat aircraft N88-29728
ROYAL AIRCRAFT ESTABLISHMENT, FARNBOROUGH (ENGLAND).
Gas turbine smoke measurement: A smoke generator for the assessment of current and future techniques N88-29930
ROYAL SIGNALS AND RADAR ESTABLISHMENT, MALVERN (ENGLAND).
Automatic prober for the dc characterisation of gallium arsenide devices. Part 2: The data sorting and display facility
[AD-A195408] N88-30111
RUTGERS - THE STATE UNIV., NEW BRUNSWICK, N. J.
Numerical simulation of nozzle flows
[AD-A195144] N88-30064
Architecture for optical digital computers
[AD-A195477] N88-30416

S

SAAB SPACE A.B., GOETEBORG (SWEDEN).
Interim Flight Opportunity (IFO). Volume 1: Executive summary
[SE/LS/AP-36-818/CN-VOL-1] N88-29849
SAARLAND UNIV., SAARBRUCKEN (WEST GERMANY).
Linguistic-technical aspects of machine translation N88-30461
SANDIA NATIONAL LABS., ALBUQUERQUE, N. MEX.
Gas phase combustion chemistry of nitramine propellants
[AD-A195082] N88-29902
SATCON TECHNOLOGY CORP., CAMBRIDGE, MASS.
Synchronous response modelling and control of an annular momentum control device
[NASA-CR-4166] N88-29995
SCHOOL OF AEROSPACE MEDICINE, BROOKS AFB, TEX.
Central serous chorioretinopathy in USAF aviators: A review
[AD-A195897] N88-30280
A field study on soft contact lens wear in USAF military transport aircraft
[AD-A195962] N88-30285
SCIENCE APPLICATIONS RESEARCH, GREENBELT, MD.
The advice taker/inquirer: A system for high-level acquisition of expert knowledge N88-30359
SCIENTIFIC RESEARCH ASSOCIATES, INC., GLASTONBURY, CONN.
Numerical simulation of the function of scientific instrumentation for measuring the speed of electron devices
[AD-A194969] N88-30103
SCRIPPS INSTITUTION OF OCEANOGRAPHY, LA JOLLA, CALIF.
Pb isotope constaints on the extent of crustal recycling into a steady state mantle N88-30215
SELENIA SPAZIO S.P.A., ROME (ITALY).
The LTPP communication processor
[CL/CP/SES/FR/004] N88-30328
SELSKAPET FOR INDUSTRIELL OG TEKNISK FORSKNING, TRONDHEIM (NORWAY).
Study of human factors engineering criteria for Extra Vehicular Activity (EVA) systems, volume 2
[STF23-F87025-VOL-2] N88-30293
Study of human factors engineering criteria for extravehicular activity (EVA) systems, volume 1
[STF23-F87025-VOL-1] N88-30296
SENER S.A., LAS ARENAS (SPAIN).
Obtaining stress intensity factors on cracks, by means of fitting techniques on numerical results calculated with the finite element method N88-30153
SENER S.A., MADRID (SPAIN).
Study of robotics spacecraft servicing and assembly in space. Volume 1: Executive summary
[ESA-CR(P)-2612-VOL-1] N88-29839
Interim Flight Opportunity (IFO). Volume 1: Executive summary
[SE/LS/AP-36-818/CN-VOL-1] N88-29849
SHEFFIELD UNIV. (ENGLAND).
Three-dimensional gas turbine combustor modelling N88-29937
Development of a more general Reynolds stress closure for swirling flow
[AD-A195121] N88-30092
SHERWIN-WILLIAMS CO., CHICAGO, ILL.
Prediction of degradation of polymeric coating materials N88-29970
SIERRA GEOPHYSICS, INC., KIRKLAND, WASH.
Discrimination studies using short-period P waves at upper mantle distances
[AD-A195468] N88-30257
SMITHSONIAN INSTITUTION, WASHINGTON, D. C.
Physical properties of surface materials on Martian volcanoes: Dust-covered lava and ash N88-30493
SOCIETE EUROPEENNE DE PROPULSION, VERNON (FRANCE).
Simulation of Vulcain engine operation at low inlet pressure
[ETN-88-93083] N88-29875
SOCIETE NATIONALE D'ETUDE ET DE CONSTRUCTION DE MOTEURS D'AVIATION, PARIS (FRANCE).
Evaluation of the advanced air breathing propulsion concepts, executive summary
[ESA-CR(P)-2540] N88-29802
SOCIETE NATIONALE INDUSTRIELLE AEROSPATIALE, CANNES (FRANCE).
Study on conceptual design of spacecraft using Computer Aided Engineering (CAE)
[SNIAS-920-CA/TS] N88-29841
Imaging instrument of the vegetation payload (SPOT 4)
[SNIAS-881-440-107] N88-30169
SOCIETE NATIONALE INDUSTRIELLE AEROSPATIALE, LES MUREAUX (FRANCE).
Interim Flight Opportunity (IFO). Volume 1: Executive summary
[SE/LS/AP-36-818/CN-VOL-1] N88-29849
Rupture of carbon fiber reinforced plastics (T300-914) composite materials: Influence of initial first ply failures on the fatigue behavior
[SNIAS-881-422-103] N88-29892
SOUTHWEST RESEARCH INST., SAN ANTONIO, TEX.
A study of the effect of random input motion on low Reynolds number flows
[AD-A195559] N88-29747
Constitutive modeling for isotropic materials
[NASA-CR-182132] N88-29811
Spray automated balancing of rotors: Methods and materials
[NASA-CR-182151] N88-29825
Evaluation of bond testing equipment for inspection of Army advanced composite airframe structures
[AD-A195795] N88-29885
Fuel effects on flame radiation and hot-section durability N88-29925
SPACE TELESCOPE SCIENCE INST., BALTIMORE, MD.
Lisp Object State Saver (LOSS): A facility used to save partial schedules of the Hubble Space Telescope N88-30360
Verification and validation of rulebased systems for Hubble Space Telescope ground support N88-30361
The guide star catalog
[NASA-CR-183253] N88-30547
Starbursts and their dynamics
[NASA-CR-180227] N88-30549
Evolutionary helium and CNO anomalies in the atmospheres and winds of massive hot stars
[NASA-CR-183254] N88-30550
Observations of faint field galaxies
[NASA-CR-183251] N88-30555
A deep redshift survey of field galaxies. Comments on the reality of the Butcher-Oemler effect
[NASA-CR-183255] N88-30558
Radio and infrared properties of young stars
[NASA-CR-183252] N88-30579
SPAR AEROSPACE LTD., STE-ANNE-DE-BELLEVUE (QUEBEC).
Study of robotics spacecraft servicing and assembly in space. Volume 1: Executive summary
[ESA-CR(P)-2612-VOL-1] N88-29839
SRI INTERNATIONAL CORP., MENLO PARK, CALIF.
Quality measures and assurance for AI (Artificial Intelligence) software
[NASA-CR-4187] N88-30304
Research on problem-solving systems
[AD-A195154] N88-30370
STANFORD UNIV., CALIF.
An experimental study of an adaptive-wall wind tunnel
[NASA-CR-183152] N88-29821
Mathematical problems of nonlinear wave propagation and of waves in heterogeneous media
[AD-A195970] N88-30057
Application of nondestructive testing techniques to materials testing
[AD-A195718] N88-30138
Spectral analysis of the Elatina varve series
[NASA-CR-183085] N88-30260
Algorithms for nonlinear least-squares problems
[AD-A196071] N88-30305
Performance prediction of concurrent systems
[NASA-CR-183175] N88-30312

Formulation and solution of economic equilibrium problems
[AD-A196034] N88-30470

STATE UNIV. OF NEW YORK, ALBANY.
Laser sensing for identification and control of distributed parameter systems
[AD-A195886] N88-30124

STEEL STRUCTURES PAINTING COUNCIL, PITTSBURGH, PA.
Reduced time frame for predicting coating performance N88-29979

STERLING FEDERAL SYSTEMS, INC., PALO ALTO, CALIF.
Nonequilibrium flow computations. 1: An analysis of numerical formulations of conservation laws
[NASA-CR-177489] N88-30384

STERLING SOFTWARE, PALO ALTO, CALIF.
An analysis of finite-difference and finite-volume formulations of conservation laws
[NASA-CR-177416] N88-30071
Supermap for Cray FORTRAN: A user's guide
[NASA-CR-177410] N88-30308
The eivaN: A forward-looking interactive orbital trajectory plotting tool for use with proximity operations (PROX OPS) and other maneuvers: Description and user's manual
[NASA-CR-177490] N88-30327

STOCKHOLM UNIV. (SWEDEN).
Global vertical mass transport by clouds: A two-dimensional model study
[CM-74] N88-30192

STRATEGIC DEFENSE INITIATIVE ORGANIZATION, WASHINGTON, D.C.
Report to congress on the strategic defense system architecture
[AD-A195476] N88-30393

STRATHCLYDE UNIV., GLASGOW (SCOTLAND).
The effect of thicker oceanic crust in the Archaean on the growth of continental crust through time N88-30254

STUTTGART UNIV. (WEST GERMANY).
Study of modern instrumentation and methods for astronomic positioning in the field
[AD-A196173] N88-30548

SUNDSTRAND ENERGY SYSTEMS, ROCKFORD, ILL.
Study of toluene stability for an Organic Rankine Cycle (ORC) space-based power system
[NASA-CR-180884] N88-29863
Study of toluene rotary fluid management device and shear flow condenser performance for a space-based organic Rankine power system
[NASA-CR-180885] N88-29872

SWEDISH INST. OF SPACE PHYSICS, UMEA.
Reconstruction of wave distribution functions in warm plasmas
[IRF-PREPRINT-104] N88-30422

SWEDISH INST. OF SPACE PHYSICS, UPPSALA.
Characteristics of solitary waves and weak double layers in the magnetospheric plasma
[IRF-PREPRINT-105] N88-30418

SYDNEY UNIV. (AUSTRALIA).
The study of hydromagnetic waves and RF heating using the TORTUS tokamak, the development of diagnostic techniques based on submillimeter lasers and the gyrotron, and gas discharge N88-30419

SYRACUSE UNIV., N. Y.
On adaptive cell-averaging CFAR (Constant False-Alarm Rate) radar signal detection
[AD-A196286] N88-30009

SYSTEMS ENGINEERING LABS., INC., GREENBELT, MD.
Analytical methods in stochastic control and nonlinear filtering
[AD-A194272] N88-30388

SYSTEMS TECHNOLOGY, INC., HAWTHORNE, CALIF.
Pilot modeling N88-29736
Pilot modeling applications N88-29737
Advances in flying qualities: Concepts and criteria for a mission oriented flying qualities specification N88-29739

T

TACAN AEROSPACE CORP., CARLSBAD, CALIF.
Spectroscopic studies with multiple quantum well materials with applications to optical signal processing at room temperature
[AD-A194171] N88-30409

TAYLOR (J.), CAMBERLEY (ENGLAND).
An interim comparison of operational CG records in turbulence on small and large civil aircraft N88-29729

TECHNICAL RESEARCH CENTRE OF FINLAND, ESPOO.
State variable approach to deformation phenomena in Face Centered Cubic (FCC) metals
[VTT-44] N88-29964
Ion exchange processes for fabrication of integrated optical waveguide structures into glass substrates
[VTT-46] N88-30405

TECHNICAL UNIV. OF ISTANBUL (TURKEY).
A dynamic analysis of piezoelectric strained elements
[AD-A196079] N88-30430

TECHNION - ISRAEL INST. OF TECH., HAIFA.
Models of cerebral-body perfusion and cerebral chemical transport
[AD-A194945] N88-30283

TECHNISCHE HOCHSCHULE, DARMSTADT (WEST GERMANY).
Large ionic species in sooting acetylene and benzene flames N88-29932

TECHNISCHE HOGESCHOOL, DELFT (NETHERLANDS).
Time-domain far-field scattering of plane electromagnetic waves by a penetrable object in the Born approximation
[PB87-176129] N88-30040

TECHNISCHE UNIV., BERLIN (WEST GERMANY).
Possibilities of economical improvements for Moon based rocket propulsion using lunar propellants
[ILR-MITT-196] N88-29871
Investigations on the modification of structural reliability by substitution of aluminum by carbon fiber reinforced plastics in aircraft construction
[ILR-MITT-195] N88-29877
The optical spectroscopy of copper-blue luminescence in zinc sulfide crystals. Zero-phonon line spectra under the influence of magnetic field, temperature and excitation intensity
[ETN-88-93122] N88-29903
Experimental and theoretical investigations of isotope shift and hyperfine structure on 5d elements (especially platinum, iridium and rhenium)
[ETN-88-93121] N88-29957
Voltage directive drive with claw pole motor and control without rotor position indicator
[ETN-88-93120] N88-30047
Spectral properties of semiconductor lasers with external resonators
[ETN-88-93119] N88-30125
Stability of stick-slip phenomenon by using constitutive friction laws of Dietrich and Ruina
[ILR-MITT-197] N88-30127

TECHNISCHE UNIV., BRUNSWICK (WEST GERMANY).
Flight test equipment for the on-board measurement of wind turbulence N88-29719

TECHNISCHE UNIV., MUNICH (WEST GERMANY).
Comparison of the performance of a reverse flow annular combustion chamber under low and high pressure conditions N88-29923

TELEDYNE GEOTECHNICAL, ALEXANDRIA, VA.
Maximum-likelihood multichannel deconvolution of P waves at seismic arrays
[AD-A194990] N88-30191
Finite-difference simulations of Rayleigh-wave scattering by shallow heterogeneity
[AD-A194961] N88-30259

TENNESSEE UNIV., KNOXVILLE.
The petrogenesis of oceanic kimberlites and included mantle megacrysts: The Malaitan alnoite N88-30232
Continental growth through time by underplating of subducted oceanic crust: Evidence from kimberlites in South Africa and SW Pacific N88-30244
Advancement of latent trait theory
[AD-A194302] N88-30289

TENNESSEE UNIV., TULLAHOMA.
Contamination and distortion of steady flow field induced by discrete frequency disturbances in aircraft gas engines
[AD-A195440] N88-30069

TEXAS A&I UNIV., KINGSVILLE.
A fiber optic collective flight control system for helicopters
[AD-A195406] N88-29818

TEXAS INSTRUMENTS, INC., DALLAS.
Stress related failures causing open metallization
[AD-A195061] N88-30150

TEXAS UNIV., ARLINGTON.
Dielectric millimeter waveguides: A feasibility study for a novel dielectric millimeter waveguide
[AD-A195104] N88-30042

TEXAS UNIV., AUSTIN.
Confirmation of slow-waves in a crosstie overlay coplanar waveguide and its application to band-reject gratings and reflectors
[AD-A194981] N88-30011
The ultrashort period dwarf nova SW Ursae Majoris N88-30553

TICRA A/S, COPENHAGEN (DENMARK).
Development of a general software package for the analysis and synthesis of planar antenna arrays for space applications
[S-247-02] N88-30000

U

UNITED KINGDOM ATOMIC ENERGY AUTHORITY, ABINGDON (ENGLAND).
The use of upwind schemes at high Reynolds number: A cautionary note
[AD-A196227] N88-30074

UNITED KINGDOM ATOMIC ENERGY AUTHORITY, HARWELL (ENGLAND).
The effects of total dose on the SEU sensitivity of CMOS static RAMS
[AERE-R-12779] N88-30401
The Single Event Upset (SEU) test facility on the Hardwell tandem generator for cosmic ray simulation
[AERE-R-12896] N88-30580

UNITED TECHNOLOGIES CORP., EAST HARTFORD, CONN.
The effects of inlet turbulence and rotor/stator interactions on the aerodynamics and heat transfer of a large-scale rotating turbine model. Volume 2: Heat transfer data tabulation. 15 percent axial spacing
[NASA-CR-179467] N88-29804

UNITED TECHNOLOGIES CORP., SOUTH WINDSOR, CONN.
Regenerative fuel cell energy storage system for a low earth orbit space station
[NASA-CR-174802] N88-30184

UNITED TECHNOLOGIES RESEARCH CENTER, EAST HARTFORD, CONN.
A study of the critical factors controlling the synthesis of ceramic matrix composites from preceramic polymers
[AD-A195405] N88-29881
Nozzle airflow influences on fuel patternation N88-29916
User's manual for three dimensional boundary layer (BL3-D) code
[NASA-CR-174899] N88-30063
Assessment of a 3-D boundary layer analysis to predict heat transfer and flow field in a turbine passage
[NASA-CR-174894] N88-30066

UNIVERSIDAD AUTONOMA DE MADRID, CANTOBLANCO (SPAIN).
Study of secondary emission properties of materials used for high power RF components in space
[ESA-CR(P)-2587] N88-30012

UNIVERSITIES SPACE RESEARCH ASSOCIATION, HUNTSVILLE, ALA.
An improvement in the numerical integration procedure used in the NASA Marshall engineering thermosphere model
[NASA-CR-179389] N88-30200

UNIVERSITY COLL. OF NORTH WALES, BANGOR.
Polymer-ceramic composites
[AD-A195789] N88-29983

UTAH UNIV., SALT LAKE CITY.
A test for interfacial effects and stress transfer in ceramic matrix composites
[NASA-CR-182873] N88-29880
Attenuated total reflectance FT-IR spectroscopy to measure interfacial reaction kinetics at silica surfaces
[AD-A196330] N88-29908

V

VANDERBILT UNIV., NASHVILLE, TENN.
Vanderbilt free electron laser project in biomedical and materials research
[AD-A195961] N88-30121

VIRGINIA POLYTECHNIC INST. AND STATE UNIV., BLACKSBURG.
Analytical study of graphite-epoxy tube response to thermal loads
[NASA-CR-183215] N88-29884
Human factors report on information management requirements for next-generation manned bombers
[AD-A195870] N88-30296

VON KARMAN INST. FOR FLUID DYNAMICS, RHODE-SAINT-GENESE (BELGIUM).
Analysis of a feed device for the pneumatic transport of noncohesive particles
[VKI-TM-44] N88-30062
Laser Doppler Velocimeter (LDV) and pressure measurements of gas particle flows in bends
[VKI-TN-163] N88-30083

W

WASHINGTON UNIV., SEATTLE.
Evidence for crustal recycling during the Archean: The parental magmas of the stillwater complex N88-30226
Passive microwave measurements of water vapor fields and rain for locating fronts in cyclonic storms
[AD-A195632] N88-30267

A model for architectural comparison
[AD-A195993] N88-30302
The triangle: A multiprocessor architecture for fast curve and surface generation
[AD-A195882] N88-30324
WAYNE STATE UNIV., DETROIT, MICH.
Range data description based on multiple characteristics N88-30351
WESTINGHOUSE ELECTRIC CORP., SEABROOK, MD.
MOORE: A prototype expert system for diagnosing spacecraft problems N88-30343
WISCONSIN UNIV., MADISON.
Initial value problems in viscoelasticity
[AD-A196052] N88-30145
Validate algorithms for the determination of rainfall rates from SSM/I microwave satellite imagery
[AD-A195426] N88-30270
On the Nash point equilibria in the calculus of variations
[AD-A194959] N88-30381
Multiple solutions and bifurcation for a class of nonlinear Sturm-Liouville eigenvalue problems on an unbounded domain
[AD-A195954] N88-30389
WORLD METEOROLOGICAL ORGANIZATION, GENEVA (SWITZERLAND).
Activities report of the World Meteorological Organization
[WMO-689] N88-30265

Typical Contract Number Index Listing

Listings in this index are arranged alphanumerically by contract number. Under each contract number the NASA accession numbers denoting documents that have been produced as a result of research done under that contract are arranged in ascending order. The NASA accession number denotes the number by which the citation is identified.

AF AFOSR-0032-88 ..... N88-30385
AF PROJ. 2311 ..... N88-30575
AF PROJ. 3005 ..... N88-29962
AF PROJ. 6670 ..... N88-30269
AF PROJ. 7659 ..... N88-29843
AF-AFOSR-0007-87 ..... N88-30057
AF-AFOSR-0025-87 ..... N88-30198
AF-AFOSR-0032-88 ..... N88-30385
AF-AFOSR-0040-87 ..... N88-30016
AF-AFOSR-0041-87 ..... N88-30390
AF-AFOSR-0049-83 ..... N88-30069
AF-AFOSR-0049-84 ..... N88-30195
AF-AFOSR-0053-87 ..... N88-29890
AF-AFOSR-0063-84 ..... N88-30138
AF-AFOSR-0082-86 ..... N88-29794
AF-AFOSR-0093-86 ..... N88-30376
AF-AFOSR-0093-87 ..... N88-30433
AF-AFOSR-0099-87 ..... N88-30124
AF-AFOSR-0101-87 ..... N88-30363
AF-AFOSR-0111-86 ..... N88-30438
AF-AFOSR-0116-84 ..... N88-30426
AF-AFOSR-0128-86 ..... N88-30290
AF-AFOSR-0143-85 ..... N88-30378
AF-AFOSR-0155-82 ..... N88-29777
AF-AFOSR-0158-87 ..... N88-30142
AF-AFOSR-0162-84 ..... N88-30155
AF-AFOSR-0164-86 ..... N88-30429
AF-AFOSR-0169-87 ..... N88-29861
AF-AFOSR-0189-86 ..... N88-30406
AF-AFOSR-0191-87 ..... N88-30145
AF-AFOSR-0202-87 ..... N88-30389
AF-AFOSR-0233-85 ..... N88-30283
AF-AFOSR-0233-86 ..... N88-29959
AF-AFOSR-0248-85 ..... N88-30092
AF-AFOSR-0294-86 ..... N88-30416
AF-AFOSR-0306-84 ..... N88-29901
AF-AFOSR-0307-85 ..... N88-30145
AF-AFOSR-0318-83 ..... N88-29851
AF-AFOSR-0318-86 ..... N88-30137
AF-AFOSR-0320-86 ..... N88-30283
AF-AFOSR-0323-85 ..... N88-30417
AF-AFOSR-0332-85 ..... N88-29999
AF-AFOSR-0392-87 ..... N88-30432
ARPA ORDER 4511 ..... N88-30191
ARPA ORDER 4952 ..... N88-30004
ARPA ORDER 5916 ..... N88-29822
DA PROJ. 1L1-61102-AH-43 ..... N88-30086
DA PROJ. 1L1-62209-A-47-A N88-30128
DA PROJ. 1L1-62209-AH-76 ..... N88-29825
DA PROJ. 1L1-62618-AH-80 ..... N88-29772
DA PROJ. 1L1-62716-A-700 ..... N88-29797
DA PROJ. 3E1-62777-A-878 ..... N88-30287
DA PROJ. 3M1-61102-BS-10 ..... N88-30008
DAAA15-86-C-0053 ..... N88-29812
DAAA15-88-C-0005 ..... N88-29797
DAAG29-84-C-0021 ..... N88-30409
DAAG29-84-K-0140 ..... N88-30313
DAAG29-85-K-0051 ..... N88-30044
DAAG29-85-K-0060 ..... N88-30400
DAAH01-87-C-1049 ..... N88-29822
DAAK70-87-C-0027 ..... N88-30140
DAAL03-86-C-0014 ..... N88-30388
DAAL03-86-K-0093 ..... N88-30021
DAAL03-86-K-0173 ..... N88-30411
DAAL03-87-K-0036 ..... N88-30145
DAAL03-87-K-0043 ..... N88-30381
N88-30389
DAAL03-88-K-0005 ..... N88-30011
DACA76-85-C-0010 ..... N88-30364
DAJA45-84-C-0043 ..... N88-30548
DAJA45-86-C-0005 ..... N88-30430
DAJA45-86-C-0034 ..... N88-29983
DAMD17-81-C-1065 ..... N88-30287
DARPA ORDER 6153 ..... N88-29881
DE-AC04-76-DP-00613 ..... N88-29980
DE-AC04-76DP-00789 ..... N88-30051
DE-AC05-84OR-21400 ..... N88-30149
N88-30306
DLA900-84-C-0910 ..... N88-29885
DLA900-85-C-4100 ..... N88-29882
DNA001-86-C-0174 ..... N88-30421
DRET-85/130 ..... N88-29945
DTRS57-85-C-00083 ..... N88-30449
N88-30452
N88-30454
N88-30455
N88-30457
N88-30468
ESA-3991-00786-FR N88-30022
ESA-5047/82-NL-HP N88-30323
ESA-5286/82-NL N88-29855
ESA-5615/83-NL-PP N88-30136
ESA-6029/84-NL-PP(SC) N88-30365
ESA-6272/85-NL-AB N88-29849
ESA-6324/85-NL-PB(SC) N88-30552
ESA-6451/85 ..... N88-30325
ESA-6521/85 ..... N88-29992
N88-29994
ESA-6569/86-NL-PP(SC) N88-29827
ESA-6787/86-NL-IW(SC) N88-30183
ESA-6822/86-F-HEW(SC) N88-29806
ESA-6823/86-HEW(SC) N88-29802
ESA-6827/86-NL-PH(SC) N88-29986
ESA-6829/86-NL-PH(SC) N88-29862
ESA-6837/86-NL-PP(SC) N88-29839
ESA-6885/86 ..... N88-29841
ESA-6917/86-NL-JG(SC) N88-30102
ESA-7190/87 ..... N88-29840
ESRIN-6297/86-HGE-I(SC) N88-30167
N88-30176
ESTEC-5313/83-NL-HP N88-30401
ESTEC-5508/83-NL-PB(SC) N88-30182
ESTEC-5635/86-NL-MA N88-30580
ESTEC-5709/83-NL-GH N88-30002
ESTEC-5966/84-NL-PR(SC) N88-30118
ESTEC-6262/85-NL-PH N88-29852
ESTEC-6377/85-NL-PR(SC) N88-29857
ESTEC-6567/85-NL-IW(SC) N88-30000
ESTEC-6577/85-NL-PB N88-30012
ESTEC-6596/86-NL-MA(SC) N88-29847
ESTEC-6828/86-NL-PH(SC) N88-29866
ESTEC-6892/86-NL-MA(SC) N88-30139
ESTEC-6950/86-NL-IW(SC) N88-30328
ESTEC-7016/87-NL-PP(SC) N88-30293
N88-30298
ESTEC-7025/87-NL-IW(SC) N88-30446
N88-30448
ESTEC-7153/87-NL-DG N88-29844
ESTEC-7211/87-NL-DG N88-30013
FC-85-563 ..... N88-29907
FINEP-537/CT N88-30185
N88-30186
FMV-FFL-82250-85-076-73-001 ..... N88-30157
F3615-84-C-0066 ..... N88-30291
F04611-87-C-0049 ..... N88-29954
F04701-85-C-0086 ..... N88-29891
N88-29953
N88-30050
N88-30120
F08606-86-C-0006 ..... N88-30191
F08606-86-C-0014 ..... N88-30257
F08635-86-C-0309 ..... N88-29926
F19628-81-C-0029 ..... N88-29843
F19628-83-C-0092 ..... N88-30256
F19628-83-K-0005 ..... N88-30017
F19628-84-C-0005 ..... N88-30269
F19628-85-C-0002 ..... N88-30005
N88-30020
F19628-85-C-0183 ..... N88-29894
F19628-86-C-0054 ..... N88-30259
F19628-86-C-0077 ..... N88-30196
F19628-87-C-0003 ..... N88-30018
F30602-81-C-0169 ..... N88-30009
F30602-81-C-0206 ..... N88-30042
F30602-85-C-0093 ..... N88-30150
F33615-83-C-3225 ..... N88-30143
F33615-84-C-2435 ..... N88-30052
F33615-84-C-2457 ..... N88-29810
F33615-84-C-2478 ..... N88-29896
F33615-84-C-3216 ..... N88-29792
F33615-84-C-5130 ..... N88-29889
F33615-84-K-3009 ..... N88-30064
F33615-85-C-2515 ..... N88-29916
F33615-85-C-3418 ..... N88-29993
F33615-85-C-3602 ..... N88-30300
F33615-85-D-0514 ..... N88-30296
F33615-86-C-3217 ..... N88-29962
F33615-87-C-1499 ..... N88-30380
F33615-87-C-5291 ..... N88-30435
F49620-85-C-0049 ..... N88-29805
F49620-85-C-0125 ..... N88-30443
F49620-85-K-0001 ..... N88-30370
F49620-86-C-0008 ..... N88-29795
N88-29796
F49620-86-C-0027 ..... N88-30271
F49620-86-C-0030 ..... N88-30004
F49620-86-C-0069 ..... N88-29870
F49620-86-K-0007 ..... N88-30428
F49620-87-C-0041 ..... N88-30439
F49620-87-C-0070 ..... N88-30103
F49620-87-C-0093 ..... N88-29881
MDA903-85-K-0072 ..... N88-30302
MDA972-87-C-0005 ..... N88-30469
MIPR-85-MM-5507 ..... N88-30008
NAGW-398 ..... N88-30543
NAGW-419 ..... N88-30312
NAGW-552 ..... N88-30571
NAGW-821 ..... N88-30542
NAGW-976 ..... N88-30427
N88-30431
N88-30437
N88-30440
NAGW-1090 ..... N88-30581
NAG1-58 ..... N88-30151
NAG1-343 ..... N88-29884
NAG1-694 ..... N88-30113
NAG2-248 ..... N88-30312
NAG2-345 ..... N88-29775
NAG2-444 ..... N88-29880
NAG2-499 ..... N88-30274
N88-30275
N88-30276
NAG3-61 ..... N88-30084
NAG3-379 ..... N88-30164
NAG3-501 ..... N88-30106
NAG3-511 ..... N88-29961
NAG3-816 ..... N88-30055
NAG5-949 ..... N88-30134
NAG8-488 ..... N88-29848
NAG8-697 ..... N88-30547
N88-30550
N88-30555
N88-30558
N88-30579
NAG9-108 ..... N88-30542
NASW-3458 ..... N88-30148
NASW-3966 ..... N88-30572
NASW-4066 ..... N88-30201
N88-30258
N88-30473
N88-30487
N88-30536
NASW-4234 ..... N88-30309
NASW-4307 ..... N88-29753
N88-29782
N88-29899
N88-29906

	N88-29909
	N88-30087
	N88-30088
	N88-30266
	N88-30444
NAS1-17067	N88-30304
NAS1-18000	N88-30329
	N88-30399
NAS1-18107	N88-29715
	N88-29716
	N88-29743
	N88-29749
	N88-30058
	N88-30079
	N88-30386
NAS1-18276	N88-29744
	N88-29745
	N88-29770
NAS1-18322	N88-29995
NAS1-18605	N88-29716
	N88-29743
	N88-30079
NAS2-11555	N88-30071
	N88-30308
	N88-30327
	N88-30384
NAS2-11665	N88-29819
NAS2-11853	N88-29815
NAS2-11927	N88-30100
NAS2-12404	N88-29790
NAS2-12419	N88-29817
NAS2-12558	N88-29816
NAS3-22234	N88-30184
NAS3-23716	N88-30063
	N88-30066
NAS3-23717	N88-29804
NAS3-23772	N88-29858
NAS3-23925	N88-29811
NAS3-24340	N88-30076
NAS3-24663	N88-29863
	N88-29872
NAS3-24738	N88-29876
NAS3-24900	N88-29835
NAS3-25052	N88-29867
NAS3-25069	N88-29825
NAS5-31500	N88-30344
NAS7-918	N88-30001
	N88-30357
NAS8-36419	N88-30181
NAS8-36639	N88-30200
NAS9-17560	N88-29846
	N88-30369
NAS9-17878	N88-29836
	N88-29837
	N88-29854
NBS-60-NAN-135D-0576	N88-29927
NCC1-99	N88-30320
NCC2-77	N88-29821
NCC2-241	N88-30297
NCC2-387	N88-30321
NCC2-478	N88-29893
NGL-05-020-272	N88-30260
NGL-39-009-003	N88-30070
NGR-05-002-160	N88-30566
NGT-36-002-800	N88-29952
NIVR-1987	N88-30323
NSF AST-82-05956-A02	N88-30562
NSF AST-86-04324	N88-30562
NSF ATM-85-12513	N88-30271
NSF DMR-84-12465	N88-30440
NSF DMS-84-20623	N88-30470
NSF DMS-86-20303	N88-30145
NSF DMS-87-12058	N88-30145
NSF DMS-87-96241	N88-30145
NSF DMS-10324-84	N88-30387
NSF DMS-16191-85	N88-30387
NSF ECS-84-07285	N88-30383
NSF ECS-87-00903	N88-30385
NSF MSM-86-15187	N88-30348
N000-14-86-K-0265	N88-29897
	N88-29907
	N88-29955
N00014-80-C-0507	N88-30425
N00014-80-C-0622	N88-30010
	N88-30014
	N88-30046
N00014-81-C-0195	N88-30035
N00014-81-C-0569	N88-30289
N00014-81-K-0742	N88-30383
N00014-82-K-0335	N88-30305
N00014-82-K-0339	N88-30096
	N88-30104
	N88-30112
N00014-82-K-0348	N88-30082
N00014-83-C-0170	N88-29905
N00014-83-K-0468	N88-29958
N00014-84-C-0018	N88-30391
N00014-85-C-0840	N88-29747
N00014-85-C-2530	N88-30442
N00014-85-K-0-0124	N88-30326
N00014-85-K-0113	N88-30392
N00014-85-K-0124	N88-30010
	N88-30014
	N88-30132
	N88-30311
	N88-30364
	N88-30386
	N88-30371
	N88-30374
	N88-30375
	N88-30379
	N88-30395
	N88-30397
N00014-85-K-0169	N88-30387
N00014-85-K-0329	N88-30318
N00014-85-K-0343	N88-30470
N00014-85-K-0474	N88-30056
N00014-85-K-0494	N88-30397
N00014-85-K-0667	N88-29878
N00014-85-K-0712	N88-29908
N00014-85-K-0782	N88-30318
N00014-85-K-0809	N88-30041
N00014-85-K-0825	N88-30045
N00014-86-C-2342	N88-30115
N00014-86-F-0049	N88-30574
	N88-30576
N00014-86-K-0180	N88-30311
	N88-30319
	N88-30379
	N88-30568
N00014-86-K-0191	N88-30414
N00014-86-K-0232	N88-30299
N00014-86-K-0264	N88-30324
N00014-86-K-0453	N88-30267
N00014-86-K-0680	N88-30451
N00014-86-K-0685	N88-30371
N00014-86-K-0711	N88-30126
N00014-86-K-2001	N88-30270
N00014-87-C-0146	N88-30121
N00014-87-C-0418	N88-30035
N00014-87-C-0665	N88-30061
N00014-87-K-0162	N88-29981
N00014-87-K-0257	N88-29904
N00014-87-K-0396	N88-30114
N00014-87-K-0432	N88-30295
N00014-87-K-0825	N88-30046
	N88-30429
N00014-88-K-0055	N88-30277
N00014-88-K-0134	N88-30389
N00600-84-D-4171	N88-29801
PROJ. RR0-4108	N88-30277
PROJ. RR0-4204	N88-30289
	N88-30392
RR0-4108	N88-29981
RR0-4209	N88-30295
R35-82	N88-30267
SWRI PROJ. 06-7576	N88-29811
TO-87-57	N88-29836
W-31-109-ENG-38	N88-29987
	N88-30051
W-7405-ENG-48	N88-29898
199-22-76-01	N88-30402
307-50-06-03	N88-29776
324-02-00	N88-29874
480-51-13-01	N88-29856
481-50-12	N88-29863
	N88-29872
505-60	N88-30071
505-60-4X	N88-30093
505-60-21-04	N88-29820
505-60-31	N88-29774
505-61-71-02	N88-29752
505-62-0K	N88-29825
505-62-21	N88-29780
	N88-29997
	N88-30084
	N88-30090
	N88-30094
	N88-30377
505-63-1B	N88-29807
505-63-21-01	N88-29754
	N88-29778
505-63-51	N88-30128
505-63-51-07	N88-30399
505-63-91-02	N88-30329
505-66-11	N88-29817
	N88-30073
505-66-51	N88-29816
505-67-01	N88-30304
505-90-21-01	N88-29715
	N88-29716
	N88-29743
	N88-29749
	N88-30058
	N88-30079
	N88-30386
506-40-11-08	N88-29744
	N88-29745
	N88-29770
506-41-21	N88-29952
506-42-21	N88-29858
506-42-31	N88-29860
	N88-29868
506-42-32	N88-29869
506-42-37	N88-29859
506-43-11-04	N88-29879
506-44-21	N88-30048
	N88-30055
506-45-31	N88-30100
506-47-31	N88-30327
506-48-91	N88-29873
506-49-31	N88-29845
506-49-31-02	N88-29850
532-06-11	N88-29790
533-04-1A	N88-29811
533-04-11	N88-29804
533-04-12	N88-30063
	N88-30066
535-03-01	N88-29771
553-04-12	N88-30164
582-01-11	N88-30078
	N88-30099
585-01-21-06	N88-29995
586-01-11	N88-29833
694-03-03	N88-30072
778-35-13	N88-30472
992-15-00-00-72	N88-30583
992-21-01	N88-29819

Typical Report Number Index Listing

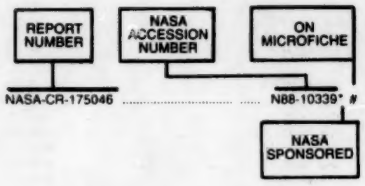

Listings in this index are arranged alphanumerically by report number. The NASA accession number denotes the number by which the citation is identified. An asterisk (*) indicates that the item is a NASA report. A pound sign (#) indicates that the item is available on microfiche.

A-86185 ..... N88-30301* #
A-86295 ..... N88-29774* #
A-87289 ..... N88-29773* #
A-88106 ..... N88-29750* #
A-88254 ..... N88-30085* #
A-88259 ..... N88-29751* #
A-88274 ..... N88-30314* #
A-88288 ..... N88-30373* #

AAMRL-TR-87-042 ..... N88-30296 #

ACSC-88-0510 ..... N88-30396 #
ACSC-88-0725 ..... N88-29842 #
ACSC-88-1015 ..... N88-29799 #
ACSC-88-1175 ..... N88-29826 #
ACSC-88-1735 ..... N88-29786 #
ACSC-88-2405 ..... N88-29791 #
ACSC-88-2805 ..... N88-29834 #
ACSC-88-2830 ..... N88-29798 #

AD-A185270 ..... N88-29772 #
AD-A187379 ..... N88-29779 #
AD-A188973 ..... N88-29966 #
AD-A189864 ..... N88-29815* #
AD-A193692 ..... N88-30299 #
AD-A194171 ..... N88-30409 #
AD-A194272 ..... N88-30388 #
AD-A194302 ..... N88-30289 #
AD-A194317 ..... N88-30077 #
AD-A194340 ..... N88-30322 #
AD-A194397 ..... N88-29786 #
AD-A194416 ..... N88-30097 #
AD-A194567 ..... N88-30014 #
AD-A194682 ..... N88-30019 #
AD-A194683 ..... N88-30003 #
AD-A194785 ..... N88-30082 #
AD-A194786 ..... N88-30363 #
AD-A194803 ..... N88-29999 #
AD-A194804 ..... N88-30049 #
AD-A194806 ..... N88-29800 #
AD-A194807 ..... N88-30307 #
AD-A194809 ..... N88-30391 #
AD-A194824 ..... N88-30450 #
AD-A194827 ..... N88-30471 #
AD-A194835 ..... N88-30286 #
AD-A194837 ..... N88-30041 #
AD-A194838 ..... N88-30425 #
AD-A194842 ..... N88-29822 #
AD-A194857 ..... N88-30020 #
AD-A194861 ..... N88-30413 #
AD-A194862 ..... N88-30404 #
AD-A194871 ..... N88-30158 #
AD-A194872 ..... N88-30362 #
AD-A194874 ..... N88-29814 #
AD-A194875 ..... N88-30163 #
AD-A194876 ..... N88-29769 #
AD-A194877 ..... N88-29829 #
AD-A194880 ..... N88-29883 #
AD-A194888 ..... N88-30053 #
AD-A194906 ..... N88-29799 #
AD-A194908 ..... N88-29834 #
AD-A194910 ..... N88-29796 #
AD-A194912 ..... N88-29642 #
AD-A194918 ..... N88-29785 #
AD-A194931 ..... N88-29861 #
AD-A194941 ..... N88-29901 #
AD-A194944 ..... N88-29895 #
AD-A194945 ..... N88-30283 #
AD-A194947 ..... N88-30284 #
AD-A194949 ..... N88-30112 #
AD-A194956 ..... N88-30104 #
AD-A194957 ..... N88-30096 #
AD-A194959 ..... N88-30381 #
AD-A194961 ..... N88-30259 #
AD-A194967 ..... N88-30278 #
AD-A194969 ..... N88-30103 #
AD-A194979 ..... N88-30052 #
AD-A194981 ..... N88-30011 #
AD-A194990 ..... N88-30191 #
AD-A194992 ..... N88-30429 #
AD-A194993 ..... N88-30387 #
AD-A194994 ..... N88-30264 #
AD-A195011 ..... N88-29896 #
AD-A195014 ..... N88-30396 #
AD-A195061 ..... N88-30150 #
AD-A195062 ..... N88-29797 #
AD-A195066 ..... N88-30046 #
AD-A195067 ..... N88-29998 #
AD-A195072 ..... N88-30006 #
AD-A195073 ..... N88-29891 #
AD-A195079 ..... N88-30394 #
AD-A195081 ..... N88-29956 #
AD-A195082 ..... N88-29902 #
AD-A195085 ..... N88-30144 #
AD-A195086 ..... N88-30034 #
AD-A195090 ..... N88-30018 #
AD-A195093 ..... N88-30451 #
AD-A195096 ..... N88-29796 #
AD-A195104 ..... N88-30042 #
AD-A195118 ..... N88-29965 #
AD-A195119 ..... N88-30004 #
AD-A195121 ..... N88-30092 #
AD-A195144 ..... N88-30064 #
AD-A195152 ..... N88-30045 #
AD-A195154 ..... N88-30370 #
AD-A195155 ..... N88-30095 #
AD-A195159 ..... N88-30411 #
AD-A195161 ..... N88-30056 #
AD-A195163 ..... N88-30193 #
AD-A195165 ..... N88-29805 #
AD-A195176 ..... N88-29985 #
AD-A195179 ..... N88-29853 #
AD-A195182 ..... N88-30443 #
AD-A195194 ..... N88-30367 #
AD-A195200 ..... N88-29791 #
AD-A195201 ..... N88-29826 #
AD-A195223 ..... N88-29993 #
AD-A195224 ..... N88-29878 #
AD-A195226 ..... N88-30137 #
AD-A195242 ..... N88-30436 #
AD-A195248 ..... N88-30126 #
AD-A195249 ..... N88-30424 #
AD-A195267 ..... N88-30442 #
AD-A195282 ..... N88-29784 #
AD-A195285 ..... N88-30400 #
AD-A195311 ..... N88-30392 #
AD-A195313 ..... N88-30161 #
AD-A195331 ..... N88-30288 #
AD-A195335 ..... N88-30017 #
AD-A195372 ..... N88-29801 #
AD-A195399 ..... N88-30044 #
AD-A195405 ..... N88-29881 #
AD-A195406 ..... N88-29818 #
AD-A195408 ..... N88-30111 #
AD-A195428 ..... N88-30270 #
AD-A195440 ..... N88-30069 #
AD-A195450 ..... N88-29905 #
AD-A195464 ..... N88-30438 #
AD-A195466 ..... N88-29954 #
AD-A195467 ..... N88-29792 #
AD-A195468 ..... N88-30257 #
AD-A195476 ..... N88-30393 #
AD-A195477 ..... N88-30416 #
AD-A195482 ..... N88-30277 #
AD-A195496 ..... N88-30290 #
AD-A195497 ..... N88-30376 #
AD-A195500 ..... N88-29851 #
AD-A195539 ..... N88-30198 #
AD-A195542 ..... N88-30010 #
AD-A195543 ..... N88-30271 #
AD-A195559 ..... N88-29747 #
AD-A195560 ..... N88-30035 #
AD-A195561 ..... N88-30383 #
AD-A195586 ..... N88-29864 #
AD-A195587 ..... N88-30303 #
AD-A195590 ..... N88-30295 #
AD-A195594 ..... N88-30140 #
AD-A195597 ..... N88-29959 #
AD-A195604 ..... N88-30142 #
AD-A195606 ..... N88-30426 #
AD-A195611 ..... N88-30417 #
AD-A195628 ..... N88-30279 #
AD-A195632 ..... N88-30267 #
AD-A195639 ..... N88-30378 #
AD-A195645 ..... N88-30385 #
AD-A195647 ..... N88-30432 #
AD-A195667 ..... N88-30159 #
AD-A195681 ..... N88-30421 #
AD-A195683 ..... N88-30016 #
AD-A195685 ..... N88-29794 #
AD-A195687 ..... N88-30008 #
AD-A195690 ..... N88-30406 #
AD-A195693 ..... N88-29890 #
AD-A195694 ..... N88-30433 #
AD-A195697 ..... N88-30280 #
AD-A195699 ..... N88-29810 #
AD-A195701 ..... N88-29981 #
AD-A195712 ..... N88-30021 #
AD-A195716 ..... N88-30138 #
AD-A195717 ..... N88-30143 #
AD-A195723 ..... N88-30175 #
AD-A195730 ..... N88-30397 #
AD-A195731 ..... N88-30439 #
AD-A195735 ..... N88-30287 #
AD-A195759 ..... N88-29830 #
AD-A195760 ..... N88-30272 #
AD-A195787 ..... N88-30300 #
AD-A195789 ..... N88-29963 #
AD-A195795 ..... N88-29885 #
AD-A195805 ..... N88-30291 #
AD-A195818 ..... N88-30380 #
AD-A195821 ..... N88-30054 #
AD-A195838 ..... N88-30372 #
AD-A195839 ..... N88-30410 #
AD-A195841 ..... N88-30197 #
AD-A195845 ..... N88-30123 #
AD-A195846 ..... N88-30033 #
AD-A195847 ..... N88-30005 #
AD-A195848 ..... N88-30256 #
AD-A195850 ..... N88-30449 #
AD-A195851 ..... N88-30455 #
AD-A195854 ..... N88-30452 #
AD-A195855 ..... N88-30457 #
AD-A195856 ..... N88-30468 #
AD-A195857 ..... N88-30454 #
AD-A195870 ..... N88-30296 #
AD-A195877 ..... N88-29787 #
AD-A195882 ..... N88-30324 #
AD-A195885 ..... N88-30155 #
AD-A195886 ..... N88-30124 #
AD-A195887 ..... N88-30390 #
AD-A195889 ..... N88-30414 #
AD-A195890 ..... N88-30059 #
AD-A195897 ..... N88-30318 #
AD-A195898 ..... N88-30428 #
AD-A195909 ..... N88-29958 #
AD-A195918 ..... N88-30199 #
AD-A195919 ..... N88-30262 #
AD-A195920 ..... N88-30568 #
AD-A195921 ..... N88-30311 #
AD-A195922 ..... N88-30375 #
AD-A195923 ..... N88-30132 #
AD-A195926 ..... N88-30374 #
AD-A195928 ..... N88-30326 #
AD-A195929 ..... N88-30371 #
AD-A195931 ..... N88-30319 #
AD-A195932 ..... N88-30366 #

REPORT

AD-A195934 ..... N88-29900 #
AD-A195937 ..... N88-30415 #
AD-A195951 ..... N88-30408 #
AD-A195952 ..... N88-30158 #
AD-A195954 ..... N88-30380 #
AD-A195961 ..... N88-30121 #
AD-A195962 ..... N88-30285 #
AD-A195970 ..... N88-30057 #
AD-A195971 ..... N88-29870 #
AD-A195972 ..... N88-30195 #
AD-A195974 ..... N88-30120 #
AD-A195975 ..... N88-29991 #
AD-A195976 ..... N88-30166 #
AD-A195977 ..... N88-30317 #
AD-A195978 ..... N88-30116 #
AD-A195982 ..... N88-30313 #
AD-A195991 ..... N88-30115 #
AD-A195993 ..... N88-30302 #
AD-A195994 ..... N88-30162 #
AD-A195995 ..... N88-29963 #
AD-A195997 ..... N88-30061 #
AD-A195999 ..... N88-29882 #
AD-A196001 ..... N88-30073 #
AD-A196014 ..... N88-30368 #
AD-A196018 ..... N88-30117 #
AD-A196023 ..... N88-30261 #
AD-A196024 ..... N88-30469 #
AD-A196025 ..... N88-30043 #
AD-A196026 ..... N88-30294 #
AD-A196028 ..... N88-30435 #
AD-A196030 ..... N88-30050 #
AD-A196034 ..... N88-30470 #
AD-A196052 ..... N88-30145 #
AD-A196059 ..... N88-29989 #
AD-A196061 ..... N88-29812 #
AD-A196071 ..... N88-30305 #
AD-A196079 ..... N88-30430 #
AD-A196089 ..... N88-29904 #
AD-A196103 ..... N88-30114 #
AD-A196111 ..... N88-29748 #
AD-A196124 ..... N88-30194 #
AD-A196129 ..... N88-29788 #
AD-A196153 ..... N88-30086 #
AD-A196154 ..... N88-29996 #
AD-A196167 ..... N88-30110 #
AD-A196168 ..... N88-29987 #
AD-A196170 ..... N88-30122 #
AD-A196173 ..... N88-30548 #
AD-A196185 ..... N88-29889 #
AD-A196187 ..... N88-29793 #
AD-A196188 ..... N88-29823 #
AD-A196190 ..... N88-30080 #
AD-A196191 ..... N88-30282 #
AD-A196202 ..... N88-30423 #
AD-A196224 ..... N88-30364 #
AD-A196225 ..... N88-29990 #
AD-A196227 ..... N88-30074 #
AD-A196228 ..... N88-30190 #
AD-A196231 ..... N88-29953 #
AD-A196232 ..... N88-30007 #
AD-A196239 ..... N88-30036 #
AD-A196240 ..... N88-30119 #
AD-A196247 ..... N88-29777 #
AD-A196263 ..... N88-29887 #
AD-A196264 ..... N88-30398 #
AD-A196265 ..... N88-30107 #
AD-A196285 ..... N88-30147 #
AD-A196286 ..... N88-30009 #
AD-A196287 ..... N88-30038 #
AD-A196290 ..... N88-30456 #
AD-A196291 ..... N88-30292 #
AD-A196297 ..... N88-30065 #
AD-A196298 ..... N88-30268 #
AD-A196310 ..... N88-30379 #
AD-A196316 ..... N88-29894 #
AD-A196325 ..... N88-30196 #
AD-A196327 ..... N88-29982 #
AD-A196328 ..... N88-30395 #
AD-A196329 ..... N88-29960 #
AD-A196330 ..... N88-29908 #

AD-E500978 ..... N88-30449 #
AD-E500978 ..... N88-30452 #
AD-E500978 ..... N88-30454 #
AD-E500978 ..... N88-30455 #
AD-E500978 ..... N88-30457 #
AD-E500978 ..... N88-30468 #
AD-E801635 ..... N88-30003 #
AD-E801635 ..... N88-30019 #
AD-E951137 ..... N88-29987 #
AD-E951144 ..... N88-30122 #
AD-E951148 ..... N88-30110 #
AD-E951149 ..... N88-30038 #
AD-E951149 ..... N88-30065 #
AD-E951149 ..... N88-30268 #
AD-E951149 ..... N88-30292 #

AD-E951149 ..... N88-30456 #

AERE-R-12779 ..... N88-30401 #
AERE-R-12896 ..... N88-30580 #

AERONOMICA-ACTA-A-330-1988 ..... N88-30070* #
AERONOMICA-ACTA-A-331-1988 ..... N88-29907
AERONOMICA-ACTA-A-332-1988 ..... N88-29897
AERONOMICA-ACTA-A-333-1988 ..... N88-29955
AERONOMICA-ACTA-A-334-1988 ..... N88-30168

AES-8609709F-1 ..... N88-29962 #

AFAL-TR-88-002 ..... N88-30049 #
AFAL-TR-88-011 ..... N88-29954 #
AFAL-TR-88-042 ..... N88-29965 #

AFGL-ERP-980 ..... N88-30190 #
AFGL-ERP-987 ..... N88-30197 #

AFGL-TR-88-0168 ..... N88-30256 #
AFGL-TR-87-0203 ..... N88-30575 #
AFGL-TR-87-0219 ..... N88-30269 #
AFGL-TR-87-0225 ..... N88-30190 #
AFGL-TR-87-0241 ..... N88-29843 #
AFGL-TR-87-0306 ..... N88-30197 #
AFGL-TR-87-0322 ..... N88-30259 #
AFGL-TR-87-0332 ..... N88-30018 #
AFGL-TR-88-0108 ..... N88-29894 #
AFGL-TR-0280 ..... N88-30196 #

AFHRL-TR-87-53 ..... N88-30291 #

AFIT/CI/NR-88-1 ..... N88-30261 #
AFIT/CI/NR-88-6 ..... N88-29748 #
AFIT/CI/NR-88-23 ..... N88-30282 #
AFIT/CI/NR-88-44 ..... N88-30060 #
AFIT/CI/NR-88-46 ..... N88-29823 #
AFIT/CI/NR-88-86 ..... N88-30194 #
AFIT/CI/NR-88-87 ..... N88-30038 #
AFIT/CI/NR-88-89 ..... N88-30456 #
AFIT/CI/NR-88-101 ..... N88-30423 #
AFIT/CI/NR-88-126 ..... N88-30292 #
AFIT/CI/NR-88-140 ..... N88-30065 #

AFIT/DS/AA/88-1 ..... N88-30158 #

AFIT/DS/ENG/88J-1 ..... N88-30382 #

AFIT/GA/AA/88J-1 ..... N88-29829 #

AFIT/GAE/AA/87D-5 ..... N88-29883 #
AFIT/GAE/AA/87D-21 ..... N88-30163 #
AFIT/GAE/AA/88J-1 ..... N88-29814 #
AFIT/GAE/AA/88J-2 ..... N88-29789 #

AFOSR-88-0046TR ..... N88-29901 #
AFOSR-88-0410TR ..... N88-29999 #
AFOSR-88-0435TR ..... N88-30383 #
AFOSR-88-0449TR ..... N88-30103 #
AFOSR-88-0478TR ..... N88-30004 #
AFOSR-88-0496TR ..... N88-30271 #
AFOSR-88-0528TR ..... N88-30428 #
AFOSR-88-0529TR ..... N88-29881 #
AFOSR-88-0530TR ..... N88-30438 #
AFOSR-88-0531TR ..... N88-30416 #
AFOSR-88-0532TR ..... N88-29959 #
AFOSR-88-0541TR ..... N88-29861 #
AFOSR-88-0544TR ..... N88-30443 #
AFOSR-88-0545TR ..... N88-30137 #
AFOSR-88-0547TR ..... N88-30290 #
AFOSR-88-0549TR ..... N88-30198 #
AFOSR-88-0563TR ..... N88-30370 #
AFOSR-88-0569TR ..... N88-30439 #
AFOSR-88-0576TR ..... N88-30426 #
AFOSR-88-0588TR ..... N88-30376 #
AFOSR-88-0600TR ..... N88-29870 #
AFOSR-88-0612TR ..... N88-30417 #
AFOSR-88-0622TR ..... N88-30195 #
AFOSR-88-0630TR ..... N88-30365 #
AFOSR-88-0633TR ..... N88-30432 #
AFOSR-88-0636TR ..... N88-30378 #
AFOSR-88-0640TR ..... N88-30069 #
AFOSR-88-0652TR ..... N88-30057 #
AFOSR-88-0653TR ..... N88-30155 #
AFOSR-88-0654TR ..... N88-30124 #
AFOSR-88-0656TR ..... N88-29777 #
AFOSR-88-0657TR ..... N88-30390 #
AFOSR-88-0661TR ..... N88-30406 #
AFOSR-88-0666TR ..... N88-29851 #
AFOSR-88-0667TR ..... N88-30138 #
AFOSR-88-0669TR ..... N88-29890 #
AFOSR-88-0670TR ..... N88-29794 #
AFOSR-88-0675TR ..... N88-30016 #
AFOSR-88-0683TR ..... N88-30433 #

AFWAL-TR-87-2087 ..... N88-29810 #
AFWAL-TR-87-2088 ..... N88-30052 #
AFWAL-TR-87-2097 ..... N88-29896 #
AFWAL-TR-87-3055-VOL-3 ..... N88-30300 #
AFWAL-TR-87-3059 ..... N88-29962 #
AFWAL-TR-87-3102 ..... N88-29993 #
AFWAL-TR-87-3110 ..... N88-30064 #
AFWAL-TR-88-1050 ..... N88-30043 #
AFWAL-TR-88-3003 ..... N88-29800 #
AFWAL-TR-88-30u6 ..... N88-30143 #
AFWAL-TR-88-4043 ..... N88-30435 #
AFWAL-TR-88-4075 ..... N88-29889 #

AFWL-TR-87-21 ..... N88-29792 #
AFWL-TR-88-28 ..... N88-30006 #

AGARD-CP-422 ..... N88-29910 #
AGARD-CP-430 ..... N88-30458 #

AGARD-LS-157 ..... N88-29735 #

AGARD-R-734 ..... N88-29725 #
AGARD-R-734-ADD ..... N88-29717 #
AGARD-R-754 ..... N88-29755 #

AI-M-946 ..... N88-30326 #
AI-M-977 ..... N88-30371 #
AI-M-1013 ..... N88-30397 #
AI-M-1028 ..... N88-30374 #
AI-M-1037 ..... N88-30366 #
AI-M-1039 ..... N88-30568 #
AI-M-1040 ..... N88-30319 #
AI-M-1041 ..... N88-30375 #
AI-M-1046 ..... N88-30132 #
AI-M-1049 ..... N88-30311 #

AI-TR-1031 ..... N88-30379 #
AI-TR-1035 ..... N88-30395 #

AIAA-88-2110 ..... N88-30093* #
AIAA-88-3091 ..... N88-30094* #
AIAA-88-3152 ..... N88-29771* #
AIAA-88-3154 ..... N88-29807* #
AIAA-88-3211 ..... N88-29860* #
AIAA-89-0205 ..... N88-29780* #

AMSEL-NV-TR-0068 ..... N88-30415 #

AMSMI/CR-RD-PR-88-1 ..... N88-29987 #

AMSMI/TR-RD-AS-87-19 ..... N88-30122 #

AMSMI/TR-RD-RE-88-1 ..... N88-30268 #
AMSMI/TR-RD-RE-88-2 ..... N88-30110 #

ANSER-TR-5362-1 ..... N88-30196 #

ARAED-TR-88009 ..... N88-29989 #

ARCCB-TR-88018 ..... N88-29960 #
ARCCB-TR-88022 ..... N88-30147 #

ARI-RR-644.1 ..... N88-29894 #

ARL/AERO-PROP-TM-446 ..... N88-30107 #

ARL/AERO-TM-394 ..... N88-30193 #

ARL/MAT-R-120 ..... N88-30398 #

ARL/STRUC-R-432 ..... N88-29887 #

ARL/STRUC-TM-467 ..... N88-30097 #
ARL/STRUC-TM-481 ..... N88-30161 #

ARO-21436.9-EL-S ..... N88-30409 #
ARO-21453.12-MA ..... N88-30313 #
ARO-21758.12-CH ..... N88-30044 #
ARO-22416.8-PH ..... N88-30400 #
ARO-23026.1-EL ..... N88-30021 #
ARO-23344.7-MA-S ..... N88-30388 #
ARO-24626.33-PH ..... N88-30411 #
ARO-25045.1-EL ..... N88-30011 #

AS-S-121 ..... N88-30017 #

ASE-88-5 ..... N88-30378 #
ASE-5343 ..... N88-29954 #

AV-FR-88/807 ..... N88-29822 #

AVSCOM-TM-88-C-003 ..... N88-30126* #

AVSCOM-TP-88-C-001 ..... N88-30094* #

AVSCOM-TR-88-C-018 ..... N88-29825* #

A4-TR-88-0546 ..... N88-29805 #

BAE-CS/TP-8359 ..... N88-30102 #

BAE-TP-8502 ..... N88-30013 #

BDM/MCL-88-0182-TR ..... N88-30004 #

BDX-613-3807 ..... N88-29980 #

BF-R-66.090-1 ..... N88-30118 #

BN-1073 ..... N88-30387 #

BRA-87-320R ..... N88-30421 #
BRA-88-W032R ..... N88-30115 #

BRDEC-2461 ..... N88-29965 #
BRDEC-2466 ..... N88-29963 #
BRDEC-2469 ..... N88-29982 #

BRL-CR-595 ..... N88-29812 #

BRL-MR-3661 ..... N88-30059 #

BRL-TR-2833 ..... N88-29772 #
BRL-TR-2893 ..... N88-30086 #
BRL-TR-2894 ..... N88-29956 #
BRL-TR-2899 ..... N88-29895 #
BRL-TR-2906 ..... N88-29902 #
BRL-TR-2907 ..... N88-29990 #
BRL-TR-2915 ..... N88-30073 #
BRL-TR-2925 ..... N88-30159 #

B8803805 ..... N88-29808 #
B8803806 ..... N88-29838 #

CCMS-88-16 ..... N88-29884* #

CE-79 ..... N88-30141 #

CL/CP/SES/FR/004 ..... N88-30328 #

CLASSIC-88-22 ..... N88-30305 #

CLM-P-835 ..... N88-30074 #

CM-74 ..... N88-30192 #

CMI-RI-TR-88-2 ..... N88-30410 #
CMI-RI-TR-88-5 ..... N88-30372 #

CMS-TSR-88-16 ..... N88-30381 #
CMS-TSR-88-27 ..... N88-30145 #
CMS-TSR-88-30 ..... N88-30389 #

CMT-111 ..... N88-30005 #

CMU-RI-TR-88-1 ..... N88-30380 #

COL-TN-AS-0059-VOL-1 ..... N88-29849 #

CONF-880435-21 ..... N88-30051 #

CRC-559 ..... N88-29991 #

CRDEC-TR-88054 ..... N88-29900 #

CRIF-MT-172 ..... N88-30146 #

CSDL-R-2055 ..... N88-29790* #
CSDL-R-2056 ..... N88-29817* #

CSDL-T-1002 ..... N88-29846* #

CSI-R1027 ..... N88-30435 #

CSL-TR-87-344 ..... N88-30312* #

CSSA-ASTRO-88-13 ..... N88-30260* #

CU-ECE-88-06 ..... N88-30417 #

CU-153-1200 ..... N88-30114 #
CU-1536935 ..... N88-30406 #

DE87-014456 ..... N88-30189 #
DE88-012061 ..... N88-30051 #
DE88-012449 ..... N88-29898 #
DE88-701554 ..... N88-30563 #
DE88-702536 ..... N88-30089 #
DE88-702704 ..... N88-30081 #
DE88-702706 ..... N88-30445 #
DE88-702707 ..... N88-30441 #
DE88-702708 ..... N88-30434 #

DFVLR-FB-87-17 ..... N88-30187 #
DFVLR-FB-87-18 ..... N88-30075 #
DFVLR-FB-87-21 ..... N88-30067 #
DFVLR-FB-87-31 ..... N88-30080 #

DFVLR-IB-222-88-A-12 ..... N88-29862 #

DFVLR-MITT-88-25 ..... N88-29767 #

DIA-DST-2700Z-002-88 ..... N88-30116 #

DMS-DB-02-VOL-1-PT-1 ..... N88-29745* #
DMS-DB-02-VOL-1-PT-2 ..... N88-29770* #
DMS-DB-02-VOL-3-PT-2 ..... N88-29744* #

DNA-TR-87-280 ..... N88-30421 #

DODA-AR-004-549 ..... N88-30097 #
DODA-AR-004-584 ..... N88-30107 #
DODA-AR-004-585 ..... N88-30398 #
DODA-AR-004-590 ..... N88-30161 #
DODA-AR-004-593 ..... N88-30193 #
DODA-AR-004-597 ..... N88-29687 #

DOE/NASA/50112-75 ..... N88-30472* #

DOT/FAA/ACS-88-1(27) ..... N88-29784 #

DOT/FAA/CT-86/33 ..... N88-29815* #

DREA-TM-88/206 ..... N88-30162 #

DRIC-BR-105535-PT-2 ..... N88-30111 #

DTRC-87/045 ..... N88-29779 #

D2-RP-AI-106 ..... N88-30325 #

E-2776 ..... N88-30164* #
E-3056 ..... N88-30472* #
E-3963 ..... N88-30055* #
E-4146 ..... N88-29746* #
E-4181 ..... N88-30128* #
E-4200 ..... N88-30099* #
E-4229 ..... N88-29907* #
E-4233 ..... N88-29833* #
E-4262 ..... N88-30094* #
E-4274 ..... N88-29860* #
E-4295 ..... N88-30090* #
E-4304 ..... N88-29874* #
E-4309 ..... N88-30072* #
E-4330 ..... N88-29859* #
E-4337 ..... N88-29869* #
E-4338 ..... N88-30377* #
E-4339 ..... N88-30048* #
E-4342 ..... N88-30078* #
E-4345 ..... N88-29952* #
E-4349 ..... N88-30084* #
E-4356 ..... N88-29868* #
E-4363 ..... N88-29997* #
E-4373 ..... N88-29780* #
E-4378 ..... N88-29873* #
E-4387 ..... N88-29771* #
E-4414 ..... N88-29845* #

EEC-202 ..... N88-29788

EEC/NOTE-5/87 ..... N88-30015

EEI-87-171 ..... N88-29836* #
EEI-87-173 ..... N88-29837* #
EEI-88-181 ..... N88-29854* #

EFI-938(89)-86 ..... N88-30563 #

EFR-014-REV-B ..... N88-29797 #

ERIM-154600-34-T ..... N88-30035 #

ERNO-OX1-002/88-VOL-1 ..... N88-29827 #

ESA-CR(P)-2539 ..... N88-29806 #
ESA-CR(P)-2540 ..... N88-29802 #
ESA-CR(P)-2544 ..... N88-29855 #
ESA-CR(P)-2546 ..... N88-30002 #
ESA-CR(P)-2547 ..... N88-30139 #
ESA-CR(P)-2548-VOL-1 ..... N88-29992 #
ESA-CR(P)-2548-VOL-2 ..... N88-29994 #
ESA-CR(P)-2551 ..... N88-30401 #
ESA-CR(P)-2558 ..... N88-30022 #
ESA-CR(P)-2560 ..... N88-29844 #
ESA-CR(P)-2563 ..... N88-30183 #
ESA-CR(P)-2565 ..... N88-29841 #
ESA-CR(P)-2568 ..... N88-30552 #
ESA-CR(P)-2569-VOL-1 ..... N88-30446 #
ESA-CR(P)-2569-VOL-2 ..... N88-30448 #

ESA-CR(P)-2572-VOL-1 ..... N88-30298 #
ESA-CR(P)-2572-VOL-2 ..... N88-30293 #
ESA-CR(P)-2577 ..... N88-30365 #
ESA-CR(P)-2578 ..... N88-30323 #
ESA-CR(P)-2579 ..... N88-30328 #
ESA-CR(P)-2580 ..... N88-30325 #
ESA-CR(P)-2581 ..... N88-30182 #
ESA-CR(P)-2582 ..... N88-30000 #
ESA-CR(P)-2583-VOL-1 ..... N88-29849 #
ESA-CR(P)-2587 ..... N88-30012 #
ESA-CR(P)-2593 ..... N88-29847 #
ESA-CR(P)-2604-PT-1 ..... N88-30167* #
ESA-CR(P)-2604-PT-2 ..... N88-30176 #
ESA-CR(P)-2605 ..... N88-30118 #
ESA-CR(P)-2606 ..... N88-29852 #
ESA-CR(P)-2609 ..... N88-29857 #
ESA-CR(P)-2610 ..... N88-29866 #
ESA-CR(P)-2612-VOL-1 ..... N88-29839 #
ESA-CR(P)-2613 ..... N88-30580 #
ESA-CR(P)-2614 ..... N88-29862 #
ESA-CR(P)-2616 ..... N88-30102 #
ESA-CR(P)-2618 ..... N88-29840 #
ESA-CR(P)-2619 ..... N88-30013 #
ESA-CR(P)-2623 ..... N88-29986 #
ESA-CR(P)-2624 ..... N88-30136 #
ESA-CR(P)-2627-VOL-1 ..... N88-29827 #

ESA-ESTL-76 ..... N88-30136 #

ESA-F09 ..... N88-29828 #

ESA-SP-1097 ..... N88-30557 #
ESA-SP-1098 ..... N88-30556 #
ESA-SP-1100 ..... N88-30447 #

ESA-TT-1082 ..... N88-29767 #
ESA-TT-1087 ..... N88-30187 #
ESA-TT-1089 ..... N88-30075 #
ESA-TT-1091 ..... N88-30067 #
ESA-TT-1100 ..... N88-30080 #

ESD-TR-88-122 ..... N88-30005 #
ESD-TR-88-156 ..... N88-30020 #

ETL-R-143 ..... N88-30175 #
ETL-R-145 ..... N88-30166 #

ETN-88-91607 ..... N88-30582 #
ETN-88-92020 ..... N88-30135 #
ETN-88-92431 ..... N88-30101 #
ETN-88-92606 ..... N88-29838 #
ETN-88-92612 ..... N88-29808 #
ETN-88-92646 ..... N88-30403 #
ETN-88-92650 ..... N88-29964 #
ETN-88-92651 ..... N88-30405 #
ETN-88-92652 ..... N88-30146 #
ETN-88-92668 ..... N88-29803 #
ETN-88-92680 ..... N88-29809 #
ETN-88-92688 ..... N88-30096 #
ETN-88-92698 ..... N88-30091 #
ETN-88-92700 ..... N88-30422 #
ETN-88-92701 ..... N88-30418 #
ETN-88-92716 ..... N88-30265 #
ETN-88-92718 ..... N88-30062 #
ETN-88-92719 ..... N88-30083 #
ETN-88-92725 ..... N88-30070* #
ETN-88-92761 ..... N88-29831 #
ETN-88-92764 ..... N88-29806 #
ETN-88-92765 ..... N88-29802 #
ETN-88-92767 ..... N88-29992 #
ETN-88-92768 ..... N88-29994 #
ETN-88-92769 ..... N88-30002 #
ETN-88-92770 ..... N88-30139 #
ETN-88-92771 ..... N88-29855 #
ETN-88-92774 ..... N88-30401 #
ETN-88-92799 ..... N88-29827 #
ETN-88-92847 ..... N88-29892 #
ETN-88-92876 ..... N88-30169 #
ETN-88-92909 ..... N88-30187 #
ETN-88-92910 ..... N88-30075 #
ETN-88-92912 ..... N88-30080 #
ETN-88-93013 ..... N88-30022 #
ETN-88-93014 ..... N88-29844 #
ETN-88-93015 ..... N88-30183 #
ETN-88-93016 ..... N88-29841 #
ETN-88-93017 ..... N88-30552 #
ETN-88-93018 ..... N88-30446 #
ETN-88-93019 ..... N88-30448 #
ETN-88-93020 ..... N88-30298 #
ETN-88-93021 ..... N88-30293 #
ETN-88-93022 ..... N88-30365 #
ETN-88-93023 ..... N88-30323 #
ETN-88-93024 ..... N88-30328 #
ETN-88-93025 ..... N88-30325 #
ETN-88-93026 ..... N88-30182 #
ETN-88-93027 ..... N88-30000 #

ETN-88-93026 ..... N88-29849 #
ETN-88-93031 ..... N88-30012 #
ETN-88-93032 ..... N88-29847 #
ETN-88-93033 ..... N88-30167* #
ETN-88-93034 ..... N88-30176 #
ETN-88-93035 ..... N88-30118 #
ETN-88-93036 ..... N88-29852 #
ETN-88-93037 ..... N88-29857 #
ETN-88-93038 ..... N88-29866 #
ETN-88-93039 ..... N88-30580 #
ETN-88-93040 ..... N88-30102 #
ETN-88-93041 ..... N88-29840 #
ETN-88-93042 ..... N88-30013 #
ETN-88-93045 ..... N88-30557 #
ETN-88-93046 ..... N88-30556 #
ETN-88-93047 ..... N88-30447 #
ETN-88-93048 ..... N88-29826 #
ETN-88-93050 ..... N88-29767 #
ETN-88-93053 ..... N88-30067 #
ETN-88-93057 ..... N88-29865 #
ETN-88-93058 ..... N88-29813 #
ETN-88-93059 ..... N88-29988 #
ETN-88-93060 ..... N88-30407 #
ETN-88-93061 ..... N88-30192 #
ETN-88-93062 ..... N88-30157 #
ETN-88-93063 ..... N88-30561 #
ETN-88-93064 ..... N88-30567 #
ETN-88-93065 ..... N88-30562 #
ETN-88-93066 ..... N88-30569 #
ETN-88-93067 ..... N88-30564 #
ETN-88-93068 ..... N88-30546 #
ETN-88-93069 ..... N88-30565 #
ETN-88-93070 ..... N88-30560 #
ETN-88-93071 ..... N88-29907
ETN-88-93072 ..... N88-29897
ETN-88-93073 ..... N88-29955
ETN-88-93074 ..... N88-30188
ETN-88-93079 ..... N88-30037 #
ETN-88-93081 ..... N88-30171 #
ETN-88-93083 ..... N88-29875 #
ETN-88-93114 ..... N88-30535 #
ETN-88-93115 ..... N88-29877 #
ETN-88-93116 ..... N88-29871 #
ETN-88-93117 ..... N88-30127 #
ETN-88-93119 ..... N88-30125 #
ETN-88-93120 ..... N88-30047 #
ETN-88-93121 ..... N88-29957 #
ETN-88-93122 ..... N88-29903 #
ETN-88-93123 ..... N88-29886 #
ETN-88-93147 ..... N88-29839 #
ETN-88-93148 ..... N88-29862 #
ETN-88-93150 ..... N88-29996 #
ETN-88-93151 ..... N88-30136 #

FCP-TR-DOS-SY-026 ..... N88-30183 #

FCR-6128 ..... N88-30184* #

FFA-TN-1987-68 ..... N88-30157 #

FOA-C-20713-2.1 ..... N88-29865 #
FOA-C-20714-2.1 ..... N88-29813 #
FOA-C-20718-2.1 ..... N88-29988 #
FOA-C-30481-3.1 ..... N88-30407 #

FR-20311-1 ..... N88-29867* #

FTD-ID(RS)T-0147-88 ..... N88-30117 #
FTD-ID(RS)T-0265-88 ..... N88-30119 #

FTMS-RP-ER-011 ..... N88-29986 #

FVI-86-22 ..... N88-30133 #

GARRETT-21-6689 ..... N88-30076* #

GDSS-SP-88-006 ..... N88-29835* #

H-1461 ..... N88-30093* #

HEL-TM-4-88 ..... N88-30294 #

HEL-TN-3-88-REV-B ..... N88-29797 #

HIC466 ..... N88-30092 #

HL-88-24 ..... N88-30151* #

IB-222-87-A-08 ..... N88-29824 #

IC-87/101 ..... N88-30089 #
IC-87/304 ..... N88-30081 #
IC-87/307 ..... N88-30445 #
IC-87/308 ..... N88-30441 #
IC-87/309 ..... N88-30434 #

ICASE-IR-1 ..... N88-30058* #

ICASE-88-43 ..... N88-29743* #
ICASE-88-44 ..... N88-30079* #
ICASE-88-45 ..... N88-29716* #
ICASE-88-46 ..... N88-29715* #
ICASE-88-47 ..... N88-29749* #
ICASE-88-49 ..... N88-30366* #

ICOMP-88-17 ..... N88-30377* #

IEPC-88-002 ..... N88-29859* #
IEPC-88-035 ..... N88-29873* #
IEPC-88-045 ..... N88-29869* #
IEPC-88-091 ..... N88-29868* #

ILR-MITT-195 ..... N88-29877 #
ILR-MITT-196 ..... N88-29871 #
ILR-MITT-197 ..... N88-30127 #

INPE-4478-PRE/1245 ..... N88-30186 #
INPE-4494-PRE/1258 ..... N88-30185 #
INPE-4537-PRE/1284 ..... N88-30173 #
INPE-4561-PRE/1302 ..... N88-30315 #
INPE-4564-PRE/1305 ..... N88-30310 #
INPE-4567-PRE/1308 ..... N88-30559 #
INPE-4569-PRE/1310 ..... N88-30178 #
INPE-4580-PRE/1314 ..... N88-30551 #
INPE-4582-PRE/1316 ..... N88-30570 #
INPE-4583-PRE/1317 ..... N88-30578 #
INPE-4587-PRE/1318 ..... N88-30170 #
INPE-4590-PRE/1320 ..... N88-30172 #
INPE-4591-PRE/1321 ..... N88-30180 #
INPE-4592-PRE/1322 ..... N88-30174 #
INPE-4593-PRE/1324 ..... N88-30168 #
INPE-4594-PRE/1324 ..... N88-30177 #
INPE-4596-PRE/1324 ..... N88-30577 #
INPE-4609-PRE/1332 ..... N88-30165 #
INPE-4610-PRE/1333 ..... N88-30316 #
INPE-4611-PRE/1334 ..... N88-30179 #
INPE-4613-PRE/1336 ..... N88-30420 #
INPE-4631-PRE/1346 ..... N88-30263 #

IRF-PREPRINT-104 ..... N88-30422 #
IRF-PREPRINT-105 ..... N88-30418 #

ISBN-0-70-581286-3 ..... N88-30401 #
ISBN-0-8330-0810-2 ..... N88-29795 #
ISBN-0-86776-251-9 ..... N88-30152 #
ISBN-9-26-310689-4 ..... N88-30265 #
ISBN-9-51-383058-6 ..... N88-29964 #
ISBN-9-51-383065-3 ..... N88-30405 #
ISBN-9-51-422421-3 ..... N88-30101 #
ISBN-92-835-0426-7 ..... N88-29725 #
ISBN-92-835-0449-6 ..... N88-30458 #
ISBN-92-835-0452-6 ..... N88-29755 #
ISBN-92-835-0458-5 ..... N88-29717 #
ISBN-92-835-0461-5 ..... N88-29735 #
ISBN-92-835-0465-8 ..... N88-29910 #
ISBN-0358-5069 ..... N88-30405 #

ISL-PU-304/87 ..... N88-30135 #

ISSN-0038-0911 ..... N88-30574 #
ISSN-0038-0911 ..... N88-30576 #
ISSN-0065-3713 ..... N88-29897
ISSN-0065-3713 ..... N88-29907
ISSN-0065-3713 ..... N88-29955
ISSN-0065-3713 ..... N88-30188
ISSN-0250-1589 ..... N88-30447 #
ISSN-0280-445X ..... N88-30192 #
ISSN-0284-1711 ..... N88-30418 #
ISSN-0284-1711 ..... N88-30422 #
ISSN-0347-3694 ..... N88-29813 #
ISSN-0347-3694 ..... N88-29865 #
ISSN-0347-3694 ..... N88-29988 #
ISSN-0347-3706 ..... N88-30407 #
ISSN-0356-1852 ..... N88-30101 #
ISSN-0358-5069 ..... N88-29964 #
ISSN-0379-6566 ..... N88-30556 #
ISSN-0379-6566 ..... N88-30557 #
ISSN-0531-4496 ..... N88-30535 #
ISSN-1010-5301 ..... N88-29828 #

JIAA-TR-87 ..... N88-29821* #

JPL-BIBL-39-29 ..... N88-30453* #

JPL-PUBL-82-68-REV-1 ..... N88-30554* #

JPRS-USP-88-001 ..... N88-30498 #

L-16405 ..... N88-29776* #
L-16435 ..... N88-29752* #
L-16462 ..... N88-30402* #

LC-79-640375 ..... N88-30574 #
LC-79-640375 ..... N88-30576 #
LC-87-28382 ..... N88-29795 #

LIDS-P-1758 ..... N88-30385 #

LIDS-TH-1771 ..... N88-30318 #

LMSC-F115808 ..... N88-30181* #

LPI-CONTRIB-650 ..... N88-30473* #
LPI-CONTRIB-660 ..... N88-30487* #

LPI-TR-88-02 ..... N88-30201* #
LPI-TR-88-04 ..... N88-30536* #
LPI-TR-88-08 ..... N88-30258* #

MANIP-217A ..... N88-29855 #

MATRA-100/CC/MLG/031/87 ..... N88-29847 #

MCR-TR-8711/12-1-VOL-2 ..... N88-29801 #

MCR-88-511 ..... N88-30469 #

MD87-50-IB-BQC-JEO ..... N88-30387 #

MEBS-38/87 ..... N88-29852 #

MIT-KBIISE-1 ..... N88-30449 #
MIT-KBIISE-2 ..... N88-30455 #
MIT-KBIISE-5 ..... N88-30452 #
MIT-KBIISE-6 ..... N88-30457 #
MIT-KBIISE-7 ..... N88-30468 #
MIT-KBIISE-8 ..... N88-30454 #

MMCIAC-000701 ..... N88-29882 #

MS-7681 ..... N88-30020 #

MTL-TR-88-11 ..... N88-30408 #
MTL-TR-88-21 ..... N88-30156 #

NAE-AN-45 ..... N88-29781 #

NAS 1.15:4040-PT-2 ..... N88-29776* #
NAS 1.15:88233 ..... N88-30301* #
NAS 1.15:88317 ..... N88-29774* #
NAS 1.15:89801 ..... N88-30573* #
NAS 1.15:100063 ..... N88-29773* #
NAS 1.15:100081 ..... N88-29750* #
NAS 1.15:100339 ..... N88-29832* #
NAS 1.15:100340 ..... N88-30412* #
NAS 1.15:100444 ..... N88-30093* #
NAS 1.15:100463 ..... N88-30583* #
NAS 1.15:100597 ..... N88-29850* #
NAS 1.15:100656 ..... N88-29856* #
NAS 1.15:100659 ..... N88-29820* #
NAS 1.15:100663 ..... N88-29778* #
NAS 1.15:100665 ..... N88-29754* #
NAS 1.15:100691 ..... N88-30039* #
NAS 1.15:100899 ..... N88-30472* #
NAS 1.15:100955 ..... N88-29746* #
NAS 1.15:100962 ..... N88-30128* #
NAS 1.15:100964 ..... N88-29807* #
NAS 1.15:101016 ..... N88-30085* #
NAS 1.15:101019 ..... N88-29751* #
NAS 1.15:101023 ..... N88-30314* #
NAS 1.15:101032 ..... N88-30373* #
NAS 1.15:101188 ..... N88-30581* #
NAS 1.15:101293 ..... N88-29860* #
NAS 1.15:101303 ..... N88-30094* #
NAS 1.15:101305 ..... N88-30090* #
NAS 1.15:101307 ..... N88-29833* #
NAS 1.15:101309 ..... N88-29874* #
NAS 1.15:101314 ..... N88-30072* #
NAS 1.15:101324 ..... N88-29859* #
NAS 1.15:101326 ..... N88-29869* #
NAS 1.15:101327 ..... N88-30377* #
NAS 1.15:101328 ..... N88-30048* #
NAS 1.15:101330 ..... N88-30078* #
NAS 1.15:101333 ..... N88-29952* #
NAS 1.15:101334 ..... N88-30084* #
NAS 1.15:101343 ..... N88-29997* #
NAS 1.15:101347 ..... N88-29780* #
NAS 1.15:101351 ..... N88-29873* #
NAS 1.15:101357 ..... N88-29771* #
NAS 1.15:101363 ..... N88-29868* #
NAS 1.15:101370 ..... N88-29845* #
NAS 1.15:101495 ..... N88-29879* #
NAS 1.21:7011(315) N88-30281*
NAS 1.26:4166 ..... N88-29995* #
NAS 1.26:4187 ..... N88-30304* #
NAS 1.26:172051 ..... N88-29854* #
NAS 1.26:172061 ..... N88-29836* #
NAS 1.26:172062 ..... N88-29837* #

NAS 1.26:172083 ..... N88-29846* #
NAS 1.26:174802 ..... N88-30184* #
NAS 1.26:174894 ..... N88-30066* #
NAS 1.26:174899 ..... N88-30063* #
NAS 1.26:175012 ..... N88-30164* #
NAS 1.26:177410 ..... N88-30308* #
NAS 1.26:177416 ..... N88-30071* #
NAS 1.26:177445 ..... N88-30100* #
NAS 1.26:177476 ..... N88-29819* #
NAS 1.26:177479 ..... N88-29816* #
NAS 1.26:177481 ..... N88-29790* #
NAS 1.26:177482 ..... N88-29817* #
NAS 1.26:177489 ..... N88-30384* #
NAS 1.26:177490 ..... N88-30327* #
NAS 1.26:178315 ..... N88-30058* #
NAS 1.26:178414-VOL-1-PT-1 ..... N88-29745* #
NAS 1.26:178414-VOL-1-PT-2 ..... N88-29770* #
NAS 1.26:178416-VOL-3-PT-2 ..... N88-29744* #
NAS 1.26:179370 ..... N88-30148* #
NAS 1.26:179373 ..... N88-30181* #
NAS 1.26:179389 ..... N88-30200* #
NAS 1.26:179467 ..... N88-29804* #
NAS 1.26:180227 ..... N88-30549* #
NAS 1.26:180884 ..... N88-29863* #
NAS 1.26:180885 ..... N88-29872* #
NAS 1.26:181198 ..... N88-30453* #
NAS 1.26:181438 ..... N88-29775* #
NAS 1.26:181483 ..... N88-29815* #
NAS 1.26:181688 ..... N88-30329* #
NAS 1.26:181689 ..... N88-30399* #
NAS 1.26:181690 ..... N88-29743* #
NAS 1.26:181693 ..... N88-30079* #
NAS 1.26:181697 ..... N88-29716* #
NAS 1.26:181698 ..... N88-29715* #
NAS 1.26:181699 ..... N88-29749* #
NAS 1.26:181706 ..... N88-30386* #
NAS 1.26:182128 ..... N88-29835* #
NAS 1.26:182132 ..... N88-29811* #
NAS 1.26:182139 ..... N88-30076* #
NAS 1.26:182145 ..... N88-29858* #
NAS 1.26:182151 ..... N88-29825* #
NAS 1.26:182157 ..... N88-29961* #
NAS 1.26:182159 ..... N88-29876* #
NAS 1.26:182160 ..... N88-29867* #
NAS 1.26:182201 ..... N88-30055* #
NAS 1.26:182214 ..... N88-30106* #
NAS 1.26:182833 ..... N88-30167* #
NAS 1.26:182873 ..... N88-29880* #
NAS 1.26:183025 ..... N88-30536* #
NAS 1.26:183037 ..... N88-30473* #
NAS 1.26:183073 ..... N88-30201* #
NAS 1.26:183074 ..... N88-30487* #
NAS 1.26:183085 ..... N88-30260* #
NAS 1.26:183113 ..... N88-30571* #
NAS 1.26:183126 ..... N88-30566* #
NAS 1.26:183132 ..... N88-30113* #
NAS 1.26:183136 ..... N88-30275* #
NAS 1.26:183137 ..... N88-30276* #
NAS 1.26:183139 ..... N88-30274* #
NAS 1.26:183142 ..... N88-29848* #
NAS 1.26:183152 ..... N88-29821* #
NAS 1.26:183157 ..... N88-30572* #
NAS 1.26:183161 ..... N88-30320* #
NAS 1.26:183166 ..... N88-30151* #
NAS 1.26:183168 ..... N88-29893* #
NAS 1.26:183169 ..... N88-30258* #
NAS 1.26:183172 ..... N88-30369* #
NAS 1.26:183175 ..... N88-30312* #
NAS 1.26:183202 ..... N88-30134* #
NAS 1.26:183206 ..... N88-30321* #
NAS 1.26:183207 ..... N88-30309* #
NAS 1.26:183215 ..... N88-29884* #
NAS 1.26:183219 ..... N88-30554* #
NAS 1.26:183229 ..... N88-30070* #
NAS 1.26:183246 ..... N88-30297* #
NAS 1.26:183251 ..... N88-30555* #
NAS 1.26:183252 ..... N88-30579* #
NAS 1.26:183253 ..... N88-30547* #
NAS 1.26:183254 ..... N88-30550* #
NAS 1.26:183255 ..... N88-30558* #
NAS 1.26:183264 ..... N88-30431* #
NAS 1.26:183265 ..... N88-30440* #
NAS 1.26:183266 ..... N88-30427* #
NAS 1.26:183267 ..... N88-30437* #
NAS 1.55:3009 ..... N88-30330* #
NAS 1.60:2830 ..... N88-30402* #
NAS 1.60:2834 ..... N88-29752* #
NAS 1.60:2840 ..... N88-30099* #
NAS 1.61:1205 ..... N88-30545* #
NAS 1.71:LAR-13740-1 ..... N88-30105* #
NAS 1.71:LAR-13777-1 ..... N88-29789* #
NAS 1.71:LAR-13889-1 ..... N88-30160* #
NAS 1.71:LAR-13898-1 ..... N88-30130* #
NAS 1.71:LEW-14203-1 ..... N88-29984* #
NAS 1.71:LEW-14698-1 ..... N88-29888* #
NAS 1.71:NPO-16987-1-CU ..... N88-30001* #
NAS 1.77:20240 ..... N88-29906* #
NAS 1.77:20310 ..... N88-29782* #
NAS 1.77:20324 ..... N88-30444* #
NAS 1.77:20330 ..... N88-30088* #
NAS 1.77:20333 ..... N88-29909* #
NAS 1.77:20342 ..... N88-30266* #
NAS 1.77:20343 ..... N88-30068* #
NAS 1.77:20347 ..... N88-30087* #
NAS 1.77:20349 ..... N88-29753* #
NAS 1.77:20352 ..... N88-29899* #
NASA-CASE-LAR-13740-1 ..... N88-30105* #
NASA-CASE-LAR-13777-1 ..... N88-29789* #
NASA-CASE-LAR-13797-1 ..... N88-30108*
NASA-CASE-LAR-13889-1 ..... N88-30160* #
NASA-CASE-LAR-13898-1 ..... N88-30130* #
NASA-CASE-LEW-14203-1 ..... N88-29984* #
NASA-CASE-LEW-14698-1 ..... N88-29888* #
NASA-CASE-MSC-20900-1 ..... N88-30131*
NASA-CASE-NPO-16987-1-CU ..... N88-30001* #
NASA-CP-3009 ..... N88-30330* #
NASA-CR-4166 ..... N88-29995* #
NASA-CR-4187 ..... N88-30304* #
NASA-CR-172051 ..... N88-29854* #
NASA-CR-172061 ..... N88-29836* #
NASA-CR-172062 ..... N88-29837* #
NASA-CR-172063 ..... N88-29846* #
NASA-CR-174802 ..... N88-30184* #
NASA-CR-174894 ..... N88-30066* #
NASA-CR-174899 ..... N88-30063* #
NASA-CR-175012 ..... N88-30164* #
NASA-CR-177410 ..... N88-30308* #
NASA-CR-177416 ..... N88-30071* #
NASA-CR-177445 ..... N88-30100* #
NASA-CR-177476 ..... N88-29819* #
NASA-CR-177479 ..... N88-29816* #
NASA-CR-177481 ..... N88-29790* #
NASA-CR-177482 ..... N88-29817* #
NASA-CR-177489 ..... N88-30384* #
NASA-CR-177490 ..... N88-30327* #
NASA-CR-178315 ..... N88-30058* #
NASA-CR-178414-VOL-1-PT-1 ..... N88-29745* #
NASA-CR-178414-VOL-1-PT-2 ..... N88-29770* #
NASA-CR-178416-VOL-3-PT-2 ..... N88-29744* #
NASA-CR-179370 ..... N88-30148* #
NASA-CR-179373 ..... N88-30181* #
NASA-CR-179389 ..... N88-30200* #
NASA-CR-179467 ..... N88-29804* #
NASA-CR-180227 ..... N88-30549* #
NASA-CR-180884 ..... N88-29863* #
NASA-CR-180885 ..... N88-29872* #
NASA-CR-181196 ..... N88-30453* #
NASA-CR-181438 ..... N88-29775* #
NASA-CR-181483 ..... N88-29815* #
NASA-CR-181688 ..... N88-30329* #
NASA-CR-181689 ..... N88-30399* #
NASA-CR-181690 ..... N88-29743* #
NASA-CR-181693 ..... N88-30079* #
NASA-CR-181697 ..... N88-29716* #
NASA-CR-181698 ..... N88-29715* #
NASA-CR-181699 ..... N88-29749* #
NASA-CR-181706 ..... N88-30386* #
NASA-CR-182128 ..... N88-29835* #
NASA-CR-182132 ..... N88-29811* #
NASA-CR-182139 ..... N88-30076* #
NASA-CR-182145 ..... N88-29858* #
NASA-CR-182151 ..... N88-29825* #
NASA-CR-182157 ..... N88-29961* #
NASA-CR-182159 ..... N88-29876* #
NASA-CR-182160 ..... N88-29867* #
NASA-CR-182201 ..... N88-30055* #
NASA-CR-182214 ..... N88-30106* #
NASA-CR-182833 ..... N88-30167* #
NASA-CR-182873 ..... N88-29880* #
NASA-CR-183025 ..... N88-30536* #
NASA-CR-183037 ..... N88-30473* #
NASA-CR-183073 ..... N88-30201* #
NASA-CR-183074 ..... N88-30487* #
NASA-CR-183085 ..... N88-30260* #
NASA-CR-183113 ..... N88-30571* #
NASA-CR-183126 ..... N88-30566* #
NASA-CR-183132 ..... N88-30113* #
NASA-CR-183136 ..... N88-30275* #
NASA-CR-183137 ..... N88-30276* #
NASA-CR-183139 ..... N88-30274* #
NASA-CR-183142 ..... N88-29848* #
NASA-CR-183152 ..... N88-29821* #
NASA-CR-183157 ..... N88-30572* #
NASA-CR-183161 ..... N88-30320* #
NASA-CR-183166 ..... N88-30151* #
NASA-CR-183168 ..... N88-29893* #
NASA-CR-183169 ..... N88-30258* #
NASA-CR-183172 ..... N88-30369* #
NASA-CR-183175 ..... N88-30312* #
NASA-CR-183202 ..... N88-30134* #
NASA-CR-183206 ..... N88-30321* #
NASA-CR-183207 ..... N88-30309* #
NASA-CR-183215 ..... N88-29884* #
NASA-CR-183219 ..... N88-30554* #
NASA-CR-183229 ..... N88-30070* #
NASA-CR-183246 ..... N88-30297* #
NASA-CR-183251 ..... N88-30555* #
NASA-CR-183252 ..... N88-30579* #
NASA-CR-183253 ..... N88-30547* #
NASA-CR-183254 ..... N88-30550* #
NASA-CR-183255 ..... N88-30558* #
NASA-CR-183264 ..... N88-30431* #
NASA-CR-183265 ..... N88-30440* #
NASA-CR-183266 ..... N88-30427* #
NASA-CR-183267 ..... N88-30437* #
NASA-RP-1205 ..... N88-30545* #
NASA-SP-7011(315) N88-30281*
NASA-TM-4040-PT-2 ..... N88-29776* #
NASA-TM-88233 ..... N88-30301* #
NASA-TM-88317 ..... N88-29774* #
NASA-TM-89801 ..... N88-30573* #
NASA-TM-100063 ..... N88-29773* #
NASA-TM-100081 ..... N88-29750* #
NASA-TM-100339 ..... N88-29832* #
NASA-TM-100340 ..... N88-30412* #
NASA-TM-100444 ..... N88-30093* #
NASA-TM-100483 ..... N88-30583* #
NASA-TM-100597 ..... N88-29850* #
NASA-TM-100656 ..... N88-29858* #
NASA-TM-100659 ..... N88-29820* #
NASA-TM-100663 ..... N88-29778* #
NASA-TM-100665 ..... N88-29754* #
NASA-TM-100891 ..... N88-30039* #
NASA-TM-100899 ..... N88-30472* #
NASA-TM-100955 ..... N88-29746* #
NASA-TM-100962 ..... N88-30128* #
NASA-TM-100964 ..... N88-29807* #
NASA-TM-101016 ..... N88-30085* #
NASA-TM-101019 ..... N88-29751* #
NASA-TM-101023 ..... N88-30314* #
NASA-TM-101032 ..... N88-30373* #
NASA-TM-101188 ..... N88-30581* #
NASA-TM-101293 ..... N88-29860* #
NASA-TM-101303 ..... N88-30094* #
NASA-TM-101305 ..... N88-30090* #
NASA-TM-101307 ..... N88-29833* #
NASA-TM-101309 ..... N88-29874* #
NASA-TM-101314 ..... N88-30072* #
NASA-TM-101324 ..... N88-29859* #
NASA-TM-101326 ..... N88-29869* #
NASA-TM-101327 ..... N88-30377* #
NASA-TM-101328 ..... N88-30048* #
NASA-TM-101330 ..... N88-30078* #
NASA-TM-101333 ..... N88-29952* #
NASA-TM-101334 ..... N88-30084* #
NASA-TM-101343 ..... N88-29997* #
NASA-TM-101347 ..... N88-29780* #
NASA-TM-101351 ..... N88-29873* #
NASA-TM-101357 ..... N88-29771* #
NASA-TM-101363 ..... N88-29868* #
NASA-TM-101370 ..... N88-29845* #
NASA-TM-101495 ..... N88-29879* #
NASA-TP-2830 ..... N88-30402* #
NASA-TP-2834 ..... N88-29752* #
NASA-TP-2840 ..... N88-30099* #
NASA-TT-20240 ..... N88-29906* #
NASA-TT-20310 ..... N88-29782* #
NASA-TT-20324 ..... N88-30444* #
NASA-TT-20330 ..... N88-30088* #
NASA-TT-20333 ..... N88-29909* #
NASA-TT-20342 ..... N88-30266* #
NASA-TT-20343 ..... N88-30068* #
NASA-TT-20347 ..... N88-30087* #
NASA-TT-20349 ..... N88-29753* #
NASA-TT-20352 ..... N88-29899* #
NATICK/TR-88/021 ..... N88-29896 #
NBS-SP-250-17 ..... N88-30109 #
NEPRF-CR-88-01 ..... N88-30267 #
NEPRF-TR-87-04 ..... N88-30262 #
NEPRF-TR-87-05 ..... N88-30199 #
NLR-MP-86072-U ..... N88-29838 #
NLR-MP-87037-U ..... N88-29808 #

NLR-TR-87076-L ..... N88-30323 #

NOSC/TR-1216 ..... N88-30288 #

NRC-27892 ..... N88-29781 #

NRL-MR-6100 ..... N88-30264 #
NRL-MR-6144 ..... N88-30053 #
NRL-MR-6154 ..... N88-30424 #

NRL-9099 ..... N88-30036 #
NRL-9103 ..... N88-30123 #
NRL-9111 ..... N88-30033 #
NRL-9119 ..... N88-30007 #

NSMRL-1108 ..... N88-30279 #

NVO-272 ..... N88-30189 #

ONR-TR-18 ..... N88-30054 #

ORNL/TM-10246 ..... N88-30306 #
ORNL/TM-10787 ..... N88-30149 #

PB87-176129 ..... N88-30040
PB88-201595 ..... N88-30109 #
PB88-212766 ..... N88-30574 #
PB88-212774 ..... N88-30576 #

PNR90423 ..... N88-29803 #
PNR90447 ..... N88-29809 #
PNR90458 ..... N88-30096 #
PNR90471 ..... N88-30091 #

PPS-187 ..... N88-30547* #
PPS-190 ..... N88-30549* #
PPS-202 ..... N88-30550* #
PPS-203 ..... N88-30579* #
PPS-204 ..... N88-30558* #
PPS-205 ..... N88-30555* #

PRF-520-1288-0353 ..... N88-30151* #

PSI-1048/TR-795 ..... N88-30061 #

PSRM-TN-0000-00-04A ..... N88-29866 #

PW-FR-19602 ..... N88-29876* #

R-3255-AF ..... N88-29795 #

R/D-4618-EN-01 ..... N88-30548 #

RADC-TR-87-160 ..... N88-30009 #
RADC-TR-88-8 ..... N88-30150 #
RADC-TR-88-22 ..... N88-30017 #
RADC-TR-88-32-VOL-2 ..... N88-30042 #

RAND/N-2499-AF ..... N88-29796 #

REPT-1-51206A-VOL-1 ..... N88-30295 #
REPT-87-158-EI/ET/AG ..... N88-30139 #
REPT-88B-121 ..... N88-30545* #
REPT-88B0212 ..... N88-30330* #
REPT-112 ..... N88-30101 #
REPT-0353-12 ..... N88-30151* #
REPT-1285-1A ..... N88-29792 #
REPT-1966-20 ..... N88-30040

RIACS-TR-88.6 ..... N88-30309* #
RIACS-TR-88.11 ..... N88-30321* #

RR-CE78 ..... N88-30154 #
RR-CE83 ..... N88-30152 #

RSRE-MEMO-4066-PT-2 ..... N88-30111 #

RU-TR-169-MAE-F ..... N88-30084 #

R85-956834 ..... N88-30068* #
R85-956834-1 ..... N88-30063* #
R87AEG ..... N88-29810 #

S-247-02 ..... N88-30060 #
S-575 ..... N88-30583* #

SC5462.FR ..... N88-29812 #

SD-RP-AI-009-VOL-1 ..... N88-30446 #
SD-RP-AI-009-VOL-2 ..... N88-30448 #

SD-TN-AI-012 ..... N88-29992 #

SD-TR-88-37 ..... N88-29953 #
SD-TR-88-51 ..... N88-29891 #
SD-TR-88-55 ..... N88-30120 #

SD-TR-88-70 ..... N88-30050 #

SE/LS/AP-36-818/CN-VOL-1 ..... N88-29849 #

SEI-TR-87-13 ..... N88-30388 #

SER-C-PREPUBL-FASC-21 ..... N88-30561 #
SER-C-PREPUBL-FASC-22 ..... N88-30567 #
SER-C-PREPUBL-FASC-23 ..... N88-30582 #
SER-C-PREPUBL-FASC-24 ..... N88-30569 #
SER-C-PREPUBL-FASC-25 ..... N88-30564 #
SER-C-PREPUBL-FASC-26 ..... N88-30546 #
SER-C-PREPUBL-FASC-27 ..... N88-30565 #
SER-C-PREPUBL-FASC-28 ..... N88-30560 #

SG-TN-AI-027-VOL-2 ..... N88-29994 #

SGD-523-PT-1 ..... N88-30574 #
SGD-523-PT-2 ..... N88-30576 #

SGI-R-88-136 ..... N88-30257 #

SLI-8707 ..... N88-29993 #

SNIAS-881-422-103 ..... N88-29892 #
SNIAS-881-440-107 ..... N88-30169 #
SNIAS-920-CA/TS ..... N88-29841 #

SR-3 ..... N88-30283 #
SR-4 ..... N88-30256 #

SR/FIS/108(87)CZ ..... N88-30552 #

SRA-R87-910024-F ..... N88-30103 #

SRI-4616 ..... N88-30304* #

STF23-F87025-VOL-1 ..... N88-30298 #
STF23-F87025-VOL-2 ..... N88-30293 #

SU-SOL-88-7 ..... N88-30470 #

SWRI-8814 ..... N88-29747 #

TGAL-87-3 ..... N88-30191 #
TGAL-87-02 ..... N88-30259 #

TL-3333 ..... N88-30365 #

TN88-7104-101-23 ..... N88-30308* #

TR-1 ..... N88-30414 #
TR-21 ..... N88-29904 #
TR-21 ..... N88-30391 #
TR-87-08-07 ..... N88-30324 #
TR-87-50 ..... N88-30387 #
TR-88-01 ..... N88-30299 #
TR-88-04-01 ..... N88-30302 #
TR-534 ..... N88-30383 #
TR-0086(6925-04)-1 ..... N88-30120 #
TR-0086(6945-02)-2 ..... N88-30050 #
TR-0086A(2935-06)-2 ..... N88-29891 #

TR0086A(2060)-3 ..... N88-29953 #

TSL-88-2 ..... N88-30082 #

TT-6705 ..... N88-29783 #

UCB/ERL-M87/74 ..... N88-30041 #
UCB/ERL-M88/21 ..... N88-30425 #

UCB/ERL-87/1 ..... N88-30439 #

UCB/R/88/A1053 ..... N88-30142 #

UCID-21410 ..... N88-29898 #

UCLA-ENG-88-8 ..... N88-29878 #

UDR-TR-88-21 ..... N88-29889 #

UILU-ENG-88-4006 ..... N88-29861 #

ULRF-433/CAR ..... N88-30256 #

UNC-TEMPIS-19 ..... N88-30451 #

US-PATENT-APPL-SN-074792 ..... N88-30108*
US-PATENT-APPL-SN-079317 ..... N88-30131*
US-PATENT-APPL-SN-203376 ..... N88-30001* #
US-PATENT-APPL-SN-205900 ..... N88-30105* #
US-PATENT-APPL-SN-210277 ..... N88-30160* #
US-PATENT-APPL-SN-210480 ..... N88-29789* #
US-PATENT-APPL-SN-219016 ..... N88-29888* #
US-PATENT-APPL-SN-225427 ..... N88-30130* #

US-PATENT-APPL-SN-231026 ..... N88-29984* #
US-PATENT-APPL-SN-831372 ..... N88-30108*

US-PATENT-CLASS-156-233 ..... N88-30108*
US-PATENT-CLASS-156-247 ..... N88-30108*
US-PATENT-CLASS-156-272.4 ..... N88-30108*
US-PATENT-CLASS-156-274.8 ..... N88-30108*
US-PATENT-CLASS-156-275.5 ..... N88-30108*
US-PATENT-CLASS-156-307.7 ..... N88-30108*
US-PATENT-CLASS-219-121.54 ..... N88-30131*
US-PATENT-CLASS-219-121.56 ..... N88-30131*
US-PATENT-CLASS-219-121.57 ..... N88-30131*
US-PATENT-CLASS-219-124.02 ..... N88-30131*
US-PATENT-CLASS-219-130.4 ..... N88-30131*

US-PATENT-4,766,286 ..... N88-30131*
US-PATENT-4,767,484 ..... N88-30108*

USAAEFA-83-13 ..... N88-29785 #
USAAEFA-86-25 ..... N88-29793 #

USAAVSCOM-TM-87-D-5 ..... N88-29768 #

USAAVSCOM-TR-87-A-7 ..... N88-29819* #

USAFSAM-TR-87-34 ..... N88-30280 #
USAFSAM-TR-88-4 ..... N88-30285 #

UTRC-R86-956480-VOL-2 ..... N88-29804* #

VKI-TM-44 ..... N88-30062 #

VKI-TN-163 ..... N88-30083 #

VLSI-MEMO-87-423 ..... N88-30014 #
VLSI-MEMO-87-424 ..... N88-30010 #
VLSI-MEMO-88-440 ..... N88-30045 #
VLSI-MEMO-88-0822 ..... N88-30046 #

VPI-E-88-25 ..... N88-29884* #

VTT-44 ..... N88-29964 #
VTT-46 ..... N88-30405 #

WES-TR-ITL-88-1 ..... N88-30307 #

WES/IR/ITL-88-1 ..... N88-30317 #

WMO-689 ..... N88-30265 #

☆ U.S. GOVERNMENT PRINTING OFFICE: 1988—241-445/80022

FEDERAL REGIONAL DEPOSITORY LIBRARIES

ALABAMA

AUBURN UNIV. AT MONTGOMERY LIBRARY
Documents Department
Montgomery, AL 36193
(205) 271-9650

UNIV. OF ALABAMA LIBRARY
Documents Dept.-Box S
University, AL 35486
(205) 348-6046

ARIZONA

DEPT. OF LIBRARY, ARCHIVES AND PUBLIC RECORDS
Third Floor—State Cap.
1700 West Washington
Phoenix, AZ 85007
(602) 255-4121

UNIVERSITY OF ARIZONA LIB.
Government Documents Dept.
Tucson, AZ 85721
(602) 621-6433

ARKANSAS

ARKANSAS STATE LIBRARY
One Capitol Mall
Little Rock, AR 72201
(501) 371-2326

CALIFORNIA

CALIFORNIA STATE LIBRARY
Govt. Publications Section
P.O. Box 2037
Sacramento, CA 95809
(916) 324-4863

COLORADO

UNIV OF COLORADO LIB.
Government Pub. Division
Campus Box 184
Boulder, CO 80309
(303) 492-8834

DENVER PUBLIC LIBRARY
Govt. Pub. Department
1357 Broadway
Denver, CO 80203
(303) 571-2131

CONNECTICUT

CONNECTICUT STATE LIBRARY
Government Documents Unit
231 Capitol Avenue
Hartford, CT 06106
(203) 566-7029

FLORIDA

UNIV. OF FLORIDA LIBRARIES
Library West
Documents Department
Gainesville, FL 32611
(904) 392-0367

GEORGIA

UNIV. OF GEORGIA LIBRARIES
Government Reference Dept.
Athens, GA 30602
(404) 542-8949

HAWAII

UNIV. OF HAWAII LIBRARY
Govt. Documents Collection
2550 The Mall
Honolulu, HI 96822
(808) 948-8230

IDAHO

UNIV. OF IDAHO LIBRARY
Documents Section
Moscow, ID 83843
(208) 885-6344

ILLINOIS

ILLINOIS STATE LIBRARY
Information Services Branch
Centennial Building
Springfield, IL 62756
(217) 782-5185

INDIANA

INDIANA STATE LIBRARY
Serials Documents Section
140 North Senate Avenue
Indianapolis, IN 46204
(317) 232-3686

IOWA

UNIV. OF IOWA LIBRARIES
Govt. Documents Department
Iowa City, IA 52242
(319) 353-3318

KANSAS

UNIVERSITY OF KANSAS
Doc. Collect—Spencer Lib.
Lawrence, KS 66045-2800
(913) 864-4662

KENTUCKY

UNIV. OF KENTUCKY LIBRARIES
Govt. Pub. Department
Lexington, KY 40506-0039
(606) 257-3139

LOUISIANA

LOUISIANA STATE UNIVERSITY
Middleton Library
Govt. Docs. Dept.
Baton Rouge, LA 70803
(504) 388-2570

LOUISIANA TECHNICAL UNIV. LIBRARY
Documents Department
Ruston, LA 71272-0046
(318) 257-4962

MAINE

UNIVERSITY OF MAINE
Raymond H. Fogler Library
Tri-State Regional Documents Depository
Orono, ME 04469
(207) 581-1680

MARYLAND

UNIVERSITY OF MARYLAND
McKeldin Lib.—Doc. Div.
College Park, MD 20742
(301) 454-3034

MASSACHUSETTS

BOSTON PUBLIC LIBRARY
Government Docs. Dept.
Boston, MA 02117
(617) 536-5400 ext.226

MICHIGAN

DETROIT PUBLIC LIBRARY
Sociology Department
5201 Woodward Avenue
Detroit, MI 48202-4093
(313) 833-1409

MICHIGAN STATE LIBRARY
P.O. Box 30007
Lansing, MI 48909
(517) 373-1593

MINNESOTA

UNIVERSITY OF MINNESOTA
Government Pubs. Division
409 Wilson Library
309 19th Avenue South
Minneapolis, MN 55455
(612) 373-7870

MISSISSIPPI

UNIV. OF MISSISSIPPI LIB.
Documents Department
University, MS 38677
(601) 232-5857

MONTANA

UNIV. OF MONTANA
Mansfield Library
Documents Division
Missoula, MT 59812
(406) 243-6700

NEBRASKA

UNIVERSITY OF NEBRASKA - LINCOLN
Love Library
Documents Department
Lincoln, NE 68588-0410
(402) 472-2562

NEVADA

UNIVERSITY OF NEVADA LIB.
Govt. Pub. Department
Reno, NV 89557-0044
(702) 784-6579

NEW JERSEY

NEWARK PUBLIC LIBRARY
5 Washington Street
Newark, NJ 07101-0630
(201) 733-7812

NEW MEXICO

UNIVERSITY OF NEW MEXICO
Zimmerman Library
Government Pub. Dept.
Albuquerque, NM 87131
(505) 277-5441

NEW MEXICO STATE LIBRARY
Reference Department
325 Don Gaspar Avenue
Santa Fe, NM 87503
(505) 827-3826

NEW YORK

NEW YORK STATE LIBRARY
Empire State Plaza
Albany, NY 12230
(518) 474-5563

NORTH CAROLINA

UNIVERSITY OF NORTH CAROLINA AT CHAPEL HILL
Davis Library
BA/SS Documents Division
Chapel Hill, NC 27515
(919) 962-1151

NORTH DAKOTA

UNIVERSITY OF NORTH DAKOTA
Chester Fritz Library
Documents Department
Grand Forks, ND 58202
(701) 777-4629
In cooperation with North Dakota State Univ. Library

OHIO

STATE LIBRARY OF OHIO
Documents Department
65 South Front Street
Columbus, OH 43266-0334
(614) 462-7051

OKLAHOMA

OKLAHOMA DEPT. OF LIB.
Government Documents
200 NE 18th Street
Oklahoma City, OK 73105
(405) 521-2502, ext. 252

OKLAHOMA STATE UNIV. LIB.
Documents Department
Stillwater, OK 74078
(405) 624-6546

OREGON

PORTLAND STATE UNIV. LIB.
Documents Department
P.O. Box 1151
Portland, OR 97207
(503) 229-3673

PENNSYLVANIA

STATE LIBRARY OF PENN.
Government Pub. Section
P.O. Box 1601
Harrisburg, PA 17105
(717) 787-3752

TEXAS

TEXAS STATE LIBRARY
Public Services Department
P.O. Box 12927—Cap. Sta.
Austin, TX 78711
(512) 475-2996

TEXAS TECH. UNIV. LIBRARY
Govt. Documents Department
Lubbock, TX 79409
(806) 742-2268

UTAH

UTAH STATE UNIVERSITY
Merrill Library, U.M.C. 30
Logan, UT 84322
(801) 750-2682

VIRGINIA

UNIVERSITY OF VIRGINIA
Alderman Lib.—Public Doc.
Charlottesville, VA 22903-2498
(804) 924-3133

WASHINGTON

WASHINGTON STATE LIBRARY
Documents Section
Olympia, WA 98504
(206) 753-4027

WEST VIRGINIA

WEST VIRGINIA UNIV. LIB.
Documents Department
Morgantown, WV 26506-6069
(304) 293-3640

WISCONSIN

MILWAUKEE PUBLIC LIBRARY
814 West Wisconsin Avenue
Milwaukee, WI 53233
(414) 278-3065

ST. HIST LIB. OF WISCONSIN
Government Pub. Section
816 State Street
Madison, WI 53706
(608) 262-4347

WYOMING

WYOMING STATE LIBRARY
Supreme Ct. & Library Bld.
Cheyenne, WY 82002
(307) 777-5919

National Aeronautics and
Space Administration
Code NTT-4
Washington, D.C.
20546

Official Business

Penalty for Private Use, $300

SPECIAL FOURTH-CLASS RATE
POSTAGE & FEES PAID
NASA
PERMIT No. G 27

NASA

POSTMASTER: If Undeliverable (Section 158
Postal Manual) Do Not Return